LIQUID BIOPSY

EDITED BY: Catherine Alix-Panabieres, George Calin and Klaus Pantel
PUBLISHED IN: Frontiers in Cell and Developmental Biology and
Frontiers in Oncology

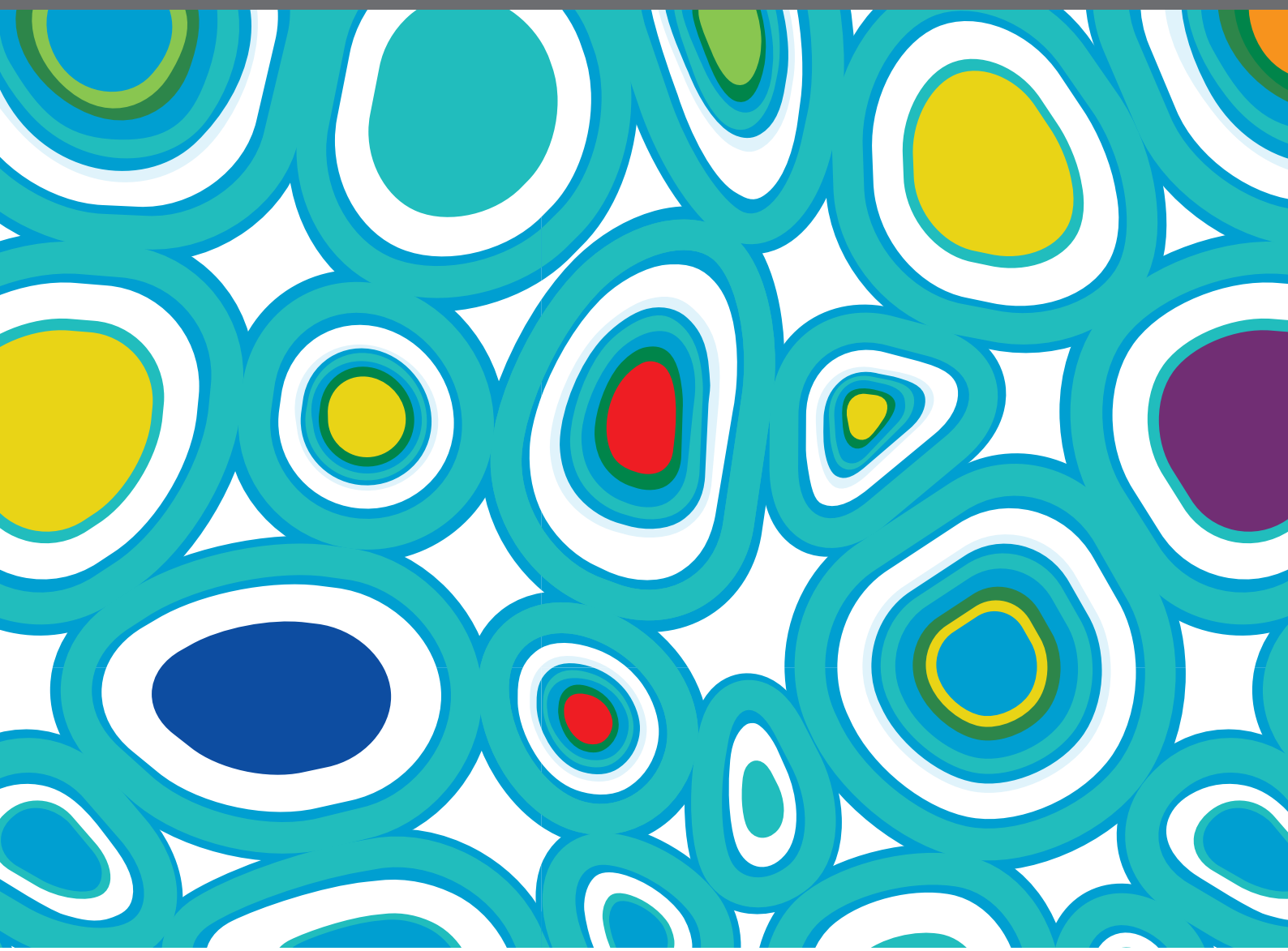

frontiers Research Topics

Frontiers eBook Copyright Statement

The copyright in the text of individual articles in this eBook is the property of their respective authors or their respective institutions or funders. The copyright in graphics and images within each article may be subject to copyright of other parties. In both cases this is subject to a license granted to Frontiers.

The compilation of articles constituting this eBook is the property of Frontiers.

Each article within this eBook, and the eBook itself, are published under the most recent version of the Creative Commons CC-BY licence. The version current at the date of publication of this eBook is CC-BY 4.0. If the CC-BY licence is updated, the licence granted by Frontiers is automatically updated to the new version.

When exercising any right under the CC-BY licence, Frontiers must be attributed as the original publisher of the article or eBook, as applicable.

Authors have the responsibility of ensuring that any graphics or other materials which are the property of others may be included in the CC-BY licence, but this should be checked before relying on the CC-BY licence to reproduce those materials. Any copyright notices relating to those materials must be complied with.

Copyright and source acknowledgement notices may not be removed and must be displayed in any copy, derivative work or partial copy which includes the elements in question.

All copyright, and all rights therein, are protected by national and international copyright laws. The above represents a summary only. For further information please read Frontiers' Conditions for Website Use and Copyright Statement, and the applicable CC-BY licence.

ISSN 1664-8714
ISBN 978-2-83250-451-2
DOI 10.3389/978-2-83250-451-2

About Frontiers

Frontiers is more than just an open-access publisher of scholarly articles: it is a pioneering approach to the world of academia, radically improving the way scholarly research is managed. The grand vision of Frontiers is a world where all people have an equal opportunity to seek, share and generate knowledge. Frontiers provides immediate and permanent online open access to all its publications, but this alone is not enough to realize our grand goals.

Frontiers Journal Series

The Frontiers Journal Series is a multi-tier and interdisciplinary set of open-access, online journals, promising a paradigm shift from the current review, selection and dissemination processes in academic publishing. All Frontiers journals are driven by researchers for researchers; therefore, they constitute a service to the scholarly community. At the same time, the Frontiers Journal Series operates on a revolutionary invention, the tiered publishing system, initially addressing specific communities of scholars, and gradually climbing up to broader public understanding, thus serving the interests of the lay society, too.

Dedication to Quality

Each Frontiers article is a landmark of the highest quality, thanks to genuinely collaborative interactions between authors and review editors, who include some of the world's best academicians. Research must be certified by peers before entering a stream of knowledge that may eventually reach the public - and shape society; therefore, Frontiers only applies the most rigorous and unbiased reviews.
Frontiers revolutionizes research publishing by freely delivering the most outstanding research, evaluated with no bias from both the academic and social point of view. By applying the most advanced information technologies, Frontiers is catapulting scholarly publishing into a new generation.

What are Frontiers Research Topics?

Frontiers Research Topics are very popular trademarks of the Frontiers Journals Series: they are collections of at least ten articles, all centered on a particular subject. With their unique mix of varied contributions from Original Research to Review Articles, Frontiers Research Topics unify the most influential researchers, the latest key findings and historical advances in a hot research area! Find out more on how to host your own Frontiers Research Topic or contribute to one as an author by contacting the Frontiers Editorial Office: frontiersin.org/about/contact

LIQUID BIOPSY

Topic Editors:
Catherine Alix-Panabieres, Centre Hospitalier Universitaire de Montpellier, France
George Calin, University of Texas MD Anderson Cancer Center, United States
Klaus Pantel, University Medical Center Hamburg-Eppendorf, Germany

Citation: Alix-Panabieres, C., Calin, G., Pantel, K., eds. (2022). Liquid Biopsy. Lausanne: Frontiers Media SA. doi: 10.3389/978-2-83250-451-2

Table of Contents

06 ***Circulating Non-coding RNAs in Renal Cell Carcinoma—Pathogenesis and Potential Implications as Clinical Biomarkers***
Dominik A. Barth, Rares Drula, Leonie Ott, Linda Fabris, Ondrej Slaby, George A. Calin and Martin Pichler

22 ***Employing Flow Cytometry to Extracellular Vesicles Sample Microvolume Analysis and Quality Control***
Joana Maia, Silvia Batista, Nuno Couto, Ana C. Gregório, Cristian Bodo, Julia Elzanowska, Maria Carolina Strano Moraes and Bruno Costa-Silva

37 ***Short-Term Circulating Tumor Cell Dynamics in Mouse Xenograft Models and Implications for Liquid Biopsy***
Amber L. Williams, Jessica E. Fitzgerald, Fernando Ivich, Eduardo D. Sontag and Mark Niedre

51 ***Real-Time Molecular Monitoring in Acute Myeloid Leukemia With Circulating Tumor DNA***
Deepshi Thakral, Ritu Gupta, Ranjit Kumar Sahoo, Pramod Verma, Indresh Kumar and Sangeeta Vashishtha

64 ***The Identification of Plasma Exosomal miR-423-3p as a Potential Predictive Biomarker for Prostate Cancer Castration-Resistance Development by Plasma Exosomal miRNA Sequencing***
Tianyu Guo, Yang Wang, Jing Jia, Xueying Mao, Elzbieta Stankiewicz, Glenda Scandura, Edwina Burke, Lei Xu, Jacek Marzec, Caitlin R. Davies, Jiaying Jasmin Lu, Prabhakar Rajan, Alistair Grey, Karen Tipples, John Hines, Sakunthala Kudahetti, Tim Oliver, Thomas Powles, Constantine Alifrangis, Manish Kohli, Greg Shaw, Wen Wang, Ninghan Feng, Jonathan Shamash, Daniel Berney, Liang Wang and Yong-Jie Lu

77 ***DNA-Loaded Extracellular Vesicles in Liquid Biopsy: Tiny Players With Big Potential?***
Susana García-Silva, Miguel Gallardo and Héctor Peinado

84 ***Next-Generation Cancer Biomarkers: Extracellular Vesicle DNA as a Circulating Surrogate of Tumor DNA***
Samuel Amintas, Véronique Vendrely, Charles Dupin, Louis Buscail, Christophe Laurent, Barbara Bournet, Jean-Philippe Merlio, Aurélie Bedel, François Moreau-Gaudry, Julian Boutin, Sandrine Dabernat and Etienne Buscail

93 ***Epigenetic Landscape of Liquid Biopsy in Colorectal Cancer***
Aitor Rodriguez-Casanova, Nicolás Costa-Fraga, Aida Bao-Caamano, Rafael López-López, Laura Muinelo-Romay and Angel Diaz-Lagares

117 ***MicroRNA-940 as a Potential Serum Biomarker for Prostate Cancer***
Smrithi Rajendiran, Sayantan Maji, Ahmed Haddad, Yair Lotan, Rajesh R. Nandy, Jamboor K. Vishwanatha and Pankaj Chaudhary

127 ***Characterizing the Genomic Landscape of Brain Glioma With Circulating Tumor DNA From Tumor* In Situ *Fluid***
Zhiyuan Sheng, Jinliang Yu, Kaiyuan Deng, Hugo Andrade-Barazarte, Ajmal Zemmar, Sijia Li, Nianxuan Li, Zhaoyue Yan, Zhongcan Chen, Yong Sun, Juha Hernesniemi and Xingyao Bu

135 ***Predict Colon Cancer by Pairing Plasma miRNAs: Establishment of a Normalizer-Free, Cross-Platform Model***
Da Qin, Qingdong Guo, Rui Wei, Si Liu, Shengtao Zhu, Shutian Zhang and Li Min

144 ***Evaluation of Monocarboxylate Transporter 4 (MCT4) Expression and Its Prognostic Significance in Circulating Tumor Cells From Patients With Early Stage Non-Small-Cell Lung Cancer***
Athina Markou, E. Tzanikou, G. Kallergi, E. Pantazaka, V. Georgoulias, A. Kotsakis and E. Lianidou

153 ***Characterization of Plasma Cell-Free DNA Integrity Using Droplet-Based Digital PCR: Toward the Development of Circulating Tumor DNA-Dedicated Assays***
Geoffroy Poulet, Fanny Garlan, Sonia Garrigou, Eleonora Zonta, Leonor Benhaim, Marie-Jennifer Carrillon, Audrey Didelot, Delphine Le Corre, Claire Mulot, Philippe Nizard, Frederic Ginot, Audrey Boutonnet-Rodat, Helene Blons, Jean-Baptiste Bachet, Julien Taïeb, Aziz Zaanan, Vanna Geromel, Laurence Pellegrina, Pierre Laurent-Puig, Shu-Fang Wang-Renault and Valerie Taly

164 ***Post-Biopsy Cell-Free DNA From Blood: An Open Window on Primary Prostate Cancer Genetics and Biology***
Marinella Corbetta, Chiara Chiereghin, Ilaria De Simone, Giulia Soldà, Monica Zuradelli, Michele Giunta, Giovanni Lughezzani, Nicolò Maria Buffi, Rodolfo Hurle, Alberto Saita, Paolo Casale, Rosanna Asselta, Massimo Lazzeri, Giorgio Guazzoni and Stefano Duga

174 ***Updates on Clinical Use of Liquid Biopsy in Colorectal Cancer Screening, Diagnosis, Follow-Up, and Treatment Guidance***
Omayma Mazouji, Abdelhak Ouhajjou, Roberto Incitti and Hicham Mansour

187 ***Detection Methods and Clinical Applications of Circulating Tumor Cells in Breast Cancer***
Hongyi Zhang, Xiaoyan Lin, Yuan Huang, Minghong Wang, Chunmei Cen, Shasha Tang, Marcia R. Dique, Lu Cai, Manuel A. Luis, Jillian Smollar, Yuan Wan and Fengfeng Cai

196 ***Genetic Characterization of Cancer of Unknown Primary Using Liquid Biopsy Approaches***
Noemi Laprovitera, Irene Salamon, Francesco Gelsomino, Elisa Porcellini, Mattia Riefolo, Marianna Garonzi, Paola Tononi, Sabrina Valente, Silvia Sabbioni, Francesca Fontana, Nicolò Manaresi, Antonia D'Errico, Maria A. Pantaleo, Andrea Ardizzoni and Manuela Ferracin

211 ***Application of Data Science in Circulating Tumor DNA Detection: A Promising Avenue Towards Liquid Biopsy***
Ming Li, Sisi Xie, Chenyu Lu, Lingyun Zhu and Lvyun Zhu

219 ***Case Report: Circulating Tumor DNA Fraction Analysis Using Ultra-Low-Pass Whole-Genome Sequencing Correlates Response to Chemoradiation and Recurrence in Stage IV Small-Cell Carcinoma of the Cervix - A Longitudinal Study***
Ata Abbas, Morgan Gruner, Jennifer Karohl, Peter G. Rose, Amy Joehlin-Price, Daniel Stover and Haider Mahdi

226 ***Low-Coverage Whole Genome Sequencing of Cell-Free DNA From Immunosuppressed Cancer Patients Enables Tumor Fraction Determination and Reveals Relevant Copy Number Alterations***
Amira Bouzidi, Karim Labreche, Marine Baron, Marianne Veyri, Jérôme Alexandre Denis, Mehdi Touat, Marc Sanson, Frédéric Davi, Erell Guillerm, Stéphanie Jouannet, Frédéric Charlotte, Franck Bielle, Sylvain Choquet, Pierre-Yves Boëlle, Jacques Cadranel, Véronique Leblond, Brigitte Autran, Jean-Marc Lacorte, Jean-Philippe Spano, Florence Coulet and the IDEATION study group

237 ***Impact of Preanalytical and Analytical Methods on Cell-Free DNA Diagnostics***
Jure Krasic, Irena Abramovic, Alen Vrtaric, Nora Nikolac Gabaj, Sasa Kralik-Oguic, Ana Katusic Bojanac, Davor Jezek and Nino Sincic

254 ***Circulating Tumor Cells in Desmoid Tumors: New Perspectives***
Alexcia C. Braun, Fernando A. B. Campos, Emne A. Abdallah, Anna P. C. Ruano, Tiago da S. Medina, Milena S. Tariki, Fabio F. E. Pinto, Celso A. L. de Mello and Ludmilla T. D. Chinen

263 ***Tumor-Educated Platelet miR-18a-3p as a Novel Liquid-Biopsy Biomarker for Early Diagnosis and Chemotherapy Efficacy Monitoring in Nasopharyngeal Carcinoma***
Kaiyu Sun, Hui Wang, Xianqun Xu, Xiuqi Wei, Jingyu Su, Kaidong Zhu and Junli Fan

271 ***Pilocytic Astrocytoma-Derived Cells in Peripheral Blood: A Case Report***
Giorgio Volpentesta, Giuseppe Donato, Elisabetta Ferraro, Chiara Mignogna, Riccardo Radaelli, Umberto Sabatini, Domenico La Torre and Natalia Malara

277 ***The Emerging Role of Exosomes in Cancer Chemoresistance***
Jing Li, Na Gao, Zhengfan Gao, Wei Liu, Bairen Pang, Xingli Dong, Yong Li and Tianli Fan

291 ***Association of Soluble B7-H4 and Circulating Tumor Cells in Blood of Advanced Epithelial Ovarian Cancer Patients***
Pawel Mach, Rainer Kimmig, Sabine Kasimir-Bauer and Paul Buderath

298 ***Deoxyribonucleic Acid 5-Hydroxymethylation in Cell-Free Deoxyribonucleic Acid, a Novel Cancer Biomarker in the Era of Precision Medicine***
Ling Xu, Yixin Zhou, Lijie Chen, Abdul Saad Bissessur, Jida Chen, Misha Mao, Siwei Ju, Lini Chen, Cong Chen, Zhaoqin Li, Xun Zhang, Fei Chen, Feilin Cao, Linbo Wang and Qinchuan Wang

frontiers in Cell and Developmental Biology

REVIEW
published: 15 September 2020
doi: 10.3389/fcell.2020.00828

Circulating Non-coding RNAs in Renal Cell Carcinoma—Pathogenesis and Potential Implications as Clinical Biomarkers

*Dominik A. Barth[1,2], Rares Drula[2,3], Leonie Ott[2,4], Linda Fabris[2], Ondrej Slaby[5,6], George A. Calin[2] and Martin Pichler[1,7]**

[1] Research Unit of Non-Coding RNAs and Genome Editing, Division of Clinical Oncology, Department of Internal Medicine, Comprehensive Cancer Center Graz, Medical University of Graz, Graz, Austria, [2] Department of Translational Molecular Pathology, The University of Texas MD Anderson Cancer Center, Houston, TX, United States, [3] Research Centre for Functional Genomics and Translational Medicine, Iuliu Hatieganu University of Medicine and Pharmacy, Cluj-Napoca, Romania, [4] Department of Tumor Biology, Center of Experimental Medicine, University Medical Center Hamburg-Eppendorf, Hamburg, Germany, [5] Central European Institute of Technology, Masaryk University, Brno, Czechia, [6] Department of Comprehensive Cancer Care, Masaryk Memorial Cancer Institute, Brno, Czechia, [7] Department of Experimental Therapeutics, The University of Texas MD Anderson Cancer Center, Houston, TX, United States

OPEN ACCESS

Edited by:
Mohd Wasim Nasser, University of Nebraska Medical Center, United States

Reviewed by:
Maria Francesca Baietti, VIB KU Leuven Center for Cancer Biology, Belgium
Ali M. Ardekani, Avicenna Research Institute (ARI), Iran
Vinay Sagar, Northwestern Medicine, United States

***Correspondence:**
Martin Pichler
martin.pichler@medunigraz.at

Specialty section:
This article was submitted to Molecular and Cellular Oncology, a section of the journal Frontiers in Cell and Developmental Biology

Received: *01 July 2020*
Accepted: *04 August 2020*
Published: *15 September 2020*

Citation:
Barth DA, Drula R, Ott L, Fabris L, Slaby O, Calin GA and Pichler M (2020) Circulating Non-coding RNAs in Renal Cell Carcinoma—Pathogenesis and Potential Implications as Clinical Biomarkers. Front. Cell Dev. Biol. 8:828. doi: 10.3389/fcell.2020.00828

Liquid biopsy—the determination of circulating cells, proteins, DNA or RNA from biofluids through a "less invasive" approach—has emerged as a novel approach in all cancer entities. Circulating non-(protein) coding RNAs including microRNAs (miRNAs), long non-coding RNAs (lncRNAs), and YRNAs can be passively released by tissue or cell damage or actively secreted as cell-free circulating RNAs, bound to lipoproteins or carried by exosomes. In renal cell carcinoma (RCC), a growing body of evidence suggests circulating non-coding RNAs (ncRNAs) such as miRNAs, lncRNAs, and YRNAs as promising and easily accessible blood-based biomarkers for the early diagnosis of RCC as well as for the prediction of prognosis and treatment response. In addition, circulating ncRNAs could also play a role in RCC pathogenesis and progression. This review gives an overview over the current study landscape of circulating ncRNAs and their involvement in RCC pathogenesis as well as their potential utility as future biomarkers in RCC diagnosis and treatment.

Keywords: biomarker, liquid biopsy, prognosis, long non-coding RNA, microRNA, prognosis, diagnosis, renal cell carcinoma

INTRODUCTION

Renal cell carcinoma (RCC) makes up for more than 90% of malignant kidney tumors, which measures up to 338,000 newly diagnosed patients each year worldwide and makes RCC the second most common urogenital malignancy in men and the third most frequent in women (Ferlay et al., 2015; Znaor et al., 2015; Siegel et al., 2019). The most frequent histological subtype is clear cell renal cell carcinoma (ccRCC) accounting for 70–80%, followed by papillary and chromophobe RCC (Rini et al., 2009). Roughly 20–30% of patients are diagnosed with an initially metastatic disease

(Janzen et al., 2003), which only allows palliative treatment strategies (Powles et al., 2017). Although patient outcomes in these treatment settings have significantly improved since the introduction of immune checkpoint inhibitor therapy and combinations with antiangiogenetic drugs, most patients eventually experience a progressive disease (Motzer et al., 2015, 2018; Cella et al., 2019; Rini et al., 2019).

To date, there are no screening programs or reliable and economically reasonable biomarkers available for the early diagnosis of RCC that would drastically improve the disease outcomes (Rossi et al., 2018). Moreover, although many easily available blood-based biomarkers for the prognosis and the prediction of treatment outcome have been assessed in different stages of treatment and disease, they have not entered clinical routine yet (Dalpiaz et al., 2017; Farber et al., 2017; Seles et al., 2017). In the recent years, liquid biopsies such as circulating tumor cells (CTCs) or circulating ribonucleic acids, obtained from, for instance, blood or urine samples, are emerging (Ellinger et al., 2016; Li G. et al., 2017; Bergerot et al., 2018; Cimadamore et al., 2019). These liquid biopsies serve as novel and promising tools for the diagnosis, prognosis prediction, and selection of appropriate treatment options in RCC patients (Cimadamore et al., 2019; Smith et al., 2020).

Circulating non-coding RNAs (ncRNAs), including microRNAs (miRNAs) and long non-coding RNAs (lncRNAs), have been repeatedly suggested as well-accessible blood-based biomarkers in numerous cancer entities, including urogenital malignancies such as prostate (Su et al., 2015), bladder (Nandagopal and Sonpavde, 2016), testicular (Dieckmann et al., 2019), and kidney cancer (Ellinger et al., 2016). miRNAs are a class of non-protein coding RNAs that are about 20 nucleotides in length (Schwarzenbacher et al., 2019). They bind to the mRNA of their target proteins at the 3′UTR, which results in limited translation and increased degradation of the mRNA (Bartel, 2004). Thus, miRNAs are regulators of many cell functions including cell growth and proliferation and therefore play a principal role in tumorigenesis and progression of RCC and thus may represent useful biomarkers (Schanza et al., 2017; Barth et al., 2019). On the other hand, lncRNAs are over 200 nucleotides in length and regulate cellular processes by different mechanisms (Novikova et al., 2013). They sponge miRNAs, thereby preventing them from binding to their respective targets, which leads to the preserved expression of these targets. Furthermore, they can act as scaffold and decoy for miRNAs or proteins or can act as guides for proteins to influence gene transcription. lncRNAs were demonstrated to regulate cancer development and progression as either oncogenic or tumor-suppressive factors (Chi et al., 2019), and thus therapeutic concepts utilizing the key role of lncRNAs in cancer have emerged over the last decade (Pan et al., 2018b; Pichler et al., 2020).

In RCC, the utility of circulating ncRNAs as biomarkers has been previously evaluated (Ellinger et al., 2016); nevertheless, in the recent years, further evidence has been added to this emerging field. The present review aims to give an update and overview on the progress of circulating ncRNAs as biomarkers across various treatment settings in RCC and highlights pathogenetic implications (see **Tables 1**, **2**).

Challenges of Circulating ncRNAs as Biomarkers in Cancer

As of yet, the development and the use of circulating RNA-based biomarkers comes with certain challenges (Zaporozhchenko et al., 2018). In contrast to cell-free DNA, which is mainly set free in the course of cell death, the largest proportion of circulating RNAs is actively secreted by normal and tumor cells and therefore could reflect current cellular processes and states to disease better, although they can be released during apoptosis and other types of cell death as well (Javidi et al., 2014; Zaporozhchenko et al., 2018). In its nature, cell-free RNA molecules are rather unstable in biofluids such as blood and urine, among others, due to the underlying environmental conditions, including pH and the enzymatic activity of ribonucleases (Tzimagiorgis et al., 2011; Bryzgunova and Laktionov, 2015; Koczera et al., 2016; Zaporozhchenko et al., 2018); nevertheless, miRNAs are astonishingly stable under these extreme conditions (Cortez et al., 2011). Interestingly, in cancer, the activity of ribonucleases in the blood may be decreased, granting a higher stability of circulating RNA products (Huang et al., 2014). Circulating RNAs are often encapsulated in microvesicles, such as exosomes or apoptotic bodies, or can be bound to lipoproteins, such as Ago2 or high-density lipoprotein, in order to protect them from degeneration (**Figure 1**) (Arroyo et al., 2011; Gallo et al., 2012; Wagner et al., 2013; Javidi et al., 2014; Zaporozhchenko et al., 2018).

Exosomes act as an intercellular communication channel, with signals encrypted in the form of the encapsulated DNA, RNA, or protein cargo. The composition of this cargo is highly cell specific and can be a status indicator of cellular homeostasis of the originating cell. Thus, the presence of a specific exosomal cargo signature, specifically miRNA composition, has been previously indicated as having indicative biomarker potential in a number of oncological diseases, including renal carcinoma (Butz et al., 2016; Du et al., 2017). Exosomes participate in intercellular communication and several cellular processes, including the regulation of angiogenesis, apoptosis, and metastasis, and may be utilized as biomarkers or therapeutic targets (Gurunathan et al., 2019; Zhang and Yu, 2019). Exosomes are actively secreted by most cell types through the endosomal sorting complexes required for transport pathway (Colombo et al., 2013), resulting in the fusion of the late endosomal multivesicular body and the cellular membrane (Trajkovic et al., 2008). Moreover, exosomes may transfer miRNAs and lncRNAs between tumor cells, thereby transferring drug resistance and metastatic potential as there is cumulative proof regarding the increased secretion and the differential miRNA signature identified in tumor-derived exosomes when compared to normal cells (Vojtech et al., 2014). While the miRNA sorting mechanisms have not been completely elucidated, recent insight points toward the interaction with a series of RNA binding proteins, such as members of the heterogeneous nuclear ribonucleoprotein family that have been proven to form vesicle-specific miRNA–protein complexes (Villarroya-Beltri et al., 2013). Other proposed mechanisms are based on the activity of the neutral sphingomyelinase 2 and the affinity of miRNAs to membrane raft-like structures containing ceramide as a possible loading mechanism (Groot and Lee, 2020). While it is not yet clear whether the currently proposed miRNA

TABLE 1 | Circulating miRNAs as diagnostic biomarkers in renal cell carcinoma.

miRNA/ panel	Tissue expression pattern	Liquid biopsy expression pattern	Sample type (liquid biopsy)	Sample size (liquid biopsy)	Validation cohort	RCC subtypes included	Diagnostic capability	References
miR-210	↑	↑	Serum	68 patients 42 controls	NA	ccRCC	AUC = 0.874, Sen 81.0%, Spe 79.4%	Zhao et al., 2013
	↑	↑	Serum exosomes	40 patients 30 controls	NA	ccRCC	AUC = 0.8779, Sen 82.5%, Spe 80.0%	Wang X. et al., 2018
	↑	↑	Serum	34 patients 23 controls	NA	ccRCC	AUC = 0.77, Sen 65%, Spe 83%	Iwamoto et al., 2014
	NA	↑	Plasma	66 patients 67 controls	NA	ccRCC	AUC = 0.6775, Sen 89.55%, Spe 48.48%	Chen et al., 2018a
	NA	↑	Serum exosomes	82 patients 80 controls	NA	ccRCC	AUC = 0.69 Sen 70%, Spe 62.2%	Zhang et al., 2018
	NA	↑	Serum	195 patients 100 controls	NA	ccRCC, pRCC, chRCC	AUC = 0.74	Fedorko et al., 2015
miR-378	NA	↑	Serum	195 patients 100 controls	NA	ccRCC, pRCC, chRCC	AUC = 0.82	Fedorko et al., 2015
	NA	↑ (not confirmed in the validation cohort)	Serum	25 patients 25 controls	117 patients 123 controls	ccRCC	NA	Hauser et al., 2012
	NA	↑	Serum	15 patients 10 controls	90 patients 30 controls	ccRCC pRCC chRCC	AUC = 0.71, Sen 70%, Spe 60%	Redova et al., 2012
miR-451	NA	↓	Serum	15 patients 10 controls	90 patients 30 controls	ccRCC pRCC chRCC	AUC = 0.77, Sen 81%, Spe 77%	Redova et al., 2012
miR-144-3p	↑	↑	Plasma	106 patients 28 angiomyolipomas 123 controls	NA	ccRCC	AUC = 0.91, Sen 87.1%, Spe 83.02%	Lou et al., 2017
miR-508-3p	NA	↓	Serum	10 patients 10 controls	85 patients 35 controls	ccRCC	AUC = 0.80	Liu et al., 2019a
miR-885-5p	NA	↑	Serum	10 patients 10 controls	85 patients 35 controls	ccRCC	AUC = 0.87	Liu et al., 2019a
miR-224	NA	↑	Plasma	66 patients 67 controls	NA	ccRCC	AUC = 0.6056, Sen 88.60%, Spe 40.91%	Chen et al., 2018a
miR-625-3p	↑	↑	Serum	50 patients 74 controls	NA	ccRCC	AUC = 0.792, Sen 70.3%, Spe 80.0%	Zhao et al., 2019a
miR-1233	NA	↑	Serum	30 patients 30 controls	84 patients 93 controls	ccRCC, pRCC, chRCC, sRCC	AUC = 0.588, Sen 77.4%, Spe 37.6%	Wulfken et al., 2011
	NA	↑	Serum exosomes	82 patients 80 controls	NA	ccRCC	AUC = 0.82 Sen 81%, Spe 76%	Zhang et al., 2018
miR-21	NA	↑	Serum	30 patients 30 controls	NA	ccRCC	AUC = 0.865, Sen 77.3%, Spe 96.4%	Tusong et al., 2017
miR-106a	NA	↑	Serum	30 patients 30 controls	NA	ccRCC	AUC = 0.819, Sen 86.7%, Spe 70%	Tusong et al., 2017
Diagnostic miRNA panels								
miR-210 miR-378	NA	NA	Serum	195 patients 100 controls	NA	ccRCC, pRCC, chRCC	AUC = 0.85, Sen 80%, Spe 78%	Fedorko et al., 2015
miR-378 mirR-451	NA	NA	Serum	15 patients 10 controls	90 patients 30 controls	ccRCC, pRCC, chRCC	AUC = 0.86, Sen 81%, Spe 83%	Redova et al., 2012

(Continued)

TABLE 1 | Continued

miRNA/ panel	Tissue expression pattern	Liquid biopsy expression pattern	Sample type (liquid biopsy)	Sample size (liquid biopsy)	Validation cohort	RCC subtypes included	Diagnostic capability	References
miR-193a-3p miR-362 miR-572 miR-28-5p miR-378	NA NA NA NA NA	↑ ↑ ↑ ↓ ↓	Serum	28 patients 28 controls	79 patients 79 controls	ccRCC	AUC = 0.807, Sen 80%, Spe 71%	Wang et al., 2015
miR-508-3p miR-885-5p	NA	↓ ↑	Serum	10 patients 10 controls	85 patients 35 controls	ccRCC	AUC = 0.90	Liu et al., 2019a
miR-224/ miR-141 ratio	NA	NA	Plasma	66 patients 67 controls			AUC = 0.9898, Sen 97.06%, Spe 98.53%	Chen et al., 2018a

RCC, renal cell carcinoma; ccRCC, clear cell renal cell carcinoma; pRCC, papillary renal cell carcinoma; chRCC, chromophobe renal cell carcinoma; sRCC, sarcomatoid renal cell carcinoma; NA, not applicable; AUC, area under the curve; Sen, sensitivity; Spe, specificity.

exosomal sorting mechanisms have any clinical relevance, the presence of specific miRNA signatures is indicated to have both mechanistic (Squadrito et al., 2014) and biomarker implications in cancer (Qu et al., 2016; Hosseini et al., 2017; Jiang N. et al., 2019; Wang et al., 2019).

As of yet, when considering cell-free circulating ncRNAs as blood-based biomarkers, differences in the study designs, including the choice of samples (serum versus plasma) and analyzing methods such as quantitative real-time PCR (qRT-PCR), next-generation sequencing, or microarrays, should be taken into account as they can heavily influence experimental outcomes (Lee et al., 2017). For instance, the total concentration of RNA extracted from samples is higher in serum as in plasma, which might be due to differences in processing, leading to the release of RNA when the blood is coagulating (Wang et al., 2012; Lee et al., 2017). Last but not least, differences in normalization of ncRNA measurements to molecules that are consistently expressed in healthy individuals and cancer patients can influence experimental outcomes. In addition, differences in sample collection, storage, and processing may impact the outcome of studies which, once again, impedes the comparability between studies, underlining the necessity of validation studies (Lee et al., 2017).

CIRCULATING miRNAs IN RCC

Circulating miRNAs as Potential Diagnostic Tools

Zhao et al. (2013) first discovered the potential of miR-210 in the diagnosis of RCC. Besides the upregulation of miR-210 in malignant tissues as compared to healthy adjacent parenchyma, they also discovered significantly increased miR-210 levels in serum samples of RCC patients as compared to healthy controls (Zhao et al., 2013). These results were later confirmed by several studies which found increased serum and plasma miR-210 levels in RCC (Iwamoto et al., 2014; Fedorko et al., 2015; Liu T. Y. et al., 2016; Dias et al., 2017; Chen et al., 2018a; Wang X. et al., 2018). Interestingly, the miR-210 serum levels were additionally reported to decline after curative surgery was performed (Fedorko et al., 2015; Wang X. et al., 2018). The serum miR-210 levels could successfully differentiate RCC patients form healthy individuals; however, both sensitivity and specificity are strongly varying and are 81 and 79.4% (Zhao et al., 2013), 67.5 and 70% (Wang X. et al., 2018), and 65 and 83% (Iwamoto et al., 2014) in the different studies, respectively. However, cutoffs for biomarker dichotomization were determined using ROC curve analysis, which makes them difficult to compare. Moreover, no validation cohorts for diagnostic testing were implemented in the studies (Zhao et al., 2013; Iwamoto et al., 2014; Wang X. et al., 2018). Therefore, although there is strong evidence for a potential clinical utility of miR-210 serum levels, future studies need to address these issues. Interestingly enough, serum-derived exosomal miR-210 may offer additional insight for its biomarker potential in comparison to free circulating miR-210 (Wang X. et al., 2018; Zhang et al., 2018). As expected, miR-210 was again upregulated in RCC tissues in a study by Wang X. et al. (2018), which also matched the patient's serum samples. This indicates that changes of miR-210 expressions in RCC cells are perfectly reflected by miR-210 circulating in the patient's blood. However, there may be significant enrichment differences between exosomal and free circulating miR-210, as the latter is increased to a comparably lesser degree. This is also reflected in the diagnostic capability of the two approaches as indicated by significantly varying sensitivity and specificity for exosomal (AUC = 0.8779, 82.5, and 80%) and exosome-free (AUC = 0.7888, 67.5, and 70%) miR-210, respectively (Wang X. et al., 2018). Furthermore, the authors demonstrated increased exosomal miR-210 secretion of RCC cell lines under hypoxic experimental conditions (Wang X. et al., 2018), which is in line with another study investigating serum miR-210 levels in RCC (Dias et al., 2017). miR-210 is strongly connected to hypoxia as it is induced by the absence of functional von Hippel–Lindau (VHL) tumor suppressor gene, which is frequently encountered in RCC tumorigenesis (Shen and Kaelin, 2013), and by increasing hypoxia-inducible factor (HIF) activity (Neal et al., 2010; McCormick et al., 2013; Liu L. L. et al., 2017). Reciprocally, miR-210 may also target hypoxia-inducible factor 1α (HIF-1α), indicating a feedback loop, and thereby suppress hypoxia-induced apoptosis (Liu L. L. et al., 2017). miR-210

TABLE 2 | Circulating miRNAs as prognostic biomarkers in renal cell carcinoma.

miRNA/panel	Sample type (liquid biopsy)	Sample size (liquid biopsy)	Validation cohort	RCC subtypes included	Endpoint	Outcome (high expression)	Hazard ratio (HR), 95% confidence interval (95%CI), *p*-value	References
miR-221	Plasma	43 patients	NA	ccRCC, others (not specified)	OS CSS	Poor	CSS: HR = 10.7, 95%CI 1.33–85.65, $p = 0.024$	Teixeira et al., 2014
miR-224	Serum exosomes	108 patients	NA	Not specified	PFS CSS OS	Poor	PFS: HR = 11, 95% CI 3.3–68.7, $p \leq 0.0001$ CSS: HR = 1.6, 95% CI 1.1–2.5, $p = 0.014$ OS: HR = 9.1, 95% CI 1.8–166.1, $p = 0.0043$	Fujii et al., 2017
miR-26a-1-3p	Plasma exosomes	44 patients	65 patients	Metastatic ccRCC, pRCC, chRCC, unspecified	OS	Good	HR = 0.43, 95% CI 0.1–0.84, $p = 0.025$	Du et al., 2017
miR-615-3p	Plasma exosomes	44 patients	65 patients	Metastatic ccRCC, pRCC, chRCC, unspecified	OS	Good	HR = 0.36, 95% CI 0.11–0.54, $p = 0.0007$	Du et al., 2017
miR-let-7i-5p	Plasma exosomes	44 patients	65 patients	Metastatic ccRCC, pRCC, chRCC, unspecified	OS	Good	HR = 0.49, 95% CI 0.21–0.84, $p = 0.018$	Du et al., 2017
miR-150	Plasma	94 patients	NA	ccRCC	CSS	Good	HR = 1.3, 95% CI 1.0–1.8, $p = 0.03$	Chanudet et al., 2017
miR-210 miR-221 miR-1233	Plasma	54 patients	NA	ccRCC, Others (not specified)	CSS	Poor	HR = 3.02, 95% CI 1.19–7.64, $p = 0.014$	Dias et al., 2017

RCC, renal cell carcinoma; ccRCC, clear cell renal cell carcinoma; pRCC, papillary renal cell carcinoma; chRCC, chromophobe renal cell carcinoma; NA, not applicable; HR, hazard ratio; 95%CI, 95% confidence interval; OS, overall survival; PFS, progression-free survival; CSS, cancer-specific survival.

upregulation under hypoxic conditions results in increased proliferation, genetic instability, angiogenesis, and metastasis and adapts mitochondrial function (Dang and Myers, 2015). An increased release of miR-210 was observed when exposing RCC cell lines to hypoxic conditions in the previously discussed study by Dias et al. (2017), corroborating these results.

Fedorko et al. (2015) also demonstrated the diagnostic potential of serum miR-210; however, in their study, significantly elevated serum levels of miR-378 were better able to differentiate RCC patients from healthy controls with AUCs of 0.74 and 0.82 for miR-210 and miR-378, respectively. Nonetheless, the discriminatory ability of miR-210 and miR-378 combined performed best and discriminated RCC cases with a sensitivity and a specificity of 80 and 78%, respectively (Fedorko et al., 2015). Even so, evidence for the utility of miR-378 in blood-based liquid biopsy is not unambiguous. Although Hauser et al. (2012) could identify serum miR-378 to be significantly higher in a set of ccRCC patients and could discriminate cancer patients form healthy controls, they could not verify their results in the validation cohort. Furthermore, another study that aimed to evaluate a diagnostic panel including five miRNAs reported the miR-378 levels to be reduced in RCC patients as compared to healthy controls (Wang et al., 2015). As opposed to this, Redova et al. (2012) again reported that miR-378 serum levels significantly increased in patients with RCC, which they could further verify in a validation cohort. Apart from miR-378, Redova et al. (2012) also analyzed the diagnostic capability of miR-451 which was found to be significantly decreased in patient serum. This was also verified in a validation cohort. However, interestingly, the combination of miR-451 with the formerly discussed miR-378 could better differentiate the serum samples of healthy individuals from RCC patients with a sensitivity of 81% and a specificity of 83% (Redova et al., 2012). The varying and partly conflicting results regarding serum miR-378 may be due to differences in cohort size as well as baseline characteristics, yet collectively the clinical utility of serum miR-378 in RCC diagnostics at that time is uncertain. In RCC, the pathogenetic role of miR-378 has not been entirely resolved; however, miR-378 may be a regulator of angiogenesis, but this hypothesis is lacking a clear experimental *in vitro* and *in vivo* evidence (Li H. C. et al., 2014). In other cancer types, a pro-angiogenetic effect of miR-378 was demonstrated (Lee et al., 2007; Krist et al., 2015),

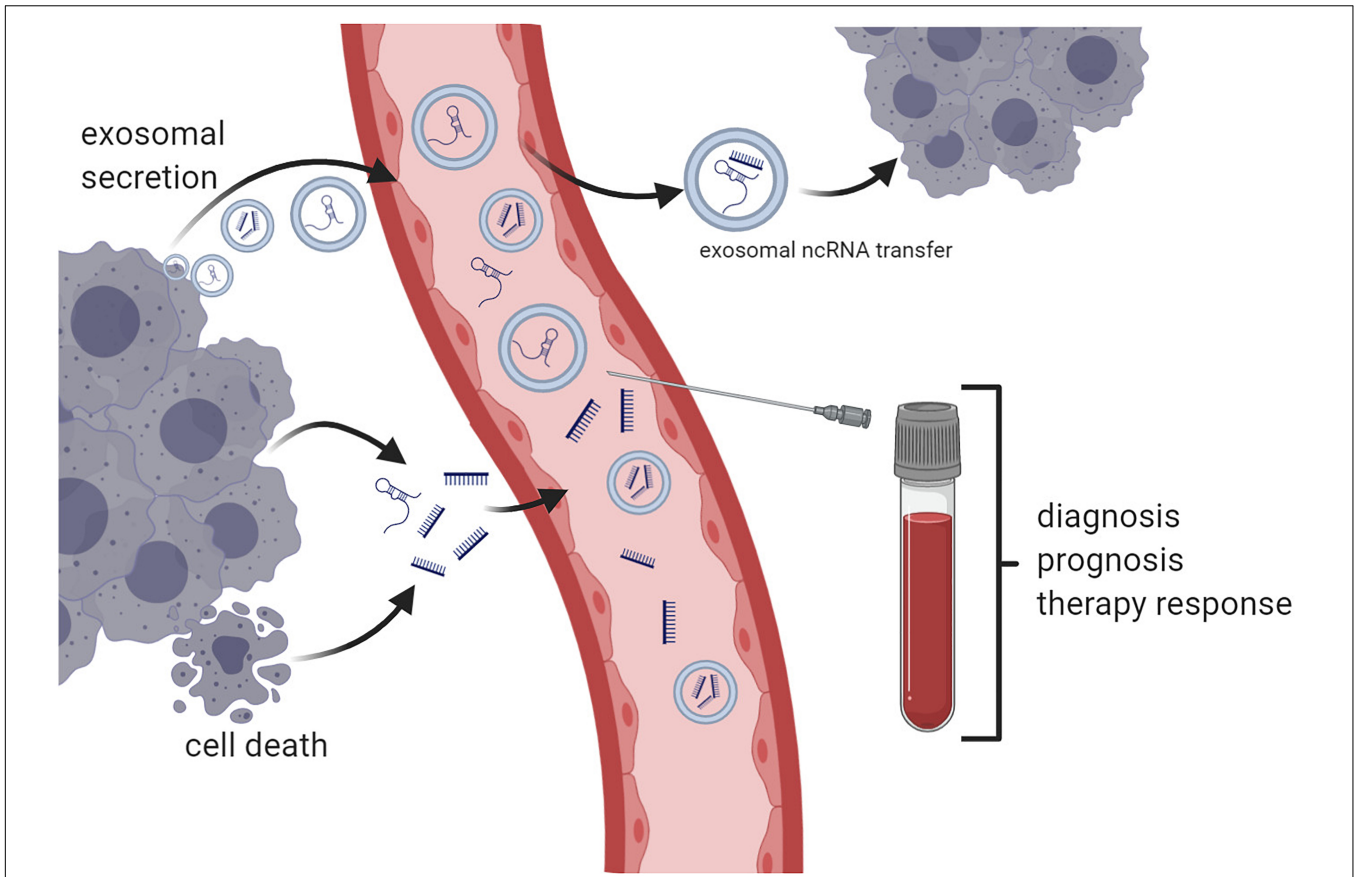

FIGURE 1 | Principles of circulating non-coding RNA (ncRNA)-based liquid biopsy. Non-coding RNA products such as microRNAs and long non-coding RNAs are either actively secreted or released in the course of cell death. Exosomal ncRNAs can be transferred between different tumor sites and thereby disseminate metastatic potential (*e.g.*, miR-19b-3p) or drug resistance (*e.g.*, lncRNA ARSR). Blood samples may be used for diagnosis or prediction of prognosis and response to cancer therapies (created with Biorender.com).

and it could serve as a biomarker for antiangiogenetic therapy in ovarian cancer (Chan et al., 2014). Its role as an oncogenic or tumor-suppressive miRNA seems to vary depending on the cancer type (Zhang et al., 2014; Chen et al., 2016; Li S. et al., 2017; Zeng et al., 2017; Ma et al., 2019), which is frequently observed in other miRNAs (Svoronos et al., 2016).

As already mentioned before, Wang et al. (2015) developed a diagnostic miRNA signature enabling the diagnosis of early ccRCC, which, besides miR-378, also includes miR-193a-3p, miR-362, miR-572, and miR-28-5p. Apart from miR-378 and miR-28-5p, which were significantly decreased, the other miRNAs contained in the diagnostic panel were significantly overexpressed in the serum of ccRCC patients. The panel was able to differentiate patients with ccRCC from non-cancerous controls, especially at the early stages of the disease, accounting for 80% sensitivity and 71% specificity in stage I ccRCC (Wang et al., 2015). However, since corresponding tissue samples were not analyzed in the study, conclusions on the altered expression levels in RCC tissue and their potential reflection in serum miRNA expression and additional involvement in ccRCC pathogenesis cannot be drawn. As for miR-193a-3p, it was shown to target the tumor suppressor phosphatase and tensin homolog (PTEN) and mediate the PI3K/Akt pathway, thereby promoting RCC cell growth and progression (Liu L. et al., 2017; Pan Y. et al., 2018). miR-572 likewise represents an oncomir in RCC pathogenesis by enhancing proliferation and invasion and inhibiting tumor cell apoptosis by suppressing NF2/Hippo signaling (Guan et al., 2018; Pan et al., 2018a). On the other hand, miR-28-5p (Wang et al., 2016) and miR-362 (Zou et al., 2016; Zhu et al., 2020) were suggested as tumor-suppressive miRNAs in RCC, although the miR-362 serum levels were increased in the study by Wang et al. (2015).

Another miRNA that was reported to qualify as liquid diagnostic biomarker is miR-144-3p, which is overexpressed in the plasma of RCC patients and could successfully discriminate RCC from both healthy individuals and patients with renal angiomyolipoma. The sensitivity and the specificity were at 87.1 and 83.02% or 75 and 71.7%, respectively (Lou et al., 2017). The miR-144-3p levels in RCC tissue were likewise increased, and the plasma levels drastically dropped after curative surgery was performed (Xiao et al., 2017). miR-144-3p may promote ccRCC progression and induce resistance to the receptor tyrosine kinase inhibitor sunitinib by targeting AT-rich interaction domain 1A (ARID1A), which is the gene of the SWI/SNF subunit in the SWI/SNF chromatin remodeling complex (Xiao et al., 2017; Mathur, 2018). ARID1A influences cell cycle, apoptosis, and

p53 targets, thus acting as a tumor suppressor (Mathur, 2018). However, the role of miR-144-3p in RCC pathogenesis may not be clear as another study conversely suggested miR-144-3p both being decreased in RCC tissue and acting as a tumor suppressor by targeting mitogen-activated protein kinase 8 (MAP3K8) (Liu F. et al., 2016).

miR-508-3p and miR-509-5p were both demonstrated to play a role in RCC pathogenesis and additionally altered tissue and plasma expression levels were reported. As for miR-508-3p, the expression levels in tissue, plasma, and serum are consistently decreased as reported by two studies (Zhai et al., 2012; Liu et al., 2019a), and serum miR-508-3p was able to differentiate RCC and non-cancer samples (AUC = 0.8), which even improved when combined with increased serum levels of miR-885-5p (AUC = 0.9) (Liu et al., 2019a). As for miR-509-5p, the evidence is not as clear since its expression was found to be decreased in the plasma of RCC patients, yet the difference was not significant in every available study although the baseline characteristics of the study population were similar (Zhai et al., 2012; Zhang et al., 2013). Nonetheless, both miR-508-3p and miR-509-5p may act as tumor suppressors in RCC by inducing apoptosis and inhibiting cell proliferation and migration *in vitro* (Zhai et al., 2012; Zhang et al., 2013; Liu et al., 2019a). Zinc finger E-box-binding homeobox 1 and nuclear factor kappa B subunit 1 may represent targets of miR-508-3p as demonstrated in cervical and gastric cancer (Huang et al., 2016; Guo et al., 2018).

Furthermore, Chen et al. (2018a) also investigated several plasmatic miRNAs for their diagnostic potential in RCC, including miR-210, which we already discussed earlier. In their study, besides miR-210, the authors included miR-224 and miR-141 and analyzed various plasmatic combinations of the three miRNAs. Interestingly, the combination of the significantly elevated miR-224 and the decreased miR-141 plasma levels in a miR-224/miR-141 ratio showed the best diagnostic capability (AUC = 0.9898, sensitivity 97.06%, specificity 98.53%), representing a promising potential diagnostic tool in RCC patients (Chen et al., 2018a). However, this was not tested in a validation cohort, and external validation is missing. Considering the varying and partly conflicting results in the analysis of miRNAs in a larger body of evidence, at this point, it should be considered hypothesis-generating until confirmed by future studies.

miR-21, which has been repeatedly shown to be overexpressed in RCC tissue and has been suggested as a prognostic marker in RCC patients (Faragalla et al., 2012; Zaman et al., 2012; Vergho et al., 2014), was also reported to be elevated in patients' serum samples and positively correlated to tumor stages, indicating a potential role as a blood-based diagnostic biomarker (Cheng et al., 2013; Tusong et al., 2017). Additionally, a decline in miR-21 serum levels after surgery was reported (Tusong et al., 2017). However, Sanders et al. (2012) could not confirm the potential clinical value of miR-21, as, in their analysis, the expression levels were highly similar between controls and urological cancers including RCC. This may be due to differences in the study populations as serum miR-21 could be correlated to tumor stages (Cheng et al., 2013). Interestingly, increased serum levels of miR-21 were observed in other cancer types as well, including prostate, lung, and breast cancer (Zhang H. L. et al., 2011; Liu et al., 2012; Schwarzenbach et al., 2012). Besides miR-21, Cheng et al. (2013) also discovered that miR-34a and miR-224 were overexpressed, and miR-141 expression was significantly decreased in the sera of RCC patients, corroborating previously discussed results of miR-224 and miR-141 (Chen et al., 2018a).

In RCC cells, miR-21 was proposed to act as an oncogenic miRNA and enhance tumor progression and proliferation while inhibiting apoptosis (Zhang A. et al., 2011; Li X. et al., 2014; Petrozza et al., 2015). Additionally, it may target VHL mRNA (Sun et al., 2019; Zang et al., 2019), the loss of which plays a major role in RCC tumorigenesis and promotes normoxic HIF signaling (Shen and Kaelin, 2013).

miR-106a is another candidate for a diagnostic miRNA in ccRCC as it was significantly overexpressed in the serum of 30 ccRCC patients with matched controls and was reduced after curative surgery, which indicates a potential use in post-surgery biomarker monitoring (Tusong et al., 2017). In addition, miR-106a could differentiate ccRCC patients from controls with an AUC of 0.819 and a sensitivity and a specificity of 86.7 and 70%, respectively (Tusong et al., 2017). However, the members of the miR-106 family miR-106a-5p and miR-106a* were previously reported to be downregulated in RCC tissue (Ma et al., 2015; Pan et al., 2017), which is in contrast to the findings of increased miR-106a levels in patient serum by Tusong et al. (2017). miR-106a-5p overexpression was shown to inhibit both cell migration and invasion *in vitro* and reduced metastases *in vivo* by targeting p21 activated kinase 5 (Pan et al., 2017). Moreover, miR-106a* was found to suppress the proliferation of RCC cell lines by inhibiting IRS-2 and thus inhibiting PI3K/Akt signaling (Ma et al., 2015). Therefore, the serum expression of miR-106a should be interpreted with caution unless validation in larger cohorts was performed.

Another miRNA which may qualify as a future marker in the diagnosis of RCC is miR-625-3p. It was reported to be overexpressed in ccRCC tissues yet decreased in the serum of ccRCC patients (Zhao et al., 2019a). A high tissue expression of miR-625-3p was an independent predictor for poor OS (HR = 2.949, 95%CI 1.413–6.152, $p = 0.004$), whereas serum expression could significantly differentiate ccRCC patients from healthy controls (AUC = 0.792, sensitivity 70.3%, specificity 80%) (Zhao et al., 2019a). However, the inconsistency in miR-625-3p expression in tumor tissue and patient serum demands further validation. In functional investigations in RCC cell lines, miR-625-3p was shown to enhance RCC cell migration and invasion and additionally inhibit apoptosis (Zhao et al., 2019a).

Wulfken et al. (2011) identified miR-1233, which showed significantly higher levels in both RCC tissue and patients' serum, as a biomarker candidate in RCC diagnostics. The diagnostic utility was verified in a multicenter validation cohort including 84 RCC patients and 93 controls, yet although miR-1233 was able to significantly discriminate RCC patients from healthy individuals, the results in the validation cohort may not support its use in clinical routine (AUC = 0.588, sensitivity 77.4%, specificity 37.6%) (Wulfken et al., 2011). Even so, the combination of miR-1233 with miR-141 could promisingly enhance the diagnostic capability, reaching a sensitivity of 100% and a specificity of

73.3% (Yadav et al., 2017). In addition, Zhang et al. (2018) found that serum exosomal miR-1233 increased in their study including 82 RCC patients and successfully differentiated RCC from non-cancer samples, corroborating previous results. The pathogenetic role of miR-1233 in RCC to date is not well investigated; however, the observed increase of miR-1233 levels upon hypoxia in RCC cell lines indicates its involvement in hypoxic cell signaling (Dias et al., 2017).

Apart from acting as biomarkers, exosomal miRNAs were suggested to promote RCC progression. Wang et al. (2019) reported that exosomal miR-19b-3p that originated from ccRCC cancer stem cells (CSC) in RCC metastases transfers EMT potential to renal cancer cells by being incorporated by the tumor cells. Mechanistically, miR-19b-3p targets the tumor suppressor PTEN and enhances lung metastases (Wang et al., 2019). This was also verified in rodent models, and CD103 overexpression in CSC exosomes was suggested to guide exosomes to their destinations in tumor and lung tissue. Corroborating these results, in a cohort of 209 ccRCC patients, CD103+ exosomes were significantly increased in patients with metastatic disease, indicating a potential use in the diagnosis and the monitoring of metastasized ccRCC (Wang et al., 2019).

Circulating miRNAs as Prognostic Biomarkers in RCC

Dias et al. (2017) aimed to analyze the potential prognostic utility of the already afore-discussed miR-210, miR-221, and miR-1233 in the blood plasma of RCC patients. Interestingly, the increased plasma levels of all investigated miRNAs were significantly associated with poor cancer-specific survival (CSS) and independently predicted for CSS when combined as a single biomarker (HR = 3.02, 95%CI 1.19–7.64, $p = 0.014$). Moreover, this miRNA panel complements prognostic parameters, such as tumor stage, Fuhrman grade, age, and gender, as it significantly improves their prognostic capacity when combined to an index with already established clinico-pathological parameters (Dias et al., 2017). As for miR-221, this corroborates the findings of Teixeira et al. (2014) who reported miR-221 to be upregulated in the plasma of RCC patients. Moreover, plasma levels were found to be even higher in patients who already had metastatic disease when first diagnosed with RCC. Increased plasmatic miR-221 expression levels represented an independent prognostic marker for OS (Teixeira et al., 2014). In the same study, miR-222, the plasmatic expression of which was also observed to be increased in RCC patients *versus* healthy controls, did not validate as an independent predictor of overall survival (OS). Interestingly, the addition of plasmatic miR-221 levels to the already established clinico-pathological parameters TNM stage, Fuhrman grade, and age combined could improve their prognostic capability (c-index 0.8, HR = 4.5, 95%CI 1.17–17.34, $p = 0.029$ *versus* c-index 0.961, HR = 10.7, 95%CI 1.33–85.65, $p = 0.26$) (Teixeira et al., 2014). Both miR-221 and miR-222 were found to be significantly overexpressed in RCC tissue *vs.* healthy renal parenchyma and have already been considered as promoters of RCC proliferation and progression in numerous studies (Lu et al., 2015; Liu et al., 2019b; Zhao et al., 2019b; Lv et al., 2020). Furthermore, both miRNAs were proposed as predictive markers for treatment response to sunitinib therapy and were demonstrated to enhance angiogenesis *via* targeting the vascular endothelial growth factor receptor 2 (VEGFR2) (Khella et al., 2015; Garcia-Donas et al., 2016). This mechanism was also shown to regulate the response to sunitinib treatment in prostate cancer (Krebs et al., 2020). miR-221 was additionally suggested in the regulation of HIF-1α, which plays a major role in RCC pathogenesis (Penolazzi et al., 2019), and beyond that, it could enhance RCC cell proliferation, migration, and invasion by targeting the tissue inhibitor of metalloproteinases 2 (TIMP2) as found in cell culture models (Lu et al., 2015).

miR-224 was already shown to have a potential diagnostic utility in the previous chapter (Chen et al., 2018a). As for its impact on RCC prognosis, Fujii et al. (2017) analyzed exosomal miR-224 in RCC patients. miR-224 was upregulated in RCC tissue and the high exosomal miR-224 in the blood of 108 RCC patients independently predicted for shorter CSS, progression-free survival (PFS), and OS (CSS: HR = 1.6, 95%CI 1.1–2.5, $p = 0.014$; PFS: HR = 11, 95%CI 3.3–68.7, $p \leq 0.0001$; OS: HR = 9.1, 95%CI 1.8–166.1, $p = 0.0043$), respectively (Fujii et al., 2017). Functional experiments revealed an oncogenic role of miR-224 in RCC pathogenesis. Exosomes containing miR-224 from a metastatic RCC cell line that were added to a cell line of primary RCC enhanced proliferation and invasion and, moreover, increased the intracellular miR-224 levels in primary cell lines (Fujii et al., 2017). This indicates the importance of exosomal miRNAs in cancer progression (Fujii et al., 2017; Kulkarni et al., 2019). Furthermore, miR-224 was shown to influence RCC progression by directly targeting alpha-2,3-sialyltransferase IV and impacting the PI3K/AKT pathway (Pan Y. et al., 2018).

Another study that investigated the prognostic utility of plasma exosomal miRNAs was conducted by Du et al. (2017). In their study, in a first step, plasma exosomal miRNA expression levels were evaluated in a discovery cohort including 44 patients with metastatic RCC. In a second step, the most promising miRNAs were confirmed in a validation cohort of 65 patients. Eventually, miR-26a-1-3p (HR = 0.43, 95%CI 0.1–0.84, $p = 0.025$), miR-615-3p (HR = 0.36, 95%CI 0.11–0.54, $p = 0.0007$), and miRNA let-7i-5p (HR = 0.49, 95%CI 0.21–0.84, $p = 0.018$) retained their prognostic value in the validation set, and decreased plasma exosomal expression was significantly associated with adverse prognosis (Du et al., 2017). Moreover, Du et al. (2017) compared the prognostic ability of the established Memorial Sloan-Kettering Cancer Center (MSKCC) score, which takes multiple clinico-pathological factors into consideration, *versus* the MSKCC score with the inclusion of let-7i-5p. In their analysis, the addition of let-7i-5p improved the prognostic capability (AUC = 0.64) as compared to the MSKCC score alone (AUC = 0.58) (HR = 3.43, 95%CI 2.73–24.15, $p = 0.0002$ for the combination) (Du et al., 2017). The miRNA let-7 family mainly exerts tumor-suppressive functions in cancer, yet several subtypes may also act as oncogenes (Chirshev et al., 2019). However, let7i-5p and its role in RCC pathogenesis have not been evaluated yet. The members of the let7-family let7b and let7c were reported to be decreased in RCC tissue and were able to suppress

proliferation and restore chemoresistance to 5-fluorouracile in *in vitro* experiments (Peng et al., 2015). In contrast, let-7g-5p and let-7i-5p were significantly overexpressed in a study including 94 ccRCC specimens (Gowrishankar et al., 2014). The differing results across the let-7 subtype underline the different biological roles of let-7 subtypes, and further research is therefore necessary to clarify the functional role of exosomal let-7i-3p in RCC. Results in other cancer types suggest a tumor-suppressive role of let-7i as, for instance, they are downregulated in ovarian and bladder cancer and inhibited tumor proliferation and chemoresistance (Yang et al., 2008; Qin et al., 2019). As for miR-615-3p, Wang Q. et al. (2018) found it to be sponged by the lncRNA HOXA transcript at the distal tip (HOTTIP) and to target insulin-like growth factor 2 in RCC. In their study, HOTTIP was shown to be upregulated in RCC tissue, and the overexpression of HOTTIP was reported to promote RCC proliferation, migration, and invasion *in vitro*, implicating a tumor-suppressive role of miR-615-3p (Wang Q. et al., 2018).

Chanudet et al. (2017) screened for circulating miRNAs in RCC using microRNA arrays in plasma samples of 94 ccRCC patients of all clinical stages and 100 healthy controls. Although they could not recommend single miRNAs or miRNA signatures for the early diagnosis of ccRCC, thereby contradicting previous results, the authors found lower miR-150 expression in the plasma of ccRCC patients to be independently associated with cancer-specific survival (HR = 1.3, 95%CI 1.0–1.8, $p = 0.03$) (Chanudet et al., 2017). Even though miR-150 has not been functionally investigated in RCC yet, the utility of exosomal serum miR-150 levels in colorectal cancer for prognosis prediction supports the notion of its future clinical utility in RCC (Zhao Y. J. et al., 2019; Zou et al., 2019). However, miR-150 may exert different functions in different cancer types as, for instance, it promotes metastasis in lung cancer, whereas it may behave as a tumor suppressor in colorectal cancer (Li et al., 2016; Chen et al., 2018b).

Circulating miRNAs as Predictive Biomarkers for Therapy Response

Circulating miRNAs might also be involved in acquiring resistance to treatment regimens in RCC. A recent study suggests that miR-35-5p carried in extracellular vesicles participates in the development of resistance to the multi-targeted receptor tyrosine kinase inhibitor sunitinib (He et al., 2020). In the study, sorafenib-sensitive cell lines were exposed to extracellular vesicles of sorafenib-resistant RCC cells, which contained increased levels of miR-31-5p. This resulted in increasing sorafenib resistance in the former treatment-sensitive cell lines, indicating transmitted therapy resistance by miR-31-5p *via* extracellular vesicles. The role of miR-31-5p in the induction of sorafenib resistance was subsequently demonstrated in further *in vitro* and *in vivo* experiments, and functional analysis revealed MutL homolog 1 (MLH1) as a direct target of miR-31-5p. The authors speculate that reduced MLH1 expression and subsequent increased genomic instability may facilitate the development of drug resistance (He et al., 2020). Ultimately, He et al. (2020) found significantly increased levels of miR-31-5p within extracellular vesicles in the serum of RCC patients, who had progressed on sorafenib-based treatment, as compared to serum levels before treatment initiation. This indicates a possible role as a predictive biomarker for the development of sorafenib resistance; however, the authors did not further investigate miR-31-5p levels and the potential impact on clinical endpoints such as PFS or response rates (He et al., 2020). Nevertheless, the role of miR-31-5p in RCC pathogenesis is not without inconsistencies. A previous study suggested that miR-31-5p may act as a tumor suppressor in RCC by inhibiting proliferation, migration, and invasion *via* targeting cyclin-dependent kinase 1 (Li et al., 2019). Moreover, the expression of miR-31-5p has been reported to be significantly lower in RCC tissue and cell lines (Li et al., 2019).

Gamez-Pozo et al. (2012) developed several predictive models of miRNA expression in the peripheral blood for resistance to sunitinib therapy in a prospective observational multicenter study including 38 metastatic RCC patients who received first-line treatment with sunitinib. Blood samples were taken before and 2 weeks after treatment initiation, and micro-array assays and subsequent verification of promising miRNA candidates with qPCR were performed. The authors developed 12 predictive models for each response group, whereas poor response was defined as progression earlier than 6 months and prolonged response was defined as progression later than 18 months after therapy initiation. The expression levels of up to four miRNAs per individual model and 28 miRNAs in total were significantly related with their respective prognostic groups. One model of the poor response group, including miR-192, miR-193-3p, and miR-501-3p, and one model of the prolonged response group, which included miR-miR-410, miR-1181, and miR-424*, prevailed their predictive ability in the validation with qRT-PCR (Gamez-Pozo et al., 2012). However, due to the relatively small patient sample, further research and validation is required.

CIRCULATING LONG NON-CODING RNAS IN RCC

Although the utility of circulating lncRNAs as biomarkers in cancer and potential pathomechanisms have been reported repeatedly, in RCC data remain limited.

The lncRNA gradually increased during hepatocarcinogenesis (GIHCG) may represent a promising biomarker in RCC (He et al., 2018). GIHCG is overexpressed in RCC tissue as compared to healthy adjacent tissue and is also elevated in the serum of RCC patients, showing a highly significant correlation with tumor tissue expression levels. Moreover, the GIHCG serum levels were able to discriminate RCC patients and healthy individuals with a sensitivity and a specificity of 87 and 84.8%, respectively (AUC = 0.920) (He et al., 2018). In addition, GIHCG retained its diagnostic ability when only early-stage RCC and healthy controls were compared, and RCC tissue expression levels were significantly associated with OS; however, no uni- and multivariate analyses were performed (He et al., 2018). GIHCG was first described in hepatocellular carcinoma, where it was demonstrated to enhance tumor cell proliferation, migration, and metastases both *in vitro* and *in vivo*

by recruiting the transcription factors EZH2 and DNMT1 to the miR-200b/a/429 promoter, thereby epigenetically silencing miR-200b/a/429 expression (Sui et al., 2016). Since then, GIHCG's oncogenic role has been reported in various cancers such as ovarian, colorectal, gastric, and cervical cancer (Yao et al., 2018; Jiang X. et al., 2019; Liu G. et al., 2019; Zhang et al., 2019). He et al. (2018) eventually confirmed this role in RCC in knockdown experiments.

Wu et al. (2016) attempted to develop a panel including several lncRNAs as a novel diagnostic marker for RCC. In their study, potential lncRNAs for further investigation were first discovered in RCC tissue, and the serum expression of lncRNA candidates was analyzed in a discovery cohort including 25 patients with ccRCC, pRCC, or chRCC in a second step. Subsequently, promising lncRNAs were evaluated in a validation set of 37 patients and 35 healthy controls. A panel of five lncRNAs, low expressed in tumor (LET), plasmacytoma variant translocation 1 (PVT1), promoter of CDKN1A antisense DNA damage activated RNA (PANDAR), phosphatase and tensin homolog pseudogene 1 (PTENP1), and linc00963, was able to successfully discriminate non-cancer from RCC patients (AUC = 0.823) and retained their diagnostic ability throughout the different clinical TNM stages, also indicating their utility as early markers for RCC (Wu et al., 2016). In an additional small clinical patient set which also included patients with benign renal tumors, the cancer patients showed significantly higher risk indices as compared to controls (Wu et al., 2016). lncRNA LET is considered a tumor suppressor in a variety of cancer types which also accounts for RCC, where LET was shown to enhance apoptosis and impair mitochondrial membrane potential by targeting miR-373-3p, thereby regulating Dickkopf 1 and tissue TIMP2 expression (Weidle et al., 2017; Ye et al., 2019). Moreover, PTENP1, too, acts as a tumor-suppressive factor in RCC by acting as a competing endogenous RNA for miR-21, which would otherwise promote cell proliferation, migration, and invasion by the suppression of PTEN, an important tumor suppressor (Zhang A. et al., 2011; Song et al., 2012; Yu et al., 2014). In contrast, PVT1 (Pan et al., 2018b; Derderian et al., 2019) and PANDAR (Li J. et al., 2017; Han et al., 2019) are well-known oncogenic lncRNAs, and their role in RCC tumorigenesis and negative impact on RCC outcome have been reported (Bao et al., 2017; Xu et al., 2017; Yang et al., 2017; Li et al., 2018). Linc00963 has not been investigated in RCC yet but was indicated to promote cancer progression in a variety of malignancies such as head and neck cancer osteosarcoma and breast cancer (Zhou et al., 2019b; Lee et al., 2020; Wu et al., 2020). However, Wu et al. (2016) found that the expression levels of PVT1 and linc00963 were significantly downregulated in the serum of RCC patients as compared to tissue expression levels.

The lncRNA activated in RCC with sunitinib resistance (ARSR) was first described by Qu et al. (2016), who suggested the involvement of exosomal ARSR in the development of resistance to sunitinib in RCC and discovered its potential pathomechanism. ARSR expression was increased in the RCC tissue of patients who were resistant to sunitinib as well as in resistant RCC cell lines. Moreover, plasma levels were significantly elevated in RCC patients as compared to healthy controls, and detectable ARSR levels dropped after surgical treatment and increased upon tumor recurrence. Higher plasma ARSR levels independently predicted for shorter PFS for sunitinib treatment (HR = 2.9, 95%CI 1.2–7.1, p = 0.017) (Qu et al., 2016). This indicates that the circulating ARSR in RCC patients is a promising biomarker for response to sunitinib (Qu et al., 2016). Interestingly, ARSR has also been associated with drug resistance in osteosarcoma and hepatocellular carcinoma (Li Y. et al., 2017; Shen and Cheng, 2020). Furthermore, Qu et al. (2016) elucidated the underlying mechanism in RCC and demonstrated that ARSR upregulation is indispensable for the development of sunitinib resistance. ARSR was shown to sponge both miR-34 and miR-449, thereby preventing them from binding to their targets AXL and c-MET, thus inhibiting their degradation. As a result, ARSR upregulation results in a likewise increase of AXL and c-MET and further activation of the downstream STAT3, AKT, and ERK signaling pathway (Qu et al., 2016). The involvement of ARSR in STAT3 and AKT regulation was confirmed in liver cancer (Li Y. et al., 2017; Yang et al., 2019). Moreover, in RCC, AKT was found to promote ARSR expression by inhibiting forkhead box protein O1/3a (FOXO1 and FOXO3a), which results in the formation of a positive feedback loop (Qu et al., 2016). Interestingly, the exosomal secretion of ARSR was reported to transfer sunitinib resistance to former sunitinib-sensitive cells both *in vitro* and *in vivo*, indicating the exosomal dissemination of sunitinib resistance. In addition, therapeutically targeting ARSR could restore sunitinib sensitivity *in vivo* (Qu et al., 2016).

CIRCULATING YRNAs IN RCC

YRNAs are small ncRNA molecules that form characteristic stem-loop formations because of their complementary 5′ and 3′ UTRs (Pruijn et al., 1993). Originally, they were reported in rheumatic diseases where they were found to be part of soluble ribonucleoproteins (Hendrick et al., 1981). YRNAs comprise the four subtypes hY1, hY3, hY4, and hY5 and are abundant in both serum and plasma (Dhahbi et al., 2013; Yeri et al., 2017). Recently, they have been suggested as circulating biomarkers in breast as well as head and neck cancer (Dhahbi et al., 2014; Victoria Martinez et al., 2015). In RCC, although Nientiedt et al. (2018) reported significant alterations in the expression levels of hY3 and hY4 in malignant *versus* healthy tissue, they could not find any differences in serum expression levels. Thus, YRNAs do not bring any additional value as easily available blood-based biomarkers in RCC (Nientiedt et al., 2018).

COMPARISON TO CURRENT STANDARDS

The early diagnosis of RCC still remains difficult due to the lack of broad screening programs and a specific panel of symptoms already noticeable at early-stage disease. Many patients are diagnosed incidentally when they present with symptoms like hematuria, abdominal mass, or flank pain (Vasudev et al., 2020).

Since many of these symptoms are non-specific, the majority of patients do not get completely evaluated within the first 6 months after initial presentation (Zhou et al., 2019a), thus reducing the number of patients diagnosed at an early stage. This is a major issue since early diagnosis is crucial for successful therapy and is associated with better patient survival (Tsui et al., 2000; Palsdottir et al., 2012). Hence, finding liquid biomarkers for early-stage disease detection might prove to be beneficial for patients. Due to the minimal invasiveness of liquid biopsies, they could be performed routinely. However, up to now, there is no established biomarker available for clinical use. RCC is reported to present with lower circulating tumor DNA (ctDNA) levels compared to other tumor entities (Smith et al., 2020), excluding it as a feasible diagnostic marker in RCC. Also, CTCs have not been established for clinical use in RCC diagnosis yet due to heterogenous surface marker expression (Bu et al., 2020), which makes an enrichment with the CellSearch^{TM} system, the only FDA-approved CTC capture platform, difficult (Bai et al., 2018). Therefore, circulating ncRNAs might represent useful and easily available biomarkers in the diagnosis and treatment of RCC. As summarized in this review, the analysis of various circulating ncRNAs can distinguish RCC patients from healthy donors. However, systematic screenings and larger-scale studies, which would be necessary for a potential clinical implementation in the diagnosis of early-stage RCC, are missing.

For prognostic purposes, the International Metastatic RCC Database Consortium (IMDC) and MSKCC risk scores are the current standard tools in RCC. Both use a panel of six or five clinical parameters to predict patient outcome, respectively (Tanaka et al., 2016). Even though they are widely validated, there are also reports showing their limitations. Indeed they performed fairly accurate in predicting OS in different cohorts of mRCC patients undergoing first- and second-line targeted therapy (Heng et al., 2009; Ko et al., 2015; Tanaka et al., 2016). Their respective prognoses for around 23% of patients in a treatment-naïve cohort undergoing the first line of targeted therapy do not match, suggesting limited prognostic capacity (Okita et al., 2019). They also do not perform well in predicting OS in patients undergoing cytoreductive nephrectomy (Westerman et al., 2020). Thus, implementation of additional or new biomarkers, to reliably stratify RCC patients in the era of targeted therapies, might be beneficial. It was already shown that the inclusion of an additional miRNA as a marker could improve the prognostic capacity of the MSKCC score (Du et al., 2017). Various ncRNAs, as described in this review, have prognostic capacities for OS (Teixeira et al., 2014) or therapy response (Gamez-Pozo et al., 2012; Li et al., 2019; He et al., 2020). In general, multiple miRNAs or lncRNAs summarized in a distinctive panel or signature appear to bring higher predictive values. Hence, comparisons of ncRNAs alone or in combination with well-established clinical scores, with scores like the MSKCC and IMDC, might be interesting to evaluate to check whether prognosis prediction in various settings can be improved.

CONCLUSION

In order to make circulating ncRNAs feasible biomarkers for diagnosis and prognosis in RCC, comparisons with current, well-established standards are necessary to determine whether they add any value. Therefore, sensitivity, specificity, and accuracy would have to be compared or added to scores like the IMDC or the MSKCC or other promising methods such as genomic profiling.

However, due to missing validations and an ongoing discussion about, for example, optimal sample processing and normalization, circulating ncRNAs are not yet to enter clinical practice in RCC, and further research is needed.

AUTHOR CONTRIBUTIONS

DB and MP conceptualized this work. DB contributed to visualization and writing—preparing the original draft. DB, RD, LO, LF, OS, GC, and MP contributed to writing—reviewing and editing the manuscript. MP supervised the study. OS, GC, and MP took charge of funding acquisition. All the authors have read and agreed to the published version of the manuscript.

FUNDING

This project has received funding from the European Union's Horizon 2020 Research and Innovation Program under the Marie Skłodowska-Curie grant agreement no. 824036.

ACKNOWLEDGMENTS

DB thanks the Society for Cancer Patients (Verein für Krebskranke) of the Medical University of Graz for the financial support during his traineeship at the MD Anderson Cancer Center.

REFERENCES

Arroyo, J. D., Chevillet, J. R., Kroh, E. M., Ruf, I. K., Pritchard, C. C., Gibson, D. F., et al. (2011). Argonaute2 complexes carry a population of circulating microRNAs independent of vesicles in human plasma. *Proc. Natl. Acad. Sci. U.S.A.* 108, 5003–5008. doi: 10.1073/pnas.1019055108

Bai, M., Zou, B., Wang, Z., Li, P., Wang, H., Ou, Y., et al. (2018). Comparison of two detection systems for circulating tumor cells among patients with renal cell carcinoma. *Int. Urol. Nephrol.* 50, 1801–1809. doi: 10.1007/s11255-018-1954-2

Bao, X., Duan, J., Yan, Y., Ma, X., Zhang, Y., Wang, H., et al. (2017). Upregulation of long noncoding RNA PVT1 predicts unfavorable prognosis in patients with clear cell renal cell carcinoma. *Cancer Biomark* 21, 55–63. doi: 10.3233/cbm-170251

Bartel, D. P. (2004). MicroRNAs: genomics, biogenesis, mechanism, and function. *Cell* 116, 281–297.

Barth, D. A., Slaby, O., Klec, C., Juracek, J., Drula, R., Calin, G. A., et al. (2019). Current concepts of non-coding RNAs in the pathogenesis of non-clear cell renal cell carcinoma. *Cancers (Basel)* 11:10.3390/cancers11101580.

Bergerot, P. G., Hahn, A. W., Bergerot, C. D., Jones, J., and Pal, S. K. (2018). The role of circulating tumor DNA in renal cell carcinoma. *Curr. Treat. Options Oncol.* 19:10.

Bryzgunova, O. E., and Laktionov, P. P. (2015). Extracellular nucleic acids in urine: sources, structure, diagnostic potential. *Acta Naturae* 7, 48–54. doi: 10.32607/20758251-2015-7-3-48-54

Bu, J., Nair, A., Kubiatowicz, L. J., Poellmann, M. J., Jeong, W. J., Reyes-Martinez, M., et al. (2020). Surface engineering for efficient capture of circulating tumor cells in renal cell carcinoma: From nanoscale analysis to clinical application. *Biosens. Bioelectron.* 162:112250. doi: 10.1016/j.bios.2020.112250

Butz, H., Nofech-Mozes, R., Ding, Q., Khella, H. W. Z., Szabo, P. M., Jewett, M., et al. (2016). Exosomal MicroRNAs are diagnostic biomarkers and can mediate cell-cell communication in renal cell carcinoma. *Eur. Urol. Focus* 2, 210–218. doi: 10.1016/j.euf.2015.11.006

Cella, D., Grunwald, V., Escudier, B., Hammers, H. J., George, S., Nathan, P., et al. (2019). Patient-reported outcomes of patients with advanced renal cell carcinoma treated with nivolumab plus ipilimumab versus sunitinib (CheckMate 214): a randomised, phase 3 trial. *Lancet Oncol.* 20, 297–310. doi: 10.1016/s1470-2045(18)30778-2

Chan, J. K., Kiet, T. K., Blansit, K., Ramasubbaiah, R., Hilton, J. F., Kapp, D. S., et al. (2014). MiR-378 as a biomarker for response to anti-angiogenic treatment in ovarian cancer. *Gynecol. Oncol.* 133, 568–574. doi: 10.1016/j.ygyno.2014.03.564

Chanudet, E., Wozniak, M. B., Bouaoun, L., Byrnes, G., Mukeriya, A., Zaridze, D., et al. (2017). Large-scale genome-wide screening of circulating microRNAs in clear cell renal cell carcinoma reveals specific signatures in late-stage disease. *Int. J. Cancer* 141, 1730–1740. doi: 10.1002/ijc.30845

Chen, Q. G., Zhou, W., Han, T., Du, S. Q., Li, Z. H., Zhang, Z., et al. (2016). MiR-378 suppresses prostate cancer cell growth through downregulation of MAPK1 in vitro and in vivo. *Tumour Biol.* 37, 2095–2103. doi: 10.1007/s13277-015-3996-8

Chen, X., Lou, N., Ruan, A., Qiu, B., Yan, Y., Wang, X., et al. (2018a). miR-224/miR-141 ratio as a novel diagnostic biomarker in renal cell carcinoma. *Oncol. Lett.* 16, 1666–1674.

Chen, X., Xu, X., Pan, B., Zeng, K., Xu, M., Liu, X., et al. (2018b). miR-150-5p suppresses tumor progression by targeting VEGFA in colorectal cancer. *Aging (Albany NY)* 10, 3421–3437. doi: 10.18632/aging.101656

Cheng, T., Wang, L., Li, Y., Huang, C., Zeng, L., and Yang, J. (2013). Differential microRNA expression in renal cell carcinoma. *Oncol. Lett.* 6, 769–776. doi: 10.3892/ol.2013.1460

Chi, Y., Wang, D., Wang, J., Yu, W., and Yang, J. (2019). Long non-coding RNA in the pathogenesis of cancers. *Cells* 8:1015. doi: 10.3390/cells8091015

Chirshev, E., Oberg, K. C., Ioffe, Y. J., and Unternaehrer, J. J. (2019). Let-7 as biomarker, prognostic indicator, and therapy for precision medicine in cancer. *Clin. Transl. Med.* 8:24.

Cimadamore, A., Gasparrini, S., Massari, F., Santoni, M., Cheng, L., Lopez-Beltran, A., et al. (2019). Emerging molecular technologies in renal cell carcinoma: liquid biopsy. *Cancers (Basel)* 11:196. doi: 10.3390/cancers11020196

Colombo, M., Moita, C., van Niel, G., Kowal, J., Vigneron, J., Benaroch, P., et al. (2013). Analysis of ESCRT functions in exosome biogenesis, composition and secretion highlights the heterogeneity of extracellular vesicles. *J. Cell. Sci.* 126(Pt 24), 5553–5565. doi: 10.1242/jcs.128868

Cortez, M. A., Bueso-Ramos, C., Ferdin, J., Lopez-Berestein, G., Sood, A. K., and Calin, G. A. (2011). MicroRNAs in body fluids–the mix of hormones and biomarkers. *Nat. Rev. Clin. Oncol.* 8, 467–477. doi: 10.1038/nrclinonc.2011.76

Dalpiaz, O., Luef, T., Seles, M., Stotz, M., Stojakovic, T., Pummer, K., et al. (2017). Critical evaluation of the potential prognostic value of the pretreatment-derived neutrophil-lymphocyte ratio under consideration of C-reactive protein levels in clear cell renal cell carcinoma. *Br. J. Cancer* 116, 85–90. doi: 10.1038/bjc.2016.393

Dang, K., and Myers, K. A. (2015). The role of hypoxia-induced miR-210 in cancer progression. *Int. J. Mol. Sci.* 16, 6353–6372. doi: 10.3390/ijms16036353

Derderian, C., Orunmuyi, A. T., Olapade-Olaopa, E. O., and Ogunwobi, O. O. (2019). PVT1 signaling is a mediator of cancer progression. *Front. Oncol.* 9:502. doi: 10.3389/fonc.2019.00502

Dhahbi, J. M., Spindler, S. R., Atamna, H., Boffelli, D., and Martin, D. I. (2014). Deep sequencing of serum small RNAs identifies patterns of 5' tRNA half and YRNA fragment expression associated with breast cancer. *Biomark Cancer* 6, 37–47.

Dhahbi, J. M., Spindler, S. R., Atamna, H., Boffelli, D., Mote, P., and Martin, D. I. (2013). 5'-YRNA fragments derived by processing of transcripts from specific YRNA genes and pseudogenes are abundant in human serum and plasma. *Physiol. Genomics* 45, 990–998. doi: 10.1152/physiolgenomics.00129.2013

Dias, F., Teixeira, A. L., Ferreira, M., Adem, B., Bastos, N., Vieira, J., et al. (2017). Plasmatic miR-210, miR-221 and miR-1233 profile: potential liquid biopsies candidates for renal cell carcinoma. *Oncotarget* 8, 103315–103326. doi: 10.18632/oncotarget.21733

Dieckmann, K. P., Radtke, A., Geczi, L., Matthies, C., Anheuser, P., Eckardt, U., et al. (2019). Serum levels of MicroRNA-371a-3p (M371 Test) as a new biomarker of testicular germ cell tumors: results of a prospective multicentric study. *J. Clin. Oncol.* 37, 1412–1423. doi: 10.1200/jco.18.01480

Du, M., Giridhar, K. V., Tian, Y., Tschannen, M. R., Zhu, J., Huang, C. C., et al. (2017). Plasma exosomal miRNAs-based prognosis in metastatic kidney cancer. *Oncotarget* 8, 63703–63714. doi: 10.18632/oncotarget.19476

Ellinger, J., Gevensleben, H., Muller, S. C., and Dietrich, D. (2016). The emerging role of non-coding circulating RNA as a biomarker in renal cell carcinoma. *Expert Rev. Mol. Diagn.* 16, 1059–1065. doi: 10.1080/14737159.2016.1239531

Faragalla, H., Youssef, Y. M., Scorilas, A., Khalil, B., White, N. M., Mejia-Guerrero, S., et al. (2012). The clinical utility of miR-21 as a diagnostic and prognostic marker for renal cell carcinoma. *J. Mol. Diagn.* 14, 385–392. doi: 10.1016/j.jmoldx.2012.02.003

Farber, N. J., Kim, C. J., Modi, P. K., Hon, J. D., Sadimin, E. T., and Singer, E. A. (2017). Renal cell carcinoma: the search for a reliable biomarker. *Transl. Cancer Res.* 6, 620–632.

Fedorko, M., Stanik, M., Iliev, R., Redova-Lojova, M., Machackova, T., Svoboda, M., et al. (2015). Combination of MiR-378 and MiR-210 serum levels enables sensitive detection of renal cell carcinoma. *Int. J. Mol. Sci.* 16, 23382–23389. doi: 10.3390/ijms161023382

Ferlay, J., Soerjomataram, I., Dikshit, R., Eser, S., Mathers, C., Rebelo, M., et al. (2015). Cancer incidence and mortality worldwide: sources, methods and major patterns in GLOBOCAN 2012. *Int. J. Cancer* 136, E359–E386.

Fujii, N., Hirata, H., Ueno, K., Mori, J., Oka, S., Shimizu, K., et al. (2017). Extracellular miR-224 as a prognostic marker for clear cell renal cell carcinoma. *Oncotarget* 8, 109877–109888. doi: 10.18632/oncotarget.22436

Gallo, A., Tandon, M., Alevizos, I., and Illei, G. G. (2012). The majority of microRNAs detectable in serum and saliva is concentrated in exosomes. *PLoS One* 7:e30679. doi: 10.1371/journal.pone.0030679

Gamez-Pozo, A., Anton-Aparicio, L. M., Bayona, C., Borrega, P., Gallegos Sancho, M. I., Garcia-Dominguez, R., et al. (2012). MicroRNA expression profiling of peripheral blood samples predicts resistance to first-line sunitinib in advanced renal cell carcinoma patients. *Neoplasia* 14, 1144–1152.

Garcia-Donas, J., Beuselinck, B., Inglada-Perez, L., Grana, O., Schoffski, P., Wozniak, A., et al. (2016). Deep sequencing reveals microRNAs predictive of antiangiogenic drug response. *JCI Insight* 1:e86051.

Gowrishankar, B., Ibragimova, I., Zhou, Y., Slifker, M. J., Devarajan, K., Al-Saleem, T., et al. (2014). MicroRNA expression signatures of stage, grade, and progression in clear cell RCC. *Cancer Biol. Ther.* 15, 329–341. doi: 10.4161/cbt.27314

Groot, M., and Lee, H. (2020). Sorting mechanisms for MicroRNAs into extracellular vesicles and their associated diseases. *Cells* 9:1044. doi: 10.3390/cells9041044

Guan, Y., Gong, Z., Xiao, T., and Li, Z. (2018). Knockdown of miR-572 suppresses cell proliferation and promotes apoptosis in renal cell carcinoma cells by targeting the NF2/Hippo signaling pathway. *Int. J. Clin. Exp. Pathol.* 11, 5705–5714.

Guo, S. J., Zeng, H. X., Huang, P., Wang, S., Xie, C. H., and Li, S. J. (2018). MiR-508-3p inhibits cell invasion and epithelial-mesenchymal transition by targeting ZEB1 in triple-negative breast cancer. *Eur. Rev. Med. Pharmacol. Sci.* 22, 6379–6385.

Gurunathan, S., Kang, M. H., Jeyaraj, M., Qasim, M., and Kim, J. H. (2019). Review of the isolation, characterization, biological function, and multifarious therapeutic approaches of exosomes. *Cells* 8:307. doi: 10.3390/cells8040307

Han, L., Wang, B., Wang, R., Wang, Z., Gong, S., Chen, G., et al. (2019). Prognostic and clinicopathological significance of long non-coding RNA PANDAR expression in cancer patients: a meta-analysis. *Front. Oncol.* 9:1337. doi: 10.3389/fonc.2019.01337

Hauser, S., Wulfken, L. M., Holdenrieder, S., Moritz, R., Ohlmann, C. H., Jung, V., et al. (2012). Analysis of serum microRNAs (miR-26a-2*, miR-191, miR-337-3p and miR-378) as potential biomarkers in renal cell carcinoma. *Cancer Epidemiol.* 36, 391–394. doi: 10.1016/j.canep.2012.04.001

He, J., He, J., Min, L., He, Y., Guan, H., Wang, J., et al. (2020). Extracellular vesicles transmitted miR-31-5p promotes sorafenib resistance by targeting MLH1 in renal cell carcinoma. *Int. J. Cancer* 146, 1052–1063. doi: 10.1002/ijc.32543

He, Z. H., Qin, X. H., Zhang, X. L., Yi, J. W., and Han, J. Y. (2018). Long noncoding RNA GIHCG is a potential diagnostic and prognostic biomarker and therapeutic target for renal cell carcinoma. *Eur. Rev. Med. Pharmacol. Sci.* 22, 46–54.

Hendrick, J. P., Wolin, S. L., Rinke, J., Lerner, M. R., and Steitz, J. A. (1981). Ro small cytoplasmic ribonucleoproteins are a subclass of La ribonucleoproteins: further characterization of the Ro and La small ribonucleoproteins from uninfected mammalian cells. *Mol. Cell. Biol.* 1, 1138–1149. doi: 10.1128/mcb.1.12.1138

Heng, D. Y., Xie, W., Regan, M. M., Warren, M. A., Golshayan, A. R., Sahi, C., et al. (2009). Prognostic factors for overall survival in patients with metastatic renal cell carcinoma treated with vascular endothelial growth factor-targeted agents: results from a large, multicenter study. *J. Clin. Oncol.* 27, 5794–5799. doi: 10.1200/jco.2008.21.4809

Hosseini, M., Khatamianfar, S., Hassanian, S. M., Nedaeinia, R., Shafiee, M., Maftouh, M., et al. (2017). Exosome-encapsulated microRNAs as potential circulating biomarkers in colon cancer. *Curr. Pharm. Des.* 23, 1705–1709. doi: 10.2174/1381612822666161201144634

Huang, T., Kang, W., Zhang, B., Wu, F., Dong, Y., Tong, J. H., et al. (2016). miR-508-3p concordantly silences NFKB1 and RELA to inactivate canonical NF-kappaB signaling in gastric carcinogenesis. *Mol. Cancer* 15:9.

Huang, W., Zhao, M., Wei, N., Wang, X., Cao, H., Du, Q., et al. (2014). Site-specific RNase A activity was dramatically reduced in serum from multiple types of cancer patients. *PLoS One* 9:e96490. doi: 10.1371/journal.pone.0096490

Iwamoto, H., Kanda, Y., Sejima, T., Osaki, M., Okada, F., and Takenaka, A. (2014). Serum miR-210 as a potential biomarker of early clear cell renal cell carcinoma. *Int. J. Oncol.* 44, 53–58. doi: 10.3892/ijo.2013.2169

Janzen, N. K., Kim, H. L., Figlin, R. A., and Belldegrun, A. S. (2003). Surveillance after radical or partial nephrectomy for localized renal cell carcinoma and management of recurrent disease. *Urol. Clin. North Am.* 30, 843–852. doi: 10.1016/s0094-0143(03)00056-9

Javidi, M. A., Ahmadi, A. H., Bakhshinejad, B., Nouraee, N., Babashah, S., and Sadeghizadeh, M. (2014). Cell-free microRNAs as cancer biomarkers: the odyssey of miRNAs through body fluids. *Med. Oncol.* 31:295.

Jiang, N., Pan, J., Fang, S., Zhou, C., Han, Y., Chen, J., et al. (2019). Liquid biopsy: Circulating exosomal long noncoding RNAs in cancer. *Clin. Chim. Acta* 495, 331–337. doi: 10.1016/j.cca.2019.04.082

Jiang, X., Li, Q., Zhang, S., Song, C., and Zheng, P. (2019). Long noncoding RNA GIHCG induces cancer progression and chemoresistance and indicates poor prognosis in colorectal cancer. *Onco Targets Ther.* 12, 1059–1070. doi: 10.2147/ott.s192290

Khella, H. W. Z., Butz, H., Ding, Q., Rotondo, F., Evans, K. R., Kupchak, P., et al. (2015). miR-221/222 are involved in response to sunitinib treatment in metastatic renal cell carcinoma. *Mol. Ther.* 23, 1748–1758. doi: 10.1038/mt.2015.129

Ko, J. J., Xie, W., Kroeger, N., Lee, J. L., Rini, B. I., Knox, J. J., et al. (2015). The international metastatic renal cell carcinoma database consortium model as a prognostic tool in patients with metastatic renal cell carcinoma previously treated with first-line targeted therapy: a population-based study. *Lancet Oncol.* 16, 293–300. doi: 10.1016/s1470-2045(14)71222-7

Koczera, P., Martin, L., Marx, G., and Schuerholz, T. (2016). The Ribonuclease A superfamily in humans: canonical RNases as the buttress of innate immunity. *Int. J. Mol. Sci.* 17:1278. doi: 10.3390/ijms17081278

Krebs, M., Solimando, A. G., Kalogirou, C., Marquardt, A., Frank, T., Sokolakis, I., et al. (2020). miR-221-3p regulates VEGFR2 expression in high-risk prostate cancer and represents an escape mechanism from sunitinib In Vitro. *J. Clin. Med.* 9:670. doi: 10.3390/jcm9030670

Krist, B., Florczyk, U., Pietraszek-Gremplewicz, K., Jozkowicz, A., and Dulak, J. (2015). The role of miR-378a in metabolism, angiogenesis, and muscle biology. *Int. J. Endocrinol.* 2015:281756.

Kulkarni, B., Kirave, P., Gondaliya, P., Jash, K., Jain, A., Tekade, R. K., et al. (2019). Exosomal miRNA in chemoresistance, immune evasion, metastasis and progression of cancer. *Drug Discov. Today* 24, 2058–2067. doi: 10.1016/j.drudis.2019.06.010

Lee, D. Y., Deng, Z., Wang, C. H., and Yang, B. B. (2007). MicroRNA-378 promotes cell survival, tumor growth, and angiogenesis by targeting SuFu and Fus-1 expression. *Proc. Natl. Acad. Sci. U.S.A.* 104, 20350–20355. doi: 10.1073/pnas.0706901104

Lee, I., Baxter, D., Lee, M. Y., Scherler, K., and Wang, K. (2017). The importance of standardization on analyzing circulating RNA. *Mol. Diagn. Ther.* 21, 259–268. doi: 10.1007/s40291-016-0251-y

Lee, S. P., Hsieh, P. L., Fang, C. Y., Chu, P. M., Liao, Y. W., Yu, C. H., et al. (2020). LINC00963 promotes cancer stemness, metastasis, and drug resistance in head and neck carcinomas via ABCB5 regulation. *Cancers (Basel)* 12:10.3390/cancers12051073.

Li, G., Zhao, A., Peoch, M., Cottier, M., and Mottet, N. (2017). Detection of urinary cell-free miR-210 as a potential tool of liquid biopsy for clear cell renal cell carcinoma. *Urol. Oncol.* 35, 294–299. doi: 10.1016/j.urolonc.2016.12.007

Li, H., Ouyang, R., Wang, Z., Zhou, W., Chen, H., Jiang, Y., et al. (2016). MiR-150 promotes cellular metastasis in non-small cell lung cancer by targeting FOXO4. *Sci. Rep.* 6:39001.

Li, H. C., Li, J. P., Wang, Z. M., Fu, D. L., Li, Z. L., Zhang, D., et al. (2014). Identification of angiogenesis-related miRNAs in a population of patients with renal clear cell carcinoma. *Oncol. Rep.* 32, 2061–2069. doi: 10.3892/or.2014.3403

Li, J., Li, Z., Zheng, W., Li, X., Wang, Z., Cui, Y., et al. (2017). PANDAR: a pivotal cancer-related long non-coding RNA in human cancers. *Mol. Biosyst.* 13, 2195–2201. doi: 10.1039/c7mb00414a

Li, S., Yang, F., Wang, M., Cao, W., and Yang, Z. (2017). miR-378 functions as an onco-miRNA by targeting the ST7L/Wnt/β-catenin pathway in cervical cancer. *Int. J. Mol. Med.* 40, 1047–1056. doi: 10.3892/ijmm.2017.3116

Li, W., Zheng, Z., Chen, H., Cai, Y., and Xie, W. (2018). Knockdown of long non-coding RNA PVT1 induces apoptosis and cell cycle arrest in clear cell renal cell carcinoma through the epidermal growth factor receptor pathway. *Oncol. Lett.* 15, 7855–7863.

Li, X., Xin, S., He, Z., Che, X., Wang, J., Xiao, X., et al. (2014). MicroRNA-21 (miR-21) post-transcriptionally downregulates tumor suppressor PDCD4 and promotes cell transformation, proliferation, and metastasis in renal cell carcinoma. *Cell Physiol. Biochem.* 33, 1631–1642. doi: 10.1159/000362946

Li, Y., Quan, J., Chen, F., Pan, X., Zhuang, C., Xiong, T., et al. (2019). MiR-31-5p acts as a tumor suppressor in renal cell carcinoma by targeting cyclin-dependent kinase 1 (CDK1). *Biomed. Pharmacother.* 111, 517–526. doi: 10.1016/j.biopha.2018.12.102

Li, Y., Ye, Y., Feng, B., and Qi, Y. (2017). Long noncoding RNA lncARSR promotes doxorubicin resistance in hepatocellular carcinoma via modulating PTEN-PI3K/Akt pathway. *J. Cell. Biochem.* 118, 4498–4507. doi: 10.1002/jcb.26107

Liu, F., Chen, N., Xiao, R., Wang, W., and Pan, Z. (2016). miR-144-3p serves as a tumor suppressor for renal cell carcinoma and inhibits its invasion and metastasis by targeting MAP3K8. *Biochem. Biophys. Res. Commun.* 480, 87–93. doi: 10.1016/j.bbrc.2016.10.004

Liu, G., Jiang, Z., Qiao, M., and Wang, F. (2019). Lnc-GIHCG promotes cell proliferation and migration in gastric cancer through miR- 1281 adsorption. *Mol. Genet. Genomic Med.* 7:e711. doi: 10.1002/mgg3.711

Liu, L., Li, Y., Liu, S., Duan, Q., Chen, L., Wu, T., et al. (2017). Downregulation of miR-193a-3p inhibits cell growth and migration in renal cell carcinoma by targeting PTEN. *Tumour Biol.* 39:1010428317711951.

Liu, L. L., Li, D., He, Y. L., Zhou, Y. Z., Gong, S. H., Wu, L. Y., et al. (2017). miR-210 protects renal cell against hypoxia-induced apoptosis by targeting HIF-1 alpha. *Mol. Med.* 23, 258–271. doi: 10.2119/molmed.2017.00013

Liu, S., Deng, X., and Zhang, J. (2019a). Identification of dysregulated serum miR-508-3p and miR-885-5p as potential diagnostic biomarkers of clear cell renal carcinoma. *Mol. Med. Rep.* 20, 5075–5083.

Liu, S., Wang, Y., Li, W., Yu, S., Wen, Z., Chen, Z., et al. (2019b). miR-221-5p acts as an oncogene and predicts worse survival in patients of renal cell cancer. *Biomed. Pharmacother.* 119:109406. doi: 10.1016/j.biopha.2019.109406

Liu, T. Y., Zhang, H., Du, S. M., Li, J., and Wen, X. H. (2016). Expression of microRNA-210 in tissue and serum of renal carcinoma patients and its effect

on renal carcinoma cell proliferation, apoptosis, and invasion. *Genet. Mol. Res.* 15:15017746.

Liu, X. G., Zhu, W. Y., Huang, Y. Y., Ma, L. N., Zhou, S. Q., Wang, Y. K., et al. (2012). High expression of serum miR-21 and tumor miR-200c associated with poor prognosis in patients with lung cancer. *Med. Oncol.* 29, 618–626. doi: 10.1007/s12032-011-9923-y

Lou, N., Ruan, A. M., Qiu, B., Bao, L., Xu, Y. C., Zhao, Y., et al. (2017). miR-144-3p as a novel plasma diagnostic biomarker for clear cell renal cell carcinoma. *Urol. Oncol.* 35, 36.e7–36.e14. doi: 10.1016/j.urolonc.2016.07.012

Lu, G. J., Dong, Y. Q., Zhang, Q. M., Di, W. Y., Jiao, L. Y., Gao, Q. Z., et al. (2015). miRNA-221 promotes proliferation, migration and invasion by targeting TIMP2 in renal cell carcinoma. *Int. J. Clin. Exp. Pathol.* 8, 5224–5229.

Lv, J., Zhu, Y., and Zhang, Q. (2020). An increased level of MiR-222-3p is associated with TMP2 suppression, ERK activation and is associated with metastasis and a poor prognosis in renal clear cell carcinoma. *Cancer Biomark.* 28, 141–149. doi: 10.3233/cbm-190264

Ma, J., Wu, D., Yi, J., Yi, Y., Zhu, X., Qiu, H., et al. (2019). MiR-378 promoted cell proliferation and inhibited apoptosis by enhanced stem cell properties in chronic myeloid leukemia K562 cells. *Biomed. Pharmacother.* 112:108623. doi: 10.1016/j.biopha.2019.108623

Ma, Y., Zhang, H., He, X., Song, H., Qiang, Y., Li, Y., et al. (2015). miR-106a* inhibits the proliferation of renal carcinoma cells by targeting IRS-2. *Tumour Biol.* 36, 8389–8398. doi: 10.1007/s13277-015-3605-x

Mathur, R. (2018). ARID1A loss in cancer: Towards a mechanistic understanding. *Pharmacol. Ther.* 190, 15–23. doi: 10.1016/j.pharmthera.2018.05.001

McCormick, R. I., Blick, C., Ragoussis, J., Schoedel, J., Mole, D. R., Young, A. C., et al. (2013). miR-210 is a target of hypoxia-inducible factors 1 and 2 in renal cancer, regulates ISCU and correlates with good prognosis. *Br. J. Cancer* 108, 1133–1142. doi: 10.1038/bjc.2013.56

Motzer, R. J., Escudier, B., McDermott, D. F., George, S., Hammers, H. J., Srinivas, S., et al. (2015). Nivolumab versus everolimus in advanced renal-cell carcinoma. *N. Engl. J. Med.* 373, 1803–1813.

Motzer, R. J., Tannir, N. M., McDermott, D. F., Aren Frontera, O., Melichar, B., Choueiri, T. K., et al. (2018). Nivolumab plus ipilimumab versus sunitinib in advanced renal-cell carcinoma. *N. Engl. J. Med.* 378, 1277–1290.

Nandagopal, L., and Sonpavde, G. (2016). Circulating biomarkers in bladder cancer. *Bladder Cancer* 2, 369–379. doi: 10.3233/blc-160075

Neal, C. S., Michael, M. Z., Rawlings, L. H., Van der Hoek, M. B., and Gleadle, J. M. (2010). The VHL-dependent regulation of microRNAs in renal cancer. *BMC Med.* 8:64. doi: 10.1186/1741-7015-8-64

Nientiedt, M., Schmidt, D., Kristiansen, G., Muller, S. C., and Ellinger, J. (2018). YRNA expression profiles are altered in clear cell renal cell carcinoma. *Eur. Urol. Focus* 4, 260–266. doi: 10.1016/j.euf.2016.08.004

Novikova, I. V., Hennelly, S. P., and Sanbonmatsu, K. Y. (2013). Tackling structures of long noncoding RNAs. *Int. J. Mol. Sci.* 14, 23672–23684. doi: 10.3390/ijms141223672

Okita, K., Hatakeyama, S., Tanaka, T., Ikehata, Y., Tanaka, T., Fujita, N., et al. (2019). Impact of disagreement between two risk group models on prognosis in patients with metastatic renal-cell carcinoma. *Clin. Genitourin. Cancer* 17, e440–e446. doi: 10.1016/j.clgc.2019.01.006

Palsdottir, H. B., Hardarson, S., Petursdottir, V., Jonsson, A., Jonsson, E., Sigurdsson, M. I., et al. (2012). Incidental detection of renal cell carcinoma is an independent prognostic marker: results of a long-term, whole population study. *J. Urol.* 187, 48–53. doi: 10.1016/j.juro.2011.09.025

Pan, X., Li, Z., Zhao, L., Quan, J., Zhou, L., Xu, J., et al. (2018a). microRNA-572 functions as an oncogene and a potential biomarker for renal cell carcinoma prognosis. *Oncol. Rep.* 40, 3092–3101.

Pan, X., Zheng, G., and Gao, C. (2018b). LncRNA PVT1: a novel therapeutic target for cancers. *Clin. Lab.* 64, 655–662.

Pan, Y., Hu, J., Ma, J., Qi, X., Zhou, H., Miao, X., et al. (2018). MiR-193a-3p and miR-224 mediate renal cell carcinoma progression by targeting alpha-2,3-sialyltransferase IV and the phosphatidylinositol 3 kinase/Akt pathway. *Mol. Carcinog.* 57, 1067–1077. doi: 10.1002/mc.22826

Pan, Y. J., Wei, L. L., Wu, X. J., Huo, F. C., Mou, J., and Pei, D. S. (2017). MiR-106a-5p inhibits the cell migration and invasion of renal cell carcinoma through targeting PAK5. *Cell Death Dis.* 8:e3155. doi: 10.1038/cddis.2017.561

Peng, J., Mo, R., Ma, J., and Fan, J. (2015). Let-7b and Let-7c are determinants of intrinsic chemoresistance in renal cell carcinoma. *World J. Surg. Oncol.* 13:175.

Penolazzi, L., Bonaccorsi, G., Gafa, R., Ravaioli, N., Gabriele, D., Bosi, C., et al. (2019). SLUG/HIF1-alpha/miR-221 regulatory circuit in endometrial cancer. *Gene* 711:143938. doi: 10.1016/j.gene.2019.06.028

Petrozza, V., Carbone, A., Bellissimo, T., Porta, N., Palleschi, G., Pastore, A. L., et al. (2015). Oncogenic MicroRNAs characterization in clear cell renal cell carcinoma. *Int. J. Mol. Sci.* 16, 29219–29225.

Pichler, M., Rodriguez-Aguayo, C., Nam, S. Y., Dragomir, M. P., Bayraktar, R., Anfossi, S., et al. (2020). Therapeutic potential of FLANC, a novel primate-specific long non-coding RNA in colorectal cancer. *Gut* doi: 10.1136/gutjnl-2019-318903 [Epub ahead of print].

Powles, T., Albiges, L., Staehler, M., Bensalah, K., Dabestani, S., Giles, R. H., et al. (2017). Updated European association of urology guidelines recommendations for the treatment of first-line metastatic clear cell renal cancer. *Eur. Urol.* 73, 311–315. doi: 10.1016/j.eururo.2017.11.016

Pruijn, G. J., Wingens, P. A., Peters, S. L., Thijssen, J. P., and van Venrooij, W. J. (1993). Ro RNP associated Y RNAs are highly conserved among mammals. *Biochim. Biophys. Acta* 1216, 395–401. doi: 10.1016/0167-4781(93)90006-y

Qin, M. M., Chai, X., Huang, H. B., Feng, G., Li, X. N., Zhang, J., et al. (2019). let-7i inhibits proliferation and migration of bladder cancer cells by targeting HMGA1. *BMC Urol.* 19:53. doi: 10.1186/s12894-019-0485-1

Qu, L., Ding, J., Chen, C., Wu, Z. J., Liu, B., Gao, Y., et al. (2016). Exosome-transmitted lncARSR promotes sunitinib resistance in renal cancer by acting as a competing endogenous RNA. *Cancer Cell* 29, 653–668. doi: 10.1016/j.ccell.2016.03.004

Redova, M., Poprach, A., Nekvindova, J., Iliev, R., Radova, L., Lakomy, R., et al. (2012). Circulating miR-378 and miR-451 in serum are potential biomarkers for renal cell carcinoma. *J. Transl. Med.* 10:55. doi: 10.1186/1479-5876-10-55

Rini, B. I., Campbell, S. C., and Escudier, B. (2009). Renal cell carcinoma. *Lancet* 373, 1119–1132.

Rini, B. I., Plimack, E. R., Stus, V., Gafanov, R., Hawkins, R., Nosov, D., et al. (2019). Pembrolizumab plus Axitinib versus Sunitinib for advanced renal-cell carcinoma. *N. Engl. J. Med.* 380, 1116–1127.

Rossi, S. H., Klatte, T., Usher-Smith, J., and Stewart, G. D. (2018). Epidemiology and screening for renal cancer. *World J. Urol.* 36, 1341–1353.

Sanders, I., Holdenrieder, S., Walgenbach-Brunagel, G., von Ruecker, A., Kristiansen, G., Muller, S. C., et al. (2012). Evaluation of reference genes for the analysis of serum miRNA in patients with prostate cancer, bladder cancer and renal cell carcinoma. *Int. J. Urol.* 19, 1017–1025. doi: 10.1111/j.1442-2042.2012.03082.x

Schanza, L. M., Seles, M., Stotz, M., Fosselteder, J., Hutterer, G. C., Pichler, M., et al. (2017). MicroRNAs associated with von hippel-lindau pathway in renal cell carcinoma: a comprehensive review. *Int. J. Mol. Sci.* 18:10.3390/ijms18112495.

Schwarzenbach, H., Milde-Langosch, K., Steinbach, B., Muller, V., and Pantel, K. (2012). Diagnostic potential of PTEN-targeting miR-214 in the blood of breast cancer patients. *Breast Cancer Res. Treat.* 134, 933–941. doi: 10.1007/s10549-012-1988-6

Schwarzenbacher, D., Klec, C., Pasculli, B., Cerk, S., Rinner, B., Karbiener, M., et al. (2019). MiR-1287-5p inhibits triple negative breast cancer growth by interaction with phosphoinositide 3-kinase CB, thereby sensitizing cells for PI3Kinase inhibitors. *Breast Cancer Res.* 21:20.

Seles, M., Posch, F., Pichler, G. P., Gary, T., Pummer, K., Zigeuner, R., et al. (2017). Blood platelet volume represents a novel prognostic factor in patients with nonmetastatic renal cell carcinoma and improves the predictive ability of established prognostic scores. *J. Urol.* 198, 1247–1252. doi: 10.1016/j.juro.2017.07.036

Shen, C., and Kaelin, W. G. Jr. (2013). The VHL/HIF axis in clear cell renal carcinoma. *Semin. Cancer Biol.* 23, 18–25. doi: 10.1016/j.semcancer.2012.06.001

Shen, P., and Cheng, Y. (2020). Long noncoding RNA lncARSR confers resistance to Adriamycin and promotes osteosarcoma progression. *Cell Death Dis.* 11:362.

Siegel, R. L., Miller, K. D., and Jemal, A. (2019). Cancer statistics, 2019. *CA Cancer J. Clin.* 69, 7–34.

Smith, C. G., Moser, T., Mouliere, F., Field-Rayner, J., Eldridge, M., Riediger, A. L., et al. (2020). Comprehensive characterization of cell-free tumor DNA in plasma and urine of patients with renal tumors. *Genome Med.* 12:23.

Song, M. S., Salmena, L., and Pandolfi, P. P. (2012). The functions and regulation of the PTEN tumour suppressor. *Nat. Rev. Mol. Cell. Biol.* 13, 283–296. doi: 10.1038/nrm3330

Squadrito, M. L., Baer, C., Burdet, F., Maderna, C., Gilfillan, G. D., Lyle, R., et al. (2014). Endogenous RNAs modulate microRNA sorting to exosomes and transfer to acceptor cells. *Cell Rep.* 8, 1432–1446. doi: 10.1016/j.celrep.2014.07.035

Su, Y. J., Yu, J., Huang, Y. Q., and Yang, J. (2015). Circulating long noncoding RNA as a potential target for prostate cancer. *Int. J. Mol. Sci.* 16, 13322–13338. doi: 10.3390/ijms160613322

Sui, C. J., Zhou, Y. M., Shen, W. F., Dai, B. H., Lu, J. J., Zhang, M. F., et al. (2016). Long noncoding RNA GIHCG promotes hepatocellular carcinoma progression through epigenetically regulating miR-200b/a/429. *J. Mol. Med. (Berl)* 94, 1281–1296. doi: 10.1007/s00109-016-1442-z

Sun, J., Jiang, Z., Li, Y., Wang, K., Chen, X., and Liu, G. (2019). Downregulation of miR-21 inhibits the malignant phenotype of pancreatic cancer cells by targeting VHL. *Onco Targets Ther.* 12, 7215–7226. doi: 10.2147/ott.s211535

Svoronos, A. A., Engelman, D. M., and Slack, F. J. (2016). OncomiR or tumor suppressor? The duplicity of MicroRNAs in cancer. *Cancer Res.* 76, 3666–3670. doi: 10.1158/0008-5472.can-16-0359

Tanaka, N., Mizuno, R., Ito, K., Shirotake, S., Yasumizu, Y., Masunaga, A., et al. (2016). External validation of the MSKCC and IMDC risk models in patients treated with targeted therapy as a first-line and subsequent second-line treatment: a Japanese multi-institutional study. *Eur. Urol. Focus* 2, 303–309. doi: 10.1016/j.euf.2015.11.001

Teixeira, A. L., Ferreira, M., Silva, J., Gomes, M., Dias, F., Santos, J. I., et al. (2014). Higher circulating expression levels of miR-221 associated with poor overall survival in renal cell carcinoma patients. *Tumour Biol.* 35, 4057–4066. doi: 10.1007/s13277-013-1531-3

Trajkovic, K., Hsu, C., Chiantia, S., Rajendran, L., Wenzel, D., Wieland, F., et al. (2008). Ceramide triggers budding of exosome vesicles into multivesicular endosomes. *Science* 319, 1244–1247. doi: 10.1126/science.1153124

Tsui, K. H., Shvarts, O., Smith, R. B., Figlin, R., de Kernion, J. B., and Belldegrun, A. (2000). Renal cell carcinoma: prognostic significance of incidentally detected tumors. *J. Urol.* 163, 426–430. doi: 10.1016/s0022-5347(05)67892-5

Tusong, H., Maolakuerban, N., Guan, J., Rexiati, M., Wang, W. G., Azhati, B., et al. (2017). Functional analysis of serum microRNAs miR-21 and miR-106a in renal cell carcinoma. *Cancer Biomark.* 18, 79–85. doi: 10.3233/cbm-160676

Tzimagiorgis, G., Michailidou, E. Z., Kritis, A., Markopoulos, A. K., and Kouidou, S. (2011). Recovering circulating extracellular or cell-free RNA from bodily fluids. *Cancer Epidemiol.* 35, 580–589. doi: 10.1016/j.canep.2011.02.016

Vasudev, N. S., Wilson, M., Stewart, G. D., Adeyoju, A., Cartledge, J., Kimuli, M., et al. (2020). Challenges of early renal cancer detection: symptom patterns and incidental diagnosis rate in a multicentre prospective UK cohort of patients presenting with suspected renal cancer. *BMJ Open* 10:e035938. doi: 10.1136/bmjopen-2019-035938

Vergho, D., Kneitz, S., Rosenwald, A., Scherer, C., Spahn, M., Burger, M., et al. (2014). Combination of expression levels of miR-21 and miR-126 is associated with cancer-specific survival in clear-cell renal cell carcinoma. *BMC Cancer* 14:25. doi: 10.1186/1471-2407-14-25

Victoria Martinez, B., Dhahbi, J. M., Nunez Lopez, Y. O., Lamperska, K., Golusinski, P., Luczewski, L., et al. (2015). Circulating small non-coding RNA signature in head and neck squamous cell carcinoma. *Oncotarget* 6, 19246–19263. doi: 10.18632/oncotarget.4266

Villarroya-Beltri, C., Gutiérrez-Vázquez, C., Sánchez-Cabo, F., Pérez-Hernández, D., Vázquez, J., Martin-Cofreces, N., et al. (2013). Sumoylated hnRNPA2B1 controls the sorting of miRNAs into exosomes through binding to specific motifs. *Nat. Commun.* 4:2980.

Vojtech, L., Woo, S., Hughes, S., Levy, C., Ballweber, L., Sauteraud, R. P., et al. (2014). Exosomes in human semen carry a distinctive repertoire of small non-coding RNAs with potential regulatory functions. *Nucleic Acids Res.* 42, 7290–7304. doi: 10.1093/nar/gku347

Wagner, J., Riwanto, M., Besler, C., Knau, A., Fichtlscherer, S., Röxe, T., et al. (2013). Characterization of levels and cellular transfer of circulating lipoprotein-bound microRNAs. *Arterioscler Thromb Vasc. Biol.* 33, 1392–1400. doi: 10.1161/atvbaha.112.300741

Wang, C., Hu, J., Lu, M., Gu, H., Zhou, X., Chen, X., et al. (2015). A panel of five serum miRNAs as a potential diagnostic tool for early-stage renal cell carcinoma. *Sci. Rep.* 5:7610.

Wang, C., Wu, C., Yang, Q., Ding, M., Zhong, J., Zhang, C. Y., et al. (2016). miR-28-5p acts as a tumor suppressor in renal cell carcinoma for multiple antitumor effects by targeting RAP1B. *Oncotarget* 7, 73888–73902. doi: 10.18632/oncotarget.12516

Wang, K., Yuan, Y., Cho, J. H., McClarty, S., Baxter, D., and Galas, D. J. (2012). Comparing the MicroRNA spectrum between serum and plasma. *PLoS One* 7:e41561. doi: 10.1371/journal.pone.0041561

Wang, L., Yang, G., Zhao, D., Wang, J., Bai, Y., Peng, Q., et al. (2019). CD103-positive CSC exosome promotes EMT of clear cell renal cell carcinoma: role of remote MiR-19b-3p. *Mol. Cancer* 18:86.

Wang, Q., Wu, G., Zhang, Z., Tang, Q., Zheng, W., Chen, X., et al. (2018). Long non-coding RNA HOTTIP promotes renal cell carcinoma progression through the regulation of the miR-615/IGF-2 pathway. *Int. J. Oncol.* 53, 2278–2288.

Wang, X., Wang, T., Chen, C., Wu, Z., Bai, P., Li, S., et al. (2018). Serum exosomal miR-210 as a potential biomarker for clear cell renal cell carcinoma. *J. Cell. Biochem.* 120, 1492–1502. doi: 10.1002/jcb.27347

Weidle, U. H., Birzele, F., Kollmorgen, G., and Ruger, R. (2017). Long non-coding RNAs and their role in metastasis. *Cancer Genomics Proteomics* 14, 143–160.

Westerman, M. E., Shapiro, D. D., Tannir, N. M., Campbell, M. T., Matin, S. F., Karam, J. A., et al. (2020). Survival following cytoreductive nephrectomy: a comparison of existing prognostic models. *BJU Int.* doi: 10.1111/bju.15160 [Epub ahead of print].

Wu, Y., Wang, Y. Q., Weng, W. W., Zhang, Q. Y., Yang, X. Q., Gan, H. L., et al. (2016). A serum-circulating long noncoding RNA signature can discriminate between patients with clear cell renal cell carcinoma and healthy controls. *Oncogenesis* 5:e192. doi: 10.1038/oncsis.2015.48

Wu, Z., Wang, W., Wang, Y., Wang, X., Sun, S., Yao, Y., et al. (2020). Long noncoding RNA LINC00963 promotes breast cancer progression by functioning as a molecular sponge for microRNA-625 and thereby upregulating HMGA1. *Cell Cycle* 19, 610–624. doi: 10.1080/15384101.2020.1728024

Wulfken, L. M., Moritz, R., Ohlmann, C., Holdenrieder, S., Jung, V., Becker, F., et al. (2011). MicroRNAs in renal cell carcinoma: diagnostic implications of serum miR-1233 levels. *PLoS One* 6:e25787. doi: 10.1371/journal.pone.0025787

Xiao, W., Lou, N., Ruan, H., Bao, L., Xiong, Z., Yuan, C., et al. (2017). Mir-144-3p promotes cell proliferation, metastasis, sunitinib resistance in clear cell Renal cell carcinoma by downregulating ARID1A. *Cell Physiol. Biochem.* 43, 2420–2433. doi: 10.1159/000484395

Xu, Y., Tong, Y., Zhu, J., Lei, Z., Wan, L., Zhu, X., et al. (2017). An increase in long non-coding RNA PANDAR is associated with poor prognosis in clear cell renal cell carcinoma. *BMC Cancer* 17:373. doi: 10.1186/s12885-017-3339-9

Yadav, S., Khandelwal, M., Seth, A., Saini, A. K., Dogra, P. N., and Sharma, A. (2017). Serum microRNA expression profiling: potential diagnostic implications of a panel of serum microRNAs for clear cell renal cell cancer. *Urology* 104, 64–69. doi: 10.1016/j.urology.2017.03.013

Yang, C., Cai, W. C., Dong, Z. T., Guo, J. W., Zhao, Y. J., Sui, C. J., et al. (2019). lncARSR promotes liver cancer stem cells expansion via STAT3 pathway. *Gene* 687, 73–81. doi: 10.1016/j.gene.2018.10.087

Yang, N., Kaur, S., Volinia, S., Greshock, J., Lassus, H., Hasegawa, K., et al. (2008). MicroRNA microarray identifies Let-7i as a novel biomarker and therapeutic target in human epithelial ovarian cancer. *Cancer Res.* 68, 10307–10314. doi: 10.1158/0008-5472.can-08-1954

Yang, T., Zhou, H., Liu, P., Yan, L., Yao, W., Chen, K., et al. (2017). lncRNA PVT1 and its splicing variant function as competing endogenous RNA to regulate clear cell renal cell carcinoma progression. *Oncotarget* 8, 85353–85367. doi: 10.18632/oncotarget.19743

Yao, N., Yu, L., Zhu, B., Gan, H. Y., and Guo, B. Q. (2018). LncRNA GIHCG promotes development of ovarian cancer by regulating microRNA-429. *Eur. Rev. Med. Pharmacol. Sci.* 22, 8127–8134.

Ye, Z., Duan, J., Wang, L., Ji, Y., and Qiao, B. (2019). LncRNA-LET inhibits cell growth of clear cell renal cell carcinoma by regulating miR-373-3p. *Cancer Cell Int.* 19:311.

Yeri, A., Courtright, A., Reiman, R., Carlson, E., Beecroft, T., Janss, A., et al. (2017). Total extracellular small RNA profiles from plasma, saliva, and urine of healthy subjects. *Sci. Rep.* 7:44061.

Yu, G., Yao, W., Gumireddy, K., Li, A., Wang, J., Xiao, W., et al. (2014). Pseudogene PTENP1 functions as a competing endogenous RNA to suppress clear-cell renal cell carcinoma progression. *Mol. Cancer Ther.* 13, 3086–3097. doi: 10.1158/1535-7163.mct-14-0245

Zaman, M. S., Shahryari, V., Deng, G., Thamminana, S., Saini, S., Majid, S., et al. (2012). Up-regulation of microRNA-21 correlates with lower kidney cancer survival. *PLoS One* 7:e31060. doi: 10.1371/journal.pone.0031060

Zang, C., Sun, J., Liu, W., Chu, C., Jiang, L., and Ge, R. (2019). miRNA-21 promotes cell proliferation and invasion via VHL/PI3K/AKT in papillary thyroid carcinoma. *Hum. Cell* 32, 428–436. doi: 10.1007/s13577-019-00254-4

Zaporozhchenko, I. A., Ponomaryova, A. A., Rykova, E. Y., and Laktionov, P. P. (2018). The potential of circulating cell-free RNA as a cancer biomarker: challenges and opportunities. *Expert Rev. Mol. Diagn.* 18, 133–145. doi: 10.1080/14737159.2018.1425143

Zeng, M., Zhu, L., Li, L., and Kang, C. (2017). miR-378 suppresses the proliferation, migration and invasion of colon cancer cells by inhibiting SDAD1. *Cell Mol. Biol. Lett.* 22:12.

Zhai, Q., Zhou, L., Zhao, C., Wan, J., Yu, Z., Guo, X., et al. (2012). Identification of miR-508-3p and miR-509-3p that are associated with cell invasion and migration and involved in the apoptosis of renal cell carcinoma. *Biochem. Biophys. Res. Commun.* 419, 621–626. doi: 10.1016/j.bbrc.2012.02.060

Zhang, A., Liu, Y., Shen, Y., Xu, Y., and Li, X. (2011). miR-21 modulates cell apoptosis by targeting multiple genes in renal cell carcinoma. *Urology* 78, 474.e13–474.e19. doi: 10.1016/j.urology.2011.03.030

Zhang, G. J., Zhou, H., Xiao, H. X., Li, Y., and Zhou, T. (2014). MiR-378 is an independent prognostic factor and inhibits cell growth and invasion in colorectal cancer. *BMC Cancer* 14:109. doi: 10.1186/1471-2407-14-109

Zhang, H. L., Yang, L. F., Zhu, Y., Yao, X. D., Zhang, S. L., Dai, B., et al. (2011). Serum miRNA-21: elevated levels in patients with metastatic hormone-refractory prostate cancer and potential predictive factor for the efficacy of docetaxel-based chemotherapy. *Prostate* 71, 326–331. doi: 10.1002/pros.21246

Zhang, L., and Yu, D. (2019). Exosomes in cancer development, metastasis, and immunity. *Biochim. Biophys. Acta Rev. Cancer* 1871, 455–468. doi: 10.1016/j.bbcan.2019.04.004

Zhang, W., Ni, M., Su, Y., Wang, H., Zhu, S., Zhao, A., et al. (2018). MicroRNAs in serum exosomes as potential biomarkers in clear-cell renal cell carcinoma. *Eur. Urol. Focus* 4, 412–419. doi: 10.1016/j.euf.2016.09.007

Zhang, W. B., Pan, Z. Q., Yang, Q. S., and Zheng, X. M. (2013). Tumor suppressive miR-509-5p contributes to cell migration, proliferation and antiapoptosis in renal cell carcinoma. *Ir. J. Med. Sci.* 182, 621–627. doi: 10.1007/s11845-013-0941-y

Zhang, X., Mao, L., Li, L., He, Z., Wang, N., and Song, Y. (2019). Long noncoding RNA GIHCG functions as an oncogene and serves as a serum diagnostic biomarker for cervical cancer. *J. Cancer* 10, 672–681. doi: 10.7150/jca.28525

Zhao, A., Li, G., Peoc'h, M., Genin, C., and Gigante, M. (2013). Serum miR-210 as a novel biomarker for molecular diagnosis of clear cell renal cell carcinoma. *Exp. Mol. Pathol.* 94, 115–120. doi: 10.1016/j.yexmp.2012.10.005

Zhao, L., Liu, K., Pan, X., Quan, J., Zhou, L., Li, Z., et al. (2019a). miR-625-3p promotes migration and invasion and reduces apoptosis of clear cell renal cell carcinoma. *Am. J. Transl. Res.* 11, 6475–6486.

Zhao, L., Quan, J., Li, Z., Pan, X., Wang, J., Xu, J., et al. (2019b). MicroRNA-222-3p promotes tumor cell migration and invasion and inhibits apoptosis, and is correlated with an unfavorable prognosis of patients with renal cell carcinoma. *Int. J. Mol. Med.* 43, 525–534.

Zhao, Y. J., Song, X., Niu, L., Tang, Y., Song, X., and Xie, L. (2019). Circulating Exosomal miR-150-5p and miR-99b-5p as diagnostic biomarkers for colorectal cancer. *Front. Oncol.* 9:1129. doi: 10.3389/fonc.2019.01129

Zhou, Y., van Melle, M., Singh, H., Hamilton, W., Lyratzopoulos, G., and Walter, F. M. (2019a). Quality of the diagnostic process in patients presenting with symptoms suggestive of bladder or kidney cancer: a systematic review. *BMJ Open* 9:e029143. doi: 10.1136/bmjopen-2019-029143

Zhou, Y., Yin, L., Li, H., Liu, L. H., and Xiao, T. (2019b). The LncRNA LINC00963 facilitates osteosarcoma proliferation and invasion by suppressing miR-204-3p/FN1 axis. *Cancer Biol. Ther.* 20, 1141–1148. doi: 10.1080/15384047.2019.1598766

Zhu, H., Wang, S., Shen, H., Zheng, X., and Xu, X. (2020). SP1/AKT/FOXO3 signaling is involved in miR-362-3p-mediated inhibition of cell-cycle pathway and EMT progression in renal cell carcinoma. *Front. Cell Dev. Biol.* 8:297. doi: 10.3389/fcell.2020.00297

Znaor, A., Lortet-Tieulent, J., Laversanne, M., Jemal, A., and Bray, F. (2015). International variations and trends in renal cell carcinoma incidence and mortality. *Eur. Urol.* 67, 519–530. doi: 10.1016/j.eururo.2014.10.002

Zou, S. L., Chen, Y. L., Ge, Z. Z., Qu, Y. Y., Cao, Y., and Kang, Z. X. (2019). Downregulation of serum exosomal miR-150-5p is associated with poor prognosis in patients with colorectal cancer. *Cancer Biomark* 26, 69–77. doi: 10.3233/cbm-190156

Zou, X., Zhong, J., Li, J., Su, Z., Chen, Y., Deng, W., et al. (2016). miR-362-3p targets nemo-like kinase and functions as a tumor suppressor in renal cancer cells. *Mol. Med. Rep.* 13, 994–1002. doi: 10.3892/mmr.2015.4632

Conflict of Interest: The authors declare that the research was conducted in the absence of any commercial or financial relationships that could be construed as a potential conflict of interest.

Copyright © 2020 Barth, Drula, Ott, Fabris, Slaby, Calin and Pichler. This is an open-access article distributed under the terms of the Creative Commons Attribution License (CC BY). The use, distribution or reproduction in other forums is permitted, provided the original author(s) and the copyright owner(s) are credited and that the original publication in this journal is cited, in accordance with accepted academic practice. No use, distribution or reproduction is permitted which does not comply with these terms.

frontiers in Cell and Developmental Biology

METHODS
published: 30 October 2020
doi: 10.3389/fcell.2020.593750

Employing Flow Cytometry to Extracellular Vesicles Sample Microvolume Analysis and Quality Control

Joana Maia[1,2], Silvia Batista[1], Nuno Couto[1,3], Ana C. Gregório[1], Cristian Bodo[1], Julia Elzanowska[1], Maria Carolina Strano Moraes[1†] and Bruno Costa-Silva[1*†]*

[1] Champalimaud Research, Champalimaud Centre for the Unknown, Lisbon, Portugal, [2] Graduate Program in Areas of Basic and Applied Biology, University of Porto, Porto, Portugal, [3] Digestive Unit, Champalimaud Clinical Centre, Lisbon, Portugal

OPEN ACCESS

Edited by:
Catherine Alix-Panabieres, Centre Hospitalier Universitaire de Montpellier, France

Reviewed by:
Adriana Franco Paes Leme, Brazilian Biosciences National Laboratory (LNBio), Brazil
Susana García-Silva, Spanish National Cancer Research Center (CNIO), Spain

***Correspondence:**
Bruno Costa-Silva
bruno.costa-silva@research.fchampalimaud.org
Maria Carolina Strano Moraes
carolina.stranomoraes@research.fchampalimaud.org

† These authors have contributed equally to this work

Specialty section:
This article was submitted to Molecular and Cellular Oncology, a section of the journal Frontiers in Cell and Developmental Biology

Received: 11 August 2020
Accepted: 30 September 2020
Published: 30 October 2020

Citation:
Maia J, Batista S, Couto N, Gregório AC, Bodo C, Elzanowska J, Strano Moraes MC and Costa-Silva B (2020) Employing Flow Cytometry to Extracellular Vesicles Sample Microvolume Analysis and Quality Control. Front. Cell Dev. Biol. 8:593750. doi: 10.3389/fcell.2020.593750

Extracellular Vesicles (EVs), membrane vesicles released by all cells, are emerging mediators of cell-cell communication. By carrying biomolecules from tissues to biofluids, EVs have attracted attention as non-invasive sources of clinical biomarkers in liquid biopsies. EVs-based liquid biopsies usually require EVs isolation before content analysis, which frequently increases sample volume requirements. We here present a Flow Cytometry (FC) strategy that does not require isolation or concentration of EVs prior to staining. By doing so, it enables population analysis of EVs in samples characterized by challenging small volumes, while reducing overall sample processing time. To illustrate its application, we performed longitudinal non-lethal population analysis of EVs in mouse plasma and in single-animal collections of murine vitreous humor. By quantifying the proportion of vesicular particles in purified and non-purified biological samples, this method also serves as a precious tool to quality control isolates of EVs purified by different protocols. Our FC strategy has an unexplored clinical potential to analyze EVs in biofluids with intrinsically limited volumes and to multiply the number of different analytes in EVs that can be studied from a single collection of biofluid.

Keywords: liquid biopsy, extracellular vesicles, exosomes, cancer flow cytometry, sample purity, microvolume, population study, longitudinal study

INTRODUCTION

Extracellular vesicles (EVs), membrane vesicles released by all cells, are emerging players in cell-cell communication. In addition to differences in size and biogenesis mechanism, EVs are highly heterogeneous in molecular composition and biological properties (Groot Kormelink et al., 2016; Kowal et al., 2016; Willms et al., 2016, 2018). Their cargo includes proteins, lipids and nucleic acids, which can be transported both locally and to distant cellular targets through the peripheral circulation. As shown by us (Peinado et al., 2012; Costa-Silva et al., 2015; Hoshino et al., 2015; Rodrigues et al., 2019) and others (Kalluri, 2016), EVs can act as messengers and carriers of biomolecules in physiological and pathological scenarios (Maia et al., 2018; Stahl and Raposo, 2019).

Extracellular vesicles have been described in all body fluids (Kalluri and LeBleu, 2020), including blood (Caby et al., 2005), urine (Pisitkun et al., 2004), saliva (Ogawa et al., 2011), and vitreous humor (Ragusa et al., 2015). They serve as non-invasive sources of liquid biopsies for

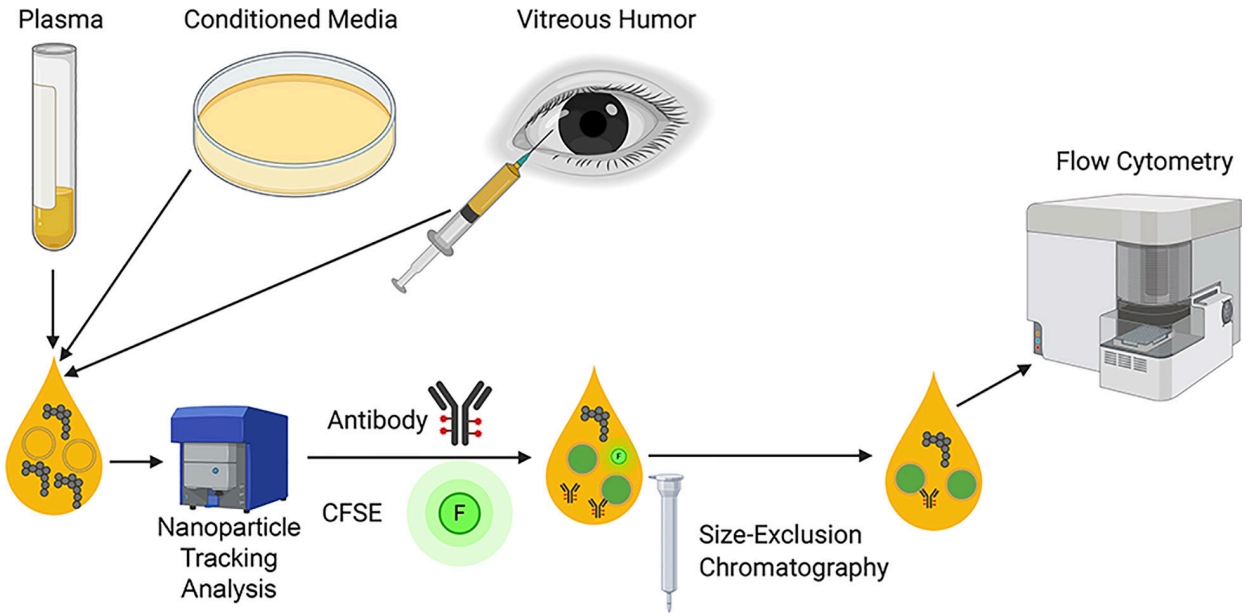

GRAPHICAL ABSTRACT

clinical biomarkers and allow longitudinal sampling to follow disease progression. However, high heterogeneity, which include differences in both quantity and quality of EVs, usually represent a challenge to the identification of specific EVs biomarkers in human samples. To contour some of these limitations, pre-clinical models are frequently employed, as they permit a higher degree of control over the experimental setup and sampling, and facilitate basic research related to EV composition, biogenesis and biological functions. Murine models in particular display a smaller degree of variability than clinical samples, which facilitates the discovery of biomarker candidates. However, sample volume requirements may complicate or even hamper the study of EVs in small volumes of individual collections mouse biofluids. This is mainly due to the general requirement for isolation of EVs before analysis, which inherently increases the sample volume consumption and potentially limits the number of EVs that can be harvested, thus restricting downstream analysis.

Several EV isolation methodologies are available, including separation of vesicles of similar size (e.g., by ultrafiltration, size exclusion chromatography, nanowire-based traps and deterministic lateral displacement systems), similar mass and/or density (e.g., by gradient-coupled ultracentrifugation and acoustic separation systems). It is worth noting that most of these techniques display high sample volume requirements, which can be difficult to achieve depending on the experimental context. To circumvent the volume issue, some technologies, like microfluidic lab-on-a-chip, have been developed. However, their full implementation still needs to overcome several hurdles (e.g., manual sample preparation and many non-automated chips) (Boriachek et al., 2018). Currently, there are no available methods to purify only EVs expressing endosomal features, nor consensus on markers that could be used to differentiate smaller endosomal-derived (i.e., exosomes) from larger membrane shedding-derived (i.e., Microvesicles) vesicles. Even molecules considered as markers of small endosomal EVs, such as HSP70, CD63 and CD9, have been reported to be present both in small and large EVs (Kowal et al., 2016). In the specific case of CD63, previous reports described EV isolates from several cell lines as lacking this molecule (Zhang et al., 2018). Thus, although the majority of our vesicles display exosomes features, including size (**Table 1**), we decided to identify them as EVs throughout the manuscript to avoid potential misidentification of our sample, following the latest MISEV's recommendations (Thery et al., 2018). Importantly, the aim of this work is not to focus our study in endosomal EVs, but instead to present a new method that can help the study of EVs populations in general.

Once purified, pooled EVs can be studied for their protein (e.g., by western blotting and mass spectrometry), lipid (e.g., by mass spectrometry) and nucleic acid (e.g., by PCR, DNA and RNA sequencing) content (Contreras-Naranjo et al., 2017; Shen et al., 2017; Guo et al., 2018). Nevertheless, these methods lack information on subpopulations and molecular heterogeneity of EVs at a single-vesicle level. Technologies based on immunoaffinity-capture surfaces and beads, such as ELISA and conventional flow cytometry, have enabled the analysis of populations of EVs expressing specific antigens (Kowal et al., 2016; Guo et al., 2018). However, by capturing heterogeneous groups of EVs containing a common molecule of interest or due to resolution limitations, these methods do not allow for single-vesicle analysis of small EVs (Arenaccio and Federico, 2017; Shah et al., 2018; Zhang et al., 2018).

By tackling some of these issues, Flow Cytometry (FC) has emerged as a promising tool for thorough single-EV studies. Recently, several groups described novel strategies to stain

TABLE 1 | Comparison of size range, sample volume and processing times between distinct isolation methods of EVs.

Sample type	Isolation method	Mean size ± standard error (nm)	Approximate sample volume for 2 × 10^9 particles	Approximate processing time
Conditioned Medium	NP	129.3 ± 4.7 nm	137 μL	3.5 h
	ExoQ	150.6 ± 4.2 nm	287 μL	19 h
	UC-I	144.9 ± 3.3 nm	1650 μL	27 h
	UC-II	137.3 ± 3.7 nm	660 μL	26 h
	UC-III	155.1 ± 2.7 nm	480 μL	6 h
	UC-IV	162.0 ± 3.2 nm	660 μL	7 h
Plasma	NP	80.5 ± 3.8 nm	1.7 μL	3.5 h
	UC-I	140.7 ± 6.2 nm	400 μL	27 h
Vitreous humor	NP	165.5 ± 2.8 nm	5.7 μL	3.5 h

purified EVs for FC (Morales-Kastresana et al., 2017), reported on the detection of EVs immune-captured by conventional FC (Campos-Silva et al., 2019), optimized imaging FC for analysis of EV samples (Gorgens et al., 2019) and developed new methodologies for the detection and sorting of EVs (Morales-Kastresana et al., 2019). However, existing protocols require EVs' isolation (Nolte-'t Hoen et al., 2012; van der Vlist et al., 2012; Pospichalova et al., 2015; Groot Kormelink et al., 2016; Morales-Kastresana et al., 2017), volume concentration (Choi et al., 2019) or immunocapture of subsets of EVs (Gorgens et al., 2019) prior to staining. All these factors increase the processing time, limit the analysis of EVs to sub-populations containing biomolecules of interest and/or prevent sample analysis of small volumes and/or low numbers of EVs.

We here present a modified FC strategy that does not require isolation of EVs or concentration prior to staining, enabling the analysis of single EVs in both purified and non-purified biological samples. Determining the optimal strategy for isolating EVs for an endpoint analysis is often a critical step. Here we show the application of our FC strategy to assess the purity of isolates of EVs prepared by different protocols, thus addressing a current concern for standardization and quality control in the field of EVs (Théry et al., 2019). We also show the application of our strategy to the analysis of non-purified populations of EVs in microvolumes of individual longitudinal non-lethal collections of mouse plasma biofluids. We also demonstrate the application of our strategy to study EVs in individual mouse vitreous humor samples.

METHODS

General Setup

The Flow Cytometry (FC) strategy presented in this manuscript is here briefly summarized and depicted in **Graphical Abstract**. Our general setup, starts with the NTA characterization of the biological samples. After that, the same number of particles is stained with antibody and CFSE. In order to remove of unbound CFSE and antibody, Size Exclusion Chromatography (SEC) columns are used and EVs-enriched fractions are pooled and analyzed with the Flow Cytometer Apogee A60-Micro-Plus (Apogee Flow Systems, United Kingdom).

Cells

The C57Bl/6 murine PAN02 cell line (also identified as Panc 02, originally induced by 3-MCA, Corbett et al., 1984) was purchased from the DTP, DCTD Tumor Repository, NIH, and cultured in RPMI 1640 (Corning 15363561, NY, United States). The medium was supplemented with 10% Fetal Bovine Serum (FBS, Biowest S181BH-500, Nuaillé, France) and 1% penicillin–streptomycin (Gibco 15-140-122, United States), and maintained in a humid incubator with 5% CO_2 at 37°C. For conditioning, cells were cultured in DMEM, High Glucose, with Glutamine, No Phenol Red (Gibco 31-053-028, United States) supplemented with 1% penicillin–streptomycin and 10% EV-depleted FBS. FBS was depleted of bovine EVs by ultracentrifugation at 100,000 *g* for 140 min. For the preparation of conditioned medium, 1 × 10^6 PAN02 cells were seeded per 150 mm culture dish containing 20 mL of medium, and the conditioned medium was collected after 72 h of culture.

Tumor Induction, and Plasma and Vitreous Humor Collection

All mouse work was performed in accordance with national animal experimentation guidelines (DGAV), animal protocol 0421/000/000/2018. Adult C57Bl/6 female mice (5–8 weeks old) were used for all experimental procedures. Mice were anesthetized using isoflurane 1.5–3%. Mouse vitreous humor was collected from naïve mice using 29G syringes (BD 324892, New Jersey, United States) inserted at a 45° angle into the vitreous cavity 2 mm posterior to the limbus. The volume of vitreous humor collected per mouse was in average 5 μL, where 5 μL of vitreous humor was diluted in 20 μL of 5,000 U-I-/mL heparin.

For tumor induction, a suspension of 1.5 × 10^6 PAN02 tumor cells, resuspended in 30 μL Matrigel (Corning 354230, NY, United States), was injected intrahepatically with 29G syringes in a total of 19 animals. The experiments had a length of 14 days. Blood was collected on the day prior (Day 0), and 7 and 14 days after intrahepatic injection of PAN02 tumors. On Day 0 and Day 7 the blood was collected by submandibular bleeding via blood collection lancets, and on Day 14 it was collected by retro-orbital bleeding via heparinized glass capillary tubes. The volume of plasma collected per mouse was in average 20 μL, which were diluted in 50 μL of 5,000 U-I-/mL heparin.

TABLE 2 | Apogee A60 configuration and laser power.

Channel number	Short channel name	Full channel name	Optical filter name	Laser wavelength	Laser power	PMT voltage
Ch1	405-SALS	Small Angle Light Scatter		405 nm	200 mW	400 V
Ch2	405-LALS	Large Angle Light Scatter		405 nm	200 mW	400 V
Ch3	405-Grn	Green Fluorescence	BP-525/50	405 nm	200 mW	500 V
Ch4	405-Org	Orange Fluorescence	LWP-590/35	405 nm	200 mW	500 V
Ch5	APC	Red Fluorescence	BP-676/36	638 nm	150 mW	550 V
Ch6	CFSE	Green Fluorescence	BP-525/50	488 nm	200 mW	525 V
Ch7	PE	Orange Fluorescence	BP-575/30	488 nm	200 mW	500 V
Ch8	488-Red	Red Fluorescence	BP-676/36	488 nm	200 mW	500 V
Ch9	488-DRed	Deep Red Fluorescence	LWP-740	488 nm	200 mW	500 V

EVs' Flow Cytometry

The A60-Micro-Plus machine (Apogee Flow Systems, United Kingdom) is equipped with three spatially separated lasers (488 nm – Position C, 405 nm – Position A and 638 nm – Position B), 7 fluorescence color detectors (525/50, LWP590, 530/30, 574/26, 590/40, 695/40, 676/36) and 3 light scatter detectors (SALS, MALS, and LALS). More details are available in **Table 2**.

As internal controls across assays, before each FC experiment we used two commercially available mixes of beads (Apogee 1493 and Apogee 1517, Apogee Flow Systems, United Kingdom). Silica and Polystyrene beads were used as reference particles for the EV detection. Using the previous described settings (**Table 2**), it is possible to detect particles that scatter light similarly to 100 nm silica (SiO_2) beads (**Figures 1Ai,ii**). In this ApogeeMix, SiO_2 beads have a refractive index (η) (η = 1.42–1.43) close to that of EVs (η ∼1.39) (Chandler et al., 2011; van der Pol et al., 2012).

To identify event coincidence and swarming regime (Libregts et al., 2018) in the experimental settings, serial dilutions of purified EVs were performed. The working range was set in the linear region within the operational range indicated by the Apogee A60-Micro-Plus manufacturer (maximum of 3,000 events/second) (**Figure 1B**). Before loading, samples were diluted in filtered PBS to bring their concentration within the working range of the equipment (maximum of 3,000 events/second). All samples were run at a flow rate of 1.5 μL/min using a 405 nm – LALS threshold of 70. For the control samples, equivalent running times is the stopping criteria utilized (e.g., 200 s). Thus, in these cases control samples are captured for equivalent amounts of time in order to fairly compare the number of positive counts between the different conditions. For the population analysis experiments, the stopping criteria utilized is the number of events acquired, so samples are acquired until a minimum of 250,000 events is reached. The 405 nm – LALS PMT was monitored and always maintained below 0.35. This number is an indicator of noise, since it displays the amount of background current, which is a function of the amount of background light reaching the photomultiplier.

For the control experiments (**Figure 1C** and **Supplementary Figures S1A,D, S4**), equivalent running times was the stopping criteria utilized. Thus, in these cases control samples were captured for equivalent amounts of time in order to fairly compare the number of positive counts between the different conditions. For the population analysis experiments depicted, the stopping criteria utilized was the number of events acquired, so samples were acquired until a minimum of 250,000 events was reached. In all experimental settings, the data was not pre-gated based on the scatter signals. The acquired data was exported and analyzed with FlowJo software v10.4.2 (FlowJo LLC, United States). All flow cytometry files are available at "flowrepository.org" under the Repository ID FR-FCM-Z2EH. The link for access to the files is:

flowrepository.org/id/RvFrS5PMa2qxxbQeAKuwxsgluJLyTsfcivorJMOOPQ0rMi6fCvkTxsQmIMXgv54S

Validation of the EVs Staining Protocol

As a simple approach to normalize the input for our staining protocol, all samples were analyzed for particle concentration and size distribution by the NS300 Nanoparticle Tracking Analysis (NTA) system with red laser (638 nm) (NanoSight – Malvern Panalytical, United Kingdom). Samples were pre-diluted in filtered PBS to achieve a concentration within the range for optimal NTA analysis. Video acquisitions were performed using a camera level of 16 and a threshold between 5 and 7. Five to nine videos of 30 s were captured per sample. Analysis of particle concentration per mL and size distribution were performed with the NTA software v3.4.

For staining, 2×10^9 particles of non-purified (NP) sample or purified EVs were mixed with 40 μL of filtered PBS containing 0.4 μg of anti-CD9 conjugated to phycoerythin (PE) (Thermo Fisher Scientific LABC 12-0091-81, Massachusetts, United States) and incubated for 1 h at 37° C. Samples were incubated with Carboxyfluorescein Diacetate Succinimidyl Ester (CFSE – Thermo Fisher Scientific LTI C34554, MA, United States) in a final concentration of 25.6 μM for 90 min at 37°C. The staining with CFSE was done after the addition of the antibody to ensure that the dye would not interfere with the antibody staining. For removal of unbound CFSE and antibody, Size Exclusion Chromatography (SEC) columns (iZON qEV original columns SP1, United Kingdom) were used. Samples containing unstained or stained EVs, and appropriate controls, were diluted up to 500 μL with filtered PBS and processed by qEV following manufacturer's instructions. EVs-enriched fractions #7, #8, and #9 (500 μL each) were then pooled and retrieved for analysis with the Flow Cytometer Apogee A60-Micro-Plus (Apogee Flow Systems, United Kingdom).

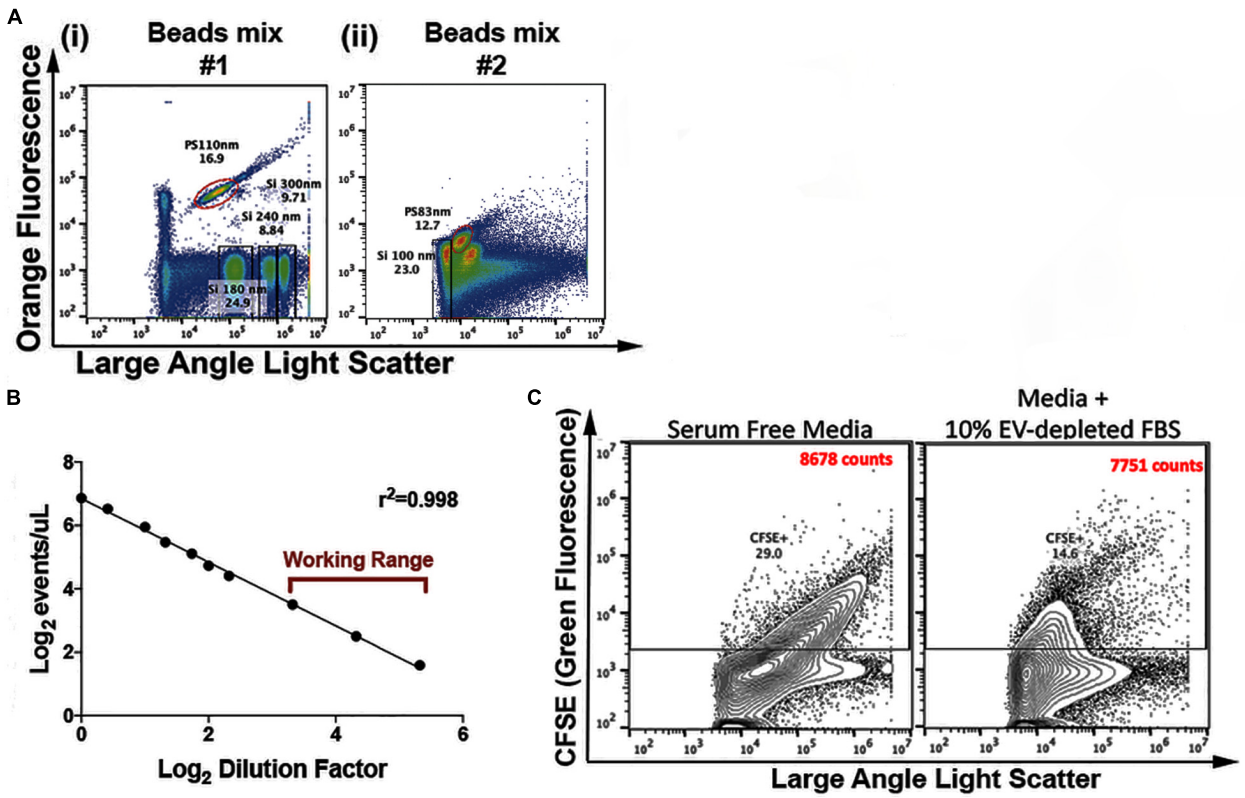

FIGURE 1 | EVs' Flow Cytometry parameters. **(A)** Flow cytometry analysis of a mix of polystyrene (PS) and silica (Si) beads. Depicted in the flow cytometric plots are: 110 nm PS, 180 nm Si, 240 nm Si, 300 nm Si (i) and 83 nm PS and 100 nm Si beads (ii) **(B)**, analysis of events/μL in relation to sample dilution factor. The utilized working range is indicated (n = 5 – representative plot). **(C)** Representative plots of CFSE-labeled serum-free and 10% EV-depleted FBS medium; the indicated counts ($CFSE^+$) correspond to the events within the $CFSE^+$ gate.

The FC strategy here presented relies on the staining of vesicular particles with CFSE, as previously described (Pospichalova et al., 2015; Morales-Kastresana et al., 2017; Mastoridis et al., 2018). A subset of the experiments shown here was performed with conditioned medium, in which cells were grown in medium containing EVs-depleted FBS. To control for the presence of serum-derived vesicles in our samples, serum-free medium and medium containing 10% of EVs-depleted FBS were stained with CFSE and analyzed using our standard settings, with flow cytometry data being acquired for similar periods of time. $CFSE^+$ events count in medium containing 10% of EVs-depleted FBS were as low as those found in serum-free medium, about 3% of the number of events acquired in EV samples from conditioned medium (**Figure 1C**).

For all subsequent analyses, quadrant thresholds were established with unstained and single-stained EVs. Vesicle-free controls containing CFSE, anti-CD9, and both CFSE and anti-CD9 are also shown. Control samples were captured using equal time periods, similar to the acquisition times of corresponding samples containing EVs (**Supplementary Figure S1A**). Increments in the concentration of CFSE didn't increase the proportion of $CFSE^+$ EVs (**Supplementary Figure S1B**), suggesting that our experimental conditions for CFSE staining are optimal. To ensure that Anti-CD9 staining was performed in optimal experimental conditions, incremental concentrations of Anti-CD9 were tested (**Supplementary Figure S1C**). The working amount of Anti-CD9 was set at 0.4 μg per staining reaction. To certify that the observed $CFSE^+$ events were indeed vesicles, purified EVs were pre-incubated with 2% NP-40 for 1 h at room temperature and analyzed using our FC strategy. A reduction of 90% of $CFSE^+$ events was found upon detergent treatment, confirming that most of the observed $CFSE^+$ events were indeed EVs (**Supplementary Figure S1D**).

NP-40 Treatment

Extracellular vesicles were lysed by incubation with 2% NP-40 (Thermo Fisher Scientific 85124, MA, United States) for 1 h at room temperature, and then stained with CFSE and analyzed by our FC strategy, as described above.

Calculation of MESF Values

Assessment of standardized unit molecules of equivalent soluble fluorochrome (MESF) values allows for cross comparisons between different instruments and laboratories (Schwartz et al., 2004; Wang and Hoffman, 2017). In this work, MESF for PE and FITC were then used to determine the fluorescence intensity of anti-CD9 and CFSE staining, respectively. The MESF

were calculated for PE and CFSE using SPERO™ Rainbow Beads Calibration Particles (Spherotech RCP-05-5, United States) according to instructions provided by the manufacturer. The MESF values were measured, with the same acquisition settings applied for all the assays and using a set of Rainbow Beads containing 4 bead populations with known equivalents of FITC molecules and 4 bead populations with known equivalents of PE molecules (**Figure 2A**). After data collection, the Median Fluorescence intensity (MFI) of these peaks was converted to Relative Channel Number (#CH) using the formula [Relative Channel# (#CH) = $(R/4)\log_{10}(MFI)$, where R is the resolution]. Then, the #CH values of the Rainbow beads were plotted against log MESF values and a linear regression was performed (**Figures 2B,C**). The MESF values for unknown samples was calculated using the equation corresponding to this linear regression. Therefore, this regression allowed for the calculation of MESF values of our experimental controls. In our experimental setting the gates for $CFSE^+$ and $CD9^+$ were defined such that the $CFSE^-$ and $CD9^-$ populations displayed approximately 517 and 371 MESF, respectively. The $CFSE^+$ population was approximately 10501 MESF whereas the PE^+ population (CD9) was approximately 1441 MESF (**Figure 2D**).

Purification and Characterization of EVs

Mouse blood (3.5 mL) and supernatant fraction of conditioned medium (80 mL) were centrifuged at 500 *g* for 10 min. The collected supernatant was then centrifuged at 3,000 *g* for 20 min (these samples are from now on referred to as "non-purified" – NP – samples), followed by another centrifugation at 12,000 *g* for 20 min. After these initial steps, purification of EVs was performed in plasma by UC-I (bellow) and in conditioned medium according to one of the following protocols (**Figure 3A**):

- (Exoquick) ExoQuick® commercial kit (System Biosciences EXOTC10A-1, Palo Alto, CA, United States), following manufacturer's instructions;
- (UC-I) 100,000 *g* for 140 min, followed by pellet resuspension in 14.5 mL of filtered Phosphate-Buffered Saline (PBS, Corning 15313581, NY, United States). This sample was pipetted on top of a 4 mL sucrose cushion (D_2O containing 1.2 g of protease-free sucrose and 96 mg of Tris base adjusted to pH 7.4), and centrifuged at 100,000 *g* for 70 min. The fraction of interest (4 mL) was aspirated with a 18G needle and taken to a final volume of 20 mL with filtered PBS. The sample was then centrifuged at 100,000 *g* for 18 h. The EV-containing pellet was resuspended in filtered PBS;
- (UC-II) 100,000 *g* for 140 min. Pellet was washed with filtered PBS and centrifuged at 100,000 *g* for 18 h. The EV-containing pellet was resuspended in filtered PBS;
- (UC-III) 100,000 *g* for 70 min, followed by resuspension of the EV-containing pellet in filtered PBS;
- (UC-IV) 100,000 *g* for 70 min. Pellet was washed with PBS and again centrifuged at 100,000 *g* for another 70 min. The EV-containing pellet was resuspended in filtered PBS.

For the non-purified samples (NP) of conditioned medium (100 μL), mouse plasma (20 μL in 50 μL of 5,000 U-I-/mL heparin) and vitreous humor (5 μL diluted in 20 μL of 5,000 U-I-/mL heparin), a first centrifugation was performed at 500 *g* for 10 min. The supernatant was collected and a second

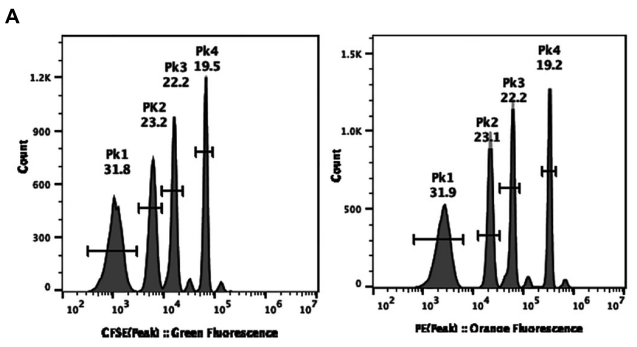

B

FITC MESF			
Peak	MFI	#CH	MESF
Pk1	1072	117,13	38
Pk2	5856	145,64	106
Pk3	15356	161,82	191
Pk4	63673	185,70	450
PE MESF			
Peak	MFI	#CH	MESF
Pk1	2478	131,20	281
Pk2	21156	167,20	1025
Pk3	58689	184,33	1899
Pk4	317832	212,69	5268

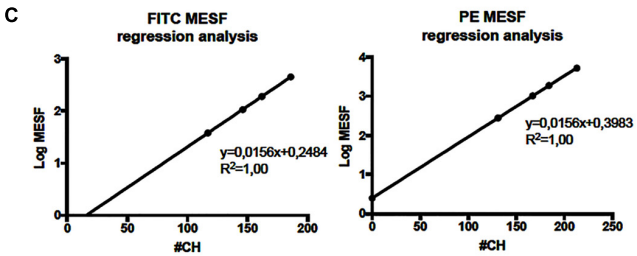

D

FITC MESF				
Sample		MFI	#CH	MESF
EVs+ CFSE	CFSE+	10274	155,07	149
	CFSE-	1066	117,04	38
PE MESF				
Sample		MFI	#CH	MESF
EVs+CD9	CD9+	8113	151,11	575
	CD9-	2395	130,63	275

FIGURE 2 | Assessment of MESF values. **(A)** Histograms of the RCP-05-5 beads in the FITC and PE channel. **(B)** The FITC and PE Median Fluorescence Intensity (MFI) of each peak was measured and converted to Relative Channel Number (#CH), and the MESF values calculated (using template provided by manufacturer). **(C)** Calibration graphs and linear regression where the MFI is plotted in the *x*-axis and log MESF is plotted in the *y*-axis. **(D)** Calculation of FITC and PE MESF values for EVs samples stained with CFSE or Anti-CD9.

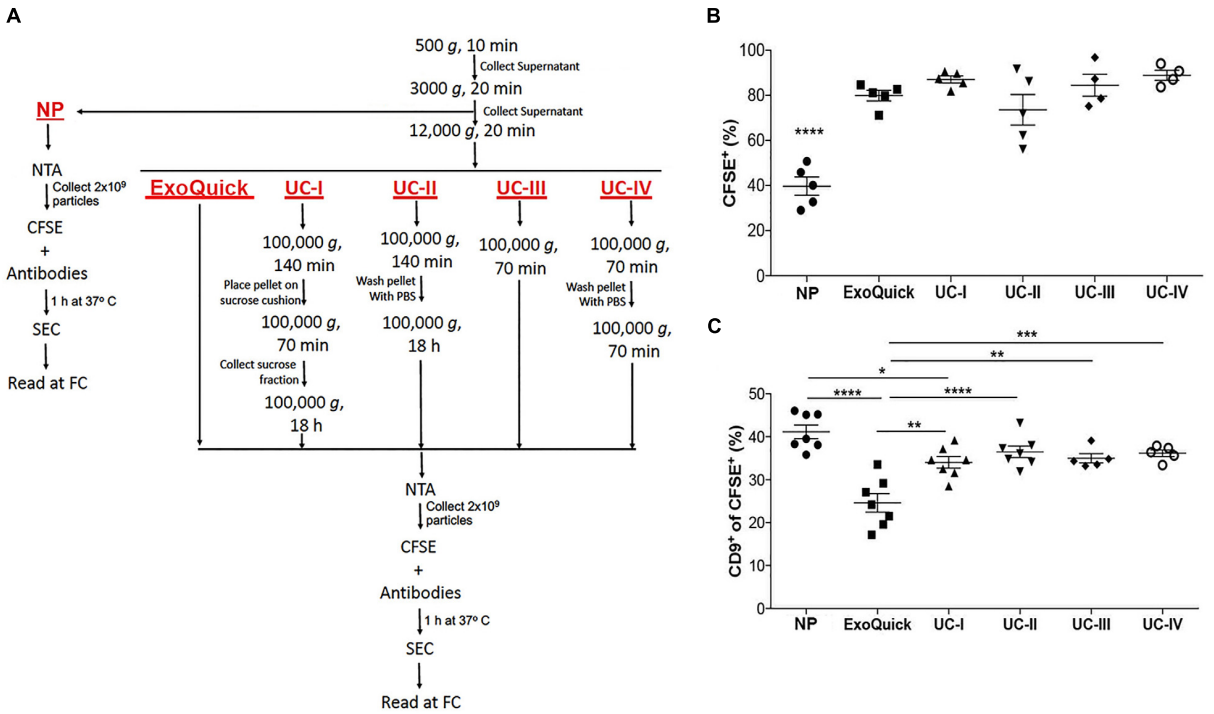

FIGURE 3 | Comparison of isolation methods of EVs. **(A)** Flow chart for sample processing by ultracentrifugation (UC), ExoQuick and for analysis of non-purified (NP) samples. **(B)** Proportion of CFSE$^+$ EVs in non-purified conditioned medium (NP) vs. conditioned medium purified by ExoQuick® or four distinct protocols of ultracentrifugation (UC-I-IV), as indicated in the **Figure 3A**. ****$P < 0.0001$ by ANOVA, with Tukey's post-test. **(C)** Proportion of CD9$^+$ events within CFSE$^+$ EVs in NP, and medium purified by ExoQuick and ultracentrifugation (UC-I-IV). ****$P < 0.0001$, ***$P < 0.001$, **$P < 0.01$, *$P < 0.05$ by ANOVA, with Tukey's post-test. All data are represented as mean ±SEM.

centrifugation step was performed at 3,000 *g* for 20 min. The supernatant after this second centrifugation corresponds to the non-purified sample.

All solutions used (PBS and sucrose cushion) were sterile (0.22 μm membrane-filtered). The ultracentrifugation (UC) steps were performed in refrigerated conditions (4°C) with rotors 50.4Ti or 70Ti (Beckman-Coulter, California, United States).

Statistical Analysis

Error bars in graphical data represent means ± SEM. Statistical significance was determined using either a two-tailed Student's *t*-test or an ANOVA test. A *P*-value under 0.05 was considered statistically significant. Statistical analyses were performed using the GraphPad Prism software (GraphPad Version 7, CA, United States). No statistical method was used to predetermine sample size. The experiments were not randomized, and the investigators were not blinded to allocation during experiments and outcome assessment.

RESULTS

Quantification of Populations of EVs in Conditioned Medium

As remarkably noted by the MISEV2018 guidelines, in a growing field as the EV research, methodologies' standardization is of the utmost importance (Thery et al., 2018). Since there is no single optimal separation method, it's critical for EV studies to choose the best suitable strategy for isolating EVs. Therefore, this decision still poses as a significant challenge in the field, where various EV isolation techniques are available.

In the light of these facts, our FC strategy was first employed in the quality and efficiency assessments of different EV isolation protocols. In order to perform such comparison, the proportion of vesicular (CFSE$^+$) and non-vesicular (CFSE$^-$) particles in samples prepared by different protocols was analyzed.

The quantification of vesicles in conditioned medium (NP) from native tumor cells by our FC strategy showed that ∼40% of particles were CFSE$^+$ (**Figure 3B** and **Supplementary Figure S2A**). On the other hand, samples purified by sucrose cushion-coupled differential ultracentrifugation (UC-I), considered a high-specificity method, contained ∼85% of CFSE$^+$ vesicles. Different EVs isolation protocols by ultracentrifugation may utilize different combinations of washing and density flotation steps. Therefore, the impact of these variations in the proportion of CFSE$^+$ vesicles in the final isolate was tested (**Figure 3B**). With the exception of samples ultracentrifuged overnight without a prior density flotation step (UC-II), in which the proportion of vesicular structures was ∼70%, all other ultracentrifugation-derived preparations contained ∼85% of vesicular structures. As in ultracentrifugation-based methods, ExoQuick® generated samples containing ∼80% of vesicular

structures (**Figure 3B**). These findings indicate in the samples purified by the selected methods the majority of particles present were $CFSE^+$ EVs.

The impact of isolation methods in populations of EVs was also tested. Based on previous reports indicating expression of CD9 in EVs of endosomal origin (Willms et al., 2016), $CFSE^+$ populations containing this tetraspanin were measured. Although displaying a slight reduction in UC-I, the proportion of $CD9^+$ in $CFSE^+$ vesicles was comparable between non-purified samples (NP) and those obtained after isolation by ultracentrifugation. On the other hand, samples processed by ExoQuick® contained lower levels of $CD9^+$ within $CFSE^+$ vesicles (**Figures 3C** and **Supplementary Figure S2B**). This suggests that isolation protocols indeed have an impact on the quality of the sample analyzed, since they may select for subpopulations of EVs.

Quantification of Populations of EVs in Plasma

In several studies of EVs as liquid biopsies, the sample volume demanded is difficult to achieve due to the nature of the experimental conditions. Therefore, a methodology that relies on non-purified biological samples may enable novel experimental approaches. Taking that into account, our FC strategy was next used to quantify EVs in purified and non-purified plasma.

The proportion of $CFSE^+$ vesicles in purified and non-purified plasma was measured. While ∼90% of particles in purified plasma samples (UC-I) were $CFSE^+$ vesicles, this percentage decreased to approximately 20% in non-purified plasma (NP) (**Figures 4A,B**). Next, the population distribution of CD9 in EVs from mouse plasma was analyzed. Between 15–32% of $CFSE^+$ plasma EVs were $CD9^+$. Importantly, this level was comparable between samples that had been purified by UC-I and in native plasma samples (**Figures 4C,D**).

Longitudinal Population Studies of EVs in Microvolumes of Plasma

After confirming that the results between samples of purified and non-purified plasma were comparable (**Figure 4D**), our FC strategy was employed in a longitudinal sampling scheme. This longitudinal experimental design was chosen due to its similarity to the ones desired for studies of EVs as liquid biopsies, e.g., to follow disease progression or treatment efficacy.

The applicability of our FC strategy to longitudinal measurements of populations of EVs was tested in microvolumes of non-purified mouse plasma. The presence of tumor cells is expected to modify the plasmatic levels of EVs during the course of the disease. Therefore, plasma from tumor-bearing mice was collected at different time points (Bebelman et al., 2018). Specifically, blood was collected from each mouse prior to intrahepatic injection of PAN02 pancreatic cancer cells (Day 0), and one (Day 7) and 2 weeks (Day 14) post-injection, as depicted in **Figure 5A**. In this longitudinal analysis of plasma from 10 animals, the proportion of $CFSE^+$ events significantly increased in eight of the experimental subjects between days 0–7, in five between days 7–14 and in nine between days 0–14 (**Figure 5B** and **Supplementary Figure S3A**). When analyzed in relation to the total concentration of particles present in each time point measured by Nanosight (**Figure 5C**), the concentration of $CFSE^+$ events *per* μL increased in 6 animals between days 0–7 and days 7–14, and in all animals between days 0–14 (**Figure 5D**).

$CD9^+$ populations were measured using the experimental settings already described. The proportion of $CD9^+$ within $CFSE^+$ events increased in 8 animals between days 0–7, in 7 animals between days 7–14 and in 9 animals between days 0–14 (**Figure 5E** and **Supplementary Figure S3B**). Similarly, when analyzing this data in relation to the concentration of particles present in plasma (**Figure 5C**), an increase of $CFSE^+CD9^+$ events *per* μL in 6 animals between days 0–7 and in 9 animals between days 7–14 and 0–14 (**Figure 5F**) was observed.

Quantification of Populations of EVs in Vitreous Humor

To further illustrate the application of our FC strategy in performing population analysis of EVs in microvolumes of samples, this workflow was used to study EVs in non-purified vitreous humor, of which 2–2.5 μL *per* mouse/*per* eye was collected. Approximately 68% of particles were $CFSE^+$ vesicles (**Figures 6A,B**). However, the levels of $CD9^+$ events in vitreous humor (<0.1% – **Figure 6B**) were as low as those found in control PBS containing CFSE and anti-CD9 during equivalent sample running times, which is in accordance with the literature (Murthy et al., 2014; Skeie et al., 2015; Zhao et al., 2018) as discussed below (**Supplementary Figure S4**).

DISCUSSION

Measurement of $CFSE^+$ Events as a Strategy to Assess Sample Purity

The lack of consensus regarding methods for purification of EVs remains a challenge, especially when reproducibility between different isolation modalities is desired. This limits EV use in clinical applications and is further complicated by the insufficient means to measure sample purity, notably in complex biological samples containing a mixture of vesicular and non-vesicular particles, such as plasma. Multiple strategies, such as measurement of protein:particle ratio (Webber and Clayton, 2013; Maiolo et al., 2015) and albumin (Baranyai et al., 2015; Veremeyko et al., 2018), have been proposed as quality control parameters for the preparation of EVs, particularly when low specificity isolation methods are employed (Théry et al., 2019). However, because they fail to provide population information, it is still unclear whether these metrics can accurately reflect the purity of preparations of EVs.

CFSE has to date been frequently used as a strategy to label EVs for FC applications (Pospichalova et al., 2015; Morales-Kastresana et al., 2017; Mastoridis et al., 2018; Morales-Kastresana et al., 2019). The suitability of different dyes to efficiently stain and identify EVs has already been addressed by the Jennifer Jones group (Morales-Kastresana et al., 2017). In a work published in 2017, the Jones' group tested several

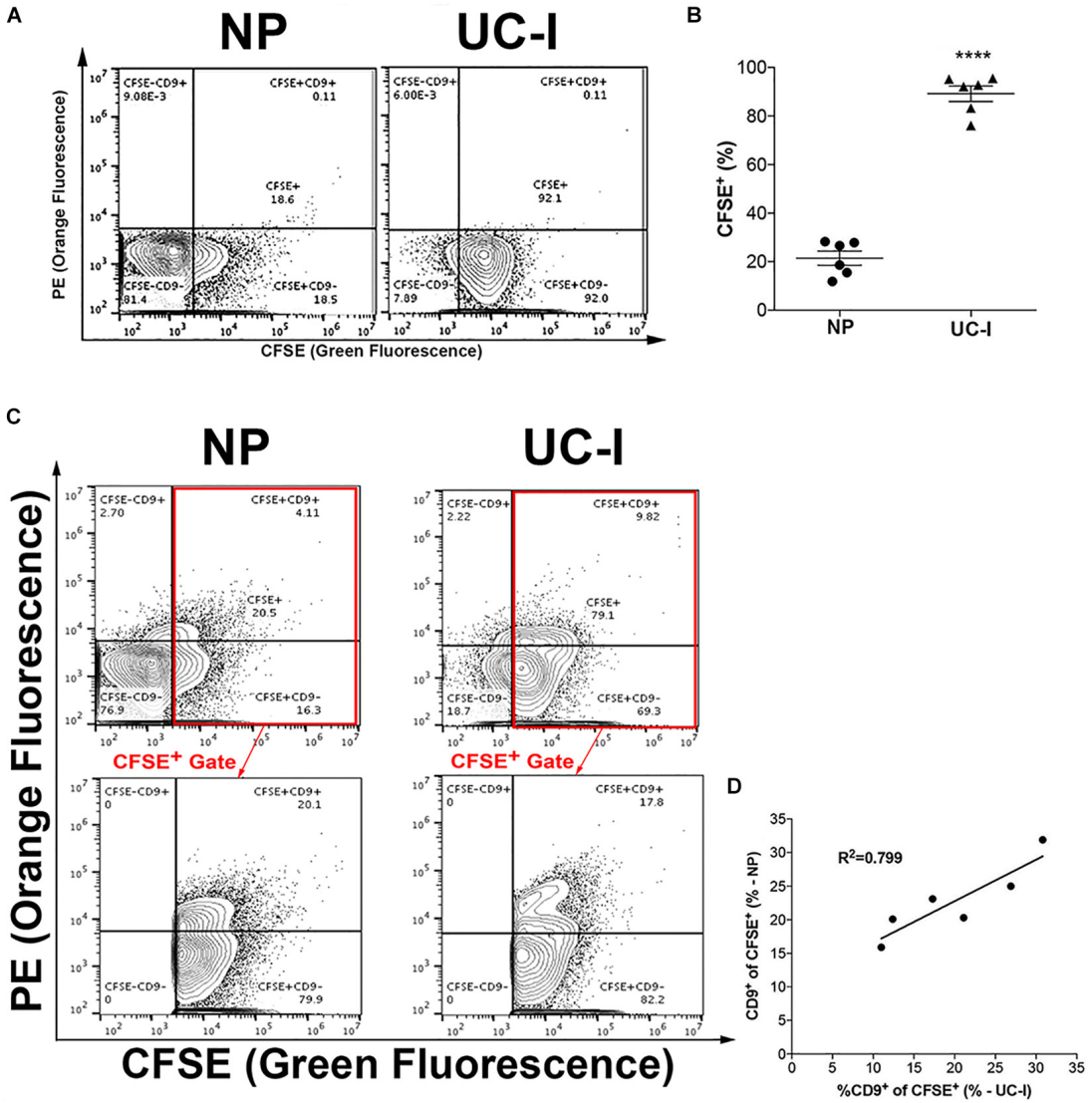

FIGURE 4 | Characterization of EVs in plasma. **(A)** Plots are representative of CFSE$^+$labeled particles from non-purified (NP) plasma, or from plasma purified by ultracentrifugation (UC-I). **(B)** Proportion of CFSE$^+$ EVs in non-purified plasma (NP) vs. plasma purified by sucrose cushion-coupled ultracentrifugation (UC - I). $^{****}P < 0.0001$ differences vs. NP by two-tailed *t*-test. Data are represented as mean ± SEM. **(C)** Representative plots of particles labeled with CFSE and anti-CD9 from NP and UC-I plasma; the lower panels indicate the CD9$^+$ and CD9$^-$ events within CFSE$^+$ particles. **(D)** Correlation analysis of CD9$^+$ events within CFSE$^+$ EVs in samples before (NP) and after purification (UC-I).

dyes, including CFSE and PHK26. While PKH26 was shown to produce 100–400 nm micelles or aggregates both in the presence of EVs or alone in solution, CFSE alone did not form such aggregates. Thus, taking this into account, in our work EVs were labeled with CFSE. The data here presented supports the vesicular labeling with CFSE as a means for determining quality control of purification protocols of EVs. As shown, the majority of particles present in samples purified by high-specificity methods were CFSE$^+$. The employment of ExoQuick® or ultracentrifugation for enrichment of EVs prior to SEC reduced the proportion of CFSE$^-$ particles. In addition, lysis of EVs with the detergent NP-40 resulted in a reduction of 90% of CFSE$^+$ events. Together, these results support the usefulness of CFSE as a tool to identify vesicular particles in biofluids, and thus the suitability of our FC strategy for quality control and quantitative comparison of isolates of EVs prepared by different protocols.

This same approach was employed to validate the depletion of EVs from the FBS used in our *in vitro* studies. Previous reports suggest that traces of bovine EVs may persist in the FBS supernatant after depletion steps (Shelke et al., 2014), which could interfere in the analysis of EVs from conditioned medium. However, comparison of serum-free medium and medium containing 10% of EVs-depleted FBS showed an equally reduced proportion of CFSE$^+$ events. This indicates that residual FBS-derived EVs was not high enough to impact our analysis. Nonetheless, future studies using our strategy for analysis of EVs

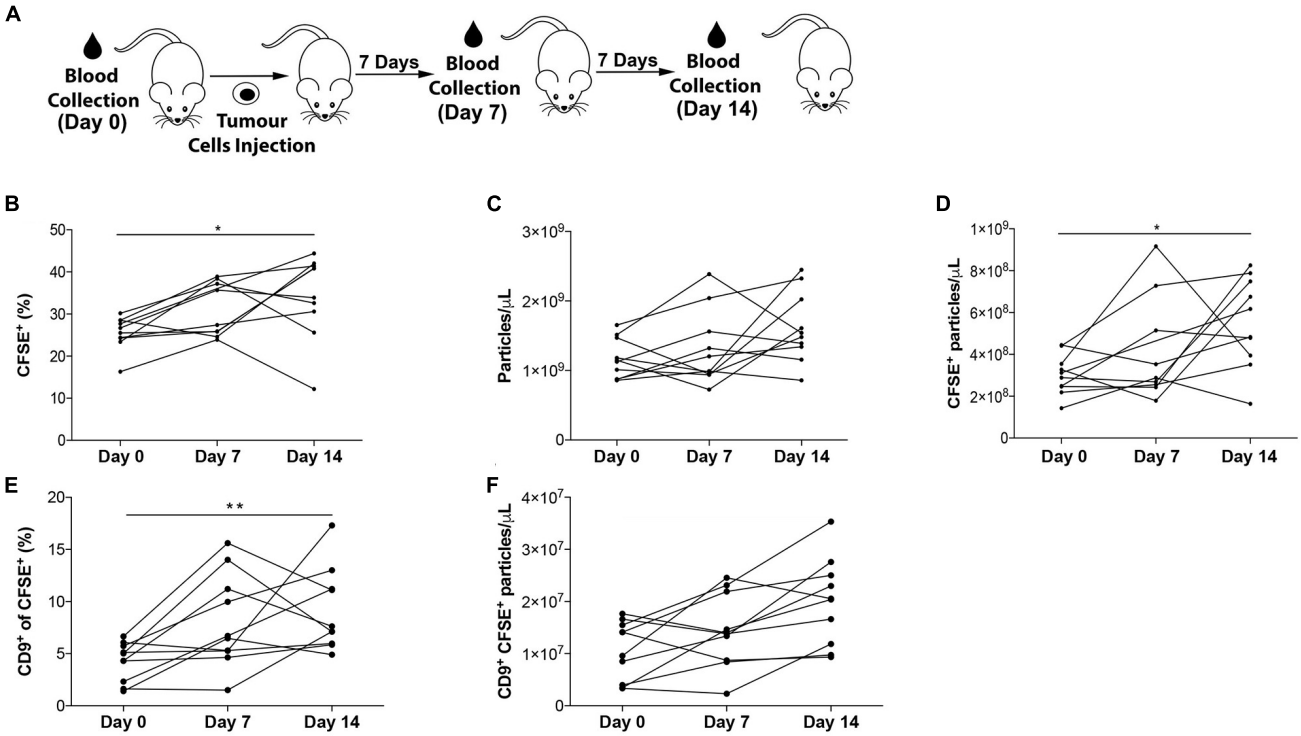

FIGURE 5 | Longitudinal analysis of EVs in plasma. **(A)** Experimental setup. **(B)** Proportion of $CFSE^+$ EVs in non-purified plasma of mice prior (Day 0), and 7 and 14 days after intrahepatic injection of PAN02 tumors. **(C)** Concentration of total particles per microliter of plasma, by NanoSight. **(D)** Concentration of $CFSE^+$ EVs per microliter of plasma. **(E)** Proportion of $CD9^+$ events within $CFSE^+$ EVs. **(F)** Concentration of $CD9^+$ $CFSE^+$ EVs per microliter of plasma. $^{**}P < 0.01$, $^{*}P < 0.05$, differences vs. Day 0 by ANOVA, with Kruskal–Wallis post-test. All data are represented as mean ±SEM.

in conditioned medium will need to account for background events on a case-by-case basis, especially when using low cell numbers, short conditioning time and/or cells producing low levels of EVs.

Results presented by others indicate that CFSE staining could not label 100% of EVs (van der Vlist et al., 2012; Pospichalova et al., 2015; de Rond et al., 2018). Thus, we reasoned that some of the $CFSE^-$ events observed in our experiments could correspond to non-stained EVs. However, unlike the results presented here, in these previous studies CFSE staining was performed in cells before (van der Vlist et al., 2012) or during medium conditioning (Pospichalova et al., 2015), and CFSE concentrations were 1.6–16 times lower (van der Vlist et al., 2012; Pospichalova et al., 2015; de Rond et al., 2018) than those we used. In addition, only ∼15% of the events in samples purified by differential ultracentrifugation coupled with sucrose cushion (UC-I) were CFSE-, and treatment of EVs with the detergent NP-40 caused a reduction of 90% of $CFSE^+$ events, indicating that this dye labels the majority of EVs in our experimental settings. While this may still suggest that CFSE is not capable of staining all EVs present in the sample, it is still unclear to which extent even high-purity isolation methods may provide 100% pure preparations of EVs. Although undesirable, protein aggregation may be present in antibody preparations. This is mainly due to solution conditions, such as ionic strength, pH, temperature, pressure and excipients (Manning et al., 1995), and intrinsic properties of antibodies, such as primary sequence, tertiary structure, non-symmetrical hydrophobicity and charge distributions (Liu et al., 2005; Roberts, 2007; Nishi et al., 2010). Therefore, the potential contribution of unbound antibody aggregates to $CFSE^-$ $Antibody^+$ events was tested. Most $CFSE^-CD9^+$ events didn't correspond to unbound antibodies, and were reduced by EVs purification (**Supplementary Figure S5**). These results suggest that the $CFSE^-$ events observed in the $CD9^+$ population analysis correspond to non-vesicular particles of specific molecular composition with similar size as compared to EVs. Future studies, including detailed morphology and composition analysis, will be necessary to further define these $CFSE^-$ non-vesicular particles.

Comparison of Purification Methods of EVs by FC

In spite of being considered a high-recovery and low-specificity method (Théry et al., 2019), isolation based on precipitation polymers such as ExoQuick® resulted in a high proportion of $CFSE^+$ EVs. This agrees with studies suggesting that EVs prepared by ultracentrifugation or precipitation polymers are comparable (Helwa et al., 2017; Prendergast et al., 2018). In samples prepared by ExoQuick®, however, we found that the proportion of $CD9^+$ $CFSE^+$ events was reduced when compared to NP and other isolation methods. This suggests that, despite providing a high yield of EVs,

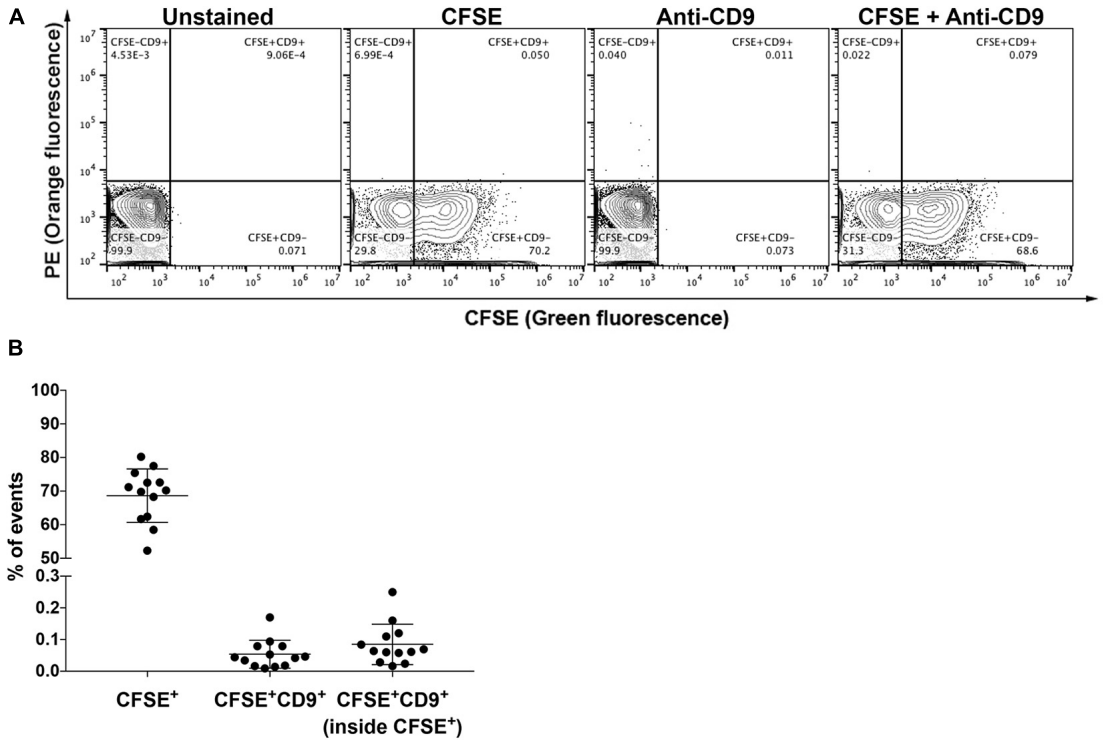

FIGURE 6 | Analysis of EVs in vitreous humor. **(A)** Representative plots of unstained and stained EVs from non-purified vitreous humor from naïve mice in single-animal collections, as indicated. (**B**) Proportion of $CFSE^+$ events, $CFSE^+CD9^+$ events and $CD9^+$ events within $CFSE^+$ EVs. All data are represented as mean ±SEM.

ExoQuick® may insert EV population bias. Also of concern, precipitating agents have previously been linked to potential loss of biological activity (Paolini et al., 2016) and structure (Gamez-Valero et al., 2016) of EVs. Thus, our data adds yet another parameter that should be carefully considered before selecting ExoQuick® as a method of choice for the isolation of EVs.

SEC is the technique of choice for many groups interested in studying the composition and biological activity of vesicles, as it allows simple, fast and affordable isolation of EVs. As SEC is a key component of our FC strategy, the proportion of $CFSE^+$ particles in our preparations was measured to access the isolation efficacy of EVs by SEC. In our experimental settings, this preparation is referred to as NP (non-purified), since SEC is used after staining, and not before as a traditional isolation method. Although considered a low recovery, high specificity method (Théry et al., 2019), conditioned medium processed by SEC contained less than 40% of $CFSE^+$ vesicular particles. This was also the case for more complex samples, such as plasma and vitreous humor, in which the percentage of $CFSE^+$ particles after SEC processing were, respectively, ∼20% and ∼68%. These findings agree with recent studies using comparative transmission electron microscopy, in which SEC-derived preparations displayed a lower proportion of structures resembling EVs when compared to samples derived from differential ultracentrifugation (Takov et al., 2019).

Differential ultracentrifugation is one of the most commonly used EV purification methods. To improve EV purity, most researchers combine ultracentrifugation with additional techniques following the primary step, such as the use of washing steps with saline as well as the use of density gradients (Thery et al., 2018). We found that the proportion of $CFSE^+$ events and $CD9^+$ events within the $CFSE^+$ gate did not differ in the absence (UC-III) or presence (UC-II and UC-IV) of washing steps with PBS or when a sucrose cushion step was used (UC-I). Our results suggest that these additional steps have no major impact in sample purity. However, a more detailed characterization of the potential impact of these washing and/or separation steps in the selection of populations of EVs with specific composition (protein, sugar, lipid, and nucleic acids) will be necessary in future studies.

Our FC strategy allows for faster processing times and also substantially decreases the sample volume requirements compared to conventional EVs isolation protocols (**Table 1**). Thus, we consider ours to be a consistent approach to be applied to control the quality of preparations of EVs.

While we used CFSE as a general EV marker, our experimental setup was performed having CD9 not only as an illustration of the capabilities of the method, but also as an analyte of interest. Our side-by-side comparison of $CFSE^+CD9^+$ events in samples submitted (UC-I) or not (NP) to isolation by ultracentrifugation showed that both strategies are comparable when analyzing

$CD9^+$ EVs populations (**Figures 4C,D**). However, although this equivalence was true for $CD9^+$ EVs, we cannot discard the possibility that other populations of EVs behave differently, specially while probably there is no validated universal EV marker that can be used as an experimental control. Every method, including differential ultracentrifugation, potentially inserts population isolation bias to EVs (as illustrated in **Figure 3C**). Such isolation bias, if existent, has yet to be studied and understood. Be it for future studies in the field of population of EVs, or be it for studies involving other vesicular molecules, we believe and strongly suggest that side-by-side validation of non-purified versus purified samples (as in **Figures 4C,D**) should be performed as a pre-validation of our approach. Thus, for every EV molecule of interest, the approach presented in our work that relies on the use of NP samples in different contexts should first be validated by a comparison study similar to the one presented in **Figures 4C,D**.

Longitudinal Study of EVs in Plasma by FC

Longitudinal composition analyses can provide precious temporal information on the dynamics of EVs in physiological and pathological settings (Eitan et al., 2017; Menon et al., 2018; Wu et al., 2018). However, these studies are often difficult in microvolumes of samples, mainly due to the limited number of EVs that can be harvested in these experimental conditions (Théry et al., 2019). This constraint frequently leads to insufficient recovery of EVs (Clayton et al., 2018), unless small volume samples are pooled from multiple individuals or collections. Moreover, in studies involving small animals, the requirement for lethal bleeding in order to collect enough plasma for the effective isolation of EVs complicates the performance of longitudinal studies and increases the demand for animals, leading to higher costs, higher sample processing complexity and potential bioethical issues. By not requiring isolation of EVs prior to staining, our FC strategy allows for the analysis of both intra- and inter-individual heterogeneity in the population of interest throughout an experiment. In our studies, the proportion of $CFSE^+$ EVs and of $CD9^+$ events within $CFSE^+$ EVs increased in the plasma of mice bearing liver metastatic pancreatic cancer lesions. Based on these results, we are currently studying the potential use of these readouts for follow-up studies of pancreatic cancer patients in the metastatic phase.

Study of EVs in Vitreous Humor by FC

The vitreous humor is a small-volume biofluid that contains low protein content, ranging from 120 to 500 ng/μL (Chowdhury et al., 2010), which is frequently considered to arise from filtration of plasma through fenestrated capillaries of the ciliary body stroma via the iris root (Freddo et al., 1990). Besides the quantitative differences in protein content, a comparison of vitreous humor and plasma proteome revealed that only 58% of the vitreous humor proteins have also been identified in human plasma (Chowdhury et al., 2010). Consistent with this, our analysis revealed that vitreous fluid contains three times more $CFSE^+$ vesicular structures when compared to plasma. Furthermore, it contained insignificant levels of $CD9^+$ events, comparable to those found in control solutions with only CFSE and anti-CD9. These results are consistent with the previously reported absence of CD9 in EVs from vitreous humor (Murthy et al., 2014; Skeie et al., 2015; Zhao et al., 2018). However, it is still unknown whether the absence of $CD9^+$ vesicles is a result of the filtration that occurs during the production of vitreous humor, uptake and degradation of this vesicle population by ocular cells, higher prevalence of non-endosomal EVs and/or other mechanisms. Although it is unclear to which extend ocular cells contribute to the collection of EVs found in vitreous humor, our FC strategy can be potentially used to study these vesicles both in pre-clinical and clinical settings as potential biomarkers and biological mediators of eye diseases.

CONCLUSION

By allowing for the analysis of conditioned medium volumes as small as 100 μL, our FC strategy can be potentially used to characterize the heterogeneity of EVs and the differential packaging of biomolecules during the biogenesis of EVs in highly controlled small-scale in vitro systems. This approach also makes it possible to study populations of EVs from as little as ∼1 μL of plasma or vitreous humor. By doing so, our strategy represents a precious tool to identify novel physiological and pathological cell-to-cell communication systemic networks involving EVs in *in vivo* models.

In regard to the use of EVs as liquid biopsies, clinical relevance relies on experimental data that is comparable/translatable to human practice. Although *in vitro* assays are very helpful, murine models are especially relevant in this context, since they capture the complexity of human processes and often are the most advanced pre-clinical models to study the biological significance of EVs in a multicellular organism, unravel novel EV biomarkers and analyze disease stages that would be inaccessible or nonviable in direct human studies. However, in this ever-growing pre-clinical field some hurdles must be overcome. Namely, the lack of EVs isolation analytical reproducibility, which limits its clinical applicability; and the sample volume requirements, which limits the application of EVs as liquid biopsies, especially with the potential for longitudinal sampling to follow disease progression. In native clinical samples, our FC strategy has an unexplored capability to be applied in the study of populations of EVs, multiplying the number of possible different analysis from a single biofluid collection. It also has a great potential to enable the study of populations of EVs in samples with intrinsically limited volumes, such as lacrimal, vitreous humor and synovial fluids, facilitating the use of these biofluids as liquid biopsies on clinical settings.

DATA AVAILABILITY STATEMENT

The original contributions presented in the study are included in the article/**Supplementary Material**, further inquiries can be directed to the corresponding author.

ETHICS STATEMENT

The animal study was reviewed and approved, being performed in accordance with national animal experimentation guidelines (DGAV), animal protocol 0421/000/000/2018.

AUTHOR CONTRIBUTIONS

JM designed and performed the all experiments. SB, NC, and AG contributed to the animal experimentation. CB contributed to the sample processing, EVs characterization and equipment maintenance. JE contributed with the Pan02 EVs samples for **Supplementary Figure S2**. MS built the experimental setup. BC-S conceived the project. All the authors wrote and reviewed the manuscript.

FUNDING

JM was supported by "Fundação para a Ciência e a Tecnologia" (PD/BD/105866/2014). SB was supported by the EMBO Installation Grant 3921. AG was supported by the grant 2017NovPCC1058 from Breast Cancer Now's Catalyst Programme, which is supported by funding from Pfizer. JE was supported by the grant 765492 from H2020-MSCA-ITN-2017. This work was supported by the Champalimaud Foundation, the grant 751547 from H2020-MSCA-IF-2016 and the grant LCF/PR/HR19/52160014 from "La Caixa" Foundation. This manuscript has been released as a pre-print at BioRxiv (Maia et al., 2020).

ACKNOWLEDGMENTS

We thank A. Vieira and D. Fortunato, for helpful discussions and technical support, and Dr. M. de Sousa for her interest in this work and in the preparation of the manuscript. **Graphical Abstract** was created with BioRender.com.

SUPPLEMENTARY MATERIAL

The Supplementary Material for this article can be found online at: https://www.frontiersin.org/articles/10.3389/fcell.2020.593750/full#supplementary-material

Supplementary Figure 1 | Internal controls and detergent lysis of EVs. **(A)** Representative plots of buffer containing CFSE only, anti-CD9 only, and CFSE and anti-CD9 (upper panels), and of unstained EVs, EVs stained with CFSE, EVs stained with anti-CD9, and EVs double stained with CFSE and anti-CD9 (lower panels); the indicated counts correspond to the events within the upper right quadrant ($CFSE^+CD9^+$). **(B)** Titration of CFSE staining. **(C)** Titration of Anti-CD9 staining. **(D)** Detergent lysis of EVs. The plots are representative of unstained and non-lysed EVs (EVs), CFSE-stained non-lysed EVs (EVs+CFSE), unstained EVs lysed with NP-40 (EVs+NP-40) and CFSE-stained EVs lysed with NP-40 (EVs+NP-40+CFSE); the counts of $CFSE^+$ particles are indicated. The graph indicates the reduction in the percentage of $CFSE^+$ EVs after lysis with NP-40. All data are represented as mean ± SEM.

Supplementary Figure 2 | Different purification methods of conditioned medium samples. **(A)** Representative plots of CFSE-labeled particles from non-purified conditioned medium (NP), and from conditioned medium purified by ExoQuick or by distinct ultracentrifugation protocols (UC-I-IV). **(B)** Representative plots of particles labeled with CFSE and anti-CD9 from NP, and from conditioned medium purified by ExoQuick or by ultracentrifugation (UC-I-IV). The lower panels indicate the CD9 status within $CFSE^+$ EVs.

Supplementary Figure 3 | Longitudinal analysis of plasma EVs. **(A)** Representative plots of $CFSE^+$labeled EVs from non-purified plasma of mice prior (Day 0), and at 7 and 14 days after intrahepatic injection of PAN02 cells. **(B)** Representative plots of particles from NP plasma double labeled with CFSE and anti-CD9; the lower panels indicate the $CD9^+$ and $CD9^-$ particles within $CFSE^+$ EVs.

Supplementary Figure 4 | $CD9^+$ events in vitreous humor. Representative plots of PBS and vitreous humor double labeled with CFSE and anti-CD9. Samples were captured during 250 s. The indicated counts ($CFSE^+CD9^+$) correspond to the events within the upper right quadrant.

Supplementary Figure 5 | Analysis of false-positive $CD9^+$ events in conditioned medium. **(A)** Calibration curve of false-positive events. Buffer containing anti-CD9, in the same concentration used in the staining reaction and pre-cleared by SEC, was analyzed by Flow Cytometry for increasing acquisition times. **(B)** Estimate percentage of false-positive events by unbound anti-CD9 within $CFSE^-CD9^+$ in each purification context. **(C)** Proportion of $CFSE^+$ (black) and $CFSE^-$ (white) events within $CD9^+$ events in NP samples and samples purified by ExoQuick and ultracentrifugation (UC-I-IV). $^{****}P < 0.0001$ by ANOVA, with Tukey's post-test. All data are represented as mean ±SEM.

REFERENCES

Arenaccio, C., and Federico, M. (2017). The Multifaceted Functions of Exosomes in Health and Disease: An Overview. *Adv. Exp. Med. Biol.* 998, 3–19. doi: 10.1007/978-981-10-4397-0_1 doi: 10.1007/978-981-10-4397-0_1

Baranyai, T., Herczeg, K., Onódi, Z., Voszka, I., Módos, K., Marton, N., et al. (2015). Isolation of Exosomes from Blood Plasma: Qualitative and Quantitative Comparison of Ultracentrifugation and Size Exclusion Chromatography Methods. *PLoS One* 10:e0145686. doi: 10.1371/journal.pone.0145686

Bebelman, M. P., Smit, M. J., Pegtel, D. M., and Baglio, S. R. (2018). Biogenesis and function of extracellular vesicles in cancer. *Pharmacol. Ther.* 188, 1–11. doi: 10.1016/j.pharmthera.2018.02.013

Boriachek, K., Islam, M. N., Möller, A., Salomon, C., Nguyen, N. T., Hossain, M. S. A., et al. (2018). Biological Functions and Current Advances in Isolation and Detection Strategies for Exosome Nanovesicles. *Small* 14:1702153 doi: 10.1002/smll.201702153

Caby, M. P., Lankar, D., Vincendeau-Scherrer, C., Raposo, G., and Bonnerot, C. (2005). Exosomal-like vesicles are present in human blood plasma. *Int. Immunol.* 17, 879–887.

Campos-Silva, C., Suárez, H., Jara-Acevedo, R., Linares-Espinós, E., Martinez-Piñeiro, L., Yáñez-Mó, M., et al. (2019). High sensitivity detection of extracellular vesicles immune-captured from urine by conventional flow cytometry. *Sci. Rep.* 9:2042. doi: 10.1038/s41598-019-38516-38518

Chandler, W. L., Yeung, W., and Tait, J. F. (2011). A new microparticle size calibration standard for use in measuring smaller microparticles using a new flow cytometer. *J. Thromb. Haemost.* 9, 1216–1224. doi: 10.1111/j.1538-7836.2011.04283.x

Choi, D., Montermini, L., Jeong, H., Sharma, S., Meehan, B., Rak, J., et al. (2019). Mapping Subpopulations of Cancer Cell-Derived Extracellular Vesicles and Particles by Nano-Flow Cytometry. *ACS Nano.* 13, 10499–10511. doi: 10.1021/acsnano.9b04480

Chowdhury, U. R., Madden, B. J., Charlesworth, M. C., and Fautsch, M. P. (2010). Proteome analysis of human aqueous humor. *Invest. Ophthalmol. Vis. Sci* 51, 4921–4931. doi: 10.1167/iovs.10-5531

Clayton, A., Buschmann, D., Byrd, J. B., Carter, D. R. F., Cheng, L., Compton, C., et al. (2018). Summary of the ISEV workshop on extracellular vesicles as disease biomarkers, held in Birmingham, UK, during December 2017. *J. Extracel. Vesic.* 7:1473707. doi: 10.1080/20013078.2018.1473707

Contreras-Naranjo, J. C., Wu, H. J., and Ugaz, V. M. (2017). Microfluidics for exosome isolation and analysis: enabling liquid biopsy for personalized medicine. *Lab. Chip.* 17, 3558–3577. doi: 10.1039/c7lc00592j

Corbett, T. H., Roberts, B. J., Leopold, W. R., Peckham, J. C., Wilkoff, L. J., Griswold, D. P. Jr., et al. (1984). Induction and chemotherapeutic response of two transplantable ductal adenocarcinomas of the pancreas in C57BL/6 mice. *Cancer Res.* 44, 717–726.

Costa-Silva, B., Aiello, N. M., Ocean, A. J., Singh, S., Zhang, H., Thakur, B. K., et al. (2015). Pancreatic cancer exosomes initiate pre-metastatic niche formation in the liver. *Nat. Cell Biol.* 17, 816–826. doi: 10.1038/ncb3169

de Rond, L., van der Pol, E., Hau, C. M., Varga, Z., Sturk, A., van Leeuwen, T. G., et al. (2018). Comparison of Generic Fluorescent Markers for Detection of Extracellular Vesicles by Flow Cytometry. *Clin. Chem.* 64, 680–689. doi: 10.1373/clinchem.2017.278978

Eitan, E., Green, J., Bodogai, M., Mode, N. A., Bæk, R., Jørgensen, M. M., et al. (2017). Age-Related Changes in Plasma Extracellular Vesicle Characteristics and Internalization by Leukocytes. *Sci. Rep.* 7:1342. doi: 10.1038/s41598-017-01386-z

Freddo, T. F., Bartels, S. P., Barsotti, M. F., and Kamm, R. D. (1990). The source of proteins in the aqueous humor of the normal rabbit. *Invest. Ophthalmol. Vis. Sci.* 31, 125–137.

Gamez-Valero, A., Monguió-Tortajada, M., Carreras-Planella, L., Franquesa, Ml, Beyer, K., Borràs, F. E., et al. (2016). Size-Exclusion Chromatography-based isolation minimally alters Extracellular Vesicles' characteristics compared to precipitating agents. *Sci. Rep.* 6:33641. doi: 10.1038/srep33641

Gorgens, A., Bremer, M., Ferrer-Tur, R., Murke, F., Tertel, T., Horn, P. A., et al. (2019). Optimisation of imaging flow cytometry for the analysis of single extracellular vesicles by using fluorescence-tagged vesicles as biological reference material. *J. Extracell. Vesicl.* 8:1587567. doi: 10.1080/20013078.2019.1587567

Groot Kormelink, T., Arkesteijn, G. J., Nauwelaers, F. A., van den Engh, G., Nolte-'t Hoen, E. N., Wauben, M. H., et al. (2016). Prerequisites for the analysis and sorting of extracellular vesicle subpopulations by high-resolution flow cytometry. *Cytometry A* 89, 135–147. doi: 10.1002/cyto.a.22644

Guo, S. C., Tao, S. C., and Dawn, H. (2018). Microfluidics-based on-a-chip systems for isolating and analysing extracellular vesicles. *J. Extracell. Vesicl.* 7:1508271. doi: 10.1080/20013078.2018.1508271

Helwa, I., Cai, J., Drewry, M. D., Zimmerman, A., Dinkins, M. B., Khaled, M. L., et al. (2017). A Comparative Study of Serum Exosome Isolation Using Differential Ultracentrifugation and Three Commercial Reagents. *PLoS One* 12:e0170628. doi: 10.1371/journal.pone.0170628

Hoshino, A., Costa-Silva, B., Shen, T. L., Rodrigues, G., Hashimoto, A., Tesic Mark, M., et al. (2015). Tumour exosome integrins determine organotropic metastasis. *Nature* 527, 329–335. doi: 10.1038/nature15756

Kalluri, R. (2016). The biology and function of exosomes in cancer. *J. Clin. Invest.* 126, 1208–1215. doi: 10.1172/JCI81135

Kalluri, R., and LeBleu, V. S. (2020). The biology, function, and biomedical applications of exosomes. *Science* 367:eaau6977 doi: 10.1126/science.aau6977

Kowal, J., Arras, G., Colombo, M., Jouve, M., Morath, J. P., Primdal-Bengtson, B., et al. (2016). Proteomic comparison defines novel markers to characterize heterogeneous populations of extracellular vesicle subtypes. *Proc. Natl. Acad. Sci. U.S.A* 113, E968–E977. doi: 10.1073/pnas.1521230113

Libregts, S., Arkesteijn, G. J. A., Nemeth, A., Nolte-'t Hoen, E. N. M., and Wauben, M. H. M. (2018). Flow cytometric analysis of extracellular vesicle subsets in plasma: impact of swarm by particles of non-interest. *J. Thromb. Haemost.* 16, 1423–1436. doi: 10.1111/jth.14154

Liu, J., Nguyen, M. D., Andya, J. D., and Shire, S. J. (2005). Reversible self-association increases the viscosity of a concentrated monoclonal antibody in aqueous solution. *J. Pharm. Sci.* 94, 1928–1940. doi: 10.1002/jps.20347

Maia, J., Batista, S., Couto, N., Gregório, A. C., Bodo, C., Elzanowska, J., et al. (2020). Population Analysis of Extracellular Vesicles in Microvolumes of Biofluids. *bioRxiv* doi: 10.1101/2020.01.10.895037

Maia, J., Caja, S., Strano Moraes, M. C., Couto, N., and Costa-Silva, B. (2018). Exosome-Based Cell-Cell Communication in the Tumor Microenvironment. *Front. Cell Dev. Biol.* 6:18. doi: 10.3389/fcell.2018.00018

Maiolo, D., Paolini, L., Di Noto, G., Zendrini, A., Berti, D., Bergese, P., et al. (2015). Colorimetric nanoplasmonic assay to determine purity and titrate extracellular vesicles. *Anal. Chem.* 87, 4168–4176. doi: 10.1021/ac504861d

Manning, M. C., Matsuura, J. E., Kendrick, B. S., Meyer, J. D., Dormish, J. J., Vrkljan, M., et al. (1995). Approaches for increasing the solution stability of proteins. *Biotechnol. Bioeng.* 48, 506–512. doi: 10.1002/bit.260480513

Mastoridis, S., Bertolino, G. M., Whitehouse, G., Dazzi, F., Sanchez-Fueyo, A., Martinez-Llordella, M., et al. (2018). Multiparametric Analysis of Circulating Exosomes and Other Small Extracellular Vesicles by Advanced Imaging Flow Cytometry. *Front. Immunol.* 9:1583. doi: 10.3389/fimmu.2018.01583

Menon, R., Debnath, C., Lai, A., Guanzon, D., Bhatnagar, S., Kshetrapal, P. K., et al. (2018). Circulating exosomal miRNA profile during term and preterm birth pregnancies - a longitudinal study. *Endocrinology* 160(2), 249–275 doi: 10.1210/en.2018-2836

Morales-Kastresana, A., Musich, T. A., Welsh, J. A., Telford, W., Demberg, T., Wood, J. C. S., et al. (2019). High-fidelity detection and sorting of nanoscale vesicles in viral disease and cancer. *J. Extracell. Vesicl.* 8:1597603. doi: 10.1080/20013078.2019.1597603

Morales-Kastresana, A., Telford, B., Musich, T. A., McKinnon, K., Clayborne, C., Braig, Z., et al. (2017). Labeling Extracellular Vesicles for Nanoscale Flow Cytometry. *Sci. Rep.* 7:1878. doi: 10.1038/s41598-017-01731-1732

Murthy, K. R., Goel, R., Subbannayya, Y., Jacob, H. K., Murthy, P. R., Manda, S. S., et al. (2014). Proteomic analysis of human vitreous humor. *Clin. Proteom.* 11:29. doi: 10.1186/1559-0275-11-29

Nishi, H., Miyajima, M., Nakagami, H., Noda, M., Uchiyama, S., Fukui, K., et al. (2010). Phase separation of an IgG1 antibody solution under a low ionic strength condition. *Pharm. Res.* 27, 1348–1360. doi: 10.1007/s11095-010-0125-127

Nolte-'t Hoen, E. N., van der Vlist, E. J., Aalberts, M., Mertens, H. C., Bosch, B. J., Bartelink, W., et al. (2012). Quantitative and qualitative flow cytometric analysis of nanosized cell-derived membrane vesicles. *Nanomedicine* 8, 712–720. doi: 10.1016/j.nano.2011.09.006

Ogawa, Y., Miura, Y., Harazono, A., Kanai-Azuma, M., Akimoto, Y., Kawakami, H., et al. (2011). Proteomic analysis of two types of exosomes in human whole saliva. *Biol. Pharm. Bull.* 34, 13–23. doi: 10.1248/bpb.34.13

Paolini, L., Zendrini, A., Di Noto, G., Busatto, S., Lottini, E., Radeghieri, A., et al. (2016). Residual matrix from different separation techniques impacts exosome biological activity. *Sci. Rep.* 6:23550. doi: 10.1038/srep23550

Peinado, H., Aleèkoviæ, M., Lavotshkin, S., Matei, I., Costa-Silva, B., Moreno-Bueno, G., et al. (2012). Melanoma exosomes educate bone marrow progenitor cells toward a pro-metastatic phenotype through MET. *Nat. Med.* 18, 883–891. doi: 10.1038/nm.2753

Pisitkun, T., Shen, R. F., and Knepper, M. A. (2004). Identification and proteomic profiling of exosomes in human urine. *Proc. Natl. Acad. Sci. U.S.A* 101, 13368–13373. doi: 10.1073/pnas.0403453101

Pospichalova, V., Svoboda, J., Dave, Z., Kotrbova, A., Kaiser, K., Klemova, D., et al. (2015). Simplified protocol for flow cytometry analysis of fluorescently labeled exosomes and microvesicles using dedicated flow cytometer. *J. Extracell. Vesicl.* 4:25530. doi: 10.3402/jev.v4.25530

Prendergast, E. N., de Souza Fonseca, M. A., Dezem, F. S., Lester, J., Karlan, B. Y., Noushmehr, H., et al. (2018). Optimizing exosomal RNA isolation for RNA-Seq analyses of archival sera specimens. *PLoS One* 13:e0196913. doi: 10.1371/journal.pone.0196913

Ragusa, M., Barbagallo, C., Statello, L., Caltabiano, R., Russo, A., Puzzo, L., et al. (2015). miRNA profiling in vitreous humor, vitreal exosomes and serum from uveal melanoma patients: Pathological and diagnostic implications. *Cancer Biol. Ther.* 16, 1387–1396. doi: 10.1080/15384047.2015.1046021

Roberts, C. J. (2007). Non-native protein aggregation kinetics. *Biotechnol. Bioeng.* 98, 927–938. doi: 10.1002/bit.21627

Rodrigues, G., Hoshino, A., Kenific, C. M., Matei, I. R., Steiner, L., Freitas, D., et al. (2019). Tumour exosomal CEMIP protein promotes cancer cell colonization in brain metastasis. *Nat. Cell Biol.* 21(11), 1403–1412. doi: 10.1038/s41556-019-0404-404

Schwartz, A., Gaigalas, A. K., Wang, L., Marti, G. E., Vogt, R. F., Fernandez-Repollet, E., et al. (2004). Formalization of the MESF unit of fluorescence intensity. *Cytomet. B Clin. Cytom.* 57, 1–6. doi: 10.1002/cyto.b.10066

Shah, R., Patel, T., and Freedman, J. E. (2018). Circulating Extracellular Vesicles in Human Disease. *N. Engl. J. Med.* 379, 958–966. doi: 10.1056/NEJMra1704286

Shelke, G. V., Lasser, C., Gho, Y. S., and Lotvall, J. (2014). Importance of exosome depletion protocols to eliminate functional and RNA-containing extracellular vesicles from fetal bovine serum. *J. Extracell. Vesicl.* 3:10.3402/jev.v3.24783. doi: 10.3402/jev.v3.24783

Shen, Y., Guo, D., Weng, L., Wang, S., Ma, Z., Yang, Y., et al. (2017). Tumor-derived exosomes educate dendritic cells to promote tumor metastasis via HSP72/HSP105-TLR2/TLR4 pathway. *OncoImmunology* 6:e1362527 doi: 10.1080/2162402x.2017.1362527

Skeie, J. M., Roybal, C. N., and Mahajan, V. B. (2015). Proteomic insight into the molecular function of the vitreous. *PLoS One* 10:e0127567. doi: 10.1371/journal.pone.0127567

Stahl, P. D., and Raposo, G. (2019). Extracellular Vesicles: Exosomes and Microvesicles, Integrators of Homeostasis. *Physiology* 34, 169–177. doi: 10.1152/physiol.00045.2018

Takov, K., Yellon, D. M., and Davidson, S. M. (2019). Comparison of small extracellular vesicles isolated from plasma by ultracentrifugation or size-exclusion chromatography: yield, purity and functional potential. *J. Extracell. Vesicl.* 8:1560809. doi: 10.1080/20013078.2018.1560809

Thery, C., Witwer, K. W., Aikawa, E., Alcaraz, M. J., Anderson, J. D., Andriantsitohaina, R., et al. (2018). Minimal information for studies of extracellular vesicles 2018 (MISEV2018): a position statement of the International Society for Extracellular Vesicles and update of the MISEV2014 guidelines. *J. Extracell. Vesicl.* 7:1535750.

Théry, C., Witwer, K. W., Aikawa, E., Alcaraz, M. J., Anderson, J. D., Andriantsitohaina, R., et al. (2019). Minimal information for studies of extracellular vesicles 2018 (MISEV2018): a position statement of the International Society for Extracellular Vesicles and update of the MISEV2014 guidelines. *J. Extracell. Vesicl.* 8:1535750. doi: 10.1080/20013078.2018.1535750

van der Pol, E., van Gemert, M. J., Sturk, A., Nieuwland, R., and van Leeuwen, T. G. (2012). Single vs. *swarm detection of microparticles and exosomes by flow cytometry*. *J. Thromb. Haemost.* 10, 919–930. doi: 10.1111/j.1538-7836.2012.04683.x

van der Vlist, E. J., Nolte-'t Hoen, E. N., Stoorvogel, W., Arkesteijn, G. J., and Wauben, M. H. (2012). Fluorescent labeling of nano-sized vesicles released by cells and subsequent quantitative and qualitative analysis by high-resolution flow cytometry. *Nat. Protoc.* 7, 1311–1326. doi: 10.1038/nprot.2012.065

Veremeyko, T., Yung, A. W. Y., Anthony, D. C., Strekalova, T., and Ponomarev, E. D. (2018). Early Growth Response Gene-2 Is Essential for M1 and M2 Macrophage Activation and Plasticity by Modulation of the Transcription Factor CEBPbeta. *Front. Immunol.* 9:2515. doi: 10.3389/fimmu.2018.02515

Wang, L., and Hoffman, R. A. (2017). Standardization, Calibration, and Control in Flow Cytometry. *Curr. Protoc. Cytom.* 79:1.3.1-1.3.27. doi: 10.1002/cpcy.14

Webber, J., and Clayton, A. (2013). How pure are your vesicles?. *J. Extracell. Vesicl.* 2:10.3402/jev.v2i0.19861. doi: 10.3402/jev.v2i0.19861

Willms, E., Cabanas, C., Mager, I., Wood, M. J. A., and Vader, P. (2018). Extracellular Vesicle Heterogeneity: Subpopulations, Isolation Techniques, and Diverse Functions in Cancer Progression. *Front. Immunol.* 9:738. doi: 10.3389/fimmu.2018.00738

Willms, E., Johansson, H. J., Mäger, I., Lee, Y., Blomberg, K. E. M., Sadik, M., et al. (2016). Cells release subpopulations of exosomes with distinct molecular and biological properties. *Sci. Rep.* 6:22519. doi: 10.1038/srep22519

Wu, X., Zhu, L., and Ma, P. C. (2018). Next-Generation Novel Noninvasive Cancer Molecular Diagnostics Platforms Beyond Tissues. *Am. Soc. Clin. Oncol. Educ. Book* 38, 964–977. doi: 10.1200/EDBK_199767

Zhang, H., Freitas, D., Kim, H. S., Fabijanic, K., Li, Z., Chen, H., et al. (2018). Identification of distinct nanoparticles and subsets of extracellular vesicles by asymmetric flow field-flow fractionation. *Nat. Cell Biol.* 20, 332–343. doi: 10.1038/s41556-018-0040-44

Zhao, Y., Weber, S. R., Lease, J., Russo, M., Siedlecki, C. A., Xu, L. C., et al. (2018). Liquid Biopsy of Vitreous Reveals an Abundant Vesicle Population Consistent With the Size and Morphology of Exosomes. *Transl. Vis. Sci. Technol.* 7:6. doi: 10.1167/tvst.7.3.6

Conflict of Interest: The authors declare that the research was conducted in the absence of any commercial or financial relationships that could be construed as a potential conflict of interest.

Copyright © 2020 Maia, Batista, Couto, Gregório, Bodo, Elzanowska, Strano Moraes and Costa-Silva. This is an open-access article distributed under the terms of the Creative Commons Attribution License (CC BY). The use, distribution or reproduction in other forums is permitted, provided the original author(s) and the copyright owner(s) are credited and that the original publication in this journal is cited, in accordance with accepted academic practice. No use, distribution or reproduction is permitted which does not comply with these terms.

frontiers in Oncology

ORIGINAL RESEARCH
published: 06 November 2020
doi: 10.3389/fonc.2020.601085

Short-Term Circulating Tumor Cell Dynamics in Mouse Xenograft Models and Implications for Liquid Biopsy

Amber L. Williams[1], *Jessica E. Fitzgerald*[1], *Fernando Ivich*[1], *Eduardo D. Sontag*[1,2,3] *and Mark Niedre*[1]*

[1] Department of Bioengineering, Northeastern University, Boston, MA, United States, [2] Department of Electrical and Computer Engineering, Northeastern University, Boston, MA, United States, [3] Laboratory of Systems Pharmacology, Harvard Medical School, Boston, MA, United States

Motivation: Circulating tumor cells (CTCs) are widely studied using liquid biopsy methods that analyze fractionally-small peripheral blood (PB) samples. However, little is known about natural fluctuations in CTC numbers that may occur over short timescales *in vivo*, and how these may affect detection and enumeration of rare CTCs from small blood samples.

Methods: We recently developed an optical instrument called "diffuse *in vivo* flow cytometry" (DiFC) that uniquely allows continuous, non-invasive counting of rare, green fluorescent protein expressing CTCs in large blood vessels in mice. Here, we used DiFC to study short-term changes in CTC numbers in multiple myeloma and Lewis lung carcinoma xenograft models. We analyzed CTC detections in over 100 h of DiFC data, and considered intervals corresponding to approximately 1%, 5%, 10%, and 20% of the PB volume. In addition, we analyzed changes in CTC numbers over 24 h (diurnal) periods.

Results: For rare CTCs (fewer than 1 CTC per ml of blood), the use of short DiFC intervals (corresponding to small PB samples) frequently resulted in no detections. For more abundant CTCs, CTC numbers frequently varied by an order of magnitude or more over the time-scales considered. This variance in CTC detections far exceeded that expected by Poisson statistics or by instrument variability. Rather, the data were consistent with significant changes in mean numbers of CTCs on the timescales of minutes and hours.

Conclusions: The observed temporal changes can be explained by known properties of CTCs, namely, the continuous shedding of CTCs from tumors and the short half-life of CTCs in blood. It follows that the number of cells in a blood sample are strongly impacted by the timing of the draw. The issue is likely to be compounded for multicellular CTC clusters or specific CTC subtypes, which are even more rare than single CTCs. However, we show that enumeration can in principle be improved by averaging multiple samples, analysis of larger volumes, or development of methods for enumeration of CTCs directly *in vivo*.

Keywords: circulating tumor cells, dynamics, optical devices, fluorescence, liquid biopsy, flow cytometry

OPEN ACCESS

Edited by:
Catherine Alix-Panabieres, Centre Hospitalier Universitaire de Montpellier, France

Reviewed by:
Talib Hassan Ali, Thi Qar University, Iraq
Francesca Benedetti, University of Maryland, United States

***Correspondence:**
Mark Niedre
m.niedre@neu.edu

Specialty section:
This article was submitted to Molecular and Cellular Oncology, a section of the journal Frontiers in Oncology

Received: *31 August 2020*
Accepted: *14 October 2020*
Published: *06 November 2020*

Citation:
Williams AL, Fitzgerald JE, Ivich F, Sontag ED and Niedre M (2020) Short-Term Circulating Tumor Cell Dynamics in Mouse Xenograft Models and Implications for Liquid Biopsy. Front. Oncol. 10:601085. doi: 10.3389/fonc.2020.601085

INTRODUCTION

Circulating tumor cells (CTCs) are of great interest in cancer research because of their importance in hematogenous metastasis. CTCs shed from the primary tumor into the peripheral blood (PB), and a small fraction may form metastases. It is these metastases that are extremely difficult to control clinically and eventually result in the majority of cancer-related deaths (1, 2). Nearly all CTC clinical and pre-clinical research involves "liquid biopsy", wherein CTCs are isolated from fractionally small PB samples (3, 4). CTCs are extremely rare, and fewer than 1 CTC per ml of PB is associated with reduced overall survival for major cancers such as breast (5), colorectal (6), and prostate (7). Although there have been a number of large clinical studies in the last decade, the clinical value of CTC enumeration by liquid biopsy remains as yet unclear (8–10). One major challenge is CTC heterogeneity, which has driven major efforts toward development next-generation liquid biopsy methods that permit genotypic and phenotypic characterization of single CTCs (11, 12).

A less-studied problem is that of *temporal* heterogeneity of CTCs and PB sampling, by which we mean the short-term fluctuations in CTC numbers in PB that may be largely invisible to liquid biopsy. Liquid biopsy implicitly assumes that the number of CTCs in a blood sample is representative of the entire PB volume (PBV). Previous work has shown that this assumption may be statistically dubious in light of the rarity of CTCs and the fractionally small volume of samples (13, 14). With respect to the latter, in CellSearch (for example), 7.5-ml PB samples are analyzed which corresponds to about 0.015% of the ~5 L human PBV (6). Other experimental microfluidic platforms analyze similarly small samples in the range of 2–10 ml (0.004%–0.02% PBV) (15–17). With respect to pre-clinical mouse studies PB collection is limited to 200 µl every two weeks for non-terminal experiments (without fluid replacement). This is equivalent to about 10% of the ~1.5- to 2-ml mouse PBV (18, 19).

The small number of previously-published theoretical treatments of this problem also assumes that CTC detection (sampling) statistics should follow a Poisson distribution (13, 20, 21). This further implicitly assumes that CTCs are well-mixed in blood, and that the average number of CTCs in circulation does not change significantly over the minutes or hours surrounding the blood draw. However, there is relatively little experimental pre-clinical or clinical data to support these assumptions (7, 20, 22, 23). The relative infrequency and small PBV of blood draws are major challenges. In small animal models, the rarity of CTCs in mouse models also means that the entire PBV often must be drawn and analyzed. Such terminal experiments preclude serial study in the same mouse. In summary, little is currently known about short-term fluctuations in CTC numbers *in vivo*.

"*In vivo* flow cytometry" (IVFC) is a general term for optical instrumentation designed to detect and enumerate circulating cells directly *in vivo*, most often using either fluorescence or photoacoustic contrast (19, 24). We recently developed "diffuse *in vivo* flow cytometry" (DiFC) specifically for enumeration of rare green fluorescent protein (GFP)-expressing CTCs in mouse models of metastasis (25–29). DIFC uses diffuse light to non-invasively and continuously interrogate PB flowing in large, deeply-seated vessels. We recently used DiFC to monitor CTC dissemination in multiple myeloma (MM) and Lewis lung carcinoma (LLC) (27, 29) mouse xenograft models. We showed that DiFC permitted longitudinal study of CTCs and CTC multi-cellular clusters (CTCCs) in individual mice at burdens below 1 CTC per ml of PB.

In our previous work, we used DiFC to study only the *time-averaged* (mean) number of CTCs in circulation on a given day, but did not consider the *short-term* dynamics of CTC detections over timescales of minutes or hours. These short-term variations are measured by DiFC and therefore potentially provide unique insights into temporal dynamics of CTCs *in vivo*. In this work, we analyzed more than 100 h of DiFC data taken in mice, and considered sample intervals equivalent to approximately 1%, 5%, 10%, and 20% of the PBV. We analyzed how CTC numbers fluctuated over the timescales of minutes and hours. As we show, CTC numbers were far from steady state, and exhibited variability far exceeding that expected by Poisson statistics or DiFC operator variability. As we show, this suggests that CTCs are not well-mixed in PB in general, and that the mean number of CTCs may change significantly over relatively short timescales. This can be explained by the short half-life of CTCs in circulation coupled with intermittent shedding behavior of CTCs. It also follows that the number of cells in a blood sample and the subsequent CTC enumeration accuracy may be strongly impacted by the timing of the draw. This data is also generally consistent with the small number of previously published preclinical and clinical studies on this issue. However, our analysis also shows that accuracy may be markedly improved by analysis of larger blood volumes, averaging of multiple blood samples, or continuous *in vivo* monitoring.

MATERIALS AND METHODS

DiFC Instrument and Signal Processing

The DiFC instrument (**Figure 1A**) and data processing algorithms were described in detail previously (26, 27, 29). Briefly, two specially designed fiber-optic probes (**Figure 1B**) are placed in-line along a major blood vessel (in this case, the ventral caudal bundle in the tail) as shown in **Figure 1C**. The probes have integrated lenses and filters that allow efficient fluorescent light collection and rejection of non-specific tissue autofluorescence. GFP-expressing CTCs are detected by laser-induced fluorescence as they pass through the DiFC field of view (**Figure 1D**, also see **Supplementary Materials and Methods 1.1**). DiFC therefore permits detection of moving CTCs in large blood vessels 1-2 mm deep in tissue. Analysis of peak amplitude, width, and order of detection between the two channels allows us to discriminate arterial from venous flow directions (26).

Detections of CTCs during a DiFC scan may be visualized using temporal raster plots, where each vertical black line represents a detection of a CTC (**Figure 1E**). Example DiFC data sets from our previous studies in an LLC sub-cutaneous (s.c.) flank tumor model (**Figures 1F–H**) and an MM disseminated xenograft model (**Figures 1I–K**) are shown (27, 29). As we discuss in more detail below, these two models provide complementary cases for analysis of CTC dynamics, namely, i) very rare CTCs disseminating from a single

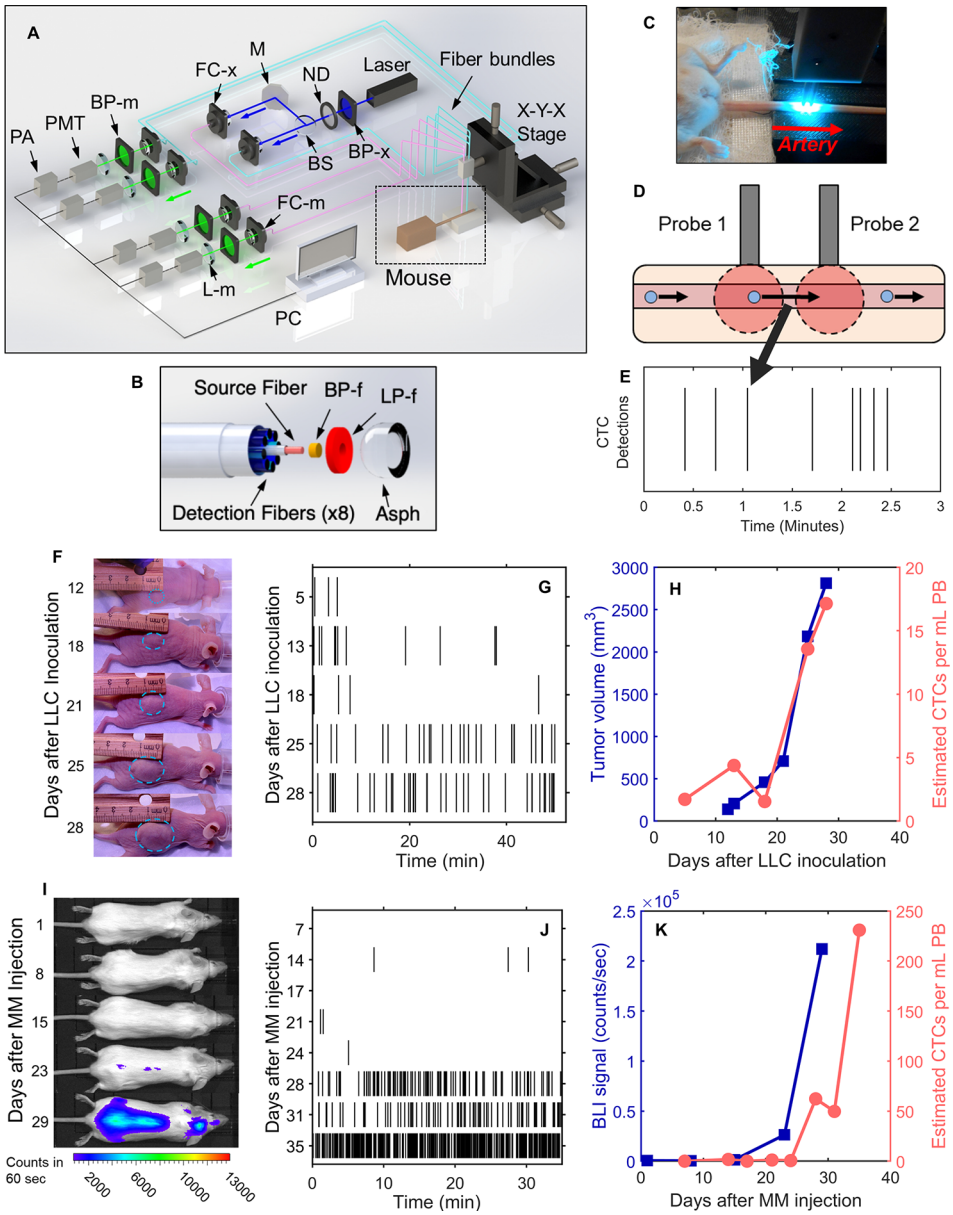

FIGURE 1 | DiFC allows non-invasive *in vivo* enumeration of rare circulating tumor cells (CTCs) in mice without drawing blood samples. **(A)** The DiFC instrument was described in detail previously (27, 29). The specially designed DiFC probes use two specially designed **(B)** optical fiber bundles that are placed on the **(C)** skin surface over the ventral side of the tail of a mouse. **(D)** When GFP-expressing CTCs pass through the DiFC field of view, the GFP is excited and the resulting fluorescent emission is detected by the probes. **(E)** The emission is identified as a CTC detection in time, which is visualized as a vertical black line on a raster plot. **(F–H)** A representative data set collected from an s.c. LLC-tumor bearing mouse. **(F)** Photographs of LLC tumor growth. **(G)** DiFC raster of CTC detections during tumor growth. **(H)** The tumor volume (blue squares) and mean rate of CTC detections (pink circles) over time. **(I–K)** Example MM-DXM mouse data. **(I)** Bioluminescence (BLI) images during MM growth. **(J)** DiFC raster plots of MM CTC detections. **(K)** BLI signal (blue squares) and mean rate of CTC detections (pink circles) over time. Panels **(A, B)** reproduced with permission from Patil et al. (27).

solid tumor (LLC) and, ii) more abundant CTCs disseminating from tumor distributed throughout the skeleton (MM).

We conservatively estimated that DiFC samples approximately 50 µl of PB per minute (27). As such, DiFC allows sampling of the complete ~1.5–2 ml mouse PBV (potentially more than once) with single CTC sensitivity in a single, 30- to 60-min scan. Central to our analysis here is the assumption that the CTC count in a specific DiFC *time interval* is equivalent to the number of CTCs that would be counted in a *blood sample* of corresponding volume drawn from the same blood vessel at that time. For example, assuming that a mouse has 2 ml of PB, a 24 s DiFC scan interval is equivalent to approximately 20 µl of blood, or about 1% of the PBV. We note

this percentage is approximate and is intended to give a physical interpretation of DiFC scan intervals to the reader. Moreover, the percentage itself is not used in any calculations so that if the true PBV were slightly higher or lower than 2 ml it would have no impact on results presented here. Mice used in each model were also approximately the same weight (~25 g), so that this percentage would likewise be approximately consistent between mice. In this work, we considered all 24 s, 2 min, 4 min and 8 min DiFC scan intervals, equivalent to 20, 100, 200, and 400 µl, or approximately 1%, 5%, 10%, and 20% of the mouse PBV.

DiFC Data Sets

In this work, we analyzed five data sets as follows:

Lewis Lung Carcinoma (LLC) Metastasis Model

We re-analyzed previously reported DiFC data measured in s.c. Lewis lung carcinoma tumor bearing mice (29). In that study, we considered only the mean CTC numbers on each day but not short-term fluctuations as we do here. Briefly, 10^6 LLC cells expressing GFP (LL/2.GFP.Luc) cells were injected s.c. in the rear flank of 42 nude mice and allowed to grow for up to 3 weeks. DiFC was performed for 40- to 50-min, at least once per week. CTCs were observed in circulation as early as 5 days after inoculation, and there was a general increase in CTC detection rate with increasing primary tumor volume (**Figures 1F–H**). However, significant inter-mouse heterogeneity was observed in terms of both CTC numbers and lung metastasis formation. We used DiFC scans from this study where at least one CTC was detected (N = 102 DiFC scans). CTC detection rates ranged from 0.019 to 1.05 CTCs per min, which is equivalent to 0.38 to 21.1 CTCs per ml of PB based on the DiFC sampling rate. We subsequently refer to these data as the "*LLC dataset*" below. A subset of 18 representative raster plots from this data set is shown in **Supplementary Figure 1**.

Multiple Myeloma (MM) Disseminated Xenograft Model (DXM)

We re-analyzed our previously reported DiFC data from an MM disseminated xenograft mouse model (DXM) (27). Briefly, 5×10^6 GFP-expressing MM.1S.GFP.Luc cells were injected intravenously (*i.v.*) via the tail vein of 10 SCID mice. After injection MM cells rapidly homed to the bone marrow niche, wherein they steadily proliferated and eventually re-entered circulation by the third week. DiFC was performed for 35 min twice weekly for up to 5 weeks. CTCs were relatively abundant (compared to the LLC model) and increased monotonically with bulk MM growth over time. Example data for an MM-DXM mouse is shown in **Figures 1I–K**. In the analysis here, we used data sets from this study where DiFC detection rates exceeded 0.5 CTCs per minute only (N = 18), and ranged from 0.6 to 19.6 CTCs per minute, which is equivalent to 12 to 392 CTCs per ml of PB. We refer to this as the "*MM 35-min dataset*" below. The complete set of DiFC raster plots are shown in **Supplementary Figure 2**.

Twenty-Four-Hour DiFC Measurements in MM-DXM Mice

We also performed new experiments in MM-DXM mice. All mice were handled in accordance with Northeastern University's Institutional Animal Care and Use Committee (IACUC) policies on animal care. Animal experiments were carried out under Northeastern University IACUC protocol #15-0728R. All experiments and methods were performed with an approval from and in accordance with relevant guidelines and regulations of Northeastern University IACUC.

We performed *i.v.* injection of 5×10^6 MM.1S.GFP.Luc cells in six, 8-week-old male severe combined immunodeficient SCID/Bg mice (Charles River) as in the MM-DXM model above (27). We performed cycles of four, 50-min DiFC scans over a 24-h period, beginning 4 weeks after inoculation. Institutional mouse housing followed a 7 am–to–7 pm light, and 7 pm–to–7 am dark cycle. To minimize possible bias in the start time for each cycle, the first DiFC scan was performed at either 7 am (N = 7 data sets) or 7 pm (N = 7 data sets). DiFC scans were performed by one of three human operators, and the first operator was also randomized. CTC detection rates for these data ranged from 0 to 42 CTCs per minute, equivalent to 0 to 840 CTCs per ml of blood. We refer to these as the "*MM 24-h dataset*" below. The complete set of 24-h DiFC measurements is shown in **Supplementary Figure 3**.

Since 24-h measurements required three human operators performing four alignments (physical repositioning) of the DiFC probe on the mouse tail in 24-h periods, we also measured the inherent inter- and intra-operator variability in DiFC measurements (for details see **Supplementary Materials and Methods 1.2**). These data are referred to as "*1-operator-with-reposition dataset*" (N = 7 data sets) and "2-*operators-with-reposition dataset*" (N = 6 data sets) below.

Limb-Mimicking Optical Phantom With Fluorescent Microspheres

We also used a limb-mimicking optical flow phantom model as we have previously (27). We used Dragon Green fluorescence level 5 (DG5) reference microspheres (Cat. DG06M, Bangs Laboratories, Inc., Fishers, IN) suspended in PBS at concentrations of 200 or 400 microspheres per ml pumped through the phantom at linear flow speeds of 15, 30, or 60 mm/s. We performed DiFC at the six concentration-speed combinations in triplicate for 35 min in each case (N = 18). Microsphere suspensions were first sonicated to prevent aggregation and clumping and then mixed well to produce as homogenous a suspension as possible. In principle, this should yield DiFC detections that follow Poisson distributions. More details on these experiments are provided in **Supplementary Materials and Methods 1.3**.

Simulated DiFC Data

We also simulated Poisson-distributed sequences of DiFC data *in silico*. We generated 54, 35-min data sets using custom written code in Matlab (The Mathworks Inc., Natick, MA) with mean rates of detection in the same range as those measured in MM DXM mice. To compare MM mouse data to processes that are not described by a single Poisson, we also generated 35-min Poisson simulations where the mean CTC detection rate increased by a factor of two halfway through the scan, i.e., Poisson detections with mean rate λ_1 in the first 17.5 min and $\lambda_2 = 2\lambda_1$ in the second 17.5 min. We generated 54 such data sets. We also simulated DiFC data sets of the sum of two concurrent

(simultaneous or merged) 35-min, Poisson-distributed sequences of mean λ_1 and $\lambda_2 = 2\lambda_1$. More details are provided in **Supplementary Materials and Methods 1.4**.

RESULTS

For Rare CTCs Small Samples Frequently Resulted in No CTC Detections

We re-analyzed previously reported DiFC data from an LLC s.c. flank metastasis model (29). In this model, CTCs were rare throughout tumor growth. Specifically, in 102 DiFC scans, CTC count rates corresponded to approximately 0.38 to 21.1 CTCs per ml of PB. Representative DiFC raster plots illustrating the range of the data set are shown in **Figures 2A–C**. Eighteen additional example data sets are also shown in **Supplementary Figure 1**.

We considered the number of CTCs detected in 24-s, 2-min, 4-min, and-8 min intervals during the DiFC scans. As above, these intervals were equivalent to approximately 20, 100, 200, and 400 µl of PB, or about 1%, 5%, 10%, and 20% of the mouse PBV. Histograms of the number of CTC detections (for the data shown in **Figures 2A–C**) are shown for 24 s (**Figures 2D–F**), 2 min (**Figures 2G–I**), 4 min (**Figures 2J–L**), and 8 min (**Figures 2M–O**) intervals, respectively. These data show that the probability that at least one CTC was detected in a small temporal sample was in general very low. For example, considering a 1% PBV sample size and 0.4 CTCs per mL, no CTCs were detected in 99% of equivalent blood samples (intervals) over the entire scan. Even for relatively high CTC burdens (14 CTCs per ml; **Figure 2C**), 1% PBV sample sizes yielded zero CTC detections 79% of the time (**Figure 2F**). As would be expected, this probability improved significantly when larger time intervals (equivalent blood samples) were considered. For example, for a CTC burden of 14 CTCs per ml and an equivalent 20% PBV sample (**Figure 2O**), at least one CTC was detected 100% of the time.

Visualizing the data another way, the fraction of intervals for which at least 1 CTC was detected for all DiFC scans in the LLC dataset are shown in **Figures 2P–S**. In combination, these data underscore the fact that analysis of fractionally small blood samples (1%–5% PBV) frequently resulted in detection of no CTCs, even though CTCs were present in the blood in all cases. Hence these data provide direct experimental validation of the notion that "more blood is better" for detection of CTCs (14). Analysis of larger blood samples would further improve this: for example, analysis of 30% of the PBV would usually (> 50% of possible PBV samples) result in detection of at least 1 CTC in half of the LLC data sets here.

CTC Counts in Small Samples Were Generally Quantitively Inaccurate

We also considered CTC enumeration accuracy from fractionally small blood samples. To study this, we used DiFC data measured in MM xenograft mice ("*MM 35-min dataset*"), (27) where CTCs were

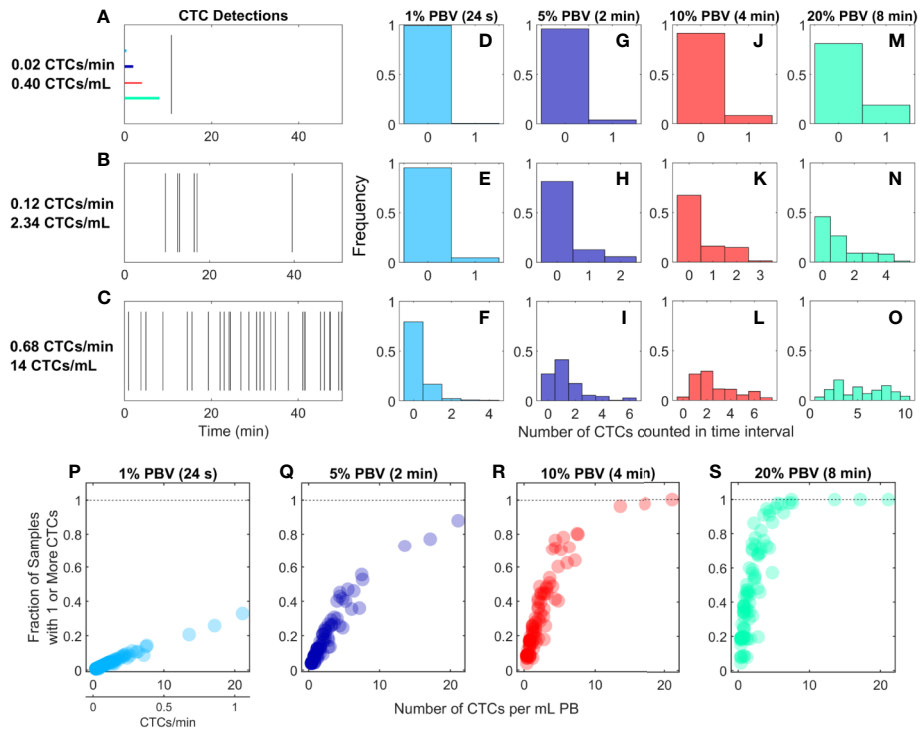

FIGURE 2 | For rare CTCs, small blood samples frequently resulted in no DiFC detections. **(A–C)** Representative DiFC raster plots of LLC-CTC detections for average count rates of **(A)** 0.4, **(B)** 2.3, and **(C)** 14 CTCs per ml PB. Colored horizontal lines show the relative length of approximately 1% (24 s), 5% (2 min), 10% (4 min), and 20% (8 min) intervals (blood sample size). Distributions of CTC counts in detections intervals are shown for **(D–F)** 1% PBV, **(G–I)** 5%, **(J–L)** 10%, and **(M–O)** 20% PBV DiFC scan intervals. The fraction of intervals where 1 or more CTCs were detected for **(P)** 1%, **(Q)** 5%, **(R)** 10%, and **(S)** 20% PBV scan intervals.

more abundant than in the LLC tumor model above. A representative 35-min DiFC raster plot from an MM xenograft mouse, measured 31 days after engraftment of MM cells is shown in **Figure 3A**. (The full set of 18 DiFC scans from this data set is shown in **Supplementary Figure 2**.) The number of CTCs counted in sliding ~1%, 5%, 10%, and 20% PBV intervals are shown in **Figures 3B–E**, respectively. We also calculated the mean number of CTCs over the entire DiFC scan (black horizontal line in each case). By inspection, CTC counts varied significantly during the scan, with periods of relatively high and low detection rates.

These data illustrate the large range of CTC detection rates measured over 35-min scans. For example, considering a 5% PBV interval (which is typical volume for a mouse blood collection experiment), equivalent detection rates ranged from 0 to 38 CTCs per sample. In other words, if PB was collected from this blood vessel, 100-µl samples drawn at different times (separated by just a few minutes) would have yielded order-of-magnitude or more differences in CTC numbers.

The histograms of these data (i.e., the number of CTC detections for all possible 1%, 5%, 10%, and 20% PBV intervals) are shown in **Figures 3F–I**, along with the mean number of CTCs detected over the full scan (vertical black lines). We compared the measured distributions to Poisson distributions which, as noted above, are frequently assumed for liquid biopsy of PB (13, 20, 21). These are indicated by the black dotted curves in **Figures 3F–I**. By inspection, the DiFC-measured distribution of count rates did not appear to follow the Poisson distribution, particularly for larger (2–8 min) equivalent blood samples. The implications of this observation are discussed in more detail below.

We also computed the "deviation from the scan mean" (DFSM) for each observation (blood sample):

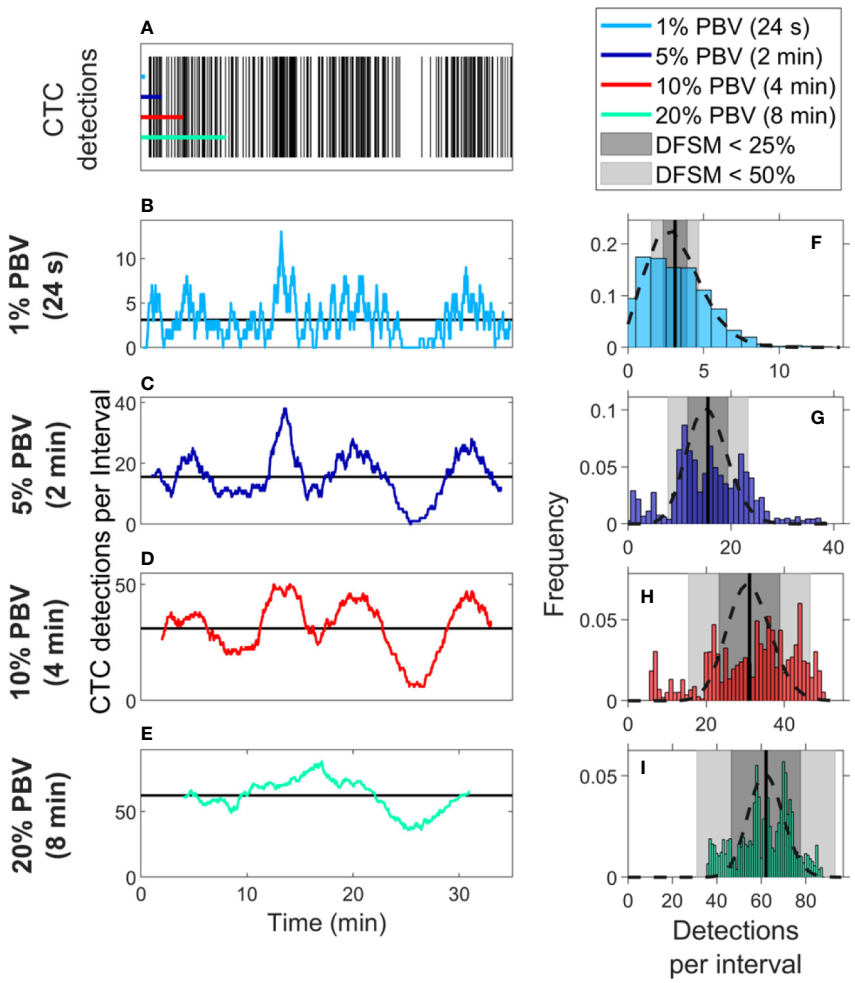

FIGURE 3 | Significant temporal fluctuation in CTC numbers were observed over the timescale of minutes. **(A)** Representative DiFC raster plot measured from a MM DXM bearing mouse. Colored horizontal lines show the length of each time interval (blood sample size). The number of CTCs counted in sliding **(B)** 1%, **(C)** 5%, **(D)** 10%, and **(E)** 20% equivalent PBV intervals are shown. Black horizontal lines identify the scan mean number of CTCs per interval. **(F–I)** The corresponding distributions of CTC counts for each equivalent PBV are shown. Black dashed lines indicate the distributions that would be expected from Poisson statistics. Black vertical lines show the mean number of CTCs. Gray shading denotes the range of DFSM < 25% (light gray) and < 50% (dark gray).

$$DFSM_i = \frac{|C_i - \lambda|}{\lambda} * 100\,\% \quad (1)$$

where C_i is the number of CTCs in the i^{th} equivalent sample and λ is the mean number of CTC detections over the full scan for each sample size. The cumulative fraction of blood samples within 0-100% DFSM for the data in **Figures 3F–I** are shown in **Figure 4A**. The cumulative fraction of samples for Poisson distributions of the same mean are also shown (dotted lines, same colors), again suggesting that experimental data diverged substantially from the Poisson behavior.

For example, these data can be interpreted as, "39% of randomly selected 5% PBV blood samples would yield a CTC count within 25% of the scan mean, whereas Poisson statistics predict that this number should be 69%". It should also be noted that the large disagreement between expected Poisson behavior and measured behavior occurred in about half of the data sets. A representative plot from another DiFC scan where closer agreement was observed is shown in **Figure 4B**.

We next considered the fraction of intervals where the DFSM was equal to or less than 25% and 50% for all sample sizes in the complete "*MM 35-min dataset*". These data are summarized in **Figures 4C, D**. Our use of 25% and 50% DFSM thresholds were selected since they are illustrative of sufficiently large error to affect prognostic classification—for example, in determining whether a sample has 4 or 5 CTCs (breast and prostate cancer) or 2 or 3 CTCs (colorectal cancer) (6–8).

Taken together, these data show that quantitative estimation of CTC numbers from single samples in mice is extremely challenging. For example, for 5% PBV samples, the median probability for all scans of randomly obtaining a CTC count within 25% of the scan mean was only 41.9% (**Figure 4C**). Likewise, the probability of obtaining a CTC count within 50% of the mean was 72.1% (**Figure 4D**). All else being equal, use of larger blood sample volumes yielded higher probability of obtaining accurate count than smaller samples (14).

There Were Significant Variations in CTC Detection Rates in 24-h Periods

We also studied the 24-h variability in CTC detection rates in MM xenograft mice by performing four, 50-min DiFC scans over 24-h periods ("*MM 24-h dataset*"). Half of the data sets began at

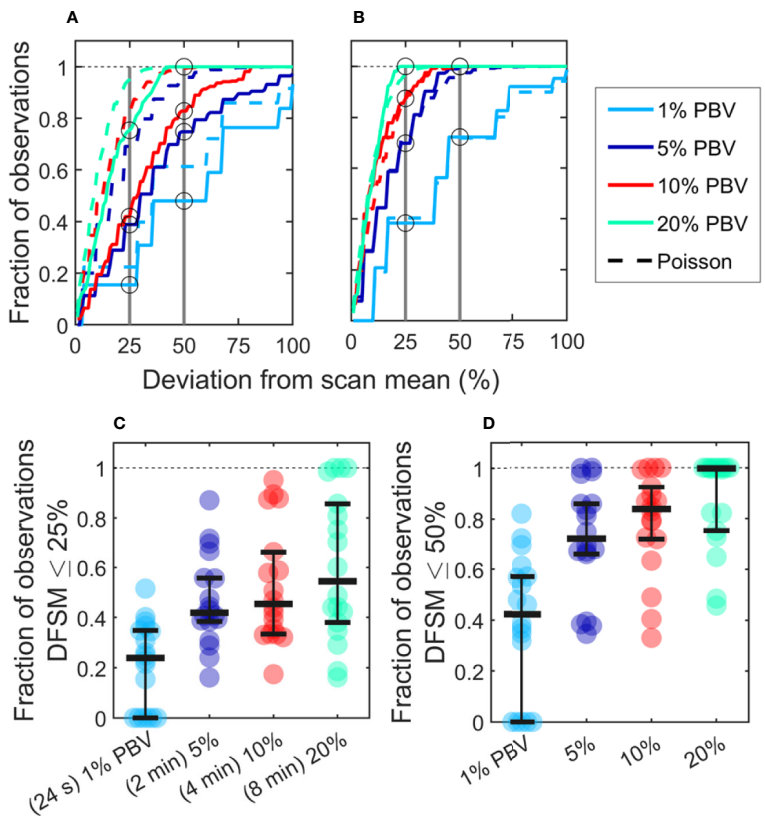

FIGURE 4 | CTC counts in small equivalent blood samples were generally quantitatively inaccurate. **(A)** Analysis of a representative DiFC data set measured in an MM xenograft mouse, showing the impact of the sample size on the percentage deviation of CTC counts in an interval from the scan mean (DFSM; see text for details). The fraction of observations within a given DFSM is shown in each case. Dotted lines indicate the expected distribution based on Poisson statistics. **(B)** A second example data set that more closely followed the expected Poisson behavior. **(C)** The fraction of equivalent blood samples with CTC counts within 25% of the scan mean (DFSM < 25%) for all 18 DiFC scans in the MM 35-min dataset. **(D)** The fraction of samples within 50% of scan mean (DFSM < 50%). Horizontal bars indicate the median, and first and third quartile for each blood sample size.

7PM, and half began at 7 am to rule out the possibility that the start time could affect the measurements. In addition, the starting DiFC human operator (one of 3) was randomized. Two representative DiFC data sets from 24-h sessions are shown in **Figures 5A–C**. CTC detection rates in moving 2 min (5% PBV) intervals are shown in **Figures 5A, B**. The 50-min average of each DiFC scan is also shown (dotted horizontal lines), as well as the average over the 24-h period (solid horizontal lines). The mean count rates over the four DiFC scans for both mice are summarized for clarity in **Figure 5C**. As shown, the average measured detection rates changed by more than an order of magnitude depending on the time of day. The complete set of 14, 24-h DiFC scan sets from this data set are shown in **Supplementary Figure 3**.

To better quantify the 24-h variability, the ratios of the maximum-to-minimum CTC detection rates for each scan are shown in the first column of **Figure 5D**. As shown, this varied from 2.5 to 152. We note that we did not observe any specific circadian pattern to the data as others have reported for MM (23). Rather, the CTC count rates were seemingly randomly higher or lower at different times of days.

This 24-h variability was also greater than the fluctuations observed over a short timescale (as in **Figure 3**). To show this, DiFC scans from the "*MM 35-min dataset*" were each divided into the first 15 and last 15 min (separated by 5 min), and the same maximum-to-minimum count rates ratios were calculated. These ranged from 1.05 to 4.4 (**Figure 5D**, column 2).

We note that 24-h measurements required up to three human operators performing four alignments (physical repositioning) of the DiFC probe on the mouse tail in each 24-h dataset. To rule out the possibility that the observed variability in CTC detection rates (**Figure 5C**) was due to repositioning of the DiFC probe on the skin surface between scans (which could affect the collection efficiency of the system) and not biological fluctuations, we tested

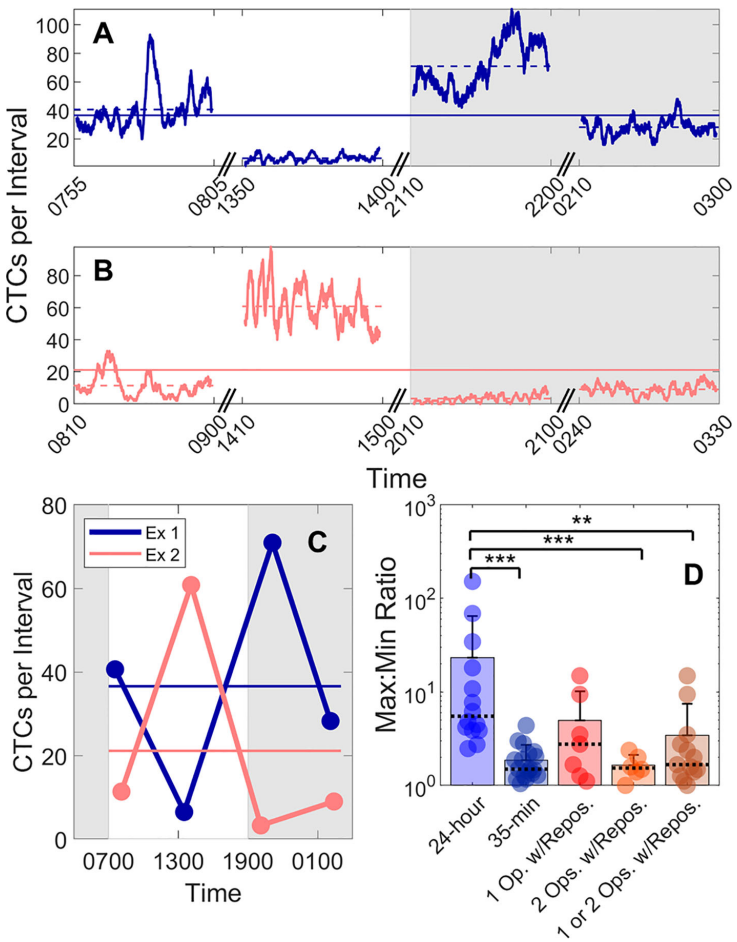

FIGURE 5 | Large fluctuations in CTC numbers were observed over 24-h cycles. **(A, B)** Example DiFC measurements taken over 24 h in two MM-bearing mice. The number of CTCs counted in 2 min (5% PBV) sliding intervals is shown. The solid horizontal lines in each figure show the 24-h mean number of CTCs per 2 min interval, and the dashed horizontal lines show the local mean of the 50-min DiFC scan. Dark hours are shaded gray. **(C)** The mean DiFC count rates over the 24-h period are shown. **(D)** Ratios of maximum-to-minimum DiFC count rates are shown for MM 24-h, MM 35-min (no repositioning), 1-operator-with-reposition, and 2-operators-with-reposition data sets. Bars represent the mean values with standard deviation error bars and dotted lines to identify the median values. Note the logarithmic y-axis. Kolmogorov-Smirnov test significance indicated by ** (p-value < 0.01) and *** (p-value < 0.001).

the intra-operator reproducibility of DiFC count rates. To do this, we tested the intra- ("*1-operator-with-reposition*") and inter-operator ("*2-operators-with-reposition*") reproducibility of DiFC count rates. The corresponding maximum-to-minimum DiFC count rate ratios ranged from 1.1 to 14.9 (**Figure 5D** column 3) and 1.0 to 2.4 (**Figure 5D** column 4), respectively.

Statistical analysis showed that the variability in mean DiFC count rate measured over 24 h was much larger than expected from either intra- or inter-operator repositioning variability. Specifically, when comparing *MM 24-h* data (N = 14) to *MM 35-min* (N = 18), *1-operator-with-reposition* (N = 7), *2-operators-with-reposition* (N = 6), and all reposition data (N = 13) by a two-sided, two-sample Kolmogorov-Smirnov test (MATLAB version 9.6), p-values were $p < 0.001$, $p = 0.058$, $p < 0.001$, and $p < 0.01$, respectively. In addition, the intra- and inter-operator variability, as well as short-term fluctuations were not significantly different from each other (all $p > 0.15$).

Variability in CTC Detection Rates *In Vivo* Was Higher Than Predicted by Poisson Statistics

Because CTC detection is a random process, some inherent measurement variability is expected. However, as already noted the variability observed in DiFC data *in vivo* frequently exceeded that expected by Poisson statistics. To better study this, we plotted the variance of the CTC counts per interval against the mean. This was repeated for 24 s, 2 min, 4 min, and 8 min intervals. Since the mean and variance of an ideal Poisson distribution are equal, if Poisson distributed CTC measurements should fall approximately along the 1:1 curve. However, as shown in **Figures 6A–D**, the measurement variance for the "*MM 35-min dataset*" was larger than the mean for about half the measurements. This deviation was significantly larger when considering the "*MM 24-h dataset*", where fluctuations were observed over 24-h periods (**Figures 6E–H**). Linear fits with a fixed intercept at zero resulted in slopes larger than 1, demonstrating that the variance generally exceed the mean.

We note that in computing the mean and variances we analyzed all possible intervals in the DiFC scans (a "sliding window"). While this approach yielded significant overlap (non-independence) between measurements, we showed explicitly that when large numbers of overlapping intervals are considered the variance converges to the non-overlapping case (see **Supplementary Materials and Methods 1.5**).

To rule out the possibility that this deviation from Poisson behavior was an artifact of DiFC measurement or data analysis methods, we repeated the analysis on *in silico* simulated data sets, where detections were Poisson distributed as shown in **Figures 6I–L**. We also performed DiFC measurements in a limb-mimicking optical flow phantom with suspensions of fluorescent microspheres that were well-mixed as shown in **Figures 6M–P**. In both cases, the variance more closely agreed with the scan mean, and linear fitting yielded slopes that were generally close to 1. The slightly larger slopes observed in the phantom data likely resulted from microspheres settling in the syringe pump over the course of the DiFC scans, i.e., the spheres were not perfectly mixed.

The physical interpretation of these data is that the mean number of CTCs in the PB fluctuated significantly (i.e., was not in quasi-steady-state) over the time-scale of the DiFC experiments. To further test this, we simulated Poisson-distributed data sets where the mean number of CTCs doubled halfway through the scan (**Figures 6Q–T**). These data more closely resemble the *in vivo* experimental data (**Figures 6A–H**). It is also worth noting that the *in vivo* DiFC data is *not* consistent with multiple *concurrent* Poisson processes. As shown in **Figures 6U–X** (and by the properties of Poisson statistics) this summation would exhibit Poisson behavior.

The implications of these data are discussed in more detail below. However, in practice, this means simply that the expected variability in CTC numbers in a single, randomly-drawn blood sample is actually much worse than would be expected by Poisson statistics as others have assumed (13, 20).

Quantification of CTCs Can Be Improved by Averaging Multiple Samples

Previous studies have shown that analysis of larger blood samples provides more accurate quantification of CTCs than smaller blood samples (14). The large temporal variability and deviation from Poisson behavior observed in our data further predicts that averaging multiple small blood samples over 24-h periods should yield more quantitatively accurate estimates (versus the average) than a single, larger blood sample. As summarized in **Figure 7**, we considered a number of sample sizes and sample number combinations. We computed the number of samples where the DFSM ≤ 25% for each case. These are shown for (**Figure 7A**) 1%, 2%, two 1%, 4%, four 1%, 20%, 80%, and four 20% samples. Here, multiple samples were selected at least 6 h apart.

We then compared paired differences for equivalent total blood volumes taken continuously or throughout the 24-h period as shown in **Figure 7B**. For example, we compared two, averaged 1% PBV (24s) samples to a single 2% PBV (2 min) measurement. Similarly, we compared four, 1% PBV samples (each taken at least 6 h apart) to a single 4% PBV sample, as well as four, 20% PBV samples to one single 80% PBV sample (32 min). For nearly every data set, averaging multiple smaller blood samples yielded a higher likelihood of accurately estimating the 24-h CTC rate compared to single, larger blood samples. This data demonstrates that while larger blood samples do improve the likelihood of accurately estimating CTC numbers, further improvements may be made by averaging smaller samples taken at different times of the day.

DISCUSSION

Although CTCs are widely studied using liquid biopsy, methods that involve analysis of single, fractionally-small PB samples inherently do not resolve temporal fluctuations in CTC numbers that can occur over the timescale of minutes or hours. As we have noted, DiFC samples large volumes of circulating PB continuously and non-invasively, and therefore provides unique insights into *in vivo* CTC dynamics in mouse models of metastasis. Our data in two xenograft models here showed that

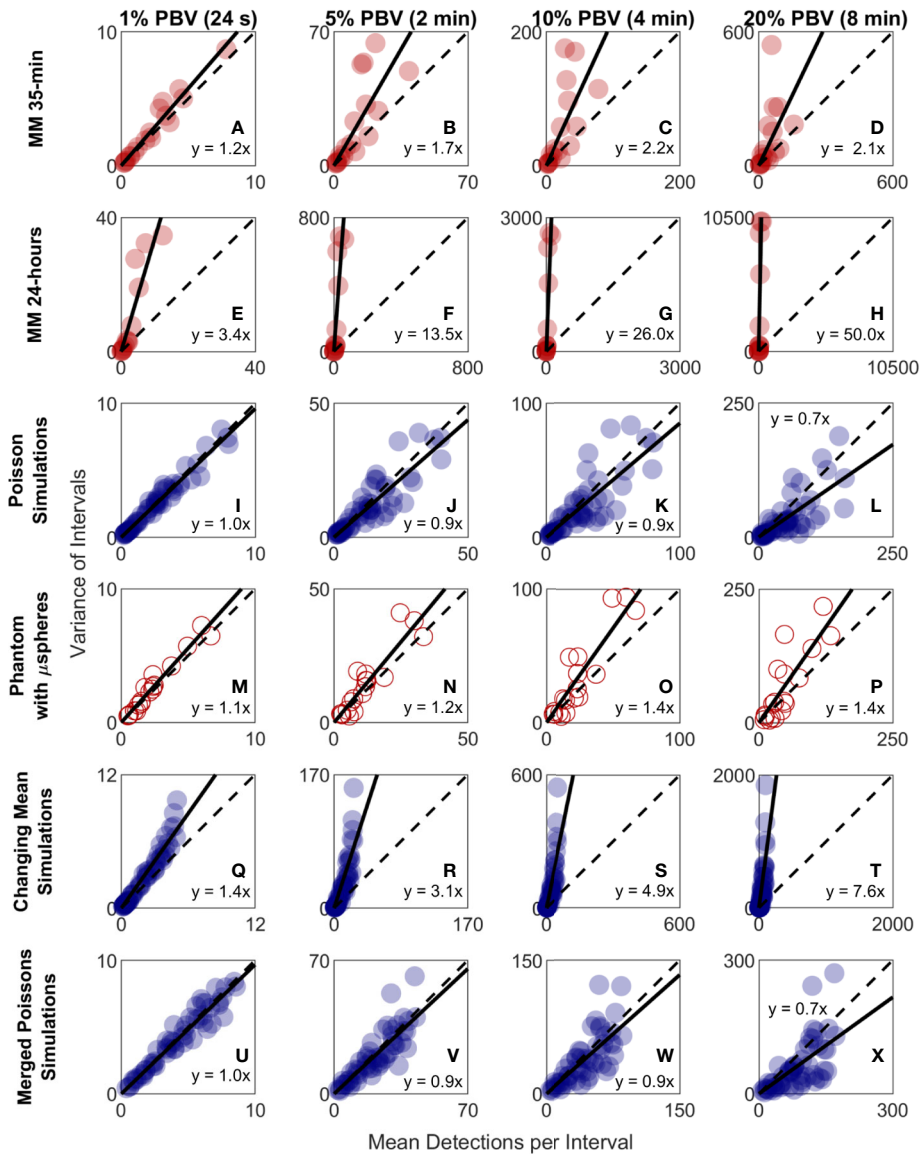

FIGURE 6 | The variability in DiFC count rate measured in mice far exceeded that expected by Poisson statistics. Measured variance in CTC counts compared to the scan mean count in DiFC data is shown for **(A–D)** MM 35-min mice, **(E–H)** MM 24-h mice, **(I–L)** simulated Poisson DiFC data, and **(M–P)** phantoms with suspensions of well-mixed microspheres. The dashed diagonal lines indicate the expected 1:1 variance-to-mean relationship for Poisson-distributed data. **(Q–T)** Simulations show that the higher than expected variance in MM 35-min data is consistent with a Poisson process with changing mean (see text for details). **(U–X)** By contrast, two or more simultaneous (merged) Poisson processes would not be consistent with the higher-than-expected variance. Equations and solid lines indicate a linear fit to each data set.

for rare CTCs (LLC bearing mice), any single small sampling interval (equivalent blood sample) frequently resulted in no CTC detections. For more abundant CTCs (MM bearing mice), small samples were unlikely to yield a quantitatively accurate estimate of mean CTC numbers. Data taken over 24-h periods also showed that CTC numbers varied by up to two orders-of-magnitude, with variance well in excess of that expected by Poisson statistics or operator variability.

In combination, it follows that that CTCs are not well mixed in the PB. This is consistent with two known properties of CTCs, i) that CTCs have a short half-life in circulation, and ii) that CTCs shed continuously from primary tumor(s). For the former, the small number of clinical estimates of CTC half-life range between 6 min and 2.4 h (15, 30, 31). Estimates of CTC half-life in mouse models also range from 10 to 60 min for different cell types and mouse strains (29, 32–37). In addition, many CTCs are cleared in minutes in the "first-pass effect" in the lungs, liver, or spleen (38, 39). With respect to the kinetics of CTC shedding, it has been previously shown that tumors disseminate CTCs at a rate of about 10^6 cells per gram of tumor tissue per day (40). We

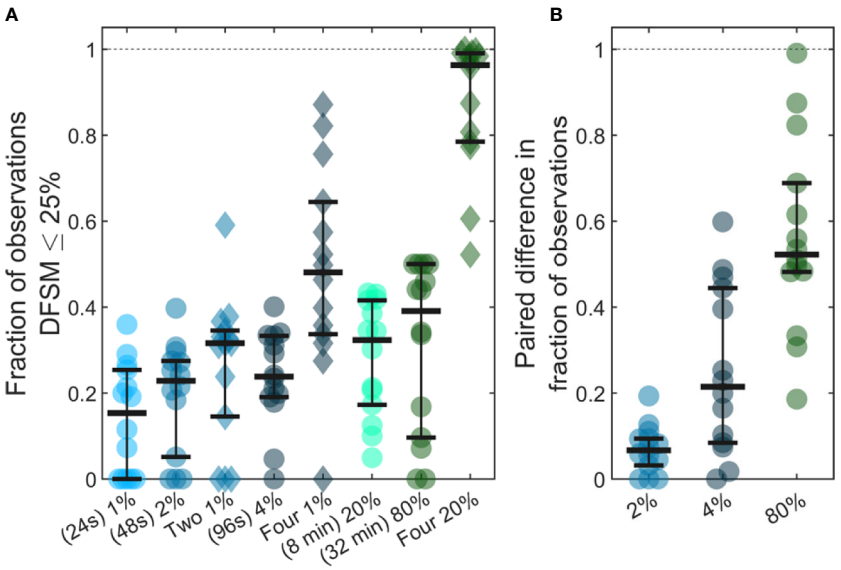

FIGURE 7 | Use of larger blood samples and averaging multiple blood samples yields improved enumeration of CTCs. **(A)** Fraction of samples of different sizes where the DFSM was less than or equal to 25% for 1%, 2%, two 1%, 4%, four 1%, 20%, 80%, and four 20% PBV samples. **(B)** Paired difference in the fraction of samples were the DFSM <= 25% between the averaged samples (two 1%, four 1%, and four 20% PBV) and a single continuous sample of equivalent size (2%, 4%, and 80% PBV).

were unable to find any specific information on the short-term dynamics of CTC shedding from the primary tumor; however, it is conceivable that this—like other tumor processes—varies over the timescale of minutes. For example, it has been shown that tumors cycle through hypoxia states on similar timescales (41). This suggests that CTCs are continuously and dynamically being shed into and cleared from circulation. For example, in one LLC data set (**Figure 3A**), only a single detection was observed in a 50-min DiFC scan suggesting that the CTC cleared from circulation before it could be detected a second time.

DiFC data support the alternate hypothesis that CTC numbers are better described using a kinetic model that oscillates between states of relatively high or low shedding, as opposed to a steady Poisson process. Specifically, CTC data from MM-DXM bearing mice was more consistent with our *in silico* simulated data sets where the mean CTC rate increased partway through the scan (**Figures 6Q–T**). These simulations suggested that CTC rates may change by approximately a factor of two over a 35-min scan, and by larger factors over 24-h periods. The disseminated nature of the MM tumor also implies that there may be multiple (many) sites of CTC shedding. However, as we noted, multiple simultaneous Poisson-distributed CTC sources would not produce the observed *in vivo* DiFC data (**Figures 6U–X**). This suggests that the changing numbers of CTCs in circulation is in response to systemic factors such as hormonal or cardiovascular effects. Despite the similarities in data, our simulations of a doubling in detection rate midway through the scan are, of course, not necessarily representative of what occurs biologically. In general, the magnitude and frequency of CTC rate changes is not known, and moreover is expected to vary with cancer type and mouse strain. Determining an accurate model of these changes is the subject of ongoing work in our group.

Since our observations were made in mouse xenograft models, a natural question is whether similar short-term temporal fluctuations occur in humans. While this requires further study, the general findings here are consistent with the small number of clinical studies in the literature. For example, (22) studied CTC numbers in blood samples taken at 12-h intervals from 51 breast cancer patients. While they concluded that there was no diurnal pattern, blood samples taken on the same day yielded differences by up to a factor of 3.8. Some patients had CTCs detected in one blood sample and no CTCs in the second blood sample, and several switched between prognostic categories (i.e., numbers above or below the 5 CTC threshold). Likewise, (23) showed 24-h variability of up to a factor of 7 in MM patients, and suggested a circadian rhythm to the fluctuations. (42) took three sequential 3 ml PB samples from each of 7 stage IV melanoma patients, and found also found significant variation in CTC number (by up to a factor of 4), including four patients where no CTCs were detected in some of the samples. However, direct comparison is difficult since these previously reported observations were made using a small number of fractionally small blood samples. As such, they did not permit study of continuous changes in CTC numbers that occur over the timescale of minutes as we do here. Moreover, the limited temporal data did not permit comparison with assumed kinetic or sampling models (such as Poisson statistics).

Together our findings suggest a number of practical implications for the use of liquid biopsy in CTC enumeration.

As noted the clinical value of CTC numbers as a diagnostic or predictive biomarker is still unclear (8–10, 43, 44). This has in part driven major efforts toward development of next-generation liquid biopsy technology for characterization of CTC genotypic and phenotypic heterogeneity (12–14). Assuming that the CTC behavior observed here extends to humans, these data may provide a simple complementary explanation (to CTC heterogeneity) for these challenges: CTCs enumerated in fractionally small blood samples is inherently sensitive to the timing of the blood draw because of the natural temporal fluctuations. As shown, these fluctuations could result in change of prognostic category (CTC positive or negative) when simple numerical thresholds are applied.

Second, these data are consistent with the notion that improved clinical CTC enumeration could be achieved by analysis of larger blood samples (13, 14), either by liquid biopsy or by development of *in vivo* methods for counting or capturing CTCs (45). Our analysis suggests that averaging of multiple small blood samples taken over the course of hours should yield even further improved accuracy. Alternatively, new *in vivo* methods could scan larger blood volumes over time and in principle yield more accurate enumeration of CTCs. In this regard, because DiFC is inherently scalable to larger tissue volumes, we are already exploring the possible translation of DiFC to humans through the use of highly specific fluorescence molecular probes (46).

Third, CTC clusters (CTCCs) are even more rare than CTCs (they occur at a frequency of less than 10% of single CTCs) but are of great interest because they are known to have significantly higher metastatic potential (47). Although we did not explicitly consider CTCCs in the analysis here, DiFC does permit detection of CTCCs (27, 29). The relative rarity of CTCCs implies that the challenges of enumeration with liquid biopsy of small PB samples are likely to be compounded. This is also true when considering accurate enumeration of specific, more-rare CTC phenotypes (11).

Last, the fast turnover of CTCs in PB also suggests that anti-CTC therapeutic strategies such as "CTC dialysis" that have been proposed (48–50) are unlikely to succeed unless performed continuously, for example using a wearable device.

In summary, analysis of DiFC data in two mouse models of metastasis shows that CTC numbers are far from steady-state *in vivo* and undergo significant fluctuations on the timescales of minutes and hours. This can (at least in these models) cause significant error in CTC detection and enumeration using small blood samples and motivates new methods for analyzing larger blood volumes *in vivo*. Ongoing work by our team includes the application of DiFC to other mouse xenograft models, investigating future clinical use of DiFC, and development of mathematical models to more accurately describe CTC dynamics.

DATA AVAILABILITY STATEMENT

The datasets generated and analyzed for this study can be found in the Blackfynn repository DOI: 10.26275/x9xq-e4wu. Additional data and code used to process data can be found in the Github repository https://github.com/NiedreLab/Williams-CTC-Dynamics-2020 (DOI: 10.5281/zenodo.4005939).

ETHICS STATEMENT

The animal study was reviewed and approved by Northeastern University IACUC protocol #15-0728R.

AUTHOR CONTRIBUTIONS

AW and MN designed research. AW, JF, and FI performed research. AW, JF, FI, and ES analyzed data. AW, ES, and MN conceived analysis. AW, ES, and MN wrote the paper. All authors contributed to the article and approved the submitted version.

FUNDING

This work was supported by the National Institutes of Health (NIH) (R01HL124315; NHLBI).

ACKNOWLEDGMENTS

We thank Dr. Paul Mathew (Tufts Medical Center, Boston, MA), Prof. Dana Brooks (Northeastern University, Boston, MA), and Prof. Daniel Ocone (Rutgers University, Piscataway, NJ) for their helpful comments and suggestions on our work. We also sincerely thank Dr. Miguel Martin (Universidad Complutense, Madrid, Spain) for kindly sharing data. This manuscript has been released as a pre-print at https://doi.org/10.1101/814368 (51).

SUPPLEMENTARY MATERIAL

The Supplementary Material for this article can be found online at: https://www.frontiersin.org/articles/10.3389/fonc.2020.601085/full#supplementary-material

SUPPLEMENTARY FIGURE 1 | Raster plots of 18 representative DiFC scans from LLC tumor bearing mice ("LLC data set"). Each solid vertical line represents a CTC detection. The dashed lines mark the end of each scan, which were of slightly different lengths. The plots are shown in ascending order of DiFC detection rate.

SUPPLEMENTARY FIGURE 2 | Raster event plots for all 18 DiFC scans in the "MM 35-min date set". Each vertical line represents a CTC detection. The plots are in ascending order of DiFC detection rate.

SUPPLEMENTARY FIGURE 3 | Fluctuations in the mean CTC count rate over 24-h periods for all DiFC scans the "MM 24-h data set". Triangle markers identify the first scan of the 24-h cycle. N = 7 cycles started ~0700 (7 am) and N = 7 sessions began at ~1900 (7 pm). Animal housing followed a 0700 to 1900 light (white background) and 1900 and 0700 dark (gray background) light cycles.

REFERENCES

1. Gupta GP, Massague J. Cancer metastasis: building a framework. *Cell* (2006) 127(4):679–95. doi: 10.1016/j.cell.2006.11.001
2. Steeg PS, Theodorescu D. Metastasis: a therapeutic target for cancer. *Nat Clin Pract Oncol* (2008) 5(4):206–19. doi: 10.1038/ncponc1066
3. Alix-Panabieres C, Pantel K. Circulating tumor cells: liquid biopsy of cancer. *Clin Chem* (2013) 59(1):110–8. doi: 10.1373/clinchem.2012.194258
4. Mader S, Pantel K. Liquid biopsy: current status and future perspectives. *Oncol Res Treat* (2017) 40(7-8):404–8. doi: 10.1159/000478018
5. Cristofanilli M, Budd GT, Ellis MJ, Stopeck A, Matera J, Miller MC, et al. Circulating tumor cells, disease progression, and survival in metastatic breast cancer. *N Engl J Med* (2004) 351(8):781–91. doi: 10.1056/NEJMoa040766
6. Cohen SJ, Punt CJ, Iannotti N, Saidman BH, Sabbath KD, Gabrail NY, et al. Relationship of circulating tumor cells to tumor response, progression-free survival, and overall survival in patients with metastatic colorectal cancer. *J Clin Oncol* (2008) 26(19):3213–21. doi: 10.1200/JCO.2007.15.8923
7. Moreno JG, Miller MC, Gross S, Allard WJ, Gomella LG, Terstappen LW. Circulating tumor cells predict survival in patients with metastatic prostate cancer. *Urology* (2005) 65(4):713–8. doi: 10.1016/j.urology.2004.11.006
8. Smerage JB, Barlow WE, Hortobagyi GN, Winer EP, Leyland-Jones B, Srkalovic G, et al. Circulating tumor cells and response to chemotherapy in metastatic breast cancer: SWOG S0500. *J Clin Oncol* (2014) 32(31):3483–9. doi: 10.1200/JCO.2014.56.2561
9. Raimondi C, Gradilone A, Naso G, Cortesi E, Gazzaniga P. Clinical utility of circulating tumor cell counting through CellSearch((R)): the dilemma of a concept suspended in Limbo. *Onco Targets Ther* (2014) 7:619–25. doi: 10.2147/OTT.S46200
10. Alix-Panabieres C, Pantel K. Challenges in circulating tumour cell research. *Nat Rev Cancer* (2014) 14(9):623–31. doi: 10.1038/nrc3820
11. Polzer B, Medoro G, Pasch S, Fontana F, Zorzino L, Pestka A, et al. Molecular profiling of single circulating tumor cells with diagnostic intention. *EMBO Mol Med* (2014) 6(11):1371–86. doi: 10.15252/emmm.201404033
12. Bardia A, Haber DA. Solidifying liquid biopsies: can circulating tumor cell monitoring guide treatment selection in breast cancer? *J Clin Oncol* (2014) 32 (31):3470–1. doi: 10.1200/JCO.2014.57.1505
13. Allan AL, Keeney M. Circulating tumor cell analysis: technical and statistical considerations for application to the clinic. *J Oncol* (2010) 2010:426218. doi: 10.1155/2010/426218
14. Lalmahomed ZS, Kraan J, Gratama JW, Mostert B, Sleijfer S, Verhoef C. Circulating tumor cells and sample size: the more, the better. *J Clin Oncol* (2010) 28(17):e288–9; author reply e90. doi: 10.1200/JCO.2010.28.2764
15. Stott SL, Lee RJ, Nagrath S, Yu M, Miyamoto DT, Ulkus L, et al. Isolation and characterization of circulating tumor cells from patients with localized and metastatic prostate cancer. *Sci Transl Med* (2010) 2(25):25ra3. doi: 10.1126/scitranslmed.3000403
16. Karabacak NM, Spuhler PS, Fachin F, Lim EJ, Pai V, Ozkumur E, et al. Microfluidic, marker-free isolation of circulating tumor cells from blood samples. *Nat Protoc* (2014) 9(3):694–710. doi: 10.1038/nprot.2014.044
17. Au SH, Edd J, Stoddard AE, Wong KHK, Fachin F, Maheswaran S, et al. Microfluidic Isolation of Circulating Tumor Cell Clusters by Size and Asymmetry. *Sci Rep* (2017) 7(1):2433. doi: 10.1038/s41598-017-01150-3
18. Hoff J. Methods of blood collection in the mouse. *Lab Anim* (2000) 29(10):47–53.
19. Hartmann C, Patil R, Lin CP, Niedre M. Fluorescence detection, enumeration and characterization of single circulating cells in vivo: technology, applications and future prospects. *Phys Med Biol* (2017) 63(1):01TR. doi: 10.1088/1361-6560/aa98f9
20. Tibbe AG, Miller MC, Terstappen LW. Statistical considerations for enumeration of circulating tumor cells. *Cytometry A* (2007) 71(3):154–62. doi: 10.1002/cyto.a.20369
21. Coumans FA, Ligthart ST, Terstappen LW. Interpretation of changes in circulating tumor cell counts. *Transl Oncol* (2012) 5(6):486–91. doi: 10.1593/tlo.12247
22. Martin M, Garcia-Saenz JA, Maestro De las Casas ML, Vidaurreta M, Puente J, Veganzones S, et al. Circulating tumor cells in metastatic breast cancer: timing of blood extraction for analysis. *Anticancer Res* (2009) 29(10):4185–7.
23. Paiva B, Paino T, Sayagues JM, Garayoa M, San-Segundo L, Martin M, et al. Detailed characterization of multiple myeloma circulating tumor cells shows unique phenotypic, cytogenetic, functional, and circadian distribution profile. *Blood* (2013) 122(22):3591–8. doi: 10.1182/blood-2013-06-510453
24. Tuchin VV, Tarnok A, Zharov VP. In vivo flow cytometry: a horizon of opportunities. *Cytometry A* (2011) 79(10):737–45. doi: 10.1002/cyto.a.21143
25. Zettergren E, Vickers D, Runnels J, Murthy SK, Lin CP, Niedre M. Instrument for fluorescence sensing of circulating cells with diffuse light in mice in vivo. *J BioMed Opt* (2012) 17(3):37001. doi: 10.1117/1.JBO.17.3.037001
26. Tan X, Patil R, Bartosik P, Runnels JM, Lin CP, Niedre M. In vivo flow cytometry of extremely rare circulating cells. *Sci Rep* (2019) 9(1):3366. doi: 10.1038/s41598-019-40143-2
27. Patil R, Tan X, Bartosik P, Detappe A, Runnels JM, Ghobrial I, et al. Fluorescence monitoring of rare circulating tumor cell and cluster dissemination in a multiple myeloma xenograft model in vivo. *J BioMed Opt* (2019) 24(8):1–11. doi: 10.1117/1.JBO.24.8.085004
28. Di W, Tan X, Calderon IAC, Neal Reilly AE, Niedre M, Clark HA. Real-time particle-by-particle detection of erythrocyte-camouflaged microsensor with extended circulation time in the bloodstream. *Proc Natl Acad Sci U S A* (2020) 117(7):3509–17. doi: 10.1073/pnas.1914913117
29. Fitzgerald JE, Byrd BK, Patil RA, Strawbridge RR, Davis SC, Bellini C, et al. Heterogeneity of circulating tumor cell dissemination and lung metastases in a subcutaneous Lewis lung carcinoma model. *BioMed Opt Express* (2020) 11 (7):3633–47. doi: 10.1364/BOE.395289
30. Meng S, Tripathy D, Frenkel EP, Shete S, Naftalis EZ, Huth JF, et al. Circulating tumor cells in patients with breast cancer dormancy. *Clin Cancer Res* (2004) 10(24):8152–62. doi: 10.1158/1078-0432.CCR-04-1110
31. Aceto N, Bardia A, Miyamoto DT, Donaldson MC, Wittner BS, Spencer JA, et al. Circulating tumor cell clusters are oligoclonal precursors of breast cancer metastasis. *Cell* (2014) 158(5):1110–22. doi: 10.1016/j.cell.2014.07.013
32. Georgakoudi I, Solban N, Novak J, Rice WL, Wei X, Hasan T, et al. In vivo flow cytometry: a new method for enumerating circulating cancer cells. *Cancer Res* (2004) 64(15):5044–7. doi: 10.1158/0008-5472.CAN-04-1058
33. Sipkins DA, Wei X, Wu JW, Runnels JM, Cote D, Means TK, et al. In vivo imaging of specialized bone marrow endothelial microdomains for tumour engraftment. *Nature* (2005) 435(7044):969–73. doi: 10.1038/nature03703
34. He W, Wang H, Hartmann LC, Cheng JX, Low PS. In vivo quantitation of rare circulating tumor cells by multiphoton intravital flow cytometry. *Proc Natl Acad Sci U S A* (2007) 104(28):11760–5. doi: 10.1073/pnas.0703875104
35. Runnels JM, Carlson AL, Pitsillides C, Thompson B, Wu J, Spencer JA, et al. Optical techniques for tracking multiple myeloma engraftment, growth, and response to therapy. *J BioMed Opt* (2011) 16(1):011006. doi: 10.1117/1.3520571
36. Pestana N, Mortensen LJ, Runnels JP, Vickers D, Murthy SK, Lin CP, et al. Improved diffuse fluorescence flow cytometer prototype for high sensitivity detection of rare circulating cells in vivo. *J BioMed Opt* (2013) 18(7):77002. doi: 10.1117/1.JBO.18.7.077002
37. Pera V, Tan X, Runnels J, Sardesai N, Lin CP, Niedre M. Diffuse fluorescence fiber probe for in vivo detection of circulating cells. *J BioMed Opt* (2017) 22 (3):37004. doi: 10.1117/1.JBO.22.3.037004
38. Mizuno N, Kato Y, Izumi Y, Irimura T, Sugiyama Y. Importance of hepatic first-pass removal in metastasis of colon carcinoma cells. *J Hepatol* (1998) 28 (5):865–77. doi: 10.1016/s0168-8278(98)80238-9
39. Fischer UM, Harting MT, Jimenez F, Monzon-Posadas WO, Xue H, Savitz SI, et al. Pulmonary passage is a major obstacle for intravenous stem cell delivery: the pulmonary first-pass effect. *Stem Cells Dev* (2009) 18(5):683–92. doi: 10.1089/scd.2008.0253
40. Butler TP, Gullino PM. Quantitation of cell shedding into efferent blood of mammary adenocarcinoma. *Cancer Res* (1975) 35(3):512–6.
41. Dewhirst MW. Relationships between cycling hypoxia, HIF-1, angiogenesis and oxidative stress. *Radiat Res* (2009) 172(6):653–65. doi: 10.1667/RR1926.1
42. Juratli MA, Sarimollaoglu M, Nedosekin DA, Melerzanov AV, Zharov VP, Galanzha EI. Dynamic fluctuation of circulating tumor cells during cancer progression. *Cancers (Basel)* (2014) 6(1):128–42. doi: 10.3390/cancers6010128
43. de Bono JS, Scher HI, Montgomery RB, Parker C, Miller MC, Tissing H, et al. Circulating tumor cells predict survival benefit from treatment in metastatic castration-resistant prostate cancer. *Clin Cancer Res* (2008) 14(19):6302–9. doi: 10.1158/1078-0432.CCR-08-0872

44. Toss A, Mu Z, Fernandez S, Cristofanilli M. CTC enumeration and characterization: moving toward personalized medicine. *Ann Transl Med* (2014) 2(11):108. doi: 10.3978/j.issn.2305-5839.2014.09.06
45. Saucedo-Zeni N, Mewes S, Niestroj R, Gasiorowski L, Murawa D, Nowaczyk P, et al. A novel method for the in vivo isolation of circulating tumor cells from peripheral blood of cancer patients using a functionalized and structured medical wire. *Int J Oncol* (2012) 41(4):1241–50. doi: 10.3892/ijo.2012.1557
46. Patil RA, Srinivasarao M, Amiji MM, Low PS, Niedre M. Fluorescence labeling of circulating tumor cells with a folate receptor-targeted molecular probe for diffuse In vivo flow cytometry. *Mol Imaging Biol* (2020) 22:1280–9. doi: 10.1007/s11307-020-01505-9
47. Hong Y, Fang F, Zhang Q. Circulating tumor cell clusters: What we know and what we expect (Review). *Int J Oncol* (2016) 49(6):2206–16. doi: 10.3892/ijo.2016.3747
48. Faltas B. Cornering metastases: therapeutic targeting of circulating tumor cells and stem cells. *Front Oncol* (2012) 2:68. doi: 10.3389/fonc.2012.00068
49. Kim YR, Yoo JK, Jeong CW, Choi JW. Selective killing of circulating tumor cells prevents metastasis and extends survival. *J Hematol Oncol* (2018) 11 (1):114. doi: 10.1186/s13045-018-0658-5
50. Galanzha EI, Menyaev YA, Yadem AC, Sarimollaoglu M, Juratli MA, Nedosekin DA, et al. In vivo liquid biopsy using Cytophone platform for photoacoustic detection of circulating tumor cells in patients with melanoma. *Sci Transl Med* (2019) 11(496):eaat5857. doi: 10.1126/scitranslmed.aat5857
51. Williams AL, Fitzgerald JE, Ivich F, Sontag ED, Niedre M. Short-term circulating tumor cell dynamics in mouse xenograft models and implications for liquid biopsy. *bioRxiv* (2020) Preprint:814368. doi: 10.1101/814368

Conflict of Interest: The authors declare that the research was conducted in the absence of any commercial or financial relationships that could be construed as a potential conflict of interest.

Copyright © 2020 Williams, Fitzgerald, Ivich, Sontag and Niedre. This is an open-access article distributed under the terms of the Creative Commons Attribution License (CC BY). The use, distribution or reproduction in other forums is permitted, provided the original author(s) and the copyright owner(s) are credited and that the original publication in this journal is cited, in accordance with accepted academic practice. No use, distribution or reproduction is permitted which does not comply with these terms.

frontiers in Cell and Developmental Biology

REVIEW
published: 11 December 2020
doi: 10.3389/fcell.2020.604391

Real-Time Molecular Monitoring in Acute Myeloid Leukemia With Circulating Tumor DNA

Deepshi Thakral[1], Ritu Gupta[1]*, Ranjit Kumar Sahoo[2], Pramod Verma[1], Indresh Kumar[1] and Sangeeta Vashishtha[1]*

[1] Laboratory Oncology Unit, Dr. BRA IRCH, All India Institute of Medical Sciences, New Delhi, India, [2] Department of Medical Oncology, Dr. BRA IRCH, All India Institute of Medical Sciences, New Delhi, India

The clonal evolution of acute myeloid leukemia (AML), an oligoclonal hematological malignancy, is driven by a plethora of cytogenetic abnormalities, gene mutations, abnormal epigenetic patterns, and aberrant gene expressions. These alterations in the leukemic blasts promote clinically diverse manifestations with common characteristics of high relapse and drug resistance. Defining and real-time monitoring of a personalized panel of these predictive genetic biomarkers is rapidly being adapted in clinical setting for diagnostic, prognostic, and therapeutic decision-making in AML. A major challenge remains the frequency of invasive biopsy procedures that can be routinely performed for monitoring of AML disease progression. Moreover, a single-site biopsy is not representative of the tumor heterogeneity as it is spatially and temporally constrained and necessitates the understanding of longitudinal and spatial subclonal dynamics in AML. Hematopoietic cells are a major contributor to plasma cell-free DNA, which also contain leukemia-specific aberrations as the circulating tumor-derived DNA (ctDNA) fraction. Plasma cell-free DNA analysis holds immense potential as a minimally invasive tool for genomic profiling at diagnosis as well as clonal evolution during AML disease progression. With the technological advances and increasing sensitivity for detection of ctDNA, both genetic and epigenetic aberrations can be qualitatively and quantitatively evaluated. However, challenges remain in validating the utility of liquid biopsy tools in clinics, and universal recommendations are still awaited towards reliable diagnostics and prognostics. Here, we provide an overview on the scope of ctDNA analyses for prognosis, assessment of response to treatment and measurable residual disease, prediction of disease relapse, development of acquired resistance and beyond in AML.

Keywords: plasma cell free DNA, cfDNA, circulating tumor DNA, ctDNA, acute myeloid leukemia, genomic profiling, measurable residual disease, hematological malignancies

OPEN ACCESS

Edited by:
Catherine Alix-Panabieres, Centre Hospitalier Universitaire de Montpellier, France

Reviewed by:
Giovannino Silvestri, University of Maryland, United States
Apollonia Tullo, Institute of Biomembranes, Bioenergetics and Molecular Biotechnologies, National Research Council, Italy

****Correspondence:***
Deepshi Thakral
deepshithakral@gmail.com
Ritu Gupta
drritugupta@gmail.com

Specialty section:
This article was submitted to Molecular and Cellular Oncology, a section of the journal Frontiers in Cell and Developmental Biology

Received: *09 September 2020*
Accepted: *21 October 2020*
Published: *11 December 2020*

Citation:
Thakral D, Gupta R, Sahoo RK, Verma P, Kumar I and Vashishtha S (2020) Real-Time Molecular Monitoring in Acute Myeloid Leukemia With Circulating Tumor DNA. Front. Cell Dev. Biol. 8:604391. doi: 10.3389/fcell.2020.604391

Abbreviations: AML, acute myeloid leukemia; AlloSCT, allogeneic stem cell transplantation; CAPP-Seq, cancer personalized profiling by deep sequencing; CHIP, clonal hematopoiesis of indeterminate potential; cfDNA, cell-free DNA; ctDNA, circulating tumor-derived DNA; CpG, cytosine and guanine dinucleotides; CN-AML, cytogenetically normal karyotype AML; CTCs, circulating tumor cells; ddPCR, droplet digital PCR; dsDNA, double-stranded DNA; EGFR, epidermal growth factor receptor; ELN, European Leukemia Net; FDA, Food and Drug Administration; FISH, fluorescence *in situ* hybridization; HPLC-MS, high performance liquid chromatography based mass spectrometry; IGH, immunoglobulin heavy chain; ISLB, International Society of Liquid Biopsy; MALDI-TOF MS, matrix-assisted laser desorption ionization time-of-flight mass spectrometry; MDS, myelodysplastic syndrome; MRD, measurable residual disease (also known as molecular or minimal residual disease); NCCN, National Comprehensive Cancer Network; NGS, next-generation sequencing; PCR, polymerase chain reaction; qPCR, quantitative PCR; Safe-SeqS, safe-sequencing system; Tam-Seq, tagged amplicon deep sequencing; TCR, T cell receptor; TMB, tumor mutation burden; VAF, variant allelic frequency; WHO, World Health Organization.

INTRODUCTION

Acute myeloid leukemia (AML) is a rapidly progressing hematological malignancy that display varied clinicopathological features as well as treatment outcomes (Estey and Döhner, 2006; Döhner et al., 2015; De Kouchkovsky and Abdul-Hay, 2016). With an annual incidence of 4.3 per 100,000 (age-adjusted cases from 2013 to 2017), the median age at diagnosis of AML is 68 years and 5-year relative survival is 28.7% in the United States alone [National Cancer Institute, 2017; SEER Cancer Stat Facts: Acute Myeloid Leukemia (accessed at https://seer.cancer.gov/statfacts/html/amyl.html; on 20th August, 2020)]. The expanding knowledge of its genomics has revealed the molecular complexity of the abnormal leukemogenesis in AML, which has immensely contributed to the refinement of risk stratification and personalized therapeutic strategies for these patients (Welch et al., 2012; Ley, 2013; Papaemmanuil et al., 2016; Leisch et al., 2019). Of the several novel treatment options approved by the U.S. Food and Drug Administration (FDA) that target specific gene mutations, surface markers, or regulators of apoptosis, epigenetic, or micro-environmental pathways; eight of these drugs have recently been incorporated into clinical practice to guide patient-specific treatment in AML in addition to the standard chemotherapy (Tiong and Wei, 2019; Green and Konig, 2020). Nevertheless, the long-term survival is less than 30% in patients below the age of 60 years and worse in older AML patients with comorbidities (Appelbaum et al., 2006; Almeida and Ramos, 2016). A significant proportion of AML patients eventually encounter disease relapse or become refractory even after initially achieving complete remission (CR) post-induction chemotherapy (Schlenk et al., 2017; Shlush et al., 2017).

In the current scenario with several options of standard chemotherapy, low-intensity regimens, combination chemoimmunotherapy, and clinical trials, AML patients may certainly benefit from the provision of concurrent real-time longitudinal monitoring of disease burden. The persistence of patient-specific genetic alterations in the due course of disease progression holds potential prognostic value. Monitoring these alterations may further guide strategies for maintenance of remission in the long term. Since liquid biopsy techniques are extensively being explored as non-invasive methods for tumor diagnosis and disease monitoring, these can provide early insights into treatment efficacy as well as predict recurrence of the disease. Here, we present an overview of the scope of molecular analysis of ctDNA in tracking relevant genetic markers for longitudinal monitoring of disease burden in AML.

TRANSFORMING CLASSIFICATION OF AML POST-GENOMICS ERA

Ever since the World Health Organization (WHO) introduced a new classification system of AML based on recurrent cytogenetic abnormalities in 2001 (Jaffe et al., 2001; Vardiman et al., 2002) and subsequently revised it in 2008 (Vardiman et al., 2009; Swerdlow et al., 2017) and further refined it based on molecular alterations in 2016 (Swerdlow et al., 2016, 2017), AML genome sequencing has further revealed a wide spectrum of driver and co-occurring mutations in majority of the patients (Ley et al., 2008; Mardis et al., 2009). The advent of next-generation sequencing (NGS) has deciphered the heterogeneous molecular complexity of AML genome specifically with cytogenetically normal karyotype (CN-AML) (Welch et al., 2012; Ley et al., 2013; Martelli et al., 2013). This category of CN-AML comprises almost half of the newly diagnosed AML cases (Ghanem et al., 2012; Martelli et al., 2013). In addition to the abnormal myeloid differentiation (gene rearrangements in *RUNX1, CBFB*, *RARA*, and alterations in other transcription factors), it has become evident that more than 95% of AML patients carry known driver and co-occurring mutations that are implicated in the survival of the neoplastic clone or subclones (Gupta, 2016; Papaemmanuil et al., 2016). Somatic mutations became apparent as an independent prognostic factor for risk stratification in CN-AML (Grimwade et al., 2016). Henceforth, WHO classification was updated by incorporating subcategories based on recurrent cytogenetic abnormalities and mutations such as AML with mutated *NPM1* and *CEBPA* as full entities and mutated *RUNX1* as provisional entity in the revised 2016 classification (Arber et al., 2016). The timeline of various milestones highlighting the transition toward genomic classification of AML is shown in **Figure 1**.

FUNCTIONAL GENOMIC LANDSCAPE AND RISK ASSESSMENT IN AML

Next-generation sequencing of AML genome has revealed the gene mutation map of driver events that led to a genomic classification of AML with significant clinical correlation (Ley et al., 2013; Papaemmanuil et al., 2016; Bullinger et al., 2017). These mutated genes are now segregated into nine categories based on their biological function (**Table 1**). Data from the mutational profiling of AML patients by either whole-genome or whole-exome sequencing was obtained by The Cancer Genome Atlas (TCGA) project (Ley et al., 2013). This study documented an average number of 13 coding mutations (single nucleotide variations and insertions/deletions) per patient suggesting a coordinated interaction of these gene alterations in AML pathogenesis (Grimwade et al., 2016). An average of less than one gene fusion event and a median of one somatic copy-number variant (e.g., trisomies or monosomies) were few other findings. Moreover, AML genomes with complex cytogenetic profile strongly associated with mutations in *TP53* gene. The updated European Leukemia Net (ELN) recommendation for risk stratification of AML patients into favorable, intermediate, and adverse groups is governed by a comprehensive integrated genomic profiling that includes recurrent chromosomal abnormalities, gene mutations, and *FLT3-ITD* allelic ratio (Döhner et al., 2017). Currently, most AML cases are assigned prognostically distinct subcategories based on the considerations of clinical presentation and presence or co-occurrence of cytogenetic and molecular aberrations (Hou et al., 2014). Comprehensive molecular profiling is gradually becoming the mainstay for improved diagnosis, prognostication, measurable residual disease (MRD) assessment, eligibility for

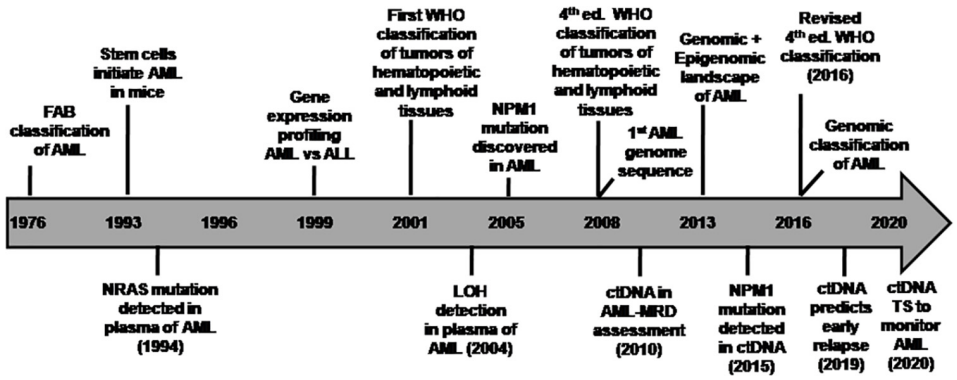

FIGURE 1 | Timeline of various milestones in the evolution of genomic classification of AML (Adapted from TCGA project Ley et al., 2013) and studies on circulating tumor DNA in AML. Initially, AML was classified by the French-American-British (FAB) Cooperative Group (1976) based on the cell lineage of leukemic cells and their differentiation status derived from the cell morphology as well as cytochemical staining of BM cells (Bennett et al., 1976). This approach had limitations in risk stratification in majority of AML cases. The discovery of recurrent cytogenetic abnormalities led to a novel classification system by the World Health Organization [WHO] (2001), which was revised in 2008 and later in the 2016 WHO Classification. Few research highlights of various studies on ctDNA analysis in AML disease monitoring are indicated in the timeline as a co-evolution with advances in AML genomics. ALL, acute lymphoblastic leukemia; AML, acute myeloid leukemia; ctDNA, circulating tumor-derived DNA; ed., edition; LOH, loss of helerozygosity; MRD, measurable residual disease; TS, targeted sequencing; WHO, World Health Organization.

TABLE 1 | Functional categorization of common genetic alterations and their clinical significance in AML (Adapted from Ley et al., 2013; Thakral and Gupta, 2019).

Functional category	Genetic alteration	Functional outcome	Clinical significance/risk stratification
Class I Transcription factor fusions by gene rearrangements	*t(8;21)* *inv16/t(16;16)*	Transcriptional deregulation and impaired hematopoietic differentiation	Favorable risk (absence of KIT*/*FLT3**)
Class II Myeloid transcription factors	*CEBPA* *RUNX1* *GATA2*	Transcriptional deregulation and impaired hematopoietic differentiation	Intermediate to adverse risk
Class III Nucleophosmin 1	*NPM1*	Aberrant cytoplasmic localization of NPM1	Favorable risk (absence of *FLT3**)
Class IV Tumor suppressor	*TP53* *PHF6* *WT1*	Transcriptional deregulation and impaired degradation	Adverse prognosis
Class V Signaling genes	*FLT3* *KIT* *KRAS/NRAS* *PTPN11*	Proliferative advantage conferred by activation of RAS/RAF, JAK/STAT, and PI3K/AKT signaling pathways	Midostaurin, a multikinase inhibitor approved by FDA for oral use. Adverse prognosis in CBF AML Diagnostic markers
Class VI DNA methylation-associated genes	*DNMT3A* *DNMT3B* *IDH1* *IDH2* *TET1* *TET2*	Deregulation of DNA methylation, transcriptional deregulation	Adverse prognosis in CN-AML IDH1/2 anti-metabolite enzyme inhibitors Associated with adverse prognosis
Class VII Chromatin modifiers	*ASXL1* *EZH2* *KMT2A* fusions *KMT2A*-PTD	Deregulation of chromatin modification and transcriptional deregulation	Adverse prognosis
Class VIII Spliceosome-complex genes	*SRSF2* *SF3B1* *U2AF1* *ZRSR2*	Impaired spliceosome function; aberrant splicing	Adverse prognosis
Class IX Cohesin complex genes	*RAD21* *SMC1/SMC2* *STAG2*	Possible impairment of chromosome segregation and transcriptional regulation	Under investigation

**Mutations in the indicated gene.*

targeted therapy, and monitoring for better patient management in AML (Pollyea, 2018; Schuurhuis et al., 2018).

For the initial diagnostic work-up of AML, the conventional approach of morphologic assessment of the bone marrow remains the universal recommendation by the World Health Organization (World Health Organization [WHO], 2016), the European Leukemia Net (ELN), and the National Comprehensive Cancer Network (NCCN) guidelines (Arber et al., 2016; Döhner et al., 2017; Tallman et al., 2019). The combined information obtained from a battery of tests including flow cytometry, cytogenetics, fluorescence *in situ* hybridization (FISH), and PCR or NGS-based molecular analyses, primarily performed on the bone marrow sample, guides prognostication as well as therapeutic choices for individual patients. The current practice for the evaluation of both remission and MRD for response assessments rely on bone marrow sampling, whereas peripheral blood evaluation may be adequate for monitoring of relapse in most cases (Komanduri and Levine, 2016; Percival et al., 2017).

Once complete clinical remission is achieved post-therapy, the frequency of follow-up bone marrow biopsies is not well defined. Moreover, the clinical utility of monitoring residual leukemic burden during initial induction therapy is currently not known (Wong et al., 2019). Most commonly, once patients attain clinical remission, they undergo repeat bone marrow aspiration every 2 to 3 months during the first year and every 3 to 6 months for the next 2 years as the risk of relapse is maximum during the initial 2 years after the end of consolidation chemotherapy (Percival et al., 2017). A long-standing question remains whether this uncomfortable and inconvenient procedure of bone marrow evaluation can be avoided during certain situations of disease monitoring.

For assurance to a patient in clinical remission to sustain in a clinically disease-free state, several issues remain. These include (i) sampling error introduced from a single bone marrow specimen that represents only a very small fraction of the total bone marrow cellular population (Percival et al., 2017); (ii) spatial heterogeneity and clonal evolution of leukemia (Walter et al., 2012); (iii) occurrence of extramedullary disease at relapse or diagnosis (Ganzel et al., 2016; Solh et al., 2016); (iv) limitation of the sensitivity of routine tests for residual disease monitoring (Ravandi et al., 2018); (v) patient risk stratification; and (vi) monitoring treatment efficacy. Therefore, the search for novel biomarkers that could provide additional predictive and/or prognostic information is ongoing. Subsequent development and validation of these biomarkers may contribute in clinical-decision making and better AML disease management.

MRD ASSESSMENT IN AML AND CURRENT CHALLENGES

Measurable, molecular, or minimal residual disease (MRD) has emerged as an independent prognostic indicator in AML (Schuurhuis et al., 2018). The current practice for treatment of AML patients post-remission is guided by genetic profile of leukemic blasts at diagnosis and on the MRD-level post-induction and consolidation chemotherapy. The MRD is used as an important tool for early response assessment for prediction of final treatment outcome in AML patients. Unlike the AML NCCN guidelines, the AML European Leukemia Net MRD working group recommends individualized patient-specific reliable tool to monitor MRD for response assessment and risk stratification (Arber et al., 2016; Schuurhuis et al., 2018). Multiparameteric flow cytometry, assessment of fusion transcript levels (i.e., *RUNX1-RUNX1T1*, *CBFB-MYH11*, and *PML-RARα*) or mutations (*NPM1*, *FLT3* allelic ratio) by quantitative PCR (qPCR) and more recently NGS are commonly used tools for MRD assessment (Jongen-Lavrencic et al., 2018; Voso et al., 2019; Yoest et al., 2020). The ELN is constantly improvising these guidelines for the standardization of methodology and frequency of MRD monitoring.

For MRD assessment, the sample of choice is bone marrow, although, peripheral blood is easy to obtain and lacks immature normal populations of cells that may interfere with analysis by multiparameteric flow cytometry. However, the sensitivity of MRD analysis of the peripheral blood circulating tumor cells (CTCs) is apparently lower than that of bone marrow and requires a lower MRD threshold to be prognostic. Numerous technical challenges remain regarding MRD monitoring in AML including (i) preferred source material (blood versus bone marrow); (ii) ideal sampling time; (iii) sampling interval; (iv) duration of screening for relapse; (v) identifiable and reliable molecular marker/s; and (vi) thorough validation and standardization of MRD assays for each individual marker.

Certain biological concerns include the spectrum of molecular lesions detected in AML clones that predispose them to variable proliferation potential, resulting in temporal difference between the emergence of positive MRD and hematologic relapse. Depending on the AML clone, more frequent MRD monitoring is essential for fast progressors whereas more prolonged MRD monitoring is desirable for slow progressors (Ding et al., 2012). Other confounding factors during MRD analysis include (i) asynchronous development of leukemic clones at different sites; (ii) minor residual leukemic subclones of potentially treatment-resistant nature maybe missed; and (iii) co-occurrence of clonal hematopoiesis of indeterminate potential (CHIP) mutations (e.g., *DNMT3A*, *TET2*, and *ASXL1*) that are associated with age-related clonal hematopoiesis, rather than residual leukemic cells (Busque et al., 2012; Genovese et al., 2014; Jaiswal et al., 2014).

In the rapidly evolving genomic era of precision medicine, a transition towards dynamic monitoring of tumor molecular characteristics is being witnessed. In this regard, easily accessible markers that would reflect the entire heterogeneity of the tumor such as liquid biopsy including CTCs, circulating tumor-derived DNA (ctDNA), plasma cell-free DNA (cfDNA), microRNAs (miRNA), and exosomes have emerged as biomarkers with immense potential (Bronkhorst et al., 2019; Cervena et al., 2019; Silvestri et al., 2020). Plasma cfDNA facilitates non-invasive peripheral blood sampling of tumor-associated actionable alterations that are present in its ctDNA fraction and is gradually finding clinical utility in several cancers. ctDNA has the potential to capture intratumor heterogeneity that maybe missed by tissue biopsy (Bettegowda et al., 2014). An additional advantage of cfDNA analysis may be its utility in cases where

the sample quality to perform molecular analysis such as NGS is compromised, with high failure rates. Moreover, integration of cfDNA NGS analysis showed significant increase in the detection of actionable mutations that facilitated molecularly guided therapy (Aggarwal et al., 2019).

CLINICAL STUDIES ON THE CHARACTERIZATION AND UTILITY OF PLASMA CELL-FREE DNA IN AML

Extracellular circulating DNA fragments were initially documented in the human peripheral blood in 1948 (Mandel and Metais, 1948), but its clinical relevance came to light only a few decades later. Circulating DNA was first demonstrated by the presence of anti-dsDNA antibodies detected against a nuclear non-histone substance in the sera of patients with autoimmune disease (Tan et al., 1966). Henceforth, elevated levels of circulating DNA were reported in plasma from cancer patients as compared with healthy controls (Leon et al., 1977) and detectable amounts of cfDNA fragments were also shown in other biofluids (Fleischhacker and Schmidt, 2007). Subsequently, it was demonstrated by Stroun et al. (1989) that only a fraction of the plasma cfDNA was derived from tumor cells characterized by decreased strand stability of cancer cell DNA. This led to the dawn of the concept of liquid biopsy when in 1994, Vasioukhin and Stroun's collaboration demonstrated that cfDNA carried *N-RAS* point mutations in patients with AML and myelodysplastic syndrome (MDS) (Vasioukhin et al., 1994).

The easy accessibility and usefulness of plasma cfDNA analysis for detection and monitoring of myeloid disorders was subsequently demonstrated by a few promising studies (summarized in **Table 2**). Preferential detection of *N-RAS* mutations in plasma cfDNA than in DNA obtained from blood cells or bone marrow suggested that a bone marrow biopsy or aspiration may not necessarily contain all the malignant clones involved in the disease (Vasioukhin et al., 1994). These findings were further corroborated by the detection of chromosomal abnormalities, such as loss of heterozygosity and X-chromosome inactivation, preferentially in plasma cfDNA than bone marrow cells obtained from AML patients at diagnosis and post-therapy (Rogers et al., 2004). Furthermore, the alterations of cfDNA levels during the initial phase of induction chemotherapy showed promise as a valuable marker for the early assessment of therapy response and prognostic tool in AML patients (Holdenrieder et al., 2001; Mueller et al., 2006).

For monitoring MRD and AML disease progression, the changes in the plasma cfDNA concentration and integrity index were shown as potential markers (Gao et al., 2010). Another study demonstrated the clinical utility of plasma DNA quantification by duplex real-time quantitative PCR for the evaluation of therapeutic responses and monitoring relapse in AML patients (Jiang et al., 2012). At diagnosis, the concentration of plasma DNA ranged from 73.4 to 245.1 ng/ml (median value = 168.5), which was significantly higher relative to the control groups and had a male preponderance in patients with AML. Differences in the alterations of plasma cfDNA levels post-chemotherapy between remission and non-remission patients were reported. The documented cfDNA levels in cancer patients ranges between 0 and >1,000 ng/ml of blood (average, 180 ng of cfDNA/ml) and less than 10 to 100 ng/ml (average, 30 ng/ml) in healthy controls (Fleischhacker and Schmidt, 2007). Genetic and epigenetic alterations that are unique characteristics of the tumor of origin can also be analyzed using circulating DNA (Wan et al., 2017; van der Pol and Mouliere, 2019). Indeed, plasma DNA tends to show changes in CpG global methylation early on as compared with peripheral blood cells as shown in patients with MDS (Iriyama et al., 2012).

A limitation of majority of the studies focusing on plasma cfDNA levels was a lack of assessment of tumor mutation burden (TMB), defined as the total number of non-synonymous mutations in the coding regions of the genes. A significant correlation between TMB and efficacy of targeted therapy is emerging. The clinical utility of assessing TMB using plasma cfDNA, which contains ctDNA, as a surrogate specimen to biopsy has been proposed (Cao et al., 2019; Fancello et al., 2019). To investigate the association of circulating *NPM1* (a tetra nucleotide duplication of TCTG in exon 12) mutation levels with clinical characteristics of AML patients, researchers quantitated the copies per milliliter of *NPM1*-A mutation in plasma cfDNA (Quan et al., 2015). This group demonstrated that the plasma is indeed enriched with tumor DNA and suggested the utility of monitoring *NPM1*-mutated AML using circulating DNA as a complementary assay to the routine molecular protocols. Furthermore, the utility of plasma ctDNA was demonstrated by detection of monoclonal IGH and TCR rearrangement for MRD monitoring in patients with AML (Zhong et al., 2018). During follow-up, recurrence of these rearrangements in cfDNA was observed 1-3 months earlier than bone marrow relapse indicating cfDNA as a useful tool for MRD monitoring in patients with AML.

The technological advancement in the genomic profiling of ctDNA facilitated the tracking of driver mutations and karyotypic abnormalities in AML and MDS for disease monitoring and assessment of treatment response. Highlights of the co-evolution of important breakthroughs in AML genomics and utility of cfDNA analysis are shown in **Figure 1**. A customized 55 genes panel for targeted deep sequencing of known recurrent mutations in MDS and AML was used for ctDNA analysis to monitor therapeutic response and clonal evolution in MDS (Yeh et al., 2017). These findings supported that ctDNA dynamics correlated with tumor burden during therapy for MDS. In another retrospective study, the utility of ctDNA analysis was evaluated for the identification of high-risk AML/MDS patients for relapse post-myeloablative allogeneic stem cell transplantation (alloSCT) (Nakamura et al., 2019). Nakamura et al. (2019) identified the driver mutations by NGS in each sample at diagnosis, which were then tracked using ctDNA analysis using personalized droplet digital PCR (ddPCR) for MRD quantification. Promisingly, ctDNA analysis-based MRD positivity in a few MRD-negative patients by conventional bone marrow sampling suggested the potential of ctDNA as a better representative of residual AML in these patients. The benefit of ctDNA-based MRD positivity especially in cytopenic patients after alloSCT could predict

TABLE 2 | Overview of various studies demonstrating the utility of ctDNA for molecular characterization, disease monitoring, and clinical outcome in acute myeloid leukemia.

Study focus	Patients/controls	Molecular method	Gene target	Major findings	Clinical significance	References
Point mutation	10	Southern hybridization/allele-specific PCR	N-RAS	Plasma is easily accessible and useful for detection and monitoring of myeloid disorders	Diagnostic Prognostic	Vasioukhin et al. (1994)
LOH	45/30	Multiplex PCR of microsatellite markers, sequencer	5q, 7q, 8, 17p, 20q	PB plasma is enriched in ctDNA; carry genomic aberrations	Diagnostic	Rogers et al. (2004)
DNA concentration	25	Spectrophotometry	–	Nucleosomal DNA is valuable marker for early prediction of therapeutic efficacy.	Diagnostic Prognostic therapy response	Mueller et al. (2006)
DNA concentration and integrity	60/30	qPCR	*ACTB*	Plasma DNA integrity is increased in acute leukemia and useful for monitoring MRD	Prognostic	Gao et al. (2010)
DNA concentration	66/100	Duplex real-time qPCR		Quantification of plasma DNA is useful for evaluating therapeutic effects and monitoring relapse	Diagnostic Prognostic	Jiang et al. (2012)
Mutation	100	qRT-PCR	*NPM1*	Circulating *NPM* mutations DNA assay serves as a complementary to routine investigative protocol	Diagnostic	Quan et al. (2015)
Gene rearrangement	235	qPCR	IGH or TCR gene rearrangement	Monoclonal IGH and TCR rearrangement in cfDNA may represent a useful tool for MRD monitoring	Prognostic	Zhong et al. (2018)
Mutations	53	NGS, ddPCR	57 targets	ctDNA predicts relapse post-alloSCT in AML and MDS	Diagnostic Prognostic	Nakamura et al. (2019)
Mutations	22	Targeted NGS	28 targets	cfDNA and bone marrow may be complementary in the assessment and monitoring of patients with AML.	Diagnostic Prognostic	Short et al. (2020)

relapse within a month after alloSCT and correlated with shorter overall survival. Although, this approach is potentially limited by the requirement for a unique digital PCR assays for each alteration and therefore is most suitable for recurrent mutations (*IDH1/2* genes and hotspot mutations in other genes).

Sequencing of cfDNA may identify clinically relevant mutations not detected in the bone marrow and may play a role in the assessment of MRD and prediction of relapse as further corroborated in a recent study. Targeted NGS of plasma cfDNA and bone marrow at the time of diagnosis and after achieving remission was conducted in 22 patients with AML (Short et al., 2020). Among 28 genes sequenced, a total of 39 unique somatic mutations were detected. Five mutations (13%) were detected exclusively in cfDNA, and 15 (38%) were detected only in the bone marrow. Among the 19 mutations detected in both sources, high concordance of variant allelic frequency (VAF) was observed by both methods although, sequencing of cfDNA detected new or persistent leukemia-associated mutations during remission that predicted relapse. It appears that when the VAF was <10%, either method may miss small subclonal populations suggesting that cfDNA and bone marrow analyses may be complementary in the assessment and monitoring of patients with AML. It is recommended that ctDNA may therefore be examined by error-corrected NGS, and the most convenient and reproducible approach will need to be established by individual laboratories as described in the next section (Rolfo et al., 2020).

The studies so far demonstrate a great potential for ctDNA in AML MRD assessment and thus may relieve patients from frequent risk-prone painful bone marrow punctures. Monitoring ctDNA enhances detection of relapse and defines molecular remission better. Early intervention at the stage of minimal tumor burden maybe possible by serial monitoring of ctDNA. Indeed, our experience with longitudinal molecular monitoring of plasma ctDNA during the course of AML disease progression supports these findings as described below.

CASE STUDY

In a case of AML with *RUNX1-RUNX1T1* recurrent abnormality and *KIT* D816V mutation, we retrospectively determined the fractional abundance of *KIT* D816V mutation by droplet digital PCR. Paired samples of plasma cfDNA and bone marrow aspirates were collected at baseline, for MRD assessment, at CR

after consolidation and relapse (**Supplementary Data**). A strong concordance was observed between the fractional abundance of *KIT* mutation but not the plasma cfDNA levels in both plasma and bone marrow samples at various indicated time points (**Figure 2**). Indeed, at relapse, the VAF of *KIT* mutation was represented better in the plasma cfDNA indicating it as a superior method for improved detection of persistent leukemia-associated mutation during remission that may predict early relapse. The higher turnover rate of leukemic cells than normal cells possibly contributes to the elevated cfDNA levels into circulation as was evident by increase in the levels of cfDNA post-induction. Therefore, mutation burden seems to be a more reliable marker for early treatment response than the plasma cfDNA levels. It is suggested that more frequent monitoring of ctDNA for the persistent mutations would allow an early prediction of relapse. Nevertheless, our findings need to be validated in a larger cohort.

CURRENT STATUS OF ULTRASENSITIVE TECHNOLOGY PLATFORMS FOR GENOTYPING ctDNA

The ctDNA accounts for <1% of the total cfDNA, which is a concoction of DNA fragments released by necrosis, apoptosis, and active secretion (Bettegowda et al., 2014; Diaz and Bardelli, 2014; Kustanovich et al., 2019). Depending on the disease burden, cellular turnover, stage, and treatment response, the detection and quantification of small quantities of ctDNA is challenging specially with low disease burden where the total amount of ctDNA might be 0.01% of the total cfDNA (Diehl et al., 2008; Forshew et al., 2012; Bettegowda et al., 2014; Kennedy et al., 2014; Newman et al., 2014; Gorgannezhad et al., 2018). With the currently available technologies for ctDNA characterization, a targeted or an untargeted approach may be used depending on the tumor burden. The targeted strategy is useful for tracking specific tumor mutations detected at the time of disease diagnosis at baseline (Siravegna et al., 2019; Cristofanilli and Braun, 2010). The untargeted methods focus on whole genome or exome sequencing that may detect copy number alterations or novel point mutations (Elazezy and Joosse, 2018; Gorgannezhad et al., 2018).

Various ultrasensitive technologies for detection of ctDNA include qPCR, digital PCR, targeted NGS, and mass spectrometry. These techniques offer both high sensitivity (VAF as low as ∼0.01%) and specificity (Cristofanilli and Braun, 2010; Freidin et al., 2015). Technological advances in real-time qPCR have made it possible to detect mutations with <10% VAF with higher sensitivity. This approach utilizes enrichment of common variant alleles by preferential amplification by blocking amplification at the oligo 3′ end (Elazezy and Joosse, 2018). Droplet digital PCR and Beads, Emulsions, Amplification, and Magnetic (BEAMing) technologies are two common digital platforms for liquid biopsy, which may detect mutant alleles with a high sensitivity of 0.001–0.01% (Vogelstein and Kinzler, 1999; Kristensen and Hansen, 2009). The principle of droplet digital PCR is based on water-oil emulsion droplet technology. Both the mutated and wild-type DNA samples are partitioned into thousands of droplets, and PCR amplification of each template occurs in individual droplets. Real-time PCR fluorescent-specific probes can be used for the detection of fluorescent-positive and fluorescent-negative droplets for quantitation of the absolute DNA copies using ddPCR (Kristensen and Hansen, 2009). This methodology is limited by the number of genomic targets that can be multiplexed. Another important technique is BEAMing that combines emulsion PCR, magnetic separation of the PCR product, hybridization with base-pair–specific fluorescent probes to distinguish wild-type and mutant alleles, and flow cytometry to identify and quantify specific somatic mutations present in the DNA (Thress et al., 2015). Although, digital PCR offers cost-effective platform as compared with NGS, a unique assay needs to be designed for each mutation whereas NGS allows evaluation of multiple genomic aberrations simultaneously.

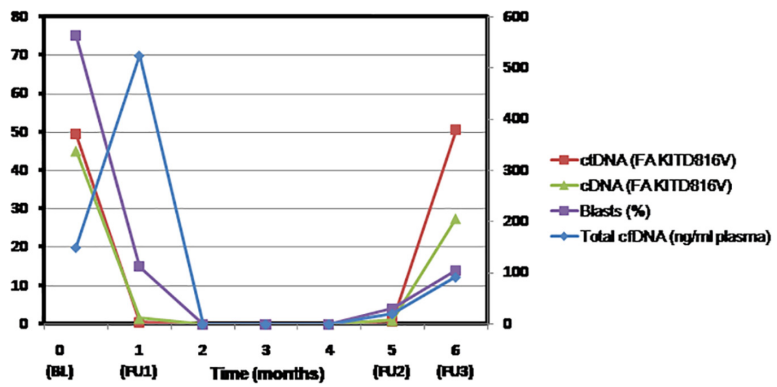

FIGURE 2 | The fractional abundance of *KIT* mutation in circulating tumor-derived DNA but not the levels of plasma cell free DNA represent residual AML better and may predict early relapse. Molecular monitoring of plasma cell-free DNA and bone marrow samples of AML patient was performed by droplet digital PCR at the indicated time points. Shown in the line graph are blast percentage (violet square), total plasma cfDNA concentration in nanograms per milliliter plasma (blue diamond), fractional abundance of *KIT* D816V mutation in cfDNA (red square), and bone marrow (green triangle) at baseline (BL = Day 0), MRD assessment (FU1 = Day 30), clinical remission (FU2 = 5 months), and after consolidation and relapse (FU3 = 6 months). BL, baseline; cDNA, complementary DNA; cfDNA, cell-free DNA; ctDNA, circulating tumor-derived DNA; FA, fractional abundance; FU, follow-up; MRD, measurable residual disease.

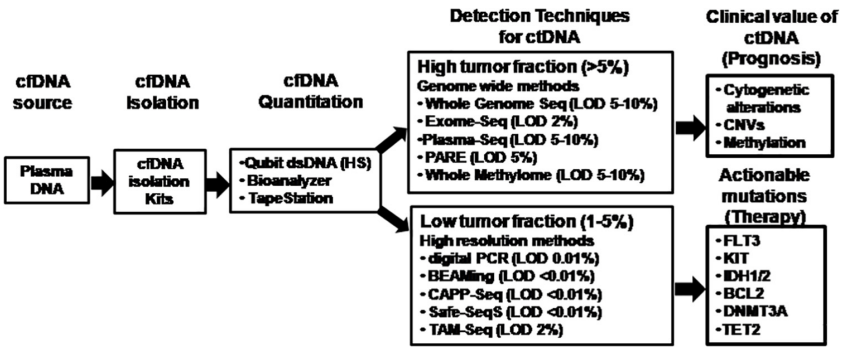

FIGURE 3 | Comparison of technology platforms for analysis of cell-free DNA. The analytical workflow for cell-free DNA characterization and analysis are depicted showing key steps of isolation, quantitation, and various options of the technology platforms available for molecular analysis of circulating tumor-derived DNA depending on the target region and tumor burden. cfDNA, cell-free DNA; ctDNA, circulating tumor-derived DNA; CAPP-Seq, cancer personalized profiling by deep sequencing; CNVs, copy number variations; dsDNA (HS), double-stranded DNA (high sensitivity); LOD, limit of detection; PARE, parallel analyses of RNA ends; Safe-SeqS, safe-sequencing system; Tam-Seq, tagged amplicon deep sequencing.

The major technical revolution witnessed is the range of ultrasensitive NGS platforms available for optimized detection of multiple somatic alterations simultaneously using ctDNA. The choice of target regions to be identified governs the selection of the NGS platform (**Figure 3**). Ultra-Deep NGS allowed quantitation of low-abundance DNA variants with high coverage in ctDNA by using error suppression multiplexed deep sequencing strategy with a limit of detection of approximately 0.02% (Narayan et al., 2012; Uchida et al., 2015). Several protocols including safe-sequencing system (Safe-SeqS) (Kinde et al., 2011), tagged amplicon deep sequencing (Tam-Seq) (Forshew et al., 2012), cancer-personalized profiling by deep sequencing (CAPP-Seq) (Newman et al., 2014), bias-corrected targeted NGS (Paweletz et al., 2016), and multiplex PCR NGS (Abbosh et al., 2017) have been evaluated. Safe-SeqS is based on assignment of unique identifiers to prespecified DNA templates, amplification of each tagged region into families and sequencing of the amplification products (Kinde et al., 2011). Tam-Seq is a protocol optimized for low-frequency hotspot mutations in circulating DNA at allele frequencies as low as 2%, with sensitivity and specificity of >97% (Forshew et al., 2012). CAPP-Seq is a capture-based NGS method that enriches for defined genomic regions prior to sequencing by hybridization of target regions to antisense oligonucleotides with a theoretical detection limit of 0.00025% VAF (Newman et al., 2014). Bias-corrected targeted NGS uses multifunctional markers including sample and sequence tags that bind to small capture probes which are amplified with high specificity (Paweletz et al., 2016). Finally, multiplex-PCR NGS is the combination of targeting clonal and subclonal single nucleotide variants selected to track phylogenetic tumor branches in plasma by high-throughput PCR amplification and sequencing reaching 99% sensitivity for the detection of mutations in the target regions (Abbosh et al., 2017).

Amplification-based methods including PCR and NGS are limited by the need for specific primers to initiate the amplification process. In this scenario, the utility and flexibility of HPLC-based mass spectrometry methods for the analysis of short DNA sequences is promising (Sharma et al., 2011). The short oligonucleotide mass analysis combines PCR amplification, restriction digestion, and electrospray ionization mass spectrometry and is more sensitive than restriction fragment length polymorphism-PCR for detection of specific mutations from circulating cfDNA. The more popular technique is matrix-assisted laser desorption ionization time-of-flight mass spectrometry (MALDI-TOF MS) for analyzing point mutations in cfDNA samples. Moreover, quantitative analysis of DNA methylation based on unique masses of methylated and unmethylated products by MALDI-TOF-MS MassARRAY system detects CpG sites.

APPLICATIONS OF ctDNA ANALYSIS IN AML

The applications of ctDNA analysis go beyond initial diagnosis, treatment stratification and monitoring, prognosis, assessment of MRD, and prediction of relapse (Mader and Pantel, 2017; Wan et al., 2017; Corcoran and Chabner, 2018; Heitzer et al., 2019; Pantel and Alix-Panabières, 2019; Cescon et al., 2020). cfDNA is an ideal non-invasive tool that allows periodic multiple tests over time and provides real-time data on tumor dynamics and evolution. Furthermore, longitudinal monitoring of ctDNA allows tracking of both genomic and epigenomic alterations (van der Pol and Mouliere, 2019; Erger et al., 2020). In addition to its use in personalized medicine, ctDNA analysis holds considerable promise as a surrogate marker for several applications such as (i) cancer screening in asymptomatic individuals (Chen and Zhao, 2019); (ii) early detection of cancer occurrence (Chen and Zhao, 2019); (iii) tumor localization and staging (van der Pol and Mouliere, 2019); (iv) monitoring of clonal evolution of malignant cells in real-time (De Mattos-Arruda et al., 2014; Fittall and Van Loo, 2019); (v) longitudinal ctDNA dynamics reflect tumor burden during treatment through serial sampling; (vi) identification of acquired drug resistance mechanisms (Russo and Bardelli, 2017; Diao et al., 2020); (vii) representative sampling of unreachable and non-resectable cancers; and (viii) utility in clinical trials (Ulrich and Paweletz, 2018; Araujo et al., 2019; Cescon et al., 2020). Potential integration of real-time ctDNA

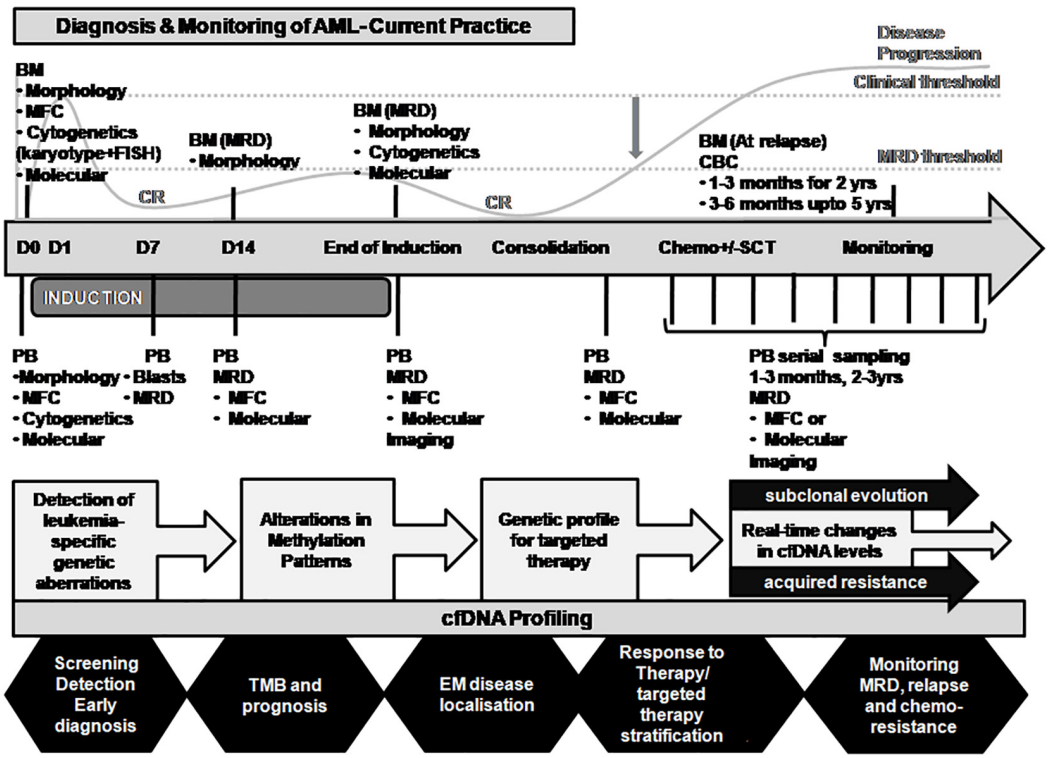

FIGURE 4 | Proposed integration of ctDNA profiling with AML diagnosis and disease monitoring. The current practice for AML diagnosis and disease monitoring is primarily dependent on the bone marrow sampling. A representation of the disease course is merged with the major time-points of investigation for evaluation of response to treatment (top panel). A critical time point post-chemotherapy needs to be defined when the disease is in occult stage and the MRD threshold is maintained (indicated by the gray downward arrow). Residual AML disease monitoring by serial sampling of circulating cfDNA analysis for patient-specific genetic alterations may prove informative when MRD threshold is breached (indicated in the middle panel). cfDNA profiling may provide several other applications in AML disease monitoring in real time as shown (bottom panel). BM, bone marrow; CBC, complete blood count; cfDNA, cell-free DNA; CR, clinical remission; MFC, multiparametric flow cytometry; MRD, measurable residual disease; PB, peripheral blood; SCT, stem cell transplantation; TMB, tumor mutation burden.

profiling and its applications in AML disease monitoring are depicted in **Figure 4**.

CURRENT CHALLENGES IN cfDNA ANALYSES

The International Society of Liquid Biopsy (ISLB) has recently elaborated on the various challenges associated with cfDNA analysis such as technological, biological, reporting-related, socio-economic, and regulatory (Rolfo et al., 2020). It is established that the plasma is a preferred choice because of the genomic DNA contamination in the serum (Steinman, 1979). The technological challenges primarily deal with preanalytical and analytical considerations which have been described earlier by our group (Thakral et al., 2020) and others (Merker et al., 2018; Volckmar et al., 2018; Kerachian et al., 2019; Li et al., 2019; Geeurickx and Hendrix, 2020; Rolfo et al., 2020). The sensitivity of cfDNA analysis is dependent on several variables from sample collection and processing, for which recommendations have been proposed to circumvent these issues (Rolfo et al., 2020). Since cfDNA levels alter during the course of the disease and are influenced by treatment, therefore, the dynamics of cfDNA can be potentially used as a real-time monitoring method (Malapelle and Rolfo, 2020). However, because of low abundance of cfDNA in certain cases, alternate methodologies are being developed for improved detection of genetic alterations such as analysis of circulating tumor RNA (ctRNA) for evaluation of fusion transcripts (Benayed et al., 2019).

One of the primary biological challenges in context of AML is CHIP. Presence of specific recurrent genetic variants (e.g., *DNMT3A*, *TET2*, and *ASXL1*) drive asymptomatic proliferation of blood cells arising from hematopoietic stem cells harboring them. These age-related CHIP mutations become a potential source of false positives in cfDNA in the absence of a hematological malignancy (Busque et al., 2012; Genovese et al., 2014). As mentioned earlier, their presence poses a challenge for MRD assessment as well as early cancer detection. To overcome this issue, a novel CHIP-filtering approach has been evaluated recently that is based on whole blood cell sequencing and cfDNA analysis with a sensitivity equivalent to droplet digital PCR (Abbosh et al., 2019; Liu et al., 2019). Another issue that might be applicable to extramedullary disease in AML is that of cfDNA shedding (Solh et al., 2016). As the sites of disease progression influence the cfDNA levels and may result in false negativity, this needs to be investigated further.

Till date, no universal consensus exists on the minimal requirement of NGS panels or their cost-effectiveness and

therefore most commercial or customized platforms attempt to incorporate detection of genetic alterations covering actionable targets. A limitation of such platforms designed using hotspots alone is that they tend to miss on novel mutations. It is recommended to use a broader gene panel that allows improved stratification of patients for clinical trials and repurposing of FDA-approved drugs. With regard to AML, detection of gene fusions maybe challenging to detect using cfDNA because of the variability in the available hybrid capture techniques. Moreover, vendor and reporting related issues remain that commercially available plasma NGS platforms should be used with caution in clinical practice as indiscriminate use of clinical suggestions of FDA-approved drugs, clinical trials, and bioinformatics based-therapies is indicated. It is recommended to evaluate the information so obtained in context of a molecular tumor board and use of standardized criteria to define actionability through the use of evidence-based scales such as OncoKB (Chakravarty et al., 2017) and ESCAT (Mateo et al., 2018).

A rigorous validation is mandatory before clinical utilization of cfDNA-based assays. To accelerate this process, a two-tier system has been created, one for the development and validation of assays (Blood Profiling Atlas in Cancer aka Blood PAC) and a regulatory body the International Liquid Biopsy Alliance (ILBA) that includes ISLB and regulatory agencies with a goal of increasing efficiency, minimizing duplication and expedition of the inclusion of liquid biopsy based assays into routine clinical practice. So far, the only FDA-approved liquid biopsy tests include Cobas EGFR mutation assay for non-small-cell lung carcinoma (Kwapisz, 2017) and Therascreen PIK3CA RGQ mutation detection assay in breast cancer.

FUTURE DIRECTION AND CONCLUSION

Liquid biopsy technologies for qualitative and quantitative analysis of cfDNA have immensely broadened our ability to assess cancer, specifically in its cryptic stage without the need for invasive sampling. A serial longitudinal monitoring of AML using cfDNA analysis from the peripheral blood may provide a series of screenshots that can potentially be coalesced together to generate a time-lapse movie of clonal evolution of leukemia. With an almost excellent concordance with matched bone marrow aspirates, cfDNA can quantify disease burden by providing mutational landscape as well as identify acquired drug resistance mechanisms which may guide clinical management in real time.

As rapid diagnosis of genetic alterations is required to opt for appropriate induction therapy by the oncologists, therefore, a quick turnaround time for comprehensive cfDNA sequencing may provide actionable information to guide clinical management. In this regard, the convenience of sample acquisition and storage of cfDNA provides added procedural advantage over currently practiced protocols. So far, the small cohorts evaluated for cfDNA necessitates further validation with a certain sample size to examine the frequency of the gene mutations in AML patients that may facilitate significant statistical power for meaningful comparisons. Initiatives have been taken by researchers through multicentric studies, cooperative-group trials, and regulatory bodies are formulated to devise universal guidelines. Further investigations will have to define the role of cfDNA as a diagnostic tool by determining clinically relevant tumor thresholds relative to currently used routine parameters.

The use of ultrasensitive sequencing technologies has facilitated the reliable detection of very low amounts of ctDNA that excellently complement the currently used methods. Therefore, an immediate clinical application of cfDNA genotyping in AML may be its incorporation in larger prospective clinical trials for the identification of patients carrying actionable mutations and their longitudinal genetic monitoring during targeted therapy administration. Monitoring of ctDNA may provide surrogate end-points for clinical outcomes. This can reduce the extended follow-up durations as well as become more cost-effective for clinical trials related to adjunct therapies. Moreover, ctDNA analyses based MRD estimation may aid the discovery of novel drugs targeted at elimination or control of residual tumor in high-risk AML patients prone to relapse (Pantel and Alix-Panabières, 2019).

Plasma ctDNA may be used for the study of virtually all genomic abnormalities including both coding and non-coding regions, loss of heterozygosity, microsatellite loci, mutations, polymorphisms, methylation, and copy number variations. Deep sequencing as a standalone for ctDNA analyses may get a boost by additional assessment of epigenetic modifications, immune signatures, platelets, exosomes, and miRNA analyses. Moreover, a better understanding of the dynamics of ctDNA in AML disease progression may be necessary before blood can be routinely used as a source to monitor tumor burden. Nevertheless, longitudinal monitoring of AML patients by ctDNA analysis could complement bone marrow cells as a diagnostic marker without sampling bias.

AUTHOR CONTRIBUTIONS

DT and RG designed and conducted the study, performed the data interpretation, statistical analysis, and wrote the manuscript. RKS is the medical oncologist who treated the patient included in the case study. PV performed the ddPCR experiments. IK performed NGS experiments. SV conducted RT-PCR and fragment analysis assays. All authors contributed to the article and approved the submitted version.

FUNDING

This work was supported by intramural research grant from All India Institute of Medical Sciences, New Delhi (Grant No. 8-607/A-607/2018/RS) to Dr. DT and grant from Indian Council of Medical Research (ICMR), Govt. of India (Grant No. Coord/7(7)/CARE-AML/18-NCD-II) to Prof. RG.

SUPPLEMENTARY MATERIAL

The Supplementary Material for this article can be found online at: https://www.frontiersin.org/articles/10.3389/fcell.2020.604391/full#supplementary-material

REFERENCES

Abbosh, C., Birkbak, N. J., Wilson, G. A., Jamal-Hanjani, M., Constantin, T., Salari, R., et al. (2017). Phylogenetic CtDNA analysis depicts early-stage lung cancer evolution. *Nature* 545, 446–451. doi: 10.1038/nature22364

Abbosh, C., Swanton, C., and Birkbak, N. J. (2019). Clonal haematopoiesis: a source of biological noise in cell-free DNA analyses. *Ann. Oncol.* 30, 358–359. doi: 10.1093/annonc/mdy552

Aggarwal, C., Thompson, J. C., Black, T. A., Katz, S. I., Fan, R., Yee, S. S., et al. (2019). Clinical implications of plasma-based genotyping with the delivery of personalized therapy in metastatic non-small cell lung cancer. *JAMA Oncol.* 5, 173–180. doi: 10.1001/jamaoncol.2018.4305

Almeida, A. M., and Ramos, F. (2016). Acute Myeloid Leukemia in the Older Adults. *Leuk. Res. Rep.* 6, 1–7. doi: 10.1016/j.lrr.2016.06.001

Appelbaum, F. R., Gundacker, H., Head, D. R., Slovak, M. L., Willman, C. L., Godwin, J. E., et al. (2006). Age and acute myeloid leukemia. *Blood* 107, 3481–3485.

Araujo, D. V., Bratman, S. V., and Siu, L. L. (2019). Designing circulating Tumor DNA-based interventional clinical trials in oncology. *Genome Med.* 11:22. doi: 10.1186/s13073-019-0634-x

Arber, D. A., Orazi, A., Hasserjian, R., Thiele, J., Borowitz, M. J., Le Beau, M. M., et al. (2016). The 2016 revision to the world health organization classification of myeloid neoplasms and acute leukemia. *Blood* 127, 2391–2405.

Benayed, R., Offin, M., Mullaney, K., Sukhadia, P., Rios, K., Desmeules, P., et al. (2019). High yield of RNA sequencing for targetable kinase fusions in lung adenocarcinomas with no mitogenic driver alteration detected by DNA sequencing and low tumor mutation burden. *Clin. Cancer Res.* 25, 4712–4722.

Bennett, J. M., Catovsky, D., Marie-Theregse, D., Flandrin, G., Galton, D. A. G., Gralnick, H. R., et al. (1976). Proposals for the classification of the acute Leukaemias French-American-British (FAB) Co-operative Group. *Br. Haematol. J.* 33, 451–458. doi: 10.1111/j.1365-2141.1976.tb03563.x

Bettegowda, C., Sausen, M., Leary, R. J., Kinde, I., Wang, Y., Agrawal, N., et al. (2014). Detection of circulating tumor DNA in early- and late-stage human malignancies. *Sci. Transl. Med.* 6:224ra24. doi: 10.1126/scitranslmed.3007094

Bronkhorst, A. J., Ungerer, V., and Holdenrieder, S. (2019). The emerging role of cell-free DNA as a molecular marker for cancer management. *Biomol. Detect. Quantif.* 17:100087. doi: 10.1016/j.bdq.2019.100087

Bullinger, L., Döhner, K., and Dohner, H. (2017). Genomics of acute myeloid leukemia diagnosis and pathways. *Clin. J. Oncol.* 35, 934–946. doi: 10.1200/JCO.2016.71.2208

Busque, L., Patel, J. P., Figueroa, M. E., Vasanthakumar, A., Provost, S., Hamilou, Z., et al. (2012). Recurrent somatic TET2 mutations in normal elderly individuals with clonal hematopoiesis. *Nat. Genet.* 44, 1179–1181. doi: 10.1038/ng.2413

Cao, D., Xu, H., Xu, X., Guo, T., and Ge, W. (2019). High tumor mutation burden predicts better efficacy of immunotherapy: a pooled analysis of 103078 cancer patients. *Oncoimmunology* 8, 1–12. doi: 10.1080/2162402X.2019.1629258

Cervena, K., Vodicka, P., and Vymetalkova, V. (2019). Diagnostic and prognostic impact of cell-free DNA in human cancers: systematic review. *Mutat. Res. Rev. Mut. Res.* 781, 100–129. doi: 10.1016/j.mrrev.2019.05.002

Cescon, D. W., Bratman, S. V., Chan, S. M., and Siu, L. L. (2020). Circulating Tumor DNA and Liquid Biopsy in Oncology. *Nature Cancer* 1, 276–290.

Chakravarty, D., Gao, J., Phillips, S., Kundra, R., Zhang, H., Wang, J., et al. (2017). OncoKB: a precision oncology knowledge base. *JCO Precis. Oncol.* 1, 1–16. doi: 10.1200/po.17.00011

Chen, M., and Zhao, H. (2019). Next-generation sequencing in liquid biopsy: cancer Screening and early detection. *Hum. Genomics* 13:34.

Corcoran, R. B., and Chabner, B. A. (2018). Application of Cell-Free DNA Analysis to Cancer Treatment. *Engl. N. Med. J.* 379, 1754–1765. doi: 10.1056/NEJMra1706174

Cristofanilli, M., and Braun, S. (2010). Circulating Tumor Cells Revisited. *JAMA* 303, 1092–1093. doi: 10.1001/jama.2010.292

De Kouchkovsky, I., and Abdul-Hay, M. (2016). Acute myeloid Leukemia: a comprehensive review and 2016 update. *Blood Cancer J.* 6:e441. doi: 10.1038/bcj.2016.50

De Mattos-Arruda, L., Weigelt, B., Cortes, J., Won, H. H., Ng, C. K. Y., Nuciforo, P., et al. (2014). Capturing Intra-tumor genetic heterogeneity by *de novo* mutation profiling of circulating cell-free tumor DNA: a proof-of-principle. *Ann. Oncol.* 215, 213–230. doi: 10.1093/annonc/mdu239

Diao, Z., Han, Y., Zhang, R., and Li, J. (2020). Circulating tumour DNA: a new biomarker to monitor resistance in NSCLC patients treated with EGFR-TKIs. *Biochim. Biophys. Acta. Rev. Cancer* 1873:188363. doi: 10.1016/j.bbcan.2020.188363

Diaz, L. A., and Bardelli, A. (2014). Liquid biopsies: genotyping circulating tumor DNA. *J. Clin. Oncol.* 32, 579–586. doi: 10.1200/JCO.2012.45.2011

Diehl, F., Schmidt, K., Choti, M. A., Romans, K., Goodman, S., Li, M., et al. (2008). Circulating mutant DNA to assess tumor dynamics. *Nat. Med.* 14, 985–990. doi: 10.1038/nm.1789

Ding, L., Ley, T. J., Larson, D. E., Miller, C. A., Koboldt, D. C., Welch, J. S., et al. (2012). Clonal evolution in relapsed acute myeloid leukaemia revealed by whole-genome sequencing. *Nature* 481, 506–510. doi: 10.1038/nature10738

Döhner, H., Estey, E., Grimwade, D., Amadori, S., Appelbaum, F. R., Büchner, T., et al. (2017). Diagnosis and management of AML in adults: 2017 ELN recommendations from an international expert panel. *Blood* 129, 424–447.

Döhner, H., Weisdorf, D. J., and Bloomfield, C. D. (2015). Acute Myeloid Leukemia. *N. Engl. J. Med.* 373, 1136–1152. doi: 10.1002/9780470987001.ch16

Elazezy, M., and Joosse, S. A. (2018). Techniques of using circulating tumor DNA as a liquid biopsy component in cancer management. *Comput. Struct. Biotechnol.* 16, 370–378. doi: 10.1016/j.csbj.2018.10.002

Erger, F., Nörling, D., Borchert, D., Leenen, E., Habbig, S., Wiesener, M. S., et al. (2020). CfNOMe - a single assay for comprehensive epigenetic analyses of cell-free DNA. *Genome Med.* 12, 1–14. doi: 10.1186/s13073-020-00750-5

Estey, E., and Döhner, H. (2006). Acute myeloid leukaemia. *Lancet* 368, 1894–1907.

Fancello, L., Gandini, S., Pelicci, P. G., and Mazzarella, L. (2019). Tumor mutational burden quantification from targeted gene panels: major advancements and challenges. *J. Immunother. Cancer* 7:183.

Fittall, M. W., and Van Loo, P. (2019). Translating insights into tumor evolution to clinical practice: promises and challenges. *Genome Med.* 11:20. doi: 10.1186/s13073-019-0632-z

Fleischhacker, M., and Schmidt, B. (2007). Circulating nucleic acids (CNAs) and cancer-A survey. *Biochim. Biophys. Acta Rev. Cancer* 1775, 181–232. doi: 10.1016/j.bbcan.2006.10.001

Forshew, T., Murtaza, M., Parkinson, C., Gale, D., Tsui, D. W. Y., Kaper, F., et al. (2012). Noninvasive identification and monitoring of cancer mutations by targeted deep sequencing of plasma DNA. *Sci. Transl. Med.* 4:136ra68. doi: 10.1126/scitranslmed.3003726

Freidin, M. B., Freydina, D. V., Leung, M., Fernandez, A. M., Nicholson, A. G., and Lim, E. (2015). Circulating tumor DNA outperforms circulating tumor cells for KRAS mutation detection in thoracic malignancies. *Clin. Chem.* 61, 1299–1304. doi: 10.1373/clinchem.2015.242453

Ganzel, C., Manola, J., Douer, D., Rowe, J. M., Fernandez, H. F., Paietta, E. M., et al. (2016). Extramedullary disease in adult acute myeloid leukemia is common but lacks independent significance: analysis of patients in ECOG-ACRIN cancer research group trials, 1980-2008. *Clin. J. Oncol.* 34, 3544–3553. doi: 10.1200/JCO.2016.67.5892

Gao, Y. J., He, Y. J., Yang, Z. L., Shao, H. Y., Zuo, Y., Bai, Y., et al. (2010). Increased integrity of circulating cell-free DNA in plasma of patients with acute Leukemia. *Clin. Chem. Lab. Med.* 48, 1651–1656. doi: 10.1515/CCLM.2010.311

Geeurickx, E., and Hendrix, A. (2020). Targets, pitfalls and reference materials for liquid biopsy tests in cancer diagnostics. *Mol. Aspects Med.* 72:100828. doi: 10.1016/j.mam.2019.10.005

Genovese, G., Kähler, A. K., Handsaker, R. E., Lindberg, J., Rose, S. A., Bakhoum, S. F., et al. (2014). Clonal hematopoiesis and blood-cancer risk inferred from blood DNA sequence. *N. Engl J. Med.* 371, 2477–2487. doi: 10.1056/NEJMoa1409405

Ghanem, H., Tank, N., and Tabbara, I. A. (2012). Prognostic implications of genetic aberrations in acute myelogenous leukemia with normal cytogenetics. *Am. J. Hematol.* 87, 69–77. doi: 10.1002/ajh.22197

Gorgannezhad, L., Umer, M., Islam, M. N., Nguyen, N. T., and Shiddiky, M. J. A. (2018). Circulating tumor DNA and liquid biopsy: opportunities, challenges, and recent advances in detection technologies. *Lab Chip* 18, 1174–1196. doi: 10.1039/c8lc00100f

Green, S. D., and Konig, H. (2020). Treatment of acute myeloid leukemia in the Era of genomics—achievements and persisting challenges. *Front. Genet.* 11:480. doi: 10.3389/fgene.2020.00480

Grimwade, D., Ivey, A., and Huntly, B. J. P. (2016). Molecular landscape of acute myeloid leukemia in younger adults and its clinical relevance. *Blood* 127, 29–41.

Gupta, R. (2016). Genomic classification of acute myeloid leukaemia: an incessantly evolving concept. *Natl. Med. J. India* 29, 283–285.

Heitzer, E., Haque, I. S., Roberts, C. E. S., and Speicher, M. R. (2019). Current and future perspectives of liquid biopsies in genomics-driven oncology. *Nat. Rev. Genet.* 20, 71–88.

Holdenrieder, S., Stieber, P., Bodenmüller, H., Busch, M., Von Pawel, J., Schalhorn, A., et al. (2001). Circulating nucleosomes in serum. *Ann. N. Y. Acad. Sci.* 945, 93–102. doi: 10.1111/j.1749-6632.2001.tb03869.x

Hou, H. A., Lin, C. C., Chou, W. C., Liu, C. Y., Chen, C. Y., Tang, J. L., et al. (2014). Integration of cytogenetic and molecular alterations in risk stratification of 318 patients with *de novo* Non-M3 acute myeloid Leukemia. *Leukemia* 28, 50–58. doi: 10.1038/leu.2013.236

Iriyama, C., Tomita, A., Hoshino, H., Adachi-Shirahata, M., Furukawa-Hibi, Y., Yamada, K., et al. (2012). Using peripheral blood circulating DNAs to Detect CpG global methylation status and genetic mutations in patients with Myelodysplastic Syndrome. *Biochem. Biophys. Res. Commun.* 419, 662–669. doi: 10.1016/j.bbrc.2012.02.071

Jaffe, E. S., Harris, N. L., Stein, H., and Vardiman, J. W. (eds) (2001). "World health organization classification of tumours", *Pathology and Genetics of Tumours of Haematopoietic and Lymphoid Tissues*, Lyon: IARC Press.

Jaiswal, S., Fontanillas, P., Flannick, J., Manning, A., Grauman, P. V., Mar, B. G., et al. (2014). Age-related clonal hematopoiesis associated with adverse outcomes. *N. Engl J. Med.* 371, 2488–2498. doi: 10.1056/NEJMoa1408617

Jiang, Y., Pan, S. Y., Xia, W. Y., Chen, D., Wang, H., Zhang, L. X., et al. (2012). [Dynamic Monitoring of plasma circulating DNA in patients with acute myeloid leukemia and its clinical significance]. *J. Exp. Hematol.* 20, 53–56.

Jongen-Lavrencic, M., Grob, T., Hanekamp, D., Kavelaars, F. G., Al Hinai, A., Zeilemaker, A., et al. (2018). Molecular minimal residual disease in acute myeloid Leukemia. *N. Engl. J. Med.* 378, 1189–1199. doi: 10.1056/NEJMoa1716863

Kennedy, S. R., Schmitt, M. W., Fox, E. J., Kohrn, B. F., Salk, J. J., Ahn, E. H., et al. (2014). Detecting ultralow-frequency mutations by duplex sequencing. *Nat. Protoc.* 9, 2586–2606. doi: 10.1038/nprot.2014.170

Kerachian, M. A., Poudineh, A., and Thiery, J. P. (2019). Cell free circulating tumor nucleic acids, a revolution in personalized cancer medicine. *Crit. Rev. Oncol. Hematol.* 144:102827. doi: 10.1016/j.critrevonc.2019.102827

Kinde, I., Wu, J., Papadopoulos, N., Kinzler, K. W., and Vogelstein, B. (2011). Detection and Quantification of Rare Mutations with Massively Parallel Sequencing. *Proc. Natl. Acad. Sci. U.S.A.* 108, 9530–9535. doi: 10.1073/pnas.1105422108

Komanduri, K. V., and Levine, R. L. (2016). Diagnosis and therapy of acute myeloid leukemia in the Era of molecular risk stratification. *Annu. Rev. Med.* 67, 59–72. doi: 10.1146/annurev-med-051914-021329

Kristensen, L. S., and Hansen, L. L. (2009). PCR-based methods for detecting single-locus DNA methylation biomarkers in cancer diagnostics, prognostics, and response to treatment. *Clin. Chem.* 55, 1471–1483. doi: 10.1373/clinchem.2008.121962

Kustanovich, A., Schwartz, R., Peretz, T., and Grinshpun, A. (2019). Life and death of circulating cell-free DNA. *Cancer Biol. Ther.* 20, 1057–1067. doi: 10.1080/15384047.2019.1598759

Kwapisz, D. (2017). The first liquid biopsy test approved. Is it a new Era of mutation testing for non-small cell lung cancer? *Ann. Transl. Med.* 5:46. doi: 10.21037/atm.2017.01.32

Leisch, M., Jansko, B., Zaborsky, N., Greil, R., and Pleyer, L. (2019). Next generation sequencing in AML-on the way to becoming a new standard for treatment initiation and/or Modulation? *Cancers* 11:252.

Leon, S. A., Shapiro, B., Sklaroff, D. M., and Yaros, M. J. (1977). Free DNA in the serum of cancer patients and the effect of therapy. *Cancer Res.* 37, 646–650.

Ley, T. J. (2013). Genomic and Epigenomic landscapes of adult *de novo* acute myeloid leukemia the cancer genome atlas research network. *N. Engl. J. Med.* 368, 2059–2074. doi: 10.1056/NEJMoa1301689

Ley, T. J., Mardis, E. R., Ding, L., Fulton, B., McLellan, M. D., Chen, K., et al. (2008). DNA sequencing of a cytogenetically normal acute myeloid Leukaemia genome. *Nature* 456, 66–72. doi: 10.1038/nature07485

Ley, T. J., Miller, C., Ding, L., Raphael, B. J., Mungall, A. J., Robertson, G., et al. (2013). Genomic and epigenomic landscapes of adult *de novo* acute myeloid Leukemia. *N. Engl. J. Med.* 368, 2059–2074.

Li, Z., Yi, L., Gao, P., Zhang, R., and Li, J. (2019). The cornerstone of integrating circulating tumor DNA into cancer management. *Biochim. Biophys. Acta. Rev. Cancer* 1871, 1–11. doi: 10.1016/j.bbcan.2018.11.002

Liu, J., Chen, X., Wang, J., Zhou, S., Wang, C. L., Ye, M. Z., et al. (2019). Biological background of the genomic variations of Cf-DNA in healthy individuals. *Ann. Oncol.* 30, 464–470. doi: 10.1093/annonc/mdy513

Mader, S., and Pantel, K. (2017). Liquid biopsy: current status and future perspectives. *Oncol. Res. Treat.* 40, 404–408. doi: 10.1159/000478018

Malapelle, U., and Rolfo, C. (2020). Liquid biopsy as a follow-up tool: comment on longitudinal monitoring of somatic genetic alterations in circulating cell-free DNA during treatment with epidermal growth factor receptor–tyrosine kinase inhibitors. *Cancer* 126, 22–25. doi: 10.1002/cncr.32482

Mandel, P., and Metais, P. (1948). Les Acides Nucléiques Du Plasma Sanguin Chez l'homme. *C. R. Acad. Sci. Paris* 142, 241–243.

Mardis, E. R., Ding, L., Dooling, D. J., Larson, D. E., McLellan, M. D., Chen, K., et al. (2009). Recurring mutations found by sequencing an acute myeloid leukemia genome. *N. Engl. J. Med.* 361, 1058–1066. doi: 10.1056/NEJMoa0903840

Martelli, M. P., Sportoletti, P., Tiacci, E., Martelli, M. F., and Falini, B. (2013). Mutational landscape of AML with normal cytogenetics: biological and clinical implications. *Blood Rev.* 27, 13–22. doi: 10.1016/j.blre.2012.11.001

Mateo, J., Chakravarty, D., Dienstmann, R., Jezdic, S., Gonzalez-Perez, A., Lopez-Bigas, N., et al. (2018). A framework to rank genomic alterations as targets for cancer precision medicine: the ESMO scale for clinical actionability of molecular targets (ESCAT). *Ann. Oncol.* 29, 1895–1902. doi: 10.1093/annonc/mdy263

Merker, J. D., Oxnard, G. R., Compton, C., Diehn, M., Hurley, P., Lazar, A. J., et al. (2018). Circulating Tumor DNA analysis in patients with cancer: American society of clinical oncology and college of american pathologists joint review. *J. Clin Oncol.* 36, 1631–1641. doi: 10.1200/JCO.2017.76.8671

Mueller, S., Holdenrieder, S., Stieber, P., Haferlach, T., Schalhorn, A., Braess, J., et al. (2006). Early prediction of therapy response in patients with acute myeloid Leukemia by Nucleosomal DNA Fragments. *BMC Cancer* 6:143. doi: 10.1186/1471-2407-6-143

Nakamura, S., Yokoyama, K., Shimizu, E., Yusa, N., Kondoh, K., Ogawa, M., et al. (2019). Prognostic impact of circulating tumor DNA Status Post–Allogeneic Hematopoietic Stem Cell Transplantation in AML and MDS. *Blood* 133, 2682–2695.

Narayan, A., Carriero, N. J., Gettinger, S. N., Kluytenaar, J., Kozak, K. R., Yock, T. I., et al. (2012). Ultrasensitive measurement of hotspot mutations in tumor DNA in blood using error-suppressed multiplexed deep sequencing. *Cancer Res.* 72, 3492–3498.

National Cancer Institute (2017). *SEER Cancer Stat Facts: Acute Myeloid Leukemia*. Available online at: Https://Seer.Cancer.Gov/Statfacts/Html/Amyl.Html (accessed August 20, 2020).

Newman, A. M., Bratman, S. V., To, J., Wynne, J. F., Eclov, N. C. W., Modlin, L. A., et al. (2014). An ultrasensitive method for quantitating circulating tumor DNA with broad patient coverage. *Nat. Med.* 20, 548–554. doi: 10.1038/nm.3519

Pantel, K., and Alix-Panabières, C. (2019). Liquid biopsy and minimal residual disease — latest advances and implications for cure. *Nat. Rev. Clin. Oncol.* 16, 409–424.

Papaemmanuil, E., Gerstung, M., Bullinger, L., Gaidzik, V. I., Paschka, P., Roberts, N. D., et al. (2016). Genomic classification and prognosis in acute myeloid Leukemia. *N. Engl J. Med.* 374, 2209–2221. doi: 10.1056/NEJMoa1516192

Paweletz, C. P., Sacher, A. G., Raymond, C. K., Alden, R. S., O'Connell, A., MacH, S. L., et al. (2016). Bias-corrected targeted next-generation sequencing for rapid, multiplexed detection of actionable alterations in cell-free DNA from advanced lung cancer patients. *Clin. Cancer Res.* 22, 915–922. doi: 10.1158/1078-0432.CCR-15-1627-T

Percival, M. E., Lai, C., Estey, E., and Hourigan, C. S. (2017). Bone marrow evaluation for diagnosis and monitoring of acute myeloid Leukemia. *Blood Rev.* 31, 185–192. doi: 10.1016/j.blre.2017.01.003

Pollyea, D. A. (2018). New drugs for acute myeloid leukemia inspired by genomics and when to use them. *Hematology* 2018, 45–50. doi: 10.1182/asheducation-2018.1.45

Quan, J., Gao, Y. J., Yang, Z. L., Chen, H., Xian, J. R., Zhang, S. S., et al. (2015). Quantitative detection of circulating nucleophosmin mutations DNA in the plasma of patients with acute myeloid Leukemia. *Int. Med. J. Sci.* 12, 17–22. doi: 10.7150/ijms.10144

Ravandi, F., Walter, R. B., and Freeman, S. D. (2018). Evaluating measurable residual disease in acute myeloid Leukemia. *Blood Adv.* 2, 1356–1366. doi: 10.1182/bloodadvances.2018016378

Rogers, A., Joe, Y., Manshouri, T., Dey, A., Jilani, I., Giles, F., et al. (2004). Relative increase in Leukemia-specific DNA in peripheral blood plasma from patients with acute myeloid Leukemia and Myelodysplasia. *Blood* 103, 2799–2801.

Rolfo, C., Cardona, A. F., Cristofanilli, M., Paz-Ares, L., Diaz Mochon, J. J., Duran, I., et al. (2020). Challenges and opportunities of CfDNA analysis implementation in clinical practice: perspective of the international society of liquid biopsy (ISLB). *Crit. Rev. Oncol. Hematol.* 151:102978. doi: 10.1016/j.critrevonc.2020.102978

Russo, M., and Bardelli, A. (2017). Lesion-directed therapies and monitoring tumor evolution using liquid biopsies. *CSH Perspect. Med.* 7:a029587. doi: 10.1101/cshperspect.a029587

Schlenk, R. F., Müller-Tidow, C., Benner, A., and Kieser, M. (2017). Relapsed/refractory acute myeloid Leukemia: Any Progress? *Curr. Opin. Oncol.* 29, 467–473. doi: 10.1097/CCO.0000000000000404

Schuurhuis, G. J., Heuser, M., Freeman, S., Béne, M. C., Buccisano, F., Cloos, J., et al. (2018). Minimal/Measurable Residual Disease in AML: a consensus document from the European LeukemiaNet MRD Working Party. *Blood* 131, 1275–1291.

Sharma, V. K., Vouros, P., and Glick, J. (2011). Mass spectrometric based analysis, characterization and applications of Circulating Cell Free DNA Isolated from Human Body Fluids. *Int. J. Mass Spectrom.* 304, 172–183. doi: 10.1016/j.ijms.2010.10.003

Shlush, L. I., Mitchell, A., Heisler, L., Abelson, S., Stanley Ng, W. K., Trotman-Grant, A., et al. (2017). Tracing the origins of relapse in acute myeloid Leukaemia to stem cells. *Nature* 547, 104–108. doi: 10.1038/nature22993

Short, N. J., Patel, K. P., Albitar, M., Franquiz, M., Luthra, R., Kanagal-Shamanna, R., et al. (2020). Targeted next-generation sequencing of circulating cell-free DNA vs bone marrow in patients with acute myeloid Leukemia. *Blood Adv.* 4, 1670–1677. doi: 10.1182/bloodadvances.2019001156

Silvestri, G., Trotta, R., Stramucci, L., Ellis, J. J., Harb, J. G., Neviani, P., et al. (2020). Persistence of Drug-resistant leukemic stem cells and impaired NK cell immunity in CML patients depend on MIR300 Antiproliferative and PP2A-activating functions. *Blood Cancer Discov.* 1, 48–67.

Siravegna, G., Mussolin, B., Venesio, T., Marsoni, S., Seoane, J., Dive, C., et al. (2019). How liquid biopsies can change clinical practice in oncology. *Ann. Oncol.* 30, 1580–1590. doi: 10.1093/annonc/mdz227

Solh, M., Solomon, S., Morris, L., Holland, K., and Bashey, A. (2016). Extramedullary acute myelogenous Leukemia. *Blood Rev.* 30, 333–339. doi: 10.1016/j.blre.2016.04.001

Steinman, C. R. (1979). Circulating DNA in Systemic Lupus Erythematosus. Association with Central Nervous System Involvement and Systemic Vasculitis. *Am. J. Med.* 67, 429–435.

Stroun, M., Anker, P., Maurice, P., Lyautey, J., Lederrey, C., and Beljanski, M. (1989). Neoplastic characteristics of the DNA found in the plasma of cancer patients. *Oncology* 46, 318–322. doi: 10.1159/000226740

Swerdlow, S. H., Campo, E., Harris, N. L., Jaffe, E. S., Pileri, S. A., Stein, H., et al. (2017). "WHO classification of tumours of haematopoietic and lymphoid tissues," in *WHO Classification of Tumours*, Vol. 2, 4th Edn, (Lyon: IARC), 439. doi: 10.1182/blood-2011-01-293050

Swerdlow, S. H., Campo, E., SPileri, A., NHarris, L., Stein, H., Siebert, R., et al. (2016). The 2016 Revision of the World health organization classification of lymphoid neoplasms. *Blood* 127, 2375–2390.

Tallman, M. S., Wang, E. S., Altman, J. K., Appelbaum, F. R., Bhatt, V. R., Bixby, D., et al. (2019). Acute myeloid leukemia, Version 3.2019, NCCN Clinical Practice Guidelines in Oncology. *J. Natl. Compr. Cancer Netw.* 17, 721–749. doi: 10.6004/jnccn.2019.0028

Tan, E. M., Schur, P. H., Carr, R. I., and Kunkel, H. G. (1966). Deoxybonucleic Acid (DNA) and Antibodies to DNA in the serum of patients with systemic lupus erythematosus. *J. Clin. Invest.* 45, 1732–1740. doi: 10.1172/JCI105479

Thakral, D., Das, N., Basnal, A., and Gupta, R. (2020). Cell-Free DNA for genomic profiling and minimal residual disease monitoring in myeloma- Are We There Yet? *Am. J. Blood Res.* 10, 26–45.

Thakral, D., and Gupta, R. (2019). "Acute Myeloid Leukemia: an Update," in *Hematopathology*, eds R. Saxena and H. Pati (Singapore: Springer), 163–182.

Thress, K. S., Brant, R., Carr, T. H., Dearden, S., Jenkins, S., Brown, H., et al. (2015). EGFR Mutation Detection in CtDNA from NSCLC Patient Plasma: a cross-platform comparison of leading technologies to support the clinical development of AZD9291. *Lung Cancer* 90, 509–515. doi: 10.1016/j.lungcan.2015.10.004

Tiong, I. S., and Wei, A. H. (2019). New drugs creating new challenges in acute myeloid Leukemia. *Genes Chromosomes Cancer* 58, 903–914. doi: 10.1002/gcc.22750

Uchida, J., Kato, K., Kukita, Y., Kumagai, T., Nishino, K., Daga, H., et al. (2015). Diagnostic Accuracy of Noninvasive Genotyping of EGFR in Lung Cancer Patients by Deep Sequencing of Plasma Cell-Free DNA. *Clin. Chem.* 61, 1191–1196. doi: 10.1373/clinchem.2015.241414

Ulrich, B. C., and Paweletz, C. P. (2018). Cell-Free DNA in oncology: gearing up for clinic. *Ann. Lab. Med.* 38, 1–8. doi: 10.3343/alm.2018.38.1.1

van der Pol, Y., and Mouliere, F. (2019). Toward the early detection of cancer by decoding the epigenetic and environmental fingerprints of cell-free DNA. *Cancer Cell* 36, 350–368. doi: 10.1016/j.ccell.2019.09.003

Vardiman, J. W., Harris, N. L., and Brunning, R. D. (2002). The World Health Organization (WHO) Classification of the Myeloid Neoplasms. *Blood* 100, 2292–2302.

Vardiman, J. W., Thiele, J., Arber, D. A., Brunning, R. D., Borowitz, M. J., Porwit, A., et al. (2009). The 2008 Revision of the World Health Organization (WHO) Classification of Myeloid Neoplasms and Acute Leukemia: rationale and important changes. *Blood* 114, 937–951.

Vasioukhin, V., Anker, P., Maurice, P., Lyautey, J., Lederrey, C., and Stroun, M. (1994). Point Mutations of the N-Ras Gene in the Blood Plasma DNA of Patients with Myelodysplastic Syndrome or Acute Myelogenous Leukaemia. *Br. J. Haematol.* 86, 774–779. doi: 10.1111/j.1365-2141.1994.tb04828.x

Vogelstein, B., and Kinzler, K. W. (1999). Digital PCR. *Proc. Natl. Acad. Sci. U.S.A.* 96, 9236–9241. doi: 10.1073/pnas.96.16.9236

Volckmar, A. L., Sültmann, H., Riediger, A., Fioretos, T., Schirmacher, P., Endris, V., et al. (2018). A field guide for cancer diagnostics using cell-free DNA: from principles to practice and clinical applications. *Gene Chromosome Cancer* 57, 123–139. doi: 10.1002/gcc.22517

Voso, M. T., Ottone, T., Lavorgna, S., Venditti, A., Maurillo, L., Lo-Coco, F., et al. (2019). MRD in AML: the role of new techniques. *Front. Oncol.* 9:655. doi: 10.3389/fonc.2019.00655

Walter, M. J., Shen, D., Ding, L., Shao, J., Koboldt, D. C., Chen, K., et al. (2012). Clonal architecture of secondary acute myeloid Leukemia. *N. Engl. J. Med.* 366, 1090–1098. doi: 10.1056/NEJMoa1106968

Wan, J. C. M., Massie, C., Garcia-Corbacho, J., Mouliere, F., Brenton, J. D., Caldas, C., et al. (2017). Liquid biopsies come of age: towards implementation of circulating tumour DNA. *Nat. Rev. Cancer* 17, 223–238. doi: 10.1038/nrc.2017.7

Welch, J. S., Ley, T. J., Link, D. C., Miller, C. A., Larson, D. E., Koboldt, D. C., et al. (2012). The origin and evolution of mutations in acute myeloid Leukemia. *Cell* 150, 264–278. doi: 10.1016/j.cell.2012.06.023

Wong, H. Y., Sung, A. D., Lindblad, K. E., Sheela, S., Roloff, G. W., Rizzieri, D., et al. (2019). Molecular measurable residual disease testing of blood during aml cytotoxic therapy for early prediction of clinical response. *Front. Oncol.* 8:669. doi: 10.3389/fonc.2018.00669

Yeh, P., Dickinson, M., Ftouni, S., Hunter, T., Sinha, D., Wong, S. Q., et al. (2017). Molecular disease monitoring using circulating tumor DNA in Myelodysplastic Syndromes. *Blood* 29, 1685–1690.

Yoest, J. M., Shirai, C. L., and Duncavage, E. J. (2020). Sequencing-based measurable residual disease testing in acute myeloid Leukemia. *Front. Cell Dev. Biol.* 8:249. doi: 10.3389/fcell.2020.00249

Zhong, L., Chen, J., Huang, X., Li, Y., and Jiang, T. (2018). Monitoring immunoglobulin heavy chain and T-Cell receptor gene rearrangement in CfDNA as minimal residual disease detection for patients with acute myeloid Leukemia. *Oncol. Lett.* 16, 2279–2288. doi: 10.3892/ol.2018.8966

Conflict of Interest: The authors declare that the research was conducted in the absence of any commercial or financial relationships that could be construed as a potential conflict of interest.

Copyright © 2020 Thakral, Gupta, Sahoo, Verma, Kumar and Vashishtha. This is an open-access article distributed under the terms of the Creative Commons Attribution License (CC BY). The use, distribution or reproduction in other forums is permitted, provided the original author(s) and the copyright owner(s) are credited and that the original publication in this journal is cited, in accordance with accepted academic practice. No use, distribution or reproduction is permitted which does not comply with these terms.

frontiers in Cell and Developmental Biology

ORIGINAL RESEARCH
published: 07 January 2021
doi: 10.3389/fcell.2020.602493

The Identification of Plasma Exosomal miR-423-3p as a Potential Predictive Biomarker for Prostate Cancer Castration-Resistance Development by Plasma Exosomal miRNA Sequencing

Tianyu Guo[1,2], Yang Wang[1,3], Jing Jia[4], Xueying Mao[1], Elzbieta Stankiewicz[1], Glenda Scandura[1], Edwina Burke[1], Lei Xu[1,5], Jacek Marzec[1,6], Caitlin R. Davies[1], Jiaying Jasmin Lu[1], Prabhakar Rajan[1,7,8,9], Alistair Grey[7,8], Karen Tipples[7], John Hines[7,9], Sakunthala Kudahetti[1], Tim Oliver[1], Thomas Powles[1], Constantine Alifrangis[7,9], Manish Kohli[10,11], Greg Shaw[7,8,9], Wen Wang[12], Ninghan Feng[3], Jonathan Shamash[13], Daniel Berney[1], Liang Wang[4] and Yong-Jie Lu[1,3]

[1] Centre for Cancer Biomarker and Biotherapeutics, Barts Cancer Institute, Queen Mary University of London, London, United Kingdom, [2] Department of Cell Biology, Zhejiang University School of Medicine, The Second Affiliated Hospital, Hangzhou, China, [3] Department of Urology, Affiliated Wuxi No. 2 Hospital of Nanjing Medical University, Wuxi, China, [4] Department of Tumor Biology, H. Lee Moffitt Cancer Center, Tampa, FL, United States, [5] Department of Urology, Zhongshan Hospital, Fudan University, Shanghai, China, [6] Centre for Cancer Research, University of Melbourne, Melbourne, VIC, Australia, [7] Department of Urology, Barts Health NHS, London, United Kingdom, [8] Division of Surgery and Interventional Sciences, University College London, London, United Kingdom, [9] Department of Uro-oncology, University College London NHS Foundation Trust, London, United Kingdom, [10] Department of Medicine, University of Utah, Huntsman Cancer Institute, Salt Lake City, UT, United States, [11] Department of Oncology, Mayo Clinic, Rochester, MN, United States, [12] Division of Bioengineering, School of Engineering and Materials Science, Queen Mary University of London, London, United Kingdom, [13] Department of Medical Oncology, Barts Health NHS, London, United Kingdom

Castration-resistant prostate cancer (CRPC) is the major cause of death from prostate cancer. Biomarkers to improve early detection and prediction of CRPC especially using non-invasive liquid biopsies could improve outcomes. Therefore, we investigated the plasma exosomal miRNAs associated with CRPC and their potential for development into non-invasive early detection biomarkers for resistance to treatment. RNA-sequencing, which generated approximately five million reads per patient, was performed to identify differentially expressed plasma exosomal miRNAs in 24 treatment-naive prostate cancer and 24 CRPC patients. RT-qPCR was used to confirm the differential expressions of six exosomal miRNAs, miR-423-3p, miR-320a, miR-99a-5p, miR-320d, miR-320b, and miR-150-5p ($p = 7.3 \times 10^{-8}$, 0.0020, 0.018, 0.0028, 0.0013, and 0.0058, respectively) firstly in a validation cohort of 108 treatment-naive prostate cancer and 42 CRPC patients. The most significant differentially expressed miRNA, miR-423-3p, was shown to be associated with CRPC with area under the ROC curve (AUC) = 0.784. Combining miR-423-3p with prostate-specific antigen (PSA) enhanced the prediction of CRPC (AUC = 0.908). A separate research center validation with 30 treatment-naive and 30 CRPC patients also confirmed the differential expression of miR-423-3p ($p = 0.016$). Finally, plasma exosomal miR-423-3p expression in CRPC patients was compared to

OPEN ACCESS

Edited by:
George Calin,
University of Texas MD Anderson Cancer Center, United States

Reviewed by:
Eddie Luidy Imada,
Johns Hopkins Medicine, United States
Fuming Li,
University of Pennsylvania, United States

***Correspondence:**
Yong-Jie Lu
y.j.lu@qmul.ac.uk

Specialty section:
This article was submitted to Molecular and Cellular Oncology, a section of the journal Frontiers in Cell and Developmental Biology

Received: 03 September 2020
Accepted: 30 November 2020
Published: 07 January 2021

Citation:
Guo T, Wang Y, Jia J, Mao X, Stankiewicz E, Scandura G, Burke E, Xu L, Marzec J, Davies CR, Lu JJ, Rajan P, Grey A, Tipples K, Hines J, Kudahetti S, Oliver T, Powles T, Alifrangis C, Kohli M, Shaw G, Wang W, Feng N, Shamash J, Berney D, Wang L and Lu Y-J (2021) The Identification of Plasma Exosomal miR-423-3p as a Potential Predictive Biomarker for Prostate Cancer Castration-Resistance Development by Plasma Exosomal miRNA Sequencing. Front. Cell Dev. Biol. 8:602493. doi: 10.3389/fcell.2020.602493

36 non-CRPC patients under androgen depletion therapy, which showed significantly higher expression in CRPC than treated non-CRPC patients ($p < 0.0001$) with AUC = 0.879 to predict CRPC with no difference between treatment-naive and treated non-CRPC patients. Therefore, our findings demonstrate that a number of plasma exosomal miRNAs are associated with CRPC and miR-423-3p may serve as a biomarker for early detection/prediction of castration-resistance.

Keywords: prostate cancer, castration-resistance development, biomarker, plasma exosome miRNA, miR-423-3p

INTRODUCTION

Prostate cancer (PCa) is the most frequently diagnosed male cancer and the second-leading cause of oncological mortality in the USA, with estimated 174,650 new cases and 31,620 deaths in 2019 (Siegel et al., 2019). Androgen deprivation therapy (ADT) has been the standard of care for initial management of locally advanced and metastatic PCa. However, patients inevitably progress to castration-resistant PCa (CRPC) within 1–3 years from the start of primary ADT, despite the initial benefits (Chandrasekar et al., 2015). The prognosis of CRPC patients is historically poor, with median overall survival after ADT failure being 2–3 years (West et al., 2014; Ryan et al., 2015). Prognostic biomarkers for patients with CRPC have been investigated in many studies (Armstrong et al., 2012; Olmos et al., 2012; Ross et al., 2012; Huang et al., 2015; Pantel et al., 2019) and circulating tumor cell analysis has been approved by the FDA as a prognostic biomarker for patients with metastatic CRPC (Pantel et al., 2019). In contrast, biomarkers to predict or monitor CRPC development are rarely investigated (Varenhorst et al., 2016), despite the fact that prediction and early detection of CRPC and earlier modifications to treatment may be more effective in controlling the disease than changing therapy after clinically apparent CRPC has developed.

Currently, CRPC is usually diagnosed based on biochemical and radiographic progression (Cornford et al., 2017). Biochemical progression relies on measuring the serum prostatic-specific antigen (PSA) level. However, the serum PSA level does not always correlate with the clinical status of CRPC (Mizokami et al., 2017). Radiographic progression reflects well-developed CRPC and necessitates frequent bone and CT scans. These issues may lead to delays in treatment changes, missing the opportunity to eradicate small subclones of CRPC cells when it is easier to cure. Thus, it is important to further investigate the molecular mechanisms of CRPC development and identify additional liquid biopsy biomarkers, which can be more easily utilized to efficiently detect/predict early CRPC to promptly change treatment into one of the effective therapies developed in recent years for CRPC patients (Afshar et al., 2015).

Exosomes are small cell secreted vesicles (30–150 nm), which contain numerous molecular constituents, including lipids, proteins, RNA and DNA, and mediate cell-cell communication by transferring these exosomal components between cells (Rana et al., 2013; Matei et al., 2017; Chen et al., 2018). MicroRNAs (miRNAs) are enriched in exosomes (Valadi et al., 2007) and can be transferred between cells via exosomes to regulate various biological processes associated with cancer development and progression (Rana et al., 2013; Sánchez et al., 2016). MiRNAs in exosomes are protected from degradation in the circulation (Ge et al., 2014) and studies have demonstrated the potential of exploiting exosomal miRNAs as non-invasive and dynamic biomarkers in cancer diagnosis and prognosis (Hu et al., 2012). Plasma exosomal miRNAs have been previously reported as valuable prognostic biomarkers in patients who have already developed CRPC (Huang et al., 2013, 2015; Yuan et al., 2016). However, no studies on the association of plasma exosomal miRNA with CRPC development have been reported.

Identification of plasma exosomal miRNAs associated with CRPC would not only improve our understanding of CRPC development mechanisms, but more importantly help the development of biomarkers to predict/detect the early occurrence of CRPC, enabling prompt alteration of therapeutic regimens before CRPC is fully developed. We therefore investigated plasma exosomal miRNAs associated with CRPC and evaluated their potential as predictive biomarkers for CRPC occurrence.

MATERIALS AND METHODS

Patients

Blood samples from 24 treatment-naive PCa patients and 24 CRPC patients for RNA next-generation sequencing (RNA-seq) and 108 treatment-naive PCa and 42 CRPC patients (including the 24 CRPC patients used for RNA-seq) in the validation cohort I were collected with patients' informed consent from St Bartholomew's Hospital, BartsHealth NHS, London, UK, between 2015 and 2018. Samples from an additional cohort of treated non-CRPC patients included 36 PCa patients who had started initial hormone-therapy <3 months before blood collection was obtained also from St Bartholomew's Hospital. Blood samples from 30 treatment-naive PCa patients and 30 CRPC patients in the independent validation cohort II were collected from Mayo Clinic, Rochester, US between 2009 and 2012 with patients' informed consent. All CRPC patients had been treated with ADT and had evidence of disease progression with rising PSA and/or imaging-based progression. Patients' clinical data is summarized in **Table 1**. Use of patient blood samples and clinical data in this study was approved by London City & East Research Ethics Committee (09/H0704/4+5) and Institutional Review Board of Medical College of Wisconsin (PRO00017780). RNA-seq and validation workflow is presented in **Figure 1**.

TABLE 1 | Clinical characteristics of patients in the RNA-sequencing and RT-qPCR validation cohorts.

	RNA-sequencing cohort		Validation cohort I		Treated non-CRPC	Validation cohort II	
	Treatment-naive	CRPC	Treatment-naive	CRPC[a]		Treatment-naive	CRPC
Case number	24	24	108	42	36	30	30
Age, yr, median (IQR)	65.15 (56.13-70.73)	75.55 (68.75-81.89)	65.90 (57.89–72.10)	72.65 (68.38–80.88)	65.90 (61.10–73.55)	67.30 (63.38–80.55)	71.70 (65.85–76.58)
Gleason score at diagnosis							
≤6	8	1	36	1	1	2	4
7	16	2	58	7	11	14	9
8	0	5	6	8	5	3	4
≥9	0	9	8	16	14	8	10
unknown	0	7	0	10	5	3	3
Median PSA at sample collection, ng/ml (IQR)	9.9 (6.9–12.75)	51 (17.75–241.8)	8.9 (5.75–13)	57 (21.5–192.3)	15.5 (6.255–112.7)	7 (1.75–28.55)[b]	47.7 (9.35–119)

Yr, year; IQR, interquartile range; CRPC, castration-resistant prostate cancer; PSA, prostate-specific antigen. [a]including 24 patients used for RNA-sequencing; [b]one patient's data is missing.

Exosome Isolation

Plasma was isolated within 2 h of blood draw by centrifugation of whole blood at 1,200 g for 10 min, followed by another centrifugation of the supernatant at 2,000 g for 10 min. The supernatant was taken as plasma and stored at −80°C for future use. Two hundred microliter of plasma from each case was used. Prior to exosome precipitation, plasma samples were treated with RNase A to remove free circulating RNAs and then RNase A was inactivated with RNase inhibitor. Exosomes were isolated using the Total Exosome Isolation Kit (from plasma) (Invitrogen™) following manufacturer's instructions. For the validation cohort at Mayo Clinic, US, exosomes were isolated using ExoQuick Plasma prep and Exosome precipitation kit (System Biosciences) without RNase pre-treatment.

RNA Extraction

The exosome pellet was re-suspended in Buffer RLT (Qiagen) with 0.25 μg/μl Proteinase K and incubated at 50°C for 30 min. Exosomal RNA was then extracted using miRNeasy Micro Kit (Qiagen) and QIAzol Lysis Reagent (Qiagen) according to the manufacturer's protocol. PC3 cell miRNAs were extracted using AllPrep® DNA/RNA/Protein Mini kit (Qiagen) and miReasy micro kit (Qiagen) according to the recommended protocol.

RNA-Seq and Data Analysis

Indexed libraries were prepared from the exosomal RNA as instructed by the NEBNext Multiplex Small RNA Library Prep Set for Illumina (NEB) without size selection. RNA-seq was performed on Illumina NextSeq 500 platform. The data was trimmed with trimgalore (end minimum quality level 30 and minimum read length 15) and aligned to human reference genome build hg19 with Bowtie 0.12.8 (seed mismatch limit 1 and seed length 10) implemented in BaseSpace (Illumina, CA). BAM files were uploaded into Partek Genomic Suite (Partek Inc) and annotated against mirBase 20 mature miRNA. Samples were sequenced twice and read counts from two runs were combined for data analysis. The raw data was deposited to Gene Expression Omnibus (accession number: GSE136321). MiRNAs expressed in <25% of samples were removed from differential expression analysis. The miRNA read counts were analyzed using four pipelines to identify differentially expressed miRNAs (**Figure 1**): (1) Counts per million (CPM), (2) The trimmed mean of M-value normalization (TMM) (Robinson and Oshlack, 2010), (3) Limma (Ritchie et al., 2015), and (4) DESeq2 (Love et al., 2014). For CPM analysis, filtered read counts were transformed to CPM using the cpm() function implemented in edgeR package (version 2.4.0) and then Welch's *t*-test was performed in SPSS 24. TMM was performed using functions implemented in the edgeR. Filtered read counts were input as a DGEList in R (v4.0.2). TMM normalization was performed using calcNormFactors() function implemented in edgeR() package. EstimateCommonDisp() was performed to estimate the common dispersion parameter and the ExactTest() functions in edgeR were used to detect differentially expressed miRNAs. The results were then written out as a csv file. Pipeline combining functions in Limma and edgeR were performed using functions implemented in both software packages in R. Filtered read counts were input as a DGEList and normalized with calcNormFactors() function. The normalized data was voom transformed with voom() function. Then a linear model was fitted using lmfit() and the empirical Bayes statistics was applied with eBayes() function to smooth the standard errors. The results were then written out as a csv file. DESeq2 differential expression analysis was performed using functions in the DESeq2 R package (v4.0.2). A DESeq data set was generated with filtered read counts using DESeqDataSetFromMatrix() function implemented in DESeq2() package. Normalization and differentially expressed gene analysis was done using DESeq() function. The results were then written out as a csv file.

Reverse Transcription Quantitative Real-Time Polymerase Chain Reaction (RT-qPCR)

The reverse transcription was performed using miScript II RT kit (Qiagen). RT-qPCR was performed with miScript primer assays (Qiagen) (MS00004179—Hs_miR-423_1 miScript Primer, MS00008932—Hs_miR-193a-5p_1 miScript Primer,

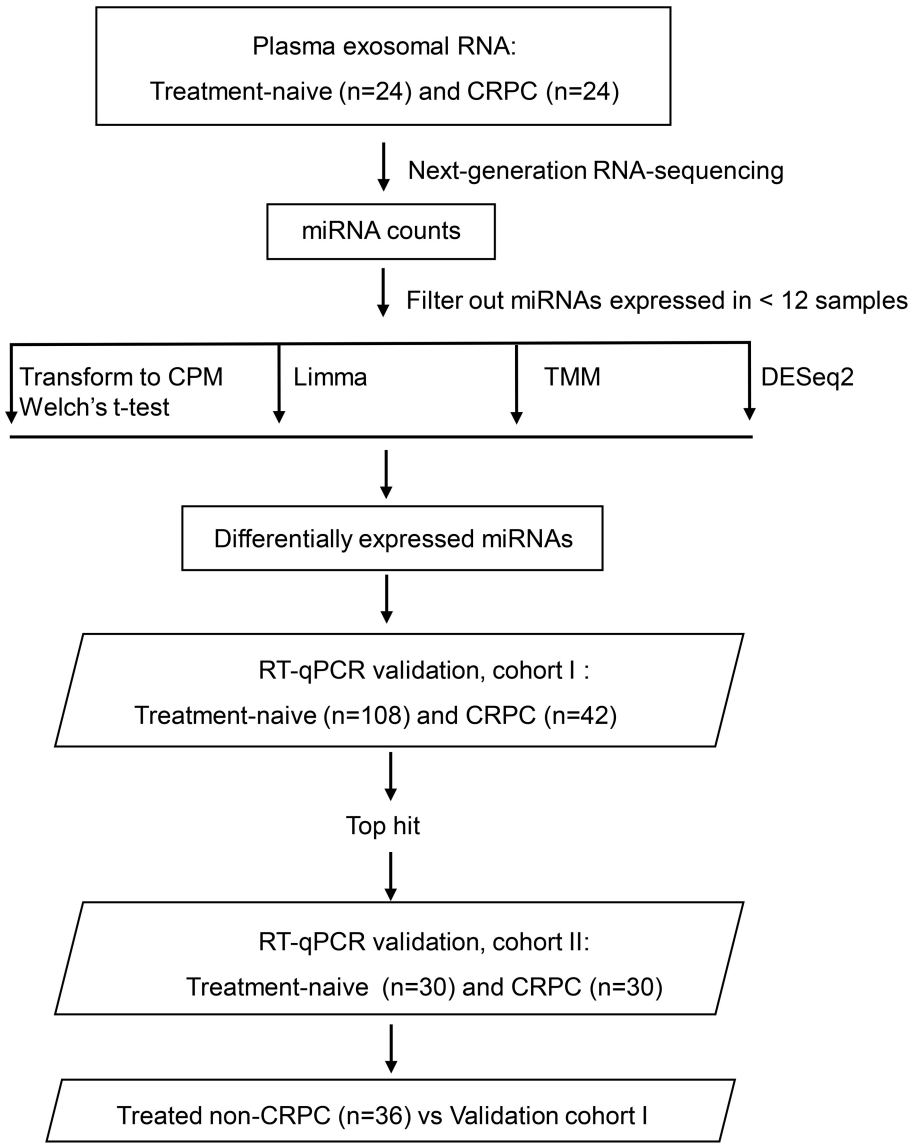

FIGURE 1 | Overview of the plasma exosomal miRNA analysis workflow. CRPC, castration-resistant prostate cancer; CPM, counts per million transformation; Limma, linear models for microarray and RNA-sequencing data; TMM, the trimmed mean of M-value normalization.

MS00003738—Hs_miR-200a_1 miScript Primer, MS00032158—Hs_miR-99a_2 miScript Primer, MS00014707—Hs_miR-320a_1 miScript Primer, MS00031710—Hs_miR-320d_2 miScript Primer, MS00031703—Hs_miR-320b_2 miScript Primer, MS00006552—Hs_miR-24_1 miScript Primer, MS00010752—Hs_miR-9_1 miScript Primer, MS00007350—Hs_miR-30a-5p_1 miScript Primer, MS00003129—Hs_let-7c_1 miScript Primer, MS00008372—Hs_miR-101_3 miScript Primer, MS00003556—Hs_miR-148a_1 miScript Primer, MS00003577—Hs_miR-150_1 miScript Primer, MS00031829—Hs_miR-375_2 miScript Primer, MS00004242—Hs_miR-451_1 miScript Primer) and miScript SYBR® Green PCR Kit (Qiagen) on Quantstudio™ real-time PCR system (ThermoFisher Scientific). Let-7c-5p and miR-30a-5p were selected as endogenous reference genes based on their small variation across all samples in our sequencing data and previous publication (Huang et al., 2015). $\Delta Ct = (Ct^{miRNA} - \text{average } Ct^{referencegenes})$ and where PC3 cell line miRNA was used to normalize multiple RT-qPCR plates, ΔCt was calculated as sample $(Ct^{miRNA} - \text{average } Ct^{referencegenes}) - PC3\ (Ct^{miRNA} - \text{average } Ct^{referencegenes})$. The relative expression level of miRNAs in exosomes was calculated as $2^{-\Delta Ct}$. All reactions were run in triplicate.

Pathway Over-Representation Analysis

Targets of miRNAs were retrieved from TarBase v7.0 and pathway overrepresentation analysis was performed using KEGG pathways via online tool DIANA-miRPath v3.0 (http://snf-515788.vm.okeanos.grnet.gr/) (Vlachos et al.,

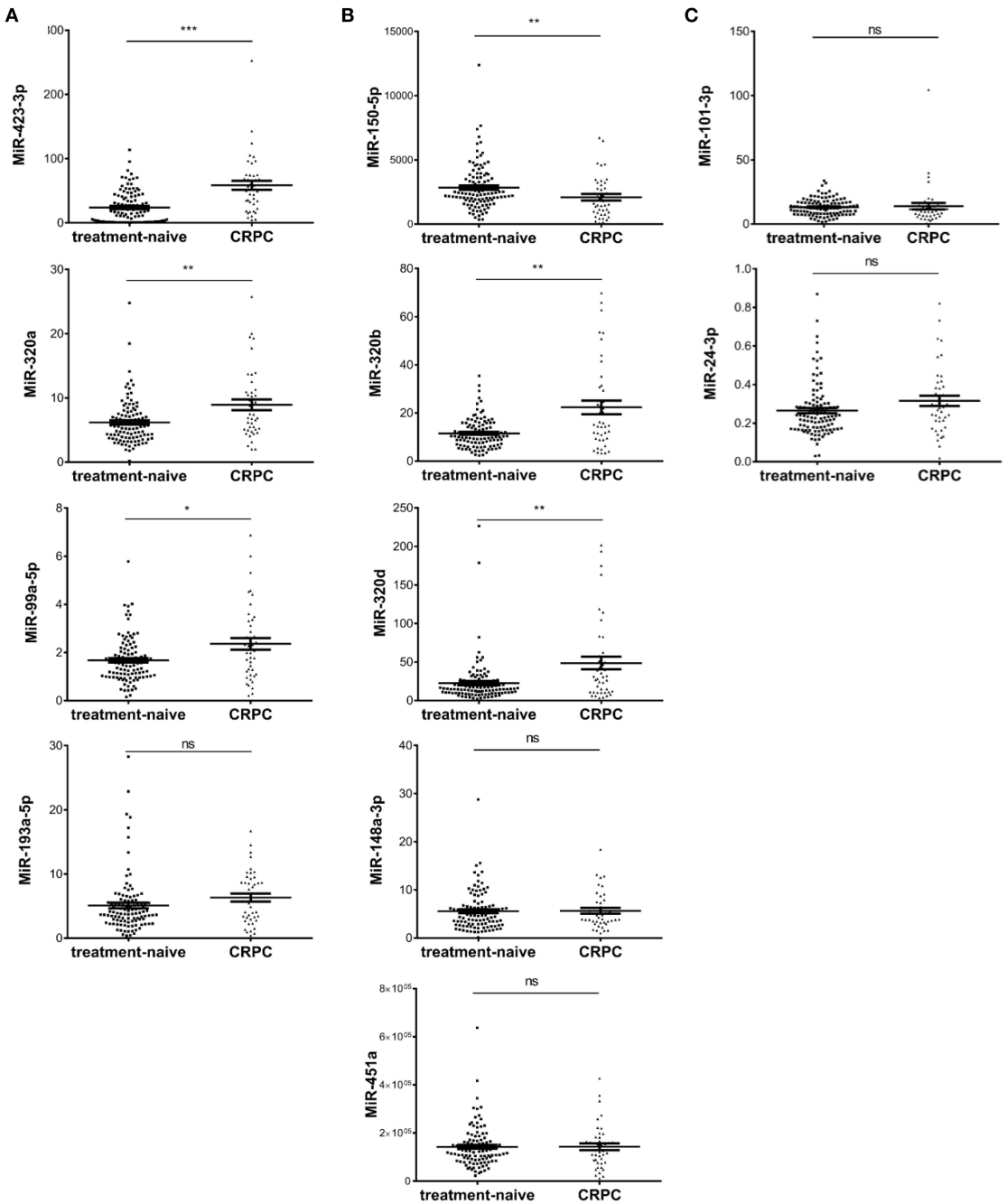

FIGURE 2 | Scatter plots of plasma exosomal miRNA expression levels evaluated by RT-qPCR in validation cohort I of 108 treatment-naive prostate cancer and 42 castration resistant prostate cancer (CRPC) patients. **(A)** The five significant differentially expressed miRNAs from RNA-seq identified by four RNA-seq analysis methods; **(B)** The six significant differentially expressed miRNAs from RNA-seq identified by three RNA-seq analysis methods; **(C)** The differentially expressed miRNAs from RNA-seq identified by two RNA-seq analysis methods. The y-axis shows the relative expression level of miRNAs calculated by $2^{-\Delta Ct}$. The error bars show the mean ± standard error of mean (SEM). $^{*}p < 0.05$, $^{**}p < 0.01$, $^{***}p < 0.001$, ns, not significant.

2015). The CRPC associated miRNAs identified in this study were input and analyzed using TarBase to retrieve target genes of the miRNAs. Pathways union mode was used to identify all the pathways significantly targeted by the selected miRNAs. False Discovery Rate correction was applied. *P*-value threshold was set at 0.05 and microT threshold was defaulted at 0.8. Fisher's exact test was selected as the enrichment analysis method. To generate heatmap for each miRNA, significance clusters/heatmap option was selected.

Statistical Analysis

Analysis of the RNA-seq data was described in previous section. Unpaired Mann-Whitney U tests were performed on RT-qPCR relative expression levels to identify differences in exosomal miRNA expression levels between treatment-naive PCa, treated non-CRPC and CRPC and were performed in GraphPad Prism 7. Receiver operating characteristic (ROC) curves were generated and the area under the curve (AUC) was used to evaluate the prediction values of parameters for CRPC. ROC curve and AUC was generated in GraphPad Prism 7. Binomial logistic regression was performed with miR-423-3p relative expression level and PSA level as predictors for CRPC (yes, no) using the binomial logistic regression function in SPSS 24. A combination model (CM) was computed as the linear predictor of the fitted bivariate logistic model with PSA and 423-3p relative expression level as only predictors as a*PSA+b*miR-423-3p, where the values of "a" and "b" are the covariance factors of PSA and miR-423-3p relative expression level, respectively. Univariate logistic regression analyses were performed separately for miR-423-3p relative expression level and PSA level to evaluate and compare their association with CRPC. The miR-423-3p relative expression and PSA level were treated as continuous variables, and CRPC status was considered as a categorical variable. To examine the independent association of miR-423-3p expression with CRPC status and adjust it for PSA level a multivariate logistic regression analysis was performed. All statistical tests were two sided. We did not apply multiple event testing correction to exosomal RNA-seq data analysis, since there are only a small number of miRNAs for the analysis and the differential miRNA expression was identified by different analysis tools to select candidates (more than selected based on adjusted *p*-value) for experimental validation. Bonferroni correction test was performed to modify *p*-values for RT-qPCR result multiple tests through dividing the critical *p*-value by the number of comparisons being made.

RESULTS

The Plasma Exosomal miRNA Expression Profiles in Patients With Treatment-Naive PCa and CRPC

To identify candidate plasma exosomal miRNAs associated with CRPC development, RNA-seq was performed in a screening cohort of 24 treatment-naive PCa patients and 24 CRPC patients. Combing two runs of data, the RNA-seq produced an average of five million reads per sample. This data enabled us to detect 612 plasma exosomal miRNAs in total, with 483 detected in treatment-naive PCa and 499 in CRPC patients (**Supplementary Table 1**). There were 37 miRNAs which were consistently detected in all individual samples, while 45 miRNAs detected in all CRPC samples and 45 miRNAs detected in all treatment-naive PCa samples (**Supplementary Table 2**). On average, miR-451a was the most abundant miRNA in both treatment-naive PCa and CRPC. The top ten most abundant miRNAs detected in these two groups are listed in **Supplementary Table 3**.

Identification of Differential Expression of miRNAs by RNA-Seq Comparing Patients With Treatment-Naive PCa and CRPC

To identify differentially expressed plasma exosomal miRNAs between the treatment-naive PCa and CRPC patients, we employed four methods (CPM, TMM, Limma, and DESeq2) to analyze the RNA-seq data. MiRNAs expressed in <25% of samples were filtered out from the analysis. From the remaining 185 miRNAs, we identified 13, 13, 11, and 14 differentially expressed miRNAs by Limma, TMM, CPM, and DESeq2 methods, respectively, at $p < 0.01$ (**Table 2** and **Supplementary Table 4**). Among them, five miRNAs (miR-423-3p, miR-99a-5p, miR-320a, miR-200a-3p, and miR-193a-5p) were identified by all four methods and they were all present at higher levels in CRPC than treatment naive PCa patient samples. Six miRNAs (miR-375, miR-451a, miR-320b, miR-148a-3p, miR-150-5p, miR-320d) were detected by three of the methods and three miRNAs (miR-101-3p, miR-9-5p, miR-24-3p) by two of the methods. Of note, all of the miRNAs with $p < 0.01$ from DESeq2 were also detected by one of the other methods. Except for DESeq2, the other three methods presented some unique miRNAs which were not detected by others.

Validation of Plasma Exosomal miRNAs as Potential Biomarkers for CRPC by RT-qPCR

To validate candidate plasma exosomal miRNAs as biomarkers for CRPC development, we performed RT-qPCR and tested all the five miRNAs with $p < 0.01$ in all four RNA-seq analysis methods, the six miRNAs with $p < 0.01$ in three methods, and three miRNAs with $p < 0.01$ in two methods in validation cohort I, consisting of 108 treatment-naive PCa and 42 CRPC patients collected in St Bartholomew's Hospital. Of the five miRNAs identified by all four sequencing data analysis methods, the expression of miR-200a-3p was too low to be detected by RT-qPCR. Out of the remaining four miRNAs, three miRNAs, miR-423-3p, miR-320a, and miR-99a-5p were significantly differentially expressed between treatment-naive PCa patients and CRPC ($p = 7.3 \times 10^{-8}$, 0.002 and 0.0186, respectively) (**Figure 2A**), while miR-193a-5p showed a trend without a statistically significant difference ($p = 0.0547$). After multiple testing correction, miR-423-3p and miR-320a remained statistically significant. Consistent with the RNA-seq data, these miRNAs were expressed at higher levels in CRPC compared to treatment-naive PCa patients.

Among the six miRNAs which showed significant difference in three of the four RNA-seq analysis methods, miR-375 could not be detected efficiently by our RT-qPCR method. Of the remaining five miRNAs, three miRNAs, miR-320d, miR-320b, and miR-150-5p were significantly differentially expressed ($p = 0.0028$, 0.0013, and 0.0058, respectively) (**Figure 2B**) and all remained statistically significant after multiple testing correction. miR-148a-3p and miR-451a showed no significant difference between treatment-naive PCa and CRPC ($p = 0.95$ and 0.98, respectively) (**Figure 2B**).

TABLE 2 | Differentially expressed plasma exosomal miRNAs at $p < 0.01$ between treatment-naive prostate cancer and CRPC by RNA-sequencing analyses.

Limma		TMM		CPM		DESeq2	
MiRNA	***p*-value**	**MiRNA**	***p*-value**	**MiRNA**	***p*-value**	**MiRNA**	***p*-value**
miR-375	3.73×10^{-04}	miR-375	5.71×10^{-11}	**miR-423-3p**	4.20×10^{-04}	miR-375	7.79×10^{-07}
miR-193a-5p	3.93×10^{-04}	**miR-193a-5p**	1.32×10^{-05}	miR-21-5p	1.06×10^{-03}	**miR-193a-5p**	2.36×10^{-05}
miR-101-3p	9.07×10^{-04}	miR-9-5p	1.56×10^{-05}	**miR-320a**	1.10×10^{-03}	miR-320b	1.53×10^{-04}
miR-451a	1.70×10^{-03}	miR-184	9.39×10^{-05}	**miR-193a-5p**	2.07×10^{-03}	**miR-200a-3p**	2.73×10^{-04}
miR-320b	1.73×10^{-03}	**miR-200a-3p**	4.00×10^{-04}	miR-451a	2.61×10^{-03}	**miR-320a**	2.83×10^{-04}
miR-320a	3.07×10^{-03}	miR-320b	4.90×10^{-04}	miR-24-3p	3.25×10^{-03}	**miR-99a-5p**	5.40×10^{-04}
miR-423-3p	4.79×10^{-03}	miR-148a-3p	1.04×10^{-03}	**miR-99a-5p**	4.74×10^{-03}	**miR-423-3p**	6.32×10^{-04}
miR-148a-3p	5.33×10^{-03}	**miR-99a-5p**	1.70×10^{-03}	miR-146a-5p	7.78×10^{-03}	miR-9-5p	6.39×10^{-04}
miR-150-5p	5.87×10^{-03}	miR-150-5p	2.63×10^{-03}	**miR-200a-3p**	8.33×10^{-03}	miR-150-5p	8.47×10^{-04}
miR-342-5p	6.39×10^{-03}	miR-320d	2.90×10^{-03}	miR-22-5p	9.21×10^{-03}	miR-148a-3p	1.09×10^{-03}
miR-200a-3p	6.55×10^{-03}	**miR-320a**	3.26×10^{-03}	miR-320d	9.82×10^{-03}	miR-320d	2.86×10^{-03}
miR-99a-5p	8.05×10^{-03}	**miR-423-3p**	3.27×10^{-03}			miR-101-3p	5.31×10^{-03}
miR-30c-5p	8.84×10^{-03}	miR-122-5p	7.07×10^{-03}			miR-451a	5.62×10^{-03}
						miR-24-3p	6.09×10^{-03}

CRPC, castration-resistant prostate cancer; CPM, counts per million transformation; TMM, the trimmed mean of M-value normalization. MiRNAs in bold are these differentially expression by all four analysis methods.

Among the three miRNAs which showed significant difference in only two of the four RNA-seq analysis methods, miR-9 had too low an expression to be detected. MiR-101-3p and miR-24-3p showed no significant difference ($p = 0.086$ and 0.075, respectively) (**Figure 2C**).

As treatment-naive PCa is mostly of low Gleason score (6 and 7) and more than half of the CRPC cases have a high Gleason score (8 or higher), we interrogated Gleason score associations in the treatment-naive PCa cohort, where we have sufficient number of patients for subgroup analysis. We found no significant association of Gleason score with the expression of any of the six miRNAs (**Supplementary Figure 1**).

To evaluate the predictive value of the plasma exosomal miRNAs for CRPC, we performed ROC curves analysis based on the RT-qPCR results. Comparing the treatment-naive PCa and CRPC, the AUC of miR-423-3p, miR-320a, miR-99a-5p, miR-320d, miR-320b, miR-150-5p was 0.784 (95% confidence interval (CI): 0.707–0.860, $p < 0.0001$), 0.663 (95% CI: 0.562–0.764, $p = 0.0020$), 0.624 (95% CI: 0.514–0.734, $p = 0.019$), 0.657 (95% CI: 0.549–0.766, $p = 0.0028$), 0.670 (95% CI: 0.560–0.779, $p = 0.0013$), and 0.645 (95% CI: 0.539–0.751, $p = 0.0058$), respectively (**Figure 3A**). When miR-423-3p, which showed the best predictive value, was combined with PSA (AUC = 0.837, 95% CI: 0.740–0.934) with a logistic binominal regression model (combination model = 0.026*PSA+0.033*miR-423-3p), the performance improved to AUC = 0.908 (95% CI: 0.861–0.955, $p < 0.0001$) with 80.95% (95% CI: 65.88–91.4%) sensitivity and 82.41% (73.9–89.06%) specificity (**Figure 3B**). Using a multivariate logistic regression analysis, including miR-423-3p expression and PSA level as variables, we found that both exosomal miR-423-3p expression ($p = 7.29 \times 10^{-05}$) and PSA level ($p = 0.000557$) were independently associated with CRPC status.

Pathway Analysis of Differentially Expressed Exosomal miRNAs

After identified plasma exosomal miRNAs associated with CRPC, we sought to explore the potential pathways in which these miRNAs are involved. We performed functional pathway analysis of targets for the six validated CRPC associated miRNAs, miR-423-3p, miR-320a, miR-99a-5p, miR-320d, miR-320b, and miR-150-5p. Targets of miRNAs were retrieved from TarBase v7.0 and pathway overrepresentation analysis was performed using KEGG pathways via DIANA-miRPath v3.0. Most of the significantly enriched pathways were cancer-associated. Hippo signaling pathway, TGF-beta signaling pathway and Adherens junction were the three most significant pathways as shown in the collected target analysis of the six differentially expressed miRNAs in **Table 3**. Additionally, we also explored the significantly enriched pathways (corrected $p < 0.05$) for each miRNA (**Figure 4**).

Additional Sample Cohort Validation of Plasma Exosomal miR-423-3p as a CRPC Biomarker

To further validate the CRPC association of exosomal miR-423-3p, which showed the most significant difference between treatment-naive PCa and CRPC, its expression was investigated in an independent validation cohort II. This cohort consisted of 30 treatment-naive PCa and 30 CRPC patients from Mayo Clinic, where patients in the untreated PCa group were selectively enriched for metastatic disease (16/30). Plasma exosomal miRNAs were extracted by a different protocol to validation cohort I as described previously in materials and methods. Comparing the 30 treatment-naive PCa to the 30 CRPC patients, miR-423-3p was again expressed at a significantly ($p = 0.016$)

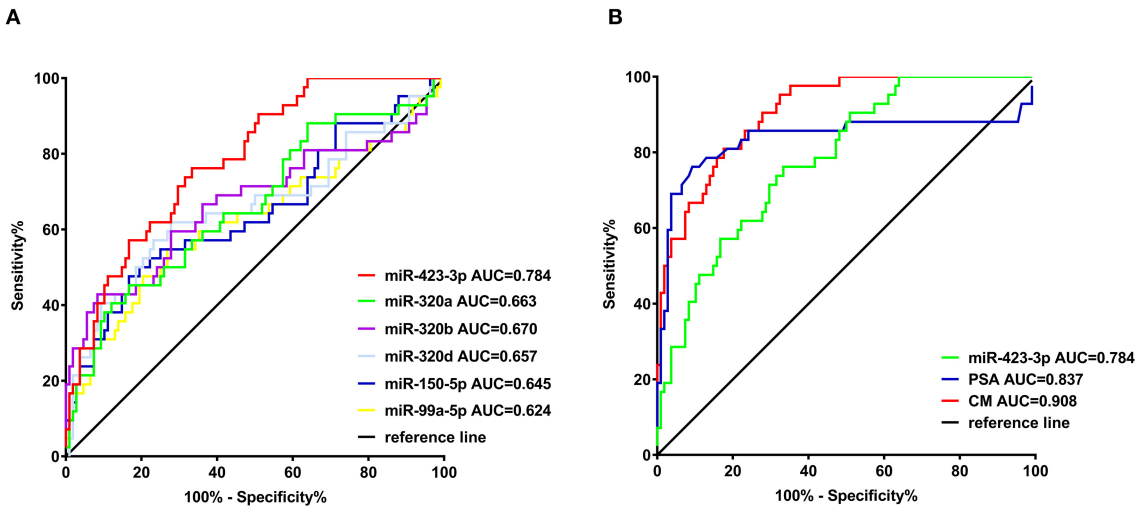

FIGURE 3 | Receiver operating characteristic (ROC) analysis of the efficiencies of classifiers in discriminating castration-resistant prostate cancer (CRPC) from treatment-naive prostate cancer. **(A)** ROC analysis of the six confirmed plasma exosomal miRNAs significantly different between treatment-naive and CRPC patients in validation cohort I; **(B)** ROC analysis of miR-423-3p, serum prostate-specific antigen (PSA) and the combination model (CM) of miR-423-3p and PSA in predicting CRPC in validation cohort I.

TABLE 3 | KEGG pathway analysis of target genes of six plasma exosomal miRNAs.

KEGG pathway	*p*-value	Number of target genes	miRNAs
Hippo signaling pathway	2.20×10^{-09}	20	3
TGF-beta signaling pathway	1.71×10^{-08}	15	2
Adherens junction	3.02×10^{-08}	16	4
Transcriptional misregulation in cancer	8.04×10^{-06}	32	2
Pathways in cancer	2.58×10^{-05}	72	3
Viral carcinogenesis	5.26×10^{-05}	43	3
Proteoglycans in cancer	6.67×10^{-05}	25	2
Glioma	1.06×10^{-04}	17	2
Glycosphingolipid biosynthesis—lacto and neolacto series	6.23×10^{-04}	2	1
Colorectal cancer	1.05×10^{-03}	16	2
Renal cell carcinoma	4.98×10^{-03}	5	1
Central carbon metabolism in cancer	6.43×10^{-03}	4	1
Chronic myeloid leukemia	0.012	19	2
Endometrial cancer	0.024	5	1
Pancreatic cancer	0.035	11	1

higher level in plasma exosomes from CRPC than treatment-naive PCa patients (**Figure 5A**), which confirmed the association of plasma exosomal miR-423-3p with CRPC regardless of different cohorts and different detection methods.

Increase of Plasma Exosomal miR-423-3p Expression Is Correlated With CRPC Development but Not in Response to ADT

To exclude the possibility that the increase of plasma exosomal miR-423-3p in CRPC as compared to treatment naive PCa is the result of ADT rather than castration resistance development, we further performed RT-qPCR analysis of plasma exosomal miR-423-3p in a group of 36 early stage treatment non-CRPC patients, who had been receiving ADT for <3 months. We found that the expression of plasma exosomal miR-423-3p was not significantly different between treatment-naive PCa and ADT-treated non-CRPC patients ($p = 0.3353$), indicating that ADT does not affect plasma exosomal miR-423-3p levels (**Figure 5B**). However, miR-423-3p expression was consistently and significantly ($p < 0.0001$) higher in CRPC than treated non-CRPC patients (**Figure 5B**). Based on the data from this cohort, plasma exosomal miR-423-3p alone had an excellent CRPC prediction value of AUC = 0.879 (95% CI: 0.7981–0.9599, $p < 0.0001$) (**Figure 5C**).

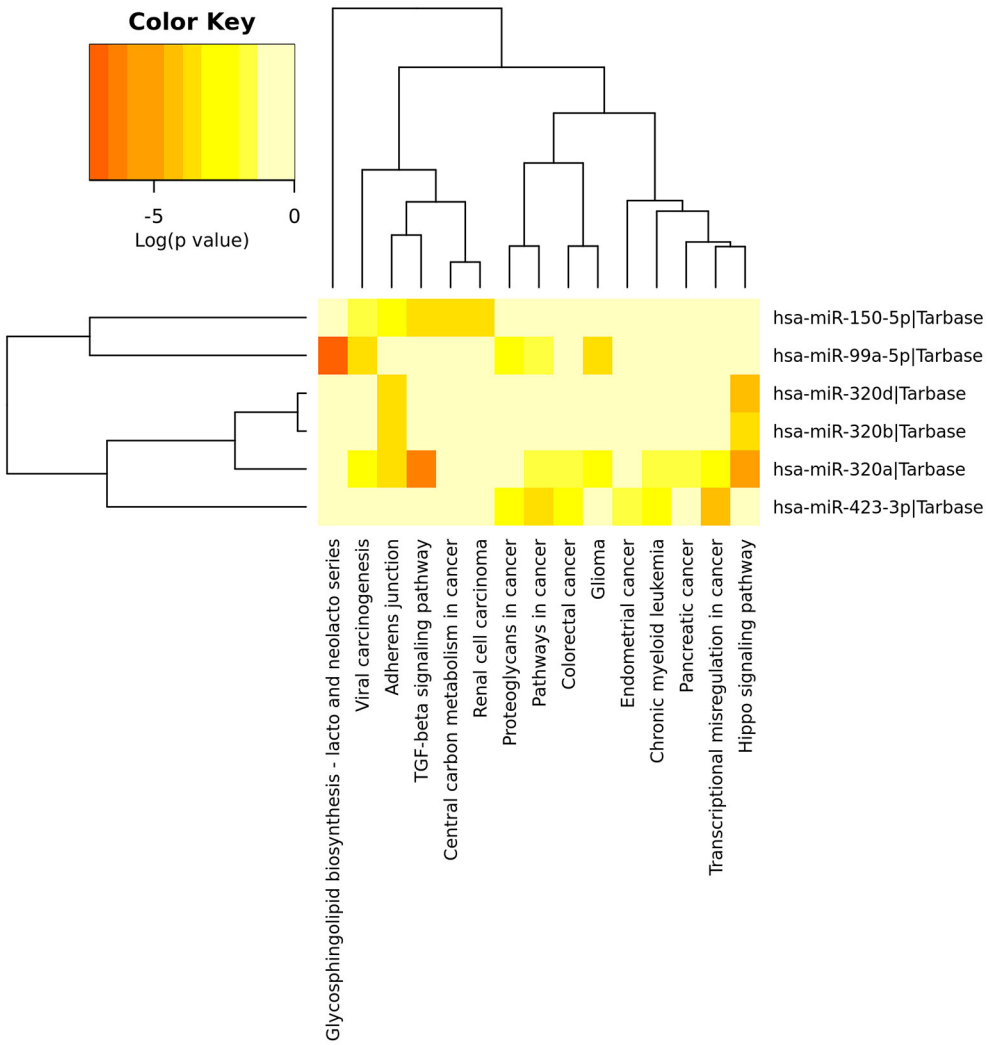

FIGURE 4 | Heatmap of significant pathways predicted by DIANA-miRPath (v.3.0) for six differentially expressed plasma exosomal miRNAs between treatment-naive prostate cancer and castration-resistant prostate cancer patients. Pathways are depicted on the x-axis and miRNAs on the y-axis. The color code represents the log (*p*-value), with the most significant predicted miRNA-pathway interactions in red.

DISCUSSION

The development of CRPC is a major clinical problem in the management of advanced PCa. While a number of studies have investigated biomarkers for CRPC prognosis (Armstrong et al., 2012; Olmos et al., 2012; Ross et al., 2012; Huang et al., 2015; Pantel et al., 2019), there are limited investigations into biomarkers predicting or monitoring CRPC development (Varenhorst et al., 2016). In this study, we generated plasma exosomal miRNA profiles in treatment-naive PCa and CRPC by RNA-seq and identified plasma exosomal miRNAs associated with CRPC. We validated six differentially expressed miRNAs, miR-423-3p, miR-320a, miR-99a-5p, miR-320d, miR-320b, and miR-150-5p in a larger cohort of treatment-naive PCa and CRPC samples by RT-qPCR, with multicenter validation of miR-423-3p differential expression, which is the most significantly associated miRNA with CRPC. Furthermore, we showed that increased plasma exosomal miR-423-3p expression in CRPC is not associated with the response to ADT treatment, confirming that its expression increase is a cause or result of CRPC development. Our results show the potential of using plasma exosomal miRNAs as biomarkers to predict/monitor CRPC development, which might enable an early treatment change before CRPC is well-established.

Blood-based test has a number of advantages for clinical utility. It is non-invasive and can provide real-time information on patient status. MiRNAs in plasma exosomes serve as good candidates for blood biomarkers as they are protected from degradation, allowing for their stable and easy detection by methods such as RT-qPCR assays. In a previous study, Huang et al. generated extracellular vesicle RNA profiles from CRPC and a small number of hormone-sensitive PCa patients (Yuan et al.,

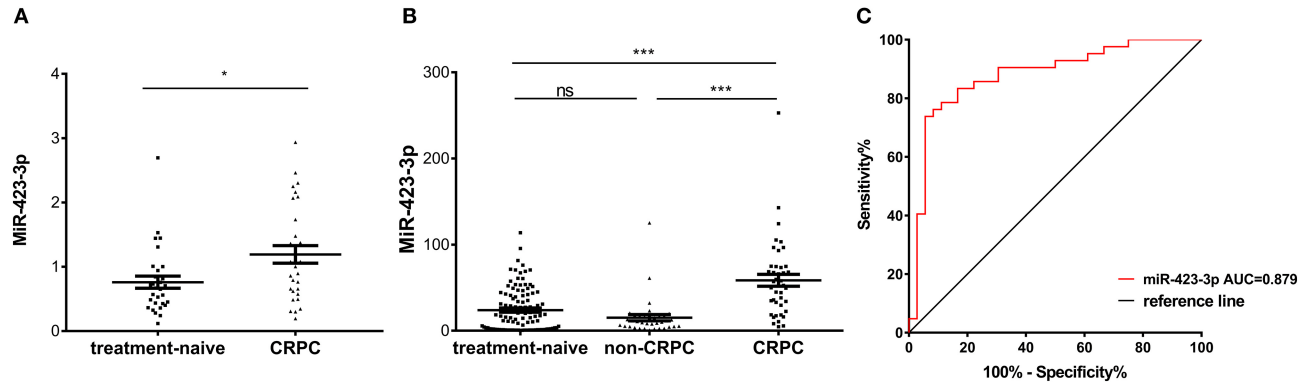

FIGURE 5 | Plasma exosomal miR-423-3p expression levels evaluated by RT-qPCR in validation cohort II and treated non-CRPC. **(A)** Scatter plot of plasma exosomal miR-423-3p expression levels evaluated by RT-qPCR in validation cohort II of 30 treatment-naive prostate cancer patients and 30 castration-resistant prostate cancer (CRPC) patients; **(B)** Scatter plot of plasma exosomal miR-423-3p expression levels evaluated by RT-qPCR in treated non-CRPC patients in comparison to patients in validation cohort I; **(C)** Receiver operating characteristic (ROC) analysis of the plasma exosomal miR-423-3p in discriminating CRPC in cohort I from treated non-CRPC. In scatter plots, the y-axis show the relative expression level of miR-423-3p calculated by $2^{-\Delta Ct}$ and the error bars are showing the mean ± standard error of mean (SEM). *$p<0.05$, ***$p < 0.001$, ns, not significant.

2016) without exosomal miRNA analysis in association with CRPC. Using a modified plasma exosome isolation and RNA-seq method, we identified in a large patient cohort several plasma exosomal miRNAs significantly correlated to CRPC, which were validated by RT-qPCR method in a larger cohort of patients. Our data, showing that there was no significant expression difference of the six miRNAs between different Gleason grade groups, ruled out the influence of Gleason grade on the correlation of these miRNA expression with CRPC. The association of miR-423-3p with CRPC development was further supported by its differential expression in the comparison between ADT treated and CRPC cohorts and the independent validation cohort II, where the Gleason grade distribution was similar between the groups. We identified miR-423-3p as the most significantly differentially expressed miRNA between treatment-naive PCa and CRPC and the correlation of its increase with CRPC was also validated in a separate sample cohort from an independent research center. In a previous study by Watahiki et al. with a small patient cohort, higher levels of plasma miR-423-3p has been reported in patients with metastatic CRPC (n=25) compared to treatment-naive localized PCa ($n = 25$) (Watahiki et al., 2013). However, while their results are consistent with ours regarding the potential of using miR-423-3p as a circulating biomarker for metastatic CRPC prediction, we are the first to demonstrate that miR-423-3p exists in the plasma exosomes and presents at different expression levels during PCa development. This is important, as it means that plasma miR-423-3p is not just released from dying cells, but is actively secreted by cells, which can be involved in cell-cell communication to promote CRPC development. Furthermore, the result from the study by Watahiki et al. (2013) cannot rule out whether the increase of plasma miR-423-3p was the consequence of ADT treatment or CRPC development. We demonstrated that plasma exosomal miR-423-3p was associated with CRPC development instead of ADT treatment by comparing newly treated PCa patients who were at the responsive stage with those who had developed CRPC. Our study suggests that plasma exosomal miR-423-3p has strong potential to be developed in a biomarker for monitoring CRPC development and its predictive value for CRPC development should be further validated in a longitudinal study of pre-hormone therapy patients with CRPC development follow-up data.

The limited studies published to date, using patient samples to investigate genes or biomarkers associated with CRPC development, mainly compared treatment-naive PCa and CRPC samples (Nguyen et al., 2013; Watahiki et al., 2013; Goto et al., 2015). A potential issue affecting the reliability of the CRPC association is that one group of patients is untreated and the other group of patients is treated. Therefore, the genetic/molecular changes could be induced by the treatment. In this study, we have confirmed the CRPC specific association of a potential biomarker by comparing androgen depletion treated non-CRPC patients to treatment-naive PCa and CRPC patients. Therefore, we have developed a robust approach for the investigation of CRPC associated genetic changes or biomarkers using clinical samples and identified potential clinically valuable biomarkers for the early detection/prediction of CRPC occurrence.

Several normalization methods for RNA-seq data have been proposed, but no standard method has currently been established. We employed four most commonly used methods to analyze our sequencing data, CPM, Limma, TMM, and DESeq2, each with their advantages (Dillies et al., 2013; Tam et al., 2015). In our study, the miRNAs identified as differentially expressed by four and three RNA-seq analysis methods gave more reproducible results in RT-qPCR validation than those identified only by two of these methods. As there is no gold-standard method for miRNA sequencing data analysis, our results indicate that the combination of different analysis methods should be used to identify candidate miRNAs for further validation.

In addition to biomarker potential, the identified plasma exosomal miRNAs may have important functions in CRPC development. Emerging evidence shows that exosomes play a key role in cell-cell crosstalk, which may impact tumor cell

growth, metastasis, angiogenesis and cancer microenvironment (Maia et al., 2018). The involvement of these six miRNAs in CRPC development has been previously reported. Consistent to our findings of miR-150-5p under-expression in CRPC patients, previous studies showed low miR-150-5p expression in CRPC tissue compared to PCa and non-PCa tissue (Okato et al., 2017) and its role as a tumor suppressor (Okato et al., 2017; Osako et al., 2017). Paradoxically, while we detected the overexpression of miR-320a, miR-320b, miR-320d, and miR-99a-5p in CRPC patient plasma exosomes, miR-320 and miR-99a-5p have been reported to suppress prostate carcinogenesis (Hsieh et al., 2013; Arai et al., 2018), and lower expression levels of miR-320a and miR-99a-5p in CRPC tissues have been reported by comparing a small number of CRPC with untreated PCa cases (Okato et al., 2016; Arai et al., 2018). The tumor suppressor role of these miRNAs does not necessarily conflict with our observations in plasma exosomes. Regarding the deregulation of these miRNAs in the metastatic CRPC tissues, these observations have to be validated in larger cohorts. The opposite results for the expression levels of miRNAs in plasma and tissue samples are not uncommon as previously found in the studies of miR-320 in glioblastoma (Roth et al., 2011; Dong et al., 2014; Manterola et al., 2014) and of miR-99a in endometrioid endometrial carcinoma (Torres et al., 2012). The pathway overrepresentation analysis identified the Hippo signaling pathway as the most significantly enriched pathway. Hippo signaling pathway has been intensively studied in cancer development which showed an important regulation role of PCa development (Salem and Hansen, 2019). Therefore, it would be interesting to further investigate if multiple miRNAs regulate Hippo signaling and cell-cell communication and play a potential role in the development of CRPC. Thus, the functional roles of these plasma exosomal miRNAs warrant further investigation.

MiR-423-3p is the most significantly dysregulated miRNA in our study. Functional studies have demonstrated the cancer promoting role of miR-423-3p in other cancer types (Guan et al., 2014; Li et al., 2015; Kong et al., 2017; Xu et al., 2018). miR-423-3p overexpression has been reported in many human cancers including lung, breast, gastric and colorectal cancers, where it acts in an oncogenic manner via enhancing cell proliferation, cell cycle progression, cell migration and invasion (Murria Estal et al., 2013; Li et al., 2015; Zhao et al., 2015; Kong et al., 2017; Sun et al., 2019; Wang et al., 2019). A study investigating brain-metastasis related miRNAs in lung adenocarcinoma found that miR-423-3p over expression directly contributed to brain metastasis by increasing cancer cell proliferation, migration and invasion (Sun et al., 2019). In Colorectal cancer, it was found that miR-423-3p was overexpressed in cancer compared to normal tissues and as a result increased cell proliferation, migration and invasion through inhibiting P21 (Li et al., 2015). However, its functional role in PCa has not yet been reported. Further studies to investigate miR-423-3p, in particular exosomal miR-423-3p, in CRPC development are warranted.

In conclusion, by analyzing the exosomal miRNA signature of multiple cohorts of treatment-naive PCa and CRPC patients with RNA-seq and RT-qPCR validation, we identified plasma exosomal miRNAs potentially associated with CRPC. Our multicenter validation as well as inclusion of androgen depletion treated non-CRPC patients confirmed the association of plasma exosomal miR-423-3p specifically with CRPC development. We demonstrated that plasma exosomal miRNAs may serve as biomarkers for non-invasive real-time monitoring of PCa status and the prediction of CRPC occurrence, which would have great potential to improve PCa treatment.

DATA AVAILABILITY STATEMENT

The datasets presented in this study can be found in online repositories. The names of the repository/repositories and accession number(s) can be found at: https://www.ncbi.nlm.nih.gov/geo/query/acc.cgi?acc=GSE136321.

ETHICS STATEMENT

The studies involving human participants were reviewed and approved by London City & East Research Ethics Committee; Institutional Review Board of Medical College of Wisconsin. The patients/participants provided their written informed consent to participate in this study.

AUTHOR CONTRIBUTIONS

Y-JL and TG conceived the study. TG and YW conducted the experiments at Barts Cancer Institute. JJ conducted experiment at MCW Cancer Center. TG, JM, and Y-JL analyzed the data. XM, GSc, EB, LX, ES, SK, PR, AG, KT, JH, TO, TP, CA, GSh, WW, NF, JS, DB, MK, JL, and CD helped with sample and data collection. PR, AG, KT, JH, TO, TP, CA, GSh, WW, NF, JS, DB, LW, and Y-JL were involved in data collection and interpretation. TG, Y-JL, JM, XM, EB, LX, ES, GSh, JS, LW, and CD were involved in drafting the manuscript. Y-JL supervised the study. All authors read and approved the final manuscript.

FUNDING

This work was supported by Orchid, Cancer Research UK (C16420/A18066), Chinese Scholarship Council, and partially supported by the National Institutes of Health to LW (R01CA212097).

ACKNOWLEDGMENTS

We thank Eva Wozniak, Anna Terry, and Charles Meins at QMUL Genome Center for the technical assistance with RNA sequencing. We also thank all patients and healthy donors participating in this study.

SUPPLEMENTARY MATERIAL

The Supplementary Material for this article can be found online at: https://www.frontiersin.org/articles/10.3389/fcell.2020.602493/full#supplementary-material

REFERENCES

Afshar, M., Evison, F., James, N. D., and Patel, P. (2015). Shifting paradigms in the estimation of survival for castration-resistant prostate cancer: a tertiary academic center experience. *Urol. Oncol.* 33, e331–337. doi: 10.1016/j.urolonc.2015.05.003

Arai, T., Okato, A., Yamada, Y., Sugawara, S., Kurozumi, A., Kojima, S., et al. (2018). Regulation of NCAPG by miR-99a-3p (passenger strand) inhibits cancer cell aggressiveness and is involved in CRPC. *Cancer Med.* 7, 1988–2002. doi: 10.1002/cam4.1455

Armstrong, A. J., Eisenberger, M. A., Halabi, S., Oudard, S., Nanus, D. M., Petrylak, D. P., et al. (2012). Biomarkers in the management and treatment of men with metastatic castration-resistant prostate cancer. *Eur. Urol.* 61, 549–559. doi: 10.1016/j.eururo.2011.11.009

Chandrasekar, T., Yang, J. C., Gao, A. C., and Evans, C. P. (2015). Mechanisms of resistance in castration-resistant prostate cancer (CRPC). *Transl. Androl. Urol.* 4, 365–380. doi: 10.3978/j.issn.2223-4683.2015.05.02

Chen, G., Huang, A. C., Zhang, W., Zhang, G., Wu, M., Xu, W., et al. (2018). Exosomal PD-L1 contributes to immunosuppression and is associated with anti-PD-1 response. *Nature* 560, 382–386. doi: 10.1038/s41586-018-0392-8

Cornford, P., Bellmunt, J., Bolla, M., Briers, E., de Santis, M., Gross, T., et al. (2017). EAU-ESTRO-SIOG guidelines on prostate cancer. Part II: treatment of relapsing, metastatic, and castration-resistant prostate cancer. *Eur. Urol.* 71, 630–642. doi: 10.1016/j.eururo.2016.08.002

Dillies, M. A., Rau, A., Aubert, J., Hennequet-Antier, C., Jeanmougin, M., Servant, N., et al. (2013). A comprehensive evaluation of normalization methods for Illumina high-throughput RNA sequencing data analysis. *Brief. Bioinformatics* 14, 671–683. doi: 10.1093/bib/bbs046

Dong, L., Li, Y., Han, C., Wang, X., She, L., and Zhang, H. (2014). miRNA microarray reveals specific expression in the peripheral blood of glioblastoma patients. *Int. J. Oncol.* 45, 746–756. doi: 10.3892/ijo.2014.2459

Ge, Q., Zhou, Y., Lu, J., Bai, Y., Xie, X., and Lu, Z. (2014). miRNA in plasma exosome is stable under different storage conditions. *Molecules* 19, 1568–1575. doi: 10.3390/molecules19021568

Goto, Y., Kojima, S., Nishikawa, R., Kurozumi, A., Kato, M., Enokida, H., et al. (2015). MicroRNA expression signature of castration-resistant prostate cancer: the microRNA-221/222 cluster functions as a tumour suppressor and disease progression marker. *Br. J. Cancer* 113, 1055–1065. doi: 10.1038/bjc.2015.300

Guan, G., Zhang, D., Zheng, Y., Wen, L., Yu, D., Lu, Y., et al. (2014). microRNA-423-3p promotes tumor progression via modulation of AdipoR2 in laryngeal carcinoma. *Int. J. Clin. Exp. Pathol.* 7, 5683–5691.

Hsieh, I. S., Chang, K. C., Tsai, Y. T., Ke, J. Y., Lu, P. J., Lee, K. H., et al. (2013). MicroRNA-320 suppresses the stem cell-like characteristics of prostate cancer cells by downregulating the Wnt/beta-catenin signaling pathway. *Carcinogenesis* 34, 530–538. doi: 10.1093/carcin/bgs371

Hu, G., Drescher, K. M., and Chen, X. M. (2012). Exosomal miRNAs: biological properties and therapeutic potential. *Front. Genet.* 3:56. doi: 10.3389/fgene.2012.00056

Huang, X., Yuan, T., Liang, M., Du, M., Xia, S., Dittmar, R., et al. (2015). Exosomal miR-1290 and miR-375 as prognostic markers in castration-resistant prostate cancer. *Eur. Urol.* 67, 33–41. doi: 10.1016/j.eururo.2014.07.035

Huang, X., Yuan, T., Tschannen, M., Sun, Z., Jacob, H., Du, M., et al. (2013). Characterization of human plasma-derived exosomal RNAs by deep sequencing. *BMC Genomics* 14:319. doi: 10.1186/1471-2164-14-319

Kong, P., Zhu, X., Geng, Q., Xia, L., Sun, X., Chen, Y., et al. (2017). The microRNA-423-3p-Bim axis promotes cancer progression and activates oncogenic autophagy in gastric cancer. *Mol. Ther.* 25, 1027–1037. doi: 10.1016/j.ymthe.2017.01.013

Li, H. T., Zhang, H., Chen, Y., Liu, X. F., and Qian, J. (2015). MiR-423-3p enhances cell growth through inhibition of p21Cip1/Waf1 in colorectal cancer. *Cell. Physiol. Biochem.* 37, 1044–1054. doi: 10.1159/000430230

Love, M. I., Huber, W., and Anders, S. (2014). Moderated estimation of fold change and dispersion for RNA-seq data with DESeq2. *Genome Biol.* 15:550. doi: 10.1186/s13059-014-0550-8

Maia, J., Caja, S., Strano Moraes, M. C., Couto, N., and Costa-Silva, B. (2018). Exosome-based cell-cell communication in the tumor microenvironment. *Front. Cell Dev. Biol.* 6:18. doi: 10.3389/fcell.2018.00018

Manterola, L., Guruceaga, E., Gállego Pérez-Larraya, J., González-Huarriz, M., Jauregui, P., Tejada, S., et al. (2014). A small noncoding RNA signature found in exosomes of GBM patient serum as a diagnostic tool. *Neurooncology* 16, 520–527. doi: 10.1093/neuonc/not218

Matei, I., Kim, H. S., and Lyden, D. (2017). Unshielding exosomal RNA unleashes tumor growth and metastasis. *Cell* 170, 223–225. doi: 10.1016/j.cell.2017.06.047

Mizokami, A., Izumi, K., Konaka, H., Kitagawa, Y., Kadono, Y., Narimoto, K., et al. (2017). Understanding prostate-specific antigen dynamics in monitoring metastatic castration-resistant prostate cancer: implications for clinical practice. *Asian J. Androl.* 19, 143–148. doi: 10.4103/1008-682X.179159

Murria Estal, R., Palanca Suela, S., de Juan Jiménez, I., Egoavil Rojas, C., García-Casado, Z., Juan Fita, M. J., et al. (2013). MicroRNA signatures in hereditary breast cancer. *Breast Cancer Res. Treat.* 142, 19–30. doi: 10.1007/s10549-013-2723-7

Nguyen, H. C., Xie, W., Yang, M., Hsieh, C. L., Drouin, S., Lee, G. S., et al. (2013). Expression differences of circulating microRNAs in metastatic castration resistant prostate cancer and low-risk, localized prostate cancer. *Prostate* 73, 346–354. doi: 10.1002/pros.22572

Okato, A., Arai, T., Kojima, S., Koshizuka, K., Osako, Y., Idichi, T., et al. (2017). Dual strands of pre-miR150 (miR1505p and miR1503p) act as antitumor miRNAs targeting SPOCK1 in naive and castration-resistant prostate cancer. *Int. J. Oncol.* 51, 245–256. doi: 10.3892/ijo.2017.4008

Okato, A., Goto, Y., Kurozumi, A., Kato, M., Kojima, S., Matsushita, R., et al. (2016). Direct regulation of LAMP1 by tumor-suppressive microRNA-320a in prostate cancer. *Int. J. Oncol.* 49, 111–122. doi: 10.3892/ijo.2016.3522

Olmos, D., Brewer, D., Clark, J., Danila, D. C., Parker, C., Attard, G., et al. (2012). Prognostic value of blood mRNA expression signatures in castration-resistant prostate cancer: a prospective, two-stage study. *Lancet Oncol.* 13, 1114–1124. doi: 10.1016/S1470-2045(12)70372-8

Osako, Y., Seki, N., Koshizuka, K., Okato, A., Idichi, T., Arai, T., et al. (2017). Regulation of SPOCK1 by dual strands of pre-miR-150 inhibit cancer cell migration and invasion in esophageal squamous cell carcinoma. *J. Hum. Genet.* 62, 935–944. doi: 10.1038/jhg.2017.69

Pantel, K., Hille, C., and Scher, H. I. (2019). Circulating tumor cells in prostate cancer: from discovery to clinical utility. *Clin. Chem* 65, 87–99. doi: 10.1373/clinchem.2018.287102

Rana, S., Malinowska, K., and Zöller, M. (2013). Exosomal tumor microRNA modulates premetastatic organ cells. *Neoplasia* 15, 281–295. doi: 10.1593/neo.122010

Ritchie, M. E., Phipson, B., Wu, D., Hu, Y., Law, C., and Shi, W., et al. (2015). limma powers differential expression analyses for RNA-sequencing and microarray studies. *Nucleic Acids Res.* 43:e47. doi: 10.1093/nar/gkv007

Robinson, M. D., and Oshlack, A. (2010). A scaling normalization method for differential expression analysis of RNA-seq data. *Genome Biol.* 11:R25. doi: 10.1186/gb-2010-11-3-r25

Ross, R. W., Galsky, M. D., Scher, H. I., Magidson, J., Wassmann, K., Lee, G. S., et al. (2012). A whole-blood RNA transcript-based prognostic model in men with castration-resistant prostate cancer: a prospective study. *Lancet Oncol.* 13, 1105–1113. doi: 10.1016/S1470-2045(12)70263-2

Roth, P., Wischhusen, J., Happold, C., Chandran, P. A., Hofer, S., Eisele, G., et al. (2011). A specific miRNA signature in the peripheral blood of glioblastoma patients. *J. Neurochem.* 118, 449–457. doi: 10.1111/j.1471-4159.2011.07307.x

Ryan, C. J., Smith, M. R., Fizazi, K., Saad, F., Mulders, P. F., Sternberg, C. N., et al. (2015). Abiraterone acetate plus prednisone versus placebo plus prednisone in chemotherapy-naive men with metastatic castration-resistant prostate cancer (COU-AA-302): final overall survival analysis of a randomised, double-blind, placebo-controlled phase 3 study. *Lancet Oncol.* 16, 152–160. doi: 10.1016/S1470-2045(14)71205-7

Salem, O., and Hansen, C. G. (2019). The hippo pathway in prostate cancer. *Cells* 8:370. doi: 10.3390/cells8040370

Sánchez, C. A., Andahur, E. I., Valenzuela, R., Castellón, E. A., Fullá, J. A., Ramos, C. G., et al. (2016). Exosomes from bulk and stem cells from human prostate cancer have a differential microRNA content that contributes cooperatively over local and pre-metastatic niche. *Oncotarget* 7, 3993–4008. doi: 10.18632/oncotarget.6540

Siegel, R. L., Miller, K. D., and Jemal, A. (2019). Cancer statistics, 2019. *CA Cancer J. Clin.* 69, 7–34. doi: 10.3322/caac.21551

Sun, G., Ding, X., Bi, N., Wang, Z., Wu, L., Zhou, W., et al. (2019). Molecular predictors of brain metastasis-related microRNAs in lung adenocarcinoma. *PLoS Genet.* 15:e1007888. doi: 10.1371/journal.pgen.1007888

Tam, S., Tsao, M. S., and McPherson, J. D. (2015). Optimization of miRNA-seq data preprocessing. *Brief. Bioinformatics* 16, 950–963. doi: 10.1093/bib/bbv019

Torres, A., Torres, K., Pesci, A., Ceccaroni, M., Paszkowski, T., Cassandrini, P., et al. (2012). Deregulation of miR-100, miR-99a and miR-199b in tissues and plasma coexists with increased expression of mTOR kinase in endometrioid endometrial carcinoma. *BMC Cancer* 12:369. doi: 10.1186/1471-2407-12-369

Valadi, H., Ekström, K., Bossios, A., Sjöstrand, M., Lee, J. J., and Lötvall, J. O. (2007). Exosome-mediated transfer of mRNAs and microRNAs is a novel mechanism of genetic exchange between cells. *Nat. Cell Biol.* 9, 654–U672. doi: 10.1038/ncb1596

Varenhorst, E., Klaff, R., Berglund, A., Hedlund, P. O., Sandblom, G., and Network Scandinavian Prostate Cancer Group Trial (2016). Predictors of early androgen deprivation treatment failure in prostate cancer with bone metastases. *Cancer Med.* 5, 407–414. doi: 10.1002/cam4.594

Vlachos, I. S., Zagganas, K., Paraskevopoulou, M., D., Georgakilas, G., Karagkouni, D., Vergoulis, T., et al. (2015). DIANA-miRPath v3.0: deciphering microRNA function with experimental support. *Nucleic Acids Res.* 43, W460–466. doi: 10.1093/nar/gkv403

Wang, R., Li, G., Zhuang, G., Sun, S., and Song, Z. (2019). Overexpression of microRNA-423-3p indicates poor prognosis and promotes cell proliferation, migration, and invasion of lung cancer. *Diagn. Pathol.* 14:53. doi: 10.1186/s13000-019-0831-3

Watahiki, A., Macfarlane, R. J., Gleave, M. E., Crea, F., Wang, Y., Helgason, C. D., et al. (2013). Plasma miRNAs as biomarkers to identify patients with castration-resistant metastatic prostate cancer. *Int. J. Mol. Sci.* 14, 7757–7770. doi: 10.3390/ijms14047757

West, T. A., Kiely, B. E., and Stockler, M. R. (2014). Estimating scenarios for survival time in men starting systemic therapies for castration-resistant prostate cancer: a systematic review of randomised trials. *Eur. J. Cancer* 50, 1916–1924. doi: 10.1016/j.ejca.2014.04.004

Xu, J., He, J., Huang, H., Peng, R., and Xi, J. (2018). MicroRNA-423-3p promotes glioma growth by targeting PANX2. *Oncol. Lett.* 16, 179–188. doi: 10.3892/ol.2018.8636

Yuan, T., Huang, X., Woodcock, M., Du, M., Dittmar, R., Wang, Y., et al. (2016). Plasma extracellular RNA profiles in healthy and cancer patients. *Sci. Rep.* 6:19413. doi: 10.1038/srep19413

Zhao, H., Gao, A., Zhang, Z., Tian, R., Luo, A., Li, M., et al. (2015). Genetic analysis and preliminary function study of miR-423 in breast cancer. *Tumour Biol.* 36, 4763–4771. doi: 10.1007/s13277-015-3126-7

Conflict of Interest: The authors declare that the research was conducted in the absence of any commercial or financial relationships that could be construed as a potential conflict of interest.

Copyright © 2021 Guo, Wang, Jia, Mao, Stankiewicz, Scandura, Burke, Xu, Marzec, Davies, Lu, Rajan, Grey, Tipples, Hines, Kudahetti, Oliver, Powles, Alifrangis, Kohli, Shaw, Wang, Feng, Shamash, Berney, Wang and Lu. This is an open-access article distributed under the terms of the Creative Commons Attribution License (CC BY). The use, distribution or reproduction in other forums is permitted, provided the original author(s) and the copyright owner(s) are credited and that the original publication in this journal is cited, in accordance with accepted academic practice. No use, distribution or reproduction is permitted which does not comply with these terms.

frontiers in Cell and Developmental Biology

OPINION
published: 21 January 2021
doi: 10.3389/fcell.2020.622579

DNA-Loaded Extracellular Vesicles in Liquid Biopsy: Tiny Players With Big Potential?

Susana García-Silva[1]*, *Miguel Gallardo*[2] *and Héctor Peinado*[1]*

[1] Microenvironment and Metastasis Laboratory, Molecular Oncology Programme, Spanish National Cancer Research Center (CNIO), Madrid, Spain, [2] H12O - CNIO Hematological Malignancies Clinical Research Unit, Clinical Research Programme, Spanish National Cancer Research Center (CNIO), Madrid, Spain

Keywords: extracellular vesicles, exosomes, cancer, liquid biopsy, plasma, cfDNA

INTRODUCTION

Liquid biopsy in cancer is a revolutionary diagnostic concept defined by the analysis of biological material of tumor origin that extravasate to body fluids. Most common liquid biopsy studies use circulating tumor cells (CTCs) or circulating tumor-derived factors, in particular, circulating tumor DNA (ctDNA) (Alix-Panabières and Pantel, 2016; Perakis and Speicher, 2017). In the last 5 years, cutting-edge technologies such as next-generation sequencing (NGS) or digital PCR (dPCR) have been applied to detect blood-based, tumor-specific biomarkers such as CTCs and ctDNA (Husain and Velculescu, 2017; Pantel and Alix-Panabières, 2019). The quantification of circulating DNA molecules or CTCs showed *per se* prognostic value in many cancers (Haber and Velculescu, 2014). Besides this immediate analysis, another advantage of these biomarkers resides in the possibility of testing specific mutations, methylation profiles, and other DNA patterns (cfDNA and CTCs) and alternatively, proteins and the possibility of generating patient-derived xenografts (PDX) from the most aggressive cells in the tumor that putatively could initiate metastatic outgrowth (CTCs). Furthermore, the development of high sensitivity and specificity techniques enabled the identification of minimal residual disease (MRD) in cancer patient's follow-up blood samples (Pantel and Alix-Panabières, 2019). Complementary to these biomarkers, extracellular vesicles (EVs) are emerging as powerful biomarkers to provide information about the tumor and the systemic changes occurring during the disease. EVs are a broad and heterogenous group of vesicles secreted by almost any kind of cell that display a wide range of sizes (30 nm−5 μm in diameter Witwer and Théry, 2019) and are composed of a lipid bilayer enclosing nucleic acids, proteins, lipids, metabolites (Colombo et al., 2014). EVs are considered as a mechanism of cell-cell communication regulating paracrine and distal cell communication (Tkach and Théry, 2016). According to this, EVs have been detected in most biological fluids (Wiklander et al., 2019). The isolation of EVs allows for the subsequent analysis of their content that is defined by the cell of origin of the vesicle. Due to their heterogeneous content (protein, nucleic acids, lipids, metabolites, etc.), their ubiquitous production by body cells and detection in most biological fluids, circulating EVs could be useful for specific or multiplatform analyses to provide an accurate evaluation of cancer disease at early time points, during progression, therapy and post-treatment facilitating the detection of minimal residual disease and relapse anticipation (LeBleu and Kalluri, 2020).

EV-SHED DNA, CHARACTERISTICS AND CONSIDERATIONS

Since 2010, several studies have shown the presence of different DNA species in EVs such as ssDNA (Balaj et al., 2011), dsDNA (Kahlert et al., 2014; Thakur et al., 2014) and mtDNA (Cai et al., 2016; Lötvall et al., 2016). Although it is widely accepted that EVs carry DNA, the origins, localization

OPEN ACCESS

Edited by:
Catherine Alix-Panabieres, Centre Hospitalier Universitaire de Montpellier, France

Reviewed by:
Davide Zocco, Exosomics Siena SpA, Italy

***Correspondence:**
Susana García-Silva
sgsilva@cnio.es
Héctor Peinado
hpeinado@cnio.es

Specialty section:
This article was submitted to Molecular and Cellular Oncology, a section of the journal Frontiers in Cell and Developmental Biology

Received: *28 October 2020*
Accepted: *18 December 2020*
Published: *21 January 2021*

Citation:
García-Silva S, Gallardo M and Peinado H (2021) DNA-Loaded Extracellular Vesicles in Liquid Biopsy: Tiny Players With Big Potential? Front. Cell Dev. Biol. 8:622579. doi: 10.3389/fcell.2020.622579

and biological properties of this DNA are not entirely understood (Malkin and Bratman, 2020). Some works support that DNA secretion in EVs is an integral mechanism of clearing cytosolic DNA to maintain cellular homeostasis and avoid senescence and apoptosis (Takahashi et al., 2017). Another report suggests that DNA is a danger-associated signal secreted by dying cells promoting inflammation and anti-tumor immune responses (Kitai et al., 2017). A role for EV-associated DNA in priming and conferring protection to dendritic cells against pathogen infection has also been described (Torralba et al., 2018). Regarding the mechanism involved in DNA secretion on EVs, although microvesicles and exosomes have been proposed to carry DNA, a detailed analysis of the involved mechanism is missing. In a landmark study, Coffey and colleagues found that small EVs did not contain detectable amounts of dsDNA (Jeppesen et al., 2019). Surprisingly, they found that dsDNA was associated with non-vesicular particles that can be co-isolated in the same fraction than small EVs.

Regardless of their origin and mechanism, it appears clear that most of the EV-shed DNA is located on the outside surface of the EVs (Lazaro-Ibanez et al., 2019). However, after DNAse treatment, still a small proportion of DNA remains inside the vesicles (Thakur et al., 2014; Lazaro-Ibanez et al., 2019). Surface-associated DNA confers increased zeta-potential to vesicles, favors exosome-cell adhesion and contributes to the vesicle internalization in the target cell (Fischer et al., 2016; Lötvall et al., 2016; Németh et al., 2017).

Interestingly, all chromosomes are represented in EV-shed DNA with no specific regions overrepresented (Lazaro-Ibanez et al., 2019) suggesting the absence of a sequence-specific loading of DNA species in vesicles. Despite the lower amount of EV-enclosed DNA compared to EV surface-associated DNA, inner DNA displays a better quality and performance in NGS (Lazaro-Ibanez et al., 2019). Remarkably, compared to cfDNA, the reported average fragment length is longer in EVs. Thus, together with a nucleosome-associated pattern, fragments up to 4 kb are observed in exosome-derived DNA (Vagner et al., 2018; Lazaro-Ibanez et al., 2019; Malkin and Bratman, 2020) and chromosomal DNA has been found in large EVs such as oncosomes in prostate cells and in plasma of prostate cancer patients (Vagner et al., 2018).

Several works have reported that EV-shed DNA allows the detection of mutations that reliably reflects the mutational state in the tumor of origin (Kahlert et al., 2014; Thakur et al., 2014; Vagner et al., 2018; García-Romero et al., 2019; Garcia-Silva et al., 2019; Kunz et al., 2019). As a consequence of this, the use of EV-derived DNA for liquid biopsy purposes has begun to be exploited (**Table 1**). The first studies with plasma-derived EVs focused on the analysis of EGFR in lung cancer and glioblastoma (Figueroa et al., 2017; Krug et al., 2017; Castellanos-Rizaldos et al., 2018) and KRAS in pancreatic cancer (Allenson et al., 2017; Yang et al., 2017). More recently, predictive detection of BRAF mutation in circulating EV-DNA from pediatric central nervous system tumors has been described (García-Romero et al., 2019) together with the use of this mutation in seroma obtained post-lymphadenectomy in melanoma patients as a measure of minimal residual disease (Garcia-Silva et al., 2019). These and other studies demonstrate that the analysis of circulating EV-DNA can provide a prognostic value in diverse cancer types.

AN OVERVIEW OF cfDNA-BASED LIQUID BIOPSIES

Compared to EV-DNA, cfDNA has been much more extensively used in liquid biopsies. cfDNA is DNA freely circulating in the bloodstream. It is estimated that circulating tumor DNA might only be <0.01% of the total cfDNA (Pantel and Alix-Panabières, 2019). It is mainly originated during the apoptotic process, although senescence and necrosis also influence cfDNA release kinetics (Rostami et al., 2020). As a consequence of its origin, it is a highly fragmented nucleic acid.

cfDNA-based liquid biopsy can be used to detect specific tumor aberrations such as point mutations, loss of heterozygosity (LOH) or amplifications (Kerachian et al., 2019). These specific tumor genetic alterations (or a panel of them) are analyzed by targeting DNA sequencing techniques such as digital PCR (dPCR), beads–emulsion–amplification–magnetics (BEAMing), safe-sequencing system (Safe-SeqS), cancer personalized profiling by deep sequencing (CAPP-Seq), and tagged-amplicon deep sequencing (TAmSeq) (Heitzer et al., 2019). Alternatively, a non-targeted next-generation sequencing (NGS), commonly a whole-genome/exome sequencing can also be applied to cfDNA in order to extract information about copy number alterations (CNAs), DNA rearrangements or detection of subclonal mutations. The biggest drawback of this approach is the lower overall sensitivity (above 1–5%) and the need for higher concentrations of ctDNA whereas targeted DNA sequencing techniques can reach a limit of detection (LOD) minor than 0.01% (Pantel and Alix-Panabières, 2019). However, ultra-sensitive detection in plasma cfDNA samples can be achieved by analyzing hundreds to thousands of mutations previously identified by tumor genotyping (Wan et al., 2020) or by using genome-wide mutational integration (Zviran et al., 2020).

The most frequent application of cfDNA-based liquid biopsy is the monitoring of therapy response and the analysis of minimal residual disease (MRD) in clinical samples in order to anticipate the relapse of the disease before its detection with current clinical techniques (e.g., CT or PET/CT, multiparametric flow cytometry, immunohistochemistry) (Cheng et al., 2019; Pantel and Alix-Panabières, 2019). In colon cancer, the positive detection of mutations in cfDNA efficiently demonstrated prognostic value in a cohort of 230 colorectal cancer patients in which cfDNA positive status was associated to inferior recurrence-free survival (Tie et al., 2016). In breast cancer, the use of ddPCR on cfDNA samples to validate previously identified chromosome rearrangements reached a sensitivity of 93% and a specificity of 100% (Olsson et al., 2015). Targeted capture sequencing analysis of ctDNA defined MRD-associated mutations and even predict the genetic events of subsequent metastatic relapse more accurately than sequencing of the primary breast cancer (Garcia-Murillas et al., 2019). In a landmark study in lung cancer, Swanton and colleagues developed a NGS-based mutational panel of 12–30 SNVs, with addition of clinical and radiological

TABLE 1 | Summary of the main reports performing DNA-EV analyses for liquid biopsy tests.

References	Body fluid	Tumor type	Method	EV type	DNAase	Yield	DNA size	Biomarkers/ platform
Krug et al. (2017)	Plasma	NSCLC	Exo-Elution™ Plus extraction kit	Small and large EVs	No	ND	ND	EGFR T790M by NGS
Castellanos-Rizaldos et al. (2018)	Plasma	NSCLC	Exo-Elution™ Plus extraction kit	Small and large EVs	No	ND	ND	EGFR mutations by NGS
Allenson et al. (2017)	Plasma	Pancreatic cancer	Ultracentrifugation	Small EVs	No	ND	ND	KRAS mutations by ddPCR
Yang et al. (2017)	Serum	Pancreatic cancer	Ultracentrifugation	Small EVs	No	ND	ND	KRAS and TP53 mutations by ddPCR
San Lucas et al. (2016)	Pleural fluid	Pancreatic cancer	Ultracentrifugation	Small EVs	No	ND	>10kb	Tumor profiling by Illumina Hiseq2500
Figueroa et al. (2017)	CSF	Glioblastoma	Ultracentrifugation	Small EVs	Yes	ND	ND	EGFRvIII mutation by QPCR
Garcia-Silva et al. (2019)	Lymphatic exudate	Melanoma	Exo-Elution™ Plus extraction kit	Small and large EVs	No	ND	ND	BRAF V600E by QPCR
Hur et al. (2019)	BALF	NSCLC	Ultracentrifugation	Small EVs	No	ND	ND	EGFR mutations by QPCR
Song et al. (2019)	Pleural effusion fluid	NSCLC	Exo-Elution™ Plus extraction kit	Small and large EVs	No	ND	ND	Targeted-NGS
Lee et al. (2018)	Urine	Bladder cancer	ExoQuick-TC	Small EVs	No	ND	ND	Mutation analysis by target capture sequencing /CNV by whole genome sequencing

CFS, cerebrospinal fluid; BALF, bronchoalveolar lavage fluid; NSCLC, non-small cell lung cancer; PDAC, pancreatic ductal adenocarcinoma; ND, not determined.

evaluations. The detection of SNVs in ctDNA seemed to correlate with clinical evidence of NSCLC relapse with a ctDNA detection threshold <0.1% (Abbosh et al., 2017). These and other studies (Reinert et al., 2016; Chaudhuri et al., 2017; Schøler et al., 2017) demonstrate how targeted and genome-wide DNA sequencing techniques provide an accurate information during disease monitoring.

cfDNA *VS.* EV-NA, WHO IS THE WINNER?

It should be first noticed that when defining blood-derived cfDNA it is unclear the physical state/source of it. It can be effectively circulating DNA, or circulating in association with protein complexes or even associated to EVs (Jahr et al., 2001; Thierry et al., 2016). Importantly, standard protocols for cfDNA isolation do not exclude EV-shed DNA although neither concentrate nor select for it as other approaches do.

An overview of the differences between EV-DNA and cfDNA are summarized in **Figure 1**. EV-DNA is more stable than cfDNA whose half-life is estimated in <2 h (Cheng et al., 2016) forcing fast protocols of sample collection. On the contrary, EVs and their cargo show a considerable long-term stability in body fluids that facilitate their analysis in biobanked samples (Kalra et al., 2013). In addition, the fragmented nature of cfDNAs makes it difficult to generate a reliable genomic characterization for NGS, which in turn requires barcode and deep sequencing (Mouliere et al., 2011). On the other side, the presence of long EV-DNA fragments, that in cases display a chromatin structure favors amplification and better performance in NGS (Lazaro-Ibanez et al., 2019). Nevertheless, to date, most liquid biopsy studies focused on GWA and non-targeted sequencing have been performed in cfDNA such as methylation analyses (Sprang et al., 2020), DNA fragmentation patterns (Cristiano et al., 2019), or microbiome-DNA signatures (Poore et al., 2020) probably due to the delay in the application of those techniques to EV-based liquid biopsy.

Another advantage of exosomes and other EVs-based liquid biopsy is the possibility of multiplexing analyses of DNA with other EV cargo such as miRNA, long-non coding RNA, proteins, etc., that can provide a highly accurate information about the disease and will facilitate personalized and time-shaped medicine (LeBleu and Kalluri, 2020).

Few studies provide insights about the comparison of both cfDNA and EV-DNA in plasma. In a cohort of 84 non-small cell lung cancer patients, the combined use of exosomal-RNA and ctDNA sequencing improved the detection of EGFR (epidermal growth factor receptor)-activating mutations up to 98 vs. 84% for ctDNA alone (Krug et al., 2017). Remarkably, the

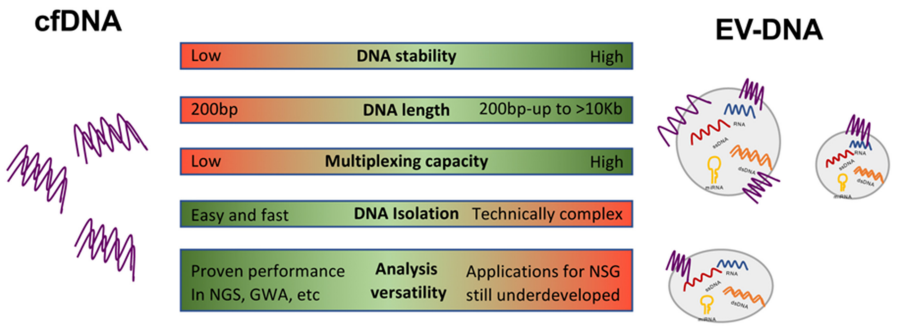

FIGURE 1 | Advantages and disadvantages of EV-associated DNA and cfDNA. Circulating cell-free (cfDNA) shows a half-life of 2 h. However, extracellular vesicles (EVs) and associated content are stable for longer times. EVs display a wide range of DNA fragment sizes compared to highly fragmented cfDNA. Multiple EV cargo allows for polyvalent multiplexed analysis. DNA isolation is easy and fast for cfDNA but is technically more complex and time-consuming in the case of EVs. Non-targeted sequence-based analyses in EV-DNA are still underdeveloped while cfDNA has proven remarkable performance in next-generation sequencing techniques (NSG) and studies based in gene-wide analysis (GWA).

best improvement was observed in the group of patients with intrathoracic metastatic disease known to have low levels of cfDNA. Moreover, the combined use of EV-RNA/DNA (EV-NA) together with cfDNA overcame the limited abundance of the EGFR T790M mutation and other EGFR mutations and obtained improved sensitivity and specificity than cfDNA alone (Castellanos-Rizaldos et al., 2018, 2019). These studies highlight the enhanced performance of combining EV-associated nucleic acids together with cfDNA vs. cfDNA analysis alone.

Following with the improved performance of EV-DNA tests, in a recent study, the assessment of Rhesus D genotype and gender by coupling quantitative PCR to EV-DNA and cfDNA isolation from maternal blood gave successful results with both approaches although only EV-DNA achieved a 100% of sensitivity and specificity for both assays (Yaşa et al., 2020).

An important drawback in EV-DNA tests is the lack of standardized isolation methods compared to cfDNA that implies additional steps of optimization, that are technically more complex and required clinical validation (Théry et al., 2006; Royo et al., 2020).

THERE IS FUTURE BEYOND PLASMA! USE OF CIRCULATING EV IN OTHER BIOFLUIDS

The secretion of EVs is a universal process and consequently EVs have been detected, isolated and analyzed in many biological fluids such as plasma, urine, cerebrospinal fluid (CSF) or bronchoalveolar lavage fluid (BALF) suggesting that these fluids can be explored for EV-based liquid biopsy tests (González and Falcón-Pérez, 2015; Gui et al., 2015; Broggi et al., 2019; Carnino et al., 2019; Kim et al., 2020). Until now, most of the studies based on other biofluids than blood have been focused on the quantification of exosomes or specific protein biomarkers. However, the analysis of mutations suggests that other fluids could be enriched in EV-associated DNA compared to plasma providing increase sensitivity. This is the case for lymphatic exudate also called exudative seroma in melanoma (Garcia-Silva et al., 2019). A combined approach isolating EV-associated nucleic acids together with cfDNA yield 600 times more copies of BRAFwt in this biofluid than in plasma. Thus, the limit of detection and sensitivity of the technique can be improved by choosing a fluid anatomically close to the tumor that would be enriched in tumor-derived EVs and consequently in EV-NA cargo. Another example of such an improvement is the analysis of CSF as an alternative to the scarce detection of biomarkers in blood for brain neoplasms. Thus, in glioblastoma patients, the use of CSF-derived EVs yield high specificity for the detection of tumor-associated EGFR amplifications (Figueroa et al., 2017). Additionally, profiling of BRAFV600E mutation in exudative seroma-derived EV-NA obtained after lymphadenectomy efficiently detected minimal residual disease and showed a strong prognostic value in a small cohort of stage III melanoma patients (Garcia-Silva et al., 2019). This study implies that malignancies such as breast cancer, melanoma, or others in which lymphadenectomy is performed could benefit from testing seroma-derived EV-NA for detection of minimal residual disease. It has been also proposed that NGS using EVs isolated from pleural fusions and urine could effectively replace tissue-based NGS in cases where there is a shortage of tissue (Lee et al., 2018; Song et al., 2019). Recent studies have demonstrated that EVs successfully isolated from BALF of lung cancer patients contain an abundant amount of dsDNA, and that liquid biopsy for EGFR genotyping using BALF is tissue-specific and extremely sensitive compared to cfDNA analysis (Hur et al., 2019; Kim et al., 2020). In summary, these works drive attention to the relevance of the selection of the ideal fluid as a source of EVs. The anatomical proximity to the tumor or disease and the intrinsic EV concentration certainly impact in the yield of the isolation process and consequently in the sensibility of the tests.

CONCLUDING REMARKS

Compared to other types of liquid biopsy biomarkers, EV-DNA tests are in their early steps. However, they could provide

additional analytical power to more established diagnostic methods due to the relatively abundant cargo of nucleic acids displaying increased stability compared to cfDNA. Although a few studies suggest that EV-NA-based tests could perform slightly better than cfDNA tests, more comparative analyses will be required to evaluate EV-NA capacity to overcome or complement cfDNA-based liquid biopsy. Combined EV-DNA/RNA with cfDNA approaches could amplify disease information and improved the specificity and the limit of detection in the tests, for example in the detection of some tumor mutations known to be underrepresented in cfDNA. On the other hand, there is a need for increased sensitivity that could boost non-invasive early detection and also enhance the analysis of minimal residual disease. Due to the heterogeneity of EV cargo, multiplexed assays combining DNA analysis with additional information on other biomolecules could also serve for a more personalized medicine. In addition, alternative biofluids are coming on the scene demonstrating improved performance than blood-based tests due to their enrichment in tumor-specific EVs. Finally, together with targeted-sequencing techniques, the development of diverse types of GWA and the capacities of machine learning to combine multiple layers of information, will definitively expand the applicability of EV-DNA-based liquid biopsy.

AUTHOR CONTRIBUTIONS

HP and SG-S conceived and designed the manuscript. SG-S, MG, and HP wrote the manuscript. All authors contributed to the article and approved the submitted version.

FUNDING

The authors gratefully acknowledged the support of the following sources of funding: H.P. RETOS SAF2017-82924-R (AEI/10.13039/501100011033/FEDER-UE), Fundación AECC: LABAE19027PEIN, Fundación Ramón Areces, and Translational NeTwork for the CLinical application of Extracellular VesicleS, TeNTaCLES, RED2018-102411-T (AEI/10.13039/501100011033). MC contra el Cancer foundation, ISCIII (CP19/00140, PI18/00295).

ACKNOWLEDGMENTS

We thank the reviewer and editor for their helpful comments.

REFERENCES

Abbosh, C., Birkbak, N. J., Wilson, G. A., Jamal-Hanjani, M., Constantin, T., Salari, R., et al. (2017). Phylogenetic ctDNA analysis depicts early-stage lung cancer evolution. *Nature* 545, 446–451. doi: 10.1038/nature 22364

Alix-Panabières, C., and Pantel, K. (2016). Clinical applications of circulating tumor cells and circulating tumor DNA as liquid biopsy. *Cancer Discov.* 6, 479–491. doi: 10.1158/2159-8290.cd-15-1483

Allenson, K., Castillo, J., San Lucas, F. A., Scelo, G., Kim, D. U., Bernard, V., et al. (2017). High prevalence of mutant KRAS in circulating exosome-derived DNA from early-stage pancreatic cancer patients. *Ann. Oncol.* 28, 741–747. doi: 10.1093/annonc/mdx004

Balaj, L., Lessard, R., Dai, L., Cho, Y. J., Pomeroy, S. L., Breakefield, X. O., et al. (2011). Tumour microvesicles contain retrotransposon elements and amplified oncogene sequences. *Nat. Commun.* 2:180. doi: 10.1038/ncomms1180

Broggi, M. A. S., Maillat, L., Clement, C. C., Bordry, N., Corthesy, P., Auger, A., et al. (2019). Tumor-associated factors are enriched in lymphatic exudate compared to plasma in metastatic melanoma patients. *J. Exp. Med.* 216, 1091–1107. doi: 10.1084/jem.20181618

Cai, J., Wu, G., Jose, P. A., and Zeng, C. (2016). Functional transferred DNA within extracellular vesicles. *Exp. Cell Res.* 349, 179–183. doi: 10.1016/j.yexcr.2016.10.012

Carnino, J. M., Lee, H., and Jin, Y. (2019). Isolation and characterization of extracellular vesicles from Broncho-alveolar lavage fluid: a review and comparison of different methods. *Respir. Res.* 20:240. doi: 10.1186/s12931-019-1210-z

Castellanos-Rizaldos, E., Grimm, D. G., Tadigotla, V., Hurley, J., Healy, J., Neal, P. L., et al. (2018). Exosome-based detection of EGFR T790M in plasma from non-small cell lung cancer patients. *Clin. Cancer Res.* 24, 2944–2950. doi: 10.1158/1078-0432.CCR-17-3369

Castellanos-Rizaldos, E., Zhang, X., Tadigotla, V. R., Grimm, D. G., Karlovich, C., Raez, L. E., et al. (2019). Exosome-based detection of activating and resistance EGFR mutations from plasma of non-small cell lung cancer patients. *Oncotarget* 10, 2911–2920. doi: 10.18632/oncotarget.26885

Chaudhuri, A. A., Chabon, J. J., Lovejoy, A. F., Newman, A. M., Stehr, H., Azad, T. D., et al. (2017). Early detection of molecular residual disease in localized lung cancer by circulating tumor DNA profiling. *Cancer Discov.* 7, 1394–1403. doi: 10.1158/2159-8290.cd-17-0716

Cheng, F., Su, L., and Qian, C. (2016). Circulating tumor DNA: a promising biomarker in the liquid biopsy of cancer. *Oncotarget* 7, 48832–48841. doi: 10.18632/oncotarget.9453

Cheng, F. T., Lapke, N., Wu, C. C., Lu, Y. J., Chen, S. J., Yu, P. N., et al. (2019). Liquid biopsy detects relapse five months earlier than regular clinical follow-up and guides targeted treatment in breast cancer. *Case Rep. Oncol. Med.* 2019:6545298. doi: 10.1155/2019/6545298

Colombo, M., Raposo, G., and Thery, C. (2014). Biogenesis, secretion, and intercellular interactions of exosomes and other extracellular vesicles. *Annu. Rev. Cell Dev. Biol.* 30, 255–289. doi: 10.1146/annurev-cellbio-101512-122326

Cristiano, S., Leal, A., Phallen, J., Fiksel, J., Adleff, V., Bruhm, D. C., et al. (2019). Genome-wide cell-free DNA fragmentation in patients with cancer. *Nature* 570, 385–389. doi: 10.1038/s41586-019-1272-6

Figueroa, J. M., Skog, J., Akers, J., Li, H., Komotar, R., Jensen, R., et al. (2017). Detection of wild-type EGFR amplification and EGFRvIII mutation in CSF-derived extracellular vesicles of glioblastoma patients. *Neuro Oncol.* 19, 1494–1502. doi: 10.1093/neuonc/nox085

Fischer, S., Cornils, K., Speiseder, T., Badbaran, A., Reimer, R., Indenbirken, D., et al. (2016). Indication of horizontal DNA gene transfer by extracellular vesicles. *PLoS ONE* 11:e0163665. doi: 10.1371/journal.pone.0163665

Garcia-Murillas, I., Chopra, N., Comino-Méndez, I., Beaney, M., Tovey, H., Cutts, R. J., et al. (2019). Assessment of molecular relapse detection in early-stage breast cancer. *JAMA Oncol.* 5, 1473–1478. doi: 10.1001/jamaoncol.2019.1838

García-Romero, N., Carrión-Navarro, J., Areal-Hidalgo, P., Ortiz de Mendivil, A., Asensi-Puig, A., Madurga, R., et al. (2019). BRAF V600E detection in liquid biopsies from pediatric central nervous system tumors. *Cancers* 12:66. doi: 10.3390/cancers12010066

Garcia-Silva, S., Benito-Martin, A., Sanchez-Redondo, S., Hernandez-Barranco, A., Ximenez-Embun, P., Nogues, L., et al. (2019). Use of extracellular vesicles from lymphatic drainage as surrogate markers of melanoma progression and BRAF (V600E) mutation. *J. Exp. Med.* 216, 1061–1070. doi: 10.1084/jem.20181522

González, E., and Falcón-Pérez, J. M. (2015). Cell-derived extracellular vesicles as a platform to identify low-invasive disease biomarkers. *Expert Rev. Mol. Diagn.* 15, 907–923. doi: 10.1586/14737159.2015.1043272

Gui, Y., Liu, H., Zhang, L., Lv, W., and Hu, X. (2015). Altered microRNA profiles in cerebrospinal fluid exosome in Parkinson disease and Alzheimer disease. *Oncotarget* 6, 37043–37053. doi: 10.18632/oncotarget.6158

Haber, D. A., and Velculescu, V. E. (2014). Blood-based analyses of cancer: circulating tumor cells and circulating tumor DNA. *Cancer Discov.* 4, 650–661. doi: 10.1158/2159-8290.cd-13-1014

Heitzer, E., Haque, I. S., Roberts, C. E. S., and Speicher, M. R. (2019). Current and future perspectives of liquid biopsies in genomics-driven oncology. *Nat. Rev. Genet.* 20, 71–88. doi: 10.1038/s41576-018-0071-5

Hur, J. Y., Lee, J. S., Kim, I. A., Kim, H. J., Kim, W. S., and Lee, K. Y. (2019). Extracellular vesicle-based EGFR genotyping in bronchoalveolar lavage fluid from treatment-naive non-small cell lung cancer patients. *Transl. Lung Cancer Res.* 8, 1051–1060. doi: 10.21037/tlcr.2019.12.16

Husain, H., and Velculescu, V. E. (2017). Cancer DNA in the circulation: the liquid biopsy. *JAMA* 318, 1272–1274. doi: 10.1001/jama.2017.12131

Jahr, S., Hentze, H., Englisch, S., Hardt, D., Fackelmayer, F. O., Hesch, R. D., et al. (2001). DNA fragments in the blood plasma of cancer patients: quantitations and evidence for their origin from apoptotic and necrotic cells. *Cancer Res.* 61, 1659–1665.

Jeppesen, D. K., Fenix, A. M., Franklin, J. L., Higginbotham, J. N., Zhang, Q., Zimmerman, L. J., et al. (2019). Reassessment of exosome composition. *Cell* 177, 428–445 e418. doi: 10.1016/j.cell.2019.02.029

Kahlert, C., Melo, S. A., Protopopov, A., Tang, J., Seth, S., Koch, M., et al. (2014). Identification of double-stranded genomic DNA spanning all chromosomes with mutated KRAS and p53 DNA in the serum exosomes of patients with pancreatic cancer. *J. Biol. Chem.* 289, 3869–3875. doi: 10.1074/jbc.C113.532267

Kalra, H., Adda, C. G., Liem, M., Ang, C. S., Mechler, A., Simpson, R. J., et al. (2013). Comparative proteomics evaluation of plasma exosome isolation techniques and assessment of the stability of exosomes in normal human blood plasma. *Proteomics* 13, 3354–3364. doi: 10.1002/pmic.201300282

Kerachian, M. A., Poudineh, A., and Thiery, J. P. (2019). Cell free circulating tumor nucleic acids, a revolution in personalized cancer medicine. *Crit. Rev. Oncol. Hematol.* 144:102827. doi: 10.1016/j.critrevonc.2019.102827

Kim, I. A., Hur, J. Y., Kim, H. J., Lee, S. E., Kim, W. S., and Lee, K. Y. (2020). Liquid biopsy using extracellular vesicle-derived DNA in lung adenocarcinoma. *J. Pathol. Transl. Med.* 54, 453–461. doi: 10.4132/jptm.2020.08.13

Kitai, Y., Kawasaki, T., Sueyoshi, T., Kobiyama, K., Ishii, K. J., Zou, J., et al. (2017). DNA-containing exosomes derived from cancer cells treated with topotecan activate a STING-dependent pathway and reinforce antitumor immunity. *J. Immunol.* 198, 1649–1659. doi: 10.4049/jimmunol.1601694

Krug, A. K., Enderle, D., Karlovich, C., Priewasser, T., Bentink, S., Spiel, A., et al. (2017). Improved EGFR mutation detection using combined exosomal RNA and circulating tumor DNA in NSCLC patient plasma. *Ann. Oncol.* 29:2143. doi: 10.1093/annonc/mdx765

Kunz, F., Kontopoulou, E., Reinhardt, K., Soldierer, M., Strachan, S., Reinhardt, D., et al. (2019). Detection of AML-specific mutations in pediatric patient plasma using extracellular vesicle-derived RNA. *Ann. Hematol.* 98, 595–603. doi: 10.1007/s00277-019-03608-y

Lazaro-Ibanez, E., Lasser, C., Shelke, G. V., Crescitelli, R., Jang, S. C., Cvjetkovic, A., et al. (2019). DNA analysis of low- and high-density fractions defines heterogeneous subpopulations of small extracellular vesicles based on their DNA cargo and topology. *J. Extracell Vesicles* 8:1656993. doi: 10.1080/20013078.2019.1656993

LeBleu, V. S., and Kalluri, R. (2020). Exosomes as a multicomponent biomarker platform in cancer. *Trends Cancer* 6, 767–774. doi: 10.1016/j.trecan.2020.03.007

Lee, D. H., Yoon, H., Park, S., Kim, J. S., Ahn, Y. H., Kwon, K., et al. (2018). Urinary exosomal and cell-free DNA detects somatic mutation and copy number alteration in urothelial carcinoma of bladder. *Sci. Rep.* 8:14707. doi: 10.1038/s41598-018-32900-6

Lötvall, G. S., Jang, S. C., Yin, Y., Lässer, C., and Lötvall, J. (2016). Human mast cells release extracellular vesicle-associated-DNA. *Matters.* doi: 10.19185/matters.201602000034

Malkin, E. Z., and Bratman, S. V. (2020). Bioactive DNA from extracellular vesicles and particles. *Cell Death Dis.* 11:584. doi: 10.1038/s41419-020-02803-4

Mouliere, F., Robert, B., Arnau Peyrotte, E., Del Rio, M., Ychou, M., Molina, F., et al. (2011). High fragmentation characterizes tumour-derived circulating DNA. *PLoS ONE* 6:e23418. doi: 10.1371/journal.pone.0023418

Németh, A., Orgovan, N., Sódar, B. W., Osteikoetxea, X., Pálóczi, K., Szabó-Taylor, K., et al. (2017). Antibiotic-induced release of small extracellular vesicles (exosomes) with surface-associated DNA. *Sci. Rep.* 7:8202. doi: 10.1038/s41598-017-08392-1

Olsson, E., Winter, C., George, A., Chen, Y., Howlin, J., Tang, M. H., et al. (2015). Serial monitoring of circulating tumor DNA in patients with primary breast cancer for detection of occult metastatic disease. *EMBO Mol. Med.* 7, 1034–1047. doi: 10.15252/emmm.201404913

Pantel, K., and Alix-Panabières, C. (2019). Liquid biopsy and minimal residual disease - latest advances and implications for cure. *Nat. Rev. Clin. Oncol.* 16, 409–424. doi: 10.1038/s41571-019-0187-3

Perakis, S., and Speicher, M. R. (2017). Emerging concepts in liquid biopsies. *BMC Med.* 15:75. doi: 10.1186/s12916-017-0840-6

Poore, G. D., Kopylova, E., Zhu, Q., Carpenter, C., Fraraccio, S., Wandro, S., et al. (2020). Microbiome analyses of blood and tissues suggest cancer diagnostic approach. *Nature* 579, 567–574. doi: 10.1038/s41586-020-2095-1

Reinert, T., Schøler, L. V., Thomsen, R., Tobiasen, H., Vang, S., Nordentoft, I., et al. (2016). Analysis of circulating tumour DNA to monitor disease burden following colorectal cancer surgery. *Gut* 65, 625–634. doi: 10.1136/gutjnl-2014-308859

Rostami, A., Lambie, M., Yu, C. W., Stambolic, V., Waldron, J. N., and Bratman, S. V. (2020). Senescence, necrosis, and apoptosis govern circulating cell-free DNA release kinetics. *Cell Rep.* 31:107830. doi: 10.1016/j.celrep.2020.107830

Royo, F., Théry, C., Falcón-Pérez, J. M., Nieuwland, R., and Witwer, K. W. (2020). Methods for separation and characterization of extracellular vesicles: results of a worldwide survey performed by the ISEV rigor and standardization subcommittee. *Cells* 9:1955. doi: 10.3390/cells9091955

San Lucas, F. A., Allenson, K., Bernard, V., Castillo, J., Kim, D. U., Ellis, K., et al. (2016). Minimally invasive genomic and transcriptomic profiling of visceral cancers by next-generation sequencing of circulating exosomes. *Ann. Oncol.* 27, 635–641. doi: 10.1093/annonc/mdv604

Schøler, L. V., Reinert, T., Ørntoft, M. W., Kassentoft, C.G., Árnadóttir, S. S., Vang, S., et al. (2017). Clinical implications of monitoring circulating tumor dna in patients with colorectal cancer. *Clin. Cancer Res.* 23, 5437–5445. doi: 10.1158/1078-0432.ccr-17-0510

Song, Z., Cai, Z., Yan, J., Shao, Y. W., and Zhang, Y. (2019). Liquid biopsies using pleural effusion-derived exosomal DNA in advanced lung adenocarcinoma. *Transl. Lung Cancer Res.* 8, 392–400. doi: 10.21037/tlcr.2019.08.14

Sprang, M., Paret, C., and Faber, J. (2020). CpG-islands as markers for liquid biopsies of cancer patients. *Cells* 9:1820. doi: 10.3390/cells9081820

Takahashi, A., Okada, R., Nagao, K., Kawamata, Y., Hanyu, A., Yoshimoto, S., et al. (2017). Exosomes maintain cellular homeostasis by excreting harmful DNA from cells. *Nat. Commun.* 8:15287. doi: 10.1038/ncomms15287

Thakur, B. K., Zhang, H., Becker, A., Matei, I., Huang, Y., Costa-Silva, B., et al. (2014). Double-stranded DNA in exosomes: a novel biomarker in cancer detection. *Cell Res.* 24, 766–769. doi: 10.1038/cr.2014.44

Théry, C., Amigorena, S., Raposo, G., and Clayton, A. (2006). Isolation and characterization of exosomes from cell culture supernatants and biological fluids. *Curr. Protoc. Cell Biol.* 3:Unit 3.22. doi: 10.1002/0471143030.cb0322s30

Thierry, A. R., El Messaoudi, S., Gahan, P. B., Anker, P., and Stroun, M. (2016). Origins, structures, and functions of circulating DNA in oncology. *Cancer Metastasis Rev.* 35, 347–376. doi: 10.1007/s10555-016-9629-x

Tie, J., Wang, Y., Tomasetti, C., Li, L., Springer, S., Kinde, I., et al. (2016). Circulating tumor DNA analysis detects minimal residual disease and predicts recurrence in patients with stage II colon cancer. *Sci. Transl. Med.* 8:346–392. doi: 10.1126/scitranslmed.aaf6219

Tkach, M., and Théry, C. (2016). Communication by extracellular vesicles: where we are and where we need to go. *Cell* 164, 1226–1232. doi: 10.1016/j.cell.2016.01.043

Torralba, D., Baixauli, F., Villarroya-Beltri, C., Fernández-Delgado, I., Latorre-Pellicer, A., Acín-Pérez, R., et al. (2018). Priming of dendritic cells by DNA-containing extracellular vesicles from activated T cells through antigen-driven contacts. *Nat. Commun.* 9:2658. doi: 10.1038/s41467-018-05077-9

Vagner, T., Spinelli, C., Minciacchi, V. R., Balaj, L., Zandian, M., Conley, A., et al. (2018). Large extracellular vesicles carry most of the tumour DNA circulating in prostate cancer patient plasma. *J. Extracell Vesicles* 7:1505403. doi: 10.1080/20013078.2018.1505403

Wan, J. C. M., Heider, K., Gale, D., Murphy, S., Fisher, E., Mouliere, F., et al. (2020). ctDNA monitoring using patient-specific sequencing and integration of variant reads. *Sci. Transl. Med.* 12:aaz8084. doi: 10.1126/scitranslmed.aaz8084

Wiklander, O. P. B., Brennan, M., Lötvall, J., Breakefield, X. O., and El Andaloussi, S. (2019). Advances in therapeutic applications of extracellular vesicles. *Sci. Transl. Med.* 11:eaav8521. doi: 10.1126/scitranslmed.aav8521

Witwer, K. W., and Théry, C. Extracellular vesicles or exosomes? On primacy, precision, and popularity influencing a choice of nomenclature. *J. Extracell. Vesic.* (2019) 8:1648167. doi: 10.1080/20013078.2019.1648167

Yang, S., Che, S. P., Kurywchak, P., Tavormina, J. L., Gansmo, L. B., Correa de Sampaio, P., et al. (2017). Detection of mutant KRAS and TP53 DNA in circulating exosomes from healthy individuals and patients with pancreatic cancer. *Cancer Biol. Ther.* 18, 158–165. doi: 10.1080/15384047.2017.1281499

Yaşa, B., Sahin, O., Öcüt, E., Seven, M., and Sözer, S. (2020). Assessment of fetal rhesus D and gender with cell-free DNA and exosomes from maternal blood. *Reprod. Sci*. doi: 10.1007/s43032-020-00321-4

Zviran, A., Schulman, R. C., Shah, M., Hill, S. T. K., Deochand, S., Khamnei, C. C., et al. (2020). Genome-wide cell-free DNA mutational integration enables ultra-sensitive cancer monitoring. *Nat. Med.* 26, 1114–1124. doi: 10.1038/s41591-020-0915-3

Conflict of Interest: The authors declare that the research was conducted in the absence of any commercial or financial relationships that could be construed as a potential conflict of interest.

Copyright © 2021 García-Silva, Gallardo and Peinado. This is an open-access article distributed under the terms of the Creative Commons Attribution License (CC BY). The use, distribution or reproduction in other forums is permitted, provided the original author(s) and the copyright owner(s) are credited and that the original publication in this journal is cited, in accordance with accepted academic practice. No use, distribution or reproduction is permitted which does not comply with these terms.

frontiers in Cell and Developmental Biology

MINI REVIEW
published: 02 February 2021
doi: 10.3389/fcell.2020.622048

Next-Generation Cancer Biomarkers: Extracellular Vesicle DNA as a Circulating Surrogate of Tumor DNA

Samuel Amintas[1,2,3], Véronique Vendrely[1,2,3], Charles Dupin[1,2,3], Louis Buscail[4,5], Christophe Laurent[1,2,3], Barbara Bournet[4], Jean-Philippe Merlio[1,3,6], Aurélie Bedel[1,2,3], François Moreau-Gaudry[1,2,3], Julian Boutin[1,2,3], Sandrine Dabernat[1,2,3]† and Etienne Buscail[4,7]†*

[1] Département des Sciences Biologiques et Médicales, Université de Bordeaux, Bordeaux, France, [2] U1035 Institut National de la Santé et de la Recherche Médicale (INSERM), Bordeaux, France, [3] Centre Hospitalier Universitaire (CHU) de Bordeaux, Bordeaux, France, [4] Centre Hospitalier Universitaire (CHU) de Toulouse, Toulouse, France, [5] INSERM UMR 1037, Toulouse Centre for Cancer Research, University of Toulouse III, Toulouse, France, [6] INSERM U1053, Bordeaux, France, [7] INSERM, UMR-1220, IRSD, University of Toulouse III, Toulouse, France

OPEN ACCESS

Edited by:
Catherine Alix-Panabieres, Centre Hospitalier Universitaire de Montpellier, France

Reviewed by:
Pierre-Jean Lamy, Groupe Inovie, France
Natasa Zarovni, Exosomics Siena SpA, Italy

***Correspondence:**
Sandrine Dabernat
sandrine.dabernat@u-bordeaux.fr

† These authors have contributed equally to this work

Specialty section:
This article was submitted to Molecular and Cellular Oncology, a section of the journal Frontiers in Cell and Developmental Biology

Received: 27 October 2020
Accepted: 17 December 2020
Published: 02 February 2021

Citation:
Amintas S, Vendrely V, Dupin C, Buscail L, Laurent C, Bournet B, Merlio J-P, Bedel A, Moreau-Gaudry F, Boutin J, Dabernat S and Buscail E (2021) Next-Generation Cancer Biomarkers: Extracellular Vesicle DNA as a Circulating Surrogate of Tumor DNA. Front. Cell Dev. Biol. 8:622048. doi: 10.3389/fcell.2020.622048

Extracellular vesicles (EVs) are produced by healthy tissues and tumor cells and are released in various bodily fluids, including blood. They are limited by bilayer phospholipidic membranes, and they carry a rich content in biomolecules. Their release cleanses the cells of their waste or serves as functional local and distant cell–cell communication and molecular exchange particles. This rich and heterogeneous content has been given intense attention in cancer physiopathology because EVs support cancer control and progression. Because of their specific active cargo, they are being evaluated as carriers of liquid biopsy biomarkers. Compared to soluble circulating biomarkers, their complexity might provide rich information on tumor and metastases status. Thanks to the acquired genomic changes commonly observed in oncogenic processes, double-stranded DNA (dsDNA) in EVs might be the latest most promising biomarker of tumor presence and complexity. This review will focus on the recent knowledge on the DNA inclusion in vesicles, the technical aspects of EV-DNA detection and quantification, and the use of EV-DNA as a clinical biomarker.

Keywords: circulating biomarker, cancer, liquid biopsy, extracellular vesicles, microvesicles, exosomes, EV-DNA

INTRODUCTION

Extracellular vesicles (EVs) have long been observed, but they were mostly considered as garbage bags to get rid of unusable intracellular constituents (Johnstone, 1992). In the mid-1990s, researchers started to report other functions for EVs. In B cells, internal vesicles rich in membrane major histocompatibility complex [MHC] class II could be released as small vesicles by exocytosis. They were considered to facilitate antigen presentation (Guescini et al., 2010). EVs could bring complex signals not only through their membrane but also by releasing the content of their lumen in the recipient cell, enabling horizontal transfer of proteins and RNAs (Cocucci et al., 2009). These concepts shed a new light on cell–cell communication, thought to occur until then only by soluble signals decoded upon receptor binding or by connexons. Within the EVs, exosomes were found

vectors of intercellular communication in physiological and pathological conditions (reviewed by Kalluri, 2016). Consequently, a swift increase in EV literature occurred, and a lot of attention was given to the identification of the protein and RNA (including miRs) cargoed in EVs as biomarkers in cancer. Now, another important type of EV biomolecules emerges as relevant for cancer biology: the EV-DNA. The aim of this review is not to propose a complete description of EV generation, release, and outcome but to focus on their DNA content as a valuable material for cell–cell communication and a relevant biomarker in cancer clinical biology.

CIRCULATING CELL FREE DNA AND EVs

As liquid biopsies have been given more and more consideration for cancer patient management, a lot of attention and technical development aimed at detecting circulating cell free DNA (cfDNA), especially circulating tumor DNA (ctDNA) within total cfDNA. Circulating cfDNA, and a fortiori ctDNA, originates from healthy or tumor tissues. In plasma, it can be free, released from dying healthy or tumor cells (necrosis or necrosis-related programmed cell death; **Figure 1**). In addition, decondensed neutrophil DNA can be ejected by NETosis as a pathogen trap (Cahilog et al., 2020; Zhen et al., 2020). Otherwise, cfDNA can be embedded in bilayer lipid biomembranes. Besides the apoptotic vesicles, in which compaction favors dead cell disposal, two major modes of EV release coexist: the exocytosis of multivesicular bodies (MVBs) and shedding vesicles directly budded from the plasma membrane (**Figure 1**). These processes are considered active, and the content of the released vesicles may be selective. Vesicles from MVBs are also known as exosomes. These distinct origins diversify their content, including their DNA. In fact, plasma cfDNA concentration analysis showed that more than 93% of amplifiable cfDNA is located in plasma EVs (Fernando et al., 2017). Thus, EVs are potential valuable materials for circulating DNA-based biomarker discovery.

The size of circulating cfDNA differs according to its origin. Apoptotic bodies carry short genomic fragments of double-stranded DNA (dsDNA), in which sizes correspond to the DNA covered by nucleosomes, protected from the apoptosis-induced endonucleases (around 160–180 base pairs) (Bortner et al., 1995). Thus, any genomic locus, a byproduct of cell death, can be embedded in apoptotic vesicles under a highly compacted form (Serrano-Heras et al., 2019). Vesicle-free DNA ongoing non-specific degradation after necrosis-related cell death or NETosis presents wider ranges of lengths from less than 100 bp for mitochondrial DNA (mtDNA) to several thousands of bp (**Figure 1**). The fragments encompass the whole genome due to the non-specific destruction of the cell and its components. Interestingly, besides transferring various proteins, lipids, and RNAs to recipient cells, cultured tumor cells and tumor cells xenografted in mice also released EVs carrying DNA, which reflected the genetic status of the tumor, including the amplification of the oncogene c-Myc (Balaj et al., 2011). Exosomes can also work as vesicular carriers of mtDNA (Guescini et al., 2010). Exosome double-stranded DNA (exoDNA) from cell lines, with sizes ranging from 100 to 2.5 kbp, can represent the entire genome and reflect the mutational status of tumor parental cells (Thakur et al., 2014; Vagner et al., 2018). Moreover, EV-mediated horizontal high molecular weight DNA transfer might contribute to creating cellular diversity in healthy cells and promote cancer progression (Fischer et al., 2016). Although rare, the authors also observed a propagation of the transferred DNA to daughter cells, likely through an integrative event. These observations suggest that the DNA inclusion in EVs is a selective active process, dedicated to share specific parts of the tumor genome (Lázaro-Ibáñez et al., 2014). Interestingly, most of studies focused on dsDNA and made no mention of single-strand DNA (ssDNA) associated to EVs.

How DNA species are sorted into EVs is also far from being resolved. The inhibition of exosome secretion results in accumulation of nuclear DNA in the cytosol, provoking a senescence-like phenotype, with cell cycle arrest and eventually apoptosis (Takahashi et al., 2017). This suggests that DNA embedding in exosomes is important for keeping cell homeostasis. DNA secretion through exosomes protects tumor cells from the inflammatory reaction induced by a DNA-triggered stimulator of interferon response (STING) signaling (Harding et al., 2017; Le Naour et al., 2020). DNA fragments can arise from damaged genomic DNA, packaged in micronuclei, which are cytosolic vesicles enveloped by a nuclear membrane (Fenech et al., 2011). Following nuclear membrane collapse of micronuclei, released genomic DNA can interact with exosomal tetraspanins, leading to the shuttling of the damaged DNA in MVBs (**Figure 1**; Yokoi et al., 2019). The same study found that exoDNA reflected copy number variation of ovarian cancer primary tumors. In addition, vesicular mtDNA might arise from distinct vesicles produced by oxidized mitochondria reaching the endolysosomal system to form MVBs (reviewed in Picca et al., 2020). These EVs can, in turn, transfer their mtDNA to cells with impaired metabolism, leading to the restoration of metabolic activity and treatment resistance (Sansone et al., 2017).

Recent studies contradict the vesicular nature of cfDNA. Although very scarce, evidence shows that EV-DNA could be bound to the outer lipid layer of EV membranes (Németh et al., 2017). High-resolution density gradient fractionation, to avoid aggregation of vesicles and obtain a pure fraction of exosomes, showed that exosomes or any other type of small EVs actually did not contain any dsDNA nor histones H2A, H3, or H4 (Jeppesen et al., 2019). Instead, active secretion of DNA and histones occurred through an amphisome-dependent mechanism, involving CD63-positive multivesicular endosomes-like structures (MVE). Amphisomes are hybrid organelles appearing from the fusion of an autophagosome and an MVE. The authors propose a new model, yet to be confirmed, in which the dsDNA might be secreted by amphisome fusion to the plasma membrane in a non-vesicular way. This non-vesicular pathway could be the recently described nanoparticular exomeres actively secreted by cells and different from mere aggregates (Zhang et al., 2018). DsDNA was found in both exomere and exosome fractions. Whether exomere-DNA can be functional as the exomere protein cargo needs to be confirmed (Zhang et al., 2019). By contrast, fractions from high-resolution iodixanol density

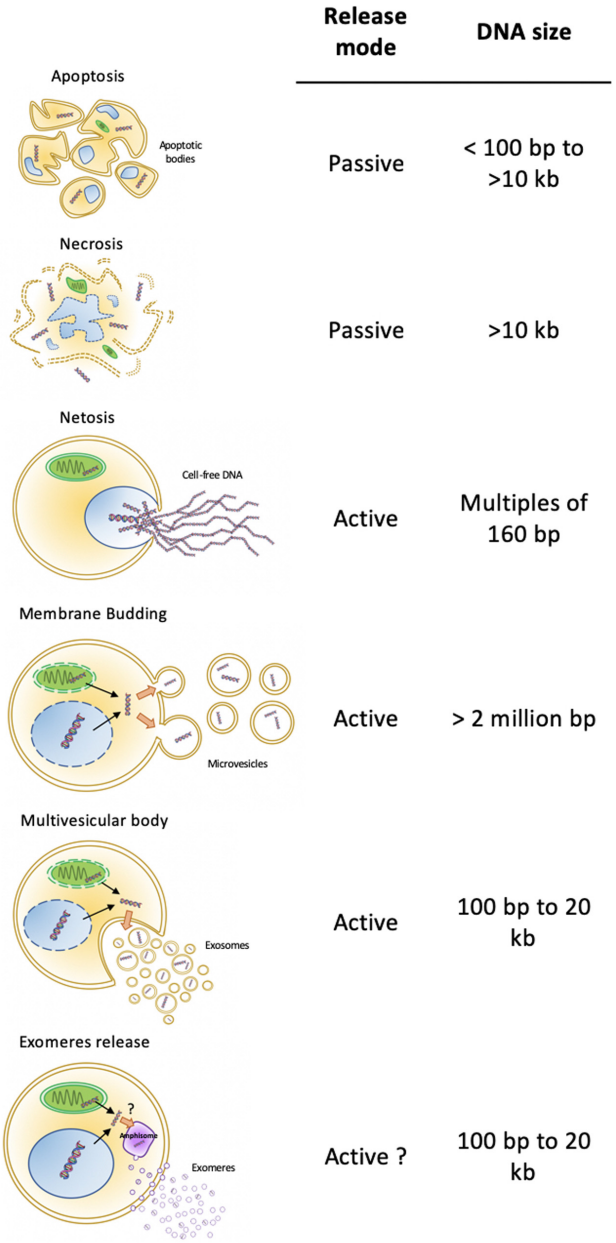

FIGURE 1 | Cell-free DNA cell sources. DNA can be released by active or passive mechanisms. Apoptosis is a passive mechanism releasing apoptotic bodies with fragmented genomic DNA, in which sizes encompass a range of 100 bp to more than 10 kb. Necrosis is a passive way of DNA release, with free and non-vesicular all sizes fragments. Active mechanisms of DNA release include NETosis, with projection of very long, decondensed genomic DNA, microvesicles budding from a plasma membrane, exosomes secretion from multivesicular bodies, and exomeres released from amphisomes. Depending on the active mechanism, DNA fragment length varies between 100 bp (exosomes and exomeres) and reaching more than 2 million bp (Microvesicles).

gradients were recently found positive for DNA fragments and exosome markers such as CD63, CD9, CD81, flotillin-1, and TSG101 (Lázaro-Ibáñez et al., 2019).

In conclusion, more work is needed to ascertain the embedding mechanism and the final location of DNA in EVs and nanoparticles.

TECHNICAL ASPECTS

Exosomes and EVs Isolation

To ascertain the presence of DNA in EV, the first step before analysis of EV-DNA is the correct and specific isolation of EVs. This is crucial to obtain pure material and to have minimal impact on DNA extraction and further analyses. Various isolation and purification methods for EVs have been recently reviewed in literature (Yang et al., 2020). Even if ultracentrifugation is still the gold standard for EV enrichment, alternative technologies allow for the purification of subpopulations of EVs such as exosomes. For instance, size exclusion chromatography seems to emerge as a promising method because it significantly limits vesicle structural damages, such as aggregation induced by high-speed centrifugation (An et al., 2018; Royo et al., 2020; Sidhom et al., 2020). This method separates vesicles according to their sizes, which is not necessarily related to their functions. Some authors report optimal vesicle enrichment and soluble protein removal with a combination of ultrafiltration and size exclusion chromatography (Diaz et al., 2018). Five different methods for isolation and separation of EVs from protein and lipid particles in human serum were compared. The authors concluded that sequential use of two or more techniques greatly improved the depletion of lipoprotein and protein contaminants but significantly reduced the yield of EVs (Brennan et al., 2020). The choice of the appropriate isolation method depends on the initial quantity of available material and the desirable amount of EVs.

Microfluidic platforms represent another auspicious technology in the field of EV research. In particular, in the line of single cell analysis, new integrated microfluidic techniques facilitate combinatorial exosome isolation and analysis based on their physical and biochemical properties (Yang et al., 2020). A recent publication describes a microfluidic device allowing the rapid isolation of tumor derived exosomes from the plasma of pancreatic ductal adenocarcinoma (PDAC) patients (Kamyabi et al., 2020). EVs or exosomes are captured by antibodies against CD63, CD9, and CD81 surface protein (exosome) or membrane EPCAM (tumor). The antibody/antigen bounds are then ruptured to recover the immobilized EVs. After DNA extraction, the authors were able to identify *KRAS* mutations by droplet digital PCR in EV-DNA. Of note, they recovered more total exoDNA in CD9/CD63/CD81 vesicles than in EPCAM-positive EVs, but this latter fraction contained more mutant *KRAS* DNA.

EV-DNA Properties and Extraction Methods

Unlike cfDNA, EV-DNA is protected by a lipid bilayer membrane, which has a protective function against nucleases, thus increasing stability. Protected DNA is particularly adapted to lab routine analysis (Jin et al., 2016). Moreover, tumor EV-DNA amounts vary depending on distinct vesicle types separated by iodixanol density gradient. Like for protein and RNA, genomic

DNA (gDNA) identified specific EV subpopulations also positive for exosomal proteins (Lázaro-Ibáñez et al., 2019). In the same way, different gDNA contents characterized apoptotic bodies, microvesicles, and exosomes (Lázaro-Ibáñez et al., 2014). After a differential centrifugation fractionation, the authors searched for specific genes and sequences within the different EV fractions. A 108 bp intron fragment for MLH1 was found in most EV types. Mutant *TP53* and *PTEN* suppressor gene sequences were present in apoptotic bodies, but in very small amounts in EVs and exosomes. Thus, it seems that higher DNA concentrations are associated with larger vesicles (Vagner et al., 2018; Lázaro-Ibáñez et al., 2019), and higher gDNA rates were packed in microvesicles from tumor as compared to normal cells (Balaj et al., 2011). Thus, paralleling the still obscure embedding mechanism of EV-DNA, identifying the best fractions for analysis remains challenging.

As mentioned in the previous chapter, gDNA was found associated to the surface of EVs, which may interfere with intravesicular DNA characterization. As extraneous DNA was found at the urinary exosome surface, a protocol to avoid contaminations and isolate internal gDNA only may be needed (Miranda et al., 2010). In the same way, DNase sensitive nucleic acids have been identified on the surface of mast cell EVs (Shelke et al., 2016) and EVs isolated from melanoma patients' plasma (Zocco et al., 2020). Although intracytoplasmic uptake of those nucleic acids occurred in recipient cells, no observable functional impact was relayed intracellularly. More recently, Vagner et al. (2018) concluded that most of the DNA content was localized on the outside or the surface of EVs, with only a small portion being internalized in EVs, but again, the functionality of this surface DNA was not described.

Regardless of the analyzed vesicles, EV-DNA extraction slightly differs from conventional DNA extraction from cells or tissues but seems to be shared by many authors. Briefly, a lysis step followed by washing and elution on spin columns are often reported. EV-DNA extraction kits are now available from several commercial suppliers, with similar methods. Moreover, in order to avoid surface-associated DNA contamination, most procedures include a DNAse I or exonuclease I pretreatment.

In conclusion, all EV types seem to be distinct in their DNA content, but the sorting of the different loci and/or mutant DNA molecules is far from being understood. Additionally, heterogeneity resides in the definitions of EV fractions. Consensual agreement will define subcategories of large and small EVs, most likely by the presence of specific biomarkers, in order to better characterize their content and functional properties, as elegantly proposed recently (Jeppesen et al., 2019). On the technical aspect, future comparison between labs is needed to validate the full process of EV enrichment and DNA extraction.

EV-DNA REFLECTS TUMOR GENOME HALLMARKS

Tumor Genome and Exome

After whole genome sequencing (WGS), human PDAC tumor genome DNA and exoDNA shared 92% of the reads, suggesting that exoDNA is representative of all chromosomes (Kahlert et al., 2014). Moreover, 65–91% coverage of the human genome was found in pancreaticobiliary cancer exosomes (San Lucas et al., 2016). In the same way, the murine tumor intestinal epithelial cell line RAS-3 EV-DNA covered more than 90% of the parental cell genome (Lee et al., 2014). Interestingly, exoDNA human sequences were 95–99% identical to the exomes of solid tumors (Vagner et al., 2018; Lázaro-Ibáñez et al., 2019). The same conclusions were drawn with serum exoDNA from pheochromocytoma (PCC) and paraganglioma (PGL) patients (Wang et al., 2018). Human prostate cancer exoDNA even spanned mtDNA (Vagner et al., 2018). Consistent with previous observations, WGS revealed that EV-DNA derived from human mast and erythroleukemic cell lines spanned all chromosomes and mtDNA (Lázaro-Ibáñez et al., 2019).

Taken together, these results confirm that exoDNA is at least representative of the entire tumor exome and may be even the whole genome.

Tumor-Specific Sequence Variations

As carriers of tumor genome and/or exome, EV-DNA allows for the detection of specific gene mutations and gene amplification originally present in the primary tumor and its metastases. Based on preclinical results, multiple studies describe the identification of oncogenic alterations or tumor suppressor gene mutations in EV-DNA. For instance, Balaj et al. (2011) found typical *c-myc* amplification in EV-DNA extracted from cultured medulloblastoma cell lines as well as medulloblastoma tumor bearing mouse sera. Similarly, inactivating point mutations of tumor suppressors *TP53* and *PTEN* were identified in exoDNA from prostate cancer cell lines bearing these mutations (Lázaro-Ibáñez et al., 2014). Stepping toward clinical applications, Kahlert et al. (2014) identified matched *KRAS* and *TP53* hotspot mutations in serum exosomal DNA and solid tumor DNA from PDAC patients. The same observations were made for *RET*, *HIF2A*, *VHL*, and *SDHB* point mutations in PCCs and PGLs bared by patients or mice (Wang et al., 2018). More recently, androgen receptor gene (*AR*) amplifications have been identified in 12 of 15 patients from a castration-resistant prostate cancer (CRPC) cohort using DNA extracted from EV-enriched plasmas (Foroni et al., 2020; **Table 1**). The detection of *AR* T878A mutation was more challenging.

Besides serum and plasma, other physiological or pathological body fluids contain EVs. A high clinical value was carried by pleural effusion EVs from lung cancer patients to determine the EGFR mutational status. Indeed, exosomal DNA *EGFR* mutational status correlated with gDNA from matched tumor tissues with 100% sensitivity, 96% specificity and 98% coincidence rate (Qu et al., 2019). More modestly, a comparative genomic profiling of solid bladder tumor DNA and matched urinary exoDNA from nine patients revealed a 65% (12/17) concordance rate for somatic mutation detection. ExoDNA and tumor samples presented a similar pattern of copy number aberrations (Lee et al., 2018).

Other molecular features of tumors can be identified by EV-DNA analysis. Frameshift mutation patterns in microsatellite

TABLE 1 | Results of the main clinical studies assessing the performance of EV-DNA biomarkers.

Mutation(s) detected	Stage of tumors: localized, metastatic, all stages	Mutant DNA localization	Type of sample	Clinical relevance and potential application	References
Ovarian cancer					
DROSHA, *LIG4*, *MACROD2*, *SATB1*, *RASSF6*, and *BIRC2*	Metastatic	Internal double-stranded exoDNA	Ascites and plasma	Treatment with genotoxic drugs resulted in increased cancer cell micronuclei and genomic DNA and other nuclear contains into exosomes	Yokoi et al., 2019
Glioblastoma					
IDH1G395A	All stages (II–IV)	Internal and external	Peripheral blood and surgical tissue sample	*IDH1G395* mutation is detected in exosomes, correlation with diagnostic and prognostic in all stages, DNA-containing EVs can cross the disrupted blood–brain barrier	García-Romero et al., 2017
Non-small cell lung cancer					
EGFR	Advance non-small cell lung cancer	ExoDNA (internal) and ctDNA	Plasma and matched baseline plasma and tissue biopsy samples	Combining exoDNA and ctDNA increased the sensitivity for EGFR mutation detection in plasma. Useful in M0/M1a patients	Krug et al., 2018
EGFR T790M	All stages and healthy controls	ExoDNA/RNA (internal) and ctDNA	Plasma	The combination of exoDNA/RNA and ctDNA for *EGFR T790M* has a better sensitivity and specificity than ctDNA alone	Castellanos-Rizaldos et al., 2018
EGFR	All stages	ExoDNA (internal)	Plasma	Diagnostic and prognosis	Hur et al., 2019
EGFR T790M	All stages	ExoDNA (internal) and ctDNA	Plasma and bronchial washing	Diagnosis and prognosis	Park et al., 2020
Urothelial carcinoma of bladder					
MDM2, *ERBB2*, *CCND1*, *CCNE1*, *CDKN2A*, *PTEN*, *RB1*	T2, T3, T4, N0, N2	ExoDNA (internal) and ctDNA	Urine samples	Identification of somatic mutation and copy number variation using ctDNA and exoDNA in urine samples	Lee et al., 2018
Prostate cancer					
P53, *MLH1*, *PTEN*	T1c, T3	ExoDNA internal and external	Plasma	EVs contain dsgDNA fragments that could be used to detect specific mutation. EVs could be used as potential biomarkers for diagnostic and prognosis	Lázaro-Ibáñez et al., 2014
AR gene amplification, AR-V7 transcript, and T878A mutation	Metastatic castration-resistant prostate cancer	ExoDNA and exoRNA internal and external	Plasma	Selective isolation of a subset of circulating exosomes enriched for tumor origin increases sensitivity and specificity for the detection of specific alterations	Foroni et al., 2020
MYC, *PTEN*	Metastatic castration-resistant prostate cancer	Single-stranded and double-stranded DNA	Plasma	EVs contain extracellular DNA and suggest that it could be used to monitor metastatic prostate cancer	Vagner et al., 2018
Melanoma					
$BRAF^{V600E}$	T3, T4	ExoDNA (internal and external) and cfDNA	Plasma	Significant improvement in $BRAF^{V600E}$ mutation detection combining cfDNA and EV-DNA analysis using peptide affinity assay	Zocco et al., 2020
Pancreatic cancer					
KRAS	All stages	ExoDNA (internal) and ctDNA	Plasma	Higher *KRAS* exo-DNA MAF was associated with decreased DFS in patients with localized disease	Allenson et al., 2017
$KRAS^{G12D}$, $TP53^{R273H}$	Resectable	ExoDNA (internal)	Plasma	ExoDNA could be an interesting tool to diagnose pancreatic malignancies	Yang et al., 2017
KRAS	All stages	ExoDNA (internal) and ctDNA	Plasma	MAF > 5% is correlated with worse DFS and OS	Bernard et al., 2019

MAF, mutant allele frequency. ExoDNA, exosomal DNA. Exo-DNA internal, a DNAse step was carried out prior to tumor DNA detection in exosomes. DFS, disease free survival. OS, overall survival. ctDNA, circulating tumor DNA. cfDNA, cell-free DNA. EV, extracellular vesicles. gDNA, genomic DNA. dsgDNA, double-stranded genomic DNA.

stretches of *TGFBR2* and other microsatellite instability (MSI) target genes were found in the DNA cargo of MSI^{+} HCT-116 colorectal cancer cell line-derived exosomes Fricke et al., 2017. Thus, tumor MSI status could potentially be determined by EV-DNA analysis.

Tumor-Specific Epigenetics

Yamamoto et al. (2016) analyzed the methylation status of BarH-like 2 homeobox protein (*BARHL2*), a gene known to be hypermethylated in gastric cancers (GC), in gastric wash-derived DNA and/or gastric juice-derived exoDNA of GC and healthy

patients. Deeper analysis revealed that the *BARHL2* methylation status provided an area under the curve of 0.923 with 90% sensitivity and 100% specificity for the discrimination of GC patients from non-GC controls. Furthermore, the analysis of *LINE-1* and *SOX-2* methylation status was performed using DNA extracted from both GC cell lines and GC patients' gastric juice microvesicles. Similar levels of methylation for *LINE-1* and *SOX-2* were obtained in EV-DNA compared to GC cell lines or patients' tumor genomic DNA (Yamamoto, 2014). Therefore, as observed for the mutational status and sequence variations, epigenetic modifications such as methylations are shared between EV-DNA and the gDNA of their tumor of origin. More cancers need to be examined to confirm these encouraging results.

EV-DNA AS A CLINICALLY RELEVANT BIOMARKER

In cancer, exosomes can oppose or potentiate the development of an aggressive tumor microenvironment, and thus impact tumor progression and metastatic and clinical outcome (Tai et al., 2018). EVs have also become choice materials for translational studies especially as liquid biopsy tools. In addition, the non-invasive and potentially repetitive nature of their analysis is applicable to both diagnosis and cancer follow-up. Routine tissue biopsy mutation status has been useful to step forward in targeted therapy, while ctDNA was proposed for the diagnosis and tumor monitoring. Although important technical advances have improved the sensitivity of ctDNA detection, and the fact that numerous studies have explored its diagnostic and prognostic values, the balance between translational research and application to routine lab use remains low.

Analysis of circulating EVs from patients with prostate cancer found tumor-related DNA, in particular *TP53* and *PTEN* mutations [**Table 1**, $n = 4$ (Lázaro-Ibáñez et al., 2014)], further confirmed in very few samples from metastatic castration-resistant cancers ($n = 4$; Vagner et al., 2018). The relevance of plasma EV-DNA remained underrated because efforts were produced for ctDNA detection. Therefore, only a few studies have compared ctDNA and EV-DNA diagnostic performances. Using ctDNA as a "gold standard" of DNA-based liquid biopsy of PDAC, stem studies by Alvarez's group demonstrated that *KRAS* mutation detection in EV-DNA was superior to ctDNA for prognosis on large cohorts (Allenson et al., 2017; Bernard et al., 2019). The clinical performance of EV-DNA was somewhat disappointing since diagnostic accuracies ranked between 35 and 69% when compared to tissue biopsy (Bernard et al., 2019; Allenson et al., 2017, respectively). However, EV-DNA showed relevance in PDAC management since a correlation with non-recurrence survival was found in both studies, but limited to patients with metastatic disease (Allenson et al., 2017; Bernard et al., 2019). Moreover, although of good prognostic value, exoDNA based on mutant *KRAS* detection with highly sensitive detection techniques might not be suitable alone for general population screening as it yields high false-positive rates (Allenson et al., 2017; Bernard et al., 2019). More work needs to be carried out to associate this detection/quantification with another marker to increase specificity, such as combined liquid biopsy approaches (Cohen et al., 2017; Buscail et al., 2019a,b). Yang et al. (2017) highlighted the diagnostic value of PCR detection of $KRAS^{G12D}$ and $TP53^{R273H}$ that could differentiate healthy controls from patients with pancreatic cancer. This method, however, showed low performance to discriminating non-invasive (e.g., chronic pancreatitis, $n = 9$ and pancreatic cysts, $n = 12$) from malignant pancreatic pathologies. The very low number of patients makes definitive conclusions very risky, though. A high concordance rate (>95%) was found between circulating cfDNA (ct or EV) and primary tumors (Bernard et al., 2019) in a good size cohort.

According to the anatomical position of the primary tumor or its metastases, other biological fluids may be relevant for EV-DNA-based liquid biopsy. Interestingly, EVs carrying the $IDH1^{G395A}$ mutation emitted by glioblastomas could cross the blood–brain barrier and be assayed intact in the bloodstream (García-Romero et al., 2017). Patients with mutated *IDH1* have a better prognosis than individuals with the wild-type allele, but with similar histology. In the same way, the genetic alterations of plasma or urine ctDNA and urine EV-DNA matched the mutational profiles of primary tumors in urothelial bladder carcinoma (Lee et al., 2018). The typical amplifications of *MDM2*, *ERBB2*, *CCND1*, and *CCNE1* and deletions of *CDKN2A*, *PTEN*, and *RB1* were characterized in only nine patients. More recently, exoDNA performed better for the diagnostic of non-small cell lung cancer (NSCLC) compared to EV-excluded cell-free DNA in bronchial wash fluid by the detection of $EGFR^{T790M}$. The overall detection sensitivity of *EGFR* mutation was 89.7 and 31%, respectively, with 100% specificity (Park et al., 2020).

In conclusion, although very preliminary, combined recent analyses propose EV-DNA as an alternative to reach the promises of ctDNA, but more work is needed and more cancers must be evaluated to reach a final decision on whether to consider clinical lab development of this emerging biomarker.

CONCLUSION AND FUTURE DEVELOPMENTS

In the era of personalized medicine, molecular and epigenetic cancer profiling, using primary tumor tissue, takes up an ever greater place in a patient's management and care. These modern molecular analyses help diagnosis, prediction of disease progression, and also adaptation and optimization of therapeutic decisions. Exosomal and EV-associated DNA seem promising as circulating biomarkers for cancer profiling as they can reflect the primary tumor and its metastases.

The mechanisms involved in active DNA release by tumor cells remain elusive; in particular, the way DNA species are sorted into EVs is far from being resolved. The recently reported amphisome-driven secretion in non-vesicular particles (Zhang et al., 2018) needs independent confirmation. In the same way, the final location of vesicle-associated DNA deserves more in depth exploration since EV-DNA can be bound to the outer lipid layer of EV membranes (Németh et al., 2017). Moreover, intra-EV

tumor DNA might be less frequent than ctDNA (Klump et al., 2018). Therefore, the best extracellular compartment for tumor DNA detection and quantification is still debated.

The functional representation of EV-DNA of tumor behavior might also be partly diminished by the fact that a large part of ctDNA within cfDNA is released by dying tumor cells. This complexifies its cancer-relevant analysis. Furthermore, more work needs to be done to determine whether cfDNA is a good surrogate of tumor heterogeneity. Lee et al. (2018) reported the detection of additional somatic mutations in urinary exoDNA compared to bladder primary tumor DNA, suggesting that, although present in tumors, these mutations were missed by standard tissue biopsy genome analysis. However, those observations must be considered carefully because the authors increased the depth of exoDNA sequencing by 2.6 folds compared to tissue DNA analysis, which allows the detection of very rare (relevant?) mutations. In the same way, it will be necessary to determine which between the intraluminal and surface associated DNA better reflects tumor heterogeneity or tumor entire genome.

A major common limitation of studies interested in the clinical value of tumor EV-DNA is the minimal size of the patient's cohorts (from as little as a few patients), reflecting that this topic is still emerging in the liquid biopsy field. By contrast, research on CTCs (circulating tumor cells) and ctDNA resulted in some indications for routine assessment. The other crucial development needed in the field is to implement a sufficient number of studies comparing the clinical values (with sufficient numbers of patients) of EV-DNA and ctDNA. Up to now, such kinds of studies are limited to PDAC and CRPC. Further external validation by other teams and in more cancers are needed.

One of the latest developments in tumor genetics is the characterization of epigenetic marks associated to tumor progression and/or severity (Costa-Pinheiro et al., 2015). Tumor epigenetic marks can as well constitute biomarkers with a theranostic value, since they permit the identification of targetable gene alterations and can be pharmacologically modified as personalized medicine approaches (see review Li et al., 2019). The extension of this knowledge to EV-DNA might be of particular interest to test whether EV-transferred DNA retains the epigenetic marks. If so, it would be worthwhile to ask whether they are stably kept during the journey and transferred in and impact recipient cells. Moreover, the traceability of EV can definitely link the primary tumor origin of epigenetic marks. Finally, finding the retention of tumor epigenetic marks in tumor EVs might position tumor EV-DNA as the ultimate circulating tumor biomarker, keeping both typical marks of tumor DNA: sequence variations and epigenetics.

Taken together, this review highlights the budding value of EV-DNA approaches to test and follow tumor liquid biopsies. Obviously, more work is needed with robust methodology to ascertain the clinical relevance of tumor EV-DNA as actual cancer biomarkers. However, the available literature tends to consider this approach very promising.

AUTHOR CONTRIBUTIONS

SA, SD, and EB involved in the manuscript writing, figure design, and table conception. VV, CD, JB, AB, J-PM, and FM-G performed the literature searching, articles selection, discussion on mechanisms and identification of DNA contents, manuscript editing, and final approval. LB, BB, and CL performed the manuscript organization, figure design, search of literature on clinical aspects, discussion on clinical relevance, manuscript editing, and final approval. All authors contributed to the article and approved the submitted version.

FUNDING

The authors received grants from the following granting agencies: Ligue régionale contre le cancer Aquitaine Charentes, Groupement Interrégional de Recherche Clinique et d'Innovation Sud-Ouest Outre-Mer Hospitalier (GIRCI SOHO), Fonds Patrick Brou de Laurière, Association Française pour la recherche contre le cancer du pancréas (AFRCP), and Cancéropôle Grand Sud-Ouest (GSO).

REFERENCES

Allenson, K., Castillo, J., San Lucas, F. A., Scelo, G., Kim, D. U., Bernard, V., et al. (2017). High prevalence of mutant KRAS in circulating exosome-derived DNA from early-stage pancreatic cancer patients. *Ann. Oncol. Off. J. Eur. Soc. Med. Oncol.* 28, 741–747. doi: 10.1093/annonc/mdx004

An, M., Wu, J., Zhu, J., and Lubman, D. M. (2018). Comparison of an optimized ultracentrifugation method versus size-exclusion chromatography for isolation of exosomes from human serum. *J. Proteome Res.* 17, 3599–3605. doi: 10.1021/acs.jproteome.8b00479

Balaj, L., Lessard, R., Dai, L., Cho, Y.-J., Pomeroy, S. L., Breakefield, X. O., et al. (2011). Tumour microvesicles contain retrotransposon elements and amplified oncogene sequences. *Nat. Commun.* 2:180. doi: 10.1038/ncomms1180

Bernard, V., Kim, D. U., San Lucas, F. A., Castillo, J., Allenson, K., Mulu, F. C., et al. (2019). Circulating nucleic acids are associated with outcomes of patients with pancreatic cancer. *Gastroenterology* 156, 108–118.e4. doi: 10.1053/j.gastro.2018.09.022

Bortner, C. D., Oldenburg, N. B., and Cidlowski, J. A. (1995). The role of DNA fragmentation in apoptosis. *Trends Cell Biol.* 5, 21–26. doi: 10.1016/s0962-8924(00)88932-88931

Brennan, K., Martin, K., FitzGerald, S. P., O'Sullivan, J., Wu, Y., Blanco, A., et al. (2020). A comparison of methods for the isolation and separation of extracellular vesicles from protein and lipid particles in human serum. *Sci. Rep.* 10:1039. doi: 10.1038/s41598-020-57497-57497

Buscail, E., Alix-Panabières, C., Quincy, P., Cauvin, T., Chauvet, A., Degrandi, O., et al. (2019a). High clinical value of liquid biopsy to detect circulating tumor cells and tumor exosomes in pancreatic ductal adenocarcinoma patients eligible for up-front surgery. *Cancers* 11:1656. doi: 10.3390/cancers11111656

Buscail, E., Chauvet, A., Quincy, P., Degrandi, O., Buscail, C., Lamrissi, I., et al. (2019b). CD63-GPC1-positive exosomes coupled with CA19-9 offer good diagnostic potential for resectable pancreatic ductal Adenocarcinoma. *Transl. Oncol.* 12, 1395–1403. doi: 10.1016/j.tranon.2019.07.009

Cahilog, Z., Zhao, H., Wu, L., Alam, A., Eguchi, S., Weng, H., et al. (2020). The role of neutrophil NETosis in organ injury: novel inflammatory cell death mechanisms. *Inflammation* 43, 1–12. doi: 10.1007/s10753-020-01294-x

Castellanos-Rizaldos, E., Grimm, D. G., Tadigotla, V., Hurley, J., Healy, J., Neal, P. L., et al. (2018). Exosome-based detection of EGFR T790M in plasma from non-small cell lung cancer patients. *Clin. Cancer Res. Off. J. Am. Assoc. Cancer Res.* 24, 2944–2950. doi: 10.1158/1078-0432.CCR-17-3369

Cocucci, E., Racchetti, G., and Meldolesi, J. (2009). Shedding microvesicles: artefacts no more. *Trends Cell Biol.* 19, 43–51. doi: 10.1016/j.tcb.2008.11.003

Cohen, J. D., Javed, A. A., Thoburn, C., Wong, F., Tie, J., Gibbs, P., et al. (2017). Combined circulating tumor DNA and protein biomarker-based liquid biopsy for the earlier detection of pancreatic cancers. *Proc. Natl. Acad. Sci. U.S.A.* 114, 10202–10207. doi: 10.1073/pnas.1704961114

Costa-Pinheiro, P., Montezuma, D., Henrique, R., and Jerónimo, C. (2015). Diagnostic and prognostic epigenetic biomarkers in cancer. *Epigenomics* 7, 1003–1015. doi: 10.2217/epi.15.56

Diaz, G., Bridges, C., Lucas, M., Cheng, Y., Schorey, J. S., Dobos, K. M., et al. (2018). Protein digestion, ultrafiltration, and size exclusion chromatography to optimize the isolation of exosomes from human blood plasma and serum. *J. Vis. Exp.* 134:57467. doi: 10.3791/57467

Fenech, M., Kirsch-Volders, M., Natarajan, A. T., Surralles, J., Crott, J. W., Parry, J., et al. (2011). Molecular mechanisms of micronucleus, nucleoplasmic bridge and nuclear bud formation in mammalian and human cells. *Mutagenesis* 26, 125–132. doi: 10.1093/mutage/geq052

Fernando, M. R., Jiang, C., Krzyzanowski, G. D., and Ryan, W. L. (2017). New evidence that a large proportion of human blood plasma cell-free DNA is localized in exosomes. *PLoS One* 12:e0183915. doi: 10.1371/journal.pone.0183915

Fischer, S., Cornils, K., Speiseder, T., Badbaran, A., Reimer, R., Indenbirken, D., et al. (2016). Indication of horizontal DNA gene transfer by extracellular vesicles. *PLoS One* 11:e0163665. doi: 10.1371/journal.pone.0163665

Fricke, F., Lee, J., Michalak, M., Warnken, U., Hausser, I., Suarez-Carmona, M., et al. (2017). TGFBR2-dependent alterations of exosomal cargo and functions in DNA mismatch repair-deficient HCT116 colorectal cancer cells. *Cell Commun. Signal.* 15:14. doi: 10.1186/s12964-017-0169-y

Foroni, C., Zarovni, N., Bianciardi, L., Bernardi, S., Triggiani, L., Zocco, D., et al. (2020). When less is more: specific capture and analysis of tumor exosomes in plasma increases the sensitivity of liquid biopsy for comprehensive detection of multiple androgen receptor phenotypes in advanced prostate cancer patients. *Biomedicines* 8:131. doi: 10.3390/biomedicines8050131

García-Romero, N., Carrión-Navarro, J., Esteban-Rubio, S., Lázaro-Ibáñez, E., Peris-Celda, M., Alonso, M. M., et al. (2017). DNA sequences within glioma-derived extracellular vesicles can cross the intact blood-brain barrier and be detected in peripheral blood of patients. *Oncotarget* 8, 1416–1428. doi: 10.18632/oncotarget.13635

Guescini, M., Genedani, S., Stocchi, V., and Agnati, L. F. (2010). Astrocytes and Glioblastoma cells release exosomes carrying mtDNA. *J. Neural Transm.* 117, 1–4. doi: 10.1007/s00702-009-0288-288

Harding, S. M., Benci, J. L., Irianto, J., Discher, D. E., Minn, A. J., and Greenberg, R. A. (2017). Mitotic progression following DNA damage enables pattern recognition within micronuclei. *Nature* 548, 466–470. doi: 10.1038/nature23470

Hur, J. Y., Lee, J. S., Kim, I. A., Kim, H. J., Kim, W. S., and Lee, K. Y. (2019). Extracellular vesicle-based EGFR genotyping in bronchoalveolar lavage fluid from treatment-naive non-small cell lung cancer patients. *Transl. Lung Cancer Res.* 8, 1051–1060. doi: 10.21037/tlcr.2019.12.16

Jeppesen, D. K., Fenix, A. M., Franklin, J. L., Higginbotham, J. N., Zhang, Q., Zimmerman, L. J., et al. (2019). Reassessment of exosome composition. *Cell* 177, 428–445.e18. doi: 10.1016/j.cell.2019.02.029

Jin, Y., Chen, K., Wang, Z., Wang, Y., Liu, J., Lin, L., et al. (2016). DNA in serum extracellular vesicles is stable under different storage conditions. *BMC Cancer* 16:753. doi: 10.1186/s12885-016-2783-2782

Johnstone, R. M. (1992). The jeanne manery-fisher memorial Lecture 1991. Maturation of reticulocytes: formation of exosomes as a mechanism for shedding membrane proteins. *Biochem. Cell Biol. Biochim. Biol. Cell.* 70, 179–190. doi: 10.1139/o92-028

Kahlert, C., Melo, S. A., Protopopov, A., Tang, J., Seth, S., Koch, M., et al. (2014). Identification of double-stranded genomic DNA spanning all chromosomes with mutated KRAS and p53 DNA in the serum exosomes of patients with pancreatic cancer. *J. Biol. Chem.* 289, 3869–3875. doi: 10.1074/jbc.C113.532267

Kalluri, R. (2016). The biology and function of exosomes in cancer. *J. Clin. Invest.* 126, 1208–1215. doi: 10.1172/JCI81135

Kamyabi, N., Abbasgholizadeh, R., Maitra, A., Ardekani, A., Biswal, S. L., and Grande-Allen, K. J. (2020). Isolation and mutational assessment of pancreatic cancer extracellular vesicles using a microfluidic platform. *Biomed. Microdevices* 22:23. doi: 10.1007/s10544-020-00483-7

Klump, J., Phillipp, U., Follo, M., Eremin, A., Lehmann, H., Nestel, S., et al. (2018). Extracellular vesicles or free circulating DNA: where to search for BRAF and cKIT mutations? *Nanomed. Nanotechnol. Biol. Med.* 14, 875–882. doi: 10.1016/j.nano.2017.12.009

Krug, A. K., Enderle, D., Karlovich, C., Priewasser, T., Bentink, S., Spiel, A., et al. (2018). Improved EGFR mutation detection using combined exosomal RNA and circulating tumor DNA in NSCLC patient plasma. *Ann. Oncol. Off. J. Eur. Soc. Med. Oncol.* 29, 700–706. doi: 10.1093/annonc/mdx765

Lázaro-Ibáñez, E., Lässer, C., Shelke, G. V., Crescitelli, R., Jang, S. C., Cvjetkovic, A., et al. (2019). DNA analysis of low- and high-density fractions defines heterogeneous subpopulations of small extracellular vesicles based on their DNA cargo and topology. *J. Extracell. Ves.* 8:1656993. doi: 10.1080/20013078.2019.1656993

Lázaro-Ibáñez, E., Sanz-Garcia, A., Visakorpi, T., Escobedo-Lucea, C., Siljander, P., Ayuso-Sacido, A., et al. (2014). Different gDNA content in the subpopulations of prostate cancer extracellular vesicles: apoptotic bodies, microvesicles, and exosomes. *Prostate* 74, 1379–1390. doi: 10.1002/pros.22853

Le Naour, J., Zitvogel, L., Galluzzi, L., Vacchelli, E., and Kroemer, G. (2020). Trial watch: sting agonists in cancer therapy. *Oncoimmunology* 9:1777624. doi: 10.1080/2162402X.2020.1777624

Lee, D. H., Yoon, H., Park, S., Kim, J. S., Ahn, Y.-H., Kwon, K., et al. (2018). Urinary Exosomal and cell-free DNA detects somatic mutation and copy number alteration in urothelial carcinoma of bladder. *Sci. Rep.* 8:14707. doi: 10.1038/s41598-018-32900-32906

Lee, T. H., Chennakrishnaiah, S., Audemard, E., Montermini, L., Meehan, B., and Rak, J. (2014). Oncogenic ras-driven cancer cell vesiculation leads to emission of double-stranded DNA capable of interacting with target cells. *Biochem. Biophys. Res. Commun.* 451, 295–301. doi: 10.1016/j.bbrc.2014.07.109

Li, Y., Li, Z., and Zhu, W.-G. (2019). Molecular mechanisms of epigenetic regulators as activatable targets in cancer theranostics. *Curr. Med. Chem.* 26, 1328–1350. doi: 10.2174/0929867324666170921101947

Miranda, K. C., Bond, D. T., McKee, M., Skog, J., Păunescu, T. G., Da Silva, N., et al. (2010). Nucleic acids within urinary exosomes/microvesicles are potential biomarkers for renal disease. *Kidney Int.* 78, 191–199. doi: 10.1038/ki.2010.106

Németh, A., Orgovan, N., Sódar, B. W., Osteikoetxea, X., Pálóczi, K., Szabó-Taylor, K. É, et al. (2017). Antibiotic-induced release of small extracellular vesicles (exosomes) with surface-associated DNA. *Sci. Rep.* 7:8202. doi: 10.1038/s41598-017-08392-8391

Park, J., Lee, C., Eom, J. S., Kim, M.-H., and Cho, Y.-K. (2020). Detection of EGFR mutations using bronchial washing-derived extracellular vesicles in patients with non-small-cell lung carcinoma. *Cancers* 12:2822. doi: 10.3390/cancers12102822

Picca, A., Guerra, F., Calvani, R., Coelho-Junior, H. J., Bossola, M., Landi, F., et al. (2020). Generation and release of mitochondrial-derived vesicles in health. *Aging Dis. J. Clin. Med.* 9:1440. doi: 10.3390/jcm9051440

Qu, X., Li, Q., Yang, J., Zhao, H., Wang, F., Zhang, F., et al. (2019). Double-stranded DNA in exosomes of malignant pleural effusions as a novel DNA source for EGFR mutation detection in lung adenocarcinoma. *Front. Oncol.* 9:931. doi: 10.3389/fonc.2019.00931

Royo, F., Théry, C., Falcón-Pérez, J. M., Nieuwland, R., and Witwer, K. W. (2020). Methods for separation and characterization of extracellular vesicles: results of a worldwide survey performed by the isev rigor and standardization subcommittee. *Cells* 9:1955. doi: 10.3390/cells9091955

San Lucas, F. A., Allenson, K., Bernard, V., Castillo, J., Kim, D. U., Ellis, K., et al. (2016). Minimally invasive genomic and transcriptomic profiling of visceral cancers by next-generation sequencing of circulating exosomes. *Ann. Oncol. Off. J. Eur. Soc. Med. Oncol.* 27, 635–641. doi: 10.1093/annonc/mdv604

Sansone, P., Savini, C., Kurelac, I., Chang, Q., Amato, L. B., Strillacci, A., et al. (2017). Packaging and transfer of mitochondrial DNA via exosomes regulate

escape from dormancy in hormonal therapy-resistant breast cancer. *Proc. Natl. Acad. Sci. U.S.A.* 114, E9066–E9075. doi: 10.1073/pnas.1704862114

Serrano-Heras, G., Díaz-Maroto, I., Carrión, B., Perona-Moratalla, A. B., Gracia, J., Arteaga, S., et al. (2019). Isolation and quantification of blood apoptotic bodies in neurological patients. *bioRxiv* [Preprint], doi: 10.1101/757872

Shelke, G. V., Jang, S. C., Yin, Y., Lässer, C., and Lötvall, J. (2016). Human mast cells release extracellular vesicle-associated DNA. *Matters* 2:e201602000034. doi: 10.19185/matters.201602000034

Sidhom, K., Obi, P. O., and Saleem, A. (2020). A review of exosomal isolation methods: is size exclusion chromatography the best option? *Int. J. Mol. Sci.* 21:6466. doi: 10.3390/ijms21186466

Tai, Y.-L., Chen, K.-C., Hsieh, J.-T., and Shen, T.-L. (2018). Exosomes in cancer development and clinical applications. *Cancer Sci.* 109, 2364–2374. doi: 10.1111/cas.13697

Takahashi, A., Okada, R., Nagao, K., Kawamata, Y., Hanyu, A., Yoshimoto, S., et al. (2017). Exosomes maintain cellular homeostasis by excreting harmful DNA from cells. *Nat. Commun.* 8:15287. doi: 10.1038/ncomms15287

Thakur, B. K., Zhang, H., Becker, A., Matei, I., Huang, Y., Costa-Silva, B., et al. (2014). Double-stranded DNA in exosomes: a novel biomarker in cancer detection. *Cell Res.* 24, 766–769. doi: 10.1038/cr.2014.44

Vagner, T., Spinelli, C., Minciacchi, V. R., Balaj, L., Zandian, M., Conley, A., et al. (2018). Large extracellular vesicles carry most of the tumour DNA circulating in prostate cancer patient plasma. *J. Extracell. Ves.* 7:1505403. doi: 10.1080/20013078.2018.1505403

Wang, L., Li, Y., Guan, X., Zhao, J., Shen, L., and Liu, J. (2018). Exosomal double-stranded DNA as a biomarker for the diagnosis and preoperative assessment of pheochromocytoma and paraganglioma. *Mol. Cancer* 17:128. doi: 10.1186/s12943-018-0876-z

Yamamoto, H. (2014). Detection of DNA methylation of gastric juice-derived exosomes in gastric cancer. *Integr. Mol. Med.* 1, 1–5. doi: 10.15761/IMM.1000105

Yamamoto, H., Watanabe, Y., Oikawa, R., Morita, R., Yoshida, Y., Maehata, T., et al. (2016). BARHL2 methylation using gastric wash DNA or gastric juice exosomal DNA is a useful marker for early detection of gastric cancer in an *H. pylori*-independent manner. *Clin. Transl. Gastroenterol.* 7:e184. doi: 10.1038/ctg.2016.40

Yang, D., Zhang, W., Zhang, H., Zhang, F., Chen, L., Ma, L., et al. (2020). Progress, opportunity, and perspective on exosome isolation - efforts for efficient exosome-based theranostics. *Theranostics* 10, 3684–3707. doi: 10.7150/thno.41580

Yang, S., Che, S. P. Y., Kurywchak, P., Tavormina, J. L., Gansmo, L. B., Correa de Sampaio, P., et al. (2017). Detection of mutant KRAS and TP53 DNA in circulating exosomes from healthy individuals and patients with pancreatic cancer. *Cancer Biol. Ther.* 18, 158–165. doi: 10.1080/15384047.2017.1281499

Yokoi, A., Villar-Prados, A., Oliphint, P. A., Zhang, J., Song, X., Hoff, P. D., et al. (2019). Mechanisms of nuclear content loading to exosomes. *Sci. Adv.* 5:eaax8849. doi: 10.1126/sciadv.aax8849

Zhang, H., Freitas, D., Kim, H. S., Fabijanic, K., Li, Z., Chen, H., et al. (2018). Identification of distinct nanoparticles and subsets of extracellular vesicles by asymmetric flow field-flow fractionation. *Nat. Cell Biol.* 20, 332–343. doi: 10.1038/s41556-018-0040-44

Zhang, Q., Higginbotham, J. N., Jeppesen, D. K., Yang, Y.-P., Li, W., McKinley, E. T., et al. (2019). Transfer of functional cargo in exomeres. *Cell Rep.* 27, 940–954.e6. doi: 10.1016/j.celrep.2019.01.009

Zhen, C., Zhao, H., Wu, L., Alam, A., Shiori, E., Hao, W., et al. (2020). The role of neutrophil NETosis in organ injury: novel inflammatory cell death mechanisms. *Inflammation* 43, 2021–2032. doi: 10.1007/s10753-020-01294-x

Zocco, D., Bernardi, S., Novelli, M., Astrua, C., Fava, P., Zarovni, N., et al. (2020). Isolation of extracellular vesicles improves the detection of mutant DNA from plasma of metastatic melanoma patients. *Sci. Rep.* 10:15745. doi: 10.1038/s41598-020-72834-72836

Conflict of Interest: The authors declare that the research was conducted in the absence of any commercial or financial relationships that could be construed as a potential conflict of interest.

Copyright © 2021 Amintas, Vendrely, Dupin, Buscail, Laurent, Bournet, Merlio, Bedel, Moreau-Gaudry, Boutin, Dabernat and Buscail. This is an open-access article distributed under the terms of the Creative Commons Attribution License (CC BY). The use, distribution or reproduction in other forums is permitted, provided the original author(s) and the copyright owner(s) are credited and that the original publication in this journal is cited, in accordance with accepted academic practice. No use, distribution or reproduction is permitted which does not comply with these terms.

frontiers in Cell and Developmental Biology

REVIEW
published: 05 February 2021
doi: 10.3389/fcell.2021.622459

Epigenetic Landscape of Liquid Biopsy in Colorectal Cancer

Aitor Rodriguez-Casanova [1,2†], Nicolás Costa-Fraga [1†], Aida Bao-Caamano [1†], Rafael López-López [2,3,4], Laura Muinelo-Romay [4,5] and Angel Diaz-Lagares [1,4*]*

[1] Cancer Epigenomics Laboratory, Translational Medical Oncology Group (Oncomet), Health Research Institute of Santiago (IDIS), University Clinical Hospital of Santiago (CHUS/SERGAS), Santiago de Compostela, Spain, [2] Roche-Chus Joint Unit, Translational Medical Oncology Group (Oncomet), Health Research Institute of Santiago (IDIS), Santiago de Compostela, Spain, [3] Translational Medical Oncology Group (Oncomet), Health Research Institute of Santiago (IDIS), University Clinical Hospital of Santiago (CHUS/SERGAS), Santiago de Compostela, Spain, [4] Centro de Investigación Biomédica en Red Cáncer (CIBERONC), Madrid, Spain, [5] Liquid Biopsy Analysis Unit, Translational Medical Oncology Group (Oncomet), Health Research Institute of Santiago (IDIS), University Clinical Hospital of Santiago (CHUS/SERGAS), Santiago de Compostela, Spain

OPEN ACCESS

Edited by:
Catherine Alix-Panabieres, Centre Hospitalier Universitaire de Montpellier, France

Reviewed by:
Shiaw-Yih Lin, University of Texas MD Anderson Cancer Center, United States
Evi Lianidou, National and Kapodistrian University of Athens, Greece

***Correspondence:**
Laura Muinelo-Romay
lmuirom@gmail.com
Angel Diaz-Lagares
angel.diaz.lagares@sergas.es

[†] These authors share first authorship

Specialty section:
This article was submitted to Molecular and Cellular Oncology, a section of the journal Frontiers in Cell and Developmental Biology

Received: 28 October 2020
Accepted: 05 January 2021
Published: 05 February 2021

Citation:
Rodriguez-Casanova A, Costa-Fraga N, Bao-Caamano A, López-López R, Muinelo-Romay L and Diaz-Lagares A (2021) Epigenetic Landscape of Liquid Biopsy in Colorectal Cancer. Front. Cell Dev. Biol. 9:622459. doi: 10.3389/fcell.2021.622459

Colorectal cancer (CRC) is one of the most common malignancies and is a major cause of cancer-related deaths worldwide. Thus, there is a clinical need to improve early detection of CRC and personalize therapy for patients with this disease. In the era of precision oncology, liquid biopsy has emerged as a major approach to characterize the circulating tumor elements present in body fluids, including cell-free DNA and RNA, circulating tumor cells, and extracellular vesicles. This non-invasive tool has allowed the identification of relevant molecular alterations in CRC patients, including some indicating the disruption of epigenetic mechanisms. Epigenetic alterations found in solid and liquid biopsies have shown great utility as biomarkers for early detection, prognosis, monitoring, and evaluation of therapeutic response in CRC patients. Here, we summarize current knowledge of the most relevant epigenetic mechanisms associated with cancer development and progression, and the implications of their deregulation in cancer cells and liquid biopsy of CRC patients. In particular, we describe the methodologies used to analyze these epigenetic alterations in circulating tumor material, and we focus on the clinical utility of epigenetic marks in liquid biopsy as tumor biomarkers for CRC patients. We also discuss the great challenges and emerging opportunities of this field for the diagnosis and personalized management of CRC patients.

Keywords: epigenetics, liquid biopsy, biomarkers, colorectal cancer, precision oncology, circulating nucleic acids, CTCs, extracellular vesicles

INTRODUCTION

Colorectal cancer (CRC) is the third most frequently detected cancer in both sexes worldwide. In particular, this tumor type accounts for ∼10% of all diagnosed cancer cases, with ∼1.8 million new cases estimated in 2018. Importantly, CRC is the second leading cause of cancer mortality in the world, being responsible for ∼9% of all cancer deaths (Bray et al., 2018). Surgery remains the most common treatment for non-metastatic CRC, while the administration of adjuvant chemotherapy is mainly restricted to stage III tumors. Importantly, most CRC patients are diagnosed at an advanced stage because symptoms normally appear after disease progression (John et al., 2011). The 5-year survival rate after surgery of localized CRC patients is over 90%, while patients affected by stage III

and IV tumors, exhibiting local lymph node invasion or distant metastases, respectively, normally show poor overall survival rates (Mattiuzzi et al., 2019). The high incidence and mortality of CRC highlight the clinical need for novel strategies to improve early CRC detection and personalize the management of patients with this type of tumor.

Currently, various screening assays are being used to detect CRC at an early stage. These detection strategies include the fecal immunochemical test (FIT), a non-invasive and cost-effective assay for detecting the presence of fecal hemoglobin (Song and Li, 2016). A positive result of this test implies the recommendation of a colonoscopy, which is the gold standard diagnostic technique for CRC detection. However, this method is clearly invasive, requires considerable patient preparation, and can eventually lead to serious complications (Triantafillidis et al., 2015).

Importantly, a refined understanding of the molecular aspects of CRC has recently been achieved owing to the application of next generation sequencing (NGS)-based approaches, which revealed a wide intratumor heterogeneity and general genomic instability (Molinari et al., 2018). Based on the advances in the molecular characterization of CRC, new biological drugs targeting vascular endothelial growth factors (VEGFRs), such as bevacizumab (Rosen et al., 2017), or epidermal growth factors (EGFRs), including cetuximab and panitumumab (Qin et al., 2018; Taniguchi et al., 2020), have improved the survival of patients, mainly in the context of metastatic CRC (mCRC). In addition, promising targeted therapies for mCRC are being evaluated in pre-clinical and clinical studies, including new drugs directed against different components of EGF/EGFR, VEGF/VEGFR, and HGF/c-MET pathways (Xie Y. H. et al., 2020). On the other hand, several recent pre-clinical studies have shown that blocking the PD-1/PD-L1 interaction or CTLA-4 with immune checkpoint inhibitors prevents colorectal tumor cells to escape from immune surveillance (Fiegle et al., 2019; Zhang Y. et al., 2020). In this sense, the use of immune checkpoint inhibitors has provided good outcomes in the treatment of mCRC with microsatellite instability (MSI) (Overman et al., 2018), which can be detected in ∼15% of CRC patients (Ward et al., 2001; Le et al., 2015). Importantly, several molecular biomarkers, such as the presence of *KRAS/NRAS/BRAF* mutations and MSI markers, have been approved for supporting the selection of targeted therapies (Lo Nigro et al., 2016). However, these predictive biomarkers are currently analyzed in tumor tissue samples, which are not always available during the disease evolution and can provide partial information of the molecular profile of colorectal tumors, mainly in the metastatic setting.

Liquid biopsy has emerged in recent years as an important approach to address and overcome such limitations. Indeed, this non-invasive strategy allows to observe the molecular landscape of circulating tumor elements in body fluids to obtain diagnostic, prognostic, and therapy response biomarkers that improve the management of cancer patients (Siravegna et al., 2017). The analysis of these liquid biopsy components in several body fluids of CRC patients has highlighted relevant molecular alterations, such as those depending on epigenetic mechanisms (Lofton-Day et al., 2008; Maminezhad et al., 2020). Importantly, the combination of liquid biopsy and detection of epigenetic alterations represents a great opportunity in cancer research for the identification of new non-invasive clinical biomarkers to improve the detection of CRC and personalize the management of this disease.

In this review, we provide an overview of the epigenetic landscape of liquid biopsies in CRC. We describe the concept and clinical application of liquid biopsy, the most relevant epigenetic mechanisms (DNA modifications, histone modifications and nucleosome positioning, and non-coding RNAs), and the implications of their deregulation in cancer cells and liquid biopsy. Furthermore, we summarize the methodologies used for detecting these epigenetic modifications in liquid biopsy, and describe the clinical utility of epigenetic marks in liquid biopsy as tumor biomarkers for CRC patients. Finally, we discuss the great challenges and opportunities of liquid biopsy epigenetics for the detection of CRC and management of CRC patients.

LIQUID BIOPSY

In the era of precision oncology, liquid biopsies represent a key element for cancer detection, to guide treatment selection and monitor tumor evolution in real time. A liquid biopsy consists of any body fluid that contains tumor material suitable for molecular characterization. Therefore, this term includes blood, the most used human liquid sample, but also other fluids such as urine, ascitic fluid, pleural effusion, cerebrospinal fluid, and saliva. Both primary tumors and metastases can release tumor material into these body fluids, mainly consisting of circulating tumor cells (CTCs), nucleic acids (cNAs), and extracellular vesicles (cEVs). These circulating elements constitute a valuable source of non-invasive biomarkers and information about the molecular mechanisms underpinning tumor dissemination and evolution (Siravegna et al., 2017).

Although Thomas Ashworth described the presence of tumor cells in the blood of breast cancer patients for the first time in 1869 (Ashworth, 1869), it was not until recent years that the scientific community focused their attention on the study of blood CTCs. Like most circulating tumor elements, CTCs are poorly concentrated in blood, and thus require the implementation of highly sensitive and specific strategies for their enrichment and subsequent detection. Initially, the most common strategy to isolate CTCs was immune enrichment, based on the presence of cell surface markers such as the epithelial cell adhesion molecule (EpCAM) (Allard et al., 2004). For example, the Food and Drug Administration (FDA)-approved CellSearch System can isolate EpCAM-positive cells and determine the number of CTCs in a sample after an immunofluorescence assay to detect epithelial and hematopoietic markers (Cristofanilli et al., 2004). This platform has been employed in numerous studies to quantify CTCs in CRC patients, demonstrating the clinical value of CTC enumeration as a prognostic and follow-up biomarker (Cohen et al., 2008; Sastre et al., 2012; Bork et al., 2015). However, this strategy has not been widely adopted as a clinical tool, mainly due to the lack of clear benefits in terms of accuracy of treatment decisions. Nevertheless, the

technology for isolating and characterizing CTCs has continued to improve during the last decade, mainly through the application of antigen-independent technologies allowing to isolate a broader and more molecularly heterogeneous CTC population (Barbazan et al., 2017). Despite the difficulty of translating CTCs into the clinical context, their molecular characterization has provided valuable information for understanding how colorectal tumor cells are able to disseminate, implant at distant locations, and generate metastasis (Barbazan et al., 2012, 2017). Such molecular characterization, including epigenetic mechanisms, is vital for unraveling the biological aspects of CRC and identifying new clinical and therapeutic biomarkers to manage this disease.

In contrast to the limited translation of CTCs into routine clinical practice, the analysis of cNAs has started to be applied to oncologic therapy selection. These analyses mainly focus on circulating cell-free DNA (cfDNA), released as a consequence of cell death and characterized by a high fragmentation in biological fluids (size, 160–180 bp). cfDNA generally contains small fractions of circulating tumor DNA (ctDNA), in a range as low as 0.01–1% in patients with advanced tumors (Thierry et al., 2016). Of note, several genetic alterations, such as point mutations, copy number variations, small indels, and translocations, together with epigenetic modifications, can be studied in cfDNA from different body fluids in a non-invasive and comprehensive way (Bardelli and Pantel, 2017). Furthermore, in 2014 Bettegowda et al. demonstrated that ctDNA is detectable in most patients with mCRC and in a considerable percentage of non-metastatic patients (Bettegowda et al., 2014). These results provided the basis for numerous studies that have demonstrated that it is possible to characterize the molecular alterations of CRC with high accuracy, thereby predicting the information obtained by standard image-based follow-up. For example, there is clear scientific evidence of the robustness of ctDNA analyses to monitor RAS mutational status without the need for invasive tissue biopsies. This approach is also interesting for improving the selection of anti-EGFR therapy at different time points of disease evolution (Siravegna et al., 2015; Vidal et al., 2017). Moreover, recent technological improvements have favored the application of ctDNA analysis in patients with early CRC as well as for the detection of minimal residual disease (MRD) after surgery (Cohen et al., 2018).

Among cNAs, numerous non-coding RNAs (ncRNAs) can be detected in liquid biopsy. Several studies have highlighted the role of ncRNAs in cell-to-cell communication through the promotion of differential gene expression in tumor cells and stroma, which has a relevant impact on cancer progression and therapy resistance (Anfossi et al., 2018; Pardini et al., 2019). Although cNA-based applications for CRC are still in the clinical validation phase, current genetic and epigenetic data are promising and will soon support a more extensive use of cNA analysis to manage this type of cancer.

Other circulating elements of great interest found in liquid biopsy are cEVs. These vesicles are a complex population of cell-derived membranous structures released by cells through different mechanisms, which can be grouped into exosomes (ranging from 30 to 100 nm), microvesicles (50–2,000 nm), and apoptotic bodies (500–4,000 nm) (Akers et al., 2013; van Niel et al., 2018). These vesicles play an important role in cancer, mediating the interaction between tumor and stromal cells, promoting cell proliferation and invasion, and significantly contributing to the establishment of pre-metastatic niches (de la Fuente et al., 2015; Becker et al., 2016). Such functions are mediated by their membrane components, but also their molecular cargo, composed of proteins, messenger RNAs (mRNAs), ncRNAs, and single- or double-stranded DNA (van Niel et al., 2018). Importantly, cEVs can be found in different body fluids at high concentrations. Their isolation is mainly achieved by ultracentrifugation, immunoaffinity, or precipitation strategies (Bu et al., 2019; Jayaseelan, 2020), and the selection of the optimal isolation strategy is a crucial point, significantly influencing the characteristics of the isolated vesicles. The presence of relevant molecular alterations has been described in exosomal DNA from cancer patients (Hao et al., 2017; Castellanos-Rizaldos et al., 2018). Furthermore, exosomal ncRNAs obtained from serum and plasma have also been explored in connection with CRC, with promising results (Matsumura et al., 2015).

In summary, the study of cNAs, CTCs, and cEVs has shown significant potential for early CRC diagnosis, therapy selection, and disease monitoring, through the analysis of several molecular alterations such as those depending on various epigenetic mechanisms, which are examined in detail in the present review.

THE EPIGENETIC MACHINERY AND CANCER

The concept of epigenetics was postulated for the first time in 1942 by Waddington (2012), and can now be defined as the study of hereditary changes in the activity and expression of genes that take place without alterations of the DNA sequence (Holliday, 1987; Berger et al., 2009). The epigenetic machinery has several mechanisms (**Figure 1**), including DNA methylation and hydroxymethylation, histone modifications and nucleosomes positioning, and ncRNAs (Rodriguez-Paredes and Esteller, 2011). These mechanisms play an important role in regulating gene expression during many biological processes, such as embryonic development, imprinting, and tissue differentiation (Sharma et al., 2010). However, the deregulation of all these epigenetic layers has important implications for cancer development and progression (Mari-Alexandre et al., 2017).

DNA Modifications: Methylation and Hydroxymethylation

DNA methylation is the most widely described epigenetic mechanism. This covalent modification of DNA consists in the incorporation of a methyl group (CH_3) to the 5′ carbon of cytosines in cytosine-phosphate-guanine (CpG) dinucleotides to produce 5-methylcytosine (5mC) (Portela and Esteller, 2010). Such incorporation is regulated by DNA methyltransferases (DNMTs), including DNMT1, DNMT3A, and DNMT3B, which catalyze the transfer of methyl groups from S-adenosyl-L-methionine (SAM) to cytosines. In particular, DNMT3A and DNMT3B participate in producing *de novo* methylation patterns

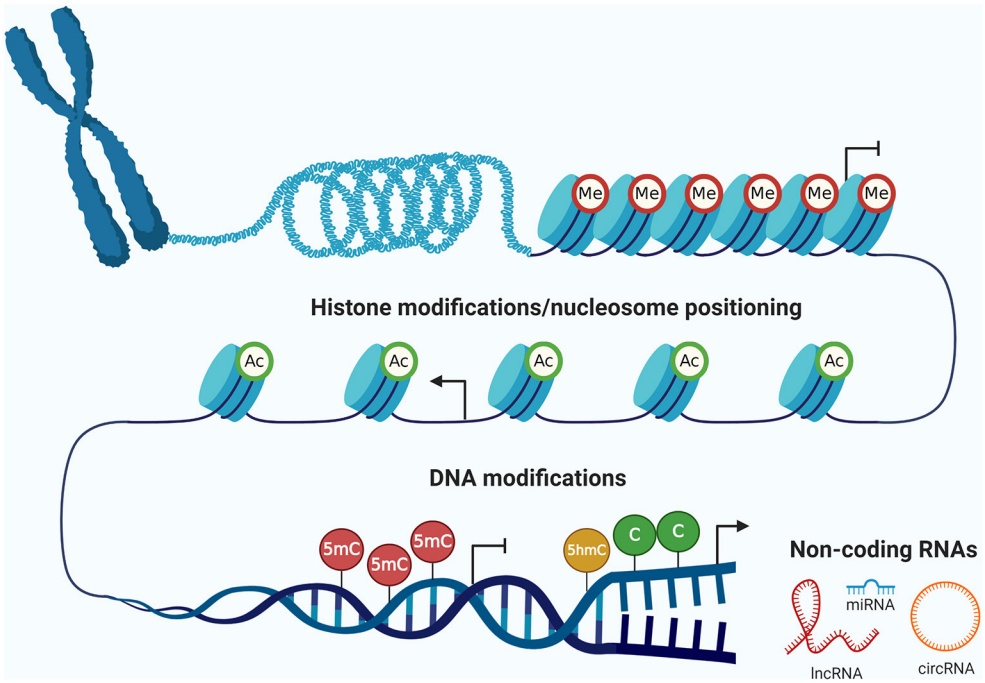

FIGURE 1 | The epigenetic machinery. There are three fundamental epigenetic mechanisms, represented by (i) DNA modifications (methylation and hydroxymethylation), (ii) post-translational modifications of histones and nucleosome positioning, and (iii) non-coding RNAs. These epigenetic layers are highly interrelated among them and regulate gene expression of relevant biological processes in normal cells. However, these mechanisms can be deregulated in tumor cells leading to cancer development and progression. Me, methylation of histones; Ac, acetylation of histones; 5mC, 5-methylcytosine; 5hmC, 5-hydroxymethylcytosine; C, cytosine; lncRNA, long non-coding RNA; miRNA, microRNA; circRNA, circular RNA. Created with BioRender.com.

in cells, while DNMT1 maintains the parental methylation profile in each cell division (Gowher and Jeltsch, 2002; Jaenisch and Bird, 2003). DNA methylation usually occurs in specific regions of the genome with high density of CpG dinucleotides, called CpG islands (CGIs). These CpG-enriched sequences are usually located in the promoter regions of genes but can also be present in intragenic regions, including gene bodies (Diaz-Lagares et al., 2016a; Arechederra et al., 2018). According to their distance from CGIs, genomic sequences can be defined as CGI shores (up to 2 kb from CGIs), shelves (2–4 kb from CGIs), and open sea (>4 kb from CGIs) (Qu et al., 2014). In addition, DNA methylation can affect not only the intragenic but also the intergenic regions of the genome, increasing the complexity of this layer of epigenetic regulation (Zhao S. G. et al., 2020).

DNA methylation plays an important role in regulating gene expression as well as in maintaining the integrity and conformation of DNA, thereby protecting it from the potential damage by mobile genetic elements (Herceg and Vaissiere, 2011). This epigenetic modification can be enhanced (hypermethylation) or suppressed (hypomethylation) in different regions of the genome (Portela and Esteller, 2010). In cancer, hypermethylation of CGIs in promoters is usually linked to silencing of both coding and non-coding tumor suppressors (Diaz-Lagares et al., 2016a,b). However, hypomethylation of CpG-poor regions has been associated with proto-oncogene expression, genomic instability, and malignant transformation of tumors (Esteller, 2008; Sheaffer et al., 2016).

In human cells, DNA methylation can be reversed by TET (ten-eleven translocation) enzymes, which induce the oxidation of 5mC to 5-hydroxymethylcytosine (5hmC) in a process defined as DNA hydroxymethylation (Tahiliani et al., 2009). This demethylation mechanism can modulate gene expression by adjusting the methylation levels (Xu and Gao, 2020). In cancer, deregulation of TET enzymes can alter the balance of genomic 5mC/5hmC levels, inducing cancer transformation (Chen et al., 2017). In addition, DNA methylation can be reversed through epigenetic-based drugs (epidrugs), which can decrease the methylation levels of hypermethylated genes (Berdasco and Esteller, 2019). For example, 5-azacytidine (5-AZA-CR) and 5-aza-2′-deoxycytidine (5-AZA-CdR, decitabine) are nucleoside analogs approved by the FDA, acting as DNA methyltransferase inhibitors (DNMTi) (Quintas-Cardama et al., 2010).

Histone Modifications and Nucleosome Positioning

Nucleosomes were first described in 1974 by Kornberg (1974) and represent the basic functional units of chromatin. They are composed of 147 bp of DNA wrapped around an octamer consisting of two copies of four core histone proteins (H2A, H2B, H3, and H4) (Kouzarides, 2007). This core of histones is organized into two H2A–H2B dimers and one H3–H4 tetramer. In addition, nucleosomes bind the linker histone H1, which protects the ∼20–50 bp of free DNA (linker DNA) located between neighboring nucleosomal particles (Portela and

Esteller, 2010). Nucleosomal histones can undergo different types of reversible post-translational modifications (PTMs), such as acetylation, methylation, phosphorylation, ubiquitylation, and sumoylation, that mainly occur in the histone tail and are enzymatically regulated (Kouzarides, 2007). Importantly, histone PTMs have demonstrated to play a relevant role in normal development and pathogenesis associated with transcriptional regulation, DNA repair and replication, or chromatin condensation (Bannister and Kouzarides, 2011; Bates, 2020). Specifically, multiple histone PTMs related to gene activation or silencing have been described, in particular histone acetylation and methylation. The balance of these types of PTMs is regulated by histone acetyltransferases (HATs), histone deacetylases (HDACs), histone methyltransferases (HMTs), and histone demethylases (HDMs). The possible combinations of PTMs provide various histone modification patterns that have been proposed to constitute a "histone code" associated with open/closed states of chromatin and gene regulation (Strahl and Allis, 2000; Rando, 2012).

In addition to PTMs, the positioning of nucleosomes has shown to be importantly involved in the regulation of chromatin accessibility. Indeed, variations in the position of nucleosomes modulate the binding of RNA polymerase or transcription factors to regulatory elements that control gene expression (Kurup et al., 2019; Huertas et al., 2020). Nucleosome positioning is controlled by chromatin-remodeling proteins (called movers) that shift nucleosomes and allow gene expression (Bates, 2020). Active genes usually present nucleosome-depleted regions (NDR) around their transcription start sites (TSS) that facilitate the accessibility of transcription regulatory proteins (Mavrich et al., 2008). The organization of nucleosomes is dynamically regulated and their turnover in active promoters and enhancers is higher than in inactive regions (Deal et al., 2010; Klemm et al., 2019). Interestingly, nucleosome positioning not only regulates gene expression but also influences the type of DNA fragmentation that can occur in different cellular processes, such as apoptosis, resulting in a non-random fragmentation of DNA (Matassov et al., 2004; Ivanov et al., 2015).

In cancer, epigenetic mechanisms such as nucleosome positioning and PTMs of histones, and/or the enzymes that regulate these modifications, are often deregulated (Hesson et al., 2014; Yang et al., 2014). For example, mutations in histone-modifying enzymes can lead to cancer development due to alterations in the PTM balance of histones (Morin et al., 2010). However, the alteration of histone modifications can be reversed in some types of tumors through the administration of certain epidrugs approved by the FDA (Hoy, 2020).

Non-coding RNAs

Non-coding transcripts are important regulatory molecules that represent the vast majority of the transcriptome (∼98%) (Kapranov et al., 2007). The number of identified ncRNAs has been rapidly increasing in recent years, and currently multiple types of ncRNAs build up the non-coding transcriptome. Similar to other epigenetic mechanisms, ncRNAs have relevant functions in controlling gene expression (Dragomir et al., 2018). Non-coding transcripts are usually classified based on their nucleotide length. Using this criterion, ncRNAs can be divided into: (i) small ncRNAs (sncRNAs), which are shorter than 200 nt and include microRNAs (miRNAs), small interfering RNAs (siRNAs), and piwi-interacting RNAs (piRNAs); and (ii) long ncRNAs (lncRNAs), which are longer than 200 nt and encompass long intergenic ncRNAs (lincRNAs) and long intronic ncRNAs (intronic lncRNAs) (Taft et al., 2010; Esteller, 2011; Memczak et al., 2013). Of note, some ncRNAs have variable lengths and might be attributed to both classes at the same time. This is the case of enhancer RNAs (eRNAs), which originate from transcriptional enhancers, and circular RNAs (circRNAs), which are circularization products arising from splicing events (Leveille et al., 2015; Zhang et al., 2019).

Among sncRNAs, miRNAs have been the most widely described ncRNAs. miRNAs are single-stranded molecules of 18–25 nt that bind to specific regions of target mRNAs, mediating post-transcriptional gene silencing by two possible mechanisms: blocking transcription or triggering mRNA degradation (Lee and Calin, 2011). As a consequence, a single miRNA can control the expression of hundreds of genes, regulating key pathways for cancer tumorigenesis and progression (Garzon et al., 2009). Importantly, miRNAs can have a dual effect in cancer, functioning either as tumor suppressors or oncogenes (oncomiRs) (Volinia et al., 2006; Bayraktar et al., 2017). In addition, different types of cancers have shown specific miRNA signatures, defining the molecular characteristics of tumors (Lu et al., 2005).

Although miRNAs are the most studied ncRNAs, lncRNAs have recently been shown to represent the vast majority of non-coding transcripts (Hon et al., 2017). LncRNAs do not have the potential to encode proteins, but they may exhibit some mRNA-like properties, such as multiexonic gene structures, polyadenylation, presence of 5′ caps, and transcription by RNA polymerase II (Guttman et al., 2009; Derrien et al., 2012). LncRNAs have relevant regulatory functions in the process of gene expression, for example during transcriptional regulation and splicing (Kotake et al., 2011; Leveille et al., 2015). Nevertheless, currently few lncRNAs have been well-characterized, although several studies have shown their implications in cancer, where they act by suppressing (Leveille et al., 2015; Diaz-Lagares et al., 2016a) or promoting the tumoral process (Gupta et al., 2010; Gutschner et al., 2013).

Interplay Between Epigenetic Mechanisms

In normal mammalian cells, epigenetic modifications can regulate each other through the interplay among distinct epigenetic players, forming a complex regulatory network (Caley et al., 2010; Rose and Klose, 2014). However, this crosstalk is also evident in cancer, where specific methylation and histone modification patterns regulate the expression of different types of ncRNAs, including miRNAs and lncRNAs (Shin et al., 2009; Leveille et al., 2015). Conversely, the disruption of ncRNA expression in cancer cells may alter histone PTMs and DNA methylation levels (Gupta et al., 2010).

TABLE 1 | Methods used for the analysis of epigenetic marks in liquid biopsy.

Feature	Approach	Method	Characteristics of the analysis	References
Methylation	LS	MSP	CpG sites by PCR	Herman et al., 1996
		qMSP	CpG sites by qPCR	Danese et al., 2013
		Methylight	CpG sites with fluorescent probes by qPCR	Eads et al., 2000
		MS-HRM	Regions with CpGs by qPCR and melting curves	Yang et al., 2015
		Multiplexed-scAEBs	CpGs sites in multiple loci by Sanger sequencing	Pixberg et al., 2017
		Methyl-BEAMing	CpG sites by emulsion dPCR	Li et al., 2009
		ddPCR	CpG sites by ddPCR	Picardo et al., 2019
		MBD-ddPCR	Immunoprecitation and ddPCR	Shinjo et al., 2020
	GW	WGBS	CpG sites in whole genome by NGS	Li et al., 2018
		MCTA-seq	Analysis of CpG islands by NGS	Liu X. et al., 2019
		TBS	Target CpG sites analysis by NGS	Liu M. C. et al., 2020
		cf-RRBS	Enzymatic digestion with MspI and NGS	De Koker et al., 2019
		Microarrays	∼850.000 CpG sites	Gallardo-Gomez et al., 2018
		cfMeDIP-seq	Immunoprecipitation and NGS	Shen et al., 2018
Hydroxymethylation	GW	5hmC-Seal	Genomic 5hmC analysis by NGS	Li et al., 2017
Histone modifications	LS	ChiP	Chromatin immunoprecipitation and qPCR	Gezer et al., 2012
	GW	cfChIP-seq	Chromatin immunoprecipitation and NGS	Vad-Nielsen et al., 2020
Nucleosome positioning	GW	WGS	Analysis of DNA fragmentation by NGS	Mouliere et al., 2018
NcRNAs	LS	Nanostring	Panel of transcripts without amplification	Shukla et al., 2018
		RT-qPCR	Transcript detection by qPCR	Cojocneanu et al., 2020
		ddPCR	Transcript analysis by ddPCR	Gasparello et al., 2020
		Isothermic	Amplification at single temperature	Miao et al., 2016
		PNA-based biosensor	Transcript analysis without amplification	Metcalf et al., 2016
		ISH-LNA	ISH and LNA for transcript detection in CTCs	Ortega et al., 2015
		Droplet microfluidic	Multiple transcripts in CTCs with droplet microfluidic	Li et al., 2019
		Microarrays	Multiple transcripts by microarrays	Cojocneanu et al., 2020
	GW	RNA-seq	Transcriptomic analysis by NGS	Amorim et al., 2017

LS, locus-specific; GW, genome-wide; MSP, methylation-specific PCR; qMSP, quantitative methylation-specific PCR; MS-HRM, methylation specific high resolution melting; scAEBS, single-cell agarose-embedded bisulfite sequencing; BEAMing, beads, emulsion, amplification, and magnetics dPCR, digital PCR; ddPCR, droplet digital PCR; MBD, methyl-CpG binding protein; WGBS, whole genome bisulfite sequencing; NGS, next-generation sequencing; MCTA-seq, methylated CpG tandem amplification and sequencing; TBS, targeted bisulfite sequencing; cf-RRBS, cell-free DNA reduced representation bisulfite sequencing; cfMeDIP-seq, cell-free methylated DNA immunoprecipitation and high-throughput sequencing; 5hmC, 5-hydroxymethylcytosine; ChiP, chromatin immunoprecipitation; cfChIP-seq, chromatin immunoprecipitation followed by sequencing of cell-free nucleosomes; WGS, whole genome sequencing; RT-qPCR, quantitative reverse transcription PCR; PNA, peptide nucleic acids; ISH-LNA, in situ hybridization-locked nucleic acid; RNA-seq, RNA sequencing.

These are only some examples of the important crosstalk that usually occurs among the different components of the epigenetic machinery.

METHODS FOR DETECTING EPIGENETIC MARKS IN LIQUID BIOPSY

Multiple methodologies have been described at genome-wide or locus-specific level for the analysis of the status of different types of epigenetic marks (Bao-Caamano et al., 2020). However, it is important to consider the advantages and limitations of each method in order to choose the most appropriate approach depending on the type of epigenetic mechanism under investigation and on the conditions of the assay (Kurdyukov and Bullock, 2016). **Table 1** shows the most representative methods used for detecting epigenetic marks in liquid biopsy.

DNA Modifications: Methylation and Hydroxymethylation

The detection of DNA methylation patterns is based on methods that (i) depend on sodium bisulfite conversion or (ii) are independent of sodium bisulfite, such as approaches based on immunoprecipitation and methyl-sensitive restriction enzymes (MSRE) (Huang and Wang, 2019). Methodologies that use bisulfite conversion are considered the gold standard for methylation analyses. These approaches are based on the principle that after sodium bisulfite treatment, methylcytosines do not undergo any change, whereas cytosine residues are converted into uracils (Frommer et al., 1992).

At the locus-specific scale, common bisulfite-based methods used in liquid biopsy include methylation-specific PCR (MSP), quantitative methylation-specific PCR (qMSP), MethyLight assay, methylation-sensitive high-resolution melting (MS-HRM), and more recently, digital PCR (dPCR)-based approaches (Li et al., 2009; Bao-Caamano et al., 2020). In particular, the detection

of methylation by dPCR represents a quantitative and highly sensitive method that allows the analysis of very low amounts of DNA. Therefore, several dPCR-based methods, including methyl-BEAMing (Barault et al., 2015) and droplet digital PCR (ddPCR) (Boeckx et al., 2018), have been used for methylation analysis in cfDNA. Regarding CTCs, the first studies describing DNA methylation alterations in these cells were reported using MSP (Chimonidou et al., 2011). Recently, a new method has been described for methylation analysis of CTCs, based on agarose-embedded bisulfite treatment (AEBS), allowing to analyze the DNA methylation status of multiple loci of single CTCs by multiplex PCR (multiplexed-scAEBS) (Pixberg et al., 2017).

Moreover, genome-wide bisulfite-based approaches based on NGS allow to evaluate the whole methylome in liquid biopsy. For instance, whole-genome bisulfite sequencing (WGBS) has proved useful for the inspection of the whole methylation landscape of not only cfDNA from cancer patients (Li et al., 2018), but also of single CTCs and CTC clusters (Gkountela et al., 2019). Although WGBS is highly informative, the high cost of this approach is a limitation for its general implementation in a clinical setting (Legendre et al., 2015; Zhang et al., 2020). Therefore, other high-throughput bisulfite-based approaches, not allowing to analyze the complete methylome but enabling to assay a great number of CpGs in a genome-wide scale, have been proposed. For instance, by MCTA-seq (methylated CpG tandem amplification and sequencing) it is possible to analyze the methylation status of CGIs in cfDNA (Liu et al., 2019). Similarly, CpG-targeted bisulfite sequencing methods have proved useful for the analysis of methylation in cfDNA. In this regard, Liu et al. introduced a novel approach by which, after bisulfite treatment of plasma cfDNA, regions of interest are pulled down and sequenced, and the results are analyzed in combination with machine learning (Liu M. C. et al., 2020). Recently, cfDNA reduced representation bisulfite sequencing (cf-RRBS) has been developed as an alternative genome-wide bisulfite sequencing method to analyze the cfDNA methylome (De Koker et al., 2019). This new method is based on the reduced representation bisulfite sequencing (RRBS) technology, which was first described by Meissner et al. (2005). In cf-RRBS, cfDNA is dephosphorylated prior to enzymatic digestion by the methylation-insensitive restriction enzyme MspI and sequencing. This approach represents a cost-effective method that allows methylation profiling of cfDNA in liquid biopsy (Van Paemel et al., 2020). In addition to NGS methods, DNA methylation can also be analyzed at the genome-wide level in liquid biopsy using methylation microarrays. This methodology implies the use of bisulfite-converted DNA and has been applied to the study of cfDNA and CTCs from cancer patients (Friedlander et al., 2014; Gallardo-Gomez et al., 2018). These genome-wide approaches based on NGS and microarrays are very promising, but have still been used in a small number of works. Therefore, more studies are necessary to validate their application for the analysis of epigenetic alterations in liquid biopsy.

One of the advantages of bisulfite conversion-based approaches is that they allow methylome profiling at base resolution (Sun et al., 2015). However, the use of bisulfite treatment for methylation analysis has some limitations, such as a potentially high degradation of DNA or an incomplete bisulfite conversion (Grunau et al., 2001; Rand et al., 2002). To overcome these limitations, Shen et al. recently developed a genome-wide method based on cell-free methylated DNA immunoprecipitation and high-throughput sequencing (cfMeDIP-seq) (Shen et al., 2018). In contrast to bisulfite single-base resolution technologies, cfMeDIP-seq is a region-based method that unravels the methylation status of genomic regions of at least 100 bp in length (Shen et al., 2019). This new bisulfite-free method was adapted from a previous methylated DNA immunoprecipitation (MeDIP) protocol based on the use of anti-methylcytosine antibodies (Taiwo et al., 2012). cfMeDIP-seq is a low-input (requiring 1 to 10 ng of DNA) and sensitive (with a detection limit down to 0.001%) approach that can be used for both early- and late-stage detection of multiple types of tumors (Shen et al., 2018, 2019). Recently, another enrichment method based on immunoprecipitation was developed to detect cfDNA methylation. This new locus-specific method is based on the immunoprecipitation of methyl-CpG binding (MBD) proteins coupled with ddPCR (MBD–ddPCR) (Shinjo et al., 2020). This highly sensitive technique allows the detection of methylation sites in cfDNA.

Similar to DNA methylation, genome-wide hydroxymethylation profiles can be obtained from cfDNA of cancer patients. This can be achieved by 5hmC-Seal, a robust and efficient sequencing method that has proved useful for detecting 5hmC in cfDNA with high sensitivity and specificity (Li et al., 2017).

Histone Modifications and Nucleosome Positioning

The global distribution of specific PTMs of histones in cells can be assayed by chromatin immunoprecipitation with massively parallel DNA sequencing (ChIP-seq) (Barski et al., 2007). Recently, Sadeh et al. developed a method to perform ChIP-seq of cell-free nucleosomes (cfChIP-seq). This method enables the capture of circulating nucleosomes with different active chromatin marks that maintain the cell-of-origin genomic distribution of modifications and expression patterns (Sadeh et al., 2019). Other similar approaches have been used to quantify the level of histone marks associated with circulating cell-free nucleosomes in plasma of cancer patients (Vad-Nielsen et al., 2020). In addition to these high-throughput technologies, circulating nucleosomes can also be analyzed by chromatin immunoprecipitation (ChIP) followed by quantitative PCR to detect histone modifications in individual genes (Gezer et al., 2012). Other methods, such as enzyme-linked immunosorbent assay (ELISA), are used to quantify the occurrence of specific histone marks based on their levels in circulating nucleosomes (Rahier et al., 2017).

In addition, the fragmentation patterns of cfDNA depending on nucleosome positioning can be analyzed using genome-wide fragmentation methods, based on the combination of NGS and machine learning. These approaches require a

very low input of cfDNA from different types of fluids, allowing even early detection of cancer (Mouliere et al., 2018). Other genome-wide fragmentation methods, such as DNA evaluation of fragments for early interception (DELFI), have been recently proposed (Cristiano et al., 2019). These kinds of fragmentation approaches are based on prior knowledge on the different lengths of cfDNA fragments originating from tumor and non-tumor cells (Jiang et al., 2015). Moreover, the landscape of cfDNA fragmentation is associated with nucleosome occupancy and epigenetic regulation (Ivanov et al., 2015). In turn, nucleosome occupancy of cfDNA correlates well with the nuclear architecture, gene structure, and gene expression observed in cells (Snyder et al., 2016), providing relevant information about nucleosome organization and the tissue of origin (Ivanov et al., 2015; Mouliere et al., 2018; Cristiano et al., 2019).

Non-coding RNAs

Genome-wide expression analyses, based on microarrays or NGS technologies, enable the detection of a large number of ncRNAs in a high-throughput manner. Therefore, microarrays and NGS have been used in liquid biopsy for the detection of several types of ncRNAs, including miRNAs, lncRNAs, and circRNAs (Amorim et al., 2017; Cojocneanu et al., 2020; Gasparello et al., 2020). Although both methods allow a comprehensive analysis of ncRNA transcripts, NGS displays higher sensitivity than microarrays and does not require previous knowledge of the target transcripts (Hurd and Nelson, 2009; Wang et al., 2019). On the other hand, several methods and instruments are based on targeted detection of transcripts in liquid biopsy. This is the case of the NanoString nCounter, a platform that directly detects the expression levels of a wide panel of ncRNAs without any enzymatic amplification (Shukla et al., 2018). Other technologies, such as reverse transcription quantitative PCR (RT-qPCR) and ddPCR, despite requiring enzyme-assisted amplification, allow to quantify the expression levels of specific ncRNA transcripts in liquid biopsy with high sensitivity. Importantly, RT-qPCR and ddPCR are usually used as gold standard methods to validate the results obtained by genome-wide approaches (Sole et al., 2019; Cojocneanu et al., 2020; Gasparello et al., 2020). However, since these PCR-based methods require several cycles of temperature variations, isothermal amplification approaches, which use a single temperature, have been developed for ncRNA analysis in liquid biopsy (Miao et al., 2016). In contrast, other methods for miRNA detection, such as the use of peptide nucleic acids (PNAs)-based fluorogenic biosensors, do not require amplification (Metcalf et al., 2016). Some targeted approaches have also been shown to be specifically useful for the analysis of ncRNAs, especially miRNAs, in CTCs. Among these, *in situ* hybridization (ISH) with locked-nucleic-acid (LNA) probes has been successfully applied for the detection of miRNAs in CTCs (Ortega et al., 2015), since the use of LNA probes increases the efficiency of ISH for the detection of miRNAs (Kubota et al., 2006). Other methods for the analysis of CTCs have been recently developed, based on signal amplification in microfluidic droplets for single-cell analysis of multiple miRNAs (Li et al., 2019).

DEREGULATION OF EPIGENETIC MECHANISMS IN COLORECTAL CANCER AND LIQUID BIOPSY

CRC originates from an accumulation of both genetic and epigenetic alterations in normal colon epithelial cells, leading to their transformation, first into adenomas and then into adenocarcinomas (Fearon and Vogelstein, 1990; Lao and Grady, 2011). Epigenetic alterations are involved in all the steps of the adenoma-carcinoma sequence, participating in the initiation, progression, and metastasis of CRC (Kim et al., 2006; Wendt et al., 2006; Silva-Fisher et al., 2020). Importantly, the disruption of the epigenetic machinery has been proposed as a hallmark of cancer by several authors (Esteller, 2007; Bates, 2020).

Promoter hypermethylation of single TSGs has been widely described in colorectal tumor cells. In particular, the hypermethylation of CGIs in promoters of relevant genes (*p16/CDKN2A, MLH1, MGMT, APC,* and *TIMP3*, among others) is associated with CRC pathogenesis (Gonzalez-Zulueta et al., 1995; Hiltunen et al., 1997; Kane et al., 1997; Esteller et al., 1999; Lee et al., 2004). In addition, the hypermethylation of specific groups of genes has shown implications for this disease. In this sense, Toyota et al. described for the first time the CpG island methylator phenotype (CIMP), characterized by the hypermethylation of CGIs in the promoter regions of a panel of TSGs from a subset of CRC and adenoma tissues (Toyota et al., 1999). CIMP-High (CIMP-H) is considered a molecular subtype of sporadic CRC characterized by a high degree of methylation in CIMP-specific loci. Most studies have defined CIMP using a classic methylated-in-tumor (MINT) marker panel: *p16/CDKN2A, MLH1, MINT1, MINT2,* and *MINT31* (Nazemalhosseini Mojarad et al., 2013). However, subsequent studies have used other types and number of genes to define CIMP, thereby increasing the difficulty of its implementation in the clinic (Weisenberger et al., 2006; Ogino et al., 2007). On the other hand, recent advances in the characterization of genome-wide DNA methylation patterns have allowed the discovery of methylation signatures based on multiple CpG sites associated with CRC (Sandoval et al., 2011; Luo et al., 2014). This type of epigenomic methodology has revealed that the disruption of methylation in colorectal tumor cells can affect both coding and non-coding genes, such as those producing miRNAs and lncRNAs (Mori et al., 2011; Diaz-Lagares et al., 2016a). In addition to the hypermethylation of TSGs, colorectal tumors are also characterized by global hypomethylation, presenting a low methylation status in LINE-1 repetitive sequences (Suter et al., 2004). On the other hand, total 5hmC levels are reduced in colon tumor cells compared to normal cells (Gilat et al., 2017). However, tumor cells can also show high levels of 5hmC in transcriptionally active regions, associated with the expression of particular coding and non-coding genes; this phenomenon contributes to CRC pathogenesis, even in early stages (Hu et al., 2017; Gao et al., 2019).

Colorectal tumors are also characterized by the disruption of histone modification patterns, such as methylation [e.g., methylation of lysine 9 on H3 (H3K9me)] and acetylation

[e.g., acetylation of lysine 27 on H3 (H3K27ac)] (Liu et al., 2013; Karczmarski et al., 2014). In addition, the positioning of nucleosomes can also be modified in tumors, and such alteration has implications for the reorganization of chromatin and gene expression (Hesson et al., 2014). In summary, the positioning of nucleosomes over the TSS and differences in the occurrence of histone epigenetic marks can regulate gene expression in colorectal tumor cells (Gimeno-Valiente et al., 2019).

The expression of several types of ncRNAs, including miRNAs and lncRNAs, is usually dysregulated in CRC. For instance, the overexpression of particular miRNAs, such as miR-21, is associated with the activation of relevant specific pathways that promote pathogenesis of colorectal tumor cells (Xiong et al., 2013). In addition, recent transcriptomic analyses have revealed CRC-specific expression signatures of miRNAs, lncRNAs, and other types of ncRNAs (Di et al., 2020; Li et al., 2020; Song et al., 2020). One of the epigenetic mechanisms that may control the expression levels of these ncRNAs in colorectal tumor cells is DNA methylation. For instance, this is the case of the lncRNA TP53TG1, which exerts tumor suppressor activity in gastrointestinal tumors and participates in the p53 response to DNA damage (Diaz-Lagares et al., 2016a).

Of note, advances in our understanding of aberrant epigenetics have led to the identification of epigenetic alterations in liquid biopsy elements (cNAs, CTCs, and cEVs) associated with all steps of CRC progression (Gasch et al., 2015; Zeng et al., 2018; Jung et al., 2020). Disruption of epigenetic mechanisms has great relevance in cancer dissemination and metastasis of solid tumors, which remains the leading cause of cancer-related death (Gupta and Massague, 2006). For example, hypermethylation of TSGs (e.g., *CDKN2A*), in both tumor tissue and cfDNA, is broadly associated with distant metastasis in CRC patients (Mitomi et al., 2010). In addition, hypomethylation of LINE-1 in plasma cfDNA of CRC patients is also correlated with disease progression; this association is stronger in tumors with higher size, lymph node affectation, and distant metastasis (Nagai et al., 2017). More recently, the epigenetic markers of CTCs have been explored to better understand cancer progression (Chimonidou et al., 2011). In particular, Lyberopoulou et al. were the first to determine the DNA methylation profile of cancer-related genes in CTCs of CRC patients. This study revealed that CTCs from CRC patients are characterized by hypermethylation of the *SFRP2* promoter and exon 1 of *VIM* (Lyberopoulou et al., 2017), which are genes related to epithelial-to-mesenchymal transition (EMT) and CRC metastasis (Shirahata et al., 2009; Loboda et al., 2011; Vincent and Postovit, 2017). In recent years, the analysis of single CTCs with genome-wide methylation (Gkountela et al., 2019) or multiplex approaches (Pixberg et al., 2017) has provided relevant information on cancer dissemination. However, the study of epigenetic alterations in CTCs from CRC patients remains limited.

In addition to CTCs, cancer-derived EVs play a major role in cancer progression as they participate in pre-metastatic niche formation (de la Fuente et al., 2015; Becker et al., 2016). For example, it has been shown that exosomal miR-25-3p from CRC cells regulates the expression of target genes, promoting vascular permeability, angiogenesis, and the formation of liver and lung metastasis in preclinical models (Zeng et al., 2018). Of note, plasma exosomal miR-25-3p levels are significantly higher in metastasic CRC patients than in those with no metastases, indicating a role for this miRNA in pre-metastatic niche formation (Zeng et al., 2018). On the other hand, the fact that serum exosomal miR-375 is less abundant in CRC patients with liver metastasis, together with functional studies, suggests its role as a tumor suppressor through the inhibition of the Bcl-2 pathway (Zaharie et al., 2015). Furthermore, recent results have indicated that decreased levels of serum exosomal miR-638 (Yan et al., 2017) and miR-548c-5p (Peng et al., 2018) are associated with liver metastasis in CRC patients.

Considering the relevance of epigenetic alterations in cancer dissemination and progression, there is a great interest in the development of epigenetic modifiers that can function as epidrugs. Importantly, some of these epigenetic modifiers have been tested preclinically or in early-phase clinical trials for CRC, representing a promising field for the treatment of this tumor (Baretti and Azad, 2018).

CLINICAL UTILITY OF EPIGENETIC MARKS IN LIQUID BIOPSY AS CRC BIOMARKERS

Alterations in epigenetic marks have shown great utility in both tissue and liquid biopsies as tumor biomarkers for early detection, prognosis, monitoring, and evaluation of therapeutic response in CRC (Jung et al., 2020). Of these epigenetic alterations, changes in DNA methylation patterns and ncRNA expression are among the most well-known epigenetic biomarkers of CRC in liquid biopsy. Epigenetic biomarkers have been detected in all the components of liquid biopsy as well as in multiple biological fluids (**Figure 2**). Although blood is the most explored biological fluid for the study of these types of biomarkers, other fluids (such as stool and saliva) have also been considered as a relevant source of epigenetic tumor biomarkers for CRC. **Tables 2–7** include examples of representative circulating epigenetic biomarkers analyzed in blood and other fluids associated with clinical applications for CRC patients.

Blood-Based Circulating Epigenetic Biomarkers

DNA Modifications: Methylation and Hydroxymethylation

A plethora of epigenetic biomarkers based on altered methylation have been evaluated in blood-derived cfDNA for the management of CRC (**Table 2**). Among them, plasma SEPTIN9 (*SEPT9*) methylation is one of the most studied epigenetic biomarkers for the screening and early detection of this tumor (Lofton-Day et al., 2008; Church et al., 2014). Epi proColon was the first commercially available test for the detection of plasma *SEPT9* methylation, and Epi proColon 2.0 constitutes the improved second generation of this test. This qualitative assay is based on the detection of methylation in the promoter region of the *SEPT9* gene from plasma cfDNA by

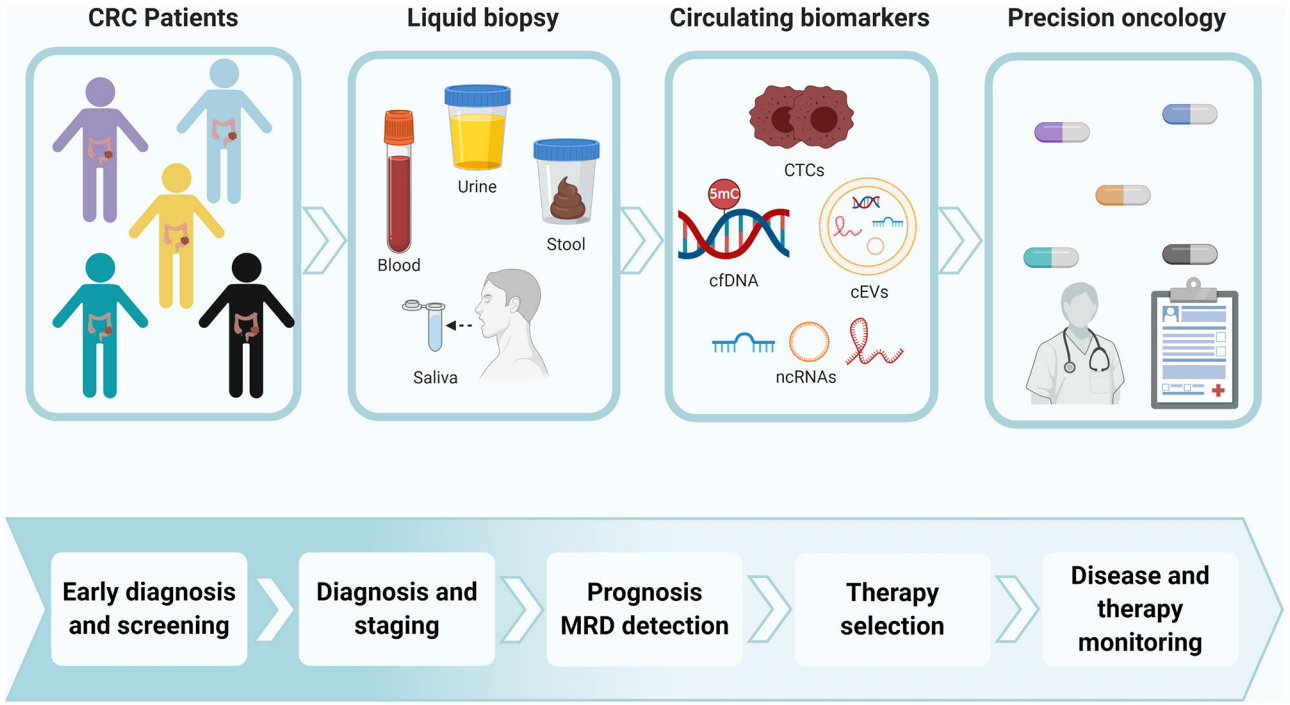

FIGURE 2 | Epigenetic biomarkers in liquid biopsy for precision oncology of CRC patients. Colorectal primary tumors and metastasis can release epigenetic biomarkers into different types of biological fluids. The disruption of these epigenetic mechanisms can be detected in circulating tumor cells (CTCs), nucleic acids (cNAs) and extracellular vesicles (cEVs), showing clinical relevance as therapeutic targets and tumor biomarkers for early detection, prognosis, monitoring, therapy selection, and evaluation of therapeutic response in CRC. The detection of these epigenetic biomarkers in liquid biopsy have a great value to personalize the management of CRC patients. CRC, colorectal cancer; CTCs, circulating tumor cells; cfDNA, cell-free DNA; ncRNAs, non-coding RNAs; MRD, minimal residual disease. Created with BioRender.com.

real-time PCR. Importantly, the Epi proColon test was the first blood-based assay approved by the FDA for the screening of CRC (Pickhardt, 2016; Issa and Noureddine, 2017). According to several studies, assessing the promoter methylation status of *SEPT9* allows to differentiate between CRC patients and healthy individuals with high overall sensitivity and specificity (Wang et al., 2018), although this assay has a limited capacity to predict precancerous lesions or adenomas (Church et al., 2014). In addition to this limitation, there are other aspects that have hampered the clinical implementation of this assay, including the high heterogeneity of the analytical characteristics among studies and its poor cost effectiveness in comparison with other methods (Wang et al., 2018). Recently, the combined analysis of *SEPT9* and *SDC2* methylation levels in blood has led to the development of a new test (ColoDefense) allowing significantly improved detection of CRC and adenomas, and thus representing a promising tool for tumor screening and early detection (Zhao G. et al., 2019). Other studies have described how the combined analysis of the methylation profiles of several genes in plasma allows for discrimination between healthy controls and patients with adenomas or CRC. For example, the analysis of a gene panel including *SFRP1*, *SFRP2*, *SDC2*, and *PRIMA1* allowed to distinguish between CRC patients and healthy controls with high sensitivity and specificity (Bartak et al., 2017). Similarly, with the SpecColon test it was possible to analyze the methylation patterns of plasma *SFRP2* and *SDC2* simultaneously, thereby accurately detecting CRC and advanced adenomas (Zhao et al., 2020b). In another study, the analysis of methylation patterns in a three-gene panel (*C9orf50*, *KCNQ5*, and *CLIP4*) in plasma, through a test called TriMeth, enabled early detection of CRC with good sensitivity and specificity (Jensen et al., 2019).

Furthermore, approaches based on methylation microarrays and NGS have been used to identify epigenetic biomarkers in cfDNA for cancer detection. For instance, the analysis of ∼850,000 CpGs in pooled cfDNA samples by MethylationEPIC array highlighted 1,384 differentially methylated CpG sites that discriminate CRC patients from healthy controls (Gallardo-Gomez et al., 2018). Moreover, the combination of NGS with machine learning has enabled the development of a test based on ∼1 million CpG sites capable of detecting and localizing more than 50 tumor types, including CRC (Liu M. C. et al., 2020). Another research group designed a targeted NGS assay based on 9,223 hypermethylated CpG sites obtained from The Cancer Genome Atlas (TCGA), which proved useful for identifying advanced CRC as well as other tumor types (Liu et al., 2018). In addition, the PanSeer assay, which considers 10,613 CpG sites, allowed the detection of five cancer types, including CRC, regardless of the tissue of origin. Importantly, this assay enabled to detect the presence of cancer in asymptomatic individuals years before standard diagnosis (Chen et al., 2020). Another

TABLE 2 | DNA modifications in cfDNA of blood as epigenetic biomarkers of CRC.

Feature	Biomarker/Assay	Clinical application	References
Methylation	Epi proColon (*SEPT9*)	Diagnosis	Lofton-Day et al., 2008
	ColoDefense (*SEPT9*, *SDC2)*	Diagnosis	Zhao G. et al., 2019
	SFRP1, SFRP2, SDC2, PRIMA1	Diagnosis	Bartak et al., 2017
	SpecColon (*SFRP2*, *SDC2*)	Diagnosis	Zhao et al., 2020b
	TriMeth (*C9orf50, KCNQ5, CLIP4*)	Diagnosis	Jensen et al., 2019
	Methylation of multiple CpG sites	Diagnosis	Liu M. C. et al., 2020
	Methylation of genomic regions	Diagnosis	Shen et al., 2018
	HPP1, HLTF	Prognosis	Wallner et al., 2006
	RARB, RASSF1A	Prognosis	Rasmussen et al., 2018
	EYA4, GRIA4, ITGA4, MAP3K14-AS1, MSC	Monitoring	Barault et al., 2018
	SEPT9, DCC, BOLL, SFRP2	Monitoring	Bhangu et al., 2018
	WIF1, NPY	Monitoring	Garrigou et al., 2016
	BCAT1, IKZF1	Monitoring	Young et al., 2016
Hydroxy-methylation	5hmC	Diagnosis/ Prognosis	Gao et al., 2019

TABLE 3 | Histone/nucleosomes in blood as epigenetic biomarkers of CRC.

Feature	Biomarker/Assay	Clinical application	References
Histone modifications	H3K9me3, H4K20me3, H3K27me3	Diagnosis	Gezer et al., 2013, 2015
	H2AK119Ub, H3K9Ac, H3K27Ac	Diagnosis	Rahier et al., 2017
	H2AK119Ub, H3K9Ac, H4K20me3	Diagnosis	Rahier et al., 2017
Nucleosomes	Concentration levels	Prognosis	Fahmueller et al., 2012
	Concentration levels	Monitoring	Holdenrieder et al., 2001
	DNA fragmentation	Diagnosis	Cristiano et al., 2019
	DNA fragmentation	Therapy response	Kitahara et al., 2016

approach for the analysis of cfDNA methylation patterns, based on the combination of immunoprecipitation and NGS (cfMeDIP), was demonstrated to be effective for the detection of CRC and other tumor types (Shen et al., 2018).

At the prognosis level, several studies have revealed that the analysis of DNA methylation in liquid biopsy is useful to predict the outcome of patients. The potential prognostic biomarker for CRC that has been most studied is the hypermethylation of the *p16* promoter in blood, which has been associated with worse overall survival (Xing et al., 2013). Similarly, several studies have analyzed the methylation status of other genes, such as *HPP1* and *HLTF*, showing that hypermethylation of these genes in serum samples indicates worse prognosis and higher mortality of CRC patients (Wallner et al., 2006; Philipp et al., 2012). Another study demonstrated that the median number of hypermethylated promoter regions was higher in CRC patients with distant metastasis than in those without metastasis. These authors also found that the hypermethylation of *RARB* and *RASSF1A* was associated with the aggressiveness of the disease, representing an independent predictive factor of worse overall survival (Rasmussen et al., 2018).

Circulating DNA methylation can also be analyzed in series of fluid samples to monitor tumor burden and evaluate the therapeutic response of CRC patients to different types of treatments, including chemotherapy and anti-EGFR therapy (Barault et al., 2018; Bhangu et al., 2018). In this regard, the hypermethylation of two genes (*WIF1* and *NPY*) in cfDNA has been described as a surrogate biomarker of tumor burden and applied to monitor patients without the need for mutational analysis in liquid biopsy (Garrigou et al., 2016). Of note, these types of circulating epigenetic alterations correlate with tumor volume and recurrence better than classical biomarkers, such as carcinoembryonic antigen (CEA) and carbohydrate antigen (CA) 19-9 (Young et al., 2016; Bhangu et al., 2018; Symonds et al., 2020). In line with these results, the analysis of circulating methylation markers has also shown consistency with the output of imaging tests in the assessment of response to therapy and surgery (Boeckx et al., 2018). All these findings indicate the potential of the analysis of circulating DNA methylation for improving the clinical evaluation of CRC patients and, if necessary, promptly redefining the treatment strategy.

The analysis of DNA methylation has also been explored in CTCs isolated from blood, although the number of studies focused on this circulating tumor population is still very low. Interestingly, when comparing the methylation levels of *VIM* and *SFRP2* in CTCs of CRC patients with those of tumor tissues, researchers found a strong correlation between the methylation status of the *SFRP2* promoter in CTCs and that of the corresponding tissue, but a weaker correlation in the case of *VIM*. Therefore, although the CTC population can show a different methylation pattern than tumor cells located in primary tissue and metastasis due to the gain of specific characteristics in the bloodstream, these data demonstrated that methylation profiling of CTCs in CRC patients represents a promising non-invasive approach for tumor detection (Lyberopoulou et al., 2017).

In addition to methylation, differential hydroxymethylation patterns of plasma cfDNA have been observed between patients with CRC and healthy controls, suggesting that markers of this epigenetic modification could also be used as a non-invasive tool for early detection and prognosis in CRC (**Table 2**). Importantly, the efficiency by which the presence of 5hmC in cfDNA points at CRC was shown to be similar to that in tumor tissues, and higher than that of well-known biomarkers, such as CEA, CA 19-9, and methylated *SEPT9* (Li et al., 2017).

Histones and Nucleosomes

The study of histone modifications in blood-circulating nucleosomes (**Table 3**) has revealed that they can also contribute to CRC detection. For example, low levels of the circulating histone marks H3K9me3, H4K20me3, and H3K27me3 have

TABLE 4 | Non-coding cfRNAs in blood as epigenetic biomarkers of CRC.

Feature	Biomarker/Assay	Clinical application	References
MiRNAs	miR-21	Diagnosis	Peng et al., 2017
	miR-601, miR-760	Diagnosis	Wang et al., 2012
	miR-532-3p, miR-331, miR-195, miR-17, miR-142-3p, miR-15b, miR-532, miR-652	Diagnosis	Kanaan et al., 2013
	miR-431, miR-15b, miR-139-3p	Diagnosis	Kanaan et al., 2013
	miR-19a, miR-19b, miR-15b, miR-29a, miR-335, miR-18a	Diagnosis	Herreros-Villanueva et al., 2019
	miR-210	Prognosis	Wang et al., 2017
	miR-141	Prognosis	Cheng et al., 2011
	miR-23b	Prognosis	Kou et al., 2016
	miR-96, miR-203, miR-141, miR-200b	Prognosis	Sun et al., 2016
	miR-29a, miR-200b, miR-203, miR-31	Prognosis	Yuan et al., 2017
	miR-31, miR-141, miR-16	Monitoring	Yuan et al., 2017
	miR-126	Therapy response	Hansen et al., 2015
	miR-21, miR-221, miR-760	Therapy response	Schirripa et al., 2019)
LncRNAs	HOTAIR, CCAT1	Diagnosis	Zhao et al., 2015
	91H, PVT-1, MEG3	Diagnosis	Liu et al., 2019
	XLOC_006844, LOC152578, XLOC_000303	Diagnosis	Shi et al., 2015
	SNHG11	Diagnosis	Xu et al., 2020
	HOTAIR	Diagnosis/Prognosis	Svoboda et al., 2014
CircRNAs	circ-CCDC66, circ-ABCC1, circ-STIL	Diagnosis	Lin et al., 2019
	hsa_circ_0082182, hsa_circ_0000370, hsa_circ_0035445	Diagnosis	Ye et al., 2019
	hsa_circ_0007534	Diagnosis/Prognosis	Zhang et al., 2018
	hsa_circ_0002320	Prognosis	Yang N. et al., 2020

TABLE 5 | Non-coding RNAs in EVs of blood as epigenetic biomarkers of CRC.

Feature	Biomarker/Assay	Clinical application	References
MiRNAs	miR-19a, miR-20a, miR-143, miR-145, miR-150, let-7a	Diagnosis	Maminezhad et al., 2020
	miR-139-3p	Diagnosis/ Metastasis monitoring	Liu W. et al., 2020
	miR-17-5p, miR-92a-3p	Prognosis	Fu et al., 2018
	miR-19a	Prognosis	Matsumura et al., 2015
	miR-21-5p, miR-1246, miR-1229-5p, miR-96-5p	Therapy response	Jin et al., 2019
LncRNAs	LINC02418	Diagnosis	Zhao Y. et al., 2019
	RPPH1	Diagnosis	Liang et al., 2019
	HOTTIP	Prognosis	Oehme et al., 2019
CircRNAs	circ-PNN	Diagnosis	Xie Y. et al., 2020

been proposed as biomarkers for the diagnosis of CRC (Gezer et al., 2013, 2015). The combination of different PTMs detected in circulating nucleosomes has also proved useful for CRC screening (Rahier et al., 2017). In addition, high concentrations of circulating nucleosomes in CRC patients have been associated with disease progression, poor therapy response, and reduced survival (Fahmueller et al., 2012). Notably, the levels of nucleosomes in cancer patients are dynamic and thus can be useful to indicate the response to therapy in real time (Holdenrieder et al., 2001).

Nucleosome occupancy is closely related to the fragmentation patterns of cfDNA (Ivanov et al., 2015). Notably, Mouliere et al. found that in multiple cancer types, including CRC, plasma cfDNA fragments exhibited different sizes between healthy individuals and cancer patients (Mouliere et al., 2018). Therefore, these authors proposed cfDNA fragmentation patterns as epigenetic biomarkers for early cancer detection. Consistently, fragmentation profiling of plasma cfDNA proved effective for CRC diagnosis, even when the tumor origin was initially unknown (Cristiano et al., 2019). The level of cfDNA fragmentation can also be associated with the prognosis of CRC patients, as patients displaying higher fragmentation showed worse prognosis (El Messaoudi et al., 2016). In addition, the analysis of cfDNA fragmentation patterns has proved useful for early detection of MRD after surgery and to predict the response of CRC patients to immunochemotherapy (**Table 3**).

Non-coding RNAs

Similar to other epigenetic alterations, the presence of ncRNAs in blood is a relevant source of biomarkers for CRC management (**Table 4**). For instance, a recent meta-analysis revealed that circulating miR-21 is a promising biomarker for CRC detection, and that its diagnostic properties can be improved by combining it with other biomarkers (Peng et al., 2017). Moreover, numerous studies have identified circulating miRNA signatures and applied them for non-invasive early detection of CRC; this enabled to distinguish healthy controls, patients with precancerous lesions

TABLE 6 | DNA modifications in non-blood fluids as epigenetic biomarkers of CRC.

Feature	Sample	Biomarker/Assay	Clinical application	References
Methylation	Stool	*FBN1*	Diagnosis	Guo et al., 2013
	Stool	*SDC2, VIM*	Diagnosis	Chen et al., 2005
	Stool	*HPP1, SFRP2, MGMT*	Diagnosis/Screening	Huang et al., 2007
	Stool	miR-34a, miR-34b/c	Diagnosis	Kalimutho et al., 2011; Wu et al., 2014
	Stool	ColoGuard (*NDRG4, BMP3*)	Diagnosis	Imperiale et al., 2014
	Stool	ColoSure (*VIM*)	Diagnosis	Ned et al., 2011
	Stool	ColoDefense (*SEPT9, SDC2*)	Diagnosis	Zhao et al., 2020a
	Urine	*VIM*	Diagnosis/Screening	Song et al., 2012
	Urine	*NDRG4*	Diagnosis	Xiao et al., 2015
	Urine	*WIF1*	Diagnosis	Amiot et al., 2014
	Bowel lavage	mir-34b/c	Diagnosis	Kamimae et al., 2011
	Bowel lavage	miR-124-3, LOC386758, *SFRP1*	Diagnosis	Harada et al., 2014
Hydroxymethylation	Urine	5-hydroxymethylated cytosine nucleosides	Diagnosis	Guo et al., 2018

TABLE 7 | Non-coding cfRNAs in non-blood fluids as epigenetic biomarkers of CRC.

Feature	Sample	Biomarker/Assay	Clinical application	References
MiRNAs	Stool	miR-451a, miR-144-5p	Diagnosis	Wu et al., 2017
	Stool	miR-20a	Diagnosis	Wu et al., 2017
	Stool	miR-421, miR-27a-3p	Diagnosis	Duran-Sanchon et al., 2020
	Stool	miR-21	Diagnosis	Wu et al., 2012
	Saliva	miR-21	Diagnosis	Sazanov et al., 2017
	Saliva	miR-186-5p, miR-29a-3p, miR-29c-3p, miR-766-3p, and miR-491-5p	Diagnosis/Prognosis	Rapado-Gonzalez et al., 2019

(advanced adenomas), and CRC patients with high sensitivity and specificity (Wang et al., 2012; Kanaan et al., 2013; Herreros-Villanueva et al., 2019). The analysis of miRNAs in blood can also provide prognostic information. For instance, increased levels of circulating miR-210 and miR-141 are associated with shorter survival rates (Cheng et al., 2011; Wang et al., 2017). In contrast, high plasma levels of miR-23b are associated with longer survival (Kou et al., 2016). The levels of different miRNAs in blood can also provide information about the patient's disease stage (Sun et al., 2016), and represent a valuable tool for early detection of recurrence after surgery (Yuan et al., 2017) and the evaluation of response to therapy in CRC patients (Hansen et al., 2015; Schirripa et al., 2019).

Other ncRNAs, such as lncRNAs, are also deregulated in CRC and can provide relevant clinical information (**Table 4**). For example, elevated plasma levels of the lncRNA HOTAIR, alone or in combination with other lncRNAs, have proved useful not only for CRC screening, but also as a biomarker associated with worse prognosis and higher mortality (Svoboda et al., 2014; Zhao et al., 2015). Of note, other studies have proposed different combinations of circulating lncRNAs as diagnostic biomarkers for the detection of CRC and precancerous lesions (Shi et al., 2015; Liu et al., 2019; Xu et al., 2020). In addition to lncRNAs, the analysis of circRNAs in blood, as biomarkers with relevant clinical properties for CRC diagnosis and prognosis, has raised considerable interest (Lin et al., 2019; Yang N. et al., 2020).

Finally, ncRNA levels have also been analyzed in cEVs, especially in exosomes, of CRC patients (**Table 5**). Exosomal miRNAs (e.g., miR-21 and miR-139-3p) can be more or less abundant than normal in the blood of CRC patients and their analysis represents a valuable tool for CRC diagnosis and prognosis (Fu et al., 2018; Liu W. et al., 2020). Furthermore, the analysis of miRNAs in circulating exosomes has revealed important strategies for the identification of treatment-resistant patients (Jin et al., 2019). For example, the exosomal levels of the lncRNAs HOTTIP, LINC02418, and RPPH1 were found deregulated in CRC and thus proposed as potential markers for the diagnosis of CRC, as well as in other clinical contexts (Liang et al., 2019; Oehme et al., 2019; Zhao Y. et al., 2019). Finally, recent studies have focused on exosomal circRNAs (e.g., circ-133 and circ-PNN), suggesting a relevant role of these ncRNAs as biomarkers for CRC (Xie Y. et al., 2020; Yang et al., 2020).

Circulating Epigenetic Biomarkers in Alternative Fluids

DNA Modifications: Methylation and Hydroxymethylation

Numerous studies have reported the application of DNA methylation patterning in stool (**Table 6**) for the detection of

CRC or precancerous lesions (Raut et al., 2020). In particular, methylation of the promoter region of *FBN1*, *SDC2*, or *VIM* has been reported as a biomarker for early CRC diagnosis (Chen et al., 2005; Guo et al., 2013; Han et al., 2019). In addition, the hypermethylation of a three-gene panel (*HPP1*, *SFRP2*, and *MGMT*) in stool showed clinical value for detecting CRC and precancerous colorectal lesions (Huang et al., 2007). Other studies have also highlighted the hypermethylation of the promoters of numerous genes in stool samples from patients affected by CRC or adenomas, such as *HIC1*, *COL4A1*, *COL4A2*, *GATA4*, *ITGA4*, *OSMR*, and *TLX2* (Lenhard et al., 2005; Kim et al., 2009; Liu et al., 2020). In addition, the methylation status of various miRNAs (e.g., miR-34a and miR-34b/c) was found to be altered in stool of CRC patients, and studied as a source of potential biomarkers (Kalimutho et al., 2011; Wu et al., 2014).

Importantly, some of the methylated biomarkers detected at an increased concentration in stool samples from CRC patients have been translated into clinical tests. This is the case of Cologuard, which is the first multi-target stool panel approved by the FDA for CRC screening (Pickhardt, 2016). The Cologuard assay combines the analysis of *NDRG4* and *BMP3* methylation, *KRAS* mutation, β-actin levels, and hemoglobin levels by immunochemistry. This multiparameter stool assay displays a high sensitivity in CRC detection, higher than that of FIT; however, Cologuard yields lower specificity in the case of asymptomatic patients, which represents a limit for its clinical implementation (Imperiale et al., 2014). Another similar FDA-approved test, ColoSure, allows to analyze *VIM* methylation in stool samples to identify the presence of precancerous adenomas or malignant colorectal tumors (Ned et al., 2011). Another strategy for addressing the methylation of known promoters is the application of the ColoDefense test to stool samples, which enables to detect the methylation status of *SEPT9* and *SDC2* with high sensitivity and specificity (Zhao et al., 2020a).

Similar to other biofluids, urine also contains cfDNA suitable for epigenetic analyses (**Table 6**). For instance, the *VIM* promoter in cfDNA from urine samples was found to display higher methylation in CRC patients than in controls, and thus methylation profiling of this promoter was proposed as a useful test for CRC screening (Song et al., 2012). The methylation status of *NDRG4* has also been explored in urine from CRC patients, showing higher diagnostic properties than that in blood and stool (Xiao et al., 2015). The easier manipulation of urine samples with respect to stool supports the value of this approach as a potential clinical method for CRC detection. The methylation levels of *WIF1*, *ALX4*, and *VIM* were also assessed in either urine or serum samples of CRC patients and controls with promising results for CRC diagnosis in the case of *WIF1* (Amiot et al., 2014). In addition, several epigenetic markers, including aberrant levels of methylated and hydroxymethylated cytosine nucleosides, have been analyzed in urine samples with promising results, and may be applied as potential biomarkers of CRC (Guo et al., 2018).

Interestingly, there are also other types of fluids that can be obtained from CRC patients. For example, mucosal wash fluid, in which DNA methylation is also detectable, can be collected during colonoscopy (Kamimae et al., 2011). Moreover, the release of cancer cells by the most aggressive tumors might impact the levels of methylated biomarkers in wash samples. To verify this hypothesis, the methylation levels of 15 genes were assessed in bowel lavage fluid (BLF) samples from a large cohort of individuals with CRC, adenomas, and small polyps, as well as from healthy individuals. The methylation levels of three gene promoters (*mir-124-3*, *LOC386758*, and *SFRP1*) showed good correlation with CRC, confirming that methylation studies in BLF samples represent a source of potential biomarkers for CRC detection (**Table 6**) (Harada et al., 2014).

Histones and Nucleosomes

As previously mentioned, nucleosome occupancy is closely related to the fragmentation patterns of cfDNA (Ivanov et al., 2015). In this regard, the different length of the DNA fragments present in stool has also been proposed as a good tool to discriminate CRC patients from healthy donors. Within this line of research, the integrity of stool DNA from CRC patients was analyzed using an oligonucleotide-based hybrid capture strategy to quantify DNA fragments of 200, 400, 800 bp, 1.3, 1.8, and 24 kb, unraveling the association between high-molecular-weight fragments and this tumor type (Boynton et al., 2003). The presence of long DNA fragments was also found to be increased in CRC patients with respect to healthy controls through the use of fluorescent primers and capillary electrophoresis (Calistri et al., 2004). Such presence of long DNA fragments in stool samples has been reported in several studies as a potential biomarker, either alone (Zou et al., 2006) or in combination with the presence of oncogenic mutations in different genes (*KRAS*, *APC*, or *p53*) (Ahlquist et al., 2000) or with altered methylation patterns (Ahlquist et al., 2012).

Non-coding RNAs

NcRNAs (mainly miRNAs) are stable in stool samples, and thus represent a relevant source of non-coding biomarkers (**Table 7**). For instance, the analysis of miR-451a and miR-144-5p levels enables to differentiate between patients with CRC and healthy donors with high sensitivity and specificity (Wu et al., 2017), while that of miR-20a levels is more suitable to discriminate CRC patients from both adenoma patients and healthy controls (Yau et al., 2016). In addition, the combined investigation of miR-421 and miR-27a-3p levels with hemoglobin quantification in stool was described as a valuable tool to improve the sensitivity of current screening strategies (Duran-Sanchon et al., 2020). Similarly, increased accumulation of several miRNAs (e.g., miR-21) has also been detected in stool from CRC patients with respect to that from healthy individuals or adenoma patients, and has thus been proposed as a potential screening tool (Wu et al., 2012).

On the other hand, several studies have demonstrated the potential of saliva as a source of biomarkers for non-oral cancer detection (**Table 7**). In particular, two studies have validated the feasibility of detecting increased levels of miRNAs in the saliva of CRC patients. In one of these studies, miR-21 levels were found to be increased in both plasma and saliva of patients with stage II–IV CRC compared to those of healthy individuals. Importantly, the sensitivity and specificity of CRC identification were higher when analyzing saliva samples (Sazanov et al., 2017). On the other hand, Rapado-González et al. performed a unique massive

profiling of miRNAs in saliva samples from both CRC patients and healthy donors, and found a total of 22 miRNAs whose accumulation was specifically altered in CRC patients. The levels of most of these miRNAs had been previously described as altered in tissue or plasma samples from CRC patients. Moreover, five of these altered miRNAs (miR-186-5p, miR-29a-3p, miR-29c-3p, miR-766-3p, and miR-491-5p) showed potential as diagnostic tools to detect CRC. Overall, these two studies demonstrated that salivary miRNA analysis represents a novel approach to detect cancer-associated epigenetic alterations with potential clinical value (Rapado-Gonzalez et al., 2019).

MiRNA content was also investigated in cEVs isolated from peritoneal lavage fluid and ascites of CRC patients and control individuals. Such global characterization of cEV-associated miRNAs provided a list of 210 miRNAs whose abundance is significantly altered in CRC patients, most of which were less abundant. From this altered pattern of miRNA accumulation, the authors could identify a 10-miRNA signature with clinical value for CRC detection (Roman-Canal et al., 2019).

Circulating Epigenetic Biomarkers in Blood vs. Alternative Fluids

As we have already described, nowadays there are several body fluids that can serve as liquid biopsies to interrogate epigenetic biomarkers in CRC. Beyond the great value of blood samples as a source of tumor material, stool, and other alternative liquid biopsies showed great potential to analyze clinically relevant biomarkers. Although liquid biopsy has the advantage of being non-invasive and accessible, the diagnostic utility of the different epigenetic biomarkers can be conditioned by the type of body fluid and biomarker analyzed. For example, the detection of some epigenetic biomarkers can be more sensitive in stool than plasma samples. Thus, some studies compared the performance of methylation biomarkers in plasma and stool in parallel, finding relevant differences. This is the case of *SEPT9* methylation, which was evaluated in stool and plasma from patients with adenomas and malignant CRC tumors. Both strategies showed similar sensitivity and specificity for the detection of CRC at all stages, however, the methylation levels of *SEPT9* in stool showed higher sensitivity for detecting adenomas and early CRC tumors, indicating that the methylation analysis of this gene in stool can improve CRC screening (Liu Y. et al., 2020). The higher diagnostic accuracy observed in stool respect to blood samples could be explained due to biomarkers can be released directly from tumor cells to the intestinal lumen (Osborn and Ahlquist, 2005). Similar results were obtained for the methylation analysis of *VIM*. Although in advanced CRC this biomarker showed similar diagnostic utility in both types of samples, in early stages the methylation of *VIM* offered higher diagnostic accuracy in stool than in plasma (Chen et al., 2005; Itzkowitz et al., 2007; Li et al., 2009). On the other hand, in independent studies the levels of methylated *SFRP2* in stool and plasma showed similar results in terms of sensitivity and specificity to detect adenomas (Zhang et al., 2014; Bartak et al., 2017). MiRNA biomarkers can also show differences between stool and blood samples. Thus, although the analysis of miR-92a expression was described as a good diagnostic tool in both types of fluids, the sensitivity of miR-92a for adenomas detection was higher in blood than stool (Ng et al., 2009; Wu et al., 2012). In addition, miR-21 was found to have a similar value for discriminating CRC patients from advanced adenomas in blood and stool, but in stool samples the data variability was higher (Peng et al., 2017). In this sense, it is important to mention that stool samples represent a very heterogeneous biological material difficult to normalize among individuals for the quantitative analysis of miRNAs. Standardization of procedures from stool collection and amount of starting material to RNA extraction and detection methods, have been proposed for the detection of CRC with fecal miRNAs (Marcuello et al., 2019).

Similar to stool samples, urine represents a completely non-invasive body fluid that can be collected without pain or risk for the patient, making the sample very suitable for mass-screening of epigenetic biomarkers in CRC. This fluid has shown promising results to analyze the methylation of some genes, such as *NDRG4*, which provided higher diagnostic power to detect CRC than the same biomarker analyzed in blood and stool (Xiao et al., 2015). Additionally, saliva also has some advantages as a diagnostic tool in comparison with blood samples. Its collection is even less invasive than blood and without causing any discomfort for the patient. Recently, miR-21 expression was assessed in peripheral blood and saliva samples obtained from patients with CRC at different stages and healthy controls. Although miR-21 levels in both saliva and plasma, showed diagnostic value for CRC screening, the analysis of saliva demonstrated higher sensitivity and specificity than blood (Sazanov et al., 2017).

Overall, the selection of the most appropriated body fluid source to analyze the different tumor epigenetic marks will depend on the specific biomarker, the clinical context and the level of clinical validation, which is nowadays higher in blood and stool samples than in other alternative body fluids.

CONCLUSIONS AND FUTURE PERSPECTIVES

The interest in epigenetic alterations associated with CRC development and progression as potential clinical biomarkers or therapeutic targets has increased significantly in recent years. In the present review, we provide an overview of the different epigenetic mechanisms that regulate key steps of CRC development. Because of the clear advantage of epigenetic analysis in liquid biopsies as a non-invasive method for the dynamic characterization of CRC, we also summarize the techniques currently applied to characterize epigenetic modifications in liquid biopsy, and describe the circulating epigenetic biomarkers identified in different body fluids and their clinical potential for the personalized management of CRC.

There is a wide range of epigenetic mechanisms that are altered in CRC, including DNA methylation and hydroxymethylation, nucleosome positioning, histone modifications, and the expression of different ncRNAs (miRNAs, lncRNAs, and circRNAs). All these alterations can be explored in different fluid samples such as blood, stool, urine, or saliva,

and represent a valuable source of clinical biomarkers. In fact, as detailed in this review, the differential methylation status of several gene promoters in CRC constitutes the rationale of several commercialized screening tests, such as Cologuard or Epi ProColon. However, substantial optimization is required prior to the general implementation of circulating epigenetic markers in the clinic to guide the management of CRC patients.

Indeed, some technical factors clearly hamper the potential translation of circulating biomarkers into the clinical routine. For example, CTCs, cNAs, and cEVs released by tumor and metastases into body fluids are usually poorly concentrated with respect to circulating non-tumor elements. Therefore, the methodology employed for their detection must be very sensitive in both localized and advanced CRC. On the other hand, new NGS-based strategies, together with ddPCR-based approaches, display improved sensitivity for the detection of epigenetic signatures in cfDNA, opening new avenues for early diagnosis of CRC. However, these approaches usually require sophisticated laboratory equipment, and are too laborious and expensive to be generically implemented into the clinical routine. Epigenetic patterns are starting to be explored also in CTCs, but mainly with the aim of characterizing the specific signatures associated with the disseminative behavior of these tumor cells, due to the difficulty of isolating CTCs even in metastatic patients. Together with their sensitivity, the specificity of epigenetic biomarkers represents a critical factor affecting their clinical utility. In fact, poor specificity of screening tests would result in unnecessary invasive evaluations and undesired side effects.

Molecular intratumoral heterogeneity also represents a clinical and technical challenge for the translation of epigenetic biomarkers in the clinical setting. It is well-acknowledged that CRC tumors are composed of multiple tumor clones with different biological properties. This heterogeneity also has an impact on the variability of several epigenetic marks, with possible clinical implications. Therefore, technical improvement is required for the study of epigenetic changes in single CTCs, which will be of great value to achieve a better understanding of CRC biology.

Another important aspect is the need for standardized protocols for sample collection, processing, and storage to improve the reproducibility of studies. In particular, sample collection and pretreatment are key steps for methylation studies, and a source of heterogeneity (Pharo et al., 2016; Merker et al., 2018; Zavridou et al., 2018). Therefore, efforts should be made to harmonize pre-analytical and analytical protocols according to the epigenetic alteration, circulating element, or body fluid under investigation. Hopefully, this standardization will be possible in the near future thanks to the commitment of international initiatives and scientific societies.

A major consideration for the clinical translation of epigenetic biomarkers is the cost effectiveness of the analyses. Nowadays, most technologies consist in time-demanding, mainly NGS-based approaches, which include library preparation and bioinformatic interpretation. However, in the future, these strategies should be associated with more adjusted costs and user-friendly bioinformatic solutions. To this purpose, it would be convenient to stimulate the technological development and commercial interest of epigenetic-based tests, thereby creating a competitive environment that will lead to significant benefits in terms of pricing and effectiveness.

Of note, the scientific community have focused their attention on the great potential of epigenomic approaches in the analysis of liquid biopsy for diagnostic purposes. For instance, one of the emerging trends is the use of broad panels of methylated biomarkers in cfDNA for pan-cancer detection. Moreover, recent studies on cfDNA have revealed the importance of NGS-based approaches for the analysis of methylation signatures, nucleosome positioning, or fragmentation footprints, opening a new scenario for epigenetics in liquid biopsy (Snyder et al., 2016; Liu et al., 2018; Cristiano et al., 2019; Liu M. C. et al., 2020). In addition, there is great interest in increasing the knowledge of the epigenetic characteristics of CTCs and cEVs also in terms of other epigenetic layers, such as 5hmC levels, differential presence of various types of ncRNAs, and epitranscriptomic modifications.

The methylation analysis of *SEPT9* (Epi proColon test) was the first blood-based assay approved by the FDA (Pickhardt, 2016; Issa and Noureddine, 2017), opening great opportunities for the clinical applications of circulating epigenetic biomarkers. One of the most challenging goals to be addressed is the clinical validation of the numerous epigenetic biomarkers that have provided promising results but have not yet reached a routine use, in order to assess their prognostic value for the outcome of patients with CRC. Indeed, the translation of the results obtained with epigenetic biomarkers into diagnostic tools is still limited, probably due to the lack of standardization and the limited number of large independent cohorts that have been analyzed. Therefore, more clinical trials, including the study of the dynamics of these epigenetics biomarkers, are warranted to validate their impact in terms of survival benefit. Similarly, numerous studies have shown that epigenetic alterations can be reversed through pharmacological intervention. However, evidence supporting the benefit of epigenetic modifiers in patients with CRC is still faint (Rezapour et al., 2019).

In summary, epigenetic circulating biomarkers have demonstrated a great potential for diagnosis of CRC, as well as for monitoring the progression and therapy response of CRC patients in a non-invasive and dynamic way. However, although significant progress has been made in the clinical translation of these biomarkers in recent years, further research is required to overcome some technologic and clinical barriers. Indeed, the translation of circulating epigenetic biomarkers into the clinical setting will require large multicenter studies to demonstrate the clinical benefit of their use. Such studies should be carried out in the near future and are expected to yield valuable results, toward a more personalized management of CRC patients.

AUTHOR CONTRIBUTIONS

RL-L, LM-R, and AD-L designed the work. AR-C, NC-F, AB-C, LM-R, and AD-L wrote the original manuscript and prepared the tables. NC-F, LM-R, and AD-L designed all the figures. AR-C, NC-F, AB-C, LM-R, RL-L, and AD-L reviewed the manuscript. LM-R and AD-L supervised the work.

All the authors contributed to the article and approved the submitted version.

FUNDING

This work was co-funded by the ISCIII (PI18/00307) and the European Regional Development Fund (FEDER). AD-L was funded by a contract Juan Rodés from ISCIII (JR17/00016). AB-C was funded by a predoctoral contract PFIS from ISCIII (FI19/00240) co-funded by Fondo Social Europeo (FSE). AR-C was supported by Roche-Chus Joint Unit (IN853B 2018/03) funded by GAIN, Consellería de Economía, Emprego e Industria. NC-F was funded by a predoctoral contract from Xunta de Galicia (IN606A-2020/004). LM-R was supported by AECC.

REFERENCES

Ahlquist, D. A., Skoletsky, J. E., Boynton, K. A., Harrington, J. J., Mahoney, D. W., Pierceall, W. E., et al. (2000). Colorectal cancer screening by detection of altered human DNA in stool: feasibility of a multitarget assay panel. *Gastroenterology* 119, 1219–1227. doi: 10.1053/gast.2000.19580

Ahlquist, D. A., Zou, H., Domanico, M., Mahoney, D. W., Yab, T. C., Taylor, W. R., et al. (2012). Next-generation stool DNA test accurately detects colorectal cancer and large adenomas. *Gastroenterology* 142, 248–256; quiz e225–246. doi: 10.1053/j.gastro.2011.10.031

Akers, J. C., Gonda, D., Kim, R., Carter, B. S., and Chen, C. C. (2013). Biogenesis of extracellular vesicles (EV): exosomes, microvesicles, retrovirus-like vesicles, and apoptotic bodies. *J. Neurooncol.* 113, 1–11. doi: 10.1007/s11060-013-1084-8

Allard, W. J., Matera, J., Miller, M. C., Repollet, M., Connelly, M. C., Rao, C., et al. (2004). Tumor cells circulate in the peripheral blood of all major carcinomas but not in healthy subjects or patients with nonmalignant diseases. *Clin. Cancer Res.* 10, 6897–6904. doi: 10.1158/1078-0432.CCR-04-0378

Amiot, A., Mansour, H., Baumgaertner, I., Delchier, J. C., Tournigand, C., Furet, J. P., et al. (2014). The detection of the methylated Wif-1 gene is more accurate than a fecal occult blood test for colorectal cancer screening. *PLoS ONE* 9:e99233. doi: 10.1371/journal.pone.0099233

Amorim, M. G., Valieris, R., Drummond, R. D., Pizzi, M. P., Freitas, V. M., Sinigaglia-Coimbra, R., et al. (2017). A total transcriptome profiling method for plasma-derived extracellular vesicles: applications for liquid biopsies. *Sci. Rep.* 7:14395. doi: 10.1038/s41598-017-14264-5

Anfossi, S., Babayan, A., Pantel, K., and Calin, G. A. (2018). Clinical utility of circulating non-coding RNAs - an update. *Nat. Rev. Clin. Oncol.* 15, 541–563. doi: 10.1038/s41571-018-0035-x

Arechederra, M., Daian, F., Yim, A., Bazai, S. K., Richelme, S., Dono, R., et al. (2018). Hypermethylation of gene body CpG islands predicts high dosage of functional oncogenes in liver cancer. *Nat. Commun.* 9:3164. doi: 10.1038/s41467-018-05550-5

Ashworth, T. (1869). A case of cancer in which cells similar to those in the tumors were seen in the blood after death. *Med. J. Aust.* 14, 146–147.

Bannister, A. J., and Kouzarides, T. (2011). Regulation of chromatin by histone modifications. *Cell Res.* 21, 381–395. doi: 10.1038/cr.2011.22

Bao-Caamano, A., Rodriguez-Casanova, A., and Diaz-Lagares, A. (2020). Epigenetics of circulating tumor cells in breast cancer. *Adv. Exp. Med. Biol.* 1220, 117–134. doi: 10.1007/978-3-030-35805-1_8

Barault, L., Amatu, A., Bleeker, F. E., Moutinho, C., Falcomata, C., Fiano, V., et al. (2015). Digital PCR quantification of MGMT methylation refines prediction of clinical benefit from alkylating agents in glioblastoma and metastatic colorectal cancer. *Ann. Oncol.* 26, 1994–1999. doi: 10.1093/annonc/mdv272

Barault, L., Amatu, A., Siravegna, G., Ponzetti, A., Moran, S., Cassingena, A., et al. (2018). Discovery of methylated circulating DNA biomarkers for comprehensive non-invasive monitoring of treatment response in metastatic colorectal cancer. *Gut* 67, 1995–2005. doi: 10.1136/gutjnl-2016-313372

Barbazan, J., Alonso-Alconada, L., Elkhatib, N., Geraldo, S., Gurchenkov, V., Glentis, A., et al. (2017). Liver metastasis is facilitated by the adherence of circulating tumor cells to vascular fibronectin deposits. *Cancer Res.* 77, 3431–3441. doi: 10.1158/0008-5472.CAN-16-1917

Barbazan, J., Alonso-Alconada, L., Muinelo-Romay, L., Vieito, M., Abalo, A., Alonso-Nocelo, M., et al. (2012). Molecular characterization of circulating tumor cells in human metastatic colorectal cancer. *PLoS ONE* 7:e40476. doi: 10.1371/journal.pone.0040476

Bardelli, A., and Pantel, K. (2017). Liquid biopsies, what we do not know (Yet). *Cancer Cell* 31, 172–179. doi: 10.1016/j.ccell.2017.01.002

Baretti, M., and Azad, N. S. (2018). The role of epigenetic therapies in colorectal cancer. *Curr. Probl. Cancer* 42, 530–547. doi: 10.1016/j.currproblcancer.2018.03.001

Barski, A., Cuddapah, S., Cui, K., Roh, T. Y., Schones, D. E., Wang, Z., et al. (2007). High-resolution profiling of histone methylations in the human genome. *Cell* 129, 823–837. doi: 10.1016/j.cell.2007.05.009

Bartak, B. K., Kalmar, A., Peterfia, B., Patai, A. V., Galamb, O., Valcz, G., et al. (2017). Colorectal adenoma and cancer detection based on altered methylation pattern of SFRP1, SFRP2, SDC2, and PRIMA1 in plasma samples. *Epigenetics* 12, 751–763. doi: 10.1080/15592294.2017.1356957

Bates, S. E. (2020). Epigenetic therapies for cancer. *N. Engl. J. Med* 383, 650–663. doi: 10.1056/NEJMra1805035

Bayraktar, R., Pichler, M., Kanlikilicer, P., Ivan, C., Bayraktar, E., Kahraman, N., et al. (2017). MicroRNA 603 acts as a tumor suppressor and inhibits triple-negative breast cancer tumorigenesis by targeting elongation factor 2 kinase. *Oncotarget* 8, 11641–11658. doi: 10.18632/oncotarget.14264

Becker, A., Thakur, B. K., Weiss, J. M., Kim, H. S., Peinado, H., and Lyden, D. (2016). Extracellular vesicles in cancer: cell-to-cell mediators of metastasis. *Cancer Cell* 30, 836–848. doi: 10.1016/j.ccell.2016.10.009

Berdasco, M., and Esteller, M. (2019). Clinical epigenetics: seizing opportunities for translation. *Nat. Rev. Genet.* 20, 109–127. doi: 10.1038/s41576-018-0074-2

Berger, S. L., Kouzarides, T., Shiekhattar, R., and Shilatifard, A. (2009). An operational definition of epigenetics. *Genes Dev.* 23, 781–783. doi: 10.1101/gad.1787609

Bettegowda, C., Sausen, M., Leary, R. J., Kinde, I., Wang, Y., Agrawal, N., et al. (2014). Detection of circulating tumor DNA in early- and late-stage human malignancies. *Sci. Transl. Med.* 6:ra224. doi: 10.1126/scitranslmed.3007094

Bhangu, J. S., Beer, A., Mittlbock, M., Tamandl, D., Pulverer, W., Schonthaler, S., et al. (2018). Circulating free methylated tumor DNA markers for sensitive assessment of tumor burden and early response monitoring in patients receiving systemic chemotherapy for colorectal cancer liver metastasis. *Ann. Surg.* 268, 894–902. doi: 10.1097/SLA.0000000000002901

Boeckx, N., Op de Beeck, K., Beyens, M., Deschoolmeester, V., Hermans, C., De Clercq, P., et al. (2018). Mutation and methylation analysis of circulating tumor DNA can be used for follow-up of metastatic colorectal cancer patients. *Clin. Colorectal Cancer* 17, e369–e379. doi: 10.1016/j.clcc.2018.02.006

Bork, U., Rahbari, N. N., Scholch, S., Reissfelder, C., Kahlert, C., Buchler, M. W., et al. (2015). Circulating tumour cells and outcome in non-metastatic colorectal cancer: a prospective study. *Br. J. Cancer* 112, 1306–1313. doi: 10.1038/bjc.2015.88

Boynton, K. A., Summerhayes, I. C., Ahlquist, D. A., and Shuber, A. P. (2003). DNA integrity as a potential marker for stool-based detection of colorectal cancer. *Clin. Chem.* 49, 1058–1065. doi: 10.1373/49.7.1058

Bray, F., Ferlay, J., Soerjomataram, I., Siegel, R. L., Torre, L. A., and Jemal, A. (2018). Global cancer statistics 2018: GLOBOCAN estimates of incidence and mortality worldwide for 36 cancers in 185 countries. *CA Cancer J. Clin.* 68, 394–424. doi: 10.3322/caac.21492

Bu, H., He, D., He, X., and Wang, K. (2019). Exosomes: isolation, analysis, and applications in cancer detection and therapy. *Chembiochem* 20, 451–461. doi: 10.1002/cbic.201800470

Caley, D. P., Pink, R. C., Trujillano, D., and Carter, D. R. (2010). Long noncoding RNAs, chromatin, and development. *Sci.World J.* 10, 90–102. doi: 10.1100/tsw.2010.7

Calistri, D., Rengucci, C., Lattuneddu, A., Francioni, G., Polifemo, A. M., Nanni, O., et al. (2004). Detection of colorectal cancer by a quantitative fluorescence determination of DNA amplification in stool. *Neoplasia* 6, 536–540. doi: 10.1593/neo.04190

Castellanos-Rizaldos, E., Grimm, D. G., Tadigotla, V., Hurley, J., Healy, J., Neal, P. L., et al. (2018). Exosome-based detection of EGFR T790M in plasma from non-small cell lung cancer patients. *Clin. Cancer Res.* 24, 2944–2950. doi: 10.1158/1078-0432.CCR-17-3369

Chen, J. Y., Luo, C. W., Lai, Y. S., Wu, C. C., and Hung, W. C. (2017). Lysine demethylase KDM2A inhibits TET2 to promote DNA methylation and silencing of tumor suppressor genes in breast cancer. *Oncogenesis* 6:e369. doi: 10.1038/oncsis.2017.71

Chen, W. D., Han, Z. J., Skoletsky, J., Olson, J., Sah, J., Myeroff, L., et al. (2005). Detection in fecal DNA of colon cancer-specific methylation of the nonexpressed vimentin gene. *J. Natl. Cancer Inst.* 97, 1124–1132. doi: 10.1093/jnci/dji204

Chen, X., Gole, J., Gore, A., He, Q., Lu, M., Min, J., et al. (2020). Non-invasive early detection of cancer four years before conventional diagnosis using a blood test. *Nat. Commun.* 11:3475. doi: 10.1038/s41467-020-17316-z

Cheng, H., Zhang, L., Cogdell, D. E., Zheng, H., Schetter, A. J., Nykter, M., et al. (2011). Circulating plasma MiR-141 is a novel biomarker for metastatic colon cancer and predicts poor prognosis. *PLoS ONE* 6:e17745. doi: 10.1371/journal.pone.0017745

Chimonidou, M., Strati, A., Tzitzira, A., Sotiropoulou, G., Malamos, N., Georgoulias, V., et al. (2011). DNA methylation of tumor suppressor and metastasis suppressor genes in circulating tumor cells. *Clin. Chem.* 57, 1169–1177. doi: 10.1373/clinchem.2011.165902

Church, T. R., Wandell, M., Lofton-Day, C., Mongin, S. J., Burger, M., Payne, S. R., et al. (2014). Prospective evaluation of methylated SEPT9 in plasma for detection of asymptomatic colorectal cancer. *Gut* 63, 317–325. doi: 10.1136/gutjnl-2012-304149

Cohen, J. D., Li, L., Wang, Y., Thoburn, C., Afsari, B., Danilova, L., et al. (2018). Detection and localization of surgically resectable cancers with a multi-analyte blood test. *Science* 359, 926–930. doi: 10.1126/science.aar3247

Cohen, S. J., Punt, C. J., Iannotti, N., Saidman, B. H., Sabbath, K. D., Gabrail, N. Y., et al. (2008). Relationship of circulating tumor cells to tumor response, progression-free survival, and overall survival in patients with metastatic colorectal cancer. *J. Clin. Oncol.* 26, 3213–3221. doi: 10.1200/JCO.2007.15.8923

Cojocneanu, R., Braicu, C., Raduly, L., Jurj, A., Zanoaga, O., Magdo, L., et al. (2020). Plasma and tissue specific miRNA expression pattern and functional analysis associated to colorectal cancer patients. *Cancers* 12:843. doi: 10.3390/cancers12040843

Cristiano, S., Leal, A., Phallen, J., Fiksel, J., Adleff, V., Bruhm, D. C., et al. (2019). Genome-wide cell-free DNA fragmentation in patients with cancer. *Nature* 570, 385–389. doi: 10.1038/s41586-019-1272-6

Cristofanilli, M., Budd, G. T., Ellis, M. J., Stopeck, A., Matera, J., Miller, M. C., et al. (2004). Circulating tumor cells, disease progression, and survival in metastatic breast cancer. *N. Engl. J. Med* 351, 781–791. doi: 10.1056/NEJMoa040766

Danese, E., Minicozzi, A. M., Benati, M., Montagnana, M., Paviati, E., Salvagno, G. L., et al. (2013). Epigenetic alteration: new insights moving from tissue to plasma - the example of PCDH10 promoter methylation in colorectal cancer. *Br. J. Cancer* 109, 807–813. doi: 10.1038/bjc.2013.351

De Koker, A., Van Paemel, R., De Wilde, B., De Preter, K., and Callewaert, N. (2019). A versatile method for circulating cell-free DNA methylome profiling by reduced representation bisulfite sequencing. *bioRxiv* 663195. doi: 10.1101/663195

de la Fuente, A., Alonso-Alconada, L., Costa, C., Cueva, J., Garcia-Caballero, T., Lopez-Lopez, R., et al. (2015). M-Trap: exosome-based capture of tumor cells as a new technology in peritoneal metastasis. *J. Natl. Cancer Inst.* 107:djv184. doi: 10.1093/jnci/djv184

Deal, R. B., Henikoff, J. G., and Henikoff, S. (2010). Genome-wide kinetics of nucleosome turnover determined by metabolic labeling of histones. *Science* 328, 1161–1164. doi: 10.1126/science.1186777

Derrien, T., Johnson, R., Bussotti, G., Tanzer, A., Djebali, S., Tilgner, H., et al. (2012). The GENCODE v7 catalog of human long noncoding RNAs: analysis of their gene structure, evolution, and expression. *Genome Res.* 22, 1775–1789. doi: 10.1101/gr.132159.111

Di, Z., Di, M., Fu, W., Tang, Q., Liu, Y., Lei, P., et al. (2020). Integrated analysis identifies a nine-microrna signature biomarker for diagnosis and prognosis in colorectal cancer. *Front. Genet.* 11:192. doi: 10.3389/fgene.2020.00192

Diaz-Lagares, A., Crujeiras, A. B., Lopez-Serra, P., Soler, M., Setien, F., Goyal, A., et al. (2016a). Epigenetic inactivation of the p53-induced long noncoding RNA TP53 target 1 in human cancer. *Proc. Natl. Acad. Sci. U.S.A.* 113, E7535–E7544. doi: 10.1073/pnas.1608585113

Diaz-Lagares, A., Mendez-Gonzalez, J., Hervas, D., Saigi, M., Pajares, M. J., Garcia, D., et al. (2016b). A novel epigenetic signature for early diagnosis in lung cancer. *Clin. Cancer Res.* 22, 3361–3371. doi: 10.1158/1078-0432.CCR-15-2346

Dragomir, M., Mafra, A. C. P., Dias, S. M. G., Vasilescu, C., and Calin, G. A. (2018). Using microRNA Networks to Understand Cancer. *Int. J. Mol. Sci.* 19:1871. doi: 10.3390/ijms19071871

Duran-Sanchon, S., Moreno, L., Auge, J. M., Serra-Burriel, M., Cuatrecasas, M., Moreira, L., et al. (2020). Identification and validation of microRNA profiles in fecal samples for detection of colorectal cancer. *Gastroenterology* 158, 947–957 e944. doi: 10.1053/j.gastro.2019.10.005

Eads, C. A., Danenberg, K. D., Kawakami, K., Saltz, L. B., Blake, C., Shibata, D., et al. (2000). MethyLight: a high-throughput assay to measure DNA methylation. *Nucleic Acids Res.* 28:E32. doi: 10.1093/nar/28.8.e32

El Messaoudi, S., Mouliere, F., Du Manoir, S., Bascoul-Mollevi, C., Gillet, B., Nouaille, M., et al. (2016). Circulating DNA as a strong multimarker prognostic tool for metastatic colorectal cancer patient management care. *Clin. Cancer Res.* 22, 3067–3077. doi: 10.1158/1078-0432.CCR-15-0297

Esteller, M. (2007). Epigenetic gene silencing in cancer: the DNA hypermethylome. *Hum. Mol. Genet.* 16, R50–R59. doi: 10.1093/hmg/ddm018

Esteller, M. (2008). Epigenetics in cancer. *N. Engl. J. Med.* 358, 1148–1159. doi: 10.1056/NEJMra072067

Esteller, M. (2011). Non-coding RNAs in human disease. *Nat. Rev. Genet.* 12, 861–874. doi: 10.1038/nrg3074

Esteller, M., Hamilton, S. R., Burger, P. C., Baylin, S. B., and Herman, J. G. (1999). Inactivation of the DNA repair gene O6-methylguanine-DNA methyltransferase by promoter hypermethylation is a common event in primary human neoplasia. *Cancer Res.* 59, 793–797.

Fahmueller, Y. N., Nagel, D., Hoffmann, R. T., Tatsch, K., Jakobs, T., Stieber, P., et al. (2012). Predictive and prognostic value of circulating nucleosomes and serum biomarkers in patients with metastasized colorectal cancer undergoing Selective Internal Radiation Therapy. *BMC Cancer* 12:5. doi: 10.1186/1471-2407-12-5

Fearon, E. R., and Vogelstein, B. (1990). A genetic model for colorectal tumorigenesis. *Cell* 61, 759–767. doi: 10.1016/0092-8674(90)90186-i

Fiegle, E., Doleschel, D., Koletnik, S., Rix, A., Weiskirchen, R., Borkham-Kamphorst, E., et al. (2019). Dual CTLA-4 and PD-L1 blockade inhibits tumor growth and liver metastasis in a highly aggressive orthotopic mouse model of colon cancer. *Neoplasia* 21, 932–944. doi: 10.1016/j.neo.2019.07.006

Friedlander, T. W., Ngo, V. T., Dong, H., Premasekharan, G., Weinberg, V., Doty, S., et al. (2014). Detection and characterization of invasive circulating tumor cells derived from men with metastatic castration-resistant prostate cancer. *Int. J. Cancer* 134, 2284–2293. doi: 10.1002/ijc.28561

Frommer, M., McDonald, L. E., Millar, D. S., Collis, C. M., Watt, F., Grigg, G. W., et al. (1992). A genomic sequencing protocol that yields a positive display of 5-methylcytosine residues in individual DNA strands. *Proc. Natl. Acad. Sci. U.S.A.* 89, 1827–1831. doi: 10.1073/pnas.89.5.1827

Fu, F., Jiang, W., Zhou, L., and Chen, Z. (2018). Circulating exosomal miR-17-5p and miR-92a-3p predict pathologic stage and grade of colorectal cancer. *Transl. Oncol.* 11, 221–232. doi: 10.1016/j.tranon.2017.12.012

Gallardo-Gomez, M., Moran, S., Paez de la Cadena, M., Martinez-Zorzano, V. S., Rodriguez-Berrocal, F. J., Rodriguez-Girondo, M., et al. (2018). A new approach to epigenome-wide discovery of non-invasive methylation biomarkers for colorectal cancer screening in circulating cell-free DNA using pooled samples. *Clin. Epigenetics* 10:53. doi: 10.1186/s13148-018-0487-y

Gao, P., Lin, S., Cai, M., Zhu, Y., Song, Y., Sui, Y., et al. (2019). 5-Hydroxymethylcytosine profiling from genomic and cell-free DNA for colorectal cancers patients. *J. Cell. Mol. Med.* 23, 3530–3537. doi: 10.1111/jcmm.14252

Garrigou, S., Perkins, G., Garlan, F., Normand, C., Didelot, A., Le Corre, D., et al. (2016). A study of hypermethylated circulating tumor DNA as a universal colorectal cancer biomarker. *Clin. Chem.* 62, 1129–1139. doi: 10.1373/clinchem.2015.253609

Garzon, R., Calin, G. A., and Croce, C. M. (2009). MicroRNAs in cancer. *Annu. Rev. Med.* 60, 167–179. doi: 10.1146/annurev.med.59.053006.104707

Gasch, C., Plummer, P. N., Jovanovic, L., McInnes, L. M., Wescott, D., Saunders, C. M., et al. (2015). Heterogeneity of miR-10b expression in circulating tumor cells. *Sci. Rep.* 5:15980. doi: 10.1038/srep15980

Gasparello, J., Papi, C., Allegretti, M., Giordani, E., Carboni, F., Zazza, S., et al. (2020). A Distinctive microRNA (miRNA) signature in the blood of colorectal cancer (CRC) patients at surgery. *Cancers* 12:2410. doi: 10.3390/cancers12092410

Gezer, U., Mert, U., Ozgur, E., Yoruker, E. E., Holdenrieder, S., and Dalay, N. (2012). Correlation of histone methyl marks with circulating nucleosomes in blood plasma of cancer patients. *Oncol. Lett.* 3, 1095–1098. doi: 10.3892/ol.2012.600

Gezer, U., Ustek, D., Yoruker, E. E., Cakiris, A., Abaci, N., Leszinski, G., et al. (2013). Characterization of H3K9me3- and H4K20me3-associated circulating nucleosomal DNA by high-throughput sequencing in colorectal cancer. *Tumour Biol.* 34, 329–336. doi: 10.1007/s13277-012-0554-5

Gezer, U., Yoruker, E. E., Keskin, M., Kulle, C. B., Dharuman, Y., and Holdenrieder, S. (2015). Histone methylation marks on circulating nucleosomes as novel blood-based biomarker in colorectal cancer. *Int. J. Mol. Sci* 16, 29654–29662. doi: 10.3390/ijms161226180

Gilat, N., Tabachnik, T., Shwartz, A., Shahal, T., Torchinsky, D., Michaeli, Y., et al. (2017). Single-molecule quantification of 5-hydroxymethylcytosine for diagnosis of blood and colon cancers. *Clin. Epigenetics* 9:70. doi: 10.1186/s13148-017-0368-9

Gimeno-Valiente, F., Riffo-Campos, A. L., Vallet-Sanchez, A., Siscar-Lewin, S., Gambardella, V., Tarazona, N., et al. (2019). ZNF518B gene up-regulation promotes dissemination of tumour cells and is governed by epigenetic mechanisms in colorectal cancer. *Sci. Rep.* 9:9339. doi: 10.1038/s41598-019-45411-9

Gkountela, S., Castro-Giner, F., Szczerba, B. M., Vetter, M., Landin, J., Scherrer, R., et al. (2019). Circulating tumor cell clustering shapes DNA methylation to enable metastasis seeding. *Cell* 176, 98–112 e114. doi: 10.1016/j.cell.2018.11.046

Gonzalez-Zulueta, M., Bender, C. M., Yang, A. S., Nguyen, T., Beart, R. W., Van Tornout, J. M., et al. (1995). Methylation of the 5' CpG island of the p16/CDKN2 tumor suppressor gene in normal and transformed human tissues correlates with gene silencing. *Cancer Res.* 55, 4531–4535

Gowher, H., and Jeltsch, A. (2002). Molecular enzymology of the catalytic domains of the Dnmt3a and Dnmt3b DNA methyltransferases. *J. Biol. Chem.* 277, 20409–20414. doi: 10.1074/jbc.M202148200

Grunau, C., Clark, S. J., and Rosenthal, A. (2001). Bisulfite genomic sequencing: systematic investigation of critical experimental parameters. *Nucleic Acids Res.* 29, E65–65. doi: 10.1093/nar/29.13.e65

Guo, C., Xie, C., Chen, Q., Cao, X., Guo, M., Zheng, S., et al. (2018). A novel malic acid-enhanced method for the analysis of 5-methyl-2'-deoxycytidine, 5-hydroxymethyl-2'-deoxycytidine, 5-methylcytidine and 5-hydroxymethylcytidine in human urine using hydrophilic interaction liquid chromatography-tandem mass spectrometry. *Anal. Chim. Acta* 1034, 110–118. doi: 10.1016/j.aca.2018.06.081

Guo, Q., Song, Y., Zhang, H., Wu, X., Xia, P., and Dang, C. (2013). Detection of hypermethylated fibrillin-1 in the stool samples of colorectal cancer patients. *Med. Oncol.* 30, 695. doi: 10.1007/s12032-013-0695-4

Gupta, G. P., and Massague, J. (2006). Cancer metastasis: building a framework. *Cell* 127, 679–695. doi: 10.1016/j.cell.2006.11.001

Gupta, R. A., Shah, N., Wang, K. C., Kim, J., Horlings, H. M., Wong, D. J., et al. (2010). Long non-coding RNA HOTAIR reprograms chromatin state to promote cancer metastasis. *Nature* 464, 1071–1076. doi: 10.1038/nature08975

Gutschner, T., Hammerle, M., Eissmann, M., Hsu, J., Kim, Y., Hung, G., et al. (2013). The noncoding RNA MALAT1 is a critical regulator of the metastasis phenotype of lung cancer cells. *Cancer Res.* 73, 1180–1189. doi: 10.1158/0008-5472.CAN-12-2850

Guttman, M., Amit, I., Garber, M., French, C., Lin, M. F., Feldser, D., et al. (2009). Chromatin signature reveals over a thousand highly conserved large non-coding RNAs in mammals. *Nature* 458, 223–227. doi: 10.1038/nature07672

Han, Y. D., Oh, T. J., Chung, T. H., Jang, H. W., Kim, Y. N., An, S., et al. (2019). Early detection of colorectal cancer based on presence of methylated syndecan-2 (SDC2) in stool DNA. *Clin. Epigenetics* 11:51. doi: 10.1186/s13148-019-0642-0

Hansen, T. F., Carlsen, A. L., Heegaard, N. H., Sorensen, F. B., and Jakobsen, A. (2015). Changes in circulating microRNA-126 during treatment with chemotherapy and bevacizumab predicts treatment response in patients with metastatic colorectal cancer. *Br. J. Cancer* 112, 624–629. doi: 10.1038/bjc.2014.652

Hao, Y. X., Li, Y. M., Ye, M., Guo, Y. Y., Li, Q. W., Peng, X. M., et al. (2017). KRAS and BRAF mutations in serum exosomes from patients with colorectal cancer in a Chinese population. *Oncol. Lett.* 13, 3608–3616. doi: 10.3892/ol.2017.5889

Harada, T., Yamamoto, E., Yamano, H. O., Nojima, M., Maruyama, R., Kumegawa, K., et al. (2014). Analysis of DNA methylation in bowel lavage fluid for detection of colorectal cancer. *Cancer Prev. Res.* 7, 1002–1010. doi: 10.1158/1940-6207.CAPR-14-0162

Herceg, Z., and Vaissiere, T. (2011). Epigenetic mechanisms and cancer: an interface between the environment and the genome. *Epigenetics* 6, 804–819. doi: 10.4161/epi.6.7.16262

Herman, J. G., Graff, J. R., Myohanen, S., Nelkin, B. D., and Baylin, S. B. (1996). Methylation-specific PCR: a novel PCR assay for methylation status of CpG islands. *Proc. Natl. Acad. Sci. U.S.A.* 93, 9821–9826. doi: 10.1073/pnas.93.18.9821

Herreros-Villanueva, M., Duran-Sanchon, S., Martin, A. C., Perez-Palacios, R., Vila-Navarro, E., Marcuello, M., et al. (2019). Plasma microRNA signature validation for early detection of colorectal cancer. *Clin. Transl. Gastroenterol.* 10:e00003. doi: 10.14309/ctg.0000000000000003

Hesson, L. B., Sloane, M. A., Wong, J. W., Nunez, A. C., Srivastava, S., Ng, B., et al. (2014). Altered promoter nucleosome positioning is an early event in gene silencing. *Epigenetics* 9, 1422–1430. doi: 10.4161/15592294.2014.970077

Hiltunen, M. O., Alhonen, L., Koistinaho, J., Myohanen, S., Paakkonen, M., Marin, S., et al. (1997). Hypermethylation of the APC (adenomatous polyposis coli) gene promoter region in human colorectal carcinoma. *Int. J. Cancer* 70, 644–648. doi: 10.1002/(sici)1097-0215(19970317)70:6<644::aid-ijc3>3.0.co;2-v

Holdenrieder, S., Stieber, P., Bodenmuller, H., Busch, M., Fertig, G., Furst, H., et al. (2001). Nucleosomes in serum of patients with benign and malignant diseases. *Int. J. Cancer* 95, 114–120. doi: 10.1002/1097-0215(20010320)95:2<114::aid-ijc1020>3.0.co;2-q

Holliday, R. (1987). The inheritance of epigenetic defects. *Science* 238, 163–170. doi: 10.1126/science.3310230

Hon, C. C., Ramilowski, J. A., Harshbarger, J., Bertin, N., Rackham, O. J., Gough, J., et al. (2017). An atlas of human long non-coding RNAs with accurate 5' ends. *Nature* 543, 199–204. doi: 10.1038/nature21374

Hoy, S. M. (2020). Tazemetostat: First Approval. *Drugs* 80, 513–521. doi: 10.1007/s40265-020-01288-x

Hu, H., Shu, M., He, L., Yu, X., Liu, X., Lu, Y., et al. (2017). Epigenomic landscape of 5-hydroxymethylcytosine reveals its transcriptional regulation of lncRNAs in colorectal cancer. *Br. J. Cancer* 116, 658–668. doi: 10.1038/bjc.2016.457

Huang, J., and Wang, L. (2019). Cell-Free DNA methylation profiling analysis-technologies and bioinformatics. *Cancers* 11:1741. doi: 10.3390/cancers11111741

Huang, Z. H., Li, L. H., Yang, F., and Wang, J. F. (2007). Detection of aberrant methylation in fecal DNA as a molecular screening tool for colorectal cancer and precancerous lesions. *World J. Gastroenterol.* 13, 950–954. doi: 10.3748/wjg.v13.i6.950

Huertas, J., MacCarthy, C. M., Scholer, H. R., and Cojocaru, V. (2020). Nucleosomal DNA dynamics mediate Oct4 pioneer factor binding. *Biophys. J.* 118, 2280–2296. doi: 10.1016/j.bpj.2019.12.038

Hurd, P. J., and Nelson, C. J. (2009). Advantages of next-generation sequencing versus the microarray in epigenetic research. *Brief. Funct. Genomics Proteomics* 8, 174–183. doi: 10.1093/bfgp/elp013

Imperiale, T. F., Ransohoff, D. F., Itzkowitz, S. H., Levin, T. R., Lavin, P., Lidgard, G. P., et al. (2014). Multitarget stool DNA testing for colorectal-cancer screening. *N. Engl. J. Med.* 370, 1287–1297. doi: 10.1056/NEJMoa1311194

Issa, I. A., and Noureddine, M. (2017). Colorectal cancer screening: an updated review of the available options. *World J. Gastroenterol.* 23, 5086–5096. doi: 10.3748/wjg.v23.i28.5086

Itzkowitz, S. H., Jandorf, L., Brand, R., Rabeneck, L., Schroy, P. C. III., Sontag, S., et al. (2007). Improved fecal DNA test for colorectal cancer screening. *Clin. Gastroenterol. Hepatol* 5, 111–117. doi: 10.1016/j.cgh.2006.10.006

Ivanov, M., Baranova, A., Butler, T., Spellman, P., and Mileyko, V. (2015). Non-random fragmentation patterns in circulating cell-free

DNA reflect epigenetic regulation. *BMC Genomics* 16 (Suppl. 13):S1. doi: 10.1186/1471-2164-16-S13-S1

Jaenisch, R., and Bird, A. (2003). Epigenetic regulation of gene expression: how the genome integrates intrinsic and environmental signals. *Nat. Genet.* 33(Suppl.), 245–254. doi: 10.1038/ng1089

Jayaseelan, V. P. (2020). Emerging role of exosomes as promising diagnostic tool for cancer. *Cancer Gene Ther.* 27, 395–398. doi: 10.1038/s41417-019-0136-4

Jensen, S. O., Ogaard, N., Orntoft, M. W., Rasmussen, M. H., Bramsen, J. B., Kristensen, H., et al. (2019). Novel DNA methylation biomarkers show high sensitivity and specificity for blood-based detection of colorectal cancer-a clinical biomarker discovery and validation study. *Clin. Epigenetics* 11:158. doi: 10.1186/s13148-019-0757-3

Jiang, P., Chan, C. W., Chan, K. C., Cheng, S. H., Wong, J., Wong, V. W., et al. (2015). Lengthening and shortening of plasma DNA in hepatocellular carcinoma patients. *Proc. Natl. Acad. Sci. USA* 112, E1317–1325. doi: 10.1073/pnas.1500076112

Jin, G., Liu, Y., Zhang, J., Bian, Z., Yao, S., Fei, B., et al. (2019). A panel of serum exosomal microRNAs as predictive markers for chemoresistance in advanced colorectal cancer. *Cancer Chemother. Pharmacol.* 84, 315–325. doi: 10.1007/s00280-019-03867-6

John, S. K., George, S., Primrose, J. N., and Fozard, J. B. (2011). Symptoms and signs in patients with colorectal cancer. *Colorectal Dis.* 13, 17–25. doi: 10.1111/j.1463-1318.2010.02221.x

Jung, G., Hernandez-Illan, E., Moreira, L., Balaguer, F., and Goel, A. (2020). Epigenetics of colorectal cancer: biomarker and therapeutic potential. *Nat. Rev. Gastroenterol. Hepatol.* 17, 111–130. doi: 10.1038/s41575-019-0230-y

Kalimutho, M., Di Cecilia, S., Del Vecchio Blanco, G., Roviello, F., Sileri, P., Cretella, M., et al. (2011). Epigenetically silenced miR-34b/c as a novel faecal-based screening marker for colorectal cancer. *Br. J. Cancer* 104, 1770–1778. doi: 10.1038/bjc.2011.82

Kamimae, S., Yamamoto, E., Yamano, H. O., Nojima, M., Suzuki, H., Ashida, M., et al. (2011). Epigenetic alteration of DNA in mucosal wash fluid predicts invasiveness of colorectal tumors. *Cancer Prev. Res.* 4, 674–683. doi: 10.1158/1940-6207.CAPR-10-0214

Kanaan, Z., Roberts, H., Eichenberger, M. R., Billeter, A., Ocheretner, G., Pan, J., et al. (2013). A plasma microRNA panel for detection of colorectal adenomas: a step toward more precise screening for colorectal cancer. *Ann. Surg.* 258, 400–408. doi: 10.1097/SLA.0b013e3182a15bcc

Kane, M. F., Loda, M., Gaida, G. M., Lipman, J., Mishra, R., Goldman, H., et al. (1997). Methylation of the hMLH1 promoter correlates with lack of expression of hMLH1 in sporadic colon tumors and mismatch repair-defective human tumor cell lines. *Cancer Res.* 57, 808–811

Kapranov, P., Cheng, J., Dike, S., Nix, D. A., Duttagupta, R., Willingham, A. T., et al. (2007). RNA maps reveal new RNA classes and a possible function for pervasive transcription. *Science* 316, 1484–1488. doi: 10.1126/science.1138341

Karczmarski, J., Rubel, T., Paziewska, A., Mikula, M., Bujko, M., Kober, P., et al. (2014). Histone H3 lysine 27 acetylation is altered in colon cancer. *Clin. Proteomics* 11:24. doi: 10.1186/1559-0275-11-24

Kim, M. S., Louwagie, J., Carvalho, B., Terhaar Sive Droste, J. S., Park, H. L., Chae, Y. K., et al. (2009). Promoter DNA methylation of oncostatin m receptor-beta as a novel diagnostic and therapeutic marker in colon cancer. *PLoS ONE* 4:e6555. doi: 10.1371/journal.pone.0006555

Kim, Y. H., Petko, Z., Dzieciatkowski, S., Lin, L., Ghiassi, M., Stain, S., et al. (2006). CpG island methylation of genes accumulates during the adenoma progression step of the multistep pathogenesis of colorectal cancer. *Genes Chromosomes Cancer* 45, 781–789. doi: 10.1002/gcc.20341

Kitahara, M., Hazama, S., Tsunedomi, R., Takenouchi, H., Kanekiyo, S., Inoue, Y., et al. (2016). Prediction of the efficacy of immunotherapy by measuring the integrity of cell-free DNA in plasma in colorectal cancer. *Cancer Sci.* 107, 1825–1829. doi: 10.1111/cas.13085

Klemm, S. L., Shipony, Z., and Greenleaf, W. J. (2019). Chromatin accessibility and the regulatory epigenome. *Nat. Rev. Genet.* 20, 207–220. doi: 10.1038/s41576-018-0089-8

Kornberg, R. D. (1974). Chromatin structure: a repeating unit of histones and DNA. *Science* 184, 868–871. doi: 10.1126/science.184.4139.868

Kotake, Y., Nakagawa, T., Kitagawa, K., Suzuki, S., Liu, N., Kitagawa, M., et al. (2011). Long non-coding RNA ANRIL is required for the PRC2 recruitment to and silencing of p15(INK4B) tumor suppressor gene. *Oncogene* 30, 1956–1962. doi: 10.1038/onc.2010.568

Kou, C. H., Zhou, T., Han, X. L., Zhuang, H. J., and Qian, H. X. (2016). Downregulation of mir-23b in plasma is associated with poor prognosis in patients with colorectal cancer. *Oncol. Lett.* 12, 4838–4844. doi: 10.3892/ol.2016.5265

Kouzarides, T. (2007). Chromatin modifications and their function. *Cell* 128, 693–705. doi: 10.1016/j.cell.2007.02.005

Kubota, K., Ohashi, A., Imachi, H., and Harada, H. (2006). Improved *in situ* hybridization efficiency with locked-nucleic-acid-incorporated DNA probes. *Appl. Environ. Microbiol.* 72, 5311–5317. doi: 10.1128/AEM.03039-05

Kurdyukov, S., and Bullock, M. (2016). DNA methylation analysis: choosing the right method. *Biology* 5:3. doi: 10.3390/biology5010003

Kurup, J. T., Campeanu, I. J., and Kidder, B. L. (2019). Contribution of H3K4 demethylase KDM5B to nucleosome organization in embryonic stem cells revealed by micrococcal nuclease sequencing. *Epigenetics Chromatin* 12:20. doi: 10.1186/s13072-019-0266-9

Lao, V. V., and Grady, W. M. (2011). Epigenetics and colorectal cancer. *Nat. Rev. Gastroenterol. Hepatol.* 8, 686–700. doi: 10.1038/nrgastro.2011.173

Le, D. T., Uram, J. N., Wang, H., Bartlett, B. R., Kemberling, H., Eyring, A. D., et al. (2015). PD-1 blockade in tumors with mismatch-repair deficiency. *N. Engl. J. Med.* 372, 2509–2520. doi: 10.1056/NEJMoa1500596

Lee, S., Hwang, K. S., Lee, H. J., Kim, J. S., and Kang, G. H. (2004). Aberrant CpG island hypermethylation of multiple genes in colorectal neoplasia. *Lab. Invest.* 84, 884–893. doi: 10.1038/labinvest.3700108

Lee, S. K., and Calin, G. A. (2011). Non-coding RNAs and cancer: new paradigms in oncology. *Discov. Med.* 11, 245–254.

Legendre, C., Gooden, G. C., Johnson, K., Martinez, R. A., Liang, W. S., and Salhia, B. (2015). Whole-genome bisulfite sequencing of cell-free DNA identifies signature associated with metastatic breast cancer. *Clin. Epigenetics* 7:100. doi: 10.1186/s13148-015-0135-8

Lenhard, K., Bommer, G. T., Asutay, S., Schauer, R., Brabletz, T., Goke, B., et al. (2005). Analysis of promoter methylation in stool: a novel method for the detection of colorectal cancer. *Clin. Gastroenterol. Hepatol.* 3, 142–149. doi: 10.1016/s1542-3565(04)00624-x

Leveille, N., Melo, C. A., Rooijers, K., Diaz-Lagares, A., Melo, S. A., Korkmaz, G., et al. (2015). Genome-wide profiling of p53-regulated enhancer RNAs uncovers a subset of enhancers controlled by a lncRNA. *Nat. Commun.* 6:6520. doi: 10.1038/ncomms7520

Li, L., Lu, M., Fan, Y., Shui, L., Xie, S., Sheng, R., et al. (2019). High-throughput and ultra-sensitive single-cell profiling of multiple microRNAs and identification of human cancer. *Chem. Commun.* 55, 10404–10407. doi: 10.1039/c9cc05553c

Li, M., Chen, W. D., Papadopoulos, N., Goodman, S. N., Bjerregaard, N. C., Laurberg, S., et al. (2009). Sensitive digital quantification of DNA methylation in clinical samples. *Nat. Biotechnol.* 27, 858–863. doi: 10.1038/nbt.1559

Li, W., Li, Q., Kang, S., Same, M., Zhou, Y., Sun, C., et al. (2018). CancerDetector: ultrasensitive and non-invasive cancer detection at the resolution of individual reads using cell-free DNA methylation sequencing data. *Nucleic Acids Res.* 46:e89. doi: 10.1093/nar/gky423

Li, W., Yu, W., Jiang, X., Gao, X., Wang, G., Jin, X., et al. (2020). The construction and comprehensive prognostic analysis of the LncRNA-associated competitive endogenous RNAs network in colorectal cancer. *Front. Genet.* 11:583. doi: 10.3389/fgene.2020.00583

Li, W., Zhang, X., Lu, X., You, L., Song, Y., Luo, Z., et al. (2017). 5-Hydroxymethylcytosine signatures in circulating cell-free DNA as diagnostic biomarkers for human cancers. *Cell Res.* 27, 1243–1257. doi: 10.1038/cr.2017.121

Liang, Z. X., Liu, H. S., Wang, F. W., Xiong, L., Zhou, C., Hu, T., et al. (2019). LncRNA RPPH1 promotes colorectal cancer metastasis by interacting with TUBB3 and by promoting exosomes-mediated macrophage M2 polarization. *Cell Death Dis.* 10:829. doi: 10.1038/s41419-019-2077-0

Lin, J., Cai, D., Li, W., Yu, T., Mao, H., Jiang, S., et al. (2019). Plasma circular RNA panel acts as a novel diagnostic biomarker for colorectal cancer. *Clin. Biochem.* 74, 60–68. doi: 10.1016/j.clinbiochem.2019.10.012

Liu, H., Ye, D., Chen, A., Tan, D., Zhang, W., Jiang, W., et al. (2019). A pilot study of new promising non-coding RNA diagnostic biomarkers for early-stage colorectal cancers. *Clin. Chem. Lab. Med.* 57, 1073–1083. doi: 10.1515/cclm-2019-0052

Liu, L., Toung, J. M., Jassowicz, A. F., Vijayaraghavan, R., Kang, H., Zhang, R., et al. (2018). Targeted methylation sequencing of plasma cell-free DNA for cancer detection and classification. *Ann. Oncol.* 29, 1445–1453. doi: 10.1093/annonc/mdy119

Liu, M. C., Oxnard, G. R., Klein, E. A., Swanton, C., and Seiden, M. V. (2020). Sensitive and specific multi-cancer detection and localization using methylation signatures in cell-free DNA. *Ann. Oncol.* 31, 745–759. doi: 10.1016/j.annonc.2020.02.011

Liu, W., Yang, D., Chen, L., Liu, Q., Wang, W., Yang, Z., et al. (2020). Plasma exosomal miRNA-139-3p is a novel biomarker of colorectal cancer. *J. Cancer* 11, 4899–4906. doi: 10.7150/jca.45548

Liu, X., Ren, J., Luo, N., Guo, H., Zheng, Y., Li, J., et al. (2019). Comprehensive DNA methylation analysis of tissue of origin of plasma cell-free DNA by methylated CpG tandem amplification and sequencing (MCTA-Seq). *Clin. Epigenetics* 11:93. doi: 10.1186/s13148-019-0689-y

Liu, X., Wen, J., Li, C., Wang, H., Wang, J., and Zou, H. (2020). High-yield methylation markers for stool-based detection of colorectal cancer. *Dig. Dis. Sci.* 65, 1710–1719. doi: 10.1007/s10620-019-05908-9

Liu, Y., Zhao, G., Miao, J., Li, H., Ma, Y., Liu, X., et al. (2020). Performance comparison between plasma and stool methylated SEPT9 tests for detecting colorectal cancer. *Front. Genet.* 11:24. doi: 10.3389/fgene.2020.00324

Liu, Y., Zheng, P., Liu, Y., Ji, T., Liu, X., Yao, S., et al. (2013). An epigenetic role for PRL-3 as a regulator of H3K9 methylation in colorectal cancer. *Gut* 62, 571–581. doi: 10.1136/gutjnl-2011-301059

Lo Nigro, C., Ricci, V., Vivenza, D., Granetto, C., Fabozzi, T., Miraglio, E., et al. (2016). Prognostic and predictive biomarkers in metastatic colorectal cancer anti-EGFR therapy. *World J. Gastroenterol.* 22, 6944–6954. doi: 10.3748/wjg.v22.i30.6944

Loboda, A., Nebozhyn, M. V., Watters, J. W., Buser, C. A., Shaw, P. M., Huang, P. S., et al. (2011). EMT is the dominant program in human colon cancer. *BMC Med. Genomics* 4:9. doi: 10.1186/1755-8794-4-9

Lofton-Day, C., Model, F., Devos, T., Tetzner, R., Distler, J., Schuster, M., et al. (2008). DNA methylation biomarkers for blood-based colorectal cancer screening. *Clin. Chem.* 54, 414–423. doi: 10.1373/clinchem.2007.095992

Lu, J., Getz, G., Miska, E. A., Alvarez-Saavedra, E., Lamb, J., Peck, D., et al. (2005). MicroRNA expression profiles classify human cancers. *Nature* 435, 834–838. doi: 10.1038/nature03702

Luo, Y., Wong, C. J., Kaz, A. M., Dzieciatkowski, S., Carter, K. T., Morris, S. M., et al. (2014). Differences in DNA methylation signatures reveal multiple pathways of progression from adenoma to colorectal cancer. *Gastroenterology* 147, 418–429 e418. doi: 10.1053/j.gastro.2014.04.039

Lyberopoulou, A., Galanopoulos, M., Aravantinos, G., Theodoropoulos, G. E., Marinos, E., Efstathopoulos, E. P., et al. (2017). Identification of methylation profiles of cancer-related genes in circulating tumor cells population. *Anticancer Res.* 37, 1105–1112. doi: 10.21873/anticanres.11423

Maminezhad, H., Ghanadian, S., Pakravan, K., Razmara, E., Rouhollah, F., Mossahebi-Mohammadi, M., et al. (2020). A panel of six-circulating miRNA signature in serum and its potential diagnostic value in colorectal cancer. *Life Sci.* 258:118226. doi: 10.1016/j.lfs.2020.118226

Marcuello, M., Vymetalkova, V., Neves, R. P. L., Duran-Sanchon, S., Vedeld, H. M., Tham, E., et al. (2019). Circulating biomarkers for early detection and clinical management of colorectal cancer. *Mol. Aspects Med.* 69, 107–122. doi: 10.1016/j.mam.2019.06.002

Mari-Alexandre, J., Diaz-Lagares, A., Villalba, M., Juan, O., Crujeiras, A. B., Calvo, A., et al. (2017). Translating cancer epigenomics into the clinic: focus on lung cancer. *Transl. Res.* 189, 76–92. doi: 10.1016/j.trsl.2017.05.008

Matassov, D., Kagan, T., Leblanc, J., Sikorska, M., and Zakeri, Z. (2004). Measurement of apoptosis by DNA fragmentation. *Methods Mol. Biol.* 282, 1–17. doi: 10.1385/1-59259-812-9:001

Matsumura, T., Sugimachi, K., Iinuma, H., Takahashi, Y., Kurashige, J., Sawada, G., et al. (2015). Exosomal microRNA in serum is a novel biomarker of recurrence in human colorectal cancer. *Br. J. Cancer* 113, 275–281. doi: 10.1038/bjc.2015.201

Mattiuzzi, C., Sanchis-Gomar, F., and Lippi, G. (2019). Concise update on colorectal cancer epidemiology. *Ann. Transl. Med.* 7:609. doi: 10.21037/atm.2019.07.91

Mavrich, T. N., Ioshikhes, I. P., Venters, B. J., Jiang, C., Tomsho, L. P., Qi, J., et al. (2008). A barrier nucleosome model for statistical positioning of nucleosomes throughout the yeast genome. *Genome Res.* 18, 1073–1083. doi: 10.1101/gr.078261.108

Meissner, A., Gnirke, A., Bell, G. W., Ramsahoye, B., Lander, E. S., and Jaenisch, R. (2005). Reduced representation bisulfite sequencing for comparative high-resolution DNA methylation analysis. *Nucleic Acids Res.* 33, 5868–5877. doi: 10.1093/nar/gki901

Memczak, S., Jens, M., Elefsinioti, A., Torti, F., Krueger, J., Rybak, A., et al. (2013). Circular RNAs are a large class of animal RNAs with regulatory potency. *Nature* 495, 333–338. doi: 10.1038/nature11928

Merker, J. D., Oxnard, G. R., Compton, C., Diehn, M., Hurley, P., Lazar, A. J., et al. (2018). Circulating tumor DNA analysis in patients with cancer: American Society of Clinical Oncology and College of American Pathologists Joint Review. *J. Clin. Oncol.* 36, 1631–1641. doi: 10.1200/JCO.2017.76.8671

Metcalf, G. A., Shibakawa, A., Patel, H., Sita-Lumsden, A., Zivi, A., Rama, N., et al. (2016). Amplification-free detection of circulating microRNA biomarkers from body fluids based on fluorogenic oligonucleotide-templated reaction between engineered peptide nucleic acid probes: application to prostate cancer diagnosis. *Anal. Chem.* 88, 8091–8098. doi: 10.1021/acs.analchem.6b01594

Miao, X., Ning, X., Li, Z., and Cheng, Z. (2016). Sensitive detection of miRNA by using hybridization chain reaction coupled with positively charged gold nanoparticles. *Sci. Rep.* 6:32358. doi: 10.1038/srep32358

Mitomi, H., Fukui, N., Tanaka, N., Kanazawa, H., Saito, T., Matsuoka, T., et al. (2010). Aberrant p16((INK4a)) methylation is a frequent event in colorectal cancers: prognostic value and relation to mRNA expression and immunoreactivity. *J. Cancer Res. Clin. Oncol.* 136, 323–331. doi: 10.1007/s00432-009-0688-z

Molinari, C., Marisi, G., Passardi, A., Matteucci, L., De Maio, G., and Ulivi, P. (2018). Heterogeneity in colorectal cancer: a challenge for personalized medicine? *Int. J. Mol. Sci.* 19:3733. doi: 10.3390/ijms19123733

Mori, Y., Olaru, A. V., Cheng, Y., Agarwal, R., Yang, J., Luvsanjav, D., et al. (2011). Novel candidate colorectal cancer biomarkers identified by methylation microarray-based scanning. *Endocr. Relat. Cancer* 18, 465–478. doi: 10.1530/ERC-11-0083

Morin, R. D., Johnson, N. A., Severson, T. M., Mungall, A. J., An, J., Goya, R., et al. (2010). Somatic mutations altering EZH2 (Tyr641) in follicular and diffuse large B-cell lymphomas of germinal-center origin. *Nat. Genet.* 42, 181–185. doi: 10.1038/ng.518

Mouliere, F., Chandrananda, D., Piskorz, A. M., Moore, E. K., Morris, J., Ahlborn, L. B., et al. (2018). Enhanced detection of circulating tumor DNA by fragment size analysis. *Sci. Transl. Med.* 10:eaat4921. doi: 10.1126/scitranslmed.aat4921

Nagai, Y., Sunami, E., Yamamoto, Y., Hata, K., Okada, S., Murono, K., et al. (2017). LINE-1 hypomethylation status of circulating cell-free DNA in plasma as a biomarker for colorectal cancer. *Oncotarget* 8, 11906–11916. doi: 10.18632/oncotarget.14439

Nazemalhosseini Mojarad, E., Kuppen, P. J., Aghdaei, H. A., and Zali, M. R. (2013). The CpG island methylator phenotype (CIMP) in colorectal cancer. *Gastroenterol. Hepatol. Bed Bench* 6, 120–128.

Ned, R. M., Melillo, S., and Marrone, M. (2011). Fecal DNA testing for Colorectal Cancer Screening: the ColoSure test. *PLoS Curr.* 3:RRN1220. doi: 10.1371/currents.RRN1220

Ng, E. K., Chong, W. W., Jin, H., Lam, E. K., Shin, V. Y., Yu, J., et al. (2009). Differential expression of microRNAs in plasma of patients with colorectal cancer: a potential marker for colorectal cancer screening. *Gut* 58, 1375–1381. doi: 10.1136/gut.2008.167817

Oehme, F., Krahl, S., Gyorffy, B., Muessle, B., Rao, V., Greif, H., et al. (2019). Low level of exosomal long non-coding RNA HOTTIP is a prognostic biomarker in colorectal cancer. *RNA Biol.* 16, 1339–1345. doi: 10.1080/15476286.2019.1637697

Ogino, S., Kawasaki, T., Kirkner, G. J., Kraft, P., Loda, M., and Fuchs, C. S. (2007). Evaluation of markers for CpG island methylator phenotype (CIMP) in colorectal cancer by a large population-based sample. *J. Mol. Diagn.* 9, 305–314. doi: 10.2353/jmoldx.2007.060170

Ortega, F. G., Lorente, J. A., Garcia Puche, J. L., Ruiz, M. P., Sanchez-Martin, R. M., de Miguel-Perez, D., et al. (2015). miRNA *in situ* hybridization in circulating tumor cells–MishCTC. *Sci. Rep.* 5:9207. doi: 10.1038/srep09207

Osborn, N. K., and Ahlquist, D. A. (2005). Stool screening for colorectal cancer: molecular approaches. *Gastroenterology* 128, 192–206. doi: 10.1053/j.gastro.2004.10.041

Overman, M. J., Lonardi, S., Wong, K. Y. M., Lenz, H. J., Gelsomino, F., Aglietta, M., et al. (2018). Durable clinical benefit with nivolumab plus ipilimumab in DNA mismatch repair-deficient/microsatellite instability-high metastatic colorectal cancer. *J. Clin. Oncol.* 36, 773–779. doi: 10.1200/JCO.2017.76.9901

Pardini, B., Sabo, A. A., Birolo, G., and Calin, G. A. (2019). Noncoding RNAs in extracellular fluids as cancer biomarkers: the new frontier of liquid biopsies. *Cancers* 11:1170. doi: 10.3390/cancers11081170

Peng, Q., Zhang, X., Min, M., Zou, L., Shen, P., and Zhu, Y. (2017). The clinical role of microRNA-21 as a promising biomarker in the diagnosis and prognosis of colorectal cancer: a systematic review and meta-analysis. *Oncotarget* 8, 44893–44909. doi: 10.18632/oncotarget.16488

Peng, Z. Y., Gu, R. H., and Yan, B. (2018). Downregulation of exosome-encapsulated miR-548c-5p is associated with poor prognosis in colorectal cancer. *J. Cell. Biochem*. doi: 10.1002/jcb.27291. [Epub ahead of print].

Pharo, H. D., Honne, H., Vedeld, H. M., Dahl, C., Andresen, K., Liestol, K., et al. (2016). Experimental factors affecting the robustness of DNA methylation analysis. *Sci. Rep.* 6:33936. doi: 10.1038/srep33936

Philipp, A. B., Stieber, P., Nagel, D., Neumann, J., Spelsberg, F., Jung, A., et al. (2012). Prognostic role of methylated free circulating DNA in colorectal cancer. *Int. J. Cancer* 131, 2308–2319. doi: 10.1002/ijc.27505

Picardo, F., Romanelli, A., Muinelo-Romay, L., Mazza, T., Fusilli, C., Parrella, P., et al. (2019). Diagnostic and Prognostic Value of B4GALT1 Hypermethylation and its clinical significance as a novel circulating cell-free DNA biomarker in colorectal cancer. *Cancers* 11:1598. doi: 10.3390/cancers11101598

Pickhardt, P. J. (2016). Emerging stool-based and blood-based non-invasive DNA tests for colorectal cancer screening: the importance of cancer prevention in addition to cancer detection. *Abdom. Radiol.* 41, 1441–1444. doi: 10.1007/s00261-016-0798-4

Pixberg, C. F., Raba, K., Muller, F., Behrens, B., Honisch, E., Niederacher, D., et al. (2017). Analysis of DNA methylation in single circulating tumor cells. *Oncogene* 36, 3223–3231. doi: 10.1038/onc.2016.480

Portela, A., and Esteller, M. (2010). Epigenetic modifications and human disease. *Nat. Biotechnol.* 28, 1057–1068. doi: 10.1038/nbt.1685

Qin, S., Li, J., Wang, L., Xu, J., Cheng, Y., Bai, Y., et al. (2018). Efficacy and tolerability of first-line cetuximab plus leucovorin, fluorouracil, and oxaliplatin (FOLFOX-4) versus FOLFOX-4 in patients with RAS wild-type metastatic colorectal cancer: the open-label, randomized, phase III TAILOR trial. *J. Clin. Oncol.* 36, 3031–3039. doi: 10.1200/JCO.2018.78.3183

Qu, Y., Lennartsson, A., Gaidzik, V. I., Deneberg, S., Karimi, M., Bengtzen, S., et al. (2014). Differential methylation in CN-AML preferentially targets non-CGI regions and is dictated by DNMT3A mutational status and associated with predominant hypomethylation of HOX genes. *Epigenetics* 9, 1108–1119. doi: 10.4161/epi.29315

Quintas-Cardama, A., Santos, F. P., and Garcia-Manero, G. (2010). Therapy with azanucleosides for myelodysplastic syndromes. *Nat. Rev. Clin. Oncol.* 7, 433–444. doi: 10.1038/nrclinonc.2010.87

Rahier, J. F., Druez, A., Faugeras, L., Martinet, J. P., Gehenot, M., Josseaux, E., et al. (2017). Circulating nucleosomes as new blood-based biomarkers for detection of colorectal cancer. *Clin. Epigenetics* 9:53. doi: 10.1186/s13148-017-0351-5

Rand, K., Qu, W., Ho, T., Clark, S. J., and Molloy, P. (2002). Conversion-specific detection of DNA methylation using real-time polymerase chain reaction (ConLight-MSP) to avoid false positives. *Methods* 27, 114–120. doi: 10.1016/s1046-2023(02)00062-2

Rando, O. J. (2012). Combinatorial complexity in chromatin structure and function: revisiting the histone code. *Curr. Opin. Genet. Dev.* 22, 148–155. doi: 10.1016/j.gde.2012.02.013

Rapado-Gonzalez, O., Majem, B., Alvarez-Castro, A., Diaz-Pena, R., Abalo, A., Suarez-Cabrera, L., et al. (2019). A novel saliva-based miRNA signature for colorectal cancer diagnosis. *J. Clin. Med.* 8:2029. doi: 10.3390/jcm 8122029

Rasmussen, S. L., Krarup, H. B., Sunesen, K. G., Johansen, M. B., Stender, M. T., Pedersen, I. S., et al. (2018). The prognostic efficacy of cell-free DNA hypermethylation in colorectal cancer. *Oncotarget* 9, 7010–7022. doi: 10.18632/oncotarget.24097

Raut, J. R., Guan, Z., Schrotz-King, P., and Brenner, H. (2020). Fecal DNA methylation markers for detecting stages of colorectal cancer and its precursors: a systematic review. *Clin. Epigenetics* 12:122. doi: 10.1186/s13148-020-00904-7

Rezapour, S., Hosseinzadeh, E., Marofi, F., and Hassanzadeh, A. (2019). Epigenetic-based therapy for colorectal cancer: prospect and involved mechanisms. *J. Cell. Physiol.* 234, 19366–19383. doi: 10.1002/jcp.28658

Rodriguez-Paredes, M., and Esteller, M. (2011). Cancer epigenetics reaches mainstream oncology. *Nat. Med.* 17, 330–339. doi: 10.1038/nm.2305

Roman-Canal, B., Tarragona, J., Moiola, C. P., Gatius, S., Bonnin, S., Ruiz-Miro, M., et al. (2019). EV-associated miRNAs from peritoneal lavage as potential diagnostic biomarkers in colorectal cancer. *J. Transl. Med.* 17:208. doi: 10.1186/s12967-019-1954-8

Rose, N. R., and Klose, R. J. (2014). Understanding the relationship between DNA methylation and histone lysine methylation. *Biochim. Biophys. Acta* 1839, 1362–1372. doi: 10.1016/j.bbagrm.2014.02.007

Rosen, L. S., Jacobs, I. A., and Burkes, R. L. (2017). Bevacizumab in colorectal cancer: current role in treatment and the potential of biosimilars. *Target. Oncol.* 12, 599–610. doi: 10.1007/s11523-017-0518-1

Sadeh, R., Sharkia, I., Fialkoff, G., Rahat, A., Gutin, J., Chappleboim, A., et al. (2019). ChIP-seq of plasma cell-free nucleosomes identifies cell-of-origin gene expression programs. *bioRxiv* 638643. doi: 10.1101/638643

Sandoval, J., Heyn, H., Moran, S., Serra-Musach, J., Pujana, M. A., Bibikova, M., et al. (2011). Validation of a DNA methylation microarray for 450,000 CpG sites in the human genome. *Epigenetics* 6, 692–702. doi: 10.4161/epi.6.6.16196

Sastre, J., Maestro, M. L., Gomez-Espana, A., Rivera, F., Valladares, M., Massuti, B., et al. (2012). Circulating tumor cell count is a prognostic factor in metastatic colorectal cancer patients receiving first-line chemotherapy plus bevacizumab: a Spanish Cooperative Group for the Treatment of Digestive Tumors study. *Oncologist* 17, 947–955. doi: 10.1634/theoncologist.2012-0048

Sazanov, A. A., Kiselyova, E. V., Zakharenko, A. A., Romanov, M. N., and Zaraysky, M. I. (2017). Plasma and saliva miR-21 expression in colorectal cancer patients. *J. Appl. Genet.* 58, 231–237. doi: 10.1007/s13353-016-0379-9

Schirripa, M., Borelli, B., D'Aurizio, R., Lubrano, S., Cremolini, C., Zucchelli, G., et al. (2019). Early modifications of circulating microRNAs levels in metastatic colorectal cancer patients treated with regorafenib. *Pharmacogenomics J.* 19, 455–464. doi: 10.1038/s41397-019-0075-3

Sharma, S., Kelly, T. K., and Jones, P. A. (2010). Epigenetics in cancer. *Carcinogenesis* 31, 27–36. doi: 10.1093/carcin/bgp220

Sheaffer, K. L., Elliott, E. N., and Kaestner, K. H. (2016). DNA hypomethylation contributes to genomic instability and intestinal cancer initiation. *Cancer Prev. Res.* 9, 534–546. doi: 10.1158/1940-6207.CAPR-15-0349

Shen, S. Y., Burgener, J. M., Bratman, S. V., and De Carvalho, D. D. (2019). Preparation of cfMeDIP-seq libraries for methylome profiling of plasma cell-free DNA. *Nat. Protoc.* 14, 2749–2780. doi: 10.1038/s41596-019-0202-2

Shen, S. Y., Singhania, R., Fehringer, G., Chakravarthy, A., Roehrl, M. H. A., Chadwick, D., et al. (2018). Sensitive tumour detection and classification using plasma cell-free DNA methylomes. *Nature* 563, 579–583. doi: 10.1038/s41586-018-0703-0

Shi, J., Li, X., Zhang, F., Zhang, C., Guan, Q., Cao, X., et al. (2015). Circulating lncRNAs associated with occurrence of colorectal cancer progression. *Am. J. Cancer Res.* 5, 2258–2265.

Shin, S., Lee, E. M., Cha, H. J., Bae, S., Jung, J. H., Lee, S. M., et al. (2009). MicroRNAs that respond to histone deacetylase inhibitor SAHA and p53 in HCT116 human colon carcinoma cells. *Int. J. Oncol.* 35, 1343–1352. doi: 10.3892/ijo_00000452

Shinjo, K., Hara, K., Nagae, G., Umeda, T., Katsushima, K., Suzuki, M., et al. (2020). A novel sensitive detection method for DNA methylation in circulating free DNA of pancreatic cancer. *PLoS ONE* 15:e0233782. doi: 10.1371/journal.pone.0233782

Shirahata, A., Sakata, M., Sakuraba, K., Goto, T., Mizukami, H., Saito, M., et al. (2009). Vimentin methylation as a marker for advanced colorectal carcinoma. *Anticancer Res.* 29, 279–281.

Shukla, N., Yan, I. K., and Patel, T. (2018). Multiplexed detection and quantitation of extracellular vesicle RNA expression using nanostring. *Methods Mol. Biol* 1740, 177–185. doi: 10.1007/978-1-4939-7652-2_14

Silva-Fisher, J. M., Dang, H. X., White, N. M., Strand, M. S., Krasnick, B. A., Rozycki, E. B., et al. (2020). Long non-coding RNA RAMS11 promotes metastatic colorectal cancer progression. *Nat. Commun.* 11:2156. doi: 10.1038/s41467-020-15547-8

Siravegna, G., Marsoni, S., Siena, S., and Bardelli, A. (2017). Integrating liquid biopsies into the management of cancer. *Nat. Rev. Clin. Oncol.* 14, 531–548. doi: 10.1038/nrclinonc.2017.14

Siravegna, G., Mussolin, B., Buscarino, M., Corti, G., Cassingena, A., Crisafulli, G., et al. (2015). Clonal evolution and resistance to EGFR blockade in the blood of colorectal cancer patients. *Nat. Med.* 21, 795–801. doi: 10.1038/nm.3870

Snyder, M. W., Kircher, M., Hill, A. J., Daza, R. M., and Shendure, J. (2016). Cell-free DNA comprises an *in vivo* nucleosome footprint that informs its tissues-of-origin. *Cell* 164, 57–68. doi: 10.1016/j.cell.2015.11.050

Sole, C., Tramonti, D., Schramm, M., Goicoechea, I., Armesto, M., Hernandez, L. I., et al. (2019). The circulating transcriptome as a source of biomarkers for melanoma. *Cancers* 11:70. doi: 10.3390/cancers11010070

Song, B. P., Jain, S., Lin, S. Y., Chen, Q., Block, T. M., Song, W., et al. (2012). Detection of hypermethylated vimentin in urine of patients with colorectal cancer. *J. Mol. Diagn.* 14, 112–119. doi: 10.1016/j.jmoldx.2011.12.003

Song, L. L., and Li, Y. M. (2016). Current noninvasive tests for colorectal cancer screening: an overview of colorectal cancer screening tests. *World J. Gastrointest. Oncol.* 8, 793–800. doi: 10.4251/wjgo.v8.i11.793

Song, W., Ren, J., Wang, C., Ge, Y., and Fu, T. (2020). Analysis of circular RNA-related competing endogenous RNA identifies the immune-related risk signature for colorectal cancer. *Front. Genet.* 11:505. doi: 10.3389/fgene.2020.00505

Strahl, B. D., and Allis, C. D. (2000). The language of covalent histone modifications. *Nature* 403, 41–45. doi: 10.1038/47412

Sun, Y., Liu, Y., Cogdell, D., Calin, G. A., Sun, B., Kopetz, S., et al. (2016). Examining plasma microRNA markers for colorectal cancer at different stages. *Oncotarget* 7, 11434–11449. doi: 10.18632/oncotarget.7196

Sun, Z., Cunningham, J., Slager, S., and Kocher, J. P. (2015). Base resolution methylome profiling: considerations in platform selection, data preprocessing and analysis. *Epigenomics* 7, 813–828. doi: 10.2217/epi.15.21

Suter, C. M., Martin, D. I., and Ward, R. L. (2004). Hypomethylation of L1 retrotransposons in colorectal cancer and adjacent normal tissue. *Int. J. Colorectal Dis.* 19, 95–101. doi: 10.1007/s00384-003-0539-3

Svoboda, M., Slyskova, J., Schneiderova, M., Makovicky, P., Bielik, L., Levy, M., et al. (2014). HOTAIR long non-coding RNA is a negative prognostic factor not only in primary tumors, but also in the blood of colorectal cancer patients. *Carcinogenesis* 35, 1510–1515. doi: 10.1093/carcin/bgu055

Symonds, E. L., Pedersen, S. K., Murray, D., Byrne, S. E., Roy, A., Karapetis, C., et al. (2020). Circulating epigenetic biomarkers for detection of recurrent colorectal cancer. *Cancer* 126, 1460–1469. doi: 10.1002/cncr.32695

Taft, R. J., Pang, K. C., Mercer, T. R., Dinger, M., and Mattick, J. S. (2010). Non-coding RNAs: regulators of disease. *J. Pathol.* 220, 126–139. doi: 10.1002/path.2638

Tahiliani, M., Koh, K. P., Shen, Y., Pastor, W. A., Bandukwala, H., Brudno, Y., et al. (2009). Conversion of 5-methylcytosine to 5-hydroxymethylcytosine in mammalian DNA by MLL partner TET1. *Science* 324, 930–935. doi: 10.1126/science.1170116

Taiwo, O., Wilson, G. A., Morris, T., Seisenberger, S., Reik, W., Pearce, D., et al. (2012). Methylome analysis using MeDIP-seq with low DNA concentrations. *Nat. Protoc.* 7, 617–636. doi: 10.1038/nprot.2012.012

Taniguchi, H., Yamanaka, T., Sakai, D., Muro, K., Yamazaki, K., Nakata, S., et al. (2020). Efficacy of panitumumab and cetuximab in patients with colorectal cancer previously treated with bevacizumab; a combined analysis of individual patient data from ASPECCT and WJOG6510G. *Cancers* 12:1715. doi: 10.3390/cancers12071715

Thierry, A. R., El Messaoudi, S., Gahan, P. B., Anker, P., and Stroun, M. (2016). Origins, structures, and functions of circulating DNA in oncology. *Cancer Metastasis Rev.* 35, 347–376. doi: 10.1007/s10555-016-9629-x

Toyota, M., Ahuja, N., Ohe-Toyota, M., Herman, J. G., Baylin, S. B., and Issa, J. P. (1999). CpG island methylator phenotype in colorectal cancer. *Proc. Natl. Acad. Sci. U.S.A.* 96, 8681–8686. doi: 10.1073/pnas.96.15.8681

Triantafillidis, J. K., Vagianos, C., and Malgarinos, G. (2015). Colonoscopy in colorectal cancer screening: current aspects. *Indian J. Surg. Oncol.* 6, 237–250. doi: 10.1007/s13193-015-0410-3

Vad-Nielsen, J., Meldgaard, P., Sorensen, B. S., and Nielsen, A. L. (2020). Cell-free Chromatin Immunoprecipitation (cfChIP) from blood plasma can determine gene-expression in tumors from non-small-cell lung cancer patients. *Lung Cancer* 147, 244–251. doi: 10.1016/j.lungcan.2020.07.023

van Niel, G., D'Angelo, G., and Raposo, G. (2018). Shedding light on the cell biology of extracellular vesicles. *Nat. Rev. Mol. Cell Biol.* 19, 213–228. doi: 10.1038/nrm.2017.125

Van Paemel, R., De Koker, A., Vandeputte, C., van Zogchel, L., Lammens, T., Laureys, G., et al. (2020). Minimally invasive classification of paediatric solid tumours using reduced representation bisulphite sequencing of cell-free DNA: a proof-of-principle study. *Epigenetics* 1–13. doi: 10.1080/15592294.2020.1790950. [Epub ahead of print].

Vidal, J., Muinelo, L., Dalmases, A., Jones, F., Edelstein, D., Iglesias, M., et al. (2017). Plasma ctDNA RAS mutation analysis for the diagnosis and treatment monitoring of metastatic colorectal cancer patients. *Ann. Oncol.* 28, 1325–1332. doi: 10.1093/annonc/mdx125

Vincent, K. M., and Postovit, L. M. (2017). A pan-cancer analysis of secreted Frizzled-related proteins: re-examining their proposed tumour suppressive function. *Sci. Rep.* 7:42719. doi: 10.1038/srep42719

Volinia, S., Calin, G. A., Liu, C. G., Ambs, S., Cimmino, A., Petrocca, F., et al. (2006). A microRNA expression signature of human solid tumors defines cancer gene targets. *Proc. Natl. Acad. Sci. U.S.A.* 103, 2257–2261. doi: 10.1073/pnas.0510565103

Waddington, C. H. (2012). The epigenotype. 1942. *Int. J. Epidemiol.* 41, 10–13. doi: 10.1093/ije/dyr184

Wallner, M., Herbst, A., Behrens, A., Crispin, A., Stieber, P., Goke, B., et al. (2006). Methylation of serum DNA is an independent prognostic marker in colorectal cancer. *Clin. Cancer Res.* 12, 7347–7352. doi: 10.1158/1078-0432.CCR-06-1264

Wang, Q., Huang, Z., Ni, S., Xiao, X., Xu, Q., Wang, L., et al. (2012). Plasma miR-601 and miR-760 are novel biomarkers for the early detection of colorectal cancer. *PLoS ONE* 7:e44398. doi: 10.1371/journal.pone.0044398

Wang, W., Qu, A., Liu, W., Liu, Y., Zheng, G., Du, L., et al. (2017). Circulating miR-210 as a diagnostic and prognostic biomarker for colorectal cancer. *Eur. J. Cancer Care* 26:e12448. doi: 10.1111/ecc.12448

Wang, Y., Chen, P. M., and Liu, R. B. (2018). Advance in plasma SEPT9 gene methylation assay for colorectal cancer early detection. *World J. Gastrointest. Oncol.* 10, 15–22. doi: 10.4251/wjgo.v10.i1.15

Wang, Y. M., Trinh, M. P., Zheng, Y., Guo, K., Jimenez, L. A., and Zhong, W. (2019). Analysis of circulating non-coding RNAs in a non-invasive and cost-effective manner. *Trends Analyt. Chem.* 117, 242–262. doi: 10.1016/j.trac.2019.07.001

Ward, R., Meagher, A., Tomlinson, I., O'Connor, T., Norrie, M., Wu, R., et al. (2001). Microsatellite instability and the clinicopathological features of sporadic colorectal cancer. *Gut* 48, 821–829. doi: 10.1136/gut.48.6.821

Weisenberger, D. J., Siegmund, K. D., Campan, M., Young, J., Long, T. I., Faasse, M. A., et al. (2006). CpG island methylator phenotype underlies sporadic microsatellite instability and is tightly associated with BRAF mutation in colorectal cancer. *Nat. Genet.* 38, 787–793. doi: 10.1038/ng1834

Wendt, M. K., Johanesen, P. A., Kang-Decker, N., Binion, D. G., Shah, V., and Dwinell, M. B. (2006). Silencing of epithelial CXCL12 expression by DNA hypermethylation promotes colonic carcinoma metastasis. *Oncogene* 25, 4986–4997. doi: 10.1038/sj.onc.1209505

Wu, C. W., Cao, X., Berger, C. K., Foote, P. H., Mahoney, D. W., Simonson, J. A., et al. (2017). Novel approach to fecal occult blood testing by assay of erythrocyte-specific microRNA markers. *Dig. Dis. Sci.* 62, 1985–1994. doi: 10.1007/s10620-017-4627-6

Wu, C. W., Ng, S. S., Dong, Y. J., Ng, S. C., Leung, W. W., Lee, C. W., et al. (2012). Detection of miR-92a and miR-21 in stool samples as potential screening biomarkers for colorectal cancer and polyps. *Gut* 61, 739–745. doi: 10.1136/gut.2011.239236

Wu, X. D., Song, Y. C., Cao, P. L., Zhang, H., Guo, Q., Yan, R., et al. (2014). Detection of miR-34a and miR-34b/c in stool sample as potential screening biomarkers for noninvasive diagnosis of colorectal cancer. *Med. Oncol* 31, 894. doi: 10.1007/s12032-014-0894-7

Xiao, W., Zhao, H., Dong, W., Li, Q., Zhu, J., Li, G., et al. (2015). Quantitative detection of methylated NDRG4 gene as a candidate biomarker for diagnosis of colorectal cancer. *Oncol. Lett.* 9, 1383–1387. doi: 10.3892/ol.2014.2815

Xie, Y., Li, J., Li, P., Li, N., Zhang, Y., Binang, H., et al. (2020). RNA-seq profiling of serum exosomal circular RNAs reveals Circ-PNN as a potential biomarker for human colorectal cancer. *Front. Oncol.* 10:982. doi: 10.3389/fonc.2020.00982

Xie, Y. H., Chen, Y. X., and Fang, J. Y. (2020). Comprehensive review of targeted therapy for colorectal cancer. *Signal Transduct. Target Ther.* 5:22. doi: 10.1038/s41392-020-0116-z

Xing, X. B., Cai, W. B., Luo, L., Liu, L. S., Shi, H. J., and Chen, M. H. (2013). The prognostic value of p16 hypermethylation in cancer: a meta-analysis. *PLoS ONE* 8:e66587. doi: 10.1371/journal.pone.0066587

Xiong, B., Cheng, Y., Ma, L., and Zhang, C. (2013). MiR-21 regulates biological behavior through the PTEN/PI-3 K/Akt signaling pathway in human colorectal cancer cells. *Int. J. Oncol* 42, 219–228. doi: 10.3892/ijo.2012.1707

Xu, T., and Gao, H. (2020). Hydroxymethylation and tumors: can 5-hydroxymethylation be used as a marker for tumor diagnosis and treatment? *Hum. Genomics* 14:15. doi: 10.1186/s40246-020-00265-5

Xu, W., Zhou, G., Wang, H., Liu, Y., Chen, B., Chen, W., et al. (2020). Circulating lncRNA SNHG11 as a novel biomarker for early diagnosis and prognosis of colorectal cancer. *Int. J. Cancer* 146, 2901–2912. doi: 10.1002/ijc.32747

Yan, S., Han, B., Gao, S., Wang, X., Wang, Z., Wang, F., et al. (2017). Exosome-encapsulated microRNAs as circulating biomarkers for colorectal cancer. *Oncotarget* 8, 60149–60158. doi: 10.18632/oncotarget.18557

Yang, H., Salz, T., Zajac-Kaye, M., Liao, D., Huang, S., and Qiu, Y. (2014). Overexpression of histone deacetylases in cancer cells is controlled by interplay of transcription factors and epigenetic modulators. *FASEB J.* 28, 4265–4279. doi: 10.1096/fj.14-250654

Yang, H., Zhang, H., Yang, Y., Wang, X., Deng, T., Liu, R., et al. (2020). Hypoxia induced exosomal circRNA promotes metastasis of Colorectal Cancer via targeting GEF-H1/RhoA axis. *Theranostics* 10, 8211–8226. doi: 10.7150/thno.44419

Yang, N., Xu, B., Kong, P., Han, M., and Li, B. H. (2020). Hsa_circ_0002320: a novel clinical biomarker for colorectal cancer prognosis. *Medicine* 99:e21224. doi: 10.1097/MD.0000000000021224

Yang, X., Dai, W., Kwong, D. L., Szeto, C. Y., Wong, E. H., Ng, W. T., et al. (2015). Epigenetic markers for noninvasive early detection of nasopharyngeal carcinoma by methylation-sensitive high resolution melting. *Int. J. Cancer* 136, E127–135. doi: 10.1002/ijc.29192

Yau, T. O., Wu, C. W., Tang, C. M., Chen, Y., Fang, J., Dong, Y., et al. (2016). MicroRNA-20a in human faeces as a non-invasive biomarker for colorectal cancer. *Oncotarget* 7, 1559–1568. doi: 10.18632/oncotarget.6403

Ye, D. X., Wang, S. S., Huang, Y., and Chi, P. (2019). A 3-circular RNA signature as a noninvasive biomarker for diagnosis of colorectal cancer. *Cancer Cell Int.* 19:276. doi: 10.1186/s12935-019-0995-7

Young, G. P., Pedersen, S. K., Mansfield, S., Murray, D. H., Baker, R. T., Rabbitt, P., et al. (2016). A cross-sectional study comparing a blood test for methylated BCAT1 and IKZF1 tumor-derived DNA with CEA for detection of recurrent colorectal cancer. *Cancer Med.* 5, 2763–2772. doi: 10.1002/cam4.868

Yuan, Z., Baker, K., Redman, M. W., Wang, L., Adams, S. V., Yu, M., et al. (2017). Dynamic plasma microRNAs are biomarkers for prognosis and early detection of recurrence in colorectal cancer. *Br. J. Cancer* 117, 1202–1210. doi: 10.1038/bjc.2017.266

Zaharie, F., Muresan, M. S., Petrushev, B., Berce, C., Gafencu, G. A., Selicean, S., et al. (2015). Exosome-carried microRNA-375 inhibits cell progression and dissemination via Bcl-2 blocking in colon cancer. *J. Gastrointestin. Liver Dis.* 24, 435–443. doi: 10.15403/jgld.2014.1121.244.375

Zavridou, M., Mastoraki, S., Strati, A., Tzanikou, E., Chimonidou, M., and Lianidou, E. (2018). Evaluation of preanalytical conditions and implementation of quality control steps for reliable gene expression and DNA methylation analyses in liquid biopsies. *Clin. Chem.* 64, 1522–1533. doi: 10.1373/clinchem.2018.292318

Zeng, Z., Li, Y., Pan, Y., Lan, X., Song, F., Sun, J., et al. (2018). Cancer-derived exosomal miR-25-3p promotes pre-metastatic niche formation by inducing vascular permeability and angiogenesis. *Nat. Commun.* 9:5395. doi: 10.1038/s41467-018-07810-w

Zhang, H., Dong, P., Guo, S., Tao, C., Chen, W., Zhao, W., et al. (2020). Hypomethylation in HBV integration regions aids non-invasive surveillance to hepatocellular carcinoma by low-pass genome-wide bisulfite sequencing. *BMC Med.* 18:200. doi: 10.1186/s12916-020-01667-x

Zhang, H., Zhu, Y. Q., Wu, Y. Q., Zhang, P., and Qi, J. (2014). Detection of promoter hypermethylation of Wnt antagonist genes in fecal samples for diagnosis of early colorectal cancer. *World J. Gastroenterol.* 20, 6329–6335. doi: 10.3748/wjg.v20.i20.6329

Zhang, P., Wu, W., Chen, Q., and Chen, M. (2019). Non-coding RNAs and their integrated networks. *J. Integr. Bioinform.* 16:20190027. doi: 10.1515/jib-2019-0027

Zhang, W., Yang, S., Liu, Y., Wang, Y., Lin, T., Li, Y., et al. (2018). Hsa_circ_0007534 as a blood-based marker for the diagnosis of colorectal cancer and its prognostic value. *Int. J. Clin. Exp. Pathol.* 11, 1399–1406.

Zhang, Y., Dong, X., Bai, L., Shang, X., and Zeng, Y. (2020). MUC1-induced immunosuppression in colon cancer can be reversed by blocking the PD1/PDL1 signaling pathway. *Oncol. Lett.* 20:317. doi: 10.3892/ol.2020.12180

Zhao, G., Li, H., Yang, Z., Wang, Z., Xu, M., Xiong, S., et al. (2019). Multiplex methylated DNA testing in plasma with high sensitivity and specificity for colorectal cancer screening. *Cancer Med.* 8, 5619–5628. doi: 10.1002/cam4.2475

Zhao, G., Liu, X., Liu, Y., Li, H., Ma, Y., Li, S., et al. (2020a). Aberrant DNA methylation of SEPT9 and SDC2 in stool specimens as an integrated biomarker for colorectal cancer early detection. *Front. Genet.* 11:643. doi: 10.3389/fgene.2020.00643

Zhao, G., Ma, Y., Li, H., Li, S., Zhu, Y., Liu, X., et al. (2020b). A novel plasma based early colorectal cancer screening assay base on methylated SDC2 and SFRP2. *Clin. Chim. Acta* 503, 84–89. doi: 10.1016/j.cca.2020.01.010

Zhao, S. G., Chen, W. S., Li, H., Foye, A., Zhang, M., Sjostrom, M., et al. (2020). The DNA methylation landscape of advanced prostate cancer. *Nat. Genet.* 52, 778–789. doi: 10.1038/s41588-020-0648-8

Zhao, W., Song, M., Zhang, J., Kuerban, M., and Wang, H. (2015). Combined identification of long non-coding RNA CCAT1 and HOTAIR in serum as an effective screening for colorectal carcinoma. *Int. J. Clin. Exp. Pathol.* 8, 14131–14140.

Zhao, Y., Du, T., Du, L., Li, P., Li, J., Duan, W., et al. (2019). Long noncoding RNA LINC02418 regulates MELK expression by acting as a ceRNA and may serve as a diagnostic marker for colorectal cancer. *Cell Death Dis.* 10:568. doi: 10.1038/s41419-019-1804-x

Zou, H., Harrington, J. J., Klatt, K. K., and Ahlquist, D. A. (2006). A sensitive method to quantify human long DNA in stool: relevance to colorectal cancer screening. *Cancer Epidemiol. Biomarkers Prev.* 15, 1115–1119. doi: 10.1158/1055-9965.EPI-05-0992

Conflict of Interest: RL-L has received honoraria for participation in Advisory Boards from Roche, AstraZeneca, Merck, MSD, Bayer, BMS, Novartis, Janssen, Lilly, Pfizer and Leo; travel, accommodations and expenses from Pharmamar, Roche, BMS and Pierre Fabre; research funding from Roche and Merck; and is co-founder and shareholder in Nasasbiotech, S.L., Mtrap Inc.

The remaining authors declare that the research was conducted in the absence of any commercial or financial relationships that could be construed as a potential conflict of interest.

Copyright © 2021 Rodriguez-Casanova, Costa-Fraga, Bao-Caamano, López-López, Muinelo-Romay and Diaz-Lagares. This is an open-access article distributed under the terms of the Creative Commons Attribution License (CC BY). The use, distribution or reproduction in other forums is permitted, provided the original author(s) and the copyright owner(s) are credited and that the original publication in this journal is cited, in accordance with accepted academic practice. No use, distribution or reproduction is permitted which does not comply with these terms.

frontiers in Oncology

ORIGINAL RESEARCH
published: 19 March 2021
doi: 10.3389/fonc.2021.628094

MicroRNA-940 as a Potential Serum Biomarker for Prostate Cancer

Smrithi Rajendiran[1], *Sayantan Maji*[1], *Ahmed Haddad*[2], *Yair Lotan*[2], *Rajesh R. Nandy*[3], *Jamboor K. Vishwanatha*[1,4] *and Pankaj Chaudhary*[1,4]*

[1] Department of Microbiology, Immunology, and Genetics, University of North Texas Health Science Center, Fort Worth, TX, United States, [2] Department of Urology, University of Texas Southwestern Medical Center, Dallas, TX, United States, [3] School of Public Health, University of North Texas Health Science Center, Fort Worth, TX, United States, [4] Texas Center for Health Disparities, University of North Texas Health Science Center, Fort Worth, TX, United States

Prostate cancer is one of the leading causes of death despite an astoundingly high survival rate for localized tumors. Though prostate specific antigen (PSA) test, performed in conjunction with digital rectal examinations, is reasonably accurate, there are major caveats requiring a thorough assessment of risks and benefits prior to conducting the test. MicroRNAs, a class of small non-coding RNAs, are stable molecules that can be detected in circulation by non-invasive methods and have gained importance in cancer prognosis and diagnosis in the recent years. Here, we investigate circulating miR-940, a miRNA known to play a role in prostate cancer progression, in both cell culture supernatants as well as patient serum and urine samples to determine the utility of miR-940 as a new molecular marker for prostate cancer detection. We found that miR-940 was significantly higher in serum from cancer patients, specifically those with clinically significant tumors (GS $\geq$ 7). Analysis of receiver operating characteristic curve demonstrated that miR-940 in combination with PSA had a higher area under curve value (AUC: 0.818) than the miR-940 alone (AUC: 0.75) for the diagnosis of prostate cancer. This study provides promising results suggesting the use of miR-940 for prostate cancer diagnosis.

Keywords: prostate cancer, miR-940, serum, circulating miRNA, PSA

OPEN ACCESS

Edited by:
George Calin,
University of Texas MD Anderson Cancer Center, United States

Reviewed by:
Boye Schnack Nielsen,
Bioneer, Denmark
Catalin Marian,
Victor Babes University of Medicine and Pharmacy, Romania
Lorenzo Sempere,
Michigan State University, United States

***Correspondence:**
Pankaj Chaudhary
pankaj.chaudhary@unthsc.edu

Specialty section:
This article was submitted to Molecular and Cellular Oncology, a section of the journal Frontiers in Oncology

Received: *11 November 2020*
Accepted: *23 February 2021*
Published: *19 March 2021*

Citation:
Rajendiran S, Maji S, Haddad A, Lotan Y, Nandy RR, Vishwanatha JK and Chaudhary P (2021) MicroRNA-940 as a Potential Serum Biomarker for Prostate Cancer. Front. Oncol. 11:628094. doi: 10.3389/fonc.2021.628094

INTRODUCTION

Prostate cancer is one of the leading causes of cancer related death among men in the US despite the advances in biomarkers (1). About 20% of all estimated new cases and 10% of estimated deaths in men are expected to be due to prostate cancer (2). Though many prostate cancers are slow growing, some forms are very aggressive and metastatic, resulting in death. Depending on the racial background and family history, some men are advised to undergo digital rectal exam (DRE) and serum total prostate specific antigen (PSA) screening at as early as 40 years of age. Some people inherently have high levels of PSA as a result of enlarged prostate, resulting in extensive evaluation with repeat biopsies. Most patients with abnormal PSA have insignificant prostate cancer, thus PSA screening has the potential for over-diagnosis and unnecessary treatments (3). Additionally, a report by U.S. Preventive Services Task Force recommended against PSA-based screening unless men express a preference for screening after being informed of and understanding the benefits and risks (4–6). Though prostate cancer antigen 3

(PCA3) urine test is under consideration as a better prognostic marker, there is insufficient evidence of extensive improvements in sensitivity and specificity compared to PSA (7, 8). Additionally, though the test marginally improves the diagnostic accuracy of prostate cancer, it does not predict short-term or long-term outcomes or the need for biopsies (7, 9–11). Further, the PCA3 test does not necessarily help distinguish aggressive from indolent disease (12, 13). Thus, there is a need for a more reliable and cost-effective tool for prostate cancer screening.

MicroRNAs (miRNAs) are a class of small non-coding RNA that regulate gene expression post-transcriptionally (14, 15). Various studies report miRNAs to be highly deregulated in prostate cancer (14, 16, 17). Additionally, miRNAs are highly stable in the serum, providing potential for using these circulating molecules as molecular diagnostic markers of cancer (17–21). The miRNA signatures are also helpful in determination of the primary site in tumors of unknown origin (22–24). Use of the miRNAs as blood-based markers has tremendous potential when used in combination with the existing PSA screening techniques for the status of the disease—cancer or not (25–27), and course of treatment (28–31).

We have identified miR-940, expressed on chromosome 16 in humans, as a novel miRNA that impedes prostate cancer progression in an *in vitro* system by regulating MIEN1 (32). Various other groups have shown dysregulation of miR-940 in other cancers. In hepatocellular carcinoma, glioma, non-small cell lung carcinoma, pancreatic ductal adenocarcinoma, triple negative breast cancer, and ovarian cancer, miR-940 inhibits cancer progression (33–39); while the opposite effects are observed in endometrial and cervical cancers (40–42).

Here, we aim to determine if circulating miR-940 could be used for early detection of prostate cancer and to distinguish between the clinically significant (GS $\geq$ 7) and insignificant (GS = 6) tumors, leading to improved management. Analysis of miR-940 in the prostate cancer and immortalized normal cell culture supernatants and serum samples from normal donors and cancer patients provides promise for considering miR-940 as a potential biomarker for prostate cancer. MiR-940 distinguishes between clinically insignificant and significant tumors, but owing to the small sample cohorts in the various groups, the statistical significance we observed is not appreciably better than the existing test (PSA) characteristics (43). Interestingly, we were also able to detect miR-940 in the urine of patients with cancer of GS $\geq$ 6; but this was at much lower levels than in the serum and was not different between clinically insignificant and clinically significant tumor samples suggesting a higher probability of success in prostate cancer diagnosis when using serum for miR-940 detection.

MATERIALS AND METHODS

Cell Lines and Cell Culture

Human prostate carcinoma cells DU-145 (ATCC HTB-81) was maintained in RPMI 1640 media with 10% fetal bovine serum (Life Technologies). Immortalized non-tumorigenic prostate epithelial cell line PWR-1E (ATCC CRL-11611) was maintained in Keratinocyte-SFM (Life Technologies) supplemented with bovine pituitary extract (25 μg/ml) and recombinant epidermal growth factor (0.15 ng/ml). Cells were cultured at 37°C with 5% CO_2.

Exosome Isolation From Cell Culture Supernatant

Exosomes from cell culture supernatant were isolated as described previously (44). Briefly, the cells were grown in serum free medium for at least 24 h. The conditioned medium was transferred to conical tubes and centrifuged at 300 × g for 10 min at 4°C to pellet the cells. Next, the supernatant was transferred to ultracentrifuge tubes and centrifuged at 16,500 × g for 20 min at 4°C to further remove cells and cell debris. The supernatant was passed through a 0.2 μm filter to remove particles larger than 200 nm. Next, the filtered supernatant was transferred to new ultracentrifuge tubes and centrifuged at 120,000 × g for 70 min at 4°C to pellet the exosomes. The supernatant was discarded and resuspended in TRIzol and processed for RNA isolation.

Serum and Urine Sample Collection From Normal and Prostate Cancer Patients

Serum samples ($n = 32$) from prostate cancer patients who had not undergone any treatment at the time of sample collection were obtained by Dr. Yair Lotan between 2001 and 2010 and scored based on pathology scoring criteria at the time of collection. Of this pool, the pathological Gleason Score was $\geq$ 7 in 25 patients and Gleason Score 6 in 7 patients. Normal serum samples ($n = 25$) was collected by the University of North Texas Health Science Center, Fort Worth, TX, through a collaboration with Dallas Methodist Hospital at Dallas, TX, during prostate cancer education and screening program from healthy males, who at the time of sample collection had no obvious indication of prostate cancer. The collection process was the standard blood draw procedure, performed by a well-trained phlebotomist at the respective sites. The urine samples were collected from patients at the time of their biopsy by Dr. Yair Lotan in 2015. Subjects were consented to the study and no personal health information was revealed. In short, for serum collection, venous blood was collected from each patient and centrifuged. Similarly, for urine miRNA, urine was collected and centrifuged. The supernatants (serum and urine) were recovered, aliquoted and stored at −80°C until further use. The study protocol was approved by the Institutional Review Boards of the University of North Texas Health Science Center, Fort Worth, TX (IRB # 2007-110, and 2013-016) and the University of Texas Southwestern Medical Center, Dallas, TX (IRB # STU 032011-187).

RNA Isolation and qPCR

Total RNA was isolated from the exosomes collected using TRIzol (Life Technologies) according to the standard protocol. Total RNA from the serum was isolated using the miRVANA PARIS kit (Life Technologies), according to the instructions provided by manufacturer. Equal amount of quantified RNA was used for the first step of cDNA synthesis using NCode

VILO miRNA cDNA Synthesis Kit (Life Technologies). For the expression of the miRNA, first the miRNA specific forward primers (mature and precursor) and normalization control specific forward primers were designed as described by Kramer 2011 (45) using Primer 3 (46) software and synthesized by Integrated DNA Technologies (Coralville, IA). The specificity of both mature and precursor primers were further confirmed by NCBI BLAST software (47). Next, using EXPRESS SYBR GreenER miRNA qRT-PCR Kits (Life Technologies), the qPCR for the miRNA and controls were carried out, according to the protocol provided by manufacturer on a Mastercycler ep gradient S realplex^2 thermal cycler (Eppendorf). Normalization of samples was carried out with respect to RNU6-2 expression. The average of the ΔCt values of all the normal samples was used to obtain the ΔΔCt values for each individual sample (normal and cancer). This ΔΔCt was then used to determine the fold change (the normalized expression values). For urine analysis, equal amounts of urine samples (625 μL per sample) was used to isolate the total RNA using miRVANA PARIS Kit, according to the manufacturer's protocol. In brief, we measured and transferred the aqueous phase, post-phenol-chloroform centrifugation, into two tubes, equally. Then, one of the tubes was precipitated with 1.25 volumes of room temperature 100% ethanol to extract total RNA from the sample and the other tube with 0.33 volume of room temperature 100% ethanol to extract enriched small RNAs. The qPCR analysis was performed as described above. ΔCt values for qPCR were obtained as Ct of miR-940 in enriched fraction—Ct of miR-940 in total RNA fraction and then compared to the averages obtained from the clinically insignificant (GS = 6) samples.

Statistical Analyses

Column graphs were generated as mean ± standard error of means (SEM) where applicable. The Scatter plots were generated as mean ± SEM. and *p*-value was calculated according to unpaired *t*-test with or without Welch's correction according to the distribution using GraphPad Prism 8 (GraphPad Software, CA). Receiver operating characteristic (ROC) curve and area under the curve (AUC) value were generated based on the sensitivity and the specificity of the different data points by the GraphPad Prism 8. Sensitivity and the specificity values for the ROC curves with individual predictors (PSA or miR-940) are calculated empirically. However, for combined predictors (PSA and miR-940), sensitivity and the specificity values cannot be obtained empirically. Instead, these values were calculated by fitting a logistic regression model with PSA and miR-940 as predictors. Spearman correlation coefficient between PSA and miR-940 was also calculated in GraphPad Prism.

RESULTS

Prostate Cancer Cells Secrete More miR-940 Than Normal Cells

We have previously demonstrated the role of miR-940 in prostate cancer progression *via* the regulation of MIEN1 (32). Here, we hypothesized that miR-940 is a secretory miRNA that could be used as a non-invasive molecular marker for a positive diagnosis of prostate cancer. To test this, we evaluated the expression of miR-940 in the exosomes derived from the serum/supplement free cell culture supernatants of PWR-1E and DU-145 cells by qPCR. Higher levels of both the precursor (Pre-miR-940) and mature (miR-940) miRNA were detected in the exosomes derived from the DU-145 cancer cells compared to the PWR-1E immortalized normal cells (**Figure 1A**). This was in stark contrast to the lower expression of miR-940 in DU-145 cell lysate compared to PWR-1E cell lysate as reported in our previous study (32). Since, the expression of miRNAs detected in both cell lines were isolated from the serum/supplement free cell culture supernatants, the observed differences are biologically relevant and not an artifact arising from intrinsic differences in the growth media for the two cell lines. Next, we quantified the proportion of miR-940 released in the exosomes to their levels within the cells for both the cell types. The ratio indicated that a higher proportion of miR-940 was secreted into the supernatant from DU-145 cells (Pre-miR-940: ∼40-fold more; miR-940: ∼3-fold more) than from PWR-1E (**Figure 1B**). This inverse expression pattern of miR-940 within and outside the cells suggested that miR-940 could be secreted out of the cells during cancer progression, in order to prevent the function of miR-940 mediated suppression of cancer, similar to what has been reported in ovarian cancer (48).

Circulating miR-940 Is High in Serum Samples of Prostate Cancer Patients

The expression of miR-940 was next assessed in a cohort of serum samples obtained from healthy or cancer patients with varying PSA levels: 0.01–15.10 ng/mL in normal samples and 2.00–38.67 ng/mL in cancer serum. As shown in **Figure 2A**, the mean concentration of serum PSA levels in normal controls was 4.64 ± 0.86 ng/mL ($n = 25$), whereas that in prostate cancer patients was 12.95 ± 1.84 ng/mL ($n = 32$, p-value = 0.0002). Similarly, the levels of miR-940 were significantly higher in serum from cancer ($n = 32$, 2.07 ± 0.18 fold, p-value = 0.0008) patients compared to the normal ($n = 25$, 1.24 ± 0.14 fold) serum (**Figure 2B**). The area under the curve (AUC) for a receiver operating characteristic (ROC) curve determining the sensitivity and specificity of the test with miR-940 in serum as the disease indicator, is 0.75 [**Figure 2C**; 95% confidence interval (CI) = 0.622 to 0.877, p-value = 0.0013] and for PSA is 0.79 (95% CI = 0.670–0.909, p-value = 0.0002). The combination of the conventional prostate cancer serum biomarker of PSA and miR-940 generated an increased diagnostic AUC value of 0.818 (95% CI = 0.710–0.925), which is better than the PSA or miR-940 AUC alone. We have also compared model fits using logistic regression (PSA only vs. PSA + miR-940 as predictors). Under the null hypothesis of no improvement by adding miR-940 as a predictor, the p-value is 0.03, indicating statistical significance. Additionally, Spearman correlation coefficient between miR-940 fold-change and PSA is 0.3914 (0.1379–0.5967) with a significance of 0.0026, indicating that the use of miR-940 along with PSA is likely to improve the diagnostic accuracy of prostate cancer detection.

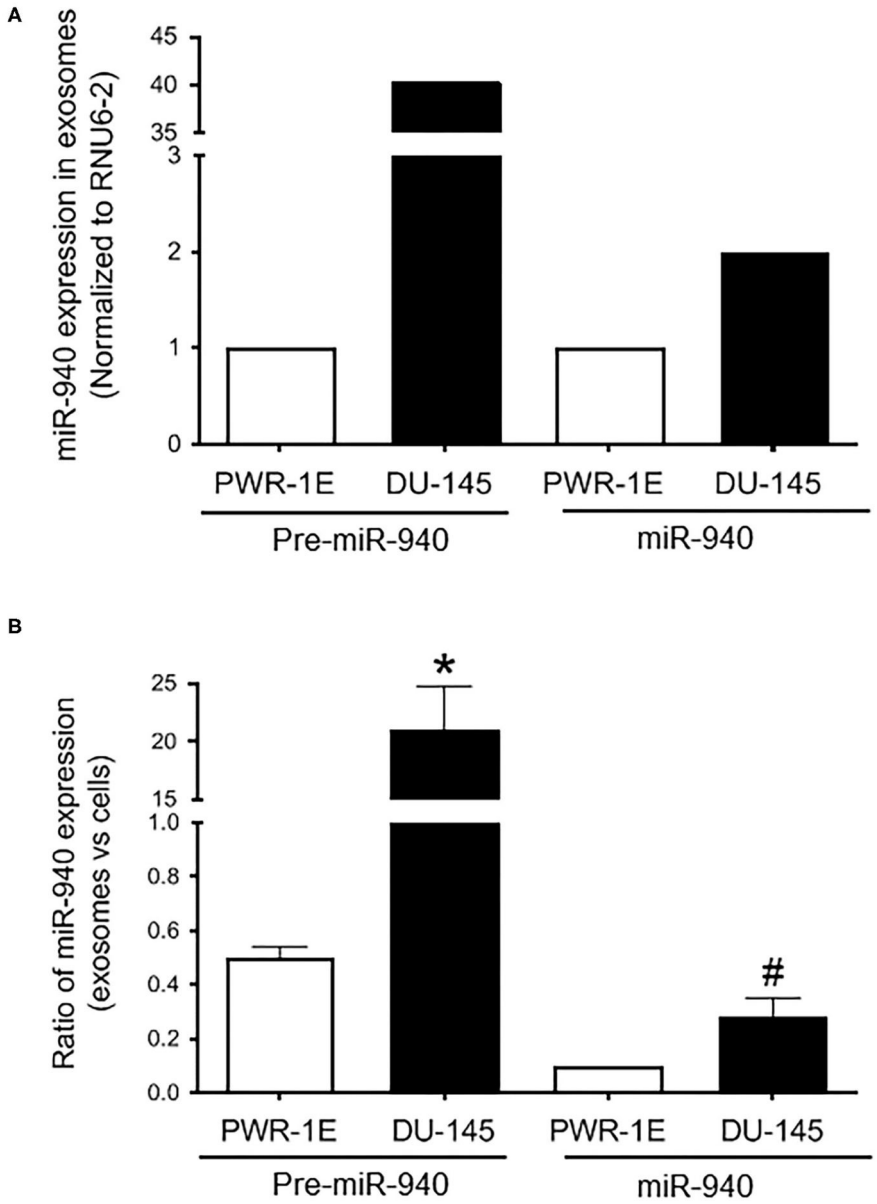

FIGURE 1 | Expression of miR-940 in cell culture supernatant. **(A)** Higher levels of both precursor (Pre-miR-940) and mature (miR-940) miRNA are detected in the exosomes derived from the cell culture supernatant of the DU-145 cancer cells compared to the normal PWR-1E cells as measured by qPCR (normalized to RNU6-2). **(B)** Ratio of miR-940 from the secreted exosomes to miR-940 within the cells, as determined by qPCR, is plotted as a fold change in the normal and cancer cells. The experiment was repeated two independent times. $^{\#}p$-value ≤ 0.1; $^{*}p$-value ≤ 0.05.

Serum miR-940 Can Potentially Distinguish Well-Differentiated From Poorly Differentiated Tumors

We classified the tumor serum further into moderately-poorly differentiated clinically significant (GS $\geq$ 7; PSA 2.0–38.67 ng/mL) and well-differentiated clinically insignificant (GS = 6; PSA 4.1–18.0 ng/mL) tumors, based on the pathological Gleason scoring rendered to the tumors during biopsy. There was an overall significant increase in miR-940 in moderately and poorly differentiated ($n = 25$, 2.24 $\pm$ 0.22 fold, p-value = 0.0148) tumor serum samples compared to clinically insignificant (n = 7, 1.49 $\pm$ 0.17-fold) tumors (**Figure 3A**). Similarly, the mean concentration of serum PSA levels in clinically insignificant tumors was 6.91 $\pm$ 1.86 ng/mL ($n = 7$), whereas that in clinically significant tumors was 14.65 $\pm$ 2.19 ng/mL ($n = 25$, p-value = 0.0134; **Figure 3B**). The degree of prediction using miR-940, in these well-differentiated and poorly differentiated samples, was however not better than the prediction based on PSA

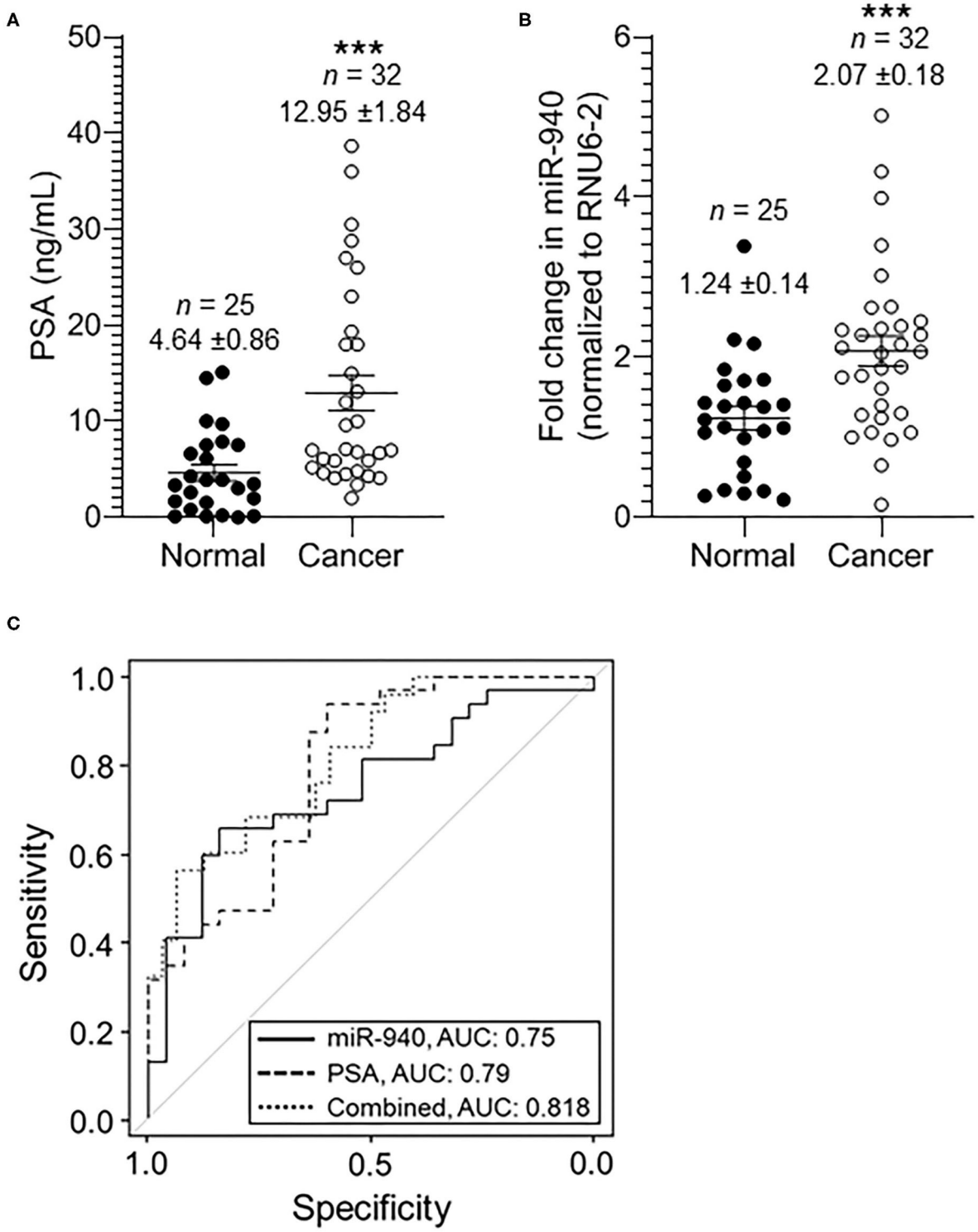

FIGURE 2 | The expression of miR-940 and PSA in serum samples of prostate cancer patients and normal healthy males. **(A)** Scatter plot analysis of PSA expression in serum samples of normal healthy ($n = 25$) controls and prostate cancer ($n = 32$) patients. The data are expressed as the mean ± SEM (***p-value = 0.0005; two-tailed Student's t-test). **(B)** Scatter plot analysis of miR-940-fold expression in serum samples of healthy normal controls ($n = 25$) and prostate cancer patients ($n = 32$). The data are expressed as the mean ± SEM (***p-value = 0.0013; two-tailed Student's t-test). **(C)** ROC curve for **(B)** depicts the sensitivity (true positive: cancer in reality and according to test variable; i.e., fold change in miR-940) and specificity (100%—false positive: 100%—normal in reality with fold change in miR-940 predicting cancer) for the use of secreted miR-940 as an independent variable to determine cancer vs. normal states. The AUC values are shown on the graph.

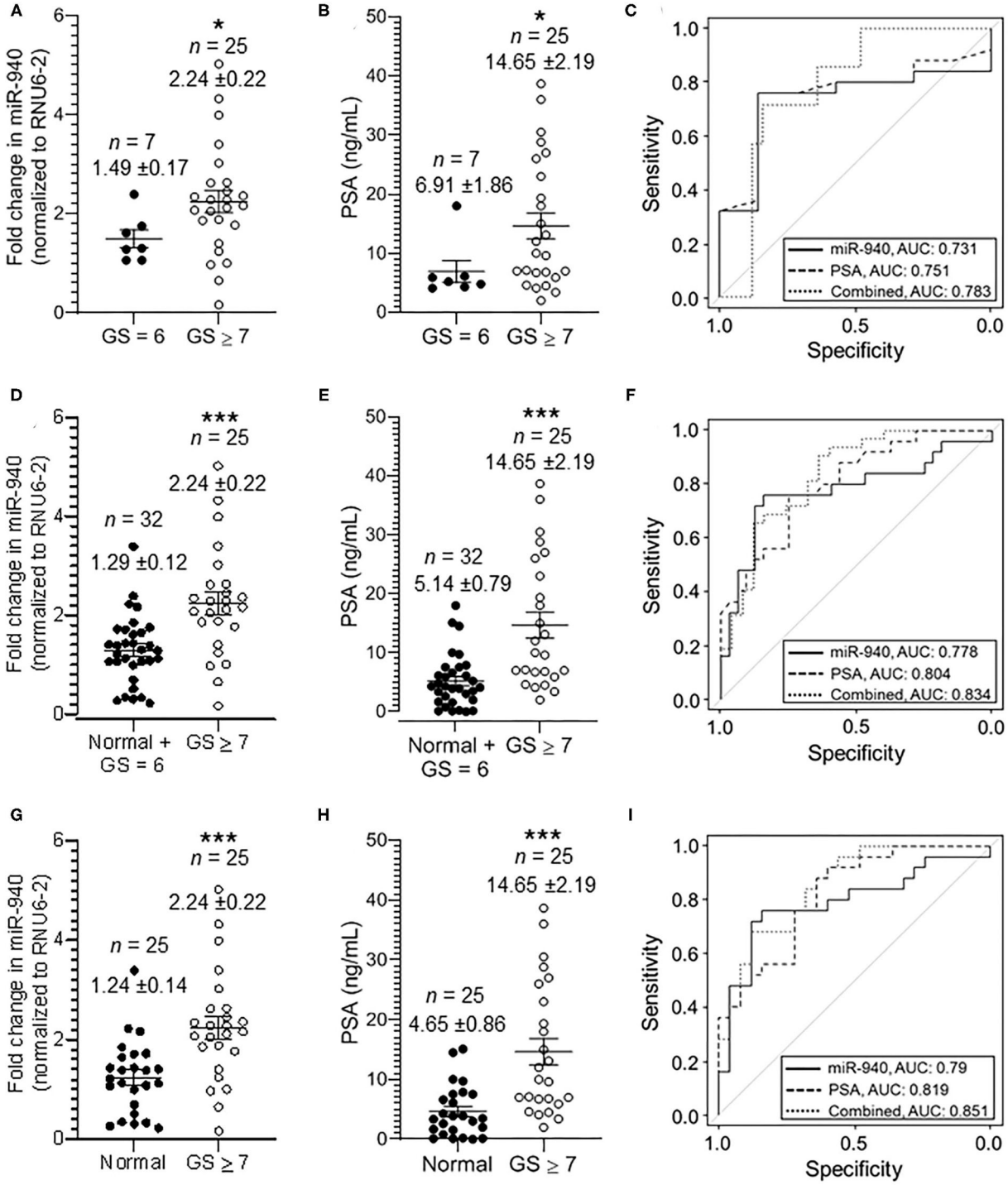

FIGURE 3 | Secreted miR-940 and PSA from serum is significantly higher in patients with clinically significant tumors. **(A)** Serum from patients who had GS 7 and above in their biopsy were grouped together as clinically significant tumor serum (GS ≥ 7, $n = 25$) and the ones with biopsy GS 6 as clinically insignificant tumor serum (GS = 6, $n = 7$). The fold change in the miR-940 was quantified using qPCR. The data are expressed as the mean ± SEM (*p-value = 0.0148; two-tailed Student's t-test). **(B)** Scatter plot analysis of PSA expression in serum samples of clinically insignificant ($n = 25$) and clinically significant ($n = 32$) prostate cancer patients. The data are expressed as the mean ± SEM (*p-value = 0.0134; two-tailed Student's t-test). **(C)** ROC curve for both miR-940, PSA, and combined (miR-940 and PSA) comparing clinically insignificant to clinically significant tumors. **(D)** Scatter plot analysis of miR-940 expression in serum samples of combined normal and clinically insignificant (Normal + GS 6, $n = 32$) tumors and clinically significant tumors (GS ≥ 7, $n = 25$) patients. The data are expressed as the mean ± SEM (***p-value = 0.0006; two-tailed Student's t-test). **(E)** PSA expression in serum samples of combined normal and clinically insignificant (Normal + GS 6, $n = 32$) tumors and clinically significant (GS ≥ 7, $n = 25$) tumors patients. (***p-value = 0.0003; two-tailed Student's t-test) **(F)** ROC curve for fold change in miR-940 to determine clinically significant cancers (GS ≥ 7) vs. normal and clinically insignificant cancers (healthy controls + GS = 6). **(G)** Scatter plot analysis of miR-940

(Continued)

FIGURE 3 | expression in serum samples of normal ($n = 25$) healthy controls and clinically significant tumors (GS $\geq$ 7, $n = 25$) patients. The data are expressed as the mean ± SEM (***p-value = 0.0005; two-tailed Student's t-test). **(H)** PSA expression in serum samples of normal ($n = 25$) controls and clinically significant tumors (GS $\geq$ 7, $n = 25$) patients. (***p-value = 0.0002; two-tailed Student's t-test) **(I)** ROC curve for fold change in miR-940 to determine clinically significant cancers (GS $\geq$ 7) vs. normal (healthy controls).

(**Figure 3C**). AUC for miR-940 ROC curve is 0.731 (95% CI = 0.541–0.921, p-value = 0.0649), while AUC for PSA ROC curve is 0.751 (95% CI = 0.566–0.936, p-value = 0.0449) and the combined (miR-940 + PSA) AUC is 0.783 (95% CI = 0.610–0.956). In this case, the improvement in model fit for logistic regression is not statistically significant (p-value = 0.18). The AUC for the ROC curve, however, increased to 0.778 (95% CI = 0.645–0.909, p-value = 0.0004) from the previously observed 0.75 (**Figure 2C**), when we combined the normal and clinically insignificant tumors (Normal + GS 6, $n = 32$, 1.29 ± 0.12-fold) into one category and compared them to clinically significant tumors (GS $\geq$ 7, $n = 25$, 2.24 ± 0.22-fold, p-value = 0.0006) for miR-940 (**Figures 3D**,**F**). In addition, AUC for PSA ROC curve was found to be 0.804 (95% CI = 0.693–0.916; p-value = 0.0001), when we combined the normal and clinically insignificant tumors (Normal + GS 6, $n = 32$, 5.14 ± 0.79 ng/mL) and compared them to clinically significant tumors (GS $\geq$ 7, $n = 25$, 14.65 ± 2.19 ng/mL, p-value = 0.0003) for PSA alone (**Figure 3E**), and similarly increased to 0.834 (95% CI = 0.726–0.942) for the combined (miR-940 + PSA) ROC curve (**Figures 3E**,**F**). In this case, the improvement in model fit for logistic regression is found to be statistically significant (p-value = 0.01). Comparing the normal miR-940 expression levels ($n = 25$, 1.24 ± 0.14-fold) to well-differentiated tumor serum (GS = 6, $n = 7$, 1.49 ± 0.17-fold) samples did not yield any significant difference (p-value = 0.2931). So, we next excluded the clinically insignificant tumor samples from the analysis to test the diagnostic accuracy of miR-940 levels between normal and clinically significant tumors. We observed that the miR-940 levels in serum from moderately-poorly differentiated tumors were significantly elevated (GS $\geq$ 7, $n = 25$, 2.24 ± 0.22 fold, p-value = 0.0005) compared to their levels in normal serum ($n = 25$, 1.24 ± 0.14-fold, **Figure 3G**), leading to a further improved AUC of 0.79 (**Figure 3I**; 95% CI = 0.658–0.922, p-value = 0.0004) for miR-940. Similarly, PSA levels were also significantly elevated in serum samples of clinically significant tumors (GS $\geq$ 7, $n = 25$, 14.65 ± 2.19 ng/mL, p-value = 0.0001) compared to normal sera ($n = 25$, 4.65 ± 0.86 ng/mL; **Figure 3H**). The AUC value was increased to 0.819 (95% CI = 0.705–0.933, p-value = 0.0001) for PSA, while improving the combined miR-940 and PSA value to 0.851 (95% CI = 0.748–0.955, p-value = 0.02; **Figure 3I**). With the use of a logistic regression model, we found that the combination of miR-940 along with PSA are able to reliably discriminate the clinically significant samples and healthy control samples, and are slightly better than PSA alone.

Circulating miR-940 Is Detected in Urine Samples of Prostate Cancer Patients

In this pilot study, we also quantified both precursor and mature miR-940 in the urine sample of prostate cancer patients. Although there were significantly lower amounts of RNA detected in the urine compared to the blood in general, we were still able to detect traces of miR-940, but this was not significantly different between clinically insignificant and clinically significant tumors (**Figure 4**; Pre-miR-940: 1.15 ± 0.45-fold and 3.11 ± 2.13-fold; miR-940: 1.04 ± 0.21-fold and 1.12 ± 0.42-fold from clinically insignificant and significant tumors, respectively).

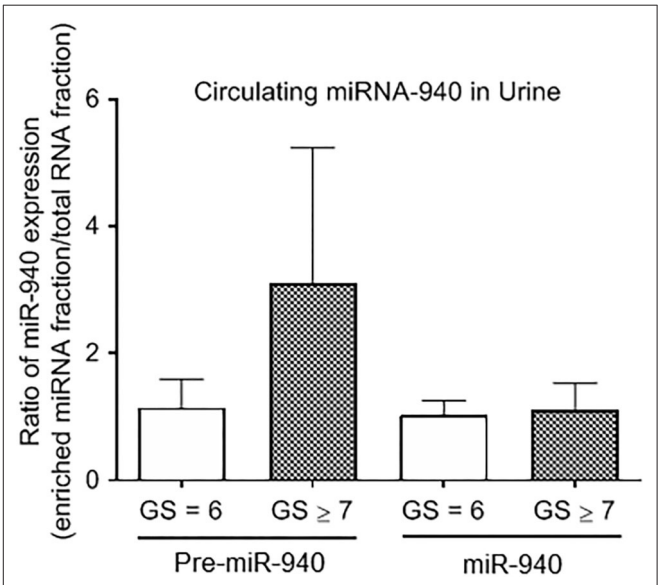

FIGURE 4 | The expression of miR-940 in urine of prostate cancer patients. Relative expression of Pre-miR-940 and miR-940 in the urine from clinically insignificant (GS $\geq$ 7) prostate cancer patients relative to clinically insignificant (GS = 6) patients ($n = 3$ and 5 respectively).

DISCUSSION

The current standard for prostate cancer detection includes DRE with PSA, followed by biopsies, for confirmation of the clinical diagnosis (4–6). With the relatively low diagnostic accuracy of PSA, and secondary infections associated with biopsy, there has been a clinical deadlock in prostate cancer diagnosis. To overcome this predicament, extensive research is underway to find reliable non-invasive markers which will not only increase the precision of diagnosis but also reduce patient discomfort. This study presents the possible use of circulating miR-940 as a secondary diagnostic biomarker for prostate cancer (in addition to the PSA). In this pilot study we have shown that miR-940 levels are high in serum from cancer patients compared to healthy controls. Although, we have primarily used equal amount of total RNA from different serum samples to detect miR-940 levels, we have also normalized to RNU6-2 (49, 50). Given that RNU6-2 is not a miRNA itself and could be released and expressed at different levels between normal and cancer patients, based on the results, we could also speculate that the

miR-940/RNU6-2 combination in cancer serum is higher than in normal serum. We acknowledge that our study also has some limitations including the relatively small sample sizes and the lack of follow up information of the patients. Also, although some of our healthy controls had high PSA with no history of prostate cancer diagnosis, they did not have a biopsy. Hence, further studies with patients who demonstrate elevated PSA but a negative biopsy and/or more samples with normal PSA as the healthy control group are needed to obtain a better diagnostic value for miR-940 by itself. Despite these drawbacks, the strong correlation of PSA to circulating miR-940 in the serum still suggests potential improvement in diagnostic accuracy for prostate cancer.

Our previous study has shown miR-940 to be highly expressed in normal cells and tissues compared to cancer counterparts (32). The expression of miR-940 in the serum is contradictory to this intracellular pattern as observed in a study conducted in breast cancer where 28 miRNAs were opposing in terms of their expression patterns between the tissue and the serum (51). This may be attributed to the many ways miRNAs are trafficked between cells or exported out of the cells, if their intracellular targets are oncogenes or tumor suppressors or to facilitate cell-cell communication (52–54). There are contradicting evidences for the presence of miR-940 in the serum: while some did not observe detectable levels of miR-940 (25), other detected miR-940 in circulation (55–57). Although we assume that the miR-940 detected in the serum is primarily from the prostate cells, we cannot with absolute certainty exclude the miRNA secretion from other cells. However, since the primary difference between the cohorts of healthy or prostate cancer patient samples is the prostate cancer disease status, we assume that at least a larger part of the secreted miRNA could be associated with the cancer cells.

Here, we speculate a bimodal role for miR-940 that could explain its increase in serum from cancer patients: (1) miR-940 is exported out of the cancer cells to prevent the down regulation of MIEN1, and other proteins predicted as targets inside the cell that aid in cancer progression (32–34, 36, 58) and (2) the secreted miR-940 facilitates the microenvironment remodeling to allow cancer progression (40, 59).

In the recent years, a few studies have identified the contradictory roles of circulating miR-940 in various cancers, either its increase or decrease is associated with cancer diagnosis (25, 33, 40, 55–57, 59, 60). Since the origin of the circulating miRNAs in serum cannot be identified, the use of just miR-940 in the serum has to be made with utmost caution and supported by other tests in order to maximize its use as a diagnostic biomarker. Here, even though we show that the miR-940 levels by themselves can distinguish cancer from normal, we still use PSA as a supportive diagnostic variable and suggest that the use of miR-940 with PSA will be more powerful than using PSA alone for the diagnosis of prostate cancer. Considering that this study strongly alludes to miR-940 being a biomarker for prostate cancer, larger scale validations are warranted.

DATA AVAILABILITY STATEMENT

The raw data supporting the conclusions of this article will be made available by the authors, without undue reservation.

ETHICS STATEMENT

The studies involving human participants were reviewed and approved by Institutional Review Boards of the University of North Texas Health Science Center, Fort Worth, TX (IRB # 2007-110, and 2013-016) and the University of Texas Southwestern Medical Center, Dallas, TX (IRB # STU 032011-187). The patients/participants provided their written informed consent to participate in this study.

AUTHOR CONTRIBUTIONS

SR, JV, and PC conceived, designed the study, and wrote the paper. SR performed all the experiments, except for exosome isolation, and analyzed the data. SM performed exosome isolations from cell culture supernatant. YL, JV, and PC collected most of the serum and urine samples. SR, AH, YL, RN, JV, and PC interpreted the results. All authors contributed to the article and approved the submitted version.

FUNDING

Research reported in this publication was supported by the National Institutes of Health Award Number CA220273, CA233355, MD012472, and MD006882.

REFERENCES

1. Duffy MJ. Biomarkers for prostate cancer: prostate-specific antigen and beyond. *Clin Chem Lab Med*. (2020) 58:326–39. doi: 10.1515/cclm-2019-0693
2. Siegel RL, Miller KD, Jemal A. Cancer statistics, 2020. *CA Cancer J Clin*. (2020) 70:7–30. doi: 10.3322/caac.21590
3. Bhavsar T, McCue P, Birbe R. Molecular diagnosis of prostate cancer: are we up to age? *Semin Oncol*. (2013) 40:259–75. doi: 10.1053/j.seminoncol.2013.04.002
4. Moyer VA, U.S. Preventive Services Task Force. Screening for prostate cancer: U.S. preventive services task force recommendation statement. *Ann Intern Med*. (2012) 157:120–34. doi: 10.7326/0003-4819-157-2-201207170-00459
5. US Preventive Services Task Force, Grossman DC, Curry SJ, Owens DK, Bibbins-Domingo K, Caughey AB, et al. Screening for Prostate cancer: US preventive services task force recommendation statement. *JAMA*. (2018) 319:1901–13. doi: 10.1001/jama.2018.3710
6. Jemal A, Fedewa SA, Ma J, Siegel R, Lin CC, Brawley O, et al. Prostate cancer incidence and PSA testing patterns in relation to USPSTF screening recommendations. *JAMA*. (2015) 314:2054–61. doi: 10.1001/jama.2015.14905
7. Ferro M, Bruzzese D, Perdona S, Marino A, Mazzarella C, Perruolo G, et al. Prostate health index (Phi) and prostate cancer antigen 3 (PCA3) significantly improve prostate cancer detection at initial biopsy in a total PSA range of 2-10 ng/ml. *PLoS ONE*. (2013) 8:e67687. doi: 10.1371/journal.pone.0067687
8. Fujita K, Nonomura N. Urinary biomarkers of prostate cancer. *Int J Urol*. (2018) 25:770–9. doi: 10.1111/iju.13734
9. Bradley LA, Palomaki GE, Gutman S, Samson D, Aronson N. Comparative effectiveness review: prostate cancer antigen 3 testing for the diagnosis

and management of prostate cancer. *J Urol*. (2013) 190:389–98. doi: 10.1016/j.juro.2013.02.005
10. Rodon N, Trias I, Verdu M, Roman R, Dominguez A, Calvo M, et al. Diagnostic and predictive value of urine PCA3 gene expression for the clinical management of patients with altered prostatic specific antigen. *Actas Urol Esp*. (2014) 38:150–5. doi: 10.1016/j.acuroe.2013.11.012
11. Rubio-Briones J, Casanova J, Dumont R, Rubio L, Fernandez-Serra A, Casanova-Salas I, et al. Optimizing prostate cancer screening; prospective randomized controlled study of the role of PSA and PCA3 testing in a sequential manner in an opportunistic screening program. *Actas Urol Esp*. (2014) 38:217–23. doi: 10.1016/j.acuroe.2014.02.005
12. Becerra MF, Bhat A, Mouzannar A, Atluri VS, Punnen S. Serum and urinary biomarkers for detection and active surveillance of prostate cancer. *Curr Opin Urol*. (2019) 29:593–7. doi: 10.1097/MOU.0000000000000670
13. Ruffion A, Devonec M, Champetier D, Decaussin-Petrucci M, Rodriguez-Lafrasse C, Paparel P, et al. PCA3 and PCA3-based nomograms improve diagnostic accuracy in patients undergoing first prostate biopsy. *Int J Mol Sci*. (2013) 14:17767–80. doi: 10.3390/ijms140917767
14. Di Leva G, Garofalo M, Croce CM. MicroRNAs in cancer. *Annu Rev Pathol*. (2014) 9:287–314. doi: 10.1146/annurev-pathol-012513-104715
15. Rupaimoole R, Calin GA, Lopez-Berestein G, Sood AK. miRNA deregulation in cancer cells and the tumor microenvironment. *Cancer Discov*. (2016) 6:235–46. doi: 10.1158/2159-8290.CD-15-0893
16. Ayub SG, Kaul D, Ayub T. Microdissecting the role of microRNAs in the pathogenesis of prostate cancer. *Cancer Genet*. (2015) 208:289–302. doi: 10.1016/j.cancergen.2015.02.010
17. Ceder Y. Non-coding RNAs in prostate cancer: from discovery to clinical applications. *Adv Exp Med Biol*. (2016) 886:155–70. doi: 10.1007/978-94-017-7417-8_8
18. Armand-Labit V, Pradines A. Circulating cell-free microRNAs as clinical cancer biomarkers. *Biomol Concepts*. (2017) 8:61–81. doi: 10.1515/bmc-2017-0002
19. Fabris L, Ceder Y, Chinnaiyan AM, Jenster GW, Sorensen KD, Tomlins S, et al. The potential of MicroRNAs as prostate cancer biomarkers. *Eur Urol*. (2016) 70:312–22. doi: 10.1016/j.eururo.2015.12.054
20. Kanwal R, Plaga AR, Liu X, Shukla GC, Gupta S. MicroRNAs in prostate cancer: functional role as biomarkers. *Cancer Lett*. (2017) 407:9–20. doi: 10.1016/j.canlet.2017.08.011
21. Madhavan D, Cuk K, Burwinkel B, Yang R. Cancer diagnosis and prognosis decoded by blood-based circulating micro RNA signatures. *Front Genet*. (2013) 4:116. doi: 10.3389/fgene.2013.00116
22. Ferracin M, Pedriali M, Veronese A, Zagatti B, Gafa R, Magri E, et al. MicroRNA profiling for the identification of cancers with unknown primary tissue-of-origin. *J Pathol*. (2011) 225:43–53. doi: 10.1002/path.2915
23. Rosenwald S, Gilad S, Benjamin S, Lebanony D, Dromi N, Faerman A, et al. Validation of a microRNA-based qRT-PCR test for accurate identification of tumor tissue origin. *Mod Pathol*. (2010) 23:814–23. doi: 10.1038/modpathol.2010.57
24. Varadhachary GR, Spector Y, Abbruzzese JL, Rosenwald S, Wang H, Aharonov R, et al. Prospective gene signature study using microRNA to identify the tissue of origin in patients with carcinoma of unknown primary. *Clin Cancer Res*. (2011) 17:4063–70. doi: 10.1158/1078-0432.CCR-10-2599
25. Cochetti G, Poli G, Guelfi G, Boni A, Egidi MG, Mearini E. Different levels of serum microRNAs in prostate cancer and benign prostatic hyperplasia: evaluation of potential diagnostic and prognostic role. *Onco Targets Ther*. (2016) 9:7545–53. doi: 10.2147/OTT.S119027
26. McDonald AC, Vira M, Walter V, Shen J, Raman JD, Sanda MG, et al. Circulating microRNAs in plasma among men with low-grade and high-grade prostate cancer at prostate biopsy. *Prostate*. (2019) 79:961–8. doi: 10.1002/pros.23803
27. Mello-Grand M, Gregnanin I, Sacchetto L, Ostano P, Zitella A, Bottoni G, et al. Circulating microRNAs combined with PSA for accurate and non-invasive prostate cancer detection. *Carcinogenesis*. (2019) 40:246–53. doi: 10.1093/carcin/bgy167
28. Cheng HH, Plets M, Li H, Higano CS, Tangen CM, Agarwal N, et al. Circulating microRNAs and treatment response in the Phase II SWOG S0925 study for patients with new metastatic hormone-sensitive prostate cancer. *Prostate*. (2018) 78:121–7. doi: 10.1002/pros.23452
29. Fletcher CE, Sulpice E, Combe S, Shibakawa A, Leach DA, Hamilton MP, et al. Androgen receptor-modulatory microRNAs provide insight into therapy resistance and therapeutic targets in advanced prostate cancer. *Oncogene*. (2019) 38:5700–24. doi: 10.1038/s41388-019-0823-5
30. Lin H-M, Mahon KL, Spielman C, Gurney H, Mallesara G, Stockler MR, et al. Phase 2 study of circulating microRNA biomarkers in castration-resistant prostate cancer. *Br J Cancer*. (2017) 116:1002–11. doi: 10.1038/bjc.2017.50
31. Liu RSC, Olkhov-Mitsel E, Jeyapala R, Zhao F, Commisso K, Klotz L, et al. Assessment of serum microRNA biomarkers to predict reclassification of prostate cancer in patients on active surveillance. *J Urol*. (2018) 199:1475–81. doi: 10.1016/j.juro.2017.12.006
32. Rajendiran S, Parwani AV, Hare RJ, Dasgupta S, Roby RK, Vishwanatha JK. MicroRNA-940 suppresses prostate cancer migration and invasion by regulating MIEN1. *Mol Cancer*. (2014) 13:250. doi: 10.1186/1476-4598-13-250
33. Ding D, Zhang Y, Yang R, Wang X, Ji G, Huo L, et al. MiR-940 suppresses tumor cell invasion and migration *via* regulation of CXCR2 in hepatocellular carcinoma. *Biomed Res Int*. (2016) 2016:7618342. doi: 10.1155/2016/7618342
34. Gu GM, Zhan YY, Abuduwaili K, Wang XL, Li XQ, Zhu HG, et al. MiR-940 inhibits the progression of NSCLC by targeting FAM83F. *Eur Rev Med Pharmacol Sci*. (2018) 22:5964–71. doi: 10.26355/eurrev_201809_15927
35. Hou L, Chen M, Yang H, Xing T, Li J, Li G, et al. MiR-940 inhibited cell growth and migration in triple-negative breast cancer. *Med Sci Monit*. (2016) 22:3666–72. doi: 10.12659/MSM.897731
36. Jiang K, Zhao T, Shen M, Zhang F, Duan S, Lei Z, et al. MiR-940 inhibits TGF-β-induced epithelial-mesenchymal transition and cell invasion by targeting Snail in non-small cell lung cancer. *J Cancer*. (2019) 10:2735–44. doi: 10.7150/jca.31800
37. Song B, Zhang C, Li G, Jin G, Liu C. MiR-940 inhibited pancreatic ductal adenocarcinoma growth by targeting MyD88. *Cell Physiol Biochem*. (2015) 35:1167–77. doi: 10.1159/000373941
38. Wang F, Wang Z, Gu X, Cui J. MiR-940 upregulation suppresses cell proliferation and induces apoptosis by targeting PKC-delta in ovarian cancer OVCAR3 cells. *Oncol Res*. (2017) 25:107–14. doi: 10.3727/096504016X14732772150145
39. Xu T, Zhang K, Shi J, Huang B, Wang X, Qian K, et al. MicroRNA-940 inhibits glioma progression by blocking mitochondrial folate metabolism through targeting of MTHFD2. *Am J Cancer Res*. (2019) 9:250–69.
40. Hashimoto K, Ochi H, Sunamura S, Kosaka N, Mabuchi Y, Fukuda T, et al. Cancer-secreted hsa-miR-940 induces an osteoblastic phenotype in the bone metastatic microenvironment *via* targeting ARHGAP1 and FAM134A. *Proc Natl Acad Sci USA*. (2018) 115:2204–9. doi: 10.1073/pnas.1717363115
41. Su K, Wang CF, Zhang Y, Cai YJ, Zhang YY, Zhao Q. MiR-940 upregulation contributes to human cervical cancer progression through p27 and PTEN inhibition. *Int J Oncol*. (2017) 50:1211–20. doi: 10.3892/ijo.2017.3897
42. Zhou Z, Xu YP, Wang LJ, Kong Y. MiR-940 potentially promotes proliferation and metastasis of endometrial carcinoma through regulation of MRVI1. *Biosci Rep*. (2019) 39:BSR20190077 doi: 10.1042/BSR20190077
43. Thompson IM, Ankerst DP, Chi C, Lucia MS, Goodman PJ, Crowley JJ, et al. Operating characteristics of prostate-specific antigen in men with an initial PSA level of 3.0 ng/ml or lower. *JAMA*. (2005) 294:66–70. doi: 10.1001/jama.294.1.66
44. Maji S, Chaudhary P, Akopova I, Nguyen PM, Hare RJ, Gryczynski I, et al. Exosomal annexin II promotes angiogenesis and breast cancer metastasis. *Mol Cancer Res*. (2017) 15:93–105. doi: 10.1158/1541-7786.MCR-16-0163
45. Kramer MF. Stem-loop RT-qPCR for miRNAs. *Curr Protoc Mol Biol*. (2011) 95:15.10. doi: 10.1002/0471142727.mb1510s95
46. Koressaar T, Remm M. Enhancements and modifications of primer design program Primer3. *Bioinformatics*. (2007) 23:1289–91. doi: 10.1093/bioinformatics/btm091
47. Mount DW. Using the basic local alignment search tool (BLAST). *CSH Protoc*. (2007) 2007:pdb.top17. doi: 10.1101/pdb.top17
48. Rashed MH, Kanlikilicer P, Rodriguez-Aguayo C, Pichler M, Bayraktar R, Bayraktar E, et al. Exosomal miR-940 maintains SRC-mediated oncogenic activity in cancer cells: a possible role for exosomal disposal of tumor suppressor miRNAs. *Oncotarget*. (2017) 8:20145–64. doi: 10.18632/oncotarget.15525
49. Schaefer A, Jung M, Miller K, Lein M, Kristiansen G, Erbersdobler A, et al. Suitable reference genes for relative quantification of miRNA

expression in prostate cancer. *Exp Mol Med*. (2010) 42:749–58. doi: 10.3858/emm.2010.42.11.076
50. Rice J, Roberts H, Rai SN, Galandiuk S. Housekeeping genes for studies of plasma microRNA: a need for more precise standardization. *Surgery*. (2015) 158:1345–51. doi: 10.1016/j.surg.2015.04.025
51. Zhu J, Zheng Z, Wang J, Sun J, Wang P, Cheng X, et al. Different miRNA expression profiles between human breast cancer tumors and serum. *Front Genet*. (2014) 5:149. doi: 10.3389/fgene.2014.00149
52. Akao Y, Khoo F, Kumazaki M, Shinohara H, Miki K, Yamada N. Extracellular disposal of tumor-suppressor miRs-145 and−34a *via* microvesicles and 5-FU resistance of human colon cancer cells. *Int J Mol Sci*. (2014) 15:1392–401. doi: 10.3390/ijms15011392
53. Chen X, Liang H, Zhang J, Zen K, Zhang C-Y. Secreted microRNAs: a new form of intercellular communication. *Trends Cell Biol*. (2012) 22:125–32. doi: 10.1016/j.tcb.2011.12.001
54. Taylor MA. Circulating microRNAs as biomarkers and mediators of cell-cell communication in cancer. *Biomedicines*. (2015) 3:270–81. doi: 10.3390/biomedicines3040270
55. Li H, Liu J, Chen J, Wang H, Yang L, Chen F, et al. A serum microRNA signature predicts trastuzumab benefit in HER2-positive metastatic breast cancer patients. *Nat Commun*. (2018) 9:1614. doi: 10.1038/s41467-018-03537-w
56. Liu X, Kwong A, Sihoe A, Chu KM. Plasma miR-940 may serve as a novel biomarker for gastric cancer. *Tumor Biol*. (2016) 37:3589–97. doi: 10.1007/s13277-015-4019-5
57. Pascut D, Krmac H, Gilardi F, Patti R, Calligaris R, Crocè LS, et al. A comparative characterization of the circulating miRNome in whole blood and serum of HCC patients. *Sci Rep*. (2019) 9:1–11. doi: 10.1038/s41598-019-44580-x
58. Luo H, Xu R, Chen B, Dong S, Zhou F, Yu T, et al. MicroRNA-940 inhibits glioma cells proliferation and cell cycle progression by targeting CKS1. *Am J Transl Res*. (2019) 11:4851–65.
59. Xie Z, Yin X, Gong B, Nie W, Wu B, Zhang X, et al. Salivary microRNAs show potential as a noninvasive biomarker for detecting resectable pancreatic cancer. *Cancer Prev Res (Phila)*. (2015) 8:165–73. doi: 10.1158/1940-6207.CAPR-14-0192
60. Liu W, Xu Y, Guan H, Meng H. Clinical potential of miR-940 as a diagnostic and prognostic biomarker in breast cancer patients. *Cancer Biomarkers*. (2018) 22:487–93. doi: 10.3233/CBM-171124

Conflict of Interest: The authors declare that the research was conducted in the absence of any commercial or financial relationships that could be construed as a potential conflict of interest.

Copyright © 2021 Rajendiran, Maji, Haddad, Lotan, Nandy, Vishwanatha and Chaudhary. This is an open-access article distributed under the terms of the Creative Commons Attribution License (CC BY). The use, distribution or reproduction in other forums is permitted, provided the original author(s) and the copyright owner(s) are credited and that the original publication in this journal is cited, in accordance with accepted academic practice. No use, distribution or reproduction is permitted which does not comply with these terms.

frontiers in Oncology

ORIGINAL RESEARCH
published: 31 March 2021
doi: 10.3389/fonc.2021.584988

Characterizing the Genomic Landscape of Brain Glioma With Circulating Tumor DNA From Tumor *In Situ* Fluid

*Zhiyuan Sheng[1], Jinliang Yu[1], Kaiyuan Deng[1], Hugo Andrade-Barazarte[1], Ajmal Zemmar[1], Sijia Li[3], Nianxuan Li[2], Zhaoyue Yan[1], Zhongcan Chen[1], Yong Sun[1], Juha Hernesniemi[1] and Xingyao Bu[1]**

[1] Department of Neurosurgery, Zhengzhou University People's Hospital, Henan Provincial People's Hospital, Zhengzhou, China, [2] School of Basic Medicine, Henan University of Chinese Medicine, Zhengzhou, China, [3] Department of Neurology, The Fifth Affiliated Hospital of Zhengzhou University, Zhengzhou, China

OPEN ACCESS

Edited by:
George Calin,
University of Texas MD Anderson Cancer Center, United States

Reviewed by:
Zuheir Alshehabi,
Tishreen University, Syria
Juliano Andreoli Miyake,
Federal University of Santa Catarina, Brazil

***Correspondence:**
Xingyao Bu
buxingyao@126.com

Specialty section:
This article was submitted to Molecular and Cellular Oncology, a section of the journal Frontiers in Oncology

Received: 24 July 2020
Accepted: 08 March 2021
Published: 31 March 2021

Citation:
Sheng Z, Yu J, Deng K, Andrade-Barazarte H, Zemmar A, Li S, Li N, Yan Z, Chen Z, Sun Y, Hernesniemi J and Bu X (2021) Characterizing the Genomic Landscape of Brain Glioma With Circulating Tumor DNA From Tumor In Situ Fluid. Front. Oncol. 11:584988. doi: 10.3389/fonc.2021.584988

Tumor *in situ* fluid (TISF) refers to the fluid at the local surgical cavity. We evaluated the feasibility of TISF-derived circulating tumor DNA (ctDNA) characterizing the genomic landscape for glioma. This retrospective study included TISF and tumor samples from 10 patients with glioma, we extracted cell-free DNA (cfDNA) from the TISF and then performed deep sequencing on that. And we compared genomic alterations between TISF and tumor tissue. Results showed that the concentration of cfDNA fragments from the patients for TISF ranged from 7.2 to 1,397 ng/ml. At least one tumor-specific mutation was identified in all 10 patients (100%). Further analysis of TISF ctDNA revealed a broad spectrum of genetic mutations, which have been reported to have clinical relevance. The analysis of concordance between TISF and tumor tissue reflected the spatiotemporal heterogeneity of glioma. Collectively, TISF ctDNA was a powerfully potential source for characterizing the genomic landscape of glioma, which provided new possibilities for precision medicine in patients with glioma.

Keywords: tumor *in situ* fluid, circulating tumor DNA, glioma, precision medicine, liquid biopsy

INTRODUCTION

Glioma is a tumor with high molecular heterogeneity, its constantly evolving genetic landscape can be a huge obstacle to the clinical management of patients (1). Studies about sequential glioma biopsies have unearthed enormous divergence of the cancer genome between the initial and recurrent tumor from the same patient (2, 3). The need for precision medicine is to characterize the real-time molecular status of the tumor, which is believed to have therapeutic significance for glioma patients (4). However, serial biopsies constitute a high risk to patients and are not realistic in clinical practice.

Liquid biopsy, defined as biofluids used for molecular diagnostics (5), has brought new hope and possibilities to precision medicine. For example, blood-based circulating tumor DNA (ctDNA)

Abbreviations: TISF, tumor *in situ* fluid; ctDNA, circulating tumor DNA.

detection has proved to be of great clinical significance for a variety of solid tumors (5), such as breast (6), gastric (7), and esophageal (8) cancers. However, regarding the CNS, identifying detectable ctDNA in plasma remains challenging (9). Current studies reported that cerebrospinal fluid (CSF) could be a promising reservoir of ctDNA for brain glioma (10, 11), but with the concomitant imperfection that tumor shedding DNA to the CSF is affected by tumor burden and tumor abutting CSF (11).

The body fluid for liquid biopsy should include any conceivable stable-acquired fluid collection (12). The surgical resection for glioma always creates a cavity at the tumor site, inside exists fluid that connects or does not connect with the CSF reservoir. Here, we coined the term "Tumor *in situ* fluid (TISF)" to describe the fluid in the local surgical cavity. It is known that most gliomas relapse at the local site (13, 14), thus tumor-shed biomarkers would congregate in TISF over the process of treatment resistance and tumor progression. Moreover, with an intraoperatively implanted reservoir, obtaining TISF postoperatively is clinically feasible and uninjurious. Based on this hypothesis, we retrospectively investigated whether ctDNA from TISF could be a new source of liquid biopsy for precision medicine for patients with glioma.

MATERIALS AND METHODS

Patients and Ethics Statement

This study included tumor *in situ* fluid (TISF) and tumor samples from 10 patients who were diagnosed as glioma (WHO grade III or IV) and treated in Henan Provincial People's Hospital (HPPH). All patients received surgical treatment with a reservoir implanted into the surgical cavity intraoperatively and TISF were collected after surgery. The retrospective study was approved by the institutional review board and ethics committee of HPPH (Zhengzhou, China). Written informed consent was signed by all patients and/or their legal representatives.

Sample Collection

As mentioned above, a reservoir for postoperative local chemotherapy was indwelled into the resection cavity during the surgery for every patient. After surgery, 0.5 to 1 ml TISF was collected for every patient using the indwelled reservoir (**Figure 1**). Unstained paraffin-embedded tumor tissues (UPETT) were collected, and tumor DNA was isolated for 9 of the 10 cases (90%). Blood samples (5 ml) for germline DNA control from each patient were also obtained.

Isolation of Tumor DNA and Germline DNA

As described elsewhere (10), EDTA tubes containing biofluids (TISF or CSF or blood) were centrifuged at 1,900*g* for 10 min, after that, the supernatants from those were additionally centrifuged at 16,000*g* for 10 min. And then samples were stored at −80°C before extraction. Genomic DNA was extracted from UPETT with the QIAamp DNA Tissue & Blood Kit (Qiagen; Germantown, MD, USA). Cell-free DNA (cfDNA) was extracted from biofluids using the MagMAX™ CellFree DNA Isolation Kit (ThermoFisher Scientific; Waltham, MA, USA). Finally, all segregated DNA was quantified using

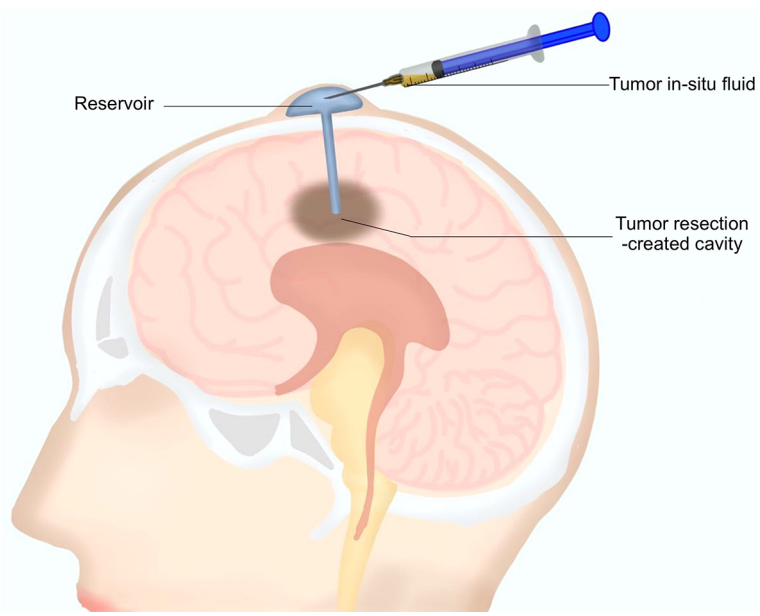

FIGURE 1 | A diagram for the tumor *in situ* fluid (TISF) collection. A reservoir was implanted into the resection cavity during the resection surgery. The dome end was placed beneath the scalp attached to the catheter that was inserted within the brain leading to the tumor resection-created cavity. A small amount of fluid could be extracted with a disposable milliliter syringe from the resection cavity *via* this reservoir postoperatively.

the Qubit 2.0 Fluorometer with the Qubit dsDNA HS Assay kit (Life Technologies; Carlsbad, CA, USA) following the advised protocol.

NGS Library and Sequencing Data Analysis

As described elsewhere, the DNA libraries were captured with a designed panel of 68 genes for brain tumors (GenetronHealth; Beijing, China) (10), those genes containing major brain tumor-related genes. The DNA sequencing was based on novaseq high-throughput sequencing platform.

Statistical Analysis

The log-rank test was used to compare the survival difference between different groups, and the nonparametric Mann Whitney test was for difference analysis between the two groups.

RESULT

Patient Characteristics

This cohort included seven female and three male who were diagnosed as WHO grade III or IV glioma, Specifically, six IDH wild-type glioblastoma (GBM) (60%), three IDH mutant low-grade (III) glioma and 1 IDH mutant GBM (40%) according to the 2016 WHO brain tumor classification with IDH status (15). The mean age was 52.7 years (33–66 years). Four tumors were located at the frontal lobe, three at the temporoparietal lobe, two at the temporal lobe, and the last one at the thalamus. Patients' characteristics were summarized in **Table 1**. All patients received concurrent chemoradiotherapy (CRT) followed by adjuvant temozolomide (TMZ) combining with local Methotrexate chemotherapy after surgery. Clinical courses of patients were presented in **Figure 2**.

TISF ctDNA Represented the Genetic Landscape of Glioma

The concentration of cfDNA from TISF ranged between 7.2 and 1,397 ng/ml (**Figure 3C**), which was high enough to minimize analytic errors in subsequent analysis. In total, 83 alterations of 37 different genes were detected. The average number of mutations detected in the TISF-derived ctDNA of respective individuals was 7.55 ± 6.79 (range, 1 to 22). The most frequently altered genes were TP53 (50%), SETD2 (40%), NF1 (30%), PTEN (30%), RELA (30%), DAXX (30%), EGFR (30%), and FAT1

TABLE 1 | Patients characteristics.

Patients	Sex	Age	WHO grade	Histopathology	IDH status	Tumor location	Interval since surgery (months)
1	F	45	4	GBM	wild type	thalamus	3.9
2	M	60	4	GBM	wild type	temporal	3.2
3	F	66	4	GBM	wild type	temporoparietal	8.0
4	F	55	4	GBM	wild type	frontal	5.7
5	M	52	4	GBM	wild type	temporoparietal	8.7
6	F	65	4	GBM	wild type	temporal	10.8
7	F	33	4	GBM	mutant	frontal	16.4
8	F	44	3	AO	mutant	frontal	12.8
9	F	54	3	AO	mutant	temporoparietal	14.7
10	M	53	3	AO	mutant	frontal	15.7

F, female; GBM, glioblastoma; AO, anaplastic oligodendroglioma.

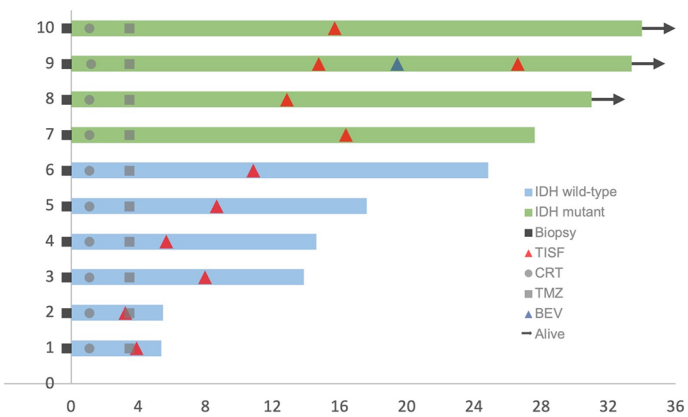

FIGURE 2 | Clinical courses of included patients. Each patient began from the primary surgery (Biopsy). TISF, tumor *in situ* fluid; CRT, concurrent chemoradiotherapy; TMZ, adjuvant temozolomide chemotherapy; BEV, bevacizumab.

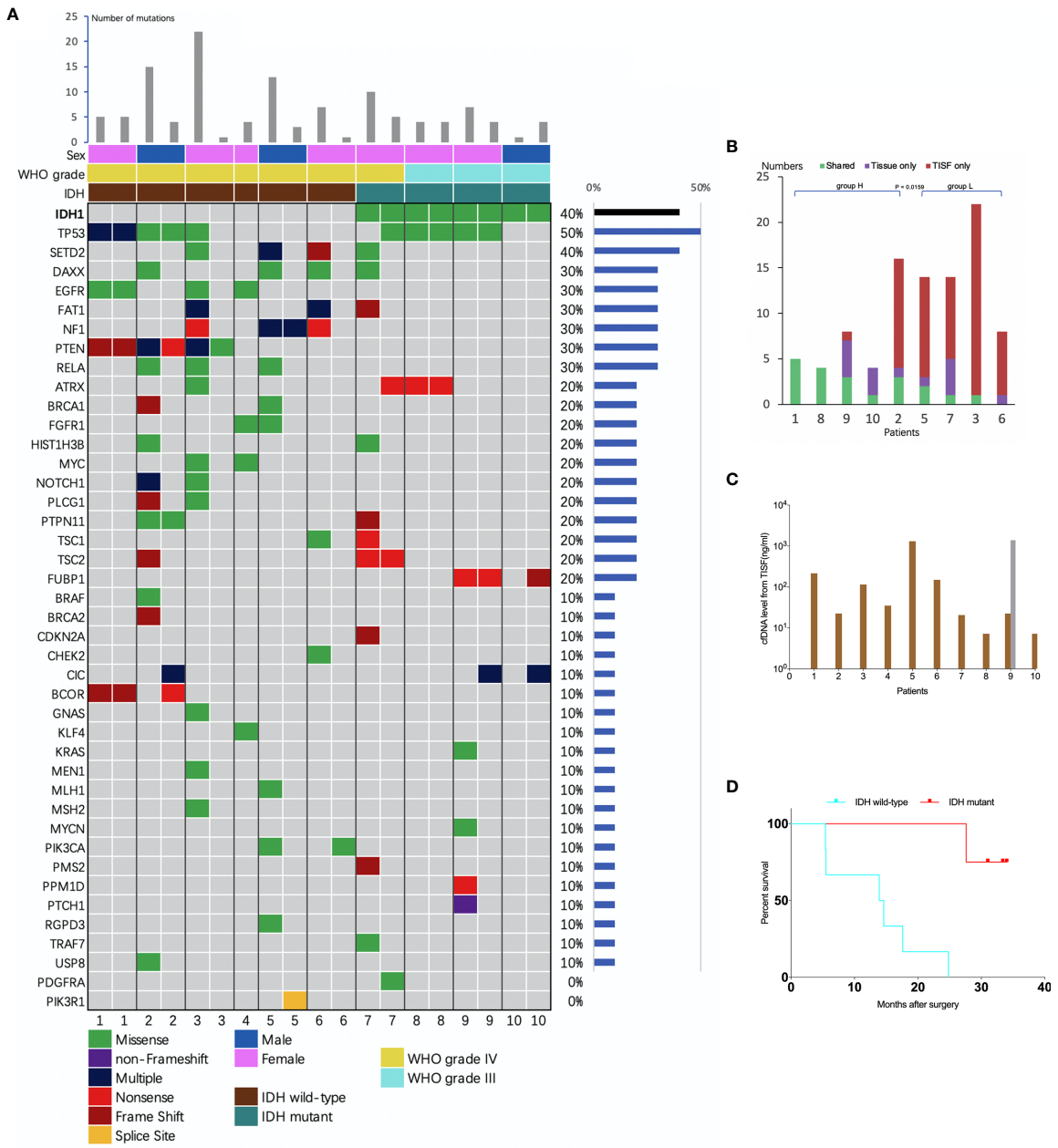

FIGURE 3 | Analysis of tumor DNA from TISF and tumor tissue. **(A)** the mutational landscape for both TISF and tumor tissue. For each patient, the left column represented TISF-derived ctDNA and the right column represented tumor tissue, patient 4 just had one column for the TISF. **(B)** Concordance of tumor DNA between TISF and tumor tissue. The percentage of shared mutations varied from 0% to 100% (median 30.0%). **(C)** Cell-free DNA (cfDNA) levels from TISF. The concentration of cfDNA from TISF ranged between 7.2 and 1397 ng/ml. For patient 9, the second time TISF cfDNA experienced a significant increase. **(D)** Survival curve for patients with different IDH status. In all 10 patients (including 6 IDH wild type and 4 IDH mutant gliomas), the IDH status was accordant between the TISF and tumor tissue (100%). Median overall survival after the primary surgery was 14.2 and 32.2 months (P = 0.0038) for TISF wild-type IDH and TISF mutant IDH glioma, respectively.

(30%). The most common category of mutation was missense mutation (65.1%), followed by frame-shifting mutation (18.1%) and nonsense mutation (13.3%) (**Figure 3A**).

To identify whether TISF ctDNA could reflect the genome alterations of glioma, we analyzed the sequencing results in depth. Firstly, IDH status was included to determining the diagnosis for glioma in the WHO 2016 classification (15). We examined whether this genetic alteration could be detected in the TISF and matched that of the tumor tissue. In all 10 patients (including six IDH wild type and four IDH mutant gliomas), the

IDH status was accordant between the TISF and tumor tissue (100%). Median overall survival after the primary surgery was 14.2 and 32.2 months for wild-type IDH and mutant IDH glioma (P = 0.0038), respectively (**Figure 3D**).

Further analysis of TISF ctDNA revealed a broad spectrum of genetic mutations which have been reported to have clinical relevance. For example, mutations of PTEN, TSC2, TSC1, NF1, and PIK3CA have been demonstrated activating PI3K/AKT/mTOR pathways, which will then boost the growth and progression of the tumor (16); FAT1 alteration is reported closely related to Wnt signaling pathway (17); modification on tumor suppressor genes, including TP53, BRCA1, BRCA2, CHEK2, and PTCH1 and on cell cycle genes, such as CDKN2A (18, 19). Many of these mutations are promising targets of precision therapeutic regimens (**Table 2**). Additionally, TMZ as an alkylating agent can induce the mutations of mis-match repair (MMR) genes, which is related to treatment resistance (20). We identified MMR gene mutations (MSH2, MLH1, and PMS2) in three patients (patients 3, 5, and 7), including two IDH wild-type GBM and one IDH-mutant GBM, all of them received systematic TMZ treatment previously, and we did not detect this signature in their tumor tissues.

Collectively, these results indicated that ctDNA from TISF was capable to characterize the genomic landscape of glioma during its progression process.

Concordance Between TISF and Tumor Tissue

We compared the sequencing results of tumor DNA from TISF and UPETT for nine patients (**Figure 4**). The median interval between biopsy (surgery) and the first TISF collection was 10.8 months (3.2–16.4 months). The percentage of shared mutations varied from 0% to 100% (median, 31.6%) (**Figure 3B**). We further divided the 9 patients into 2 groups: group H (n=5, patients 1, 2, 8, 9, 10) included patients with low-grade glioma ((WHO grade III)) or underwent a short interval between TISF collection and tumor tissue biopsy (less than 4 months); group L included the remaining four patients (patients 3, 5, 6, 7). Subsequently, the median for the percentages of shared mutations of group H came at 54.5% (31.6%–100%), and the median for group L became 8.3% (0–25%), there was a significant difference between the two groups (P = 0.0159) (**Figure 3B**).

Despite those considerable divergences between TISF and tumor tissue, for some key genes, on the other hand, high concordance was observed between TISF and tumor tissue, one is the above-mentioned IDH1, another example is the PTEN mutation (three patients, 100%) which can activate the PI3K/AKT/mTOR signaling pathways (18). Furthermore, for patient 9 (WHO grade III anaplastic oligodendroglioma), we collected another TISF for ctDNA analysis at 26.6 months after surgery. We observed more shared mutations with tumor tissue than the first TISF (3 vs. 0) and higher accordance (60% vs. 0).

TISF ctDNA Was Before Imaging Progression

Postoperatively, all patients had serial follow-up MRI. We noticed that TISF collection was performed at time points when apparent signs could not be spotted on the MRI scans for five patients. And it was until 2 to 4 months after TISF collection when doubtless recurrence signs could be observed on the images (**Figure 4**). However, we presumed that shedding DNA to TISF was a universal property of glioma because of the special location of TISF, thus ctDNA-positive in TISF could not be a biomarker for predicting the recurrence of glioma, and tumor progression should be determined by the specific genetic results as described above.

DISCUSSION

Dynamically characterizing the heterogeneity of glioma with liquid-based biomarkers is a powerful tool for precision medicine, which has been increasing the likelihood of curing malignancies (5). Here we originally demonstrated the feasibility of TISF as a steady source of liquid biopsy for glioma, providing new insight to precision medicine for brain tumors.

We identified abundant alterations derived from glioma in TISF, in-depth analysis proved that those mutations could reflect the genomic landscape of glioma during the treatment process. The landscape included PI3K/AKT/mTOR pathways-related genes, tumor suppressor genes, cell cycle genes, etc. This evidenced that multiple mechanisms contribute to the genesis and development of glioma, many of them are potential targets of precision therapies (**Table 2**).

TABLE 2 | Potential beneficial targeted medicine for patients.

Mutations	FDA approved for this cancer	FDA approved for other cancers	Phase II/III clinical trials
CDKN2A		Palbociclib, Ribociclib	Defactinib
PIK3CA		Everolimus、Temsirolimus	Ipatasertib, GDC-0077
PTEN		Alpelisib, Copanlisib	Ipatasertib, GSK2636771
TSC1, TSC2		Everolimus, Temsirolimus	Sapanisertib, LY3023414
BRAF		Encorafenib+Binimetinib	Ulixertinib, PLX8394
BRCA2		Rucaparib, Talazoparib	
KRAS		Cobimetinib, Binimetinib	
NF1		Temsirolimus, Cobimetinib	
IDH1		Ivosidenib	
PTCH1		Vismodegi, Sonidegib	

FDA, food and durg administration. Currently, very limited medicine has been approved for treating glioma. This will be improved with the development of precision medicine.

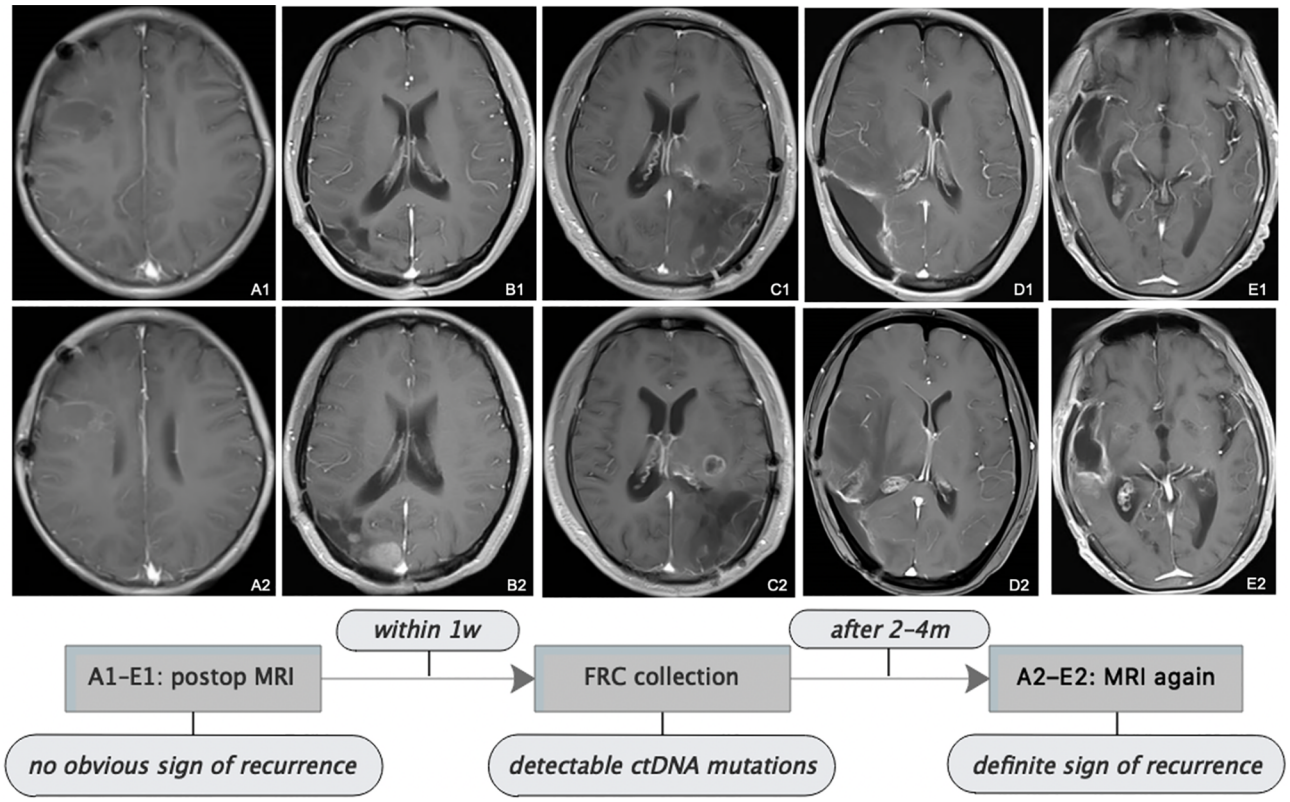

FIGURE 4 | Follow-up MRI showed tumor progression. All patients received serial MRI as the standard of care. As presented in the images and the illustrative flowchart, A1–E1 stand for a postoperative representative timepoint, at which we could not notice an obvious sign of tumor progression on the MRI scans, but at which we suspected tumor progression according to the comprehensive conditions of patients, then TISF was collected, in which tumor-specific ctDNA mutations were detected. 2–4 months later, as shown in the images A2–E2, definite radiologic sign of tumor recurrence appeared. This is interesting but we still presume that the simple signature of ctDNA-positive in TISF could not be a biomarker for early predicting the recurrence of glioma, because of the special location of TISF, which is at the local site of the tumor. The tumor progression should be determined by a specific genetic analysis.

In a previous CSF-based liquid biopsy study, Miller et al. observed a considerable divergence of shared mutations between CSF samples and tumor tissues (0–100%) across patients. Meantime, they found that samples collected at a closer interval (<3 weeks) had a higher percentage of shared mutations (79%) than those collected at a longer interval (>1,000 days) (29%) (11). Here we observed a comparable phenomenon in this pilot study. All samples were collected at a long interval (>3 months) and the percentage of shared mutations varied considerably from 0% to 100% (median, 31.6%). Interestingly, when we divided patients into two groups, i.e., group H containing patients with low-grade glioma or with a shorter interval (<4 months) and group L including the remaining patients, the fact came that group H had a higher percentage of shared mutations (median 54.5%) than group L did (median 8.3%). Several scenarios might account for these divergences. One is the spatial heterogeneity of glioma, i.e., the observation that tumor cells can show distinct genetic characteristics and one tumor biopsy usually only represents a part of tumor heterogeneity. Two is the temporal heterogeneity of glioma, which refers to that tumor can develop clonal and subclonal evolution with time, as it did in patient 9, who received two-time TISF ctDNA collection, we observed higher concordance with tumor tissue and higher cfDNA level than of the first TISF. This dynamic variation was expected correlated with the decrease in tumor burden attributed to the surgical resection and then the gradually clonal together with subclonal progression of the tumor. Another factor is due to the therapeutic pressure, which typically affects the genetic evolution of a tumor (21, 22). For example, it has been elucidated that TMZ application can induce the MMR deficit with the hypermutation ensuring in the glioma genome, which then gives contributions to the TMZ treatment resistance (20). We observed MMR gene mutations in three patients in our cohort, which was attributed to TMZ treatment. Despite those divergences and dynamics, we also noted that certain mutations were present in both tumor tissue and TISF, such as IDH1 and PTEN, which support the perspective that certain mutations or pathways occurred at the early stage of tumorigenesis and contribute to the tumor growth and progression throughout the life of the tumor (22, 23). In a word, these phenomenon and features of the tumor greatly evidenced the urgent need of precision characterization of genomic status for

glioma in real time. Future frequent TISF-based liquid biopsies would be able to depict the genomic dynamics under therapeutic pressure and based on that to guide the modification of treatment combinations.

Imaging-based assessment of tumor progression for glioma cannot overcome the hysteresis and cannot reflect the molecular status of the tumor, which makes it impossible for clinicians to monitor the microscope progression of glioma from the early stage of postoperative management. In this study, we noted that detectable mutations of ctDNA from TISF were prior to clear evidence of radiologic recurrence. It was interesting but we still presumed that the simple signature of ctDNA-positive in TISF could not be a biomarker for early predicting the recurrence of glioma, because of the special location of TISF, which is at the local site of the tumor. It could be a universal property of glioma to shed tumor DNA into TISF at any stage. And we hypothesized that potential biomarkers would appear locally in high concentrations in TISF and might then be found diluted in the CSF and eventually plasma, the latter two signatures might be the adverse prognostic factors. The tumor progression should be determined by a specific genetic analysis.

In conclusion, we proved the feasibility of TISF ctDNA for characterizing the genomic landscape of glioma, this original insight provided new perspectives and possibilities for precision medicine in patients with glioma.

DATA AVAILABILITY STATEMENT

The data sets presented in this study can be found in online repositories. The names of the repository/repositories and accession number(s) can be found below: https://figshare.com/articles/dataset/original_gene_analysis_reports_zip/12672692.

ETHICS STATEMENT

The studies involving human participants were reviewed and approved by the Institutional Review Board (IRB) and Ethics Committee of Henan Provincial People's Hospital (Zhengzhou, China). All methods were carried out in accordance with the approved guidelines. Written informed consent was obtained from all patients. Written informed consent was obtained from the minor(s)' legal guardian/next of kin for the publication of any potentially identifiable images or data included in this article.

AUTHOR CONTRIBUTIONS

XB and ZS conceived and designed the study. JY, NL, KD, and ZS collected the clinical data and samples. ZS and XB performed the data analysis. ZS wrote the manuscript. SL produced the figures. JH, HA-B, and AZ reviewed the data and revised the manuscript. YS, ZC, and ZY gave the conceptual advice. All authors contributed to the article and approved the submitted version.

FUNDING

This work was supported by the Science and Technology Tackle Program of Henan Province (grant 192102310126).

ACKNOWLEDGMENTS

We thank Juntao Li and Xiang Sun for their help in collecting and shipping samples. We thank Guangqi An, who assisted in the illustration for **Figure 1**.

REFERENCES

1. Nicholson JG, Fine HA. Diffuse Glioma Heterogeneity and Its Therapeutic Implications. *Cancer Discovery* (2021) 11(3):575–90. doi: 10.1158/2159-8290.CD-20-1474
2. Lee JK, Wang J, Sa JK, Ladewig E, Lee HO, Lee IH, et al. Spatiotemporal genomic architecture informs precision oncology in glioblastoma. *Nat Genet* (2017) 49(4):594–9. doi: 10.1038/ng.3806
3. Georgescu MM, Olar A. Genetic and histologic spatiotemporal evolution of recurrent, multifocal, multicentric and metastatic glioblastoma. *Acta Neuropathol Commun* (2020) 8(1):10. doi: 10.1186/s40478-020-0889-x
4. Tan AC, Ashley DM, López GY, Malinzak M, Friedman HS, Khasraw M. Management of glioblastoma: State of the art and future directions. *CA Cancer J Clin* (2020) 70:299–312. doi: 10.3322/caac.21613
5. Pantel K, Alix-Panabières C. Liquid biopsy and minimal residual disease — latest advances and implications for cure. *Nat Rev Clin Oncol* (2019) 16 (7):409–24. doi: 10.1038/s41571-019-0187-3
6. Chen YH, Hancock BA, Solzak JP, Brinza D, Scafe C, Miller KD, et al. Next-generation sequencing of circulating tumor DNA to predict recurrence in triple-negative breast cancer patients with residual disease after neoadjuvant chemotherapy. *NPJ Breast Cancer* (2017) 3:24. doi: 10.1038/s41523-017-0028-4
7. Leal A, van Grieken NCT, Palsgrove DN, Phallen J, Medina JE, Hruban C, et al. White blood cell and cell-free DNA analyses for detection of residual disease in gastric cancer. *Nat Commun* (2020) 1(1):525. doi: 10.1038/s41467-020-14310-3
8. Azad TD, Chaudhuri AA, Fang P, Qiao Y, Esfahani MS, Chabon JJ, et al. Circulating Tumor DNA Analysis for Detection of Minimal Residual Disease After Chemoradiotherapy for Localized Esophageal Cancer. *Gastroenterology* (2020) 158(3):494–505.e6. doi: 10.1053/j.gastro.2019.10.039
9. Sareen H, Garrett C, Lynch D, Powter B, Brungs D, Cooper A, et al. The role of liquid biopsies in detecting molecular tumor biomarkers in brain cancer patients. *Cancers (Basel)* (2020) 12(7):1831. doi: 10.3390/cancers 12071831
10. Pan C, Diplas BH, Chen X, Wu Y, Xiao X, Jiang L, et al. Molecular profiling of tumors of the brainstem by sequencing of CSF-derived circulating tumor DNA. *Acta Neuropathol* (2019) 137:297–306. doi: 10.1007/s00401-018-1936-6
11. Miller AM, Shah RH, Pentsova EI, Pourmaleki M, Briggs S, Distefano N, et al. Tracking tumour evolution in glioma through liquid biopsies of cerebrospinal fluid. *Nature* (2019) 565:654–8. doi: 10.1038/s41586-019-0882-3
12. Le Rhun E, Seoane J, Salzet M, Soffietti R, Weller M. Liquid biopsies for diagnosing and monitoring primary tumors of the central nervous system. *Cancer Lett* (2020) 480:24–8. doi: 10.1016/j.canlet.2020.03.021
13. Fukuya Y, Ikuta S, Maruyama T, Nitta M, Saito T, Tsuzuki S, et al. Tumor recurrence patterns after surgical resection of intracranial low-grade gliomas. *J Neurooncol* (2019) 144:519–28. doi: 10.1007/s11060-019-03250-8

14. Spiteri I, Caravagna G, Cresswell GD, Vatsiou A, Nichol D, Acar A, et al. Evolutionary dynamics of residual disease in human glioblastoma. *Ann Oncol* (2019) 30(3):456–63. doi: 10.1093/annonc/mdy506
15. Louis DN, Perry A, Reifenberger G, von Deimling A, Figarella-Branger D, Cavenee WK, et al. The 2016 World Health Organization Classification of Tumors of the Central Nervous System: a summary. *Acta Neuropathol* (2016) 131(6):803–20. doi: 10.1007/s00401-016-1545-1
16. Esposito A, Viale G, Curigliano G. Safety, Tolerability, and Management of Toxic Effects of Phosphatidylinositol 3-Kinase Inhibitor Treatment in Patients with Cancer: A Review. *JAMA Oncol* (2019) 5(9):1347–54. doi: 10.1001/jamaoncol.2019.0034
17. Bugter JM, Fenderico N, Maurice MM. Mutations and mechanisms of WNT pathway tumour suppressors in cancer. *Nat Rev Cancer* (2021) 21(1):5–21. doi: 10.1038/s41568-020-00307-z
18. Chen L, Liu S, Tao Y. Regulating tumor suppressor genes: post-translational modifications. *Signal Transduct Target Ther* (2020) 5(1):90. doi: 10.1038/s41392-020-0196-9
19. Hafner A, Bulyk ML, Jambhekar A, Lahav G. The multiple mechanisms that regulate p53 activity and cell fate. *Nat Rev Mol Cell Biol* (2019) 20(4):199–210. doi: 10.1038/s41580-019-0110-x
20. Touat M, Li YY, Boynton AN, Spurr LF, Iorgulescu JB, Bohrson CL, et al. Mechanisms and therapeutic implications of hypermutation in gliomas. *Nature* (2020) 580:517–23. doi: 10.1038/s41586-020-2209-9
21. Johnson BE, Mazor T, Hong C, Barnes M, Aihara K, McLean CY, et al. Mutational analysis reveals the origin and therapy-driven evolution of recurrent glioma. *Sci (80-)* (2014) 343(6167):189–93. doi: 10.1126/science.1239947
22. Barthel FP, Johnson KC, Varn FS, Moskalik AD, Tanner G, Kocakavuk E, et al. Longitudinal molecular trajectories of diffuse glioma in adults. *Nature* (2019) 576(7785):112–20. doi: 10.1038/s41586-019-1775-1
23. Körber V, Yang J, Barah P, Wu Y, Stichel D, Gu Z, et al. Evolutionary Trajectories of IDH WT Glioblastomas Reveal a Common Path of Early Tumorigenesis Instigated Years ahead of Initial Diagnosis. *Cancer Cell* (2019) 35(4):692–704.e12. doi: 10.1016/j.ccell.2019.02.007

Conflict of Interest: The authors declare that the research was conducted in the absence of any commercial or financial relationships that could be construed as a potential conflict of interest.

Copyright © 2021 Sheng, Yu, Deng, Andrade-Barazarte, Zemmar, Li, Li, Yan, Chen, Sun, Hernesniemi and Bu. This is an open-access article distributed under the terms of the Creative Commons Attribution License (CC BY). The use, distribution or reproduction in other forums is permitted, provided the original author(s) and the copyright owner(s) are credited and that the original publication in this journal is cited, in accordance with accepted academic practice. No use, distribution or reproduction is permitted which does not comply with these terms.

frontiers in Oncology

ORIGINAL RESEARCH
published: 22 April 2021
doi: 10.3389/fonc.2021.561763

Predict Colon Cancer by Pairing Plasma miRNAs: Establishment of a Normalizer-Free, Cross-Platform Model

Da Qin, Qingdong Guo, Rui Wei, Si Liu, Shengtao Zhu, Shutian Zhang and Li Min**

Department of Gastroenterology, Beijing Friendship Hospital, Capital Medical University, National Clinical Research Center for Digestive Disease, Beijing Digestive Disease Center, Beijing Key Laboratory for Precancerous Lesion of Digestive Disease, Beijing, China

OPEN ACCESS

Edited by:
Catherine Alix-Panabieres, Centre Hospitalier Universitaire de Montpellier, France

Reviewed by:
Giuseppe Palma, Istituto Nazionale Tumori Fondazione G. Pascale (IRCCS), Italy
Richa Shrivastava, Birla Institute of Technology and Science, India

***Correspondence:**
Li Min
minli@ccmu.edu.cn
Shutian Zhang
zhangshutian@ccmu.edu.cn

Specialty section:
This article was submitted to Molecular and Cellular Oncology, a section of the journal Frontiers in Oncology

Received: *10 September 2020*
Accepted: *29 March 2021*
Published: *22 April 2021*

Citation:
Qin D, Guo Q, Wei R, Liu S, Zhu S, Zhang S and Min L (2021) Predict Colon Cancer by Pairing Plasma miRNAs: Establishment of a Normalizer-Free, Cross-Platform Model. Front. Oncol. 11:561763. doi: 10.3389/fonc.2021.561763

Background: Plasma miRNAs are emerging biomarkers for colon cancer (CC) diagnosis. However, the lack of robust internal references largely limits their clinical application. Here we propose a ratio-based, normalizer-free algorithm to quantitate plasma miRNA for CC diagnosis.

Methods: A miRNA-pair matrix was established by pairing differentially expressed miRNAs in the training group from GSE106817. LASSO regression was performed to select variables. To maximize the performance, four algorithms (LASSO regression, random forest, logistic regression, and SVM) were tested for each biomarker combination. Data from GSE106817 and GSE112264 were used for internal and external verification. RT-qPCR data acquired from another cohort were also used for external validation.

Results: After validation through four algorithms, we obtained a 4-miRNA pair model (miR-1246 miR-451a; miR-1246 miR-4514; miR-654-5p miR-575; miR-4299 miR-575) that showed good performance in differentiating CC from normal controls with a maximum AUC of 1.00 in internal verification and 0.93 in external verification. Tissue validation showed a maximum AUC of 0.81. Further external validation using RT-qPCR data exhibited good classifier ability with an AUC of 0.88.

Conclusion: We established a cross-platform prediction model robust against sample-specific disturbance, which is not only well-performed in predicting CC but also promising in the diagnosis of other diseases.

Keywords: colon adenocarcinoma, miRNA, circulation miRNA, miRNA-pair, miRNA standardization

INTRODUCTION

With 1.9 million new cases, colon cancer (CC) ranks third among all cancers in incidence worldwide (1). The number of CC patients grows rapidly during the past decade, which has become a major global health problem (2). Early-stage CC patients could be cured by minimally invasive surgery and showed a 5-year survival rate of 74% (3). Thus, detection of CC at a resectable stage is a long-term pursuit of gastroenterologists (4).

Plasma microRNAs (miRNAs), representing an emerging direction of liquid biopsy, are bringing new insights to early detection of CC. Many efforts have been made to evaluate plasma miRNAs to predict CC (5, 6). Among the main existing miRNA detection methods, omics tools such as miRNA-sequencing and miRNA chip are costly and not suitable for large-scale population cancer screening. Real-time quantitative PCR (RT-qPCR) is a cost-effective alternative to the omics tools in miRNA detection. However, the absence of a proper standardization method for RT-qPCR data of plasma miRNA largely limited its reliability and repeatability in quantification assays (7). Thus, although dozens of miRNA biomarkers have been proposed in different labs, few of them were reproducible by other researchers and could eventually be applied to large-scale population screening of cancers.

In this study, we proposed a miRNA paired ratio-based standardization method for plasma miRNA quantification. We calculated the ratio of two given miRNAs in the same plasma sample, used this ratio as a new kind of variables, and constructed a prediction system based on these ratios to predict risks of CC. This ratio-based system performed well in both miRNA chip data and RT-qPCR data by eliminating possible sample-specific disturbance. We believe that this system is not only well-performed in predicting CC but also promising in the diagnosis of other diseases.

MATERIALS AND METHODS

Patients Cohorts

Plasma miRNA chip data from GSE106817 (8) and GSE112264 (9) in GEO database were obtained for analysis. GSE106817 was divided into a training group and a testing group by random number. GSE112264 was used for external verification. Furthermore, miRNA chip data of tissue samples from GSE115513 (10) was also used for validation in tissue samples. 104 plasma samples of CC patients and normal controls from Beijing Friendship Hospital were collected for RT-qPCR data validation. Clinical details of these subjects were shown in **Supplementary File 1**. All participants had signed the informed consent, and this study was approved by the ethics committee of Beijing Friendship Hospital. Flowchart of this study was shown in **Figure 1**.

Abbreviations: CC, colon cancer; RT-qPCR, real-time quantitative polymerase chain reaction; LASSO, least absolute shrinkage and selection operator; miRNAs, microRNAs; DE, Differentially expressed; SVM, Support vector machine; ROC, Receiver operator characteristic; AUC, area under the curve.

Differentially Expressed miRNA Analysis and miRNA-Pair Matrix Construction

Differentially expressed (DE) miRNA analysis was performed to training group derived from GSE106817 using "limma" package (11) in R 3.5.2. Then, miRNA paired ratios were calculated from any two DE miRNAs expression values in the same sample. Subsequently, univariate logistic regression was used to exclude pairs not associated with cancer occurrence and constructed a final miRNA-pair matrix for the training group.

Prediction Model Construction

LASSO regression was performed to select variables in the miRNA-pair matrix using "glmnet" package (12) in R 3.5.2. Models enrolled 1, 2, 3, 4 miRNA-pairs were successively established by a step-wise variable selection process by controlling lambda values in a LASSO regression. Then, the logistic prediction model for each of these models were constructed by "glm" function in R. Random forest models were established by "randomForest" package. Support vector machine (SVM) models were designed using "e1071" package. Furthermore, area under the curve (AUC) of all these prediction models were calculated to evaluate their performance.

Internal and External Verification by miRNA Chip Data

The testing group of GSE106817 was used for internal verification of the models. Receiver operator characteristic (ROC) curves of these models were drawn by using "plotROC" package (13) and "ggplot2" package. GSE112264 was used for external verification of these models. Furthermore, we also evaluated the diagnostic validity of those models in tissue miRNA chip data from GSE115513. AUC values of internal and external verification for each model were calculated.

RT-qPCR Validation

104 plasma samples from Beijing Friendship Hospital were used for external validation (**Supplementary File 1**). Total RNA isolated from plasma was obtained using TRIzol following the manufacturer's protocol (Takara, Shiga, Japan). Total RNA was reverse-transcribed and cDNA was synthesized using miR-specific stem-loop RT primers and components of the High-Capacity cDNA Reverse Transcription kit (Takara, Shiga, Japan, RR036a). The amplification of cDNA was performed in 10-μl reaction system following the SYBRGREEN life assays manufacturer's instructions. Primers used in RT-qPCR validation were shown in **Supplementary File 2**.

GSEA Analysis, Gene Ontology Analysis and KEGG Pathway Analysis

Target genes of selected miRNAs were predicted by TargetScan (14). Gene ontology analysis was then performed to identify ontologies (MF, molecular functions; BP, biological processes; CC, cellular component) enriched in the target genes of those miRNAs using clusterProfiler (15) package in R software. KEGG pathway and GSEA enrichment analysis (16) was also performed to find out the potential pathways which may be affected by those miRNAs.

Statistical Analysis

All statistical analyses were calculated by R software (version 3.5.2; https://www.r-project.org/). DE miRNAs were identified by "limma" package (version 3.38.3). ROC curves were graphed using "plotROC" package (version 2.2.1). LASSO regression was performed using "glmnet" package (version 2.0-18). Random forest regression and SVM were performed using "randomForest" package (version 4.6-14) and e1071 package (version 1.7-2). Statistical significance was defined as $P < 0.05$.

RESULTS

DE miRNA Identification and miRNA-Pair Matrix Construction

387 DE miRNAs were identified after DE analysis in the training group (91 CC and 157 NC) of GSE106817 (**Figure 1**). Any two of these 387 DE miRNAs were paired, which constructed a miRNA-pair matrix containing 74,691 miRNA-pairs. Univariate logistic regression was subsequently performed to screen for cancer-related miRNA-pairs. Finally, a miRNA-pair matrix with 61,939 miRNA-pairs was obtained.

Prediction Model Construction and Internal Verification by miRNA Chip Data

LASSO regression was performed to select the most effective variables from all miRNA-pairs to construct multivariate prediction models. Models included 1, 2, 3, 4 miRNA-pairs were established successively by a step-wise variable selection process in a LASSO regression, which is shown in **Table 1** (**Figure 2A**).

Plasma miRNA chip data of 24 CC and 73 NC from the testing group was used for internal validation. To fully maximize the performance of these models, four methods (LASSO regression, random forest, logistic regression and SVM) were simultaneously tested. High AUC results of at least 0.9 in each model were obtained, which suggested a good efficacy in CC detection (**Figures 2B–E**).

External Verification of Prediction Models by miRNA Chip Data

Another dataset (GSE112264) with plasma miRNA chip data of 50 CC and 41 NC was used for external verification. Four algorithms (LASSO regression, random forest, logistic regression and SVM) were applied to validate each of these models, and we finally obtained high AUC levels of over 0.7 in

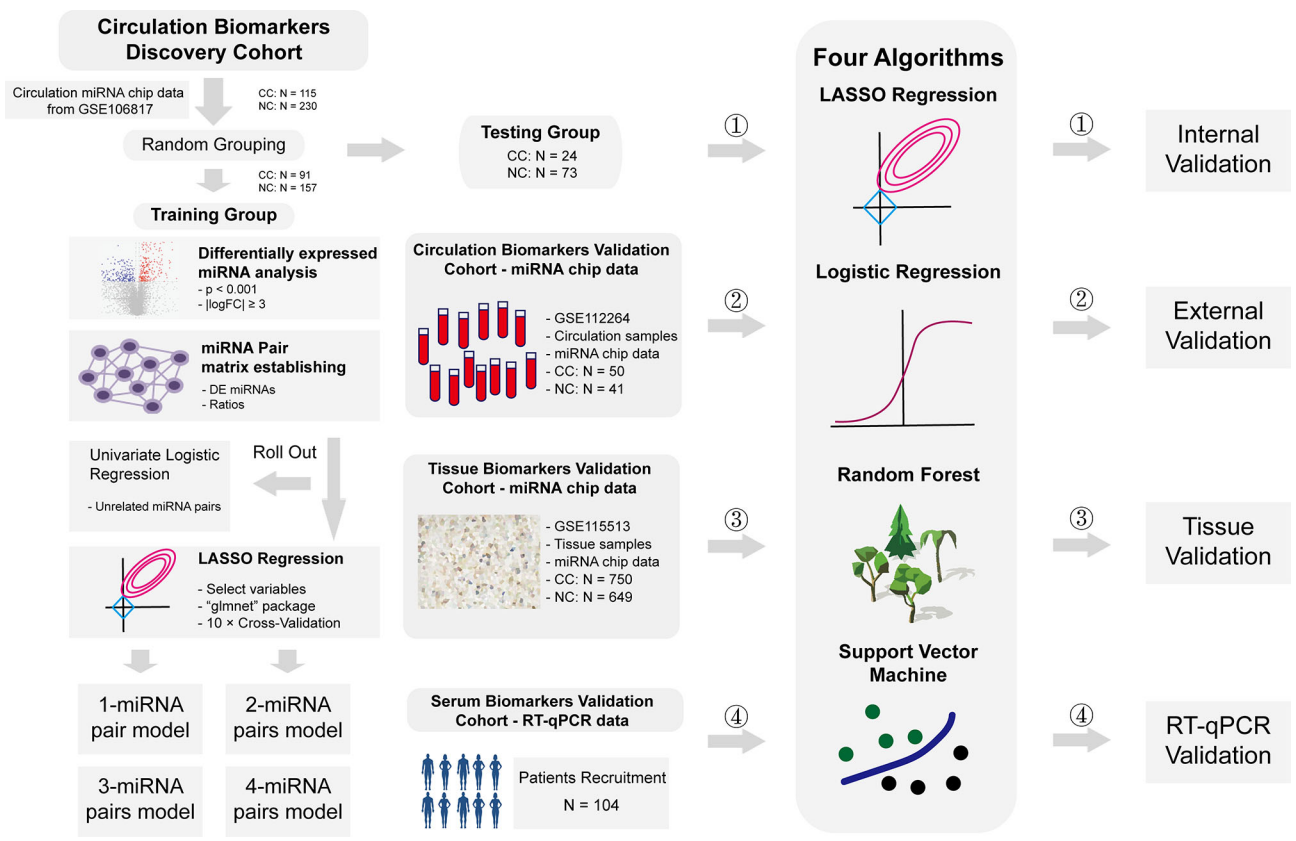

FIGURE 1 | Flowchart of study. Flowchart of this study. In short, we calculated the ratio of two given miRNAs in the same plasma sample, used this ratio as a new kind of variables, constructed a prediction system based on these ratios to predict risks of CC, and validated these models in internal level, external level, tissue level and RT-qPCR level.

TABLE 1 | Gene models established by LASSO regression.

miRNA-pair models	miRNA-pairs	coefficient	Lambda	AUC
1-miRNA-pair model	hsa-miR-1246/hsa-miR-451a	0.031	0.32	0.9683
2-miRNA-pair model	hsa-miR-1246/hsa-miR-451a	0.170	0.23	0.9686
	hsa-miR-1246/hsa-miR-4514	0.004		
3-miRNA-pair model	hsa-miR-1246/hsa-miR-451a	0.206	0.2	0.9719
	hsa-miR-1246/hsa-miR-4514	0.034		
	hsa-miR-654-5p/hsa-miR-575	0.0003		
4-miRNA-pair model	hsa-miR-1246/hsa-miR-451a	0.223	0.18	0.9753
	hsa-miR-1246/hsa-miR-4514	0.059		
	hsa-miR-654-5p/hsa-miR-575	0.002		
	hsa-miR-4299/hsa-miR-575	6.075		

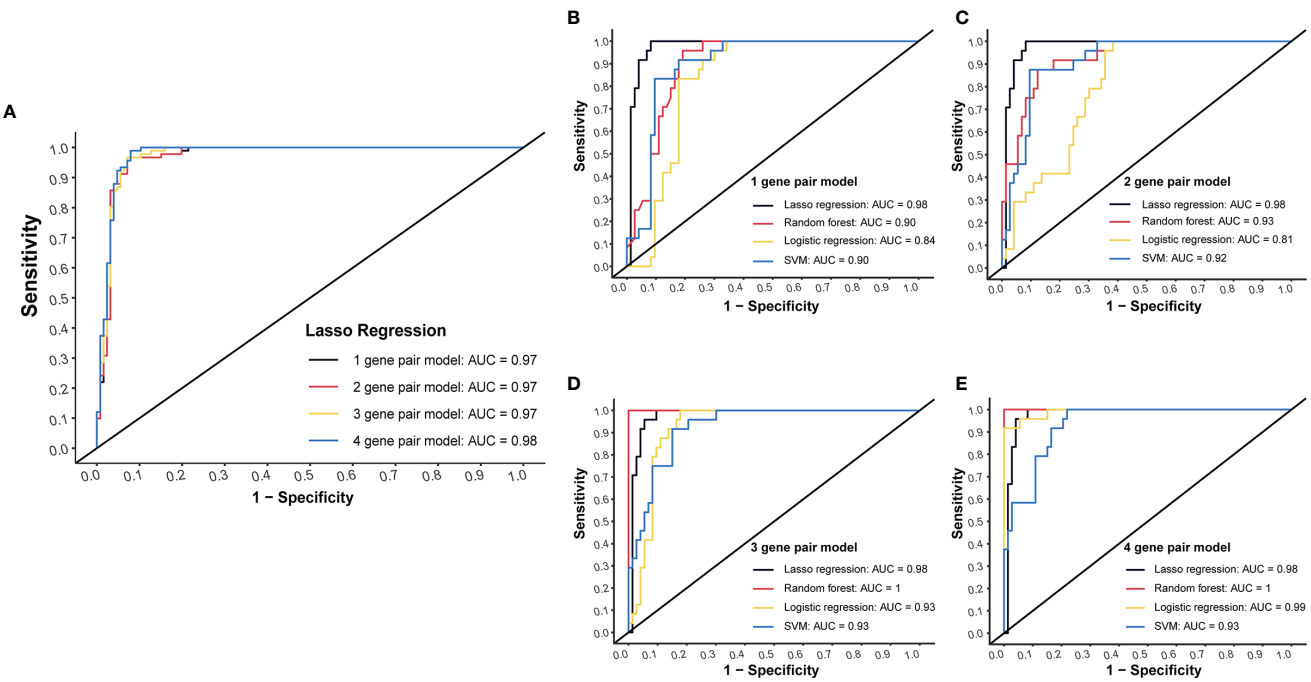

FIGURE 2 | Internal validation of four models by four methods. **(A)** Models included 1, 2, 3, 4 miRNA-pairs were established successively by a step-wise variable selection process in a LASSO regression. AUC levels of them were all more than 0.97. **(B)** Internal validation of 1-gene pair model using LASSO regression, random forest, logistic regression and SVM methods. **(C)** Internal validation of 2-gene pair model. **(D)** Internal validation of 3-gene pair model. **(E)** Internal validation of 4-gene pair model.

each model (**Figures 3A–D**). Especially, for the 4-miRNA-pair models, AUC of different algorithms was 0.8556, 0.9346, 0.7985, 0.7759, respectively (**Figure 3D**). Those results suggested a good reproducibility of our models in different cohorts.

Tissue Verification of Prediction Models by miRNA Chip Data

Generally, 3-miRNA-pair models and 4-miRNA-pair models with an AUC >0.8 could be considered as possibly applicable in clinical scenarios. To better understand their rationality, we further validated those constructed models in a tissue sample-derived miRNA chip dataset (GSE115513). For 3-miRNA-pair models, the SVM method could reach an AUC value of 0.71, while the AUC value of the logistic regression was 0.80 (**Figure 4A**). For 4-miRNA-pair models, the logistic regression method could reach an AUC value of 0.81 (**Figure 4B**). Those results exhibited reliable diagnostic performance of our prediction models in tissue samples.

Validation for Potential Clinical Application by RT-qPCR

Next, we conducted RT-qPCR assays to validate those models. For the 3-miRNA-pair model, SVM method could reach an AUC value of 0.71, which could boost to 0.82 when taking clinical information such as age and gender into consideration. However, logistic regression models gave a lower AUC level as compared to

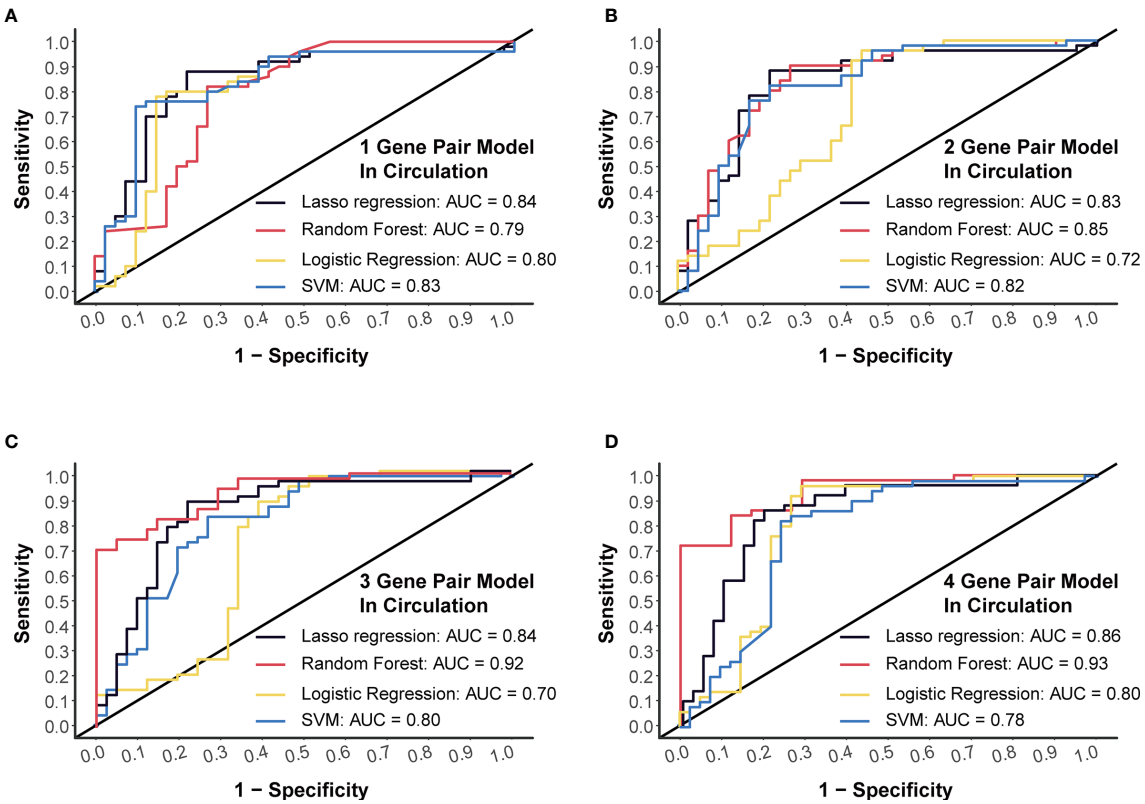

FIGURE 3 | External validation of four models using miRNA chip data. **(A)** External validation of 1-gene pair model using LASSO regression, random forest, logistic regression and SVM methods. **(B)** External validation of 2-gene pair model. **(C)** External validation of 3-gene pair model. **(D)** External validation of 4-gene pair model.

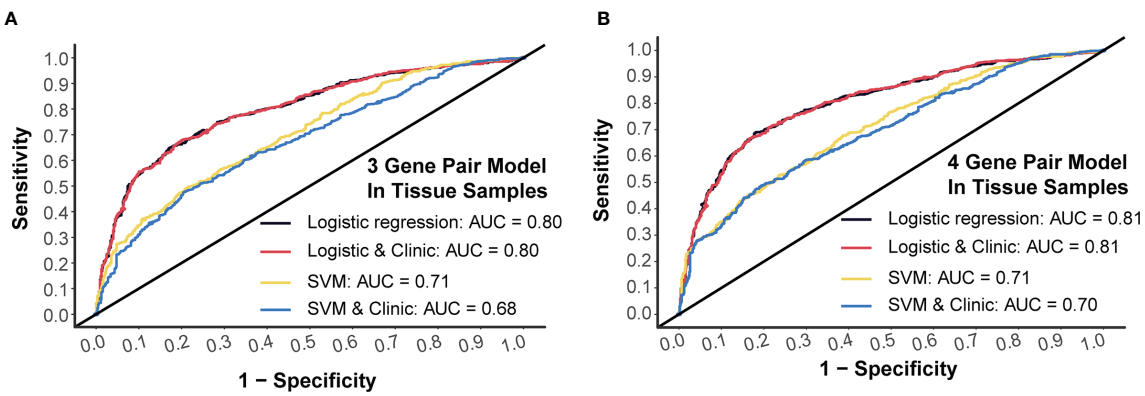

FIGURE 4 | External validation of prediction models in tissue samples. **(A)** Tissue validation of 3-gene pair model using logistic regression and SVM methods. **(B)** Tissue validation of 4-gene pair model using logistic regression and SVM methods.

SVM (**Figure 5A**). For the 4-miRNA-pair model, AUC of SVM was 0.78 and could increase to 0.88 when adding age and gender into this model (**Figure 5B**).

Then we performed subgroup analysis focusing on early CC patients and advanced CC patients, respectively. An AUC of 0.83 in the 3-miRNA-pair SVM model and an AUC of 0.92 in the 4-miRNA-pair SVM model were obtained when applying those models to distinguish 16 early CC patients from 48 normal controls (**Figures 5C, D**). Similarly, a sub-cohort consists of 40 advanced CC patients and 48 normal controls was also analyzed. The AUC reached to 0.81 in the 3-miRNA-pair SVM model and 0.85 in the 4-miRNA-pair SVM model (**Figures 5E, F**).

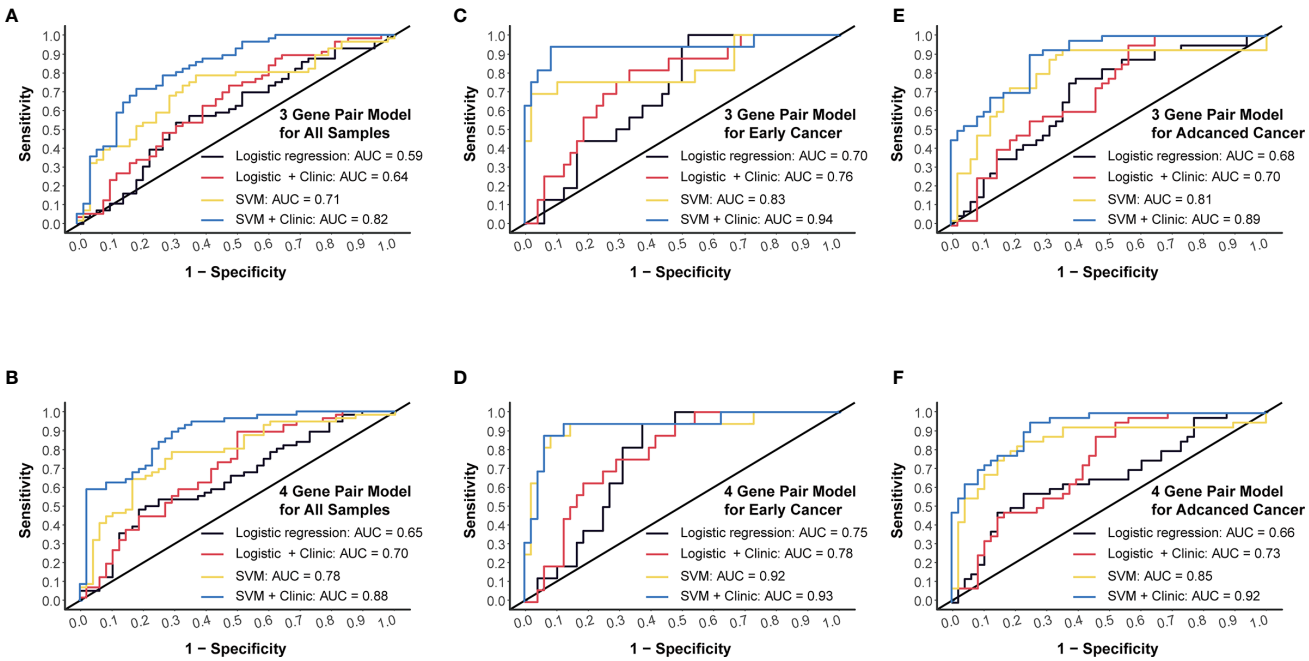

FIGURE 5 | External validation and subgroup analysis of selected models using plasma miRNA q-PCR data from Beijing Friendship Hospital. **(A)** External validation of 3-gene pair model using logistic regression and SVM methods. Red and blue lines represent adding patients' age and gender into consideration. **(B)** External validation of 4-gene pair model. **(C)** ROC assessment of 3-gene pair model predicting early cancer. **(D)** ROC assessment of 4-gene pair model predicting early cancer. **(E)** ROC assessment of 3-gene pair model predicting advanced CC. **(F)** ROC assessment of 4-gene pair model predicting advanced CC.

The comparable efficiencies between detecting early CC and advanced CC are inspiring, but the sample size is too small to draw a definite conclusion.

GSEA Analysis, GO Analysis and KEGG Pathway Analysis for the Involved miRNAs

Target genes of selected miRNAs were predicted by TargetScan based on their seed positions, which were shown in **Table 2**. GSEA analysis was then applied and showed target genes were mostly related to colorectal adenoma and colorectal cancer (**Figures 6A, B**).

KEGG analysis and GO analysis were also performed to find out gene functions and pathways affected by these miRNAs. KEGG analysis showed that target genes were mainly involved in HSV-1 infection and MAPK signaling pathway (**Figure 6C**). GO analysis showed that they were involved in regulation of cell morphogenesis (biological processes, **Figure 6D**), neuronal cell body (cellular component, **Figure 6E**), and small GTPase binding (molecular functions, **Figure 6F**).

TABLE 2 | Target gene analysis of miRNAs in prediction model.

miRNA	Target genes
hsa-miR-1246	CDR1as, FAM169B, GSG1L, ZNF23, ZNF267, ZNF83, MEIS3, ZFP69B, FAM53C, C12orf71
hsa-miR-451a	OSR1, ATF2, MIF, PSMB8, TSC1, S1PR2, C11orf30, AEBP2, GK, VAPA
hsa-miR-4514	AGO2, NBPF20, NBPF12, PRX, C19orf77, LCE1E, ZNF460, CYP4A22, NOTCH2, LCE1D
hsa-miR-654-5p	RSPO4, PRX, GUCA2B, GNG13, SYNDIG1L, PVRL1, FAM222B, PIP5K1C, PLEKHM1, RASD2
hsa-miR-575	ASPHD1, AC073610.5, HTN3, A4GNT, NANOGNB, AGAP2-AS1, BID, FOXRED1, PRSS46, REG4
hsa-miR-4299	ZNF256, ZIK1, SHISA7, MCTS1, ZNF584, BRIX1, SSMEM1, TEX12, ZNF772, DAZ4

DISCUSSION

Early detection of CC is clinically crucial but technically difficult, since the patients are hardly to exhibit any symptoms until turning into advanced stages (17). Traditional biomarkers (e.g., CEA and CA19-9) showed low sensitivity and specificity in cancer detection, which may cause missed and delayed diagnosis. Recently, an increasing number of researches focused on new biomarker types, such as plasma miRNAs (18). Plasma miRNAs are stable under various storage conditions and resistant to degradation, which made them good candidates for cancer biomarkers (6). For example, Vychytilova-Faltejskova et al. enrolled 144 colon cancer patients and 96 healthy controls, and sequencing 20 libraries each containing pooled RNA of 12 different cases (19). They constructed models by logistic regression and validated them in RT-qPCR data of 427 patients. This study had a large sample size and recorded many clinical details; however, only logistic regression was used for model construction, and the normalization method used in serum miRNA RT-qPCR quantification wasn't provided. María et al. enrolled 123 patients (63 with CRC, 60 with advanced

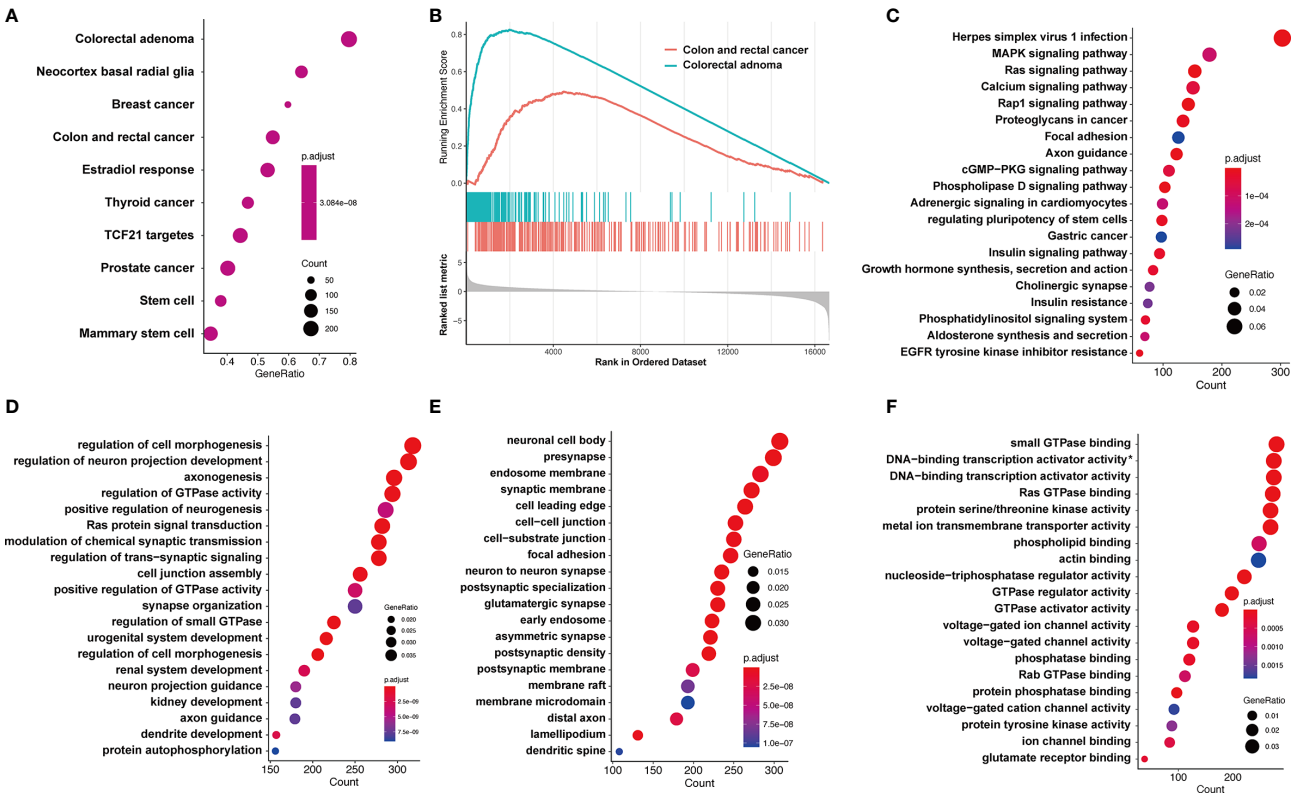

FIGURE 6 | GO analysis and KEGG pathway analysis. **(A, B)** GSEA analysis showed target genes were mostly related to colorectal adenoma and colorectal cancer. **(C)** KEGG analysis showed that target genes of miR-4299 were mainly involved in HSV-1 infection and MAPK signaling pathway. DEF. GO analysis showed that these target genes were involved in regulation of cell morphogenesis **(D)**, neuronal cell body **(E)** and small GTPase binding **(F)**. *: RNA polymerase II–specific.

adenomas) and 73 healthy controls, and identified 6 plasma miRNAs for CRC detection, which also represented good classifier abilities to advanced adenomas (20). This study had large sample volume and selected a relatively stable miRNA (miR-16) as internal reference; however, a proper modeling algorithm could make its diagnostic value better.

Among all detection methods, RT-qPCR is a proper method for clinical application for its low-cost as compared to miRNA-seq and miRNA chips (21). However, its accuracy was often questioned due to the low concentration of miRNAs in plasma and no reliable normalizer for quantification. There are two regular methods for plasma miRNA standardization. The most popular method is using traditional reference genes, such as U6 (22) and miR-16 (23), which have been considered stably expressed in human cells. However, even those reference miRNA could be dysregulated and exhibited a altered abundance in the circulation system in a disease-specific manner (24, 25). Consequently, those reference RNAs are not suitable for data normalization in circulating miRNA quantification. Spike-in exogenous miRNAs such as cel-miR-39, cel-miR-54, SV40 were also used as external references to partially eliminate deviations from experimental processes. However, these external controls could not correct sample specific deviations (26). Here we proposed a miRNA-pair ratio-based algorithm to quantitate plasma miRNA. We calculated the ratio of any two candidate miRNAs in the same sample, and taking these ratios as new variables to predict cancer occurrence. Considering that expression levels of two miRNAs were simultaneously measured under same conditions, their ratio could reflect true fold change ratio by canceling disturbance of different reference genes, which has been mathematically proved (27).

The thought using miRNA ratios to establish a prediction system for disease evaluation began in 2011. Mattia Boeri et al. performed a miRNA ratio signature study and found that signatures of miRNA ratios could reflect the prognosis of lung cancer patients with an AUC value >0.85 (28). However, the small sample size and a lack of demonstration of theoretical rationality largely weaken the confidence of their results. Then, Yu et al. mathematically verified miRNA-pair ratios to be independent of internal or external controls, which means miRNA ratios would remain stable no matter what inference genes were chosen (27). Thus, using miRNA-pair ratios instead of miRNA quantification could fully eliminate both experimental processes derived deviations and sample specific deviations. Here, for the first time, we constructed a full pipeline by using miRNA-pair ratio to construct prediction models for cancer diagnosis. Enrolled three independent cohorts with both miRNA

profiling and RT-qPCR data, we rigorously proved the robustness and cross-platform stability of this approach.

Our results suggested that a 4-miRNA-pair model could well differentiate CC patients from healthy controls with an AUC of 0.78. Stability is the major advantage of this algorithm. No matter which detection method was adopted and which reference gene was chosen, miRNA ratios would remain stable in a certain sample. Here we found that our prediction models could stay effective in both miRNA chip verification and RT-qPCR validation. This cross-platform property makes it more easily to be clinical applied, creates an opportunity for its further application in new detection methods such as microfluidics and thermophoresis.

Although we have assessed this new method in the field of cancer diagnosis and achieved good classifier ability, there were still many other fields worth exploring such as distinguishing chemotherapy/radiotherapy-sensitive CC patients, diagnosis of other cancers or noncancerous diseases, monitoring therapeutic responses. Moreover, although we have analyzed the potential pathways and biological processes involved in these miRNAs, inner connections and biological interaction between those miRNA-pairs still need in-depth investigation.

In conclusion, we have established a cross-platform prediction model robust against sample-specific disturbance, which is not only well-performed in predicting CC but also promising in the diagnosis of other diseases.

DATA AVAILABILITY STATEMENT

The original contributions presented in the study are included in the article/**Supplementary Material**. Further inquiries can be directed to the corresponding authors.

ETHICS STATEMENT

The studies involving human participants were reviewed and approved by Beijing Friendship Hospital Ethics Committee. The patients/participants provided their written informed consent to participate in this study.

AUTHOR CONTRIBUTIONS

DQ, LM, and SZha conceived and designed the study. DQ, RW, and QG performed all experiments. RW, SL, and SZhu helped to collect, reformat, and analyze the primary data. DQ and LM draft the manuscript. LM and SZha proofread and revise the manuscript. All authors contributed to the article and approved the submitted version.

FUNDING

This work was fully supported by National Natural Science Foundation of China (82073390, 81702314), Beijing Science and Technology Nova Program (Z191100001119128), Beijing Municipal Science and Technology Project (Z191100006619081), Beijing Municipal Administration of Hospitals' Youth Program (QML20180108), and The Digestive Medical Coordinated Development Center of Beijing Municipal Administration of Hospitals (XXZ02, XXZ01).

ACKNOWLEDGMENTS

The authors thank all the individuals who participated in this study.

SUPPLEMENTARY MATERIAL

The Supplementary Material for this article can be found online at: https://www.frontiersin.org/articles/10.3389/fonc.2021.561763/full#supplementary-material

REFERENCES

1. Sung H, Ferlay J, Siegel RL, Laversanne M, Soerjomataram I, Jemal A, et al. Global Cancer Statistics 2020: GLOBOCAN Estimates of Incidence and Mortality Worldwide for 36 Cancers in 185 Countries. *CA A Cancer J Clin* (2021), caac.21660. doi: 10.3322/caac.21660
2. Keum N, Giovannucci E. Global Burden of Colorectal Cancer: Emerging Trends, Risk Factors and Prevention Strategies. *Nat Rev Gastroenterol Hepatol* (2019) 16:713–32. doi: 10.1038/s41575-019-0189-8
3. Amin MB, Greene FL, Edge SB, Compton CC, Gershenwald JE, Brookland RK, et al. The Eighth Edition AJCC Cancer Staging Manual: Continuing to Build a Bridge From a Population-Based to a More "Personalized" Approach to Cancer Staging. *CA Cancer J Clin* (2017) 67:93–9. doi: 10.3322/caac.21388
4. Pawlik TM. Colon Cancer. *Surg Oncol Clin N Am* (2018) 27:xiii–xiv. doi: 10.1016/j.soc.2017.11.013
5. Melki G, Ghrewati M, Mohamed H, Barham S, Kapoor A, Ayoub F, et al. Re-Educating Residents About non-Invasive Colorectal Cancer Screening: an Approach to Improving Colon Cancer Screening Compliance. *Gastroenterol Res* (2019) 12:312–4. doi: 10.14740/gr1205
6. McDermott AM, Kerin MJ, Miller N. Identification and Validation of Mirnas as Endogenous Controls for RQ-PCR in Blood Specimens for Breast Cancer Studies. *PLoS One* (2013) 8:e83718. doi: 10.1371/journal.pone.0083718
7. Schwarzenbach H, da Silva AM, Calin G, Pantel K. Data Normalization Strategies for Microrna Quantification. *Clin Chem* (2015) 61:1333–42. doi: 10.1373/clinchem.2015.239459
8. Yokoi A, Matsuzaki J, Yamamoto Y, Yoneoka Y, Takahashi K, Shimizu H, et al. Integrated Extracellular Microrna Profiling for Ovarian Cancer Screening. *Nat Commun* (2018) 9:4319. doi: 10.1038/s41467-018-06434-4
9. Urabe F, Matsuzaki J, Yamamoto Y, Kimura T, Hara T, Ichikawa M, et al. Large-Scale Circulating Microrna Profiling for the Liquid Biopsy of Prostate Cancer. *Clin Cancer Res* (2019) 25:3016–25. doi: 10.1158/1078-0432.CCR-18-2849
10. Slattery ML, Herrick JS, Pellatt DF, Stevens JR, Mullany LE, Wolff E, et al. Microrna Profiles in Colorectal Carcinomas, Adenomas and Normal Colonic

Mucosa: Variations in Mirna Expression and Disease Progression. *Carcinogenesis* (2016) 37:245–61. doi: 10.1093/carcin/bgv249
11. Ritchie ME, Phipson B, Wu D, Hu Y, Law CW, Shi W, et al. Limma Powers Differential Expression Analyses for RNA-Sequencing and Microarray Studies. *Nucleic Acids Res* (2015) 43:e47–7. doi: 10.1093/nar/gkv007
12. Friedman J, Hastie T, Tibshirani R. Regularization Paths for Generalized Linear Models Via Coordinate Descent. *J Stat Softw* (2010) 33:1–22.
13. Sachs MC. Plotroc: a Tool for Plotting ROC Curves. *J Stat Softw* (2017) 79:2. doi: 10.18637/jss.v079.c02
14. Lewis BP, Burge CB, Bartel DP. Conserved Seed Pairing, Often Flanked by Adenosines, Indicates That Thousands of Human Genes are Microrna Targets. *Cell* (2005) 120:15–20. doi: 10.1016/j.cell.2004.12.035
15. Yu G, Wang L-G, Han Y, He Q-Y. Clusterprofiler: an R Package for Comparing Biological Themes Among Gene Clusters. *OMICS* (2012) 16:284–7. doi: 10.1089/omi.2011.0118
16. Kanehisa M, Goto S. KEGG: Kyoto Encyclopedia of Genes and Genomes. *Nucleic Acids Res* (2000) 28:27–30. doi: 10.1093/nar/28.1.27
17. Jung G, Hernández-Illán E, Moreira L, Balaguer F, Goel A. Epigenetics of Colorectal Cancer: Biomarker and Therapeutic Potential. *Nat Rev Gastroenterol Hepatol* (2020) 17:111–30. doi: 10.1038/s41575-019-0230-y
18. Cojocneanu R, Braicu C, Raduly L, Jurj A, Zanoaga O, Magdo L, et al. Plasma and Tissue Specific Mirna Expression Pattern and Functional Analysis Associated to Colorectal Cancer Patients. *Cancers* (2020) 12:843. doi: 10.3390/cancers12040843
19. Vychytilova-Faltejskova P, Radova L, Sachlova M, Kosarova Z, Slaba K, Fabian P, et al. Serum-Based Microrna Signatures in Early Diagnosis and Prognosis Prediction of Colon Cancer. *Carcinogenesis* (2016) 37:941–50. doi: 10.1093/carcin/bgw078
20. Giráldez MD, Lozano JJ, Ramírez G, Hijona E, Bujanda L, Castells A, et al. Circulating Micrornas as Biomarkers of Colorectal Cancer: Results From a Genome-Wide Profiling and Validation Study. *Clin Gastroenterol Hepatol* (2013) 11:681–8.e3. doi: 10.1016/j.cgh.2012.12.009
21. Donati S, Ciuffi S, Brandi ML. Human Circulating Mirnas Real-Time Qrt-PCR-Based Analysis: an Overview of Endogenous Reference Genes Used for Data Normalization. *Int J Mol Sci* (2019) 20:4353. doi: 10.3390/ijms20184353
22. Xiang M, Zeng Y, Yang R, Xu H, Chen Z, Zhong J, et al. U6 is Not a Suitable Endogenous Control for the Quantification of Circulating Micrornas. *Biochem Biophys Res Commun* (2014) 454:210–4. doi: 10.1016/j.bbrc.2014.10.064
23. Ge W, Yu D-C, Li Q-G, Chen X, Zhang C-Y, Ding Y-T. Expression of Serum Mir-16, Let-7f, and Mir-21 in Patients With Hepatocellular Carcinoma and Their Clinical Significances. *Clin Lab* (2014) 60:427–34. doi: 10.7754/clin.lab.2013.130133
24. Chugh P, Dittmer DP. Potential Pitfalls in Microrna Profiling. *Wiley Interdiscip Rev RNA* (2012) 3:601–16. doi: 10.1002/wrna.1120
25. Benz F, Roderburg C, Vargas Cardenas D, Vucur M, Gautheron J, Koch A, et al. U6 is Unsuitable for Normalization of Serum Mirna Levels in Patients With Sepsis or Liver Fibrosis. *Exp Mol Med* (2013) 45:e42. doi: 10.1038/emm.2013.81
26. Occhipinti G, Giulietti M, Principato G, Piva F. The Choice of Endogenous Controls in Exosomal Microrna Assessments From Biofluids. *Tumour Biol* (2016) 37:11657–65. doi: 10.1007/s13277-016-5164-1
27. Deng Y, Zhu Y, Wang H, Khadka VS, Hu L, Ai J, et al. Ratio-Based Method to Identify True Biomarkers by Normalizing Circulating Ncrna Sequencing and Quantitative PCR Data. *Anal Chem* (2019) 91:6746–53. doi: 10.1021/acs.analchem.9b00821
28. Boeri M, Verri C, Conte D, Roz L, Modena P, Facchinetti F, et al. Microrna Signatures in Tissues and Plasma Predict Development and Prognosis of Computed Tomography Detected Lung Cancer. *Proc Natl Acad Sci U S A* (2011) 108:3713–8. doi: 10.1073/pnas.1100048108

Conflict of Interest: The authors declare that the research was conducted in the absence of any commercial or financial relationships that could be construed as a potential conflict of interest.

Copyright © 2021 Qin, Guo, Wei, Liu, Zhu, Zhang and Min. This is an open-access article distributed under the terms of the Creative Commons Attribution License (CC BY). The use, distribution or reproduction in other forums is permitted, provided the original author(s) and the copyright owner(s) are credited and that the original publication in this journal is cited, in accordance with accepted academic practice. No use, distribution or reproduction is permitted which does not comply with these terms.

frontiers in Cell and Developmental Biology

ORIGINAL RESEARCH
published: 22 April 2021
doi: 10.3389/fcell.2021.641978

Evaluation of Monocarboxylate Transporter 4 (*MCT4*) Expression and Its Prognostic Significance in Circulating Tumor Cells From Patients With Early Stage Non-Small-Cell Lung Cancer

Athina Markou[1], E. Tzanikou[1], G. Kallergi[2], E. Pantazaka[2], V. Georgoulias[3], A. Kotsakis[4] and E. Lianidou[1]*

[1] Analysis of Circulating Tumor Cells, Lab of Analytical Chemistry, Department of Chemistry, University of Athens, Athens, Greece, [2] Division of Genetics, Cell and Developmental Biology, Department of Biology, University of Patras, Patras, Greece, [3] First Department of Medical Oncology, IASO General Hospital of Athens, Athens, Greece, [4] Department of Medical Oncology, University General Hospital of Larissa, Thessaly, Greece

OPEN ACCESS

Edited by:
Catherine Alix-Panabieres, Centre Hospitalier Universitaire de Montpellier, France

Reviewed by:
Holger Kalthoff, University of Kiel, Germany
Talib Hassan Ali, University of ThiQar, Iraq

***Correspondence:**
Athina Markou
atmarkou@chem.uoa.gr

Specialty section:
This article was submitted to Molecular and Cellular Oncology, a section of the journal Frontiers in Cell and Developmental Biology

Received: *15 December 2020*
Accepted: *23 March 2021*
Published: *22 April 2021*

Citation:
Markou A, Tzanikou E, Kallergi G, Pantazaka E, Georgoulias V, Kotsakis A and Lianidou E (2021) Evaluation of Monocarboxylate Transporter 4 (MCT4) Expression and Its Prognostic Significance in Circulating Tumor Cells From Patients With Early Stage Non-Small-Cell Lung Cancer. Front. Cell Dev. Biol. 9:641978. doi: 10.3389/fcell.2021.641978

Purpose: Monocarboxylate transporter 4 (*MCT4*) can influence the amount of lactate in the tumor microenvironment and further control cancer cell proliferation, migration, and angiogenesis. We investigated for the first time the expression of *MCT4* in circulating tumor cells (CTCs) derived from early stage Non-Small Cell Lung Cancer patients (NSCLC) and whether this is associated with clinical outcome.

Experimental Design: A highly sensitive RT-qPCR assay for quantification of *MCT4* transcripts was developed and validated and applied to study *MCT4* expression in CTC isolated through the Parsortix size-dependent microfluidic device from 53 and 9 peripheral blood (PB) samples of NSCLC patients at baseline (pre-surgery) and at relapse, respectively, as well as the "background noise" was evaluated using peripheral blood samples from 10 healthy donors (HD) in exactly the same way as patients.

Results: *MCT4* was differentially expressed between HD and NSCLC patients. Overexpression of *MCT4* was detected in 14/53 (26.4%) and 3/9 (33.3%) patients at baseline and at progression disease (PD), respectively. The expression levels of *MCT4* was found to increase in CTCs at the time of relapse. Kaplan-Meier analysis showed that the overexpression of *MCT4* was significantly ($P = 0.045$) associated with progression-free survival (median: 12.5 months, range 5–31 months).

Conclusion: *MCT4* overexpression was observed at a high frequency in CTCs from early NSCLC patients supporting its role in metastatic process. *MCT4* investigated as clinically relevant tumor biomarker characterizing tumor aggressiveness and its potential value as target for cancer therapy. We are totally convinced that *MCT4* overexpression in CTCs merits further evaluation as a non-invasive circulating tumor biomarker in a large and well-defined cohort of patients with NSCLC.

Keywords: liquid biopsy, CTCs, NSCLC, *MCT4*, RT-qPCR, EMT 3

INTRODUCTION

Lung cancer remains the most commonly diagnosed cancer and the leading cause of cancer death globally. Non-Small Cell Lung Cancer (NSCLC) is the common histological subtype of the disease, accounting for 85% of all lung cancer diagnoses (Molina et al., 2008). Almost 45% of patients with operable early stage NSCLC relapse within the first 18 months and the probability of patients' survival depends on the possibility of early detection of relapse (Siegel et al., 2015). The use of targeted therapy such as tyrosine kinase inhibitors (TKIs) and/or immunotherapy has led to unprecedented survival benefits in selected patients (Wu et al., 2020). Moreover, the use of therapeutic modalities against the Minimal Residual Disease (MRD) and before the development of clinically detectable metastatic lesions seems to be emerged as an important advancement in the management of early stage NSCLC. Indeed, it has been recently reported that the administration of Osimertinib in the context of adjuvant treatment in resected EGFR mutant NSCLC significantly reduced the relapse rate and prolonged the overall survival (Wu et al., 2020). The possibility of probing the early detection of NSCLC via a blood draw –termed as "liquid biopsy"- has attracted remarkable interest among the oncology community (Pawlikowska et al., 2019; Tamminga et al., 2019; Frick et al., 2020). Different tumor-derived components can be isolated from blood, including Circulating Tumor Cells (CTCs), circulating tumor DNA (ctDNA), cellfree RNA (cfRNA), exosomes, and tumor-educated platelets (TEP), providing information about the dynamic tumor profile over time (Heidrich et al., 2020). The FDA has approved the use of ctDNA for the response prediction and monitoring development resistance to EGFR TKI therapy in NSCLC patients (Wang et al., 2017; Zhang et al., 2017).

The application of liquid biopsy in NSCLC is being used for the diagnosis, prognosis and monitoring of disease based on signature molecular markers (Luo et al., 2018). However, the clinical significance of CTC enumeration in NSCLC is yet to be established since due to the EMT process, EpCAM-independent methods are required in order to isolate and characterize CTCs from NSCLC patients. Indeed, molecular characterization of CTCs got potential for the improvement of our knowledge in the field of metastatic process, the identification of new treatment predictive markers and stratification of patients into prognostic groups.

The CellSearch® system, which is the only FDA approved assay for CTC detection in metastatic breast, colorectal and prostate cancers but is able to identify CTCs only in about 23–39% of stage IV NSCLC patients (Krebs et al., 2012). Detection of CTCs in NSCLC has been challenging due to the rarity of these cells in circulation and the presence of non-epithelial characteristics due to epithelial mesenchymal transition (EMT) (Lianidou et al., 2015). EMT is characterized by down-regulation of epithelial markers, such as cytokeratin's (CKs), and up-regulation of mesenchymal markers like *Vimentin* (*VIM*).

Three metabolic properties of cancer cells (a) glucose uptake, (b) lactate secretion and (c) oxygen availability constitute the Warburg effect which attracts the interest of the scientific community for a many years (Warburg, 1956; DeBerardinis and Chandel, 2020). Moreover, Reprogramming Energy Metabolism is an Emerging Hallmark for cancer (Hanahan and Weinberg, 2011). Monocarboxylic acids including lactate play a crucial role in cellular metabolism, and their regulation has become a new target for understanding the pathogenesis of abnormal cellular processes such as oncogenesis (Poole and Halestrap, 1993; Halestrap and Price, 1999). These acids must be rapidly transported across the plasma membrane of cells and this transportation is mediated by proton-linked monocarboxylate transporters (MCTs). *MCT4* is highly expressed in glycolytic tissues such as white skeletal muscle fibers, astrocytes, white blood cells, and chondrocytes, and it plays an important role in lactate efflux from cells (Meredith and Christian, 2008). *MCT4* can control the amount of lactate in the tumor microenvironment regulating cancer cell proliferation, migration, and angiogenesis. *MCT4* expression in the tumor microenvironment has been associated with decreased overall survival (OS) (Nakayama et al., 2012; Baek et al., 2014; Doyen et al., 2014; Zhu et al., 2014), and decreased disease-free survival (DFS) in cancer patients (Curry et al., 2013; Doyen et al., 2014; Zhu et al., 2014). Moreover, *MCT4* has been proposed as a new therapeutic target in several tumor types including NSCLC (Kim et al., 2018; Kuo et al., 2020; Puri and Juvale, 2020).

In the current study, we first developed and validated a highly sensitive RT-qPCR assay for the quantification of *MCT4* transcripts, and report for the first time that *MCT4* is overexpressed in CTC isolated from patients with early NSCLC. We further evaluated whether *MCT4* overexpression in CTC is associated with DFS. Our findings indicate that *MCT4* overexpression in CTCs should be prospectively evaluated as a potential biomarker for early relapse in patients with resected NSCLC.

MATERIALS AND METHODS

Clinical Samples

Fifty three patients with early stage NSCLC were enrolled in the study and 62 peripheral blood samples (25 mL in EDTA tubes) from these patients were prospectively collected; 53 samples were obtained at baseline (pre-surgery), and 9 samples at the time of relapse whilst 10 peripheral blood samples from healthy donors (HD) were used as controls. For 12 patients that have been randomly chosen, 10 mL peripheral blood from the same blood draws were used to perform CTCs' IF analysis. The first 5 mL of blood were discarded in order, to avoid contamination from skin epithelial cells. All patients gave a written informed consent to participate in the study, which was approved by the Ethics and Scientific Committee of Thoracic Diseases General Hospital Sotiria. All HD had no known illness or fever at the time of draw, no history of malignant disease, and were $\geq$35 years old. Clinical samples were collected from 32 men and 21 women (median age: 65.2 years, range: 39–81) and all patients were diagnosed with operable (stage IA–IIIA) NSCLC. 23 patients were diagnosed with adenocarcinoma (ADC), 26 with Squamous Cell Carcinoma (SCC) and 4 with undifferentiated (NOS) NSCLC. Thirty-eight (71.6%) patients

had no evidence of disease infiltration in resected lymph nodes (N0 disease). The main patients' characteristics are summarized in **Supplementary Table 1**.

CTCs Enrichment Using the Parsortix Size-Based Microfluidic Device

Micro-fluidic device named as Parsortix (ANGLE plc, United Kingdom) (Hvichia et al., 2016) was used to for the isolation of CTCs from 25 mL whole blood. A microscope slide sized disposable cassette was used for the division of blood components (Chudziak et al., 2016; Porras et al., 2018). After that, CTCs were collected in a total volume of 200 μL of PBS into tubes. The isolation of total RNA from enriched CTCs was performed by TRIZOL-LS (Thermo Fisher Scientific, United States), and finally cDNA synthesis of the extracted total RNA was carried out as previously described (Strati et al., 2017; Zavridou et al., 2018).

CTCs Isolation by ISET System

For the isolation of CTCs with the ISET (Isolation by SizE of Tumor cells) platform (Rarecells Diagnostics, France) 10 mL of peripheral blood was used. At first, each sample was diluted in 1:10 ISET buffer (Rarecells Diagnostics) and was incubated for 10 min at room temperature (RT). 100 mL of the diluted sample was filtered using a depression tab adjusted at −10 kPa. Finally, the membrane was dried for 2 h at RT and stored at −20°C. Each membrane spot was used for identification of CTCs after immunostaining and fluorescence microscopy analysis (Kallergi et al., 2016).

RT-qPCR Assay for M*CT4* Expression

In silico study for the design of the primers and TaqMan probes for *MCT4* and *B2M* (used as a reference gene) was carefully performed using Primer Premier 5.0 software. In order to ensure the specificity of all primers and probe sequences BLAST analysis was carried out (NCBI, nucleotide BLAST). Moreover, we carefully designed our primers and probes to completely avoid primer–dimer formation, false priming sites, formation of hairpin structures and hybridization to genomic DNA. The sequences of primers and probes are available in **Supplementary Table 3**.

RT-qPCR was performed in the LightCycler® 480 instrument (Roche, Germany). Detailed optimization experiments were carried out (results not shown). The amplification reaction mixture for *MCT4* contained 2 μL of the PCR synthesis buffer (5×), 1 μL $MgCl_2$ (25 mM), 0.2 μL dNTPs (10 mM), 0.15 μL BSA (10 μg/μL), 0.1 μL Hot-Start DNA polymerase (Promega), 0.3 μL of forward and reverse primer (10 μM), 1 μL hydrolysis probe (3 μM) and H_2O to a final volume of 10 μL while the amplification reaction mixture for B2M contained 1 μL of PCR synthesis buffer (5×), 1.2 μL $MgCl_2$ (25 mM), 0.15 μL dNTPs (10 mM), 0.3 μL BSA (10 μg/μL), 0.1 μL Hot-Start DNA polymerase (Promega), 0.25 μL of forward and reverse primer (10 μM), 0.83 μL hydrolysis probe (3 μM) and H_2O to a final volume of 10 μL. Each experimental procedure included one positive and one negative control. cDNA from MCF-7 cell line was used as a positive control. In order to ensure that amplification of gDNA was completely avoided, four genomic DNAs at high concentrations were used as templates. None of these DNA samples were amplified. *B2M* was used as a reference gene for RT-qPCR. In addition, single RT-qPCR was performed for epithelial markers *(CK-19*, *CK-8*, *CK-18)* and for EMT markers (*TWIST-1* and *VIM*) as previously described (Markou et al., 2018; Strati et al., 2019).

RT-qPCR data for *MCT4* expression were normalized in respect to *B2M* expression in the same cDNAs, using the $2^{-\Delta\Delta Ct}$ approach (Livak and Schmittgen, 2001). CTCs isolated through micro-fluidics device are not 100% pure; since the presence of co-isolated PBMC in CTC fractions could affect the specificity of the MCT4 assay, we evaluated this "background noise" by analyzing peripheral blood samples from 10 HD in exactly the same way as patients. We estimated a cut-off based on *MCT4* normalized expression in respect to *B2M* expression in this control group. Using this approach we defined a sample as positive for *MCT4* overexpression (MCT4 positive) based on the fold change of *MCT4* expression in the CTC fraction in respect to the corresponding fraction in the group of the 10 HD.

Immunostaining and Confocal Imaging

ISET filters were washed with PBS and permeabilized with 0.5% Triton-X-100 in PBS for 10 min at 20°C. Non-specific antibody binding was blocked by incubation with 10% FBS in PBS for 1 h at 20°C. To identify CK, filters were incubated with a cocktail of mouse anti-CK7 antibody (Invitrogen, United States; 1:100 dilution in PBS with 1% FBS) and mouse A45 B/B3 anti-human cytokeratin (Amgen, United States); 1:70 dilution in PBS with 1% FBS) for 1 h at 20°C. Filters were washed (3 × 5 min) with PBS and then incubated with goat anti-mouse Alexa Fluor® 488 secondary antibody (Life Technologies, United States; 1:500 dilution in PBS with 1% FBS) for 45 min at 20°C. Filters were washed (3 × 5 min) with PBS and then incubated with rabbit anti-VIM antibody (Abcam, 1:500 dilution in PBS with 1% FBS) for 1 h at 20°C. After washing (3 × 5 min) with PBS, filters were incubated with goat anti-rabbit Alexa Fluor® 555 secondary antibody (Life Technologies; 1:600 dilution in PBS with 1% FBS) for 45 min at 20°C. Filters were washed (3 × 5 min) with PBS and mounted in Prolong anti-fade mounting medium containing DAPI (Cell signaling, United States). Slides were stored at −20°C before confocal imaging.

Cytospins with H1299 cells were used as controls (**Supplementary Figure 1**). One positive control (stained with all antibodies) and two negative controls (omitting one of the first antibodies) were used. Slides were washed with PBS and cells were fixed/permeabilized with ice-cold acetone/methanol (9:1) for 20 min and, thereafter, non-specific antibody binding was blocked by incubation with 5% FBS overnight at 4°C.

All imaging used a Leica (Germany) TCS SP8 confocal microscope with a ×40 oil-immersion objective. In all dual-labeling analyses we confirmed, with the use of the controls, that there was no bleed-through between the two wavelengths. Cyto-morphological criteria proposed by Meng et al. (2004) (such as high nuclear/cytoplasmic ratio, etc.) were used in order to characterize a CK-positive cell as a CTC.

Statistical Analysis

SPSS program was used for the statistical analysis of our data (SPSS Statistics 25.0, company, Armonk, NY, United States). In order to estimate the differences between groups chi-square test of independence or Fisher exact test (SPSS, version 25.0) was used. Kaplan–Meier analysis used to evaluate "time-to-event" data. Parametric and non-parametric tests were used to compare continuous variables between groups. Non-parametric tests were used to analyze the relationship between *MCT4* expression and various clinicopathological characteristics for each patient (the Mann–Whitney and χ^2-test between 2 groups and the Kruskall Wallis test for 3 or more groups). All *P*-values are two-sided. A level of $P < 0.05$ is considered statistically significant unless specified otherwise.

RESULTS

The outline of the study is shown in **Figure 1**.

Phenotypic Evaluation of *CK* and *VIM* in CTCs

CTCs were detected in 14 of 16 (87.5%) patients with early stage NSCLC. The mean and median numbers of CTCs per patient were 4.6 and 1 (range, 0–20), respectively. The absolute number of CTCs per patient for each distinct phenotype is shown in **Table 1**. Double-staining experiments (*VIM/CK*) and confocal laser scanning analysis revealed an heterogeneous expression of *CK* and *VIM*. Indeed, CTCs had low expression of *CKs* (lower than the CK expression in control H1299 cells) (**Supplementary Figure 2**); $VIM^{+}CK^{low}$ CTCs could be detected in 12 out of 16 patients (75%) and $VIM^{-}CK^{low}$CTCs in 37.5% (6 of 16) of patients.

TABLE 1 | The absolute number of CTCs per patient for $CK^{low}VIM^{+}$ and $CK^{low}VIM^{-}$ phenotype.

	Number of cells	
PATIENT	**$CK^{low}VIM^{+}$**	**$CK^{low}VIM^{-}$**
#1	8	6
#2	5	0
#3	5	2
#4	4	0
#5	3	0
#6	20	0
#7	0	2
#8	3	0
#9	11	1
#10	6	0
#11	3	0
#12	0	0
#13	1	0
#14	3	1
#15	0	0
#16	0	3

Gene Expression of CTCs Using RT-qPCR

Epithelial Markers

cDNAs isolated from clinical samples were further analyzed for epithelial markers (*CK8, CK18, CK19*) using our previously developed and analytically validated RT-qPCR assays. At baseline, *CK8* expression was detected in 8/53 (15.1%), while *CK18* and *CK19* were detected in 14/53 (26.4%) and 14/53 (26.4%), respectively. In total, in 27/53 (50.9%) samples were detected at least one CK marker (**Figure 2**).

EMT Markers

The expression of EMT markers *TWIST-1* and *VIM* was also evaluated in the same cDNAs, using our previously developed and analytically validated RT-qPCR assay (Markou et al., 2018; Strati et al., 2019). *TWIST-1* was overexpressed in 11/53 (20.7%) of samples, while *VIM* in 35/53 (66%) of samples. In total, at least one EMT marker was detected in 41/53 (77.3%) samples (**Figure 2**).

MCT4 Expression in CTC of Healthy Individuals and NSCLC Patients

Overexpression of *MCT4* transcripts could be detected in 14/53 (26.4%) patient samples. The evaluation of the differences in the expression of *MCT4* in CTC between HD and early stage NSCLC patients revealed a significantly higher expression of *MCT4*. As can be seen in **Figure 3**, the overexpression of *MCT4* differed significantly in patient's samples compared to HD's samples ($P = 0.036$; **Figure 3**). For a subgroup of these patients ($n = 9$), peripheral blood samples were available both at baseline and at the time of relapse. In this group, *MCT4* overexpression was observed in 6/18 (33.3%) CTC fraction samples [in 3/9 (33.3%) at baseline and 3/9 (33.3%) at disease progression. In two of these three cases both CTC fractions at baseline and time of relapse were found to be positive for *MCT4* overexpression. There was one case where *MCT4* overexpression was detected only in the baseline, but not at progression disease whereas there was one case where the sample was found to be positive for *MCT4* overexpression in the time of relapse. Moreover, there was only one case where the patient was identified to decrease the expression levels of MCT4 at the time of relapse in respect to the baseline sample but it seemed to remain overexpressed (**Figure 4**).

Prognostic Significance of MCT4 Expression in CTCs

The correlation between the expression levels of *MCT4* in CTCs and prognosis was further analyzed. During of follow-up period (median: 12.5, range: 5–31 months) 14/53 (26.4%) NSCLC patients developed metastases. Kaplan–Meier survival analysis demonstrated that patients who overexpressed *MCT4* ($n = 14$) had a significantly shorter DFI than those without *MCT4* overexpression ($P = 0.045$; **Figure 5**). Moreover, as can been seen in **Supplementary Table 2**, *MCT4* overexpression was not correlated with gender, smoking history, tumor size, lymph node status, and stage of disease in the population studied ($P > 0.05$).

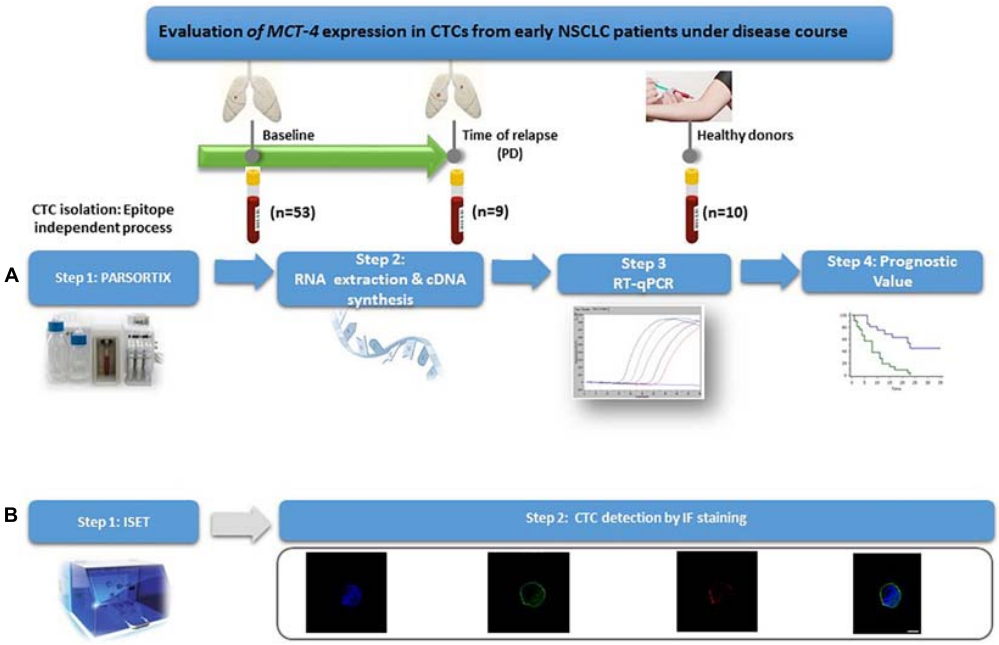

FIGURE 1 | Outline of the experimental procedure. **(A)** Gene expression profiling of CTCs. **(B)** Phenotypic evaluation of CTCs.

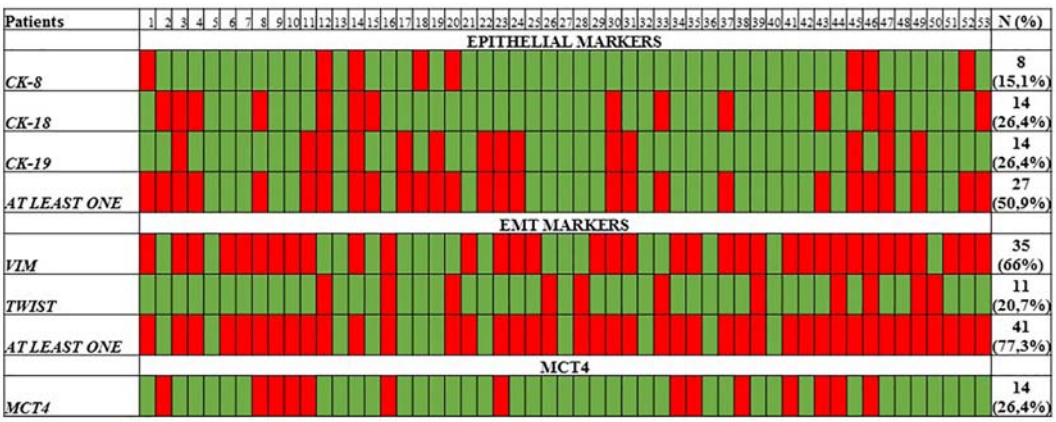

FIGURE 2 | Heat map of *CK-8/CK-18/CK-19* epithelial markers, *VIM*, *TWIST-1,* and *MCT4* as quantified by RT-qPCR.

DISCUSSION

Increased rates of glycolysis is one of the molecular mechanisms that has been studied for initiation of cancer cell metastasis (Wang et al., 2015). Warburg et al. (1927) have shown that cancer cells have an increased rate of glucose uptake and favored production of lactate, even in the normoxic conditions. It is well-known that cancer cells in order to avoid apoptosis and cellular acidosis export the intracellular lactate and monocarboxylate transporters (MCTs) play a critical role in this exportation (Halestrap and Price, 1999). This mainly performed through the action of *MCT1* and *MCT4* that control intracellular pH in cells relying on high glycolysis rates, such as red blood cells, skeletal muscle cells and tumor cells (Halestrap and Price, 1999; Halestrap, 2013). Although the expression of MCT4 in the tumor microenvironment has been associated with poor prognosis (Nakayama et al., 2012; Baek et al., 2014) and MCT4 has been studied as a new therapeutic target (Kim et al., 2018; Puri and Juvale, 2020). Immunofluoresence has been used for the detection of MCT 1 and MCT4 in cancer patient's CTC by Kershaw et al. (2015) but so far there is no any other reference on *MCT4* expression at the mRNA level on CTCs.

In the present study, we evaluated for the first time *MCT4* expression in CTC fractions isolated by a size- based EpCAM independent technology (Parsortix) from early stage NSCLC patients using a highly sensitive and specific RT-qPCR

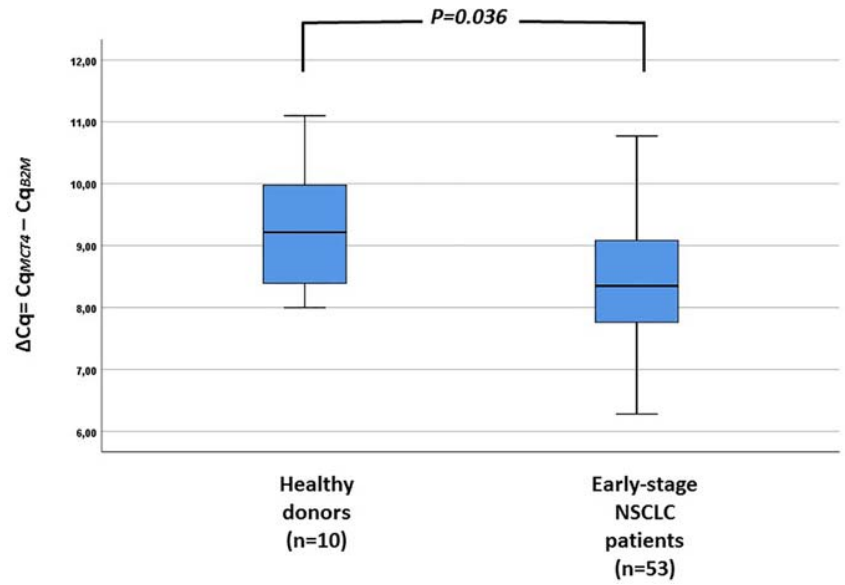

FIGURE 3 | Expression levels of *MCT4* in CTC fractions of HD (n = 10) and early stage NSCLC patients (n = 53).

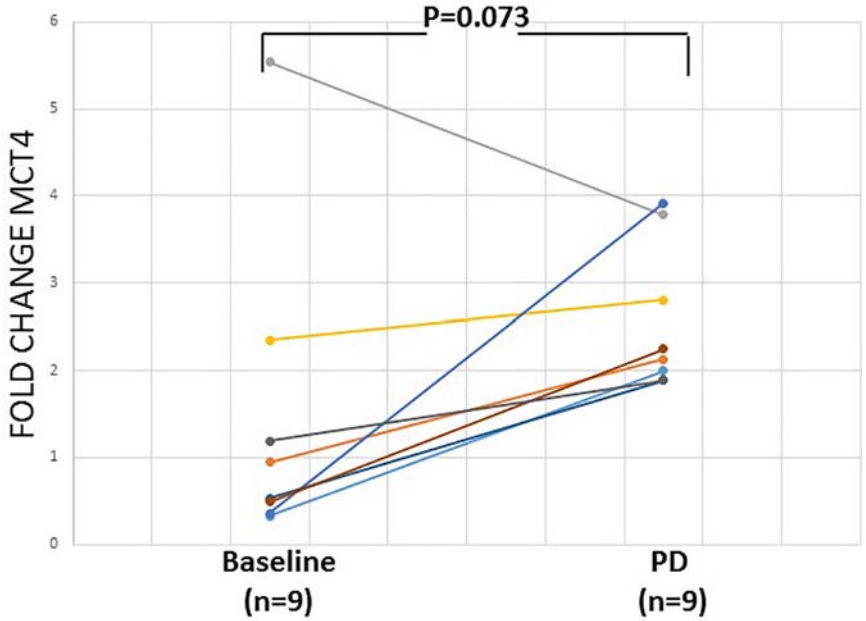

FIGURE 4 | Relative fold change ($2^{-\Delta\Delta Cq}$) of *MCT4 in* CTCs of 9 pairs of early stage NSCLC patient samples at the baseline and at the time of relapse.

assay. *MCT4* plays a critical role in energy production, tumor proliferation and invasion since lactic acid is secreted by cancer cells and acidify the tumor microenvironment (Shu et al., 2016). The inhibition of *MCT4* protein has been suggested as a novel therapeutic approach for many malignancies including NSCLC (Kuo et al., 2020). Bioinformatic analyses of the TCGA datasets demonstrated that *MCT4* is elevated in 9% of lung adenocarcinomas cases. Our findings indicate that *MCT4* is overexpressed at 14/53 (26.4%) on CTC fractions of early stage NSCLC patients. A similar positivity rate (26.4%) was also detected for epithelial markers (*CK18* and *CK19*) while the positivity rate was increased (66%) regarding the EMT marker *VIM* indicating that in NSCLC a large fraction of CTCs is under EMT status which is further supported by the observation that 13 out of 14 (92.8%) of *MCT4* overexpressed samples were found to express at least one EMT marker; conversely, the correspondent proportion of blood samples harboring at least one epithelial marker was 50%.These findings are consistent with previous

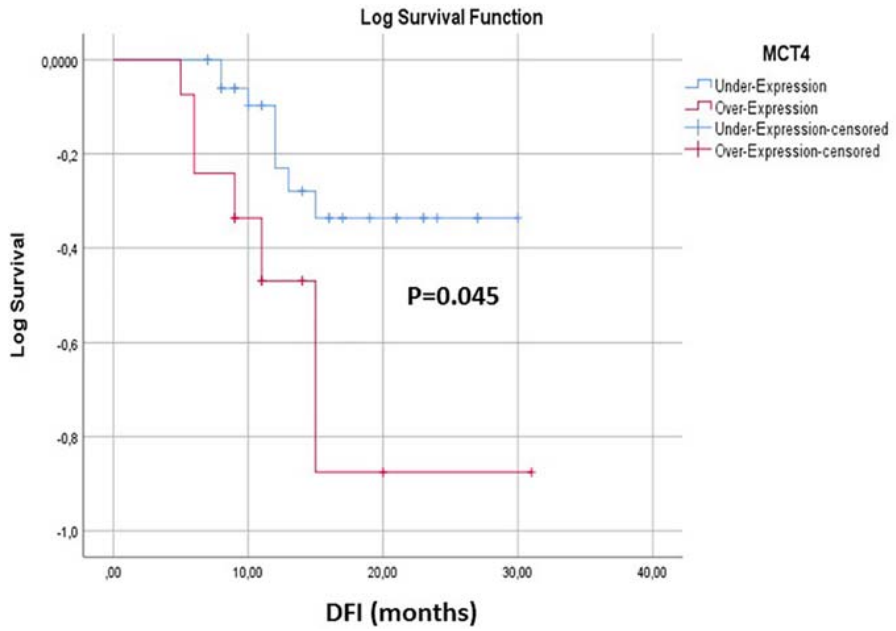

FIGURE 5 | Kaplan–Meier estimates of DFI of early stage NSCLC patients in respect to MCT4 overexpression in CTCs.

studies demonstrating that the vast majority of CTC in NSCLC patients express EMT markers (Allard et al., 2004; Lecharpentier et al., 2011; Zhang et al., 2019).

The expression of *MCT4* in the CTC fraction of patients was significantly higher than that observed in the corresponding "PBMC" fraction of HD (P = 0.036). Moreover, a higher expression level of *MCT4* in CTC were observed at the time of tumor relapse. This finding, which is in agreement with the reported increased tumoral expression of *MCT4* when the tumor progress to higher grade or metastasis, strongly which suggests that *MCT4* expression is associated with the migration and/or invasion of cancer cells (Gerlinger et al., 2012; Choi et al., 2014; Kim et al., 2015).

According to our results, overexpression of *MCT4* had a prognostic implication for early stage NSCLC patients, since it was associated with significantly reduced DFI; but conversely, there was no correlation with other patients' clinic-pathological characteristics. On the contrary, neither the expression of epithelial markers nor EMT markers provided prognostic information for NSCLC patients. However, these observations and conclusions have to be been taken with cautious because of the relatively small number of enrolled patients in the study and the low number of observed relapses during the follow-up period and need further confirmation in larger future studies. In a previous study, Ruan et al. (2017) reported that the expression *MCT-4*protein in the primary tumor cells was significantly associated with the depth of tumoral invasion (P = 0.034) and with a decreased overall survival (P = 0.001).

In recent years, MCT4 inhibitors are still in the discovery phase. Very recently Kuo et al. (2020) suggested a new therapeutic approach for the control of MCT4 in the aerobic glycolysis-preference NSCLC cell subtype. Moreover, the elimination of lactace secretion could be more effective by developing drugs that co-inhibit MCT1 and MCT4. The experimental approach *in vivo* or *in vitro* establishes that not only the inhibition of MCTs can be useful, but also MCTs could serve as vehicles for new anticancer drugs (Baltazar et al., 2014).

CONCLUSION

In conclusion, we show that overexpression *MCT4* in CTCs has prognostic significance in early stage NSCLC patients. It would be valuable to extend this study in a prospective large study as well as in different cancers, since most studies so far are based on the expression of *MCT4* in paired fresh frozen tissues. Taking into account the importance of *MCT4* in cancer, its promising potential as a new specific liquid biopsy prognostic biomarker as well as molecular targets for the development of novel cancer therapeutics, we strongly believe that our results will be of importance for both clinical researchers and those who design novel cancer therapeutics.

DATA AVAILABILITY STATEMENT

The data that support the findings of this study are available from the corresponding author (AM), upon reasonable request.

ETHICS STATEMENT

The studies involving human participants were reviewed and approved by Ethics and Scientific Committee of Thoracic

Diseases General Hospital Sotiria. The patients/participants provided their written informed consent to participate in this study.

AUTHOR CONTRIBUTIONS

AM conceived the original idea, supervised the findings of this work, and supervised the project. GK and EP contributed to immunostaining and confocal imaging. VG and AK contributed to provision of clinical samples. ET carried out the experiment. AM wrote the manuscript in consultation with EL and VG. EL helped supervise the project. All authors contributed to the article and approved the submitted version.

FUNDING

This project has received funding from the Hellenic Foundation for Research and Innovation (HFRI) and the General Secretariat for Research and Technology (GSRT), under Grant Agreement No. 1964.

SUPPLEMENTARY MATERIAL

The Supplementary Material for this article can be found online at: https://www.frontiersin.org/articles/10.3389/fcell.2021.641978/full#supplementary-material

Supplementary Figure 1 | Positive and negative controls of CK/A45/VIM staining. **(A)** Cytospin with H1299 cells stained with CK/A45 (green) anti-mouse, Alexa 488 anti-mouse, VIM (red) anti-rabbit and Alexa 555 anti-rabbit (positive control). **(B)** Cytospin with H1299 cells stained with Alexa 488 anti-mouse, VIM (red) anti-rabbit and Alexa 555 anti-rabbit (negative control for CK). **(C)** Cytospin with H1299 cells stained with CK/A45 (green) anti-mouse, Alexa 488 anti-mouse and Alexa 555 anti-rabbit (negative control for VIM).

Supplementary Figure 2 | Phenotypic characterization of CK^{low}/CK^{-} CTCs. Patients' samples were stained with DAPI (blue; first column), CK/A45 (green; second column) and VIM (red; third column). The fourth column shows overlays. Representative images from confocal laser scanning microscopy of (A) $CK^{low}/CK^{-}/VIM^{-}$ and (B) $CK^{low}/CK^{-}/VIM^{+}$ CTCs. Scale bars = 10 μm.

Supplementary Table 1 | Patients clinicopathological characteristics.

Supplementary Table 2 | *MCT4* overexpression in respect to patients clinicopathological characteristics.

Supplementary Table 3 | Primers and probe sequence for the RT-qPCR of *MCT4*.

REFERENCES

Allard, W. J., Matera, J., Miller, M. C., Repollet, M., Connelly, M. C., Rao, C., et al. (2004). Tumor cells circulate in the peripheral blood of all major carcinomas but not in healthy subjects or patients with nonmalignant diseases. *Clin. Cancer Res.* 10, 6897–6904. doi: 10.1158/1078-0432.CCR-04-0378

Baek, G., Tse, Y. F., Hu, Z., Cox, D., Buboltz, N., McCue, P., et al. (2014). MCT4 defines a glycolytic subtype of pancreatic cancer with poor prognosis and unique metabolic dependencies. *Cell Rep.* 9, 2233–2249. doi: 10.1016/j.celrep.2014.11.025

Baltazar, F., Pinheiro, C., Morais-Santos, F., Azevedo-Silva, J., Queirós, O., Preto, A., et al. (2014). Monocarboxylate transporters as targets and mediators in cancer therapy response. *Histol. Histopathol.* 29, 1511–1524. doi: 10.14670/HH-29.1511

Choi, J. W., Kim, Y., Lee, J. H., and Kim, Y. S. (2014). Prognostic significance of lactate/proton symporters MCT1, MCT4, and their chaperone CD147 expressions in urothelial carcinoma of the bladder. *Urology* 84, 245.e9–245.e15. doi: 10.1016/j.urology.2014.03.031

Chudziak, J., Burt, D. J., Mohan, S., Rothwell, D. G., Mesquita, B., Antonello, J., et al. (2016). Clinical evaluation of a novel microfluidic device for epitope-independent enrichment ofcirculatingtumour cells in patients with small cell lung cancer. *Analyst* 141, 669–678. doi: 10.1039/c5an02156a

Curry, J. M., Tuluc, M., Whitaker-Menezes, D., Ames, J. A., Anantharaman, A., Butera, A., et al. (2013). Cancer metabolism, stemness and tumor recurrence: MCT1 and MCT4 are functional biomarkers of metabolic symbiosis in head and neck cancer. *Cell Cycle* 12, 1371–1384. doi: 10.4161/cc.24092

DeBerardinis, R. J., and Chandel, N. S. (2020). We need to talk about the Warburg effect. *Nat. Metab.* 2, 127–129. doi: 10.1038/s42255-020-0172-2

Doyen, J., Trastour, C., Ettore, F., Peyrottes, I., Toussant, N., Gal, J., et al. (2014). Expression of the hypoxia-inducible monocarboxylate transporter MCT4 is increased in triple negative breast cancer and correlates independently with clinical outcome. *Biochem. Biophys. Res. Commun.* 451, 54–61. doi: 10.1016/j.bbrc.2014.07.050

Frick, M. A., Feigenberg, S. J., Jean-Baptiste, S. R., Aguarin, L. A., Mendes, A., Chinniah, C., et al. (2020). Circulating tumor cells are associated with recurrent disease in patients with early-stage non-small cell lung cancer treated with stereotactic body radiotherapy. *Clin. Cancer Res.* 26:2380.

Gerlinger, M., Santos, C. R., Spencer-Dene, B., Martinez, P., Endesfelder, D., Burrell, R. A., et al. (2012). Genome-wide RNA interference analysis of renal carcinoma survival regulators identifies MCT4 as a Warburg effect metabolic target. *J. Pathol.* 227, 146–156. doi: 10.1002/path.4006

Halestrap, A. P. (2013). The SLC16 gene family - structure, role and regulation in health and disease. *Mol. Aspects Med.* 34, 337–349. doi: 10.1016/j.mam.2012.05.003

Halestrap, A. P., and Price, N. T. (1999). The proton-linked monocarboxylate transporter (MCT) family: structure, function and regulation. *Biochem. J.* 343(Pt 2), 281–299. doi: 10.1042/0264-6021:3430281

Hanahan, D., and Weinberg, R. A. (2011). Hallmarks of cancer: the next generation. *Cell* 144, 646–674. doi: 10.1016/j.cell.2011.02.013

Heidrich, I., Ačkar, L., MossahebiMohammadi, P., and Pantel, K. (2020). Liquid biopsies: potential and challenges. *Int. J. Cancer* 148, 528–545. doi: 10.1002/ijc.33217

Hvichia, G. E., Parveen, Z., Wagner, C., Janning, M., Quidde, J., Stein, A., et al. (2016). A novel microfluidic platform for size and deformability based separation and the subsequent molecular characterization of viable circulating tumor cells. *Int. J. Cancer* 138, 2894–2904. doi: 10.1002/ijc.30007

Kallergi, G., Politaki, E., Alkahtani, S., Stournaras, C., and Georgoulias, V. (2016). Evaluation of isolation methods for circulating tumor cells (CTCs). *Cell Physiol. Biochem.* 40, 411–419. doi: 10.1159/000452556

Kershaw, S., Cummings, J., Morris, K., Tugwood, J., and Dive, C. (2015). Optimisation of immunofluorescence methods to determine MCT1 and MCT4 expression in circulating tumour cells. *BMC Cancer* 15:387. doi: 10.1186/s12885-015-1382-y

Kim, H. K., Lee, I., Bang, H., Kim, H. C., Lee, W. Y., Yun, S. H., et al. (2018). MCT4 expression is a potential therapeutic target in colorectal cancer with peritoneal carcinomatosis. *Mol. Cancer Ther.* 17, 838–848. doi: 10.1158/1535-7163.MCT-17-0535

Kim, Y., Choi, J. W., Lee, J. H., and Kim, Y. S. (2015). Expression of lactate/H? symporters MCT1 and MCT4 and their chaperone CD147 predicts tumor progression in clear cell renal cell carcinoma: immunohistochemical and The Cancer Genome Atlas data analyses. *Hum. Pathol.* 46, 104–112. doi: 10.1016/j.humpath.2014.09.013

Krebs, M. G., Hou, J. M., Sloane, R., Lancashire, L., Priest, L., Nonaka, D., et al. (2012). Analysis of circulating tumor cells in patients with non-small cell lung cancer using epithelial marker-dependent and -independent approaches. *J. Thorac. Oncol.* 7, 306–315. doi: 10.1097/jto.0b013e31823c5c16

Kuo, T. C., Huang, K. Y., Yang, S. C., Wu, S., Chung, W. C., Chang, Y. L., et al. (2020). Monocarboxylate transporter 4 is a therapeutic target in non-small

cell lung cancer with aerobic glycolysis preference. *Mol. Ther. Oncolytics* 18, 189–201. doi: 10.1016/j.omto.2020.06.012

Lecharpentier, A., Vielh, P., Perez-Moreno, P., Planchard, D., Soria, J. C., and Farace, F. (2011). Detection of circulating tumour cells with a hybrid (epithelial/mesenchymal) phenotype in patients with metastatic non-small cell lung cancer. *Br. J. Cancer* 105, 1338–1341. doi: 10.1038/bjc.2011.405

Lianidou, E. S., Markou, A., and Strati, A. (2015). The role of CTCs as tumor biomarkers. *Adv. Exp. Med. Biol.* 867, 341–367. doi: 10.1007/978-94-017-7215-0_21

Livak, K. J., and Schmittgen, T. D. (2001). Analysis of relative gene expression data using real-time quantitative PCR and the 2(-Delta DeltaC(T)) method. *Methods* 25, 402–408. doi: 10.1006/meth.2001.1262

Luo, W., Rao, M., Qu, J., and Luo, D. (2018). Applications of liquid biopsy in lung cancer-diagnosis, prognosis prediction, and disease monitoring. *Am. J. Transl. Res.* 10, 3911–3923.

Markou, A., Lazaridou, M., Paraskevopoulos, P., Chen, S., Swierczewska, M., Budna, J., et al. (2018). Multiplex gene expression profiling of in vivo isolated circulating tumor cells in high-risk prostate cancer patients. *Clin. Chem.* 64, 297–306. doi: 10.1373/clinchem.2017.275503

Meng, S., Tripathy, D., Frenkel, E. P., Shete, S., Naftalis, E. Z., Huth, J. F., et al. (2004). Circulating tumor cells in patients with breast cancer dormancy. *Clin. Cancer Res.* 10, 8152–8162.

Meredith, D., and Christian, H. C. (2008). The SLC16 monocaboxylate transporter family. *Xenobiotica* 38, 1072–1106. doi: 10.1080/00498250802010868

Molina, J. R., Yang, P., Cassivi, S. D., Schild, S. E., and Adjei, A. A. (2008). Non-small cell lung cancer: epidemiology, risk factors, treatment, and survivorship. *Mayo Clin. Proc.* 83, 584–594. doi: 10.4065/83.5.584

Nakayama, Y., Torigoe, T., Inoue, Y., Minagawa, N., Izumi, H., Kohno, K., et al. (2012). Prognostic significance of monocarboxylate transporter 4 expression in patients with colorectal cancer. *Exp. Ther. Med.* 3, 25–30. doi: 10.3892/etm.2011.361

Pawlikowska, P., Faugeroux, V., Oulhen, M., Aberlenc, A., Tayoun, T., Pailler, E., et al. (2019). Circulating tumor cells (CTCs) for the noninvasive monitoring and personalization of non-small cell lung cancer (NSCLC) therapies. *J. Thorac. Dis.* 11, S45–S56.

Poole, R. C., and Halestrap, A. P. (1993). Transport of lactate and other monocarboxylates across mammalian plasma membranes. *Am. J. Physiol.* 264, C761–C782. doi: 10.1152/ajpcell.1993.264.4.C761

Porras, T. B., Kaur, P., Ring, A., Schechter, N., and Lang, J. E. (2018). Challenges in using liquid biopsies for gene expression profiling. *Oncotarget* 9, 7036–7053. doi: 10.18632/oncotarget.24140

Puri, S., and Juvale, K. (2020). Monocarboxylate transporter 1 and 4 inhibitors as potential therapeutics for treating solid tumours: a review with structure-activity relationship insights. *Eur. J. Med. Chem.* 199:112393. doi: 10.1016/j.ejmech.2020.112393

Ruan, Y., Zeng, F., Cheng, Z., Zhao, X., Fu, P., and Chen, H. (2017). High expression of monocarboxylate transporter 4 predicts poor prognosis in patients with lung adenocarcinoma. *Oncol. Lett.* 14, 5727–5734. doi: 10.3892/ol.2017.6964

Shu, Q. H., Ge, Y. S., Ma, H. X., Gao, X. Q., Pan, J., Liu, D., et al. (2016). Prognostic value of polarized macrophages in patients with hepatocellular carcinoma after curative resection. *J. Mol. Med.* 94, 155–171.

Siegel, R. L., Miller, K. D., and Jemal, A. (2015). Cancer statistics, 2015. *CA Cancer J. Clin.* 65, 5–29. doi: 10.3322/caac.21254

Strati, A., Koutsodontis, G., Papaxoinis, G., Angelidis, I., Zavridou, M., Economopoulou, P., et al. (2017). Prognostic significance of PD-L1 expression on circulating tumor cells in patients with head and neck squamous cell carcinoma. *Ann. Oncol.* 28, 1923–1933. doi: 10.1093/annonc/mdx206

Strati, A., Nikolaou, M., Georgoulias, V., and Lianidou, E. S. (2019). Prognostic significance of TWIST1, CD24, CD44, and ALDH1 transcript quantification in EpCAM-positive circulating tumor cells from early stage breast cancer patients. *Cells* 8:652. doi: 10.3390/cells8070652

Tamminga, M., de Wit, S., Schuuring, E., Timens, W., Terstappen, L. W. M. M., Hiltermann, T. J. N., et al. (2019). Circulating tumor cells in lung cancer are prognostic and predictive for worse tumor response in both targeted- and chemotherapy. *Transl. Lung Cancer Res.* 8, 854–861. doi: 10.21037/tlcr.2019.11.06

Wang, R., Lu, Y. Y., and Fan, D. M. (2015). Reasons for cancer metastasis: a holistic perspective. *Mol. Clin. Oncol.* 3, 1199–1202. doi: 10.3892/mco.2015.623

Wang, W., Song, Z., and Zhang, Y. A. (2017). Comparison of ddPCR and ARMS for detecting EGFR T790M status in ctDNA from advanced NSCLC patients with acquired EGFR-TKI resistance. *Cancer Med.* 6, 154–162. doi: 10.1002/cam4.978

Warburg, O. (1956). On the origin of cancer cells. *Science* 123, 309–314. doi: 10.1126/science.123.3191.309

Warburg, O., Wind, F., and Negelstein, E. (1927). The metabolism of tumors in the body. *J. Gen. Physiol.* 8, 519–530. doi: 10.1085/jgp.8.6.519

Wu, Y. L., Tsuboi, M., He, J., John, T., Grohe, C., Majem, M., et al. (2020). Osimertinib in resected *EGFR*-mutated non-small-cell lung cancer. *N. Engl. J. Med.* 383, 1711–1723. doi: 10.1056/NEJMoa2027071

Zavridou, M., Mastoraki, S., Strati, A., Tzanikou, E., Chimonidou, M., and Lianidou, E. (2018). Evaluation of preanalytical conditions and implementation of quality control steps for reliable gene expression and DNA methylation analyses in liquid biopsies. *Clin. Chem.* 64, 1522–1533. doi: 10.1373/clinchem.2018.292318

Zhang, X., Chang, N., Yang, G., Zhang, Y., Ye, M., Cao, J., et al. (2017). A comparison of ARMS-Plus and droplet digital PCR for detecting EGFR activating mutations in plasma. *Oncotarget* 8, 112014–112023. doi: 10.18632/oncotarget.22997

Zhang, X., Wei, L., Li, J., Zheng, J., Zhang, S., and Zhou, J. (2019). Epithelial-mesenchymal transition phenotype of circulating tumor cells is associated with distant metastasis in patients with NSCLC. *Mol. Med. Rep.* 19, 601–608.

Zhu, J., Wu, Y. N., Zhang, W., Zhang, X. M., Ding, X., Li, H. Q., et al. (2014). Monocarboxylate transporter 4 facilitates cell proliferation and migration and is associated with poor prognosis in oral squamous cell carcinoma patients. *PLoS One* 9:e87904. doi: 10.1371/journal.pone.0087904

Conflict of Interest: The authors declare that the research was conducted in the absence of any commercial or financial relationships that could be construed as a potential conflict of interest.

Copyright © 2021 Markou, Tzanikou, Kallergi, Pantazaka, Georgoulias, Kotsakis and Lianidou. This is an open-access article distributed under the terms of the Creative Commons Attribution License (CC BY). The use, distribution or reproduction in other forums is permitted, provided the original author(s) and the copyright owner(s) are credited and that the original publication in this journal is cited, in accordance with accepted academic practice. No use, distribution or reproduction is permitted which does not comply with these terms.

frontiers in Oncology

ORIGINAL RESEARCH
published: 06 May 2021
doi: 10.3389/fonc.2021.639675

Characterization of Plasma Cell-Free DNA Integrity Using Droplet-Based Digital PCR: Toward the Development of Circulating Tumor DNA-Dedicated Assays

Geoffroy Poulet[1,2†], Fanny Garlan[1†], Sonia Garrigou[1], Eleonora Zonta[1], Leonor Benhaim[1,3], Marie-Jennifer Carrillon[1], Audrey Didelot[1], Delphine Le Corre[1], Claire Mulot[1,4], Philippe Nizard[1], Frederic Ginot[5], Audrey Boutonnet-Rodat[5], Helene Blons[1,6], Jean-Baptiste Bachet[1,7,8,9], Julien Taïeb[1,6,9], Aziz Zaanan[1,6], Vanna Geromel[2], Laurence Pellegrina[2], Pierre Laurent-Puig[1,6], Shu-Fang Wang-Renault[1] and Valerie Taly[1]**

[1] Centre de Recherche des Cordeliers, INSERM, CNRS, Sorbonne Université, USPC, Université de Paris, Equipe labellisée Ligue Nationale Contre le Cancer, CNRS SNC 5096, Paris, France, [2] Eurofins-Biomnis, Specialized Medical Biology Laboratory, Lyon, France, [3] Department of Visceral and Surgical Oncology, Gustave Roussy, Villejuif, France, [4] CIC-EC4 URC, HEGP, Hôpitaux Universitaires Paris Ouest AP-HP, Paris, France, [5] Adelis, ID-solutions, Labège, France, [6] Department of Oncology, European Georges-Pompidou Hospital, AP-HP, Paris Descartes University, Paris, France, [7] Sorbonne Universités, UPMC Université, Paris, France, [8] Department of Hepato-gastroenterology, Groupe Hospitalier Pitié Salpêtrière, Paris, France, [9] AGEO (Association des Gastroentérologues Oncologues), Paris, France

Background: Cellular-cell free-DNA (ccfDNA) is being explored as a diagnostic and prognostic tool for various diseases including cancer. Beyond the evaluation of the ccfDNA mutational status, its fragmentation has been investigated as a potential cancer biomarker in several studies. However, probably due to a lack of standardized procedures dedicated to preanalytical and analytical processing of plasma samples, contradictory results have been published.

Methods: ddPCR assays allowing the detection of *KRAS* wild-type and mutated sequences (*KRAS* p.G12V, pG12D, and pG13D) were designed to target different fragments sizes. Once validated on fragmented and non-fragmented DNA extracted from cancer cell lines, these assays were used to investigate the influence of the extraction methods on the non-mutated and mutated ccfDNA integrity reflected by the DNA integrity index (DII). The DII was then analyzed in two prospective cohorts of metastatic colorectal cancer patients (RASANC study $n = 34$; PLACOL study $n = 12$) and healthy subjects ($n = 49$).

Results and Discussion: Our results demonstrate that ccfDNA is highly fragmented in mCRC patients compared with healthy individuals. These results strongly suggest that the characterization of ccfDNA integrity hold great promise toward the development of a universal biomarker for the follow-up of mCRC patients. Furthermore, they support the importance of standardization of sample handling and processing in such analysis.

Keywords: circulating tumor DNA, picoliter-droplet digital PCR, cancer biomarker, apoptosis, necrosis, DNA integrity index, circulating cell-free DNA

OPEN ACCESS

Edited by:
Catherine Alix-Panabieres, Centre Hospitalier Universitaire de Montpellier, France

Reviewed by:
Jillian Phallen, Johns Hopkins University, United States
Theresa D. Ahrens, University of Copenhagen, Denmark

***Correspondence:**
Shu-Fang Wang-Renault
shufang.renault@parisdescartes.fr
Valerie Taly
valerie.taly@parisdescartes.fr

†These authors have contributed equally to this work

Specialty section:
This article was submitted to Molecular and Cellular Oncology, a section of the journal Frontiers in Oncology

Received: *09 December 2020*
Accepted: *16 February 2021*
Published: *06 May 2021*

Citation:
Poulet G, Garlan F, Garrigou S, Zonta E, Benhaim L, Carrillon M-J, Didelot A, Le Corre D, Mulot C, Nizard P, Ginot F, Boutonnet-Rodat A, Blons H, Bachet J-B, Taïeb J, Zaanan A, Geromel V, Pellegrina L, Laurent-Puig P, Wang-Renault S-F and Taly V (2021) Characterization of Plasma Cell-Free DNA Integrity Using Droplet-Based Digital PCR: Toward the Development of Circulating Tumor DNA-Dedicated Assays. Front. Oncol. 11:639675. doi: 10.3389/fonc.2021.639675

INTRODUCTION

The presence of circulating cell-free DNA (ccfDNA) in body effluents has been largely described (1), and increased amounts of ccfDNA have been found in blood samples of patients affected by several disorders (2) including cancer (3, 4). The main sources of ccfDNA in healthy individuals have been described as apoptosis, active cellular release, and necrosis (5). Its integrity (defined as a metric describing size distribution) may differ depending on the involved cell-death mechanism and/or on the cell origin. In particular, it has been suggested that ccfDNA originating from tumor cells presents a different fragmentation profile than the ccfDNA originating from healthy cells (6, 7). Nevertheless, it should be taken into account that ccfDNA extracted from plasma of cancer patients is therefore composed at various proportions of tumor and non-tumor ccfDNA fractions. In recent years, the ccfDNA analysis, and more precisely its tumor fraction (ctDNA) has been largely developed, for the diagnosis, prognosis, follow-up, and treatment management of cancer patients (6, 8). Moreover, recent technological development of sensitive procedures such as droplet-based digital-PCR (ddPCR) or newly optimized next-generation sequencing (NGS) have greatly facilitated such applications (9).

The presence of ctDNA is generally assessed by the detection of tumor-specific genetic or epigenetic alterations (10–12). The quantity of ctDNA is suggested to reflect tumor burden and progression (13). In cancer, it has also been shown that disease-related cell death may lead to specific profiles of circulating nucleic acids (5). The ccfDNA integrity has thus been proposed as a potential non-invasive diagnostic biomarker especially pertinent in cancer (14, 15).

Quantitative PCR (qPCR) analysis based on the measurement of the relative amount of DNA amplicons of different sizes has long been the reference method for DNA integrity assessment (16–18). A wide range of strategies including high-sensitivity electrophoresis fragment separation (19) or NGS (20) has now been developed for such analysis. Even if the characterization of ccfDNA fragmentation profile has gained increasing interest in recent years as a cancer biomarker, contradictory results have been published (6, 16, 21). Such discrepancies could be linked with differences in the strategies used for ccfDNA fragmentation analysis. The latest findings tend to demonstrate a higher fragmentation level for ctDNA than for the non-tumor ccfDNA fraction (15, 21, 22). Using IntPlex, an optimized qPCR technique, Moulière et al. found a larger quantity of smaller fragments in plasma of colorectal cancer (CRC) patients compared with healthy subjects (23). Jiang et al. demonstrated by massive parallel sequencing that the size of ccfDNA in hepatocellular carcinoma (HCC) patients was inversely correlated with the concentrations of ctDNA in plasma (20). Comparing fragment lengths from cell-free DNA between melanoma patients (bearing *BRAF* V600E allele) and healthy subject (*BRAF* wild-type allele), Underhill et al. observed that the BRAF V600E mutant allele occurred more commonly at a shorter fragment length than the fragment length of the wild-type allele (132–145 bp vs. 165 bp, respectively) (24). Recently, using a novel technology (BIABooster system) based on electro-hydrodynamic actuation, we also suggested the pertinence of total ccfDNA quantification and size profiling for several cancers including melanoma, CRC, non-small cell lung cancer (NSCLC) and prostate cancer (19). To circumvent potential bias linked to the strategy chosen for ccfDNA integrity characterization and to increase the accuracy of such measurement, there is a growing need for highly sensitive and specific approaches.

In this article, we developed a ccfDNA integrity index (DII) dedicated-ddPCR assays and coupled it to fragment-based analysis by BIABooster system to investigate the pertinence of the characterization of total ccfDNA integrity in mCRC patients and propose its potential use as biomarker for mCRC patients. Moreover, our work also highlighted the crucial importance of the standardization of the preanalytical strategy for ccfDNA integrity investigation.

Abbreviations: bp, base pairs; ccfDNA, circulating cell-free DNA; ctDNA, circulating tumor DNA; ddPCR, droplet-based digital PCR; DII, DNA Integrity Index; qPCR, quantitative PCR; mCRC, metastatic colorectal cancer; MT, mutant; NGS, next-generation sequencing; nt, nucleotide; WT, wild-type; *KRAS*, v-Ki-ras2 Kirsten rat sarcoma viral oncogene homolog.

MATERIALS AND METHODS

Patients and Study Design

Samples from two prospective cohorts of mCRC patients were included for a total of 81 samples. In the AGEO RASANC cohort, 69 patients were included with plasma samples collected in BCT Streck Tube (STRECK, Cat. N°:218997) (25). In the PLACOL cohort, 12 patients were included with plasma sampled in EDTA Tube (Greiner Bio-One International, Cat. No. 456043) (26). The basic clinical characteristics of healthy subjects and mCRC patients included in the study are summarized in **Supplementary Table 1**. All samples from AGEO RASANC study have been analyzed by NGS with the Panel Colon-Lung Cancer V2 (study results already published) (25). Both studies have received ethical approval from the "Ile-de-France ethics committee," and the patients provided written informed consent. The research protocols were registered in clinicaltrials.gov (NCT02502656 and NCT01983098 for AGEO RASANC and PLACOL studies, respectively).

For both cohorts, the preanalytic conditions including blood collection tubes and plasma ccfDNA extraction kits were different. We thus added two control groups composed of samples from healthy patients that we processed with the same preanalytic conditions.

The DNA integrity was evaluated by ddPCR in 46 mCRC samples and 49 healthy samples. The size profiling of ccfDNA was investigated by BIAbooster System in 33 mCRC samples and 10 healthy samples. The workflow of the study is summarized in **Figure 1**.

In parallel, to determine the impact of the extraction method on the ccfDNA integrity, two different ccfDNA purification kits used in PLACOL and AGEO RASANC studies (respectively, 1° QIAmp® Circulating Nucleic Acid Kit and 2° RSC Automated Maxwell) have been compared on eight healthy plasmas. The workflow of the study is listed in **Supplementary Figure 1**.

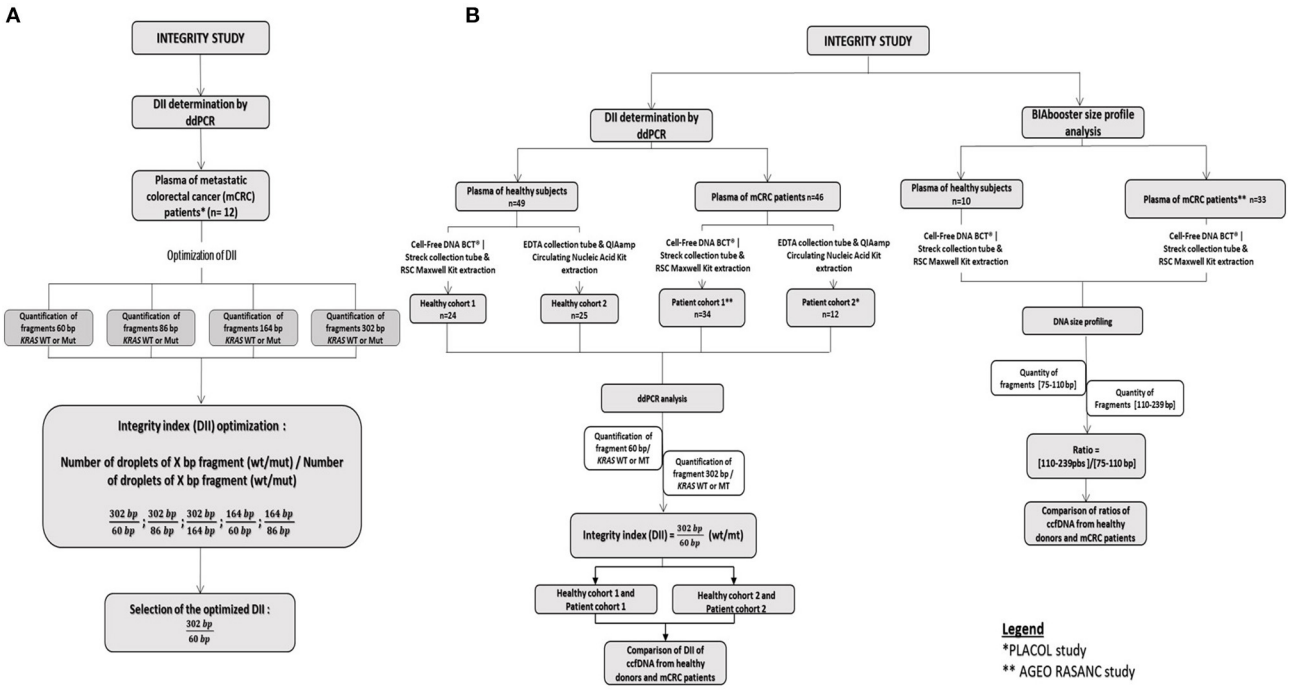

FIGURE 1 | Workflow of the integrity study. **(A)** Development of the DII using the PLACOL cohort ($n = 11$ samples analyzed). DNA hasbeen quantified using, respectively, 60, 86, 164, and 302 bp amplicons. Several combinations have been tested to determine the optimal DNA integrity index. Finally, the 302/60 bp ratio turned out to be the most clinically relevant. **(B)** Samples from two prospective cohorts of patients presenting a mCRC were included, AGEO RASANC ($n = 67$) and PLACOL ($n = 12$) cohort with a total of 81 metastatic CRC samples. Circulating cell-free DNA integrity of 34 patients (AGEO RASANC cohort) and 12 patients (PLACOL cohort) was analyzed by ddPCR, and ccfDNA size profiling of 33 patients (AGEO RASANC cohort) was analyzed by BIAbooster System. As the preanalytic conditions (blood collection tubes, plasma ccfDNA extraction kits) are different for these two prospective cohorts of patients, the corresponding control groups were included; 8.5 ml blood per tube from 59 healthy subjects are used as negative controls and split into two groups (control groups A and B). Thirty-four healthy blood samples were collected in cell-free DNA BCT from Streck, and circulating DNA has been extracted with Maxwell RSC ccfDNA Plasma Kit from the plasma samples associated, and 25 blood tubes were sampled in EDTA tubes and circulating DNA purified by the QIAmp® Circulating Nucleic Acid Kit (Qiagen) from plasma samples associated. Among control A and B healthy subjects' samples, DNA integrity of 49 plasma was analyzed by droplet-based digital PCR, and ccfDNA size profiling of 10 plasma was analyzed by BIAbooster System.

Plasma ccfDNA Preparation

In the AGEO RASANC and corresponding control group, plasma from healthy individuals or mCRC patients were collected in Cell-Free DNA BCT® | Streck tubes and extracted with the use of the Maxwell RSC ccfDNA Plasma kit (Promega; called Ext.kit 1 in the manuscript) using Maxwell® RSC Instrument.

In the PLACOL study and corresponding control group, plasma from healthy individuals or mCRC patients were collected in EDTA tubes and extracted with the QIAmp® Circulating Nucleic Acid Kit (QIAGEN; called Ext.kit 2 in the manuscript) according to the manufacturer's instructions. See **Supplementary Materials and Methods** for full protocol description.

Cell Line DNA Extraction, Fragmentation, and Quantification

DNA was extracted from two cell lines SW620 (mutated *KRAS* c.35G>T, p.G12V) and LoVo cell lines (mutated c.38G>A, p.G13D) using the QIAamp DNA Blood Mini Kit (QIAGEN) according to the manufacturer's instructions and eluted into 200 µl of Tris 10 mM/pH 8 before storage at −20°C.

The extracted DNA was fragmented by sonication (S220 Covaris Focused-Ultrasonicator sonicator) to obtain fragments ranging from 50 to 700 bp. The experimental parameters are described in **Supplementary Table 2**. The size distribution of fragmented DNA was confirmed by the miniaturized electrophoresis Caliper system, LabChip® GX/GXII Microfluidic system (Perkin-Elmer) using DNA assay 5K reagent kit (Perkin-Elmer) (see **Supplementary Figure 2** for size distribution).

Integrity Index Determination

Droplet-Based Digital PCR Analysis

Droplet-based digital PCR assays targeting three frequent mutations of the *KRAS* oncogene (p.G13D, p.G12V, or p.G12D) and its wild-type sequence were designed. These assays allowed to amplify sequences of 60, 86, 164, and 302 bp for both targeted mutant (MT) and wild-type (WT) *KRAS* sequences (probe bearing a FAM or VIC fluorophore respectively) for each targeted amplicon size (see **Figure 2A**; **Supplementary Table 3**). Droplet digital PCR was carried out with the Raindrop system (Raindance Technologies, Bio-Rad) as previously described (25, 26).

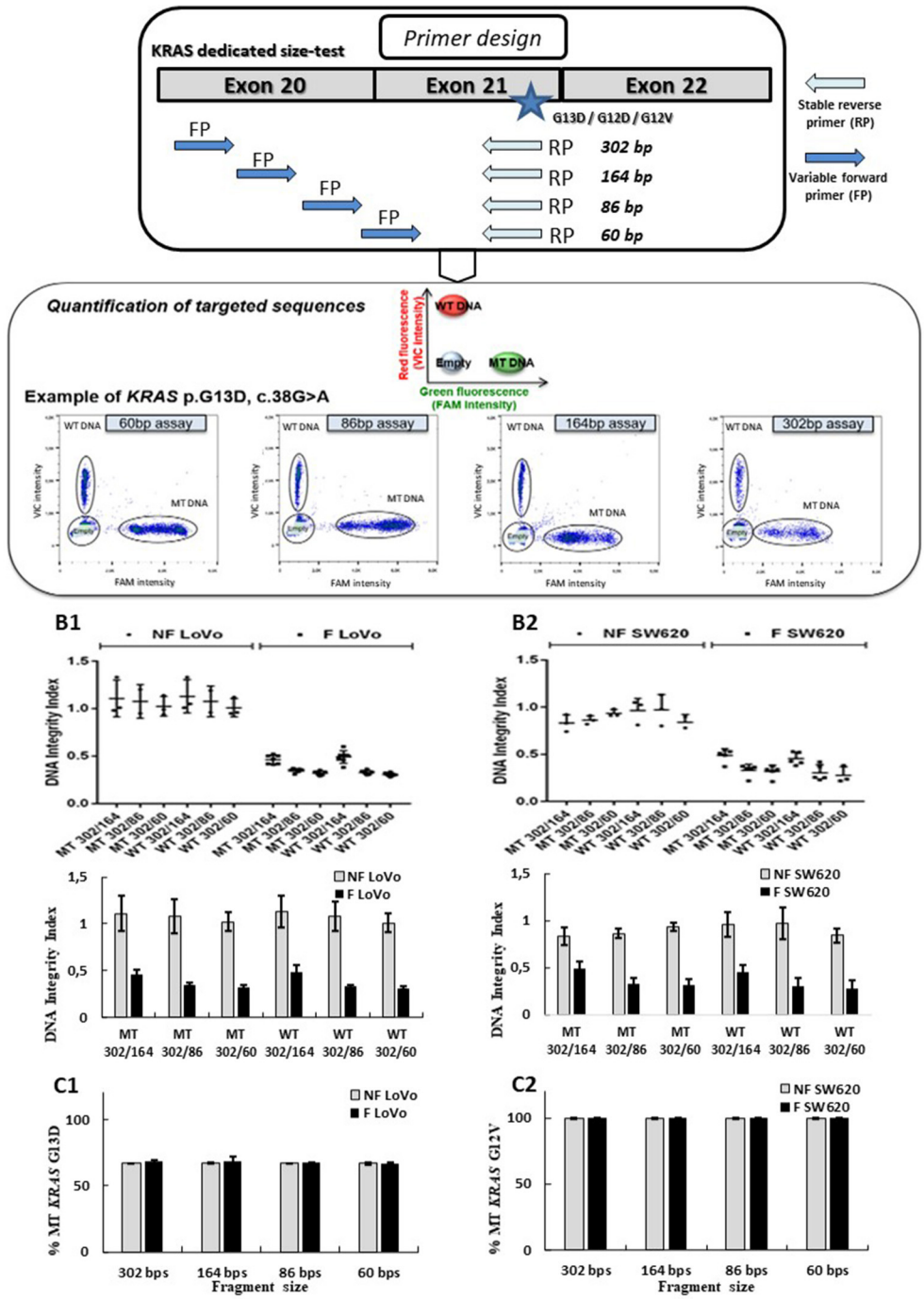

FIGURE 2 | Design and validation of ddPCR assays for ccfDNA integrity analysis with the use of fragmented and non-fragmented cell line DNA. Droplet-based digital PCR duplex assays amplifying different sizes of *KRAS* wild-type (WT) and mutant (MT) fragments (60, 86, 184, and 302 bp) were designed and optimized **(A)**. The LOB for the 302-, 164-, 86-, and 60-bp *KRAS* assays were, respectively, 0, 0, 3, and 1, irrespective of the mutation status. Fragmented (F) and non-fragmented (NF) DNA from LoVo (**B1**, **C1**) and SW620 CRC line (**B2**, **C2**) were used. DNA integrity index (DII) were analyzed using 302 bp amplicon (corresponding to the long fragments) and 60, 84, and 184 bp amplicons as short fragments (**B1**, **B2**). Percentage of *KRAS*-mutated alleles for F and NF DNA of each cell lines are given in (**C1**, **C2**). Nevertheless, PCR efficiency of the primers has not been determined by qPCR for each amplicon size on fragmented and unfragmented DNA.

Detailed Description of Droplet-Based Digital PCR Assays and DII Calculation

Taqman® Genotyping Master Mix (Life Technologies) at 12.5 µl was mixed with the assay solution containing: 0.75 µl of 40 mM dNTP Mix (New England BioLabs), 0.5 µl of 25 mM $MgCl_2$, 1 µl 25× Droplet Stabilizer (RainDance Technologies), 1.25 µl 20× Assay Mix containing 8 µM of forward and reverse primers, 4 µM of 6-FAM and 4 µM of VIC Taqman®-labeled probes, and cell line DNA or plasma DNA to a final reaction volume of 25 µl.

All PCR assay mixes were prepared as shown in a pre-PCR room to limit risks of contamination. TaqMan® (from Life Technologies-Thermo Fisher Scientific) probes were tested. In classic TaqMan® assay, the probe bearing VIC-fluorophore (λex 538 nm/λem 554 nm) was designed to be specific to the WT allele, while the probe bearing FAM-fluorophore (λex 494 nm/λem 518 nm) was able to specifically hybridize to the mutated sequence. The emulsifications of DNA samples were generated according to manufacturer protocol (Raindance, Bio-Rad Laboratories). The emulsion was thermal cycled following the different PCR programs described in **Supplementary Table 4** (PCR programs). After completion, the emulsions were either stored at 4°C or processed immediately to measure the end-point fluorescence signal from each droplet.

A limit of blank (LOB) has been calculated as described previously (1). It is defined by the frequency of positive droplets measured in genomic DNA (non-mutated) ($n = 10$ minimum). The calculated LOB was subtracted from each sample. The LOB for the 302, 164, 86, and 60 bp *KRAS* assays were, respectively, 0, 0, 3, and 1, irrespective of the mutation status. Data were analyzed according to manufacturer's instructions (Raindance Analyst Flow-Jo software). Since the number of droplets reveals the quantity of amplifiable target DNA, the fraction of amplifiable DNA in patients' samples could be determined. The number of droplets was determined using the software RainDrop Analyst (Bio-Rad Laboratories). All data were normalized to 5,000,000 droplets (corresponding to the theorical number of droplets generated by automation). A LOB correction (subtraction) has been performed to calculate the final number of positive MT droplets. Starting from the same amount of DNA, amplified fragmented copies of long and short fragments were counted to calculate the DNA Integrity Index. The PCR programs are given in **Supplementary Table 4**.

Starting from the same amount of DNA, DII was defined as a ratio between the number of amplified copies of long (302 bp) and "short" (60, 86, and 164 bp) DNA fragments. DIIs were calculated separately for WT and MT sequences. An example of DII calculation is as follows:

$$(E1)\ DII\ WT = \frac{Quantity\ of\ fluorescent\ droplets\ corresponding\ to\ 302\ bp\ fragment\ (WT)}{Quantity\ of\ fluorescent\ droplets\ corresponding\ to\ 60\ bp\ fragment\ (WT)} \quad (1)$$

For samples (i.e., Placol_5 and RASANC_10) that did not present detectable 302 bp fragments for the mutated allele, the DII was evaluated as follows : DII MT < 1/[quantity of fluorescent droplets corresponding to 60 or 86 or 164 bp fragments (MT)]. These two samples were however excluded from final statistical analysis.

BIAbooster Analysis

The size profiles and concentration analysis of ccfDNA from healthy individuals and mCRC patients were also performed using BIAbooster System (Picometrics technologies, ID-Solution) as previously described (19). The system is based on the principle of DNA fragment migration by capillary electrophoresis coupled to LED-induced fluorescence (LEDIF) detectors. It allows performing size and concentration analysis of double-stranded DNA with a sensitivity of 10 fg/µl in an operating time of 20 min. Based on the quantity of the different fragments obtained, a ratio highlighting the size distribution of the tested sample is calculated by BIAbooster technology as follows (E2):

$$(E2)\ ratio = \frac{Detected\ Quantity\ of\ fragments\ with\ a\ size\ ranging\ between\ 110 and\ 239\ bp}{Detected\ Quantity\ of\ fragments\ with\ a\ size\ ranging\ between\ 75 and\ 110\ bp} \quad (2)$$

The description of the statistical analysis is provided in the **Supplementary Materials and Methods**.

RESULTS

Validation of ddPCR Assays for ccfDNA Integrity Analysis Using Fragmented and Non-fragmented Cell Line DNA as a Model

Even if the characterization of ccfDNA fragmentation profile has gained increasing interest in recent years as a cancer biomarker, contradictory results have been published (6, 16, 21). Such discrepancies could be linked with differences in the strategies used for ccfDNA fragmentation analysis. The first step of this study was thus to evaluate the pertinence of ddPCR in this context using model samples containing DNA of controlled sizes.

Several Taqman® assays targeting *KRAS* sequence fragments of different lengths were designed (see **Figure 2A**). We used mechanically fragmented DNA (sonicated) and non-fragmented DNA from LoVo and SW620 CRC cell lines bearing WT and/or MT *KRAS* genes. Length of fragments evaluated using the miniaturized electrophoresis Caliper system, LabChip® GX/GXII Microfluidic system (see section **MATERIALS AND METHODS**), varied from 50 to 70 bp to 700 to 800 bp with higher amounts of large-size fragments (see **Supplementary Figure 2**). In order to determine the performance of the developed assay, we compared DII and mutant allelic fraction determination of fragmented and non-fragmented DNA of two cancer cell lines (however, PCR efficiencies of the primers for both types of DNA were not determined). Using our ddPCR strategy, a stable DII (see **equation E1**) of 1 was observed when analyzing non-fragmented DNA (gray bars) from both cell lines (60, 86, and 164 bp amplicons were used for determination of the quantity of short

fragments while 302 bp was used for the determination of the quantity of the long fragment). These results suggested that a comparable amount of DNA was amplified regardless of the size of the tested fragments (**Figures 2B1,2**). When analyzing fragmented DNA (black bars), DII were inversely correlated with the size of amplicon selected as short fragments (164, 86, and 60 bp). Higher amounts of input DNA could be detected with the shorter amplicons. Meanwhile, as expected, similar DII were observed for the *KRAS* MT or WT sequences for both cell lines (**Figures 2B1,B2**, MT vs. WT bars). The percentage of *KRAS* MT DNA remained stable for the different analyses (**Figures 2C1,C2**), suggesting no detection bias of MT sequences over WT sequences. These results validate the pertinence of the developed ddPCR assays for the integrity analysis of both mutant and WT alleles.

Detection of ctDNA Concentration in mCRC Patients Depends on the Amplicon Size Used for ddPCR Assays

Using ddPCR assays in duplex format (as shown in **Figure 2A**), *KRAS* WT and MT DNA sequences could be precisely quantified, allowing to calculate the concentrations of each allele in the patient's samples. As shown in **Figures 3A1,A2**, ctDNA concentration and its proportion within total ccfDNA was linked to the targeted amplicon size used in the ddPCR integrity assay with smaller targeted amplicons leading to the detection of higher concentration of ctDNA (highlighted by the detection of *KRAS* MT alleles). Such results are in favor of a higher fragmentation of ctDNA and confirmed more efficient detection of ctDNA by ddPCR assays when targeting short amplicons.

Determination of ctDNA Integrity in mCRC Patients by ddPCR

Droplet-based digital PCR integrity analysis targeting 60, 86, and 302 bp amplicons were performed in plasma ccfDNA of mCRC patients (PLACOL study, $n = 12$). As expected, a high fragmentation of ctDNA was observed in ccfDNA. DII results for the detection of MT allele are, respectively, 0.05 and 0.04 for the 302/86 and 302/60 bp amplicons. For the detection of WT allele, DII results are, respectively, 0.09 and 0.11 for 302/86 and 302/60. Significant differences between MT and WT alleles are observed (Wilcoxon test, $p = 0.03$ and 0.0075, respectively, for DII 302/86 and DII 302/60). Analysis of the MT fraction of ccfDNA highlighted an even stronger fragmentation with very low amount of 302 bp sequences detected compared with the WT sequence (**Supplementary Table 5**). The calculated DII of *KRAS* WT sequences was found significantly higher than the one calculated for *KRAS* MT sequences (**Figure 3B**, Wilcoxon test, $p < 0.05$). Since WT sequences can be released by both normal and tumor cells while MT sequences by tumor cells only, such results suggest a higher fragmentation of ctDNA as compared with the non-mutated fraction of ccfDNA. This was not observed when using 164 bp amplicon as long fragments for DII calculation (**Figure 3C**). Moreover, the concentration and fraction of ctDNA in patient samples detected by the *KRAS* MT allele appeared slightly higher when using 60 bp amplicon compared with the 86-bp one (**Supplementary Figure 3**). Based on these results, 60 bp amplicon was chosen as the short fragment and 302 bp amplicon as the long fragment to calculate ccfDNA and ctDNA DII in the following ddPCR experiments.

Extraction Conditions Could Influence ccfDNA Integrity Profiles

No significant differences of DII were observed between eight healthy plasma samples collected at the same time on K2-EDTA tube and cell-free DNA BCT° (STRECK) suggesting an absence of influence of the collection tube on ccfDNA fragmentation profile. (**Supplementary Table 6**; **Supplementary Figure 4**). We thus mainly focused on ccfDNA extraction methods on the ccfDNA quantity and DII in this study (workflow is described in **Supplementary Figure 1**). The results showed that a higher quantity of ccfDNA were extracted when using QIAmp® Circulating Nucleic Acid Kit (Ext.kit 2) as compared with the Maxwell RSC ccfDNA Plasma Kit (Ext.kit 1) (see **Figure 4A**) although the difference between the concentrations of 60 bp fragments was not statistically significant ($p = 0.45$). Moreover, DIIs calculated by ddPCR on the DNA extracted by the two methods appeared different ($p = 0.0017$) (**Figure 4B**). Such results confirmed the pertinence of preanalytic condition standardization not only for ccfDNA integrity determination but also in general for ccfDNA studies.

Comparison of ccfDNA Integrity Index Between mCRC Patients and Healthy Individuals

The DII of ccfDNA determined by ddPCR from both mCRC patients group were significantly lower than those from corresponding healthy plasma (**Figure 5A1** for AGEO RASANC study, $p = 2.5e{-}08$ and **Figure 5A2** for PLACOL study, $p = 1.2e{-}05$). However, when analyzing separately the DII of the *KRAS* WT and *KRAS* MT sequences in the two patient groups, a significant difference was observed for the PLACOL study ($p = 0.0058$) and not for the RASANC study ($p = 0.27$) (**Figures 5A1,A2**).

Circulating cell-free DNA size profiles from healthy individuals and mCRC patients was also compared using the BIAbooster System (**Figures 5B1,B2**). To better characterize small, fragmented DNA fraction, we characterized ccfDNA fragments between 75 and 110 bp (shorter than mono-nucleosomal DNA fragment lengths) and between 110 and 239 bp (comprising expected mono-nucleosomal DNA fragment lengths (140–180 bp). However, since the PLACOL cohort was extracted using the QIAamp Circulating Nucleic Acid Kit that implies the use of RNA carrier that can compromise BIAbooster fragments analysis, only the sample from AGEO RASANC cohort were analyzed here. As shown in **Figure 5B1**, a higher quantity of short fragments (75–110 bp) was observed in mCRC patients than in healthy individuals (**Figure 5B1**) and no difference was found for 110–239 bp fragments. Furthermore, similar DII differences were observed by ddPCR. The ratio of the quantity of fragments between 110 and 239 bp and 75 and

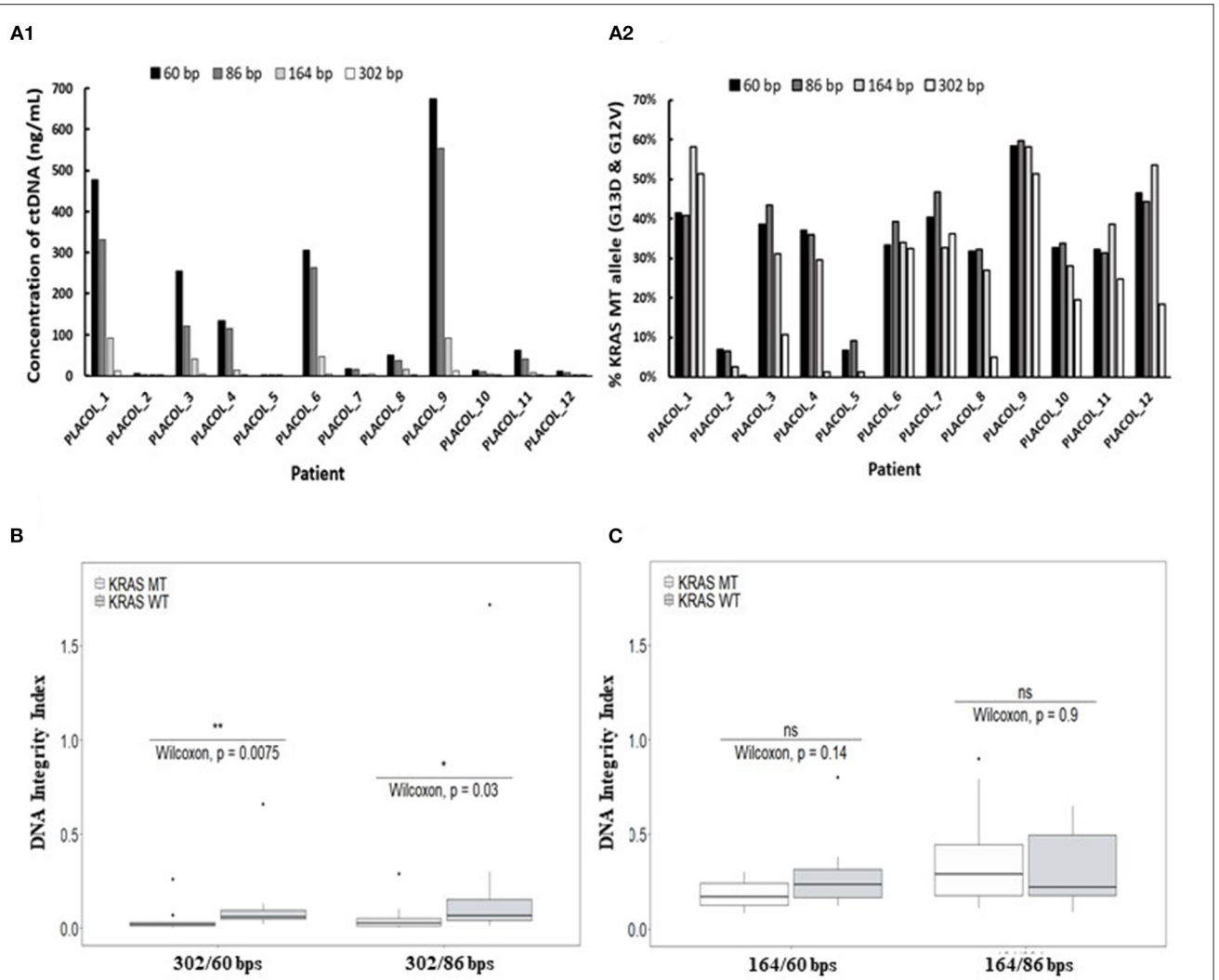

FIGURE 3 | Characterization of ctDNA by droplet-based digital PCR using assays targeting increasing amplicon sizes. Concentration of plasma ctDNA **(A1)** and percentage of *KRAS*-mutated alleles **(A2)** in mCRC patients and DNA integrity indexes (DII) calculated with the use of 302 bp **(B)** or 164 bp amplicon **(C)** (corresponding to the long fragments) by ddPCR. *KRAS* WT and MT ddPCR duplex assays amplifying different sizes of fragments (60, 86, 164, and 302 bp) were used for measuring ctDNA concentration and percentage of *KRAS*-mutated alleles (**A1**,**A2**) for 11 mCRC patients (one patient excluded since no 302 bp MT fragments were detectable). DII were calculated based on the amplification of sequences with different lengths as described in the section **MATERIALS AND METHODS**. For DII calculation, 60 bp amplicons were used as the short fragments and either 302 bp **(B)** or 164 bp amplicon **(C)** as the long fragments. Mann–Whitney *U*-test was used for statistical significance analysis. $^{*}p < 0.05$; $^{**}p < 0.01$.

110 bp was also significantly different between mCRC patients and healthy individuals (**Figure 5B2**). These results further reinforced the potentiality of using ccfDNA integrity and its size profiling as a diagnostic or follow-up tool for mCRC patients.

DISCUSSION

Up to now, most strategies of ctDNA detection are based on the targeting of tumor-specific mutations which implies the conception of a numerous assays or large NGS gene panels to cover a maximum of possible mutations. The use of epigenetic alterations such as hypermethylated sequences has been recently described in mCRC (27) but remains cancer specific. The characterization of DNA integrity has long been suggested as a potentially "universal" cancer marker (6). However, contradictory results have limited researchers' interest, which drew our attention on the importance of standardization.

The necessary normalization of the preanalytical conditions has been highlighted (28–30) and is also central to large research/network initiatives (31). As different clinical studies could present different preanalytical treatments, it is necessary to investigate the potential impact of preanalytical methods on the efficiency of purification of the different sizes of DNA fragments.

Several studies have recalled the impact of the collection tube on the ccfDNA integrity (32–34). The collection tubes mostly

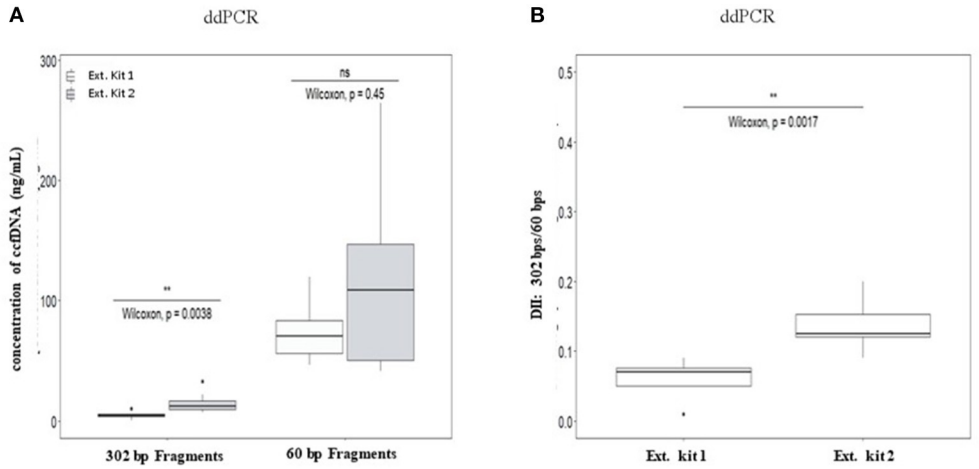

FIGURE 4 | Comparison of the influence of ccfDNA extraction methods on the resulting ccfDNA fragment concentrations **(A)** and DNA integrity **(B)** by ddPCR. Plasma from 10 healthy individuals were used in this analysis (see workflow in **Supplementary Figure 1**). Maxwell RSC ccfDNA Plasma Kit (extraction kit 1) (Promega) and QIAmp® Circulating Nucleic Acid Kit (extraction kit 2) (Qiagen) were used for ccfDNA extraction. DII were calculated for ddPCR using 302 bp amplicon as the long fragment and 60 bp amplicon as the short fragment ($n = 8$, two individuals were excluded as no ccfDNA was available) **(B)**. Wilcoxon test was used for significance analysis. *$p < 0.05$; **$p < 0.01$; ***$p < 0.001$.

differs on their content in preservative agents that prevent blood cell hemolysis (35). We did not observe such impact in our study (**Supplementary Figure 4**). This could be linked to the low number of healthy individuals studied. It could also be explain by the fact that the EDTA collection tubes were processed early after collection within the PLACOL study (26), limiting unwanted DNA fragmentation. Indeed, it has been shown that when tubes are not handled adequately, the genomic DNA coming from the blood cell could be released. This genomic DNA could both dilute the ccfDNA tumor fraction and disturb its fragmentation profile. The increase of multicentric clinical studies and the centralization of the analysis platforms could cause uncontrolled delays between blood collection and plasma separation. For these reasons, several ccfDNA preservative tubes have been developed, such as the BCT Streck tubes used in this study (36), that could become a reference collection tube dedicated to liquid biopsy (30).

Recent studies that compared extraction methods for the isolation of ccfDNA from plasma samples have concluded that they can affect both ccfDNA yield and fragmentation (32, 37). Our work confirmed these results showing significant differences both in terms of fragmentation and ccfDNA concentration.

Originator studies that have analyzed the DNA integrity in cancers, relied on the qPCR analysis of repetitive unspecific DNA sequences (ALU, LINE1) (16). Recent works however, have been developed to specifically measure integrity indexes while targeting cancer-specific mutated sequences by qPCR (23). These studies are nevertheless limited by the sensitivity and accuracy of basic bulk PCR techniques. Emerging methods based on droplet-based digital PCR could reach both high sensitivity and accuracy (38, 39) especially when following the Digital MIQE Guidelines (40). Moreover, innovative procedures have also been developed for fragment-based highly sensitive detection (19, 24). Our results demonstrated, using two independent strategies, a significant difference of ccfDNA fragmentation in plasma of mCRC patients compared with healthy subjects. Moreover, when specifically targeting the fraction of ccfDNA bearing cancer-specific mutations (and thus discriminating ctDNA) by ddPCR, significant differences were also observed between DNA bearing cancer-specific mutation(s) and non-mutated DNA in the patients from the PLACOL cohort. Such results confirmed the high fragmentation of ctDNA (with most fragments below 150 bp as highlighted by both strategies used), which is consistent with other studies (18, 41, 42). BIAbooster system provided complementary data to the ddPCR assay, evoking that a major part of the ctDNA could even be smaller than 110 bp (**Figure 5B1**; **Supplementary Figure 5**). The two methods lead to complementary information. Indeed digital-PCR assay quantifies amplifiable DNA fragments larger than a chosen size (i.e., if a 60-bp amplicon is amplified, detected DNA fragments be larger than 60 bp including the targeted sequence) whereas BIAbooster system determines the quantity of DNA fragments within a given size range (for example, between 75 and 110 bp).

In addition to pursuing the development of DII measurement of ccfDNA as a universal cancer marker, such results have strong implications with regard to future assay design. Indeed, we showed that assay targeting short amplicons allowed more sensitive and precise quantification of ctDNA, which is especially relevant for the analysis of low concentrated plasma samples. Interestingly, using IntPlex, Moulière et al. demonstrated that the targeting of small fragments within ccfDNA permits to increase the efficiency of the detection of ctDNA (23). In a more recent work, they also improved the detection of ctDNA by analyzing the shorter fragments after adding an either *in vitro* or *in silico* size selection step

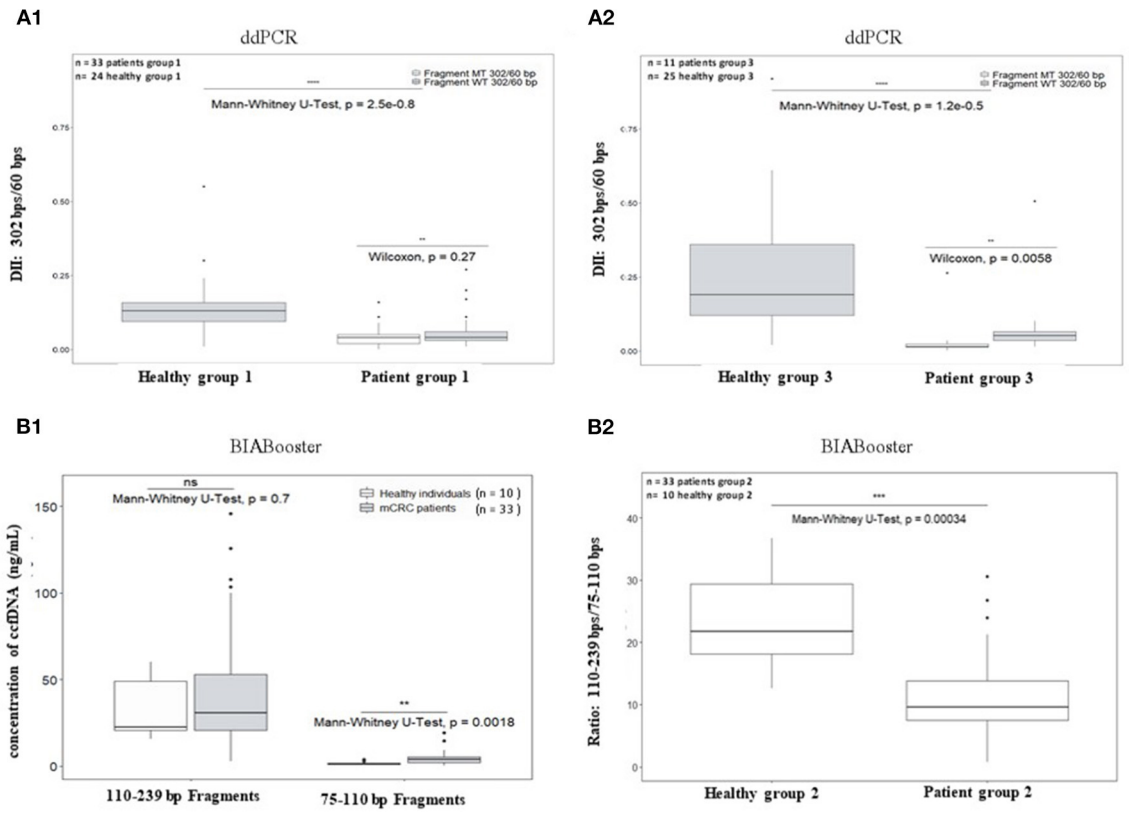

FIGURE 5 | Comparison of plasma ccfDNA integrity and ccfDNA size profiling between healthy individuals and metastatic CRC patients. As ccfDNA from different patients' groups were prepared with different preanalytic conditions (blood collection tubes and ccfDNA extraction kits), DII comparative analysis was performed for each patient group samples using healthy subject samples collected and treated with the same procedure (see workflow **Figure 2**). To calculate DII by ddPCR, 302 bp amplicon was used as long fragment and 60 bp amplicon as short fragment (**A1**: AGEO RASANC cohort and **A2**: PLACOL cohort). Two samples (one from AGEO RASANC study and one from PLACOL study) have been excluded due to an absence of detection of droplets bearing DNA-mutated fragments of 302 bp or more. To investigate different size distributions by the BIAbooster System, fragments with size ranging from 110 to 239 bp were used as long fragments and fragments with size ranging from 75 to 110 bp as short fragments (**B1**,**B2**: AGEO RASANC cohort only). Mann–Whitney *U*-test was used for significance analysis. $^{*}p < 0.05$; $^{**}p < 0.01$; $^{***}p < 0.001$; $^{***}p < 0.0005$. Fragmentation of *KRAS* WT and MT alleles within ccfDNA for mCRC patients is shown in (**A1**,**A2**). Mutant-allele frequency determined with the DII assay was compared with the one determined previously using other assays for the RASANC samples [BPER NGS, Bachet et al. Ann Oncol. (25)] and PLACOL samples [ddPCR targeting 86 bp amplicon, Garlan et al. CCR. (26)]. Linear regression model is given in **Supplementary Figure 6**.

(43). Xiao Liu et al. also enhanced the detection of pancreatic cancer by developing a new single-strand library preparation and hybrid-capture-based ccfDNA sequencing (SLHC-seq) to analyze small ccfDNA fragments (<100 bp) (44).

In conclusion, with the combined consideration of the importance of the standardization of preanalytical and analytical procedures as well as the increase of the sensibility and accuracy of analytical methods, the measure of DNA integrity should be an interesting parameter to develop new clinical biomarker in oncology. In particular, even if differences have been observed between sample preparation procedures, the crucial point appeared to ensure method consistency within a single study. Indeed, even if the ext.kit 2 may allow for highest purification of small DNA fragments (and thus probably of tumoral DNA enriched fraction) as compared with ext.kit 1, it also seems to lead to strongest variations in extraction efficiency (see **Figure 4**).Further analyses, involving a larger number of samples are required to allow for definitive conclusions. Moreover, the described procedures will allow conducting similar studies on newly developed ccfDNA extraction kits. The optimizations of the described ddPCR method could involve the development of multiplex assay that allows the measurement of different fragment sizes in a single pot. Yet, the limited number of patients in our study also requires further investigations. Another limitation is that we limited our analysis to patients with mCRC. Moreover, to fully validate the DII as cancer biomarker, further investigations about the cfDNA biology, in particular about the potential influence of aging on cfDNA fragmentation could be of interest. In order to assess its role in a more general setting, further studies should involve various cancer stages as well as other primary tumors. Moreover, investigating the processes leading to the observed differences of fragmentation profiles between tumor and healthy cells derived DNA would greatly contribute to the use of DII measurement as a universal cancer marker.

DATA AVAILABILITY STATEMENT

The datasets presented in this study can be found in online repositories. The names of the repository/repositories and accession number(s) can be found in the article/**Supplementary Material**.

ETHICS STATEMENT

The studies involving human participants were reviewed and approved by NCT02502656 (AGEO RASANC). The patients/participants provided their written informed consent to participate in this study.

AUTHOR CONTRIBUTIONS

All authors listed have made a substantial, direct and intellectual contribution to the work, and approved it for publication.

FUNDING

This work was supported by the Ministère de l'Enseignement Supérieur et de la Recherche, the Université Paris-Descartes, the Centre National de la Recherche Scientifique (CNRS), the Institut National de la Santé et de la Recherche Médicale (INSERM), the Institut National du Cancer (INCA, n° 2009-1-RT-03-US-1 and 2009-RT-03-UP5-1), the Association pour la recherche contre le cancer (ARC, no. SL220100601375), the Agence Nationale de la Recherche (ANR Nanobiotechnologies; no. ANR-10-NANO-0002-09), the SIRIC CARPEM, the ligue nationale contre le cancer (LNCC, Program Equipe labelisée LIGUE; no. EL2016.LNCC/VaT), and Advanced Merieux Research Grant (PL-P and VT). GP was supported by a CIFRE (N°2018/0368) funding from the Association Nationale Recherche Technologie (ANRT) and Eurofins-Biomnis. FGa thanks the Fondation Servier for a fellowship within the Frontiers in Life Science Ph.D. program (FdV). The RASANC trial was sponsored by AGEO and supported by a grant from Merck Serono s.a.s. (France) (no grant numbers apply), an affiliate of Merck KGaA (Darmstadt, Germany). The AGEO Group sponsored the trial and investigators were responsible for study design, data collection, data analysis, and data interpretation. Merck Serono s.a.s. (France), an affiliate of Merck KGaA (Darmstadt, Germany), supported this trial through grants to AGEO, but had no role in study design, data collection, data analysis, data interpretation, or writing of the report.

ACKNOWLEDGMENTS

The authors thank Dr. Antonio Alberdi and his colleagues from the Technological platform, Research Institute Saint-Louis Haematology, Immunology, Oncology Department, AP-NP for assistance to generate and validate fragmented DNA with ultrasonication (Covaris).

SUPPLEMENTARY MATERIAL

The Supplementary Material for this article can be found online at: https://www.frontiersin.org/articles/10.3389/fonc.2021.639675/full#supplementary-material

REFERENCES

1. Bardelli A, Pantel K. Liquid biopsies, what we do not know (Yet). *Cancer Cell.* (2017) 31:172–9. doi: 10.1016/j.ccell.2017.01.002
2. Butt AN, Swaminathan R. Overview of circulating nucleic acids in plasma/serum. *Annals N Y Acad Sci.* (2008) 1137:236–42. doi: 10.1196/annals.1448.002
3. Panabières CA, Pantel K. Clinical applications of circulating tumor cells and circulating tumor dna as liquid biopsy. *Cancer Discovery.* (2016) 6:479–91. doi: 10.1158/2159-8290.CD-15-1483
4. Bettegowda C, Sausen M, Leary RJ, Kinde I, Wang Y, Agrawal N, et al. Detection of circulating tumor DNA in early- and late-stage human malignancies. *Sci Trans Med.* (2014) 6:224ra24. doi: 10.1158/1538-7445.AM2014-5606
5. Aucamp J, Bronkhorst AJ, Badenhorst CPS, Pretorius PJ. The diverse origins of circulating cell-free DNA in the human body: a critical re-evaluation of the literature. *Biol Rev.* (2018) 93:1649–83. doi: 10.1111/brv.12413
6. Schwarzenbach H, Hoon DSB, Pantel K. Cell-free nucleic acids as biomarkers in cancer patients. *Nat Rev Cancer.* (2011) 11:426–37. doi: 10.1038/nrc3066
7. Mouliere F, Thierry AR. The importance of examining the proportion of circulating DNA originating from tumor, microenvironment and normal cells in colorectal cancer patients. *Expert Opinion Biol Therapy.* (2012) 12(Suppl. 1):S209–215. doi: 10.1517/14712598.2012.688023
8. Crowley E, Di Nicolantonio F, Loupakis F, Bardelli A. Liquid biopsy: monitoring cancer-genetics in the blood. *Nat Rev Clini Oncol.* (2013) 10:472–84. doi: 10.1038/nrclinonc.2013.110
9. Postel M, Roosen A, Laurent-Puig P, Taly V, Wang-Renault SF. Droplet-based digital PCR and next generation sequencing for monitoring circulating tumor DNA: a cancer diagnostic perspective. *Expert Rev Mol Diagnostics.* (2018) 18:7–17. doi: 10.1080/14737159.2018.1400384
10. Cortés-Hernandez LE, Eslami-S Z, Alix-Panabières C. Circulating tumor cell as the functional aspect of liquid biopsy to understand the metastatic cascade in solid cancer | Elsevier Enhanced Reader. *Mol Aspects Med.* (2019) 72:100816. doi: 10.1016/j.mam.2019.07.008
11. Cohen JD, Li L, Wang Y, Thoburn C, Afsari B, Danilova L, et al. Detection and localization of surgically resectable cancers with a multi-analyte blood test. *Science.* (2018) 359:926–30. doi: 10.1126/science.aar3247
12. Poulet G, Massias J, Taly V. Liquid biopsy: general concepts. *Acta Cytol.* (2019) 63:449–55. doi: 10.1159/000499337
13. Schøler LV, Reinert T, Ørntoft M-BW, Kassentoft CG, Andersen CL. Clinical implications of monitoring circulating tumor dna in patients with colorectal cancer. *Clin Cancer Res.* (2017) 23:5437–45. doi: 10.1158/1078-0432.CCR-17-0510
14. Arko-Boham B, Aryee NA, Blay RM, Owusu EDA, Tagoe EA, Doris Shackie E-S, et al. Circulating cell-free DNA integrity as a diagnostic and prognostic marker for breast and prostate cancers. *Cancer Genetics.* (2019) 235–236:65–71. doi: 10.1016/j.cancergen.2019.04.062
15. El Messaoudi S, Mouliere F, Du Manoir S, Gillet B, Thierry AR. Circulating DNA as a strong multimarker prognostic tool for metastatic colorectal cancer patient management care. *Clinical Cancer Res.* (2016) 22:3067–77. doi: 10.1158/1078-0432.CCR-15-0297
16. Umetani N, Kim J, Hiramatsu S, Reber HA, Hines OJ, Bilchik AJ, et al. Increased integrity of free circulating DNA in sera of patients with colorectal or periampullary cancer: direct quantitative PCR for ALU repeats. *Clin Chem.* (2006) 52:1062–9. doi: 10.1373/clinchem.2006.068577

17. Zonta E, Taly V, Nizard P. Assessment of DNA integrity, applications for cancer research. *Adv Clin Chem.* (2015) 70:197–246. doi: 10.1016/bs.acc.2015.03.002
18. Vizza E, Corrado G, De Angeli M, Carosi M, Mancini E, Baiocco E, et al. Serum DNA integrity index as a potential molecular biomarker in endometrial cancer. *J Exp Clin Cancer Res.* (2018) 37:16. doi: 10.1186/s13046-018-0708-4
19. Andriamanampisoa CL, Bancaud A, Boutonnet-Rodat A, Didelot A, Fabre J, Fina F, et al. BIABooster: online DNA concentration and size profiling with a limit of detection of 10 fg/μL and application to high-sensitivity characterization of circulating cell-free DNA. *Anal Chem.* (2018) 90:3766–74. doi: 10.1021/acs.analchem.7b04034
20. Jiang P, Chan CWM, Chan KCA, Cheng SH, Wong J, Wong VW-S, et al. Lengthening and shortening of plasma DNA in hepatocellular carcinoma patients. *Proc Natl Acad Sci USA.* (2015) 112:3178–9. doi: 10.1073/pnas.1500076112
21. Mouliere F, Robert B, Arnau Peyrotte E, Del Rio M, Ychou M, Molina F, et al. High fragmentation characterizes tumour-derived circulating DNA. Lee T, editor. *PLoS ONE.* (2011) 6:e23418. doi: 10.1371/journal.pone.0023418
22. Thierry AR, Mouliere F, Gongora C, Ollier J, Robert B, Ychou M, et al. Origin and quantification of circulating DNA in mice with human colorectal cancer xenografts. *Nucleic Acids Res.* (2010) 38:6159–75. doi: 10.1093/nar/gkq421
23. Mouliere F, El Messaoudi S, Gongora C, Guedj A-S, Robert B, Del Rio M, et al. Circulating cell-free DNA from colorectal cancer patients may reveal high KRAS or BRAF mutation load. *Trans Oncol.* (2013) 6:319–28. doi: 10.1593/tlo.12445
24. Underhill HR, Kitzman JO, Hellwig S, Welker NC, Daza R, Baker DN, et al. Fragment length of circulating tumor DNA. *PLoS Genet.* (2016) 12:e1006162. doi: 10.1371/journal.pgen.1006162
25. Bachet JB, Bouché O, Taieb J, Dubreuil O, Garcia ML, Meurisse A, et al. RAS mutation analysis in circulating tumor DNA from patients with metastatic colorectal cancer: the AGEO RASANC prospective multicenter study. *Ann Oncol.* (2018) 29:1211–9. doi: 10.1093/annonc/mdy061
26. Garlan F, Laurent-Puig P, Blons H, Taly V. Early evaluation of circulating tumor DNA as marker of therapeutic efficacy in metastatic colorectal cancer patients (PLACOL Study). *Clinical Cancer Res.* (2017) 23:5416–25. doi: 10.1158/1078-0432.CCR-16-3155
27. Garrigou S, Perkins G, Garlan F, Normand C, Didelot A, Le Corre D, et al. A study of hypermethylated circulating tumor DNA as a universal colorectal cancer biomarker. *Clin Chem.* (2016) 62:1129–39. doi: 10.1373/clinchem.2015.253609
28. Lampignano R, Neumann MHD, Weber S, Heitzer E. Multicenter evaluation of circulating cell-free DNA extraction and downstream analyses for the development of standardized (pre)analytical work flows. *Clin Chem.* (2019) 65:306837. doi: 10.1373/clinchem.2019.306837
29. Meddeb R, Pisareva E, Thierry AR. Guidelines for the preanalytical conditions for analyzing circulating cell-free DNA. *Clin Chem.* (2019) 65:623–33. doi: 10.1373/clinchem.2018.298323
30. Nikolaev S, Lemmens L, Koessler T, Nouspiked T. Circulating tumoral DNA: preanalytical validation and quality control in a diagnostic laboratory. *Anal Biochem.* (2018) 542:34–9. doi: 10.1016/j.ab.2017.11.004
31. Cancer-ID. Cancer treatment and monitoring through identification of circulating tumor cells and tumor related nucleic acids in blood [Internet]. Available online at: https://www.cancer-id.eu
32. Sorber L, Zwaenepoel K, Deschoolmeester V, Roeyen G, Lardon F, Rolfo C, et al. A comparison of cell-free DNA isolation kits: isolation and quantification of cell-free DNA in plasma. *J Mol Diagn.* (2017) 19:162–8. doi: 10.1016/j.jmoldx.2016.09.009
33. Norton SE, Luna KK, Lechner JM, Qin J, Fernando MR. A new blood collection device minimizes cellular dna release during sample storage and shipping when compared to a standard device. *J Clin Lab Anal.* (2013) 27:305–11. doi: 10.1002/jcla.21603
34. Almazi JG, Pockney P, Craig G, Smith ND, Hondermarck H, Verrills NM, et al. Cell-free DNA blood collection tubes are appropriate for clinical proteomics: a demonstration in colorectal cancer. *Proteomics Clin Applic.* (2018) 12:e1700121. doi: 10.1002/prca.201700121
35. Zhao Y, Li Y, Li S, Luo J, Xia H. Performance comparison of blood collection tubes as liquid biopsy storage system for minimizing cfDNA contamination from genomic DNA. *J Clin Lab Anal.* (2019) 33:e22670. doi: 10.1002/jcla.22670
36. Diaz IM, Nocon A, Mehnert DH, Fredebohm J, Diehl F, Holtrup F. Performance of Streck cfDNA blood collection tubes for liquid biopsy testing. *PLoS ONE.* (2016) 11:e0166354. doi: 10.1371/journal.pone.0166354
37. Pérez-Barrios C, Nieto-Alcolado I, Torrente M, Jiménez-Sánchez C, Calvo V, Gutierrez-Sanz L, et al. Comparison of methods for circulating cell-free DNA isolation using blood from cancer patients: impact on biomarker testing. *Translational Lung Cancer Research.* (2016) 5:665–72. doi: 10.21037/tlcr.2016.12.03
38. Yoshida R, Sasaki T, Umekage Y, Tanno S, Ono Y, Ogata M, et al. Highly sensitive detection of ALK resistance mutations in plasma using droplet digital PCR. *BMC Cancer.* (2018) 18:1136. doi: 10.1186/s12885-018-5031-0
39. Pekin D, Skhiri Y, Baret J-C, Le Corre D, Mazutis L, Ben Salem C, et al. Quantitative and sensitive detection of rare mutations using droplet-based microfluidics. *Lab on a Chip.* (2011) 11:2156–66. doi: 10.1039/c1lc20128j
40. Huggett JF, Foy CA, Benes V, Emslie K, Garson JA, Bustin SA. The digital MIQE guidelines: minimum information for publication of quantitative digital PCR experiments | clinical chemistry. *Clinical Chemistry.* (2019) 59:892–902. doi: 10.1373/clinchem.2013.206375
41. Sobhani, N, Generali, D, Zanconati F, Bortul M. Cell-free DNA integrity for the monitoring of breast cancer: future perspectives? *World J Clin Oncol.* (2018) 9:26–32. doi: 10.5306/wjco.v9.i2.26
42. Cheng J, Holland-Letz T, Wallwiener M, Surowy H, Cuk K, Schott S, et al. Circulating free DNA integrity and concentration as independent prognostic markers in metastatic breast cancer. *Breast Cancer Res Treat.* (2018) 169:69–82. doi: 10.1007/s10549-018-4666-5
43. Mouliere F, Chandrananda D, Piskorz AM, Moore EK, Morris J, Ahlborn LB, et al. Enhanced detection of circulating tumor DNA by fragment size analysis. *Sci Transl Med.* (2018) 10:eaat4921. doi: 10.1126/scitranslmed.aat4921
44. Liu X, Liu L, Ji Y, Li C, Wei T, Yang X, et al. Enrichment of short mutant cell-free DNA fragments enhanced detection of pancreatic cancer. *EBioMedicine.* (2019) 41:345–56. doi: 10.1016/j.ebiom.2019.02.010

Conflict of Interest: VT: Honoraria from Raindance Technologies and Boerhinger Ingehleim; cofounder emulseo; board emulseo. JT: Honoraria from Merck, Amgen, Roche, Pierre Fabre, MSD, Sanofi, and Lilly, Servier, and Astra-Zeneca. AZ: consulting and/or advisory boards for: Roche, Merck Serono, Amgen, Sanofi, and Lilly. PL-P: Honoraria and board: Amgen, Merck-Serono, Boehringer Ingelheim, Sanofi, Roche, and Lilly. HB: Honoraria Astra-Zeneca, BMS, MSD. JT: Honoraria from Merck, AMGEN, ROCHE, SIRTEX, BAXALTA, SANOFI, Lilly, and Servier. AZ: Consulting and/or advisory boards for Roche, Merck Serono, Amgen, Sanofi, and Lilly. GP, LP, and VG: Eurofins-Biomnis employee. FGa: Bio-Rad employee. AB and FGi were employed by company ADELIS.

The remaining authors declare that the research was conducted in the absence of any commercial or financial relationships that could be construed as a potential conflict of interest.

Copyright © 2021 Poulet, Garlan, Garrigou, Zonta, Benhaim, Carrillon, Didelot, Le Corre, Mulot, Nizard, Ginot, Boutonnet-Rodat, Blons, Bachet, Taïeb, Zaanan, Geromel, Pellegrina, Laurent-Puig, Wang-Renault and Taly. This is an open-access article distributed under the terms of the Creative Commons Attribution License (CC BY). The use, distribution or reproduction in other forums is permitted, provided the original author(s) and the copyright owner(s) are credited and that the original publication in this journal is cited, in accordance with accepted academic practice. No use, distribution or reproduction is permitted which does not comply with these terms.

frontiers in Oncology

ORIGINAL RESEARCH
published: 24 May 2021
doi: 10.3389/fonc.2021.654140

Post-Biopsy Cell-Free DNA From Blood: An Open Window on Primary Prostate Cancer Genetics and Biology

*Marinella Corbetta[1], Chiara Chiereghin[2], Ilaria De Simone[1,2], Giulia Soldà[1,2], Monica Zuradelli[1,3], Michele Giunta[1], Giovanni Lughezzani[1,2], Nicolò Maria Buffi[1,2], Rodolfo Hurle[2], Alberto Saita[2], Paolo Casale[2], Rosanna Asselta[1,2], Massimo Lazzeri[1], Giorgio Guazzoni[1,2] and Stefano Duga[1,2]**

[1] Department of Biomedical Sciences, Humanitas University, Milan, Italy, [2] IRCCS Humanitas Research Hospital, Milan, Italy, [3] IRCCS Humanitas Research Hospital, Humanitas Cancer Center, Milan, Italy

Circulating cell-free DNA (ccfDNA), released from normal and cancerous cells, is a promising biomarker for cancer detection as in neoplastic patients it is enriched in tumor-derived DNA (ctDNA). ctDNA contains cancer-specific mutations and epigenetic modifications, which can have diagnostic/prognostic value. However, in primary tumors, and in particular in localized prostate cancer (PCa), the fraction of ctDNA is very low and conventional strategies to study ccfDNA are unsuccessful. Here we demonstrate that prostate biopsy, by causing multiple injuries to the organ, leads to a significant increase in plasma concentration of ccfDNA ($P<0.0024$) in primary PCa patients. By calculating the minor allele fraction at patient-specific somatic mutations pre- and post-biopsy, we show that ctDNA is significantly enriched (from 3.9 to 164 fold) after biopsy, representing a transient "molecular window" to access and analyze ctDNA. Moreover, we show that newly released ccfDNA contains a larger fraction of di-, tri- and multi-nucleosome associated DNA fragments. This feature could be exploited to further enrich prostate-derived ccfDNA and to analyze epigenetic markers. Our data represent a proof-of-concept that liquid tumor profiling from peripheral blood performed just after the biopsy procedure can open a "valuable molecular metastatic window" giving access to the tumor genetic asset, thus providing an opportunity for early cancer detection and individual genomic profiling in the view of PCa precision medicine.

Keywords: circulating cell-free DNA, circulating tumor DNA, primary prostate cancer, biopsy, biomarker

OPEN ACCESS

Edited by:
Catherine Alix-Panabieres, Centre Hospitalier Universitaire de Montpellier, France

Reviewed by:
Gabriella Guida, University of Bari Aldo Moro, Italy
Carlo V. Bruschi, University of Salzburg, Austria

***Correspondence:**
Stefano Duga
stefano.duga@hunimed.eu

Specialty section:
This article was submitted to Molecular and Cellular Oncology, a section of the journal Frontiers in Oncology

Received: *15 January 2021*
Accepted: *23 April 2021*
Published: *24 May 2021*

Citation:
Corbetta M, Chiereghin C, De Simone I, Soldà G, Zuradelli M, Giunta M, Lughezzani G, Buffi NM, Hurle R, Saita A, Casale P, Asselta R, Lazzeri M, Guazzoni G and Duga S (2021) Post-Biopsy Cell-Free DNA From Blood: An Open Window on Primary Prostate Cancer Genetics and Biology. Front. Oncol. 11:654140. doi: 10.3389/fonc.2021.654140

INTRODUCTION

The analysis of circulating cell-free DNA (ccfDNA) represents one of the most promising strategies for non-invasive disease monitoring (1). In cancer management, it has been effectively used to follow tumor evolution and acquisition of resistance, as well as for guiding treatment decisions in multiple non-hematologic diseases. ccfDNA is thought to be released into the bloodstream by all cells, both by active secretion and as a consequence of death by apoptosis or necrosis, in response to both physiological processes (i.e. exercise), as well as malignant and non-malignant pathological conditions, such as inflammation and tissue damage (2). Although the first description of ccfDNA in plasma dates back to 1948 (3), abnormalities in patients with cancer were observed only decades later (4, 5), and the exact mechanism of its release and its biological properties still remain unclear.

During cancer development, tumor-derived DNA is released in the circulation (circulating tumor DNA, ctDNA) since early stages of the disease and mixes with a larger amount of physiologically released nonmalignant DNA, which is mostly derived from hematopoietic cells (6, 7). The fraction of cancer-derived ccfDNA is highly variable, and mainly depends on two factors: i) the advancement of the disease, with more ctDNA reflecting a greater disease burden, and ii) the location of the tumor, with colon, gastroduodenal tract, breast, pancreas, liver, and skin cancers releasing large amounts of ctDNA, whereas glioma, thyroid, kidney, and prostate tumors are associated with the smallest amount of ctDNA in plasma (8, 9). These tissue differences have been explained by the presence of the blood-brain barrier for gliomas and of an organ capsule/pseudocapsule for thyroid, prostate, and kidney cancer, limiting the diffusion of ctDNA into blood (9).

Once released in the circulation, ccfDNA undergoes a rapid degradation by nucleases (10, 11), with an estimated half-life of fewer than 2 h (12, 13). Therefore, most ccfDNA presents as a 160- to 170-bp peak, roughly corresponding to the portion of DNA protected by the interaction with histones in nucleosomes (14, 15). Larger fragments, of about 360 to 400 bp and more, have also been reported, likely representing multimers of nucleosomes (16). Dying cells and tumors undergoing cell necrosis were shown to release additional longer fragments, up to 10 kb (14). Tissue-specific methylation signatures and nucleosome phasing analysis have been effectively used to derive the organ of origin of ccfDNA (7, 15, 17). Recently, the fragment length of ctDNA from different cancers was found to be more variable compared to non-cancer ccfDNA, probably reflecting tumor-specific changes in chromatin structure and epigenetics marks, suggesting that ccfDNA fragmentation could serve as a biomarker for cancer detection (18).

Concerning prostate cancer (PCa), only few studies have explored ctDNA as a potential biomarker in localized disease to distinguish PCa from benign prostatic hyperplasia in patients with elevated prostate-specific antigen (PSA) (19), to provide prognostic information in patients undergoing radical prostatectomy (20), or to follow-up patients with PCa (21). More recently, Hennigan and colleagues confirmed that in localized PCa, allele-specific alterations in ctDNA are below the threshold for detection, even in high-risk patients who will eventually develop disease recurrence (22). A larger number of studies, conversely, explored the feasibility to use ctDNA in advanced metastatic and castration-resistant disease, demonstrating that ctDNA from liquid biopsies can be used to get insights into the mutational burden of metastatic PCa, without the need for direct tissue sampling, and as prognostic biomarker of response to therapy (23–29).

It has been clearly demonstrated that certain conditions, including inflammation, exercise, or tissue injury, substantially increase the ccfDNA level. In particular, it was shown that ccfDNA levels may increase by more than an order of magnitude during surgery (12). Similarly, we could hypothesize that prostate biopsy, by requiring multiple punctures of the organ, would release a large amount of prostate DNA representative of all analyzed regions, creating a sort of temporary time window for ccfDNA analysis, which may allow getting genetic information for a precision-decision making, even in localized PCa. Hence, we tested the hypothesis that prostate biopsy may generate a transient increase in prostate-derived ccfDNA, which is also likely to be enriched in ctDNA, and could provide molecular data on the tumor of diagnostic, prognostic, and theranostic relevance.

MATERIALS AND METHODS

Study Cohort and Sample Collection

The study was approved by the Humanitas Clinical and Research Center Ethics Committee (336/19) and all participants signed an appropriate informed consent. We enrolled 38 patients who underwent prostate biopsy for suspected PCa according to indications from their referring urologists. Twenty-one patients already had a prostate biopsy in the past that detected PCa Gleason 3 + 3 in 10 and 3 + 4 in 1 patient. Inclusion criteria were the following: i) patients >45 years of age with or without a positive digital rectal examination (DRE); ii) total PSA >2 ng/ml, according to Hybritech B&C calibration and suspected mpMRI for PCa (Prostate Imaging-Recording and Data System [PI-RADS] v.2 – score >=3). Patients with a previous diagnosis of PCa who were under active surveillance and high-grade prostatic intraepithelial neoplasia or atypical small acinar proliferation were also considered as cases. Exclusion criteria were the following: i) patients with bacterial acute prostatitis in the 3 months prior to biopsy; ii) patients subjected to previous endoscopic surgery of the prostate; iii) patients being treated with dutasteride or finasteride. Subjects with chronic renal failure, marked blood protein alterations (plasma normal range, 6–8 g/100 ml), hemophiliacs, or those previously submitted to multiple blood transfusions were not included in the study, as these conditions may alter the analysis. mpMRI/TRUS software assisted fusion-guided biopsy was performed in 31 patients by two experienced urologists (ML and GL) with more than 500 procedure each one. The prostate profile and regions of interest (ROIs) were manually contoured by the expert urologists and radiologists. Images of the prostate and mpMRI derived ROIs were fused in real time for biopsy. The procedures were performed by transperineal or transrectal approach and two

or more cores for single ROI were sampled plus a systematic random biopsy (12 cores) according to EAU Guideline for biopsy-naïve patients. Seven patients received a trans rectal ultrasound guided systematic (12 core) biopsy. In patients whose biopsies were studied by RNA sequencing, the analyzed core was harvested from the highest PIRADS ROI or mpMRI index lesion.

After the diagnosis of PCa, 18 patients underwent radical prostatectomy, including two patients under active surveillance (AS) who were up-graded to clinical significant PCa. Four patients under AS, who were upgraded, opted for androgen deprivation therapy or radiotherapy and seven continued their follow-up according to Prostate Cancer Research International Active Surveillance (PRIAS) protocol. One patient with a very high risk disease received radiotherapy and ADT. Five patients who presented benign prostate hyperplasia received a medical therapy. Three patients were referred to their general practitioner.

Fresh-needle biopsies and blood samples were collected from all 38 patients, whose clinicopathological information are summed up in **Table 1**. Fresh-needle biopsies were immersed into the RNAlater stabilization solution (Sigma-Aldrich, St Louis, MO, USA) immediately after withdrawal and were left overnight at 4°C to allow the solution enter the sample. After RNAlater removal, biopsies were stored at −80°C. Blood samples, approximately 3 ml each, were collected in Vacutainer® EDTA tubes and withdrawn from patients prior and after biopsy, at different time points (10, 30, 60, and 120 minutes after the procedure).

Isolation of ccfDNA

Isolation of ccfDNA was performed within 1 hour from blood withdrawal; samples were centrifuged to isolate plasma for 10 minutes at 2000g at room temperature. To ensure that the cellular component was completely removed, plasma was centrifuged again at 2000g for 10 minutes at room temperature. The collected plasma was either immediately processed for ccfDNA extraction with the Maxwell RSC ccfDNA Plasma Kit (Promega, Madison, WI, USA) using the Maxwell instrument (Promega), or stored at −20°C until use. DNA was quantified using a fluorometer (Thermo Fisher Scientific, Waltham, MA, USA) with the Qubit™ dsDNA HS Assay Kit (Thermo Fisher Scientific). Qualitative analysis was performed with the Agilent High Sensitivity D5000 ScreenTape System on Agilent-4200 TapeStation (Agilent Technologies; Santa Clara, CA, USA).

RNA Extraction From Biopsies

Molecular analyses were performed on a total of 28 patients. Biopsy samples were disrupted and homogenized in presence of Tungsten Carbide Beads, 3 mm diameter (QIAGEN, Hilden, Germany) with the TissueLyser II (QIAGEN). RNA was extracted from the homogenized samples using the Maxwell® RSC miRNA Tissue Kit, with the automated Maxwell instrument, according to the manufacturer's protocol. RNA was quantified by Qubit fluorometer with Qubit™ RNA HS Assay Kit (Thermo Fisher Scientific) and RNA quality was assessed with the Agilent High Sensitivity RNA Screen Tape (Agilent Technologies) on an Agilent-4200 Tapestation, obtaining a mean RNA integrity number (RIN) value of 7.05 (max value 10, min value 3.7).

Next-Generation Sequencing (NGS) Analysis

Targeted RNA sequencing was performed using the TruSight RNA Pan-Cancer Panel (Illumina, San Diego, CA, USA). Libraries were prepared starting from 55 to 75 ng of RNA, following the manufacturer's protocol. cDNA libraries, synthesized from fragmented RNA, were sequenced as 76-bp paired-end reads on a NextSeq550 platform (Illumina).

Sequencing data were analyzed using the RNAseq alignment v. 2.0.10 pipeline on BaseSpace (Illumina). Briefly, input reads were filtered against abundant sequences, such as mitochondrial or ribosomal sequences, using Bowtie 0.12.9 (30), and then aligned to the reference human genome (UCSC hg19) and the RefSeq annotation of transcripts using the Spliced Transcripts Alignment to a Reference (STAR) program (v. 2.6.1a) (31). Single nucleotide variants (SNVs) were identified with the Strelka Variant Caller v.2.9.9 (32), and the presence of fusion transcripts was detected with the Manta Structural Variant Caller v.1.4.0 (33).

Somatic SNV Selection From Patients' Bioptic Tissue

The variant call lists were filtered to identify somatic SNVs. Five rare variants (with minor allele frequency, MAF, <0.01, for annotated variants) covered by at least 50 reads and falling

TABLE 1 | Patient characteristics and biopsy results.

Status*	N	Age, years (mean ± SD; range)	Pre-biopsy PSA level, ng/mL (median; [IQR])	% positive cores (mean ± SD; range)	Prostate volume, mm^3 (mean ± SD; range)
No cancer	5	67 ± 10; 52–76	6.00 [3.97–11.62]	0	n.a.
3+3	7	65 ± 5; 57–71	5.40 [5.10–10.55]	14.8 ± 20.4; 12.5–57.1	40.3 ± 15.9; 22–49.8
3+4	13	67 ± 6; 51–74	8.20 [5.89–12.90]	31.8 ± 17.9; 15.8–60	33.2 ± 19.7; 12.48–60
4+3	5	72 ± 4; 69–78	9.96 [5.25–17.80]	36.1 ± 25.2; 18.8–80	42.7 ± 18; 31.8–63.4
4+4	6	63 ± 7; 55–70	13.54 [10.67–24.48]	68 ± 39; 6.3–100	68.6 ± 3.67; 66–72.8
4+5	1	56	23.14	100	n.a.
5+5	1	80	20	58.3	n.a.

Pre-biopsy PSA level is indicated as median and interquartile range (IQR) expressed as [quartile 1- quartile 3]. All other parameters are indicated as mean ± standard deviation (SD). N, number; n.a., not available; PSA, prostate-specific antigen.

**Patients with PCa were classified according to the Gleason Score.*

into exonic regions were selected and verified by Sanger sequencing. For all chosen variants, one primer pair spanning the region containing the SNV of interest was designed. Genomic DNA was extracted from the cellular components of blood samples recovered after plasma separation. 1.5 mL of phosphate buffered saline (PBS) 1x was added to blood cellular components and the extractions were performed from 400 µL of resuspended cells with the Maxwell 16 Blood DNA Purification kit (Promega). PCR reactions were conducted by using the GoTaq® G2 Flexi DNA Polymerase (Promega), according to the manufacturer's instructions. Sequencing reactions were performed using the BigDye Terminator Cycle Sequencing Ready Reaction Kit v1.1 (Thermo Fisher Scientific) and then loaded on an ABI-3500 sequencer (Thermo Fisher Scientific). Electropherograms were analyzed with the FinchTV software. All primers were purchased from Sigma. Primer sequences and PCR cycling conditions for each amplicon are available on request.

Detection of Selected Somatic Mutations in ccfDNA

To amplify the genomic regions containing the selected somatic variants in pre- and post-biopsy ccfDNA, PCR assays were designed and performed using the low-error rate Q5® High-Fidelity DNA Polymerase (New England BioLabs, Ipswich, MA, USA). Each reaction was carried out in a final volume of 50 µL, following the manufacturer's instructions, and starting from at least 1 ng of ccfDNA. For each variant, the same PCR was performed starting from pre- and post-ccfDNA of the relevant patient. Purified PCR products were quantified with the Qubit™ dsDNA HS Assay Kit on the Qubit fluorometer. NGS analysis of amplicons was carried out with the NEBNext® Ultra™ II DNA Library Prep Kit for Illumina (New England BioLabs). In this regard, two different amplicon pools were generated: a pre-biopsy ccfDNA and a post-biopsy ccfDNA amplicon pool; in each pool amplicons were equally represented. Libraries were prepared following the manufacturer's instructions, starting from the same amount of material for each coupled pre- and post-biopsy pool, varying from a minimum of 195 ng to a maximum of 490 ng. Libraries were sequenced on the NextSeq550 platform obtaining a mean depth of 235,367x. Read number and base count of each variant were reported following BAM alignment on the hg19 reference genome, through visualization with the Integrative Genomics Viewer tool (34).

Statistical Analysis

All statistical analyses were performed using GraphPad Prism version 7.01 for Windows (GraphPad software, San Diego, California USA, www.graphpad.com). Wilcoxon matched-pairs signed rank test was applied to calculate statistical significance of the observed differences in ccfDNA levels between pre- and post-biopsy conditions at all analyzed time points. The same statistical test was also used to evaluate the size increase of ccfDNA peaks pre- and post-biopsy.

RESULTS

Clinical and Histological Features of Analyzed Subjects

A total of 38 patients referred to prostate biopsy for suspected PCa were enrolled in the study (**Table 1**). The median preoperative PSA of these patients was 9.96 ng/mL [IQR 5.35 ng/mL to 17.8 ng/mL]. Upon biopsy analysis, 5 patients had no evidence of PCa, 7 had lSUP1 (Gleason score <3+4), 18 had ISUP2 or 3 (Gleason score 3 + 4 and 4 + 3, respectively), and 8 had ISUP4 or 5 (Gleason score >4+3).

Prostate Biopsy Increases ccfDNA Levels in Blood

A first blood sample for ccfDNA extraction was taken from 32 patients immediately before the biopsy procedure. A second blood sample was collected either 60 (N=13) or 120 (N=19) minutes after the biopsy. The amount of ccfDNA extracted from 1 mL of plasma was measured using a QubitVR 2.0 Fluorometer.

As shown in **Figure 1**, the total amount of ccfDNA was significantly increased in the post-biopsy samples compared to pre-biopsy ones at both time points (60 min: pre-biopsy median 2.76 ng/mL, IQR: 2.29–4.07 ng/mL vs post-biopsy median 3.62 ng/mL, IQR: 3.12–5.19 ng/mL, P=0.0024; 120 min: pre-biopsy 5.1 ng/mL, IQR: 4.22–5.58 ng/mL vs post-biopsy, median 7.05 ng/mL, IQR: 5.98–7.5 ng/mL, P=0.0023). No correlation between post-biopsy ccfDNA levels and Gleason score was observed (data not show).

Kinetics of ccfDNA Increase After Prostate Biopsy

Six additional patients were analyzed to describe the time course of ccfDNA release after biopsy. For this purpose, in addition to the pre-biopsy sample, a total of 4 blood samples at different time points (10, 30, 60, and 120 min after the procedure) were taken for each patient. The extracted ccfDNA was then analyzed for size and concentration. Comparing the profiles of each patient at different time points (see as an example the quali/quantitative reports in **Figure 2**) we could confirm a significant increase in the size of ccfDNA fragments after the biopsy. In particular, at both 60 and 120 minutes after biopsy, we observed the presence of a significant amount of ccfDNA fragments longer than 350 bp (up to 1.5 kb), likely corresponding to DNA associated to multiple nucleosomes (**Figure 2**).

Moreover, in all six cases, the kinetics of ccfDNA release in circulation showed an increase in ccfDNA levels with time, with the highest average ccfDNA concentration observed 1 hour after the procedure; however, only some patients showed a peak in ccfDNA at 1 hour, while in others the increase continued at 2 hours post biopsy (**Figure 3**).

Size Distribution Analysis of ccfDNA

In pre-biopsy samples, a typical ccfDNA size-pattern was found, with a main 160 to 165 bp peak and a minor 360 to 400 bp peak, representing mono and di-nucleosomal lengths, respectively (**Figure 4**). Comparing pre- and post-biopsy samples, the

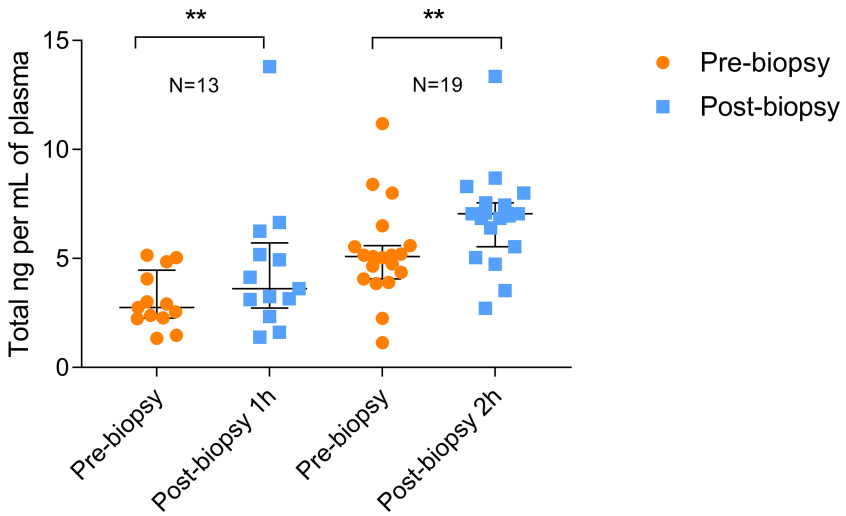

FIGURE 1 | Quantitation of pre- and post-biopsy ccfDNA from blood. ccfDNA extracted from blood immediately before the biopsy and after 1 or 2 hours from the end of the procedure. Scatter plots (with median and interquartile range) show the amount of ccfDNA expressed as ng/mL of plasma. The number of analyzed individuals in shown above the plots (** P<0.01; Wilcoxon test for paired samples).

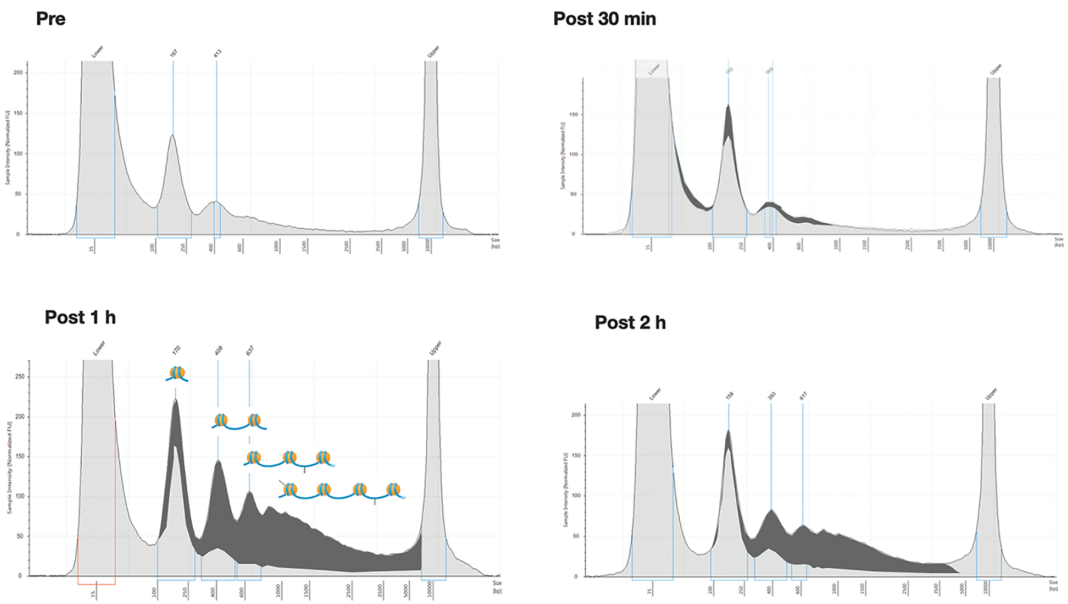

FIGURE 2 | Overall size distribution of ccfDNA pre- and post-biopsy. Representative Tape station electropherograms showing DNA fragment size distribution in ccfDNA isolated from plasma of a single patient (P20) pre-biopsy and after 30 min, 1 hour, and 2 hours from the procedure. The longer fragments appearing after 1 and 2 hours post-biopsy are highlighted in dark grey as the portion of the area under the curve after subtracting the profile obtained for pre-biopsy ccfDNA. In the 1h panel a schematic representation of the predicted nucleosomal structure of the detected fragments is depicted above the profiles.

increase in the area of the 360-bp peak was significantly higher than the one measured for the 160-bp peak (75.11% vs. 37.46%, P=0.0007), confirming that post-biopsy ccfDNA contains qualitatively different DNA. Moreover, in post-biopsy ccfDNA, additional peaks were visible at about 630 bp and 870 bp, likely representing further nucleosomal multimers, as well as fragments larger than 1 kb (**Figure 4**).

ctDNA Enrichment in Post-Biopsy ccfDNA

The significant increase in ccfDNA after the biopsy is likely to derive from the tissue damage caused by the needle puncture injury. So, we hypothesized that the ccfDNA released in the bloodstream should be enriched in prostate-derived DNA and, particularly, in ctDNA. To validate this hypothesis, we searched for patient-specific somatic mutations in the tumor tissue

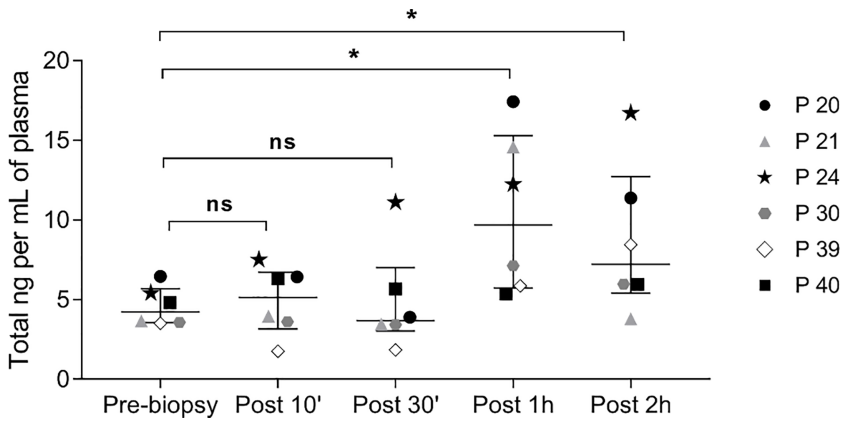

FIGURE 3 | Kinetics of ccfDNA release in circulation after prostate biopsy. Scatter plots, with median and interquartile range, of ccfDNA concentration (ng/mL plasma) as quantified by the Qubit fluorometer in the plasma of 6 patients at different time points. ns, not significant; * P< 0.05; Wilcoxon test for paired samples.

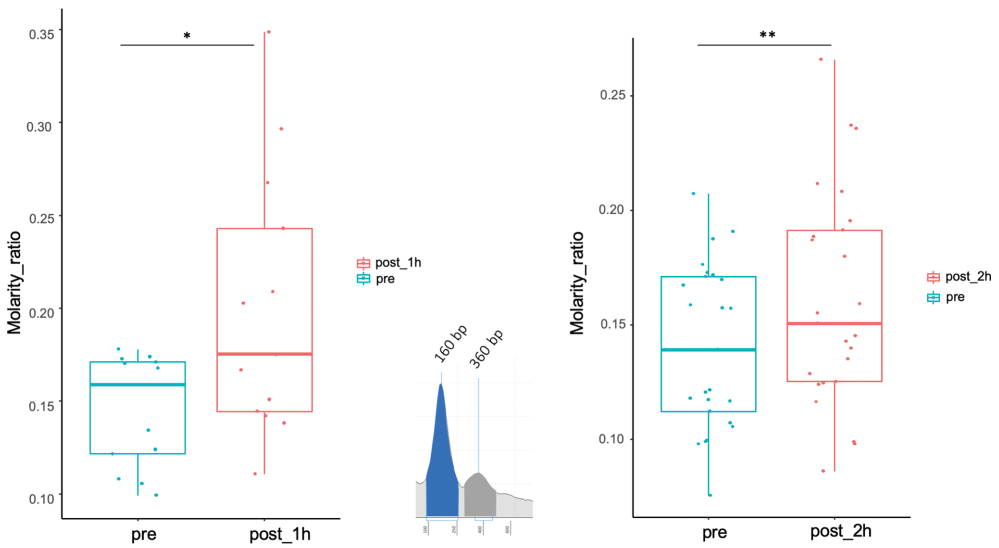

FIGURE 4 | Size shift in post-biopsy ccfDNA vs. pre-biopsy ccfDNA. Boxplots show the molarity ratio between the 360 bp (DNA associated to two consecutive nucleosomes) and the 160 bp (DNA associated with a single nucleosome) peaks obtained by measuring the peak area, one hour and 2 hours from the biopsy procedure. Boxes define the interquartile range; the central line refers to the median. The number of analyzed individuals in shown below the graph (*P < 0.05, **P < 0.01; Wilcoxon test for paired samples).

(obtained from a fresh biopsy of the index lesion) by targeted RNAseq using the TruSight RNA Pan-Cancer kit, which enriches for 1,385 cancer-related genes, including some of the most frequently mutated genes in PCa. A total of 28 patients were selected for molecular analysis. We obtained a mean number of reads per patient of 22.7 M with an average of 98% of aligned reads to the reference genome. Coding regions were covered with an average depth of 721.7×. Variant calling on NGS data found on average 4,112 SNVs per patient. To identify likely somatic variants, we selected only exonic SNVs with an alternative allele fraction ≤0.35, MAF<0.01 in the general population, and covered by at least 50 reads. Variants that were recurrently found in more than 25% of the samples were excluded as putative sequencing artifacts. After prioritization, a total of 188 candidate somatic variants (on average 7 per patient) in 87 genes were left (**Figure 5**). Of these, 106 were missense, 76 were synonymous/silent, and 6 nonsense.

Five variants, namely NM_005338.7(HIP1):c.2167G>A (p.Glu723Lys), NM_000546.5 (TP53):c.747G>C/T(p.Arg249Ser), NM_014991.5(WDFY3):c.718A>G(p.Met240Val), NM_022455.5 (NSD1):c.3049A>T(p.Thr1017Ala), and NM_015001.3(SPEN): c.2500C>T(p.Gln834Ter), in four patients were selected and validated by Sanger sequencing. Absence in germline DNA confirmed that all selected variants (one nonsense, four missense)

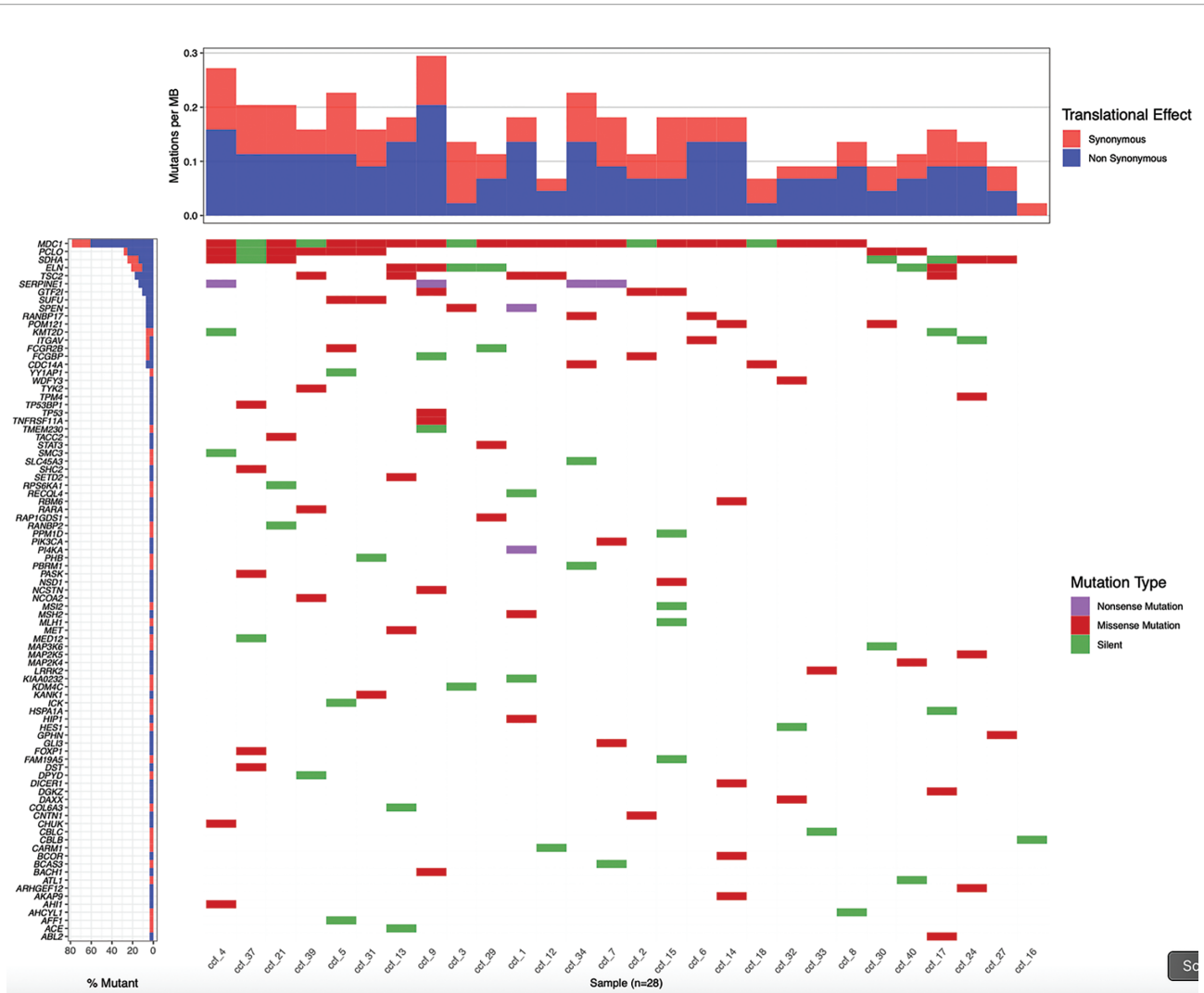

FIGURE 5 | Patient-specific candidate PCa somatic variants from biopsy samples. Waterfall plot representing 188 candidate somatic variants detected in 28 prostate biopsy samples by targeted RNA sequencing. Each column represents a sample and each row a gene. Mutations are colored according to the predicted functional consequence. The plot was generated using the GenVisR Bioconductor package.

were somatic. We then performed tumor-guided personalized deep sequencing in each patient's ccfDNA, by amplifying the relevant DNA fragment and submitting the pool of amplified fragments to NGS. The number of mutated reads divided by the total reads at each of the mutation sites in post-biopsy ccfDNA was calculated and compared with the same ratio calculated on ccfDNA before the biopsy procedure. In all cases, a dramatic enrichment in ctDNA was found, ranging from 3.9 to 164 times the amount present in circulation before the surgical procedure (**Table 2**).

DISCUSSION

As the debate continues on the merits of PCa detection, urologists are struggling to balance benefits from early detection and treatment of lethal PCa from overdiagnosis and overtreatment of clinically insignificant PCa. The landscape of PCa early detection approach and management continues to evolve thanks to the understanding of the value of PSA isoforms (35), as well as of other molecular and imaging biomarkers (36). However, there are still many areas of research where efforts to optimize patient selection for diagnosis and risk stratification for treatment are ongoing. The emerging data on somatic and germline mutations in PCa have provided additional insights into the importance of genetic testing to identify clinically significant PCa (37). There is, therefore, a strong unmet clinical need for non-invasive biomarkers in early disease for better stratifying patients with aggressive tumors from those not in need of further intervention. Such an approach should discriminate cancer patients from healthy subjects, distinguish clinically significant from indolent PCa, guide therapy, and predict prognosis and follow-up.

TABLE 2 | Enrichment in ctDNA post biopsy.

Gene	Pre ccfDNA					Post ccfDNA					Fold enrichment			
	A	T	C	G	Tot counts	A	T	C	G	Tot counts	A	T	C	G
SPEN	395	56	344,112	71	344,634	384	2,228	366,751	75	369,440	0.9	**37.1**	1.0	1.0
HIP1	273	67	514,588	138	515,067	193	9,007	413,019	95	422,316	0.9	**163.9**	1.0	0.8
TP53	1.231	36	278,734	162	280,167	2,517	39	263,754	601	266,912	**2.2**	1.1	1.0	**3.9**
NSD1	27.761	55	0	7	27,823	23,025	52	0	151	23,228	1.0	1.1		**25.8**
WDFY3	15	64,070	8	3	64,096	13	39,801	169	2	39,987	1.4	1.0	**33.9**	1.1

The fold increase of ctDNA was calculated by dividing the proportion of the reads supporting each of the four nucleotide calls on the total number of reads in the post biopsy ccfDNA by the proportion of reads of the same nucleotide in the pre-biopsy sample. Fold enrichments of the analyzed somatic variants are marked in bold.

The data currently present in the literature suggest that in patients with primary PCa it is not possible to exploit the analysis of ctDNA as the quantity of ctDNA released into the circulation is insufficient (22). Here we set up and tested an alternative approach, which uses the inherent characteristics/consequences of the prostate biopsy procedure as a way to obtain increased amounts of prostate-derived ccfDNA and, possibly, ctDNA from blood. By measuring the amount of ccfDNA before and after a prostate biopsy (index lesion plus a standard 12-core schema) we were able to describe, for the first time, the size profile and the kinetics of ccfDNA release in circulation after prostate biopsy. Moreover, by looking at patient-specific somatic mutations we showed that post-biopsy ccfDNA is significantly enriched in tumor-derived ctDNA. We found no correlation between post-biopsy ccfDNA levels and Gleason score, which suggests that probably malignancy does not correlate directly with the number of undifferentiated cells. Differences in post-biopsy ccfDNA levels might depend on the level of traumatism induced during the surgical procedure.

As a crucial biological property of ccfDNA, size profile has been assessed by a variety of methods, including gel electrophoresis, atomic force microscopy (AFM), quantitative real-time PCR (qPCR), and NGS (38). In most cases, the size profile of ccfDNA was distributed as a "ladder" pattern with a major peak at ~166 bp. However, by using AFM, Mouliere and colleagues showed that 80% of ccfDNA in colorectal cancer patients is <145 bp (39) and, by qPCR, that the ccfDNA with *KRAS* mutation is more fragmented than the wild-type ccfDNA in colorectal cancer patients (40). Also, by using NGS, it was reported that short ccfDNA fragments preferentially carried the tumor-associated aberrations in hepatocellular carcinoma patients (41). Therefore, tumor ccfDNA is generally considered to be shorter than non-tumor ccfDNA, although some evidence points to the opposite: for example, by NGS, it was reported that the median overall size of ccfDNA in tumor patients is around 163.8 bp (18). Furthermore, the ccfDNA isolated from early stages of pancreatic and breast cancer was observed to be longer than that found in metastatic patients (42, 43). Concerning PCa, it is interesting to note that in seminal fluid fragments longer than 1000 bp were shown to be more abundant than in healthy subjects (44). These discrepancies, besides deriving from the different techniques used to measure the ccfDNA size, may also reflect different subnucleosomal fragmentation patterns of ccfDNA. In particular, hypomethylation of DNA, a frequent finding in cancer, may increase the accessibility of ccfDNA to nucleases, giving reason for the shorter size distribution of ccfDNA in most cancer patients. Our experiments measured ccfDNA immediately after a surgical procedure, which is likely to damage a large number of cells and create the condition for the subsequent death of nearby cells, promoting a release of ccfDNA mainly due to cell break than to apoptotic pathways. This is probably the reason why we could observe a significant increase in the size of ccfDNA, as demonstrated by the increased ratio between the single-nucleosome and the double-nucleosome DNA peaks. This difference in fragment lengths could be exploited to enhance sensitivity for detecting the presence of ctDNA and for noninvasive genomic analysis of cancer by performing a first PCR step with long amplicons, thus selecting longer ccfDNA fragments, more likely to come from the damaged prostate tissue. This would be an approach similar, even though opposite, to the one recently described by Mouliere and colleagues (45). Further studies will evaluate whether, with this enrichment step, it is possible to detect somatic mutations directly from ccfDNA in primary PCa.

The release of ctDNA from the prostate can also be exploited to check for epigenetic modifications, which represent useful markers to improve the stratification of patients with aggressive and indolent PCa (46, 47). In particular, a four-gene prognostic model was derived by analyzing DNA methylation changes in 12 genes associated with disease progression and validated to improve the prediction of recurrence in patients with PCa after surgery (48).

In conclusion, our experiments pave the way to perform ccfDNA analysis also in primary PCa by exploiting the transient release in circulation of prostate ctDNA immediately after the biopsy procedure. This can give easy access to DNA from the entire organ, being superior (and cheaper) compared to the analysis of single biopsies, in the view of the frequent multifocal nature of PCa. ctDNA obtained after biopsy can be studied for the presence of somatic mutations or epigenetic alterations, thus allowing to anticipate a precision medicine-based approach to therapy.

DATA AVAILABILITY STATEMENT

The datasets presented in this study have been deposited in the Zenodo repository under the accession number: 10.5281/zenodo.4454599. The datasets presented in this article are not readily available because it includes sensitive data. Requests to access the datasets should be directed to the corresponding author.

ETHICS STATEMENT

The study was reviewed and approved by the Humanitas Clinical and Research Center Ethics Committee (336/19). The patients/participants provided their written informed consent to participate in this study.

AUTHOR CONTRIBUTIONS

Conception and design: SD, RA, and ML. Acquisition of data: CC, IS, MZ, MG, GL, NMB, RH, AS, and PC. Analysis and interpretation of data: SD, RA, CC, and ML. Drafting of the manuscript: MC. Critical revision of the manuscript for important intellectual content: SD, RA, MZ, ML, GS, and GG. Statistical analysis: RA. Obtaining funding: GG. Administrative, technical, or material support supervision: SD. All authors contributed to the article and approved the submitted version.

FUNDING

This work was supported by the Ministero della Salute (Ricerca Finalizzata, grant number RF-2018-12367080) and by intramural funding (Fondazione Humanitas per la Ricerca). We would also like to acknowledge the financial aid of a number of friends who supported our research with personal donations.

REFERENCES

1. Pantel K, Alix-Panabières C. Liquid Biopsy and Minimal Residual Disease - Latest Advances and Implications for Cure. *Nat Rev Clin Oncol* (2019) 16:409–24. doi: 10.1038/s41571-019-0187-3
2. Jahr S, Hentze H, Englisch S, Hardt D, Fackelmayer FO, Hesch RD, et al. DNA Fragments in the Blood Plasma of Cancer Patients: Quantitations and Evidence for Their Origin From Apoptotic and Necrotic Cells. *Cancer Res* (2001) 61:1659–65.
3. Mandel P, Metais P. Les Acides Nucléiques Du Plasma Sanguin Chez L'Homme. *C. R Seances Soc Biol Fil* (1948) 142:241–24.
4. Leon SA, Shapiro B, Sklaroff DM, Yaros MJ. Free DNA in the Serum of Cancer Patients and the Effect of Therapy. *Cancer Res* (1977) 37:646–50.
5. Stroun M, Anker P, Lyautey J, Lederrey C, Maurice PA. Isolation and Characterization of DNA From the Plasma of Cancer Patients. *Eur J Cancer Clin Oncol* (1987) 23:707–12. doi: 10.1016/0277-5379(87)90266-5
6. Lui YY, Chik KW, Chiu RW, Ho CY, Lam CW, Lo YM. Predominant Hematopoietic Origin of Cell-Free DNA in Plasma and Serum After Sex-Mismatched Bone Marrow Transplantation. *Clin Chem* (2002) 48:421–7. doi: 10.1093/clinchem/48.3.421
7. Sun K, Jiang P, Chan KC, Wong J, Cheng YK, Liang RH, et al. Plasma DNA Tissue Mapping by Genome-Wide Methylation Sequencing for Noninvasive Prenatal, Cancer, and Transplantation Assessments. *Proc Natl Acad Sci USA* (2015) 112:E5503–5512. doi: 10.1073/pnas.1508736112
8. Bettegowda C, Sausen M, Leary RJ, Kinde I, Wang Y, Agrawal N, et al. Detection of Circulating Tumor DNA in Early- and Late-Stage Human Malignancies. *Sci Transl Med* (2014) 6:224ra224. doi: 10.1158/1538-7445.AM2014-5606
9. Khier S, Lohan L. Kinetics of Circulating Cell-Free DNA for Biomedical Applications: Critical Appraisal of the Literature. *Future Sci OA* (2018) 4: FSO295. doi: 10.4155/fsoa-2017-0140
10. Tamkovich SN, Cherepanova AV, Kolesnikova EV, Rykova EY, Pyshnyi DV, Vlassov VV, et al. and Dnase Activity in Human Blood. *Ann N Y Acad Sci* (2006) 1075:191–6. doi: 10.1196/annals.1368.026
11. Yao W, Mei C, Nan X, Hui L. Evaluation and Comparison of in Vitro Degradation Kinetics of DNA in Serum, Urine and Saliva: A Qualitative Study. *Gene* (2016) 590:142–8. doi: 10.1016/j.gene.2016.06.033
12. Diehl F, Schmidt K, Choti MA, Romans K, Goodman S, Li M, et al. Circulating Mutant DNA to Assess Tumor Dynamics. *Nat Med* (2008) 14:985–90. doi: 10.1038/nm.1789
13. Yu SC, Lee SW, Jiang P, Leung TY, Chan KC, Chiu RW, et al. High-Resolution Profiling of Fetal DNA Clearance From Maternal Plasma by Massively Parallel Sequencing. *Clin Chem* (2013) 59:1228–37. doi: 10.1373/clinchem.2013.203679
14. Jiang P, Lo YMD. The Long and Short of Circulating Cell-Free DNA and the Ins and Outs of Molecular Diagnostics. *Trends Genet* (2016) 32:360–71. doi: 10.1016/j.tig.2016.03.009
15. Snyder MW, Kircher M, Hill AJ, Daza RM, Shendure J. Cell-Free DNA Comprises an in Vivo Nucleosome Footprint That Informs Its Tissues-of-Origin. *Cell* (2016) 164:57–68. doi: 10.1016/j.cell.2015.11.050
16. Rumore PM, Steinman CR. Endogenous Circulating DNA in Systemic Lupus Erythematosus. Occurrence as Multimeric Complexes Bound to Histone. *J Clin Invest* (1990) 86:69–74. doi: 10.1172/JCI114716
17. Lehmann-Werman R, Neiman D, Zemmour H, Moss J, Magenheim J, Vaknin-Dembinsky A, et al. Identification of Tissue-Specific Cell Death Using Methylation Patterns of Circulating DNA. *Proc Natl Acad Sci USA* (2016) 113:E1826–1834. doi: 10.1073/pnas.1519286113
18. Cristiano S, Leal A, Phallen J, Fiksel J, Adleff V, Bruhm DC, et al. Genome-Wide Cell-Free DNA Fragmentation in Patients With Cancer. *Nature* (2019) 570:385–9. doi: 10.1038/s41586-019-1272-6
19. Feng J, Gang F, Li X, Jin T, Houbao H, Yu C, et al. and Its DNA Integrity as Biomarker to Distinguish Prostate Cancer From Benign Prostatic Hyperplasia in Patients With Increased Serum Prostate-Specific Antigen. *Int Urol Nephrol* (2013) 45:1023–8. doi: 10.1007/s11255-013-0491-2
20. Bastian PJ, Palapattu GS, Yegnasubramanian S, Lin X, Rogers CG, Mangold LA, et al. Prognostic Value of Preoperative Serum Cell-Free Circulating DNA in Men With Prostate Cancer Undergoing Radical Prostatectomy. *Clin Cancer Res* (2007) 13:5361–7. doi: 10.1158/1078-0432.CCR-06-2781
21. Wroclawski ML, Serpa-Neto A, Fonseca FL, Castro-Neves-Neto O, Pompeo AS, Machado MT, et al. Cell-Free Plasma DNA as Biochemical Biomarker for the Diagnosis and Follow-Up of Prostate Cancer Patients. *Tumour Biol* (2013) 34:2921–7. doi: 10.1007/s13277-013-0854-4
22. Hennigan ST, Trostel SY, Terrigino NT, Voznesensky OS, Schaefer RJ, Whitlock NC, et al. Low Abundance of Circulating Tumor DNA in Localized Prostate Cancer. *JCO Precis Oncol* (2019) 3:PO.19.00176. doi: 10.1200/PO.19.00176
23. Ulz P, Belic J, Graf R, Auer M, Lafer I, Fischereder K, et al. Whole-Genome Plasma Sequencing Reveals Focal Amplifications as a Driving Force in Metastatic Prostate Cancer. *Nat Commun* (2016) 7:12008. doi: 10.1038/ncomms12008
24. Carreira S, Romanel A, Goodall J, Grist E, Ferraldeschi R, Miranda S, et al. Tumor Clone Dynamics in Lethal Prostate Cancer. *Sci Transl Med* (2014) 6:254ra125. doi: 10.1126/scitranslmed.3009448
25. Conteduca V, Wetterskog D, Sharabiani MTA, Grande E, Fernandez-Perez MP, Jayaram A, et al. Androgen Receptor Gene Status in Plasma DNA Associates With Worse Outcome on Enzalutamide or Abiraterone for Castration-Resistant Prostate Cancer: A Multi-Institution Correlative Biomarker Study. *Ann Oncol* (2017) 28:1508–16. doi: 10.1093/annonc/mdx155
26. Lallous N, Volik SV, Awrey S, Leblanc E, Tse R, Murillo J, et al. Functional Analysis of Androgen Receptor Mutations That Confer Anti-Androgen Resistance Identified in Circulating Cell-Free DNA From Prostate Cancer Patients. *Genome Biol* (2016) 17:10. doi: 10.1186/s13059-015-0864-1
27. Wyatt AW, Azad AA, Volik SV, Annala M, Beja K, McConeghy B, et al. Genomic Alterations in Cell-Free DNA and Enzalutamide Resistance in Castration-Resistant Prostate Cancer. *JAMA Oncol* (2016) 2:1598–606. doi: 10.1001/jamaoncol.2016.0494
28. Azad AA, Volik SV, Wyatt AW, Haegert A, Le Bihan S, Bell RH, et al. Androgen Receptor Gene Aberrations in Circulating Cell-Free DNA: Biomarkers of Therapeutic Resistance in Castration-Resistant Prostate Cancer. *Clin Cancer Res* (2015) 21:2315–24. doi: 10.1158/1078-0432.CCR-14-2666

29. Mehra N, Dolling D, Sumanasuriya S, Christova R, Pope L, Carreira S, et al. Plasma Cell-Free DNA Concentration and Outcomes From Taxane Therapy in Metastatic Castration-Resistant Prostate Cancer From Two Phase III Trials (FIRSTANA and PROSELICA). *Eur Urol* (2018) 74:283–91. doi: 10.1016/j.eururo.2018.02.013
30. Langmead B, Trapnell C, Pop M, Salzberg SL. Ultrafast and Memory-Efficient Alignment of Short DNA Sequences to the Human Genome. *Genome Biol* (2009) 10:R25. doi: 10.1186/gb-2009-10-3-r25
31. Dobin A, Davis CA, Schlesinger F, Drenkow J, Zaleski C, Jha S, et al. STAR: Ultrafast Universal RNA-Seq Aligner. *Bioinformatics* (2013) 29:15–21. doi: 10.1093/bioinformatics/bts635
32. Kim S, Scheffler K, Halpern AL, Bekritsky MA, Noh E, Källberg M, et al. Strelka2: Fast and Accurate Calling of Germline and Somatic Variants. *Nat Methods* (2018) 15:591–4. doi: 10.1038/s41592-018-0051-x
33. Chen X, Schulz-Trieglaff O, Shaw R, Barnes B, Schlesinger F, Källberg M, et al. Manta: Rapid Detection of Structural Variants and Indels for Germline and Cancer Sequencing Applications. *Bioinformatics* (2016) 32:1220–2. doi: 10.1093/bioinformatics/btv710
34. Robinson JT, Thorvaldsdóttir H, Winckler W, Guttman M, Lander ES, Getz G, et al. Integrative Genomics Viewer. *Nat Biotechnol* (2011) 29:24–6. doi: 10.1038/nbt.1754
35. Skidmore ZL, Wagner AH, Lesurf R, Campbell KM, Kunisaki J, Griffith OL, et al. Genvisr: Genomic Visualizations in R. *Bioinformatics* (2016) 32:3012–4. doi: 10.1093/bioinformatics/btw325
36. Chiu PK, Ng CF, Semjonow A, Zhu Y, Vincendeau S, Houlgatte A, et al. A Multicentre Evaluation of the Role of the Prostate Health Index (PHI) in Regions With Differing Prevalence of Prostate Cancer: Adjustment of PHI Reference Ranges is Needed for European and Asian Settings. *Eur Urol* (2018) 75:558–61. doi: 10.1016/j.eururo.2018.10.047
37. Lughezzani G, Buffi NM, Lazzeri M. Diagnostic Pathway of Patients With a Clinical Suspicion of Prostate Cancer: Does One Size Fit All? *Eur Urol* (2018) 74:400–1. doi: 10.1016/j.eururo.2018.05.013
38. Lazzeri M, Lughezzani G. Re: Inherited DNA-Repair Gene Mutations in Men With Metastatic Prostate Cancer. *Eur Urol* (2016) 70:703–4. doi: 10.1016/j.eururo.2016.07.039
39. Shi J, Zhang R, Li J, Zhang R. Size Profile of Cell-Free DNA: A Beacon Guiding the Practice and Innovation of Clinical Testing. *Theranostics* (2020) 10:4737–48. doi: 10.7150/thno.42565
40. Mouliere F, El Messaoudi S, Pang D, Dritschilo A, Thierry AR. Multi-Marker Analysis of Circulating Cell-Free DNA Toward Personalized Medicine for Colorectal Cancer. *Mol Oncol* (2014) 8:927–41. doi: 10.1016/j.molonc.2014.02.005
41. Mouliere F, El Messaoudi S, Gongora C, Guedj AS, Robert B, Del Rio M, et al. Circulating Cell-Free DNA From Colorectal Cancer Patients May Reveal High Kras or Braf Mutation Load. *Transl Oncol* (2013) 6:319–28. doi: 10.1593/tlo.12445
42. Jiang P, Chan CW, Chan KC, Cheng SH, Wong J, Wong VW, et al. Lengthening and Shortening of Plasma DNA in Hepatocellular Carcinoma Patients. *Proc Natl Acad Sci USA* (2015) 112:E1317–25. doi: 10.1073/pnas.1500076112
43. Lapin M, Oltedal S, Tjensvoll K, Buhl T, Smaaland R, Garresori H, et al. Fragment Size and Level of Cell-Free DNA Provide Prognostic Information in Patients With Advanced Pancreatic Cancer. *J Transl Med* (2018) 16:300. doi: 10.1186/s12967-018-1677-2
44. Madhavan D, Wallwiener M, Bents K, Zucknick M, Nees J, Schott S, et al. Plasma DNA Integrity as a Biomarker for Primary and Metastatic Breast Cancer and Potential Marker for Early Diagnosis. Breast Cancer Res. *Treat* (2014) 146:163–74. doi: 10.1007/s10549-014-2946-2
45. Ponti G, Maccaferri M, Manfredini M, Micali S, Torricelli F, Milandri R, et al. Quick Assessment of Cell-Free DNA in Seminal Fluid and Fragment Size for Early Non-Invasive Prostate Cancer Diagnosis. *Clin Chim Acta* (2019) 497:76–80. doi: 10.1016/j.cca.2019.07.011
46. Mouliere F, Chandrananda D, Piskorz AM, Moore EK, Morris J, Ahlborn LB, et al. Enhanced Detection of Circulating Tumor DNA by Fragment Size Analysis. *Sci Transl Med* (2018) 10:eaat4921. doi: 10.1126/scitranslmed.aat4921
47. Murphy K, Murphy BT, Boyce S, Flynn L, Gilgunn S, O'Rourke CJ, et al. Integrating Biomarkers Across Omic Platforms: An Approach to Improve Stratification of Patients With Indolent and Aggressive Prostate Cancer. *Mol Oncol* (2018) 12:1513–25. doi: 10.1002/1878-0261.12348
48. Jeyapala R, Kamdar S, Olkhov-Mitsel E, Savio AJ, Zhao F, Cuizon C, et al. An Integrative DNA Methylation Model for Improved Prognostication of Postsurgery Recurrence and Therapy in Prostate Cancer Patients. *Urol Oncol* (2020) 38:39.e1–9. doi: 10.1016/j.urolonc.2019.08.017

Conflict of Interest: The authors declare that the research was conducted in the absence of any commercial or financial relationships that could be construed as a potential conflict of interest.

Copyright © 2021 Corbetta, Chiereghin, De Simone, Soldà, Zuradelli, Giunta, Lughezzani, Buffi, Hurle, Saita, Casale, Asselta, Lazzeri, Guazzoni and Duga. This is an open-access article distributed under the terms of the Creative Commons Attribution License (CC BY). The use, distribution or reproduction in other forums is permitted, provided the original author(s) and the copyright owner(s) are credited and that the original publication in this journal is cited, in accordance with accepted academic practice. No use, distribution or reproduction is permitted which does not comply with these terms.

frontiers in Cell and Developmental Biology

MINI REVIEW
published: 24 May 2021
doi: 10.3389/fcell.2021.660924

Updates on Clinical Use of Liquid Biopsy in Colorectal Cancer Screening, Diagnosis, Follow-Up, and Treatment Guidance

*Omayma Mazouji[1], Abdelhak Ouhajjou[2], Roberto Incitti[3] and Hicham Mansour[1]**

[1]GES-LCM2E, FPN, Mohamed First University, Oujda, Morocco, [2]Al-Azhar Oncology Center, Rabat, Morocco, [3]Computational Bioscience Research Center (CBRC), King Abdullah University of Science and Technology (KAUST), Thuwal, Saudi Arabia

OPEN ACCESS

Edited by:
George Calin,
University of Texas MD Anderson Cancer Center, United States

Reviewed by:
Bianca Vezzani,
University of Ferrara, Italy
Bandana Chakravarti,
Sanjay Gandhi Post Graduate Institute of Medical Sciences (SGPGI), India

***Correspondence:**
Hicham Mansour
h.mansour@ump.ac.ma

Specialty section:
This article was submitted to Molecular and Cellular Oncology, a section of the journal Frontiers in Cell and Developmental Biology

Received: 29 January 2021
Accepted: 30 March 2021
Published: 24 May 2021

Citation:
Mazouji O, Ouhajjou A, Incitti R and Mansour H (2021) Updates on Clinical Use of Liquid Biopsy in Colorectal Cancer Screening, Diagnosis, Follow-Up, and Treatment Guidance. Front. Cell Dev. Biol. 9:660924. doi: 10.3389/fcell.2021.660924

Colorectal cancer (CRC) is one of the most common cancers worldwide, being the third most diagnosed in the world and the second deadliest. Solid biopsy provides an essential guide for the clinical management of patients with colorectal cancer; however, this method presents several limitations, in particular invasiveness, and cannot be used repeatedly. Recently, clinical research directed toward the use of liquid biopsy, as an alternative tool to solid biopsy, showed significant promise in several CRC clinical applications, as (1) detect CRC patients at early stage, (2) make treatment decision, (3) monitor treatment response, (4) predict relapses and metastases, (5) unravel tumor heterogeneity, and (6) detect minimal residual disease. The purpose of this short review is to describe the concept, the characteristics, the genetic components, and the technologies used in liquid biopsy in the context of the management of colorectal cancer, and finally we reviewed gene alterations, recently described in the literature, as promising potential biomarkers that may be specifically used in liquid biopsy tests.

Keywords: colorectal cancer, liquid biopsy, biomarker, screening, diagnosis, prognosis, targeted therapy, circulating tumor DNA

INTRODUCTION

The World Health Organization projected that, in the next few years, cancer will kill more than a dozen million people every year worldwide. The figures exceed those of all other death causes, such as infection, cardiovascular diseases, traffic accidents, and other registered so far (World Health Organization, 2020b). The global prevalence of cancer is predicted to increase by 75% by 2030 (Ferlay et al., 2019; World Health Organization, 2020b). This rise is projected to be significantly larger in developing countries and could reach 90% in the poorest countries (Ferlay et al., 2019; World Health Organization, 2020b). Despite the advances in diagnostic tools and treatments, colorectal cancer (CRC) remains one of the leading causes of cancer mortality worldwide, accounting for more than 9% of all cancer deaths (Boyle and Langman, 2000; Ferlay et al., 2019). According to a recent report from the GLOBOCAN database, the second

highest mortality rates among cancers were observed for CRC, with an estimated number of 935,173 deaths (both sexes and all ages; Ferlay et al., 2019; World Health Organization, 2020a). Prognosis for CRC depends on several parameters, among which the two most important are age and stage at diagnosis.

Several large studies have shown that the risk of developing CRC begins to increase noticeably after the age of 50. After that, the risk continues to double approximately with each succeeding decade (Haggar and Boushey, 2009). Although young age is associated with more advanced disease stage and unfavorable tumor characteristics, young age was shown to be a prognostic factor for better survival (Li et al., 2014). Less advanced stage I tumors are associated with a higher 5-year survival amounting to more than 80%, as compared to more advanced tumors like stage IV, which is associated with a 5-year survival rate of less than 5% (O'Connell et al., 2004; Noone et al., 2018). Unfortunately, most CRC cases are diagnosed at advanced stages, when curative surgical treatment is not sufficient, and chemotherapy or targeted therapy must be used. In contrast, CRC is preventable and curable when diagnosed early (Hamzehzadeh et al., 2017). These statistics show how crucial it would be to have screening tools to accurately detect CRC tumors at the early stage, enabling more successful fighting CRC and reduction of mortality caused by this cancer. In diagnosis, the golden standard for the determination of CRC status is the pathological analysis of tissue biopsy. Obtaining such biopsy requires relatively costly and complex medical devices as colonoscopy or flexible sigmoidoscopy, and well-trained staff (Baxter and Rabeneck, 2009). Nevertheless, biopsy has several important limitations: it is invasive, is expensive, is uncomfortable, is difficult to be performed in serial tests, has technical limitations associated with tumor location, and is not efficient in targeting tumor cells subpopulations (Fernández-Lázaro et al., 2020). Tissue extraction carries also risks, and it is inaccessible for some cases (Baxter and Rabeneck, 2009). Moreover, it gives tumor picture only at a single location, and it could ignore spatial tumor genetic heterogeneity. Therefore, it cannot be used in screening programs to detect CRC at early stage and it is not suitable for longitudinal monitoring (Baxter and Rabeneck, 2009; Hamzehzadeh et al., 2017; Fernández-Lázaro et al., 2020). In contrast to tissue biopsy, liquid biopsy has several advantages in CRC management. In this review, we describe the concept of liquid biopsy and its applications in the management of colorectal cancer patients.

LIQUID BIOPSY BACKGROUND

The concept of liquid biopsy is that of searching circulating biomarkers to detect tumor traces released from primary tumor and/or metastasis sites (Peng et al., 2017; Fernández-Lázaro et al., 2020). The extensive clinical research conducted to date clearly showed that liquid biopsy can provide information on the molecular status of CRC at any disease stage of the tumor, whether primary or metastasis stage (Wang et al., 2019), and in a comprehensive way which could strongly help oncologists in treatment guidance, particularly in identifying abnormalities leading to cancer initiation, to make treatment decisions and to monitor patient response to treatment (Cheung et al., 2018; Cortés-Hernández et al., 2020; Fernández-Lázaro et al., 2020).

In the field of noninvasive genetic tests, the first study that provided a conceptual framework and a practical basis for a new molecular approach to detect CRC was related to the development of the first assays based on the detection of the presence of gene mutations in DNA extracted from the stool (Sidransky et al., 1992; Mansour, 2014). This finding raised considerable hope of a possibility of developing a noninvasive genetic test using stool of CRC patients. Subsequent work assessed several biomarkers in stool and in other body fluids (Ebert et al., 2006; Roperch et al., 2013; Amiot et al., 2014; Mansour, 2014). Using information from detection of genetic anomalies affords a sensitivity (i.e., the ability to avoid individuals with CRC being falsely diagnosed as healthy) which can be substantially high, while still maintaining reasonably high specificity (Ebert et al., 2006; Roperch et al., 2013; Amiot et al., 2014; van Lanschot et al., 2017). The use of this molecular approach was also tentatively extended to post-therapeutic surveillance (Imperiale et al., 2014).

Molecular assays for CRC detection currently in use or under development are based on assessing genetic and/or epigenetic anomalies or a combination (Palmirotta et al., 2018). While other type of markers exists, such as proteins or RNA biomarkers, they might not be suitable for routine tests, because, before performing detection experiments, these assays need special patient preparations, stabilizing buffers, and adequate temperature for sample storage. The process is long, is error-prone, and may be a barrier for patients' adherence to the CRC detection and monitoring protocols. Unlike protein or RNA-based assays, genetic assays are based on a more streamlined analytical experiment. In addition to that, genetic assays depend much less on setting varying thresholds on relevant experimental parameters when specified for distinguishing cancer patients from the controls (Robertson and Imperiale, 2015). Moreover, many genetic biomarkers can be combined in a single assay, which is more challenging with protein-based assays (this is not a problem with RNA-based ones). In addition to that, the large development of massively parallel sequencing tools and the evolution of our knowledge and understanding of genetics show that genetic variations and epigenetic modifications can strongly impact screening, diagnosis, and prognosis options of CRC-affected patients, as well as how patients may respond to specific therapy. Several noninvasive epigenetic and genetic tests are now available, having high sensitivity and specificity and being low-risk, cost-effective, and easy to implement in clinical settings or across a large population for CRC patient screening (Ebert et al., 2006; Mansour et al., 2012; Roperch et al., 2013).

SIGNIFICANCE OF LIQUID BIOPSY

The extensive clinical research progress and advancements that have been made since the human genome was first sequenced have greatly increased our knowledge on cancer genetics and have participated in the development of new cutting-edge molecular biology tools. Several genetic and epigenetic alterations

have been shown to initiate and sustain specific deregulated cellular signaling pathways involved in CRC tumors. Today, these alterations can be easily detected in body fluids without the need to investigate the initial tumor site. From a simple blood collection, we can extract circulating tumor cells (CTC), circulating tumor DNAs (ctDNAs), and/or other extracellular vesicles (EV) and monitor molecular alterations in CRC patients. This procedure can be frequently repeated over time in order to monitor changes that occur during treatment, serving as an early indicator of tumor recurrence, drug resistance, or metastasis with a view to adapting, escalating, or changing the treatment strategy.

Liquid biopsy has several advantages: it is a noninvasive, fast, and easy tool to perform. In terms of noninvasiveness, sampling body fluids (blood or stool) does not require sophisticated equipment or highly skilled human intervention (Neumann et al., 2018; Fernández-Lázaro et al., 2020). For instance, some companies provide kits to individuals who can take the stool samples at home, thus speeding up the clinical process. The result can be obtained in a few hours, as compared to tissue extraction and pathological analysis, which can take several days. Moreover, liquid biopsy generates less morbidity than the conventional method due to its minimally invasive or noninvasive nature. Performing a series of liquid biopsies instead of solid biopsies avoids unnecessary health risks for the patient (Vymetalkova et al., 2018; Fernández-Lázaro et al., 2020), such as hyper-vascularized tumor rupture leading to catastrophic bleeding and hemorrhage risk and tumor seeding, regarding which several studies have shown that through aspiration cytology and biopsy extraction, many patients developed cancer at multiple sites (Shyamala et al., 2014).

CRC is known for its wide temporal and spatial intratumor heterogeneity; there are three major molecular pathways that produce this heterogeneity: genomic instability, microsatellite instability, and CpG island methylator phenotype (Dang et al., 2020). Detecting this heterogeneity through an invasive solid biopsy represents a great challenge, while this could be possible in some cases through a liquid biopsy (Vacante et al., 2020).

LIQUID BIOPSY COMPONENTS

The main types of tumor traces targeted in liquid biopsy are CTC, circulating tumor exosomes, ctDNAs, and circulating tumor RNAs (ctRNAs; Heitzer et al., 2015; Jia et al., 2017; Vymetalkova et al., 2018; Ding et al., 2020; Eslami-S et al., 2020; **Figure 1**).

FIGURE 1 | The main types of tumor traces targeted in liquid biopsy (circulating tumor cells, circulating tumor exosomes, circulating tumor DNA, circulating tumor RNA). The molecular biology tools routinely used are flow cytometry, real-time-PCR, next-generation sequencing (NGS), microarray, and BEAMing technology.

Circulating tumor cells are cells released into the bloodstream from the primary or metastatic high-dividing tumor cells (Shen et al., 2017; Muinelo-Romay et al., 2018). CTCs are the first tumor biomolecules discovered in 1869 by Ashworth in the blood of a deceased patient with metastatic cancer. CTCs exist in various forms: as single cells with several epithelio-mesenchyme transition (EMT) phenotypes or as clusters bound to platelets, macrophages, and/or reactivated stromal cells (Satelli et al., 2015). CTCs are present in a few cells to hundreds per milliliter of whole blood; in addition, CTCs are larger than white blood cells and measure between 15 and 25 μm (Yang et al., 2019). Several groups have been working on CTC detection methods and have developed a variety of methods to overcome technical challenges to efficiently capture CTCs in the blood (Shen et al., 2017; Yang et al., 2019). The application of these tools in gastrointestinal malignancies was promising for early diagnosis, treatment planning, prognostic stratification, and metastasis monitoring (Pantel and Alix-Panabieres, 2017; Yang et al., 2019).

Exosomes are EV and homogeneous particles, stable and easily detectable in terms of their size. Exosomes are detected in almost all body fluids and express specific markers, such as HSP70 and ALIX, that distinguish exosomes from other subcellular vesicles (Halvaei et al., 2018; Zhou et al., 2020). Exosomes can be considered as diagnostic and prognostic biomarkers in cancer. Many commercial kits provide rapid and efficient separation of exosomes from a small amount of human body fluid. In the case of CRC, the ExoScreen technique detects circulating exosomes in patients' blood samples (Fernández-Lázaro et al., 2020).

Circulating tumor DNAs are DNA fragments found in the bloodstream following different events, such as apoptosis, necrosis, and macrophage digestion. Some of them derive from malignant tumor cells, thus providing information about specific mutations in cancer (Takeda et al., 2019). In 1948, Mandel et al. were the first who hinted at the occurrence of circulating free-DNA (cfDNA) in plasma from different diseases. Despite this early discovery, the concept of liquid biopsy using ctDNA did not start being used until 1977, when other researchers identified the presence of ctDNAs in the body fluid of patients with cancer (Aghamir et al., 2020). The size range of ctDNAs varies between 150 and 10,000 bp, but the vast majority of ctDNAs are found with a size of 166 bp, like nucleosomes. Possibly, ctDNAs might be released during cell apoptosis, necrosis, or following cell lysis by immune cells (Shen et al., 2017). In CRC, a high degree of concordance between somatic mutations detected in tumor tissue and those in ctDNAs was described in blood samples from patients with early or advanced tumors, which means that the ctDNAs retain the same genetic signatures as those present in tumor tissue (Vidal et al., 2017; Li et al., 2019). The sheer amount of ctDNA found in peripheral blood differs between normal individuals and those with colorectal cancer. Indeed, circulating tumor DNA levels are higher in cancer patients than in normal individuals. The number of mutant DNA fragments can range between 1 and 1800 fragments per milliliter of plasma (Diehl et al., 2008). This quantity is low in patients with early-stage CRC, while in the case of metastatic CRC, the quantity can largely exceed these values (Shen et al., 2017). These quantities are present as a small fraction of the total cfDNA, ranging from 0.01 to 50% depending on tumor stage (Diehl et al., 2008). It is also important to mention that the information gathered from ctDNA varies depending on tumor type, since not all tumors release ctDNA. Moreover, ctDNA in cancer patients occurs in low amounts in blood compared to cfDNA; this is due to several factors such as cancer stage, tumor vascularization, tumor burden, metastasis event, and rates of cell necrosis and apoptosis.

Circulating RNAs. In addition to ctDNAs and CTCs, free ctRNAs can be used as noninvasive tumor markers in colorectal cancer. The denomination of ctRNA includes several RNA types, as micro-RNA (miRNA), other noncoding RNA (ncRNA), and messenger RNA (mRNA; Fernández-Lázaro et al., 2020). miRNAs are the most studied over the past decade and may be the most widely described noninvasive biomarkers in colorectal cancer (**Table S1**). They are detected in both serum and fecal samples and have attracted more attention, due to their stability and resistance to RNase-mediated degradation (Toiyama et al., 1870). They can be released into the bloodstream in two forms, either in association with RNA binding proteins or packaged in exosomes, both providing protection and stability of RNAs in body fluids (Shigeyasu et al., 2017; Fernández-Lázaro et al., 2020).

Significant research effort has been focused on the detection of ctDNAs in cancer and provides an overview of the detection performance across cancer types, experimental conditions, and clinical practice (Vymetalkova et al., 2018). Regarding CRC, clinical research studies have shown that information gathered by ctDNAs can afford good sensitivity, specificity, and predictive power both in the diagnosis and in the follow-up of CRC patients (Mansour, 2014). There is now large evidence that liquid biopsy represents an essential tool in oncology, through the collection of samples of minimally invasive fluids. Targeting ctDNAs or other cell components in liquid biopsy is an appropriate method to detect genetic abnormalities harbored by tumor cells. In this context, liquid biopsy can detect tumor heterogeneity, monitor molecular changes during and after treatment (Diehl et al., 2008; Toledo et al., 2017; Trojan et al., 2017), and allow to set up a molecular profile on the tumor burden in patients with colorectal cancer, as well as with other types of cancers (Arneth, 2018; Cheung et al., 2018; Tadimety et al., 2018). In clinical practice, liquid biopsy has several advantages in filling the gaps generated by conventional methods, in particular solid biopsy, in that it can allow (1) the early detection of mutations, and in particular "actionable" (i.e., therapeutically targetable) mutations, and (2) avoiding the use of therapies associated with tumor resistance.

MOLECULAR BIOLOGY APPROACHES IN LIQUID BIOPSY

To date, several technologies based on the molecular biology of ctDNAs or DNA/RNAs from CTC or EV have been adapted

for achieving ctDNAs identification, and analysis (**Figure 1**). They can be classified into two approaches: massively parallel sequencing technologies or next-generation sequencing (NGS) and digital genomic techniques such as digital PCR (dPCR). NGS can target any gene or regulatory region in ctDNA by selecting genomic regions of the target of interest, before sequencing and during the library preparation. This approach assures the analysis of large parts of the genome and allows the identification of several types of genetic alterations with high technical sensitivity (Osumi et al., 2019).

In case of presence of rare alleles and limited amount of input DNA material, the sensitivity of ctDNA detection can be further improved by using dPCR (Osumi et al., 2019). This approach provides increased identification and absolute quantification of ctDNA by dividing samples into multiple independent quantitative PCR reactions. The reactions performed contain ideally one target sequence, or few targets or none, so that the total concentration of the target sequence is obtained by a fraction of the positive amplification partitions. This partitioning of samples ensures a better detection of genetic abnormalities, including rare mutations that are difficult to detect (Quan et al., 2018; Chin et al., 2019). Digital genomic technologies offer higher technical sensitivity compared to most massively parallel sequencing technologies and have been used as an orthogonal method for validation of results and for the quantification of ctDNA. The dPCR can identify rare frequent alleles with high accuracy (Cheung et al., 2018). The NGS can also detect rare mutations but with a lower technical sensitivity than dPCR, unless (potentially costly) high sequencing depth is reached (Cheung et al., 2018; Mansour et al., 2020). In contrast to dPCR, massively parallel sequencing approaches can be designed to detect somatic mutations in either known or unknown driver genes. Besides these methods, there are other technologies allowing precise detection of ctDNA at high sensitivity, such as digital droplet PCR (ddPCR), BEAMing technology, and microarray (García-Foncillas et al., 2017; Wu et al., 2020). In **Table 1**, we give a brief description of these techniques highlighting their limitations.

A number of technologies based on the biological or physical properties of CTCs have been developed for CTC isolation and identification (Shen et al., 2017; Yang et al., 2019). CTCs are detected by an immunomagnetic separation technology based on the combination of surface antigens with magnetic beads attached to specific antibodies. For example, an antibody against the epithelial cell adhesion molecule (EpCAM) is used, then the antigen-antibody complex formed is separated under the effect of a magnetic field (Cheung et al., 2018; Marrugo-Ramírez et al., 2018; Siskova et al., 2020). This technology is commercialized as a kit called CellSearch, which is the only kit presently approved by the FDA as a method of detecting CTCs in patients with metastatic colorectal, breast, or prostate cancers (Cheung et al., 2018; Vafaei et al., 2020; Wu et al., 2020). The CellSearch kit allows detection of CTCs at a density of few tumor cells in whole blood sampling and represents high performance of 99 and 97% for specificity and sensitivity, respectively (Fernández-Lázaro et al., 2020). The limitation of this technique is described in **Table 1**. Besides the CellSearch kit, there are other tests based on the same principle, CellCollector, CellMax CMx, Cytelligen, AdnaTest, DEPArray, and others. All these tests allow the detection of CTCs to be monitored in the patients during treatment, with the main aim of either predicting recurrence of tumor or being used for downstream molecular profiling experiments (Shen et al., 2017).

LIQUID BIOPSY APPLICATIONS

In Early Diagnosis and Screening of CRC

The most studied noninvasive tools for CRC detection are hemoccult test and fecal immunochemical test (FIT). Several years of assessment highlighted important limitations of these tools. Hemoccult test and FIT showed less than satisfactory performances and difficulties in the interpretation of results (Lieberman, 2010; Imperiale et al., 2014; Lou and Shaukat, 2021). To overcome those limitations, liquid biopsy has been investigated as an alternative for more than two decades and has shown consistent and satisfactory performance, thanks to the development of cutting-edge molecular biology instruments, which enable the analysis of released tumor traces ctDNA and CTC in the body fluids. ctDNA quantity and CTC numbers in body fluids are observed at high levels in colorectal cancer cases, especially at advanced stages. For instance, the mean concentration of ctDNA in blood or stool is 5–50 times higher in CRC patients than in healthy subjects (Pindler et al., 2015; Vymetalkova et al., 2018), and regarding CTC, CRC patients could contain 5–50 CTCs per few mL of whole blood (Gold et al., 2015; Pantel and Alix-Panabieres, 2017).

Recently, the detection of several tumor markers in ctDNA or in CTC has attracted considerable attention in CRC screening as well as in diagnosis. Detecting colorectal cancer at the early stage based on liquid biopsy is an effective strategy in reducing patient mortality and in increasing overall survival (OS) in affected patients. The use of noninvasive samples can be a valuable tool for unraveling the genetic and epigenetic abnormalities involved in tumorigenesis (Gold et al., 2015). The CRC molecular assays currently in use are based on the assessment of genetic or epigenetic modifications or both. The main gene alterations known to date are as follows.

Currently, mutations in the KRAS, BRAF, APC, and TP53 genes have been widely detected in the ctDNA of CRC patients. The analysis of the mutations found for these genes in tumor tissue and plasmatic ctDNA showed significant concordance, up to 100% (Vidal et al., 2017; Vymetalkova et al., 2018; Li et al., 2019). The **KRAS** gene is mutated in 35–45% of CRCs, with a high frequency in codons 12, 13, 59, 61, and 146. In advanced colorectal cancers, more than 50 different **BRAF** mutations have been documented for CRC, with 90% consisting of a change from thymine to single base adenine at position 1799, located in exon 15 and producing a substitution at codon 600 that replaces glutamine with valine (V600E; Wang et al., 2017). In addition to that, mutational inactivation of

TABLE 1 | The limitations of techniques routinely used for the detection of ctDNA or CTC.

Method	Description	Limits	References
Digital PCR (dPCR)	dPCR ensures increased identification and absolute quantification of circulating tumor DNA by amplification of the target in the presence of fluorescent dye.	- The dPCR's multiplexing (simultaneous assay of several targets) is limited. - Unable to detect all alteration types that could occur within a single target. - Needs protocol optimization for each alteration type. - Unable to simultaneously detect gene expression and gene alteration. - Detect only known mutations.	Mansour et al., 2012; Fernández-Lázaro et al., 2020
Next-generation-sequencing (NGS)	NGS allows analysis of large parts of the genome and can identify multiple mutations with increased sensitivity.	- Library and sequencing kits are expensive and time-consuming. - Sample procession and library preparation need experienced specialists. - Primary and secondary data analysis require bioinformatics expertise. - Raw data can be noisy. - Need adequate sequencing coverage. - Can miss low-frequency variants. - Need orthogonal validation.	Noone et al., 2018; Wang et al., 2019; Fernández-Lázaro et al., 2020
Droplet digital PCR (ddPCR)	DdPCR represents a highly sensitive and absolute quantification strategy that allows detection of low-frequency variants by amplification of single DNA molecules. This strategy is based on splitting the sample into several individual droplets and each droplet undergoes a PCR reaction that will then be analyzed to determine the positive fractions in the original sample.	- Presence of technical false negative and false positive results. - Lack of full automation of the technique. - Detection of only known mutations.	Peng et al., 2017; Wang et al., 2019; Fernández-Lázaro et al., 2020
BEAMing technology (beads, emulsion, amplification, and magnetics)	BEAMing allows the detection of ctDNAs based on the amplification of the DNA segment by ePCR, then identification and quantification of the beads containing the mutation by flow cytometry.	- Technical complexity difficult to tackle for routine analysis. - The success rate of emulsion PCR is low. - Targets only a small number of alterations. - Detection only known mutations. - Introduction of biases due to requirement of pre-amplification of the target sequence.	Cheung et al., 2018; Wang et al., 2019; Fernández-Lázaro et al., 2020
CELLTRACKS® AUTOPREP® System and CELLTRACKS ANALYZER II® System (CellSearch Kit)	CellSearch is based on the selection of circulating epithelial cells from peripheral blood samples by the use of magnetic beads and under the influence of a magnetic field.	- CTCs with mesenchymal features cannot be detected. - Only CTCs that retain epithelial features can be detected. - The test requires the collection of large volume of blood for analysis. - Only few cells are detected.	Neumann et al., 2018; Noone et al., 2018; Cortés-Hernández et al., 2020; World Health Organization, 2020a

the **APC** gene was detected in about 85% of sporadic cases and frequently seen in distal rather than proximal colon cancer sites (Markowitz and Bertagnolli, 2009). Also, germline mutation of the APC gene was described and is inherited in familial adenomatous polyposis (FAP) patients (Powell et al., 1993). Mutation of the APC gene leads to the activation of the tumor suppressor genes DCC/DPC4 and TP53 and to the activation of oncogenes such as COX2 and KRAS (Markowitz and Bertagnolli, 2009). The **TP53** gene mutation has been widely detected in non-hypermutated colorectal cancers with a percentage of approximately 55–60% and represents the second abnormality observed after the APC mutation (Nakayama and Oshima, 2019). The majority of TP53 mutations occur at exons 4, 5, 6, 7, and 8, especially between codons 100 and 300 (Li et al., 2019). In addition to the previously described molecular alterations seen in CRC, epigenetic phenomena such as CpG island methylator phenotype (CIMP) are also involved in CRC carcinogenesis; this alteration accounts for nearly 10–40% of all sporadic cases (Freitas et al., 2018). As an example of the epigenetic modification, methylation of the promoter region of the **MLH1** gene is strongly linked to the so-called methylator phenotype; it is reported in 22–49% of CIMP-positive tumors (Levine et al., 2016). Our group and other researchers identified several noninvasive methylation biomarkers, which in combination have demonstrated their diagnostic effect in CRC detection, such as **WIF**, **NPY**, **PENK**, **SEPT9**, **VIM**, **ALX4**, and others (Amiot et al., 2014; Jung et al., 2020).

Measuring the genetic and epigenetic information of a combination of several regions of genomic DNA sequence is useful in developing sensitive and highly specific noninvasive tumor diagnosis tests for early-stage CRC detection. In clinical practice, the liquid biopsy tests developed for screening use either genetic or epigenetic targets or a combination.

These biomarkers have passed several clinical trial validations and have been used to build new classes of assays; some are already approved by the FDA or designed as breakthrough devices and can be found in the market. The main tests are the following:

- The Epi proColon test, also known as the mSEPT9 test, is the first blood test designed for the identification of SEPT9 methylation in patients with colorectal cancer. This test is based on the extraction of ctDNA in the plasma and the amplification of the methylated DNA fragments by PCR (deVos et al., 2009). The Epi proColon Kit was approved by the Chinese Food and Drug Administration and the United States FDA in 2015 and 2016, respectively. The SEPT9 methylation test has good detection sensitivity. Numerous studies compared the performance of the mSEPT9 test with the FIT test. Research carried out showed that the mSEPT9 test is more sensitive than the FIT test (Johnson et al., 2014; Jin et al., 2015; Wu et al., 2016). The sensitivity of mSEPT9 is slightly higher ranging from 73 to 77% against 58 to 74% for the FIT test. The specificity of the two tests is high reaching 94% for mSEPT9 and 97% for the FIT test (Johnson et al., 2014; Jin et al., 2015; Wu et al., 2016).
- The monoplex assay for methylated VIM is currently marketed as a laboratory-developed test under the name of ColoSure™. This test is a single-marker test used to identify methylation of Vimentin in colorectal cancer. The test was developed by the Laboratory Corporation of America (LabCorp; Ned et al., 2011). Through several clinical studies, aberrant methylation of VIM alone has been detected with good sensitivity and specificity in CRC and pre-cancerous adenomas (Ned et al., 2011). The ColoSure test shows good performance ranging from 72 to 83% and from 53 to 86% for sensitivity and specificity, respectively. In addition, the ColoSure test represents an alternative screening method recommended especially in patients who cannot use standard diagnosis methods such as colonoscopy (Ned et al., 2011; Hamzehzadeh et al., 2017).
- The Cologuard test, also known as the mt-sDNA screening test, is a technology that allows the detection of DNA biomarkers in fecal samples. The Cologuard Screening test was developed by EXACT SCIENCES Corporation and Mayo Clinic, approved by the FDA in 2014 as a CRC screening tool and recommended by the College of American Pathologists. This test is recommended for asymptomatic subjects with average or high risk to develop CRC. The Cologuard test allows the quantification of a panel of distinct biomarkers consisting of the mutated KRAS gene; the methylation of the DNA promoter regions of genes NDRG4, BMP3, VIM, and TFP12; and the assessment of the fecal occult blood (Imperiale et al., 2014). In a clinical trial that screened 9,989 subjects, the effectiveness of Cologuard was established. In comparison to the FIT test, the Cologuard test was shown to be more accurate in detecting cancers and advanced adenomas, 92 vs. 74% for CRCs and 42 vs. 24% for advanced adenomas. However, the specificity of Cologuard was lower than for FIT, and it gave a negative screening result for only 87% of the normal subjects, while FIT provided accurate negative results for 95% of these normal subjects (Imperiale et al., 2014).

In CRC Prognosis

Liquid biopsy has other potential applications in clinical practice such as CRC patient's follow-up. Among the biomolecules detected in body fluids, ctDNA has shown prognostic value in patients with metastatic colorectal cancer (mCRC; Pindler et al., 2015). Numerous studies have shown that an increased ctDNA level is associated with shorter OS in patients with mCRC, while patients with low plasma ctDNA levels are associated with a longer OS (Pindler et al., 2015; Shen et al., 2017; Osumi et al., 2019). More specifically, KRAS or BRAF mutations in ctDNA have a prognostic aspect in mCRC and are correlated with shorter progression-free survival (PFS) and OS (El Messaoudi et al., 2016; Shen et al., 2017). Besides ctDNA, several biomarkers, which allow the detection of CTC, are considered as prognostic markers in CRC, like CK20-positive markers, leading to shorter OS. Other biomarkers, such as CK19, CD133, GCC, EPCAM, SURVIVIN, MUC 1, MUC 2, and hTERT, have shown their prognostic effect in CRC (Vafaei et al., 2019). In recent years, some biomarkers resulting from methylation aberration have also shown their prognostic value in CRC, taking as an example the methylation of the following genes: TAC1, IGFBP3, CDKN2A (p16), SEPT9, HPP1, TFPA2E, EVL, HLTF, CD109, BNIP3, NRCAM, MLH1, MGMT, CDKN2A (p14), and APC (Ma et al., 2019). Despite that the literature approves that methylation biomarkers have a prognostic effect, those biomarkers are not clinically applicable yet, due to the lack of validation studies (Draht et al., 2018).

Treatment Guidance and Post-treatment Monitoring

The identification of molecular anomalies associated with CRC has progressed in recent years. Liquid biopsy is a new strategy in performing a comprehensive tumor genomic profiling to aid for cancer treatment. Based upon genomic drivers of tumorigenesis, oncologists can make treatment recommendations and ensure the use of the right targeted therapy to the right patient. The use of targeted therapies has dramatically improved the OS of patients with mCRC (Martini et al., 2017). The detection of gene anomalies in liquid biopsy has been improved considerably; it constitutes a potential tool to identify actionable mutation, which could be targeted by a specific therapy (Martini et al., 2017). The following are the gene alterations used in CRC treatment (**Figure 2**):

- Patients harboring EGFR gene mutation, which constitutively activates the EGF receptor, could be treated with anti-EGFR drugs, such as cetuximab or panitumumab. In some cases, this strategy remains ineffective due to the presence of resistant mutant proteins, which act in the EGFR downstream signaling pathway. Indeed, ctDNA enables the early detection of possible resistance and guide for other treatment options (Ohhara et al., 2016; Martini et al., 2017). Cetuximab or panitumumab binds to EGFR, causing antitumor activity.

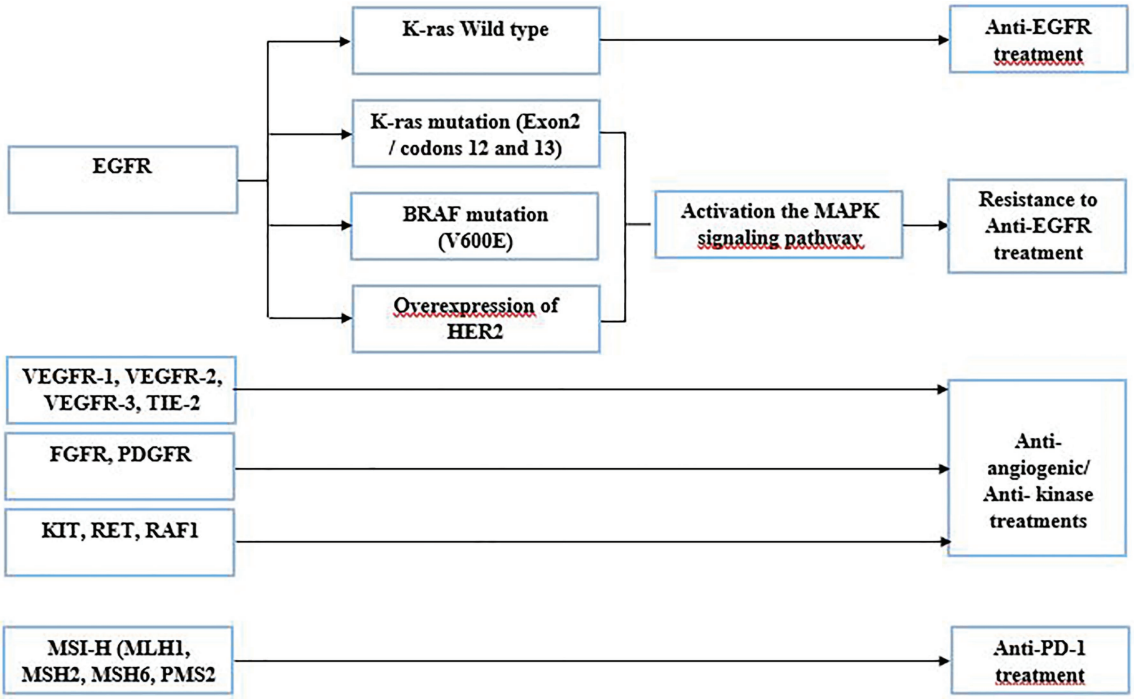

FIGURE 2 | Gene alterations used in CRC treatment.

In some cases, these drugs are not functional due to molecular aberrations in effectors of the EGFR pathway, such as mutations in exon 2 (codons 12 and 13) of the KRAS gene. These mutations involve activation of the MAPK pathway, thus leading to resistance to anti-EGFR treatment (Bronte et al., 2015). Before determining the targeted therapy, confirmation of the tumor status of the RAS gene is required and liquid biopsy can help in that respect as well.

- HER2 and EGFR share many downstream pathways, such as RAS/RAF/MEK and PI3K/AKT. Thus, amplification of the HER gene could confer resistance to anti-EGFR treatment (Xie et al., 2020). Also, it was described that PI3K mutations and PTEN loss might be associated with EGFR blockade resistance (Xie et al., 2020).
- BRAF gene mutations are also known to be an indicator of poor prognosis, and they are also identified as an adversely predictive biomarker of anti-EGFR treatment (Guo et al., 2019). Despite the blockage of EGFR, the BRAF mutation (V600E) provides resistance to treatment by activating the MAPK signaling pathway which promotes proliferation and survival of tumor cells. The resistance of the BRAF mutation to anti-EGFR therapy has been identified in several clinical trials (Zhao et al., 2017). These assays demonstrate a strong relationship between the presence of the BRAF mutation (V600E) and resistance to anti-EGFR therapy in colorectal cancer (Zhao et al., 2017).
- Several genes encoding protein kinases can be found frequently mutated in CRC with gain of function. Regorafenib is a multi-targeting inhibitor introduced in the clinical setting of mCRC (Arai et al., 2019), involving the blocking of aberrant activation of a panoply of protein kinases. These protein kinases are related either to the angiogenic pathway (VEGFR-1, VEGFR-2, VEGFR-3, and TIE-2) or to the oncogenic pathway (KIT, RET, RAF1, and BRAF). In two randomized phase III trials CORRECT and CONCUR, conducted in a population of patients with mCRC, regorafenib significantly increased OS and PFS with a reported benefit of 6.4 vs. 5.0 months and 1.9 vs. 1.7 months compared to placebo, respectively (Ohhara et al., 2016).
- Two other genes are found altered in CRC, the fibroblast growth factor receptor (FGFR) and the platelet-derived growth factor receptor (PDGFR). The aberrated FGFR form ends up behaving as an oncogene, playing a crucial role in the migration, proliferation, angiogenesis, and survival of cancer cells. Mutation of FGFRs leads to deregulation of downstream pathways leading to the formation of mitotic and anti-apoptotic cells (Cha et al., 2018). PDGFs are often mutated or overexpressed, leading to deregulation in the PDGF/PDGFR signaling pathway. This dysfunction is associated with angiogenesis, metastasis, invasion, and resistance to targeted therapies in CRC patients (Manzat Saplacan et al., 2017; García-Aranda and Redondo, 2019). PDGFR plays an important role in cell growth, cell division, and blood vessel formation in cancer. Regorafenib could be used to block the aberrant activity of the FGFR and the PDGFR (Bignucolo et al., 2017).
- Lastly, some CRC patients will have tumors that are microsatellite unstable, also known as microsatellite-high (MSI-H). The MSI-H phenotype is associated with germline defects in the following genes: MLH1, MSH2, MSH6, and PMS2. A programmed cell death protein 1 (PD-1) antibody is recommended in patients with microsatellite-unstable tumors (Overman et al., 2018; Oliveira et al., 2019).

Based on the genomic profile provided by the liquid biopsy test, oncologists can make treatment recommendations. The assessment of the genetic status of validated biomarkers in a noninvasive manner can be used as companion test for targeted therapies. These targeted therapies have shown to increase the quality of life of affected patients compared to standard chemotherapies. Moreover, the use of liquid biopsy is an effective tool in posttreatment monitoring and can provide a comprehensive genetic profile of tumor heterogeneity, which could change over time (Reece et al., 2019).

PROMISING CRC BIOMARKERS

We performed a literature search to capture identified tumor-related markers in body fluids (blood, stool, and urine), reported to be used for screening, diagnosis, or monitoring of CRC patients. Thereby, the search yielded 60 relevant biomarkers. The output data are reviewed and summarized in **Table S1**. We identified several classes of alterations: gene mutation, gene methylation, and changes in RNA expression and protein levels. The performance of these tumor markers remains relatively encouraging ranging from 6 to 99% and 29 to 100% for sensitivity and specificity, respectively, but with a largely variable cohort size, ranging from 29 to 2,975 recruited subjects (Okugawa et al., 2015; Rodia et al., 2016). The development of noninvasive genetic assays raises considerable hope for the possibility of reducing CRC mortality. A promising alternative to gene methylation and mutation is miRNA expression, which can also be detected in both serum and stool. These molecules are particularly interesting, being small, much more resistant to degradation than coding RNA, and easily profiled in body fluids. In addition, in many studies they show good performance in distinguishing CRC-affected patients from healthy subjects.

TECHNICAL LIMITATIONS AND THE FUTURE OF THE LIQUID BIOPSY

The advantages of liquid biopsy are unquestionable; however, we should admit that in clinical routine, we have still been facing several limitations. These include the following: (1) contamination by fragmented constitutive DNA adds to the critical need for adequate storage/quick processing after sampling and that of special precaution having to be taken for sample preservation, by using a specific buffer to avoid cell lysis and DNA/RNA release from hematological cells. (2) Not all tumors are shedding CTC or ctDNA and the use of liquid biopsy for these patients is therefore useless. (3) Usually, ctDNA in cancer patients occurs in low amounts in the blood compared to cfDNA. This fact is due to several factors such as cancer stage, tumor vascularization, tumor burden, metastatic potential of cancer cells, and the rate of necrosis and apoptosis. (4) The small size of ctDNA fragments makes it difficult to identify large-scale DNA rearrangements. (5) Methylation anomalies are rarely investigated, because assays need DNA treatment by sodium bisulfite, which consumes large quantities of DNA. (6) The volume of blood to be collected is high, compared to most blood tests, with at least 7 ml of whole blood being required. (7) Several platforms can be used for liquid biopsy testing, but many of them rely on technologies which are prone to errors, especially for those who need pre-amplification steps. (8) Some tumor-specific mutations can be extremely low, as low as 0.01% of total cfDNA, which can make the detection of low-frequency variants particularly challenging. (9) The only technology able to detect unknown variants is the NGS; however, to be able to detect low-frequency variants, large and potentially costly base coverage of the targeted region, defined as the number of reads covering a base, is an important prerequisite for reliable variant detection from NGS data. (10) The identification of genomic alterations with unknown significance or unclear effect on the gene function makes the interpretation difficult. (11) The use of exosomes and CTCs in routine diagnostics is limited; only CTCs that maintain epithelial features can be detected by the EpCAM, excluding CTCs with other characteristics (Vacante et al., 2020). Regarding exosomes, one of the main challenges limiting the clinical use of these EV is the lack of standardization and consistency regarding their isolation methods, which requires difficult and laborious methods (Drula et al., 2020). In addition, the high cost of the equipment and reagents intended for the most used technology in bioscience, NGS hinders the routine use of liquid biopsy in the clinical laboratory. Moreover, there is the need of expert and experienced specialists for sample handling from EV extraction to library preparation and the need for elaborate bioinformatics pipelines for data treatment and analysis.

Liquid biopsy still resists to be used routinely in clinical setting for CRC patient management (Arneth, 2018). Currently in clinical practice, liquid biopsy is used as a supplement to the conventional method, specifically when the tissue biopsy cannot be performed and/or the patient is resistant to any invasive procedure. In the field of the diagnosis of CRC, we still rely on the gold standard which is tissue biopsy rather liquid biopsy, to evaluate accurately the tumor cells and their microenvironment (Arneth, 2018).

Overall, the usefulness of liquid biopsy in the management of colorectal cancer is limited, but these limitations may be overcome soon. Liquid biopsy may provide a better real-time understanding of the dynamic of tumor growth and its evolution, which will lead to counter cancer development and metastasis. In terms of CRC treatment, drug development is lagging far away from the huge quantity of genetic information generated by liquid biopsy. The synchronization will be a huge trigger for the next level in personalized medicine in CRC.

CONCLUSION

Liquid biopsy is an emerging field in the management of colorectal cancer, whose relevance as a potential diagnostic, prognostic, monitoring, and therapeutic tool makes it a viable strategy in clinical practice of CRC patients. Liquid biopsy also has certain limitations, but they seem to be at the reach of near-future technological development.

AUTHOR CONTRIBUTIONS

HM planned and supervised the work. OM and HM wrote the paper. RI and AO reviewed and edited the paper. All authors contributed to the article and approved the submitted version.

FUNDING

The research funding of the university has supported this work. Publication fees supported by the Cancer Research Institute IRC, Kingdom of Morocco (www.irc.ma).

ACKNOWLEDGMENTS

We thank Majda Llbiyi undergraduate student for drawing **Figure 1**.

SUPPLEMENTARY MATERIAL

The Supplementary Material for this article can be found online at: https://www.frontiersin.org/articles/10.3389/fcell.2021.660924/full#supplementary-material

REFERENCES

Aghamir, S. M. K., Heshmat, R., Ebrahimi, M., and Khatami, F. (2020). Liquid biopsy: the unique test for chasing the genetics of solid tumors. *Epigenet Insights* 13:2516865720904052. doi: 10.1177/2516865720904052

Amiot, A., Mansour, H., Baumgaertner, I., Delchier, J. C., Tournigand, C., Furet, J. P., et al. (2014). The detection of the methylated Wif-1 gene is more accurate than a fecal occult blood test for colorectal cancer screening. *PLoS One* 9:e99233. doi: 10.1371/journal.pone.0099233

Annaházi, A., Ábrahám, S., Farkas, K., Rosztóczy, A., Inczefi, O., Földesi, I., et al. (2016). A pilot study on faecal MMP-9: a new noninvasive diagnostic marker of colorectal cancer. *Br. J. Cancer* 114, 787–792. doi: 10.1038/bjc.2016.31

Arai, H., Battaglin, F., Wang, J., Lo, J. H., Soni, S., Zhang, W., et al. (2019). Molecular insight of regorafenib treatment for colorectal cancer. *Cancer Treat. Rev.* 81:101912. doi: 10.1016/j.ctrv.2019.101912

Arneth, B. (2018). Update on the types and usage of liquid biopsies in the clinical setting: a systematic review. *BMC Cancer* 18:527. doi: 10.1186/s12885-018-4433-3

Bastaminejad, S., Taherikalani, M., Ghanbari, R., Akbari, A., Shabab, N., and Saidijam, M. (2017). Investigation of microRNA-21 expression levels in serum and stool as a potential non-invasive biomarker for diagnosis of colorectal cancer. *Iran. Biomed. J.* 21, 106–113. doi: 10.18869/acadpub.ibj.21.2.106

Baxter, N., and Rabeneck, L. (2009). New findings about the risks and limitations of colonoscopy used in the early detection of colorectal cancer. *Healthc. Q.* 12, 24–25. doi: 10.12927/hcq.2009.20675

Bengs, S., Becker, E., Busenhart, P., Spalinger, M. R., Raselli, T., Kasper, S., et al. (2019). β_6-integrin serves as a novel serum tumor marker for colorectal carcinoma. *Int. J. Cancer* 145, 678–685. doi: 10.1002/ijc.32137

Bhardwaj, M., Weigl, K., Tikk, K., Benner, A., Schrotz-King, P., and Brenner, H. (2020). Multiplex screening of 275 plasma protein biomarkers to identify a signature for early detection of colorectal cancer. *Mol. Oncol.* 14, 8–21. doi: 10.1002/1878-0261.12591

Bignucolo, A., De Mattia, E., Cecchin, E., Roncato, R., and Toffoli, G. (2017). Pharmacogenomics of targeted agents for personalization of colorectal cancer treatment. *Int. J. Mol. Sci.* 18:1522. doi: 10.3390/ijms18071522

Boyle, P., and Langman, J. S. (2000). ABC of colorectal cancer: epidemiology. *BMJ* 321, 805–808. doi: 10.1136/bmj.321.7264.805

Bronte, G., Silvestris, N., Castiglia, M., Galvano, A., Passiglia, F., Sortino, G., et al. (2015). New findings on primary and acquired resistance to anti-EGFR therapy in metastatic colorectal cancer: do all roads lead to RAS? *Oncotarget* 6, 24780–24796. doi: 10.18632/oncotarget.4959

Cha, Y., Kim, H. P., Lim, Y., Han, S. W., Song, S. H., and Kim, T. Y. (2018). FGFR2 amplification is predictive of sensitivity to regorafenib in gastric and colorectal cancers in vitro. *Mol. Oncol.* 12, 993–1003. doi: 10.1002/1878-0261.12194

Chen, W. Y., Zhao, X. J., Yu, Z. F., Hu, F. L., Liu, Y. P., Cui, B. B., et al. (2015). The potential of plasma miRNAs for diagnosis and risk estimation of colorectal cancer. *Int. J. Clin. Exp. Pathol.* 8, 7092–7101.

Cheung, A. H., Chow, C., and To, K. F. (2018). Latest development of liquid biopsy. *J. Thorac. Dis.* 10 (Suppl. 14), S1645–S1651. doi: 10.21037/jtd.2018.04.68

Chin, R. I., Chen, K., Usmani, A., Chua, C., Harris, P. K., Binkley, M. S., et al. (2019). Detection of solid tumor molecular residual disease (MRD) using circulating tumor DNA (ctDNA). *Mol. Diagn. Ther.* 23, 311–331. doi: 10.1007/s40291-019-00390-5

Cortés-Hernández, L. E., Eslami-S, Z., and Alix-Panabières, C. (2020). Circulating tumor cell as the functional aspect of liquid biopsy to understand the metastatic cascade in solid cancer. *Mol. Asp. Med.* 72:100816. doi: 10.1016/j.mam.2019.07.008

Dang, H. X., Krasnick, B. A., White, B. S., Grossman, J. G., Strand, M. S., and Zha, J. (2020). The clonal evolution of metastatic colorectal cancer. *Sci. Adv.* 6:eaay9691. doi: 10.1126/sciadv.aay9691

deVos, T., Tetzner, R., Model, F., Weiss, G., Schuster, M., Distler, J., et al. (2009). Circulating methylated SEPT9 DNA in plasma is a biomarker for colorectal cancer. *Clin. Chem.* 55, 1337–1346. doi: 10.1373/clinchem.2008.115808

Diehl, F., Schmidt, K., Choti, M. A., Romans, K., Goodman, S., Li, M., et al. (2008). Circulating mutant DNA to assess tumor dynamics. *Nat. Med.* 14, 985–990. doi: 10.1038/nm.1789

Ding, Y., Li, W., Wang, K., Xu, C., Hao, M., and Ding, L. (2020). Perspectives of the application of liquid biopsy in colorectal cancer. *Biomed. Res. Int.* 2020:6843180. doi: 10.1155/2020/6843180

Draht, M. X. G., Goudkade, D., Koch, A., Grabsch, H. I., Weijenberg, M. P., van Engeland, M., et al. (2018). Prognostic DNA methylation markers for sporadic colorectal cancer: a systematic review. *Clin. Epigenetics* 10:35. doi: 10.1186/s13148-018-0461-8

Drula, R., Ott, L. F., Berindan-Neagoe, I., Pantel, K., and Calin, G. A. (2020). MicroRNAs from liquid biopsy derived extracellular vesicles: recent advances in detection and characterization methods. *Cancer* 12:2009. doi: 10.3390/cancers12082009

Ebert, M. P., Model, F., Mooney, S., Hale, K., Lograsso, J., Tonnes-Priddy, L., et al. (2006). Aristaless-like homeobox-4 gene methylation is a potential marker for colorectal adenocarcinomas. *Gastroenterology* 131, 1418–1430. doi: 10.1053/j.gastro.2006.08.034

El Messaoudi, S., Mouliere, F., Du Manoir, S., Bascoul-Mollevi, C., Gillet, B., Nouaille, M., et al. (2016). Circulating DNA as a strong multimarker prognostic tool for metastatic colorectal cancer patient management care. *Clin. Cancer Res.* 22, 3067–3077. doi: 10.1158/1078-0432.CCR-15-0297

Eslami-S, Z., Cortés-Hernández, L. E., Cayrefourcq, L., and Alix-Panabières, C. (2020). The different facets of liquid biopsy: a kaleidoscopic view. *Cold Spring Harb. Perspect. Med.* 10:a037333. doi: 10.1101/cshperspect.a037333

Fang, Z., Tang, J., Bai, Y., Lin, H., You, H., Jin, H., et al. (2015). Plasma levels of microRNA-24, microRNA-320a, and microRNA-423-5p are potential biomarkers for colorectal carcinoma. *J. Exp. Clin. Cancer Res.* 34:86. doi: 10.1186/s13046-015-0198-6

Fei, W., Chen, L., Chen, J., Shi, Q., Zhang, L., Liu, S., et al. (2017). RBP4 and THBS2 are serum biomarkers for diagnosis of colorectal cancer. *Oncotarget* 8, 92254–92264. doi: 10.18632/oncotarget.21173

Ferlay, J., Colombet, M., Soerjomataram, I., Mathers, C., Parkin, D. M., Piñeros, M., et al. (2019). Estimating the global cancer incidence and mortality in 2018: GLOBOCAN sources and methods. *Int. J. Cancer* 144, 1941–1953. doi: 10.1002/ijc.31937

Fernández-Lázaro, D., García Hernández, J. L., García, A. C., Córdova Martínez, A., Mielgo-Ayuso, J., and Cruz-Hernández, J. J. (2020). Liquid biopsy as novel tool in precision medicine: origins, properties, identification and clinical perspective of cancer's biomarkers. *Diagnostics* 10:215. doi: 10.3390/diagnostics10040215

Fernández-Lázaro, D., Hernández, J. L. G., García, A. C., Castillo, A. C. D., Hueso, M. V., and Cruz-Hernández, J. J. (2020). Clinical perspective and

translational oncology of liquid biopsy. *Diagnostics* 10:443. doi: 10.3390/diagnostics10070443

Freitas, M., Ferreira, F., Carvalho, S., Silva, F., Lopes, P., Antunes, L., et al. (2018). A novel DNA methylation panel accurately detects colorectal cancer independently of molecular pathway. *J. Transl. Med.* 16:45. doi: 10.1186/s12967-018-1415-9

Fung, K. Y., Tabor, B., Buckley, M. J., Priebe, I. K., Purins, L., Pompeia, C., et al. (2015). Blood-based protein biomarker panel for the detection of colorectal cancer. *PLoS One* 10:e0120425. doi: 10.1371/journal.pone.0120425

García-Aranda, M., and Redondo, M. (2019). Targeting receptor kinases in colorectal cancer. *Cancer* 11:433. doi: 10.3390/cancers11040433

García-Foncillas, J., Alba, E., Aranda, E., Díaz-Rubio, E., López-López, R., Tabernero, J., et al. (2017). Incorporating BEAMing technology as a liquid biopsy into clinical practice for the management of colorectal cancer patients: an expert taskforce review. *Ann. Oncol.* 28, 2943–2949. doi: 10.1093/annonc/mdx501

Gold, B., Cankovic, M., Furtado, L. V., Meier, F., and Gocke, C. D. (2015). Do circulating tumor cells, exosomes, and circulating tumor nucleic acids have clinical utility? A report of the association for molecular pathology. *J. Mol. Diagn.* 17, 209–224. doi: 10.1016/j.jmoldx.2015.02.001

Guo, T. A., Wu, Y. C., Tan, C., Jin, Y. T., Sheng, W. Q., Cai, S. J., et al. (2019). Clinicopathologic features and prognostic value of KRAS, NRAS and BRAF mutations and DNA mismatch repair status: a single-center retrospective study of 1,834 Chinese patients with stage I-IV colorectal cancer. *Int. J. Cancer* 145, 1625–1634. doi: 10.1002/ijc.32489

Haggar, F. A., and Boushey, R. P. (2009). Colorectal cancer epidemiology: incidence, mortality, survival, and risk factors. *Clin. Colon Rectal Surg.* 22, 191–197. doi: 10.1055/s-0029-1242458

Halvaei, S., Daryani, S., Eslami-S, Z., Samadi, T., Jafarbeik-Iravani, N., Bakhshayesh, T. O., et al. (2018). Exosomes in cancer liquid biopsy: a focus on breast cancer. *Mol. Ther. Nucleic Acids* 10, 131–141. doi: 10.1016/j.omtn.2017.11.014

Hamzehzadeh, L., Yousefi, M., and Ghaffari, S. H. (2017). Colorectal cancer screening: a comprehensive review to recent non-invasive methods. *Int. J. Hematol. Oncol. Stem Cell Res.* 11, 250–261.

Han, Y. D., Oh, T. J., Chung, T. H., Jang, H. W., Kim, Y. N., An, S., et al. (2019). Early detection of colorectal cancer based on presence of methylated syndecan-2 (SDC2) in stool DNA. *Clin. Epigenetics* 11:51. doi: 10.1186/s13148-019-0642-0

Hao, T. B., Shi, W., Shen, X. J., Qi, J., Wu, X. H., Wu, Y., et al. (2014). Circulating cell-free DNA in serum as a biomarker for diagnosis and prognostic prediction of colorectal cancer. *Br. J. Cancer* 111, 1482–1489. doi: 10.1038/bjc.2014.470

Heitzer, E., Ulz, P., and Geigl, J. B. (2015). Circulating tumor DNA as a liquid biopsy for cancer. *Clin. Chem.* 61, 112–123. doi: 10.1373/clinchem.2014.222679

Imperiale, T. F., Ransohoff, D. F., Itzkowitz, S. H., Levin, T. R., Lavin, P., Lidgard, G. P., et al. (2014). Multitarget stool DNA testing for colorectal-cancer screening. *N. Engl. J. Med.* 370, 1287–1297. doi: 10.1056/NEJMoa1311194

Jensen, S. Ø., Øgaard, N., Ørntoft, M. W., Rasmussen, M. H., Bramsen, J. B., Kristensen, H., et al. (2019). Novel DNA methylation biomarkers show high sensitivity and specificity for blood-based detection of colorectal cancer-a clinical biomarker discovery and validation study. *Clin. Epigenetics* 11:158. doi: 10.1186/s13148-019-0757-3

Jeun, M., Lee, H. J., Park, S., Do, E. J., Choi, J., Sung, Y. N., et al. (2019). A novel blood-based colorectal cancer diagnostic technology using electrical detection of colon cancer secreted protein-2. *Adv. Sci.* 6:1802115. doi: 10.1002/advs.201802115

Jia, S., Zhang, R., Li, Z., and Li, J. (2017). Clinical and biological significance of circulating tumor cells, circulating tumor DNA, and exosomes as biomarkers in colorectal cancer. *Oncotarget* 8, 55632–55645. doi: 10.18632/oncotarget.17184

Jin, P., Kang, Q., Wang, X., Yang, L., Yu, Y., Li, N., et al. (2015). Performance of a second-generation methylated SEPT9 test in detecting colorectal neoplasm. *J. Gastroenterol. Hepatol.* 30, 830–833. doi: 10.1111/jgh.12855

Johnson, D. A., Barclay, R. L., Mergener, K., Weiss, G., König, T., Beck, J., et al. (2014). Plasma Septin9 versus fecal immunochemical testing for colorectal cancer screening: a prospective multicenter study. *PLoS One* 9:e98238. doi: 10.1371/journal.pone.0098238

Jung, G., Hernández-Illán, E., Moreira, L., Balaguer, F., and Goel, A. (2020). Epigenetics of colorectal cancer: biomarker and therapeutic potential. *Nat. Rev. Gastroenterol. Hepatol.* 17, 111–130. doi: 10.1038/s41575-019-0230-y

Levine, A. J., Phipps, A. I., Baron, J. A., Buchanan, D. D., Ahnen, D. J., Cohen, S. A., et al. (2016). Clinicopathologic risk factor distributions for MLH1 promoter region methylation in CIMP-positive tumors. *Cancer Epidemiol. Biomark. Prev.* 25, 68–75. doi: 10.1158/1055-9965.EPI-15-0935

Li, Q., Cai, G., Li, D., Wang, Y., Zhuo, C., and Cai, S. (2014). Better long-term survival in young patients with non-metastatic colorectal cancer after surgery, an analysis of 69,835 patients in SEER database. *PLoS One* 9:e93756. doi: 10.1371/journal.pone.0093756

Li, G., Pavlick, D., Chung, J. H., Bauer, T., Tan, B. A., Peguero, J., et al. (2019). Genomic profiling of cell-free circulating tumor DNA in patients with colorectal cancer and its fidelity to the genomics of the tumor biopsy. *J. Gastrointest. Oncol.* 10, 831–840. doi: 10.21037/jgo.2019.05.05

Li, H., Zhang, J., Tong, J. H. M., Chan, A. W. H., Yu, J., Kang, W., et al. (2019). Targeting the oncogenic p53 mutants in colorectal cancer and other solid tumors. *Int. J. Mol. Sci.* 20:5999. doi: 10.3390/ijms20235999

Lieberman, D. (2010). Progress and challenges in colorectal cancer screening and surveillance. *Gastroenterology* 138, 2115–2126. doi: 10.1053/j.gastro.2010.02.006

Loktionov, A. (2020). Biomarkers for detecting colorectal cancer non-invasively: DNA, RNA or proteins? *World J. Gastrointest. Oncol.* 12, 124–148. doi: 10.4251/wjgo.v12.i2.124

Lou, S., and Shaukat, A. (2021). Noninvasive strategies for colorectal cancer screening: opportunities and limitations. *Curr. Opin. Gastroenterol.* 37, 44–51. doi: 10.1097/MOG.0000000000000688

Ma, Z., Williams, M., Cheng, Y. Y., and Leung, W. K. (2019). Role of methylated DNA biomarkers in patients with colorectal cancer. *Dis. Markers* 2019, 1–8. doi: 10.1155/2019/2673543

Mansour, H. (2014). Cell-free nucleic acids as noninvasive biomarkers for colorectal cancer detection. *Front. Genet.* 5:182. doi: 10.3389/fgene.2014.00182

Mansour, H., Incitti, R., and Bajic, V. (2012). *Composite Biomarker for Non-Invasive Screening, Diagnosis and Prognosis of Colorectal Cancer*. Patent No. PCT/IB2012/002515.

Mansour, H., Ouhajjou, A., Bajic, V. B., and Incitti, R. (2020). Next-generation sequencing at high sequencing depth as a tool to study the evolution of metastasis driven by genetic change events of lung squamous cell carcinoma. *Front. Oncol.* 10:1215. doi: 10.3389/fonc.2020.01215

Manzat Saplacan, R. M., Balacescu, L., Gherman, C., Chira, R. I., Craiu, A., Mircea, P. A., et al. (2017). The role of PDGFs and PDGFRs in colorectal cancer. *Mediat. Inflamm.* 2017:4708076. doi: 10.1155/2017/4708076

Markowitz, S. D., and Bertagnolli, M. M. (2009). Molecular origins of cancer: molecular basis of colorectal cancer. *N. Engl. J. Med.* 361, 2449–2460. doi: 10.1056/NEJMra0804588

Marrugo-Ramírez, J., Mir, M., and Samitier, J. (2018). Blood-based cancer biomarkers in liquid biopsy: a promising non-invasive alternative to tissue biopsy. *Int. J. Mol. Sci.* 19:2877. doi: 10.3390/ijms19102877

Martini, G., Troiani, T., Cardone, C., Vitiello, P., Sforza, V., Ciardiello, D., et al. (2017). Present and future of metastatic colorectal cancer treatment: a review of new candidate targets. *World J. Gastroenterol.* 23, 4675–4688. doi: 10.3748/wjg.v23.i26.4675

Melotte, V., Yi, J. M., Lentjes, M. H., Smits, K. M., Van Neste, L., Niessen, H. E., et al. (2015). Spectrin repeat containing nuclear envelope 1 and forkhead box protein E1 are promising markers for the detection of colorectal cancer in blood. *Cancer Prev. Res.* 8, 157–164. doi: 10.1158/1940-6207.CAPR-14-0198

Meng, C., Yin, X., Liu, J., Tang, K., Tang, H., and Liao, J. (2018). TIMP-1 is a novel serum biomarker for the diagnosis of colorectal cancer: a meta-analysis. *PLoS One* 13:e0207039. doi: 10.1371/journal.pone.0207039

Muinelo-Romay, L., Casas-Arozamena, C., and Abal, M. (2018). Liquid biopsy in endometrial cancer: new opportunities for personalized oncology. *Int. J. Mol. Sci.* 19:2311. doi: 10.3390/ijms19082311

Nakayama, M., and Oshima, M. (2019). Mutant p53 in colon cancer. *J. Mol. Cell Biol.* 11, 267–276. doi: 10.1093/jmcb/mjy075

Ned, R. M., Melillo, S., and Marrone, M. (2011). Fecal DNA testing for colorectal cancer screening: the ColoSure™ test. *PLOS Curr.* 3:RRN1220. doi: 10.1371/currents.RRN1220

Neumann, M. H. D., Bender, S., Krahn, T., and Schlange, T. (2018). ctDNA and CTCs in liquid biopsy—current status and where we need to progress. *Comput. Struct. Biotechnol. J.* 16, 190–195. doi: 10.1016/j.csbj.2018.05.002

Ng, L., Wan, T. M., Man, J. H., Chow, A. K., Iyer, D., Chen, G., et al. (2017). Identification of serum miR-139-3p as a non-invasive biomarker for colorectal cancer. *Oncotarget* 8, 27393–27400. doi: 10.18632/oncotarget.16171

Nian, J., Sun, X., Ming, S., Yan, C., Ma, Y., Feng, Y., et al. (2017). Diagnostic accuracy of methylated SEPT9 for blood-based colorectal cancer detection: a systematic review and meta-analysis. *Clin. Transl. Gastroenterol.* 8:e216. doi: 10.1038/ctg.2016.66

Noone, AM, Howlader, N, Krapcho, M, Miller, D, Brest, A, Yu, M, et al. (eds). (2018). SEER Cancer Statistics Review, 1975–2015. Bethesda, MD. National Cancer Institute. Available at: https://seer.cancer.gov/csr/1975_2015/ (Accessed December 01, 2020).

O'Connell, J. B., Maggard, M. A., and Ko, C. Y. (2004). Colon cancer survival rates with the new American joint committee on Cancer sixth edition staging. *J. Natl. Cancer Inst.* 96, 1420–1425. doi: 10.1093/jnci/djh275

Ohhara, Y., Fukuda, N., Takeuchi, S., Honma, R., Shimizu, Y., Kinoshita, I., et al. (2016). Role of targeted therapy in metastatic colorectal cancer. *World J. Gastrointest. Oncol.* 8, 642–655. doi: 10.4251/wjgo.v8.i9.642

Okugawa, Y., Grady, W. M., and Goel, A. (2015). Epigenetic alterations in colorectal cancer: emerging biomarkers. *Gastroenterology* 149, 1204.e12–1225.e12. doi: 10.1053/j.gastro.2015.07.011

Oliveira, A. F., Bretes, L., and Furtado, I. (2019). Review of PD-1/PD-L1 inhibitors in metastatic dMMR/MSI-H colorectal cancer. *Front. Oncol.* 9:396. doi: 10.3389/fonc.2019.00396

Osumi, H., Shinozaki, E., Yamaguchi, K., and Zembutsu, H. (2019). Clinical utility of circulating tumor DNA for colorectal cancer. *Cancer Sci.* 110, 1148–1155. doi: 10.1111/cas.13972

Overman, M. J., Ernstoff, M. S., and Morse, M. A. (2018). Where we stand with immunotherapy in colorectal cancer: deficient mismatch repair, proficient mismatch repair, and toxicity management. *Am. Soc. Clin. Oncol. Educ. Book* 38, 239–247. doi: 10.1200/EDBK_200821

Palmirotta, R., Lovero, D., Cafforio, P., Felici, C., Mannavola, F., Pellè, E., et al. (2018). Liquid biopsy of cancer: a multimodal diagnostic tool in clinical oncology. *Ther. Adv. Med. Oncol.* 10:1758835918794630. doi: 10.1177/1758835918794630

Pantel, K., and Alix-Panabieres, C. (2017). Liquid biopsy in 2016: circulating tumour cells and cell-free DNA in gastrointestinal cancer. *Nat. Rev. Gastroenterol. Hepatol.* 14, 73–74. doi: 10.1038/nrgastro.2016.198

Peng, M., Chen, C., Hulbert, A., Brock, M. V., and Yu, F. (2017). Non-blood circulating tumor DNA detection in cancer. *Oncotarget* 8, 69162–69173. doi: 10.18632/oncotarget.19942

Peng, J., Ou, Q., Pan, Z., Zhang, R., Zhao, Y., Deng, Y., et al. (2018). Serum CNPY2 isoform 2 represents a novel biomarker for early detection of colorectal cancer. *Aging* 10, 1921–1931. doi: 10.18632/aging.101512

Pindler, K. L., Pallisgaard, N., Andersen, R. F., Brandslund, I., and Jakobsen, A. (2015). Circulating free DNA as biomarker and source for mutation detection in metastatic colorectal cancer. *PLoS One* 10:e0108247. doi: 10.1371/journal.pone.0108247

Powell, S. M., Petersen, G. M., Krush, A. J., Booker, S., Jen, J., Giardiello, F. M., et al. (1993). Molecular diagnosis of familial adenomatous polyposis. *N. Engl. J. Med.* 329, 1982–1987. doi: 10.1056/NEJM199312303292702

Quan, P. L., Sauzade, M., and Brouzes, E. (2018). dPCR: a technology review. *Sensors* 18:1271. doi: 10.3390/s18041271

Reece, M., Saluja, H., Hollington, P., Karapetis, C. S., Vatandoust, S., Young, G. P., et al. (2019). The use of circulating tumor DNA to monitor and predict response to treatment in colorectal cancer. *Front. Genet.* 10:1118. doi: 10.3389/fgene.2019.01118

Robertson, D. J., and Imperiale, T. F. (2015). Stool testing for colorectal cancer screening. *Gastroenterology* 149, 1286–1293. doi: 10.1053/j.gastro.2015.05.045

Rodia, M. T., Ugolini, G., Mattei, G., Montroni, I., Zattoni, D., Ghignone, F., et al. (2016). Systematic large-scale meta-analysis identifies a panel of two mRNAs as blood biomarkers for colorectal cancer detection. *Oncotarget* 7, 30295–30306. doi: 10.18632/oncotarget.8108

Roperch, J. P., Incitti, R., Forbin, S., Bard, F., Mansour, H., Mesli, F., et al. (2013). Aberrant methylation of NPY, PENK, and WIF1 as a promising marker for blood-based diagnosis of colorectal cancer. *BMC Cancer* 13:566. doi: 10.1186/1471-2407-13-566

Satelli, A., Mitra, A., Brownlee, Z., Xia, X., Bellister, S., Overman, M. J., et al. (2015). Epithelial-mesenchymal transitioned circulating tumor cells capture for detecting tumor progression. *Clin. Cancer Res.* 21, 899–906. doi: 10.1158/1078-0432.CCR-14-0894

Shen, Z., Wu, A., and Chen, X. (2017). Current detection technologies for circulating tumor cells. *Chem. Soc. Rev.* 46, 2038–2056. doi: 10.1039/C6CS00803H

Shigeyasu, K., Toden, S., Zumwalt, T. J., Okugawa, Y., and Goel, A. (2017). Emerging role of microRNAs as liquid biopsy biomarkers in gastrointestinal cancers. *Clin. Cancer Res.* 23, 2391–2399. doi: 10.1158/1078-0432.CCR-16-1676

Shimura, T., Iwasaki, H., Kitagawa, M., Ebi, M., Yamada, T., Yamada, T., et al. (2019). Urinary cysteine-rich protein 61 and trefoil factor 3 as diagnostic biomarkers for colorectal cancer. *Transl. Oncol.* 12, 539–544. doi: 10.1016/j.tranon.2018.12.006

Shyamala, K., Girish, H. C., and Murgod, S. (2014). Risk of tumor cell seeding through biopsy and aspiration cytology. *J. Int. Soc. Prev. Community Dent.* 4, 5–11. doi: 10.4103/2231-0762.129446

Sidransky, D., Tokino, T., Hamilton, S. R., Kinzler, K. W., Levin, B., Frost, P., et al. (1992). Identification of ras oncogene mutations in the stool of patients with curable colorectal tumors. *Science* 256, 102–105. doi: 10.1126/science.1566048

Siskova, A., Cervena, K., Kral, J., Hucl, T., Vodicka, P., and Vymetalkova, V. (2020). Colorectal adenomas-genetics and searching for new molecular screening biomarkers. *Int. J. Mol. Sci.* 21:3260. doi: 10.3390/ijms21093260

Tadimety, A., Closson, A., Li, C., Yi, S., Shen, T., and Zhang, J. X. J. (2018). Advances in liquid biopsy on-chip for cancer management: technologies, biomarkers, and clinical analysis. *Crit. Rev. Clin. Lab. Sci.* 55, 140–162. doi: 10.1080/10408363.2018.1425976

Takeda, K., Yamada, T., Takahashi, G., Iwai, T., Ueda, K., Kuriyama, S., et al. (2019). Analysis of colorectal cancer-related mutations by liquid biopsy: utility of circulating cell-free DNA and circulating tumor cells. *Cancer Sci.* 110, 3497–3509. doi: 10.1111/cas.14186

Toiyama, Y., Okugawa, Y., Fleshman, J., Richard Boland, C., and Goel, A. (1870). MicroRNAs as potential liquid biopsy biomarkers in colorectal cancer: a systematic review. *Biochim. Biophys. Acta Rev. Cancer* 2018, 274–282. doi: 10.1016/j.bbcan.2018.05.006

Toledo, R. A., Cubillo, A., Vega, E., Garralda, E., Alvarez, R., de la Varga, L. U., et al. (2017). Clinical validation of prospective liquid biopsy monitoring in patients with wild-type RAS metastatic colorectal cancer treated with FOLFIRI-cetuximab. *Oncotarget* 8, 35289–35300. doi: 10.18632/oncotarget.13311

Trojan, J., Klein-Scory, S., Koch, C., Schmiegel, W., and Baraniskin, A. (2017). Clinical application of liquid biopsy in targeted therapy of metastatic colorectal cancer. *Case Rep. Oncol. Med.* 2017:6139634. doi: 10.1155/2017/6139634

Uppara, M., Adaba, F., Askari, A., Clark, S., Hanna, G., Athanasiou, T., et al. (2015). A systematic review and meta-analysis of the diagnostic accuracy of pyruvate kinase M2 isoenzymatic assay in diagnosing colorectal cancer. *World J. Surg. Oncol.* 13:48. doi: 10.1186/s12957-015-0446-4

Vacante, M., Ciuni, R., Basile, F., and Biondi, A. (2020). The liquid biopsy in the management of colorectal cancer: an overview. *Biomedicine* 8:308. doi: 10.3390/biomedicines8090308

Vafaei, S., Fattahi, F., Ebrahimi, M., Janani, L., Shariftabrizi, A., and Madjd, Z. (2019). Common molecular markers between circulating tumor cells and blood exosomes in colorectal cancer: a systematic and analytical review. *Cancer Manag. Res.* 11, 8669–8698. doi: 10.2147/CMAR.S219699

Vafaei, S., Roudi, R., Madjd, Z., Aref, A. R., and Ebrahimi, M. (2020). Potential theranostics of circulating tumor cells and tumor-derived exosomes application in colorectal cancer. *Cancer Cell Int.* 20:288. doi: 10.1186/s12935-020-01389-3

van Lanschot, M. C., Carvalho, B., Coupé, V. M., van Engeland, M., Dekker, E., and Meijer, G. A. (2017). Molecular stool testing as an alternative for surveillance colonoscopy: a cross-sectional cohort study. *BMC Cancer* 17:116. doi: 10.1186/s12885-017-3078-y

Vidal, J., Muinelo, L., Dalmases, A., Jones, F., Edelstein, D., Iglesias, M., et al. (2017). Plasma ctDNA RAS mutation analysis for the diagnosis and treatment monitoring of metastatic colorectal cancer patients. *Ann. Oncol.* 28, 1325–1332. doi: 10.1093/annonc/mdx125

Vymetalkova, V., Cervena, K., Bartu, L., and Vodicka, P. (2018). Circulating cell-free DNA and colorectal cancer: a systematic review. *Int. J. Mol. Sci.* 19:3356. doi: 10.3390/ijms19113356

Wang, J., Koo, K. M., Wang, Y., and Trau, M. (2019). Engineering state-of-the-art plasmonic nanomaterials for SERS-based clinical liquid biopsy applications. *Adv. Sci.* 6:1900730. doi: 10.1002/advs.201900730

Wang, X., Wei, Q., Gao, J., Li, J., Li, J., Gong, J., et al. (2017). Clinicopathologic features and treatment efficacy of Chinese patients with BRAF-mutated metastatic colorectal cancer: a retrospective observational study. *Chin. J. Cancer* 36:81. doi: 10.1186/s40880-017-0247-y

World Health Organization (2020a). IARC, The Global Cancer Observatory Available at: https://gco.iarc.fr/today/data/factsheets/cancers/8-Colon-fact-sheet.pdf (Accessed December 01, 2020).

World Health Organization (2020b). Projected global deaths for selected causes, 2004–2030, r 2004. Available at: https://www.who.int/healthinfo/global_burden_disease/GBD_report_2004update_full.pdf

Worm Ørntoft, M. B. (2018). Review of blood-based colorectal cancer screening: how far are circulating cell-free DNA methylation markers from clinical implementation? *Clin. Colorectal Cancer* 17, e415–e433. doi: 10.1016/j.clcc.2018.02.012

Wu, J., Hu, S., Zhang, L., Xin, J., Sun, C., Wang, L., et al. (2020). Tumor circulome in the liquid biopsies for cancer diagnosis and prognosis. *Theranostics* 10, 4544–4556. doi: 10.7150/thno.40532

Wu, Y., Yang, L., Zhao, J., Li, C., Nie, J., Liu, F., et al. (2015). Nuclear-enriched abundant transcript 1 as a diagnostic and prognostic biomarker in colorectal cancer. *Mol. Cancer* 14:191. doi: 10.1186/s12943-015-0455-5

Wu, D., Zhou, G., Jin, P., Zhu, J., Li, S., Wu, Q., et al. (2016). Detection of colorectal cancer using a simplified SEPT9 gene methylation assay is a reliable method for opportunistic screening. *J. Mol. Diagn.* 18, 535–545. doi: 10.1016/j.jmoldx.2016.02.005

Xiao, W., Zhao, H., Dong, W., Li, Q., Zhu, J., Li, G., et al. (2015). Quantitative detection of methylated NDRG4 gene as a candidate biomarker for diagnosis of colorectal cancer. *Oncol. Lett.* 9, 1383–1387. doi: 10.3892/ol.2014.2815

Xie, Y. H., Chen, Y. X., and Fang, J. Y. (2020). Comprehensive review of targeted therapy for colorectal cancer. *Signal Transduct. Target. Ther.* 5:22. doi: 10.1038/s41392-020-0116-z

Xu, J., Ye, Y., Zhang, H., Szmitkowski, M., Mäkinen, M. J., Li, P., et al. (2016). Diagnostic and prognostic value of serum interleukin-6 in colorectal cancer. *Medicine* 95:e2502. doi: 10.1097/MD.0000000000002502

Xue, Y., Yu, F., Yan, D., Cui, F., Tang, H., Wang, X., et al. (2014). Zinc-α-2-glycoprotein: a candidate biomarker for colon cancer diagnosis in Chinese population. *Int. J. Mol. Sci.* 16, 691–703. doi: 10.3390/ijms16010691

Yang, C., Chen, F., Wang, S., and Xiong, B. (2019). Circulating tumor cells in gastrointestinal cancers: current status and future perspectives. *Front. Oncol.* 9:1427. doi: 10.3389/fonc.2019.01427

Zhao, G., Ma, Y., Li, H., Li, S., Zhu, Y., Liu, X., et al. (2020). A novel plasma based early colorectal cancer screening assay base on methylated SDC2 and SFRP2. *Clin. Chim. Acta* 503, 84–89. doi: 10.1016/j.cca.2020.01.010

Zhao, B., Wang, L., Qiu, H., Zhang, M., Sun, L., Peng, P., et al. (2017). Mechanisms of resistance to anti-EGFR therapy in colorectal cancer. *Oncotarget* 8, 3980–4000. doi: 10.18632/oncotarget.14012

Zhou, B., Xu, K., Zheng, X., Chen, T., Wang, J., Song, Y., et al. (2020). Application of exosomes as liquid biopsy in clinical diagnosis. *Signal Transduct. Target. Ther.* 5:144. doi: 10.1038/s41392-020-00258-9

Conflict of Interest: RI and HM are founders and shareholders of OncoDiag, a company specialized in biomarkers for noninvasive cancer diagnostics. AO is a cofunder of Al Azhar Oncology Center.

The remaining author declares that the research was conducted in the absence of any commercial or financial relationships that could be construed as a potential conflict of interest.

Copyright © 2021 Mazouji, Ouhajjou, Incitti and Mansour. This is an open-access article distributed under the terms of the Creative Commons Attribution License (CC BY). The use, distribution or reproduction in other forums is permitted, provided the original author(s) and the copyright owner(s) are credited and that the original publication in this journal is cited, in accordance with accepted academic practice. No use, distribution or reproduction is permitted which does not comply with these terms.

frontiers in Oncology

REVIEW
published: 02 June 2021
doi: 10.3389/fonc.2021.652253

Detection Methods and Clinical Applications of Circulating Tumor Cells in Breast Cancer

Hongyi Zhang[1†], Xiaoyan Lin[1†], Yuan Huang[2†], Minghong Wang[3], Chunmei Cen[1], Shasha Tang[1], Marcia R. Dique[1], Lu Cai[4], Manuel A. Luis[1], Jillian Smollar[5], Yuan Wan[5] and Fengfeng Cai[1]*

[1] Department of Breast Surgery, Yangpu Hospital, Tongji University School of Medicine, Shanghai, China, [2] Cellomics International Limited, Hong Kong, China, [3] Shanghai Public Health Clinical Center, Fudan University, Shanghai, China, [4] Department of General Surgery, Zhongshan Hospital, Fudan University, Shanghai, China, [5] Department of Biomedical Engineering, The City College of New York, New York, NY, United States

OPEN ACCESS

Edited by:
George Calin,
University of Texas MD Anderson Cancer Center, United States

Reviewed by:
Ramray Bhat,
Indian Institute of Science (IISc), India
Zuheir Alshehabi,
Tishreen University, Syria

***Correspondence:**
Fengfeng Cai
caifengfeng@tongji.edu.cn

[†]These authors have contributed equally to this work

Specialty section:
This article was submitted to Molecular and Cellular Oncology, a section of the journal Frontiers in Oncology

Received: 05 February 2021
Accepted: 29 April 2021
Published: 02 June 2021

Citation:
Zhang H, Lin X, Huang Y, Wang M, Cen C, Tang S, Dique MR, Cai L, Luis MA, Smollar J, Wan Y and Cai F (2021) Detection Methods and Clinical Applications of Circulating Tumor Cells in Breast Cancer. Front. Oncol. 11:652253. doi: 10.3389/fonc.2021.652253

Circulating Tumor Cells (CTCs) are cancer cells that split away from the primary tumor and appear in the circulatory system as singular units or clusters, which was first reported by Dr. Thomas Ashworth in 1869. CTCs migrate and implantation occurs at a new site, in a process commonly known as tumor metastasis. In the case of breast cancer, the tumor cells often migrate into locations such as the lungs, brain, and bones, even during the early stages, and this is a notable characteristic of breast cancer. Survival rates have increased significantly over the past few decades because of progress made in radiology and tissue biopsy, making early detection and diagnosis of breast cancer possible. However, liquid biopsy, particularly that involving the collection of CTCs, is a non-invasive method to detect tumor cells in the circulatory system, which can be easily isolated from human plasma, serum, and other body fluids. Compared to traditional tissue biopsies, fluid sample collection has the advantages of being readily available and more acceptable to the patient. It can also detect tumor cells in blood earlier and in smaller numbers, possibly allowing for diagnosis prior to any tumor detection using imaging methods. Because of the scarcity of CTCs circulating in blood vessels (only a few CTCs among billions of erythrocytes and leukocytes), thorough but accurate detection methods are particularly important for further clinical applications.

Keywords: CTCs, breast cancer, clinical application, liquid biopsy, detection methods

INTRODUCTION

Breast cancer has overtaken lung cancer in 2020 to become the most common type of cancer in the world. The metastatic nature of breast cancer is also of great concern, as metastasis accounts for 90% of malignancy deaths, because of distal progressions of primary tumors (1). One hypothesis is that tumor metastasis is triggered *via* CTCs (circulating tumor cells) that are found in patients' blood (2). In a successful dispersal process, cancer cells of breast tumors in primary site infiltrate surrounding tissues, enter blood and lymphatic vessels, followed by translocation to distant sites. The ability to

escape from blood vessels and adapt to novel microenvironments in the body allow cancer cells to successfully implant, colonize and proliferate in a new site.

Compared to primary cancer cells, circulating tumor cells show a more aggressive ability to mutate, accumulating genetic changes similar to or larger than those of the original tumor through somatic cell mutations and acquisition of additional characteristics within circulation (3). As the dissemination of tumors appears to be mostly *via* the blood, circulating tumor cells that have penetrated the blood vessels to infiltrate potential metastatic sites are of obvious interest (4); for example, many studies have concluded that the blood-borne dissemination is contributed by EMT (epithelial-mesenchymal transition) in patients with breast cancer (5). Recently, many investigations into liquid biopsy have been conducted; a considerable number showed the potential of CTC detection as an effective method for the evaluation of chemotherapy efficacy, early diagnoses and malignancy recurrence, and choice of drug sensitivity (6). Liquid biopsies of CTCs have the following advantages over other tumor markers in the blood: (1) easy to collect, (2) persistent assessment, (3) analysis of the overall tumors burden rather than a limited part of tumors. Given the many benefits of CTCs have in relation to the early diagnosis and treatment of breast tumors, early stage detection of CTCs in blood appears to be the most critical. However, because of the extremely low concentration of CTCs in human blood, detection has always been a technical challenge. This has led to more research and development in relation to detection methods. Recently, the detection and clinical application of CTCs have been gradually incorporated into the field of nanotechnology and genetics. The detection methods of CTCs are changing dramatically, and the clinical applications are becoming increasingly extensive (7). As a result of the increased attention on this critical subject, multiple detection methods have been developed, and these methods can be used to detect circulating tumor cells *in vivo* as well as *in vitro*.

This article sets out the current state of recent developments relating to detection methods, commercial systems, and clinical applications of CTCs, as well as the limitations and prospects of each method for reference during clinical processes and as guidance for researchers and clinicians.

DETECTION METHODS OF CTCS

CTCs are infrequent neoplastic cells, and a high-level detection platform, appropriate equipment and techniques are needed to detect its rather low concentration in blood, as approximately one CTC per milliliter of blood can escape from primary neoplasms or metastases. The properties to detect and separate heterogeneous CTCs of all types, as well as to separate out the large blood and white cells in blood, are necessary to for a CTC testing platform. With results of negative or positive enrichment, and recognizing circulating tumor cells or removing hematopoietic cells through immune affinity strategy, the selection of CTCs is commonly the first stage of detection. The detection procedure then further distinguishes (and possibly characterizes) CTC from other regular cells. Then, CTCs are identified and isolated from other normal blood cells (8).

In Vitro Detection Methods

CTCs counts have long been seen as a preferred tool in clinical diagnosis. Recently, accurate detection of CTCs may soon be achieved due to many advanced techniques being developed. Enrichment as well as detection procedures are basics for these novel techniques. The gathering and detection methods of CTCs are based on biological or physical features. The latter depends on size, electrical properties, and other physical characteristics of tumor cells, while the former depends on antigen-antibody combinations and the differences of DNA and RNA which distinguish CTCs from normal cells.

Detection Methods Relying on Physical Properties

CTCs can be identified from normal cells in blood, such as leukocytes, through physical isolation, without any biomarker labeling. The isolation tactics focus on several distinctions in physical characteristics between cells in blood and CTCs, as set out in **Table 1**.

1. *ISET (Isolation by Size of Epithelial Tumor cells):* Because of their larger size compared to leukocytes in blood, CTCs can be easily isolated by diameter. An identical hypothesis, the nucleoporeassay, is also based on size differences (9, 10). Overall, ISET equipment allows the isolation of CTM (circulating tumor microemboli) and CTCs from all kinds of malignancies as intact cells, without any previous selection based on immune system. However, proof of the existence of CTCs smaller than 8 μm has not yet been explored, leaving questions about the sensitivities of the method.
2. *ScreenCell system:* Through utilizing a microporous membrane filter, ScreenCell systems separate CTCs by cell size screen, making later characterization and sorting possible. Filtration membranes, based on microfiltration technology, enable nucleated cells to pass while holding up CTCs. The potential to achieve high throughput persistent processing of large volumes of blood has been demonstrated. This method has some advantages, for example, related cellular and molecular biological techniques, and techniques that are related to the figures and identification

TABLE 1 | The strategies for isolation based on physical properties of CTCs.

Physical characteristics	
Base on Density	Ficoll-Paque® (Density Medium Centrifugation)
Charge on Surface	depFFF (Dielectrophoretic field-flow fractionation) ApoStream®
Both Size and Density	Onco-Quick® (Porous barrier for size-based separation and density-based centrifugation)
Both Size and Deformability	Vortex chip Microfluid vortex capture
Size Only	DFF (Dean Flow Fractionation) SSA (Selective size amplification) in conjunction with MOA (multi obstacle architecture) ISET® (Isolation by Size of Epithelial tumor cells) ScreenCell (Microporous membrane filter)

of CTCs and their latent gene abnormalities, can conveniently analyze neoplasm cells extracted onto the filter. Furthermore, cells isolated from blood can undergo tissue culture to be used in future experiments, without the usage of any assay based on antibody, which can open up a broad range of isolation areas for cancer cells, covering non-epithelial originated cells.

3. *Electrical features (Surface charge):*

The majority of cells of mammals have a net negatively-charged surface, especially in physiological situation. However, because of the existence of some macromolecules that have polarized particles, some cell surfaces have complex dielectric features, such as proteins, nucleic acids and polypeptides.

For example, compared to leukocytes in blood, neoplasm cells (e.g. CTCs) have a surface with more zeta potential or negative charge, which has been demonstrated by studies. In addition, these cells, compared to white blood cells, were also proven to have lower cytoplasmic conductivity as well as higher unit membrane capacitance (11).

Detection Methods Based on Immunological Properties

This method identifies CTCs by proteins on the cell surface or DNA/RNA in cancer cells. Antibodies in blood can identify and combine with specific markers, usually proteins, on cell surfaces. For instance, epithelial markers are commonly used to identify and separate blood cells and malignancy cells, due to features commonly expressed on epithelial and epithelial cancer cells, which are rarely expressed on the mesenchymal white blood cells.

Immunology-based technology commonly uses specific protein biomarkers, expressed by either cancer cells or blood cells only, and their complementary antibodies. Circulating tumor cells isolation tactics based on proteins can be categorized into 3 types, as set out in **Table 2**.

1. Positive selection: Specific markers usually expressed on the surface of epithelial cancer cells or normal cells, such as epithelial markers, are combined with antibodies, a design to identify CTCs in samples of liquid biopsy. Usually, two steps are involved in these technologies, firstly CTC-enrichment, followed by the step of enumeration and CTC detection. Current positive selection detection procedures include the CellSearch® system, Adnatest® system, MagSweeper™, CTC Chips and Herringbone Chips, EPHESIA CTC Chips, IsoFlux, Velcro-like devices, GEDI microdevices, and DEPArray®.

For instance, the US FDA (Food and Drug Administration) has approved the CellSearch® test system, which combines immune-driven nano-magnetic beads with epithelial cell adhesion molecules (EpCAM) through fluorescent specific CTC reaction recognition. It can be applied to breast carcinoma and other malignancies treatment in addition to patient monitoring after chemotherapy or surgeries. However, independent validations of this novel technology are lacking.

2. *Negative selection*: Opposite to the former technology, based on surface markers of cells that are quite different to non-CTCs, consumption procedures are used by negative selection technology to remove white blood cells (WBCs) and other blood cells. In negative CTC enrichment, WBCs are depleted using antibodies of specificity against various biomarkers, such as CD66b or CD45; this makes the selection of leukocytes appearing in blood possible. However, not all nucleated cells in blood are positive for CD66b or CD45. Negative selection methods include white blood cells depletion kits, CTC Chips, RosetteSep method, and Easysep method.

For instance, the Easysep method is quick, simple, and does not require a separation column of immune cells using magnetic separation technology, along with other advantages. This method depends on the TAC technology: normal cells are labeled with antigen-antibody complex, under the action of immune magnetic beads, and normal cells were placed in the EasySep™ magnetic pole, while CTCs were allowed to be negatively selected and can thereafter be extracted from peripheral blood mononuclear cells (PBMCs).

3. *Selection-free* CTCs can express EpCAM at varying levels (12). Selection-free techniques for CTC recognition have been developed, in that some cells express both mesenchymal and epithelial phenotypes. This method combines high throughput microscopy, flow cytometry and RT-PCR. No extra loss of CTCs during a selection procedure is one of the advantages of these methods. Nevertheless, these methods also have some restrictions, for example, CTCs and WBCs need to be distinguished by imperfect biological markers. Examples of selection-free methods include Epic Sciences and AccuCyte® – CyteFinder®.

TABLE 2 | The strategies for isolation relied on biological features of CTCs.

Biological characteristics	
Positive Selection	EPHESIA CTC-Chip
	CellSearch® system
	MagSweeper™
	CTC-Chip and Herringbone-Chip
	IsoFlux
	Adnatest® system
	Velcro-like device
	GEDI microdevice
	DEPArray®
Negative Selection	leukocytes depletion kits
	RosetteSep method
	CTC-iChip
Selection-free	Epic Sciences
	AccuCyte® – CyteFinder®

In Vivo Detection Methods

Optical Imaging Technology

Clinically, commonly used imaging technologies include MRI (magnetic resonance imaging), PAT (Photoacoustic tomography),

OCT (optical coherence tomography), CT (computed tomography) and PET (positron emission tomography). Optical imaging technologies, such as PAT and OCT, are much higher in velocity and resolution than those of CT, MRI, and PET, and can even identify circulating tumor cells *in vivo*. Optical imaging has been proposed for real-time imaging of rapidly flowing cells in blood vessels, including cancer cells (13). Zerda et al., successfully detected free RPMI-8226 myeloma cells in the blood vessels of rat ears by means of speckle-modulating OCT (SM-OCT), which can modulate speckle noise (13) and gold nanorods (~100 nm× 30 nm) were exploited as contrast agents to label cancer cells. OCT technology was first used for single cell detection in the circulatory system within animals. The results show that optical imaging techniques with high resolution can be taken to capture fluorescence-labeled cancer cells and non-labeled melanoma cells or intravascular nanoparticles. However, precisely quantifying the dynamic change of CTCs in fast flowing blood is still very difficult because of the slow imaging velocity of these technologies.

In *in vitro* flow cytometry (IVFC), as each cell passes through the laser beam, fluorescent markers on cell surfaces can be suddenly activated to emit a fluorescence. Quantification of the fluorescent-labeled cells is done through data processing and analysis. The natural blood circulation is directly exploited by IVFC as the fluid flow system to quantitatively analyze the changes of fast flowing target cells in real-time. Different signals are produced by target cells (CTCs) and other cells using different methods such as contrast, fluorescence, photothermal, photoacoustic, light scattering intensity, etc. The methodology for each type of flow cytometry is based on those signals, such as *in vivo* fluorescence flow cytometry, *in vivo* photoacoustic flow cytometry. Fluorescence IVFC (IVFFC) and photoacoustic IVFC (IVPAFC) are the most widely used for CTC detection.

Fluorescence Flow Cytometry

A novel small animal research tool was developed by Tan et al. called "Diffuse *in vivo* Flow Cytometry" (DiFC), which is used to directly detect CTCs in blood, that are fluorescently-labeled. Near-infrared diffuse photons are used in this technique, making it possible to count and identify cells flowing in veins and large superficial arteries, and drawing of blood samples is not necessary. The speed and depth can be measured and individual cells of different directions in arterial or venous can be counted when DiFC is combined with a new signal processing algorithm. The experiment shows that all the blood of a mouse can be easily monitored in under 10 minutes, while a false positive rate of 0.014 per minute is maintained by DiFC, which means DiFC is a credible tool to detect CTCs at concentration levels even below 1 cell per milliliter. Therefore, DiFC is a promising technology to be applied in biological applications. In summary, IVFFC has been widely used to monitor the dynamic changes of fluorescently labeled CTCs in the blood circulation system of animal tumor models, including single CTCs, CTC clusters and apoptotic CTCs (14).

Photoacoustic Flow Cytometry

IVPAFC was first developed by Zharov et al. of Arkansas University. The mechanism of action is as follows: IVPAFC irradiates blood vessels with a high-frequency pulse laser and detects the instantaneous ultrasonic signals generated by target cells flowing through the blood vessel through ultrasonic detectors placed on the surface of tissue. The target cells absorb light energy and then convert the light energy into heat energy, when the tissue is irradiated. This causes the local temperature to rise, which initiates a thermoelastic change in the tissues, producing an ultrasonic wave (i.e., photoacoustic signal). Compared to detection methods of CTCs *in vitro*, IVPAFC has distinct merits. For instance, in the case of CTCs metastases along lymphatic vessels, lymphatic system and vessels should be enhanced and displayed by contrast agents because of the small structure of lymphatic vessels, as well as the transparent lymph liquid in the lymph vessels.

Besides, the collection amount of lymph fluid is often too small with long-term intubation, causing multiple restrictions in the analysis of CTCs in lymph-based *in vitro* detection methods. In CTC detection by IVPAFC, the background noise in photoacoustic signals produced by colorless lymph is low, which has significant advantages. In the study, the researchers used gold-plated carbon nanotubes and ligand-functionalized iron trioxide magnetic nanoparticles to specifically mark breast tumor cells MDA-MB-231 to evaluate detection levels of target cells. Based on the same technique, others evaluated the detection of CD44 expressing breast cancer stem cells. They used IVPAFC to detect whether CTCs in breast cancer patients have transferred to bone tissue and cerebrospinal fluid, and eventually proved that not only can IVPAFC detect melanoma CTCs *in vivo* in real-time, it can also eradicate melanoma cells and have significant therapeutic effects.

Scaffold Implants

The implanted *in vivo* scaffold-based capturing technology mainly stimulates the microenvironment *in vivo*, through biomaterial scaffolds, to induce the migration of cancer cells into the scaffolds. Shea et al. (15) implanted a Polylactide-co-Glycolide (PLG) scaffold into mice and the results showed that PLG scaffolds have the abilities to regulate the local immune microenvironment, capture and recruit metastatic cancer cells, and even decrease solid organs' tumor burden. All the biomaterials that used have great biocompatibility and can be made into tissue engineering scaffolds or drug sustained-release carriers, etc., which have broad biomedical applications. Furthermore, other types of scaffolds could be used as targets for SUM1315 breast tumor cells to metastasize in mice, such as BMSCs (human bone stromal cells) and BMP-2 (bone morphogenetic protein-2). For such patients, particularly those with a high risk of recurrence, Scaffolds implantation can not only help find tumor metastasis at a relatively early stage, but also treat breast cancer with a relatively low burden.

Intravenous Indwelling Needle Device

Intravenous indwelling needles (IINs) mainly consist of a puncture needle core and an endovascular catheter. The surface of the needle core tip is functionalized, allowing high affinity ligands such as antibody and aptamer to bind specifically to CTCs. Another method is when the needle core is replaced

with other biologically compatible materials, whereby CTCs can be captured by inserting a catheter into blood vessels.

Presently, GILUPI CellCollector® is the first and only technology approved by US FDA that captures CTCs through IINs. The functionalized thread was laxly pushed into the elbow venous vessel through the indwelling needle's catheter (blood flow was about 20 mL per min) and stayed about 30 minutes in order to capture CTCs. Thereafter, the thread was taken out, washed, fixed, sealed and immunostained it, and observed and CTCs were counted under a microscope. CTCs are recognised when cells show positive EpCAM or cytokeratin (CK) 4, 5, 8, 9, 18 and are between 10 and 50 micrometers in size and have a high cytoplasmic ratio. The benefit of this method is that it is straightforward and quick, brings little trauma and is easily accepted by patients with breast cancer.

Microfluidic Chip

Based on a sorting chip microfluidic cell, through an arteriovenous shunt implanted in mice, the microfluidic chip system has been tested when it is continuously connected to a conscious mouse. When the blood passes through the equipment, microfluidic valves which are pneumatically controlled are able to capture CTCs, and the remaining blood without CTCs will be go back into the mouse. An optofluidic system presented by Hamza (16) showed that the system continuously collected CTCs labeled by fluorescence from a genetically engineered mouse model (GEMM) for several hours per day over various days or weeks. Two-step microfluidic chips were developed by Hyun (17), which can not only sort out heterogeneous CTCs based on their features, but also isolate CTCs from cells in blood. In conclusion, the microfluidic chips are beneficial to research on heterogeneity of CTCs, and by extension, personalized tumor therapy. However, because of the traumatic features of the insertion of catheter in veins and arteries as well as the sterility requirement of CTCs sorting devices and the materials' biotoxicity, the application of microfluidic chip is limited.

CLINICAL APPLICATION OF CTCS IN BREAST CANCER AND OTHER CANCERS

In 2020, breast cancer is on the top of malignancy lists in the world, especially in developed areas. Identifying/diagnosing cancer and metastatic tumors in an early stage is critically important for clinicians to detect and treat breast cancer patients. Although the prognosis is better than lung cancer and other malignancies, a prominent characteristic of breast cancer is early metastasis, to areas such as lungs, bones and brain, causing the elevated mortality rates of breast cancer. As a prognostic tumor marker of treatment efficacy and metastatic progress with huge potential, CTCs count has been proven and studied by multiple researchers (18). Compared to conventional imaging diagnosis and tissue biopsy, CTC is expected to be a non-invasive tumor screening method for clinical application. In addition, compared to conventional tissue biopsy, liquid biopsy captures the heterogeneous essence of tumors, given the dual sources of primary and metastatic tumors (19,20). Because of that, increasingly more attention has been paid to clinical applications of CTC detection in breast cancer.

Screening and Early Detection of Cancer

Early diagnosis plays a key role in decreasing mortality of breast cancer, while various grades and types of breast cancer have different significance. For instance, the progress speed of grade I is much more slow than grades II and III of breast cancer, which means early diagnosis when the diameter of tumors is smaller than two centimeters can improve prognosis and OR (overall survival) of patients with breast cancer (21). CTC detection plays a critical part in the screening, diagnosis, early detection and treatment of breast cancer.

A quick CTCs detection method with great sensitivity has been created by Kruspe et al. (22). CTCs-derived nucleases, a special enzyme that are usually elevated in multiple malignancies, are used for signal amplification in the study. The result shows that probes activated by fluorescent nucleases are able to detect CTCs levels quickly, and can be an economical and effective detection method of CTCs for early diagnosis of breast cancer. Although CTC detection can detect breast cancer earlier than conventional detection methods, further research on CTC detection and its application in tumor diagnosis still needs to be conducted, as using CTC for cancer diagnosis is still in the preliminary phase of development.

Predicting Recurrence and Prognosis in Breast Cancer

It is commonly accepted that breast cancer malignant tumors have a strong invasive ability that can migrate into remote organs, such as bones and lungs, at an early stage. Therefore, forecasting prognosis and cancer recurrence in breast cancer *via* CTC detection plays a critical role in the treatment. There is a plethora of studies which shows, as an independent predictor, that the number of CTCs in blood before therapies have a significant implication in both OR (overall survival) and progression-free survival of breast cancer patients (23).

The largest multicenter study was published by Rack and his colleagues (24). In this study, they recruited 2,026 early breast cancer patients in group 1 and 1,492 patients in group 2. Group 1 consists of patients before adjuvant chemotherapy, while group 2 consists of patients after chemotherapy, and both groups are treated with the CellSearch System to count the number of CTCs.

According to the study, 21.5% of patients examined were detected with CTCs in their blood, while CTCs can be found in 22.4% of node-positive patients and 19.6% of node-negative patients. 22.1% of patients were detected with CTCs even after chemotherapy. The continuous existence of CTCs in peripheral blood is related to a worse prognosis, in the other words, increased risk of recurrence in primary sites is related to an elevated number of CTCs detected, before or after adjuvant chemotherapy. Another similar study by Madic et al. (25) probed the correlations of CTC and ctDNA plasma level with the prognosis in patients with TNBC (triple negative breast cancer). The study showed that worse prognosis and lower

overall survival and time of progression were related to those patients with higher CTC counts. These studies point toward the critical role of CTCs in forecasting relapse and prognosis in patients with breast cancer.

Recognition of Resistance Mechanisms and Therapeutic Targets

ER/PR and HER-2 are therapeutic targets of breast cancer. Clinical data show that in approximately 30% of cases, the HER-2 status of distant metastatic tumor cells and CTCs are significantly different from that of cells in the primary site, suggesting that drugs targeting the primary tumor may not be appropriate for metastatic tumors. Detecting new properties and characteristics of tumors through conventional tissue biopsy may hurt patients; a non-invasive method like CTCs is an ideal alternative. Other than ER/PR and HER-2, in recent years, the discovery of immune checkpoint regulators such as PD-L1 has made the successful therapy of advanced breast cancer possible, which has become an exciting new therapeutic target. The evidence that PD-L1 is expressed on the surface of CTCs in breast cancer patients with ER or PR(+) and HER2(-) was first found by Mazel and his colleagues (26), and the established assays of CTC/PD-L1 will be used for liquid biopsy in future clinical experiments of breast cancer patients who are experiencing the immune checkpoint.

Real-Time Monitoring of Therapies

After therapy such as surgery or chemotherapy, real time detection of the level of CTCs in patients is needed to monitor and evaluate their conditions and furthermore, predict and assess survival period. During chemotherapy, the clinical validity of CTCs quantification *via* CellSearch method for monitoring was assessed in metastatic breast cancer patients through analyzing each patients' real-time data of CTCs (27). Bidard et al. (28) contacted 51 European centres and requested them to offer both reported and unreported anonymized data for individual metastatic breast cancer patients who took part in experiments between January 2003 and July 2012. They concluded that when added to full clinicopathological predictive models, CTCs count can improve metastatic breast cancer's prognostication, while tumor markers in serum cannot, which means real time monitoring of CTCs can not only detect and identify deterioration, but also be used in the assessment and monitoring of therapies.

The Clinical Application of CTCs of Other Common Cancers

Through current techniques of CTCs detection, different cancer types can be identified, this is usually done based on the physical, chemical, and biological properties of the tumor cells. For example, the source of the tumor can be determined by detecting CTC phenotypes, immunohistochemistry, and examining the genes of the cells. For example, KRT7 and TTF-1 positive CTCs are associated with lung cancer, PSA and PSMA positive cells are associated with prostate cancer, and KRT20 and CDX2 positive cells are associated with colorectal cancer. Therefore, the tumor type can be identified through the characteristics of circulating tumor cells. In addition to breast cancer, CTC detection technology is also widely used in clinical detection and clinical treatment of a variety of tumors, such as prostate cancer, digestive tract cancer, small cell lung cancer, etc. The CellSearch® system is the only US FDA-approved test platform for CTC isolation, primarily for breast, prostate, and colorectal cancer, and is considered the gold standard for CTC testing. In metastatic prostate cancer, breast cancer, and colorectal cancer, ≥5 circulating tumor cells per 7.5 mL of blood are often associated with poor overall survival and prognosis (23, 29, 30).

Prostate cancer is the most commonly occurring cancer, besides breast cancer. Several large phase II and III trials have established the prognostic value of CTCs in advanced prostate cancer, especially metastatic castrated prostate cancer. The test of CTC has gone beyond traditional PSA measurements to prove to be the strongest independent predictor of survival and has been approved by the FDA for monitoring prostate cancer treatment (30, 31). However, in the hormone-sensitive stage and early stage of prostate cancer, the clinical application of CTC is still a huge challenge due to the very low level of CTCs. In other words, the clinical application of CTC in prostate cancer largely depends on the progression stage of the prostate cancer itself.

Although the CellSearch® system has not been approved for CTCs detection for lung cancer, a large number of clinical trials have proved that CTCs detection has high clinical value in lung cancer, and CTCs technology has been proven to be a predictor of lung cancer prognosis. The number of CTCs in small cell lung cancer is ten times that in non-small cell lung cancer, so circulating tumor cells detection methods are mainly used in small cell lung cancer (32–34). Real-time monitoring of CTCs in the treatment of lung cancer enables prediction of disease progression before clinical deterioration occurs. Similar to breast cancer, a decrease in the number of CTCs in the blood after surgery or chemoradiotherapy often indicates remission of the disease. On the contrary, an increase in the number of CTCs is often indicative of tumor metastasis and recurrence. Interestingly, when He's team detected CTCs in 165 patients with benign pulmonary nodules, they found 5 CTC-positive patients, and all of these patients developed lung cancer in the next four years, suggesting that CTCs may have a unique role in predicting the occurrence of lung cancer. T J N Hiltermann (35) pointed out that the number of CTCs at baseline and the dynamic change of CTCs after one month chemotherapy is an independent predictor of small cell lung cancer. The number of CTCs has no correlation with tumor response in small cell lung cancer, so when forecasting the survival rate of the patients, compared to the size and volume of tumor, spread of CTCs in blood is more important. In addition, the role of CTCs in the clinical prognosis of cancer has been widely recognized, and it is used as an influencing factor to complement the traditional TNM staging system, and is widely used in the diagnosis, screening, long-term monitoring of lung cancer, as well as to guide the treatment of lung cancer patients.

In non-metastatic urinary carcinoma of the bladder, the detection of CTCs was positively correlated with worse progression-free survival, overall survival, tumor-specific survival and relapse-free survival. In addition, in pure and variant urinary carcinomas of the bladder, CTCs are an independent prognostic factor (36). However, the presence of CTCs in patients with seminogenic and non-seminogenic testicular germ cell tumors is currently unknown (37). Although EpCAM is often negative or very low in renal cell carcinoma, one study claimed that it can detect CTC in 16% of patients with metastatic renal cell carcinoma, and although the detection level is low, it offers a glimmer of hope for the application of CTCs in kidney cancer.

CTC detection technology is also widely used in digestive tract tumors, and CTC count is significantly correlated with the metastasis and recurrence of digestive tract tumors, especially colorectal cancer (36). Guus van Dalum et al. (38) conducted a 5-year follow-up of 183 colorectal cancer patients from Mayo Hospital in the United States, and found that tumor patients with a higher level of CTCs before surgery, had a shorter disease-free survival and poorer prognosis after surgery. Surprisingly, the appearance of CTCS a few weeks after surgery was not significantly correlated with RFS (recurrence-free survival) and CCRD, while the appearance of CTCS two or three years after surgery was significantly correlated with RFS and CCRD. Preoperative CTCs in stage I-III CRC patients were associated with significantly reduced RFS and CCRS. This suggests that the preoperative level of CTCs can guide the chemotherapy of cancer patients. Similarly, in esophageal and gastric cancers, higher preoperative CTCs were associated with poorer postoperative outcomes (39). In pancreatic cancer, the detection rate of CTCs in metastatic pancreatic cancer is significantly higher than that in non-metastatic pancreatic cancer, and the level of CTCs has been shown to be one of the independent influencing factors for overall survival after surgery. However, it is difficult to detect circulating tumor cells from pancreatic cancer in peripheral blood, because CTCs are mostly blocked by the liver in the portal vein. The presence of a large number of CTCs in the portal vein is often indicative of liver metastasis. Therefore, a low level of CTC in peripheral blood and a high level in the portal vein is an important feature of the blood distribution in CTC analysis of pancreatic cancer. A study of 88 patients with cholangiocarcinoma (CCA) by Ju Dong Yang et al. (40) showed that CTCs were detectable in patients with CCA and were an independent predictor of survival in patients with CCA.However, given the small sample size of the study and the absence of continuous blood tests, it is not possible to determine whether CTCs predict overall survival in patients with CCA.

Although CTC applications can be used in a wide range of carcinoma, such as breast, prostate, rectal, small cell lung cancer and pancreatic cancer, CTC detection is not suitable for all tumors (41). According to some studies, the detection of CTCs in a small number of gynecological tumors, neuroendocrine tumors, head and neck tumors, and melanoma has not achieved significant results. This may be related to the mode of metastasis of the tumor itself, the affinity of antigens and antibodies on the tumor surface, and the low number of CTCs in the blood. For example, in recent years, although trace amounts of CTCs have been detected in squamous cell carcinoma of the head and neck, this largely depends on the test method, the timing of blood collection, and the patient's clinical stage. Therefore, it is difficult to apply CTC detection techniques in the clinical treatment of head and neck tumors. However, if CTCs could be captured under EMT, it would greatly improve the detection of CTCs in head and neck tumors. Therefore, large-scale clinical trials are necessary for head and neck tumors, melanoma and other tumors with very low numbers of CTCs.

CONCLUSION AND DISCUSSION

Breast cancer is a malignant tumor usually known for its early metastasis and high heterogeneity and cure rates. Early detection and treatment can significantly elevate survival rates in breast cancer patients. CTCs have been proven to play a critically important part in the diagnosis and therapy of breast cancer. There are numerous CTC detection methods, which can be generally divided into *in vivo* and *in vitro* methods, and can be chosen on the basis of the requirements of the specific disease. At present, in order to isolate CTCs with integrity, high vitality and high purity, *in vitro* detection technology is able to capture and release CTCs mildly, construct the negative selection method of specific enrichment and remove normal blood cells to obtain CTCs, and integrate the modules of *in situ* culture and analyze the enriched CTCs immediately. There are two main methods for quantitative analysis of CTCs *in vivo*. One is optic-based IVFCs, which counts CTCs by optical signals. The other is to capture CTCs, then stain tumor cells, and count the number of cells under a microscope. Among them, the commercial CellCollector is the most representative. The currently developed *in vivo* capture technology of CTCs effectively ensures the quality of CTCs before and during capture, but downstream analysis of CTCs after *in vivo* capture is faced with such problems as cell inactivation; new techniques need to be developed to meet standards of CTC culture and molecular analyses. In any case, the detection and molecular characterization of CTCs remains challenging in that they are exceedingly rare and the number of samples available is extremely limited. Therefore, there is an urgent demand to develop a novel system with higher sensitivity, convenience, and efficiency. Clinically, compared with the conventional "gold standard" of tissue biopsy, CTC detection and monitoring can be acquired by routine blood sampling and is an innovative technique using less invasive methods that can sample consistently and repeatedly, so it is safer and timelier.

However, CTCs face many problems in terms of detection technology, clinical application and biological challenges. At present, there are many techniques and methods to detect CTCs in blood, but all of them are faced with the issue of poor sensitivity, which may lead to the delay of detection of tumor cell metastasis in patients, thus delaying treatment. Compared with traditional two-dimensional scaffolds, the implantation of three-dimensional scaffolds and the increase of antibody loading can greatly improve the sensitivity of CTC capture. In addition, although there are

many different detection techniques, not one single technique can detect all different types of circulating tumor cells.

Through the detection of CTCs, we not only expect to obtain the dynamic change in the number of CTCs with the development of the tumor, but also hope to obtain biological information related to the phenotype, genome, transcriptome, proteome and metabolome of the primary tumor from CTCs, which are of vital importance in the field of clinical treatment and biological research. Current biological techniques only guarantee the activity of CTCs before and during capture, but *in vitro* downstream analysis of CTCs is faced with problems such as cell inactivation and distortion, which greatly affects the application of CTCs in clinical and biological engineering. Therefore, there is an urgent need to develop a method to isolate CTCs *in vitro* with a mild and specific technique for releasing captured CTCs, so that CTCs can be completely released from the surface of detection system. There is currently a lack of broad consensus on CDC isolation, extraction, collection and preservation of samples, and selection of biomarkers. In order to improve the accuracy of CTCs tests, a standard set of performance assessment criteria should be developed, including enrichment, cell viability and release efficiency, capture efficiency, and purity. This will improve the sensitivity and specificity of CTC detection and maximize the use of CTCs in the blood (which are already scarce).

Although CTCs have great potential in real-time monitoring, prognosis and diagnosis of tumors, CTCs alone cannot be used as an effective indicator to guide the formulation of clinical treatment plans for tumors. Large-scale clinical studies can be carried out in combination with CTCs and other tumor markers, so as to develop the index of circulating tumor cells combined with tumor markers to guide the formulation of clinical tumor programs, which will bring more far-reaching significance and improvements to the applications of circulating tumor cells in clinical and bioengineering. For example, CTC testing in combination with LDH measurements has been shown to be superior to baseline serum LDH measurements alone, in the evaluation of therapeutic efficacy (31). In addition, the biomolecular properties of CTCs have extremely important properties, which can be used to evaluate tumor consistency, prediction of site, specific metastasis, drug resistance map and identification of new drug targets, etc. Therefore, different subsets of CTCs may lead to different clinical outcomes. This gives us an important clue that the analysis of biomolecular properties of individual circulating tumor cells can be used as a novel prognostic or predictive marker to improve patient clinical outcomes. In recent years, CTC research on single biological molecular characteristics has made great progress, but due to the complex detection technology of CTCs, there is still no single enrichment method that can collect each and every CTC in blood, and separate the target cells and unspecific cells completely.

In general, the detection technology of CTCs is improving with each passing day. It is hoped that the current difficulties will be overcome in the near future, and CTC technology will be more widely applied in clinical practice. As an emerging diagnosis and treatment method, CTCs provides the possibility to find and treat breast cancer even at a stage before imaging methods can be used, guide treatment in conjunction with other tumor markers, monitor the treatment of patients after surgery, and predict the prognosis of patients. In addition, there is growing evidence that the current technology can be partially personalized for tumor types, and CTCs can also be applied to other cancers, such as prostate cancer, small cell lung cancer, straight colon cancer, etc., indicating that CTCs will significantly advance the development of precision oncology in the coming decades. However, CTCs still face great clinical and biological challenges, such as low sensitivity, small numbers, loss of cell activity and so on. Although it will be challenging to improve the detection rate of CTCs, make full use of CTCs for gene analysis of the primary tumor, and guide new treatments according to the molecular targets on the surface of CTCs, this also brings great hope for the further development of biology and emerging immunotherapy techniques.

AUTHOR CONTRIBUTIONS

HZ, XL, YH, MW, CC, ST, MD, LC, ML, JS, YW, and FC contributed to the writing and editing of the manuscript. All authors contributed to the article and approved the submitted version.

FUNDING

The present study was supported by the Shanghai Yangpu District Health and Family Planning Commission Fund for Hao Yi Shi Training Project (Grant nos. 201742, 2020-2023) and the Natural Science Foundation of Shanghai (Grant no. 18ZR1436000).

ACKNOWLEDGMENTS

The authors would like to thank Tongji university and Yangpu Centre Hospital for providing equipment and excellent technical support for our CTCs study.

REFERENCES

1. Lambert AW, Pattabiraman DR, Weinberg RA. Emerging Biological Principles of Metastasis. *Cell* (2017) 168(4):670–91. doi: 10.1016/j.cell.2016.11.037
2. Baccelli I, Schneeweiss A, Riethdorf S, Stenzinger A, Schillert A, Vogel V, et al. Identification of a Population of Blood Circulating Tumor Cells From Breast Cancer Patients That Initiates Metastasis in a Xenograft Assay. *Nat Biotechnol* (2013) 31(6):539–44. doi: 10.1038/nbt.2576
3. Perumal V, Corica T, Dharmarajan AM, Sun Z, Dhaliwal SS, Dass CR, et al. Circulating Tumour Cells (Ctc), Head and Neck Cancer and Radiotherapy; Future Perspectives. *Cancers* (2019) 11(3):367. doi: 10.3390/cancers11030367
4. Plaks V, Koopman CD, Werb Z. Cancer. Circulating Tumor Cells. *Science* (2013) 341(6151):1186–8. doi: 10.1126/science.1235226
5. Yu M, Bardia A, Wittner BS, Stott SL, Smas ME, Ting DT, et al. Circulating Breast Tumor Cells Exhibit Dynamic Changes in Epithelial and Mesenchymal Composition. *Science* (2013) 339(6119):580–4. doi: 10.1126/science.1228522

6. De Toro J, Herschlik L, Waldner C, Mongini C. Emerging Roles of Exosomes in Normal and Pathological Conditions: New Insights for Diagnosis and Therapeutic Applications. *Front Immunol* (2015) 6:203. doi: 10.3389/fimmu.2015.00203
7. Pereira B, Chin SF, Rueda OM, Vollan HK, Provenzano E, Bardwell HA, et al. The Somatic Mutation Profiles of 2,433 Breast Cancers Refines Their Genomic and Transcriptomic Landscapes. *Nat Commun* (2016) 7:11479. doi: 10.1038/ncomms11479
8. Ferreira MM, Ramani VC, Jeffrey SS. Circulating Tumor Cell Technologies. *Mol Oncol* (2016) 10(3):374–94. doi: 10.1016/j.molonc.2016.01.007
9. Kanwar N, Hu P, Bedard P, Clemons M, McCready D, Done SJ. Identification of Genomic Signatures in Circulating Tumor Cells From Breast Cancer. *Int J Cancer* (2015) 137(2):332–44. doi: 10.1002/ijc.29399
10. Gasch C, Oldopp T, Mauermann O, Gorges TM, Andreas A, Coith C, et al. Frequent Detection of PIK3CA Mutations in Single Circulating Tumor Cells of Patients Suffering From HER2-Negative Metastatic Breast Cancer. *Mol Oncol* (2016) 10(8):1330–43. doi: 10.1016/j.molonc.2016.07.005
11. Alix-Panabières C, Pantel K. Challenges in Circulating Tumour Cell Research. *Nat Rev Cancer* (2014) 14(9):623–31. doi: 10.1038/nrc3820
12. Massoner P, Thomm T, Mack B, Untergasser G, Martowicz A, Bobowski K, et al. EpCAM is Overexpressed in Local and Metastatic Prostate Cancer, Suppressed by Chemotherapy and Modulated by MET-Associated miRNA-200c/205. *Br J Cancer* (2014) 111(5):955–64. doi: 10.1038/bjc.2014.366
13. Dutta R, Liba O, SoRelle ED, Winetraub Y, Ramani VC, Jeffrey SS, et al. Real-Time Detection of Circulating Tumor Cells in Living Animals Using Functionalized Large Gold Nanorods. *Nano Lett* (2019) 19(4):2334–42. doi: 10.1021/acs.nanolett.8b05005
14. Cai F, Cai L, Zhou Z, Pan X, Wang M, Chen S, et al. Prognostic Role of Tif1γ Expression and Circulating Tumor Cells in Patients With Breast Cancer. *Mol Med Rep* (2019) 19(5):3685–95. doi: 10.3892/mmr.2019.10033
15. Azarin SM, Yi J, Gower RM, Aguado BA, Sullivan ME, Goodman AG, et al. In Vivo Capture and Label-Free Detection of Early Metastatic Cells. *Nat Commun* (2015) 6:8094. doi: 10.1038/ncomms9094
16. Hamza B, Ng SR, Prakadan SM, Delgado FF, Chin CR, King EM, et al. Optofluidic Real-Time Cell Sorter for Longitudinal CTC Studies in Mouse Models of Cancer. *Proc Natl Acad Sci USA* (2019) 116(6):2232–6. doi: 10.1073/pnas.1814102116
17. Hyun KA, Lee TY, Lee SH, Jung HI. Two-Stage Microfluidic Chip for Selective Isolation of Circulating Tumor Cells (CTCS). *Biosens Bioelectron* (2015) 67:86–92. doi: 10.1016/j.bios.2014.07.019
18. Nolan J, Nedosekin DA, Galanzha EI, Zharov VP. Detection of Apoptotic Circulating Tumor Cells Using In Vivo Fluorescence Flow Cytometry. *Cytom A* (2019) 95(6):664–71. doi: 10.1002/cyto.a.23642
19. Wan L, Pantel K, Kang Y. Tumor Metastasis: Moving New Biological Insights Into the Clinic. *Nat Med* (2013) 19(11):1450–64. doi: 10.1038/nm.3391
20. Krebs MG, Metcalf RL, Carter L, Brady G, Blackhall FH, Dive C. Molecular Analysis of Circulating Tumour Cells-Biology and Biomarkers. *Nat Rev Clin Oncol* (2014) 11(3):129–44. doi: 10.1038/nrclinonc.2013.253
21. Lannin DR, Wang S. Are Small Breast Cancers Good Because They Are Small or Small Because They are Good? *N Engl J Med* (2017) 376(23):2286–91. doi: 10.1056/NEJMsr1613680
22. Kruspe S, Dickey DD, Urak KT, Blanco GN, Miller MJ, Clark KC, et al. Rapid and Sensitive Detection of Breast Cancer Cells in Patient Blood With Nuclease-Activated Probe Technology. *Mol Ther Nucleic Acids* (2017) 8:542–57. doi: 10.1016/j.omtn.2017.08.004
23. Cristofanilli M, Budd GT, Ellis MJ, Stopeck A, Matera J, Miller MC, et al. Circulating Tumor Cells, Disease Progression, and Survival in Metastatic Breast Cancer. *N Engl J Med* (2004) 351(8):781–91. doi: 10.1056/NEJMoa040766
24. Rack B, Schindlbeck C, Jückstock J, Andergassen U, Hepp P, Zwingers T, et al. Circulating Tumor Cells Predict Survival in Early Average-to-High Risk Breast Cancer Patients. *J Natl Cancer Inst* (2014) 106(5). doi: 10.1093/jnci/dju066
25. Madic J, Kiialainen A, Bidard FC, Birzele F, Ramey G, Leroy Q, et al. Circulating Tumor DNA and Circulating Tumor Cells in Metastatic Triple Negative Breast Cancer Patients. *Int J Cancer* (2015) 136(9):2158–65. doi: 10.1002/ijc.29265
26. David R. Pd-L1 Expression by Circulating Breast Cancer Cells. *Lancet Oncol* (2015) 16(7):e321. doi: 10.1016/S1470-2045(15)00074-1
27. Cai F, Cen C, Cai L, Falar LM, Biskup E. Application of Circulation Tumor Cells Detection in Diagnosis and Treatment of Breast Tumors. *Rejuvenation Res* (2019) 22(6):498–502. doi: 10.1089/rej.2018.2154
28. Bidard FC, Peeters DJ, Fehm T, Nolé F, Gisbert-Criado R, Mavroudis D, et al. Clinical Validity of Circulating Tumour Cells in Patients With Metastatic Breast Cancer: A Pooled Analysis of Individual Patient Data. *Lancet Oncol* (2014) 15(4):406–14. doi: 10.1016/S1470-2045(14)70069-5
29. de Bono JS, Scher HI, Montgomery RB, Parker C, Miller MC, Tissing H, et al. Circulating Tumor Cells Predict Survival Benefit From Treatment in Metastatic Castration-Resistant Prostate Cancer. *Clin Cancer Res* (2008) 14(19):6302–9. doi: 10.1158/1078-0432.CCR-08-0872
30. Cohen SJ, Punt CJ, Iannotti N, Saidman BH, Sabbath KD, Gabrail NY, et al. Prognostic Significance of Circulating Tumor Cells in Patients With Metastatic Colorectal Cancer. *Ann Oncol* (2009) 20(7):1223–9. doi: 10.1093/annonc/mdn786
31. Scher HI, Jia X, de Bono JS, Fleisher M, Pienta KJ, Raghavan D, et al. Circulating Tumour Cells as Prognostic Markers in Progressive, Castration-Resistant Prostate Cancer: A Reanalysis of IMMC38 Trial Data. *Lancet Oncol* (2009) 10(3):233–9. doi: 10.1016/S1470-2045(08)70340-1
32. Krebs MG, Sloane R, Priest L, Lancashire L, Hou JM, Greystoke A, et al. Evaluation and Prognostic Significance of Circulating Tumor Cells in Patients With non-Small-Cell Lung Cancer. *J Clin Oncol* (2011) 29(12):1556–63. doi: 10.1200/JCO.2010.28.7045
33. Kapeleris J, Kulasinghe A, Warkiani ME, Vela I, Kenny L, O'Byrne K, et al. The Prognostic Role of Circulating Tumor Cells (CTCS) in Lung Cancer. *Front Oncol* (2018) 8:311. doi: 10.3389/fonc.2018.00311
34. Crosbie PA, Shah R, Krysiak P, Zhou C, Morris K, Tugwood J, et al. Circulating Tumor Cells Detected in the Tumor-Draining Pulmonary Vein Are Associated With Disease Recurrence After Surgical Resection of NSCLC. *J Thorac Oncol* (2016) 11(10):1793–7. doi: 10.1016/j.jtho.2016.06.017
35. Hou JM, Krebs MG, Lancashire L, Sloane R, Backen A, Swain RK, et al. Clinical Significance and Molecular Characteristics of Circulating Tumor Cells and Circulating Tumor Microemboli in Patients With Small-Cell Lung Cancer. *J Clin Oncol* (2012) 30(5):525–32. doi: 10.1200/JCO.2010.33.3716
36. Rink M, Chun FK, Dahlem R, Soave A, Minner S, Hansen J, et al. Prognostic Role and HER2 Expression of Circulating Tumor Cells in Peripheral Blood of Patients Prior to Radical Cystectomy: A Prospective Study. *Eur Urol* (2012) 61(4):810–7. doi: 10.1016/j.eururo.2012.01.017
37. Riethdorf S, O'Flaherty L, Hille C, Pantel K. Clinical Applications of the CellSearch Platform in Cancer Patients. *Adv Drug Delivery Rev* (2018) 125:102–21. doi: 10.1016/j.addr.2018.01.011
38. van Dalum G, Stam GJ, Scholten LF, Mastboom WJ, Vermes I, Tibbe AG, et al. Importance of Circulating Tumor Cells in Newly Diagnosed Colorectal Cancer. *Int J Oncol* (2015) 46(3):1361–8. doi: 10.3892/ijo.2015.2824
39. Khoja L, Backen A, Sloane R, Menasce L, Ryder D, Krebs M, et al. A Pilot Study to Explore Circulating Tumour Cells in Pancreatic Cancer as a Novel Biomarker. *Br J Cancer* (2012) 106(3):508–16. doi: 10.1038/bjc.2011.545
40. Yang JD, Campion MB, Liu MC, Chaiteerakij R, Giama NH, Ahmed MH, et al. Circulating Tumor Cells Are Associated With Poor Overall Survival in Patients With Cholangiocarcinoma. *Hepatology* (2016) 63(1):148–58. doi: 10.1002/hep.27944
41. Kulasinghe A, Perry C, Jovanovic L, Nelson C, Punyadeera C. Circulating Tumour Cells in Metastatic Head and Neck Cancers. *Int J Cancer* (2015) 136(11):2515–23. doi: 10.1002/ijc.29108

Conflict of Interest: Author YH was employed by company Cellomics International Limited.

The remaining authors declare that the research was conducted in the absence of any commercial or financial relationships that could be construed as a potential conflict of interest.

Copyright © 2021 Zhang, Lin, Huang, Wang, Cen, Tang, Dique, Cai, Luis, Smollar, Wan and Cai. This is an open-access article distributed under the terms of the Creative Commons Attribution License (CC BY). The use, distribution or reproduction in other forums is permitted, provided the original author(s) and the copyright owner(s) are credited and that the original publication in this journal is cited, in accordance with accepted academic practice. No use, distribution or reproduction is permitted which does not comply with these terms.

frontiers in Cell and Developmental Biology

ORIGINAL RESEARCH
published: 10 June 2021
doi: 10.3389/fcell.2021.666156

Genetic Characterization of Cancer of Unknown Primary Using Liquid Biopsy Approaches

*Noemi Laprovitera[1,2†], Irene Salamon[1,3†], Francesco Gelsomino[1,4], Elisa Porcellini[1], Mattia Riefolo[1,5], Marianna Garonzi[6], Paola Tononi[6], Sabrina Valente[1], Silvia Sabbioni[3], Francesca Fontana[6], Nicolò Manaresi[6], Antonia D'Errico[1,5], Maria A. Pantaleo[1,4], Andrea Ardizzoni[1,4] and Manuela Ferracin[1]**

[1] Department of Experimental, Diagnostic and Specialty Medicine (DIMES), University of Bologna, Bologna, Italy, [2] Department of Life Sciences and Biotechnologies, University of Ferrara, Ferrara, Italy, [3] Center for Applied Biomedical Research (CRBA), University of Bologna, Italy, [4] Divisione di Oncologia Medica, IRCCS Azienda Ospedaliero-Universitaria di Bologna, Bologna, Italy, [5] Pathology Unit, Sant'Orsola Hospital, IRCCS Azienda Ospedaliero-Universitaria di Bologna, Bologna, Italy, [6] Menarini Silicon Biosystems S.p.A, Bologna, Italy

OPEN ACCESS

Edited by:
Catherine Alix-Panabieres, Centre Hospitalier Universitaire de Montpellier, France

Reviewed by:
Ignacio Matos, University College London, United Kingdom
Emanuela Grassilli, University of Milano Bicocca, Italy

***Correspondence:**
Manuela Ferracin
manuela.ferracin@unibo.it

† These authors have contributed equally to this work

Specialty section:
This article was submitted to Molecular and Cellular Oncology, a section of the journal Frontiers in Cell and Developmental Biology

Received: 09 February 2021
Accepted: 03 May 2021
Published: 10 June 2021

Citation:
Laprovitera N, Salamon I, Gelsomino F, Porcellini E, Riefolo M, Garonzi M, Tononi P, Valente S, Sabbioni S, Fontana F, Manaresi N, D'Errico A, Pantaleo MA, Ardizzoni A and Ferracin M (2021) Genetic Characterization of Cancer of Unknown Primary Using Liquid Biopsy Approaches. Front. Cell Dev. Biol. 9:666156. doi: 10.3389/fcell.2021.666156

Cancers of unknown primary (CUPs) comprise a heterogeneous group of rare metastatic tumors whose primary site cannot be identified after extensive clinical–pathological investigations. CUP patients are generally treated with empirical chemotherapy and have dismal prognosis. As recently reported, CUP genome presents potentially druggable alterations for which targeted therapies could be proposed. The paucity of tumor tissue, as well as the difficult DNA testing and the lack of dedicated panels for target gene sequencing are further relevant limitations. Here, we propose that circulating tumor cells (CTCs) and circulating tumor DNA (ctDNA) could be used to identify actionable mutations in CUP patients. Blood was longitudinally collected from two CUP patients. CTCs were isolated with CELLSEARCH® and DEPArray™ NxT and Parsortix systems, immunophenotypically characterized and used for single-cell genomic characterization with *Ampli*1™ kits. Circulating cell-free DNA (ccfDNA), purified from plasma at different time points, was tested for tumor mutations with a CUP-dedicated, 92-gene custom panel using SureSelect Target Enrichment technology. In parallel, FFPE tumor tissue was analyzed with three different assays: FoundationOne CDx assay, DEPArray LibPrep and OncoSeek Panel, and the SureSelect custom panel. These approaches identified the same mutations, when the gene was covered by the panel, with the exception of an insertion in *APC* gene. which was detected by OncoSeek and SureSelect panels but not FoundationOne. *FGFR2* and *CCNE1* gene amplifications were detected in single CTCs, tumor tissue, and ccfDNAs in one patient. A somatic variant in *ARID1A* gene (p.R1276*) was detected in the tumor tissue and ccfDNAs. The alterations were validated by Droplet Digital PCR in all ccfDNA samples collected during tumor evolution. CTCs from a second patient presented a pattern of recurrent amplifications in *ASPM* and *SEPT9* genes and loss of *FANCC*. The 92-gene custom panel identified 16 non-synonymous somatic alterations in ccfDNA, including a deletion (I1485Rfs*19) and a somatic mutation (p.

A1487V) in *ARID1A* gene and a point mutation in *FGFR2* gene (p.G384R). Our results support the feasibility of non-invasive liquid biopsy testing in CUP cases, either using ctDNA or CTCs, to identify CUP genetic alterations with broad NGS panels covering the most frequently mutated genes.

Keywords: CTC, cell-free tumor DNA, cancer of unknown primary, liquid biopsy, precision oncology

INTRODUCTION

Malignant solid tumors that are not fully eradicated at an early stage are doomed to spread to nearby lymph nodes and organs and eventually give origin to distant metastases. A diagnosis of metastatic cancer considerably reduces the chances to eliminate the tumor and cure the patient. The metastatic process is made possible by the progressive acquirement of genetic alterations in tumor cells, which eventually become anchorage independent and self-sufficient for cell growth. Disseminated tumor cells, including circulating tumor cells (CTCs) and CTC clusters, are highly metastatic (Aceto et al., 2014), and their number in the blood correlates with patient prognosis in several cancer types (Riethdorf et al., 2007; Joosse et al., 2015; Sparano et al., 2018).

The epitome of advanced cancers could be considered a particularly aggressive metastatic disease known as cancer of unknown primary (CUP, also occult primary cancer). CUP is a rare syndrome of metastatic cancers whose primary site cannot be identified after detailed physical examinations, blood analyses, imaging, and immunohistochemical (IHC) testing (Fizazi et al., 2015). CUPs make up 3–5% of newly diagnosed cancers worldwide and represent an important clinical problem (Varadhachary and Raber, 2014; Laprovitera et al., 2021), specifically when considering that current therapeutic protocols are primary site oriented. As a final result, CUP patients receive empirical cytotoxic chemotherapy regimens and have poor prognosis [average overall survival (OS) 4–9 months, about 20% survive more than 1 year]. It has been reported that CUPs present actionable genetic alterations (Ross et al., 2015; Varghese et al., 2017), and these alterations can be identified in circulating tumor DNA (ctDNA) (Kato et al., 2017). Therefore, an improvement in CUP treatment and outcome could derive from clinical trials where patients are treated in accordance to their specific actionable mutations (Conway et al., 2019), as in NCT02628379 based on FoundationOne CDx target sequencing (Roche Foundation Medicine), or basket trials extended to CUP patients. Moreover, recent studies evidenced how CUP patients could benefit from treatment with immune checkpoint inhibitors (Haratani et al., 2019), and clinical trials have been opened and are currently recruiting (NCT04131621) or positively concluded (UMIN000030649). In this clinical trial, 56 CUP patients, of whom 45 previously treated, were treated with anti PD-1 nivolumab; the objective response rate (ORR) in the overall population was 21.4%, with a median progression-free survival (PFS) and OS of 5.1 (95% CI, 2.7–5.6) and 15.9 months (95% CI, 8.4–not reached), respectively (Tanizaki et al., 2020).

CUP genetic testing is currently limited by the scarcity of tumor biopsy material and reduced biopsy DNA quality; therefore, a liquid biopsy approach could be of the outmost interest. Several works demonstrated the utility of ctDNA and CTC testing to monitor cancer patient prognosis and guide treatment decisions (Ignatiadis and Dawson, 2014). In addition, ctDNA variant allele frequency was found to be associated with a worse prognosis in patients with metastatic disease (Pairawan et al., 2020); moreover, CTCs became an important clinical prognostic biomarker (Amintas et al., 2020) with potential application in *in vitro* (Zhao et al., 2019) and *in vivo* disease modeling (Drapkin et al., 2018) and drug testing (Yu et al., 2014). Size-based or antigen-based technologies for CTC isolation and/or enumeration have been developed in the past 10 years, each one presenting advantages and limitations (Yu et al., 2011).

CUP patients are usually diagnosed with an advanced metastatic disease; therefore, they are likely to have a high number of CTCs and CTC clusters in the circulation. Given the CUP undifferentiated status and variable presentation, it is yet to demonstrate whether CUP CTCs could be isolated using tumor antigen selection (Komine et al., 2014). In this study, we explored liquid biopsy, specifically ctDNA- and CTC-based applications, as approaches to detect CUP druggable mutations. We compared two methods to isolate CTCs, one antigen-based, size-agnostic (CELLSEARCH, Menarini Silicon Biosystems) and another antigen-agnostic, size-based (Parsortix, ANGLE plc). CTCs and ctDNA were detectable in the blood of CUP patients and analyzed for genomic alterations, which were further compared with genomic alterations identified in tumor biopsy.

MATERIALS AND METHODS

Sample Collection

Two patients (Pt#71 and Pt#95) with a diagnosis of cancer of unknown origin (CUP) were recruited at Bologna University Hospital, Italy. The study was conducted in accordance with the Declaration of Helsinki, and the protocol was approved by the Ethics Committee Center Emilia-Romagna Region—Italy (protocol 130/2016/U/Tess). Patients provided written informed consent.

Metastatic tissue from lymph node (Pt#71) and ampulla of Vater (Pt#95) was formalin-fixed and paraffin-embedded (FFPE) and used for tumor DNA collection. For Pt#71, blood sampling was performed at three different time points: (A) at diagnosis (August 2018), (B) during FOLFOX-4 treatment (stable disease, November 2018), and (C) at disease progression (May 2019). For Pt#95, blood sampling was performed at diagnosis.

Plasma separation was performed *via* centrifugation at 1,900 × *g* for 10 min at 4°C. A variable number (N = 2–5) of plasma aliquots (1 ml) for each patient was collected and stored at –80°C prior to isolation of circulating cell-free DNA (ccfDNA). PBMCs were isolated from peripheral blood of Pt#95 using Ficoll-Paque Plus (17-1440-02, GE Healthcare, Chicago, IL,

United States). Briefly, after plasma depletion, an equal volume of PBS was added to the remaining blood in EDTA tubes. Following, 4 ml of diluted blood was stratified on 3 ml of Ficoll-Paque Plus and centrifuged at 400 × *g* for 30 min at room temperature in a swinging-bucket rotor. The PBMC ring was carefully removed by pipetting and the pellet was washed with PBS and centrifuged at 100 × *g* for 5 min. Finally, the pellet was stored at −80°C prior to proceeding with DNA extraction.

CTC Isolation With CELLSEARCH and DEPArray NxT

Pt#71 and Pt#95 blood samples were collected at diagnosis. CELLSEARCH® system (Menarini Silicon Biosystems, Castel Maggiore, Italy) was used to enrich and enumerate CTCs, followed by single-cell isolation with the DEPArray® NxT system (Menarini Silicon Biosystems). Briefly, 7.5 ml of blood was loaded in CELLSEARCH Autoprep® for EpCAM-based immunomagnetic capture of CTCs, followed by immunofluorescent staining (CK-FITC, PD-L1-PE, CD45-APC, and DAPI using the CELLSEARCH CXC kit in one patient, and CK-PE, CD45-APC, and DAPI with the CELLSEARCH CTC kit in the other patient). After CTC enumeration with the CellTrack Analyzer II, the sample was loaded into a DEPArray Cartridge and single CTCs and leukocytes were isolated with the DEPArray NxT system (Menarini Silicon Biosystems) from each sample. A variable number of CTCs and leukocytes, used as control, were isolated as single cells and then subjected to whole-genome amplification employing the *Ampli*1 WGA Kit (Menarini Silicon Biosystems).

CTC Isolation With the Parsortix System

For Pt#95, tumor cells were enriched from peripheral blood also using the Parsortix system (ANGLE plc, Guildford, United Kingdom). Blood cells were forced to pass through a 6.5-μm separator cassette that can capture CTCs based on their size and deformability properties. Then, to confirm the CTC nature of retained cells, we stained CTCs using a combination of anti-human EpCAM-FITC, anti-human CD45-APC (BD 561864/555485), and DAPI for cell nuclei staining. Images were acquired using a Leica DMI6000 B inverted fluorescence microscope (Leica Microsystems, Wetzlar, Germany).

DNA Extraction

DNA was extracted from the tumor area after selection by an expert pathologist, with the guidance of the hematoxylin–eosin-stained section. The DNA from different areas of FFPE unstained slides was extracted using the QIAamp DNA FFPE Tissue Kit (Cat No: 56404, Qiagen, Hilden, Germany) following the manufacturer's guidelines (as described in Cinausero et al., 2019). Normal DNA was extracted from a non-tumor area in formalin-fixed paraffin-embedded (FFPE) tissue for Pt#71 and from PBMC for Pt#95. DNA from PBMCs was extracted using the QIAamp DNA Micro kit (Cat No: 56304, Qiagen, Hilden, Germany). Ten slices of Pt#71 FFPE tumor tissue were sent to Roche Foundation Medicine (Cambridge, MA, United States) for comprehensive genomic profile analysis with FoundationOne CDx (F1CDx) assay.

ccfDNA was purified from 1 ml of plasma by Maxwell RSC instrument (Cat No: AS4500, Promega, Madison, WI, United States) using the Maxwell RSC ccfDNA Plasma Kit (Cat No: AS1480, Promega). Genomic and ccfDNA were quantified using the Qubit 4.0 Fluorometer (Cat No: Q33238, Thermo Fisher Scientific, Waltham, MA, United States) and the Qubit dsDNA High Sensitivity Assay Kit (Cat No: Q32854, Thermo Fisher Scientific).

We assessed yields and quality of FFPE-derived gDNAs using the NGS FFPE QC Kit (Cat No: G9700B, Agilent Technologies, Santa Clara, CA, United States) according to the producer's protocol (G9700-90000, v. E1, May 2018, Agilent Technologies).

Analysis of Tumor Genetic Alterations

A 1.2-Mb custom SureSelect capture bait library (Agilent Technologies, Santa Clara, CA, United States) was designed to target 92 genes (listed in **Supplementary Table 1**), selected to be the most frequently mutated genes in CUPs, as reported in MSK Impact study CUP cohort (Zehir et al., 2017), including druggable or potentially actionable alterations. The panel was designed using Agilent SureDesign web application (v. 7.0, Agilent Technologies)[1] to cover coding exons and UTRs, with 25 flanking bases from 3′ and 5′ ends. This panel comprehends up to 51,466 probes included in five probe groups, with 2 × tiling density, balanced boosting, and 86% of probes with the most stringent masking. Libraries were prepared using the custom gene panel following *SureSelectXT HS/SureSelectXT Low Input Target Enrichment with Pre-Capture Pooling* protocol (G9702-90005, v. A0, June 2019, Agilent Technologies). An input of 50 ng of gDNA (normal and tumor) underwent enzymatic fragmentation according to *SureSelect Enzymatic Fragmentation* protocol (G9702-90050, Revision B0, January 2020, Agilent Technologies). Libraries from ccfDNAs of Pt #71 (A, C) and Pt#95 were prepared starting from 25 ng of DNA bypassing the fragmentation step, as described in a published application note (Barber et al., 2017). Libraries were sequenced on NextSeq 500 (Illumina) platform using High Output 2 × 75-bp flow cells. Variant calling and paired analyses (tumor vs. normal) were performed using SureCall software (v. 4.2), applying a filter for all samples at 5%, and at 1% for ccfDNAs. Somatic alterations were filtered to only keep exonic non-synonymous single-nucleotide variants (SNVs), insertions, deletions, multiple nucleotide variants, and long deletions not detected in the normal sample.

Alterations with population allele frequency (Genome Aggregation Database, GnomAD; Karczewski et al., 2020) higher than 0.5% in Non-Finnish European (NFE) population were also filtered out. All variants reported had a coverage higher than 100. Target sequencing data (92-gene custom panel) were used to assess copy number variants using panelcn.MOPS pipeline (Povysil et al., 2017). Variants triage and clinical classification was obtained with Alissa Interpret software (Agilent Technologies). Variants were also annotated using ANNOVAR (Wang et al., 2010). Bioinformatic pathogenicity prediction, reported in

[1]https://earray.chem.agilent.com/suredesign/

Tables 1, **2**, of the identified variants was performed consulting the prediction score/outcome of SIFT (Sort Intolerated From Tolerated; Vaser et al., 2016), Polyphen2 HVAR (Polymorphism Phenotyping v2; Adzhubei et al., 2010), LRT (Likelihood Ratio Test; Chun and Fay, 2009), Mutation Taster (Schwarz et al., 2014), Mutation Assessor (Reva et al., 2011), FATHMM (Functional Analysis Through Hidden Markov Model; Shihab et al., 2013), CADD (Combined Annotation Dependent Depletion; Kircher et al., 2014), and VEST (Variant Effect Scoring Tool; Douville et al., 2016). Genes with evidence for actionability and the FDA-approved drugs reported in **Tables 1**, **2** were obtained consulting OncoKB (Chakravarty et al., 2017).

Single-cell genomic DNA from DEPArray NxT sorted cells, amplified using the *Ampli*1™ WGA Kit, was processed to obtain Illumina-compatible libraries using the *Ampli*1™ OncoSeek Panel and the *Ampli*1™ LowPass kits. Conversely, tumor gDNA was directly processed with DEPArray™ LibPrep and DEPArray™ OncoSeek Panel kits. After sequencing on MiSeq platforms, raw data were analyzed using assay-specific applications on the MSBiosuite platform (Menarini Silicon Biosystems).

FFPE tumor tissue of Pt#71 was eligible for genetic testing using FoundationOne CDx (F1CDx) assay. F1CDx is performed exclusively as a laboratory service using DNA extracted from FFPE tumor samples. A library was prepared with a hybrid capture−based target enrichment approach and whole−genome shotgun library construction to detect substitutions, indels, copy number alterations, and selected rearrangements in a total of 324 genes. Sequencing was performed using the Illumina HiSeq 4000 platform, obtaining a >500 × median coverage. F1CDx specimens were also simultaneously profiled for tumor mutation burden (TMB) and microsatellite instability (MSI) status (further technical information is available at https://www.foundationmedicine.com/genomic-testing/foundation-one-cdx).

Droplet Digital PCR Validation

Droplet Digital PCR technology (Bio-Rad, Hercules, CA, United States) along with Mutational and Copy Number Determination assays (Bio-Rad) were used to validate specific alterations in both genomic and ccfDNAs. A Copy Number Variation assay was used to assess the amplification of *FGFR2* gene (dHsaCB2500320, Bio-Rad) using *RPP30* as reference gene (dHsaCP2500350, Bio-Rad). A digestion with *Hae*III restriction enzyme was performed during ddPCR, according to the manufacturer's instruction. Mutational assay for wild-type and mutated *ARID1A* (p.R1276*) was performed with a custom IDT assay (02516372). For this assay, DNA digestion with *Hin*dIII restriction enzyme was performed only for gDNA. Probe-based Droplet Digital PCR experiment was performed according to the manufacturer's instruction and thermal cycling conditions were 95°C for 10 min, 94°C for 30 s and 58°C for 1 min for 40 cycles, 98°C for 10 min, and an infinite hold at 4°C (ramping rate reduced to 2%). Droplet selection was performed individually for each well using QuantaSoft software v 1.7 (Bio-Rad) obtaining the final copy number variation or the wild-type/mutated allele fractions.

RESULTS

Case Presentation

Pt#71

A 49-year-old woman with a history of primary biliary cholangitis (PBC) was admitted at Bologna University Hospital in June 2018 due to enlarged left cervical lymph nodes associated with severe asthenia, pruritus, and fever. A contrast-enhanced computed tomography (CT) scan showed multiple pathologic abdominal (epigastrium, mesogastrium, stomach curvature, hepatic hilum, pancreatic, and retroperitoneal regions) and left supraclavicular lymph nodes, confirmed also by a F-Fluorodeoxyglucose positron emission tomography/computed tomography (18-F-FDG PET/CT) scan. The patient underwent abdominal surgery leading to the excision of two lymph nodes. Pathological examination confirmed the presence of nodal metastasis from adenocarcinoma.

Immunohistochemistry staining reported positivity for keratin 7, keratin 20, and CDX2, and negativity for neuroendocrine markers (chromogranin, synaptophysin, and CD56). Therefore, the conclusive pathological diagnosis was suggestive of lymph node metastasis from adenocarcinoma of the gastrointestinal tract. Esophagogastroduodenoscopy (EGDS) and pancoloscopy (PC) failed to identify any neoplastic lesion. In addition, molecular analyses for the determination of MSI, HER2, ALK, and PD-L1 status (by IHC); *KRAS*, *NRAS*, *BRAF* mutational status and *MGMT* methylation status (by pyrosequencing); and *ROS1* and *MET* (by FISH) were all negative. Among the serum oncomarkers, the positive ones were Ca19.9 (291 U/ml, n.v < 40 U/ml), Ca125 (130.9 U/ml, n.v < 35 U/ml), and NSE (34 μg/L, n.v < 12 μg/L).

Taking into account the history of PBC and its association with a higher risk of cholangiocarcinoma, a magnetic resonance cholangiopancreatography (MRCP) and MRI with contrast was performed and ruled out the presence of any tumor lesion. Then, the patient was treated with FOLFOX-4 as first-line treatment every 2 weeks up to 11 courses, obtaining a partial response. A maintenance treatment based on De Gramont regimen (FULCV) was continued for four courses followed by a worsening of patient's clinical condition and the appearance of pleural and abdominal effusions. Blood was collected for CTC analysis with CELLSEARCH and DEPArray at November 2018. Treatment with Pazopanib, a novel multi-kinase inhibitor (VEGFR1, VEGFR2, VEGFR3, PDGFR, FGFR, c-Kit, and c-Fms/CSF1R), was proposed due to the presence of *FGFR2* amplification (F1CDx testing). However, death occurred in June 2019 due to progressive disease and hepato-renal syndrome.

Pt#95

A 63-year-old woman was admitted at Bologna University Hospital in February 2019 due to an edema of the upper limb. Echo-Doppler scanning revealed thrombosis in basilica, axillary, subclavian, internal jugular, and external jugular veins. The patient experienced weight loss, asthenia, nausea, and cough.

A contrast-enhanced total body CT showed the presence of supra- and infradiaphragmatic enlarged lymph nodes associated

TABLE 1 | Mutation report of tumor, ccfDNA, and CTCs from Pt#71.

				SureSelect 92-gene panel (Agilent Technologies)	SureSelect 92-gene panel (Agilent Technologies)	SureSelect 92-gene panel (Agilent Technologies)	Foundati-One CDx (Roche)	Ampli1(TM OncoSeek and LowPass Kit (Menarini Silicon Biosystem)	DEPArray(TM OncoSeek and LowPass Kit (Menarini Silicon Biosystem)	Pathogenicity Prediction								Actional genes/approved drugs [OncoKB (Chakravarty et al., 2017)]
Gene	**Position**	**Coding change**	**Amino acidic change**	**Tumor FFPE**	**ccfDNA at diagnosis**	**ccfDNA at PD**	**Tumor FFPE**	**CTCs**	**Tumor FFPE**	**SIFT (Vaser et al., 2016)**	**Polyphen2 (Adzhubei et al., 2010)**	**LRT (Chun and Fay, 2009)**	**Mutation Taster (Schwarz et al., 2014)**	**Mutation Assessor (Reva et al., 2011)**	**FATHMM (Shihab et al., 2013)**	**CADD (Kircher et al., 2014)**	**VEST3 (Douville et al., 2016)**	
APC	chr5:112840254	4607insA	p.T1556fs*3	9.8%	22.6%	29.9%	ND	90.2%-99.2%	14.0%	–	–	–	–	–	–	–	–	–
ARID1A	chr1:26773456	c.C3826T	p.R1276X	8.9%	28.5%	22.8%	7.3%	NI	NI	–	–	–	DC	–	–	HF	–	–
ERBB3	chr12:56085144	c.C384A	p.S128R	9.8%	20.7%	20.4%	8.5%	NI	NI	–	PS	DT	DC	NFL	TL	BG	HF	–
NTRK1	chr1:156881475	C2206T	p.Q736X	8.3%	26.0%	22.3%	7.6%	NI	NI	DT	–	DT	DC	–	–	HF	–	–
KEAP1	chr19:10499630	c.G404A	p.R135H	9.0%	22.6%	19.5%	7.0%	NI	NI	TL	PD	DT	DC	NFL	TL	HF	HF	–
PALB2	chr16:23629735	C2419T	p.P807S	9.0%	19.1%	16.6%	6.0%	NI	NI	TL	BG	NL	PM	NFN	TL	BG	BG	Level 1/Olaparib*
KMT2C	chr7:152265209	c.C1013T	p.S338L	ND	5.5%	4.3%	NI	NI	NI	TL	PD	U	DC	NFL	DG	BG	BG	–
KMT2C	chr7:152247975	c.C2459T	p.T820I	ND	1.1%	1.1%	NI	NI	NI	DT	PS	DT	DC	NFL	DG	HF	HF	–
PTPRD	chr9:8404618	c.T2908G	p.L970V	ND	5.1%	3.5%	NI	NI	NI	–	PD	DT	DC	FCM	TL	BG	HF	–
TP53	chr9:8404618	c.T316C	p.C106R	ND	2.1%	ND	ND	ND	ND	DT	PD	DT	DC	FCM	DG	HF	HF	Levels 1–3/no drug
TP53	chr17:7674251	c.G315C	p.M105I	ND	1.8%	ND	ND	ND	ND	DT	PD	DT	DC	FCM	DG	HF	HF	Levels 1–3/no drug
TP53	chr17:7674252	c.A355G	p.I119V	ND	1.7%	ND	ND	ND	ND	DT	PD	DT	DC	FCM	DG	HF	HF	Levels 1–3/no drug
TP53	chr17:7674212	c.C9G	p.C3W	ND	1.2%	ND	ND	ND	ND	DT	PD	DT	DC	FCM	DG	BG	HF	Levels 1–3/no drug
ALK	chr2:29328463	c.A1301G	p.K434R	ND	ND	7.0%	ND	OTR	OTR	–	BG	U	DC	NFN	TL	HF	BG	Level 1/Lorlatinib, Brigatinib*
EPHA5	chr4:65420551	c.A1417C	p.T473P	ND	ND	8.3%	NI	NI	NI	TL	PS	NL	DC	NFL	TL	BG	HF	–
FAT1	chr4:186707744	c.A2084C	p.N695T	ND	ND	2.6%	NI	NI	NI	TL	BG	NL	PM	NFN	TL	BG	BG	–
MGA	chr15:41736268	c.T4004C	p.L1335P	ND	ND	1.6%	NI	NI	NI	DT	PD	NL	DC	NFN	TL	BG	HF	–
KMT2C	chr7:152248206	c.C2228T	p.P743L	ND	ND	1.6%	NI	NI	NI	TL	BG	NL	PM	NFN	DG	BG	BG	–
KMT2C	chr7:152235897	c.C2689T	p.R897X	ND	ND	1.4%	NI	NI	NI	–	–	–	DC	–	–	HF	–	–
PTPRD	chr9:8389280	c.A3117C	p.Q1039H	ND	ND	6.8%	ND	NI	NI	–	PD	DT	DC	FCM	DG	BG	HF	–
ABL1	chr9:133760790	c.C3113T	p. A1038V	NI	NI	NI	52.8%	OTR	OTR	–	BG	–	–	NFN	–	HF	–	–
GRM3	chr7:86415916	c.C808T	p.R270C	NI	NI	NI	7.0%	NI	NI	–	PS	–	–	FCM	–	HF	–	–
MAP3K1	chr5:56177843	c.C2816G	p.S939C	NI	NI	NI	49.6%	NI	NI	–	BG	–	–	–	–	HF	–	–
MSH3	chr5:80149992	c.A2857T	p.M953L	NI	NI	NI	46.1%	NI	NI	–	PD	–	–	FCM	–	HF	–	–
MSH6	chr2:48028273	c.G3151A	p.V1051I	NI	NI	NI	50.0%	OTR	OTR	–	BG	–	–	NFL	–	BG	–	–
PTPRO	chr12:15475691	c.G31T	p.A11S	NI	NI	NI	52.2%	NI	NI	–	BG	–	–	NFN	–	BG	–	–

*NI, not included; ND, not detected; OTR, out of target region; TL, tolerated; DT, deleterious; BG, benign; PD, Probably Damaging; PS, Possibly damaging; U, Unknown, NL, normal; DC, Disease causing; PM, polymorphism; NFN, non-functional neutral; NFL, non-functional low; FCM, functional medium; DG, Damaging; HF, harmful. *Approved for cancer types different from CUP.*

TABLE 2 | Mutation report of tumor, ccfDNA and CTCs from Pt#95.

				SureSelect 92-gene panel (Agilent Technologies)	SureSelect 92-gene panel (Agilent Technologies)	Ampli1 OncoSeek and LowPass Kit (Menarini Silicon Biosystem)	Pathogenicity Prediction								Actional genes/drugs [OncoKB (Chakravarty et al., 2017)]
Gene	**Position**	**Coding change**	**Amino acidic change**	**ccfDNA at diagnosis**	**Tumor FFPE**	**CTCs**	**SIFT** (Vaser et al., 2016)	**Polyphen2** (Adzhubei et al., 2010)	**LRT** (Chun and Fay, 2009)	**Mutation Taster** (Schwarz et al., 2014)	**Mutation Assessor** (Reva et al., 2011)	**FATHMM** (Shihab et al., 2013)	**CADD** (Kircher et al., 2014)	**VEST3** (Douville et al., 2016)	
ARID1A	chr1:26774679	c.4454_4457delTACA	p.I1485Rfs*19	32.6%	25%	NI	-	-	-	-	-	-	-	-	-
ARID1A	chr1:26774687	c.C4460T	p.A1487V	33.2%	27%	NI	TL	BG	DT	DC	NFN	TL	BG	HF	-
SPEN	chr1:15937527	c.G10391C	p.G3464A	31.0%	24%	NI	TL	BG	-	DC	NFL	TL	BG	BG	-
PIK3CG	chr7:106872869	c.G2218A	p.E740K	22.0%	8%	NI	TL	BG	NL	DC	NFL	TL	BG	BG	-
FGFR2	chr10:121515254	c.G814A	p.G272R	19.0%	NC	OTR	DT	PD	DT	DC	FCM	DG	HF	HF	Level 4/Debio1347, AZD4547, BGJ398, Erdafitinib
KMT2D	chr12:49031574	c.G13131A	p.W4377X	17.0%	FLQ	NI	DT	–	NL	DC†	–	–	HF	–	Level 3/no drug
FAT1	chr4:186621042	c.A5544C	p.Q1848H	13.1%	NC	NI	TL	PD	DT	DC	NFL	TL	BG	HF	–
KMT2C	chr7:152265180	c.G1042A	p.D348N	9.8%	FLQ	NI	TL	PD	U	DC	NFL	DG	BG	BG	–
KMT2C	chr7:152248140	c.A2294G	p.E765G	7.8%	ND	NI	TL	BG	DT	DC	NFL	DG	BG	BG	–
KMT2C	chr7:152235876	c.C2710T	p.R904X	7.5%	FLQ	NI	TL	–	NL	DC	–	–	HF	–	–
KMT2C	chr7:152235929	c.G2657A	p.R886H	6.8%	ND	NI	DT	PS	DT	DC	FCM	DG	HF	BG	–
KMT2C	chr7:152235861	c.A2725G	p.R909G	6.6%	ND	NI	TL	PD	DT	DC	FCM	DG	BG	HF	–
KMT2C	chr7:152248143	c.C2291T	p.S764F	4.9%	FLQ	NI	DT	BG	NL	DC	NFL	DG	BG	BG	–
KMT2C	chr7:152265209	c.C1013T	p.S338L	4.9%	ND	NI	TL	PD	U	DC	NFL	DG	BG	BG	–
KMT2C	chr7:152273774	c.G943A	p.G315S	4.9%	NC	NI	DT	PD	DT	DC	FCM	TL	HF	HF	–
KMT2C	chr7:152247966	c.T2468C	p.I823T	2.3%	NC	NI	TL	PD	DT	DC	NFL	DG	BG	HF	–
MGA	chr15:41767261	c.C8552T	p.P2851L	NC	5.20%	NI	TL	PS	NL	DC	NFN	DG	BG	BG	–
KMT2C	chr7:152163206	c.C10371A	p.D3457E	NC	6.30%	NI	TL	BG	NL	DC	NFL	DG	BG	BG	–
PTPRD	chr9:8521304	c.G904A	p.E302K	NC	5.00%	NI	–	PD	DT	DC	FCM	TL	HF	HF	–
ASXL2	chr2:25743628	c.G1929T	p.Q643H	NC	5.10%	NI	DT	PD	NL	DC	FCM	TL	BG	BG	–

NI, not included; NC, not covered region; FLQ, filtered for low quality; ND, not detected; OTR, out of target region; TL, tolerated; DT, deleterious; BG, benign; PD, Probably Damaging; PS, Possibly damaging; U, Unknown, NL, normal; DC, Disease causing; NFN, non-functional neutral; NFL, non-functional low; FCM, functional medium; DG, Damaging; HF, harmful. †Known to be disease causing.

with edema and diffuse suffusion of mesenteric and perivisceral tissues suggestive of peritoneal carcinosis, confirmed also by a 18F-FDG-PET/CT scan.

A CT-guided biopsy of a left paraortic lymph node led to a pathological diagnosis of node metastasis from poorly differentiated carcinoma with microglandular and signet-ring architecture. At immunohistochemistry, cells presented a focal positivity for K7 and CDX2 and negativity to K20 and synaptophysin. The immunophenotypical findings suggested to suspect a gastric primary tumor. Blood was collected for CTC analysis with CELLSEARCH and DEPArray and Parsortix at December 2019.

In May 2019, molecular analyses for the determination of MSI and HER2 status (by IHC) were negative, as well as *KRAS*, *NRAS*, *BRAF*, mutational status, and MGMT methylation status (by pyrosequencing). The patient underwent EGDS with ecoendoscopy, which found a suspicious area in the ampulla of Vater. Histological examination confirmed the presence of poorly differentiated adenocarcinoma with mixed, micro-glandular pattern, and signet-ring cells and a lymphangitic infiltration of the mucosa of duodenal type. IHC analysis reported a strong immunoreactivity to MUC1, MUC5AC, MUC6, and a complete negativity to MUC2 in addition to the previously identified $K7^+/K20^-/CDX2^+$ profile, suggesting a likely bilio-pancreatic origin.

Starting from May 2019, the patient was treated with FOLFOX-4 regimen up to nine cycles, obtaining an initial partial response. In October 2019, the patient was admitted at the Emergency room of the Bologna University Hospital due to dyspnea and bilateral pleural effusion. The patient underwent pleural drainage and cytological examination, followed by video-assisted thoracoscopy and pleurodesis. The cell block was tested by IHC and the identified tumor cells were found to be reactive for BEREP4, K7, and CDX2 and negative for TTF1 and calretinin. Molecular analysis on pleural-derived cytological specimen was performed in the diagnostic setting. The analysis reported a pathogenic alteration in *FGFR2* gene (c.1150G > A, p. Gly384Arg, AF:33.4%); no gene amplification or fusion was detected. In December 2019, the patient started weekly gemcitabine regimen as second-line treatment. After 2 weeks from the first administration, the patient had uncontrolled ascitic effusion. Abdominal CT with and without contrast showed progressive disease due to evident radiological signs of peritoneal carcinosis. The patient died in January 2020 due to further progressive disease.

Identification and Characterization of CTCs From CUP Patients Using CELLSEARCH and DEPArray or Parsortix Systems

CTCs from patients' peripheral blood were isolated by combining CELLSEARCH and the DEPArray system. For Pt#71, 66 ($CK^+/CD45^-/DAPI^+$) cells (none of which was positive for PD-L1) were captured with immunomagnetic beads. The isolated cells were then loaded on DEPArray that retrieved $n = 12$ CTCs. Three CTCs and one leukocyte as control were subjected to single-cell whole-genome amplification and sequencing.

For Pt#95, CELLSEARCH captured 133 CTCs cells (defined as above) from which DEPArray recovered 34 putative CTCs (**Figure 1** and **Supplementary Figure 1**). A total number of 32 CTCs and four leukocytes ware subjected to single-cell whole-genome amplification, and 10 CTCs passed quality control criteria for low-pass whole-genome analysis.

Pt#95 whole blood was also used to isolate CTCs with the Parsortix system (ANGLE plc). Large cells were isolated with a 6.5 μm Parsortix cassette. Some EpCAM-positive and CD45-negative CTCs were captured in the cassette (**Figure 2**), together with EpCAM-positive and CD45-positive cells of unknown significance (**Figure 2**).

Mutational Analysis of CTCs, ctDNA, and Tumor

Pt#71

F1CDx testing reported the amplification of *FGFR2* (Copy Number, CN: 49) and *CCNE1* (CN: 8) genes along with a somatic variant in *ARID1A* gene (p.R1276*) with an allele frequency (AF) of 7.3%. Moreover, F1CDx reported an intermediate tumor mutational burden (13 mutations/Mb). Single-cell genome-wide characterization of CTCs (*Ampli*1 LowPass, Menarini Silicon Biosystems) allowed sub-chromosomal losses detection, including a LOH region comprising the *APC* gene, and pattern of extensive gains, including *FGFR2* and *CCNE1* genes (**Figure 3**).

The same alterations were confirmed on bulk tumor DNA. Moreover, targeted sequencing (*Ampli*1 OncoSeek panel, Menarini Silicon Biosystems) was able to detect the presence of *FGFR2* amplification in 3/3 CTCs and the inactivating homozygous somatic variant in *APC* gene (p.T1556Nfs*3, AF: 90.2–99.2%). The APC somatic variant, which was missed by F1CDx, was detected (**Figure 3**) in two out of three analyzed CTCs, while the third CTC shows no coverage in the APC region (L5589, grayed out), in agreement with the deletion detected by the LowPass copy number profile in this cell, and a single-WBC control from the same sample (L5601) was wild type, as expected. The tumor gDNA target sequencing (DEPArray OncoSeek panel, Menarini Silicon Biosystems) confirmed the *FGFR2* amplification and reported the same frameshift variant in *APC*, even though with a lower allele frequency (p.T1556Nfs*3, AF: 14%), likely due to contamination by normal cells. The single-copy homozygous variant in APC found in CTCs is coherent with a ∼15% variant frequency in the presence of 70% of normal cells in FFPE. Indeed, when setting the contamination parameter to 70% in the FFPE low-pass analysis, the bioinformatic pipeline was able to call, out of the increased noise, some CNA regions similar to those detected in CTCs, which were otherwise undetectable without the correction factor (**Supplementary Figure 2**).

The SureSelect 92-gene custom panel detected the APC insertion in bulk tumor DNA (AF:9.8%) and also in circulating cfDNAs analyzed at two different time points (ccfDNA at diagnosis, AF: 22.6% and ccfDNA at the progression of the disease, AF:29.9%). The tool *panelcn.MOPS* (Povysil et al., 2017) used to analyze target sequencing data confirmed the

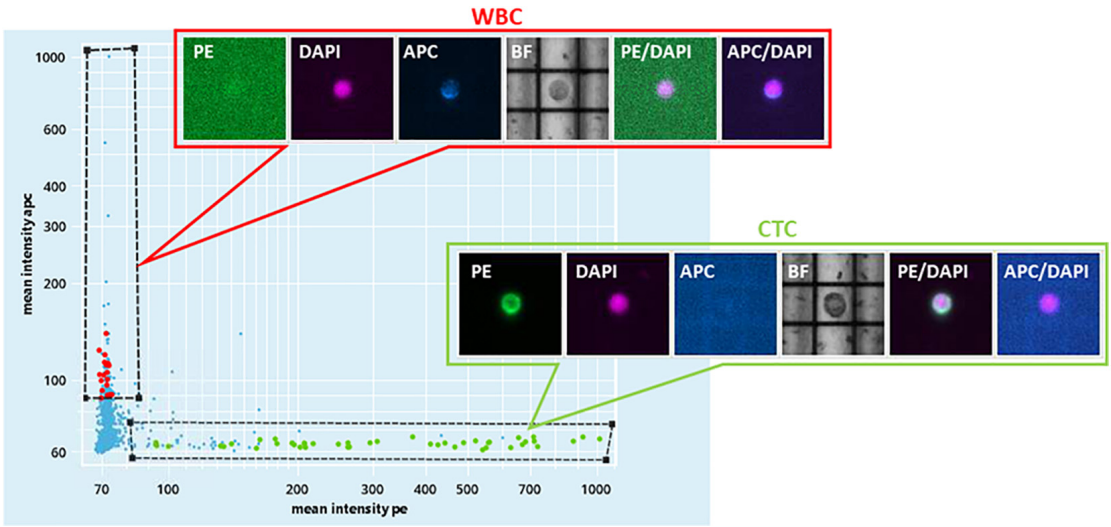

FIGURE 1 | DEPArray NxT analysis. Scatter plot of the enriched blood sample of patient#95. On the *X*-axis, the mean intensity fluorescence of PE channel is reported, corresponding to the intensity of CK IF staining. On the *Y*-axis, the mean intensity of CD45-APC is represented.

FGFR2 and *CCNE1* gene amplification reporting a copy number alteration higher than four in both genes; however, no *APC* loss was detected. Moreover, we confirmed the mutation in *ARID1A* gene (p.R1276*), *ERBB3* (p.S128R), *KEAP1* (p.R135H), *PALB2* (p.P807S), and *NTRK1* (p.Q736X), previously reported by F1CDx, both in the tumor and in the ccfDNAs. All detected variants and CNVs are listed in **Tables 1**, **3**.

In **Table 1**, we reported other mutations detected by F1CDx in genes not included in the custom panel and some variants detected in ccfDNAs not observed in the tumor. Of note, we observed mutations in *ALK* (p.K434R, AF:7%), *EPHA5* (p.T473P, AF: 8.3%), *PTPRD* (p.Q1039H, AF:6.8%), and other alterations at lower frequency.

Droplet Digital PCR technology validated the *ARID1A* mutation (**Figure 4A** and **Supplementary Figure 3A**) and the *FGFR2* amplification (**Figure 4B** and **Supplementary Figure 3B**) in bulk tumor DNA and in longitudinally collected ccfDNAs at three different time points of disease evolution. Of note, the frequency of *ARID1A* mutation decreases at time point B, during FOLFOX-4 treatment, then it increases during the progression of the disease, while the *FGFR2* amplification has a decreasing trend in terms of copy number value during disease progression. The Variant Allele Frequency reported by target sequencing at two time points was found to be consistent with the Fractional Abundance (FA% = mutated copies/mutated copies + wild-type copies) measured by ddPCR.

Pt#95

Single-cell whole-genome characterization of 10 CTCs detected a recurrent amplification signal in the regions of *ASPM* and *SEPT9* genes and a deletion including *FANCC* gene in all analyzed CTCs (**Supplementary Figure 4**), as shown in the CNV profile clustering in **Figure 5**. CTCs and bulk tumor DNA-targeted sequencing (*Ampli*1 OncoSeek Panel, Menarini Silicon Biosystems) reported no somatic mutation in the regions covered by the panel.

Target sequencing performed on ccfDNA and tumor FFPE tissue with the 92-gene custom panel identified 16 non-synonymous, somatic genetic alterations not detected in the normal cells in the ccfDNA and 8 in the tumor DNA (**Table 2**), including *ARID1A* deletion (I1485Rfs*19, AF: 32.6%) and mutation (p. A1487V, AF: 33.2%) and a mutation in *FGFR2* gene (p.G272R, AF:19%). Of note, mutational analysis performed in the diagnostic setting (obtained with Oncomine Comprehensive Assay by Thermo Fisher Scientific) reported the same mutation in *FGFR2* gene; no amplifications or deletions were detected with Agilent custom panel, but regions including *ASPM*, *SEPT9*, and *FANCC* genes were not captured.

DISCUSSION

The identification of driver and actionable genetic alterations is crucial to broaden the treatment choices of cancer patients. This is particularly relevant for patients with CUP, who have reduced access to targeted and immunotherapies. One main reason resides in treatment protocols being designed in a tumor-gnostic way. Furthermore, CUPs are characterized by scarce availability of tumor material for genetic testing, due to the extensive use of tissue slices in immune-phenotypic testing required for diagnostic procedures.

In this pilot study, we took advantage of liquid biopsy approaches to genetically characterize CUP tumors using both CTCs and DNA as a source of tumor DNA, with the aim to identify druggable genetic alterations.

The isolation and counting of CTCs is becoming an important tool to evaluate aggressiveness and prognosis of different solid tumors. The CELLSEARCH system (Menarini Silicon

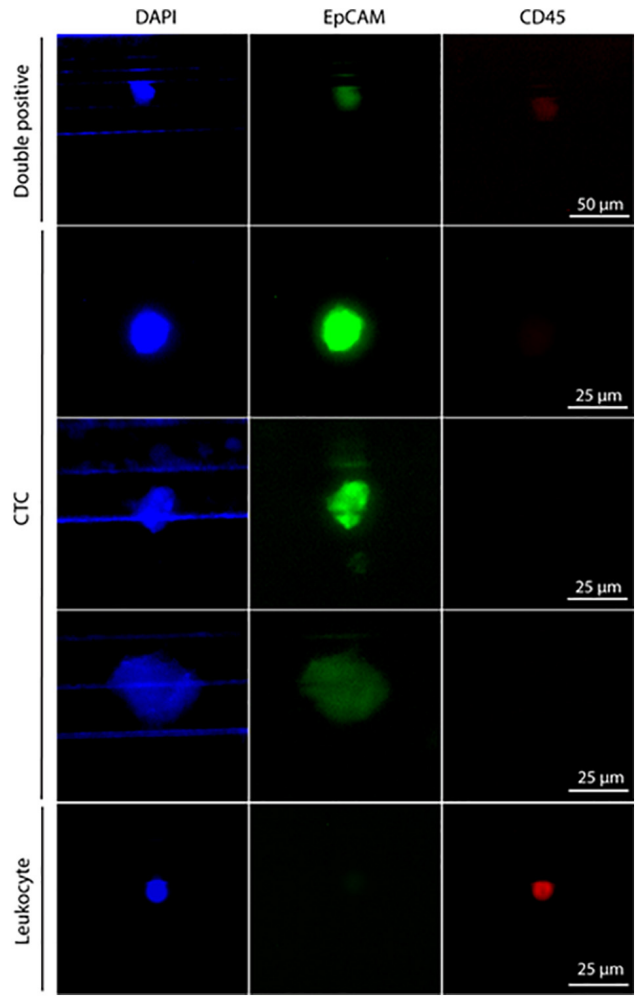

FIGURE 2 | Staining of cells isolated with Parsortix from patient #95. Cells were forced to pass through a 6.5-µm cassette in the Parsortix system and then stained with different antibodies. Nuclei stained with DAPI (blue), CD45 (red), and EpCAM (green). From top to bottom: double-positive cells ($CD45^+$, $EpCAM^+$) of unknown significance, three exemplary CTCs ($CD45^-$, $EpCAM^+$), one exemplary leucocyte ($CD45^+$, $EpCAM^-$) Scale bar, 50 µm (double-positive cells) and 25 µm (CTCs and leucocyte).

Biosystems) is to date the only platform cleared by the FDA for detecting and enumerating CTCs in metastatic breast, prostate, and colorectal cancer patients, while other technologies are at preclinical and clinical stages of development. CTC count as measured by CELLSEARCH System proved to have prognostic value in different metastatic solid tumors, including breast (Cristofanilli et al., 2004), colorectal (Cohen et al., 2008), and gastric cancers (Matsusaka et al., 2010). In addition, the detection of one or more CTCs using this system was found to predict early recurrence and a worse prognosis in chemo naïve patients with non-metastatic breast cancer (Lucci et al., 2012). A considerable number of CTCs were detected in the two CUP patients enrolled in our study, and they were successfully enriched and enumerated by CELLSEARCH and isolated with DEPArray for downstream molecular analysis (*Ampli*1 kit).

Recently, CTC isolation methods based on label-free systems were also developed. In one patient, we used the Parsortix system (ANGLE plc) for the size-based enrichment of CTCs from peripheral blood of CUP patients. This approach ensured a size-based selection of CTCs without the need of specific markers, which is a potential issue when isolating these cells from CUP patients. Some CTCs enriched with the Parsortix system proved to be positive for EpCAM marker, therefore confirming their epithelial origin, although no genetic confirmation could be produced. We also detected cells that co-express hemato-epithelial markers, as previously reported for a subpopulation of epithelial ovarian cancer tumor cells (Akhter et al., 2018). In this paper, the authors proposed a cell–cell fusion theory to explain the origin of these peculiar cell population. Indeed, $EpCAM^+$ and $CD45^+$ cells show more invasive mesenchymal properties and overexpress genes related to drug resistance, anti-apoptosis, and stemness. The detection of cells with these characteristics in circulation could be associated with CUP highly invasive phenotype and deserves further investigations.

CTCs and ccfDNA were used for CUP genetic testing. Our results from two longitudinally monitored patients suggested that CTCs and ctDNA can be isolated from the blood of CUP patients and are suitable for genetic characterization. FFPE tumor tissue was used to validate the liquid biopsy results. In addition, we analyzed and compared different targeted sequencing approaches applied to tumor FFPE tissue, CTCs, and ccfDNA: FoundationOne CDx (Roche Foundation Medicine), OncoSeek Panels (*Ampli*1 and DEPArray OncoSeek Panels, Menarini Silicon Biosystems), and an in-house developed, Agilent SureSelect panel, focusing on 92 genes frequently mutated in CUPs and metastatic solid tumors. The comprehensive genomic analysis was highly overlapping among the different approaches, when the region was covered by all panels. Clearly, these three different technologies cover a different number of genes and hot spot regions, which explains the differential detection of some variants.

Interestingly, both CUP patients presented actionable *FGFR2* aberrations. Specifically, a ∼80-fold copy number amplification (Pt#71) and a gene mutation (Pt#95), both at the tumor and CTC/ctDNA level, suggest a potential implication of this pathway in tumor progression and aggressiveness (Dienstmann et al., 2014). FGFR2 is a member of the fibroblast growth factor receptor family, whose signaling pathway activates downstream effectors that play a crucial role in cell proliferation, survival, and migration (Turner and Grose, 2010). *FGFR2* rearrangements have been detected in 10–15% of intrahepatic cholangiocarcinomas (Arai et al., 2014; Silverman et al., 2019), amplifications in up to 15% of gastric cancers (Deng et al., 2012; Seo et al., 2017) and point mutations in about 10% of endometrial cancers (Byron et al., 2012); moreover, *FGFR2* amplification has also a prognostic significance in gastric cancers (Chang et al., 2014; Seo et al., 2017). Of note, in longitudinal ccfDNAs from Pt#71, we observed a progressive reduction of *FGFR2* CN during treatments, which mirrors the initial partial response. Taking into account the chemo-naïve status of the two patients and the unavailability of clinical trials testing multi-kinase or FGFR2 inhibitors in CUP patients, the patients were treated

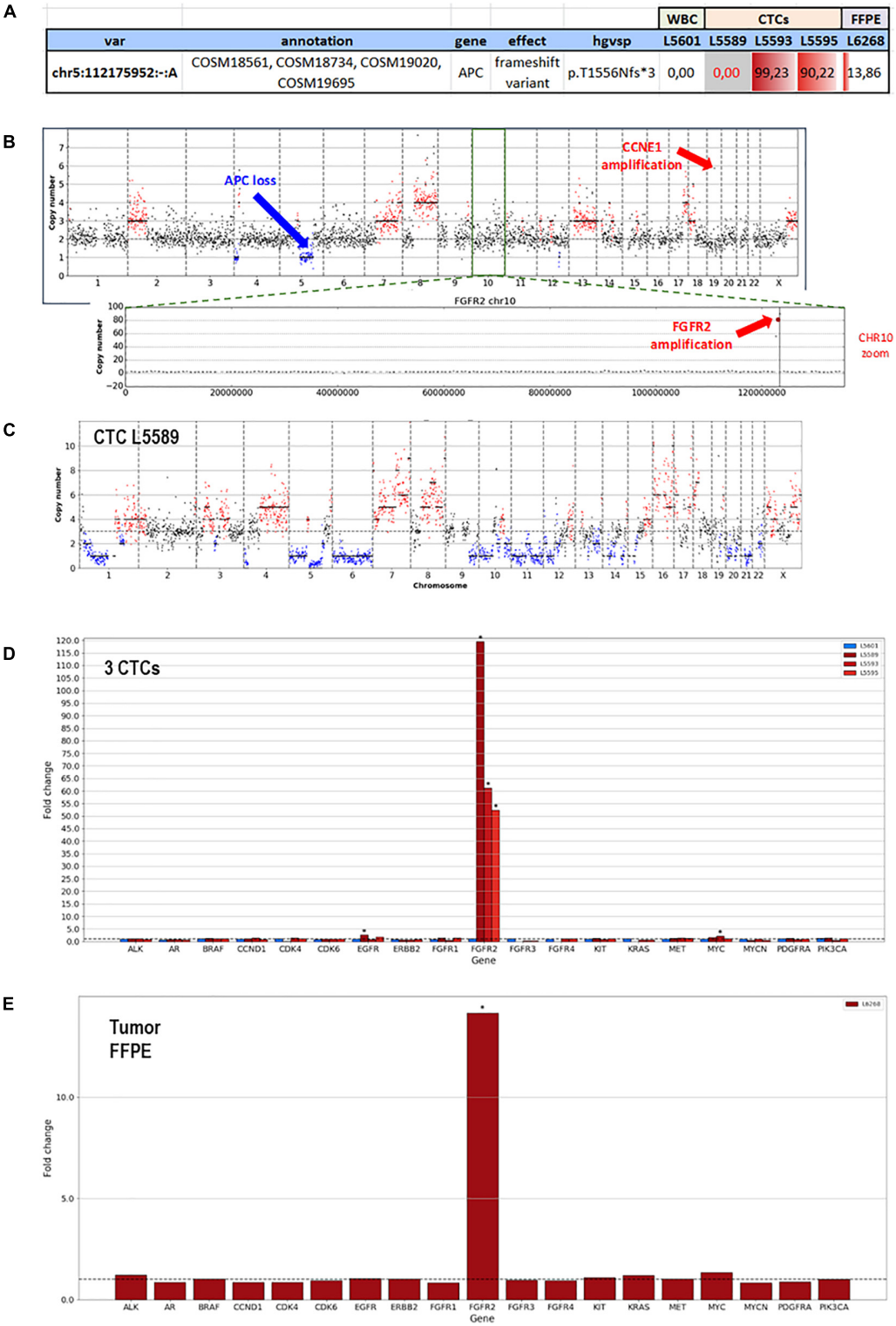

FIGURE 3 | Whole-genome copy number profiles and mutation analysis of CTCs and FFPE gDNA from patient #71. **(A)** Detection of a homozygous somatic variant (absent in a single WBC), in two out of three CTCs in *APC* gene (APC:p.T1556Nfs*3), a region also subjected to LOH, and the detection of the same variant in the FFPE tissue at lower frequency, due to the possible contamination by normal cells. **(B)** Representative copy number profile of one CTC. Amplification signal was detected for *FGFR2* and *CCNE1* genes, indicated with red arrows. The LOH region in chromosome 5, comprising the *APC* gene, is indicated with a blue arrow. **(C)** LowPass profile of L5589 CTC showing the complete deletion of *APC* genomic region, in agreement with the lack of coverage in targeted sequencing (grayed out in **A**). **(D)** Copy number aberration (CNA) distribution showing *FGFR2* amplification in all three CTCs **(D)** and FFPE biopsy **(E)**.

TABLE 3 | Copy number (CN) alterations detected in Pt#71.

		SureSelect 92-gene panel (Agilent Technologies)	SureSelect 92-gene panel (Agilent Technologies)	FoundatiOne CDx™ (Roche)	Ampli1 OncoSeek and LowPass Kit (Menarini Silicon Biosystem)	DEPArray™ OncoSeek and LowPass Kit (Menarini Silicon Biosystem)
Gene	Alteration	Tumor FFPE (CN)	ccfDNAs (CN)	Tumor FFPE (CN)	CTC (CN)	Tumor FFPE (CN)
FGFR2	Amplification	>4	>4	49	> 80	82
CCNE1	Amplification	>4	>4	8	6	5
APC	Loss/deletion	Not detected	Not detected	Not detected	Detected	Detected

with platinum salts and fluoropyrimidines, as suggested by the current guidelines.

Pt#71 also presented an amplification in *CCNE1* (Cyclin E1) gene, which is known to be associated with poor prognosis in ovarian and triple-negative breast cancer, probably involved in the emergence of resistance to chemotherapy (Nakayama et al., 2010; Huang et al., 2020).

Another common genetic feature of the two tested CUP tumors was the presence of alterations in *ARID1A* gene, which is a tumor suppressor gene encoding the DNA-binding subunit of the chromatin remodeler complex SWI/SNF (Trizzino et al., 2018). Despite not being druggable, this gene is the most frequently mutated chromatin regulator across all human cancers (Kadoch et al., 2013) and its loss impairs RNA polymerase II (RNAPII) pausing. Compromised RNAPII pausing results in transcriptional dysregulation of active genes, such as *TP53* and *ESR1*, which could explain the oncogenic effects of ARID1A loss (Trizzino et al., 2018). The recurrence of these mutation in both reported cases open an interesting prospective on the role of ARID1A in regulating the aggressiveness of CUPs. Of note, when longitudinally evaluated in ccfDNAs of Pt#71, the Fractional Abundance of *ARID1A* mutation (p.R1276*) decreased during treatment and then increases at disease progression, suggesting its potential involvement in disease worsening. Moreover, we noticed that in ccfDNAs at diagnosis and disease progression, in which the Fractional Abundance of $ARID1A_{mut}$ was high, there was also the emergence of novel mutations in *TP53, ALK, EPHA5, FAT1*, and *MGA* genes, not detected in the tumor biopsy. *In vitro* experiments demonstrated that *ARID1A* deficiency leads to DNA replication stress (Tsai et al., 2020) and impaired checkpoint activation and repair of DNA double-strand breaks (DSBs), which sensitizes to DSB-inducing treatments (Shen et al., 2015). Moreover, ARID1A normally recruits MSH2 to chromatin during DNA replication and promotes mismatch repair (MMR); however, its deficiency is associated with the impairment of MMR and thus an increase in mutagenesis and mutational load (Shen et al., 2018). As a consequence, ARID1A deficiency has been investigated as a biomarker of response to anti-PD-1/PD-L1 immunotherapy treatment (Okamura et al., 2020); alterations in this gene were found to be associated with a longer PFS in patients treated with anti-PD-1/PD-L1 immunotherapy (regardless of microsatellite and tumor mutational burden status). It has been demonstrated that 15% of CUP patients harbor alterations in *ARID1A* gene (MSK impact study; Zehir et al., 2017). Therefore, immune checkpoint inhibitors could be considered as a therapeutic option for ARID1A mutated CUP cases. In the two CUP cases investigated in this study, ARID1A-dependent accumulation of genetic alterations could explain the number of novel mutations that were longitudinally detected in the ccfDNA.

However, another explanation could be that the mutation load was boosted by the mutagenic activity of oxaliplatin (L-OHP), a DNA-alkylating-like agent,

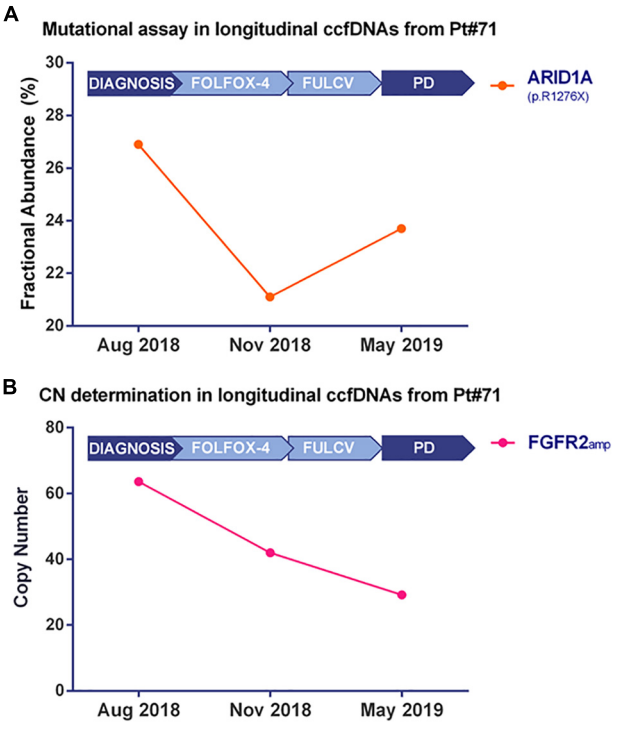

FIGURE 4 | Kinetics of mutated fractional abundance and CNV in longitudinal ccfDNAs measured by Droplet Digital PCR. The graph in **(A)** illustrates *ARID1A* mutated fractional abundance (p.R1276X) during patient's follow-up. This value decreases during treatment and later rises at the worsening of patient's conditions; on the contrary, when monitoring *FGFR2* amplification at the same time points, as reported in **(B)**, a decreasing trend was detected from the diagnosis to disease progression.

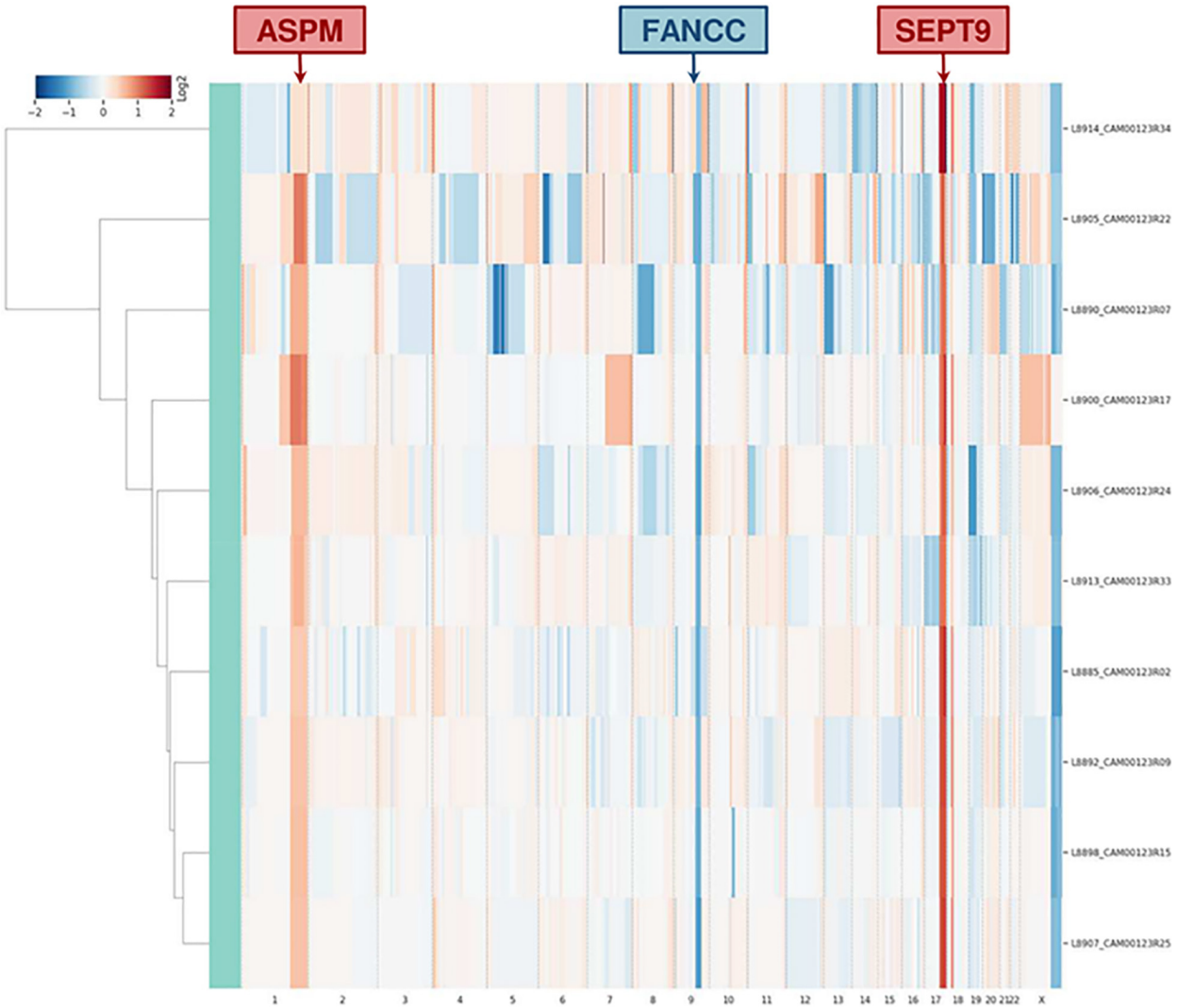

FIGURE 5 | Clustering analysis of 10 CTCs based on whole-genome copy number profile. The heatmap represents the relative copy number profiles of 10 different CTCs isolated through CELLSEARCH® and DEPArray™ technologies. Segments of gains or deletions are color-coded according their relative log2 copy number ratios.

which is included in FOLFOX-4 chemotherapy combination along with Leucovorin and 5-fluorouracil (5-FU) (Silva et al., 2005; Kawamoto et al., 2012). This chemotherapy regimen is commonly used to manage metastatic colorectal cancer (Benson et al., 2014), but also administered to CUP patients with $K20^+/K7^-/CDX2^+$ IHC signature.

Overall, our analysis constitutes the proof of concept needed to assess the relevance of liquid biopsy genetic testing in metastatic cancer of unknown origin and underlies the importance of using dedicated NGS panels to identify actionable genetic alterations.

Altogether, our results support the use of liquid biopsy, either using CTCs or ccfDNA, in the genetic characterization of CUPs and identification of driver mutations, with the advantage of a minimally invasive approach and potential longitudinal monitoring. This is a proof-of-concept study on a small number of patients, but given the rarity of the disease and the great need for effective therapies, we believe we provided valuable novel data. We can also conclude that a timely genetic testing and the use of broad or CUP-dedicated NGS panels, covering the most frequently mutated genes, are of the outmost importance to offer these patients novel therapeutic options and potentially improve their survival.

DATA AVAILABILITY STATEMENT

The datasets presented in this article are not readily available because patients have consented to the use of their individual genetic data for biomedical research, but not for unlimited public

data release. Requests to access the datasets should be directed to corresponding author.

ETHICS STATEMENT

The studies involving human participants were reviewed and approved by the Ethics Committee Center Emilia-Romagna Region – Italy (protocol 130/2016/U/Tess). The patients/participants provided their written informed consent to participate in this study.

AUTHOR CONTRIBUTIONS

NL, IS, EP, MR, MG, PT, and SV carried out the experiments and data analysis. MF wrote the manuscript with support from NL, IS, FG, AA, FF, NM, MP, and SS. AD'E and AA helped supervise the project. MF conceived the original idea and supervised the project. All authors contributed to the article and approved the submitted version.

FUNDING

The research leading to these results has received funding from AIRC under IG 2016–ID. 18464 project–P.I. Ferracin Manuela and CaMMPPO study sponsored by Menarini Silicon Biosystems S.p.A. NL was supported by eDIMES Lab funds from Bologna University. The authors would like to thank Fondazione del Monte di Bologna e Ravenna for the financial support.

SUPPLEMENTARY MATERIAL

The Supplementary Material for this article can be found online at: https://www.frontiersin.org/articles/10.3389/fcell.2021.666156/full#supplementary-material

Supplementary Figure 1 | DEPArray NxT representative CTC images from patient #95. Cell gallery acquired by DEPArray, showing single fluorescent channels and overlays, and bright field (BF) images where the DEPArray electrodes (pitch 20μm) are visible.

Supplementary Figure 2 | Patient #71: Low-Pass Whole Genome CNA profiles. **(A)** FFPE without compensation: the signal produced by normal cells impact the copy-number alterations (CNA) call. **(B)** Pure single-CTC: clear CNA calls with digital copy-number values (e.g., Chr 8q $n = 4$). **(C)** FFPE analysis set at 70% normal DNA contamination: signal is amplified and, among increased noise, some true positive CNA detected also in CTCs are called (green arrows) along with putative false-positives (orange arrows).

Supplementary Figure 3 | Mutational assay and copy number determination assay by Droplet Digital PCR. The graph reports ddPCR outputs of *ARID1A* mutated fractional abundance (p.R1276X) **(A)** and in *FGFR2* amplification **(B)** during patient's follow-up at three different time points.

Supplementary Figure 4 | Patient #95 single-CTCs images and CNA profiles. Cell gallery acquired by DEPArray, showing single fluorescent channels and overlays, and bright field (BF) images for 10 CTCs, paired with the corresponding CNA profile.

Supplementary Table 1 | List of genes and regions included in SureSelect custom panel.

REFERENCES

Aceto, N., Bardia, A., Miyamoto, D. T., Donaldson, M. C., Wittner, B. S., Spencer, J. A., et al. (2014). Circulating tumor cell clusters are oligoclonal precursors of breast cancer metastasis. *Cell* 158, 1110–1122. doi: 10.1016/j.cell.2014.07.013

Adzhubei, I. A., Schmidt, S., Peshkin, L., Ramensky, V. E., Gerasimova, A., Bork, P., et al. (2010). A method and server for predicting damaging missense mutations. *Nat Methods* 7, 248–249. doi: 10.1038/nmeth0410-248

Akhter, M. Z., Sharawat, S. K., Kumar, V., Kochat, V., Equbal, Z., Ramakrishnan, M., et al. (2018). Aggressive serous epithelial ovarian cancer is potentially propagated by EpCAM(+)CD45(+) phenotype. *Oncogene* 37, 2089–2103. doi: 10.1038/s41388-017-0106-y

Amintas, S., Bedel, A., Moreau-Gaudry, F., Boutin, J., Buscail, L., Merlio, J. P., et al. (2020). Circulating tumor cell clusters: united we stand divided we fall. *Int. J. Mol. Sci.* 21:2653. doi: 10.3390/ijms21072653

Arai, Y., Totoki, Y., Hosoda, F., Shirota, T., Hama, N., Nakamura, H., et al. (2014). Fibroblast growth factor receptor 2 tyrosine kinase fusions define a unique molecular subtype of cholangiocarcinoma. *Hepatology* 59, 1427–1434. doi: 10.1002/hep.26890

Barber, L. J., Mansukhani, S., Herman, B., Arezi, B., and Gerlinger, M. (2017). *Application Note: Ultra-sensitive Cancer Liquid Biopsy Analysis with the Agilent SureSelectXT HS Target Enrichment Workflow*. Santa Clara, CA: Agilent Technologies.

Benson, A. B. III, Venook, A. P., Bekaii-Saab, T., Chan, E., Chen, Y. J., Cooper, H. S., et al. (2014). Colon cancer, version 3.2014. *J. Natl. Compr. Canc. Netw.* 12, 1028–1059. doi: 10.6004/jnccn.2014.0099

Byron, S. A., Gartside, M., Powell, M. A., Wellens, C. L., Gao, F., Mutch, D. G., et al. (2012). FGFR2 point mutations in 466 endometrioid endometrial tumors: relationship with MSI, KRAS, PIK3CA, CTNNB1 mutations and clinicopathological features. *PLoS One* 7:e30801. doi: 10.1371/journal.pone.0030801

Chakravarty, D., Gao, J., Phillips, S., Kundra, R., Zhang, H., Wang, J., et al. (2017). OncoKB: a precision oncology knowledge base. *JCO Precis. Oncol.* 2017:PO.17.00011. doi: 10.1200/po.17.00011

Chang, J., Liu, X., Wang, S., Zhang, Z., Wu, Z., Zhang, X., et al. (2014). Prognostic value of FGFR gene amplification in patients with different types of cancer: a systematic review and meta-analysis. *PLoS One* 9:e105524. doi: 10.1371/journal.pone.0105524

Chun, S., and Fay, J. C. (2009). Identification of deleterious mutations within three human genomes. *Genome Res* 19, 1553–1561. doi: 10.1101/gr.092619.109

Cinausero, M., Laprovitera, N., De Maglio, G., Gerratana, L., Riefolo, M., Macerelli, M., et al. (2019). KRAS and ERBB-family genetic alterations affect response to PD-1 inhibitors in metastatic nonsquamous NSCLC. *Ther. Adv. Med. Oncol.* 11:1758835919885540. doi: 10.1177/1758835919885540

Cohen, S. J., Punt, C. J., Iannotti, N., Saidman, B. H., Sabbath, K. D., Gabrail, N. Y., et al. (2008). Relationship of circulating tumor cells to tumor response, progression-free survival, and overall survival in patients with metastatic colorectal cancer. *J. Clin. Oncol.* 26, 3213–3221. doi: 10.1200/JCO.2007.15.8923

Conway, A. M., Mitchell, C., and Cook, N. (2019). Challenge of the unknown: how can we improve clinical outcomes in cancer of unknown primary? *J. Clin. Oncol.* 37, 2089–2090. doi: 10.1200/jco.19.00449

Cristofanilli, M., Budd, G. T., Ellis, M. J., Stopeck, A., Matera, J., Miller, M. C., et al. (2004). Circulating tumor cells, disease progression, and survival in metastatic breast cancer. *N. Engl. J. Med.* 351, 781–791. doi: 10.1056/NEJMoa040766

Deng, N., Goh, L. K., Wang, H., Das, K., Tao, J., Tan, I. B., et al. (2012). A comprehensive survey of genomic alterations in gastric cancer reveals

systematic patterns of molecular exclusivity and co-occurrence among distinct therapeutic targets. *Gut* 61, 673–684. doi: 10.1136/gutjnl-2011-301839

Dienstmann, R., Rodon, J., Prat, A., Perez-Garcia, J., Adamo, B., Felip, E., et al. (2014). Genomic aberrations in the FGFR pathway: opportunities for targeted therapies in solid tumors. *Ann. Oncol.* 25, 552–563. doi: 10.1093/annonc/mdt419

Douville, C., Masica, D. L., Stenson, P. D., Cooper, D. N., Gygax, D. M., Kim, R., et al. (2016). Assessing the pathogenicity of insertion and deletion variants with the variant effect scoring tool (VEST-Indel). *Hum. Mutat.* 37, 28–35. doi: 10.1002/humu.22911

Drapkin, B. J., George, J., Christensen, C. L., Mino-Kenudson, M., Dries, R., Sundaresan, T., et al. (2018). Genomic and functional fidelity of small cell lung cancer patient-derived xenografts. *Cancer Discov.* 8, 600–615. doi: 10.1158/2159-8290.CD-17-0935

Fizazi, K., Greco, F. A., Pavlidis, N., Daugaard, G., Oien, K., Pentheroudakis, G., et al. (2015). Cancers of unknown primary site: ESMO clinical practice guidelines for diagnosis, treatment and follow-up. *Ann. Oncol.* 26(Suppl. 5), v133–v138. doi: 10.1093/annonc/mdv305

Haratani, K., Hayashi, H., Takahama, T., Nakamura, Y., Tomida, S., Yoshida, T., et al. (2019). Clinical and immune profiling for cancer of unknown primary site. *J. Immunother. Cancer* 7:251. doi: 10.1186/s40425-019-0720-z

Huang, X., Wu, H. M., Zhu, C., Shao, D., Guo, D., Zhou, Y., et al. (2020). Next generation sequencing reveals CCNE1 amplification as an independent prognostic factor for triple negative breast cancer (TNBC) patients. *J. Clin. Oncol.* 38:558. doi: 10.1200/JCO.2020.38.15_suppl.558

Ignatiadis, M., and Dawson, S. J. (2014). Circulating tumor cells and circulating tumor DNA for precision medicine: dream or reality? *Ann. Oncol.* 25, 2304–2313. doi: 10.1093/annonc/mdu480

Joosse, S. A., Gorges, T. M., and Pantel, K. (2015). Biology, detection, and clinical implications of circulating tumor cells. *EMBO Mol. Med.* 7, 1–11. doi: 10.15252/emmm.201303698

Kadoch, C., Hargreaves, D. C., Hodges, C., Elias, L., Ho, L., Ranish, J., et al. (2013). Proteomic and bioinformatic analysis of mammalian SWI/SNF complexes identifies extensive roles in human malignancy. *Nat. Genet.* 45, 592–601. doi: 10.1038/ng.2628

Karczewski, K. J., Francioli, L. C., Tiao, G., Cummings, B. B., Alfoldi, J., Wang, Q., et al. (2020). The mutational constraint spectrum quantified from variation in 141,456 humans. *Nature* 581, 434–443. doi: 10.1038/s41586-020-2308-7

Kato, S., Krishnamurthy, N., Banks, K. C., De, P., Williams, K., Williams, C., et al. (2017). Utility of genomic analysis in circulating tumor DNA from patients with carcinoma of unknown primary. *Cancer Res.* 77, 4238–4246. doi: 10.1158/0008-5472.CAN-17-0628

Kawamoto, Y., Tsuchihara, K., Yoshino, T., Ogasawara, N., Kojima, M., Takahashi, M., et al. (2012). KRAS mutations in primary tumours and post-FOLFOX metastatic lesions in cases of colorectal cancer. *Br. J. Cancer* 107, 340–344. doi: 10.1038/bjc.2012.218

Kircher, M., Witten, D. M., Jain, P., O'Roak, B. J., Cooper, G. M., and Shendure, J. (2014). A general framework for estimating the relative pathogenicity of human genetic variants. *Nat. Genet.* 46, 310–315. doi: 10.1038/ng.2892

Komine, K., Inoue, M., Otsuka, K., Fukuda, K., Nanjo, H., and Shibata, H. (2014). Utility of measuring circulating tumor cell counts to assess the efficacy of treatment for carcinomas of unknown primary origin. *Anticancer Res.* 34, 3165–3168.

Laprovitera, N., Riefolo, M., Ambrosini, E., Klec, C., Pichler, M., and Ferracin, M. (2021). Cancer of unknown primary: challenges and progress in clinical management. *Cancers* 13:451. doi: 10.3390/cancers13030451

Lucci, A., Hall, C. S., Lodhi, A. K., Bhattacharyya, A., Anderson, A. E., Xiao, L., et al. (2012). Circulating tumour cells in non-metastatic breast cancer: a prospective study. *Lancet Oncol.* 13, 688–695. doi: 10.1016/S1470-2045(12)70209-7

Matsusaka, S., Chin, K., Ogura, M., Suenaga, M., Shinozaki, E., Mishima, Y., et al. (2010). Circulating tumor cells as a surrogate marker for determining response to chemotherapy in patients with advanced gastric cancer. *Cancer Sci.* 101, 1067–1071. doi: 10.1111/j.1349-7006.2010.01492.x

Nakayama, N., Nakayama, K., Shamima, Y., Ishikawa, M., Katagiri, A., Iida, K., et al. (2010). Gene amplification CCNE1 is related to poor survival and potential therapeutic target in ovarian cancer. *Cancer* 116, 2621–2634. doi: 10.1002/cncr.24987

Okamura, R., Kato, S., Lee, S., Jimenez, R. E., Sicklick, J. K., and Kurzrock, R. (2020). ARID1A alterations function as a biomarker for longer progression-free survival after anti-PD-1/PD-L1 immunotherapy. *J. Immunother. Cancer.* 8:e000438. doi: 10.1136/jitc-2019-000438

Pairawan, S., Hess, K. R., Janku, F., Sanchez, N. S., Mills Shaw, K. R., Eng, C., et al. (2020). Cell-free circulating tumor DNA variant allele frequency associates with survival in metastatic cancer. *Clin. Cancer Res.* 26, 1924–1931. doi: 10.1158/1078-0432.CCR-19-0306

Povysil, G., Tzika, A., Vogt, J., Haunschmid, V., Messiaen, L., Zschocke, J., et al. (2017). panelcn.MOPS: copy-number detection in targeted ngs panel data for clinical diagnostics. *Hum. Mutat.* 38, 889–897. doi: 10.1002/humu.23237

Reva, B., Antipin, Y., and Sander, C. (2011). Predicting the functional impact of protein mutations: application to cancer genomics. *Nucleic Acids Res.* 39:e118. doi: 10.1093/nar/gkr407

Riethdorf, S., Fritsche, H., Muller, V., Rau, T., Schindlbeck, C., Rack, B., et al. (2007). Detection of circulating tumor cells in peripheral blood of patients with metastatic breast cancer: a validation study of the cell search system. *Clin. Cancer Res.* 13, 920–928. doi: 10.1158/1078-0432.CCR-06-1695

Ross, J. S., Wang, K., Gay, L., Otto, G. A., White, E., Iwanik, K., et al. (2015). Comprehensive genomic profiling of carcinoma of unknown primary site: new routes to targeted therapies. *JAMA Oncol.* 1, 40–49. doi: 10.1001/jamaoncol.2014.216

Schwarz, J. M., Cooper, D. N., Schuelke, M., and Seelow, D. (2014). MutationTaster2: mutation prediction for the deep-sequencing age. *Nat. Methods* 11, 361–362. doi: 10.1038/nmeth.2890

Seo, S., Park, S. J., Ryu, M. H., Park, S. R., Ryoo, B. Y., Park, Y. S., et al. (2017). Prognostic impact of fibroblast growth factor receptor 2 gene amplification in patients receiving fluoropyrimidine and platinum chemotherapy for metastatic and locally advanced unresectable gastric cancers. *Oncotarget* 8, 33844–33854. doi: 10.18632/oncotarget.12953

Shen, J., Ju, Z., Zhao, W., Wang, L., Peng, Y., Ge, Z., et al. (2018). ARID1A deficiency promotes mutability and potentiates therapeutic antitumor immunity unleashed by immune checkpoint blockade. *Nat. Med.* 24, 556–562. doi: 10.1038/s41591-018-0012-z

Shen, J., Peng, Y., Wei, L., Zhang, W., Yang, L., Lan, L., et al. (2015). ARID1A deficiency impairs the dna damage checkpoint and sensitizes cells to parp inhibitors. *Cancer Discov.* 5, 752–767. doi: 10.1158/2159-8290.cd-14-0849

Shihab, H. A., Gough, J., Cooper, D. N., Stenson, P. D., Barker, G. L., Edwards, K. J. I, et al. (2013). Predicting the functional, molecular, and phenotypic consequences of amino acid substitutions using hidden Markov models. *Hum. Mutat.* 34, 57–65. doi: 10.1002/humu.22225

Silva, M. J., Costa, P., Dias, A., Valente, M., Louro, H., and Boavida, M. G. (2005). Comparative analysis of the mutagenic activity of oxaliplatin and cisplatin in the Hprt gene of CHO cells. *Environ. Mol. Mutagen.* 46, 104–115. doi: 10.1002/em.20138

Silverman, I. M., Murugesan, K., Lihou, C. F., Féliz, L., Frampton, G. M., Newton, R. C., et al. (2019). Comprehensive genomic profiling in FIGHT-202 reveals the landscape of actionable alterations in advanced cholangiocarcinoma. *J. Clin. Oncol.* 37(15 Suppl.):4080. doi: 10.1200/JCO.2019.37.15_suppl.4080

Sparano, J., O'Neill, A., Alpaugh, K., Wolff, A. C., Northfelt, D. W., Dang, C. T., et al. (2018). Association of circulating tumor cells with late recurrence of estrogen receptor-positive breast cancer: a secondary analysis of a randomized clinical trial. *JAMA Oncol.* 4, 1700–1706. doi: 10.1001/jamaoncol.2018.2574

Tanizaki, J. Y., Akiyoshi, K., Minami, K., Ueda, H., Takiguchi, H., Nakayama Kondoh, H., et al. (2020). NivoCUP: an open-label phase II study on the efficacy of nivolumab in cancer of unknown primary. *J. Clin. Oncol.* 38(15 Suppl.):106. doi: 10.1200/JCO.2020.38.15_suppl.106

Trizzino, M., Barbieri, E., Petracovici, A., Wu, S., Welsh, S. A., Owens, T. A., et al. (2018). The tumor suppressor arid1a controls global transcription via pausing of RNA Polymerase II. *Cell Rep.* 23, 3933–3945. doi: 10.1016/j.celrep.2018.05.097

Tsai, S., Chang, E. Y.-c., Fournier, L.-A., Wells, J. P., Minaker, S. W., Zhu, Y. D., et al. (2020). ARID1A regulates R-loop associated DNA replication stress. *bioRxiv* [Preprint]. doi: 10.1101/2020.11.16.384446

Turner, N., and Grose, R. (2010). Fibroblast growth factor signalling: from development to cancer. *Nat. Rev. Cancer* 10, 116–129. doi: 10.1038/nrc2780

Varadhachary, G. R., and Raber, M. N. (2014). Cancer of unknown primary site. *N. Engl. J. Med.* 371, 757–765. doi: 10.1056/NEJMra1303917

Varghese, A. M., Arora, A., Capanu, M., Camacho, N., Won, H. H., Zehir, A., et al. (2017). Clinical and molecular characterization of patients with cancer of unknown primary in the modern era. *Ann. Oncol.* 28, 3015–3021. doi: 10.1093/annonc/mdx545

Vaser, R., Adusumalli, S., Leng, S. N., Sikic, M., and Ng, P. C. (2016). SIFT missense predictions for genomes. *Nat. Protoc.* 11, 1–9. doi: 10.1038/nprot.2015.123

Wang, K., Li, M., and Hakonarson, H. (2010). ANNOVAR: functional annotation of genetic variants from high-throughput sequencing data. *Nucleic Acids Res.* 38:e164. doi: 10.1093/nar/gkq603

Yu, M., Bardia, A., Aceto, N., Bersani, F., Madden, M. W., Donaldson, M. C., et al. (2014). Cancer therapy. ex vivo culture of circulating breast tumor cells for individualized testing of drug susceptibility. *Science* 345, 216–220. doi: 10.1126/science.1253533

Yu, M., Stott, S., Toner, M., Maheswaran, S., and Haber, D. A. (2011). Circulating tumor cells: approaches to isolation and characterization. *J. Cell Biol.* 192, 373–382. doi: 10.1083/jcb.201010021

Zehir, A., Benayed, R., Shah, R. H., Syed, A., Middha, S., Kim, H. R., et al. (2017). Mutational landscape of metastatic cancer revealed from prospective clinical sequencing of 10,000 patients. *Nat. Med.* 23, 703–713. doi: 10.1038/nm.4333

Zhao, P., Zhou, W., Liu, C., Zhang, H., Cheng, Z., Wu, W., et al. (2019). Establishment and characterization of a CTC cell line from peripheral blood of breast cancer patient. *J. Cancer* 10, 6095–6104. doi: 10.7150/jca.33157

Conflict of Interest: MG, PT, FF, and NM were employees of Menarini Silicon Biosystems and co-inventors in patents assigned to the company, regarding certain company products used in this study. AA received honoraria (self) for advisory board participation: BMS, MSD, ROCHE, Astra Zeneca, and Eli-Lilly Research Grants to my Institution: Celgene, BMS, Ipsen, and Roche.

The remaining authors declare that the research was conducted in the absence of any commercial or financial relationships that could be construed as a potential conflict of interest.

Copyright © 2021 Laprovitera, Salamon, Gelsomino, Porcellini, Riefolo, Garonzi, Tononi, Valente, Sabbioni, Fontana, Manaresi, D'Errico, Pantaleo, Ardizzoni and Ferracin. This is an open-access article distributed under the terms of the Creative Commons Attribution License (CC BY). The use, distribution or reproduction in other forums is permitted, provided the original author(s) and the copyright owner(s) are credited and that the original publication in this journal is cited, in accordance with accepted academic practice. No use, distribution or reproduction is permitted which does not comply with these terms.

frontiers in Oncology

MINI REVIEW
published: 21 July 2021
doi: 10.3389/fonc.2021.692322

Application of Data Science in Circulating Tumor DNA Detection: A Promising Avenue Towards Liquid Biopsy

Ming Li[†], *Sisi Xie*[†], *Chenyu Lu*, *Lingyun Zhu*[*] *and Lvyun Zhu*[*]

Department of Biology and Chemistry, College of Liberal Arts and Sciences, National University of Defense Technology, Changsha, China

The circulating tumor DNA (ctDNA), as a promising biomarker of liquid biopsy, has potential clinical relevance on the molecular diagnosis and monitoring of cancer. However, the trace concentration level of ctDNA in the peripheral blood restricts its extensive clinical application. Recently, high-throughput-based methodologies have been leveraged to improve the sensitivity and specificity of ctDNA detection, showing a promising avenue towards liquid biopsy. This review briefly summarizes the high-throughput data features concerned by current ctDNA detection strategies and the technical obstacles, potential solutions, and clinical relevance of current ctDNA profiling technologies. We also highlight future directions improving the limit of detection of ctDNA for better clinical application. This review may serve as a reference for the crosslinks between data science and ctDNA-based liquid biopsy, benefiting clinical translation in advanced cancer diagnosis.

Keywords: cancer diagnosis, ctDNA detection, data science, liquid biopsy, technological advancement

OPEN ACCESS

Edited by:
George Calin, University of Texas MD Anderson Cancer Center, United States

Reviewed by:
Svetlana Tamkovich, Novosibirsk State University, Russia
Elizabeth A. Proctor, The Pennsylvania State University, United States

***Correspondence:**
Lvyun Zhu
zhulvyun@nudt.edu.cn
Lingyun Zhu
lingyunzhu@nudt.edu.cn

[†]*These authors have contributed equally to this work*

Specialty section:
This article was submitted to Molecular and Cellular Oncology, a section of the journal Frontiers in Oncology

Received: *08 April 2021*
Accepted: *05 July 2021*
Published: *21 July 2021*

Citation:
Li M, Xie S, Lu C, Zhu L and Zhu L (2021) Application of Data Science in Circulating Tumor DNA Detection: A Promising Avenue Towards Liquid Biopsy. Front. Oncol. 11:692322. doi: 10.3389/fonc.2021.692322

INTRODUCTION

Liquid biopsy, a non-invasive real-time method, can provide diagnostic and prognostic information during cancer progression and treatment (1). Unlike tissue biopsy, liquid biopsy examines circulating tumor cells (2) or tumor-released molecules, such as DNAs (3) and RNAs (4), from the circulatory system. Circulating tumor DNA (ctDNA) is generated from tumor cells (5), which forms a small minority of the cell-free DNA (cfDNA) in circulation against a background of fragments mostly derived from normal cells in the event of cell death or exosome secretion (6, 7). Plasma ctDNA could originate from both the nuclei or the mitochondria of tumor cells (8). However, only nucleus ctDNA records sufficient information of tumor genome, revealing tumor generation, development, metastasis, and recurrence (9), while mitochondrial ctDNA often provides information noise due to its less genomic information and higher copy number (**Supplementary Figure 1**). Thus, the concentration and abnormal sequence features of nucleus ctDNA (hereinafter ctDNA for convenience) in patients' blood are significantly correlated with the course of the disease and curative effect (10), rendering it an emerging tumor marker and an

Abbreviations: CAPP-Seq, the Cancer Personalized Profiling by deep sequencing; CH, clonal hematopoietic; cfDNA, cell-free DNA; ctDNA, circulating tumor DNA; HTS, high-throughput sequencing; PCR, polymerase chain reaction.

essential part of liquid biopsy (11). Although the trace concentration of ctDNA in the peripheral blood and intense background noises challenge the clinical application of ctDNA, a series of ctDNA capture methods based on data science aiming at its biological features improves the sensitivity and accuracy of ctDNA detection and gradually clears the obstacles in the potential clinical application of ctDNA detection (12, 13). This review briefly summarizes the recent development and application of data science for highly sensitive and robust ctDNA detection. We also discuss the current challenges of ctDNA detection technologies and provide insights into the potential development direction in their future application.

DATA FEATURES UTILIZED BY CURRENT ctDNA DETECTION STRATEGIES

Current ctDNA detection strategies are developed mainly based on the fragment concentration and the sequence features, such as abnormal mutations and methylations. The dynamic concentration of ctDNA is significantly correlated with the progress of the cancer disease. Because of its short half-life of less than 2 hours (14) and its low concentration (5), ctDNA is almost undetectable in patients with primary tumors. However, along with the progression of the disease, the immune system is attenuated, and ctDNA is gradually accumulated, which could be discriminated from cfDNA under certain limits of detection (15). The increased concentration of ctDNA could identify patients with cancer from healthy cohorts and stratify patients in the early and advanced stages (16). Besides, the changes in ctDNA levels before and after drug treatment are related to the therapeutic effect for patients (17). Furthermore, for tumor-free patients after treatment, the concentration level of ctDNA indicates the risk of cancer recurrence (18).

Technically, concentration analysis of ctDNA is a challenging task because ctDNA makes up a small proportion of the total cfDNA extracted from serum (19, 20). For example, Diehl et al. found that the mean mutated allele frequency of *APC* gene of patients with colorectal cancer ranged from early stages' 0.04% to late stages 11% (21). Extraction of ctDNA information from other cfDNA noise should be an initial step for ctDNA detection. Size selection–based data selection has been widely utilized in ctDNA detection to increase the signal-to-noise ratio. The size of cfDNA generated from the apoptosis of normal cells is about 167 bp, which is due to the structure of the histone octamer (22). However, studies show that the ctDNA is shorter than cfDNA in the meaning of statistics (23) and has a typical size of less than 142 bp in low molecular weight (24). The enriched mitochondrial ctDNA is about 100 bp in size, much smaller than that of nuclear ctDNA, further displaying the size variety of ctDNA fragments (8). Notably, there are long-size cfDNA fragments that exist, such as 2 kb and 20 kb fragments, which are probably generated from cancer cell necrosis (25) and blood cell surface (26), respectively. The accurate enrichment of ctDNA in a particular interval size eliminates some background noises to some extent and relatively enhances data processing efficiency. For example, Mouliere et al. mapped the distribution of ctDNA fragments and optimized the ctDNA capture by choosing to concentrate ctDNA fragments in the size of 90–150 bp from the blood samples (27). In parallel, the interference from mitochondrial ctDNA fragments can be significantly eliminated by reducing the interval size of captured DNA fragments (28, 29), and the size selection strategy not only greatly reduces the cost of sequencing but also considerably decreases the false-positive rates of results by data analysis (30).

The sequence information carried by ctDNA can reflect the mutation load and the methylation features of tumor cells. ctDNA profiling facilitates their delineation not only on a genome-wide scale but also in some specific genes or intervals of the tumor genome. Some studies showed that the mutational spectrum constructed by ctDNA is highly consistent with that of tissue biopsy (31, 32). Besides, ctDNA, which comes from a broader range of tumor cells, represents the heterogeneity of the tumor mutational spectrum better than the tissue biopsy (31). The spatial heterogeneity with the tumor's continuous self-cloning and the temporal heterogeneity possibly resulting from drug resistance can be tracked by real-time monitoring in ctDNA fragments (33). An inspiring technology termed Cancer Personalized Profiling by deep sequencing (CAPP-Seq) preselected some specifically mutational exon regions by mining a large number of genetic mutations *in silico*. These exon-containing ctDNAs are subsequently extracted from serum cfDNAs using customized probes and then analyzed by high-throughput sequencing. This method could remarkably improve the detection sensitivity and specificity of ctDNAs by reducing the potential impact of stochastic noise and biological variability (34) (**Supplementary Figure 2**).

In addition, the methylation features of ctDNA reveal some epigenetic information of cancer patients. The methylation patterns can be maintained stably throughout the life span after *de novo* methylation (35), and the changes in the methylated patterns predict the risk of diseases (36). Because of the increased accuracy of high-throughput sequencing (HTS) technologies, the slight differences in methylation profiles between cancer patients and healthy cohorts shed light on the differential gene expression patterns at the epigenetic level and the relevance of epigenetic modification and tumor stage (37). For instance, the hypermethylation of tumor suppressor genes is strongly consistent with cancer occurrence, indicating that the methylation status of these modifications detected by ctDNA can play an essential role in the early detection of cancer and the determination of tissue of origin, and those patterns benefit machine learning for classification modeling (38).

Data mining has increasingly become a potential requirement for algorithm design of ctDNA detection. Given the rapid development in omics, the biological data in the open database online have increased exponentially, reforming the traditional data processing methods (39–41) (**Supplementary Figure 3**). By narrowing the scope of previous experimental data and using an appropriate workflow, the data mining system for ctDNA is simplified, accompanied by dramatically reduced costs of the whole research project. It provides the possibility for finding the new features of ctDNA hidden in the data structure to promote

further development of ctDNA capture (**Figure 1**). For example, Misawa et al. mined the transcriptome data and filtered out the abnormal methylations as biomarkers in ctDNA, which assists in designing a mathematical model of ctDNA detection to identify patients with human papillomavirus–associated oropharyngeal cancer (42).

TECHNICAL OBSTACLES AND POTENTIAL SOLUTIONS OF DATA PROCESSING IN ctDNA PROFILING

With the deepening understanding of biological features of ctDNA, the prevalence of ctDNA detection in cancer diagnosis inspired researchers. However, several technical shortcomings limit the clinical application of ctDNA detection.

Firstly, the sensitivity and specificity of ctDNA profiling are remarkably influenced by poor experimental conditions when facing complex biological characteristics (43). The trace amount and inevitable degradation of plasma ctDNA jeopardize ctDNA detection, especially when the blood sample is isolated and collected by centrifugation. Recent related studies demonstrate that plasma ctDNA loses about 50% after centrifugation (44, 45). The current blood storage manners are always accompanied by hemagglutination and extravasation, which considerably hamper ctDNA detection. Moreover, several commercial kits have been developed but show different extraction efficiencies and fragment size preferences, thereby challenging the repeatability and comparability of ctDNA detection resulting from different studies (46–49). Thus, the development of a universal standard protocol used for ctDNA extraction is essential in the future clinic application of ctDNA detection strategies.

Furthermore, the low signal-to-noise ratio remains a major problem for data processing of ctDNA detection. In addition to the low proportion of ctDNA in the serum cfDNA pools, as mentioned above, somatic mutations deriving from clonal hematopoietic (CH) and mitochondrial ctDNA also bring significant background noises. CH variants are cumulated with age, which could be attributed to the cloning expansion of stem cells carrying somatic mutations (50). Due to the high false-positive rate in ctDNA detection results, CH variants also interfere with the construction of the ctDNA mutation spectrum (51). Although mitochondrial ctDNA could be roughly excluded by size selection manner, the leaking information still exists during ctDNA detection (52). Given the above, the development of data analysis algorithms to increase signal-to-noise rate will facilitate the reliability of ctDNA as a tumor biomarker applied in clinical diagnosis. For instance, Nassiri et al. have developed a machine learning–based model to analyze the data generated from methylated HTS in ctDNA detection, increasing the accuracy of subtyping intracranial tumors (53). Moreover, CH variances produced by white blood cells are recognized by the combination of computational algorithms, then the false-positive rates of ctDNA detection would be decreased (54). With the help of statistical analysis and machine learning models, the CH variances spectrum can be built quickly and will be removed effectively by comparing it to the mutational spectrum of tumors constructed by ctDNA assays (30).

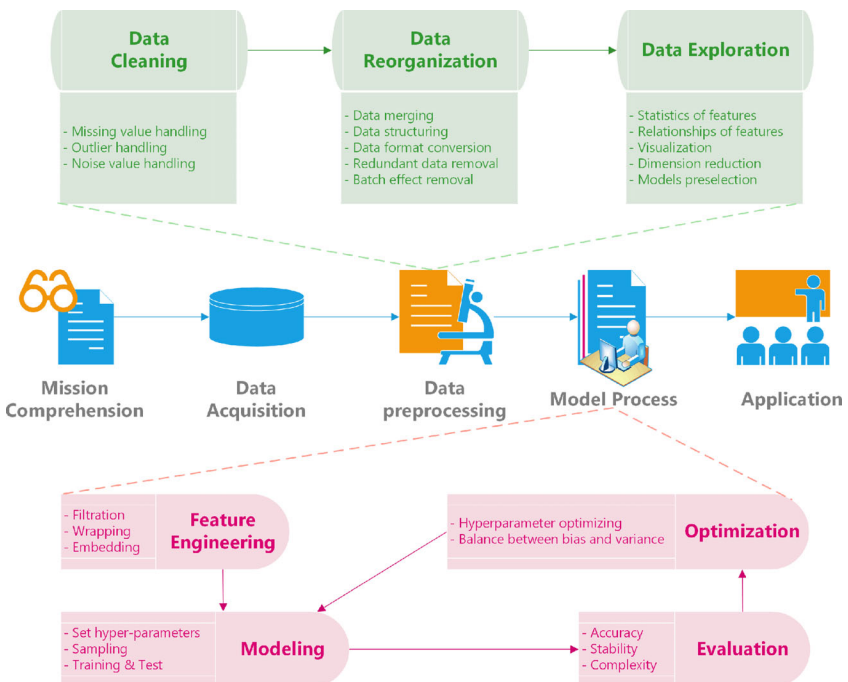

FIGURE 1 | Data mining process of ctDNA detection. ctDNA, circulating tumor DNA.

Additionally, the technological bias of HTS platforms inevitably interferes with the high-throughput ctDNA detection. These sequencing errors can be partially reduced or corrected. For instance, increased sequencing depth dilutes the error information (55), and the introduction of appropriate barcodes and indexes could evaluate the sequence duplication bias produced through polymerase chain reaction (PCR) amplification (56). The erroneous sequencing on barcodes, which affects the deduplication of unique ctDNA molecules and results in errors in aligning molecules to unique ctDNA, can be optimized by increasing the hamming edit distance between different barcodes (57). However, these additional barcodes occupy some part of reads and then reduce the actual length of target ctDNA to be sequenced, attributing to the limitation of the reading sequence length of long-read assembly technology. Therefore, the choice of proper barcodes used for HTS of ctDNA detection is the critical factor in resolving the inevitable sequencing errors, calling for new methods for pre- and post-sequencing error correction based on a statistical landscape.

CLINICAL RELEVANCE OF CURRENT ctDNA PROFILING TECHNOLOGIES

The clinical relevance of the ctDNA biomarker shows substantial potential in non-invasive liquid biopsy, which may benefit millions of patients for early detection of tumor (58, 59), determination of tissue of origin (37), prediction of therapeutic effect, especially for immunotherapies (60–62), and monitoring (15, 30). The dynamic risk stratification correlated to the tumor genesis could also be facilitated by ctDNA detection such as occupation, age, living habits, and even mutational signatures (63). With the aid of classification or non-supervisor clustering, ctDNA detection technologies are conspicuously improved in terms of accuracy, sensitivity, specificity, operational convenience, and reasonable cost.

The patterns of mutational spectrums or epigenetic profiles recognized by data mining uncover the particular clinical relevance of ctDNA detection. The genome-wide mutational landscape is conducive to the evaluation of tumor mutation burden (13), neoplasm staging (64), genotyping (11), and the choice of therapies (65). Meanwhile, the methylation profiles of ctDNA contribute to discriminating patients from healthy cohorts (37), differentiating cancer types (53), and identifying the primary tumor location (66). These profiles can complement each other in many aspects, though those meaningful patterns below them require plenty of modeling theories for recognition accuracy. The combination of mutation and methylation spectrums makes the acquirement of detailed genomic landscapes possible, provides multiple insights into the tumor heterogeneity, and evaluates the impact of tumor heterogeneity on the selection of therapies, such as non-responders or drug resistance (67, 68).

In addition to its non-invasiveness, near real-time monitoring and prognosis prediction are additional advantages of ctDNA detection over tissue biopsy (69, 70). For example, the concentration of ctDNA was correlated with the prognosis of patients treated with pembrolizumab (10). Furthermore, ctDNA detection, as an auxiliary method for low-dose computed tomography, can track the molecular minimal residual disease and predict the risk of recurrence for tumor-free patients (18, 71). Finally, the real-time information of ctDNA detection reflects patients' status and sheds light on the personalized profiling for each patient, which is essential for precision medicine (72).

FUTURE DIRECTIONS IMPROVING THE LIMIT OF DETECTION OF ctDNA

There is a definite clue that an evolution is happening in high-throughput ctDNA detection by introducing novel sequencing platforms, a combination of different biomarkers, and a development of new principles. New-generation sequencing technologies, such as nanopore sequencing, begin to be utilized in ctDNA detections (73). Compared with HTS technologies, nanopore sequencing exhibits real-time sequencing and long reads, resulting in its potentially broad application in the field of nucleic acid sequencing in the future (74). Moreover, nanopore sequencing is PCR-free, avoiding amplification bias and errors of PCR during the process of sequencing library preparation. Although nanopore sequencing remains to have some shortcomings in sequencing short DNA fragments, many efforts have been made to ameliorate these shortcomings (2, 75). For instance, Sun et al. have applied the solid-state nanopore to detect ctDNA originating from serum samples. This strategy cooperates with the hybridization chain reaction to amplify the

TABLE 1 | Comparison of techniques in ctDNA detection.

Techniques	Flux	Level	Sensitivity (%)	Specificity (%)	VAF or LOD (%)	Reference (PMID)
Lung-CLiP	HTS	somatic mutation	64, 82, and 100% for stages I, II, and III	98	0.01	32269342
iDES-enhanced CAPP-Seq	HTS	somatic mutation	90	96	0.02	27018799
CAPP-Seq	HTS	somatic mutation	50 for stage I, 100 for stages II–IV	96	0.02	24705333
TEC-Seq	HTS	somatic mutation	97.4	89	0.1	28814544
MCTA-Seq	HTS	methylation alteration	94	89	/	26516143
dPCR	PCR	somatic mutation	92.9	100	0.5	25324352
ARMS	PCR	somatic mutation	96.3	65.2	0.15	28868565
BEAMing	PCR	somatic mutation	90.4	93.5	0.001	28106345
MSP	PCR	methylation alteration	67	100	/	18006766

ctDNA, circulating tumor DNA; VAF, variant allele frequency; LOD, limit of detection. The symbol "/" means that we didn't found the exact data in that paper.

target's signals, improve data authenticity, and overcome the hurdles of nanopore application (76).

Combining multi-biomarkers in liquid biopsy, based on optimized models and algorithms, has a higher efficiency in tumor detections. The various biomarkers used as the inputs of the detection model have a complementary function because of their different sensitivity and specificity to patients. For example, combining exosome RNA and ctDNA in plasma, Krug et al. leveraged the threshold of a predefined model to detect EGFR mutations in non-small cell lung cancer, achieving a higher sensitivity than that of ctDNA detection alone (77). Cohen et al. utilized the protein biomarkers as a supplement to ctDNA detection, and a few patients with ctDNA undetectable were finally detected (78). Furthermore, the combination of multi-biomarkers provides the convenience of multi-parameters to machine learning in future liquid biopsy and promotes the development of detection tools in the diagnosis and prognosis for patients with cancer.

New principles, whether biological feature-based or data-driven, are the catalyzers of the ctDNA detection improvement. In the last decades, discovering new principles of ctDNA detection methods contributes to promoting the clinical application of this intriguing biomarker of liquid biopsy (**Table 1**). For example, the definition of recurrence index, an index equal to total unique patients with mutations covered per kb of an exon, has been introduced into CAPP-Seq as a selection principle that obviously improved the limit of detection of ctDNA (34). The continuous evolution of new technical principles of data analysis provides the substantial potential to ctDNA as a promising biomarker for its future clinical utility (79).

CONCLUSION

Embracing data science, ctDNA is a promising biomarker in cancer detection. ctDNA has several exciting characteristics, which could be handled to raise strategies to improve ctDNA detection performance. Herein, we reviewed data science that played an essential role in current strategies, such as data selection, data mining, and data correction, to overcome the technical obstacles in ctDNA detection. The recognition of the value of directing data processing indicates a possible trend to exploit ctDNA assays further. With the rapid development of data acquisition methodologies, modeling, and data processing algorithms, ctDNA detection enhanced its prevalent advantages in monitoring intrinsic tumor information. Novel high-throughput technology platforms and the combination of diverse biomarkers in liquid biopsy were also essential for this technology advancement. ctDNA-based liquid biopsies, as an alternative or even a substitutive choice of tissue biopsy, have significant clinical relevance in cancer diagnosis and prognosis. Subsequent efforts should be continued to promote the advancement of the detection technologies, theories, and principles accelerated by prosperously developed data science.

AUTHOR'S NOTE

The data of **Supplementary Figure 3** coming from the GEOdatabase, including the R script and Rdata file.

AUTHOR CONTRIBUTIONS

ML: writing—original draft, figure design, and visualization. SX: assistance with writing review and editing. CL: assistance with figure design and visualization. LiZ: necessary advice provision. LvZ: supervision, funding acquisition, writing review, and editing. All authors contributed to the article and approved the submitted version.

FUNDING

This review was supported by grants from the National Natural Science Foundation of China (31500686, 31870855), the "Huxiang Young Talents Plan" Project of Hunan Province (2019RS2030), the Natural Science Foundation of Hunan Province (2020JJ5657), Fund for NUDT Young Innovator Awards (20190104), and Postgraduate Scientific Research Innovation Project of Hunan Province.

ACKNOWLEDGMENTS

The authors thank ShineWrite for its linguistic assistance during this manuscript's preparation.

SUPPLEMENTARY MATERIAL

The Supplementary Material for this article can be found online at: https://www.frontiersin.org/articles/10.3389/fonc.2021.692322/full#supplementary-material

Supplementary Figure 1 | Origination of ctDNA. ctDNA, circulating tumor DNA; cfDNA, cell-free DNA.

Supplementary Figure 2 | The workflow of CAPP-Seq. CAPP-Seq, the Cancer Personalized Profiling by deep sequencing; ctDNA, circulating tumor DNA; cfDNA, cell-free DNA.

Supplementary Figure 3 | Rapid growth in the number of samples uploaded in the GEO (Gene Expression Omnibus) database.

REFERENCES

1. Mohan S, Foy V, Ayub M, Leong HS, Schofield P, Sahoo S, et al. Profiling of Circulating Free DNA Using Targeted and Genome-Wide Sequencing in Patients With SCLC. *J Thorac Oncol* (2020) 15(2):216–30. doi: 10.1016/j.jtho.2019.10.007
2. Li X, Zhang P, Dou L, Wang Y, Sun K, Zhang X, et al. Detection of Circulating Tumor Cells in Breast Cancer Patients by Nanopore Sensing With Aptamer-

Mediated Amplification. *ACS Sens* (2020) 5(8):2359–66. doi: 10.1021/acssensors.9b02537
3. Dawson SJ, Tsui DW, Murtaza M, Biggs H, Rueda OM, Chin SF, et al. Analysis of Circulating Tumor DNA to Monitor Metastatic Breast Cancer. *N Engl J Med* (2013) 368(13):1199–209. doi: 10.1056/NEJMoa1213261
4. Allegretti M, Casini B, Mandoj C, Benini S, Alberti L, Novello M, et al. Precision Diagnostics of Ewing's Sarcoma by Liquid Biopsy: Circulating EWS-FLI1 Fusion Transcripts. *Ther Adv Med Oncol* (2018) 10:1758835918774337. doi: 10.1177/1758835918774337
5. Jahr S, Hentze H, Englisch S, Hardt D, Fackelmayer FO, Hesch RD, et al. DNA Fragments in the Blood Plasma of Cancer Patients: Quantitations and Evidence for Their Origin From Apoptotic and Necrotic Cells. *Cancer Res* (2020) 61(4):1659–65. doi: cancerres.aacrjournals.org/content/61/4/1659
6. Bronkhorst AJ, Wentzel JF, Aucamp J, van Dyk E, du Plessis L, Pretorius PJ. Characterization of the Cell-Free DNA Released by Cultured Cancer Cells. *Biochim Biophys Acta* (2016) 1863(1):157–65. doi: 10.1016/j.bbamcr.2015.10.022
7. Jeppesen DK, Fenix AM, Franklin JL, Higginbotham JN, Zhang Q, Zimmerman LJ, et al. Reassessment of Exosome Composition. *Cell* (2019) 177(2):428–45.e18. doi: 10.1016/j.cell.2019.02.029
8. Mair R, Mouliere F, Smith CG, Chandrananda D, Gale D, Marass F, et al. Measurement of Plasma Cell-Free Mitochondrial Tumor DNA Improves Detection of Glioblastoma in Patient-Derived Orthotopic Xenograft Models. *Cancer Res* (2019) 79(1):220–30. doi: 10.1158/0008-5472.CAN-18-0074
9. Aravanis AM, Lee M, Klausner RD. Next-Generation Sequencing of Circulating Tumor DNA for Early Cancer Detection. *Cell* (2017) 168(4):571–4. doi: 10.1016/j.cell.2017.01.030
10. Bratman SV, Yang SYC, Iafolla MAJ, Liu Z, Hansen AR, Bedard PL, et al. Personalized Circulating Tumor DNA Analysis as a Predictive Biomarker in Solid Tumor Patients Treated With Pembrolizumab. *Nat Cancer* (2020) 1(9):873–81. doi: 10.1038/s43018-020-0096-5
11. Jayaram A, Wetterskog D, Attard G. Plasma DNA and Metastatic Castration-Resistant Prostate Cancer: The Odyssey to a Clinical Biomarker Test. *Cancer Discov* (2018) 8(4):392–4. doi: 10.1158/2159-8290.CD-18-0124
12. Chaudhuri AA, Chabon JJ, Lovejoy AF, Newman AM, Stehr H, Azad TD, et al. Early Detection of Molecular Residual Disease in Localized Lung Cancer by Circulating Tumor DNA Profiling. *Cancer Discov* (2017) 7(12):1394–403. doi: 10.1158/2159-8290.CD-17-0716
13. Ishii H, Azuma K, Sakai K, Naito Y, Matsuo N, Tokito T, et al. Determination of Somatic Mutations and Tumor Mutation Burden in Plasma by CAPP-Seq During Afatinib Treatment in NSCLC Patients Resistance to Osimertinib. *Sci Rep* (2020) 10(1):691. doi: 10.1038/s41598-020-57624-4
14. Diehl F, Schmidt K, Choti MA, Romans K, Goodman S, Li M, et al. Circulating Mutant DNA to Assess Tumor Dynamics. *Nat Med* (2008) 14(9):985–90. doi: 10.1038/nm.1789
15. Phallen J, Sausen M, Adleff V, Leal A, Hruban C, White J, et al. Direct Detection of Early-Stage Cancers Using Circulating Tumor DNA. *Sci Transl Med* (2017) 9(403):eaan2415. doi: 10.1126/scitranslmed.aan2415
16. Bettegowda C, Sausen M, Leary RJ, Kinde I, Wang Y, Agrawal N, et al. Detection of Circulating Tumor DNA in Early- and Late-Stage Human Malignancies. *Sci Transl Med* (2014) 6(224):224ra24. doi: 10.1126/scitranslmed.3007094
17. Blumendeller C, Boehme J, Frick M, Schulze M, Rinckleb A, Kyzirakos C, et al. Use of Plasma ctDNA as a Potential Biomarker for Longitudinal Monitoring of a Patient With Metastatic High-Risk Upper Tract Urothelial Carcinoma Receiving Pembrolizumab and Personalized Neoepitope-Derived Multipeptide Vaccinations: A Case Report. *J Immunother Cancer* (2021) 9(1):e001406. doi: 10.1136/jitc-2020-001406
18. Tie J, Wang Y, Tomasetti C, Li L, Springer S, Kinde I, et al. Circulating Tumor DNA Analysis Detects Minimal Residual Disease and Predicts Recurrence in Patients With Stage II Colon Cancer. *Sci Transl Med* (2016) 8(346):346ra92. doi: 10.1126/scitranslmed.aaf6219
19. Yang N, Li Y, Liu Z, Qin H, Du D, Cao X, et al. The Characteristics of ctDNA Reveal the High Complexity in Matching the Corresponding Tumor Tissues. *BMC Cancer* (2018) 18(1):319. doi: 10.1186/s12885-018-4199-7
20. Yong E. Cancer Biomarkers: Written in Blood. *Nature* (2014) 511(7511):524–6. doi: 10.1038/511524a
21. Diehl F, Li M, Dressman D, He Y, Shen D, Szabo S, et al. Detection and Quantification of Mutations in the Plasma of Patients With Colorectal Tumors. *Proc Natl Acad Sci U S A* (2005) 102(45):16368–73. doi: 10.1073/pnas.0507904102
22. Ivanov M, Baranova A, Butler T, Spellman P, Mileyko V. Non-Random Fragmentation Patterns in Circulating Cell-Free DNA Reflect Epigenetic Regulation. *BMC Genomics* (2015) 16 Suppl 13:S1. doi: 10.1186/1471-2164-16-S13-S1
23. Tamkovich SN, Kirushina NA, Voytsitskiy VE, Tkachuk VA, Laktionov PP. Features of Circulating DNA Fragmentation in Blood of Healthy Females and Breast Cancer Patients. *Adv Exp Med Biol* (2016) 924:47–51. doi: 10.1007/978-3-319-42044-8_10
24. Hellwig S, Nix DA, Gligorich KM, O'Shea JM, Thomas A, Fuertes CL, et al. Automated Size Selection for Short Cell-Free DNA Fragments Enriches for Circulating Tumor DNA and Improves Error Correction During Next Generation Sequencing. *PLoS One* (2018) 13(7):e0197333. doi: 10.1371/journal.pone.0197333
25. Mouliere F, Robert B, Arnau Peyrotte E, Del Rio M, Ychou M, Molina F, et al. High Fragmentation Characterizes Tumour-Derived Circulating DNA. *PLoS One* (2011) 6(9):e23418. doi: 10.1371/journal.pone.0023418
26. Tamkovich S, Laktionov P. Cell-Surface-Bound Circulating DNA in the Blood: Biology and Clinical Application. *IUBMB Life* (2019) 71(9):1201–10. doi: 10.1002/iub.2070
27. Mouliere F, Chandrananda D, Piskorz AM, Moore EK, Morris J, Ahlborn LB, et al. Enhanced Detection of Circulating Tumor DNA by Fragment Size Analysis. *Sci Transl Med* (2018) 10(466):eaat4921. doi: 10.1126/scitranslmed.aat4921
28. Zhang R, Nakahira K, Guo X, Choi AM, Gu Z. Very Short Mitochondrial DNA Fragments and Heteroplasmy in Human Plasma. *Sci Rep* (2016) 6:36097. doi: 10.1038/srep36097
29. Jiang P, Chan CW, Chan KC, Cheng SH, Wong J, Wong VW, et al. Lengthening and Shortening of Plasma DNA in Hepatocellular Carcinoma Patients. *Proc Natl Acad Sci U S A* (2015) 112(11):E1317–25. doi: 10.1073/pnas.1500076112
30. Chabon JJ, Hamilton EG, Kurtz DM, Esfahani MS, Moding EJ, Stehr H, et al. Integrating Genomic Features for Non-Invasive Early Lung Cancer Detection. *Nature* (2020) 580(7802):245–51. doi: 10.1038/s41586-020-2140-0
31. Strickler JH, Loree JM, Ahronian LG, Parikh AR, Niedzwiecki D, Pereira AAL, et al. Genomic Landscape of Cell-Free DNA in Patients With Colorectal Cancer. *Cancer Discov* (2018) 8(2):164–73. doi: 10.1158/2159-8290.CD-17-1009
32. Adalsteinsson VA, Ha G, Freeman SS, Choudhury AD, Stover DG, Parsons HA, et al. Scalable Whole-Exome Sequencing of Cell-Free DNA Reveals High Concordance With Metastatic Tumors. *Nat Commun* (2017) 8(1):1324. doi: 10.1038/s41467-017-00965-y
33. De Mattos-Arruda L, Weigelt B, Cortes J, Won HH, Ng CKY, Nuciforo P, et al. Capturing Intra-Tumor Genetic Heterogeneity by De Novo Mutation Profiling of Circulating Cell-Free Tumor DNA: A Proof-of-Principle. *Ann Oncol* (2014) 25(9):1729–35. doi: 10.1093/annonc/mdu239
34. Newman AM, Bratman SV, To J, Wynne JF, Eclov NC, Modlin LA, et al. An Ultrasensitive Method for Quantitating Circulating Tumor DNA With Broad Patient Coverage. *Nat Med* (2014) 20(5):548–54. doi: 10.1038/nm.3519
35. Dor Y, Cedar H. Principles of DNA Methylation and Their Implications for Biology and Medicine. *Lancet* (2018) 392(10149):777–86. doi: 10.1016/s0140-6736(18)31268-6
36. Easwaran H, Johnstone SE, Van Neste L, Ohm J, Mosbruger T, Wang Q, et al. A DNA Hypermethylation Module for the Stem/Progenitor Cell Signature of Cancer. *Genome Res* (2012) 22(5):837–49. doi: 10.1101/gr.131169.111
37. Moss J, Magenheim J, Neiman D, Zemmour H, Loyfer N, Korach A, et al. Comprehensive Human Cell-Type Methylation Atlas Reveals Origins of Circulating Cell-Free DNA in Health and Disease. *Nat Commun* (2018) 9(1):5068. doi: 10.1038/s41467-018-07466-6
38. Chan KC, Jiang P, Chan CW, Sun K, Wong J, Hui EP, et al. Noninvasive Detection of Cancer-Associated Genome-Wide Hypomethylation and Copy Number Aberrations by Plasma DNA Bisulfite Sequencing. *Proc Natl Acad Sci U S A* (2013) 110(47):18761–8. doi: 10.1073/pnas.1313995110
39. Resteghini C, Trama A, Borgonovi E, Hosni H, Corrao G, Orlandi E, et al. Big Data in Head and Neck Cancer. *Curr Treat Options Oncol* (2018) 19(12):62. doi: 10.1007/s11864-018-0585-2
40. Ngiam KY, Khor IW. Big Data and Machine Learning Algorithms for Health-Care Delivery. *Lancet Oncol* (2019) 20(5):e262–e73. doi: 10.1016/S1470-2045(19)30149-4

41. Kantarjian H, Yu PP. Artificial Intelligence, Big Data, and Cancer. *JAMA Oncol* (2015) 1(5):573–4. doi: 10.1001/jamaoncol.2015.1203
42. Misawa K, Imai A, Matsui H, Kanai A, Misawa Y, Mochizuki D, et al. Identification of Novel Methylation Markers in HPV-Associated Oropharyngeal Cancer: Genome-Wide Discovery, Tissue Verification and Validation Testing in ctDNA. *Oncogene* (2020) 39(24):4741–55. doi: 10.1038/s41388-020-1327-z
43. Markus H, Contente-Cuomo T, Farooq M, Liang WS, Borad MJ, Sivakumar S, et al. Evaluation of Pre-Analytical Factors Affecting Plasma DNA Analysis. *Sci Rep* (2018) 8(1):7375. doi: 10.1038/s41598-018-25810-0
44. Rikkert LG, van der Pol E, van Leeuwen TG, Nieuwland R, Coumans FAW. Centrifugation Affects the Purity of Liquid Biopsy-Based Tumor Biomarkers. *Cytomet A* (2018) 93(12):1207–12. doi: 10.1002/cyto.a.23641
45. van der Pol Y, Mouliere F. Toward the Early Detection of Cancer by Decoding the Epigenetic and Environmental Fingerprints of Cell-Free DNA. *Cancer Cell* (2019) 36(4):350–68. doi: 10.1016/j.ccell.2019.09.003
46. Sorber L, Zwaenepoel K, Deschoolmeester V, Roeyen G, Lardon F, Rolfo C, et al. A Comparison of Cell-Free DNA Isolation Kits: Isolation and Quantification of Cell-Free DNA in Plasma. *J Mol Diagn* (2017) 19(1):162–8. doi: 10.1016/j.jmoldx.2016.09.009
47. Worm Orntoft MB, Jensen SO, Hansen TB, Bramsen JB, Andersen CL. Comparative Analysis of 12 Different Kits for Bisulfite Conversion of Circulating Cell-Free DNA. *Epigenetics* (2017) 12(8):626–36. doi: 10.1080/15592294.2017.1334024
48. Torga G, Pienta KJ. Patient-Paired Sample Congruence Between 2 Commercial Liquid Biopsy Tests. *JAMA Oncol* (2018) 4(6):868–70. doi: 10.1001/jamaoncol.2017.4027
49. Kuderer NM, Burton KA, Blau S, Rose AL, Parker S, Lyman GH, et al. Comparison of 2 Commercially Available Next-Generation Sequencing Platforms in Oncology. *JAMA Oncol* (2017) 3(7):996–8. doi: 10.1001/jamaoncol.2016.4983
50. Genovese G, Kahler AK, Handsaker RE, Lindberg J, Rose SA, Bakhoum SF, et al. Clonal Hematopoiesis and Blood-Cancer Risk Inferred From Blood DNA Sequence. *N Engl J Med* (2014) 371(26):2477–87. doi: 10.1056/NEJMoa1409405
51. Hu Y, Ulrich BC, Supplee J, Kuang Y, Lizotte PH, Feeney NB, et al. False-Positive Plasma Genotyping Due to Clonal Hematopoiesis. *Clin Cancer Res* (2018) 24(18):4437–43. doi: 10.1158/1078-0432.CCR-18-0143
52. Weerts MJA, Timmermans EC, van de Stolpe A, Vossen R, Anvar SY, Foekens JA, et al. Tumor-Specific Mitochondrial DNA Variants Are Rarely Detected in Cell-Free DNA. *Neoplasia* (2018) 20(7):687–96. doi: 10.1016/j.neo.2018.05.003
53. Nassiri F, Chakravarthy A, Feng S, Shen SY, Nejad R, Zuccato JA, et al. Detection and Discrimination of Intracranial Tumors Using Plasma Cell-Free DNA Methylomes. *Nat Med* (2020) 26(7):1044–7. doi: 10.1038/s41591-020-0932-2
54. Zhang Y, Yao Y, Xu Y, Li L, Gong Y, Zhang K, et al. Pan-Cancer Circulating Tumor DNA Detection in Over 10,000 Chinese Patients. *Nat Commun* (2021) 12(1):11. doi: 10.1038/s41467-020-20162-8
55. Goodwin S, McPherson JD, McCombie WR. Coming of Age: Ten Years of Next-Generation Sequencing Technologies. *Nat Rev Genet* (2016) 17(6):333–51. doi: 10.1038/nrg.2016.49
56. Marx V. How to Deduplicate PCR. *Nat Methods* (2017) 14(5):473–6. doi: 10.1038/nmeth.4268
57. Newman AM, Lovejoy AF, Klass DM, Kurtz DM, Chabon JJ, Scherer F, et al. Integrated Digital Error Suppression for Improved Detection of Circulating Tumor DNA. *Nat Biotechnol* (2016) 34(5):547–55. doi: 10.1038/nbt.3520
58. Yokoi K, Yamashita K, Watanabe M. Analysis of DNA Methylation Status in Bodily Fluids for Early Detection of Cancer. *Int J Mol Sci* (2017) 18(4):735. doi: 10.3390/ijms18040735
59. Wan N, Weinberg D, Liu TY, Niehaus K, Ariazi EA, Delubac D, et al. Machine Learning Enables Detection of Early-Stage Colorectal Cancer by Whole-Genome Sequencing of Plasma Cell-Free DNA. *BMC Cancer* (2019) 19(1):832. doi: 10.1186/s12885-019-6003-8
60. Goldberg SB, Narayan A, Kole AJ, Decker RH, Teysir J, Carriero NJ, et al. Early Assessment of Lung Cancer Immunotherapy Response via Circulating Tumor DNA. *Clin Cancer Res* (2018) 24(8):1872–80. doi: 10.1158/1078-0432.CCR-17-1341
61. Lee JH, Long GV, Menzies AM, Lo S, Guminski A, Whitbourne K, et al. Association Between Circulating Tumor DNA and Pseudoprogression in Patients With Metastatic Melanoma Treated With Anti-Programmed Cell Death 1 Antibodies. *JAMA Oncol* (2018) 4(5):717–21. doi: 10.1001/jamaoncol.2017.5332
62. Wang Z, Duan J, Cai S, Han M, Dong H, Zhao J, et al. Assessment of Blood Tumor Mutational Burden as a Potential Biomarker for Immunotherapy in Patients With Non-Small Cell Lung Cancer With Use of a Next-Generation Sequencing Cancer Gene Panel. *JAMA Oncol* (2019) 5(5):696–702. doi: 10.1001/jamaoncol.2018.7098
63. Carroll PR, Parsons JK, Andriole G, Bahnson RR, Castle EP, Catalona WJ, et al. NCCN Guidelines Insights: Prostate Cancer Early Detection, Version 2.2016. *J Natl Compr Canc Netw* (2016) 14(5):509–19. doi: 10.6004/jnccn.2016.0060
64. Song CX, Yin S, Ma L, Wheeler A, Chen Y, Zhang Y, et al. 5-Hydroxymethylcytosine Signatures in Cell-Free DNA Provide Information About Tumor Types and Stages. *Cell Res* (2017) 27(10):1231–42. doi: 10.1038/cr.2017.106
65. Goodall J, Mateo J, Yuan W, Mossop H, Porta N, Miranda S, et al. Circulating Cell-Free DNA to Guide Prostate Cancer Treatment With PARP Inhibition. *Cancer Discov* (2017) 7(9):1006–17. doi: 10.1158/2159-8290.CD-17-0261
66. Sun K, Jiang P, Chan KC, Wong J, Cheng YK, Liang RH, et al. Plasma DNA Tissue Mapping by Genome-Wide Methylation Sequencing for Noninvasive Prenatal, Cancer, and Transplantation Assessments. *Proc Natl Acad Sci U S A* (2015) 112(40):E5503–12. doi: 10.1073/pnas.1508736112
67. Kim MS, Yamashita K, Chae YK, Tokumaru Y, Chang X, Zahurak M, et al. A Promoter Methylation Pattern in the N-Methyl-D-Aspartate Receptor 2B Gene Predicts Poor Prognosis in Esophageal Squamous Cell Carcinoma. *Clin Cancer Res* (2007) 13(22 Pt 1):6658–65. doi: 10.1158/1078-0432.CCR-07-1178
68. Claus R, Lucas DM, Stilgenbauer S, Ruppert AS, Yu L, Zucknick M, et al. Quantitative DNA Methylation Analysis Identifies a Single CpG Dinucleotide Important for ZAP-70 Expression and Predictive of Prognosis in Chronic Lymphocytic Leukemia. *J Clin Oncol* (2012) 30(20):2483–91. doi: 10.1200/JCO.2011.39.3090
69. Forshew T, Murtaza M, Parkinson C, Gale D, Tsui DW, Kaper F, et al. Noninvasive Identification and Monitoring of Cancer Mutations by Targeted Deep Sequencing of Plasma DNA. *Sci Transl Med* (2012) 4(136):136ra68. doi: 10.1126/scitranslmed.3003726
70. Burnham P, Dadhania D, Heyang M, Chen F, Westblade LF, Suthanthiran M, et al. Urinary Cell-Free DNA is a Versatile Analyte for Monitoring Infections of the Urinary Tract. *Nat Commun* (2018) 9(1):2412. doi: 10.1038/s41467-018-04745-0
71. Comino-Mendez I, Turner N. Predicting Relapse With Circulating Tumor DNA Analysis in Lung Cancer. *Cancer Discov* (2017) 7(12):1368–70. doi: 10.1158/2159-8290.CD-17-1086
72. Girotti MR, Gremel G, Lee R, Galvani E, Rothwell D, Viros A, et al. Application of Sequencing, Liquid Biopsies, and Patient-Derived Xenografts for Personalized Medicine in Melanoma. *Cancer Discov* (2016) 6(3):286–99. doi: 10.1158/2159-8290.CD-15-1336
73. Burck N, Gilboa T, Gadi A, Patkin Nehrer M, Schneider RJ, Meller A. Nanopore Identification of Single Nucleotide Mutations in Circulating Tumor DNA by Multiplexed Ligation. *Clin Chem* (2021) 67(5):753–62. doi: 10.1093/clinchem/hvaa328
74. Deamer D, Akeson M, Branton D. Three Decades of Nanopore Sequencing. *Nat Biotechnol* (2016) 34(5):518–24. doi: 10.1038/nbt.3423
75. Martignano F, Munagala U, Crucitta S, Mingrino A, Semeraro R, Del Re M, et al. Nanopore Sequencing From Liquid Biopsy: Analysis of Copy Number Variations From Cell-Free DNA of Lung Cancer Patients. *Mol Cancer* (2021) 20(1):32. doi: 10.1186/s12943-021-01327-5
76. Sun H, Yao F, Su Z, Kang XF. Hybridization Chain Reaction (HCR) for Amplifying Nanopore Signals. *Biosens Bioelectron* (2020) 150:111906. doi: 10.1016/j.bios.2019.111906
77. Krug AK, Enderle D, Karlovich C, Priewasser T, Bentink S, Spiel A, et al. Improved EGFR Mutation Detection Using Combined Exosomal RNA and Circulating Tumor DNA in NSCLC Patient Plasma. *Ann Oncol* (2018) 29(3):700–6. doi: 10.1093/annonc/mdx765
78. Cohen JD, Javed AA, Thoburn C, Wong F, Tie J, Gibbs P, et al. Combined Circulating Tumor DNA and Protein Biomarker-Based Liquid Biopsy for the Earlier Detection of Pancreatic Cancers. *Proc Natl Acad Sci U S A* (2017) 114(38):10202–7. doi: 10.1073/pnas.1704961114
79. Schiff R, Jeselsohn R. Is ctDNA the Road Map to the Landscape of the Clonal Mutational Evolution in Drug Resistance? Lessons From the PALOMA-3

Study and Implications for Precision Medicine. *Cancer Discov* (2018) 8 (11):1352–4. doi: 10.1158/2159-8290.CD-18-1084

Conflict of Interest: The authors declare that the research was conducted in the absence of any commercial or financial relationships that could be construed as a potential conflict of interest.

Copyright © 2021 Li, Xie, Lu, Zhu and Zhu. This is an open-access article distributed under the terms of the Creative Commons Attribution License (CC BY). The use, distribution or reproduction in other forums is permitted, provided the original author(s) and the copyright owner(s) are credited and that the original publication in this journal is cited, in accordance with accepted academic practice. No use, distribution or reproduction is permitted which does not comply with these terms.

frontiers in Oncology

CASE REPORT
published: 26 July 2021
doi: 10.3389/fonc.2021.652683

Case Report: Circulating Tumor DNA Fraction Analysis Using Ultra-Low-Pass Whole-Genome Sequencing Correlates Response to Chemoradiation and Recurrence in Stage IV Small-Cell Carcinoma of the Cervix - A Longitudinal Study

Ata Abbas[1‡], Morgan Gruner[2‡], Jennifer Karohl[2], Peter G. Rose[2], Amy Joehlin-Price[3], Daniel Stover[4] and Haider Mahdi[2,5,6†]*

[1] Division of Hematology and Oncology, Department of Medicine, Case Western Reserve University, Cleveland, OH, United States, [2] Division of Gynecologic Oncology, Obstetrics, Gynecology and Women's Health Institute, Cleveland Clinic, Cleveland, OH, United States, [3] Department of Anatomic Pathology, Pathology and Laboratory Medicine Institute, Cleveland Clinic, Cleveland, OH, United States, [4] Division of Medical Oncology, The Stefanie Spielman Comprehensive Breast Center, The James Cancer Hospital and Solove Research Institute at The Ohio State University Wexner Medical Center, Columbus, OH, United States, [5] Translational Hematology Oncology Research Department, Taussig Cancer Institute, Cleveland Clinic, Cleveland, OH, United States, [6] Genomic Medicine Institute, Lerner Research Institute, Cleveland Clinic, Cleveland, OH, United States

Neuroendocrine carcinoma of the cervix is a rare and aggressive form of cervical cancer that presents with frequent metastasis at diagnosis and high recurrence rates. Primary treatment is multimodal, which often includes chemotherapy with or without radiation therapy. There are no data available to guide treatment for recurrence, and second-line therapies are extrapolated from small-cell lung carcinoma data. Close monitoring of these patients for recurrence is paramount. Evaluation of circulating tumor DNA (ctDNA) in the peripheral blood is an attractive approach due to its non-invasive nature. Ultra-low-pass whole-genome sequencing (ULP-WGS) can assess tumor burden and response to therapy and predict recurrence; however, data are lacking regarding the role of ULP-WGS in small-cell carcinoma of the cervix. This study demonstrates a patient whose response to chemotherapy and cancer recurrence was accurately monitored by ctDNA analysis using ULP-WGS and confirmed with radiologic imaging findings.

Keywords: ctDNA, ULP-WGS, tumor fraction, response to chemo-radiation, small cell carcinoma, cervix

OPEN ACCESS

Edited by:
George Calin, University of Texas MD Anderson Cancer Center, United States

Reviewed by:
Pavel Sluka, Monash University, Australia
Yusra Shao, Wayne State University, United States

****Correspondence:***
Haider Mahdi
mahdihs@upmc.edu

†Present address:
Haider Mahdi, Magee Women's Hospital and Magee Women's Research Institute, University of Pittsburgh Medical Center, Pittsburgh, PA, United States

‡These authors have contributed equally to this work

Specialty section:
This article was submitted to Molecular and Cellular Oncology, a section of the journal Frontiers in Oncology

Received: *12 January 2021*
Accepted: *08 July 2021*
Published: *26 July 2021*

Citation:
Abbas A, Gruner M, Karohl J, Rose PG, Joehlin-Price A, Stover D and Mahdi H (2021) Case Report: Circulating Tumor DNA Fraction Analysis Using Ultra-Low-Pass Whole-Genome Sequencing Correlates Response to Chemoradiation and Recurrence in Stage IV Small-Cell Carcinoma of the Cervix: A Longitudinal Study. Front. Oncol. 11:652683. doi: 10.3389/fonc.2021.652683

BACKGROUND

Neuroendocrine carcinoma (NEC) of the cervix is a rare form of cervical cancer and accounts for only 2% of all invasive cervical cancers (1–3). The majority are small-cell carcinomas, which tend to behave aggressively; are characterized by a high mitotic rate, extensive necrosis, high propensity for lymphovascular space invasion (LVSI); and are frequently associated with HPV 18 (4, 5). NECs of

the cervix are highly aggressive; therefore, they require a multimodality treatment approach, which often includes platinum/etoposide-based chemotherapy with or without radiation (6). Gardner et al. published the SGO clinical document that provided treatment guidelines highlighting radical excision and chemotherapy for early-stage disease (7). NEC of the cervix tends to affect young women with a median age of 37 years. The prognosis is poor, usually a short clinical course with a median survival of less than 24 months (8, 9). In patients with recurrent disease, data to guide treatment decisions are absent for this rare cancer subtype. Second-line drugs are mostly extrapolated from small-cell lung cancer (SCLC), including chemotherapy like topotecan, paclitaxel, or VAC combination chemotherapy. However, these regimens are toxic with limited activity. Recently, the role of immunotherapy with immune checkpoint inhibition has been explored in SCLC and other high-grade neuroendocrine carcinomas (10, 11). Even though the benefit is restricted to small subgroups, the data is limited in NEC of the cervix or other gynecologic origin. Recently, Frumovitz et al. reported low activity of pembrolizumab in patients with recurrent small-cell carcinoma of the cervix and other lower female genital tract (12).

Evaluation of circulating tumor DNA (ctDNA) in the peripheral blood of patients with solid tumors represents an attractive approach given its non-invasive nature and the potential to do a serial evaluation at the time of diagnosis, during therapy, and at follow-up (13–15). However, the extent of the shedding of tumor DNA into the peripheral blood depends on many factors, including the type of cancer, the extent of disease, visceral metastasis, etc. The impact of ctDNA on the management of solid tumors has been highlighted in several aspects, including somatic genomic characterization, therapy selection, and tumor fraction, as well as molecular residual disease to predict tumor burden, prognosis, response, and resistance to therapy, and disease recurrence (15–18).

Ultra-low-pass whole-genome sequencing (ULP-WGS) represents an attractive approach to assess tumor burden and therapeutic response/resistance, given that it is affordable, is cost-effective, and does assess the whole genome with low coverage (0.1 x coverage) (18, 19). The data on the role of ctDNA in general and specifically ULP-WGS in predicting prognosis, response to chemoradiation, and recurrence in small-cell carcinoma of the cervix are lacking. ULP-WGS could be a potentially promising approach given the aggressive nature of this cancer and the tendency for the metastatic spread at the time of diagnosis and recurrences. Further, these patients tend to have a scant amount of tissue that limits extensive genomic characterization because most of them are treated with chemotherapy or chemoradiation rather than surgical resection.

In this study, we sought to investigate the tumor fraction and copy number alteration in ctDNA using ULP-WGS in the peripheral blood of a patient diagnosed with stage IV small-cell carcinoma of the cervix who underwent chemotherapy with cisplatin and etoposide concurrent with pelvic radiation and achieved complete clinical response followed by recurrent disease in the liver, adrenal gland, and brain within 6 months. Here, we show that tumor fraction assessment at the time of diagnosis and during treatment correlated with response to chemoradiation therapy and recurrent disease.

CASE PRESENTATION

Clinical Case Course

A 32-year-old female with a non-contributory past medical history presented to medical care with the complaint of brown vaginal discharge and an abnormal sensation in her vagina. A 2.5–3 cm pedunculated mass was noted on examination with cervical biopsy pathology positive for invasive high-grade neuroendocrine carcinoma, most consistent with small-cell type and associated with endocervical adenocarcinoma *in situ*. Immunostaining for p63, p40, synaptophysin, and chromogranin was performed to assist with cell typing. The carcinoma cells express neuroendocrine markers synaptophysin and chromogranin (**Figures 1A, B**). P63 stains were weakly positive, and the p40 stain was negative (data not shown). She then underwent MRI and PET/CT imaging, which was positive for uptake in the cervix region. Metastases in the liver and right adrenal gland were also noted (**Figure 1C**), leading to the final diagnosis of stage IV invasive high-grade small cell NEC of the cervix. The patient began therapy with cisplatin 75 D1 and etoposide D1, 2, 3 - Q21 days. She was transitioned to carboplatin AUC5 after C2 due to severe tinnitus. After three cycles of the above chemotherapy, a CT scan was performed, which demonstrated decreased hepatic metastasis and complete resolution of a right adrenal metastatic lesion. The patient received four additional cycles of the aforementioned carboplatin and etoposide and then underwent a repeat PET/CT scan, which demonstrated complete interval resolution of the previously seen hypermetabolic cervical mass, hepatic mass, and adrenal mass (**Figure 2A**). The patient then underwent two additional cycles (consolidation cycles) of carboplatin and etoposide after imaging confirmation of disease resolution. Simultaneously, during the consolidation chemotherapy cycles, the patient underwent EBRT to the pelvis with a total dose of 4,500 cGy in 25 fractions and HDR brachytherapy to cervix and parametria with a total dose of 1,400 cGy in two fractions. The patient completed therapy and was with no evidence of disease for 5 months. One year after her initial diagnosis and 5 months after completing therapy, she presented with new-onset dizziness. She underwent imaging, which demonstrated an interval development of hepatic and right adrenal metastatic disease (**Figure 2B**, right), as well as a heterogeneously enhancing 2.9 cm likely intra-axial mass involving the right temporal lobe (**Figure 2B**, left). She received a gamma knife to two brain targets—the right temporal lobe and left insular regions. She was then started on ipilimumab plus nivolumab immunotherapy. Newly detected spinal nerve root metastases and leptomeningeal disease were discovered, for which she underwent 20 Gy in five fractions of palliative RT to the spine. Shortly thereafter, the patient was admitted to the hospital in the

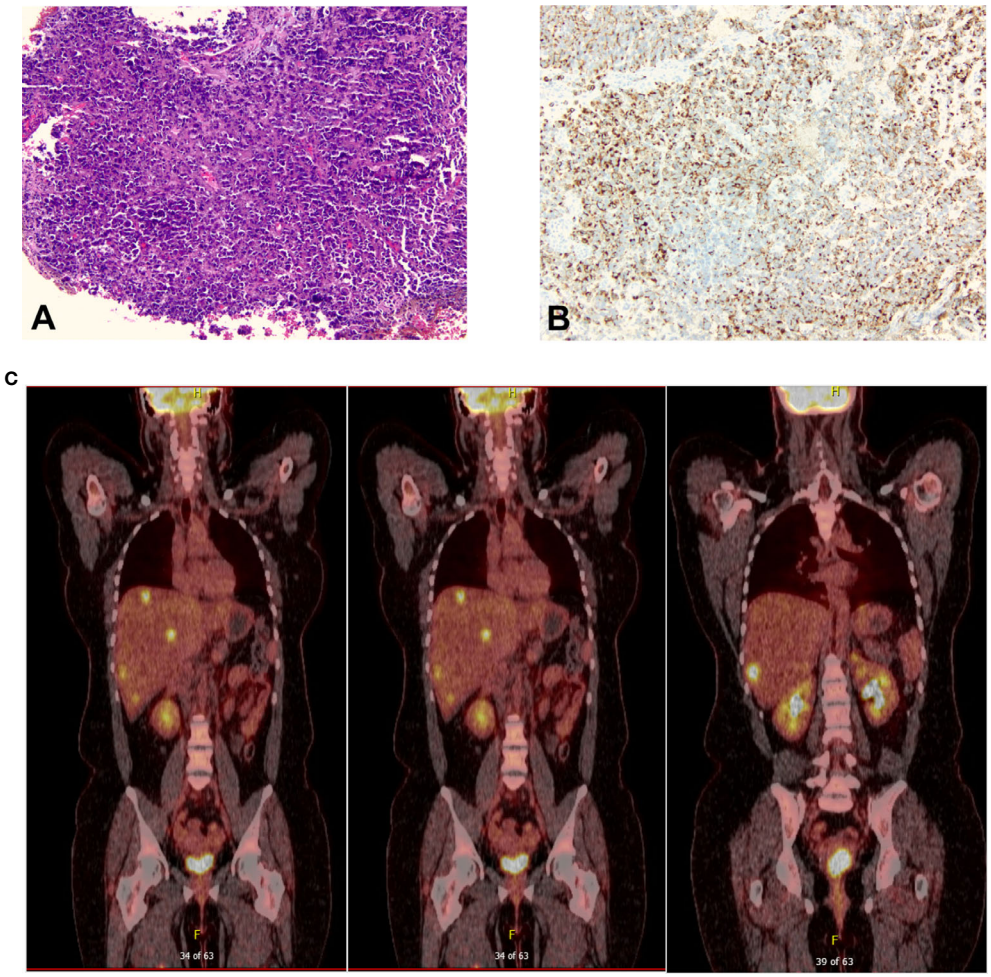

FIGURE 1 | **(A)** The initial cervical biopsy (100× magnification) demonstrated extensive mitotic activity, high-grade nuclei with hyperchromasia and nuclear molding, scant cytoplasm, and ill-defined cell borders, all characteristic of small-cell carcinoma. **(B)** The carcinoma was diffusely positive for chromogranin (100× magnification) and synaptophysin (not pictured). **(C)** Positron Emission Tomography/Computed Tomography (PET/CT) scan at the time of diagnosis that showed evidence of cervical disease, multiple hepatic metastases, and right adrenal gland metastasis.

setting of altered mental status and noted to have disease progression. The family selected hospice care, and the patient expired 15 months after the initial diagnosis (**Figure 3**).

Correlation of Tumor Fraction (TFx) Determined Using ULP-WGS With Clinical Outcome

To establish TFx as a non-invasive biomarker using cell-free DNA, first, we sought to investigate the relationship of TFx with disease burden at the time of diagnosis and during chemoradiation. We focused on the time of diagnosis, during treatment, and at the completion of treatment. At the time of diagnosis, her tumor TFx was 26%, with wide variability in somatic copy number alteration (sCNA). After completion of chemotherapy, her TFx dropped to 5%, which coincided with the finding of complete response by her PET/CT scan. Then after completion of pelvic radiation a month after, her TFx was 2.5%. Then 5 months later, she had another evaluation, and her TFx was 36%. This was consistent with the diagnosis of recurrent disease that was evident by imaging, confirming recurrent brain, multiple hepatic, and right adrenal metastasis (**Figures 4A, B**).

Comparison of Somatic Copy Number Alteration (sCNA) Between Primary Disease at Initial Diagnosis and Recurrent Disease

We sought to investigate sCNA to see if there is a difference between the primary and recurrent disease and if there are interval changes. sCNA at the time of recurrence was comparable with that at the time of initial diagnosis, but with higher amplitude, especially for amplification (**Figure 4A**). Similarly, genes-level copy number data were comparable too with evidence of additional gains at the time of recurrence as evident in selected genes that correspond to certain pathways like

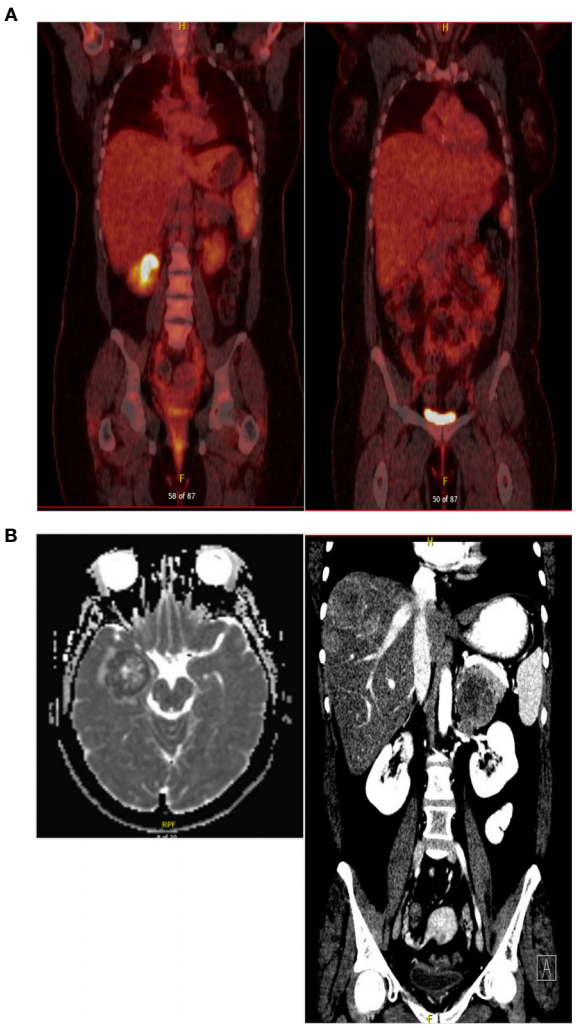

FIGURE 2 | **(A)** PET/CT scan after completing chemoradiation therapy showed no evidence of disease. **(B)** At the time of diagnosis of recurrent disease, brain MRI and CT scan of the abdomen confirming brain metastasis and multiple hepatic metastatic disease.

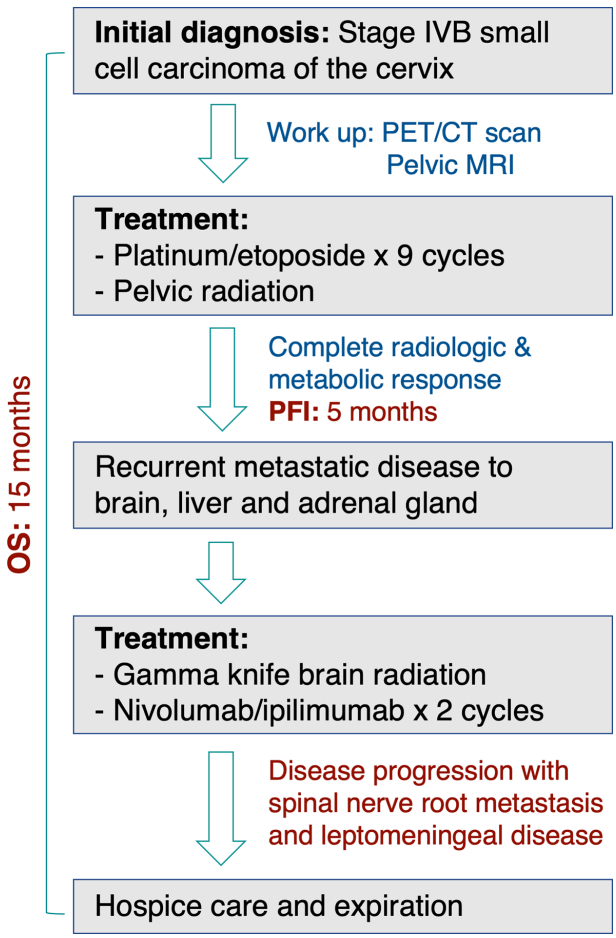

FIGURE 3 | A schematic representation showing treatment course and timeline.

PI3K/AKT, RAS/RAF, DNA-damage response, MYC/MCL, TP53, RB1, and others (**Figure 4C**).

DISCUSSION

Here, we present a case study with longitudinal monitoring of sCNA and tumor fraction using ULP-WGS in cell-free DNA of a patient diagnosed with stage IVB small-cell carcinoma of the cervix. We demonstrate that tumor fractions correlate positively with radiologic disease burden and response to chemoradiation therapy. Our data show evidence of tumor shedding into the peripheral blood at the time of diagnosis of small-cell NEC of the cervix. The decline of tumor fractions from 26 to 2.5% after treatments was correlated with PET/CT scans. Furthermore, a spike to 36% at the time of recurrent disease was also correlated with the radiologic evidence of recurrent metastatic disease. This highlights the potential use of measuring tumor fractions in cell-free DNA using ULP-WGS to monitor tumor burden, response to therapy, and disease recurrence in high-grade neuroendocrine carcinoma of the cervix.

This is the first report to the best of our knowledge that highlights the role of serial assessment of tumor fractions using ULP-WGS in NEC of the cervix. Small-cell NEC of the cervix is rare, highly aggressive, and has a poor prognosis. ctDNA may play a role in monitoring disease burden, assessing response to therapy, and predicting disease recurrence during surveillance. It is likely a more acceptable approach to these patients, especially during surveillance, due to the overall ease and safer blood draw. Further, these cancers tend to be metastatic at the time of diagnosis and less likely to be treated with surgical resection. Given that, getting adequate tissue is usually problematic, and often, there is scant tissue from biopsy to obtain a diagnosis. Therefore, ctDNA can be used to genomically characterize these cancers at diagnosis and monitor recurrence and disease progression.

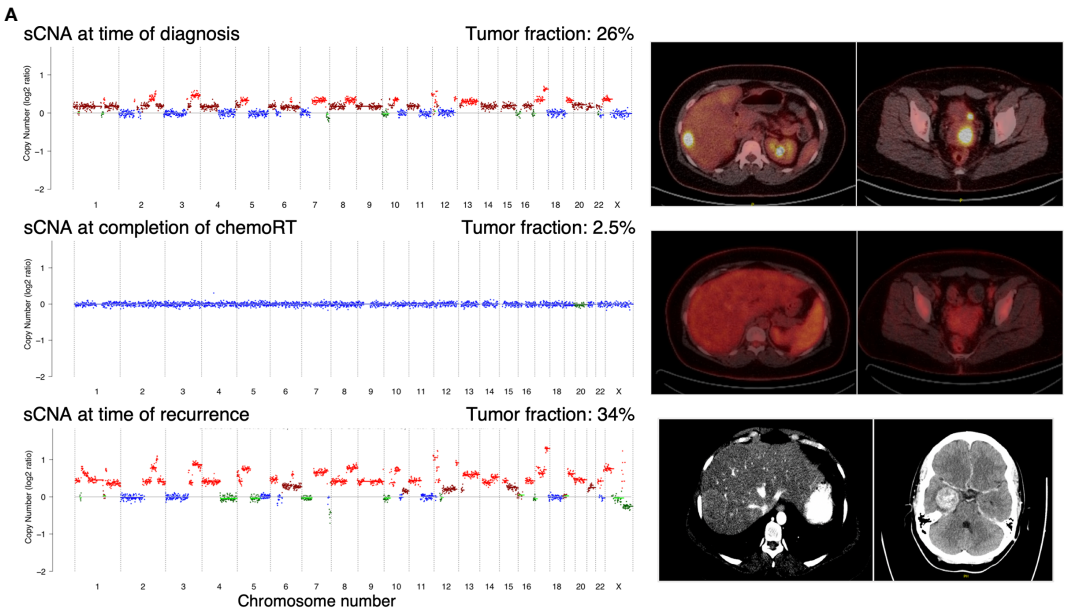

C

Gene	Chr. locus	CNA at diagnosis	CNA at recurrence	Gene	Chr. locus	CNA at diagnosis	CNA at recurrence	Gene	Chr. locus	CNA at diagnosis	CNA at recurrence
PIK3CA	3q26.23	2	2	*ERBB2*	17q12	1	1	*CHECK1*	11q24	0	1
BCL6	3q27	2	2	*FOXO1*	13q14	1	1	*FANCF*	11p14	0	1
MCU4	3q29	2	2	*ARID1A*	1P36.11	0	1	*PARP1*	1q42	0	1
MUC20	3q29	2	2	*AKT1*	14q32.33	0	1	*TSC1*	9q34	0	1
FGF12	3q28	2	2	*AKT3*	1q43	0	1	*HRAS*	11p15	0	1
AKT2	19q13.2	1	1	*MYCL*	1p34.2	0	1	*ERBB3*	12q13	0	1
TP53	17P13.1	1	1	*MCL1*	1q21.2	0	1	*PALB2*	16p12.2	-1	-1
RB1	13q14.2	1	1	*KRAS*	12p12.1	0	1	*CHEK2*	22q12.1	-1	-1
MYC	8q24.21	1	1	*NRAS*	1p13.2	0	1	*CCND1*	13q13.3	-1	-1
BRCA1	7q21.31	1	1	*BRAF*	7q34	0	-1	*ATM*	11q22	-1	-1
BRCA2	13q13.1	1	1	*JAK2*	9p24.1	0	1	*MLH1*	3p22	-1	-1
NBN	8q21.3	1	1	*EGFR*	7p11.2	0	-1	*PIK3R2*	19p13	-1	-1
RAD51C	17q22	1	1	*Mdm2*	12q15	0	1	*TSC2*	16p13	-1	-1
RAD51D	17q12	1	1	*PMS2*	7p22	0	-1	*RASSF1*	3p21	-1	-1
CCNE1	19q12	1	1	*FGFR1*	8p11	0	1				
MET	7q31.2	0	-1	*FGFR3*	4p16.3	0	1				

FIGURE 4 | **(A)** sCNA at three different time points (left panels) with copy number (log2 ratio) indicated on the y-axis and chromosome on the x-axis. PET/CT images corresponding to the time of liquid biopsy collections (right panels). **(B)** Diagrammatic representation of the serial trend of tumor fraction at diagnosis, during treatment, and at the time of recurrence. **(C)** A descriptive comparison of selected gene-level copy number data between time of diagnosis and time of recurrence. -2/-1/0/1/2 refer for homozygous deletion, heterozygous deletion, copy neutral, low gain, and high amplification, respectively.

We observed a high tumor fraction at the time of diagnosis and recurrence, possibly due to the presence of distant visceral metastasis, especially to the liver, high disease burden, and aggressive biology of this cancer. Prior studies reported that liver metastasis is associated with higher shedding of ctDNA than other metastatic sites, which could be explained by the anatomy and blood flow supporting the metastatic disease in the visceral sites (18). The potential utility is to monitor patients during surveillance for evidence of visceral metastasis, especially when other diagnostic modalities are negative like imaging and other biomarkers or those with rising biomarkers with negative imaging, which represent a real challenge in some cancers.

A critical question is whether this patient had a complete molecular response or not at the completion of therapy. Although she had a complete metabolic response with full resolution of her disease, it is not clear if there was still residual molecular disease given that the tumor fraction significantly dropped to 2.5%. Furthermore, it is not clear whether there is an optimal cutoff that can be used to make a judgment on the role of therapy duration, treatment intensification, or changing treatment regimens. These need to be investigated further in future prospective studies.

There is no reliable serologic biomarker to monitor response to therapy or recurrence during the surveillance of patients with small-cell NEC of the cervix. Therefore, longitudinal monitoring of ctDNA represents an attractive approach in managing these patients, especially if combined with radiology imaging. Remarkably, the sCNA patterns and genes-level data (**Figure 4**) at the time of recurrence were comparable to that of initial diagnosis but with higher amplitude. These data support that at least at the copy number level, the recurrent tumors of this aggressive cancer have similar molecular characteristics compared to primary disease but with a higher amplitude of amplification. These data are interesting but should be interpreted cautiously and need to be validated in the future in a prospective cohort of this aggressive cancer.

In conclusion, this case study highlights the role of serial assessment of tumor fraction and ctDNA as a potentially promising non-invasive biomarker in patients with advanced-stage small-cell NEC of the cervix. Future studies are warranted

to assess the role of ctDNA as a prognostic and predictive biomarker in this highly aggressive cancer, particularly in correlation with the extent of disease, tumor burden, and site of metastasis. Further, it will be important to explore the additional benefits by combining ctDNA analysis with radiologic imaging during follow-up of response to therapy and routine surveillance.

METHODS

Clinical Case Data Extraction

The clinicopathologic, treatment, and response evaluation data were collected retrospectively from the patient's chart.

Clinical Specimens, Circulating Tumor DNA Extraction and Quantification

Plasma samples were prospectively collected as part of an ongoing study approved by the Cleveland Clinic Institutional Review Board. Patients have consented for blood collection prospectively. Blood was collected in 10 ml of Cell-Free DNA BCT (Streck, Omaha, NE, USA). Blood was processed to collect plasma and buffy coat through standard density gradient centrifuge protocol. In brief, blood samples were centrifuged at 1,500 rpm for 6 min. The plasma was isolated and stored in 1.5 ml microfuge tubes and frozen in −80°C till further processing. Further, DNA was extracted using the standard protocol. In brief, RBC lysis buffer was used for 5–10 min then spun at 450 rcf for 5 min. The supernatant was removed, and 500 ml of PBS was added and spun for 5 min, then lysis solution was added to lyse overnight, and then samples were stored in −80°C till future use. Subsequently, for the purpose of cell-free DNA analysis, frozen aliquots of the plasma samples were thawed at room temperature and subjected to a second high-speed spin after thawing. Cell-free DNA extraction and quantification were performed as previously described (13).

Ultra-Low-Pass Whole-Genome Sequencing (ULP-WGS) and Analysis

Library construction of cell-free DNA was performed using the Kapa HyperPrep kit with custom adapters (IDT, Coralville, IA, USA). Three to 20 ng of cell-free DNA input (median, 5 ng), or approximately 1,000 to 7,000 haploid genome equivalents, was used for ultra-low-pass whole-genome sequencing. Constructed sequencing libraries were pooled and sequenced using 100-bp paired-end runs on a HiSeq2500 (Illumina, San Diego, CA, USA) to get an average genome-wide fold coverage of 0.13. Segment copy number and tumor fraction (TFx) were derived *via* ichorCNA (13). Samples were excluded if the median absolute deviation of copy ratios ($\log_2$ ratio) between adjacent bins, genome-wide, was >0.20, suggesting poor-quality sequence data.

Gene-Level Copy Number Analyses

GISTIC2.0 output (20, 21) was used for all gene-level copy number analyses. Segmented data files derived from ichorCNA were purity and ploidy corrected, then input into GISTIC2.0 with amplification/deletion threshold $\log_2$ ratio > 0.3, confidence level 0.99, and Q-value threshold 0.05. Genes were defined as gain (GISTIC value 1; corresponds to three copies) or amplification (GISTIC value 2; corresponds to four or more copies) *versus* diploid (GISTIC value 0).

DATA AVAILABILITY STATEMENT

The raw data supporting the conclusions of this article will be made available by the authors, without undue reservation.

ETHICS STATEMENT

The studies involving human participants were reviewed and approved by Cleveland Clinic IRB. The patients/participants provided their written informed consent to participate in this study.

AUTHOR CONTRIBUTIONS

All authors contributed to the article and approved the submitted version.

REFERENCES

1. Albores-Saavedra J, Larraza O, Poucell S, Rodríguez Martínez HA. Carcinoid of the Uterine Cervix: Additional Observations on a New Tumor Entity. *Cancer* (1976) 38:2328. doi: 10.1002/1097-0142(197612)38:6<2328::AID-CNCR2820380620>3.0.CO;2-J
2. Miller B, Dockter M, el Torky M, Photopulos G. Small Cell Carcinoma of the Cervix: A Clinical and Flow-Cytometric Study. *Gynecol Oncol* (1991) 42:27. doi: 10.1016/0090-8258(91)90225-T
3. Van Nagell JR Jr, Donaldson ES, Wood EG, Maruyama Y, Utley J. Small Cell Cancer of the Uterine Cervix. *Cancer* (1977) 40:2243. doi: 10.1002/1097-0142(197711)40:5<2243::AID-CNCR2820400534>3.0.CO;2-H
4. Ambros RA, Park JS, Shah KV, Kurman RJ. Evaluation fo Histologic, Morphometric, and Immunohistochemical Criteria in the Differential Diagnosis of Small Cell Carcinoma of the Cervix With Particular Reference to Human Papillomavirus Type 16 and 18. *Mod Pathol* (1991) 4:586–93.
5. Stoler MH, Mills SE, Gersell DJ, Walker AN. Small-Cell Neuroendocrine Carcinoma of the Cervix. A Human Papillomavirus Type 19-Associated Cancer. *Am J Surg Pathol* (1991) 15:28–32. doi: 10.1097/00000478-199101000-00003
6. Moertel C, Kvols L, Oconnel M, Rubin J. Treatment of Neuroendocrine Carcinomas With Combined Etoposide and Cisplatin; Evidence of Major Therapeutic Activity in the Anaplastic Variants of These Neoplasms. *Cancer* (1991) 68:227–32. doi: 10.1002/1097-0142(19910715)68:2<227::AID-CNCR2820680202>3.0.CO;2-I
7. Gardner GJ, Rediy-Lagunes D, Gehrig PA. Neuroendocrine Tumors of the Gynecologic Tract: A Society of Gynecologic Ocology (SGO) Clinical Document. *Gynecol Oncol* (2011) 122(1):190–8. doi: 10.1016/j.ygyno.2011.04.011
8. Chen J, Macdonald OK, Gaffney DK. Incidence, Mortality, and Prognostic Factors of Small Cell Carcinoma of the Cervix. *Obstet Gynecol* (2008) 111(6):1394–402. doi: 10.1097/AOG.0b013e318173570b

9. McCusker M, Cote T, Clegg L, TAvassoli F. Endocrine Tumors of the Uterine Cervix: Incidence, Demographics, and Survival With Comparison to Squamous Cell Carcinoma. *Gynecol Oncol* (2003) 88:333–9. doi: 10.1016/S0090-8258(02)00150-6
10. Antonia SJ, López-Martin JA, Bendell J, Ott PA, Taylor M, Eder JP, et al. Nivolumab Alone and Nivolumab Plus Ipilimumab in Recurrent Small-Cell Lung Cancer (CheckMate 032): A Multicentre, Open-Label, Phase 1/2 Trial. *Lancet Oncol* (2016) Jul17(7):883–95. doi: 10.1016/S1470-2045(16)30098-5
11. Ready N, Farago AF, de Braud F, Atmaca A, Hellmann MD, Schneider JG, et al. Third-Line Nivolumab Monotherapy in Recurrent SCLC: CheckMate 032. *J Thorac Oncol* (2019) 14(2):237–44. doi: 10.1016/j.jtho.2018.10.003
12. Frumovitz M, Westin SN, Salvo G, Zarifa A, Xu M, Yap TA, et al. Phase II Study of Pembrolizumab Efficacy and Safety in Women With Recurrent Small Cell Neuroendocrine Carcinoma of the Lower Genital Tract. *Gynecol Oncol* (2020) 158(3):570–5. doi: 10.1016/j.ygyno.2020.05.682
13. Adalsteinsson VA, Ha G, Freeman SS, Choudhury AD, Stover DG, Parsons HA, et al. Scalable Whole-Exome Sequencing of Cell-Free DNA Reveals High Concordance With Metastatic Tumors. *Nat Commun* (2017) 8(1):1324. doi: 10.1038/s41467-017-00965-y
14. Hovelson DH, Liu CJ, Wang Y, Kang Q, Henderson J, Gursky A, et al. Rapid, Ultra Low Coverage Copy Number Profiling of Cell-Free DNA as a Precision Oncology Screening Strategy. *Oncotarget* (2017) 8(52):89848–66. doi: 10.18632/oncotarget.21163
15. Fan G, Zhang K, Yang X, Ding J, Wang Z, Li J. Prognostic Value of Circulating Tumor DNA in Patients With Colon Cancer: Systematic Review. *PloS One* (2017) 12(2):e0171991. doi: 10.1371/journal.pone.0171991
16. Goodall J, Mateo J, Yuan W, Mossop H, Porta N, Miranda S, et al. TOPARP-A Investigators. Circulating Cell-Free DNA to Guide Prostate Cancer Treatment With PARP Inhibition. *Cancer Discov* (2017) 7(9):1006–17. doi: 10.1158/2159-8290.CD-17-0261
17. Kienel A, Porres D, Heidenreich A, Pfister D. cfDNA as a Prognostic Marker of Response to Taxane Based Chemotherapy in Patients With Prostate Cancer. *J Urol* (2015) 194(4):966–71. doi: 10.1016/j.juro.2015.04.055
18. Choudhury AD, Werner L, Francini E, Wei XX, Ha G, Freeman SS, et al. Tumor Fraction in Cell-Free DNA as a Biomarker in Prostate Cancer. *JCI Insight* (2018) 3(21):e122109. doi: 10.1172/jci.insight.122109
19. Stover DG, Parsons HA, Ha G, Freeman SS, Barry WT, Guo H, et al. Association of Cell-Free DNA Tumor Fraction and Somatic Copy Number Alterations With Survival in Metastatic Triple-Negative Breast Cancer. *J Clin Oncol* (2018) 36(6):543–53. doi: 10.1200/JCO.2017.76.0033
20. Beroukhim R, Mermel CH, Porter D, Wei G, Raychaudhuri S, Donovans J, et al. The Landscape of Somatic Copy-Number Alteration Across Human Cancers. *Nature* (2010) 463:899–905. doi: 10.1038/nature08822
21. Mermel CH, Schumacher SE, Hill B, Meyerson ML, Beroukhim R, Getz G, et al. GISTIC2.0 Facilitates Sensitive and Confident Localiza- Tion of the Targets of Focal Somatic Copy-Number Al- Teration in Human Cancers. *Genome Biol* (2011) 12:R41. doi: 10.1186/gb-2011-12-4-r41

Conflict of Interest: The authors declare that the research was conducted in the absence of any commercial or financial relationships that could be construed as a potential conflict of interest.

Publisher's Note: All claims expressed in this article are solely those of the authors and do not necessarily represent those of their affiliated organizations, or those of the publisher, the editors and the reviewers. Any product that may be evaluated in this article, or claim that may be made by its manufacturer, is not guaranteed or endorsed by the publisher.

Copyright © 2021 Abbas, Gruner, Karohl, Rose, Joehlin-Price, Stover and Mahdi. This is an open-access article distributed under the terms of the Creative Commons Attribution License (CC BY). The use, distribution or reproduction in other forums is permitted, provided the original author(s) and the copyright owner(s) are credited and that the original publication in this journal is cited, in accordance with accepted academic practice. No use, distribution or reproduction is permitted which does not comply with these terms.

frontiers in Cell and Developmental Biology

ORIGINAL RESEARCH
published: 03 August 2021
doi: 10.3389/fcell.2021.661272

Low-Coverage Whole Genome Sequencing of Cell-Free DNA From Immunosuppressed Cancer Patients Enables Tumor Fraction Determination and Reveals Relevant Copy Number Alterations

Amira Bouzidi[1†], Karim Labreche[2†], Marine Baron[3‡], Marianne Veyri[4‡], Jérôme Alexandre Denis[5], Mehdi Touat[6], Marc Sanson[6], Frédéric Davi[7], Erell Guillerm[8], Stéphanie Jouannet[9], Frédéric Charlotte[10], Franck Bielle[11], Sylvain Choquet[3], Pierre-Yves Boëlle[2], Jacques Cadranel[12], Véronique Leblond[3], Brigitte Autran[13], Jean-Marc Lacorte[1§], Jean-Philippe Spano[4§], Florence Coulet[8§] and the IDEATION study group*

[1] Sorbonne University, INSERM, Research Unit on Cardiovascular and Metabolic Disease UMR ICAN, Department of Endocrine Biochemistry and Oncology, AP-HP, Hôpital Pitié Salpêtrière, Paris, France, [2] Sorbonne University, INSERM, Pierre Louis Institute of Epidemiology and Public Health, Paris, France, [3] Sorbonne University, Center for Immunology and Infectious Diseases (CIMI-Paris), Department of Hematology, APHP, Hôpital Pitié Salpêtrière, Paris, France, [4] Sorbonne University, INSERM, Pierre Louis Institute of Epidemiology and Public Health, Theravir Team, Medical Oncology, AP-HP, Hôpital Pitié Salpêtrière, Paris, France, [5] Sorbonne University, INSERM, Saint-Antoine Research Center, Cancer Biology and Therapeutics, CRSA, Department of Endocrine Biochemistry and Oncology, AP-HP, Hôpital Pitié Salpêtrière, Paris, France, [6] Sorbonne University, INSERM, CNRS, Brain and Spine Institute, ICM, Department of Neurology 2-Mazarin, AP-HP, Hôpital Pitié Salpêtrière, Paris, France, [7] Sorbonne University, INSERM, Centre de Recherche des Cordeliers, Department of Biological Hematology, AP-HP, Hôpital Pitié Salpêtrière, Paris, France, [8] Sorbonne University, INSERM, Saint-Antoine Research Center, Microsatellites Instability and Cancer, CRSA, Genetics Department, AP-HP, Hôpital Pitié Salpêtrière, Paris, France, [9] Sorbonne University, Neurosurgery Department, AP-HP, Hôpital Pitié Salpêtrière, Paris, France, [10] Sorbonne University, Anatomy and Pathologic Cytology, AP-HP, Hôpital Pitié Salpêtrière, Paris, France, [11] Sorbonne University, Neuropathology Department, AP-HP, Hôpital Pitié Salpêtrière, Paris, France, [12] Sorbonne University, Chest Department and Thoracic Oncology, GRC 04, Theranoscan, AP-HP, Hôpital Tenon, Paris, France, [13] Sorbonne University, INSERM, CNRS, Center for Immunology and Infectious Diseases (CIMI-Paris), AP-HP, Pitié-Salpêtrière Hospital, Paris, France

OPEN ACCESS

Edited by:
Catherine Alix-Panabieres, Centre Hospitalier Universitaire de Montpellier, France

Reviewed by:
Florent Mouliere, Amsterdam University Medical Center, Netherlands
Simon Heeke, University of Texas MD Anderson Cancer Center, United States

***Correspondence:**
Florence Coulet
florence.coulet@aphp.fr

[†] These authors have contributed equally to this work and share first authorship

[‡] These authors have contributed equally to this work

[§] These authors have contributed equally to this work and share last authorship

Specialty section:
This article was submitted to Molecular and Cellular Oncology, a section of the journal Frontiers in Cell and Developmental Biology

Received: 30 January 2021
Accepted: 18 June 2021
Published: 03 August 2021

Citation:
Bouzidi A, Labreche K, Baron M, Veyri M, Denis JA, Touat M, Sanson M, Davi F, Guillerm E, Jouannet S, Charlotte F, Bielle F, Choquet S, Boëlle P-Y, Cadranel J, Leblond V, Autran B, Lacorte J-M, Spano J-P, Coulet F and the IDEATION study group (2021) Low-Coverage Whole Genome Sequencing of Cell-Free DNA From Immunosuppressed Cancer Patients Enables Tumor Fraction Determination and Reveals Relevant Copy Number Alterations. Front. Cell Dev. Biol. 9:661272. doi: 10.3389/fcell.2021.661272

Cell-free DNA (cfDNA) analysis is a minimally invasive method that can be used to detect genomic abnormalities by directly testing a blood sample. This method is particularly useful for immunosuppressed patients, who are at high risk of complications from tissue biopsy. The cfDNA tumor fraction (TF) varies greatly across cancer type and between patients. Thus, the detection of molecular alterations is highly dependent on the circulating TF. In our study, we aimed to calculate the TF and characterize the copy number aberration (CNA) profile of cfDNA from patients with rare malignancies occurring in immunosuppressed environments or immune-privileged sites. To accomplish this, we recruited 36 patients: 19 patients with non-Hodgkin lymphoma (NHL) who were either human immunodeficiency virus (HIV)-positive or organ transplant recipients, 5 HIV-positive lung cancer patients, and 12 patients with glioma. cfDNA was extracted from the patients' plasma and sequenced using low-coverage whole genome sequencing (LC-WGS). The cfDNA TF was then calculated using the ichorCNA bioinformatic

algorithm, based on the CNA profile. In parallel, we performed whole exome sequencing of patient tumor tissue and cfDNA samples with detectable TFs. We detected a cfDNA TF in 29% of immune-suppressed patients (one patient with lung cancer and six with systemic NHL), with a TF range from 8 to 70%. In these patients, the events detected in the CNA profile of cfDNA are well-known events associated with NHL and lung cancer. Moreover, cfDNA CNA profile correlated with the CNA profile of matched tumor tissue. No tumor-derived cfDNA was detected in the glioma patients. Our study shows that tumor genetic content is detectable in cfDNA from immunosuppressed patients with advanced NHL or lung cancer. LC-WGS is a time- and cost-effective method that can help select an appropriate strategy for performing extensive molecular analysis of cfDNA. This technique also enables characterization of CNAs in cfDNA when sufficient tumor content is available. Hence, this approach can be used to collect useful molecular information that is relevant to patient care.

Keywords: liquid biopsy, cfDNA, CNA profile, cancer, immunodeficiency

INTRODUCTION

Patients infected with human immunodeficiency virus (HIV) or who are organ transplant recipients are at increased risk of developing several cancers compared to the general population (Hortlund et al., 2017; Yarchoan and Uldrick, 2018). Moreover, the risk of cancer-related mortality is increased in these patients (Sigel et al., 2011; Au et al., 2019; Horner et al., 2020). Tissue biopsies performed on immunosuppressed patients entails an elevated risk of complications and demonstrates lower diagnostic yields and increased mortality (Plattner et al., 2018; Cleveland et al., 2020). Compared with tissue biopsy, liquid biopsy such as cell-free DNA (cfDNA) has several benefits. Molecular profiling of cfDNA could allow patients to undergo close, longitudinal follow-up that can enable primary diagnosis of extensive disease, optimal choice of treatment, early diagnosis of clinical progression, and identification of secondary resistance mechanisms. In addition, cfDNA analysis offers comprehensive coverage that can help address issues of tumor heterogeneity (Ilie and Hofman, 2016). Collecting and analyzing cfDNA may be particularly advantageous for immunosuppressed patients, as this approach offers a minimally invasive and cost-effective alternative to more traditional molecular profiling methods.

The cfDNA tumor fraction (TF), which is the proportion of tumor molecules that are present in a cfDNA sample, varies greatly across cancer type and between patients, and represents a clinically relevant biomarker (Adalsteinsson et al., 2017; Van Roy et al., 2017; Chen et al., 2019). The detection of tumor-associated single nucleotide variants (SNVs) in the cfDNA can be achieved by using high-depth targeted sequencing methods (Newman et al., 2014; Ishii et al., 2020) or PCR-based methods (Denis et al., 2017). Broader analyses such as whole exome sequencing (WES) at standard depth (∼150 × coverage) are generally informative when the TF is ∼5% to 10% (Cibulskis et al., 2013). Therefore, the estimation of the TF could help guide selection of the appropriate molecular approach for subsequent detection of SNVs in cfDNA.

Recently, a cost-effective approach, ichorCNA11, was established to calculate the TF of cfDNA using low-coverage whole genome sequencing (LC-WGS). This method identifies segmental/arm-level copy number aberrations (CNAs), which enables the TF to be inferred (Adalsteinsson et al., 2017).

The aim of our study was to calculate the TF and determine the CNA profile of cfDNA in immunosuppressed patients or patients with tumors located in immune-privileged sites, such as the central nervous system (CNS) using LC-WGS and ichorCNA. This approach can guide the decision to subsequently perform a targeted PCR-based method, a targeted sequencing, or a WES, based on the circulating tumor content, to provide a more comprehensive molecular analysis of cfDNA in this specific, frail population.

For this purpose, we recruited patients with cancers known to be associated with variable amounts of cfDNA (from low to high) in immunocompetent patients (Mouliere et al., 2018). Specifically, we enrolled untreated immunodeficient patients with non-Hodgkin lymphoma (NHL) (either systemic or localized to the CNS), HIV-positive patients with non-small-cell lung cancer (NSCLC), and immunocompetent patients with glioma.

MATERIALS AND METHODS

Patient Cohort

Patients were enrolled in the IDeATIon project (ClinicalTrials.gov identifier: NCT03706625), a multidisciplinary, multicentric, translational research program that focuses on severe tumors that appear in immunosuppressed patients or in immune-privileged sites such as the CNS. The protocol was approved by the French national IRB (no. 2018-A01099-46) and the "Commission Nationale de l'Informatique et des Libertés" (CNIL no. 918222).

Three types of rare and severe cancers were selected: (1) NHL (either systemic or localized to the CNS) occurring in patients with HIV or in transplant recipients, (2) NSCLC in patients with HIV, and (3) glioma. The inclusion criteria were as follows:

(1) male or female adults (age ≥ 18 years old), (2) confirmed histopathological diagnosis of one of the three types of cancer listed above, (3) anti-tumoral treatment-naive (except for some glioma patients), (4) hemoglobin level > 9 g/dl for lung cancer patients and > 7 g/dl for NHL and glioma patients, and (5) written informed consent. From July 2018 to December 2020, 118 patients were enrolled in the IDeATIon project. This study includes 36 of these prospectively enrolled patients (**Table 1**).

Spike-In Experiment

Genomic DNA (gDNA) was isolated from two human NSCLC cell lines, H2030 (ATCC® CRL-5914™) and H1975 (ATCC® CRL-5908™), and healthy donor blood using a QIAamp DNA Blood Mini Kit (Qiagen). The DNA concentrations were quantified on a Quantus™ Fluorometer (Promega) using QuantiFluor® ONE dsDNA Dye (Promega). Genomic DNA was sheared to an average size of 150 bp using The Bioruptor® Pico (Diagenode). Fragment size was confirmed on a TapeStation 4200 electrophoresis system (Agilent). To create the spike-in mix, H2030 or H1975 DNA was mixed with healthy donor DNA to a final proportion of 5% or 15%, and the samples were analyzed by LC-WGS.

Plasma Preparation and cfDNA Extraction

Blood was collected in Cell-Free DNA Collection Tubes (ROCHE), which were then centrifuged for 10 min at 820 *g*. Next, the supernatant was transferred to a fresh tube, centrifuged at 20,000 *g* for a further 10 min, and stored in 1-ml aliquots at −80°C until later extraction. cfDNA was extracted from 5 ml of plasma using the QIAamp Circulating Nucleic Acid Kit (Qiagen) following the manufacturer's instructions and eluted in a volume of 35 µl. cfDNA was quantified using a Quantus™ Fluorometer (Promega). The size distribution of the cfDNA was checked on a TapeStation 4200 electrophoresis system (Agilent) using Cell-free DNA ScreenTape.

LC-WGS and Analysis

Sequencing libraries were prepared from 4 to 10 ng of cfDNA using the SMARTer® ThruPLEX® Tag-seq Kit (Takara Bio). Libraries were quantified using a Qubit™ dsDNA HS Assay Kit (Thermo Fisher), and the fragment sizes were confirmed using a TapeStation 4200 electrophoresis system (Agilent). Equal amounts of the sequencing libraries were pooled to generate a single sample for sequencing. WGS at an average coverage of 4 × was performed on a Novaseq (Illumina) system using 2 × 150-bp paired-end sequencing. BCL2FASTQ (Illumina) was used to convert bcl files to fastq files. The coverage statistics are summarized in **Supplementary Figure 1**. Paired-end fastq files were aligned to the hg38 human reference genome using the BWA-MEM algorithm (Li and Durbin, 2009). PCR duplicates were removed, and a Base Quality Score Recalibration (BQSR) was executed with the Genome Analysis Toolkit (GATK) version 4.1 (McKenna et al., 2010) following GATK best practice.

Based on the pre-processed aligned reads, the TF in the cfDNA was calculated using the ichorCNA workflow, as described previously (Adalsteinsson et al., 2017). Briefly, using the readCounter tools from the HMMcopy suite, we calculated the read count coverage of reads with a mapping quality greater than 20 in 1-Mb-window bins across all autosomal chromosomes. The read counts were then normalized to correct for GC content and mappability bias. The copy number analysis and TF prediction were performed using the ichorCNA R software package. LC-WGS sequencing of the healthy donor sample served as the normal WIG. Adjustments were made to the standard ichorCNA settings to account for ploidy (2 or 3) and an initial normal contamination range of 0.1 to 0.99. Genotype count at genomic position on LC-WGS data were performed using bcftools mpileup command (**Supplementary Table 1**).

DNA Extraction From Tissue Biopsy

Tumor gDNA was isolated from fresh or formalin-fixed paraffin-embedded (FFPE) diagnostic tissue biopsies using a QIAamp DNA Mini Kit (Qiagen) or a QIAamp DNA FFPE Tissue Kit (Qiagen), respectively, according to the manufacturer's instructions.

WES and Tumor Tissue Analysis

Libraries were prepared and hybrid-captured using the SeqCap EZ MedExome Enrichment Kit (Roche) with 200 ng of DNA input. Sequencing was performed on an Illumina Novaseq system with 150-bp paired-end reads. Raw paired-end fastq files were pre-processed using fastp (Chen et al., 2018) for quality control, adapter trimming, and quality filtering. The filtered reads were aligned to the hg38 human reference genome using BWA-MEM (Adalsteinsson et al., 2017). Reads were pre-processed according to GATK best practice. Coverage summary statistics of the consensus coding sequence are shown in **Supplementary Figure 2**. Somatic SNVs and indels that differed between tumor–normal pairs were called using MuTecT (Cibulskis et al., 2013) and Strelka2 (Kim et al., 2018), respectively. We excluded potential oxidative damage-induced mutations as per Costello et al. (2013) using in-house scripts.

Copy number analysis for tumor biopsy WES was performed using the TitanCNA pipeline (Ha et al., 2014[1]). Briefly, we first identified heterozygous single nucleotide polymorphisms (SNPs) from the matched normal germline blood sample using the Samtools mpileup command and the Exome captured regions bed file and computed read counts for the reference SNPs and alternative genotypes from the tumor biopsy samples. Next, we computed read counts for 50-kb bins using HMMcopy (Ha et al., 2012). Centromeres were filtered based on chromosome gap coordinates obtained from UCSC for the hg38 human reference genome. The read coverage for 50-kb bins across the genome was corrected for GC content and mappability. Finally, TitanCNA was used with default values (except for alphaK = 2500 and minDepth = 20) to generate solutions with one to five clonal clusters, with the initial ploidy set to 2 and 3. The solution with the optimal number of clonal clusters was selected using the minimum S_Dbw validity index (using log ratio and allele ratio)

[1]https://github.com/gavinha/TitanCNA

TABLE 1 | Study cohort description.

	NHL	Lung cancer	Glioma
Number of patients	19	5	12
Mean age of diagnosis (range)	56 (21–76)	61 (58–74)	36 (18–62)
Sex			
Male	16 (84%)	5 (100%)	6 (50%)
Female	3 (16%)	0	6 (50%)
Immune status/localization			
immunocompromised HIV + /systemic	5 (26.3%)	NA	NA
immunocompromised PTLD/systemic	8 (42.1%)	NA	NA
immunocompromised HIV + /CNS	1 (5.2%)	NA	NA
immunocompromised PTLD/CNS	5 (26.3%)	NA	NA
immunocompromised HIV + /Lung	NA	5 (100%)	NA
Immunocompetent/CNS	0	NA	12 (100%)
Histology			
	Monomorphic B-cell PTLD (9)	Non small cell adenocarcinoma (5)	Ganglioglioma (2)
	Polymorphic PTLD (3)		Glioblastoma (4)
	DLBCL (3)		Oligodendroglioma (3)
	Burkitt lymphoma (1)		Astrocytoma(3)
	Marginal zone lymphoma (1)		
	Plasmablastic lymphoma(1)		
	HHV8 + DLBCL,NOS (1)		
Stage	**Ann Arbor for systemic NHL**	**TNM classification**	
	Stage I (4)	Stage I	Stage I (2)
	Stage II (0)	Stage II (2)	Stage II (2)
	Stage III (0)	Stage III (1)	Stage III (4)
	Stage IV (9)	Stage IV (2)	Stage IV (4)
Spreading	**Extranodal involvement**	**Metastasis**	**Metastasis**
	Yes (10)	Yes (2)	
	No (2)	No (3)	No (12)

NHL, Non-Hodgkin lymphoma. CNS, central nervous system. DLBCL, diffuse large B cell lymphoma.

as recommended. Tumor purity estimation was performed using ABSOLUTE (Carter et al., 2012).

Comparing the LC-WGS Results for the cfDNA and Matched Tumor Biopsies

We performed a $\log_2$ ratio comparison for 23 patients for whom both LC-WGS cfDNA data and matched tumor biopsy WES data were available (**Supplementary Figure 3**). We excluded LC-WGS cfDNA segments that did not overlap the tumor biopsy sample. Additionally, we restricted the comparison to segments with cellular prevalence = 1, indicating a higher proportion of tumor cells containing that event. If more than one $\log_2$ ratio was assigned to the same segments, the median value of the $\log_2$ ratios in the LC-WGS segments was retained for comparison. Similarity between each cfDNA sample and the matching tumor biopsy was calculated by computing the Spearman correlation coefficient.

WES and cfDNA Analysis

WES was performed on three cfDNA samples with a detectable TF. The same libraries prepared for LC-WGS were hybrid-captured using a SeqCap EZ MedExome Enrichment Kit (Roche). The sequencing and bioinformatic analysis were performed as described above for tumor tissue, except that variant calling was performed on SNVs only.

RNA Sequencing and Expression Analysis

RNA was extracted from tumoral tissue using an RNeasy Micro Kit (Qiagen). Libraries were prepared from 500 ng of RNA. After end repair, A-tailing, ligation, and purification, sequencing was performed on an Illumina Novaseq with 150-bp paired-end reads. Reads were aligned to the human hg38 reference genome after an index was generated using STAR v2.7.2 (Dobin et al., 2013) by applying per-sample two-pass mapping. The generated BAM files were pre-processed according to GATK v4.1 RNA-seq best practice (Mark Duplicate, SplitNcigarReads and BQSR), followed by transcript quantification using Kallisto v0.45.0 (Bray et al., 2016). To summarize transcript-level abundance estimates for gene-level analysis, we used *tximport* R packages (Soneson et al., 2015). Gene expression comparison was achieved by simple extraction of the listed genes (ABC and GCB, **Supplementary Figure 4C**) from total gene expression level, followed by Wilcoxon test to compare the regularized-logarithm transformation (rlog) of the gene count between the two gene sets.

Statistical Analysis

We used R (version 4.0.0) to perform all statistical analyses and tests. The Wilcoxon test was used to compare ploidy across the exome and LC-WGS data. Copy number variation (CNV) segment tests and *p*-values were computed using Spearman's test.

RESULTS

Cohort Description

The clinical features of the 36 patients included in our cohort are shown in **Table 1**. Twenty-four patients were immunodeficient, namely, 19 who had NHL and 5 who had NSCLC. Among the patients with NHL, 6 were HIV-positive [1 with primary central nervous system lymphoma (PCNSL) and 5 with systemic NHL] and 13 were organ transplant recipients (5 with PCNSL and 8 with systemic NHL). All five patients with NSCLC were HIV-positive. The other 12 patients in the cohort were immunocompetent and had glioma. Biological material, including blood and tumor tissue samples, was collected at the time of diagnosis and prior to any anti-tumoral treatment (except for some glioma patients).

Estimation of the TF in the cfDNA

To establish the LC-WGS protocol and ensure reproducibility, we first performed a spike-in experiment by mixing gDNA from two lung cancer cell lines (H2030 and H1975) with known genomic profiles with DNA from a healthy donor at different ratios. We found that a detectable TF using our method was a TF > 5% (**Supplementary Figure 1**). Following LC-WGS and bioinformatics analysis, the TF in cfDNA from 24 immunodeficient patients with cancer (19 NHL and 5 NSCLC-HIV) and 12 immunocompetent patients with glioma was determined. We prioritized ichorCNA solutions with a ploidy of 2, as our cohort did not exhibit high-copy genome amplification, and subjected the CNV profiles to manual review to account for bias introduced to bin $\log_2$ ratio values after GC content correction.

The calculated TF values ranged from 8 to 70% (**Figure 1A**). Thirty-two percent of immunodeficient NHL patients (6/19) and 20% of HIV-positive NSCLC patients (1/5) had a TF greater than 5%. However, no tumor-derived cfDNA was detected in any of the glioma or PCNSL patients. The estimated TF for the HIV-positive patient with NSCLC was 23%; this patient had metastatic cancer (T4 N3 M1c, stage 4B disease).

Next, we compared TF values across different groups of patients with NHL, based on localization, International Prognostic Index (IPI) score, and type of immunodeficiency (**Figure 1B**). Six of the NHL patients with detectable TF (TF = 8%, 10%, 12%, 13%, 55%, and 70%) had exclusively systemic localization. In contrast, the TF was below the limit of detection of all the patients with PCNSL. Five out of the six patients with a TF value > 5% had extranodal manifestations of disease. No difference was observed in terms of type of immunodeficiency. Finally, five out of nine patients with a high IPI score (2 or 3) exhibited detectable levels of tumor cfDNA, whereas only one in four with a low IPI score (0 or 1) had a detectable TF.

Copy Number Alteration Profile Concordance Between Tumor Biopsies and cfDNA

Next, we compared the CNA profiles for the cfDNA samples as established by LC-WGS and ichorCNA with the CNA profiles deduced from WES of matched tumor biopsies (100× to 200×, $n = 23$). These analyses involve comparison of the normalized $\log_2$ copy ratios between the two sample types from same patients. We found that the Mb-scale copy numbers correlated well in samples with a TF > 5% (ranging from $\rho = 0.34$ to $\rho = 0.81$; $p < 0.001$, **Figure 2A**), while there was no significant correlation for patients with undetectable TFs ($\rho = -0.31$ to $\rho = 0.08$; **Figure 2B**, **Supplementary Figure 3**).

Copy Number Alteration Profile Analysis of cfDNA

To evaluate whether cfDNA can serve as a proxy for tumor biopsies in cancer analyses, we analyzed the CNA profiles of cfDNA from patients with a TF > 5%.

In the HIV-positive patient with NSCLC, chromosomal gains were identified for several genes known to be associated with NSCLC, such as *SOX2* (3q), *TERT* (5p), and *EGFR* (7q). Furthermore, we found amplification of *MYC* and heterozygous deletion of the *PTEN* tumor suppressor, located at 8q and 10q, respectively (**Figure 3B**).

In the NHL group, at the chromosomal level, chromosome 12 gain was the most frequent event (encountered in 4/6 patients), followed by chromosome 15 loss (detected in 2/6 patients). These CNAs were mutually exclusive in our cohort (**Figure 3A**). Focal chromosomal alterations were also detected, including 8q24 gain and 6p22, 6q21 loss, which were identified in 3/6 and 2/6 patients, respectively. These findings were compared to known cancer-associated somatic CNAs seen in patients with NHL (Lopez et al., 2019; Cascione et al., 2020) or NSCLC (Spoerke et al., 2012; Qiu et al., 2017).

The NHL patients in our cohort exhibited two distinct CNA profiles. The first group included patients [three patients with diffuse large B-cell lymphoma (DLBCL) and one patient with Burkitt lymphoma] who exhibited gain of chromosome 12, which is where *STAT6*, *MDM2*, and *BCL7A* are located. The second group (two patients with DLBCL) exhibited neutral chromosome 12 copy numbers but had gains in a region harboring the HLA locus, *PRDM1*, and *POLG1* (**Supplementary Figure 4A**). Interestingly, patient FR-02-40 harbored alterations in genes associated with the activated B-cell (ABC) DLBCL subgroup (Testoni et al., 2015; Schmitz et al., 2018), such as *PIK3CA*, *NFKBIZ*, *BCL2*, and *SPIB*.

To confirm whether this patient belonged to the ABC molecular subgroup, we analyzed somatic mutations from WES analysis of a biopsy of the patient's tumor. We identified mutations in the tumor suppressor gene *TBL1XR1* and the proto-oncogene *PIM1* (**Supplementary Figure 4B**). In addition, RNA-seq expression analysis of

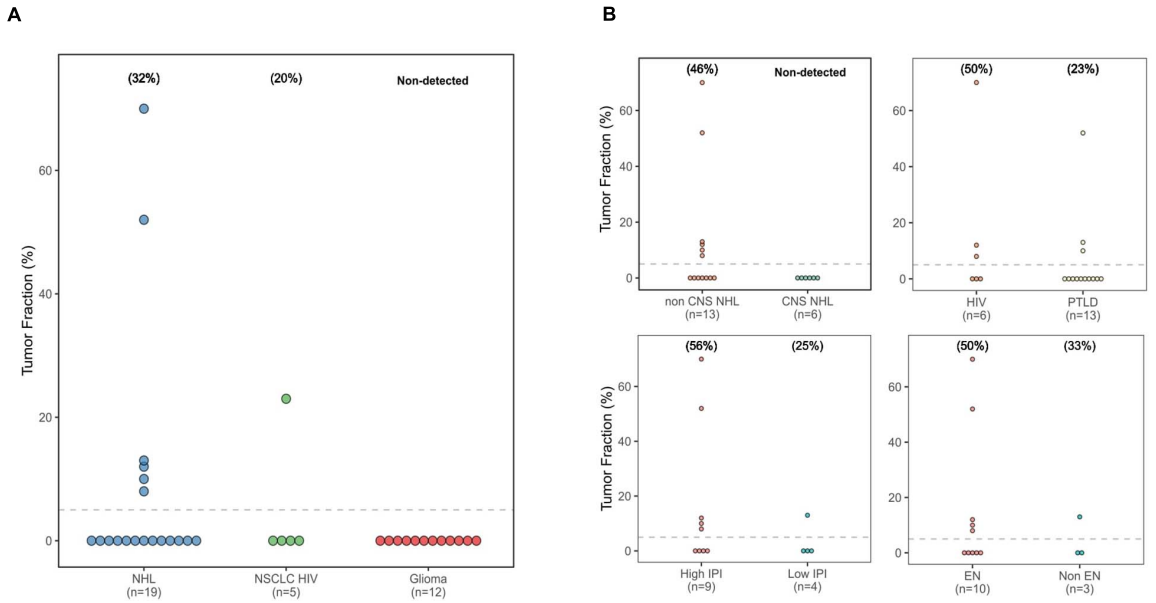

FIGURE 1 | Tumor fraction dot plots. **(A)** All three cancer types studied. **(B)** Based on non-Hodgkin lymphoma location, immunodeficiency type, nodal location, and International Prognostic Index group.

the matched tumor tissue revealed overexpression of ABC-associated genes (Alizadeh et al., 2000; Rosenwald et al., 2002) (**Supplementary Figure 4C**). Finally, immunohistochemistry analysis using the Hans algorithm classified patient FR-02-40 as non-GCB.

WES of cfDNA

The availability of sufficient tumor-derived cfDNA material allowed us to generate WES data (median coverage of 200×) on three of the cases with LC-WGS and tumor biopsy exome sequenced. We detected shared coding somatic SNV in cfDNA and tumor biopsy in FR-02-040-BP (16%), FR-02-056-LTT (28%), and FR-01-092-PA (83%). Across the common mutations, we identified mutations of known-driver genes in NSCLC as *TP53* and *MAP2K1* (Wislez et al., 2021) and recurrent mutated genes in NHL as *MYC, TBL1XR1, IGLL5, GNA13*, and *PIM1*. We found a strong correlation between the variant allele frequency (VAF) on cfDNA and the somatic VAF in tumor tissue biopsy (Pearson test, ρ = 0.7–0.78, all p-value < 0.001, **Supplementary Figure 4**). Notably, the median VAFs of shared SNV were larger as the estimated TFs were higher (**Supplementary Table 2**). In addition to somatic variant analysis, we estimated ploidy and purity in cfDNA WES data. Computed tumor purity on cfDNA was comparable to TFs calculated using LC-WGS (**Supplementary Table 2**).

DISCUSSION

Studies have shown that LC-WGS and ichorCNA analysis can accurately detect low fractions of circulating tumor DNA in blood plasma (Adalsteinsson et al., 2017; Chen et al., 2019). Calculating the TF in the cfDNA can help select a method with appropriate sensitivity for performing a comprehensive molecular analysis. Using CNAs to calculate the TF is particularly relevant, as the vast majority of cancers harbor arm-level somatic CNAs (Beroukhim et al., 2010).

Our pilot study is the first to calculate TFs and characterize somatic CNA profiles for cfDNA using LC-WGS and ichorCNA in immunosuppressed patients (HIV-positive or transplant recipients) with NHL (systemic or CNS-localized) or lung cancer. Immunocompetent patients with glioma were also included, given the location of the tumor in an immunosuppressive environment, and, for the purposes of this pilot study, were expected to exhibit a low TF in the blood (Bettegowda et al., 2014).

A TF was detectable in 29% (7/24) of the immunodeficient patients in our cohort, with a TF range of 8% to 70%.

No TFs or CNAs were detected in PCNSL and glioma patients. The failure to detect a TF in these patients was presumably caused by insufficient ctDNA levels in the blood that were below the limit of detection for ichorCNA. Indeed, the lower limit of ichorCNA sensitivity for detecting the presence of tumor is 3% (Adalsteinsson et al., 2017). Glioma-associated mutations have been detected in liquid biopsies using highly sensitive droplet digital PCR (Muralidharan et al., 2021) or by analyzing cerebrospinal fluid (CSF) instead of plasma (Mouliere et al., 2018), suggesting that it could be valuable to test LC-WGS on CSF cfDNA in PCNSL patients. Our results support the use of targeted molecular analyses with high sensitivity when the TF is not detected or is very low.

In contrast, patients with a detectable TF should be selected for further larger-scale sequencing methods, such as WES, for

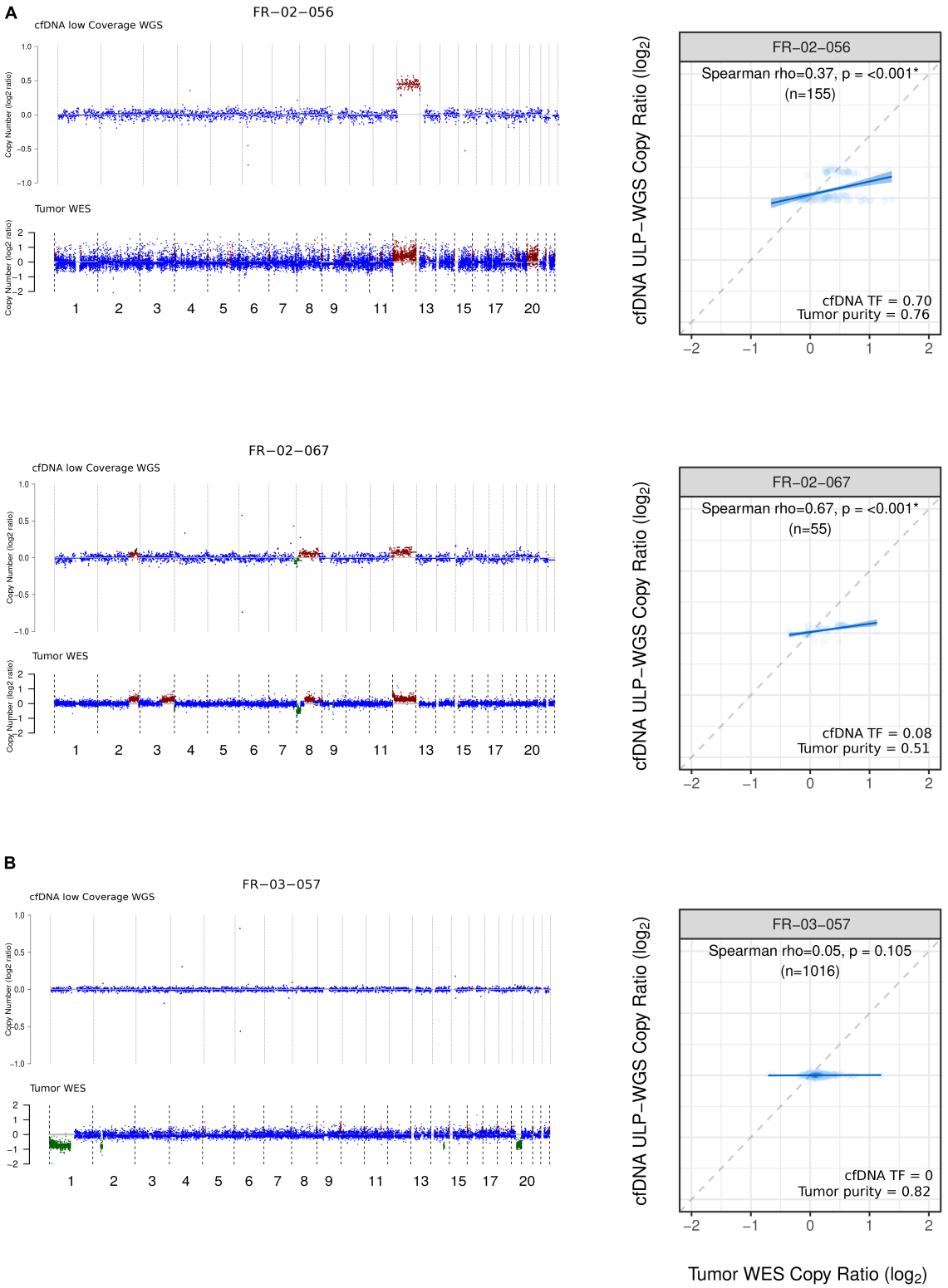

FIGURE 2 | Copy number profile and comparison from LC-WGS cfDNA and WES tumor biopsy. **(A)** Left track shows genome-wide copy number from two ID-NHL patients (FR-02-056 and FR-02-067 with the following median coverage for cfDNA 4.24X, 3.49X and for WES tumor biopsy 216X, 211X, respectively). Right track shows cfDNA tumor fraction (TF) computed using ichorCNA and Tumor purity calculated using ABSOLUTE. **(B)** Left track shows genome-wide copy number from a 1p19q codeleted glioma patient FR-03-057 with the following median coverage for 4.30X for cfDNA and 166 X for WES tumor biopsy. Right track shows Spearman rank correlation between LC-WGS cfDNA and WES tumor biopsy (see *Materials and Methods*).

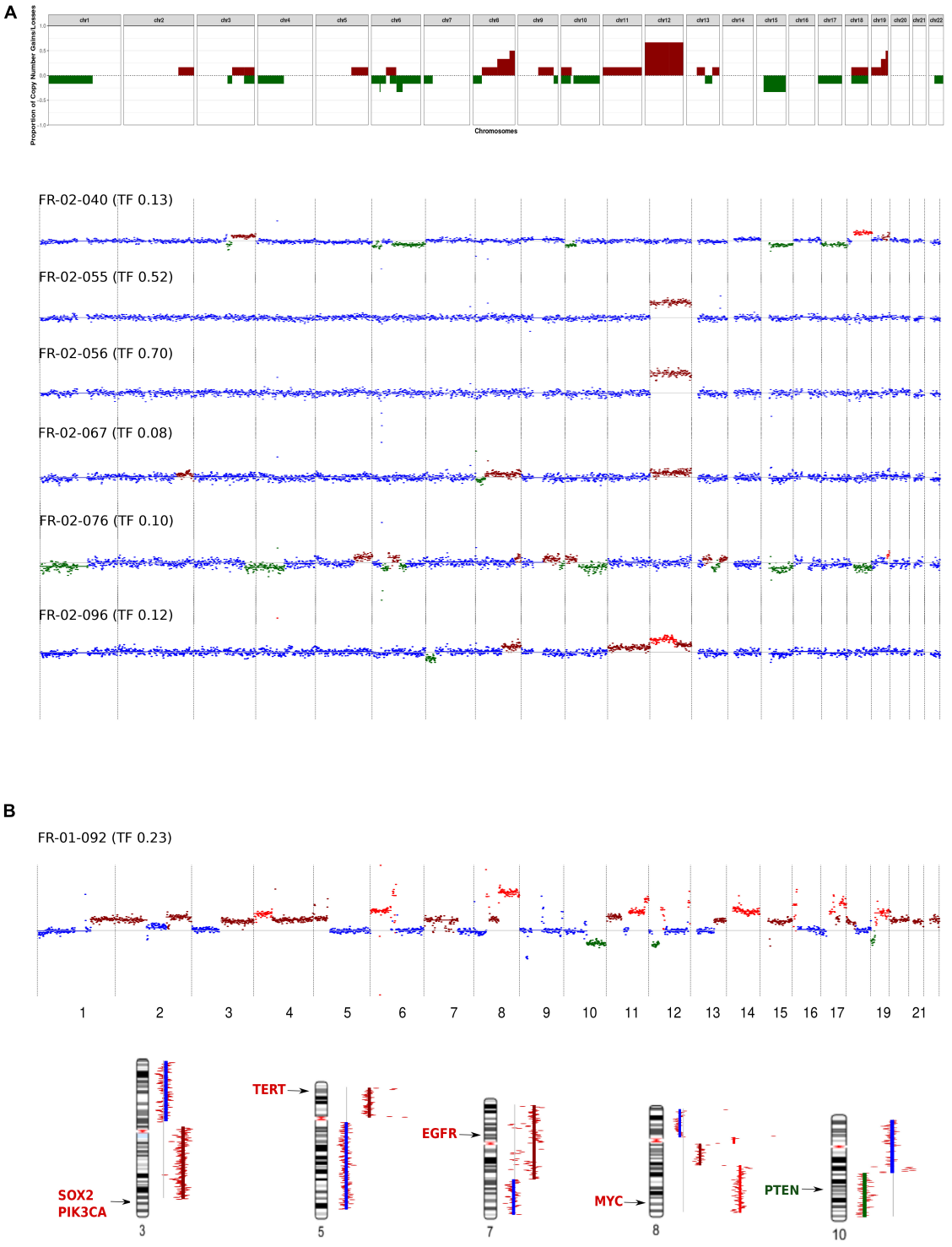

FIGURE 3 | Genome-wide copy number alteration (CNA) landscape in patients with a tumor fraction >5%. **(A)** Cell-free DNA (cfDNA) results from six immunodeficient non-Hodgkin lymphoma patients. Top, frequency of copy number variation (CNV) regions detected by low-coverage whole-genome sequencing of cfDNA. Bottom, CNV pattern for each patient. The plots show the CNV $\log_2$ ratios between the cfDNA sample and the healthy donor (HD). Neutral copy numbers are shown in blue, copy number gains are shown in dark red, copy number amplifications are shown in red, and copy number losses are shown in green. **(B)** cfDNA results from the non-small-cell lung cancer (NSCLC) patients infected with human immunodeficiency virus. Top, CNV pattern. Bottom, genes affected by CNA known to be associated with NSCLC, and their chromosomal locations.

which the calculated TF could help guide calibration of the sequencing depth.

One immunosuppressed lung cancer patient included in our study had a TF of 23%. This patient had non-small-cell adenocarcinoma, was HIV-positive, and had advanced metastatic disease (T4 N3 M1c, stage 4B disease). The CNA profile derived from the tumor tissue biopsy taken from this patient correlated well with the findings from the corresponding liquid biopsy ($\rho = 0.81$). Moreover, the CNA profile was consistent with patterns that are typically observed in patients with NSCLC (Chen et al., 2019; Raman et al., 2020). Determining the CNA profile from cfDNA could constitute an attractive method to support histological subtyping of lung cancer patients, as suggested by Raman et al.

In our study population, the immunodeficient NHL patient group had the highest proportion of patients with detectable aberrations (6/19, 32%). The proportion of patients with detectable cancer-derived cfDNA in this group was lower than that described in the literature for NHL patients. Bohers et al. identified tumor-associated mutations in the cfDNA in 19/30 patients (63%), and Rossi et al., in 20/30 patients (66.6%) (Rossi et al., 2017; Bohers et al., 2018). However, these two studies focused on targeted detection of somatic SNVs in recurrently mutated cancer genes using high-throughput targeted sequencing. It has been shown that a CNA is > 20 times more likely to be detected by LC-WGS than by arrays (Zhou et al., 2018).

Interestingly, 5/6 NHL patients with a TF $> 5\%$ had extranodal manifestations and a high IPI score. Given that our patients were untreated at the time of liquid biopsy, our results agree with a study concluding that ctDNA is a promising biomarker for identifying NHL patients at high risk of treatment failure and at risk of recurrence before clinical evidence of disease relapse (Roschewski et al., 2015).

The potential utility of cfDNA as a biomarker and as a way to molecularly characterize tumors is supported by the concordance between the cfDNA and tumor tissue CNA profiles. Despite the low number of patients with cfDNA WES data, VAF comparison and purity estimation collectively suggests an accurate sensitivity of TF estimation using LC-WGS/IchorCNA. Surprisingly, the strongest correlation was found in the patient with a TF of 23% and not in the patient with a TF of 70%. This may be attributable to the fact that several CNA events were detected in the patient with the lower TF, while only chromosome 12 gain was found in the patient with the higher TF. However, this patient harbors coding variants with high VAFs in cfDNA (median VAF = 0.28, **Supplementary Table 2**).

The CNA profiles derived from the cfDNA from the DLBCL subgroup are consistent with patterns that are usually observed in DLBCL and have been previously detected by analyzing tumor tissue (Testoni et al., 2015). However, based on events observed in the cfDNA CNA profiles, we were further able to distinguish two distinct groups of patients. These two groups (chromosome 12 gain or neutral copy number) correlate with the ABC and GCB gene expression subgroups (Schmitz et al., 2018). Furthermore, mutations in genes corresponding to one subgroup or the other were found in the matched tumor tissue. These results should be confirmed in a larger cohort.

CONCLUSION

Our pilot study showed, for the first time, that ctDNA can be detected by LC-WGS/ichorCNA in the plasma of immunosuppressed patients with advanced NHL or lung cancer. This cost-effective method accurately calculated the TF and determined the CNA profile from the cfDNA and can be used to guide the choice of molecular method for further larger-scale investigations of cfDNA. Applying this method to a larger cohort of immunodeficient patients, as well as an immunocompetent cohort, may help shed light on cancer pathogenesis, the genomic mechanisms by which tumor cells acquire treatment resistance, and the response to treatment in this specific population. Liquid biopsy can be particularly useful in immunosuppressed patients, who are at higher risk for complications during tissue biopsy. Using this approach, molecular information from ctDNA can be collected before and during treatment to help improve patient care. Future analyses could help elucidate the direct impact that immune system impairment has on the circulating TF in these patients.

MEMBERS OF THE IDEATION STUDY GROUP

Ahmed Idbaih, Noureddine Balegroune, Amélie Guihot, Ioannis Theodorou, Agusti Alentorn, Isabelle Brocheriou, Anne-Geneviève, Damien Roos Weil, and Alberto Picca.

DATA AVAILABILITY STATEMENT

The data presented in the study are deposited in the European Nucleotide Archive repository, accession number PRJEB43455, link: https://www.ebi.ac.uk/ena/browser/view/PRJEB43455.

ETHICS STATEMENT

The studies involving human participants were reviewed and approved by the IRB (no 2018-A01099-46) and "Commission Nationale de l'Informatique et des Libertés" (CNIL no 918222). The patients/participants provided their written informed consent to participate in this study.

AUTHOR CONTRIBUTIONS

AB and KL processed the experimental data, performed the analysis, drafted the manuscript, and designed the tures. AB and SJ carried out the experiments. KL and P-YB performed the bioinformatic analyses. FCo, JD, and J-ML were involved in planning and supervised the work and the manuscript draft.

J-PS and BA conceived of the project IDEATION study. MV is the project manager of IDEATION study. EG helped for experimental process. FCh and FB are anatomopathologists involved for selection of tumor tissue. MB, MT, FD, SC, VL, and JC aided in interpreting the results and worked on the manuscript. All authors discussed the results and commented on the manuscript.

FUNDING

The IDeATIon project is financially supported by the MSDAvenir endowment fund. This work was supported by a grant from SIRIC CURAMUS (Cancer United Research Associating Medicine, University & Society integrated cancer research program).

ACKNOWLEDGMENT

We thank the following individuals, belonging to the study group IDEATION, for their expertise and assistance throughout all aspects of our study: Ahmed Idbaih, Noureddine Balegroune, Amélie Guihot, Ioannis Theodorou, Agusti Alentorn, Isabelle Brocheriou, Anne-Geneviève Marcelin, Damien Roos Weil, and Alberto Picca.

SUPPLEMENTARY MATERIAL

The Supplementary Material for this article can be found online at: https://www.frontiersin.org/articles/10.3389/fcell.2021.661272/full#supplementary-material

REFERENCES

Adalsteinsson, V. A., Ha, G., Freeman, S. S., Choudhury, A. D., Stover, D. G., Parsons, H. A., et al. (2017). Scalable whole-exome sequencing of cell-free DNA reveals high concordance with metastatic tumors. *Nat. Commun.* 8:1324. doi: 10.1038/s41467-017-00965-y

Alizadeh, A. A., Eisen, M. B., Davis, R. E., Ma, C., Lossos, I. S., Rosenwald, A., et al. (2000). Distinct types of diffuse large B-cell lymphoma identified by gene expression profiling. *Nature* 403, 503–511. doi: 10.1038/35000501

Au, E. H., Chapman, J. R., Craig, J. C., Lim, W. H., Teixeira-Pinto, A., Ullah, S., et al. (2019). Overall and site-specific cancer mortality in patients on dialysis and after kidney transplant. *J. Am. Soc. Nephrol.* 30, 471–480. doi: 10.1681/ASN.2018090906

Beroukhim, R., Mermel, C. H., Porter, D., Wei, G., Raychaudhuri, S., Donovan, J., et al. (2010). The landscape of somatic copy-number alteration across human cancers. *Nature* 463, 899–905. doi: 10.1038/nature08822

Bettegowda, C., Sausen, M., Leary, R. J., Kinde, I., Wang, Y., Agrawal, N., et al. (2014). Detection of circulating tumor DNA in early– and late-stage human malignancies. *Sci. Transl. Med. 6:224ra24*. doi: 10.1126/scitranslmed.3007094

Bohers, E., Viailly, P.-J., Becker, S., Marchand, V., Ruminy P., Maingonnat, C., et al. (2018). Non-invasive monitoring of diffuse large B-cell lymphoma by cell-free DNA high-throughput targeted sequencing: analysis of a prospective cohort. *Blood Cancer J.* 8:74. doi: 10.1038/s41408-018-0111-6

Bray, N. L., Pimentel, H., Melsted, P., and Pachter, L. (2016). Near-optimal probabilistic RNA-seq quantification. *Nat. Biotechnol.* 34, 525–527. doi: 10.1038/nbt.3519

Carter, S. L., Cibulskis, K., Helman, E., McKenna, A., Shen, H., Zack, T., et al. (2012). Absolute quantification of somatic DNA alterations in human cancer. *Nat. Biotechnol.* 30, 413–421. doi: 10.1038/nbt.2203

Cascione, L., Aresu, L., Baudis, M., and Bertoni, F. (2020). DNA copy number changes in diffuse large b cell lymphomas. *Front. Oncol.* 10:584095. doi: 10.3389/fonc.2020.584095

Chen, S., Zhou, Y., Chen, Y., and Gu, J. (2018). fastp: an ultra-fast all-in-one FASTQ preprocessor. *Bioinformatics* 34, i884–i890. doi: 10.1093/bioinformatics/bty560

Chen, X., Chang, C. W., Spoerke, J. M., Yoh, K. E., Kapoor, V., Baudo, C., et al. (2019). Low-pass whole-genome sequencing of circulating cell-free dna demonstrates dynamic changes in genomic copy number in a squamous lung cancer clinical cohort. *Clin. Cancer Res.* 25, 2254–2263. doi: 10.1158/1078-0432.CCR-18-1593

Cibulskis, K., Lawrence, M. S., Carter, S. L., Sivachenko, A., Jaffe, D., Sougnez, C., et al. (2013). Sensitive detection of somatic point mutations in impure and heterogeneous cancer samples. *Nat. Biotechnol.* 31, 213–219. doi: 10.1038/nbt.2514

Cleveland, H., Chau, A., Jeng, Z., Gardner, G., Yoo, R., Zhang, W., et al. (2020). Percutaneous lung biopsy in immunocompromised pediatric patients. *J. Vasc. Interv. Radiol.* 31, 93–98. doi: 10.1016/j.jvir.2019.07.016

Costello, M., Pugh, T. J., Fennell, T. J., Stewart, C., Lichtenstein, L., Meldrim, J. C., et al. (2013). Discovery and characterization of artifactual mutations in deep coverage targeted capture sequencing data due to oxidative DNA damage during sample preparation. *Nucleic Acids Res.* 41:e67. doi: 10.1093/nar/gks1443

Denis, J. A., Guillerm, E., Coulet, F., Larsen, A. K., and Lacorte, J. M. (2017). The role of beaming and digital PCR for multiplexed analysis in molecular oncology in the era of next-generation sequencing. *Mol. Diagn. Ther.* 21, 587–600. doi: 10.1007/s40291-017-0287-7

Dobin, A., Davis, C. A., Schlesinger, F., Drenkow, J., Zaleski, C., Jha, S., et al. (2013). STAR: ultrafast universal RNA-seq aligner. *Bioinformatics*. 29, 15–21. doi: 10.1093/bioinformatics/bts635

Ha, G., Roth, A., Khattra, J., Ho, J., Yap, D., Prentice, L. M., et al. (2014). TITAN: inference of copy number architectures in clonal cell populations from tumor whole-genome sequence data. *Genome Res.* 24, 1881–1893. doi: 10.1101/gr.180281.114

Ha, G., Roth, A., Lai, D., Bashashati, A., Ding, J., Goya, R., et al. (2012). Integrative analysis of genome-wide loss of heterozygosity and monoallelic expression at nucleotide resolution reveals disrupted pathways in triple-negative breast cancer. *Genome Res.* 22, 1995–2007. doi: 10.1101/gr.137570.112

Horner, M. J., Shiels, M. S., Pfeiffer, R. M., and Engels, E. A. (2020). Deaths attributable to cancer in the United States HIV population during 2001-2015. *Clin. Infect. Dis.* 72, e224–e231. doi: 10.1093/cid/ciaa1016

Hortlund, M., Arroyo Muhr, L. S., Storm, H., Engholm, G., Dillner, J., and Bzhalava, D. (2017). Cancer risks after solid organ transplantation and after long-term dialysis. *Int. J. Cancer* 140, 1091–1101. doi: 10.1002/ijc.30531

Ilie, M., and Hofman, P. (2016). Pros: Can tissue biopsy be replaced by liquid biopsy? *Transl. Lung Cancer Res.* 5, 420–423. doi: 10.21037/tlcr.2016.08.06

Ishii, H., Azuma, K., Sakai, K., Naito, Y., Matsuo, N., Tokito, T., et al. (2020). Determination of somatic mutations and tumor mutation burden in plasma by capp-seq during afatinib treatment in nsclc patients resistance to osimertinib. *Sci. Rep.* 10:691. doi: 10.1038/s41598-020-57624-4

Kim, S., Scheffler, K., Halpern, A. L., Bekritsky, M. A., Noh, E., Kallberg, M., et al. (2018). Strelka2: fast and accurate calling of germline and somatic variants. *Nat. Methods* 15, 591–594. doi: 10.1038/s41592-018-0051-x

Li, H., and Durbin, R. (2009). Fast and accurate short read alignment with Burrows-Wheeler transform. *Bioinformatics* 25, 1754–1760. doi: 10.1093/bioinformatics/btp324

Lopez, C., Kleinheinz, K., Aukema, S. M., Rohde, M., Bernhart, S. H., Hubschmann, D., et al. (2019). Genomic and transcriptomic changes complement each other in the pathogenesis of sporadic Burkitt lymphoma. *Nat. Commun.* 10:1459. doi: 10.1038/s41467-019-08578-3

McKenna, A., Hanna, M., Banks, E., Sivachenko, A., Cibulskis, K., Kernytsky, A., et al. (2010). The Genome Analysis Toolkit: a MapReduce framework for analyzing next-generation DNA sequencing data. *Genome Res.* 20, 1297–1303. doi: 10.1101/gr.107524.110

Mouliere, F., Mair, R., Chandrananda, D., Marass, F., Smith, C. G., Su, J., et al. (2018). Detection of cell-free DNA fragmentation and copy number alterations in cerebrospinal fluid from glioma patients. *EMBO Mol. Med.* 10:e9323. doi: 10.15252/emmm.201809323

Muralidharan, K., Yekula, A., Small, J. L., Rosh, Z. S., Kang, K. M., Wang, L., et al. (2021). TERT promoter mutation analysis for blood-based diagnosis and monitoring of gliomas. *Clin. Cancer Res.* 27, 169–178. doi: 10.1158/1078-0432.CCR-20-3083

Newman, A. M., Bratman, S. V., To, J., Wynne, J. F., Eclov, N. C., Modlin, L. A., et al. (2014). An ultrasensitive method for quantitating circulating tumor DNA with broad patient coverage. *Nat. Med*. 20, 548–554. doi: 10.1038/nm.3519

Plattner, B. W., Chen, P., Cross, R., Leavitt, M. A., Killen, P. D., and Heung, M. (2018). Complications and adequacy of transplant kidney biopsies: a comparison of techniques. *J. Vasc. Access* 19, 291–296. doi: 10.1177/1129729817747543

Qiu, Z. W., Bi, J. H., Gazdar, A. F., and Song, K. (2017). Genome-wide copy number variation pattern analysis and a classification signature for non-small cell lung cancer. *Genes Chromosomes Cancer* 56, 559–569. doi: 10.1002/gcc.22460

Raman, L., Van der Linden, M., Van der Eecken, K., Vermaelen, K., Demedts, I., Surmont, V., et al. (2020). Shallow whole-genome sequencing of plasma cell-free DNA accurately differentiates small from non-small cell lung carcinoma. *Genome Med.* 12:35. doi: 10.1186/s13073-020-00735-4

Roschewski, M., Dunleavy, K., Pittaluga, S., Moorhead, M., Pepin, F., Kong, K., et al. (2015). Circulating tumour DNA and CT monitoring in patients with untreated diffuse large B-cell lymphoma: a correlative biomarker study. *Lancet Oncol.* 16, 541–549. doi: 10.1016/S1470-2045(15)70106-3

Rosenwald, A., Wright, G., Chan, W. C., Connors, J. M., Campo, E., Fisher, R. I., et al. (2002). The use of molecular profiling to predict survival after chemotherapy for diffuse large-B-cell lymphoma. *N. Engl. J. Med.* 346, 1937–1947. doi: 10.1056/NEJMoa012914

Rossi, D., Diop, F., Spaccarotella, E., Monti, S., Zanni, M., Rasi, S., et al. (2017). Diffuse large B-cell lymphoma genotyping on the liquid biopsy. *Blood* 129, 1947–1957. doi: 10.1182/blood-2016-05-719641

Schmitz, R., Wright, G. W., Huang, D. W., Johnson, C. A., Phelan, J. D., Wang, J. Q., et al. (2018). Genetics and Pathogenesis of diffuse large b-cell lymphoma. *N. Engl. J. Med.* 378, 1396–1407. doi: 10.1056/NEJMoa1801445

Sigel, K., Dubrow, R., Silverberg, M., Crothers, K., Braithwaite, S., and Justice, A. (2011). Cancer screening in patients infected with HIV. *Curr. HIV/AIDS Rep.* 8, 142–152. doi: 10.1007/s11904-011-0085-5

Soneson, C., Love, M. I., and Robinson, M. D. (2015). Differential analyses for RNA-seq: transcript-level estimates improve gene-level inferences. *F1000Research* 4:1521. doi: 10.12688/f1000research.7563.2

Spoerke, J. M., O'Brien, C., Huw, L., Koeppen, H., Fridlyand, J., Brachmann, R. K., et al. (2012). Phosphoinositide 3-kinase (PI3K) pathway alterations are associated with histologic subtypes and are predictive of sensitivity to PI3K inhibitors in lung cancer preclinical models. *Clin. Cancer Res.* 18, 6771–6783. doi: 10.1158/1078-0432.CCR-12-2347

Testoni, M., Zucca, E., Young, K. H., and Bertoni, F. (2015). Genetic lesions in diffuse large B-cell lymphomas. *Ann. Oncol.* 26, 1069–1080. doi: 10.1093/annonc/mdv019

Van Roy, N., Van Der Linden, M., Menten, B., Dheedene, A., Vandeputte, C., Van Dorpe, J., et al. (2017). Shallow whole genome sequencing on circulating cell-free dna allows reliable noninvasive copy-number profiling in neuroblastoma patients. *Clin. Cancer Res.* 23, 6305–6314. doi: 10.1158/1078-0432.CCR-17-0675

Wislez, M., Domblides, C., Greillier, L., Mazières, J., Monnet, I., Kiakouama-Maleka, L., et al. (2021). Circulating tumor DNA in advanced non-small-cell lung cancer patients with HIV is associated with shorter overall survival: Results from a Phase II trial (IFCT-1001 CHIVA). *Lung Cancer* 157, 124–130. doi: 10.1016/j.lungcan.2021.05.013

Yarchoan, R., and Uldrick, T. S. (2018). HIV-associated cancers and related diseases. *N. Engl. J. Med.* 378, 1029–1041. doi: 10.1056/NEJMra1615896

Zhou, B., Ho, S. S., Zhang, X., Pattni, R., Haraksingh, R. R., and Urban, A. E. (2018). Whole-genome sequencing analysis of CNV using low-coverage and paired-end strategies is efficient and outperforms array-based CNV analysis. *J. Med. Genet.* 55, 735–743. doi: 10.1136/jmedgenet-2018-105272

Conflict of Interest: The authors declare that the research was conducted in the absence of any commercial or financial relationships that could be construed as a potential conflict of interest.

Publisher's Note: All claims expressed in this article are solely those of the authors and do not necessarily represent those of their affiliated organizations, or those of the publisher, the editors and the reviewers. Any product that may be evaluated in this article, or claim that may be made by its manufacturer, is not guaranteed or endorsed by the publisher.

Copyright © 2021 Bouzidi, Labreche, Baron, Veyri, Denis, Touat, Sanson, Davi, Guillerm, Jouannet, Charlotte, Bielle, Choquet, Boëlle, Cadranel, Leblond, Autran, Lacorte, Spano, Coulet and the IDEATION study group. This is an open-access article distributed under the terms of the Creative Commons Attribution License (CC BY). The use, distribution or reproduction in other forums is permitted, provided the original author(s) and the copyright owner(s) are credited and that the original publication in this journal is cited, in accordance with accepted academic practice. No use, distribution or reproduction is permitted which does not comply with these terms.

frontiers in Cell and Developmental Biology

ORIGINAL RESEARCH
published: 06 September 2021
doi: 10.3389/fcell.2021.686149

Impact of Preanalytical and Analytical Methods on Cell-Free DNA Diagnostics

*Jure Krasic[1,2,3], Irena Abramovic[1,2,3], Alen Vrtaric[3,4], Nora Nikolac Gabaj[3,4,5], Sasa Kralik-Oguic[3,6], Ana Katusic Bojanac[1,3], Davor Jezek[3,7] and Nino Sincic[1,2,3]**

[1] Department of Medical Biology, School of Medicine, University of Zagreb, Zagreb, Croatia, [2] Scientific Group for Research on Epigenetic Biomarkers, School of Medicine, University of Zagreb, Zagreb, Croatia, [3] Centre of Excellence for Reproductive and Regenerative Medicine, School of Medicine, University of Zagreb, Zagreb, Croatia, [4] Department of Clinical Chemistry, Sestre Milosrdnice University Hospital Center, Zagreb, Croatia, [5] Faculty of Pharmacy and Biochemistry, University of Zagreb, Zagreb, Croatia, [6] Clinical Institute of Laboratory Diagnostics, University Hospital Centre Zagreb, Zagreb, Croatia, [7] Department of Histology and Embryology, School of Medicine, University of Zagreb, Zagreb, Croatia

OPEN ACCESS

Edited by:
George Calin,
University of Texas MD Anderson Cancer Center, United States

Reviewed by:
Carlo V. Bruschi,
University of Salzburg, Austria
Mohamed Zaiou,
Nancy-Université, France

***Correspondence:**
Nino Sincic
nino.sincic@mef.hr

Specialty section:
This article was submitted to Molecular and Cellular Oncology, a section of the journal Frontiers in Cell and Developmental Biology

Received: 26 March 2021
Accepted: 13 August 2021
Published: 06 September 2021

Citation:
Krasic J, Abramovic I, Vrtaric A, Nikolac Gabaj N, Kralik-Oguic S, Katusic Bojanac A, Jezek D and Sincic N (2021) Impact of Preanalytical and Analytical Methods on Cell-Free DNA Diagnostics. Front. Cell Dev. Biol. 9:686149. doi: 10.3389/fcell.2021.686149

While tissue biopsy has for the longest time been the gold-standard in biomedicine, precision/personalized medicine is making the shift toward liquid biopsies. Cell-free DNA (cfDNA) based genetic and epigenetic biomarkers reflect the molecular status of its tissue-of-origin allowing for early and non-invasive diagnostics of different pathologies. However, selection of preanalytical procedures (including cfDNA isolation) as well as analytical methods are known to impact the downstream results. Calls for greater standardization are made continuously, yet comprehensive assessments of the impact on diagnostic parameters are lacking. This study aims to evaluate the preanalytic and analytic factors that influence cfDNA diagnostic parameters in blood and semen. Text mining analysis has been performed to assess cfDNA research trends, and identify studies on isolation methods, preanalytical and analytical impact. Seminal and blood plasma were tested as liquid biopsy sources. Traditional methods of cfDNA isolation, commercial kits (CKs), and an in-house developed protocol were tested, as well as the impact of dithiothreitol (DTT) on cfDNA isolation performance. Fluorimetry, qPCR, digital droplet PCR (ddPCR), and bioanalyzer were compared as cfDNA quantification methods. Fragment analysis was performed by qPCR and bioanalyzer while the downstream application (cfDNA methylation) was analyzed by pyrosequencing. In contrast to blood, semen as a liquid biopsy source has only recently begun to be reported as a liquid biopsy source, with almost half of all publications on it being review articles. Experimental data revealed that cfDNA isolation protocols give a wide range of cfDNA yields, both from blood and seminal plasma. The addition of DTT to CKs has improved yields in seminal plasma and had a neutral/negative impact in blood plasma. Capillary electrophoresis and fluorometry reported much higher yields than PCR methods. While cfDNA yield and integrity were highly impacted, cfDNA methylation was not affected by isolation methodology or DTT. In conclusion, NucleoSnap was recognized as the kit with the best overall performance. DTT improved CK yields

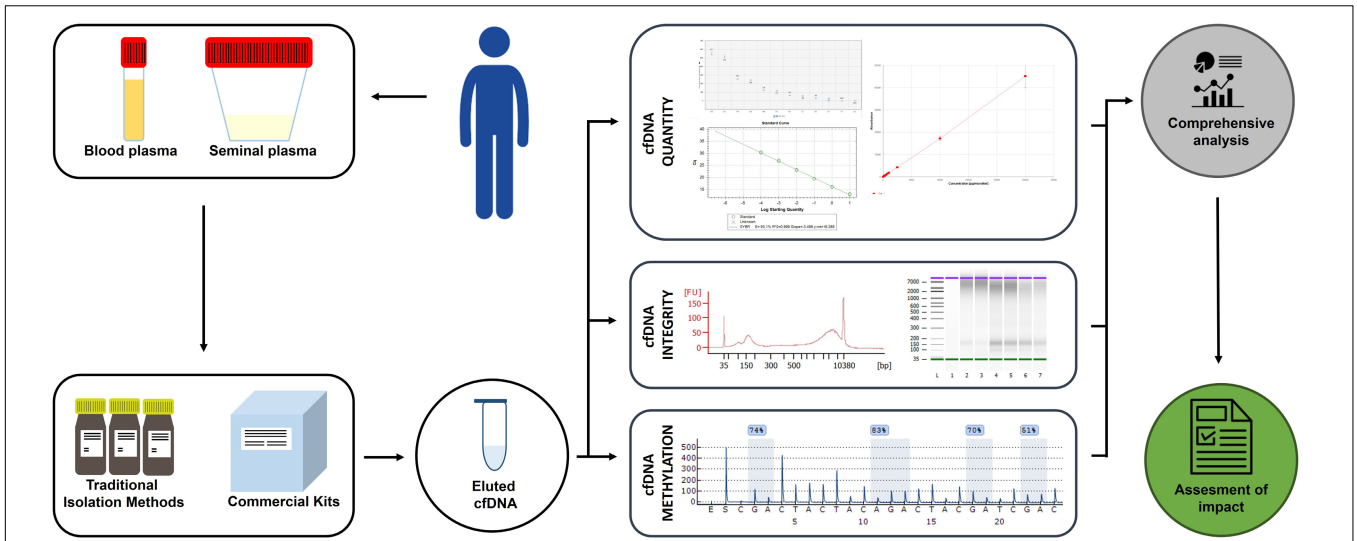

GRAPHICAL ABSTRACT | Depiction of the experimental design.

in seminal plasma. The in-house developed protocol has shown near-kit isolation performance. ddPCR LINE-1 assay for absolute detection of minute amounts of cfDNA was established and allowed for quantification of samples inhibited in qPCR. cfDNA methylation was recognized as a stable biomarker unimpacted by cfDNA isolation method. Finally, semen was found to be an abundant source of cfDNA offering potential research opportunities and benefits for cfDNA based biomarkers development related to male reproductive health.

Keywords: cell-free DNA, liquid biopsy, blood plasma, seminal plasma, preanalytics, cell-free DNA methylation, cell-free DNA integrity

INTRODUCTION

Tissue biopsies have been the gold-standard in disease diagnostics and prognostics (Constâncio et al., 2020). However, the issues with tissue biopsies have become more apparent, such as its invasiveness, the need for repetitive sampling, the problem of tumor heterogeneity, and unapproachability of certain tissues (Stewart et al., 2018; Constâncio et al., 2020; Lee E. Y. et al., 2020). With the advent of precision and personalized medicine these constraints are becoming both more evident and limiting. Utilization of the genetic material in liquid biopsies offers solutions in a reliable, cost-effective, and minimally invasive way (Lobo et al., 2019; Constâncio et al., 2020; Spiller et al., 2020; Thakral et al., 2020; Wang et al., 2020; Vandekerkhove et al., 2021).

Cell-free DNA (cfDNA) is one of the most prominent molecules present in liquid biopsies, discovered in 1948 by Mandel and Metai in human blood plasma (Aucamp et al., 2016; Cook et al., 2018; Krasic et al., 2018). Originating from apoptosis, necrosis, and direct cell secretion, cfDNA has been detected in almost all body fluids, such as urine, sputum, cerebrospinal fluid, pleural fluid, cyst fluid, saliva, bronchial lavages, and semen (Draškovič, 2017; Chen et al., 2018; Kumar et al., 2018; Johansson et al., 2019). It reflects the genetic and epigenetic characteristics of its tissue of origin, such as DNA methylation, mutations, or microsatellite alterations (Barták et al., 2019). cfDNA is double-stranded and varies in size, ranging from 180 bp up to 10,000 bp, with the majority being around 180 bp long, corresponding to the size of the DNA within the nucleosomes by apoptotic processes (Draškovič, 2017; Cook et al., 2018; Somen et al., 2019; Streleckiene et al., 2019; Li S. et al., 2020). In the blood of healthy individuals cfDNA quantity ranges from 1.8 to 44 ng/ml (Draškovič, 2017; Streleckiene et al., 2019), mostly originating from hematopoietic cells (Aucamp et al., 2016; Somen et al., 2019; Lampignano et al., 2020). Its quantity and fragment size can be increased by conditions such as physical activity, pregnancy, and various other states (Warton and Samimi, 2015; Cook et al., 2018; Barták et al., 2019; Johansson et al., 2019; Ottaviano et al., 2021). Disease-derived cfDNA primarily originates from necrotic and phagocytotic processes, such as in inflammation, sepsis, trauma, or cancer, and is elevated in quantity (Aucamp et al., 2016; Ponti et al., 2019; Somen et al., 2019; Yu et al., 2019; Li S. et al., 2020; Ottaviano et al., 2021). Among these cfDNA fractions, circulating tumor DNA (ctDNA), which originates from cancer cells, is of great interest as a novel oncological biomarker (Solassol et al., 2018; Keup et al., 2020; Ponti et al., 2020).

Biomarkers associated with different diseases have been successfully detected in cfDNA, such as copy number variations, single nucleotide polymorphisms, cfDNA integrity, and epigenetic modifications including cfDNA methylation (Vaissière et al., 2009; Vaca-Paniagua et al., 2015; Trigg et al., 2018; Lee et al., 2019; Constâncio et al., 2020; Li S. et al., 2020; Rodriguez-Casanova et al., 2021; Yin et al., 2021). In particular cfDNA quantity, integrity, and methylation have shown themselves to be the most prominent diagnostic parameters (Trigg et al., 2018; Mbaye et al., 2019; Lampignano et al., 2020; Lo et al., 2021; Vandekerkhove et al., 2021; Zhang et al., 2021). cfDNA methylation presents itself as a valuable biomarker in liquid biopsy research due to its high specificity for various biological states and robust biological stability (Constâncio et al., 2020; Miller et al., 2021), with some authors even presenting cfDNA methylation status as the universal cancer biomarker (Meddeb et al., 2019). Recent reports highlight multiple possible applications of the cfDNA methylation profiling among which are: being able to identify the tissue of origin and discern between different tissues (healthy and cancerous) (Moss et al., 2018; Stewart et al., 2018; Gaga et al., 2020; Sprang et al., 2020; Miller et al., 2021), as well as guiding therapy selection and monitoring disease prognosis (Somen et al., 2019; Tuaeva et al., 2019; Li S. et al., 2020). For example, LINE-1 cfDNA hypomethylation is associated with multiple cancer characteristics, such as risk, type, progression, and poor prognosis (Lee et al., 2019). Further research has shown a correlation between cfDNA quantity and tumor size, metastasis status, and burden (Stewart et al., 2018; Streleckiene et al., 2019). The cfDNA integrity index (CFI) is yet another biomarker for cancer diagnostics and therapy monitoring (Kumar et al., 2018; Chan et al., 2021) with longer fragments described in cancer patients (Meddeb et al., 2019; Shi et al., 2020; Chan et al., 2021). Research on the possible applications of cfDNA's size profile is ongoing in many fields such as oncology, transplantation medicine, cardiology, and infectious disease medicine (Shi et al., 2020), as well as in reproductive medicine since sperm fragmentation index has been proposed to supplement routine diagnostics in identifying subfertility issues and predict *in vitro* fertilization success (Li L. et al., 2020). Limitations of cfDNA include the relatively short half-life and the variable amount of target cfDNA fraction (Ponti et al., 2019; Sorber et al., 2019; Lampignano et al., 2020). In particular, ctDNA is detected in blood samples of over 75% pancreatic, ovarian, and colorectal cancer patients, while in prostate cancer patients significantly lower levels were found (Ponti et al., 2019) suggesting that for different pathologies different liquids should be investigated as biopsies.

In contrast to blood plasma, very little research has been done on seminal plasma despite many factors pointing to its great promise in male reproductive medicine. For example, seminal plasma has a comparatively high amount of cfDNA of heterogeneous size in relation to other body fluids (Draškovič, 2017; Ponti et al., 2019) which allows for analysis such as the genome-wide promoter methylation of the human testis and epididymis to be performed (Wu et al., 2013). Seminal plasma cfDNA levels correlate with sperm parameters, with the quantity of low molecular weight cfDNA correlating to positive sperm parameters, and higher cfDNA concentrations discriminating azoospermic patients from normozoospermic (Li et al., 2009; Chen et al., 2018; Ponti et al., 2018; Mbaye et al., 2019; Morgan and Watkins, 2020). So far, cfDNA concentrations and their electrophoretic patterns have been shown to discriminate between prostate cancer, benign prostatic hyperplasia patients, and age-matched healthy controls (Ponti et al., 2019). This could allow seminal plasma to provide a non-invasive alternative to prostate tissue biopsies which carry risks of morbidity (Drabovich et al., 2014; Ponti et al., 2018). Seminal plasma is a true non-invasive biopsy, and with the high abundance of cfDNA is suitable for both cost-effective and more advanced diagnostic methods, promising to find a place in male reproductive medicine (Li et al., 2009; Drabovich et al., 2014; Ponti et al., 2018, 2019; Mbaye et al., 2019; Morgan and Watkins, 2020).

Although progress has been made many issues have remained unsolved, leaving the integration of cfDNA into routine clinical practice facing the challenge of standardization of both the preanalytical phase and analytical assays (Lampignano et al., 2020). Currently, there are over 60 clinical trials involving cfDNA approaches, which all depend on their practical advantage and robustness in the clinical setting (Kumar et al., 2018). So far, cfDNA is only being utilized by specialized laboratories which have reported 13 different techniques for the isolation of cfDNA, 5 different methodological approaches for quantification, and 11 different genotyping methods, clearly demonstrating little inter-laboratory standardization (Haselmann et al., 2018; Kumar et al., 2018; Lampignano et al., 2020). Sample collection, preservation, blood collection tube type, storage temperature, serum or plasma preparation, and cfDNA extraction were already proven to have an impact on the amount, integrity, and purity of isolated cfDNA with a strong influence on the downstream molecular analysis (Medina Diaz et al., 2016; Sorber et al., 2019; Lee J. S. et al., 2020; Samoila et al., 2020). A number of studies are being published on assessing various preanalytical variables and technical aspects of cfDNA extraction which are calling attention to new potential issues in the employed methodology and a need for greater standardization in liquid biopsy protocols and workflows (Page et al., 2006; Malentacchi et al., 2015; Draškovič, 2017; Cook et al., 2018; Kumar et al., 2018; Mojtabanezhad Shariatpanahi et al., 2018; Barták et al., 2019; de Kock et al., 2019; Meddeb et al., 2019; Sorber et al., 2019; Streleckiene et al., 2019; Abramovic et al., 2020; Augustus et al., 2020; Bronkhorst et al., 2020; Lampignano et al., 2020; Lee E. Y. et al., 2020; Lee J. S. et al., 2020; Salvianti et al., 2020; Samoila et al., 2020). The clinical use of cfDNA also requires the development and standardization of high sensitivity methods able to analyze highly fragmented DNA (Johansson et al., 2019; Sorber et al., 2019). Despite all this, comprehensive studies examining the impact of extraction methods on cfDNA diagnostic parameters are sorely lacking in both blood and seminal plasma (Draškovič, 2017). With both the preanalytical protocols and analytical assays standardized, reference values correlating to disease states could be reliably identified and translated to clinical practice (Aucamp et al., 2017).

The aim of this study was to identify and evaluate these preanalytic and analytic factors that influence cfDNA diagnostic

parameters in blood and semen samples. For this reason, the impact of traditional cfDNA isolation methods and kit-based isolation methods was evaluated on cfDNA diagnostic parameters (cfDNA yield, integrity, and cfDNA methylation). We have employed fluorimetry, qPCR, digital droplet PCR (ddPCR), and capillary electrophoresis as the four most commonly used cfDNA detection methods. CFI was assessed using qPCR and capillary electrophoresis. The impact on cfDNA methylation was analyzed by pyrosequencing.

MATERIALS AND METHODS

Text Mining

In order to identify all studies comparing cfDNA isolation methods and cfDNA research in general, a Europe PMC based literature search was conducted, with the last update being on the 31st of December 2020. Europe PMC was selected due to it being a flexible platform with currently 1.3 billion annotations text mined from articles, and growing (Ferguson et al., 2021). Keywords were combined with Boolean operators into search terms and are listed in **Table 1**.

Sample Collection and Plasma Preparation

Blood and ejaculate samples were taken from 12 normozoospermic men. The criteria for normozoospermia were according to the guidelines of World Health Organization (WHO) (Cooper et al., 2009). Samples were drawn and plasma was prepared at the clinical hospital centers Zagreb and Sestre milosrdnice.

Of peripheral venous blood 12 ml (two 6 ml tubes) was collected into EDTA-containing tubes (Greiner Bio-One) and processed within 2 h after venipuncture. To ensure cell-free plasma collection and to prevent cellular contamination, all EDTA-blood samples were centrifuged in two steps (1400 × *g* for 10 min and then 4500 × *g* for 10 min). Blood plasma was stored at −80°C.

Ejaculate samples were obtained by masturbation after 3–5 days of sexual abstinence and were allowed to liquefy for 30–60 min at room temperature. Seminal plasma was obtained by triple centrifugation of ejaculate samples to prevent cellular contamination (400 × *g* for 10 min, 12,000 × *g* for 10 min, and 20,000 × *g* for 10 min), which is a modification of the protocol by Li et al. (2009). Seminal plasma was stored at −80°C.

Plasma samples were pooled before further processing into one blood plasma sample and one seminal plasma sample, to remove subject variance.

TABLE 1 | List of search terms used in the literature search and the goal for which they were used.

Research goal	Search term
Identification of publications on cfDNA isolation methods	("cell-free DNA" OR "cell free DNA" OR cfDNA) AND (isolation method OR extraction method OR purification method) AND (optimization OR comparison OR selection OR evaluation) AND (plasma OR serum OR blood OR urine OR ejaculate OR semen OR "seminal fluid" OR "liquid biopsy")
Identification of publications on cfDNA research	"cell-free DNA" OR "cfDNA" OR "cell free DNA"
	("cell-free DNA" OR "cfDNA" OR "cell free DNA") AND (blood)
	("cell-free DNA" OR "cfDNA" OR "cell free DNA") AND (urine)
	("cell-free DNA" OR "cfDNA" OR "cell free DNA") AND (semen OR ejaculate OR "seminal plasma" OR "seminal fluid")

cfDNA Isolation

The most commonly used traditional methods for cfDNA isolation (TIM) were selected for the study: the Triton–Heat–Phenol (THP) by Xue et al. (2009), Phenol–chloroform isoamyl alcohol isolation (PCI) protocols by Yuan et al. (2012); Schmidt et al. (2005), and Hufnagl et al. (2013), which were all done following the author's recommendations. We have also tested the salting-out method by Miller et al. (1988) which is one of the most widely used gDNA isolation methods and which has been previously used, with slight modifications in cfDNA isolation (Jorgez et al., 2006). The recommendations laid out in the original article were followed.

An in-house PCI cfDNA isolation protocol with dithiothreitol (DTT) was developed, following DTT amount recommendations for sperm gDNA isolation from the research article by Doerksen et al. (2000). Briefly, 100 μL of lysis solution (240 mM Tris–HCl pH 8.0, 1800 mM NaCl, and 120 mM EDTA), 120 μL of 10% SDS, 30 μL of proteinase-K, and 12 μL of 1 M DTT was added to 1 ml of blood plasma and seminal plasma, respectively. The plasma sample was vortexed, spun down, and left over-night in a heating block at 50°C. PCI was added 1:1 to the plasma, shaken, and incubated at room temperature for 5 min, after which the sample was centrifuged at 16,000 × *g* for 15 min. The supernatant was transferred to a new tube and the DNA was precipitated by adding 1/20 of the volume of 4 M NaCl and 1/1 volume of ice-cold ethanol and incubating at −20°C over-night. The DNA was centrifuged at maximum speed for 30 min, washed with 70% ethanol, centrifuged at maximum speed for 30 min and dissolved in 100 μL of TE buffer (10 mM Tris–HCl pH 8.0 and 1 mM EDTA).

The three most widely used commercial kits (CK) for cfDNA isolation were selected, Qiagen's QIAmp Circulating Nucleic Acid Kit which is currently the gold standard (Streleckiene et al., 2019), Zymo's Quick-cfDNA Serum & Plasma Kit, and Macherey-Nagel's NucleoSnap cfDNA. All protocols were performed according to the manufacturer's instruction, using the QIAvac 24 Plus vacuum station (Qiagen). The proteinase-K digestion step has been increased to overnight in all three kits, as it has been shown that longer digestion results in higher yields (Pérez-Barrios et al., 2016). Protocols used are depicted in **Table 2**.

TABLE 2 | List of cfDNA isolation methods used in the study along with their sources.

cfDNA isolation methods used				
Protocol	**Protocol description**	**Source**	**Previously tested on blood plasma**	**Previously tested on seminal plasma**
TIM-1	Triton–Heat–Phenol (THP)	Xue et al., 2009	Yes	No
TIM-2	PCI	Yuan et al., 2012	Yes	No
TIM-3	PCI	Hufnagl et al., 2013	Yes	No
TIM-4	PCI	Schmidt et al., 2005	Yes	No
TIM-5	Salting out	Miller et al., 1988	Yes	No
TIM-6	PCI	In-house	No	No
TIM-7	PCI – TIM-3 modified	Hufnagl et al., 2013	No	No
CK-1	QIAmp Circulating Nucleic Acid Kit	Qiagen	Yes	Yes
CK-2	Quick-cfDNA Serum & Plasma Kit	Zymo	Yes	No
CK-3	NucleoSnap cfDNA	Macherey-Nagel	Yes	No

The impact of DTT on cfDNA isolation was tested as well, with the protocols described in **Table 3**. To the CK groups, 10 mM DTT was added since it is the standard concentration used in most sperm DNA isolations. To the modified Hufnagl et al.'s (2013) 80 mM DTT was added to test if the reported higher concentrations of DTT improve isolation yields (He et al., 2017).

The cfDNA isolation protocols were performed starting with 1 ml of blood or seminal plasma which was eluted in 100 μL of elution buffer (for CK) or TE buffer (for TIM). cfDNA of the same body liquid and isolated by the same protocol was pooled for fragment analysis.

Fluorometric dsDNA Assay

To perform fluorometric quantification of cfDNA quantity Quant-iT PicoGreen dsDNA Assay Kit (Thermofisher), was used, following the manufacturer's instructions. Samples were excited at 480 nm and the fluorescence was measured at 520 nm using a TECAN Spark multimode reader. Lambda DNA was used to generate the standard curve. All samples and standards were run in triplicates.

Real-Time PCR

As described in detail in Rago et al. (2007), human LINE-1 is a retrotransposon family member with over 100,000 elements interspersed throughout the human genome. As such, quantifying human LINE-1 offers a sensitive method for quantifying human cfDNA, therefore the concentration and integrity of total cfDNA were determined by qPCR with primers targeting the second open reading frame of the human LINE-1 element.

Primers amplifying an 82-bp and a 224-bp LINE-1 region were used (Takai et al., 2015). The shorter amplicon was used to quantify total cfDNA, while the longer amplicon was used to calculate the CFI, with the ratio of longer cfDNA fragments to the shorter ones (Rostami et al., 2020). The primers used are listed in **Table 4**.

qPCR reactions were carried out in triplicate, using 1 μL of isolated cfDNA, SsoAdvanced Universal SYBR Green Supermix (Bio-Rad Laboratories), and 250 nM forward and reverse primers. Real-Time PCR amplification was performed on the CFX96 Touch Real-Time PCR Detection System (Bio-Rad Laboratories) according to the protocol: pre-cycling heat activation of DNA polymerase at 98°C for 3 min followed by 40 cycles of denaturation at 98°C for 10 s, annealing/extension at 60°C for 30 s, followed by a melting point gradient from 65 to 95°C. The analysis was performed using CFX Maestro Software (Bio-Rad Laboratories). Absolute quantification of cfDNA in each sample was determined by a standard curve with serial dilutions of human genomic DNA (Qiagen).

Droplet Digital PCR

To assess the viability of cfDNA concentration detection by ddPCR, the total 82 bp LINE-1 cfDNA fragments were quantified on the ddPCR system (Bio-Rad Laboratories), using the modified protocol from He K. et al. (2019).

Isolated cfDNA samples were diluted (with dilutions ranging from 3× to 1000×) to allow for accurate quantification of LINE-1 fragments and avoiding droplet oversaturation. Commercial human genomic DNA (Qiagen) was used to create a standard curve ranging from 3.125 to 100 pg/μL for accurate absolute cfDNA quantification. All samples and standards were *HaeIII*-digested and were ran in duplicates. The ddPCR reaction was set up using 1 μL of isolated cfDNA, QX200 ddPCR EvaGreen, Supermix (Bio-Rad Laboratories), and 100 nM forward and reverse primers (**Table 4**). Droplets were generated in the Bio-Rad QX200 droplet generator (Bio-Rad Laboratories) using the QX200 Droplet Generation Oil for EvaGreen. The droplets were transferred to a 96 well ddPCR plate (Bio-Rad Laboratories) and heat-sealed with a pierceable aluminum foil (Bio-Rad) in the PX1 PCR Plate Sealer (Bio-Rad). PCR amplification was done using the CFX96 Deep Well PCR thermal cycler (Bio-Rad Laboratories) according to the protocol: activation at 95°C for 5 min, 40 cycles of denaturation at 95°C for 30 s, and annealing/extension at 60°C for 60 s, followed by signal stabilization at 4°C for 5 min and 90°C for 5 min and the final step being an infinite hold at 4°C. All steps had a ramp rate of 2°C/s. Droplets were analyzed in the QX200 Droplet Reader (Bio-Rad Laboratories) using QuantaSoft software and quantified assuming Poisson's

TABLE 3 | List of methods used to assess the impact of DTT addition on blood and seminal plasma isolation.

DTT impact on cfDNA				
Protocol	**Protocol description**	**DTT amount (mM)**	**Previously tested on blood plasma**	**Previously tested on seminal plasma**
TIM-6	In-house developed PCI	10	No	No
TIM-7	Modification of Hufnaghl et al.	80	No	No
CK-1 +	QIAmp Circulating Nucleic Acid Kit	10	No	No
CK-2 +	Quick-cfDNA Serum & Plasma Kit	10	No	No
CK-3 +	NucleoSnap cfDNA	10	No	No

TABLE 4 | List of primers used along with their amplicon size.

Target	Description		Sequence	bp
LINE-1	Short sequence	F	5′-TCACTCAAAGCCGCTCAACTAC-3′	82
		R	5′-TCTGCCTTCATTTCGTTATGTACC-3′	
LINE-1	Long sequence	F	5′-TCTGCCTTCATTTCGTTATGTACC-3′	224
		R	5′-TCAGCACCACACCACACCTATTC-3′	
LINE-1	Pyrosequencing	F	5′-BIOTIN-TAGGGAGTGTTAGATAGTGG-3′	108
		R	5′-AACTCCCTAACCCCTTAC-3′	
		SEQ	5′-CAAATAAAACAATACCTC-3′	

random distribution. Data was acquired using one-dimensional or two-dimensional based plotting systems as recommended by the manufacturer. Thresholds were set by excluding only the true negative population, according to the no-template control which was included in each assay.

Bioanalyzer

The isolated cfDNA fragment profile and concentration were analyzed using capillary electrophoresis. The High Sensitivity DNA microchip kit (Agilent Technologies) and an Agilent 2100 Bioanalyzer (Agilent Technologies) equipped with Expert 2100 software were used to perform the analysis, according to the instructions provided by the manufacturer. After the nucleic acids were separated analogously to capillary electrophoresis, they were normalized to the two DNA markers and were visualized as a virtual band. Fragments were separated into short (223 bp and less) and long (224 bp and more), which has allowed the calculation of CFI, with the ratio of longer fragments to total quantified cfDNA.

cfDNA Methylation Analysis

Bisulfite conversion was performed using the EpiTect Plus DNA Bisulfite Kit (Qiagen) and 40 μL of the isolated cfDNA, according to the manufacturer's instructions. Bisulfite-converted cfDNA was then eluted in 30 μL of elution buffer.

For the PCR amplification of the LINE-1 repetitive region using the PyroMark PCR Kit (Qiagen) 1 μL of bisulfite-treated DNA was used as the template. Samples along with methylated and unmethylated control DNA from the EpiTect PCR Control DNA kit (Qiagen) were run in triplicates. PCR protocol was as follows: initial denaturation at 95°C for 15 min; 50 cycles of denaturation at 94°C for 30 s, annealing at 58°C for 30 s, and extension at 72°C for 30 s; final extension was at 72°C for 10 min (Daskalos et al., 2009). The biotinylated PCR product was purified using the Pyromark Q24 Vacuum Workstation (Qiagen). Methylation levels of the six CpG's were then measured by Pyromark Q24 Advanced System with PyroMark Q24 CpG Advanced Reagents (Qiagen). cfDNA methylation levels were calculated as the ratio of C/T at a CpG site using the Pyromark Q24 Advanced Software 3.0.1 (Qiagen). Global cfDNA methylation was calculated as the average value of the six CpG's. Primers used in cfDNA methylation analysis are listed in **Table 4**.

Statistical Analysis

Isolated cfDNA concentrations were statistically analyzed by the Kruskal–Wallis test with Dunn's multiple correction test using the GraphPad Prism Software (GraphPad), with the level of significance set to 0.05.

RESULTS

Literature Mining

The literature search using Europe PMC for scientific publications involving cfDNA research has found the earliest two publications in 1967 while reaching up to 10 publications per year only in 1988. This low-publishing trend on cfDNA research existed until the 2000s when more than 10 publications per year were published consistently. The following increase in publication quantity regarding cfDNA was extremely rapid, with the first 6 years of the 21st century producing more articles than the whole period from 1967 to 2000 (**Figure 1**). The increase is still ongoing with 100 publications per year being achieved in 2010, 1000 per year in 2017 while in 2020 there were 2833 publications related to cfDNA. However, of the published articles 2105 included blood as the cfDNA source, urine being a distant second with 504 published articles, and semen (seminal fluid) has lagged even further behind with only 55 published articles as a source of cfDNA.

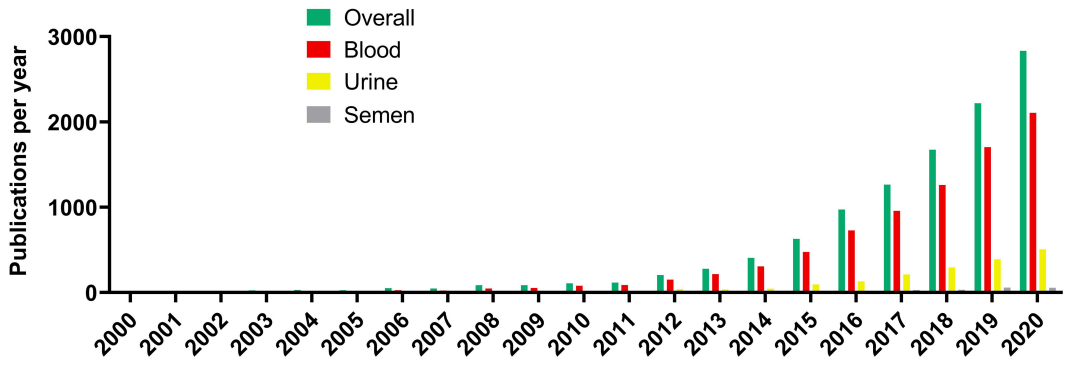

FIGURE 1 | Cell-free DNA article publication rate per year.

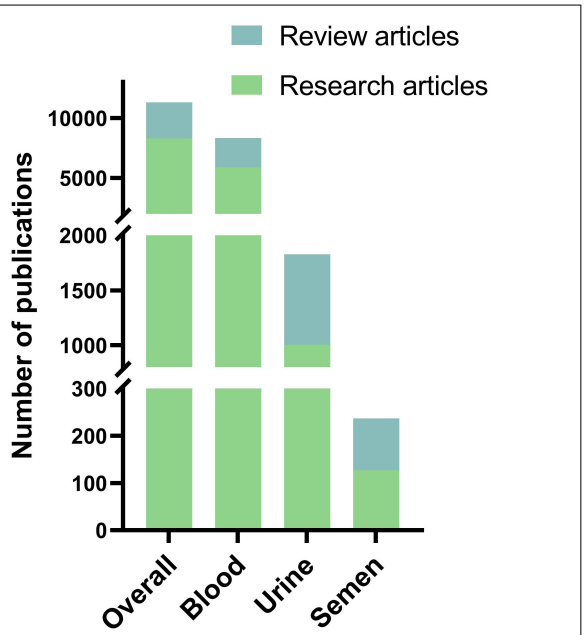

FIGURE 2 | Amount of original research articles and review articles in the total number of publications on cfDNA within respective body fluid of origin.

Publications on cfDNA research were then separated by type, being original research or review articles (**Figure 2**). Overall, review articles make up 27% of all articles published on cfDNA, 29% of all articles on blood, 45% on urine, and 46% on semen as a cfDNA source.

Next, Europe PMC literature search was carried out to identify publications that compare cfDNA isolation methods and the impact of various preanalytical factors on them. The search has produced 2198 results, of which 696 were discarded due to being reviews, thus leaving 1502 results. Poster and oral presentations were further excluded leaving 1393 results for review by title and abstract by two authors. Finally, 147 articles were left for full-text evaluation by two authors, who have additionally excluded articles with no comparison of different cfDNA isolation methods, with no investigation on the impact of preanalytical parameters on cfDNA isolation, and no usage of human samples. Eighty-three publications were obtained at the end, dating as early as 2006 with a frequency not more than a few publications per year, until 2018 where 13 articles were published. The increase in interest for cfDNA isolation methods continued in 2019 and 2020 with 21 and 20 research articles being published, respectively (**Figure 3**). The selected articles, when separated according to body fluid used for cfDNA isolation conform with the overall cfDNA article trends, blood as a liquid biopsy was generally the most explored, followed by urine and so far, only one published research was done on seminal plasma as cfDNA source dating from 2009 (**Table 5**). Most of the publications have compared the impact of different isolation methods using only one liquid biopsy source, followed by assessing the potential of body fluids (such as bronchial lavage or urine) for cfDNA isolation, while only rare studies compared the efficacy impact of different isolation methods on different body fluids.

cfDNA Yield

Fluorometric assessment of cfDNA yield has shown a significant impact of isolation methods on cfDNA yield in both blood and seminal plasma. Yields of cfDNA extracted from blood plasma according to TIM protocols were in the range from 14 to 31 ng/ml, while CK protocols have produced a narrower yield range from 5 to 15 ng/ml. Seminal plasma cfDNA yields from TIM protocols have ranged from 95 to 727 ng/ml, while CK protocols have ranged from 86 to 656 ng/ml (**Figure 4A**). As seen in blood plasma, most of the TIM's outperformed the CK's, while in seminal plasma TIM-5, TIM-6, CK-2, and CK-3 samples stood out roughly equally above the rest. Moreover, in blood plasma, the addition of DTT in three CK has led to a reduction of 5, 6, and 1% of cfDNA yield, respectively. In seminal plasma, an increase in yield by 14% in CK-1, and by 33% in CK-3 was observed, while in CK-2 a reduction of 6% was found.

Assessment of cfDNA yield by qPCR analysis of LINE-1 has again shown a significant impact of different isolation methods on blood and seminal plasma cfDNA yield (**Figure 4B**). However, contrary to the fluorometric measurement, in blood plasma, cfDNA yields from TIM protocols measured by qPCR

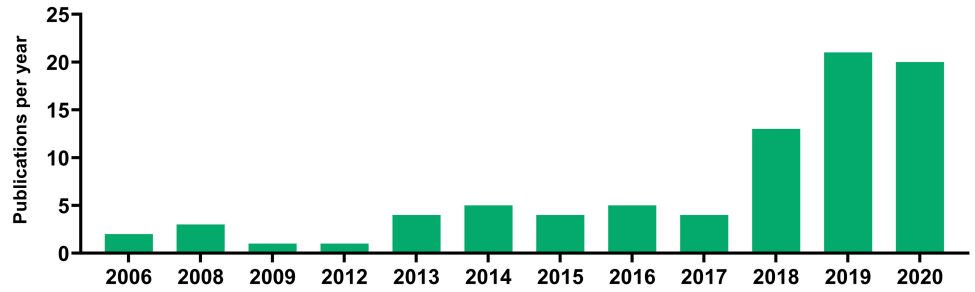

FIGURE 3 | Articles published investigating the impact of various protocols on cfDNA research and analysis.

TABLE 5 | Investigated parameters within the publications assessing the impact of various preanalytical and analytical parameters of cfDNA research.

Articles comparing cell-free DNA methods			**83**
cfDNA source		Plasma	65
	Blood		
		Serum	5
	Urine		15
	Semen		1
Comparisons		Method	58
	Isolation		
		Between liquids	9
	Centrifugation		9
	Quantification/fragment distribution		31
	Tubes/preservatives		13
	Effect of time and temperature		15
	Preanalytical impacts on analysis outcome		42

were lower (1–7 ng/ml) than those from CK samples (5–9 ng/ml). A similar trend was observed for seminal plasma, with higher (75–753 ng/ml) yields of CK samples compared to TIM (0.2–429 ng/ml). Furthermore, we observed a negative impact of DTT addition to CK protocols on cfDNA yields in blood plasma with a decrease of 3% in CK-1, 94% in CK-2, and 9% in CK-3. In seminal plasma, however, an improvement of cfDNA yields was obtained by the addition of DTT with 22% in CK-1, 9% in CK-2, and 34% in CK-3. However, both the blood and seminal plasma cfDNA samples isolated by the TIM-5 protocol failed to be detected by the qPCR measurement.

Quantification of cfDNA yield by ddPCR analysis of LINE-1 has shown the same overall trend established by qPCR analysis (**Figure 4C**). In the blood plasma processed by TIM protocols, cfDNA yields have ranged from 1 to 6 ng/ml, while in CK protocols a range of 4–7 ng/ml, was obtained. In the seminal plasma sample processed by TIM cfDNA yields have ranged from 1 to 895 ng/ml with TIM-5 having had the highest yield overall, while in CK protocols the range was a bit smaller, from 68 to 584 ng/ml. With ddPCR employed as a measurement tool, the addition of DTT to blood plasma in CK protocols has reduced cfDNA yields by 4% in CK-1, 43% in CK-2, and 14% in CK-3. The seminal plasma sample has shown an increase in cfDNA quantity by 22% when processed by CK-1, and 28% by CK-3, while a reduction of 19% was found in CK-2 protocol after the addition of DDT.

Capillary electrophoretic analysis of cfDNA quantity from blood plasma has shown similar yields to fluorometric analysis, with TIM protocol ranges having been in the range of 1–20 ng/ml and CK yields were in the range of 15–27 ng/ml. The highest yield was exhibited by CM-3 protocol at 26 ng/ml (**Figure 4D**). The TIM-5 protocol, however, was not analyzable, similarly to qPCR analysis. In seminal plasma, the same overall trend was observed, with yields again being more similar to fluorometric analysis. cfDNA yields from TIM protocols were in the range from 350 to 982 ng/ml with TIM-2 having had the highest yield at 982 ng/ml. Meanwhile, the TIM-1 protocol was not analyzable (as in both the qPCR and ddPCR analysis). As for cfDNA yields from CK protocols, they were in the range of 138–775 ng/ml. The addition of DTT to blood plasma has reduced yield in the CK-2 protocol by 67%, while it has increased the yield of the CK-3 protocol by 28%. As for the impact of DTT on the cfDNA yield of blood plasma processed by CK-1, it was not analyzable by the bioanalyzer. In seminal plasma, DDT has reduced overall yield by 8% in CK-1, by 14% in CK-2, and by 1% in CK-3.

cfDNA Integrity

Analysis of the ratio of short (82 bp) and long (224 bp) LINE-1 fragments by qPCR has allowed us to quantify the total amount of long and short LINE-1 fragments in samples, and subsequently calculate the CFI for the cfDNA isolation methods (**Figure 5A**). Blood plasma CFI has ranged from 0.22 to 0.43, while seminal plasma CFI has ranged from 0 to 0.45. Most blood plasma protocols have exhibited a similar CFI of 0.4, with the lowest CFI having been exhibited by the CK-2 protocol, which has presented a lower amount of isolated fragments in general (**Figure 5B**). Seminal plasma CFI has shown a much higher variability depending on the isolation method, with only TIM-3, TIM-4, and the CK protocols having had comparable levels of CFI. It is also noteworthy that the seminal plasma processed by TIM-7 only contained short cfDNA fragments. The addition of DTT to blood plasma increased the CFI by 6% in CK-1 but reduced it in CK-2 and CK-3 by 16%. In seminal plasma, CK-1 has produced an increase of the CFI by 22% and CK-3 by 6%, while CK-2 saw a reduction of 4% due to DDT.

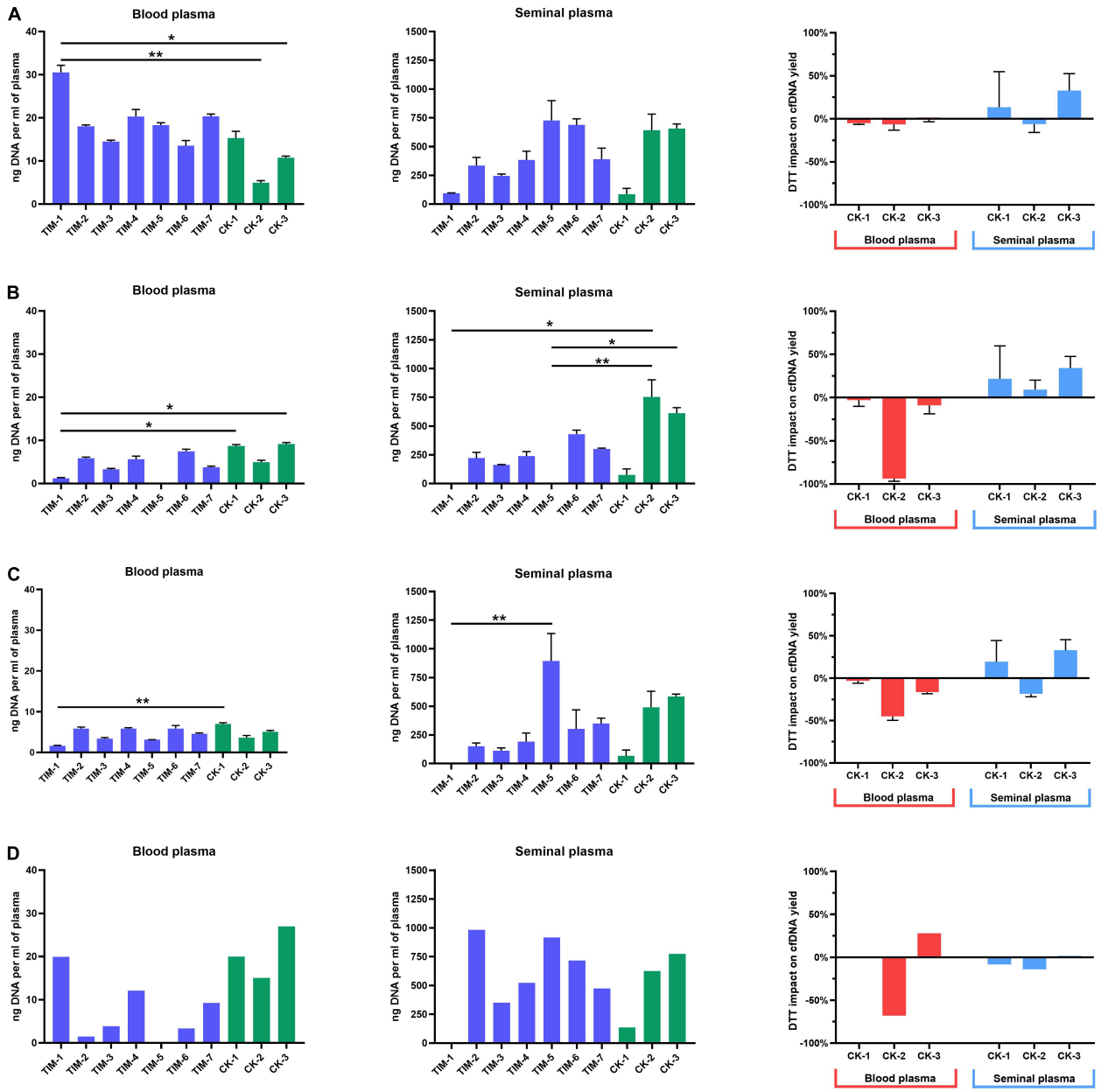

FIGURE 4 | Cell-free DNA yields from blood and seminal plasma. **(A)** Yields measured by fluorometry, with DTT impact on commercial kits depicted as percentage change; **(B)** yields measured by qPCR analysis of LINE-1, with DTT impact on commercial kits depicted as percentage change; **(C)** yields measured by ddPCR, with DTT impact on commercial kits depicted as percentage change; **(D)** yields measured by capillary electrophoresis, with DTT impact on commercial kits depicted as percentage of change. Values represented are means with SD. Asterisks were used to depict statistical significance, $^{*}P < 0.05$, $^{**}P < 0.01$.

Analysis of fragment size was performed by capillary electrophoresis as well, with the cut-off set at 223 bp to discriminate between long and short cfDNA fragments. In blood plasma, CFI has ranged from 0.2 to 1.0, along with the fact that only long fragments have been detected in the TIM-1 protocol (**Figure 5C**). In seminal plasma, the CFI has ranged from 0.1 up to 0.6, while cfDNA isolated by TIM-1 has not been able to be analyzed. The largest amount of long cfDNA fractions was isolated using TIM-2, CK-2, and CK-3 protocols in seminal plasma (**Figure 5D**). The impact of DTT addition on the CFI of blood plasma in CK protocols was not analyzable in CK-1, while a 26% reduction in CK-2 and an increase of 44% in CK-3 was observed. In seminal plasma, the addition of DTT has increased CFI in CK-1 by 9%, CK-2 by 8%, and CK-3 by 4%.

The addition of DTT to CK-3 protocol in blood plasma sample has led to increased fragmentation of isolated cfDNA, with an increase in short fragments and decrease in long ones, while DTT

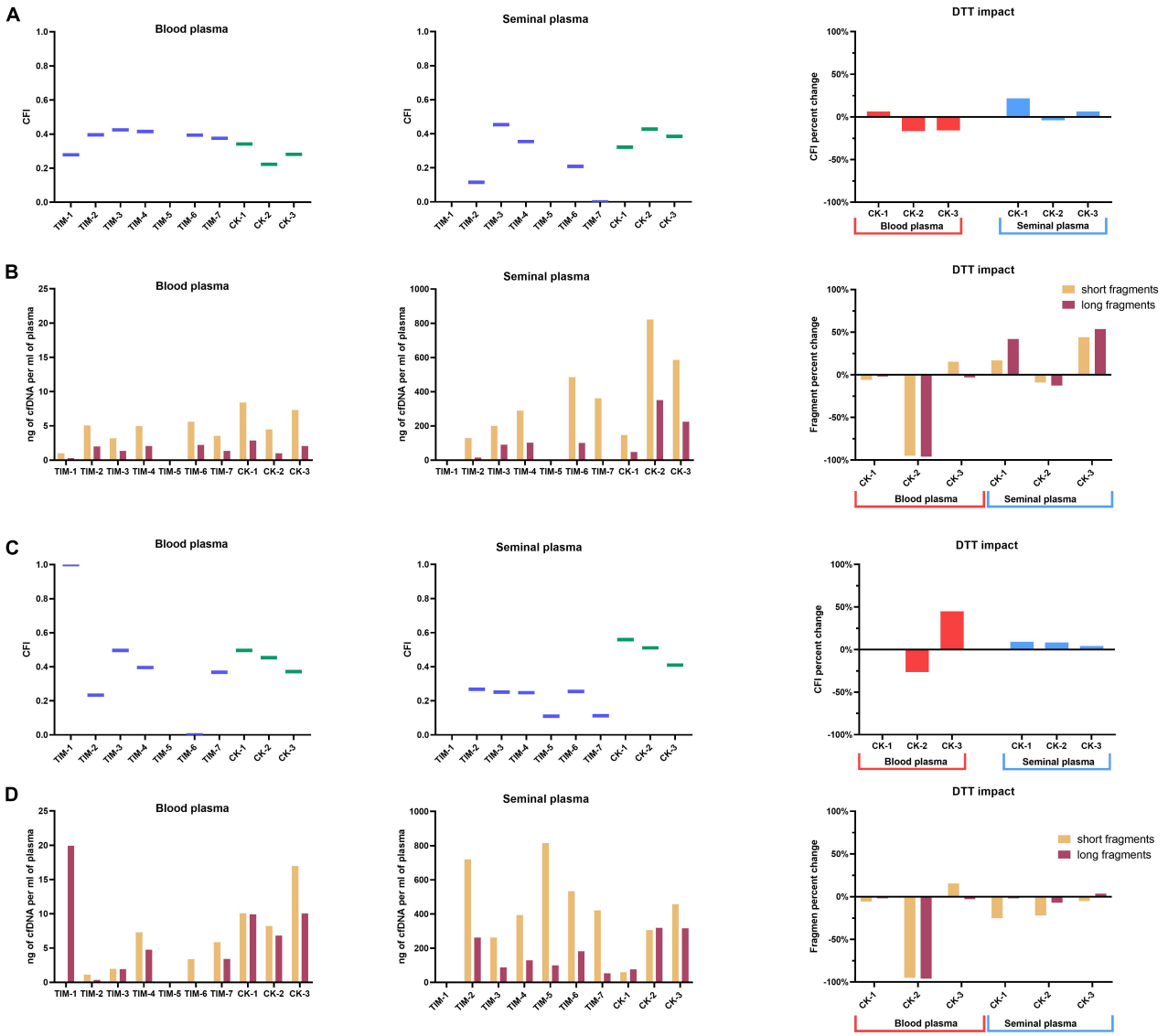

FIGURE 5 | Cell-free DNA fragmentation index. **(A)** CFI analysis by qPCR, with the impact of DDT on long fragment ratio; **(B)** total long and short LINE-1 cfDNA fragments quantified by qPCR, with the impact of DTT on total fragment yield; **(C)** CFI analysis by capillary electrophoresis, with the impact of DTT on long fragment ratio; **(D)** total long and short LINE-1 cfDNA fragments quantified by capillary electrophoresis, with the impact of DTT on total fragment yield. Values represented are means.

has usually produced either a uniform increase or decrease in both long and short fragment amount.

cfDNA Methylation

We have assessed both the global and CpG specific cfDNA methylation of LINE-1 isolated from blood and seminal plasma by pyrosequencing. Here, no impact of either cfDNA isolation methods or the addition of DTT on cfDNA methylation levels has been found (**Figure 6**). Additionally, in seminal plasma global cfDNA hypomethylation of 6% in comparison to blood plasma was detected, with the detected blood plasma cfDNA methylation level of 69% and seminal plasma level of 63%. CpG 2 had the smallest difference between blood and seminal plasma cfDNA methylation, with blood plasma having had 84% methylation compared to 82% in seminal plasma. While CpG 4 had the largest difference, with blood plasma having had 53% cfDNA methylation compared to 45% in seminal plasma.

DISCUSSION

As the literature analysis has shown, interest in cfDNA research is only increasing year to year, from 10 publications per year in the 1990s to over 2800 publications in 2020. However, this rise in popularity hasn't been followed by increased standardization

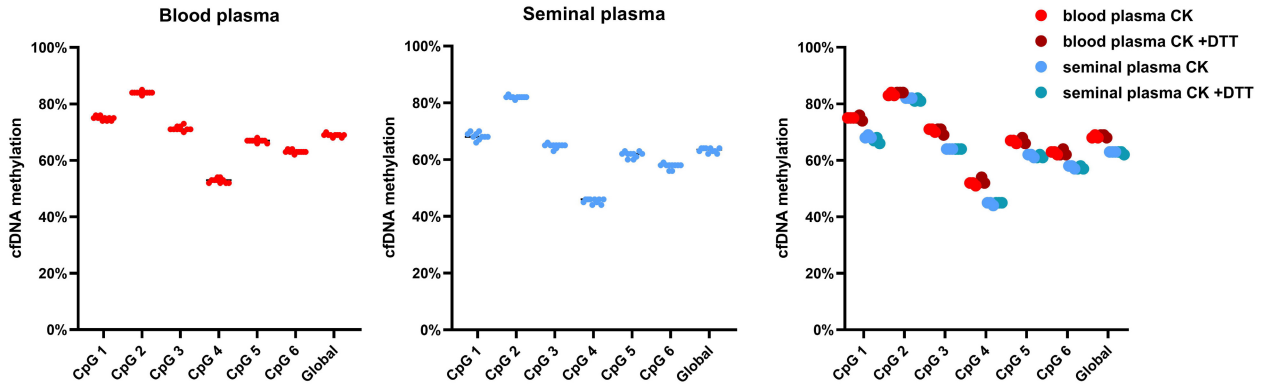

FIGURE 6 | Cell-free DNA methylation of LINE-1 in blood and seminal plasma. cfDNA methylation is depicted both as CpG specific and global, along with the impact of DTT on cfDNA methylation. Values represented are means. Every dot represents a different protocol used.

in methods for isolation, quantification, and analysis of cfDNA, all of which lead to potential pitfalls when comparing results obtained from different methodologies (Trigg et al., 2018). This is accentuated by the fact that in the last 3 years more than half of all publications investigating the impact of different isolation methods or parameters impacting cfDNA yield were published. However, there is no clear consensus on the methodology using blood plasma as the body fluid of origin for cfDNA research, and so far, only one study has investigated this in seminal plasma, meaning this is far from a closed topic. With male reproductive system disorders affecting the quality of men's lives both in their prime and in the aging population, their treatment is in part limited by the prejudice related to check up's and the absence of accurate diagnostic methods (Drabovich et al., 2014). Seminal plasma promises to complement medical imaging and blood-based tests for non-invasive diagnostics of male reproductive health, with male infertility, prostate, and testicular cancer being pathologies most likely to see the greatest benefits (Drabovich et al., 2014).

With regards to plasma preparation, centrifugation protocols widely differ but previous research has shown the least amount of cellular DNA contamination when a two-step centrifugation protocol is used, with no negative impact on cfDNA yield (Pös et al., 2020). A two-step centrifugation protocol is the most common in blood plasma preparation, consisting of a slow speed first step ($<2000 \times g$) followed by a high-speed second step ($>3000 \times g$) (Sorber et al., 2019; Pös et al., 2020). While this is sufficient for blood plasma preparation and is according to the WHO guidelines for seminal plasma preparation (Cao et al., 2011; Pös et al., 2020) we have had multiple issues with the two-step approach in seminal plasma preparation for cfDNA analysis. Despite other studies successfully using this method for seminal plasma preparation (Li et al., 2009; Ponti et al., 2019; Eikmans et al., 2020; Fraczek et al., 2020) we have found that seminal plasma processed by standard double centrifugation still has too much cellular debris present. This debris can often result in spin column blockage at worst and at best increase the time required for the sample to pass through the column by a significant amount. In this research, a three-step method with an additional centrifugation step at $20{,}000 \times g$ has removed most of the cellular debris allowing for unimpeded cfDNA isolation.

It has been demonstrated that preanalytical parameters, including cfDNA isolation methods, impact diagnostic parameters, notably the yield, quality, degree of cfDNA fragmentation, and cfDNA methylation (Barták et al., 2019; Johansson et al., 2019; Oreskovic et al., 2019). However, despite the research using cfDNA rapidly increasing very little is known on the exact degree of impact these parameters have on the diagnostic parameters and especially in semen. Furthermore, the results of cfDNA analysis vary according to the method employed (Bronkhorst et al., 2020). To investigate the impact of the selected preanalytical and analytical methods on the downstream cfDNA diagnostic parameters we have evaluated in this work the most commonly used methods of cfDNA isolation. We have analyzed both traditional methods and those based on CKs, as well as routine methods for cfDNA quantification: a fluorometric dsDNA assay, qPCR, and ddPCR assays and capillary electrophoresis (Ponti et al., 2018; Streleckiene et al., 2019). We were able to assess for potential discrepancies, downstream inhibitors, and confounding factors.

We have confirmed the previously reported higher yields of cfDNA from seminal plasma (Ponomaryova et al., 2020) regardless of the isolation method. Higher yields allow for easier overall sample processing of both high and low sensitivity downstream analytical methods allowing for greater application in male reproductive medicine, especially oncology and fertility management (Ponti et al., 2019). We have also noticed a discrepancy between PCR and fluorometric quantification of cfDNA yield both in blood and seminal plasma isolated samples, with fluorometry suggesting greater quantities for all TIM's. Fluorometric quantification of cfDNA has been reported to overestimate cfDNA quantity possibly due to cfDNA fragmentation, standards used (Sedlackova et al., 2013), or even due to the presence of carrier-RNA during isolation such as in CK-1 (Streleckiene et al., 2019). Quantification by qPCR

has shown a reduction in the obtained cfDNA yields, with the exception of TIM-1 and TIM-5 which seem to have inhibited the qPCR reaction altogether. In CK-2 and CK-3 protocols, the cfDNA yields detected correspond the most between those obtained by PCR methods and fluorimetry and also show the least variability irrespective of the detection method used. We have also reported the successful application of a modified LINE-1 ddPCR assay for cfDNA quantification from liquid biopsy samples, which has allowed for absolute quantification of cfDNA. The quantification by ddPCR was more in line with yields obtained by qPCR, which seem to suggest the fluorimetric overestimation, but has also allowed for detection of samples which were inhibited in the qPCR analysis, most notably samples TIM-1 and TIM-5. This could be of importance for highly valuable, low-volume samples or those with the presence of inhibitors, giving ddPCR a supplementary role to qPCR cfDNA quantification, which is currently the gold standard (Streleckiene et al., 2019; Yan et al., 2021). Quantification of cfDNA samples by capillary electrophoresis has shown yields more similar to the ones obtained by fluorometric analysis. However, in seminal plasma cfDNA obtained by TIM-1 and TIM-5 as well as the blood plasma cfDNA obtained by CK-1 protocol, there could be the presence of possible contaminants or inhibitory substances in the buffer which prevent the detection of molecular markers and subsequent analyses. Protocols TIM-4, TIM-6, and TIM-7, as well as CK-3, have produced the highest cfDNA yields with the highest purity in both blood and seminal plasma samples with TIM-6 and CK-3 being our recommendation.

To our knowledge, no research has been done yet on the effect of DTT on cfDNA isolation, despite the fact that DTT has been used for the purpose of increasing DNA yield in extraction protocols due to its ability to reduce disulfide bonds and keep proteins in a reduced state (Leite et al., 2019). Due to this, DTT has found a wide application in isolation of DNA from sources like bacteria, highly mucous liquids, and semen (Doerksen et al., 2000; Radford et al., 2015; Liu et al., 2018), in concentrations commonly ranging from 1 to 10 mM DTT (Doerksen et al., 2000; Pacheco et al., 2011; Radford et al., 2015). However, concentrations of DTT up to 200 mM have also been tested for the effect on DNA yield (He et al., 2017; Liu et al., 2018) where optimal DNA yields were obtained by higher (160 and 200 mM) DTT concentrations. In our research, among TIM protocols we have designed two protocols, TIM-6 and TIM-7, that included DTT in concentrations of 10 and 80 mM, respectively. While the addition of DTT has resulted in increased cfDNA yields in both seminal and blood plasma there was no further increase with higher concentrations. However, in seminal plasma cfDNA there was even a reduction in CFI with a higher concentration of DTT. This can be explained by the well-known effect of DTT, which causes single-stranded nicks in double-stranded DNA (Fjelstrup et al., 2017). The observed increase in cfDNA yield has prompted us to modify all three investigated CK protocols with the addition of 10 mM DTT. However, what we have found is that while having a negligible or even a slightly negative effect on blood plasma cfDNA yield, it has greatly increased seminal plasma cfDNA yield. The addition of DTT has also impacted the CFI of obtained cfDNA, and while in cfDNA from blood plasma there is a noticeable increase in short versus long fragments, in seminal plasma cfDNA there is also an overall increase in both short and long fragments isolated. To summarize, this effect of DTT on cfDNA isolation could be of interest when working with small liquid biopsy volumes and low amounts of cfDNA and should be investigated further.

Overall, we presented four different methods with all showing the same general trend each with its strength and weakness (Bronkhorst et al., 2020). While certain isolation methods seem more prone to inhibitions in PCR-based analysis, they might still be analyzable using fluorometry, while capillary electrophoresis can be used for a technical overestimation check-up. Conversely, PCR methods can be applied to get a more accurate estimation of usable cfDNA fragments for downstream analyses, rather than just very short (less than 40 bp) fragments, such as seen in TIM processed seminal plasma cfDNA. In addition, the previously reported greater efficacy of CKs (Mauger et al., 2015; He Z. et al., 2019) was confirmed only in seminal plasma and not in blood plasma. Finally, our results show that the comparison of cfDNA yields obtained by different isolation and quantification methods is not feasible or reliable. While PCR methods offer greater consistency there is a place for non-PCR detection methods in supplementing PCR-based methods in cfDNA analysis, especially in the case of samples processed by traditional isolation methods (Keshavarz et al., 2015; Akbariqomi et al., 2019) which can contain inhibitory substances. Concerning the variability of cfDNA yield with regard to the isolation method used, blood plasma samples show the least method-dependent variability and especially when using PCR detection methods. However, statistically significant differences were detected between different isolation protocols in both blood and semen as cfDNA source, and by different methods of cfDNA quantification. While mitigation of the analytical bias can be done by employing multiple methods (Lampignano et al., 2020), the isolation method-dependent bias can only be solved by greater inter-lab standardization, especially when using liquid biopsies other than blood.

Optimal isolation protocols should extract all cfDNA fractions present in the sample, and not have a preference for a certain size (Johansson et al., 2019). In the case of blood plasma, we observed that TIM's have a higher ratio of long cfDNA fragments, while CK's have a larger quantity of short fragments. Seminal plasma in general has exhibited a distinct electrophoretic profile, with both small and large fragments being present, while in blood plasma the 180 bp cfDNA fragment has made up the majority of the cfDNA. This distinct profile has been proposed to be of diagnostic and clinical relevance (Ponti et al., 2019), meaning parameters impacting CFI must be paid attention to when working with semen as the source of liquid biopsy, especially if the analysis should be comparable to those done by other laboratories and centers. Capillary electrophoresis of blood plasma samples seems unable to detect the presence of larger fragments analyzable by qPCR, while certain samples unable to be amplified by PCR are able to be detected by this method. Complementary usage of both methods is required for fuller characterization of investigated samples. Evaluation of the impact of isolation methods on CFI

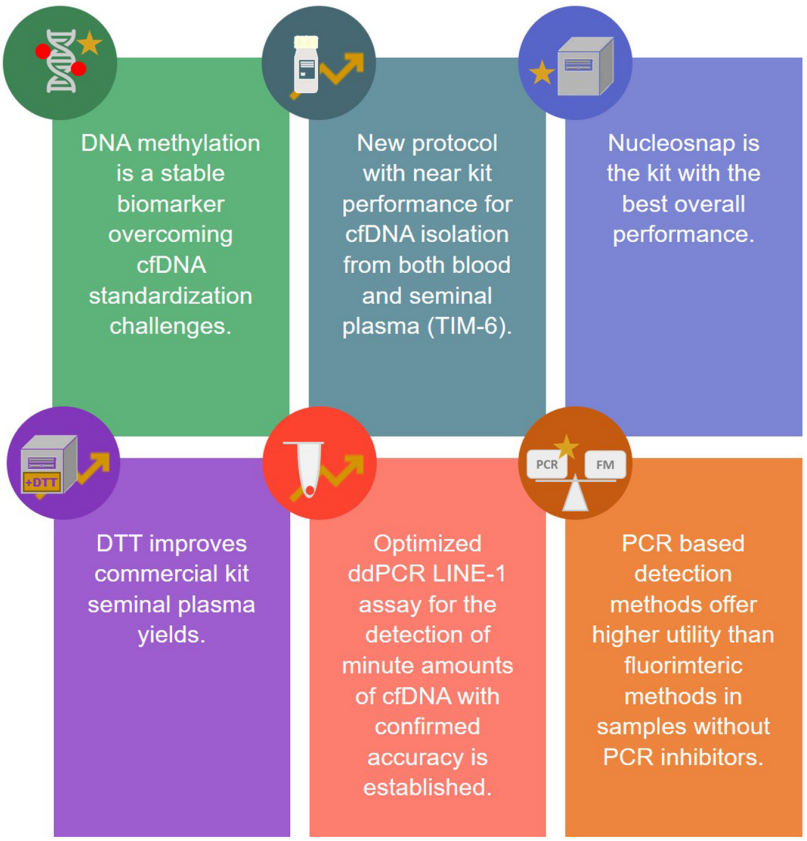

FIGURE 7 | Key points. Short depiction of the takeaway points of this study.

has revealed that the impact is higher when working with semen than with blood plasma, also that the PCR detection methods produces more uniform results. This could be due to seminal plasma possessing a higher abundance of longer fragments of cfDNA, so it is also more susceptible to procedure induced fragmentation. Thus, when working with semen, attention should be brought to both isolation and detection methods employed, to avoid inducing fragmentation and analytical bias into a diagnostic parameter.

While studies have previously reported that isolation methods could impact cfDNA methylation analysis results (Barták et al., 2019), in this study we have found no impact. LINE-1 cfDNA methylation of the six investigated CpG's as well as the average global methylation has been consistent across all analyzed isolation methods in both seminal and blood plasma. The consistency within individual CpG sites is especially important since averaging the methylation value of a CpG island often leads to a loss of relevant information (Sprang et al., 2020). Even in our case of 6% hypomethylation in seminal plasma samples without individual CpG analysis, there is no way of distinguishing if it is present in an individual site or across all sites. With pyrosequencing, we were able to reliably assess cfDNA methylation both globally and CpG site-specific even in samples with minute amounts of cfDNA and even in samples that contained PCR inhibitors. The requirement for eluted cfDNA to undergo bisulfite conversion and subsequent clean-up could have "leveled out" the different isolation protocols. This finding of the consistency of cfDNA methylation irrespective of isolation method opens new possibilities and opportunities in cfDNA biomarker research since it could bypass the whole issue of inter-lab standardization. cfDNA methylation could be reliably compared across labs and studies irrespective of preanalytical methods used.

To our knowledge, the current study is the first comprehensive investigation of preanalytical and analytical impact on diagnostic parameters of cfDNA obtained from blood and semen. According to the presented results, NucleoSnap is the best cfDNA isolation method in both blood and seminal plasma, overtaking the current *de facto* gold standard Qiagen. The in-house developed isolation protocol TIM-6 has presented itself as an inexpensive method but with near kit performance in both blood and seminal plasma cfDNA isolation (**Figure 7**). The addition of DTT could be beneficial especially when isolating cfDNA from seminal plasma. We suggest PCR based protocols for cfDNA detection due to their ease-of-use, and comparability of ddPCR and qPCR results. LINE-1 ddPCR assay is a reliable method for quantification of minute amounts of cfDNA applicable to hard-to-detect samples. Isolation methods have had no impact on cfDNA methylation results obtained

by pyrosequencing. Presented results facilitate further cfDNA biomarker development, promoting standardization in related diagnostics and research. Finally, we stress that semen offers a promising source of cfDNA for male reproductive health research and patient management.

DATA AVAILABILITY STATEMENT

The raw data supporting the conclusions of this article will be made available by the authors, without undue reservation.

ETHICS STATEMENT

The studies involving human participants were reviewed and approved by University of Zagreb School of Medicine (641-01/17-02/01). The patients/participants provided their written informed consent to participate in this study.

AUTHOR CONTRIBUTIONS

NS, JK, and AKB contributed to conception and design of the study. NS and DJ provided the funding and the resources required for the study. JK and IA performed the analysis. AV, NNG, and SK-O collected and processed the samples. NS, AKB, and DJ have administrated the project. NS, NNG, and SK-O have supervised the execution of the project. NS and JK have created the visuals for the manuscript. JK wrote the original draft of the manuscript. All authors contributed to manuscript revision, read, and approved the submitted version.

FUNDING

This publication was financed by the European Union through the European Regional Development Fund, Operational Programme Competitiveness and Cohesion, under grant agreement No. KK.01.1.1.01.0008, Regenerative and Reproductive Medicine – Exploring New Platforms and Potentials. This work has been supported by Croatian Science Foundation under the projects "Epigenetic biomarkers in blood and ejaculate of patients with testicular seminoma" (epiSem, IP-2016-06-3692) and "Epigenetic biomarkers in prostate cancer" (epiPro, UIP-2017-05-8138).

ACKNOWLEDGMENTS

We wish to acknowledge and thank Filip Rokić and Oliver Vugrek from the Ruđer Bošković Institute on their support with capillary electrophoresis.

REFERENCES

Abramovic, I., Ulamec, M., Bojanac Katusic, A., Bulic-Jakus, F., Jezek, D., and Sincic, N. (2020). MiRNA in prostate cancer: challenges toward translation. *Epigenomics* 12, 543–558. doi: 10.2217/epi-2019-0275

Akbariqomi, M., Heidari, R., Gargari, S. S., Omrani, M. D., Rigi, G., Sanikhani, N. S., et al. (2019). Evaluation and statistical optimization of a method for methylated cell-free fetal DNA extraction from maternal plasma. *J. Assist. Reprod. Genet.* 36, 1029–1038. doi: 10.1007/s10815-019-01425-w

Aucamp, J., Bronkhorst, A. J., Badenhorst, C. P. S., and Pretorius, P. J. (2016). A historical and evolutionary perspective on the biological significance of circulating DNA and extracellular vesicles. *Cell Mol. Life Sci.* 73, 4355–4381. doi: 10.1007/s00018-016-2370-3

Aucamp, J., Bronkhorst, A. J., Peters, D. L., Van Dyk, H. C., Van der Westhuizen, F. H., and Pretorius, P. J. (2017). Kinetic analysis, size profiling, and bioenergetic association of DNA released by selected cell lines in vitro. *Cell. Mol. Life Sci.* 74, 2689–2707. doi: 10.1007/s00018-017-2495-z

Augustus, E., van Casteren, K., Sorber, L., van Dam, P., Roeyen, G., Peeters, M., et al. (2020). The art of obtaining a high yield of cell-free DNA from urine. *PLoS One [Internet]* 15:e0231058. doi: 10.1371/journal.pone.0231058

Barták, B. K., Kalmár, A., Galamb, O., Wichmann, B., Nagy, Z. B., Tulassay, Z., et al. (2019). Blood collection and cell-free DNA isolation methods influence the sensitivity of liquid biopsy analysis for colorectal cancer detection. *Pathol. Oncol. Res.* 25, 915–923. doi: 10.1007/s12253-018-0382-z

Bronkhorst, A. J., Ungerer, V., and Holdenrieder, S. (2020). Comparison of methods for the isolation of cell-free DNA from cell culture supernatant. *Tumor Biol.* 42, 1–10.

Cao, X. W., Lin, K., Li, C. Y., and Yuan, C. W. (2011). A review of WHO Laboratory manual for the examination and processing of human semen (5th edition). *Zhonghua Nan Ke Xue* 17, 1059–1063.

Chan, R., Lin, P., Chen, S., Lin, S., Chen, P., Lin, B., et al. (2021). Clinical utility of a cell-free DNA assay in patients with colorectal cancer. *Front. Oncol.* 11:589673.

Chen, Y., Liao, T., Zhu, L., Lin, X., Wu, R., and Jin, L. (2018). Seminal plasma cell-free mitochondrial DNA copy number is associated with human semen quality. *Eur. J. Obstet. Gynecol. Reprod. Biol. [Internet]* 231, 164–168. doi: 10.1016/j.ejogrb.2018.10.048

Constâncio, V., Nunes, S. P., Henrique, R., and Jerónimo, C. (2020). DNA methylation-based testing in liquid biopsies as detection and prognostic biomarkers for the four major cancer types. *Cells* 9:624. doi: 10.3390/cells9030624

Cook, L., Starr, K., Boonyaratanakornkit, J., Hayden, R., Sam, S. S., and Caliendo, A. M. (2018). Does size matter? Comparison of extraction yields for different-sized DNA fragments by seven different routine and four new circulating cell-free extraction methods. *J. Clin. Microbiol.* 56, 1–13.

Cooper, T. G., Noonan, E., von Eckardstein, S., Auger, J., Baker, H. W. G., Behre, H. M., et al. (2009). World Health Organization reference values for human semen characteristics. *Hum. Reprod. Update* 16, 231–245. doi: 10.1093/humupd/dmp048

Daskalos, A., Nikolaidis, G., Xinarianos, G., Savvari, P., Cassidy, A., Zakopoulou, R., et al. (2009). Hypomethylation of retrotransposable elements correlates with genomic instability in non-small cell lung cancer. *Int. J. Cancer* 124, 81–87. doi: 10.1002/ijc.23849

de Kock, R., Deiman, B., Kraaijvanger, R., and Scharnhorst, V. (2019). Optimized (Pre) analytical conditions and workflow for droplet digital PCR analysis of cell-free DNA from patients with suspected lung carcinoma. *J. Mol. Diagnostics [Internet]* 21, 895–902. doi: 10.1016/j.jmoldx.2019.05.003

Doerksen, T., Benoit, G., and Trasler, J. M. (2000). Deoxyribonucleic acid hypomethylation of male germ cells by mitotic and meiotic exposure to 5-azacytidine is associated with altered testicular histology. *Endocrinology* 141, 3235–3244. doi: 10.1210/endo.141.9.7661

Drabovich, A. P., Saraon, P., Jarvi, K., and Diamandis, E. P. (2014). Seminal plasma as a diagnostic fluid for male reproductive system disorders. *Nat. Rev. Urol.* 11, 278–288. doi: 10.1038/nrurol.2014.74

Draškoviè, T. (2017). Isolation of cell-free DNA from seminal fluid. *J. Pharm. Pharmacol. [Internet]* 5, 554–560.

Eikmans, M., Anholts, J. D. H., Blijleven, L., Meuleman, T., van Beelen, E., van der Hoorn, M. L. P., et al. (2020). Optimization of microrna acquirement from seminal plasma and identification of diminished seminal microRNA-34B as indicator of low semen concentration. *Int. J. Mol. Sci.* 21, 1–15.

Ferguson, C., Araújo, D., Faulk, L., Gou, Y., Hamelers, A., Huang, Z., et al. (2021). Europe PMC in 2020. *Nucleic Acids Res.* 49, D1507–D1514.

Fjelstrup, S., Andersen, M. B., Thomsen, J., Wang, J., Stougaard, M., Pedersen, F. S., et al. (2017). The effects of dithiothreitol on DNA. *Sensors (Switzerland)* 17, 1–10.

Fraczek, M., Wojnar, L., Kamieniczna, M., Piasecka, M., Gill, K., Kups, M., et al. (2020). Seminal plasma analysis of oxidative stress in different genitourinary topographical regions involved in reproductive tract disorders associated with genital heat stress. *Int. J. Mol. Sci.* 21, 1–17.

Gaga, M., Chorostowska-Wynimko, J., Horváth, I., Tammemagi, M. C., Shitrit, D., Eisenberg, V. H., et al. (2020). Validation of Lung EpiCheck®, a novel methylation-based blood assay, for the detection of lung cancer in European and Chinese high-risk individuals. *Eur. Respir J.* 57:2002682. doi: 10.1183/13993003.02682-2020

Haselmann, V., Ahmad-Nejad, P., Geilenkeuser, W. J., Duda, A., Gabor, M., Eichner, R., et al. (2018). Results of the first external quality assessment scheme (EQA) for isolation and analysis of circulating tumour DNA (ctDNA). *Clin. Chem. Lab. Med.* 56, 220–228. doi: 10.1515/cclm-2017-0283

He, H., Li, R., Chen, Y., Pan, P., Tong, W., Dong, X., et al. (2017). Integrated DNA and RNA extraction using magnetic beads from viral pathogens causing acute respiratory infections. *Sci. Rep.* 7:45199.

He, K., Fujiwara, H., Zajac, C., Sandford, E., Reddy, P., Choi, S. W., et al. (2019). A pipeline for faecal host DNA analysis by absolute quantification of LINE-1 and mitochondrial genomic elements using ddPCR. *Sci. Rep.* 9: 5599.

He, Z., Tang, C., Chen, X., Liu, H., Yang, G., Xiao, Z., et al. (2019). Based on magnetic beads to develop the kit for extraction of high-quality cell-free DNA from blood of breast cancer patients. *Mater. Express* 9, 956–961. doi: 10.1166/mex.2019.1579

Hufnagl, C., Stöcher, M., Moik, M., Geisberger, R., and Greil, R. (2013). A modified Phenol-chloroform extraction method for isolating circulating cell free DNA of tumor patients. *J. Nucleic Acids Investig.* 4, 1–3. doi: 10.4081/jnai.2013.4282

Johansson, G., Andersson, D., Filges, S., Li, J., Muth, A., Godfrey, T. E., et al. (2019). Considerations and quality controls when analyzing cell-free tumor DNA. *Biomol. Detect. Quantif. [Internet]*17:100078. doi: 10.1016/j.bdq.2018.12.003

Jorgez, C. J., Dang, D. D., Simpson, J. L., Lewis, D. E., and Bischoff, F. Z. (2006). Quantity versus quality: optimal methods for cell-free DNA isolation from plasma of pregnant women. *Genet. Med.* 8, 615–619. doi: 10.1097/01.gim.0000241904.32039.6f

Keshavarz, Z., Moezzi, L., Ranjbaran, R., Aboualizadeh, F., Behzad-Behbahani, A., Abdullahi, M., et al. (2015). Evaluation of a modified DNA extraction method for isolation of cell-free fetal DNA from maternal serum. *Avicenna J. Med. Biotechnol.* 7, 85–88.

Keup, C., Benyaa, K., Hauch, S., Sprenger-Haussels, M., Tewes, M., Mach, P., et al. (2020). Targeted deep sequencing revealed variants in cell-free DNA of hormone receptor-positive metastatic breast cancer patients. *Cell. Mol. Life Sci. [Internet]* 77, 497–509. doi: 10.1007/s00018-019-03189-z

Krasic, J., Sincic, N., and Samija, I. (2018). Liquid biopsy for patients with cancer?: different. *Mol. Exp. Biol. Med.* 2, 1–8. doi: 10.1007/978-3-319-55661-1_1

Kumar, M., Choudhury, Y., Ghosh, S. K., and Mondal, R. (2018). Application and optimization of minimally invasive cell-free DNA techniques in oncogenomics. *Tumor Biol.* 40, 1–12.

Lampignano, R., Neumann, M. H. D., Weber, S., Kloten, V., Herdean, A., Voss, T., et al. (2020). Multicenter evaluation of circulating cell-free DNA extraction and downstream analyses for the development of standardized (Pre)analytical work flows. *Clin. Chem.* 66, 149–160. doi: 10.1373/clinchem.2019.306837

Lee, E. Y., Lee, E. J., Yoon, H., Lee, D. H., and Kim, K. H. (2020). Comparison of four commercial kits for isolation of urinary cell-free DNA and sample storage conditions. *Diagnostics* 10:234. doi: 10.3390/diagnostics10040234

Lee, J. S., Kim, M., Seong, M. W., Kim, H. S., Lee, Y. K., and Kang, H. J. (2020). Plasma vs. serum in circulating tumor DNA measurement: characterization by DNA fragment sizing and digital droplet polymerase chain reaction. *Clin. Chem. Lab. Med.* 58, 527–532. doi: 10.1515/cclm-2019-0896

Lee, K. H., Shin, T. J., Kim, W. H., Lee, S. Y., and Cho, J. Y. (2019). Methylation of LINE-1 in cell-free DNA serves as a liquid biopsy biomarker for human breast cancers and dog mammary tumors. *Sci. Rep. [Internet]* 9:175.

Leite, G. G. S., Morales, W., Weitsman, S., Celly, S., Parodi, G., Mathur, R., et al. (2019). Optimizing microbiome sequencing for small intestinal aspirates: validation of novel techniques through the REIMAGINE study. *BMC Microbiol.* 19:239.

Li, H. G., Huang, S. Y., Zhou, H., Liao, A. H., and Xiong, C. L. (2009). Quick recovery and characterization of cell-free DNA in seminal plasma of normozoospermia and azoospermia: implications for non-invasive genetic utilities. *Asian J. Androl. [Internet]* 11, 703–709. doi: 10.1038/aja.2009.65

Li, L., Li, H., Tian, Y., Hu, M., Le, F., Wang, L., et al. (2020). Differential microRNAs expression in seminal plasma of normospermic patients with different sperm DNA fragmentation indexes. *Reprod. Toxicol. [Internet]* 94, 8–12. doi: 10.1016/j.reprotox.2020.03.007

Li, S., Wang, L., Zhao, Q., Wang, Z., Lu, S., Kang, Y., et al. (2020). Genome-wide analysis of cell-free DNA methylation profiling for the early diagnosis of pancreatic cancer. *Front. Genet.* 11:596078.

Liu, Y., Schulze-Makuch, D., de Vera, J. P., Cockell, C., Leya, T., Baqué, M., et al. (2018). The development of an effective bacterial single-cell lysis method suitable for whole genome amplification in microfluidic platforms. *Micromachines* 9:367. doi: 10.3390/mi9080367

Lo, Y. M. D., Han, D. S. C., Jiang, P., and Chiu, R. W. K. (2021). Epigenetics, fragmentomics, and topology of cell-free DNA in liquid biopsies. *Science* 372:144.

Lobo, J., Gillis, A. J. M., van den Berg, A., Dorssers, L. C. J., Belge, G., Dieckmann, K. P., et al. (2019). . Identification and validation model for informative liquid biopsy-based microRNA biomarkers: insights from germ cell tumor in vitro, in vivo and patient-derived data. *Cells* 8:1637. doi: 10.3390/cells8121637

Malentacchi, F., Pizzamiglio, S., Verderio, P., Pazzagli, M., Orlando, C., Ciniselli, C. M., et al. (2015). Influence of storage conditions and extraction methods on the quantity and quality of circulating cell-free DNA (ccfDNA): the SPIDIA-DNAplas external quality assessment experience. *Clin. Chem. Lab. Med.* 53, 1935–1942.

Mauger, F., Dulary, C., Daviaud, C., Deleuze, J. F., and Tost, J. (2015). Comprehensive evaluation of methods to isolate, quantify, and characterize circulating cell-free DNA from small volumes of plasma. *Anal .Bioanal. Chem.* 407, 6873–6878. doi: 10.1007/s00216-015-8846-4

Mbaye, M. M., El Khalfi, B., Louanjli, N., Saadani, B., Kaarouch, I., Madkour, A., et al. (2019). Seminal cell-free DNA test for the management of male infertility. *Annu. Res. Rev. Biol.* 30, 1–10. doi: 10.9734/arrb/2018/v30i530025

Meddeb, R., Pisareva, E., and Thierry, A. R. (2019). Guidelines for the preanalytical conditions for analyzing circulating cell-free DNA. *Clin. Chem.* 65, 623–633. doi: 10.1373/clinchem.2018.298323

Medina Diaz, I., Nocon, A., Mehnert, D. H., Fredebohm, J., Diehl, F., and Holtrup, F. (2016). Performance of Streck cfDNA blood collection tubes for liquid biopsy testing. *PLoS One.* 11:e0166354. doi: 10.1371/journal.pone.0166354

Miller, B. F., Petrykowska, H. M., and Elnitski, L. (2021). Assessing ZNF154 methylation in patient plasma as a multicancer marker in liquid biopsies from colon, liver, ovarian and pancreatic cancer patients. *Sci. Rep. [Internet]* 11:221.

Miller, S. A., Dykes, D. D., and Polesky, H. F. (1988). A simple salting out procedure for extracting DNA from human nucleated cells. *Nucleic Acids Res.* 16:1215. doi: 10.1093/nar/16.3.1215

Mojtabanezhad Shariatpanahi, A., Rokni, P., Shahabi, E., Varshoee Tabrizi, F., and Kerachian, M. A. (2018). Simple and cost-effective laboratory methods to evaluate and validate cell-free DNA isolation. *BMC Res. Notes [Internet]* 11:757. doi: 10.1186/s13104-018-3866-8

Morgan, H. L., and Watkins, A. J. (2020). The influence of seminal plasma on offspring development and health. *Semin. Cell Dev. Biol. [Internet]* 97, 131–137. doi: 10.1016/j.semcdb.2019.06.008

Moss, J., Magenheim, J., Neiman, D., Zemmour, H., Loyfer, N., Korach, A., et al. (2018). Comprehensive human cell-type methylation atlas reveals origins of circulating cell-free DNA in health and disease. *Nat. Commun. [Internet]* 9:5068.

Oreskovic, A., Brault, N. D., Panpradist, N., Lai, J. J., and Lutz, B. R. (2019). Analytical comparison of methods for extraction of short cell-free DNA from urine. *J. Mol. Diagnostics [Internet]*. 21, 1067–1078. doi: 10.1016/j.jmoldx.2019.07.002

Ottaviano, M., Giuliano, M., Tortora, M., La Civita, E., Liotti, A., Longo, M., et al. (2021). A new horizon of liquid biopsy in thymic epithelial tumors: the potential utility of circulating cell-free DNA. *Front. Oncol.* 10:602153.

Pacheco, S. E., Houseman, E. A., Christensen, B. C., Marsit, C. J., Kelsey, K. T., Sigman, M., et al. (2011). Integrative DNA methylation and gene expression analyses identify DNA packaging and epigenetic regulatory genes associated with low motility sperm. *PLoS One* 6:e20280. doi: 10.1371/journal.pone.0020280

Page, K., Powles, T., Slade, M. J., Tamburo De Bella, M., Walker, R. A., Coombes, R. C., et al. (2006). The importance of careful blood processing in isolation of cell-free DNA. *Ann. N. Y. Acad. Sci.* 1075, 313–317. doi: 10.1196/annals.1368.042

Pérez-Barrios, C., Nieto-Alcolado, I., Torrente, M., Jiménez-Sánchez, C., Calvo, V., Gutierrez-Sanz, L., et al. (2016). Comparison of methods for circulating cell-free DNA isolation using blood from cancer patients: impact on biomarker testing. *Transl. Lung Cancer Res.* 5, 665–672. doi: 10.21037/tlcr.2016.12.03

Ponomaryova, A. A., Rykova, E. Y., Gervas, P. A., Cherdyntseva, N. V., Mamedov, I. Z., and Azhikina, T. L. (2020). Aberrant methylation of LINE-1 transposable elements: a search for cancer biomarkers. *Cells* 9, 1–19.

Ponti, G., Maccaferri, M., Mandrioli, M., Manfredini, M., Micali, S., Cotugno, M., et al. (2018). Seminal cell-free DNA assessment as a novel prostate cancer biomarker. *Pathol. Oncol. Res.* 24, 941–945. doi: 10.1007/s12253-018-0416-6

Ponti, G., Maccaferri, M., Manfredini, M., Micali, S., Torricelli, F., Milandri, R., et al. (2019). Quick assessment of cell-free DNA in seminal fluid and fragment size for early non-invasive prostate cancer diagnosis. *Clin. Chim. Acta [Internet]* 497, 76–80. doi: 10.1016/j.cca.2019.07.011

Ponti, G., Maccaferri, M., Percesepe, A., Tomasi, A., and Ozben, T. (2020). Liquid biopsy with cell free DNA: new horizons for prostate cancer. *Crit. Rev. Clin. Lab. Sci. [Internet]* 58, 60–76. doi: 10.1080/10408363.2020.1803789

Pös, Z., Pös, O., Styk, J., Mocova, A., Strieskova, L., Budis, J., et al. (2020). Technical and methodological aspects of cell-free nucleic acids analyzes. *Int. J. Mol. Sci.* 21, 1–43. doi: 10.4061/2010/389129

Radford, E. J., Ito, M., Shi, H., Corish, J. A., Yamazawa, K., Peters, A. H. F. M., et al. (2015). In utero undernourishment perturbs the adult sperm methylome and is linked to metabolic disease transmission. *Science* 345, 1–26.

Rago, C., Huso, D. L., Diehl, F., Karim, B., Liu, G., Papadopoulos, N., et al. (2007). Serial assessment of human tumor burdens in mice by the analysis of circulating DNA. *Cancer Res.* 67, 9364–9370. doi: 10.1158/0008-5472.can-07-0605

Rodriguez-Casanova, A., Costa-Fraga, N., Bao-Caamano, A., López-López, R., Muinelo-Romay, L., and Diaz-Lagares, A. (2021). Epigenetic landscape of liquid biopsy in colorectal cancer. *Front. Cell Dev. Biol.* 9:622459.

Rostami, A., Lambie, M., Yu, C. W., Stambolic, V., Waldron, J. N., and Bratman, S. V. (2020). Senescence, necrosis, and apoptosis govern circulating cell-free DNA release kinetics. *Cell Rep. [Internet]* 31:107830. doi: 10.1016/j.celrep.2020.107830

Salvianti, F., Gelmini, S., Costanza, F., Mancini, I., Sonnati, G., Simi, L., et al. (2020). The pre-analytical phase of the liquid biopsy. *N. Biotechnol. [Internet]* 55, 19–29. doi: 10.1016/j.nbt.2019.09.006

Samoila, A., Sosa, J., Padilla, J., Wutkowski, M., Vanness, K., Viale, A., et al. (2020). Developing quality programs for cell-free DNA (cfDNA) extraction from peripheral blood. *J. Appl. Lab. Med.* 5, 788–797. doi: 10.1093/jalm/jfaa050

Schmidt, B., Weickmann, S., Witt, C., and Fleischhacker, M. (2005). Improved method for Isolating cell-free DNA. *Clin. Chem.* 51, 1560–1561.

Sedlackova, T., Repiska, G., Celec, P., Szemes, T., and Minarik, G. (2013). Fragmentation of DNA affects the accuracy of the DNA quantitation by the commonly used methods. *Biol .Proced. Online [Internet]* 15:1.

Shi, J., Zhang, R., Li, J., and Zhang, R. (2020). Size profile of cell-free DNA: a beacon guiding the practice and innovation of clinical testing. *Theranostics* 10, 4737–4748. doi: 10.7150/thno.42565

Solassol, J., Quantin, X., Larrieux, M., Senal, R., Audran, P., Grand, D., et al. (2018). Comparison of five cell-free DNA isolation methods to detect the EGFR T790M mutation in plasma samples of patients with lung cancer. *Clin. Chem. Lab. Med.* 56, e243–e246.

Somen, E., Mioc, P., Serman, A., Vranic, S., and Serman, L. (2019). Novel epigenetic biomarkers in pregnancy-related disorders and cancers. *Cell* 18:1459. doi: 10.3390/cells8111459

Sorber, L., Zwaenepoel, K., Jacobs, J., De Winne, K., Goethals, S., Reclusa, P., et al. (2019). Circulating cell-free DNA and RNA analysis as liquid biopsy: optimal centrifugation protocol. *Cancers (Basel)* 11:458. doi: 10.3390/cancers11040458

Spiller, C. M., Lobo, J., Boellaard, W. P. A., Gillis, A. J. M., Bowles, J., and Looijenga, L. H. J. (2020). Cripto and MIR-371A-3P are serum biomarkers of testicular germ cell tumors and are detected in seminal plasma from azoospermic males. *Cancers (Basel)* 12, 1–18.

Sprang, M., Paret, C., and Faber, J. (2020). CpG-islands as markers for liquid biopsies of cancer patients. *Cells* 9:1820. doi: 10.3390/cells9081820

Stewart, C. M., Kothari, P. D., Mouliere, F., Mair, R., Somnay, S., Benayed, R., et al. (2018). The value of cell-free DNA for molecular pathology. *J. Pathol.* 244, 616–627. doi: 10.1002/path.5048

Streleckiene, G., Forster, M., Inciuraite, R., Lukosevicius, R., and Skieceviciene, J. (2019). Effects of quantification methods, isolation kits, plasma biobanking, and hemolysis on cell-free DNA analysis in plasma. *Biopreserv. Biobank.* 17, 553–561. doi: 10.1089/bio.2019.0026

Takai, E., Totoki, Y., Nakamura, H., Morizane, C., Nara, S., Hama, N., et al. (2015). Clinical utility of circulating tumor DNA for molecular assessment in pancreatic cancer. *Sci. Rep.* 5:18425.

Thakral, D., Gupta, R., Sahoo, R. K., Verma, P., Kumar, I., and Vashishtha, S. (2020). Real-time molecular monitoring in acute myeloid leukemia with circulating tumor DNA. *Front. Cell Dev. Biol.* 8:604391.

Trigg, R. M., Martinson, L. J., Parpart-Li, S., and Shaw, J. A. (2018). Factors that influence quality and yield of circulating-free DNA: a systematic review of the methodology literature. *Heliyon [Internet]* 4:e00699. doi: 10.1016/j.heliyon.2018.e00699

Tuaeva, N. O., Falzone, L., Porozov, Y. B., Nosyrev, A. E., Trukhan, V. M., Kovatsi, L., et al. (2019). Translational application of circulating DNA in oncology: review of the last decades achievements. *Cells* 8, 1–30.

Vaca-Paniagua, F., Oliver, J., Da Costa, A. N., Merle, P., McKay, J., Herceg, Z., et al. (2015). Targeted deep DNA methylation analysis of circulating cell-free DNA in plasma using massively parallel semiconductor sequencing. *Epigenomics* 7, 353–362. doi: 10.2217/epi.14.94

Vaissière, T., Cuenin, C., Paliwal, A., Vineis, P., Hainaut, P., Herceg, Z., et al. (2009). Quantitative analysis of DNA methylation after whole bisulfitome amplification of a minute amount of DNA from body fluids. *Epigenetics* 4, 221–230. doi: 10.4161/epi.8833

Vandekerkhove, G., Lavoie, J. M., Annala, M., Murtha, A. J., Sundahl, N., Walz, S., et al. (2021). Plasma ctDNA is a tumor tissue surrogate and enables clinical-genomic stratification of metastatic bladder cancer. *Nat. Commun. [Internet].* 12:184.

Wang, Y., Fang, Y. X., Dong, B., Du, X., Wang, J., Wang, X., et al. (2020). Discovery of extracellular vesicles derived miR-181a-5p in patient's serum as an indicator for bone-metastatic prostate cancer. *Theranostics* 11, 878–892. doi: 10.7150/thno.49186

Warton, K., and Samimi, G. (2015). Methylation of cell-free circulating DNA in the diagnosis of cancer. *Front. Mol. Biosci.* 2:13.

Wu, C., Ding, X., Li, H., Zhu, C., and Xiong, C. (2013). Genome-wide promoter methylation profile of human testis and epididymis: identified from cell-free seminal DNA. *BMC Genomics* 14:288. doi: 10.1186/1471-2164-14-288

Xue, X., Teare, M. D., Holen, I., Zhu, Y. M., and Woll, P. J. (2009). Optimizing the yield and utility of circulating cell-free DNA from plasma and serum. *Clin. Chim. Acta [Internet]* 404, 100–104. doi: 10.1016/j.cca.2009.02.018

Yan, Y. Y., Guo, Q. R., Wang, F. H., Adhikari, R., Zhu, Z. Y., Zhang, H. Y., et al. (2021). Cell-free DNA: hope and potential application in cancer. *Front. Cell Dev. Biol.* 9:639233.

Yin, J., Hu, W., Gu, H., and Fang, J. (2021). Combined assay of circulating tumor dna and protein biomarkers for early noninvasive detection and prognosis of non-small cell lung cancer. *J. Cancer* 12, 1258–1269. doi: 10.7150/jca.49647

Yu, D., Tong, Y., Guo, X., Feng, L., Jiang, Z., Ying, S., et al. (2019). Diagnostic value of concentration of circulating cell-free DNA in breast cancer: a meta-analysis. *Front. Oncol.* 9:95.

Yuan, H., Zhu, Z.-Z., Lu, Y., Liu, F., Zhang, W., Huang, G., et al. (2012). A modified extraction method of circulating free DNA for epidermal growth factor receptor mutation analysis. *Yonsei Med. J. [Internet]* 53:132. doi: 10.3349/ymj.2012.53.1.132

Zhang, L., Wang, C. M., Zhou, W. P., Chen, Q. P., Zhou, S., Lei, W., et al. (2021). Dynamic changes of fetal-derived hypermethylated RASSF1A and Septin 9 sequences in maternal plasma. *Reprod. Sci.* 28, 1194–1199. doi: 10.1007/s43032-020-00416-y

Conflict of Interest: The authors declare that the research was conducted in the absence of any commercial or financial relationships that could be construed as a potential conflict of interest.

Publisher's Note: All claims expressed in this article are solely those of the authors and do not necessarily represent those of their affiliated organizations, or those of the publisher, the editors and the reviewers. Any product that may be evaluated in this article, or claim that may be made by its manufacturer, is not guaranteed or endorsed by the publisher.

Copyright © 2021 Krasic, Abramovic, Vrtaric, Nikolac Gabaj, Kralik-Oguic, Katusic Bojanac, Jezek and Sincic. This is an open-access article distributed under the terms of the Creative Commons Attribution License (CC BY). The use, distribution or reproduction in other forums is permitted, provided the original author(s) and the copyright owner(s) are credited and that the original publication in this journal is cited, in accordance with accepted academic practice. No use, distribution or reproduction is permitted which does not comply with these terms.

frontiers in Oncology

ORIGINAL RESEARCH
published: 14 September 2021
doi: 10.3389/fonc.2021.622626

Circulating Tumor Cells in Desmoid Tumors: New Perspectives

Alexcia C. Braun[1], Fernando A. B. Campos[2], Emne A. Abdallah[1], Anna P. C. Ruano[1], Tiago da S. Medina[1], Milena S. Tariki[2], Fabio F. E. Pinto[3], Celso A. L. de Mello[2] and Ludmilla T. D. Chinen[1]**

[1] International Center for Research, A.C. Camargo Cancer Center, São Paulo, Brazil, [2] Department of Clinical Oncology, A. C. Camargo Cancer Center, São Paulo, Brazil, [3] Department of Orthopedics, A. C. Camargo Cancer Center, São Paulo, Brazil

OPEN ACCESS

Edited by:
George Calin,
University of Texas MD Anderson Cancer Center, United States

Reviewed by:
James Reuben,
University of Texas MD Anderson Cancer Center, United States
Chang Zou,
Jinan University, China

***Correspondence:**
Alexcia C. Braun
alexciabraun@gmail.com
Ludmilla T. D. Chinen
ltdchinen@gmail.com

Specialty section:
This article was submitted to Molecular and Cellular Oncology, a section of the journal Frontiers in Oncology

Received: 28 October 2020
Accepted: 13 August 2021
Published: 14 September 2021

Citation:
Braun AC, Campos FAB, Abdallah EA, Ruano APC, Medina TS, Tariki MS, Pinto FFE, de Mello CAL and Chinen LTD (2021) Circulating Tumor Cells in Desmoid Tumors: New Perspectives. Front. Oncol. 11:622626. doi: 10.3389/fonc.2021.622626

Introduction: Desmoid tumor (DT) is a rare neoplasm with high local recurrence rates, composed of fibroblastic cells that are characterized by the expression of key molecules, including the intermediate filament vimentin, cyclooxygenase-2 (COX-2), and nuclear β-catenin, and lack of epithelial markers. Circulating tumor cells (CTCs) isolated from the peripheral blood of patients with sarcomas and other neoplasms can be used as early biomarkers of tumor invasion and dissemination. Moreover, CTCs can also re-colonize their tumors of origin through a process of "tumor self-seeding."

Objectives: We aimed to identify CTCs in the peripheral blood of patients with DT and evaluate their expression of β-catenin, transforming growth factor receptor I (TGF-βRI), COX-2, and vimentin proteins.

Material and Methods: We conducted a prospective study of patients with initial diagnosis or relapsed DT with measurable disease. Blood samples from each patient were processed and filtered by ISET® (Rarecells, France) for CTC isolation and quantification. The CTC expression of β-catenin, COX-2, TGF-βRI, and vimentin was analyzed by immunocytochemistry (ICC).

Results: A total of 18 patients were included, and all had detectable CTCs. We found a concordance of β-catenin expression in both CTCs and primary tumors in 42.8% (6/14) of cases by using ICC and immunohistochemistry, respectively.

Conclusions: Our study identified a high prevalence of CTCs in DT patients. Concordance of β-catenin expression between primary tumor and CTCs brings new perspectives to assess the dynamics of CTCs in the blood compartment, opening new avenues for studying the biology and behavior of DT. In addition, these results open the possibility of using CTCs to predict DT dynamics at the time of disease progression and treatment. Further studies with larger sample sizes are needed to validate our findings.

Keywords: circulating tumor cells, desmoid tumor, beta catenin expression, vimentin expression, TGF-βRI expression

INTRODUCTION

Desmoid tumor (DT) is a rare non-metastasizing mesenchymal neoplasm that can show aggressive local behavior and thereby can impact the functionality and quality of life of the patients (1, 2). DTs are typically diagnosed in adults (35–40 years) and are more common in women of reproductive age (3, 4). They can affect any anatomic site but are commonly localized in the extremities, abdominal wall, and abdominal mesentery (5). The clinical outcomes of DTs are unpredictable, with some progressing to large-sized tumors with infiltration and destruction of adjacent vital structures, and others showing spontaneous regression (6). Nevertheless, reliable and validated predictive factors regarding DT evolution are still lacking (7).

The initial management of asymptomatic patients with non-life-threatening DTs is often watch-and-wait, as up to 20% will regress spontaneously (8). If treatment is indicated, options include surgery, radiation, or systemic therapy with tyrosine-kinase inhibitors or chemotherapy (6, 8). Due to the infiltrative nature of the disease, post-surgical recurrence rates can exceed 50% of cases, especially for extra-abdominal desmoids, which reinforce observation as an adequate strategy (9).

Histologically, DTs are composed of fibroblastic cells characterized on immunohistochemistry (IHC) by the expression of intermediate filament vimentin, along with cyclooxygenase-2 (COX-2) and nuclear β-catenin, and lack of epithelial markers expression (1, 10, 11). Approximately 90% of DTs are sporadic, while the remaining cases are usually related to familial adenomatous polyposis (FAP), specifically Gardner syndrome (12). In both cases, mutations that activate the Wnt/β-catenin signaling pathway are likely to play a significant role in tumorigenesis (13). Wnt/β-catenin signaling is involved in numerous processes, such as the control of gene expression and regulation of cell adhesion and polarity (14). In addition, approximately 85% of DTs are related to mutations in the exon 3 of the beta-catenin encoding gene *CTNNB1* (15). *CTNNB1* mutations of DTs generally occur at codons 41 or 45, with p.T41A (threonine to alanine), p.S45F (serine to phenylalanine), and p.S45P (serine to proline) being the most frequent ones (15–21).

Used as a new tool for diagnosing and monitoring cancer, liquid biopsies have received increasing attention. Using a simple blood test has enormous implications for the diagnosis of cancer, so it is possible to avoid invasive tissue biopsies in the future and obtain a similar result from the circulating tumor cell (CTC) test (22).

CTCs play a central role on tumor dissemination and metastasis, which are ultimately responsible for most cancer deaths. Cancer cells can enter circulation years before a tumor is diagnosed. The majority of cells die, and only a minor fraction contains viable metastatic precursors that infiltrate organs and survive for eventual relapse (23–25). The presence of CTCs and/or circulating tumor microemboli (CTMs) in the peripheral blood of patients can be early markers of tumor invasion and spread (26). The dissemination of cancer cells from a primary tumor is conventionally viewed as a unidirectional process that culminates with the metastatic colonization of distant organs. CTCs and CTMs are associated with poor prognosis in several carcinomas. Furthermore, CTCs can colonize their tumors of origin through a process of "tumor self-seeding" (27). In contrast to carcinomas, few studies have examined CTCs and CTMs in mesenchymal tumor patients (28), and to the best of our knowledge, there are no reports of CTC detection in cases of DT.

Therefore, the aims of this study were to determine whether CTCs could be detected in DT patients and analyze their expression of mesenchymal proteins [vimentin, transforming growth factor receptor I (TGF-βRI)], as well as β-catenin and COX-2.

METHODS

Patients and Samples

This was a prospective and descriptive study, conducted with DT patients treated at the A.C. Camargo Cancer Center, São Paulo, Brazil, between June 2017 and October 2019. Peripheral blood samples were obtained after written informed consent. CTCs were analyzed by ISET® assay (Rarecells Diagnostics, Paris, France). This study was approved by the local Research Ethics Board (REB protocol 2427/17). Inclusion criteria were age >18 years, diagnosis of DT, presence of measurable disease, and a negative medical history of recent surgical procedures or trauma. Patients with FAP were excluded.

ISET® Assay

Blood samples (8 ml) were drawn in EDTA tubes (BD Vacutainer®) with immediate gentle agitation after blood collection. If samples were not processed immediately after phlebotomy, the tubes were left on a blood homogenizer at room temperature for up to 4 h. The isolation by size of epithelial tumor cells (ISET) assay was performed as described previously (29). The samples were processed on the platform according to the manufacturer's instructions. Eight milliliter of whole blood (1 ml per spot) was topped up to 80 ml with erythrocyte lysis buffer containing 0.02% formaldehyde, incubated for 10 min at room temperature, and filtered through an 8-μm pore membrane. To preserve cell integrity, filtration pressure was optimized at −10 kPa. The membrane was then washed once with phosphate-buffered saline 1×. After processing, membranes were dried, wrapped in aluminum foil, and stored at −20°C until use.

Immunocytochemistry

The spot membranes were subjected to immunocytochemistry (ICC) in 24-well plates to evaluate protein expression. We made single [one protein analyzed, stained with DAB (Dako™)] or double (two proteins analyzed, stained with DAB and magenta chromogen) ICC assays. Before ICC reactions, antigen retrieval was performed using Antigen Retrieval Solution (Dako™). Cells in the ISET spots were then hydrated with tris-buffered saline (TBS) 1× for 20 min and permeabilized with TBS + Triton X-100 for 5 min. Endogenous peroxides were blocked with 3% hydrogen peroxide and kept in the dark for 15 min. The spots were incubated with antibodies diluted in TBS supplemented with 10% fetal calf serum. For single staining, antibody staining

was visualized with DAB (Dako™). To amplify the antibody signal for double staining, the spots were incubated with Envision G/2 Doublestain System, Rabbit/Mouse (Dako™), followed by a 10-min incubation with magenta chromogen to visualize the second antibody. Cells were stained with hematoxylin and analyzed by light microscopy (BX61-Olympus).

Negative and positive controls were added for each ICC staining. For positive controls, blood from healthy subjects was spiked with A549 and U-87 cell lines. According to the Human Protein Atlas (http://www.proteinatlas.org/), the A549 cell line expresses both β-catenin and TGF-βRI, whereas the U-87 cell line expresses both COX-2 and vimentin. These cell lines were acquired from ATCC® HTB-43™. For negative controls, A549 and U-87 cell lines spiked in healthy blood were not incubated with the primary antibody, to avoid cross-reactivity (**Supplementary Figure 1**). For protein expression analysis, cells were classified according to their staining characteristics. The absence of staining was considered negative, while staining of the nucleus or cytoplasm was classified as positive, as expected for each antibody. We did not perform statistical analysis to evaluate protein expression, progression-free survival, or overall survival due to the rarity of events in these patients and the short follow-up interval.

TABLE 1 | Clinical characteristics of the patients.

Variable	No.	%
Total number of patients	18	100
Age at recruitment, years		
Median (range)	43.5 (18–65)	
Gender		
Male	2	11
Female	16	89
Tumor location		
Lower limbs	5	28
Upper limbs	2	11
Supraclavicular	2	11
Abdominal wall	3	18
Scapular region	1	5
Retroperitoneum	1	5
Gluteal region	2	11
Paravertebral	2	11
Relapse		
Yes	12	67
No	6	33

RESULTS

Detection of CTCs and Protein Expression Analysis

Recently, it was shown that the limit of detection of ISET is 1 CTC/10 ml of whole blood and that despite its high sensitivity, the distribution of CTCs in membrane spots is not uniform (30). Thus, we tested all eight spots fixed with 0.02% formaldehyde to ensure the observation of all isolated CTCs.

Eighteen patients were enrolled in this study, including two males and 16 females, with median age at the time of recruitment of 43.5 years (18–65 years). DTs were diagnosed in the lower extremities of 27.7% of patients. Clinical and pathological characteristics were obtained from medical records and are summarized in **Table 1**.

CTCs were detected in all patients. Eight spots were tested for each patient. Two spots were tested for β-catenin and vimentin expression (double staining), two were single-stained for either COX-2 or TGFβ-RI, and the last spots were stained with hematoxylin for CTC visualization. In addition, the estimated CTC count was made considering the average count of the eight spots evaluated. The average number of CTCs detected by ISET® was 2.6 CTC/ml (0.5–13 CTCs/ml). One CTM, a cluster of three or more CTCs, was found in one patient. Quantification and characterization of CTCs are presented in **Table 2**, **Figure 1**, and **Supplementary Figure 2**.

CTCs of 11 patients (61.1%) expressed β-catenin. Immunohistochemical analysis of primary tumors revealed that 11 patients were positive for β-catenin (**Figure 2**) and three were negative, and the results of four patients were not reported. Five patients expressed β-catenin in both CTCs and primary tumors, and one who tested negative in the primary tumor also tested negative in CTCs. Two patients were positive for β-catenin expression in CTCs and negative in primary tumors (**Table 2**). Because i) IHC is the gold standard method for β-catenin detection in primary tumors and ii) primary tumor β-catenin expression was available in the medical records of only 14 patients, we found a concordance rate between primary tumors and CTCs of 42.8% (6 concordant/14 samples). As concordance, we considered simultaneous positive or negative expression of a given protein in both CTCs and primary tumors. Among the 18 patients evaluated for protein expression in CTCs, vimentin was observed in five patients (27.7%) (**Figure 3**), while nine were positive for TGFβ-RI (50%) and seven for COX-2 (38.8%).

DISCUSSION

Although it was our first study with DT, we have extensive experience with ISET, as we have been working with this method for a long time, with many published papers (29, 32–40) including two with sarcomas (29, 41). In the first paper with sarcoma (29), we tested the sensitivity of the method, as we were the first group to test ISET for non-solid tumors, and we proved, with cell line, that its sensitivity was high, even for mesenchymal cells. After spiking 25, 50, 100, and 150 HT1080 cells (derived from human fibrosarcoma), in triplicate, in 1 ml of blood from healthy donors and filtering the blood using ISET, we found mean numbers of 25, 54, 100, and 155 cells, respectively. The numbers found were not identical to the numbers of cells spiked because tumor cells were counted in a counting chamber, by dilution, and not one by one. In this study, we also filtered blood samples from 30 healthy donors in ISET and found no CTCs.

Since DTs do not metastasize, it is apparently counterintuitive to find CTCs in the bloodstream of these patients. However, our study showed that CTCs can be detected and isolated from DT patients even from relatively low volumes of blood samples. This finding suggests that CTCs might be playing a different role on

TABLE 2 | CTC counting and characterization.

Patient ID	β-Catenin expression in the primary tumor	Number of β-catenin-positive CTCs in 5 ml of blood	Number of TGFβ-RI-positive CTCs in 5 ml of blood	Number of vimentin-positive CTCs in 5 ml of blood	Number of COX-2-positive CTCs in 5 ml of blood	CTC/ 1 ml
1	Negative	1	0	0	1	1
2	Positive	4	0	0	1	1.8
3	Positive	0	2	2	0	3.8
4	Positive	0	1	0	2	1
5	Positive	4	0	2	2	2.6
6	Positive	0	0	0	0	0.8
7	Positive	0	4	0	8	13
8	Positive	2	1	0	0	4.8
9	Positive	0	0	0	0	2.6
10	Positive	5	8	1	0	5
11	-	2	7	2	0	4.75
12	Negative	0	0	0	0	0.5
13	-	4	2	0	0	1.75
14	Negative	1	3	0	0	10.5
15	-	3	0	0	1	5
16	–	1	0	0	0	1.25
17	Positive	6*	0	9*	1	8
18	Positive	0	1	0	0	1

CTC, circulating tumor cell; COX-2, cyclooxygenase-2.
**Patient with positive circulating tumor microemboli (CTMs) for β-catenin and vimentin.*

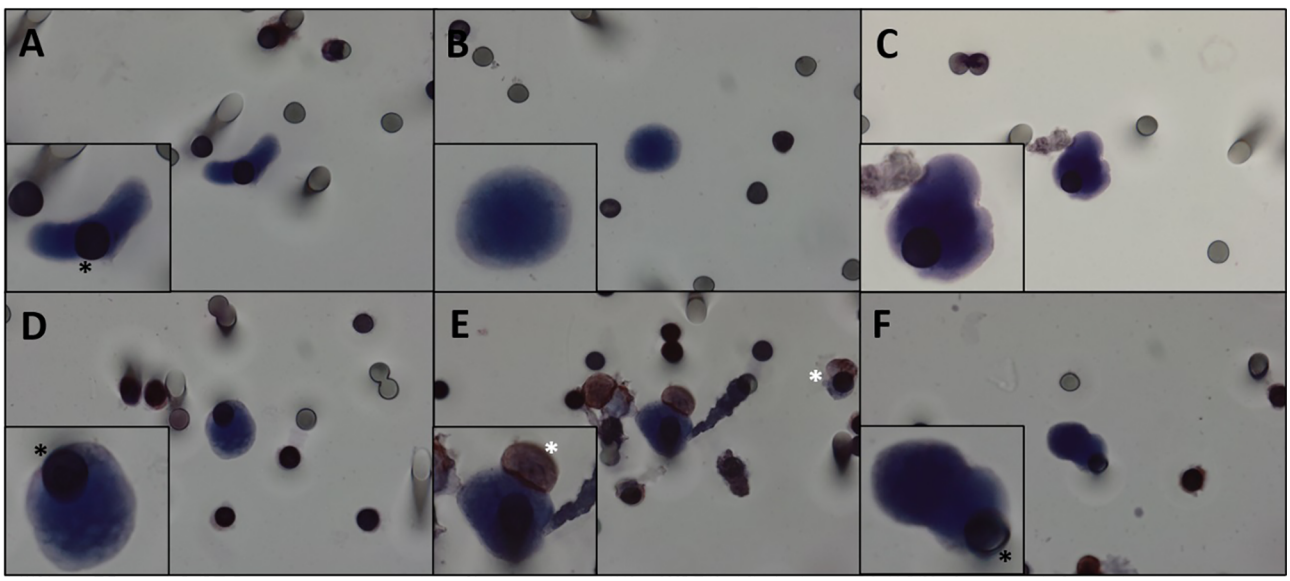

FIGURE 1 | **(A–F)** CTCs isolated from patients with DTs. Cells visualized with hematoxylin. We can observe pleomorphic desmoid tumor CTCs with all cytopathological features: nucleus size ≥ 12 μm, hyperchromatic and irregular nucleus, visible presence of cytoplasm, and a high nucleus–cytoplasm ratio (31). White asterisk: leukocytes. Black asterisk: membrane spots. Images were taken at ×600 magnification using a light microscope (Research System Microscope BX61—Olympus, Tokyo, Japan) coupled to a digital camera (SC100—Olympus, Tokyo, Japan). CTCs, circulating tumor cells; DTs, desmoid tumors.

the DT biology. That allowed us to hypothesize that CTCs can be working as vehicles that reseed the primary tumor, which could potentiate its aggressiveness. CTCs are characterized by cytomorphological features that include nucleus size ≥12 μm; hyperchromatic and irregular nuclei; visible presence of cytoplasm; and a high nucleus–cytoplasm ratio (31). We defined CTCs as cells displaying all the aforementioned characteristics, and we also observed CTC pleomorphism (**Figure 1** and **Supplementary Figure 2**). Morphologic changes resulting in more rounded or "fibroblastoid" CTCs were most likely acquired during *in vitro* cell handling or by the filtering process. In **Supplementary Figure 3**, examples of macrophages

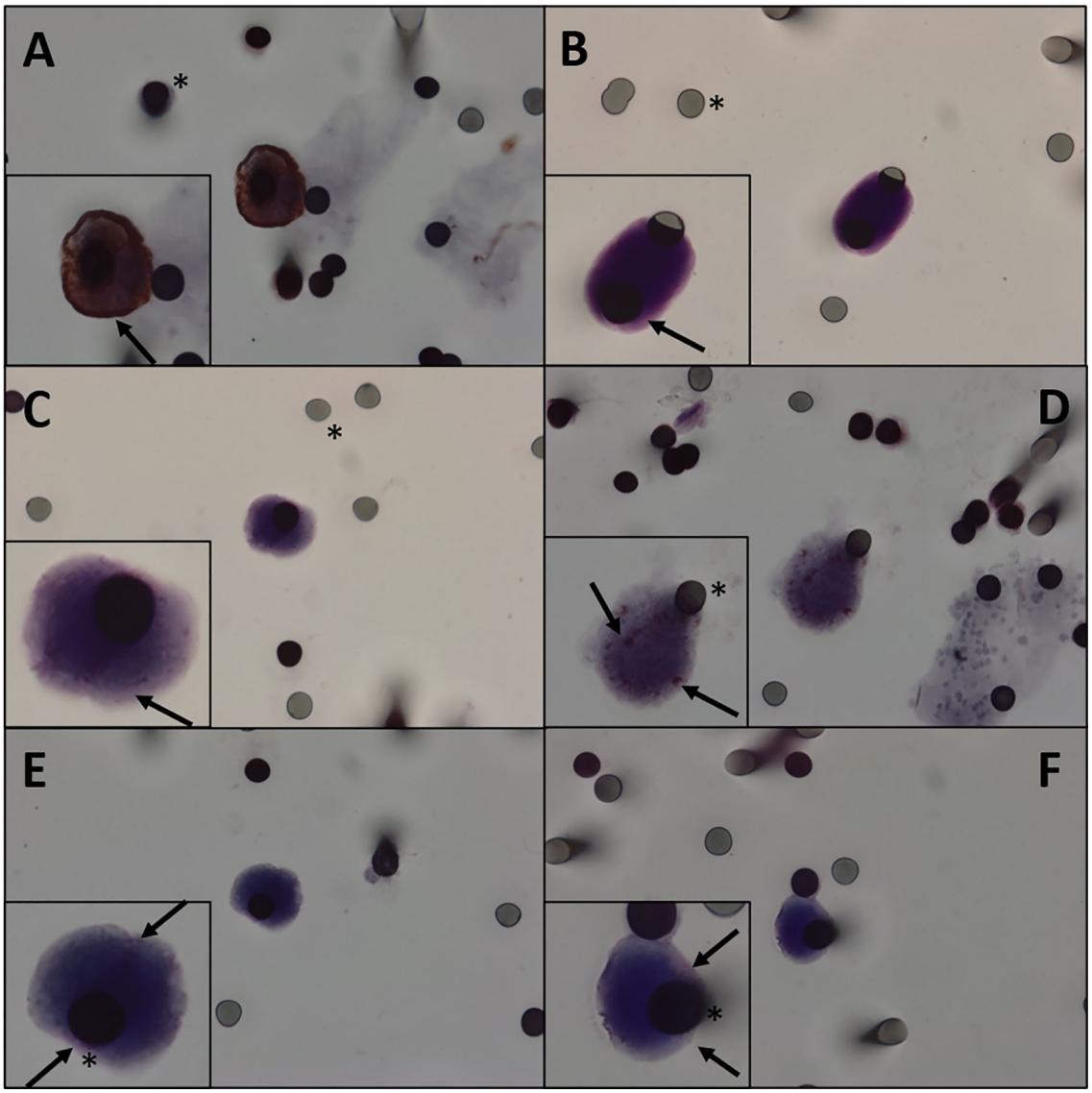

FIGURE 2 | **(A)** Immunocytochemistry of CTC with β-catenin antibody counterstaining with DAB. **(B–F)** Immunocytochemistry of CTC with β-catenin antibody and counterstaining with magenta chromogen. We can observe different degrees of staining. **(A, B)** β-Catenin highly positive staining in a patient. **(C, D)** β-Catenin middle staining in a patient. **(E, F)** β-Catenin weakly positive staining in a patient. Black asterisk: membrane spots. Black arrows: β-catenin. CTC, circulating tumor cell.

isolated from the blood of patients with DT can be appreciated, demonstrating the morphological differences between CTCs and macrophages.

The high prevalence of CTCs in our patient population might be explained by the self-seeding hypothesis. It has been proposed that self-seeding can accelerate tumor growth, angiogenesis, and stromal recruitment through seed-derived factors (27). Therefore, tumor self-seeding might explain the relationships among anaplasia, tumor size, vascularity, and prognosis and also suggests that local recurrences may result from seeding of disseminated cells following complete tumor excision (1, 42, 43).

CTMs were isolated from a single patient (**Figure 3** and **Table 2**) and were positive for β-catenin and vimentin expressions. Interestingly, it was in a 57-year-old woman whose diagnosis was in 2013 with the blood collection in this study made in September 2019 and who has not yet progressed. She has received only one treatment line (tamoxifen + celecoxib). Knowledge regarding CTMs, also called CTC clusters, has evolved over the last decade, and increasing evidence suggests that they play an essential role on the pathophysiology of metastasis (44). Preclinical and clinical studies exploiting other cancers have demonstrated that CTMs are associated with increased metastatic potential and poor prognosis (36, 45–48). Hayashi et al. detected CTMs in sarcoma patients using CellSieve™, a low-pressure microfiltration device. Our group previously isolated CTMs in sarcoma patients using ISET® but

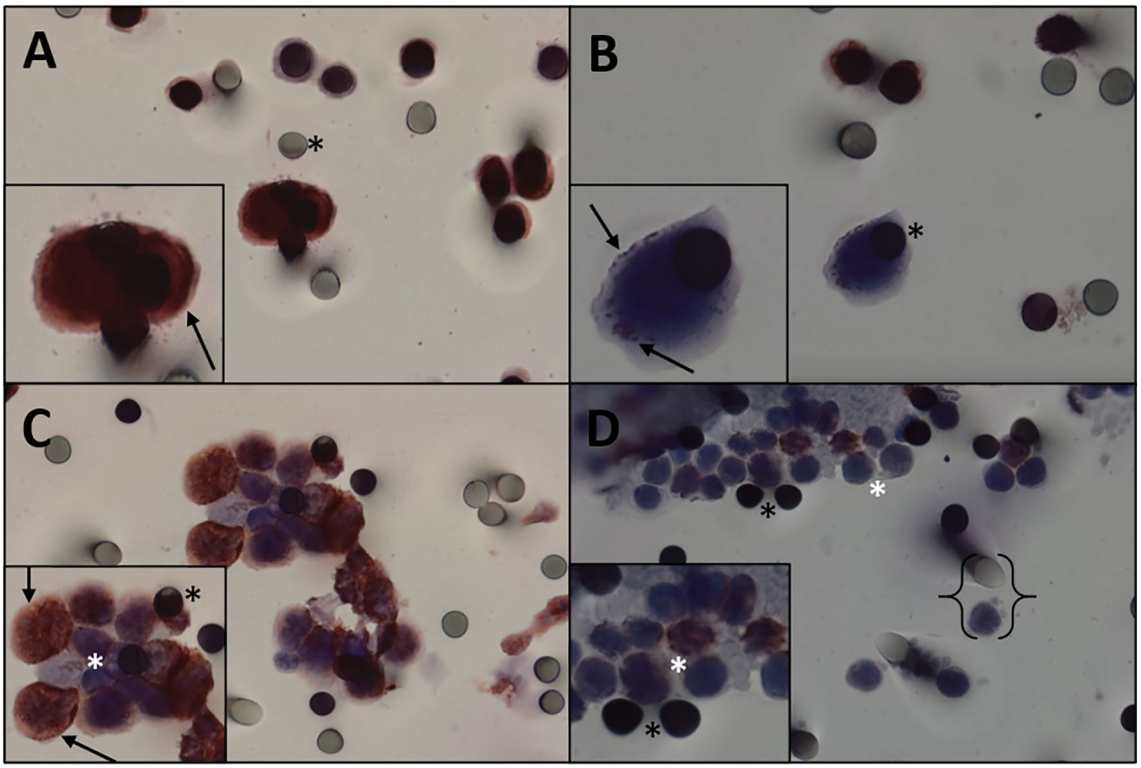

FIGURE 3 | Immunocytochemistry for vimentin. **(A, B)** Immunocytochemistry of CTC with vimentin antibody and counterstaining with DAB. **(A)** High staining. **(B)** Weak staining. **(C)** Desmoid tumor CTMs observed in the blood filtered using the ISET, stained with vimentin and counterstained with DAB chromogen. **(D)** Leukocytes from desmoid tumor patient. Black asterisk: membrane spots. Black arrows: vimentin expression. White asterisk: leukocytes. Keys: size comparison between a leukocyte and a spot. CTC, circulating tumor cell; CTMs, circulating tumor microemboli; ISET, isolation by size of epithelial tumor cells.

did not address DTs (41). Taking this into account, together with our current data, it is reasonable to hypothesize that the inability of DTs to metastasize can be explained in part by their failure to generate CTMs (as we rarely found CTMs in our cohort of 18 patients). However, this hypothesis needs to be interpreted cautiously, due to the small sample size of our cohort.

β-Catenin is broadly used for DT diagnosis. In line with this, we thought that this protein could also be expressed in CTCs. Analysis of β-catenin protein expression in CTCs showed 35.7% of concordance with primary tumors (considering both i) patients from whom reports of the primary tumor were available and ii) those patients in whom the spots analyzed for β-catenin did not present CTCs). β-Catenin is encoded by the *CTNNB1* gene in humans and is involved in cell signaling, acting primarily as a transcription factor. It has an essential role on developmental biology and cell adhesion. Mutations and overexpression of this gene are associated with several types of cancers, such as lung, breast, ovarian, endometrial, hepatocellular, and colorectal carcinomas (19–21, 49). We also identified vimentin expression in the CTCs of five patients (27.7%). Vimentin is required for plasticity of mesenchymal cells under normal physiological conditions and migration of cancer cells that have undergone epithelial/mesenchymal transition. In a previous study of sarcoma CTCs conducted by our group, we detected vimentin in CTCs of three patients in a cohort of 11 (29).

TGF-β is a secreted cytokine that regulates cell migration, differentiation, and proliferation (50). Depending on its expression level, TGF-β has both proangiogenic and antiangiogenic properties. Angiogenic factors (vascular endothelial growth factor and basic fibroblast growth factor) increase TGF-β expression when its levels are low. At high levels, TGF-β rebuilds basement membrane and inhibits the growth of endothelial cells and smooth muscle cells (51, 52). In this study, curiously, nine patients (50%) were positive for TGFβ-RI expression in CTCs. In another study by our group (37), TGF-βRI expression was associated with poor prognosis of locally advanced head and neck cancer. The identification of TGF-βRI in CTCs opens paths for the comprehensive exploitation of this pathway in DT.

COX enzymes play important roles on human physiology and various pathological conditions (53, 54). There is evidence for the critical involvement of COX-2 in many pathologies, including cancer (55, 56). Here, we also found a high frequency of DT patients expressing COX-2 in CTCs. Considering that DTs do not form metastases but show aggressive local invasion, it is possible that COX-2 plays an essential role on this process, which needs to be further investigated.

In general, we found that β-catenin was highly expressed in CTCs. Except for patient #6, we also found that at least one marker was expressed by CTCs across the whole cohort analyzed in this study, suggesting that evolution of protein expression in CTCs might be used as a biomarker that allows the non-invasive diagnosis of DT patients.

In this study, we showed that CTCs are composed of highly heterogeneous cell populations with very different phenotypes. This difference in phenotypes makes the identification of CTCs challenging, due to their similarities with other cells of the immune system, such as giant monocytes and micromegakaryocytes. However, training in analysis with the help of cytopathological criteria can overcome these difficulties. Laget et al. (30) described results that consistently show the feasibility of isolating live and fixed tumor cells with a lower limit of detection (LLOD) of a cancer cell per 10 ml of blood and an LLOD sensitivity ranging from 83% to 100%. Those results demonstrated that ISET® allows highly sensitive and impartial isolation of fixed tumor cells from blood for reliable identification of CTCs, as well as the development of immuno-molecular studies. Here, we were able to demonstrate the expression of mesenchymal proteins in CTCs by ICC, which are probably involved in tumorigenesis process.

To conclude, our study opens the prospect of using CTCs to predict desmoid dynamics throughout the course of the disease. In addition, it demonstrates that DTs release CTCs, opening new avenues for studying the biology of this tumor and improving our understanding of its high local relapse rates without distant metastasis. Additional studies with larger sample sizes should be conducted to validate our findings and explore the mechanism of DT development and progression.

DATA AVAILABILITY STATEMENT

The datasets presented in this study can be found in online repositories. The names of the repository/repositories and accession number(s) can be found in the article/**Supplementary Material**.

ETHICS STATEMENT

The studies involving human participants were reviewed and approved by AC Camargo Cancer Center. The patients/participants provided their written informed consent to participate in this study.

AUTHOR CONTRIBUTIONS

AB: design, data analysis and interpretation, manuscript writing and collection and/or assembly of data. FC, MS and FP: clinical survey/review and writing. EA and AR: collection and/or assembly of data. TM: English review. CM: conception/design and writing of the clinical part of the manuscript. LC: conception/design, data analysis and interpretation, manuscript writing, final approval of manuscript. All authors contributed to the article and approved the submitted version.

FUNDING

We thank the National Institute for Science and Tecnology in Oncogenomics and Therapeutic Innovation (INCT) for financial support for this study. ACB had a PhD fellowship from São Paulo Research Foundation FAPESP (2019/18100-8).

SUPPLEMENTARY MATERIAL

The Supplementary Material for this article can be found online at: https://www.frontiersin.org/articles/10.3389/fonc.2021.622626/full#supplementary-material

Supplementary Figure 1 | (A, B) Positive control, A549 cell line "spiked" in healthy blood and stained for β-catenin and TGF β-RI respectively. **(C, D)** Positive control, U-87 cell line "spiked" in healthy blood and stained for COX-2 and Vimentin respectively. **(E)** Negative control, A-549 cell line "spiked" in healthy blood and negative for β-catenin. Cells were analyzed by light microscopy (BX61-Olympus).

Supplementary Figure 2 | (A–I) Haematoxylin stained cells. Examples of isolated desmoid tumor CTCs with characteristic cytomorphological features (nucleus size ≥ 12 µm, hyperchromatic and irregular nucleus, visible presence of cytoplasm, and a high nucleus–cytoplasm ratio (31). White asterisk: leukocytes. Black asterisks: ISET membrane pore.

Supplementary Figure 3 | (A) Leukocytes from desmoid tumor patient. **(B, C)** Examples of macrophages isolated from the blood of patients with desmoid tumor. In **(B)**, a macrophage stained with COX-2. In **(C)**, a macrophage visualized with haematoxylin.

REFERENCES

1. Wu C, Nik-Amini S, Nadesan P, Stanford WL, Alman BA. Aggressive Fibromatosis (Desmoid Tumor) Is Derived From Mesenchymal Progenitor Cells. *Cancer Res* (2010) 70(19):7690–8. doi: 10.1158/0008-5472.CAN-10-1656
2. Ratan R, Roland CL BA. Desmoid Fibromatosis: Management in an Era of Increasing Options. *Curr Oncol Rep* (2021) 23(4):41. doi: 10.1007/s11912-021-01026-w
3. de Camargo VP, Keohan ML, D'Adamo DR, Antonescu CR, Brennan MF, Singer S, et al. Clinical Outcomes of Systemic Therapy for Patients With Deep Fibromatosis (Desmoid Tumor). *Cancer* (2010) 116(9):2258–65. doi: 10.1002/cncr.25089
4. Penel N, Coindre J-M, Bonvalot S, Italiano A, Neuville A, Le Cesne A, et al. Management of Desmoid Tumours: A Nationwide Survey of Labelled Reference Centre Networks in France. *Eur J Cancer* (2016) 58:90–6. doi: 10.1016/j.ejca.2016.02.008
5. Fiore M, MacNeill A, Gronchi A, Colombo C. Desmoid-Type Fibromatosis. *Surg Oncol Clin N Am* (2016) 25(4):803–26. doi: 10.1016/j.soc.2016.05.010
6. Garcia-Ortega DY, Martín-Tellez KS, Cuellar-Hubbe M, Martínez-Said H, Álvarez-Cano A, Brener-Chaoul M, et al. Desmoid-Type Fibromatosis. *Cancers (Basel)* (2020) 12(7):1851. doi: 10.3390/cancers12071851
7. Penel N, Chibon F, Salas S. Adult Desmoid Tumors: Biology, Management and Ongoing Trials. *Curr Opin Oncol* (2017) 29(4):268–74. doi: 10.1097/CCO.0000000000000374

8. Group DTW The Management of Desmoid Tumours: A Joint Global Consensus-Based Guideline Approach for Adult and Paediatric Patients. *Eur J Cancer* (2020) 127:96–107. doi: 10.1016/j.ejca.2019.11.013
9. Peng PD, Hyder O, Mavros MN, Turley R, Groeschl R, Firoozmand A, et al. Management and Recurrence Patterns of Desmoids Tumors: A Multi-Institutional Analysis of 211 Patients. *Ann Surg Oncol* (2012) 19(13):4036–42. doi: 10.1245/s10434-012-2634-6
10. Kotiligam D, Lazar AJF, Pollock RE, Lev D. Desmoid Tumor: A Disease Opportune for Molecular Insights. *Histol Histopathol* (2008) 23(1):117–26. doi: 10.14670/HH-23.117
11. Owens CL, Sharma R, Ali SZ. Deep Fibromatosis (Desmoid Tumor). *Cancer* (2007) 111(3):166–72. doi: 10.1002/cncr.22689
12. Koskenvuo L, Ristimäki A, Lepistö A. Comparison of Sporadic and FAP-Associated Desmoid-Type Fibromatoses. *J Surg Oncol* (2017) 116(6):716–21. doi: 10.1002/jso.24699
13. Escobar C, Munker R, Thomas JO, Li BD, Burton GV. Update on Desmoid Tumors. *Ann Oncol* (2012) 23(3):562–9. doi: 10.1093/annonc/mdr386
14. Chilov D, Sinjushina N, Rita H, Taketo MM, Mäkelä TP, Partanen J. Phosphorylated β-Catenin Localizes to Centrosomes of Neuronal Progenitors and is Required for Cell Polarity and Neurogenesis in Developing Midbrain. *Dev Biol* (2011) 357(1):259–68. doi: 10.1016/j.ydbio.2011.06.029
15. Colombo C, Bolshakov S, Hajibashi S, Lopez-Terrada L, Wang W-L, Rao P, et al. 'Difficult to Diagnose' Desmoid Tumours: A Potential Role for CTNNB1 Mutational Analysis. *Histopathology* (2011) 59(2):336–40. doi: 10.1111/j.1365-2559.2011.03932.x
16. Dômont J, Salas S, Lacroix L, Brouste V, Saulnier P, Terrier P, et al. High Frequency of β-Catenin Heterozygous Mutations in Extra-Abdominal Fibromatosis: A Potential Molecular Tool for Disease Management. *Br J Cancer* (2010) 102(6):1032–6. doi: 10.1038/sj.bjc.6605557
17. Lazar AJF, Tuvin D, Hajibashi S, Habeeb S, Bolshakov S, Mayordomo-Aranda E, et al. Specific Mutations in the β-Catenin Gene (CTNNB1) Correlate With Local Recurrence in Sporadic Desmoid Tumors. *Am J Pathol* (2008) 173 (5):1518–27. doi: 10.2353/ajpath.2008.080475
18. Braggio D, Zewdu A, Londhe P, Yu P, Lopez G, Batte K, et al. β-Catenin S45F Mutation Results in Apoptotic Resistance. *Oncogene* (2020) 39(34):5589–600. doi: 10.1038/s41388-020-1382-5
19. Lecarpentier Y, Schussler O, Hébert J-L, Vallée A. Multiple Targets of the Canonical WNT/β-Catenin Signaling in Cancers. *Front Oncol* (2019) 9:1–17. doi: 10.3389/fonc.2019.01248
20. Liu Y, Patel L, Mills GB, Lu KH, Sood AK, Ding L, et al. Clinical Significance of CTNNB1 Mutation and Wnt Pathway Activation in Endometrioid Endometrial Carcinoma. *JNCI J Natl Cancer Inst* (2014) 106(9):1–8. doi: 10.1093/jnci/dju245
21. Garcia-Rostan G, Camp RL, Herrero A, Carcangiu ML, Rimm DL, Tallini G. β-Catenin Dysregulation in Thyroid Neoplasms. *Am J Pathol* (2001) 158 (3):987–96. doi: 10.1016/S0002-9440(10)64045-X
22. Pantel K, Alix-Panabières C. Cell Lines From Circulating Tumor Cells. *Oncoscience [Internet]* (2015) 202(10):815–6. doi: 10.18632/oncoscience.195
23. Alix-Panabières C, Pantel K. Circulating Tumor Cells: Liquid Biopsy of Cancer. *Clin Chem* (2013) 59(1):110–8. doi: 10.1373/clinchem.2012.194258
24. Pantel K, Brakenhoff RH. Dissecting the Metastatic Cascade. *Nat Rev Cancer* (2004) 4(6):448–56. doi: 10.1038/nrc1370
25. Massagué J, Obenauf AC. Metastatic Colonization by Circulating Tumour Cells. *Nature* (2016) 529(7586):298–306. doi: 10.1038/nature17038
26. Paterlini-Brechot P, Benali NL. Circulating Tumor Cells (CTC) Detection: Clinical Impact and Future Directions. *Cancer Lett* (2007) 253(2):180–204. doi: 10.1016/j.canlet.2006.12.014
27. Kim M-Y, Oskarsson T, Acharyya S, Nguyen DX, Zhang XH-F, Norton L, et al. Tumor Self-Seeding by Circulating Cancer Cells. *Cell* (2009) 139 (7):1315–26. doi: 10.1016/j.cell.2009.11.025
28. Chang L, Asatrian G, Dry SM, James AW. Circulating Tumor Cells in Sarcomas: A Brief Review. *Med Oncol* (2015) 32(1):430. doi: 10.1007/s12032-014-0430-9
29. Chinen L, Mello C, Abdallah E, Ocea L, Buim M, Mingues N, et al. Isolation, Detection, and Immunomorphological Characterization of Circulating Tumor Cells (CTCs) From Patients With Different Types of Sarcoma Using Isolation by Size of Tumor Cells: A Window on Sarcoma-Cell Invasion. *Onco Targets Ther* (2014) 7:1609–17. doi: 10.2147/OTT.S62349
30. Laget S, Broncy L, Hormigos K, Dhingra DM, BenMohamed F, Capiod T, et al. Technical Insights Into Highly Sensitive Isolation and Molecular Characterization of Fixed and Live Circulating Tumor Cells for Early Detection of Tumor Invasion. *PloS One* (2017) 12(1):e0169427. doi: 10.1371/journal.pone.0169427
31. Krebs MG, Hou J-M, Sloane R, Lancashire L, Priest L, Nonaka D, et al. Analysis of Circulating Tumor Cells in Patients With Non-Small Cell Lung Cancer Using Epithelial Marker-Dependent and -Independent Approaches. *J Thorac Oncol* (2012) 7(2):306–15. doi: 10.1097/JTO.0b013e31823c5c16
32. Chinen LTD, de Carvalho FM, Rocha BMM, Aguiar CM, Abdallah EA, Campanha D, et al. Cytokeratin-Based CTC Counting Unrelated to Clinical Follow Up. *J Thorac Dis* (2013) 5(5):593–9. doi: 10.3978/j.issn.2072-1439.2013.09.18
33. Abdallah EA, Fanelli MF, Buim MEC, Machado Netto MC, Gasparini Junior JL, Souza e Silva V, et al. Thymidylate Synthase Expression in Circulating Tumor Cells: A New Tool to Predict 5-Fluorouracil Resistance in Metastatic Colorectal Cancer Patients. *Int J Cancer* (2015) 137(6):1397–405. doi: 10.1002/ijc.29495
34. Buim ME, Fanelli MF, Souza VS, Romero J, Abdallah EA, Mello C AL, et al. Detection of KRAS Mutations in Circulating Tumor Cells From Patients With Metastatic Colorectal Cancer. *Cancer Biol Ther* (2015) 16(9):1289–95. doi: 10.1080/15384047.2015.1070991
35. Abdallah EA, Fanelli MF, Souza e Silva V, Machado Netto MC, Gasparini Junior JL, Araújo DV, et al. MRP1 Expression in CTCs Confers Resistance to Irinotecan-Based Chemotherapy in Metastatic Colorectal Cancer. *Int J Cancer* (2016) 139(4):890–8. doi: 10.1002/ijc.30082
36. Corassa M, Fanelli MF, Oliveira TB, Mello CL, Machado Netto MC, Nicolau UR, et al. Circulating Tumor Microemboli as a Prognostic Factor for Locally Advanced or Metastatic Solid Tumors. *J Clin Oncol* (2016) 34(15_suppl): e23067–7. doi: 10.1200/JCO.2016.34.15_suppl.e23067
37. Fanelli MF, Oliveira TB, Braun AC, Corassa M, Abdallah EA, Nicolau UR, et al. Evaluation of Incidence, Significance, and Prognostic Role of Circulating Tumor Microemboli and Transforming Growth Factor-β Receptor I in Head and Neck Cancer. *Head Neck* (2017) 39(11):2283–92. doi: 10.1002/hed.24899
38. Abdallah EA, Braun AC, Flores BCTCP, Senda L, Urvanegia AC, Calsavara V, et al. The Potential Clinical Implications of Circulating Tumor Cells and Circulating Tumor Microemboli in Gastric Cancer. *Oncologist* (2019) 24(9):1–10. doi: 10.1634/theoncologist.2018-0741
39. Troncarelli Flores BC, Souza e Silva V, Ali Abdallah E, Mello CAL, Gobo Silva ML, Gomes Mendes G, et al. Molecular and Kinetic Analyses of Circulating Tumor Cells as Predictive Markers of Treatment Response in Locally Advanced Rectal Cancer Patients. *Cells* (2019) 8(7):641. doi: 10.3390/cells8070641
40. Abdallah EA, Souza e Silva V, Braun AC, Gasparini VA, Kupper BEC, Tariki MS, et al. A Higher Platelet-To-Lymphocyte Ratio is Prevalent in the Presence of Circulating Tumor Microemboli and is a Potential Prognostic Factor for Non-Metastatic Colon Cancer. *Transl Oncol* (2021) 14(1):100932. doi: 10.1016/j.tranon.2020.100932
41. Braun AC, de Mello CAL, Corassa M, Abdallah EA, Urvanegia AC, Alves VS, et al. EGFR Expression in Circulating Tumor Cells From High-Grade Metastatic Soft Tissue Sarcomas. *Cancer Biol Ther* (2018) 19(6):454–60. doi: 10.1080/15384047.2018.1433498
42. Sakorafas GH, Nissotakis C, Peros G. Abdominal Desmoid Tumors. *Surg Oncol* (2007) 16(2):131–42. doi: 10.1016/j.suronc.2007.07.009
43. Nieuwenhuis MH, Casparie M, Mathus-Vliegen LMH, Dekkers OM, Hogendoorn PCW, Vasen HFA. A Nation-Wide Study Comparing Sporadic and Familial Adenomatous Polyposis-Related Desmoid-Type Fibromatoses. *Int J Cancer* (2011) 129(1):256–61. doi: 10.1002/ijc.25664
44. Amintas S, Bedel A, Moreau-Gaudry F, Boutin J, Buscail L, Merlio J-P, et al. Circulating Tumor Cell Clusters: United We Stand Divided We Fall. *Int J Mol Sci* (2020) 21(7):2653. doi: 10.3390/ijms21072653
45. Aceto N, Bardia A, Miyamoto DT, Donaldson MC, Wittner BS, Spencer JA, et al. Circulating Tumor Cell Clusters Are Oligoclonal Precursors of Breast Cancer Metastasis. *Cell* (2014) 158(5):1110–22. doi: 10.1016/j.cell.2014.07.013
46. Hou J-M, Krebs MG, Lancashire L, Sloane R, Backen A, Swain RK, et al. Clinical Significance and Molecular Characteristics of Circulating Tumor Cells and Circulating Tumor Microemboli in Patients With Small-Cell Lung Cancer. *J Clin Oncol* (2012) 30(5):525–32. doi: 10.1200/JCO.2010.33.3716
47. Zhang D, Zhao L, Zhou P, Ma H, Huang F, Jin M, et al. Circulating Tumor Microemboli (CTM) and Vimentin+ Circulating Tumor Cells (CTCs)

Detected by a Size-Based Platform Predict Worse Prognosis in Advanced Colorectal Cancer Patients During Chemotherapy. *Cancer Cell Int* (2017) 17 (1):6. doi: 10.1186/s12935-016-0373-7
48. Wu G, Zhu R, Li Y, Zhao Y, Dai M. Prognostic Significance of Circulating Tumor Microemboli in Patients With Pancreatic Ductal Adenocarcinoma. *Oncol Lett* (2018) 5:7376–82. doi: 10.3892/ol.2018.8264
49. Cieply B, Zeng G, Proverbs-Singh T, Geller DA, Monga SPS. Unique Phenotype of Hepatocellular Cancers With Exon-3 Mutations in Beta-Catenin Gene. *Hepatology* (2009) 49(3):821–31. doi: 10.1002/hep.22695
50. Micalizzi DS, Farabaugh SM, Ford HL. Epithelial-Mesenchymal Transition in Cancer: Parallels Between Normal Development and Tumor Progression. *J Mammary Gland Biol Neoplasia* (2010) 15(2):117–34. doi: 10.1007/s10911-010-9178-9
51. Neuzillet C, Tijeras-Raballand A, Cohen R, Cros J, Faivre S, Raymond E, et al. Targeting the Tgfβ Pathway for Cancer Therapy. *Pharmacol Ther* (2015) 147:22–31. doi: 10.1016/j.pharmthera.2014.11.001
52. Sakurai T, Kudo M. Signaling Pathways Governing Tumor Angiogenesis. *Oncology* (2011) 81(s1):24–9. doi: 10.1159/000333256
53. Smith WL, Urade Y, Jakobsson P-J. Enzymes of the Cyclooxygenase Pathways of Prostanoid Biosynthesis. *Chem Rev* (2011) 111(10):5821–65. doi: 10.1021/cr2002992
54. Marnett LJ. The COXIB Experience: A Look in the Rearview Mirror. *Annu Rev Pharmacol Toxicol* (2009) 49(1):265–90. doi: 10.1146/annurev.pharmtox.011008.145638
55. Wang D, DuBois RN. The Role of Anti-Inflammatory Drugs in Colorectal Cancer. *Annu Rev Med* (2013) 64(1):131–44. doi: 10.1146/annurev-med-112211-154330
56. Méric J-B, Rottey S, Olaussen K, Soria J-C, Khayat D, Rixe O, et al. Cyclooxygenase-2 as a Target for Anticancer Drug Development. *Crit Rev Oncol Hematol* (2006) 59(1):51–64. doi: 10.1016/j.critrevonc.2006.01.003

Conflict of Interest: The authors declare that the research was conducted in the absence of any commercial or financial relationships that could be construed as a potential conflict of interest.

Publisher's Note: All claims expressed in this article are solely those of the authors and do not necessarily represent those of their affiliated organizations, or those of the publisher, the editors and the reviewers. Any product that may be evaluated in this article, or claim that may be made by its manufacturer, is not guaranteed or endorsed by the publisher.

Copyright © 2021 Braun, Campos, Abdallah, Ruano, Medina, Tariki, Pinto, de Mello and Chinen. This is an open-access article distributed under the terms of the Creative Commons Attribution License (CC BY). The use, distribution or reproduction in other forums is permitted, provided the original author(s) and the copyright owner(s) are credited and that the original publication in this journal is cited, in accordance with accepted academic practice. No use, distribution or reproduction is permitted which does not comply with these terms.

frontiers in Oncology

ORIGINAL RESEARCH
published: 06 October 2021
doi: 10.3389/fonc.2021.736412

Tumor-Educated Platelet miR-18a-3p as a Novel Liquid-Biopsy Biomarker for Early Diagnosis and Chemotherapy Efficacy Monitoring in Nasopharyngeal Carcinoma

Kaiyu Sun[1†], *Hui Wang*[2†], *Xianqun Xu*[3], *Xiuqi Wei*[4], *Jingyu Su*[4], *Kaidong Zhu*[4] *and Junli Fan*[3*]

[1] Department of Otolaryngology, Zhongnan Hospital of Wuhan University, Wuhan, China, [2] Department of Laboratory Medicine, Union Hospital, Tongji Medical College, Huazhong University of Science and Technology, Wuhan, China, [3] Department of Laboratory Medicine, Zhongnan Hospital of Wuhan University, Wuhan, China, [4] Department of Laboratory Medicine, Cancer Center, Union Hospital, Tongji Medical College, Huazhong University of Science and Technology, Wuhan, China

OPEN ACCESS

Edited by:
George Calin,
University of Texas MD Anderson Cancer Center, United States

Reviewed by:
Francesco Grignani,
University of Perugia, Italy
Keith R. Laderoute,
Consultant, Redwood City, CA, United States

***Correspondence:**
Junli Fan
527450105@qq.com

[†]These authors have contributed equally to this work and share first authorship

Specialty section:
This article was submitted to Molecular and Cellular Oncology, a section of the journal Frontiers in Oncology

Received: 05 July 2021
Accepted: 17 September 2021
Published: 06 October 2021

Citation:
Sun K, Wang H, Xu X, Wei X, Su J, Zhu K and Fan J (2021) Tumor-Educated Platelet miR-18a-3p as a Novel Liquid-Biopsy Biomarker for Early Diagnosis and Chemotherapy Efficacy Monitoring in Nasopharyngeal Carcinoma. Front. Oncol. 11:736412. doi: 10.3389/fonc.2021.736412

Aims: To evaluate the value of tumor-educated platelet (TEP) miR-18a-3p in the early diagnosis and chemotherapy efficacy monitoring of nasopharyngeal carcinoma (NPC).

Methods: Expression levels of miR-18a-3p in platelets and plasma were detected by relative quantitative real-time PCR in NPC patients (n=54) and normal subjects (n=36). Diagnostic values of TEP miR-18a-3p for NPC was assessed by receiver operating characteristic (ROC) curve analysis. Follow up study was carried out to observe the dynamic changes of TEP miR-18a-3p with chemotherapy on 3 NPC patients.

Results: The expression levels of TEP miR-18a-3p in NPC patients were significantly higher than that in healthy controls ($p < 0.0001$). ROC curve analysis showed that the area under the curve (AUC) value was 0.841, the sensitivity and specificity for the diagnosis of NPC were 87% and 72.7%. No correlation was found between expression levels of TEP miR-18a-3p and patients' clinical parameters and their NPC tumor-node-metastasis (TNM) stage. The positive rate of TEP miR-18a-3p and EBV DNA for NPC diagnosis were 85.4% and 66.7%. TEP miR-18a-3p expression were down-regulated after 77.8% (7 of 9) of chemotherapy, and in 66.7% (2 of 3) patients, TEP miR-18a-3p levels decreased after 3 cycles of chemotherapy.

Conclusion: The expression levels of TEP miR-18a-3p are upregulated in NPC and have a high probability to downregulated after chemotherapy, indicating a significant clinical value. TEP miR-18a-3p might serve as a novel type of liquid-biopsy biomarker for early diagnosis and chemotherapy efficacy monitoring in NPC.

Keywords: tumor-educated platelet, miR-18a-3p, liquid-biopsy, early diagnosis, chemotherapy, nasopharyngeal carcinoma

INTRODUCTION

Nasopharyngeal carcinoma (NPC) is a common malignancy arising in the nasopharynx epithelium with a remarkable ethnic and geographic distribution. NPC has a particularly high prevalence in eastern and southeastern Asia and southern China (1–3). The pathogenesis of NPC is complex and diverse, the etiology of NPC includes genetic susceptibility, dietary habits and Epstein-Barr virus (EBV) infection (4). Early symptoms of NPC include headache, neuro facial pain, neck mass, nosebleed or stuffy nose, NPC may easily be misdiagnosed since the early symptoms are non-specific (5). Radiotherapy and chemotherapy remains the mainstay of primary treatment for NPC. Non-keratinized, poorly differentiated and undifferentiated histological subtypes are particularly sensitive to chemotherapy, while radiotherapy can cure more than 90% of patients in stage I, but patients in advanced stages have a low 5-year survival rate due to local recurrence and distant metastasis (6). Therefore, early diagnosis of NPC is very important and necessary. Nasal endoscopic biopsy is the most commonly used method for diagnosis of NPC, but it is difficult to obtain tissue samples in early stage of the disease. Thus, there is an urgent need for the exploration of new biomarkers for non-invasive early detection.

MiRNAs are endogenous, small, non-coding RNA of 19 to 25 nucleotides that regulates gene expression by binding to the 3 untranslated region of target gene mRNA (7), have been demonstrated to regulate the development of many cancers by acting as tumor suppressor or oncogene in previous studies (8). MiRNAs have remarkable stability in solid and liquid specimens, so they can serve as a potential non-invasive biomarker (9), and offer a non-invasive opportunity for early diagnosis of cancer. Abnormal expression of miRNAs have been reported in the occurrence and development of NPC, such as MiR-34c, MiR124, miR-140-3p, miR-144-3p, miR-17-5p, miR-20a-5p, miR-20b-5p, and miR-205-5p (10–12). A recent study found that miR-18a was up-regulated in NPC samples, playing a role in the occurrence and development of nasopharyngeal carcinoma, and antagomir-18a might eventually be used in the treatment of NPC (13). Another study reported that miR-18a could promote proliferation of nasopharyngeal carcinoma cells by targeting miRNA processing enzyme DICER112 (14). However, the expression pattern of miR-18a-3p has not been investigated in nasopharyngeal carcinoma.

Platelets are multi-functional cell fragments best known as the cellular mediator of thrombosis. Platelets assist in sensing pathogens entering the blood stream, signaling to immune cells, releasing vascular remodeling factors, and negatively enhancing cancer metastasis. Platelets also contain a rich repertoire of RNA species, which is related to tumor biology and metastasis (15). The components in platelets can be affected by the specialized surrounding microenvironment, including tumor cells. Tumor cells appear to initiate intraplatelet signaling, resulting in splicing of platelet pre-mRNAs and enhance secretion of cytokines (15). In addition, platelet RNA appears to be dynamically affected by pathological conditions (15). It has been demonstrated that tumor cells influence platelet RNA through different mechanisms, resulting in tumor-specific RNA profiles (16). Tumor-educated platelet (TEP) RNA is involved in the progression and spread of several solid tumors, including lung, brain and breast cancer. Therefore, TEP RNA may serve as a liquid-biopsy biomarker in early diagnosis and monitoring treatment efficacy of cancer (17).

In this study, we investigated the expression levels of TEP miR-18a-3p in NPC patients and aimed to explore the value of TEP miR-18a-3p in early diagnosis and chemotherapy efficacy monitoring for NPC.

MATERIALS AND METHODS

Study Design

All samples were collected at Cancer Center, Union Hospital, Tongji Medical College, Huazhong University of Science and Technology and Zhongnan Hospital of Wuhan University from 2017 to 2019. The study was approved by the Ethics Committee of Wuhan Union Hospital, Tongji Medical College, Huazhong University of Science and Technology and the Medical Ethical Committee of Zhongnan Hospital of Wuhan University. Written informed consent was obtained from all participants. 57 NPC patients and 36 healthy donors participated in this study. 54 patients had one sample taken before any treatment to assess the diagnostic value of TEP miR-18a-3p for NPC. For the remaining 3 patients, samples were collected before and after each dose of chemotherapy to monitor dynamic change of TEP miR-18a-3p during treatment. All patients were pathologically confirmed NPC cases. The clinical and histopathological features of each participant, such as sex, age, TNM stage, history of EBV infection and pathological type, were recorded in detail.

Sample Collection

Whole blood samples (3 mL) were taken from each participant and collected into test tubes containing EDTA-K_2. The blood samples were centrifuged at 120 g for 20 minutes at room temperature and the upper layer rich in platelets (about 900 μL) were collected. The platelets were precipitated by centrifugation at 360 g for 20min at room temperature, the supernatant was plasma. Pipetting 300 μL of plasma from the supernatant into a new centrifuge tube, then discarding the remaining plasma, the precipitates were platelets. The platelets were washed twice by phosphate buffer saline. A high purity platelet preparation was determined by a ratio of < 5 karyocytes per 10^7 platelets (18). After centrifugation, platelets and plasma were added with 500 μL RNA lysate (a reagent that lysed cells and inactivated RNase included in a Liquid Total RNA Isolation Kit) and mixed for 5 minutes, respectively, then stored in -80°C refrigerator ready for RNA extraction and amplification.

RNA Extraction and Relative Real-Time Quantitative PCR (qPCR) Analysis

The total RNA was extracted from platelets or plasma using a Liquid Total RNA Isolation Kit (RP4002, BioTeke, Beijing, China). The quantity and quality of RNAs were determined by Nanodrop 2000 spectrophotometer and analyzed by an agarose gel electrophoresis. In total, 1 μg of RNAs were used for cDNA synthesis using a PrimeScript™ RT reagent Kit with gDNA

Eraser (RR047A, TAKARA, Dalian, China). The qPCR was performed using iQ™ SYBR® Green Supermix (BIO-RAD, CA, USA) on a BIO-RAD CFX96 system. The U6 was used as the internal amplification control. The primers used for amplification of miR-18a-3p and U6 are listed in **Table 1**. The URP was universal amplification primer, which was used in pairs with miR-18a-3p-S. The relative expression levels of miRNAs were calculated by $2^{-\triangle CT}$ method; while $\triangle CT = CT_{miR18a\text{-}3p} - CT_{U6}$. EBV DNA levels were determined using EB viral nucleic acid quantitative fluorescent probe PCR assay (Shengxiang Biotechnology, Hunan, China) on the Stratagene Mx3000P system (Agilent Technologies, CA, USA) at Department of Laboratory Medicine of Union Hospital.

Data Analysis

SPSS21.0 software was used for statistical analysis. MedCalc statistical software was used for ROC analysis. Mann-Whitney U test was used to compare the expression of miR-18a-3p in NPC and healthy donors, and subtypes of different TNM stages. The expression levels of miR-18a-3p were showed as (median, (lower quartiles, upper quartiles)). Independent sample t-test and Fisher' exact test were used to determine the correlation between the expression level of miR-18a-3p and the clinical parameters of the subjects. The positive rates of miR-18a-3p and EBV DNA in the diagnosis of NPC were compared by McNemar and Kappa test. A two-sided test was performed in all statistical analyses. Statistically, significant difference was set at $p < 0.05$.

RESULT

Relative Expression Levels of miR-18a-3p in Platelet and Plasma of NPC Patients and Healthy Controls

The expression levels of TEP miR-18a-3p in NPC patients [0.0914 (0.0519, 0.2155)] were significantly higher than that in healthy controls [0.0300 (0.0162, 0.0607)] ($p < 0.0001$, **Figure 1**). However, there was no significant difference in the expression levels of miR-18a-3p in plasma between the two groups ($p = 0.368$, **Figure 1**).

Evaluation of the Diagnostic Value of miR-18a-3p in NPC

ROC curve analysis was used to evaluate the diagnostic value of TEP miR-18a-3p in NPC. The area under the curve (AUC) value was 0.841 (95% CI: 0.747~0.910), Youden index was 0.5976 and the criterion was > 0.0357. The sensitivity and specificity for the diagnosis of NPC were 87% and 72.7%, respectively (**Figure 2**).

Correlations Between the Expression Levels of TEP miR-18a-3p and the Clinical Parameters of NPC

We further investigated the relationship between TEP miR-18a-3p and NPC patients' clinical parameters and their TNM stages. NPC patients were divided into high-expression group and low-expression group according to the cut-off point (0.0357) of miR-18a-3p in the Youden index analysis. The results showed that 87% (47 of 54) of the patients had high miR-18a-3p expression, but there was no significant difference in age (p=0.392, **Table 2**), gender (p=0.226, **Table 2**), hypertension (p=0.576, **Table 2**), diabetes (p>0.999, **Table 2**), Nasopharyngitis (p=0.322, **Table 2**), smoking (p>0.999, **Table 2**), alcohol drinking (p>0.999, **Table 2**), degree of differentiation (p=0.436, **Table 2**), TNM stage (p=0.806, 0.416, 0.58, respectively, **Table 2**) and EBV-DNA copies (p=0.392, **Table 2**). However, the positive rate of miR-18a-3p (85.4%) was higher than that of EBV-DNA (66.7%). Statistical analysis showed that there was no significant difference in the expression levels of miR-18a-3p among different TNM stages of NPC (p>0.05, **Figure 3** and **Table 3**).

Clinical Value of TEP miR-18a-3p in Monitoring the Efficacy of Chemotherapy for NPC

We followed up and investigated the levels of TEP miR-18a-3p of 3 NPC patients. Each patients accepted 3 times of chemotherapy, and the chemotherapy schemes of 3 patients were paclitaxel combined with cisplatin, gemcitabine combined with cisplatin, gemcitabine combined with cisplatin, respectively. TEP miR-18a-3p levels were detected before and after every chemotherapy, respectively. EBV DNA copies were obtained from the electronic medical record system according to the corresponding time. TEP miR-18a-3p expression were down-regulated after 77.8% (7 of 9) of chemotherapy, in 66.7% (2 of 3) of patients, TEP miR-18a-3p levels decreased after 3 cycles of chemotherapy. (**Figure 4**). Simultaneously, EBV DNA copies decreased after 83.3% (5 of 6) of chemotherapy, and 100% of the patents' EBV DNA copies were decreased after 3 cycles of chemotherapy (**Figure 4**). The dynamic changes of TEP miR-18a-3p and EBV DNA with chemotherapy were roughly the same.

TABLE 1 | Primers used for cDNA synthesis and real-time PCR.

Primers	Sequence (5'~3')
miR-18a-3p-S	ACACTCCAGCTGGGACTGCCCTAAGTGCTCC
miR-18a-3p-RT*	CTCAACTGGTGTCGTGGAGTCGGCAATTCAGTTGAGCCAGAAGG
URP	TGGTGTCGTGGAGTCG
U6-F	CTCGCTTCGGCAGCACA
U6-RT*	AACGCTTCACGAATTTGCGT

**cDNA synthesis primers.*

DISCUSSION

MicroRNAs are short non-coding single-stranded RNA that regulates gene expression by binding to complementary sequences in 3 or 5 untranslated region of target gene mRNA. Some studies have reported that MicroRNAs may play an important role in the pathogenesis of various human cancers (19). MicroRNAs can induce abnormal metabolism of tumor cells by affecting the process of transcription and translation of tumor cells. High expression of MiRNAs can lead to abnormal

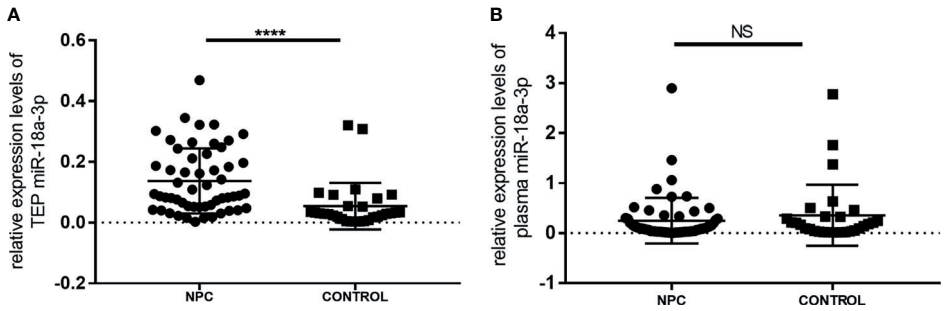

FIGURE 1 | Relative expression levels of miR-18a-3p in platelet and plasma of NPC patients and healthy controls. **(A)** The expression levels of TEP miR-18a-3p in NPC patients were significantly higher than that in healthy controls. **(B)** There was no significant difference of plasma miR-18a-3p levels between NPC and control groups. Mann–Whitney U test was used for analysis. ****$p < 0.0001$. NS, no significance.

proliferation and migration of tumor cells and induce cancer, but in other cases, the role of miRNAs may be tumor inhibition (20). MicroRNA expression profiles show that they are related to development, progression and response of tumor to therapy, suggesting that they have a great potential to be considered as diagnostic, predictive and prognostic biomarkers of tumor (7, 8).

Nasal endoscopy and clinical imaging examination are the main methods to diagnose NPC. Biopsy samples are obtained for pathological diagnosis, when no tumor is visible and the suspect index is high, blind or radiology-guided targeted biopsy will be performed. However, benign condition-like tuberculosis of the nasopharynx can also present with a similar range of symptoms, In addition, it is difficult to detect distant metastasis by computed tomography (CT) and magnetic resonance imaging (MRI) at early stage, especially when the diameter of the lesion is less than 5 mm, which will delay the detection of the tumor. At the same time, PET-CT/CT are unaffordable for most patients, especially in underdeveloped and developing countries. Nasopharyngeal tissue biopsy is the gold standard for the diagnosis of NPC, but it is invasive, which may cause some unanticipated complications in the patients at high risk, or it can only be only be effective in the middle to late stages of NPC. At this time, the effect of related treatment is not good enough (1, 21). Radiotherapy and chemotherapy remains the mainstay of primary treatment for NPC, but there are not many biomarkers used for treatment efficacy monitoring. Plasma EBV DNA is a commonly used biomarker, however, it is not applicable to NPC patients without EBV infection. Therefore, it is of great significance to find effective, non-invasive biomarkers for early diagnosis and chemotherapy efficacy monitoring in NPC.

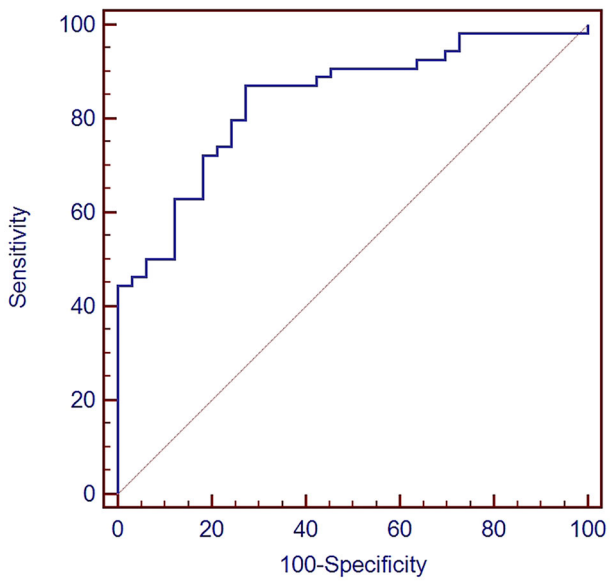

FIGURE 2 | ROC of miR-18a-3p in TEP for NPC.

Circulating tumor cells (CTCs), cell-free nucleotides, exosomes and TEPs are different sources of liquid biopsy for tumor-associated biomarkers and they play different roles in clinical application (22). Platelets are implicated in tumor biology and metastasis and can be changed on RNA and protein content by tumor cells (16, 18, 23, 24). Platelets contain a rich repertoire of RNA species and more than 500 different miRNAs have been detected in human platelets (25). Besides releasing factors, platelets can also sequester RNAs and proteins released by cancer cells. Thus, platelets actively respond to queues from local and systemic conditions, thereby altering their transcriptome and molecular content (15).We screened several RNAs that have been reported to be altered in NPC and found that the expression levels of TEP miR-18a-3p in NPC patients were significantly higher than that in normal subjects, but there were no significant difference in plasma miR-18a-3p expression levels. These data suggest that platelets may interact with tumor cells directly *via* different receptors or indirectly *via* different signaling molecules and lead to platelets RNA content changes. On the other hand, platelets may absorb and enrich miR-18a-3p released by tumor cells, therefore no difference was found between NPC patients and healthy donors in plasma. In addition, we followed-up 5 NPC patients (2 of the patients were

TABLE 2 | Correlations between expression levels of TEP miR-18a-3p and clinical parameters of NPC.

Clinical parameters	N	TEP miR-18a-3p			*p*-value
		Low	High	High%	
Age	54	45.85 ± 9.83 n=7	49.55 ± 10.67 n=47	–	0.392[b]
Gender					
Male	35	3	32	91.4	0.226
Female	19	4	15	78.9	
Hypertension	8	0	8	100	0.576
Diabetes	6	1	5	83.3	>0.999
Nasopharyngitis	11	0	11	100	0.322
Smoking	12	1	11	91.7	>0.999
Alcohol drinking	6	0	6	100	>0.999
Tumor type					
Undifferentiated	50	6	44	88.0	0.436
Differentiated	4	1	3	75.0	
T classification					
T1	2	0	2	100.0	0.806
T2	11	1	10	90.0	
T3	15	2	13	86.7	
T4	17	1	16	94.1	
Lymph node status					
N0~N1	12	0	12	100.0	0.416
N2	22	3	19	86.4	
N3	9	1	8	88.9	
Metastatic status					
M0	43	4	39	90.7	0.580
M1	3	0	3	100.0	
EBV DNA					
Negative	16	2	14	87.5	0.064[a]
Positive	32	5	27	84.4	

Positive rate of TEP miR-18a-3p: 85.4%.
Positive rate of EBV DNA: 66.7%.
[a]*McNemar and Kappa tests,* [b]*independent-samples t-test, all others are Fisher test.*

excluded) and found that TEP miR-18a-3p expression were down-regulated after 77.8% of chemotherapy, in 66.7% of patients, TEP miR-18a-3p levels decreased after 3 cycles of chemotherapy. The chemotherapy schemes included paclitaxel combined with cisplatin, gemcitabine combined with cisplatin. Suzuki reported that inhibition of miR-18a-3p reduced proliferation of mesothelioma cells and sensitizes them to cisplatin (19), Rodriguez-Aguayo reported that miR-18a-3p was related to chemotherapy-resistant ovarian cancer (26). Their findings are similar to our study and support our conclusions. Plasma load of EBV DNA has been shown to be of prognostic value (27). EBV DNA copies decreased after 83.3% of chemotherapy and all the patents' EBV DNA copies decreased after 3 cycles of chemotherapy, indicated that the treatments were effective. The dynamic changes of TEP miR-18a-3p are almost synchronized with EBV DNA copies, demonstrating the potential of TEP miR-18a-3p as an indicator of chemotherapy efficacy monitoring in NPC.

We used RT-qPCR to detect expression levels of TEP miR-18a-3p. Previous studies have demonstrated that none of the commonly used reference genes for normalization are universal for all tissue types or experimental situations (28–30). Platelet RNAs have a small amount and no reliable endogenous control miRNA has been identified in studying platelets miRNAs, U6 RNA is still the most common choice. We determined quantity and quality of RNAs and guaranteed 1 ug of RNAs were used for reverse transcription. To make the results reliable, the U6 RNA was set up as internal reference gene, and Ct value of U6 RNAs were differ within 1. TEP miR-18a-3p has certain sensitivity, specificity and accuracy in the diagnosis of NPC, and can reflect whether the chemotherapy is effective in a certain extent. These results indicate that TEP miR-18a-3p is a sensitive novel liquid-biopsy biomarker for early diagnosis and chemotherapy efficacy monitoring in NPC. However, TEP miR-18a-3p shows no difference in each TNM stage and other clinical parameters, this may be due to the small sample size, and the results can only be preliminary at this stage. Platelets are rich in peripheral blood and easy to obtained, detecting TEP RNA is convenience, economical, and non-invasive to patients. In addition, platelets have no nucleus so detecting platelets RNA can reduce interference from their own genome. Our assay is also easily applicable to clinical and automation applications since RT-qPCR is a very mature detection technology. Of course, this study has some limitations. The sample size for dynamic monitoring is small, and we only monitored the efficacy of chemotherapy, the efficacy of radiotherapy was not evaluated.

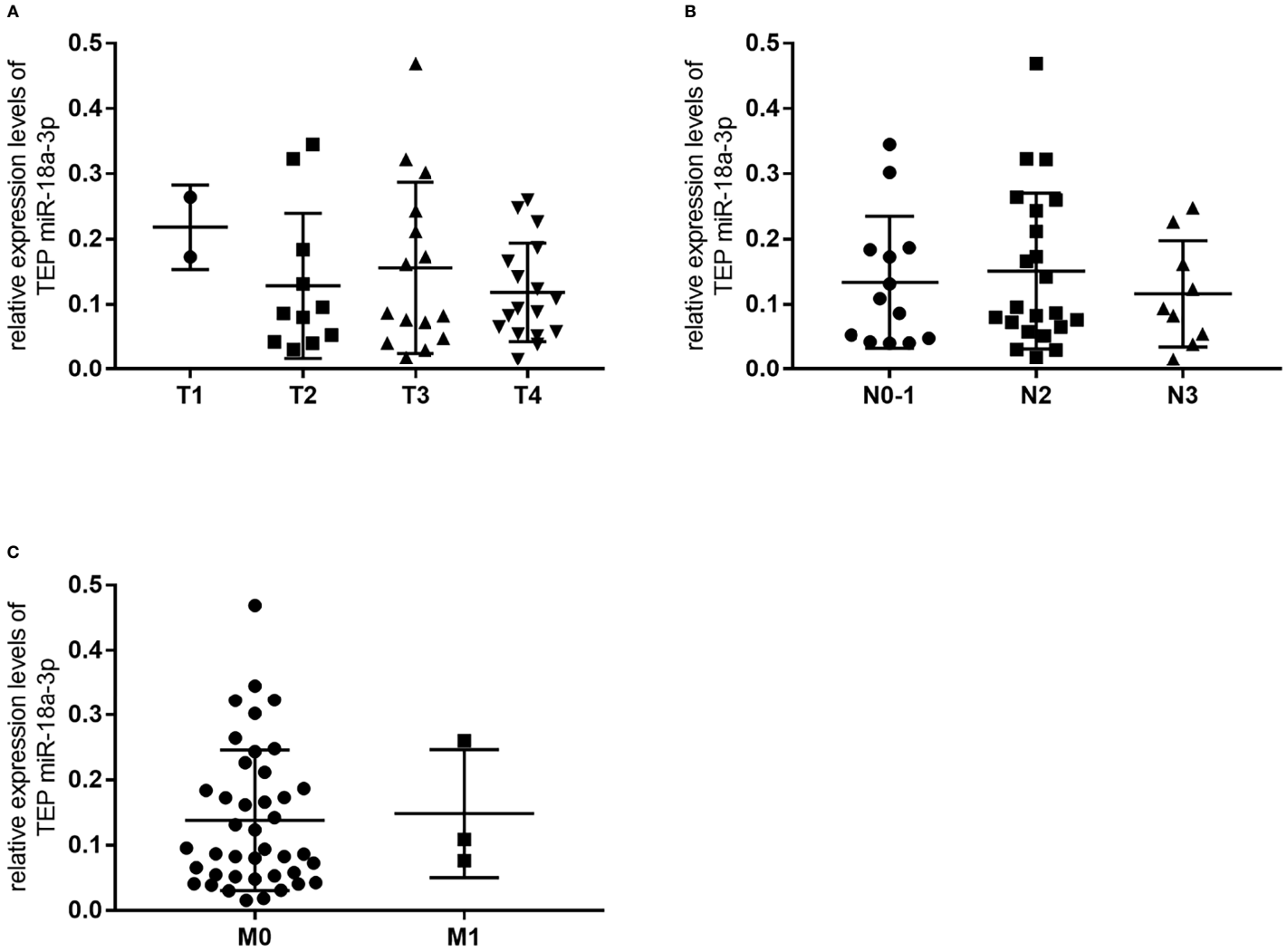

FIGURE 3 | There was no significant change in relative expression levels of TEP miR-18a-3p among different TNM stages of NPC. **(A)** Relative expression levels of TEP miR-18a-3p in T1-T4 stages; **(B)** Relative expression levels of TEP miR-18a-3p in N0~1, N2, and N3 stages; **(C)** Relative expression levels of TEP miR-18a-3p in M0 and M1 stages. Mann–Whitney U test was used for analysis.

TABLE 3 | The *p* values of comparing relative expression levels of TEP miR-18a-3p among groups with different TNM stages of NPC.

	T1-T2	T1-T3	T1-T4	T2-T3	T2-T4	T3-T4	N0~1-N2	N0~1-N3	N2-N3	M0-M1
miR-18a-3p	0.31	0.44	0.11	0.84	0.82	0.74	0.77	0.74	0.56	0.66

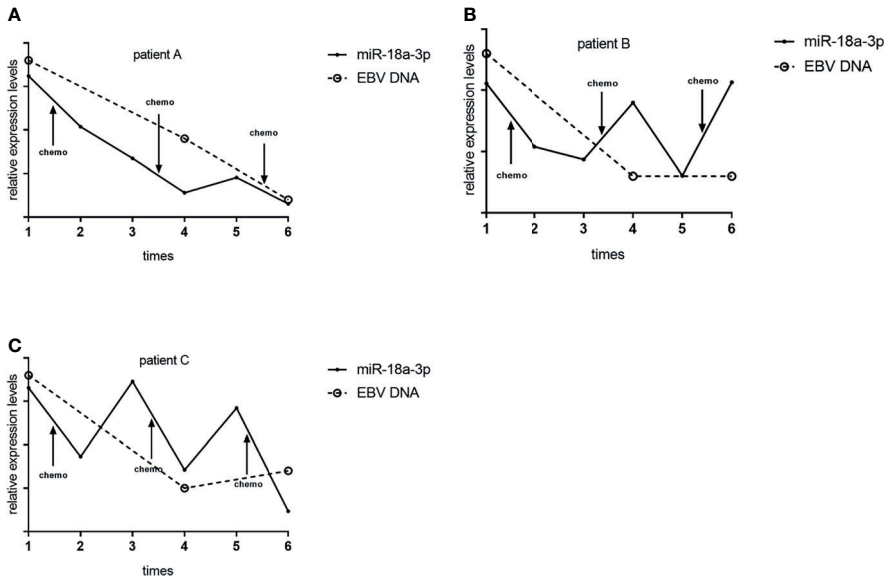

FIGURE 4 | Dynamic changes of TEP miR-18a-3p and EBV DNA with chemotherapy. **(A)** Dynamic changes of TEP miR-18a-3p and EBV DNA with chemotherapy of patient **(A, B)** Dynamic changes of TEP miR-18a-3p and EBV DNA with chemotherapy of patient **(B, C)** Dynamic changes of TEP miR-18a-3p and EBV DNA with chemotherapy of patient **(C)** chemo, chemotherapy.

These work will be completed in our follow-up research. A diagnostic consisting of more than a single miRNA might strengthen the overall approach. In general, this study found that TEP miR-18a-3p were upregulated in NPC and had a high probability to downregulated after chemotherapy. Our data suggest that TEP miR-18a-3p can potentially serve as an essential, non-invasive biomarker for early diagnosis and chemotherapy efficacy monitoring in NPC.

DATA AVAILABILITY STATEMENT

The raw data supporting the conclusions of this article will be made available by the authors, without undue reservation.

ETHICS STATEMENT

The studies involving human participants were reviewed and approved by The Ethics Committee of Wuhan Union Hospital, Tongji Medical College, Huazhong University of Science and Technology The Medical Ethical Committee of Zhongnan Hospital of Wuhan University. The patients/participants provided their written informed consent to participate in this study.

AUTHOR CONTRIBUTIONS

Conception and design: JF, KS, and HW. Development and methodology: KS, HW, XX, XW, JS, and KZ. Acquisition of data: KS, HW, and XX. Analysis and interpretation of data: KS, HW, and XW. Preparation of the paper: JF, KS, and HW.

Study supervision: JF and HW. All authors contributed to the article and approved the submitted version.

FUNDING

This work was supported by Health commission of Hubei Province scientific research project (No. WJ2019H042) to JF and Health Commission of Hubei Province scientific research project (No. WJ2019M158) to HW.

ACKNOWLEDGMENTS

We are very grateful to Dr Fubin Wang at the Department of Laboratory Medicine, Zhongnan Hospital, Wuhan University for his kind assistance in analyzing imaging data.

REFERENCES

1. Chua MLK, Wee JTS, Hui EP, Chan ATC. Nasopharyngeal Carcinoma. *Lancet* (2016) 387(10022):1012–24. doi: 10.1016/s0140-6736(15)00055-0
2. Tang LL, Chen WQ, Xue WQ, He YQ, Zheng RS, Zeng YX, et al. Global Trends in Incidence and Mortality of Nasopharyngeal Carcinoma. *Cancer Lett* (2016) 374(1):22–30. doi: 10.1016/j.canlet.2016.01.040
3. Chen Y-P, Chan ATC, Le Q-T, Blanchard P, Sun Y, Ma J. Nasopharyngeal Carcinoma. *Lancet* (2019) 394(10192):64–80. doi: 10.1016/s0140-6736(19)30956-0
4. Jiang P, Du W, Yang X. P53 and Regulation of Tumor Metabolism. *J Carcinog* (2013) 12:21–. doi: 10.4103/1477-3163.122760
5. Lee HM, Okuda KS, Gonzalez FE, Patel V. Current Perspectives on Nasopharyngeal Carcinoma. *Adv Exp Med Biol* (2019) 1164:11–34. doi: 10.1007/978-3-030-22254-3_2
6. Brigette BY, Ma ATCC. Systemic Treatment Strategies and Therapeutic Monitoring for Advanced Nasopharyngeal Carcinoma. *Expert Rev Anticancer Ther* (2006) 6(3):383–94. doi: 10.1586/14737140.6.3.383
7. Lu TX, Rothenberg ME. MicroRNA. *J Allergy Clin Immunol* (2018) 141(4):1202–7. doi: 10.1016/j.jaci.2017.08.034
8. Iorio MV, Croce CM. MicroRNA Dysregulation in Cancer: Diagnostics, Monitoring and Therapeutics. A Comprehensive Review. *EMBO Mol Med* (2012) 4(3):143–59. doi: 10.1002/emmm.201100209
9. Gustafson D, Tyryshkin K, Renwick N. microRNA-Guided Diagnostics in Clinical Samples. *Best Pract Res Clin Endocrinol Metab* (2016) 30(5):563–75. doi: 10.1016/j.beem.2016.07.002
10. Li YQ, Ren XY, He QM, Xu YF, Tang XR, Sun Y, et al. MiR-34c Suppresses Tumor Growth and Metastasis in Nasopharyngeal Carcinoma by Targeting MET. *Cell Death Dis* (2015) 6(1):e1618–e. doi: 10.1038/cddis.2014.582
11. Peng XH, H HR, Lu J, Liu X, Zhao FP, Zhang B, et al. MiR-124 Suppresses Tumor Growth and Metastasis by Targeting Foxq1 in Nasopharyngeal Carcinoma. *Mol Cancer* (2014) 13:13-186. doi: 10.1186/1476-4598-13-186
12. Zhang H, Zou X, Wu L, Zhang S, Wang T, Liu P, et al. Identification of a 7-microRNA Signature in Plasma as Promising Biomarker for Nasopharyngeal Carcinoma Detection. *Cancer Med* (2020) 9(3):1230–41. doi: 10.1002/cam4.2676
13. Mai S, Xiao R, Shi L, Zhou X, Yang T, Zhang M, et al. MicroRNA-18a Promotes Cancer Progression Through SMG1 Suppression and mTOR Pathway Activation in Nasopharyngeal Carcinoma. *Cell Death Dis* (2019) 10(11):819. doi: 10.1038/s41419-019-2060-9
14. Xi Chen JW, Cheng L, Lu M-P. miR-18a Down Regulates DICER1 and Promotes Proliferation and Metastasis of Nasopharyngeal Carcinoma. *Int J Clin Exp Med* (2014) 7(4):847–55.
15. Best MG, Vancura A, Wurdinger T. Platelet RNA as a Circulating Biomarker Trove for Cancer Diagnostics. *J Thromb Haemostasis JTH* (2017) 15(7):1295–306. doi: 10.1111/jth.13720
16. Sol N, Wurdinger T. Platelet RNA Signatures for the Detection of Cancer. *Cancer Metastasis Rev* (2017) 36(2):263–72. doi: 10.1007/s10555-017-9674-0
17. Best MG, Wesseling P, Wurdinger T. Tumor-Educated Platelets as a Noninvasive Biomarker Source for Cancer Detection and Progression Monitoring. *Cancer Res* (2018) 78(13):3407–12. doi: 10.1158/0008-5472.CAN-18-0887
18. Best MG, Sol N, Kooi I, Tannous J, Westerman BA, Rustenburg F, et al. RNA-Seq of Tumor-Educated Platelets Enables Blood-Based Pan-Cancer, Multiclass, and Molecular Pathway Cancer Diagnostics. *Cancer Cell* (2015) 28(5):666–76. doi: 10.1016/j.ccell.2015.09.018
19. Suzuki R, Amatya VJ, Kushitani K, Kai Y, Kambara T, Fujii Y, et al. Inhibition of miR-18a-3p Reduces Proliferation of Mesothelioma Cells and Sensitizes Them to Cisplatin. *Oncol Lett* (2020) 19(6):4161–8. doi: 10.3892/ol.2020.11504
20. Yi SJ, Liu P, Chen BL, Ou-Yang L, Xiong WM, Su JP. Circulating miR-31-5p may be a Potential Diagnostic Biomarker in Nasopharyngeal Carcinoma. *Neoplasma* (2019) 66(5):825–9. doi: 10.4149/neo_2018_181109N847
21. Peng H, Li Z, Long Y, Li J, Liu Z, Zhou R. Clinical Value of a Plasma Epstein-Barr Virus DNA Assay in the Diagnosis of Recurrent or Metastatic Nasopharyngeal Carcinoma: A Meta-Analysis. *Biosci Rep* (2019) 39(9):BSR20190691. doi: 10.1042/BSR20190691
22. Joosse SA, Pantel K. Tumor-Educated Platelets as Liquid Biopsy in Cancer Patients. *Cancer Cell* (2015) 28(5):552–4. doi: 10.1016/j.ccell.2015.10.007
23. Nilsson RJ, Balaj L, Hulleman E, van Rijn S, Pegtel DM, Walraven M, et al. Blood Platelets Contain Tumor-Derived RNA Biomarkers. *Blood* (2011) 118(13):3680–3. doi: 10.1182/blood-2011-03-344408
24. Calverley DC, Phang TL, Choudhury QG, Gao B, Oton AB, Weyant MJ, et al. Significant Downregulation of Platelet Gene Expression in Metastatic Lung Cancer. *Clin Trans Sci* (2010) 3(5):227–32. doi: 10.1111/j.1752-8062.2010.00226.x
25. Landry P, Plante I, Ouellet DL, Perron MP, Rousseau G, Provost P. Existence of a microRNA Pathway in Anucleate Platelets. *Nat Struct Mol Biol* (2009) 16(9):961–6. doi: 10.1038/nsmb.1651
26. Rodriguez-Aguayo C, Monroig PDC, Redis RS, Bayraktar E, Almeida MI, Ivan C, et al. Regulation of Hnrnpa1 by microRNAs Controls the miR-18a-K-RAS Axis in Chemotherapy-Resistant Ovarian Cancer. *Cell Discov* (2017) 3:17029. doi: 10.1038/celldisc.2017.29
27. Chan AT, Gregoire V, Lefebvre JL, Licitra L, Hui EP, Leung SF, et al. Nasopharyngeal Cancer: EHNS-ESMO-ESTRO Clinical Practice Guidelines for Diagnosis, Treatment and Follow-Up. *Ann Oncol Off J Eur Soc Med Oncol* (2012) 23 Suppl 7:vii83–5. doi: 10.1093/annonc/mds266
28. Vandesompele J, De Preter K, Pattyn F, Poppe B, Van Roy N, De Paepe A, et al. Accurate Normalization of Real-Time Quantitative RT-PCR Data by Geometric Averaging of Multiple Internal Control Genes. *Genome Biol* (2002) 3(7):RESEARCH0034. doi: 10.1186/gb-2002-3-7-research0034
29. Song J, Bai Z, Han W, Zhang J, Meng H, Bi J, et al. Identification of Suitable Reference Genes for qPCR Analysis of Serum microRNA in Gastric Cancer Patients. *Dig Dis Sci* (2012) 57(4):897–904. doi: 10.1007/s10620-011-1981-7
30. Dong L, Sui C, Liu Y, Yang Y, Wei J, Yang Y. Validation and Application of Reference Genes for Quantitative Gene Expression Analyses in Various Tissues of Bupleurum Chinense. *Mol Biol Rep* (2011) 38(8):5017–23. doi: 10.1007/s11033-010-0648-3

Conflict of Interest: The authors declare that the research was conducted in the absence of any commercial or financial relationships that could be construed as a potential conflict of interest.

Publisher's Note: All claims expressed in this article are solely those of the authors and do not necessarily represent those of their affiliated organizations, or those of the publisher, the editors and the reviewers. Any product that may be evaluated in this article, or claim that may be made by its manufacturer, is not guaranteed or endorsed by the publisher.

Copyright © 2021 Sun, Wang, Xu, Wei, Su, Zhu and Fan. This is an open-access article distributed under the terms of the Creative Commons Attribution License (CC BY). The use, distribution or reproduction in other forums is permitted, provided the original author(s) and the copyright owner(s) are credited and that the original publication in this journal is cited, in accordance with accepted academic practice. No use, distribution or reproduction is permitted which does not comply with these terms.

frontiers in Oncology

CASE REPORT
published: 27 October 2021
doi: 10.3389/fonc.2021.737730

Pilocytic Astrocytoma-Derived Cells in Peripheral Blood: A Case Report

*Giorgio Volpentesta[1], Giuseppe Donato[2], Elisabetta Ferraro[3], Chiara Mignogna[2], Riccardo Radaelli[1], Umberto Sabatini[4], Domenico La Torre[1] and Natalia Malara[5]**

[1] Department of Medical and Surgical Sciences, University "Magna Græcia", Catanzaro, Italy, [2] Department of Health Sciences, University Magna Græcia, Catanzaro, Italy, [3] Department of Biology, University of Pisa, Pisa, Italy, [4] Department of Medical and Surgical Sciences, University Magna Græcia, Catanzaro, Italy, [5] Department of Experimental and Clinical Medicine, University Magna Græcia, Catanzaro, Italy

Imaging limitations, invasive tissue biopsies and poor information over the course of treatment to evaluate 'real-time' tumor dynamics justify the emerging use of liquid biopsies in the field of brain tumors. Circulating tumor cells (CTCs) from high-grade astrocytomas might reach the circulation by crossing the blood–brain barrier. Here, for the first time, CTCs cytology in a case of pylocitic astrocytoma is described. An obstructive hydrocephalous due to a lateral mesencephalic tectum mass occluding the Silvio Aqueduct was diagnosed in a young, 18 years old, male. Considering the location of the tumor and the rapid deterioration of the neurological status, it has been decided to urgency treat the patient with ventriculoperitoneal shunting. Magnetic resonance imaging showed a nodular shaped lesion localized within the left lateral mesencephalic tectum. Stereotactic biopsy was not approachable due significant risk of neurological consequences. The diagnosis was performed by blood sampling, a non-invasive procedure for the patient, in order to provide tumor information. Cytopathological features on detected circulating atypical GFAP positive cells led to pilocytic diagnosis confirmed by the patient's 68 months outcome.

Keywords: pilocytic astrocytoma, diagnostic liquid biopsy, brain tumors, circulating glial cells, blood brain barrier

OPEN ACCESS

Edited by:
Catherine Alix-Panabieres, Centre Hospitalier Universitaire de Montpellier, France

Reviewed by:
Talib Hassan Ali, University of ThiQar, Iraq
Tiago Goss Dos Santos, A.C.Camargo Cancer Center, Brazil

****Correspondence:***
Natalia Malara
nataliamalara@unicz.it

Specialty section:
This article was submitted to Molecular and Cellular Oncology, a section of the journal Frontiers in Oncology

Received: *07 July 2021*
Accepted: *28 September 2021*
Published: *27 October 2021*

Citation:
Volpentesta G, Donato G, Ferraro E, Mignogna C, Radaelli R, Sabatini U, La Torre D and Malara N (2021) Pilocytic Astrocytoma-Derived Cells in Peripheral Blood: A Case Report. Front. Oncol. 11:737730. doi: 10.3389/fonc.2021.737730

INTRODUCTION

A dramatic improvement in every aspect of intracranial tumors management has occurred in the last two decades. Nevertheless, the combined analysis of clinical signs, symptoms, and magnetic resonance imaging (MRI) and computed tomography (CT)-scan findings is not always diriment to perform a diagnosis, and brain biopsy is required. Many authors have reported significant post-operative complications rate associated to the biopsy procedure (1, 2). A personalized risk assessment for each patient must be evaluated. The negative selection criteria for brain biopsy

Abbreviations: MRI, Magnetic resonance imaging; CT, Computed tomography; CTCs, Circulating tumor cells; STB, Stereotactic biopsy; H-MRS, Proton magnetic resonance spectroscopy; NAA, N-acetylaspartate; PWI, Perfusion-weighted imaging; CBV, Cerebral blood volume; CNS, Central nervous system; CSF, Cerebrospinal fluid; FLAIR, Fluid attenuation inversion recovery; H&E, Hematoxylin and eosin; GFAP, Glial fibrillary acidic protein; BBB, Blood-brain-barrier.

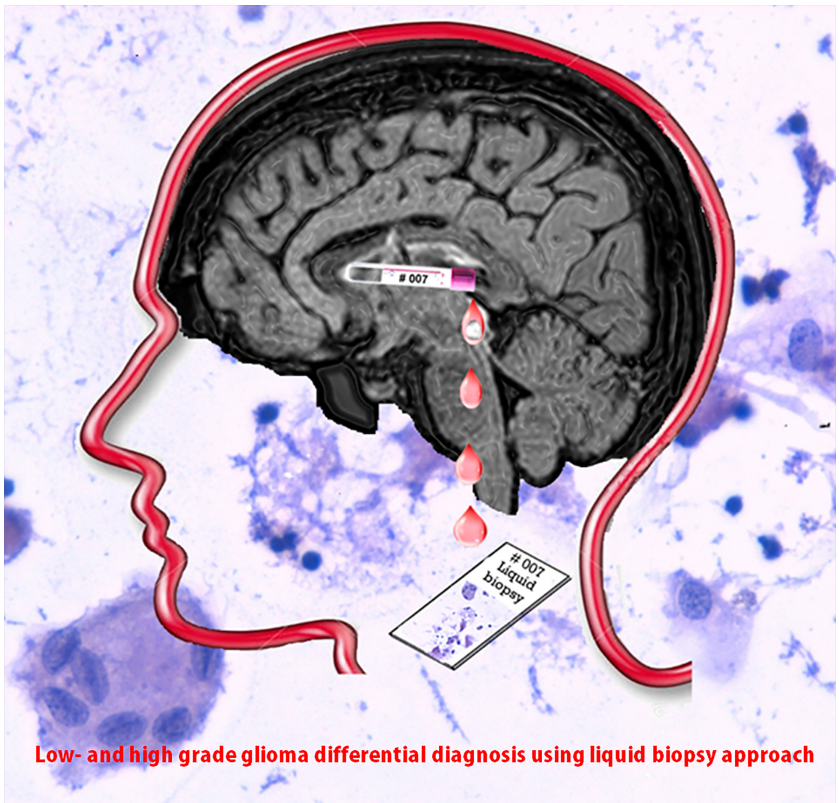

GRAPHICAL ABSTRACT

comprises the lesions located in an eloquent or deep-seated area, like brainstem. As a rule, biopsy is avoided in young adult patient with "diffuse" brainstem glioma (3). Brainstem gliomas account for approximately 10–20% of Central Nervous System (CNS) child tumors. Brainstem gliomas are categorized according to location and appearance using magnetic resonance. They are classified into two types: low grade (or focal/exophytic) and diffuse intrinsic pontine gliomas. Diffuse tumors are typically infiltrating astrocytomas, which can be grade 2–4 depending on histopathological features, and have a poorer outcomes when compared to focal neoplasms (3). In adult tumor's extension is considered "diffuse" when the lesion is poorly demarcated and is >50% of the brainstem diameter. When the biopsy is performed in the brainstem, a low-grade histology (grade II glioma) is found in up to 80% of cases (4). Occasionally, adult patients can present a rapidly growing tumor similar to the diffuse intrinsic brainstem gliomas, found in paediatric population (4). The classification based on the MRI findings, has been proposed but remains imperfect. Unfortunately, brain stem glioma has an anatomical basis that does not lend itself to easy study. The reason lies in the presence of numerous nuclei of the brain stem essential for the basic functions that alternate with stretches of the white matter. These anatomical features make biopsies and surgery here challenging. These difficulties justify to date also the limited biological knowledge of the pontine lesions of the young adult, compared to those of the child or of the gliobalstoma, identifying them as tumor entities still nosologically in definition.

To increase our knowledge about these tumor entities, characterized by a topographical anatomical dislocation that cannot be reached by conventional biopsy and/or surgical procedures, liquid biopsy represents an alternative and non-invasive strategy. In this field, liquid biopsy is intended as the procedure of isolation and analysis of circulating tumor cells, directly from a single blood sample. We have recently optimized and described an original protocol (5, 6) by which is possible to isolate from a blood sample, and short-time expand, CTCs deriving from different tumor sources included brain primitive neoplasms (7, 8). We have hypothesized that, the short-time expansion of rare circulating non-haematological cells can be useful in order to facilitate the diagnosis, thus avoiding other invasive methods. Therefore, we applied our protocol in this case in which the MRI was unable to identify lesions in the brainstem without a stereotactic biopsy (STB) approach, and the cytological examination of circulating non-haematological cells obtained from the patient blood sample and shortly cultivated led to the final diagnosis- performed by experienced pathologists- of pilocytic astrocytoma.

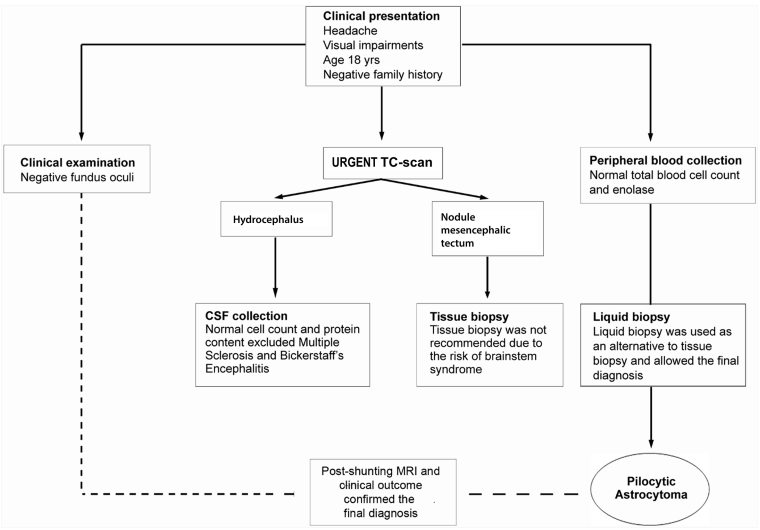

FIGURE 1 | Flow chart of diagnostic work-up. Clinical presentation with headache, visual disturbances, and the intracranial location required differential diagnosis with a wide range of CNS conditions age-related. The patient underwent to clinical examination, instrumental and biochemical analyses. During the hydrocephalus decompression procedure, a sample of CSF fluid was collected. The CSF was clear and the cell count and protein content were normal. Disorders such as multiple sclerosis and Bickerstaff's encephalitis, conceivable for the clinical symptoms and young age, were excluded. The tissue biopsy needed to exclude high-grade glioma, pineocytoma, germinoma or infectious and parasitic diseases was not recommended. Clinicians opted for performing a protocol of short-time culture on chamber slide to obtain cytological preparations from the blood. Pathological evaluation on liquid biopsy cytological specimens suggested the final diagnosis of pilocytic astrocytoma further confirmed by post-shunting MRI and 68 months of clinical outcome.

CASE PRESENTATION

A case of a 18-year-old male student having suffered from headache and visual impairments for about two months is reported. Neurological examination was negative. CT-scan performed in urgency revealed the presence of triventricular hydrocephalus caused by stenosis of the cerebral aqueduct. The most urgent therapeutic goal was mainly the management of the hydrocephalus, therefore a ventricular-peritoneal shunt placement (Medos Hakin-programmable valve) was used to provide an alternative flow pathway for the cerebrospinal fluid. The critical location of the lesion discouraged the STB procedure to obtain histopathological specimens available for the diagnosis. In addition, biochemical analysis of cerebrospinal liquor resulted normal with regard to cell count and protein content. Flow chart adopted in the diagnostic phase is reported in **Figure 1**.

Post-shunting (20 days) MRI showed a significant decrease of the ventricular size. Moreover, the MRI revealed a nodular lesion within the mesencephalic tectum with hypo-intense areas on the T1-weighted images (**Figure 2A**) and hyper intense signals on the T2-weighted sequence (**Figure 2B**). Gadolinium- T1-weighted image showed a low focal enhancement of the lesion in the periaqueductal area which suggested a reduced damage of the blood-brain barrier (**Figure 2C**). Proton magnetic resonance spectroscopy (H-MRS) revealed elevated choline peaks (choline/creatinine ratio at 1,9) in addition to reduced NAA (N-acetylaspartate) (**Figure 2D**). The perfusion-weighted imaging (PWI) of the lesion showed a low value of relative cerebral blood volume (CBV) (**Figure 2E**). The MR signal alteration was non-specific and could suggest, as alternative diagnostic hypothesis to a neoplasm, inflammatory lesions of various types, demyelinating and vascular.

The impossibility, given the mesencephalic location of the lesion, to perform a STB confirms the importance of the information which could be obtained with the cytological observation of peripheral blood CTCs shortly cultured *in vitro* and obtained applying a protocol previously described (6–8).

Biomolecular pathways and cell culture plays a pivotal role in cancer research (9–12). However, culture-induced changes in biological properties of tumor cells might profoundly affect research reproducibility and translational potential (13–15). For this reason, the cytological preparations we used in this diagnostic procedure were prepared with a protocol of short-time *in vitro* expansion, which we have widely shown to maintain phenotypic and genotypic features of CTCs (6–9). The volume of the starting blood sample was 5 ml. Briefly, adensity gradient was applied to the blood sample. The cellular suspension isolated in correspondence of the working density phase (**Figures 3a, b**) was seeded on chamber slides (**Figure 3d**) for a short-time expansion of 14 days. The procedure of expansion had two objectives: i) to unmask rare non-haematological cells with atypical proliferation ability *in vitro* and ii) to highlight rare cells numerically sufficient and viable for further characterization. After 14 days, the adherent cells were fixed and stained for cytological examination (13). The culture density of CTCs in the total cultivated cells was of 1:50. The lower rate of atypical cells in the blood-derived culture suggested finding these elements directly in peripheral blood difficult. In fact, the analysis for

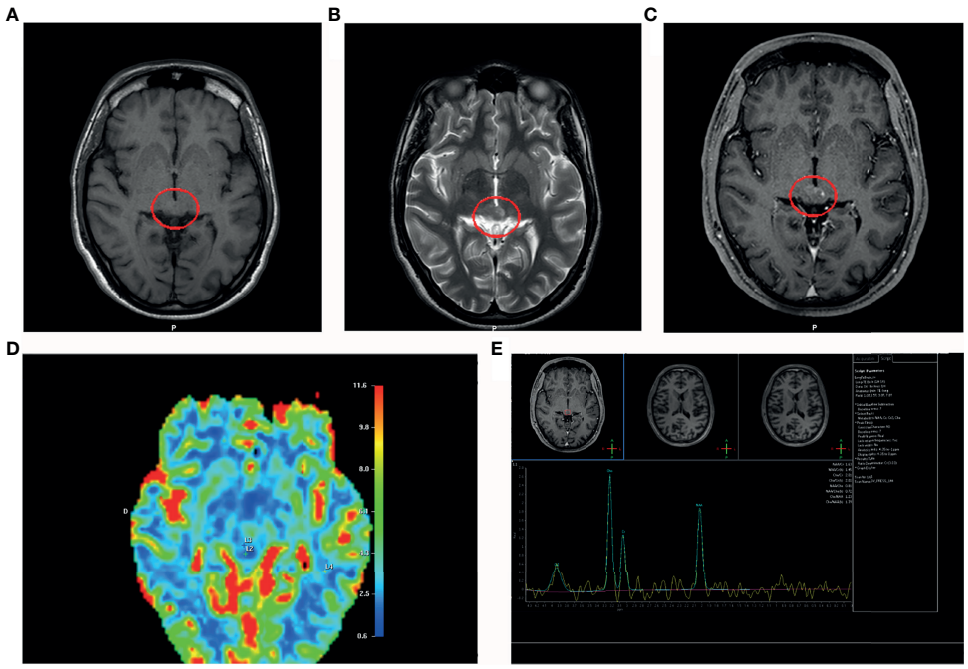

FIGURE 2 | MRI post-shunting (20 days). **(A)** MRI (T1-weighted image) shows a hypointensity signal periaqueductal area (red circle) with irregular profile suggesting the presence of the lesion. **(B)** MRI scan (T2-weighted image) shows a hyperintensity signal in the same area (red circle). **(C)** Gadolinium T1-weighted image shows a low focal contrast enhancement of the lesion in the periaqueductal area. **(D)** Proton magnetic resonance spectroscopy (MRS) reveals elevated cholin peaks (cholin/creatinine ratio at 1,9) in addition to reduced NAA (N-acetylaspartate). **(E)** Perfusion-weighted imaging (PWI) shows a low cerebral blood volume (CBV) in the area of interest.

the presence of negative CD45 cells (CD45 is a marker of the haematological population) was negative in the patient's whole blood sample.

In this case, as shown in **Figure 3**, the Hematoxylin and Eosin (H&E) stained cytological preparations revealed the presence of bulky, polinucleated or spindled cell atypical elements (**Figures 3A, B**). In addition, these atypical cells found in the blood resulted, at the immunohistochemical analysis performed through methods previously described (14), positive for the expression of the astrocytes markers S-100 (**Figures 3C, D**) and glial fibrillary acidic protein (GFAP) (**Figures 3E, F**) (14, 15). A section of brain human tissue was used as internal positive control. Moreover, as negative control, demonstrating that the reaction visualized is due to the interaction of the epitope of the target molecule and the paratope of the antibody/affinity reagent, parallel assays with the primary antibodies omitted was performed. Moreover, as positive control for the presence of CTCs from cerebral lesions in the peripheral blood we used cytological preparations obtained with the same method from peripheral blood collected (7, 8) from one case of glioblastoma and from one case of brain metastasis from melanoma (cerebral metastasis) (**Figures 3G, H**). As negative control was used the cytological pattern isolated by peripheral blood collected from a case of post-stroke frontal lobe scar (**Figure 3I**). The final cytological diagnosis was of pilocytic astrocytoma because the protean features of the proliferating glial elements (**Figures 3A–F**).

The control MRI (6 months after shunt placement) documented that the lesion was stable. Moreover, the area of altered signal at the quadrigeminal plate, hyperintense on T2/Fluid Attenuation Inversion Recovery (FLAIR), hypointense on T1-weighted images, placed at the entrance of the aqueduct of Sylvius, decreased in width. MRI was repeated evert 6 months in the first 2 years; afterwards, an annual MRI was performed, without changes in the radiological picture. Clinical outcome (68 months) supported by follow up corroborates the pathological diagnosis of pilocytic astrocytoma/low grade glioma.

The patient provided written consent in accordance with ethical principles, relevant guidelines and regulations of the Declaration of Helsinki in accordance with experimental protocols included in the study approved by the local ethical committee, with study number 2013.34. The consent includes also authorization to publish the collected data for medical/scientific purposes in accordance with local laws.

DISCUSSION AND CONCLUSIONS

In the present case, the management of hydrocephalus was the most urgent goal, while the management of tectal gliomas, due to the slow growth of this type of tumor, was conservative and included long-term monitoring (16, 17). The monitoring schedule included serial MRI imaging and repeated blood

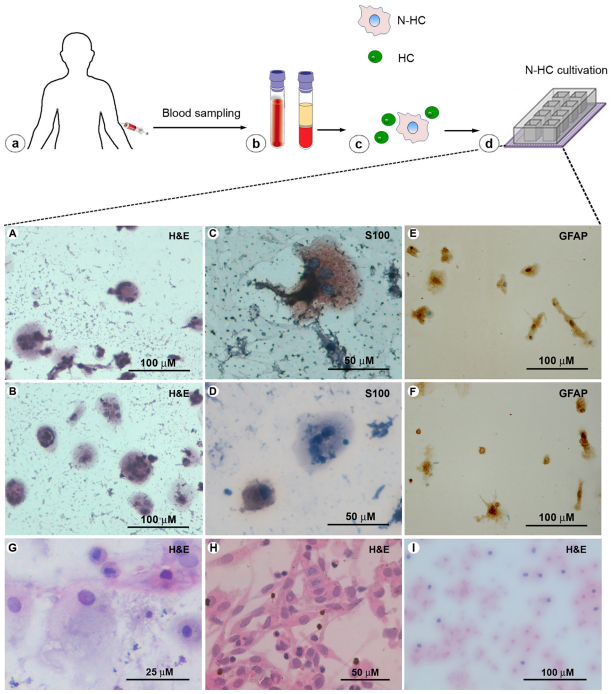

FIGURE 3 | Blood-derived glial cells in cytological preparations. **(a)** Peripheral blood sample collection. **(b)** Blood sample gradient. **(c)** From the gradient, a cellular suspension including non-haematological cells (N-HC) and residual of haematological cells (HC) was isolated. **(d)** The entire cell suspension was seeded in chamber slides and, after 14 days, adherent cells on slide were fixed for cytological analysis. **(A, B)** H&E staining of CTCs deriving from the presented case shows different cellular shapes. **(C, D)** Immunostaining shows CTCs S-100 and **(E, F)** GFAP-positive deriving from the presented case. **(G, H)** Cytological pattern of CTCs derived from one glioblastoma and one cerebral metastasis from melanoma used as positive controls. **(I)** Cytological pattern of cells from a frontal lobe scar used as negative control.

samples for cytological preparations (every six months). Clinicians did not need to prescribe any type of therapy. Clinical outcome (68 months) supported by follow up, confirmed the pathological diagnosis of pilocytic astrocytoma. Successive blood sampling to monitor the number and the pathological detection of cellular elements of interest, reported no significant variation compared to the first pathological evaluation on peripheral blood sample. The patient now is well and leads a normal life.

A major question about our results was: why circulating cells deriving from a benign cerebral lesion can be detectable in the bloodstream? Despite the MRI showed a post-contrast low enhancement of the mesencephalic lesion, this signal supports the hypothesis of the corresponding breached blood-brain barrier (BBB) according to i) the low CBV resulted by PWI findings (**Figure 2E**); ii) low vascularity showed by Gadolinium-enhanced MRI; iii) the evidence of cellular elements brain tissue derived in the bloodstream. We believe that a possible role of the shunt as vehicle of tumor cells in general circulation can be considered unlikely, because it would in turn require an explanation of the entry into the circulation of neoplastic cells at the peritoneal level. The discovery of biomarkers for BBB permeability is starting to happen. The detection of CTCs in the bloodstream could also be an early index of damage of the BBB in brain tumors that precedes in time the neuroradiological signs detectable, for example, through the signal alterations of the MRI. Furthermore, our approach for analyzying circulating tumor elements can provide a more sensitive and integrative method than neuroradiological imaging for the study of barrier damage. These integrated parameters (18) can provide a better diagnostic and prognostic value. However, to date, the identification of ideal peripheral markers to graduate the BBB damage entity remains a challenge for radiologist and neuro-oncologist (19, 20). Our approach suggested that the recognition of circulating cells of brain origin could be useful to unmask the BBB dysfunction. On these considerations, the cytological preparations from peripheral blood could be considered a precious tool also in the diagnosis and monitoring the intracranial lesions, especially in paediatric age, in order to reduce side effect of invasive procedure.

Pyloytic astrocytoma is a slow-growing, circumscribed tumor frequently occurring in children and young adults in cerebellum optic nerves or brain stem. In the brain stem, it may occur as exophytic or deep lesions that may be difficult to biopsy. Through our procedure it was possible to formulate a diagnosis that allowed to decide the patient's long-term management, avoiding further dangerous or useless diagnostic approaches. The possibility of having in short-term culture a population of cells with characteristics superimposable to single CTCs that may or may not be detected by other methods, may be an opportunity to verify the value of molecular biology techniques such as cancer genome studies and single-cell transcriptome for tumor heterogeneity. Such techniques could definitively prove their usefulness for a personalized approach to patient diagnosis and therapy (21, 22). We believe that this case highlights the strong potential of liquid biopsy to improve the diagnostic and prognostic evaluation and the quality of life in neuro-oncology.

DATA AVAILABILITY STATEMENT

The raw data supporting the conclusions of this article will be made available by the authors, without undue reservation.

ETHICS STATEMENT

The study was approved by the local ethical committee, with study number 2013.34. The patients/participants provided their written informed consent to participate in this study.

AUTHOR CONTRIBUTIONS

Conceptualization, NM and GV. Writing—original draft preparation, NM and GD. Writing—review and editing, NM,

GD, and CM. Cytological evaluation: GD and CM. Visualization, NM and RR. Supervision, GD, GV, DT, US, and NM. All authors contributed to the article and approved the submitted version.

FUNDING

This work was supported by the "Matteo's friends Association".

REFERENCES

1. Malone H, Yang J, Hershman DL, Wright JD, Bruce JN, Neugut AI. Complications Following Stereotactic Needle Biopsy of Intracranial Tumors. *World Neurosurg* (2015) 84(4):1084–9. doi: 10.1016/j.wneu.2015.05.025
2. Hargrave D, Bartels U, Bouffet E. Diffuse Brainstem Glioma in Children: Critical Review of Clinical Trials. *Lancet Oncol* (2006) 7(3):241–8. doi: 10.1016/S1470-2045(06)70615-5
3. Hassan H, Pinches A, Picton SV, Phillips RS. Survival Rates and Prognostic Predictors of High Grade Brain Stem Gliomas in Childhood: A Systematic Review and Meta-Analysis. *J Neurooncol* (2017) 135(1):13–20. doi: 10.1007/s11060-017-2546-1
4. Guillamo JS, Monjour A, Taillandier L, Devaux B, Varlet P, Haie-Meder C, et al. Brainstem Gliomas in Adults: Prognostic Factors and Classification. *Brain* (2001) 124(Pt 12):2528–39. doi: 10.1093/brain/124.12.2528
5. Malara NM, Givigliano F, Trunzo V, Macrina L, Raso C, Amodio N, et al. *In Vitro* Expansion of Tumour Cells Derived From Blood and Tumour Tissue is Useful to Redefine Personalized Treatment in Non-Small Cell Lung Cancer Patients. *J Biol Regul Homeost Agents* (2014) 28(4):717–31.
6. Malara N, Trunzo V, Foresta U, Amodio N, De Vitis S, Roveda L, et al. Ex-Vivo Characterization of Circulating Colon Cancer Cells Distinguished in Stem and Differentiated Subset Provides Useful Biomarker for Personalized Metastatic Risk Assessment. *J Transl Med* (2016) 14(1):133. doi: 10.1186/s12967-016-0876-y
7. Guadagno E, Presta I, Maisano D, Donato A, Pirrone CK, Cardillo G, et al. Role of Macrophages in Brain Tumor Growth and Progression. *Int J Mol Sci* (2018) 19(4):1005. doi: 10.3390/ijms19041005
8. Malara N, Gentile F, Coppedè N, Coluccio ML, Candeloro P, Perozziello G, et al. Superhydrophobic Lab-on-Chip Measures Secretome Protonation State and Provides a Personalized Risk Assessment of Sporadic Tumour. *NPJ Precis Oncol* (2018) 2:26. doi: 10.1038/s41698-018-0069-7
9. Gao F, Cui Y, Jiang H, Sui D, Wang Y, Jiang Z, et al. Circulating Tumor Cell is a Common Property of Brain Glioma and Promotes the Monitoring System. *Oncotarget* (2016) 7(44):71330–40. doi: 10.18632/oncotarget.11114
10. Pantel K, Denève E, Nocca D, Coffy A, Vendrell JP, Maudelonde T, et al. Circulating Epithelial Cells in Patients With Benign Colon Diseases. *Clin Chem* (2012) 58(5):936–40. doi: 10.1373/clinchem.2011.175570
11. Perozziello G, Catalano R, Francardi M, Rondanina E, Pardeo F, De Angelis F, et al. A Microfluidic Device Integrating Plasmonic Nanodevices for Raman Spectroscopy Analysis on Trapped Single Living Cells. *Microelectronic Eng* (2013) 111):314–9. doi: 10.1016/j.mee.2013.02.023
12. Perozziello G, Simone G, Candeloro P, Gentile F, Malara N, Larocca R, et al. A Fluidic Motherboard for Multiplexed Simultaneous and Modular Detection in Microfluidic Systems for Biological Application. *Micro Nanosystems* (2010) 2(4):227–38. doi: 10.2174/1876402911002040227
13. Malara NM, Leotta A, Sidoti A, Lio S, D'Angelo R, Caparello B, et al. Ageing, Hormonal Behaviour and Cyclin D1 in Ductal Breast Carcinomas. *Breast* (2006) 15(1):81–9. doi: 10.1016/j.breast.2004.12.008
14. Donato G, Presta I, Arcidiacono B, Vismara MFM, Donato A, Garo NC, et al. Innate and Adaptive Immunity Linked to Recognition of Antigens Shared by Neural Crest-Derived Tumors. *Cancers (Basel)* (2020) 12(4):840. doi: 10.3390/cancers12040840
15. Perrotta I, Carito V, Russo E, Tripepi S, Aquila S, Donato G. Macrophage Autophagy and Oxidative Stress: An Ultrastructural and Immunoelectron Microscopical Study. *Oxid Med Cell Longev* (2011) 2011:282739. doi: 10.1155/2011/282739
16. Best MG, Sol N, Zijl S, Reijneveld JC, Wesseling P, Wurdinger T. Liquid Biopsies in Patients With Diffuse Glioma. *Acta Neuropathol* (2015) 129(6):849–65. doi: 10.1007/s00401-015-1399-y
17. Onesto V, Cancedda L, Coluccio ML, Nanni M, Pesce M, Malara N, et al. Nano-Topography Enhances Communication in Neural Cells Networks. *Sci Rep* (2017) 7:9841. doi: 10.1038/s41598-017-09741-w
18. Presta I, Vismara M, Novellino F, Donato A, Zaffino P, Scali E, et al. Innate Immunity Cells and the Neurovascular Unit. *Int J Mol Sci* (2018) 319(12):3856. doi: 10.3390/ijms19123856
19. La Torre D, Conti A, Aguennouz M, De Pasquale MG, Romeo S, Angileri FF, et al. Telomere Length Modulation in Human Astroglial Brain Tumors. *PLoS One* (2013) 8(5):e64296. doi: 10.1371/journal.pone.0064296
20. La Torre D, Maugeri R, Angileri FF, Pezzino G, Conti A, Cardali SM, et al. Human Leukocyte Antigen Frequency in Human High-Grade Gliomas: A Case-Control Study in Sicily. *Neurosurgery* (2009) 64(6):1082–8. doi: 10.1227/01.NEU.0000345946.35786.92
21. Li SC, Tachiki LML, Kabeer MH, Dethlefs BA, Anthony MJ, Loudon WG. Cancer Genomic Research at the Crossroads: Realizing the Changing Genetic Landscape as Intratumoral Spatial and Temporal Heterogeneity Becomes a Confounding Factor. *Cancer Cell Int* (2014) 14:115. doi: 10.1186/s12935-014-0115-7
22. Chen X, Wen Q, Stucky A, Zeng Y, Gao S, Loudon WG, et al. Relapse Pathway of Glioblastoma Revealed by Single-Cell Molecular Analysis. *Carcinogenesis* (2018) 39(7):931–6. doi: 10.1093/carcin/bgy052

Conflict of Interest: The authors declare that the research was conducted in the absence of any commercial or financial relationships that could be construed as a potential conflict of interest.

Publisher's Note: All claims expressed in this article are solely those of the authors and do not necessarily represent those of their affiliated organizations, or those of the publisher, the editors and the reviewers. Any product that may be evaluated in this article, or claim that may be made by its manufacturer, is not guaranteed or endorsed by the publisher.

Copyright © 2021 Volpentesta, Donato, Ferraro, Mignogna, Radaelli, Sabatini, La Torre and Malara. This is an open-access article distributed under the terms of the Creative Commons Attribution License (CC BY). The use, distribution or reproduction in other forums is permitted, provided the original author(s) and the copyright owner(s) are credited and that the original publication in this journal is cited, in accordance with accepted academic practice. No use, distribution or reproduction is permitted which does not comply with these terms.

frontiers in Cell and Developmental Biology

REVIEW
published: 28 October 2021
doi: 10.3389/fcell.2021.737962

The Emerging Role of Exosomes in Cancer Chemoresistance

Jing Li[1], Na Gao[1], Zhengfan Gao[1], Wei Liu[1], Bairen Pang[2], Xingli Dong[3], Yong Li[1,2] and Tianli Fan[1]**

[1] Department of Pharmacology, School of Basic Medical Science, Zhengzhou University, Zhengzhou, China, [2] St George Hospital, St George and Sutherland Clinical School, Faculty of Medicine, UNSW Sydney, Kensington, NSW, Australia, [3] Department of Biopharmaceutical Sciences, College of Pharmacy, Harbin Medical University, Harbin, China

Chemoresistance is an impending challenge in cancer treatment. In recent years, exosomes, a subtype of extracellular vesicles with a diameter of 40–150 nm in bloodstream and other bio-fluids, have attracted increasing interest. Exosomes contain proteins, nucleic acids, and lipids, which act as important signaling molecules. Many reports indicate that exosomes play critical roles in chemoresistance through intercellular interactions, including drug removal from cells, transfer of drug resistance phenotypes to other cancer cells, and the increase in plastic stem cell subsets. Exosomes can reflect the physiological and pathological state of parent cells. Owing to their elevated stability, specificity, and sensitivity, exosomes are served as biomarkers in liquid biopsies to monitor cancer chemoresistance, progression, and recurrence. This review summarizes the exosome-mediated mechanisms of cancer chemoresistance, as well as its role in reversing and monitoring chemoresistance. The scientific and technological challenges and future applications of exosomes are also explored.

Keywords: exosome, cancer, chemoresistance, liquid biopsy, biomarker

OPEN ACCESS

Edited by:
Catherine Alix-Panabieres, Centre Hospitalier Universitaire de Montpellier, France

Reviewed by:
Weina Ke, University of North Carolina at Charlotte, United States
Richa Shrivastava, Birla Institute of Technology and Science, India

****Correspondence:***
Tianli Fan
fantianli@zzu.edu.cn
Yong Li
y.li@unsw.edu.au

Specialty section:
This article was submitted to Molecular and Cellular Oncology, a section of the journal Frontiers in Cell and Developmental Biology

Received: *07 July 2021*
Accepted: *04 October 2021*
Published: *28 October 2021*

Citation:
Li J, Gao N, Gao Z, Liu W, Pang B, Dong X, Li Y and Fan T (2021) The Emerging Role of Exosomes in Cancer Chemoresistance. Front. Cell Dev. Biol. 9:737962. doi: 10.3389/fcell.2021.737962

INTRODUCTION

Chemotherapy is vital for cancer treatment. However, the majority of cancer patients develop drug resistance after repeated treatment, first to one and then to other chemotherapeutic agents (Gottesman, 2002). Chemoresistance is a major challenge for successful anticancer therapy. Cancer-derived exosomes have been implicated in chemoresistance by providing cancer cells with nucleic acids and proteins (Namee and O'Driscoll, 2018).

Exosomes are a subclass of heterogeneous extracellular vesicles (EVs) with a diameter of 40–150 nm, which are released from a variety of cells. Exosome secretion was initially considered as a form of waste excretion by cells (Johnstone, 1992). However, subsequent advances have revealed that exosomes play an important role in both physiological and pathological processes, highlighting their involvement in cell migration and invasion, immune response and chemoresistance (Namee and O'Driscoll, 2018; Yi et al., 2020). Exosomes are a key player in communicating among protein–protein, gene–gene, and gene–microRNA (miRNA) networks, as well as intracellular and distant cellular connection routes, which bestows them with untapped application potential (Kitano, 2004). Their role in cell communication suggests a potential connection between the dysregulation of exosomal cargo and chemoresistance in cancer. Increasing evidence indicates that exosomes mediate chemoresistance (Fan et al., 2018); therefore, exploring the underlying mechanism may help identify methods to prevent and reverse chemoresistance. In addition, exosomes hold great potential to be used as biomarkers and therapeutic tools in cancer in clinical settings (Xiao et al., 2020).

In this review, we focus on discussing the mechanisms of exosome-mediated chemoresistance in cancer, the use of exosomes to reverse chemoresistance, and their application as biomarkers in liquid biopsy to monitor chemoresistance. Finally, the technological challenges and future application prospects of exosomes in cancer therapy are also explored.

EXOSOMES AND CANCER CHEMORESISTANCE

Exosomes in Cancer Research

Initially, exosomes were considered cellular waste and hence did not receive much attention. However, the characterization of nucleic acids, proteins, and lipids isolated from exosomes have advanced our understanding of the role of exosomes in intercellular communication and epigenetic regulation (Pathan et al., 2019). According to the ExoCarta database, over 9769 proteins, 3 408 mRNAs, and 2 838 miRNAs have been identified in exosomes to date. Exosomes have been found to play a vital role in mediating physiological processes and pathological conditions, wherein they mediate tumorigenesis, metastasis, angiogenesis, and drug resistance (Bach et al., 2017; Fan et al., 2018; Feng W. et al., 2019). Huang et al. (2019) demonstrated that prostate cancer-related transcript 1 (PCAT1) was present in esophageal squamous cell carcinoma (ESCC) cell-derived exosomes and promoted tumor cell growth through exosomes, and the level of exosomes was higher in the serum of ESCC patients than that in healthy volunteers. Liu X. et al. (2019) reported that miR-501 promoted tumorigenesis and chemoresistance in gastric cancer by targeting the BH3-like motif protein (BLID). As exosomes induce cancer occurrence and progression, these harmful processes can be prevented by inhibiting the production of exosomes or their uptake by target cells (Milman et al., 2019).

Under both physiological and pathological conditions, the content of exosomes is finely regulated by their parent cells, which transmit information to recipient cells and let them acquire specific functions. In turn, the functional status of parent cells can be estimated by analyzing exosome cargo. In general, exosomes act as a "double-edged sword": on the one hand, they promote cancer progression; on the other hand, they target tumor cells with anticancer drugs. Consequently, exosomes are becoming effective tools for cancer diagnosis and treatment. In the following sections, we focus on the role of exosomes in cancer chemoresistance.

The Role of Exosomes in the Tumor Microenvironment

The tumor microenvironment (TME) includes cancer cells, surrounding stromal cells (e.g., fibroblasts, inflammatory cells, and immune cells), cellular stroma, microvessels, and biomolecules. The TME is characterized by hypoxia, low pH, and high pressure. Due to these characteristics, the TME is rich in growth factors, cell chemokine factors, and proteolytic enzymes, which facilitate cancer proliferation, invasion, adhesion, angiogenesis, and chemoresistance (Cairns et al., 2006; Hui and Chen, 2015). For a long time, scientists focus exclusively on cancer cells and the use of targeted drugs to inhibit their growth. However, accumulating studies have shown that the TME plays an essential role in cancer invasion, metastasis, and chemoresistance (Hui and Chen, 2015; Ren et al., 2018). Ombrato et al. (2019) discovered that cancer-associated parenchymal cells in the TME exhibited stem cell-like characteristics, which helps cancer cells survive, spread, and develop resistance to treatment.

Exosomes provide a key communication channel between the TME and cancer cells. Wu et al. (2019) demonstrated that exosomes in the TME promoted the occurrence and progression of hepatocellular carcinoma by regulating energy metabolism and the inflammation microenvironment, as well as by inducing angiogenesis. Zhang X. et al. (2019) found that specific miRNAs carried by exosomes, including miR-193-3p, miR-210-3p, and miR-5100, promoted invasion by lung cancer cells through activation of the STAT3-induced epithelial-to-mesenchymal transition (EMT). Non-tumor cells in the TME were reported to be an important source of drug resistance, providing factors that facilitate cancer cell survival even during chemotherapy (Wilson et al., 2012). Xu et al. (2019) found that lncPSMA3-AS1 and PSMA3 were packaged into exosomes and transferred from mesenchymal stem cells to multiple myeloma, promoting proteasome inhibitor resistance (Xu et al., 2019). Binenbaum et al. (2018) shown that miR-365 in macrophage-derived exosomes inhibited the activation of gemcitabine by increasing nucleotide triphosphate levels and inducing cytidine deaminase, causing pancreatic cancer cells to become resistant to gemcitabine. From a clinical point of view, the identification of soluble resistance factors such as exosomes helps overcome drug resistance in cancer cells. This can be achieved by preventing exosomes from exerting protective effects on cancer cells and stimulating, instead, chemosensitivity.

The Mechanism Underlying Exosome-Mediated Chemoresistance

Chemoresistance is divided into primary drug resistance and multiple drug resistance (MDR). The former refers to cancer cells that are resistant to induced drugs, whereas the latter refers to cancer cells that develop resistance to induced drugs, as well as to other chemotherapeutic agents with different structures and mechanisms, to which cells were not even exposed (Gacche and Assaraf, 2018). The establishment of chemoresistance in cancer cells involves a variety of mechanisms, including increased DNA repair, downregulation of apoptosis, altered drug targets, increased drug efflux, and overexpression of MDR proteins (Housman et al., 2014; Alharbi et al., 2018). Growing evidence has demonstrated the role of exosomes in mediating cancer chemoresistance (**Figure 1**), and the following underlying mechanisms are proposed:

(1) Influencing recipient cells: exosomes induce the formation of the pre-metastatic niche between the primary cancer and remote organs and recode cell cycle and apoptosis genes of recipient cells in the TME. Organ-specific metastasis is guided by the adhesion molecules such as integrins on the surface of exosomes (Hoshino et al., 2015).

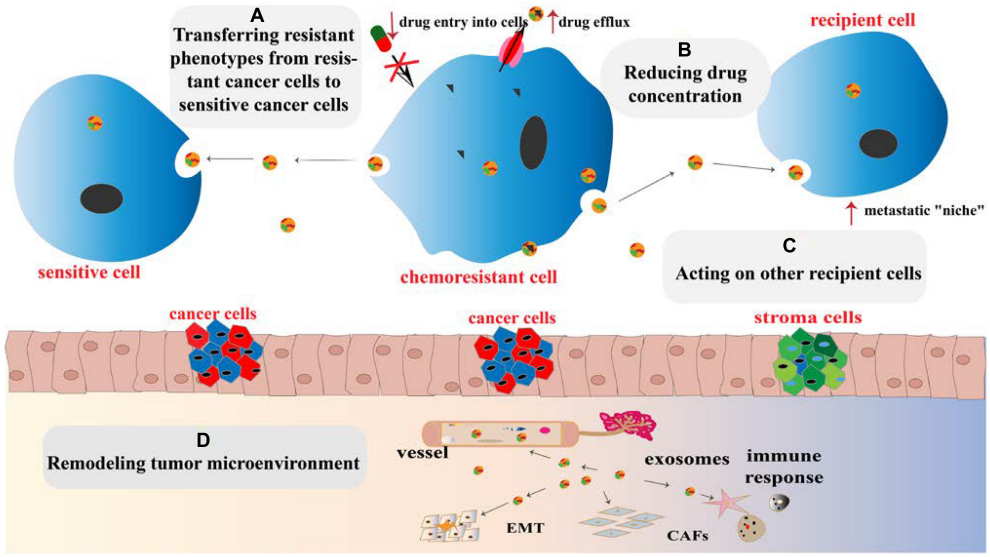

FIGURE 1 | Mechanisms for promoting chemoresistance by exosomes. **(A)** Exosomes transfer chemoresistant phenotypes from resistant cancer cells to sensitive cancer cells. **(B)** The intracellular drug concentration can be reduced by increasing drug efflux, reducing cell lysis, and isolating cytotoxic drugs via exosomes. **(C)** Exosomes acting on recipient cells induce the formation of a "niche" through transferring their contents and recoding cell cycle and apoptosis genes of recipient cells. **(D)** Exosomes remodel the TME by increasing cancer cell immune escape, promoting cancer angiogenesis, EMT, and transforming basal fibroblasts into CAFs or even cancer cells.

(2) Limiting effective drug utilization by regulating drug efflux, reducing cell cytolysis, and isolating cytotoxic drugs (Pilzer and Fishelson, 2005).

(3) Transferring chemoresistance phenotypes from drug-resistant to sensitive cells (Milman et al., 2019).

(4) Reshaping the TME: exosomes increase cancer cell immune escape, promote local cancer angiogenesis and EMT, and transform basal fibroblasts into cancer-associated fibroblasts (CAFs) or even cancer cells through TME remodeling (Wang et al., 2018).

The exosome proteins and nucleic acids mediate signal transduction and regulate gene expression by initiating signal transduction pathways or binding to cell surface receptors. We will discuss hereafter how proteins and nucleic acids in exosomes mediate chemoresistance.

Proteins in Exosome-Mediated Chemoresistance

Exosomes have been shown to transfer proteins, such as *P*-glycoprotein (*P*-gp), annexin A3, ATPase copper transporting alpha (ATP7A), ATPase copper transporting beta (ATP7B), and survivin, from drug-resistant cells to sensitive cells or to induce direct drug efflux (**Table 1**). All these processes result in chemoresistance in sensitive cancer cells.

P-gp is a 170-kDa protein encoded by the MDR-1 gene and plays a key role in maintaining appropriate intracellular drug concentration. It is currently one of the most studied proteins in cancer chemoresistance (Bebawy et al., 2009; Lv et al., 2014; Zhang et al., 2014; Kato et al., 2015). Ning et al. (2017) demonstrated that in adriamycin (ADM)-resistant human breast cancer cells (MCF7/ADM), ADM did not accumulate in the nuclei as expected but was secreted from the cells through exosomes. At the same time, a high level of *P*-gp was observed in the exosomes, together with the increased levels of its regulator transient receptor potential channel 5 (TrpC5). *P*-gp was found to be restored using a TrpC5 channel-specific

TABLE 1 | Proteins associated with exosome-mediated chemoresistance in cancer.

Cancer type	Protein	Drug-mediated resistance	References
Breast cancer	*P*-gp	Adriamycin	Ning et al., 2017
	P-gp	Docetaxel	Lv et al., 2014
	Survivin	Paclitaxel	Kreger et al., 2016
Ovarian cancer	DNMT1	Cisplatin	Cao et al., 2017
	P-gp	Paclitaxel	Zhang et al., 2014
	Annexin A3	Platinum	Yan et al., 2010; Yin et al., 2012
	ATP7A/ATP 7B/MRP1	Cisplatin	Safaei et al., 2005
Leukemia	*P*-gp	Multidrug	Bebawy et al., 2009
	MRP1	Multidrug	Lu et al., 2013
Prostate cancer	*P*-gp	Docetaxel	Kato et al., 2015
Colorectal cancer	*P*-STAT3	5-Fluorouracil	Zhang Q. et al., 2019
Pancreatic cancer	EphA2	Gemcitabine	Fan et al., 2018
Diffuse large B cell lymphoma	CA1	R-CHOP	Feng et al., 2020

ATP7A/ATP7B, ATPase copper transporting alpha/beta; CA1, carbonic anhydrase 1; DNMT1, DNA methyltransferase 1; EphA2, ephrin type-A receptor 2; MRP1, multidrug resistance protein 1; P-gp, P-glycoprotein; R-CHOP, cyclophosphamide, doxorubicin, vincristine, and prednisone, combined with rituximab.

blocker (T5E3), which limited drug efflux and increased breast cancer chemosensitivity (Ning et al., 2017). Further studies demonstrated that exosomes from MCF7/ADM cells carried ubiquitin carboxyl terminal hydrolase L1 (UCH-L1) and P-gp into the extracellular microenvironment, enabling their time-dependent integration in ADM-sensitive human breast cancer cells (MCF7/WT) and acquisition of drug-resistant phenotypes. Furthermore, the level of UCH-L1 in blood exosomes of breast cancer patients was found to correlate negatively with their prognosis. This can be explained by overexpression of UCH-L1, enhancing MDR in breast cancer through activation of the MAPK/ERK signaling pathway and upregulation of *P*-gp (Ning et al., 2017). In another study, the level of *P*-gp was reported to be significantly higher in exosomes isolated from docetaxel-resistant prostate cancer cells than in parent cells (Kato et al., 2015). The same result was observed in clinical blood samples, indicating that exosomal P-gp was associated with docetaxel resistance in prostate cancer and holds potential to be used as a biomarker to monitor docetaxel-resistant prostate cancer in clinic (Kato et al., 2015).

Annexin A3 belongs to the phospholipid-binding protein family, which is involved in intercellular interactions and is closely related to cancer cell invasion, metastasis, and chemoresistance (Donnelly and Moss, 1997; Yan et al., 2010; Yin et al., 2012). Yan et al. (2010) reported that annexin A3 was significantly enriched in Pt-resistant ovarian cancer cell lines, where it reduced the concentration of intracellular Pt-based drugs and prevented cancer cell apoptosis. Further studies showed that upregulation of annexin A3 in cancer cells led to the formation and release of multivesicular body vesicles. Western blotting and immunoelectron microscopy further confirmed the presence of annexin A3 in exosomes, suggesting that the latter transferred annexin A3 between cells to induce chemoresistance (Yan et al., 2010).

Ubiquitin proteins (survivin), DNA methyltransferase 1 (DNMT1), copper transporters (ATP7A and ATP7B), multidrug resistance protein (MRP2), P-STAT3, and carbonic anhydrase 1 (CA1) in exosomes have also been reported to induce chemoresistance (Safaei et al., 2005; Lu et al., 2013; Kreger et al., 2016; Cao et al., 2017; Zhang Q. et al., 2019; Feng et al., 2020). Survivin is a key factor in maintaining apoptosis resistance, and was frequently reported to be involved in cancer multidrug resistance (Hu et al., 2015; Han et al., 2016; Wang et al., 2016). Kreger et al. (2016) found that survivin was significantly enriched in paclitaxel-resistant breast cancer cells, where it promoted cell survival and drug resistance, and the effect that was ablated when survivin was knocked down from these exosomes. Aspe et al. (2014) reported that the dominant-negative mutant of survivin (Survivin-T34A) was shown to block survivin, inducing caspase activation and apoptosis, and enhancing the sensitivity of gemcitabine in pancreatic adenocarcinoma. Both epigenetic alterations and genetic variations play critical roles in tumorigenesis and development (Feinberg et al., 2016). DNMT1 is a key gene for DNA methylation in epigenetic modification, and the protein encoded by it is a complex enzyme with multiple regulatory functions in cancer (Ren et al., 2020). Cao et al. (2017) demonstrated that DNMT1 transcripts were significantly enriched in ovarian cancer cell lines. After the *in vivo* administration of cisplatin, DNMT1-containing exosomes were found to exacerbate xenograft progression and significantly reduce overall survival (Cao et al., 2017). The multidrug resistance of cancer cells is mainly caused by membrane protein ATP binding cassettes (ABCs), which excretes toxic substances from the body. After drug treatment, the expression of various genes involved in cells transport increased, such as ATP7A, ATP7B, and MRP2. Likewise, Safaei et al. (2005) reported greater secretion of exosomes in cisplatin-resistant ovarian cancer cell lines (2008/C13*5.25) than in sensitive cells, together with significant upregulation of ATP7A, ATP7B, and MRP2. More and more studies have reported that CA1 is related to cancer progression. Feng et al. showed that compared to diffuse large B cell lymphoma (DLBCL) parental cells, the expression of CA1 is upregulated in chemoresistant cells, and the expression level of CA1 was higher in exosomes from the blood of chemoresistant patients compared with chemosensitive patients (Feng et al., 2020). Knockdown of CA1 inhibited the growth of DLBCL cells via inhibiting the activation of the NF-kB and STAT3 signaling pathways both *in vitro* and *in vivo*. The researcher proposed that exosomal CA1 predicted prognosis and chemotherapeutic efficacy in DLBCL patients (Feng et al., 2020). Several preclinical and clinical studies have demonstrated that STAT3 is activated in many cancers and correlates with patient's survival (Birner et al., 2010). Moreover, it has been reported increased p-STAT3 levels are associated with chemoradiotherapy (Spitzner et al., 2014). Zhang X. et al. (2019) demonstrated that exosomal transfer of p-STAT3 promoted acquired 5-FU resistance in colorectal cancer cells. In summary, a growing body of evidence shows that the proteins in exosomes induce chemoresistance in sensitive cells through various mechanisms, such as the transmission of chemoresistance phenotypes and reduction of intracellular drug concentrations. It is worth noting that these proteins show promise as biomarkers for the monitoring of chemoresistance.

Nucleic Acids in Exosome-Mediated Chemoresistance

Nucleic acids in exosomes comprise DNA and RNA fragments. In recent years, several studies have demonstrated that exosomal miRNAs regulate intracellular RNA and protein levels, playing a crucial role in cancer chemoresistance (Patel et al., 2017; Qin et al., 2019).

Exosomes secreted by drug-resistant cancer cells act as paracrine regulators by transferring genetic material (O'Brien et al., 2013). The miRNAs found in exosomes secreted by chemoresistant cancer cells deliver drug-resistant phenotypes to sensitive cancer cells, thereby influencing cell growth and inducing anti-apoptotic processes (**Table 2**; Chen et al., 2014; Jin et al., 2015; Pink et al., 2015; Weiner-Gorzel et al., 2015; Au et al., 2016; Bouvy et al., 2017; Qin et al., 2017; Wei et al., 2017; Fu et al., 2018; Kanlikilicer et al., 2018; Min et al., 2018; Zhang Y. et al., 2018; Zhu et al., 2019; Han et al., 2020). Moreover, miR-501 is upregulated in lung adenocarcinoma, cervical cancer, liver cancer, and gastric cancer, suggesting that miR-501 is a carcinogenic miRNA (Fan et al., 2016;

TABLE 2 | miRNAs associated with exosome-mediated cancer chemoresistance.

Cancer type	miRNAs	Drug-mediated resistance	References
Lung cancer	miR-222-3p	Gemcitabine	Wei et al., 2017
	miR-214	Gefitinib	Zhang Y. et al., 2018
	miR-100-5p	Cisplatin	Qin et al., 2017
Breast cancer	miR-222	Docetaxel	Chen et al., 2014
	miR-567	Truzhuo	Han et al., 2020
	miR-155-3p	Paclitaxel	Au et al., 2016
Ovarian cancer	miR-21	Paclitaxel	Au et al., 2016
	miR-433	Paclitaxel	Weiner-Gorzel et al., 2015
	miR-21-3p	Cisplatin	Pink et al., 2015
	miR-1246	Paclitaxel	Kanlikilicer et al., 2018
	miR-223	Cisplatin	Zhu et al., 2019
Leukemia	miR-365	Imatinib	Min et al., 2018
	miR-19b	Multidrug	Bouvy et al., 2017
	miR-20a	Multidrug	Bouvy et al., 2017
Hepatocellular cancer	miR-32-5p	Multidrug	Fu et al., 2018
Gastric cancer	miR-21	Paclitaxel	Jin et al., 2015
	miR-501	Doxorubicin	Fan et al., 2016; Xu et al., 2018; Liu X. et al., 2019
	miR-522	Cisplatin and Paclitaxel	Zhang et al., 2020
	miR-374-5p	Oxaliplatin	Ji et al., 2019
Oral cancer	miR-21	Cisplatin	Liu et al., 2017
B-cell lymphoma	miR-99a-5p	Doxorubicin	Feng Y. et al., 2019
	miR-125b-5p	Doxorubicin	Fan et al., 2016
Colorectal cancer	miR-92a-3p	5-FU	Hu et al., 2019
Head and neck cancer	miR-196-a	Cisplatin	Qin et al., 2019
Pancreatic cancer	miR-365	Gefitinib	Binenbaum et al., 2018
	miR-210	Gefitinib	Binenbaum et al., 2018
	miR-155	Gefitinib	Patel et al., 2017

5–FU, 5-fluoro-2,4(1H,3H)-pyrimidinedione.

Xu et al., 2018; Liu X. et al., 2019). Liu X. et al. (2019) found that miR-501 promoted tumorigenesis and chemoresistance of gastric cancer by targeting BLID. Compared with exosomes (7901 Exo) secreted by sensitive gastric cancer cell lines (SGC7901), miR-501 expression was significantly upregulated in exosomes (ADR Exo) secreted by doxorubicin-resistant cell lines (SGC7901/ADR). After ADR Exo were ingested by SGC7901 cells, miR-501 was incorporated, increasing chemoresistance of gastric cancer cells to doxorubicin. Knockdown of miR-501 and overexpression of BLID, via exosome inhibitors (GW4869) or miR-501 inhibitors, restored the sensitivity of chemoresistant cells to doxorubicin and inhibited the proliferation, migration, invasion, and apoptosis of gastric cancer cells (Liu X. et al., 2019). In addition to exosomes derived from cancer cells, exosomes originating from stromal cells are also involved in cancer resistance. Hu et al. (2019) reported that CAFs directly transferred exosomes to colorectal cancer (CRC) cells and upregulated miR-92a-3p expression. In this way, CAFs were able to promote stemness, EMT, chemoresistance, and metastasis of CRC (Hu et al., 2019). In clinical studies, high expression of exosomal miR-92a-3p in serum was found to be closely related to metastasis and chemoresistance in CRC patients; hence, miR-92a-3p in exosomes secreted by CAFs is a useful biomarker for monitoring the progression of CRC (Hu et al., 2019).

In addition to miRNAs, other nucleic acids, such as long non-coding RNAs (lncRNAs) and circular RNAs (circRNAs), are also responsible for inducing chemoresistance. Qu et al. (2016) reported that during sunitinib treatment of renal cancer, the content of lncARSR in exosomes started to increase concomitantly with the development of drug resistance. Further studies found that lncARSR induced sunitinib resistance mainly through the competitive binding of miR-34/miR-449, which increased the expression of receptor tyrosine kinases (AXL and c-MET) in renal cancer cells, while promoting chemosensitivity via lncARSR inhibitors (Qu et al., 2016). Kang et al. (2018) elucidated that lncRNA PART1 was upregulated in gefitinib-resistant esophageal squamous cell carcinoma (ESCC) cells, where it regulated the miR-129/Bcl-2 pathway. Importantly, knockout of lncRNA PART1 effectively promoted gefitinib-induced cell death. Extracellular PART1 was found to enter exosomes and spread to sensitive cells, thereby inducing gefitinib resistance (Kang et al., 2018). Studies on clinical samples have shown that high levels of serum lncRNA PART1 in exosomes are associated with a poor prognosis in ESCC patients treated with gefitinib (Kang et al., 2018).

Some circRNAs are also shown to function as effective endogenous miRNA competitive molecules and have the potential to participate in cancer gene regulation. Based on both *in vitro* and *in vivo* evidence, Wang et al. (2020) demonstrated that exosomes secreted by oxaliplatin-resistant cells transferred circRNA-122 to drug-sensitive cells, wherein they enhanced glycolysis and drug resistance by upregulating the M2 isoform of pyruvate kinase and reducing miR-122 level. Knockdown of circRNA-122 was found to inhibit glycolysis and reverse drug resistance (Wang et al., 2020). Studies have also shown that mitochondrial DNA in exosomes regulates the immune escape of hormone-resistant breast cancer cells and induces chemoresistance (Sansone et al., 2017).

In summary, many preclinical and clinical studies have demonstrated that nucleic acids in exosomes play a vital role in mediating chemoresistance, leading to an increased interest in miRNA research. Inhibiting or inducing the expression of these nucleic acids can reverse chemotherapy resistance; whereas monitoring their levels can prevent chemoresistance and increase overall survival.

STRATEGIES TO COMBAT EXOSOME-MEDIATED CHEMORESISTANCE

To maximize the effect of chemotherapy, it is essential to inhibit exosome-associated chemoresistance. To this end, two possible strategies exist: (i) inhibition of exosome biogenesis and (ii) application of exosomes as delivery vehicles.

Inhibition of Exosome Biogenesis

Because exosomes induce chemoresistance in cancer cells, several studies have hypothesized that inhibition of exosome biogenesis may reverse chemoresistance. Inhibiting the formation or release of multivesicular bodies (MVBs) is the most important way to inhibit the biogenesis of exosomes (Essandoh et al., 2015; Sterzenbach et al., 2017). Hydrochloride hydrate (GW4869), a commonly used drug to inhibit the formation of exosomes, was reported to block the sprouting of MVBs mediated by ceramide, thereby inhibiting the release of exosomes from MVBs (Luberto et al., 2002). Luberto et al. (2002) found that after GW4869 treatment of cells, the exosomal proteolipid protein (PLP) and CD63 in the ultracentrifugation component were significantly reduced. Richards et al. (2017) reported that gemcitabine treatment of CAFs caused an increase in the release of chemoresistance-promoting exosomes. Treatment of gemcitabine-exposed CAFs with GW4869 significantly reduced cells survival, indicating the important role of GW4869 in reversing chemoresistance (Richards et al., 2017). Furthermore, Manumycin-A, a natural microbial metabolite, was identified as an inhibitor of exosome biogenesis and secretion in castration-resistant prostate cancer (CRPC) without affecting cell growth. Datta et al. (2017) showed that, in CRPC cells, manumycin-A suppressed exosome biogenesis and secretion via the targeted inhibition of Ras/Raf/ERK1/2 signaling and ERK-dependent inhibition of the oncogenic splicing factor hnRNP H1. Using a CRC xenograft mouse model, Gu et al. (2020) showed that neticonazole acted as a promising exosome secretion inhibitor, suppressing intestinal dysbacteriosis-induced tumorigenesis of CRC. Similarly, the exosome blocker indomethacin causes doxorubicin to effectively accumulate in the cell nuclei, instead of expelling it via exosomes. This strategy improved cytotoxicity and cell retention of the drug, thereby reversing chemoresistance (Araujo et al., 2016).

Reversing chemoresistance by inhibiting the biogenesis of exosomes is promising but challenging. Im et al. (2019) reported that the antibacterial drug sulfisoxazole exerted an antitumor effect by inhibiting the secretion of breast cancer cell exosomes. However, Fonseka et al. (2021) recently found that treating cancer cells with sulfisoxazole did not reduce the number of exosomes. This may be due to discrepancies between the two studies, such as cell lines from different passages or different equipment. Overall, drug incubation studies point to the inhibition or promotion of exosome release. This strategy is still in its infancy and requires more extensive experimental and clinical verifications in the future.

Application of Exosomes as Delivery Vehicles

In recent decades, synthetic nanoparticles (NPs) including liposomes, nanosponges, and self-assembling peptides have been widely studied for nanomedicine, especially targeted cancer therapy (Allahyari et al., 2019; Crommelin et al., 2020; Wang et al., 2021). Due to the heterogeneity of target cancer cells, the differences in biological barriers and immune systems between human and animal models, exogenous nanomaterials used to deliver drugs to target sites are facing many obstacles (Ben-David et al., 2017). One approach to overcome the limitations of synthetic NPs is developing natural carriers. Extensive evidence shows that exosomes are able to pass through lipid bilayer cell membranes, aided by their low immunogenicity, high biocompatibility, high delivery efficiency, and good stability in circulation. This property supports the potential of exosomes in drug or gene delivery.

Packing exosomes with small molecule chemotherapeutic drugs have been increasingly reported. Since the chemoresistant cells easily flush out the drugs, researchers collected the supernatant of the chemoresistant cells treated with paclitaxel and centrifuged to obtain paclitaxel-loaded exosomes to simply complete the drug loading (Yamagishi et al., 2013). It is worth mentioning that, loading drugs into exosomes improved drug stability and bioavailability and maximized their effect on target lesions. For example, Kim et al. (2016) demonstrated that, in drug-resistant cells, the incorporation of paclitaxel into exosomes increased cytotoxicity by more than 50 times, with carrier exosomes co-localizing almost completely with cancer cells. Although exosomes as delivery vehicles have achieved encouraging results in previous studies, the clinical transformation of exosomes is being challenged by large-scale production, purification, drug loading and storage. In addition, the heterogeneity between exosomes subgroups greatly hinders the quality control of manufacturing and clinical translation. In view of the shortcomings of natural exosomes, more and more researchers have developed artificial exosomes through nanobiotechnology, which brought great hope for the advanced drug delivery combined with the advantages of natural and synthetic NPs (Li et al., 2021). Given that the dissemination of exosomal cargo mediates the development of chemoresistance in tumor cells, exploring the exosomal contents may open a new avenue for the reversal of chemoresistance. Wu et al. (2020) found that upregulation of miR-193a in exosomes derived from bone marrow mesenchymal stem cells reduced cisplatin resistance of non-small cell lung cancer cells by targeting leucine-rich repeat containing 1. To improve the efficacy of cancer treatment, the above two strategies were combined. For example, miR-21 can induce 5-fluoro-2,4(1H,3H)-pyrimidinedione (5-FU) resistance in CRC cells. Liang et al. (2020) used electroporation to load miR-21 inhibitor and 5-FU into exosomes to generate a co-delivery system (THLG-EXO/5-FU/miR-21i). The latter effectively reversed drug resistance and significantly enhanced cytotoxicity in chemoresistant cells. Therefore, the successful delivery of conventional drugs and various genetic materials by exosomes offers a promising strategy for reversing chemoresistance.

USE OF EXOSOMES AS BIOMARKERS IN LIQUID BIOPSY TO MONITOR CHEMORESISTANCE

Exosomes contain a series of biomolecules, including membrane-bound proteins and soluble proteins, miRNAs, non-coding RNAs, and lipids, which are good sources of biomarkers for

cancer diagnosis and monitoring of cancer progression. Liquid biopsy allows the detection of cancer or other biomarkers in blood, urine, and other body fluids. It serves to detect the occurrence of diseases, tracks cancer progression, and predicts chemoresistance (Johann et al., 2018). Compared with traditional cancer diagnosis methods, liquid biopsy improves diagnostic precision, reduces the harm and discomfort of solid tissue biopsy, and potentially prolongs patients' survival. Commonly, liquid biopsy includes detecting circulating tumor cells (CTCs), circulating tumor DNA (ctDNA), and exosomes (Nimir et al., 2019). The use of exosomes for liquid biopsy has attracted growing attention owing to (1) high sensitivity and specificity compared to that of traditional methods, (2) detection in various body fluids via non-invasive methods, (3) high stability and durability in the extracellular environment, and (4) an indication of the physiological and pathological state of parent cells. Therefore, the use of exosomal biomarkers represents an important clinical advancement in precision medicine (Tai et al., 2018). Indeed, some diagnostic kits based on exosomes have been approved by the US Food and Drug Administration (FDA) and are currently being used for clinical diagnosis (Xiao et al., 2020).

Although promising results have been achieved in targeted cancer therapy and immunotherapy, the gradual development of chemoresistance poses a significant risk to patients' overall survival. In addition to understanding the mechanism of drug resistance and overcoming chemoresistance, the identification of suitable biomarkers helps adjust drug regimens at the earliest sign of resistance. Accumulating evidence shows that nucleic acids and proteins in exosomes are useful biomarkers for the detection of drug resistance in patients during chemotherapy (**Table 3**; Lobb et al., 2017; Lei et al., 2018; Zhang W. et al., 2018). In the quest for chemoresistance biomarkers, exosomes have been extracted from cancer cell lines, animal models, and clinical samples. To this end, high-throughput proteomics and genomics have been performed to identify proteins and/or RNAs expressed differently in exosomes secreted by chemosensitive vs. chemoresistant cells. Future experiments will determine whether certain proteins and RNAs are suitable to be used as potential biomarkers of chemoresistance in clinical settings, thus providing new strategies for targeted cancer treatment.

Exosomal Contents as Diagnostic Biomarkers for Chemoresistance

Both preclinical and clinical studies have reported the use of exosomes as biomarkers to predict cancer chemoresistance in liquid biopsy. Yang S. J. et al. (2017) demonstrated that exosomes transferred glutathione S-transferase P1 (GSTP1) from breast cancer resistant cells to sensitive cells, thereby increasing resistance to ADM. Therefore, GSTP1 can be used as a biomarker to predict anthracycline/taxane-based chemoresistance in breast cancer treatment. Hu et al. (2019) reported the elevated miR-92a-3p expression in exosomes secreted by CAFs in a study of metastatic and chemoresistant CRC patients. These exosomes promoted cancer metastasis and chemoresistance by increasing stem cell subsets and EMT of CRC cells. Accordingly, these miRNAs in CAF-exosomes hold potential as biomarkers to monitor cancer cell proliferation and chemoresistance (Hu et al., 2019).

Exosomes From Different Body Fluids as Biomarkers for Chemoresistance Diagnosis

In recent years, the use of exosomal biomarkers in urine and blood samples has become more widespread. Exosomes in urine are often used as biomarkers for the detection of prostate, bladder, kidney, and other urinary system cancers. Comparing lipid composition of urine exosomes prostate cancer patients with normal healthy subjects, Skotland et al. (2017b) found that such lipids are useful biomarkers to diagnose and track the progress of prostate cancer. Xu et al. (2019) found that the exosomes containing lncPSMA3 and proteasome subunit α7-encoding PSMA3-AS1 promoted resistance to protease inhibitors by multiple myeloma. The newly identified PSMA3/PSMA3-AS1 signaling pathway in exosomes may serve as a new therapeutic target for protease inhibitor resistance or as a biomarker for the detection of chemoresistance (Xu et al., 2019). However, blood contains a large number of proteins, making the detection of poorly expressed biomarkers difficult. Unlike blood, exosomes in saliva can be easily detected. Sun et al. (2018) identified 785 highly stable and biologically active proteins in salivary exosomes. They also demonstrated that salivary exosomal proteins could be used for the non-invasive detection of lung cancer (Sun et al., 2018). Blood-derived molecules can enter salivary glands through a transcellular or cell bypass, suggesting the use of exosomes in saliva as biomarkers of cancer progression (Yoshizawa et al., 2013). Lin et al. (2019) discussed the potential clinical application of GOLM1-NAA35 chimeric RNA (seG-NchiRNA) from salivary exosomes in ESCC and found that it could help monitor tumorigenesis and sensitivity. Exosomes in urine, blood, and saliva are useful sources as biomarkers, whereas exosomes in other body fluids, such as ascites, breast milk, and cerebrospinal fluid, can also serve as biomarkers in liquid biopsy to monitor cancer chemosensitivity (**Figure 2**).

CURRENT CHALLENGES AND FUTURE PROSPECTS

The Challenges of Applying Exosomes in Cancer Chemoresistance

At present, research on the mechanism of exosome-mediated chemoresistance is still in its infancy. The lack of biomarkers for predicting chemoresistance and methods to reverse resistance is one of the greatest challenges facing the field of cancer research. In clinical practice, further research is needed on the proteins and nucleic acids used as biomarkers to diagnose drug resistance in patients. However, the most important challenges are two-fold: (i) a lack of standardized methods for the separation and purification of exosomes and (ii) the difficulty in quantifying exosomes in different body fluids.

According to the 2015 Global International Society for Extracellular Vesicles (ISEV) survey, ultracentrifugation,

TABLE 3 | Potential exosome molecular biomarkers used in chemoresistance.

Cancer type	Exosome biomarker	Drug-mediated resistance	Investigation model	References
Lung cancer	RNA-based: miR-222-3p	Gemcitabine	A549-GR and A549-P cell lines, female severe combined immunodeficient (SCID) mice (*n* = 12), and human blood samples (*n* = 50)	Wei et al., 2017
	RNA-based: miR-214	Gefitinib	PC-9 and PC-9GR cell lines and male BALB/c nu/nu mice (*n* = 20)	Zhang Y. et al., 2018
	RNA-based: miR-100-5p	Cisplatin	A549 and A549/DDP cells lines and BABL/c athymic nude mice (*n* = 25)	Qin et al., 2017
	RNA-based: mRNA ZEB1	Multidrug	HBEC and HBECs with p53 knockdown, KRASV12 overexpression, and LKB1 knockdown cell lines	Lobb et al., 2017
	RNA-based: lncRNA H19	Gefitinib	HCC827 and HCC4006 cell lines	Lei et al., 2018
	RNA-based: lncRNA RP11-838N2.4	Erlotinib	HCC827, HCC827/R, HCC4006, and HCC4006/R cells line and serum samples (*n* = 78)	Zhang W. et al., 2018
	RNA-based: miRNA-146a-5p	Gemcitabine	Serum samples (*n* = 100) and paraffin sections of lung cancer tissues (*n* = 12)	Yuwen et al., 2017
	RNA-based: miRNA-425-3p	Cisplatin	A549, PC-9, SPCA1, H1299, H1650, H1703, H1975, and A549/DDP cell lines, serum samples (*n* = 114), and paraffin sections of lung cancer tissues (*n* = 203)	Yuwen et al., 2019
	RNA-based: lncRNA SNHG14	Trastuzumab	SKBR-3, BT474, SKBR-3/Tr, and BT474/Tr cell lines and serum samples (*n* = 72)	Dong et al., 2018
	Protein-based: *P*-gp	ADM/Docetaxel	MCF7/WT and MCF7/ADM cell lines and plasma samples (*n* = 93)	Ning et al., 2017
	Protein-based: HER2	Trastuzumab	SKBR3, BT474, and MDA-MB-231 cell lines	Ciravolo et al., 2012
	RNA-based: mRNA UCH-L1	ADM	MCF7/WT and MCF7/ADM cell lines and plasma samples (*n* = 93)	Ning et al., 2017
Ovarian cancer	RNA-based: miR-1246	Paclitaxel	HeyA8, SKOV3-ip1, A2780, HeyA8-MDR, SKOV3-TR, A2780-CP20, THP-1, and HIO180 cell lines and female athymic nude mice (*n* = 40)	Kanlikilicer et al., 2018
	Protein-based: *P*-gp	Paclitaxel	A2780, SKOV3, MCF-7, MBA-MD-231, Hel, and THP1 cell lines and female athymic nude mice (*n* = 30)	Zhu et al., 2019
	Protein-based: Annexin A3	Platinum	SKOV3, SKOV3/Cis, SKOV3/Car, A2780, A2780/Cis, and A2780/Car cell lines and tissue samples (*n* = 42)	Yan et al., 2010
Hepatocellular cancer	RNA-based: miR-32-5p	Multidrug	Bel7402, Bel/5-FU, HEK-293T, SMCC-7721, HepG2, Hep3B, and MHCC97H cell lines and tissues samples (*n* = 72)	Fu et al., 2018
	RNA-based: linc-ROR	Doxorubicin/ Camptothecin	HepG2, PLC-PRF5, and HH cell lines	Takahashi et al., 2014
	RNA-based: lnc-VLDLR	Multidrug	HepG2, Hep3B, PLC/PRF-5, Huh-7, and MzChA-1 cell lines	Takahashi et al., 2014
	RNA-based: miR-744	Sorafenib	LO2 cell line and tissue samples (*n* = 120)	Wang et al., 2019

ADM, adriamycin; HER2, human epidermal growth factor receptor-2.

polymer precipitation, immunomagnetic beads, and size exclusion chromatography are the most commonly used exosome separation techniques. However, these methods have several limitations, including cumbersome and complex operational steps, the need for expensive equipment, and low separation purity (Gardiner et al., 2016). Although ultracentrifugation is the "gold standard" for exosome separation, it causes protein contamination (Caradec et al., 2014). According to the ISEV 2018 guidelines, to achieve better specificity in exosome separation, more than one technique should be applied after the primary step, including chromatography, washing in EV-free buffer, ultrafiltration, or the application of density gradients (Thery et al., 2018). The emergence of new technologies is providing novel solutions for efficient exosome separation. Microfluidic technology has attracted attention due to its high speed, high purity, short time, and ability to process small-volume samples (Yang F. et al., 2017). Currently, microfluidic exosome separation methods comprise three categories: size-based separation, immunoaffinity-based separation, and dynamic exosome separation. Immunoaffinity-based microfluidic exosome separation has been successful for the clinical detection of cancers, thus providing a new analysis platform for cancer diagnosis and molecular typing (Yang F. et al., 2017). However, although microfluidic-based exosome separation methods have great potential, they are still in the early stages of development.

The exact quantification of exosomes remains a challenge, among other things, because their average concentration varies across body fluids (e.g., plasma, saliva, urine, and lymph). Eitan et al. (2017) determined that the average concentration of exosomes isolated from human plasma was between 1×10^9 and

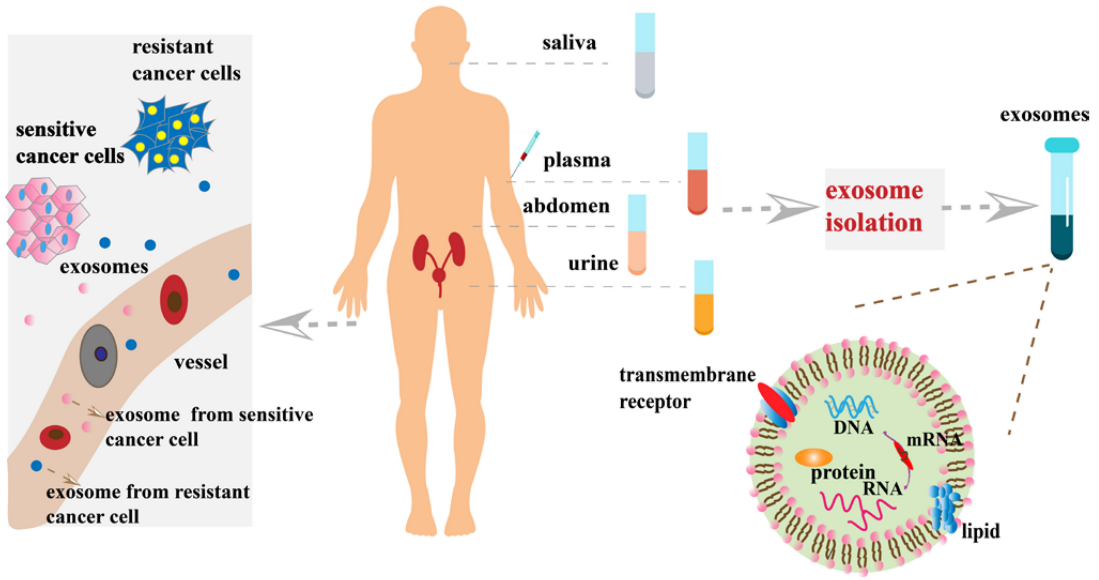

FIGURE 2 | Exosome-based analytes of liquid biopsies. At the primary cancer site, resistant cancer cells and sensitive cancer cells secrete large numbers of exosomes into the blood stream and/or invade adjacent blood vessels. Exosomes present in various body fluids (e.g., plasma, saliva, and urine) can then be separated by various methods for cancer diagnosis and monitoring progression.

3×10^{12} particles per mL. Similarly, the average concentration of exosomes was estimated to be between 2×10^{8} and 1×10^{9} in urine and between 1×10^{11} and 2×10^{12} particles per mL in lymph (Eitan et al., 2017; Gheinani et al., 2018; Broggi et al., 2019). Most clinical studies are based on very small sample sizes. However, biomarkers must be validated in large sample size studies before they are converted into clinical application tools. This requires highly specific and sensitive surface markers, which are difficult to identify for most cancer types. Another solution is to select different body fluids for exosome detection based on cancer type. Compared with peripheral blood, the pulmonary vein blood of lung cancer patients is significantly enriched with tumor-derived exosomes (Navarro et al., 2019). Similarly, Matsumura et al. (2019) demonstrated that tumor-derived exosomes were significantly enriched in the lymph compared to the plasma of melanoma patients, and lymphatic vessels were the main route of tumor tissue transport to the blood. Generally, clinical application of exosome technology could lead to numerous new discoveries and procedures.

Application Prospects of Exosomes in the Field of Cancer Chemoresistance

Exosomes have broad application potential in chemoresistance, including as biomarkers in liquid biopsy to monitor the development of chemoresistance, in the study of chemoresistance mechanisms, and in the development of new strategies for reversing chemoresistance.

Exosomes can be used as biomarkers in liquid biopsies to monitor whether cancer is resistant to chemotherapy. Traditional tissue biopsy is invasive and painful for patients, requiring repeated sampling, and hindering dynamic monitoring. The rapid development of liquid biopsy technology has paved the way for the continuous and accurate monitoring of cancer development. Because exosomes carry proteins, RNAs, and DNAs of the parent cells, they have become the "third carriage" in the field of liquid biopsy after ctDNA and CTC. Compared with ctDNA and CTC, exosomes have the advantages of comprising richer sample forms, providing more comprehensive information, harboring more stable contents, and having enormous potential and clinical application prospects. Nucleic acids and proteins in exosomes mediate the development of chemoresistance in cancer cells, and their differential expression are useful as a guide for cancer chemosensitivity, allowing clinicians to formulate a reasonable chemotherapy plan.

By exploring the mechanism of chemoresistance, new strategies for the reversal of cancer drug resistance can be developed. Exosomes, together with their nucleic acids and proteins, were previously found to mediate intercellular signal transduction and activate intracellular signaling pathways through fusion or interaction with target cells, including cancer cells. Following this approach, researchers can "take the essence and get rid of the dregs." Liu T. et al. (2019) found that the expression of miR-128-3p was significantly lower in oxaliplatin CRC cells than in parent cells. *In vivo* and *in vitro* experiments have shown that miR-128-3p reduced chemoresistance of CRC to oxaliplatin. Subsequently, co-culture of drug-resistant CRC cells with exosomes successfully transfected with miR-128-3p increased the cells' sensitivity to oxaliplatin (Liu T. et al., 2019).

In recent years, exosomes have opened up a new frontier for nano-delivery vehicles and also provided a new strategy for reversing chemoresistance due to their unique advantages (Tian et al., 2014; Logozzi et al., 2021). Compared to synthetic nanoparticles, exosomes have many advantages: (1) exosomes

can overcome biological barriers due to their small size, and have high biocompatibility and cellular uptake ability due to the membrane protein (Mulcahy et al., 2014); (2) due to proteins and lipids, exosomes as a vectorized signaling device that appears more efficient than a soluble agonist (Huber et al., 2005); (3) exosomes also have high stability, tissue specific targeting, and drug delivery through exosomes can avoid phagocytosis or degradation of macrophages (Sun et al., 2010; Haney et al., 2015). Although exosomes have these advantages, they still face many challenges as nano-delivery vehicles. At the beginning of the research, the efficiency of the simple incubation method was too low and very limited in the type of cargo to be loaded. Various improvement strategies such as electroporation, transfection, and sonication have been developed for loading therapeutic cargoes into exosomes. Tian et al. (2014) showed that doxorubicin is loaded onto iRGD peptide functional exosomes by electroporation, and the drug loading efficiency is as high as 20-fold. Due to the presence of iRGD peptide, exosomes show high tumor targeting ability and anti-tumor efficacy in *in vitro* and *in vivo* experiments (Tian et al., 2014). Another major obstacle for the clinical translation of exosomes is their low yields. In most experimental studies, exosomes are obtained through cell culture. However, the obtained exosomes are difficult to meet the clinical needs. To overcome this limitation, some researchers have found that food contains a lot of exosomes (Del et al., 2021). Compared to cell culture, milk-derived exosomes showed a 1000-fold higher yield (Betker et al., 2019; Munir et al., 2020). There are also researchers who fused exosomes and liposomes to design hybrid therapeutic nanovesicles. Cheng et al. combined the characteristics of exosomes and thermosensitive liposomes, and demonstrated the potential of hybrid nanovesicles that block CD47 immune checkpoints in drug delivery in cancer treatment (Cheng et al., 2021). Therefore, although exosomes as nano-delivery vehicles have a bright future, it is still in its infancy, and further research is needed to achieve clinical application.

Compared with nucleic acids and proteins, exosomal lipids have not been extensively studied, even though they play an important role in tumorigenesis and development. Record et al. (2014) found that exosomes rich in prostaglandin participated in cancer immune escape and promoted tumor growth. After prostaglandin is taken up by cells, it promotes phospholipid metabolism and changes the fatty acid oxidation state of target cells, thereby promoting cancer cell migration (Record et al., 2014). Aung et al. (2011) found that lipids in exosomes induced rituximab resistance in B-cell lymphoma. Skotland et al. (2017a) demonstrated that lipids in exosomes could be used as biomarkers for the diagnosis of prostate cancer. Therefore, besides their use as biomarkers, exosome lipids have a strong potential as mediators of chemoresistance. More and detailed work are warranted for studying the role of exosomes in regulating chemoresistance via lipids.

CONCLUSION

Chemoresistance is one of the main obstacles to successful cancer treatment. In recent years, exosomes have attracted attention for their role in cancer occurrence and development. They act by transmitting chemoresistance phenotypes and reducing intracellular drug concentration. The differential expression of nucleic acids and proteins in exosomes reflects the physiological and pathological conditions of cells. By the same token, exosomes could also be used to reverse chemoresistance and function as biomarkers to monitor drug resistance in cancer cells. However, our understanding of the role of exosomes in cancer chemoresistance remains limited. Furthermore, the study of exosomes faces huge challenges. As such, the successful transition of exosome research into clinical practice requires the continuous efforts of medical researchers and clinical staff.

AUTHOR CONTRIBUTIONS

JL, YL, and TF conceived the manuscript. JL wrote the manuscript and prepared the figures. NG, ZG, WL, BP, XD, YL, and TF revised the manuscript. All the authors read and approved the final manuscript.

FUNDING

This work was supported by the Key Scientific Research Projects of Colleges and Universities in Henan Province (Grant No. 20A310021 TF) and the Natural Science Foundation of Henan Province (212300410393).

REFERENCES

Alharbi, M., Zuniga, F., Elfeky, O., Guanzon, D., Lai, A., Rice, G. E., et al. (2018). The potential role of miRNAs and exosomes in chemotherapy in ovarian cancer. *Endocr. Relat. Cancer* 25, R663–R685. doi: 10.1530/ERC-18-0019

Allahyari, S., Trotta, F., Valizadeh, H., Jelvehgari, M., and Zakeri-Milani, P. (2019). Cyclodextrin-based nanosponges as promising carriers for active agents. *Expert Opin. Drug Deliv.* 16, 467–479. doi: 10.1080/17425247.2019.1591365

Araujo, C. V., Campbell, C., Goncalves-de-Albuquerque, C. F., Molinaro, R., Cody, M. J., Yost, C. C., et al. (2016). A PPARgamma agonist enhances bacterial clearance through neutrophil extracellular trap formation and improves survival in sepsis. *Shock* 45, 393–403. doi: 10.1097/SHK.0000000000000520

Aspe, J. R., Diaz, O. C., Jutzy, J. M., Deshields, S., Whang, S., and Wall, N. R. (2014). Enhancement of Gemcitabine sensitivity in pancreatic adenocarcinoma by novel exosome-mediated delivery of the Survivin-T34A mutant. *J. Extracell. Vesicles* 3:23244. doi: 10.3402/jev.v3.23244

Au, Y. C., Co, N. N., Tsuruga, T., Yeung, T. L., Kwan, S. Y., Leung, C. S., et al. (2016). Exosomal transfer of stroma-derived miR21 confers paclitaxel resistance in ovarian cancer cells through targeting APAF1. *Nat. Commun.* 7:11150. doi: 10.1038/ncomms11150

Aung, T., Chapuy, B., Vogel, D., Wenzel, D., Oppermann, M., Lahmann, M., et al. (2011). Exosomal evasion of humoral immunotherapy in aggressive B-cell lymphoma modulated by ATP-binding cassette transporter A3. *Proc. Natl. Acad. Sci. U.S.A.* 108, 15336–15341. doi: 10.1073/pnas.1102855108

Bach, D. H., Hong, J. Y., Park, H. J., and Lee, S. K. (2017). The role of exosomes and miRNAs in drug-resistance of cancer cells. *Int. J. Cancer.* 141, 220–230. doi: 10.1002/ijc.30669

Bebawy, M., Combes, V., Lee, E., Jaiswal, R., Gong, J., Bonhoure, A., et al. (2009). Membrane microparticles mediate transfer of P-glycoprotein to drug sensitive cancer cells. *Leukemia* 23, 1643–1649. doi: 10.1038/leu.2009.76

Ben-David, U., Ha, G., Tseng, Y. Y., Greenwald, N. F., Oh, C., Shih, J., et al. (2017). Patient-derived xenografts undergo mouse-specific tumor evolution. *Nat. Genet.* 49, 1567–1575. doi: 10.1038/ng.3967

Betker, J. L., Angle, B. M., Graner, M. W., and Anchordoquy, T. J. (2019). The potential of exosomes from cow milk for oral delivery. *J. Pharm. Sci.* 108, 1496–1505. doi: 10.1016/j.xphs.2018.11.022

Binenbaum, Y., Fridman, E., Yaari, Z., Milman, N., Schroeder, A., Ben, D. G., et al. (2018). Transfer of miRNA in Macrophage-Derived exosomes induces drug resistance in pancreatic adenocarcinoma. *Cancer Res.* 78, 5287–5299. doi: 10.1158/0008-5472.CAN-18-0124

Birner, P., Toumangelova-Uzeir, K., Natchev, S., and Guentchev, M. (2010). STAT3 tyrosine phosphorylation influences survival in glioblastoma. *J. Neurooncol.* 100, 339–343. doi: 10.1007/s11060-010-0195-8

Bouvy, C., Wannez, A., Laloy, J., Chatelain, C., and Dogne, J. M. (2017). Transfer of multidrug resistance among acute myeloid leukemia cells via extracellular vesicles and their microRNA cargo. *Leuk. Res.* 62, 70–76. doi: 10.1016/j.leukres.2017.09.014

Broggi, M., Maillat, L., Clement, C. C., Bordry, N., Corthesy, P., Auger, A., et al. (2019). Tumor-associated factors are enriched in lymphatic exudate compared to plasma in metastatic melanoma patients. *J. Exp. Med.* 216, 1091–1107. doi: 10.1084/jem.20181618

Cairns, R., Papandreou, I., and Denko, N. (2006). Overcoming physiologic barriers to cancer treatment by molecularly targeting the tumor microenvironment. *Mol. Cancer Res.* 4, 61–70. doi: 10.1158/1541-7786.MCR-06-0002

Cao, Y. L., Zhuang, T., Xing, B. H., Li, N., and Li, Q. (2017). Exosomal DNMT1 mediates cisplatin resistance in ovarian cancer. *Cell Biochem. Funct.* 35, 296–303. doi: 10.1002/cbf.3276

Caradec, J., Kharmate, G., Hosseini-Beheshti, E., Adomat, H., Gleave, M., and Guns, E. (2014). Reproducibility and efficiency of serum-derived exosome extraction methods. *Clin. Biochem.* 47, 1286–1292. doi: 10.1016/j.clinbiochem.2014.06.011

Chen, W. X., Cai, Y. Q., Lv, M. M., Chen, L., Zhong, S. L., Ma, T. F., et al. (2014). Exosomes from docetaxel-resistant breast cancer cells alter chemosensitivity by delivering microRNAs. *Tumour Biol.* 35, 9649–9659. doi: 10.1007/s13277-014-2242-0

Cheng, L., Zhang, X., Tang, J., Lv, Q., and Liu, J. (2021). Gene-engineered exosomes-thermosensitive liposomes hybrid nanovesicles by the blockade of CD47 signal for combined photothermal therapy and cancer immunotherapy. *Biomaterials* 275:120964. doi: 10.1016/j.biomaterials.2021.120964

Ciravolo, V., Huber, V., Ghedini, G. C., Venturelli, E., Bianchi, F., Campiglio, M., et al. (2012). Potential role of HER2-overexpressing exosomes in countering trastuzumab-based therapy. *J. Cell. Physiol.* 227, 658–667. doi: 10.1002/jcp.22773

Crommelin, D., van Hoogevest, P., and Storm, G. (2020). The role of liposomes in clinical nanomedicine development. What now? Now what? *J. Control. Release* 318, 256–263. doi: 10.1016/j.jconrel.2019.12.023

Datta, A., Kim, H., Lal, M., McGee, L., Johnson, A., Moustafa, A. A., et al. (2017). Manumycin a suppresses exosome biogenesis and secretion via targeted inhibition of Ras/Raf/ERK1/2 signaling and hnRNP H1 in castration-resistant prostate cancer cells. *Cancer Lett.* 408, 73–81. doi: 10.1016/j.canlet.2017.08.020

Del, P. L., Hazas, M., Tome-Carneiro, J., Gil-Cabrerizo, P., San-Cristobal, R., Busto, R., et al. (2021). Bovine Milk-Derived exosomes as a drug delivery vehicle for miRNA-Based therapy. *Int. J. Mol. Sci.* 22:1105. doi: 10.3390/ijms22031105

Dong, H., Wang, W., Chen, R., Zhang, Y., Zou, K., Ye, M., et al. (2018). Exosome-mediated transfer of lncRNASNHG14 promotes trastuzumab chemoresistance in breast cancer. *Int. J. Oncol.* 53, 1013–1026. doi: 10.3892/ijo.2018.4467

Donnelly, S. R., and Moss, S. E. (1997). Annexins in the secretory pathway. *Cell. Mol. Life Sci.* 53, 533–538. doi: 10.1007/s000180050068

Eitan, E., Green, J., Bodogai, M., Mode, N. A., Baek, R., Jorgensen, M. M., et al. (2017). Age-Related changes in plasma extracellular vesicle characteristics and internalization by leukocytes. *Sci. Rep.* 7:1342. doi: 10.1038/s41598-017-01386-z

Essandoh, K., Yang, L., Wang, X., Huang, W., Qin, D., Hao, J., et al. (2015). Blockade of exosome generation with GW4869 dampens the sepsis-induced inflammation and cardiac dysfunction. *Biochim. Biophys. Acta* 1852, 2362–2371. doi: 10.1016/j.bbadis.2015.08.010

Fan, D., Ren, B., Yang, X., Liu, J., and Zhang, Z. (2016). Upregulation of miR-501-5p activates the wnt/beta-catenin signaling pathway and enhances stem cell-like phenotype in gastric cancer. *J. Exp. Clin. Cancer Res.* 35:177. doi: 10.1186/s13046-016-0432-x

Fan, J., Wei, Q., Koay, E. J., Liu, Y., Ning, B., Bernard, P. W., et al. (2018). Chemoresistance transmission via exosome-mediated EphA2 transfer in pancreatic cancer. *Theranostics* 8, 5986–5994. doi: 10.7150/thno.26650

Feinberg, A. P., Koldobskiy, M. A., and Gondor, A. (2016). Epigenetic modulators, modifiers and mediators in cancer aetiology and progression. *Nat. Rev. Genet.* 17, 284–299. doi: 10.1038/nrg.2016.13

Feng, W., Dean, D. C., Hornicek, F. J., Shi, H., and Duan, Z. (2019). Exosomes promote pre-metastatic niche formation in ovarian cancer. *Mol. Cancer* 18:124. doi: 10.1186/s12943-019-1049-4

Feng, Y., Zhong, M., Tang, Y., Liu, X., Liu, Y., Wang, L., et al. (2020). The role and underlying mechanism of exosomal CA1 in chemotherapy resistance in diffuse large b cell lymphoma. *Mol. Ther. Nucleic Acids* 21, 452–463. doi: 10.1016/j.omtn.2020.06.016

Feng, Y., Zhong, M., Zeng, S., Wang, L., Liu, P., Xiao, X., et al. (2019). Exosome-derived miRNAs as predictive biomarkers for diffuse large B-cell lymphoma chemotherapy resistance. *Epigenomics UK* 11, 35–51. doi: 10.2217/epi-2018-0123

Fonseka, P., Chitti, S. V., Sanwlani, R., and Mathivanan, S. (2021). Sulfisoxazole does not inhibit the secretion of small extracellular vesicles. *Nat. Commun.* 12:977. doi: 10.1038/s41467-021-21074-x

Fu, X., Liu, M., Qu, S., Ma, J., Zhang, Y., Shi, T., et al. (2018). Exosomal microRNA-32-5p induces multidrug resistance in hepatocellular carcinoma via the PI3K/Akt pathway. *J. Exp. Clin. Cancer Res.* 37:52. doi: 10.1186/s13046-018-0677-7

Gacche, R. N., and Assaraf, Y. G. (2018). Redundant angiogenic signaling and tumor drug resistance. *Drug Resist. Updat.* 36, 47–76. doi: 10.1016/j.drup.2018.01.002

Gardiner, C., Di Vizio, D., Sahoo, S., Thery, C., Witwer, K. W., Wauben, M., et al. (2016). Techniques used for the isolation and characterization of extracellular vesicles: results of a worldwide survey. *J. Extracell. Vesicles* 5:32945. doi: 10.3402/jev.v5.32945

Gheinani, A. H., Vogeli, M., Baumgartner, U., Vassella, E., Draeger, A., Burkhard, F. C., et al. (2018). Improved isolation strategies to increase the yield and purity of human urinary exosomes for biomarker discovery. *Sci. Rep.* 8:3945. doi: 10.1038/s41598-018-22142-x

Gottesman, M. M. (2002). Mechanisms of cancer drug resistance. *Annu. Rev. Med.* 53, 615–627. doi: 10.1146/annurev.med.53.082901.103929

Gu, L., Xu, Y., Xu, W., Li, M., Su, H., Li, C., et al. (2020). The exosome secretion inhibitor neticonazole suppresses intestinal dysbacteriosis-induced tumorigenesis of colorectal cancer. *Invest. New Drugs* 38, 221–228. doi: 10.1007/s10637-019-00759-7

Han, M., Hu, J., Lu, P., Cao, H., Yu, C., Li, X., et al. (2020). Exosome-transmitted miR-567 reverses trastuzumab resistance by inhibiting ATG5 in breast cancer. *Cell Death Dis.* 11:43. doi: 10.1038/s41419-020-2250-5

Han, Z., Lee, S., Je, S., Eom, C. Y., Choi, H. J., Song, J. J., et al. (2016). Survivin silencing and TRAIL expression using oncolytic adenovirus increase anti-tumorigenic activity in gemcitabine-resistant pancreatic cancer cells. *Apoptosis* 21, 351–364. doi: 10.1007/s10495-015-1208-z

Haney, M. J., Klyachko, N. L., Zhao, Y., Gupta, R., Plotnikova, E. G., He, Z., et al. (2015). Exosomes as drug delivery vehicles for Parkinson's disease therapy. *J. Control Release* 207, 18–30. doi: 10.1016/j.jconrel.2015.03.033

Hoshino, A., Costa-Silva, B., Shen, T. L., Rodrigues, G., Hashimoto, A., Tesic, M. M., et al. (2015). Tumour exosome integrins determine organotropic metastasis. *Nature* 527, 329–335. doi: 10.1038/nature15756

Housman, G., Byler, S., Heerboth, S., Lapinska, K., Longacre, M., Snyder, N., et al. (2014). Drug resistance in cancer: an overview. *Cancers* 6, 1769–1792. doi: 10.3390/cancers6031769

Hu, J. L., Wang, W., Lan, X. L., Zeng, Z. C., Liang, Y. S., Yan, Y. R., et al. (2019). CAFs secreted exosomes promote metastasis and chemotherapy resistance by enhancing cell stemness and epithelial-mesenchymal transition in colorectal cancer. *Mol. Cancer* 18:91. doi: 10.1186/s12943-019-1019-x

Hu, Y., Xu, K., and Yague, E. (2015). MiR-218 targets survivin and regulates resistance to chemotherapeutics in breast cancer. *Breast Cancer Res. Treat.* 151, 269–280. doi: 10.1007/s10549-015-3372-9

Huang, L., Wang, Y., Chen, J., Wang, Y., Zhao, Y., Wang, Y., et al. (2019). Long noncoding RNA PCAT1, a novel serum-based biomarker, enhances cell growth by sponging miR-326 in oesophageal squamous cell carcinoma. *Cell Death Dis.* 10:513. doi: 10.1038/s41419-019-1745-4

Huber, V., Fais, S., Iero, M., Lugini, L., Canese, P., Squarcina, P., et al. (2005). Human colorectal cancer cells induce T-cell death through release of proapoptotic microvesicles: role in immune escape. *Gastroenterology* 128, 1796–1804. doi: 10.1053/j.gastro.2005.03.045

Hui, L., and Chen, Y. (2015). Tumor microenvironment: sanctuary of the devil. *Cancer Lett.* 368, 7–13. doi: 10.1016/j.canlet.2015.07.039

Im, E. J., Lee, C. H., Moon, P. G., Rangaswamy, G. G., Lee, B., Lee, J. M., et al. (2019). Sulfisoxazole inhibits the secretion of small extracellular vesicles by targeting the endothelin receptor a. *Nat. Commun.* 10:1387. doi: 10.1038/s41467-019-09387-4

Ji, R., Zhang, X., Gu, H., Ma, J., Wen, X., Zhou, J., et al. (2019). MiR-374a-5p: a new target for diagnosis and drug resistance therapy in gastric cancer. *Mol. Ther. Nucleic Acids* 18, 320–331. doi: 10.1016/j.omtn.2019.07.025

Jin, B., Liu, Y., and Wang, H. (2015). Antagonism of miRNA-21 sensitizes human gastric cancer cells to paclitaxel. *Cell Biochem. Biophys.* 72, 275–282. doi: 10.1007/s12013-014-0450-2

Johann, D. J., Steliga, M., Shin, I. J., Yoon, D., Arnaoutakis, K., Hutchins, L., et al. (2018). Liquid biopsy and its role in an advanced clinical trial for lung cancer. *Exp. Biol. Med.* 243, 262–271. doi: 10.1177/1535370217750087

Johnstone, R. M. (1992). The Jeanne Manery-Fisher Memorial Lecture 1991. Maturation of reticulocytes: formation of exosomes as a mechanism for shedding membrane proteins. *Biochem. Cell Biol.* 70, 179–190. doi: 10.1139/o92-028

Kang, M., Ren, M., Li, Y., Fu, Y., Deng, M., and Li, C. (2018). Exosome-mediated transfer of lncRNA PART1 induces gefitinib resistance in esophageal squamous cell carcinoma via functioning as a competing endogenous RNA. *J. Exp. Clin. Cancer Res.* 37:171. doi: 10.1186/s13046-018-0845-9

Kanlikilicer, P., Bayraktar, R., Denizli, M., Rashed, M. H., Ivan, C., Aslan, B., et al. (2018). Exosomal miRNA confers chemo resistance via targeting Cav1/p-gp/M2-type macrophage axis in ovarian cancer. *EBioMedicine* 38, 100–112. doi: 10.1016/j.ebiom.2018.11.004

Kato, T., Mizutani, K., Kameyama, K., Kawakami, K., Fujita, Y., Nakane, K., et al. (2015). Serum exosomal P-glycoprotein is a potential marker to diagnose docetaxel resistance and select a taxoid for patients with prostate cancer. *Urol. Oncol.* 33, 315–385. doi: 10.1016/j.urolonc.2015.04.019

Kim, M. S., Haney, M. J., Zhao, Y., Mahajan, V., Deygen, I., Klyachko, N. L., et al. (2016). Development of exosome-encapsulated paclitaxel to overcome MDR in cancer cells. *Nanomedicine* 12, 655–664. doi: 10.1016/j.nano.2015.10.012

Kitano, H. (2004). Cancer as a robust system: implications for anticancer therapy. *Nat. Rev. Cancer* 4, 227–235. doi: 10.1038/nrc1300

Kreger, B. T., Johansen, E. R., Cerione, R. A., and Antonyak, M. A. (2016). The enrichment of survivin in exosomes from breast cancer cells treated with paclitaxel promotes cell survival and chemoresistance. *Cancers* 8:111. doi: 10.3390/cancers8120111

Lei, Y., Guo, W., Chen, B., Chen, L., Gong, J., and Li, W. (2018). Tumorreleased lncRNA H19 promotes gefitinib resistance via packaging into exosomes in nonsmall cell lung cancer. *Oncol. Rep.* 40, 3438–3446. doi: 10.3892/or.2018.6762

Li, Y. J., Wu, J. Y., Liu, J., Xu, W., Qiu, X., Huang, S., et al. (2021). Artificial exosomes for translational nanomedicine. *J. Nanobiotechnol.* 19:242. doi: 10.1186/s12951-021-00986-2

Liang, G., Zhu, Y., Ali, D. J., Tian, T., Xu, H., Si, K., et al. (2020). Engineered exosomes for targeted co-delivery of miR-21 inhibitor and chemotherapeutics to reverse drug resistance in colon cancer. *J. Nanobiotechnol.* 18:10. doi: 10.1186/s12951-019-0563-2

Lin, Y., Dong, H., Deng, W., Lin, W., Li, K., Xiong, X., et al. (2019). Evaluation of salivary exosomal chimeric GOLM1-NAA35 RNA as a potential biomarker in esophageal carcinoma. *Clin. Cancer Res.* 25, 3035–3045. doi: 10.1158/1078-0432.CCR-18-3169

Liu, T., Chen, G., Sun, D., Lei, M., Li, Y., Zhou, C., et al. (2017). Exosomes containing miR-21 transfer the characteristic of cisplatin resistance by targeting PTEN and PDCD4 in oral squamous cell carcinoma. *Acta Biochim. Biophys. Sin.* 49, 808–816. doi: 10.1093/abbs/gmx078

Liu, T., Zhang, X., Du, L., Wang, Y., Liu, X., Tian, H., et al. (2019). Exosome-transmitted miR-128-3p increase chemosensitivity of oxaliplatin-resistant colorectal cancer. *Mol. Cancer* 18:43. doi: 10.1186/s12943-019-0981-7

Liu, X., Lu, Y., Xu, Y., Hou, S., Huang, J., Wang, B., et al. (2019). Exosomal transfer of miR-501 confers doxorubicin resistance and tumorigenesis via targeting of BLID in gastric cancer. *Cancer Lett.* 459, 122–134. doi: 10.1016/j.canlet.2019.05.035

Lobb, R. J., van Amerongen, R., Wiegmans, A., Ham, S., Larsen, J. E., and Moller, A. (2017). Exosomes derived from mesenchymal non-small cell lung cancer cells promote chemoresistance. *Int. J. Cancer* 141, 614–620. doi: 10.1002/ijc.30752

Logozzi, M., Di Raimo, R., Mizzoni, D., and Fais, S. (2021). What we know on the potential use of exosomes for nanodelivery. *Semin. Cancer Biol.* [Epub ahead of print]. doi: 10.1016/j.semcancer.2021.09.005

Lu, J. F., Luk, F., Gong, J., Jaiswal, R., Grau, G. E., and Bebawy, M. (2013). Microparticles mediate MRP1 intercellular transfer and the re-templating of intrinsic resistance pathways. *Pharmacol. Res.* 76, 77–83. doi: 10.1016/j.phrs.2013.07.009

Luberto, C., Hassler, D. F., Signorelli, P., Okamoto, Y., Sawai, H., Boros, E., et al. (2002). Inhibition of tumor necrosis factor-induced cell death in MCF7 by a novel inhibitor of neutral sphingomyelinase. *J. Biol. Chem.* 277, 41128–41139. doi: 10.1074/jbc.M206747200

Lv, M. M., Zhu, X. Y., Chen, W. X., Zhong, S. L., Hu, Q., Ma, T. F., et al. (2014). Exosomes mediate drug resistance transfer in MCF-7 breast cancer cells and a probable mechanism is delivery of P-glycoprotein. *Tumour Biol.* 35, 10773–10779. doi: 10.1007/s13277-014-2377-z

Matsumura, S., Minamisawa, T., Suga, K., Kishita, H., Akagi, T., Ichiki, T., et al. (2019). Subtypes of tumour cell-derived small extracellular vesicles having differently externalized phosphatidylserine. *J. Extracell. Vesicles* 8:1579541. doi: 10.1080/20013078.2019.1579541

Milman, N., Ginini, L., and Gil, Z. (2019). Exosomes and their role in tumorigenesis and anticancer drug resistance. *Drug Resist. Update* 45, 1–12. doi: 10.1016/j.drup.2019.07.003

Min, Q. H., Wang, X. Z., Zhang, J., Chen, Q. G., Li, S. Q., Liu, X. Q., et al. (2018). Exosomes derived from imatinib-resistant chronic myeloid leukemia cells mediate a horizontal transfer of drug-resistant trait by delivering miR-365. *Exp. Cell Res.* 362, 386–393. doi: 10.1016/j.yexcr.2017.12.001

Mulcahy, L. A., Pink, R. C., and Carter, D. R. (2014). Routes and mechanisms of extracellular vesicle uptake. *J. Extracell. Vesicles* 3:24641. doi: 10.3402/jev.v3.24641

Munir, J., Lee, M., and Ryu, S. (2020). Exosomes in food: health benefits and clinical relevance in diseases. *Adv. Nutr.* 11, 687–696. doi: 10.1093/advances/nmz123

Namee, N. M., and O'Driscoll, L. (2018). Extracellular vesicles and anti-cancer drug resistance. *Biochim. Biophys. Acta Rev. Cancer* 1870, 123–136. doi: 10.1016/j.bbcan.2018.07.003

Navarro, A., Molins, L., Marrades, R. M., Moises, J., Vinolas, N., Morales, S., et al. (2019). Exosome analysis in Tumor-Draining pulmonary vein identifies NSCLC patients with higher risk of relapse after curative surgery. *Cancers* 11:249. doi: 10.3390/cancers11020249

Nimir, M., Ma, Y., Jeffreys, S. A., Opperman, T., Young, F., Khan, T., et al. (2019). Detection of AR-V7 in liquid biopsies of castrate resistant prostate cancer patients: a comparison of AR-V7 analysis in circulating tumor cells, circulating tumor RNA and exosomes. *Cells* 8:688. doi: 10.3390/cells8070688

Ning, K., Wang, T., Sun, X., Zhang, P., Chen, Y., Jin, J., et al. (2017). UCH-L1-containing exosomes mediate chemotherapeutic resistance transfer in breast cancer. *J. Surg. Oncol.* 115, 932–940. doi: 10.1002/jso.24614

O'Brien, K., Rani, S., Corcoran, C., Wallace, R., Hughes, L., Friel, A. M., et al. (2013). Exosomes from triple-negative breast cancer cells can transfer phenotypic traits representing their cells of origin to secondary cells. *Eur. J. Cancer* 49, 1845–1859. doi: 10.1016/j.ejca.2013.01.017

Ombrato, L., Nolan, E., Kurelac, I., Mavousian, A., Bridgeman, V. L., Heinze, I., et al. (2019). Metastatic-niche labelling reveals parenchymal cells with stem features. *Nature* 572, 603–608. doi: 10.1038/s41586-019-1487-6

Patel, G. K., Khan, M. A., Bhardwaj, A., Srivastava, S. K., Zubair, H., Patton, M. C., et al. (2017). Exosomes confer chemoresistance to pancreatic cancer cells by promoting ROS detoxification and miR-155-mediated suppression of

key gemcitabine-metabolising enzyme, DCK. *Br. J. Cancer* 116, 609–619. doi: 10.1038/bjc.2017.18

Pathan, M., Fonseka, P., Chitti, S. V., Kang, T., Sanwlani, R., Van Deun, J., et al. (2019). Vesiclepedia 2019: a compendium of RNA, proteins, lipids and metabolites in extracellular vesicles. *Nucleic Acids Res.* 47, D516–D519. doi: 10.1093/nar/gky1029

Pilzer, D., and Fishelson, Z. (2005). Mortalin/GRP75 promotes release of membrane vesicles from immune attacked cells and protection from complement-mediated lysis. *Int. Immunol.* 17, 1239–1248. doi: 10.1093/intimm/dxh300

Pink, R. C., Samuel, P., Massa, D., Caley, D. P., Brooks, S. A., and Carter, D. R. (2015). The passenger strand, miR-21-3p, plays a role in mediating cisplatin resistance in ovarian cancer cells. *Gynecol. Oncol.* 137, 143–151. doi: 10.1016/j.ygyno.2014.12.042

Qin, X., Guo, H., Wang, X., Zhu, X., Yan, M., Wang, X., et al. (2019). Exosomal miR-196a derived from cancer-associated fibroblasts confers cisplatin resistance in head and neck cancer through targeting CDKN1B and ING5. *Genome Biol.* 20:12. doi: 10.1186/s13059-018-1604-0

Qin, X., Yu, S., Zhou, L., Shi, M., Hu, Y., Xu, X., et al. (2017). Cisplatin-resistant lung cancer cell-derived exosomes increase cisplatin resistance of recipient cells in exosomal miR-100-5p-dependent manner. *Int. J. Nanomedicine* 12, 3721–3733. doi: 10.2147/IJN.S131516

Qu, L., Ding, J., Chen, C., Wu, Z. J., Liu, B., Gao, Y., et al. (2016). Exosome-Transmitted lncARSR promotes sunitinib resistance in renal cancer by acting as a competing endogenous RNA. *Cancer Cell* 29, 653–668. doi: 10.1016/j.ccell.2016.03.004

Record, M., Carayon, K., Poirot, M., and Silvente-Poirot, S. (2014). Exosomes as new vesicular lipid transporters involved in cell-cell communication and various pathophysiologies. *Biochim. Biophys. Acta* 1841, 108–120. doi: 10.1016/j.bbalip.2013.10.004

Ren, B., Cui, M., Yang, G., Wang, H., Feng, M., You, L., et al. (2018). Tumor microenvironment participates in metastasis of pancreatic cancer. *Mol. Cancer* 17:108. doi: 10.1186/s12943-018-0858-1

Ren, W., Fan, H., Grimm, S. A., Guo, Y., Kim, J. J., Yin, J., et al. (2020). Direct readout of heterochromatic H3K9me3 regulates DNMT1-mediated maintenance DNA methylation. *Proc. Natl. Acad. Sci. U.S.A.* 117, 18439–18447. doi: 10.1073/pnas.2009316117

Richards, K. E., Zeleniak, A. E., Fishel, M. L., Wu, J., Littlepage, L. E., and Hill, R. (2017). Cancer-associated fibroblast exosomes regulate survival and proliferation of pancreatic cancer cells. *Oncogene* 36, 1770–1778. doi: 10.1038/onc.2016.353

Safaei, R., Larson, B. J., Cheng, T. C., Gibson, M. A., Otani, S., Naerdemann, W., et al. (2005). Abnormal lysosomal trafficking and enhanced exosomal export of cisplatin in drug-resistant human ovarian carcinoma cells. *Mol. Cancer Ther.* 4, 1595–1604. doi: 10.1158/1535-7163.MCT-05-0102

Sansone, P., Savini, C., Kurelac, I., Chang, Q., Amato, L. B., Strillacci, A., et al. (2017). Packaging and transfer of mitochondrial DNA via exosomes regulate escape from dormancy in hormonal therapy-resistant breast cancer. *Proc. Natl. Acad. Sci. U.S.A.* 114, E9066–E9075. doi: 10.1073/pnas.1704862114

Skotland, T., Sandvig, K., and Llorente, A. (2017b). Lipids in exosomes: current knowledge and the way forward. *Prog. Lipid Res.* 66, 30–41. doi: 10.1016/j.plipres.2017.03.001

Skotland, T., Ekroos, K., Kauhanen, D., Simolin, H., Seierstad, T., Berge, V., et al. (2017a). Molecular lipid species in urinary exosomes as potential prostate cancer biomarkers. *Eur. J. Cancer* 70, 122–132. doi: 10.1016/j.ejca.2016.10.011

Spitzner, M., Roesler, B., Bielfeld, C., Emons, G., Gaedcke, J., Wolff, H. A., et al. (2014). STAT3 inhibition sensitizes colorectal cancer to chemoradiotherapy in vitro and in vivo. *Int. J. Cancer* 134, 997–1007. doi: 10.1002/ijc.28429

Sterzenbach, U., Putz, U., Low, L. H., Silke, J., Tan, S. S., and Howitt, J. (2017). Engineered exosomes as vehicles for biologically active proteins. *Mol. Ther.* 25, 1269–1278. doi: 10.1016/j.ymthe.2017.03.030

Sun, D., Zhuang, X., Xiang, X., Liu, Y., Zhang, S., Liu, C., et al. (2010). A novel nanoparticle drug delivery system: the anti-inflammatory activity of curcumin is enhanced when encapsulated in exosomes. *Mol. Ther.* 18, 1606–1614. doi: 10.1038/mt.2010.105

Sun, Y., Huo, C., Qiao, Z., Shang, Z., Uzzaman, A., Liu, S., et al. (2018). Comparative proteomic analysis of exosomes and microvesicles in human saliva for lung cancer. *J. Proteome Res.* 17, 1101–1107. doi: 10.1021/acs.jproteome.7b00770

Tai, Y. L., Chen, K. C., Hsieh, J. T., and Shen, T. L. (2018). Exosomes in cancer development and clinical applications. *Cancer Sci.* 109, 2364–2374. doi: 10.1111/cas.13697

Takahashi, K., Yan, I. K., Wood, J., Haga, H., and Patel, T. (2014). Involvement of extracellular vesicle long noncoding RNA (linc-VLDLR) in tumor cell responses to chemotherapy. *Mol. Cancer Res.* 12, 1377–1387. doi: 10.1158/1541-7786.MCR-13-0636

Thery, C., Witwer, K. W., Aikawa, E., Alcaraz, M. J., Anderson, J. D., Andriantsitohaina, R., et al. (2018). Minimal information for studies of extracellular vesicles 2018 (MISEV2018): a position statement of the International Society for Extracellular Vesicles and update of the MISEV2014 guidelines. *J. Extracell. Vesicles* 7:1535750. doi: 10.1080/20013078.2018.1535750

Tian, Y., Li, S., Song, J., Ji, T., Zhu, M., Anderson, G. J., et al. (2014). A doxorubicin delivery platform using engineered natural membrane vesicle exosomes for targeted tumor therapy. *Biomaterials* 35, 2383–2390. doi: 10.1016/j.biomaterials.2013.11.083

Wang, G., Zhao, W., Wang, H., Qiu, G., Jiang, Z., Wei, G., et al. (2019). Exosomal MiR-744 inhibits proliferation and sorafenib chemoresistance in hepatocellular carcinoma by targeting PAX2. *Med. Sci. Monit.* 25, 7209–7217. doi: 10.12659/MSM.919219

Wang, J., Guan, X., Zhang, Y., Ge, S., Zhang, L., Li, H., et al. (2018). Exosomal miR-27a derived from gastric cancer cells regulates the transformation of fibroblasts into cancer-associated fibroblasts. *Cell. Physiol. Biochem.* 49, 869–883. doi: 10.1159/000493218

Wang, S., Xu, Y., Chan, H. F., Kim, H. W., Wang, Y., Leong, K. W., et al. (2016). Nanoparticle-mediated inhibition of survivin to overcome drug resistance in cancer therapy. *J. Control. Release.* 240, 454–464. doi: 10.1016/j.jconrel.2016.04.018

Wang, T. T., Xia, Y. Y., Gao, J. Q., Xu, D. H., and Han, M. (2021). Recent progress in the design and medical application of in situ Self-Assembled polypeptide materials. *Pharmaceutics* 13:753. doi: 10.3390/pharmaceutics13050753

Wang, X., Zhang, H., Yang, H., Bai, M., Ning, T., Deng, T., et al. (2020). Exosome-delivered circRNA promotes glycolysis to induce chemoresistance through the miR-122-PKM2 axis in colorectal cancer. *Mol. Oncol.* 14, 539–555. doi: 10.1002/1878-0261.12629

Wei, F., Ma, C., Zhou, T., Dong, X., Luo, Q., Geng, L., et al. (2017). Exosomes derived from gemcitabine-resistant cells transfer malignant phenotypic traits via delivery of miRNA-222-3p. *Mol. Cancer* 16:132. doi: 10.1186/s12943-017-0694-8

Weiner-Gorzel, K., Dempsey, E., Milewska, M., McGoldrick, A., Toh, V., Walsh, A., et al. (2015). Overexpression of the microRNA miR-433 promotes resistance to paclitaxel through the induction of cellular senescence in ovarian cancer cells. *Cancer Med.* 4, 745–758. doi: 10.1002/cam4.409

Wilson, T. R., Fridlyand, J., Yan, Y., Penuel, E., Burton, L., Chan, E., et al. (2012). Widespread potential for growth-factor-driven resistance to anticancer kinase inhibitors. *Nature* 487, 505–509. doi: 10.1038/nature11249

Wu, H., Mu, X., Liu, L., Wu, H., Hu, X., Chen, L., et al. (2020). Bone marrow mesenchymal stem cells-derived exosomal microRNA-193a reduces cisplatin resistance of non-small cell lung cancer cells via targeting LRRC1. *Cell Death Dis.* 11:801. doi: 10.1038/s41419-020-02962-4

Wu, Q., Zhou, L., Lv, D., Zhu, X., and Tang, H. (2019). Exosome-mediated communication in the tumor microenvironment contributes to hepatocellular carcinoma development and progression. *J. Hematol. Oncol.* 12:53. doi: 10.1186/s13045-019-0739-0

Xiao, Y., Zhong, J., Zhong, B., Huang, J., Jiang, L., Jiang, Y., et al. (2020). Exosomes as potential sources of biomarkers in colorectal cancer. *Cancer Lett.* 476, 13–22. doi: 10.1016/j.canlet.2020.01.033

Xu, H., Han, H., Song, S., Yi, N., Qian, C., Qiu, Y., et al. (2019). Exosome-Transmitted PSMA3 and PSMA3-AS1 promote proteasome inhibitor resistance in multiple myeloma. *Clin. Cancer Res.* 25, 1923–1935. doi: 10.1158/1078-0432.CCR-18-2363

Xu, Y. C., Liu, X., Li, M., Li, Y., Li, C. Y., Lu, Y., et al. (2018). A novel mechanism of doxorubicin resistance and tumorigenesis mediated by MicroRNA-501-5p-Suppressed BLID. *Mol. Ther. Nucleic Acids* 12, 578–590. doi: 10.1016/j.omtn.2018.06.011

Yamagishi, T., Sahni, S., Sharp, D. M., Arvind, A., Jansson, P. J., and Richardson, D. R. (2013). P-glycoprotein mediates drug resistance via a novel mechanism involving lysosomal sequestration. *J. Biol. Chem.* 288, 31761–31771. doi: 10.1074/jbc.M113.514091

Yan, X., Yin, J., Yao, H., Mao, N., Yang, Y., and Pan, L. (2010). Increased expression of annexin A3 is a mechanism of platinum resistance in ovarian cancer. *Cancer Res.* 70, 1616–1624. doi: 10.1158/0008-5472.CAN-09-3215

Yang, F., Liao, X., Tian, Y., and Li, G. (2017). Exosome separation using microfluidic systems: size-based, immunoaffinity-based and dynamic methodologies. *Biotechnol. J.* 12:1600699. doi: 10.1002/biot.201600699

Yang, S. J., Wang, D. D., Li, J., Xu, H. Z., Shen, H. Y., Chen, X., et al. (2017). Predictive role of GSTP1-containing exosomes in chemotherapy-resistant breast cancer. *Gene* 623, 5–14. doi: 10.1016/j.gene.2017.04.031

Yi, M., Xu, L., Jiao, Y., Luo, S., Li, A., and Wu, K. (2020). The role of cancer-derived microRNAs in cancer immune escape. *J. Hematol. Oncol.* 13:25. doi: 10.1186/s13045-020-00848-8

Yin, J., Yan, X., Yao, X., Zhang, Y., Shan, Y., Mao, N., et al. (2012). Secretion of annexin A3 from ovarian cancer cells and its association with platinum resistance in ovarian cancer patients. *J. Cell. Mol. Med.* 16, 337–348. doi: 10.1111/j.1582-4934.2011.01316.x

Yoshizawa, J. M., Schafer, C. A., Schafer, J. J., Farrell, J. J., Paster, B. J., and Wong, D. T. (2013). Salivary biomarkers: toward future clinical and diagnostic utilities. *Clin. Microbiol. Rev.* 26, 781–791. doi: 10.1128/CMR.00021-13

Yuwen, D., Ma, Y., Wang, D., Gao, J., Li, X., Xue, W., et al. (2019). Prognostic role of circulating exosomal miR-425-3p for the response of NSCLC to Platinum-Based chemotherapy. *Cancer Epidemiol. Biomarkers. Prev.* 28, 163–173. doi: 10.1158/1055-9965.EPI-18-0569

Yuwen, D. L., Sheng, B. B., Liu, J., Wenyu, W., and Shu, Y. Q. (2017). MiR-146a-5p level in serum exosomes predicts therapeutic effect of cisplatin in non-small cell lung cancer. *Eur. Rev. Med. Pharmacol. Sci.* 21, 2650–2658.

Zhang, F. F., Zhu, Y. F., Zhao, Q. N., Yang, D. T., Dong, Y. P., Jiang, L., et al. (2014). Microvesicles mediate transfer of P-glycoprotein to paclitaxel-sensitive A2780 human ovarian cancer cells, conferring paclitaxel-resistance. *Eur. J. Pharmacol.* 738, 83–90. doi: 10.1016/j.ejphar.2014.05.026

Zhang, H., Deng, T., Liu, R., Ning, T., Yang, H., Liu, D., et al. (2020). CAF secreted miR-522 suppresses ferroptosis and promotes acquired chemo-resistance in gastric cancer. *Mol. Cancer* 19:43. doi: 10.1186/s12943-020-01168-8

Zhang, Q., Liu, R. X., Chan, K. W., Hu, J., Zhang, J., Wei, L., et al. (2019). Exosomal transfer of p-STAT3 promotes acquired 5-FU resistance in colorectal cancer cells. *J. Exp. Clin. Cancer Res.* 38:320. doi: 10.1186/s13046-019-1314-9

Zhang, W., Cai, X., Yu, J., Lu, X., Qian, Q., and Qian, W. (2018). Exosome-mediated transfer of lncRNA RP11838N2.4 promotes erlotinib resistance in non-small cell lung cancer. *Int. J. Oncol.* 53, 527–538. doi: 10.3892/ijo.2018.4412

Zhang, X., Sai, B., Wang, F., Wang, L., Wang, Y., Zheng, L., et al. (2019). Hypoxic BMSC-derived exosomal miRNAs promote metastasis of lung cancer cells via STAT3-induced EMT. *Mol. Cancer* 18:40. doi: 10.1186/s12943-019-0959-5

Zhang, Y., Li, M., and Hu, C. (2018). Exosomal transfer of miR-214 mediates gefitinib resistance in non-small cell lung cancer. *Biochem. Biophys. Res. Commun.* 507, 457–464. doi: 10.1016/j.bbrc.2018.11.061

Zhu, X., Shen, H., Yin, X., Yang, M., Wei, H., Chen, Q., et al. (2019). Macrophages derived exosomes deliver miR-223 to epithelial ovarian cancer cells to elicit a chemoresistant phenotype. *J. Exp. Clin. Cancer Res.* 38:81. doi: 10.1186/s13046-019-1095-1

Conflict of Interest: The authors declare that the research was conducted in the absence of any commercial or financial relationships that could be construed as a potential conflict of interest.

Publisher's Note: All claims expressed in this article are solely those of the authors and do not necessarily represent those of their affiliated organizations, or those of the publisher, the editors and the reviewers. Any product that may be evaluated in this article, or claim that may be made by its manufacturer, is not guaranteed or endorsed by the publisher.

Copyright © 2021 Li, Gao, Gao, Liu, Pang, Dong, Li and Fan. This is an open-access article distributed under the terms of the Creative Commons Attribution License (CC BY). The use, distribution or reproduction in other forums is permitted, provided the original author(s) and the copyright owner(s) are credited and that the original publication in this journal is cited, in accordance with accepted academic practice. No use, distribution or reproduction is permitted which does not comply with these terms.

frontiers in Oncology

ORIGINAL RESEARCH
published: 29 October 2021
doi: 10.3389/fonc.2021.721067

Association of Soluble B7-H4 and Circulating Tumor Cells in Blood of Advanced Epithelial Ovarian Cancer Patients

Pawel Mach, Rainer Kimmig, Sabine Kasimir-Bauer and Paul Buderath*

Department of Gynecology and Obstetrics, University Hospital Essen, Essen, Germany

Introduction: Epithelial ovarian cancer (EOC) is the deadliest gynecologic malignancy worldwide. Reliable predictive biomarkers are urgently needed to estimate the risk of relapse and to improve treatment management. Soluble immune-checkpoints in EOC are promising molecules serving as prognostic biomarkers accessible *via* liquid biopsy. We thus, aimed at elucidating the role of sB7-H4 in EOC.

Material and Methods: We analyzed soluble serum B7-H4 (sB7-H4) using ELISA and circulating tumor cells (CTCs) in blood applying the AdnaTest *OvarianCancer* in 85 patients suffering from advanced EOC. Findings were correlated with clinical parameters as well as survival data.

Results: sB7-H4 was detectable in 14.1% patients, CTCs in 32.9% patients and simultaneous presence of CTCs and sB7-H4 was found in 7% patients, respectively. Although no association between sB7-H4 and CTC could be documented, each of them served as independent predictive factors for overall survival (OS).

Conclusion: sB7-H4 and CTCs are independent prognostic biomarkers for impaired survival in EOC. As they are easily accessible *via* liquid biopsy, they may be of potential benefit for the prediction of therapy response and survival for EOC patients.

Keywords: epithelial ovarian cancer, sB7-H4, circulating tumor cells (CTC), tumor micro-environment, biomarker

OPEN ACCESS

Edited by:
Klaus Pantel,
University Medical Center Hamburg-Eppendorf, Germany

Reviewed by:
Juçara Gastaldi Cominal,
Institut Imagine, France
Michal Mego,
Campus Bio-Medico University, Italy

****Correspondence:***
Pawel Mach
pawel.mach@uk-essen.de

Specialty section:
This article was submitted to Molecular and Cellular Oncology, a section of the journal Frontiers in Oncology

Received: *05 June 2021*
Accepted: *13 October 2021*
Published: *29 October 2021*

Citation:
Mach P, Kimmig R, Kasimir-Bauer S and Buderath P (2021) Association of Soluble B7-H4 and Circulating Tumor Cells in Blood of Advanced Epithelial Ovarian Cancer Patients. Front. Oncol. 11:721067. doi: 10.3389/fonc.2021.721067

INTRODUCTION

Epithelial ovarian cancer (EOC) is the deadliest gynecologic malignancy worldwide (1). In Germany, EOC is responsible for 3.2% of all malignant neoplasms and 5.3% of all cancer deaths (2). Despite a high response rate for initial therapy, most patients eventually relapse (3), leading to a relative 5-year survival of only 41 % in 2014 (2). Reliable predictive biomarkers are urgently needed to estimate the risk of relapse and improve treatment management. In this regard, it has already been demonstrated that the characterization of disseminated tumor cells (DTCs) in the bone marrow (BM) and circulating tumor cells (CTCs) in peripheral blood has identified stem cell like DTCs and CTCs, tumor cells in epithelial-mesenchymal transition (EMT) as well as resistant cells, all associated with a worse outcome and clinical platinum resistance (4–7). Interestingly, we were able to show that immunotherapy based on the intraperitoneal trifunctional bispecific antibody

Catumaxomab was successful in the elimination of DTCs and CTCs in patients with advanced EOC (8). Thus, the tumor microenvironment might play a crucial role in tumor control and tumorigenesis of these patients.

In recent years, the role of the immune system in EOC has gathered increasing attention. Several mechanisms of immune-escape have been identified in malignant tumors, including the aberrant expression of immune costimulatory ligands, such as those of the B7 family, namely programmed cell-death protein 1 (PD-1) (also known as B7-H1) and its ligands, programmed cell-death ligand 1 and 2 (PD-L1 and PD-L2). In our recent study, we show that decreased serum levels of PD-L2 were associated with poor survival and platinum-resistance, as well as the presence of DNA excision repair protein ERCC+CTC, indicating the significance of the organism's immune-response for the prevention of tumor-cell spread and the efficacy of platinum-based therapy (9).

B7-H4 is another member of the B7-family, which is highly expressed in various types of neoplasms including ovarian, endometrial, or breast cancer (BC). Its expression correlates with the progression of the disease and a poor prognosis in many cases (10, 11). Moreover, Liang et al. show that B7-H4 is more often expressed in high-grade serous EOC (12). Evaluating a serum-based, multi parametric biomarker panel in OC patients, Oikonomopoulou et al. found that high levels of B7-H4 were associated with worse overall survival (13). B7-H4 has a membrane-bound and soluble form (sB7-H4), which has also been detected in the serum of patients suffering from cancer with its expression closely related to progression and prognosis (14). However, the source and function of sB7-H4 are still unknown.

The hypothesis that immune cells in the bloodstream can expand the metastatic potential of CTCs has recently been confirmed in BC (15). Based on these findings, we hypothesize that simultaneous measurements of CTCs and sB7-H4 could help to better understand the complex interactions between the tumor microenvironment and the immune response in EOC. This study aimed to investigate the serum levels of sB7-H4 and CTCs in patients with advanced EOC and to analyze its relationship to prognosis and clinicopathological features.

MATERIAL AND METHODS

Cohort Characteristics

We analyzed data from 85 patients suffering from advanced EOC. All patients underwent primary debulking surgery including hysterectomy, bilateral salpingoovarectomy, omentectomy, peritonectomy and - in the case of macroscopic complete resection - systematic pelvic and paraaortic lymphadenectomy. Adjuvant treatment consisted of six cycles of chemotherapy with carboplatinum AUC5 and paclitaxel 175 mg/m² i.v. d1 q3w intravenously. Since 2012, patients presenting at FIGO stage IIIB or higher have been offered an additional adjuvant therapy with the antiangiogenetic antibody Bevacizumab 15 mg/kg i.v. d1 q3w for a total of 15 months. Patients were diagnosed between 2007 and 2016 at the university hospital in Essen, Germany. Clinical data were acquired from patient charts and the hospital's clinical information system. The study was approved by the local ethics committee of the University of Duisburg-Essen (Essen 05-2870 and 17-7859).

Patients recurring within six months after the end of the adjuvant platinum therapy were considered platinum-resistant. Disease-Free Survival (DFS) was calculated from the date of initial diagnosis to relapse.

An overview of patients' characteristics is given in **Table 1**.

Blood Serum Collection and Measurement of sB7-H4

Soluble (s) B7-H4 serum levels were analyzed preoperatively using the sandwich Enzyme-Linked Immunosorbent Assay Kit (Cusabio, Cologne, Germany) according to the manual instructions. For ELISA measurement, 100 µl undiluted serum samples and control samples were dispensed into wells coated with an antibody specific for B7-H4 and incubated for two hours at 37°C. Subsequently, after removing any unbound substances, a biotin-conjugated antibody specific for B7-H4 was added to the wells for one hour at 37°C. After washing three times, 100 µL of avidin conjugated Horseradish Peroxidase (HRP) were added for 1 h at 37°C. Subsequently, after washing five times, 90 µL of substrate solution containing TMB were added for 15-30 minutes at 37°C, protected from light. Color development was stopped by the addition of 50 µl stop solution to each well and the degree of enzymatic turnover of the substrate was investigated by dual-wavelength absorbance measurement at 450 and 620 nm as a reference wavelength within 5 minutes using an ELISA reader (TECAN, Model Sunrise; Austria GmbH, Grodig, Austria) and the data analysis software Magellan™ (TECAN, Mannedorf, Switzerland). To quantify the blood serum concentration levels of B7-H4, a non-linear regression model (4-parameter Marquardt) was used with a log/lin type of graph according to the manufacturer's instructions. The observed absorbance was directly proportional to the

TABLE 1 | Clinical data of patients with advanced EOC at the time of primary diagnosis.

	Total n = 85 (%)	p-value
FIGO stage		
III	61 (71.8)	0.001
IV	24 (28.2)	
Grading		
1 and 2	24 (29.3)	0.0002
3	58 (70.7)	
Nodal status		
Node negative	24 (37.5)	0.04
Node positive	40 (62.5)	
Platinum sensitivity		
Sensitive	50 (84.7)	0.0001
Resistant	23 (27.1)	
Resection status		
Complete resection	39 (48.1)	0.73
Incomplete resection	42 (51.9)	
Recurrence		
No	29 (37.7)	0.03
Yes	48 (62.3)	

concentration level of sB7-H4 in the samples, which was calculated from the calibration curve. The sB7-H4 serum levels are expressed in ng/mL according to the established standard curve (detection range: 7.8 - 500 ng/mL). The minimum detectable dose of sB7-H4 was typically less than 1.95 ng/mL. The lower limit of detection (LLD) was defined as the lowest protein concentration that could be differentiated from zero. Intra-assay variation was <8%, while inter-assay variation was <10%.

Selection and Detection of CTCs

The selection, detection, characterization and data evaluation of epithelial CTCs and CTCs in EMT in EOC has been published in detail by our group (5, 16–18).

10 ml blood was collected in EDTA tubes (Sarstedt & Co.) from each patient and processed within 4h for the enrichment of CTCs and subsequent expression analysis according to the Adnatest OvarianCancer (QIAGEN, Hilden, Germany). Briefly, CTCs were immunomagnetically selected using the AdnaTests OvarianCancerSelect and EMT-1Select. Subsequently, RNA was isolated and gene expression analysis was performed by reverse-transcription (RT) and multiplex RT-PCR detecting a) EpCAM, MUC-1, and CA-125 (AdnaTest OvarianCancerDetect; ERCC1-transcripts were investigated in a separate approach by singleplex RT-PCR) and b) PIK3CA, AKT2 and TWIST (AdnaTest EMT).

All AdnaTests were purchased from QIAGEN (Hilden, Germany). Positivity for each CTC-subtype was defined by the detection of at least one of the transcripts of each marker panel, respectively. A patient was defined as CTC-positive if epithelial CTCs and/or CTCs in EMT were detected.

Statistical Analysis

The distribution of sB7-H4 in each study group was different from normal. Descriptive statistics were computed and reported as median with interquartile range (IQR) or frequency counts (%). The differences between two groups were defined by Mann-Whitney U test. Differences in frequency counts were analyzed using the Chi-squared test. Kaplan-Meier analysis was performed to analyze DFS and overall survival (OS) probabilities. The difference between survival curves was assessed by using the log rank test. Hazard ratios (HR) with corresponding 95%-confidence intervals (95%-CI) were calculated by using Cox proportional hazards regression. The Spearman rank correlation coefficient was calculated to examine whether the sB7-H4 levels were monotonically related to CA12-5 serum levels. All analyses were performed using the MedCalc version 17.9.7 (MedCalc Software bvba, Ostend, Belgium).

RESULTS

The median age of the patients at primary diagnosis was 60 years (37 - 82, SD 11.7). The clinical data of patients included in the study are shown in **Table 1**. The majority of patients were in Figo stage III (71.3%) compared with stage IV (28.2%). High-grade tumors (G3) were found in 58 (70.7%) patients whereas Grade 1 and 2 in 24 (29.3%) of patients. 40 (62.5%) of patients had positive lymph-nodes and 24 (37.5%) negative nodal-status. When stratifying according to resection status 39 (48.1%) had complete resection (R0) compared with 42 (51.9%) patients with incomplete resection. In 48 (62.3%) patients a recurrent disease was diagnosed (**Table 1**). Among patients with platinum-resistant disease 15 (75%) had positive nodal-status, compared with 5 (25%) with negative nodal-status. In FIGO IV stage 12 (75%) patients and in FIGO III stage 28 (70%) had lymph-nodes metastasis. Follow-up was calculated from the time of diagnosis to the date of last follow-up information or death. Median follow-up time was 35.5 months (0 - 139, SD 28.1). Analyzing only patients who had died, medium time to death was 25 months (0 - 75, SD 22.8). Medium DFS was 27 months (0 - 130, SD 23.9). Patients with an OS ≤ 4 months were excluded from survival analyses in order to rule out early, surgery related deaths (n=12).

Association of sB7-H4 Concentration Levels, CTCs, and Clinicopathological Characteristics

sB7-H4 was detectable in 12/85 (14.1%) patients, CTCs in 28/85 (32.9%) patients and simultaneous presence of CTCs and sB7-H4 was found in 6/85 (7%) patients.

Epithelial CTCs were found in 10/85 (11.7%) patients and EMT-like CTCs in 18/85 (21.2%) patients. In 5/85 (5.9%) patients, expression of both epithelial and EMT-like CTCs subtypes was found. sB7-H4 positivity was significantly more common in patients without confirmed (pN0) spread to lymph nodes (25%) compared to patients with histologically confirmed (pN1) metastases in lymph nodes (12.5%, p=0.04). Moreover, sB7-H4 presence in serum was significantly associated with platinum resistance (p=0.03). CTCs presence in blood was slightly higher in platin resistant patients but the difference was not significant. There were no differences in sB7-H4 levels in serum according to clinicopathological parameters. Associations between sB7-H4 concentration levels, CTCs and clinicopathological characteristics including FIGO stage, grading, nodal status, sensibility to platin agents and resection status are presented in **Table 2**.

Impact of sB7-H4 and CTC Presence on Patients' Survival

Comparison between patients with detectable sB7-H4 serum-levels and no detectable serum levels revealed a statistically significant effect on OS. Patients with detectable sB7-H4 in blood serum showed a significantly shorter survival time than patients with no sB7-H4 detection (HR 4.42, 95% CI 1.61 – 12.13; p = 0.004). No effect on DFS could be observed (**Figure 1**).

Patients with detectable CTCs showed a significantly shorter survival time than patients in whom no CTCs were detected (HR 2.63, 95% CI 1.28 - 5.39; p = 0.008). No effect on DFS could be observed (**Figure 1**).

Univariate Cox regression analysis indicated that the presence of sB7-H4 and CTCs influenced the prognosis of our patients. Patients presenting with enhanced sB7-H4 levels and CTCs had

TABLE 2 | Associations of sB7-H4 blood serum levels, sB7-H4 presence in serum and CTCs to clinicopathological parameters.

Total n = 85	sB7-H4 ng/mL levels in serum (IQR)	p-value	sB7-H4 presence in serum (%)	p-value	CTCs presence in blood (%)	p-value
FIGO stage						
III	32.89 (5.41 - 71.9)	0.79	8 (13.1)	0.19	17 (27.8)	**0.11**
IV	31.05 (22.5 - 44.47)		6 (25)		11 (45.8)	
Grading						
I and II	30.37 (22.5 - 92.97)	0.58	4 (16.6)	0.4	11 (45.83)	0.7
III	31.73 (5.01 - 49.29)		11 (18.9)		17 (29.3)	
Lymph node status						
N0	21.79 (6.2 - 31.73)	0.24	6 (25)	0.04	3 (12.5)	0.18
N1	44.58 (17.49 - 87.6)		5 (12.5)		16 (40)	
Platinum sensitivity						
Sensitive	33.48 (4.98 - 47.76)	0.25	8 (16)	0.03	15 (30)	0.08
Resistant	31.05 (21.08 - 82.23)		6 (66.6)		13 (56.5) 23	
Resection status						
Complete resection	25.72 (5.41 - 41.28)	0.43	8 (20.5)	0.4	10 (25.6)	0.15
Incomplete resection	44.58 (22.5 - 82.23)		6 (14.3)		17 (40.47)	

Comparisons between sB7-H4 serum levels were analyzed using Mann-Whitney U test, sB7-H4- and CTC-presence using chi-square test.

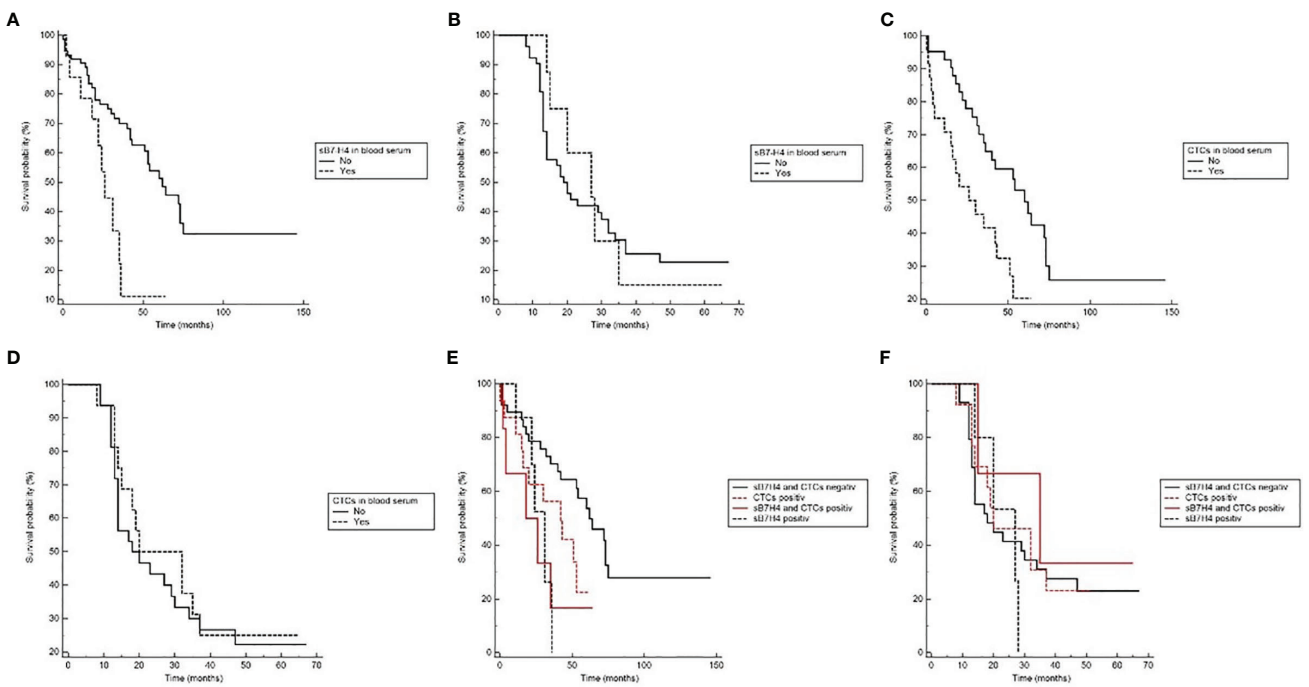

FIGURE 1 | The Kaplan-Meier plots showing prognostic relevance of sB7-H4 and CTC detection in blood serum. **(A)** Overall survival (OS) with regard to sB7-H4 detection (p=0.004). **(B)** Disease-free survival (DFS) with regard to sB7-H4 detection (ns). **(C)** Overall survival (OS) with regard to CTC detection (Log-rank p=0.008). **(D)** Disease-free survival (DFS) with regard to CTC detection (ns). **(E)** Overall survival (OS) for the different combinations of sB7-H4 and CTCs (Log-rank p=0.03). **(F)** Disease-free survival (DFS) for the different combinations of sB7-H4 and CTCs (ns).

a significantly worse OS in comparison with those patients with no detectable sB7-H4 and CTCs (HR 2.8, 95% CI 11.34 – 5.82; p=0.006 and HR 2.32, 95% CI 1.22 – 4.41; p=0.01, respectively). The clinical factors associated with prognosis including platinum-sensitivity, resection status, FIGO stadium and lymph node status also correlated with OS, however, apart from platinum-sensitivity, no effect on DFS could be observed (**Table 3**).

Multivariate Cox regression analysis including resection status, FIGO stage, grade, lymph node status, platinum-sensitivity, CTC detection and sB7-H4 presence indicated that sB7-H4 and CTCs presence were independent predictive factor for OS (HR 3.57, 95% CI 1.23 - 10.36; p=0.02 and HR 4.31, 95% CI 1.53 - 12.17; p=0.006, respectively). sB7-H4 or CTC presence did not significantly influence the adjusted hazard on developing recurrent disease (**Table 4**).

TABLE 3 | Results of univariate Cox regression analysis of patients with advanced EOC.

	OS		DFS	
	HR (95% CI)	p-value	HR (95% CI)	p-value
sB7-H4 in serum				
no	1	0.006	1	0.82
yes	2.8 (1.34 – 5.82)		0.9 (0.38 – 2.14)	
CTCs in blood				
no	1	0.01	1	0.4
yes	2.32 (1.22 – 4.41)		0.85 (0.42 – 1.69)	
Residual tumor				
no	1	0.01	1	0.16
yes	2.13 (1.17 – 3.88)		1.54 (0.84 – 2.82)	
FIGO stage				
III	1	0.12	1	0.65
IV	1.63 (0.88 – 3.04)		0.85 (0.42 – 1.72)	
Grade				
I/II	1	0.78	1	0.79
III	1.09 (0.59 – 2.03)		1.09 (0.56 – 2.08)	
Lymph node status				
N0	1	0.1	1	0.47
N1	1.95 (0.87 – 4.39)		1.35 (0.6 – 3.03)	
Platinum sensitivity				
Sensitive	1	<0.0001	1	0.03
Resistant	7.03 (4.1 – 12.08)		10.8 (1.26 – 92.74)	

CI, confidence interval; HR, hazard ratio.

TABLE 4 | Effect of sB7-H4 and CTCs presence on OS and DFS after correcting for unfavorable prognostic factors in cox proportional hazards regression model.

	OS		DFS	
	HR (95% CI)	p-value	HR (95% CI)	p-value
sB7-H4 in serum				
no	1	0.02	1	0.74
yes	3.57 (1.23 -10.36)		1.3 (0.27 – 6.08)	
CTCs in blood				
no	1	0.006	1	0.35
yes	4.31 (1.53 - 12.17)		0.59 (0.19 – 1.78)	
Residual tumor				
no	1	0.3	1	0.65
yes	1.53 (0.61 – 3.83)		1.27 (0.45 – 3.59)	
FIGO stage				
III	1	0.16	1	0.86
IV	0.47 (0.16 - 1.36)		0.89 (0.23 – 3.4)	
Grade				
I/II	1	0.22	1	0.4
III	0.58 (0.25 - 1.38)		1.5 (0.57 – 3.93)	
Lymph node status				
N0	1	0.58	1	0.73
N1	1.31 (0.5 – 3.4)		1.21 (0.41 – 3.54)	
Platinum sensitivity				
Sensitive	1	<0.0001	1	<0.0001
Resistant	7.24 (3.03 – 17.33)		59.1 (4.52 – 771.97)	

CI, confidence interval; HR, hazard ratio.

sB7-H4 and CTCs

22 out of 59 patients (37.2%) with normal sB7-H4 levels had detectable CTCs, whereas in the group of patients with detectable sB7-H4 levels, 6 out of 12 (50%) patients were positive for CTCs. However, this effect failed to reach statistical significance (p = 0.41). An overview on the presence of sB/-H4 and CTCs is given in (**Table 5**).

There were no differences in sB7-H4 serum levels between patients harboring CTCs (median 31.05, IQR13.64-63.46) or not (median 27.29, IQR 3.76-50.83) (p=0.69).

Patients with detectable sB7-H4 levels and CTCs showed a significantly shorter survival time than patients with normal sB7-H4 levels and no detectable CTCs (p = 0.03). No effects on DFS could be observed (**Figure 1**).

DISCUSSION

Our study found that detection of sB7-H4 and CTCs in blood was associated with a worse prognosis of patients with advanced EOC. However, there was no association between sB7-H4 and CTC presence. Current literature supports that high expression of B7-H4 was negatively correlated with survival outcome in OC, suggesting that B7-H4 plays an essential role in poor prognosis (16). However in a meta-analysis from Ye et al., membrane-bound B7-H4 was not related to patients' clinicopathologic characteristics (19). These results are consistent with our findings. However, it is not clear whether serum sB7-H4 levels reflect the expression of B7-H4 in tumor tissue. Similarly to the previous study for sB7-H4 and EOC (13), we found that serum sB7-H4 predicted a worse prognosis (being a predictive factor for OS), independent of clinical parameters known for worse outcomes.

In our study, patients with detectable sB7-H4 and CTCs in blood showed significantly worse survival. The function and source of sB7-H4 are still unknown but some authors have demonstrated that sB7-H4 secretion is promoted under inflammatory conditions (20–22) and in EOC, B7-H4 has been associated with a pro-inflammatory tumor microenvironment (23). On the other hand, the neutrophile-derived inflammatory response was shown to interact with CTCs expanding their metastatic potential (24). These data could be a possible explanation of the worse prognosis of EOC patients showing the simultaneous presence of sB7-H4 and CTCs in the bloodstream.

In our study sB7-H4 was found more in patients without confirmed spread to lymph-nodes, which could suggest its association with better outcome. This fact may be explained due to early way of dissemination in EOC, which is primary into

TABLE 5 | Presence of sB7-H4 and CTCs in blood serum in patients with advanced EOC.

	sB7-H4 detectable	sB7-H4 not detectable
CTCs detectable in blood serum	6	22
CTCs not detectable in blood serum	6	37

the peritoneal cavity and not into lymph-nodes. On the contrary, sB7-H4 presence was associated with platinum resistance, which is one of the most important factors connected with worse prognosis. These findings suggest that the tumor biology, rather than tumor load are responsible for sB7-H4 presence in advanced EOC.

The interaction between tumor cells and their microenvironment plays a crucial role in cancer development (25). Current data on the relationship between T-Cell regulators and CTCs in EOC are limited. However, strong evidence suggests a direct interaction between CTCs and the immune system in the peripheral blood. Mego et al. showed that patients with inflammatory BC harboring CTCs had an impaired adaptive immunity (26). In the current study, both, the presence of CTCs and sB7-H4 were associated with a worse prognosis. Postulating a function of B7-H4 as part of the tumor's immune-escape mechanisms, it seems plausible that an increased expression of the immune-checkpoint molecule increases the risk of tumor spread to the blood, indicating poor outcome. This reflects higher sB7-H4 levels in patients with positive CTCs. This is in line with our recent findings analyzing soluble PD-L1 and PD-L2 in EOC patients (9). However, we did not find any association between sB7-H4 and CTCs presence in serum. Keeping in mind that sB7-H4 and CTCs were detectable in only 15 and 28 patients, respectively, this lacking association might well be attributable to the small sample size. Nevertheless, the potential association between CTCs and soluble and membrane T-cells regulators should be further investigated since checkpoint-inhibitors showed promising results in therapy management of advanced EOC (27, 28).

Expression of immune-checkpoints on CTCs can be used as a prognostic indicator and to monitor and evaluate the efficacy of immune checkpoint inhibitors (29–33). For instance, in patients diagnosed with breast cancer, PD-L1-positive CTCs have a prognostic predictive value (33). Our data suggest that the simultaneous detection of sB7-H4 and CTCs in blood serum might have prognostic value.

The role of immune-checkpoint inhibition in the therapy of advanced EOC has been intensively investigated in recent years. It was reported that B7-H4/CD3-bispecific antibodies might be a therapeutic agent against B7-H4-expressing tumors (34). One of the biggest issues concerning checkpoint-inhibitor therapy is the identification of factors predicting therapy response. Therefore, it is crucial to identify markers that can predict the possible response to this treatment option. The presence of sB7-H4 could be a predictive marker for immunotherapy, targeting T-cells as shown by Azuma (35, 36).

There are some limitations to this study. Unfortunately, we do not have results for B7-H4 on tumor tissue for comparison studies, which should be addressed in future work. In addition, we presented a retrospective study with limited sample size. Nevertheless, our data suggest that sB7-H4 and CTCs should be considered potentially useful markers, predicting the prognosis in advanced EOC. A deeper understanding of this interaction may provide an opportunity for new therapeutic strategies.

DATA AVAILABILITY STATEMENT

The raw data supporting the conclusions of this article will be made available by the authors, without undue reservation.

ETHICS STATEMENT

The studies involving human participants were reviewed and approved by Ethics committee of the University of Duisburg-Essen (Essen 05-2870 and 17-7859). The patients/participants provided their written informed consent to participate in this study.

AUTHOR CONTRIBUTIONS

PM: study design, data acquisition, providing of blood and tissue samples, statistical analysis, and manuscript writing. RK: providing of blood and tissue samples, and manuscript editing. SK-B: study design, data acquisition, laboratory analyses, providing of blood and tissue samples, and manuscript editing. PB: study design, data acquisition, providing of blood and tissue samples, statistical analysis, and manuscript writing. All authors contributed to the article and approved the submitted version.

ACKNOWLEDGMENTS

We gratefully thank the patients and healthy controls for participation in the study and for kindly providing the samples.

REFERENCES

1. Mirza MR, Monk BJ, Herrstedt J, Oza AM, Mahner S, Redondo A, et al. Niraparib Maintenance Therapy in Platinum-Sensitive, Recurrent Ovarian Cancer. *N Engl J Med* (2016) 375(22):2154–64. doi: 10.1056/NEJMoa1611310
2. Barnes B, Kraywinkel K, Nowossadeck E, et al. *Bericht Zum Krebsgeschehen in Deutschland* In: Robert Koch-Institute. (2016).
3. Heintz AP, Odicino F, Maisonneuve P, Quinn MA, Benedet JL, Creasman WT, et al. Carcinoma of the Ovary. FIGO 26th Annual Report on the Results of Treatment in Gynecological Cancer. *Int J Gynaecol Obstet* (2006) 95 Suppl 1:S161–92. doi: 10.1016/S0020-7292(06)60033-7
4. Giannopoulou L, Kasimir-Bauer S, Lianidou ES. Liquid Biopsy in Ovarian Cancer: Recent Advances on Circulating Tumor Cells and Circulating Tumor DNA. *Clin Chem Lab Med* (2018) 56(2):186–97. doi: 10.1515/cclm-2017-0019
5. Kuhlmann JD, Wimberger P, Bankfalvi A, Keller T, Scholer S, Aktas B, et al. ERCC1-Positive Circulating Tumor Cells in the Blood of Ovarian Cancer Patients as a Predictive Biomarker for Platinum Resistance. *Clin Chem* (2014) 60(10):1282–9. doi: 10.1373/clinchem.2014.224808
6. Romero-Laorden N, Olmos D, Fehm T, Garcia-Donas J, Diaz-Padilla I. Circulating and Disseminated Tumor Cells in Ovarian Cancer: A Systematic Review. *Gynecologic Oncol* (2014) 133(3):632–9. doi: 10.1016/j.ygyno.2014.03.016

7. Chebouti I, Kasimir-Bauer S, Buderath P, Wimberger P, Hauch S, Kimmig R, et al. EMT-Like Circulating Tumor Cells in Ovarian Cancer Patients are Enriched by Platinum-Based Chemotherapy. *Oncotarget* (2017) 8(30):48820–31. doi: 10.18632/oncotarget.16179
8. Wimberger P, Heubner M, Lindhofer H, Jager M, Kimmig R, Kasimir-Bauer S. Influence of Catumaxomab on Tumor Cells in Bone Marrow and Blood in Ovarian Cancer. *Anticancer Res* (2009) 29(5):1787–91.
9. Buderath P, Schwich E, Jensen C, Horn PA, Kimmig R, Kasimir-Bauer S, et al. Soluble Programmed Death Receptor Ligands sPD-L1 and sPD-L2 as Liquid Biopsy Markers for Prognosis and Platinum Response in Epithelial Ovarian Cancer. *Front Oncol* (2019) 9:1015. doi: 10.3389/fonc.2019.01015
10. Cui Y, Li Z. B7-H4 is Predictive of Poor Prognosis in Patients With Gastric Cancer. *Med Sci Monit* (2016) 22:4233–7. doi: 10.12659/MSM.897781
11. Wang L, Yang C, Liu XB, Wang L, Kang FB. B7-H4 Overexpression Contributes to Poor Prognosis and Drug-Resistance in Triple-Negative Breast Cancer. *Cancer Cell Int* (2018) 18:100. doi: 10.1186/s12935-018-0597-9
12. Liang L, Jiang Y, Chen JS, Niu N, Piao J, Ning J, et al. B7-H4 Expression in Ovarian Serous Carcinoma: A Study of 306 Cases. *Hum Pathol* (2016) 57:1–6. doi: 10.1016/j.humpath.2016.06.011
13. Oikonomopoulou K, Li L, Zheng Y, Simon I, Wolfert RL, Valik D, et al. Prediction of Ovarian Cancer Prognosis and Response to Chemotherapy by a Serum-Based Multiparametric Biomarker Panel. *Br J Cancer* (2008) 99 (7):1103–13. doi: 10.1038/sj.bjc.6604630
14. Zhang C, Li Y, Wang Y. Diagnostic Value of Serum B7-H4 for Hepatocellular Carcinoma. *J Surg Res* (2015) 197(2):301–6. doi: 10.1016/j.jss.2015.04.034
15. Miklikova S, Minarik G, Sedlackova T, Plava J, Cihova M, Jurisova S, et al. Inflammation-Based Scores Increase the Prognostic Value of Circulating Tumor Cells in Primary Breast Cancer. *Cancers (Basel)* (2020) 12(5):1134. doi: 10.3390/cancers12051134
16. Aktas B, Kasimir-Bauer S, Heubner M, Kimmig R, Wimberger P. Molecular Profiling and Prognostic Relevance of Circulating Tumor Cells in the Blood of Ovarian Cancer Patients at Primary Diagnosis and After Platinum-Based Chemotherapy. *Int J gynecological Cancer Off J Int Gynecological Cancer Soc* (2011) 21(5):822–30. doi: 10.1097/IGC.0b013e318216cb91
17. Chebouti I, Blassl C, Wimberger P, Neubauer H, Fehm T, Kimmig R, et al. Analysis of Disseminated Tumor Cells Before and After Platinum Based Chemotherapy in Primary Ovarian Cancer. Do stem cell like cells predict prognosis? *Oncotarget* (2016) 7(18):26454–64. doi: 10.18632/oncotarget.8524
18. Chebouti I, Kuhlmann JD, Buderath P, Weber S, Wimberger P, Bokeloh Y, et al. ERCC1-Expressing Circulating Tumor Cells as a Potential Diagnostic Tool for Monitoring Response to Platinum-Based Chemotherapy and for Predicting Post-Therapeutic Outcome of Ovarian Cancer. *Oncotarget* (2017) 8 (15):24303–13. doi: 10.18632/oncotarget.13286
19. Ye Y, Wang JJ, Li SL, Wang SY, Jing FH. Does B7-H4 Expression Correlate With Clinicopathologic Characteristics and Survival in Ovarian Cancer?: A Systematic Review and PRISMA-Compliant Meta-Analysis. *Med (Baltimore)* (2018) 97(32):e11821. doi: 10.1097/MD.0000000000011821
20. Leandersson P, Kalapotharakos G, Henic E, Borgfeldt H, Petzold M, Hoyer-Hansen G, et al. A Biomarker Panel Increases the Diagnostic Performance for Epithelial Ovarian Cancer Type I and II in Young Women. *Anticancer Res* (2016) 36(3):957–65.
21. Kamimura Y, Kobori H, Piao J, Hashiguchi M, Matsumoto K, Hirose S, et al. Possible Involvement of Soluble B7-H4 in T Cell-Mediated Inflammatory Immune Responses. *Biochem Biophys Res Commun* (2009) 389(2):349–53. doi: 10.1016/j.bbrc.2009.08.144
22. Thompson RH, Zang X, Lohse CM, Leibovich BC, Slovin SF, Reuter VE, et al. Serum-Soluble B7x is Elevated in Renal Cell Carcinoma Patients and is Associated With Advanced Stage. *Cancer Res* (2008) 68(15):6054–8. doi: 10.1158/0008-5472.CAN-08-0869
23. MacGregor HL, Garcia-Batres C, Sayad A, Elia A, Berman HK, Toker A, et al. Tumor Cell Expression of B7-H4 Correlates With Higher Frequencies of Tumor-Infiltrating APCs and Higher CXCL17 Expression in Human Epithelial Ovarian Cancer. *Oncoimmunology* (2019) 8(12):e1665460. doi: 10.1080/2162402X.2019.1665460
24. Saini M, Szczerba BM, Aceto N. Circulating Tumor Cell-Neutrophil Tango Along the Metastatic Process. *Cancer Res* (2019) 79(24):6067–73. doi: 10.1158/0008-5472.CAN-19-1972
25. Worzfeld T, Pogge von Strandmann E, Huber M, Adhikary T, Wagner U, Reinartz S, et al. The Unique Molecular and Cellular Microenvironment of Ovarian Cancer. *Front Oncol* (2017) 7:24. doi: 10.3389/fonc.2017.00024
26. Mego M, Gao H, Cohen EN, Anfossi S, Giordano A, Sanda T, et al. Circulating Tumor Cells (CTC) Are Associated With Defects in Adaptive Immunity in Patients With Inflammatory Breast Cancer. *J Cancer* (2016) 7(9):1095–104. doi: 10.7150/jca.13098
27. Hamanishi J, Mandai M, Ikeda T, Minami M, Kawaguchi A, Murayama T, et al. Safety and Antitumor Activity of Anti-PD-1 Antibody, Nivolumab, in Patients With Platinum-Resistant Ovarian Cancer. *J Clin Oncol Off J Am Soc Clin Oncol* (2015) 33(34):4015–22. doi: 10.1200/JCO.2015.62.3397
28. Brahmer JR, Tykodi SS, Chow LQ, Hwu WJ, Topalian SL, Hwu P, et al. Safety and Activity of Anti-PD-L1 Antibody in Patients With Advanced Cancer. *N Engl J Med* (2012) 366(26):2455–65. doi: 10.1056/NEJMoa1200694
29. Nicolazzo C, Raimondi C, Mancini M, Caponnetto S, Gradilone A, Gandini O, et al. Monitoring PD-L1 Positive Circulating Tumor Cells in non-Small Cell Lung Cancer Patients Treated With the PD-1 Inhibitor Nivolumab. *Sci Rep* (2016) 6:31726. doi: 10.1038/srep31726
30. Kulasinghe A, Perry C, Kenny L, Warkiani ME, Nelson C, Punyadeera C. PD-L1 Expressing Circulating Tumour Cells in Head and Neck Cancers. *BMC Cancer* (2017) 17(1):333. doi: 10.1186/s12885-017-3316-3
31. Raimondi L, Raimondi FM, Di Benedetto L, Cimino G, Spinelli GP. PD-L1 Expression on Circulating Tumour Cells May Be Predictive of Response to Regorafenib in Patients Diagnosed With Chemorefractory Metastatic Colorectal Cancer. *Int J Mol Sci* (2020) 21(18):6907. doi: 10.3390/ijms21186907
32. Wang Y, Kim TH, Fouladdel S, Zhang Z, Soni P, Qin A, et al. PD-L1 Expression in Circulating Tumor Cells Increases During Radio(chemo) therapy and Indicates Poor Prognosis in Non-Small Cell Lung Cancer. *Sci Rep* (2019) 9(1):566. doi: 10.1038/s41598-018-36096-7
33. Papadaki MA, Koutsopoulos AV, Tsoulfas PG, Lagoudaki E, Aggouraki D, Monastirioti A, et al. Clinical Relevance of Immune Checkpoints on Circulating Tumor Cells in Breast Cancer. *Cancers (Basel)* (2020) 12(2):376. doi: 10.3390/cancers12020376
34. Iizuka A, Nonomura C, Ashizawa T, Kondou R, Ohshima K, Sugino T, et al. A T-Cell-Engaging B7-H4/CD3-Bispecific Fab-scFv Antibody Targets Human Breast Cancer. *Clin Cancer Res an Off J Am Assoc Cancer Res* (2019) 25 (9):2925–34. doi: 10.1158/1078-0432.CCR-17-3123
35. Azuma T, Sato Y, Ohno T, Azuma M, Kume H. Serum Soluble B7-H4 is a Prognostic Marker for Patients With non-Metastatic Clear Cell Renal Cell Carcinoma. *PloS One* (2018) 13(7):e0199719. doi: 10.1371/journal.pone.0199719
36. Ohki S, Shibata M, Gonda K, Machida T, Shimura T, Nakamura I, et al. Circulating Myeloid-Derived Suppressor Cells are Increased and Correlate to Immune Suppression, Inflammation and Hypoproteinemia in Patients With Cancer. *Oncol Rep* (2012) 28(2):453–8. doi: 10.3892/or.2012.1812

Conflict of Interest: SK-B is a consultant for Qiagen.

The remaining authors declare that the research was conducted in the absence of any commercial or financial relationships that could be construed as a potential conflict of interest.

Publisher's Note: All claims expressed in this article are solely those of the authors and do not necessarily represent those of their affiliated organizations, or those of the publisher, the editors and the reviewers. Any product that may be evaluated in this article, or claim that may be made by its manufacturer, is not guaranteed or endorsed by the publisher.

Copyright © 2021 Mach, Kimmig, Kasimir-Bauer and Buderath. This is an open-access article distributed under the terms of the Creative Commons Attribution License (CC BY). The use, distribution or reproduction in other forums is permitted, provided the original author(s) and the copyright owner(s) are credited and that the original publication in this journal is cited, in accordance with accepted academic practice. No use, distribution or reproduction is permitted which does not comply with these terms.

frontiers in Cell and Developmental Biology

REVIEW
published: 10 December 2021
doi: 10.3389/fcell.2021.744990

Deoxyribonucleic Acid 5-Hydroxymethylation in Cell-Free Deoxyribonucleic Acid, a Novel Cancer Biomarker in the Era of Precision Medicine

Ling Xu[1,2], Yixin Zhou[3], Lijie Chen[3], Abdul Saad Bissessur[1,2], Jida Chen[1], Misha Mao[1,2], Siwei Ju[1,2], Lini Chen[1,2], Cong Chen[1,2], Zhaoqin Li[1,2], Xun Zhang[1,2], Fei Chen[1,2], Feilin Cao[3], Linbo Wang[1]* and Qinchuan Wang[1]**

[1]Department of Surgical Oncology, Sir Run Run Shaw Hospital, Zhejiang University, Hangzhou, China, [2]School of Medicine, Zhejiang University, Hangzhou, China, [3]Department of Thyroid and Breast Surgery, Taizhou Hospital of Zhejiang Province Affiliated to Wenzhou Medical University, Luqiao, China

Aberrant methylation has been regarded as a hallmark of cancer. 5-hydroxymethylcytosine (5hmC) is recently identified as the ten-eleven translocase (ten-eleven translocase)-mediated oxidized form of 5-methylcytosine, which plays a substantial role in DNA demethylation. Cell-free DNA has been introduced as a promising tool in the liquid biopsy of cancer. There are increasing evidence indicating that 5hmC in cell-free DNA play an active role during carcinogenesis. However, it remains unclear whether 5hmC could surpass classical markers in cancer detection, treatment, and prognosis. Here, we systematically reviewed the recent advances in the clinic and basic research of DNA 5-hydroxymethylation in cancer, especially in cell-free DNA. We further discuss the mechanisms underlying aberrant 5hmC patterns and carcinogenesis. Synergistically, 5-hydroxymethylation may act as a promising biomarker, unleashing great potential in early cancer detection, prognosis, and therapeutic strategies in precision oncology.

Keywords: 5-hydroxymethylcytosine, cell-free DNA, ten-eleven translocase, liquid biopsy, cancer biomarker

OPEN ACCESS

Edited by:
Catherine Alix-Panabieres, Centre Hospitalier Universitaire De Montpellier, France

Reviewed by:
Daniel Hernández Sotelo, Autonomous University of Guerrero, Mexico
Fabio Ciccarone, Università Telematica San Raffaele, Italy

****Correspondence:***
Feilin Cao
drcfl@126.com
Linbo Wang
linbowang@zju.edu.cn
Qinchuan Wang
wangqinchuan@zju.edu.cn

Specialty section:
This article was submitted to Molecular and Cellular Oncology, a section of the journal Frontiers in Cell and Developmental Biology

Received: *21 July 2021*
Accepted: *29 November 2021*
Published: *10 December 2021*

Citation:
Xu L, Zhou Y, Chen L, Bissessur AS, Chen J, Mao M, Ju S, Chen L, Chen C, Li Z, Zhang X, Chen F, Cao F, Wang L and Wang Q (2021) Deoxyribonucleic Acid 5-Hydroxymethylation in Cell-Free Deoxyribonucleic Acid, a Novel Cancer Biomarker in the Era of Precision Medicine. Front. Cell Dev. Biol. 9:744990. doi: 10.3389/fcell.2021.744990

Abbreviations: 5mC, 5-methylcytosine; TSGs, Tumor suppressor genes; 5hmC, 5-hydroxymethylcytosine; TET, ten-eleven translocase; 5fC, 5-formylcytosine; 5caC, 5-carboxylcytosine; 2-OG, 2-oxoglutarate; ctDNA, circulating tumor DNA; cfDNA, cell-free DNA; HCC, hepatocellular carcinoma; CRC, colorectal cancer; AFP, alpha-fetoprotein; NSCLC, non-small cell lung cancer; PDAC, pancreatic ductal adenocarcinoma; TTS, transcription termination sites; PTC, papillary thyroid carcinoma; GBM, glioblastomas; EC, esophageal carcinoma; CCA, cholangiocarcinoma; DSS, disease-specific survival; DFS, disease-free survival; DA, diffuse astrocytomas; CSCC, cervical squamous cell carcinoma; DCP, des-gamma-carboxy prothrombin; DLBCL, diffuse large B-cell lymphoma; SCCCs, slow-cycling cancer cells; AML, acute myeloid leukemia; SVCT2 Na+-dependent Vitamin C transporter 2; BMDM, bone marrow derived macrophages; TIMP, tissue inhibitors of metalloproteinases; EMT, epithelial-mesenchymal transition; PDAC, pancreatic ductal adenocarcinoma; BLBC, basal-like breast cancer; NF-кB, nuclear factor кB; TDG, Thymine DNA glycosylase; BER, base-excision repair; 5hmU, 5-hydroxymethyluracil.

INTRODUCTION

Carcinogenesis is a multistep and complex process in which both genetic and epigenetic aberrations play substantial roles (Feinberg et al., 2016; Thomson and Meehan, 2017). 5-methylcytosine (5mC) is a major form of DNA modification observed in most mammals' CpG (Cytosine-phosphate-Guanine) dinucleotides (60–80%) (Smith and Meissner, 2013). The alteration of 5mC in DNA methylation patterns has been considered as a hallmark of cancer. Global hypomethylation leads to genomic instability, whereas hypermethylation at promoter regions leads to transcriptional silencing of tumor suppressor genes (TSGs), both of the above contributing significantly to the carcinogenesis (Sandoval and Esteller, 2012; Berdasco and Esteller, 2019). Additionally, hypomethylation and hypermethylation can regulate target gene expression by activating or silencing enhancers, respectively (Clermont et al., 2016; Ehrlich, 2019). These processes are dysregulated in many human cancers, leading to cellular de-differentiation and malignant transformation (Taberlay et al., 2014; Clermont et al., 2016). Along with 5mC, 5-hydroxymethylcytosine (5hmC) has been recently recognized as a stable modification that has multiple roles from cell pluripotency to carcinogenesis rather than merely intermedium of DNA demethylation (Putiri et al., 2014; Moen et al., 2015; López et al., 2017).

5hmC is the most abundant oxidation product of 5mC during active DNA demethylation that is mediated by ten-eleven translocase (TET) (Kriaucionis and Heintz, 2009; Tahiliani et al., 2009). TET enzymes oxidize 5mC to 5hmC, and further to 5-formylcytosine (5fC) and 5-carboxylcytosine (5caC) (Ito et al., 2011; He et al., 2011) in a 2-oxoglutarate (2-OG) and Fe (II)-dependent manner (Kohli and Zhang, 2013; Koivunen and

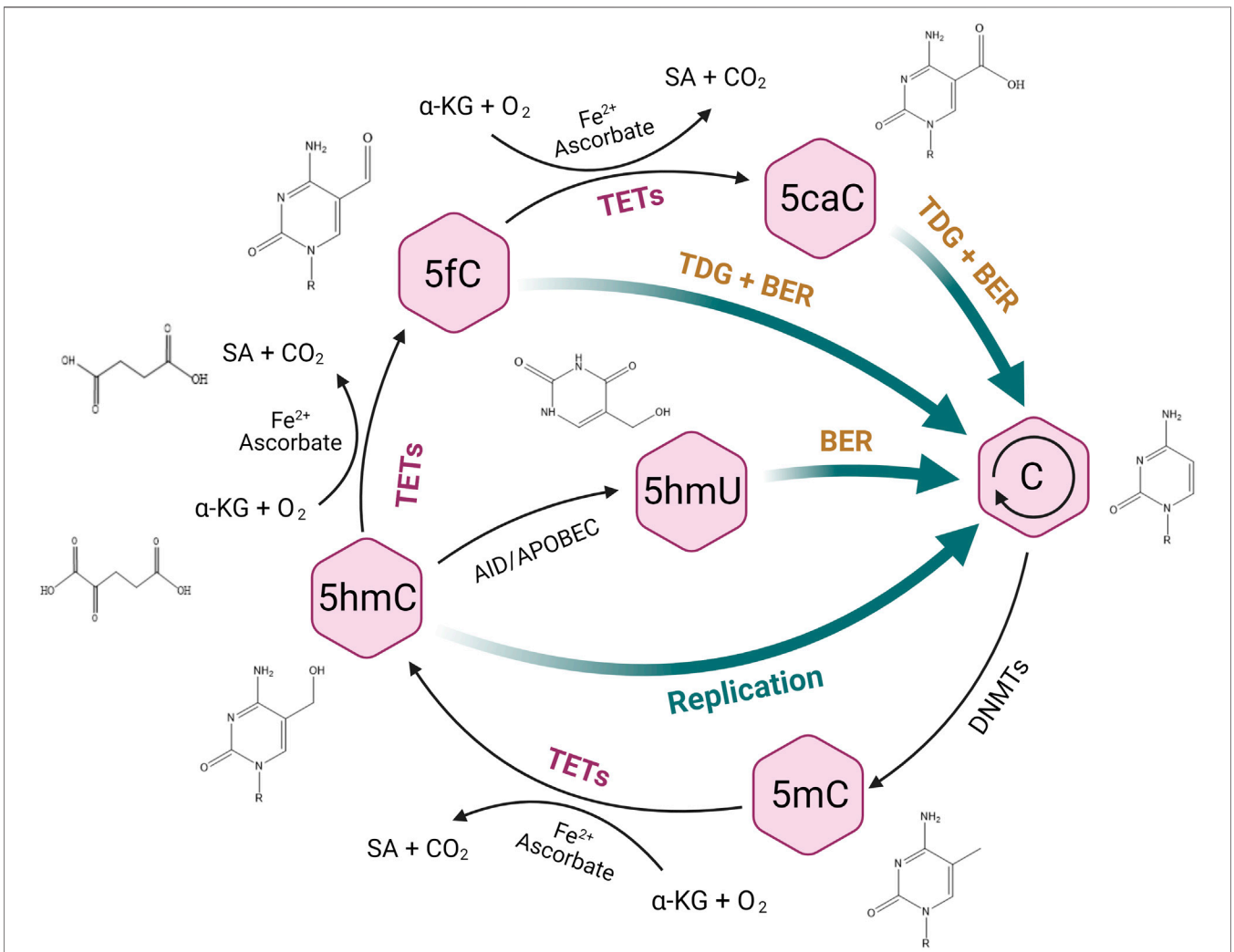

FIGURE 1 | TET-mediated DNA demethylation process. TET enzymes can oxidize 5-methylcytosine (5mC) to 5-hydroxymethylcytosine (5hmC), and further to 5-formylcytosine (5fC) and 5-carboxylcytosine (5caC), followed by the excision of 5fC and 5caC via thymine DNA glycosylase (TDG) and the replacement of unmethylated cytosine through base-excision repair (BER). 5hmC can also be deaminated to 5-hydroxymethyluracil (5hmU) by AID/APOBEC enzymes and subsequently to an unnmethylated status by BER.

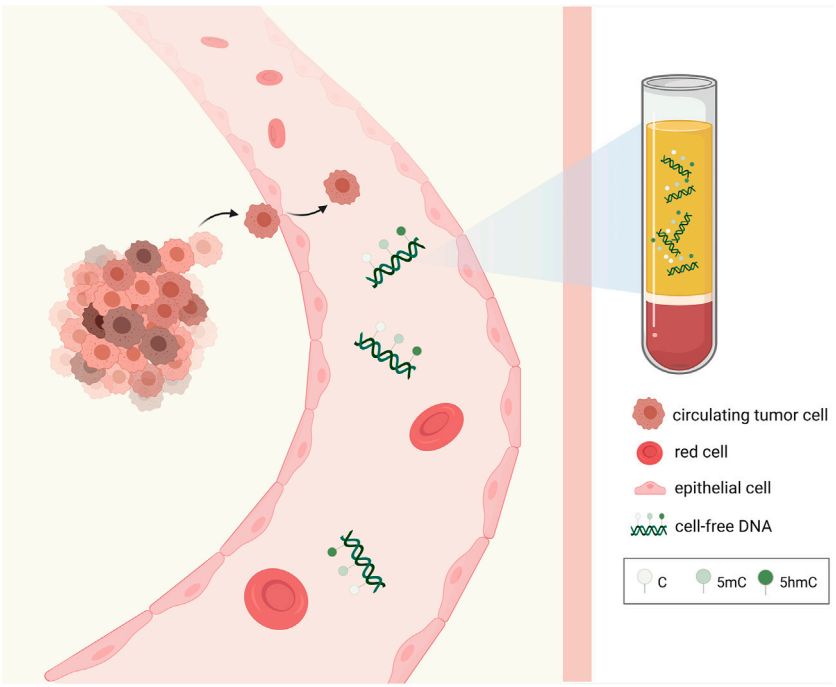

FIGURE 2 | Epigenetic alterations of cell-free DNA extracted from the blood. Tumor-derived epigenetic alterations including 5mC, 5hmC of cfDNA obtained from the blood via liquid biopsy can be utilized as novel biomarkers for cancer diagnosis, prognosis, and treatment.

Laukka, 2018) (**Figure 1**). 5hmC is found enriched over gene bodies, promoters, and enhancers upstream of transcriptional start sites, suggesting that 5hmC plays a role in the regulation of gene expression (Thomson and Meehan, 2017). 5hmC displays a cell- or tissue-specific distribution in different malignancies, and reduced global 5hmC levels were identified in multiple cancers (Lian et al., 2012; Orr et al., 2012; Chen et al., 2016; Tong et al., 2019; Wang et al., 2020), implying that 5hmC may have a promising value in cancer screen, diagnosis, progression and survival (Lian et al., 2012; Zhang et al., 2016a; Zhong et al., 2018). Moreover, 5hmC is suggested as a potential target to synergize with conventional treatment of cancer (Thomson and Meehan, 2017). Thus, 5hmC could be considered as a robust biomarker in clinical practice and promote precision medicine, although awaiting further validation.

Liquid biopsy, along with the detection of circulating tumor DNA (ctDNA) has been revolutionizing the cancer screen and treatment (Tuaeva et al., 2019). ctDNA is tumor-derived fraction of circulating cell-free DNA (cfDNA) that can reflect both genetic and epigenetic profiles of cancer (Wan et al., 2017) (**Figure 2**). The ctDNA-based liquid biopsy offers substantial advantages over traditional biopsies (Chen and Zhao, 2019; De Rubis et al., 2019; Shohdy and West, 2020). First, it is minimally invasive and it avoids the risks of tissue biopsy such as tumor seeding (Diaz and Bardelli, 2014). Second, it could provide dynamic surveillance of genetic or epigenetic changes during cancer development (Diaz and Bardelli, 2014; Wan et al., 2017). Third, it could help capture the heterogeneity of the tumor, as ctDNA fragments are derived from all clones of the cancer (Diaz and Bardelli, 2014). The detection of 5hmC in cfDNA has been reported and it is increasingly fueled by the development of high-throughput sequencing methodology (Li et al., 2017). For instance, considerable researchers used 5hmC-Seal method to capture 5hmC patterns in colorectal, gastric, hepatocellular and lung cancers (Li et al., 2017; Zhang et al., 2018; Cai et al., 2019). However, 5hmC as a biomarker in liquid biopsy of cancer remains unclear, which warrants more exploration.

In this review, we focus on the value of 5hmC detection in cfDNA as an emerging biomarker in cancer management and possible mechanisms. Specifically, we discuss how 5hmC exerts its role in the early detection, prognosis, and treatment of various malignancies. We further overview the mechanisms underlying aberrant 5hmC patterns, TETs, and carcinogenesis. Notably, we emphasize that cfDNA-based liquid biopsy combined with genome-wide sequencing of 5hmC patterns may serve as an efficient tool to implement 5hmC into clinical applications in the era of precision medicine.

DEOXYRIBONUCLEIC ACID 5-HYDROXYMETHYLATION PROMOTES EARLY DETECTION OF CANCER

Early detection of cancer leads to better outcome (Wan et al., 2017; Shohdy and West, 2020). The detection of epigenetic alterations including 5hmC could promote early detection of cancer (Jankowska et al., 2015). 5hmC modification is tissue-specific and disease-specific (Laird et al., 2013; Sproul and

Meehan, 2013; Jankowska et al., 2015), and has been reported in the process of multiple precancerous pathogenesis. For instance, the increase and decrease of 5hmC level were respectively associated with the cervical precancerous lesions (Su et al., 2019) and the breast precancerous lesions (Zhang et al., 2020). 5hmC was also involved in hepatocellular carcinoma (HCC), melanoma and esophageal cancer (Lian et al., 2012; Tian et al., 2018; Liu et al., 2019a; Krais et al., 2019). Furthermore, as cfDNA can be identified in a minimal invasively and dynamically way in body fluids, recent studies demonstrated that 5hmC in cfDNA could act as a novel biomarker in cancer detection (Li et al., 2017; Song et al., 2017), taking a substantial step toward precision medicine.

5hmC in cfDNA has been detected in multiple malignancies, including HCC (Cai et al., 2019), colorectal cancer (CRC) (Gao et al., 2019), lung cancer (Zhang et al., 2018), gastric cancer (Li et al., 2017) and pancreatic ductal adenocarcinoma (PDAC) (Song et al., 2017; Guler et al., 2020). A reduced global 5hmC level in HCC was found to be positively correlated with tumor stage (Chen et al., 2013; Chen et al., 2017; Liu et al., 2019a) and it could be observed even in chronic hepatitis without significant methylation (Wang et al., 2019). Cai et al. reported the promising value of 5hmC in cfDNA in early detection of HCC (Cai et al., 2019). The research analyzed the genome-wide 5hmC patterns in cfDNA among 2,554 Chinese HCC patients, showing that the 5hmC profile in cfDNA could effectively distinguish early HCC patients from healthy controls and liver cirrhosis. Moreover, the research designed a weighted model comprised of a 32-gene-based 5hmC marker panel, which is proved to outperform alpha-fetoprotein (AFP) in early detection of HCC (Cai et al., 2019). Likewise, lung cancer also exhibits a global loss of 5hmC (Jin et al., 2011). Song et al. found that the global level of 5hmC in cfDNA progressively decreased from early-stage lung cancer to metastatic lung cancer, indicating that 5hmC in cfDNA could contribute to the early detection and surveillance of lung cancer (Song et al., 2017). Another study based on a Chinese cohort reported that 5hmC of specific genes in cfDNA have a higher sensitivity than traditional biomarkers, including CEA, CA125, NSE, and CYFRA21-1 in the early detection of non-small cell lung cancer (NSCLC) (Zhang et al., 2018). However, 5hmC pattern in cfDNA from this study was found to exhibit global gains in gene bodies as well as promoter regions in NSCLC patients (Zhang et al., 2018). Guler et al. revealed that 5hmC peaks of cfDNA in promoter region in PDAC patients were lower than those in non-cancer patients, whereas it was significantly higher over 3′UTR, transcription termination sites (TTS) and intron regions in PDAC patients, respectively. 5hmC profile in PDAC tissues was reported could classify PDAC cfDNA, which indicates the cfDNA could mirror the 5hmC enrichment observed in tumor (Guler et al., 2020). Another study reported that 5hmC peaks gained in cfDNA were present in the gene body of representative genes in colorectal cancer tissues, compared with patients of precancerous adenomas and healthy donors, such as *BCL11A*, *KCNK9* and *NTSR1* (Gao et al., 2019). Similarly, Xiao et al. determined the genome-wide distribution of 5hmC in cfDNA, indicating that the CRC patients have the widest distribution of 5hmC, whereas the healthy donors own the narrowest distribution, and the precancerous adenomas have the moderate distribution (Xiao et al., 2021). 5hmC in cfDNA was also reported associating with molecular subtypes in non-Hodgkin lymphoma (Chiu et al., 2021). Therefore, accumulating evidences indicate that 5hmC in cfDNA, both the distribution and global level, could be served as robust biomarkers in early detection of cancer, though further research is still warranted.

Despite the fact that cfDNA could be identified in the blood, only a small fraction is from the tumor and it remains difficult to identify aberrant epigenetic profiles precisely (Jankowska et al., 2015; Shen et al., 2018). Specifically, though 5hmC profiles are apparent in tumors at an early stage, it is still challenging to detect them by next-generation sequencing, as ctDNA itself is at an imperceptible level, especially in early stage cancer (Locke et al., 2019; Kilgour et al., 2020). It is reported that ctDNA in asymptomatic cancer is not detectable based on current methodology using typical 10 ml of blood, hindering its application in cancer early detection (Fiala and Diamandis, 2018). However, the emerging 5hmC-Seal technology has been utilized to capture genome-wide profiling of 5hmC and it proved to be a highly sensitive and robust approach for genome-wide profiling of 5hmC that requires only very limited input of DNA (< 10 ng) (Han et al., 2016; Applebaum et al., 2020; Guler et al., 2020). Also, other innovative methodologies permit the implementation of ctDNA in early-stage cancer detection (Liu et al., 2019b; Hu et al., 2019). Therefore, although 5hmC in ctDNA is difficult to detect, rapidly evolving methodology permit its application in early detection of cancer.

DEOXYRIBONUCLEIC ACID 5-HYDROXYMETHYLATION PREDICTS CANCER PROGNOSIS

In the era of precision medicine, increasing studies demonstrated the potential of 5hmC, TET protein family as potential clinical biomarkers to predict the prognosis of cancer, however, the evidence remains inadequate.

The decrease of 5hmC level is closely correlated with poor prognosis in multiple malignancies, including HCC (Liu et al., 2013; Liu et al., 2014; Liu et al., 2019a), CRC (Zhong et al., 2018), NSCLC (Liao et al., 2016), breast cancer (Tsai et al., 2015), gastric cancer (Yang et al., 2013; Frycz et al., 2014), papillary thyroid carcinoma (PTC) (Tong et al., 2019), glioblastomas (GBM) (Orr et al., 2012), esophageal carcinoma (EC) (Shi et al., 2016), cholangiocarcinoma (CCA) (Dong et al., 2015; Bai et al., 2021). In HCC, it has been reported that loss of 5hmC was positively correlated with tumor size, AFP level as well as poor overall survival (Liu et al., 2013). In patients with breast cancer, especially the ER/PR-negative subtype, the reduction of 5hmC was found strongly associated with poor disease-specific survival (DSS) and disease-free survival (DFS) (Tsai et al., 2015). In patients with PTC, one study revealed that the level of 5hmC was lower in those with lymph node metastasis than those without, which indicated that 5hmC may be a useful tool in predicting the lymph node involvement of PTC (Tong et al., 2019).

Moreover, the reduction of 5hmC level showed its prognostic value in WHO grade II diffuse astrocytomas (DA) and WHO grade IV GBM (Kraus et al., 2015; Zhang et al., 2016a; Johnson et al., 2016). Low 5hmC was correlated with increased mortality and poor survival in patients with GBM (Orr et al., 2012), and it could act as a biomarker in predicting tumor infiltration instead of ki67 and H3S10p (Kraus et al., 2015). It has been revealed that the loss of 5hmC may affect normal gene transcription, which could in turn promote abnormal proliferation of tumor cells, and eventually affect the survival in cervical squamous cell carcinoma (CSCC) (Zhang et al., 2016b). On the other hand, high level of 5hmC was associated with less invasive tumor phenotype and better prognosis in colon cancer (Zhong et al., 2018), and it was also displayed as a predictor of post-operative recurrence in *TMPRSS2-ERG* negative prostate cancer (Strand et al., 2015). Therefore, the detection of 5hmC levels in various cancers serves as a promising approach in predicting cancer prognosis.

The detection of 5hmC signature in cfDNA may provide a novel tool in predicting cancer outcomes. For instance, Song et al. observed a gradual decrease of 5hmC in cfDNA in early stage and advanced metastatic lung cancer, suggesting that such stage-dependent 5hmC loss in cfDNA may be a powerful tool for outcome prediction (Song et al., 2017). Cai et al. reported a novel HCC score predicting the prognosis of HCC, which consisted of cfDNA, 5hmC, and protein biomarkers [des-gamma-carboxy prothrombin (DCP) and AFP]. The results indicated that a higher HCC score was positively associated with the risk of recurrence and metastasis (Cai et al., 2021). In addition to the global level of 5hmC, the distribution of 5hmC in cfDNA also process a prognostic value. For instance, Chiu et al. reported that in diffuse large B-cell lymphoma (DLBCL), the distinct 5hmC profile in cfDNA could reflect origin of cell, thereby distinguishing different subtypes of DLBCL, and it was associated with the events of recurrence, retreatment, or death in DLBCL (Chiu et al., 2019; Chiu et al., 2021). Collectively, these studies indicate that 5hmC has a great potential as a biomarker of cancer progression, while the detection of 5hmC in cfDNA could contribute to the development of liquid biopsy in cancer.

In summary, DNA 5-hydroxymethylation in the genome is a novel prognostic biomarker in multiple cancers. The detection of 5hmC in cfDNA could help predict the outcomes of patients with cancer. However, the research on the detection of 5hmC still needs to be explored unremittingly by researchers in the future.

TARGETING DEOXYRIBONUCLEIC ACID 5-HYDROXYMETHYLATION IN CANCER

Targeting DNA demethylation has great potential in cancer treatment. Lian et al. suggested that feasible manipulation of overexpressing TET2 could restore the 5hmC level and further suppress tumor growth and invasion in melanoma, unlatching a novel therapeutic avenue for melanoma by targeting 5hmC generating pathway to reestablish 5hmC levels or landscape in melanoma cells (Lian et al., 2012). Another study showed that TET2 plays a key role in controlling the numbers and survival of slow-cycling cancer cells (SCCCs) through controlling the expression of cell death-related genes that regulate TNF-α signaling and restraining its proapoptotic signaling (Puig et al., 2018). Slow-cycling is a temporary state preserving potential cancer initiation and increased chemo-resistance. High TET2 activity and 5hmC level were associated with resistance to chemotherapy, thereby increasing the risk of recurrence of patients. Thus, 5hmC could be served as a biomarker for identifying the increased chemo-resistant SCCCs and TET2 could be potentially targeted for treatment of SCCCs (Puig et al., 2018). Interestingly, high expression of TET1 leads to global hydroxymethylation in T-cell acute lymphoblastic leukemia (T-ALL), which protects cells from DNA damage and thereby promoting leukemic growth. Bamezai et al. outlined that PARP could induce TET1 expression, thus TET1 could be pharmacologically targeted via application of PARP inhibitor Olaparib, which showed great therapeutic potential in T-ALL treatment (Bamezai et al., 2021). Fisetin, a natural flavonol, was reported to inhibit the activity of TET1, reduce 5hmC levels in CCNY/CDK16 promoter, and further restrain the invasion and progression of renal cancer stem cells. It indicated that TET1 could be targeted and 5hmC could be a potential indicator for the treatment of fisetin in renal cancer (Si et al., 2019). Besides, Vitamin C, a cofactor for TETs to enhance 5hmC conversion, is noticeably involved in the process of DNA demethylation (Dickson et al., 2013; Minor et al., 2013; Sant et al., 2018). Sant et al. reported that the reduced expression of Na^+-dependent Vitamin C transporter 2 (SVCT2) was a primary cause of 5hmC loss in breast cancer (Sant et al., 2018). Treatment of vitamin C might make up for the deficiency of SVCT2, thus restoring 5hmC levels via activating TET activity, and inducing apoptosis in breast cancer cells (Sant et al., 2018). Moreover, it has been suggested that 5hmC or 5hmC/5mC ratio might be a potential biomarker of differentiation and proliferation in pituitary neuroendocrine tumor, which could also be used as a biomarker of the effect of decitabine (Szabó et al., 2020). Therefore, we propose that 5hmC in cancer treatment could be a promising target, although more research is warranted.

5hmC could be a biomarker in cancer immunotherapy, especially in predicting immune cell exhaustion and immune evasion. Johnson et al. found a significant age-related differentially hydroxymethylated region occurred in the intronic region of *TOX2,* which is associated with $CD8^+$ T cell exhaustion. It belongs to a family of transcription factors that modify chromatin structure during T cell development (Johnson et al., 2020). Researchers reported that circTRIM33-12 could inhibit immune evasion of HCC by sponging oncogenic miR-191 and upregulating TET1 expression, which lead to a significant increase of 5hmC levels (Wang et al., 2019). Similarly, Taylor et al. found that the immune evasion subtype of lung squamous cell carcinoma has significant enhanced EGFR signaling, which further boosted the expression of the transcription factor

ETS1. ETS1 could upregulate miR-29b, which result in the downregulation of TET1 and subsequent reduction of 5hmC level (Taylor et al., 2016). In another study, TET2 was reported promoting tumor progression in melanoma via *ARG1*, an immunosuppressive gene in tumor-associated macrophages. *ARG1* embraced a low level of 5hmC in Tet2-null bone marrow derived macrophages (BMDM) (Pan et al., 2017). Targeting TET2 and its interactors (e.g., Fe^{2+}, 2-OG, Vitamin C) could regulate the activity of B cells, T cells, and macrophages, which could contribute to immunotherapy of cancer (Jiang, 2020). Luchtel et al. reported that ascorbic acid treatment could increase the level of 5hmC in $CD8^+$ T cells and reinforce their cytotoxicity against lymphoma cells (Luchtel et al., 2020). Therefore, the 5-hydroxymethylation of DNA could be a promising biomarker and a target of cancer immunotherapy, although further studies are required.

Targeting different oncogenes in the pathways of DNA demethylation, including TETs and its cofactors, may be potential strategies in cancer treatment in the future. 5hmC in these processes can be taken as a valuable biomarker for the response to multiple therapies. In terms of immunotherapy of cancer, 5hmC provides a new approach for immunotherapy-sensitive tumors, especially in overcoming immune cell exhaustion and cancer immune evasion. Although TET or 5hmC plays a critical role in cancer treatment, the involvement of TET and 5hmC in inhibiting cancer development is still far from clarified. Some attempts have been undertaken to develop pharmaceutical drugs targeting TET or its correlated signaling pathways in cancer development. For instance, TET1 has been considered as a critical oncogenic epigenetic regulator in acute myeloid leukemia (AML), which plays its role by promoting the expression of oncogenic targets, including *HOXA9*, *MEIS1* and *PBX3*, and suppressing the expression of tumor suppressor miR-22 (Huang et al., 2013; Huang et al., 2016; Jiang et al., 2016). Jiang et al. found that application of selective inhibitors (NSC-370284 and UC-514321) could directly target STAT/TET1 signaling, which was an effective and promising therapeutic strategy to treat TET1-high AML, especially when combined with standard chemotherapy (Jiang et al., 2017). Therefore, targeting TET1 signaling might be a considerable strategy in AML treatment. Moreover, TET1 and 5hmC were reported associating with an obesity-linked pathway driving cancer stem cells in triple-negative breast cancer, which providing new understanding on the cancer prevention and treatment (Bao et al., 2020). With the development of liquid biopsy, the detection of cfDNA provides new pathways for cancer treatment (Goodall et al., 2017; Siravegna et al., 2017). For instance, a recent study investigated the alteration of 5hmC profiles during the treatment of neuroblastoma. The study showed that 5hmC profiles in cfDNA changed over time, paralleled with changes in metastatic disease burden as well as patients' response to therapy (Applebaum et al., 2020). Thus, the detection of 5hmC profiles in cfDNA may be a promising biomarker that can be widely applied in monitoring the response to cancer treatment in future.

MECHANISMS UNDERLYING DEOXYRIBONUCLEIC ACID 5-HYDROXYMETHYLATION IN CANCER

Although the alteration of DNA 5-hydroxymethylation can be utilized as potential biomarkers in cancer screen, prognosis, and treatment, the mechanisms underlying these epigenetic alterations remain obscure. Exploring how the alteration of TETs and 5hmC play roles in tumorigenesis and tumor progression could accelerate the development of cancer therapy.

The abnormal expression of TETs, or inhibition of TETs cofactors lead to the alteration in the level and localization of 5hmC, impacting the cancer development and anti-tumor immunity (Koivunen and Laukka, 2018) (**Figure 3**). Compared with TET2 which is frequently mutated in hematopoietic malignancies (Huang and Rao, 2014; Jeschke et al., 2016), TET1 mutation is a rare occurrence in cancer (Thomson and Meehan, 2017). Instead it is found both methylated and transcriptionally suppressed *in vitro* in multiple malignancies, though whether it is the cause of hypermethylation is still unclear (Wu and Brenner, 2014). In addition to the genetic or transcriptomic disruption, the activity of TETs can be regulated by its substrates, cofactors and post-translational modifications (Thomson and Meehan, 2017). It has been found that patients with hematological malignancies and gliomas often harbor mutations in *IDH1* an *IDH2*, which can convert 2-OG into 2-hydroxyglutaraye (2-HG) and thereby inhibit the catalytic activity of TET (Figueroa et al., 2010; Xu et al., 2011). The loss of 5hmC in cancer can be further explained by the post-transcriptional regulation of TET. For instance, the IDAX protein, an interacting partner of TET2 that was often proved to be mutated in tumors, leads to TET2 degradation via caspase activation (Ko et al., 2013). However, decrease in hydroxymethylation in promoters of tumor suppressor genes is scarcely reported during carcinogenesis, which may require further investigations.

TET1 is usually known as a tumor suppressor, which could inhibit cancer progression via various pathways (Hsu et al., 2012; Fu et al., 2014; Neri et al., 2015; Yan et al., 2020). TET1 directly binds to the promoter of the target genes, catalyzing 5mC to 5hmC and ultimately activating gene transcription (Pei et al., 2016). In accordance with this mechanism, one study showed that the downregulation of TET1 could reduce the hydroxymethylation at the promoter of tumor suppressor gene *AJAP1*, subsequently activating WNT/β-catenin pathway and promoting the development of bladder cancer (Yan et al., 2020). TET1 loss in prostate cancer and breast cancer was found contributing to the hypermethylation of tissue inhibitors of metalloproteinases genes (*TIMP2* and *TIMP3*), which resulted in the epithelial-mesenchymal transition (EMT) and tumor progression (Hsu et al., 2012). Another study reported the HMGA2-TET1-HOXA9 axis could regulate breast cancer cell invasion, and it holds a prognostic signature in predicting patient survival (Sun et al., 2013). TET1 is negatively regulated by HMGA2, a chromatin remodeling factor that is highly expressed in most epithelial cancers. TET1 positively modulated HOXA9 by directly binding to or inducing the

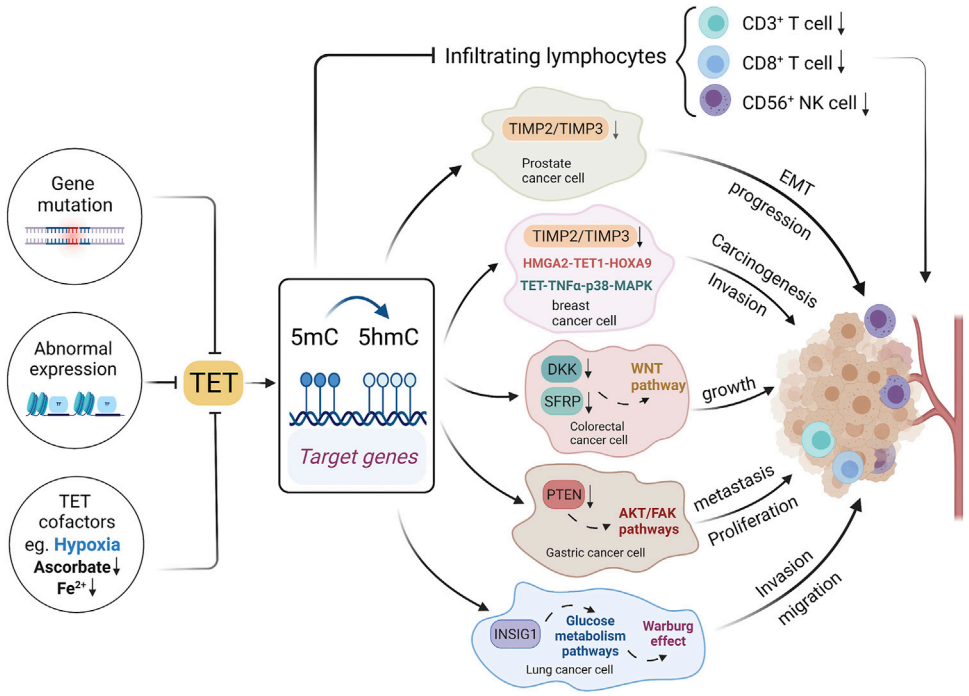

FIGURE 3 | Mechanisms underlying 5hmC and TET alterations in cancer. Gene mutations, abnormal expression and cofactors could affect TET expressions, thereby affecting DNA hydroxymethylation. The TET gene family could affect the tumor infiltrating lymphocyte, and it could also affect tumor development through multiple signal pathways.

histone binding of H3K4Me3 to the HOXA gene promoter regions, leading to local demethylation and gene transcription in breast cancer. Additionally, the downregulation of TET1 was reported to occur at the early stage and its expression could inhibit the proliferation of cancer cells in CRC (Neri et al., 2015). TET1-mediated demethylation induces a 5hmC increase at the promoter regions of *DKK* and *SFRP* genes, which were upstream inhibitors of WNT signaling pathway, hence TET downregulation can lead to cancer growth via repressing these inhibitors of WNT pathway (Neri et al., 2015). Similar mechanism was also reported in pancreatic cancer (Wu et al., 2019). Likewise, TET1 inhibits proliferation and metastasis of gastric cancer cells through demethylating PTEN promoter regions, which subsequently suppress the PTEN-inhibited AKT and FAK pathways (Pei et al., 2016). Besides DNA 5-hydroxymethylation mediated by TETs in tumor-suppressor genes, several oncogenes which encompass an acquisition of 5hmC were also reported. One study demonstrates that the 5hmC landscape in pancreatic ductal adenocarcinoma (PDAC) peaks in the gene that encodes the bromodomain-containing transcription factor BRD4, overlapping with active enhancer marks such as H3K4me1, and 5hmC acquisition by BRD4 enhancer is found to be a potential mechanism for regulating oncogenic activation (Bhattacharyya et al., 2017). In one word, 5hmC under the regulation of TETs is involved in the initiation and progression of tumors via various pathways, which is of great significance for its status as a promising biomarker in the field of precise oncology.

Besides, it is exciting to find that TETs and 5hmC changes are involved in immune signaling pathways, which may boost antitumor immunity. One study reported that in basal-like breast cancer (BLBC), the activation of nuclear factor κB (NF-κB) could suppress TET1 by binding to its promoter, highlighting a novel epigenetic-immunity connection (Collignon et al., 2018). NF-κB is a transcription factor involved in the activation of immune cells and regulation of immune signaling pathways (Gerondakis and Siebenlist, 2010; Hoesel and Schmid, 2013). Compared to TET1-high patients, low TET1 expression and subsequent 5hmC loss were associated with high infiltration of immune cells and better survival in BLBC (Collignon et al., 2018). Thus, the level of 5hmC could act as a marker of the immune response targeting tumor cells. TET2 also plays a substantial role in antitumor immunity. One study demonstrated that TET2 depletion could reduce Th1-type chemokines and PD-L1 expression by mediating the IFN-γ/JAK/STAT pathway, thereby decreasing tumor-infiltrating lymphocytes such as $CD3^+$ and $CD8^+$ T cell, and eventually it could compromise the efficacy of anti-PD-1/PD-L1 immunotherapy (Xu et al., 2019). Moreover, the 5hmC level in this study was positively correlated with the expression of chemokines and PD-L1 in tumor cells, infiltration of antitumor immune cells including $CD3^+$ T cells, $CD8^+$ T cells, and $CD56^+$ NK cells, and the response towards anti-PD-1/PD-L1 therapy. Thus, TETs and 5hmC could potentially be predictors of antitumor immunity, which may help boost the immunotherapy of cancer.

Oxygen is an essential element of TETs catalysis during demethylation (Schito and Semenza, 2016). Several studies have reported the association between TETs activity and hypoxia in different cancer (Mariani et al., 2014; Tsai et al., 2014; Wu et al., 2015). One study reported that hypoxia could reduce 5hmC levels in tumor-suppressor gene promoters by directly impairing TET oxidative activity in oncogenic process (Thienpont et al., 2016). However, in another study, hypoxia could conversely increase the expression of TET1, TET3 as well as 5hmC level in promoters, leading to carcinogenesis and poor prognosis of breast cancer patients via a TET-TNFα-p38-MAPK signaling (Wu et al., 2015). Interestingly, it was also reported that hypoxia-induced TET1 was associated with lipid metabolism in inducing EMT and cancer metastasis. 'Hypoxia-induced TET1 could increase the 5hmC level in the promoter of insulin induced gene 1 (*INSIG1*), the main regulator of cholesterol biosynthesis (Tsai et al., 2014). The knockdown of *INSIG1* could abolish the activation of mesenchymal genes, mitigating the activity of migration and invasion of lung cancer cells, and it could even decrease gene expression in the glucose metabolism pathway that contribute to the hypoxia-induced Warburg effect in tumor cells (Tsai et al., 2014). Thus, TET1 may play a crucial role in regulating cholesterol and glucose metabolism in tumor cells, although the mechanisms need to be further explored. In summary, the relationship between aberrant 5hmC patterns and carcinogenesis relies on both transcriptional state of TETs and the hypoxic environment in cancer cells (Thomson and Meehan, 2017). With further exploration of the mechanisms underlying 5hmC and carcinogenesis, the identification of new therapeutic targets and medications could be a promising field in the precise medicine of cancer.

CONCLUSION AND PERSPECTIVE

In this review, we overviewed the current research on use of DNA hydroxymethylation as a novel biomarker in the era of precision medicine. 5hmC has been highly prevailing in recent years in cancer diagnosis and prognosis. Different from genetic mutations encoded in DNA sequence, DNA hydroxymethylation is potentially reversible, which holds great promise in cancer treatment by using pharmaceutical intervention to recover normal epigenetic patterns (Thomson and Meehan, 2017). It is worth considering to effectively translate cancer-associated 5hmC patterns into clinical practice in the field of oncology.

With the development of genome-wide sequencing assays in the last few years, 5hmC profiling can be detected via ctDNA or cfDNA-based liquid biopsies, which are effective, minimally invasive tools for cancer early detection and progression surveillance. Although several studies demonstrated the detection methods of 5hmC signatures in cfDNA remain crude (Zeng et al., 2019). Another challenge is that circulating DNA from scarce tumor sub-populations can only be shown at an extremely low level in cfDNA, restraining its detection (Chen et al., 2013). This should be considered when designing novel assays and evaluating the role of 5hmC patterns in cancer by liquid biopsy. Overall, 5hmC could be a robust and pivotal biomarker in the era of liquid biopsy and precision medicine.

AUTHOR CONTRIBUTIONS

LW, FC, QW designed the review. LX researched the literature and drafted the manuscript. AB, JC, YZ, LC, MM, SJ, LC, CC, ZL, XZ, FC edited the manuscript. All authors read and approved the final manuscript.

FUNDING

The work was supported by the National Natural Science Foundation of China (No. 81972453, No. 81972597). Zhejiang Provincial Medical and Health Science and Technology (Youth Talent Program) Project No. 2020393822.The work was sponsored by Zheng Shu Medical Elite Scholarship Fund.

REFERENCES

Applebaum, M. A., Barr, E. K., Karpus, J., West-Szymanski, D. C., Oliva, M., Sokol, E. A., et al. (2020). 5-Hydroxymethylcytosine Profiles in Circulating Cell-free DNA Associate with Disease Burden in Children with Neuroblastoma. *Clin. Cancer Res.* 26 (6), 1309–1317. doi:10.1158/1078-0432.CCR-19-2829

Bai, X., Zhang, H., Zhou, Y., Nagaoka, K., Meng, J., Ji, C., et al. (2021). Ten-Eleven Translocation 1 Promotes Malignant Progression of Cholangiocarcinoma with Wild-Type Isocitrate Dehydrogenase 1. *Hepatology* 73 (5), 1747–1763. doi:10.1002/hep.31486

Bamezai, S., Demir, D., Pulikkottil, A. J., Ciccarone, F., Fischbein, E., Sinha, A., et al. (2021). TET1 Promotes Growth of T-Cell Acute Lymphoblastic Leukemia and Can Be Antagonized via PARP Inhibition. *Leukemia* 35 (2), 389–403. doi:10.1038/s41375-020-0864-3

Bao, B., Teslow, E. A., Mitrea, C., Boerner, J. L., Dyson, G., and Bollig-Fischer, A. (2020). Role of TET1 and 5hmC in an Obesity-Linked Pathway Driving Cancer Stem Cells in Triple-Negative Breast Cancer. *Mol. Cancer Res.* 18 (12), 1803–1814. doi:10.1158/1541-7786.mcr-20-0359

Berdasco, M., and Esteller, M. (2019). Clinical Epigenetics: Seizing Opportunities for Translation. *Nat. Rev. Genet.* 20 (2), 109–127. doi:10.1038/s41576-018-0074-2

Bhattacharyya, S., Pradhan, K., Campbell, N., Mazdo, J., Vasantkumar, A., Maqbool, S., et al. (2017). Altered Hydroxymethylation Is Seen at Regulatory Regions in Pancreatic Cancer and Regulates Oncogenic Pathways. *Genome Res.* 27 (11), 1830–1842. doi:10.1101/gr.222794.117

Cai, J., Chen, L., Zhang, Z., Zhang, X., Lu, X., Liu, W., et al. (2019). Genome-wide Mapping of 5-hydroxymethylcytosines in Circulating Cell-free DNA as a Non-invasive Approach for Early Detection of Hepatocellular Carcinoma. *Gut* 68 (12), 2195–2205. doi:10.1136/gutjnl-2019-318882

Cai, Z., Zhang, J., He, Y., Xia, L., Dong, X., Chen, G., et al. (2021). Liquid Biopsy by Combining 5-hydroxymethylcytosine Signatures of Plasma Cell-free DNA and Protein Biomarkers for Diagnosis and Prognosis of Hepatocellular Carcinoma. *ESMO Open* 6 (1), 100021. doi:10.1016/j.esmoop.2020.100021

Chen, K., Zhang, J., Guo, Z., Ma, Q., Xu, Z., Zhou, Y., et al. (2016). Loss of 5-hydroxymethylcytosine Is Linked to Gene Body Hypermethylation in Kidney Cancer. *Cell Res* 26 (1), 103–118. doi:10.1038/cr.2015.150

Chen, M.-L., Shen, F., Huang, W., Qi, J.-H., Wang, Y., Feng, Y.-Q., et al. (2013). Quantification of 5-methylcytosine and 5-hydroxymethylcytosine in Genomic

DNA from Hepatocellular Carcinoma Tissues by Capillary Hydrophilic-Interaction Liquid Chromatography/quadrupole TOF Mass Spectrometry. *Clin. Chem.* 59 (5), 824–832. doi:10.1373/clinchem.2012.193938

Chen, M., and Zhao, H. (2019). Next-generation Sequencing in Liquid Biopsy: Cancer Screening and Early Detection. *Hum. Genomics* 13 (1), 34. doi:10.1186/s40246-019-0220-8

Chen, Q., Yin, D., Zhang, Y., Yu, L., Li, X.-D., Zhou, Z.-J., et al. (2017). MicroRNA-29a Induces Loss of 5-hydroxymethylcytosine and Promotes Metastasis of Hepatocellular Carcinoma through a TET-SOCS1-MMP9 Signaling axis. *Cell Death Dis* 8 (6), e2906. doi:10.1038/cddis.2017.142

Chiu, B. C.-H., Chen, C., You, Q., Chiu, R., Venkataraman, G., Zeng, C., et al. (2021). Alterations of 5-hydroxymethylation in Circulating Cell-free DNA Reflect Molecular Distinctions of Subtypes of Non-hodgkin Lymphoma. *Npj Genom. Med.* 6 (1), 11. doi:10.1038/s41525-021-00179-8

Chiu, B. C.-H., Zhang, Z., You, Q., Zeng, C., Stepniak, E., Bracci, P. M., et al. (2019). Prognostic Implications of 5-hydroxymethylcytosines from Circulating Cell-free DNA in Diffuse Large B-Cell Lymphoma. *Blood Adv.* 3 (19), 2790–2799. doi:10.1182/bloodadvances.2019000175

Clermont, P. L., Parolia, A., Liu, H. H., and Helgason, C. D. (2016). DNA Methylation at Enhancer Regions: Novel Avenues for Epigenetic Biomarker Development. *Front. Biosci. (Landmark Ed.* 21, 430–446. doi:10.2741/4399

Collignon, E., Canale, A., Al Wardi, C., Bizet, M., Calonne, E., Dedeurwaerder, S., et al. (2018). Immunity Drives TET1 Regulation in Cancer through NF-Kb. *Sci. Adv.* 4 (6), eaap7309. doi:10.1126/sciadv.aap7309

De Rubis, G., Rajeev Krishnan, S., and Bebawy, M. (2019). Liquid Biopsies in Cancer Diagnosis, Monitoring, and Prognosis. *Trends Pharmacol. Sci.* 40 (3), 172–186. doi:10.1016/j.tips.2019.01.006

Diaz, L. A., Jr., and Bardelli, A. (2014). Liquid Biopsies: Genotyping Circulating Tumor DNA. *Jco* 32 (6), 579–586. doi:10.1200/jco.2012.45.2011

Dickson, K. M., Gustafson, C. B., Young, J. I., Züchner, S., and Wang, G. (2013). Ascorbate-induced generation of 5-hydroxymethylcytosine is unaffected by varying levels of iron and 2-oxoglutarate. *Biochemical and Biophysical Research Communications* 439 (4), 522–527. doi:10.1016/j.bbrc.2013.09.010

Dong, Z.-R., Zhang, C., Cai, J.-b., Zhang, P.-F., Shi, G.-M., Gao, D.-m., Sun, H.-C., Qiu, S.-J., Zhou, J., Ke, A.-W., and Fan, J. (2015). Role of 5-hydroxymethylcytosine level in diagnosis and prognosis prediction of intrahepatic cholangiocarcinoma. *Tumor Biol.* 36 (4), 2763–2771. doi:10.1007/s13277-014-2900-2

Ehrlich, M. (2019). DNA hypermethylation in disease: mechanisms and clinical relevance. *Epigenetics* 14 (12), 1141–1163. doi:10.1080/15592294.2019.1638701

Feinberg, A. P., Koldobskiy, M. A., and Göndör, A. (2016). Epigenetic modulators, modifiers and mediators in cancer aetiology and progression. *Nat Rev Genet* 17 (5), 284–299. doi:10.1038/nrg.2016.13

Fiala, C., and Diamandis, E. P. (2018). Utility of circulating tumor DNA in cancer diagnostics with emphasis on early detection. *BMC Med* 16 (1), 166. doi:10.1186/s12916-018-1157-9

Figueroa, M. E., Abdel-Wahab, O., Lu, C., Ward, P. S., Patel, J., Shih, A., Li, Y., Bhagwat, N., Vasanthakumar, A., Fernandez, H. F., Tallman, M. S., Sun, Z., Wolniak, K., Peeters, J. K., Liu, W., Choe, S. E., Fantin, V. R., Paietta, E., Löwenberg, B., Licht, J. D., Godley, L. A., Delwel, R., Valk, P. J. M., Thompson, C. B., Levine, R. L., and Melnick, A. (2010). Leukemic IDH1 and IDH2 mutations result in a hypermethylation phenotype, disrupt TET2 function, and impair hematopoietic differentiation. *Cancer cell* 18 (6), 553–567. doi:10.1016/j.ccr.2010.11.015

Frycz, B. A., Murawa, D., Borejsza-Wysocki, M., Marciniak, R., Murawa, P., Drews, M., Kołodziejczak, A., Tomela, K., and Jagodziński, P. P. (2014). Decreased expression of ten-eleven translocation 1 protein is associated with some clinicopathological features in gastric cancer. *Biomedicine & Pharmacotherapy* 68 (2), 209–212. doi:10.1016/j.biopha.2013.12.011

Fu, H.-L., Ma, Y., Lu, L.-G., Hou, P., Li, B.-J., Jin, W.-L., et al. (2014). TET1 Exerts its Tumor Suppressor Function by Interacting with P53-EZH2 Pathway in Gastric Cancer. *J. Biomed. Nanotechnology* 10 (7), 1217–1230. doi:10.1166/jbn.2014.1861

Gao, P., Lin, S., Cai, M., Zhu, Y., Song, Y., Sui, Y., et al. (2019). 5-Hydroxymethylcytosine Profiling from Genomic and Cell-free DNA for Colorectal Cancers Patients. *J. Cel Mol Med* 23 (5), 3530–3537. doi:10.1111/jcmm.14252

Gerondakis, S., and Siebenlist, U. (2010). Roles of the NF- B Pathway in Lymphocyte Development and Function. *Cold Spring Harbor Perspect. Biol.* 2 (5), a000182. doi:10.1101/cshperspect.a000182

Goodall, J., Mateo, J., Yuan, W., Mossop, H., Porta, N., Miranda, S., et al. (2017). Circulating Cell-free DNA to Guide Prostate Cancer Treatment with PARP Inhibition. *Cancer Discov.* 7 (9), 1006–1017. doi:10.1158/2159-8290.cd-17-0261

Guler, G. D., Ning, Y., Ku, C.-J., Phillips, T., McCarthy, E., Ellison, C. K., et al. (2020). Detection of Early Stage Pancreatic Cancer Using 5-hydroxymethylcytosine Signatures in Circulating Cell Free DNA. *Nat. Commun.* 11 (1), 5270. doi:10.1038/s41467-020-18965-w

Han, D., Lu, X., Shih, A. H., Nie, J., You, Q., Xu, M. M., et al. (2016). A Highly Sensitive and Robust Method for Genome-wide 5hmC Profiling of Rare Cell Populations. *Mol. Cel.* 63 (4), 711–719. doi:10.1016/j.molcel.2016.06.028

He, Y.-F., Li, B.-Z., Li, Z., Liu, P., Wang, Y., Tang, Q., et al. (2011). Tet-mediated Formation of 5-carboxylcytosine and its Excision by TDG in Mammalian DNA. *Science* 333 (6047), 1303–1307. doi:10.1126/science.1210944

Hoesel, B., and Schmid, J. A. (2013). The Complexity of NF-Kb Signaling in Inflammation and Cancer. *Mol. Cancer* 12, 86. doi:10.1186/1476-4598-12-86

Hsu, C.-H., Peng, K.-L., Kang, M.-L., Chen, Y.-R., Yang, Y.-C., Tsai, C.-H., et al. (2012). TET1 Suppresses Cancer Invasion by Activating the Tissue Inhibitors of Metalloproteinases. *Cel Rep.* 2 (3), 568–579. doi:10.1016/j.celrep.2012.08.030

Hu, L., Liu, Y., Han, S., Yang, L., Cui, X., Gao, Y., et al. (2019). Jump-seq: Genome-wide Capture and Amplification of 5-Hydroxymethylcytosine Sites. *J. Am. Chem. Soc.* 141 (22), 8694–8697. doi:10.1021/jacs.9b02512

Huang, H., Jiang, X., Li, Z., Li, Y., Song, C.-X., He, C., et al. (2013). TET1 Plays an Essential Oncogenic Role in MLL-Rearranged Leukemia. *Proc. Natl. Acad. Sci.* 110 (29), 11994–11999. doi:10.1073/pnas.1310656110

Huang, H., Jiang, X., Wang, J., Li, Y., Song, C.-X., Chen, P., et al. (2016). Identification of MLL-fusion/MYC⊣miR-26⊣TET1 Signaling Circuit in MLL-Rearranged Leukemia. *Cancer Lett.* 372 (2), 157–165. doi:10.1016/j.canlet.2015.12.032

Huang, Y., and Rao, A. (2014). Connections between TET Proteins and Aberrant DNA Modification in Cancer. *Trends Genet.* 30 (10), 464–474. doi:10.1016/j.tig.2014.07.005

Ito, S., Shen, L., Dai, Q., Wu, S. C., Collins, L. B., Swenberg, J. A., et al. (2011). Tet Proteins Can Convert 5-methylcytosine to 5-formylcytosine and 5-carboxylcytosine. *Science* 333 (6047), 1300–1303. doi:10.1126/science.1210597

Jankowska, A. M., Millward, C. L., and Caldwell, C. W. (2015). The Potential of DNA Modifications as Biomarkers and Therapeutic Targets in Oncology. *Expert Rev. Mol. Diagn.* 15 (10), 1325–1337. doi:10.1586/14737159.2015.1084229

Jeschke, J., Collignon, E., and Fuks, F. (2016). Portraits of TET-Mediated DNA Hydroxymethylation in Cancer. *Curr. Opin. Genet. Development* 36, 16–26. doi:10.1016/j.gde.2016.01.004

Jiang, S. (2020). Tet2 at the Interface between Cancer and Immunity. *Commun. Biol.* 3 (1), 667. doi:10.1038/s42003-020-01391-5

Jiang, X., Hu, C., Arnovitz, S., Bugno, J., Yu, M., Zuo, Z., et al. (2016). miR-22 Has a Potent Anti-tumour Role with Therapeutic Potential in Acute Myeloid Leukaemia. *Nat. Commun.* 7, 11452. doi:10.1038/ncomms11452

Jiang, X., Hu, C., Ferchen, K., Nie, J., Cui, X., Chen, C.-H., et al. (2017). Targeted Inhibition of STAT/TET1 axis as a Therapeutic Strategy for Acute Myeloid Leukemia. *Nat. Commun.* 8 (1), 2099. doi:10.1038/s41467-017-02290-w

Jin, S.-G., Jiang, Y., Qiu, R., Rauch, T. A., Wang, Y., Schackert, G., et al. (2011). 5-Hydroxymethylcytosine Is Strongly Depleted in Human Cancers but its Levels Do Not Correlate with IDH1 Mutations. *Cancer Res.* 71 (24), 7360–7365. doi:10.1158/0008-5472.can-11-2023

Johnson, K. C., Houseman, E. A., King, J. E., von Herrmann, K. M., Fadul, C. E., and Christensen, B. C. (2016). 5-Hydroxymethylcytosine Localizes to Enhancer Elements and Is Associated with Survival in Glioblastoma Patients. *Nat. Commun.* 7, 13177. doi:10.1038/ncomms13177

Johnson, N. D., Huang, L., Li, R., Li, Y., Yang, Y., Kim, H. R., et al. (2020). Age-related DNA Hydroxymethylation Is Enriched for Gene Expression and Immune System Processes in Human Peripheral Blood. *Epigenetics* 15 (3), 294–306. doi:10.1080/15592294.2019.1666651

Kilgour, E., Rothwell, D. G., Brady, G., and Dive, C. (2020). Liquid Biopsy-Based Biomarkers of Treatment Response and Resistance. *Cancer Cell* 37 (4), 485–495. doi:10.1016/j.ccell.2020.03.012

Ko, M., An, J., Bandukwala, H. S., Chavez, L., Äijö, T., Pastor, W. A., et al. (2013). Modulation of TET2 Expression and 5-methylcytosine Oxidation by the CXXC Domain Protein IDAX. *Nature* 497 (7447), 122–126. doi:10.1038/nature12052

Kohli, R. M., and Zhang, Y. (2013). TET Enzymes, TDG and the Dynamics of DNA Demethylation. *Nature* 502 (7472), 472–479. doi:10.1038/nature12750

Koivunen, P., and Laukka, T. (2018). The TET Enzymes. *Cell. Mol. Life Sci.* 75 (8), 1339–1348. doi:10.1007/s00018-017-2721-8

Krais, A. M., Park, Y. J., Reifenberger, G., Meister, M., Plass, C., and Schmeiser, H. H. (2019). Sensitive Detection of Hydroxymethylcytosine Levels in normal and Neoplastic Cells and Tissues. *Electrophoresis* 40 (9), 1293–1297. doi:10.1002/elps.201800523

Kraus, T. F. J., Kolck, G., Greiner, A., Schierl, K., Guibourt, V., and Kretzschmar, H. A. (2015). Loss of 5-hydroxymethylcytosine and Intratumoral Heterogeneity as an Epigenomic Hallmark of Glioblastoma. *Tumor Biol.* 36 (11), 8439–8446. doi:10.1007/s13277-015-3606-9

Kriaucionis, S., and Heintz, N. (2009). The Nuclear DNA Base 5-hydroxymethylcytosine Is Present in Purkinje Neurons and the Brain. *Science* 324 (5929), 929–930. doi:10.1126/science.1169786

Laird, A., Thomson, J. P., Harrison, D. J., and Meehan, R. R. (2013). 5-hydroxymethylcytosine Profiling as an Indicator of Cellular State. *Epigenomics* 5 (6), 655–669. doi:10.2217/epi.13.69

Li, W., Zhang, X., Lu, X., You, L., Song, Y., Luo, Z., et al. (2017). 5-Hydroxymethylcytosine Signatures in Circulating Cell-free DNA as Diagnostic Biomarkers for Human Cancers. *Cel Res* 27 (10), 1243–1257. doi:10.1038/cr.2017.121

Lian, C. G., Xu, Y., Ceol, C., Wu, F., Larson, A., Dresser, K., et al. (2012). Loss of 5-hydroxymethylcytosine Is an Epigenetic Hallmark of Melanoma. *Cell* 150 (6), 1135–1146. doi:10.1016/j.cell.2012.07.033

Liao, Y., Gu, J., Wu, Y., Long, X., Ge, D., Xu, J., et al. (2016). Low Level of 5-Hydroxymethylcytosine Predicts Poor Prognosis in Non-small Cell Lung Cancer. *Oncol. Lett.* 11 (6), 3753–3760. doi:10.3892/ol.2016.4474

Liu, C., Liu, L., Chen, X., Shen, J., Shan, J., Xu, Y., et al. (2013). Decrease of 5-hydroxymethylcytosine Is Associated with Progression of Hepatocellular Carcinoma through Downregulation of TET1. *PLoS One* 8 (5), e62828. doi:10.1371/journal.pone.0062828

Liu, J., Jiang, J., Mo, J., Liu, D., Cao, D., Wang, H., et al. (2019). Global DNA 5-Hydroxymethylcytosine and 5-Formylcytosine Contents Are Decreased in the Early Stage of Hepatocellular Carcinoma. *Hepatology* 69 (1), 196–208. doi:10.1002/hep.30146

Liu, W.-R., Tian, M.-X., Jin, L., Yang, L.-X., Ding, Z.-B., Shen, Y.-H., et al. (2014). High Expression of 5-hydroxymethylcytosine and Isocitrate Dehydrogenase 2 Is Associated with Favorable Prognosis after Curative Resection of Hepatocellular Carcinoma. *J. Exp. Clin. Cancer Res.* 33, 32. doi:10.1186/1756-9966-33-32

Liu, Y., Siejka-Zielińska, P., Velikova, G., Bi, Y., Yuan, F., Tomkova, M., et al. (2019). Bisulfite-free Direct Detection of 5-methylcytosine and 5-hydroxymethylcytosine at Base Resolution. *Nat. Biotechnol.* 37 (4), 424–429. doi:10.1038/s41587-019-0041-2

Locke, W. J., Guanzon, D., Ma, C., Liew, Y. J., Duesing, K. R., Fung, K. Y. C., et al. (2019). DNA Methylation Cancer Biomarkers: Translation to the Clinic. *Front. Genet.* 10, 1150. doi:10.3389/fgene.2019.01150

López, V., Fernández, A. F., and Fraga, M. F. (2017). The Role of 5-hydroxymethylcytosine in Development, Aging and Age-Related Diseases. *Ageing Res. Rev.* 37, 28–38. doi:10.1016/j.arr.2017.05.002

Luchtel, R. A., Bhagat, T., Pradhan, K., Jacobs, W. R., Jr., Levine, M., Verma, A., et al. (2020). High-dose Ascorbic Acid Synergizes with Anti-PD1 in a Lymphoma Mouse Model. *Proc. Natl. Acad. Sci. USA* 117 (3), 1666–1677. doi:10.1073/pnas.1908158117

Mariani, C. J., Vasanthakumar, A., Madzo, J., Yesilkanal, A., Bhagat, T., Yu, Y., et al. (2014). TET1-mediated Hydroxymethylation Facilitates Hypoxic Gene Induction in Neuroblastoma. *Cel Rep.* 7 (5), 1343–1352. doi:10.1016/j.celrep.2014.04.040

Minor, E. A., Court, B. L., Young, J. I., and Wang, G. (2013). Ascorbate Induces Ten-Eleven Translocation (Tet) Methylcytosine Dioxygenase-Mediated Generation of 5-hydroxymethylcytosine. *J. Biol. Chem.* 288 (19), 13669–13674. doi:10.1074/jbc.c113.464800

Moen, E. L., Mariani, C. J., Zullow, H., Jeff-Eke, M., Litwin, E., Nikitas, J. N., et al. (2015). New Themes in the Biological Functions of 5-methylcytosine and 5-hydroxymethylcytosine. *Immunol. Rev.* 263 (1), 36–49. doi:10.1111/imr.12242

Neri, F., Dettori, D., Incarnato, D., Krepelova, A., Rapelli, S., Maldotti, M., et al. (2015). TET1 Is a Tumour Suppressor that Inhibits colon Cancer Growth by Derepressing Inhibitors of the WNT Pathway. *Oncogene* 34 (32), 4168–4176. doi:10.1038/onc.2014.356

Orr, B. A., Haffner, M. C., Nelson, W. G., Yegnasubramanian, S., and Eberhart, C. G. (2012). Decreased 5-hydroxymethylcytosine Is Associated with Neural Progenitor Phenotype in normal Brain and Shorter Survival in Malignant Glioma. *PLoS One* 7 (7), e41036. doi:10.1371/journal.pone.0041036

Pan, W., Zhu, S., Qu, K., Meeth, K., Cheng, J., He, K., et al. (2017). The DNA Methylcytosine Dioxygenase Tet2 Sustains Immunosuppressive Function of Tumor-Infiltrating Myeloid Cells to Promote Melanoma Progression. *Immunity* 47 (2), 284–297. doi:10.1016/j.immuni.2017.07.020

Pei, Y.-F., Tao, R., Li, J.-F., Su, L.-P., Yu, B.-Q., Wu, X.-Y., et al. (2016). TET1 Inhibits Gastric Cancer Growth and Metastasis by PTEN Demethylation and Re-expression. *Oncotarget* 7 (21), 31322–31335. doi:10.18632/oncotarget.8900

Puig, I., Tenbaum, S. P., Chicote, I., Arqués, O., Martínez-Quintanilla, J., Cuesta-Borrás, E., et al. (2018). TET2 Controls Chemoresistant Slow-Cycling Cancer Cell Survival and Tumor Recurrence. *J. Clin. Invest.* 128 (9), 3887–3905. doi:10.1172/jci96393

Putiri, E. L., Tiedemann, R. L., Thompson, J. J., Liu, C., Ho, T., Choi, J.-H., et al. (2014). Distinct and Overlapping Control of 5-methylcytosine and 5-hydroxymethylcytosine by the TET Proteins in Human Cancer Cells. *Genome Biol.* 15 (6), R81. doi:10.1186/gb-2014-15-6-r81

Sandoval, J., and Esteller, M. (2012). Cancer Epigenomics: beyond Genomics. *Curr. Opin. Genet. Development* 22 (1), 50–55. doi:10.1016/j.gde.2012.02.008

Sant, D. W., Mustafi, S., Gustafson, C. B., Chen, J., Slingerland, J. M., and Wang, G. (2018). Vitamin C Promotes Apoptosis in Breast Cancer Cells by Increasing TRAIL Expression. *Sci. Rep.* 8 (1), 5306. doi:10.1038/s41598-018-23714-7

Schito, L., and Semenza, G. L. (2016). Hypoxia-Inducible Factors: Master Regulators of Cancer Progression. *Trends Cancer* 2 (12), 758–770. doi:10.1016/j.trecan.2016.10.016

Shen, S. Y., Singhania, R., Fehringer, G., Chakravarthy, A., Roehrl, M. H. A., Chadwick, D., et al. (2018). Sensitive Tumour Detection and Classification Using Plasma Cell-free DNA Methylomes. *Nature* 563 (7732), 579–583. doi:10.1038/s41586-018-0703-0

Shi, X., Yu, Y., Luo, M., Zhang, Z., Shi, S., Feng, X., et al. (2016). Loss of 5-Hydroxymethylcytosine Is an Independent Unfavorable Prognostic Factor for Esophageal Squamous Cell Carcinoma. *PLoS One* 11 (4), e0153100. doi:10.1371/journal.pone.0153100

Shohdy, K. S., and West, H. (2020). Circulating Tumor DNA Testing-Liquid Biopsy of a Cancer. *JAMA Oncol.* 6 (5), 792. doi:10.1001/jamaoncol.2020.0346

Si, Y., Liu, J., Shen, H., Zhang, C., Wu, Y., Huang, Y., et al. (2019). Fisetin Decreases TET1 Activity and CCNY/CDK16 Promoter 5hmC Levels to Inhibit the Proliferation and Invasion of Renal Cancer Stem Cell. *J. Cel Mol Med* 23 (2), 1095–1105. doi:10.1111/jcmm.14010

Siravegna, G., Marsoni, S., Siena, S., and Bardelli, A. (2017). Integrating Liquid Biopsies into the Management of Cancer. *Nat. Rev. Clin. Oncol.* 14 (9), 531–548. doi:10.1038/nrclinonc.2017.14

Smith, Z. D., and Meissner, A. (2013). DNA Methylation: Roles in Mammalian Development. *Nat. Rev. Genet.* 14 (3), 204–220. doi:10.1038/nrg3354

Song, C.-X., Yin, S., Ma, L., Wheeler, A., Chen, Y., Zhang, Y., et al. (2017). 5-Hydroxymethylcytosine Signatures in Cell-free DNA Provide Information about Tumor Types and Stages. *Cel Res* 27 (10), 1231–1242. doi:10.1038/cr.2017.106

Sproul, D., and Meehan, R. R. (2013). Genomic Insights into Cancer-Associated Aberrant CpG Island Hypermethylation. *Brief. Funct. Genomics* 12 (3), 174–190. doi:10.1093/bfgp/els063

Strand, S. H., Hoyer, S., Lynnerup, A.-S., Haldrup, C., Storebjerg, T. M., Borre, M., et al. (2015). High Levels of 5-hydroxymethylcytosine (5hmC) Is an Adverse Predictor of Biochemical Recurrence after Prostatectomy in ERG-Negative Prostate Cancer. *Clin. Epigenet* 7, 111. doi:10.1186/s13148-015-0146-5

Su, P.-H., Hsu, Y.-W., Huang, R.-L., Chen, L.-Y., Chao, T.-K., Liao, C.-C., et al. (2019). TET1 Promotes 5hmC-dependent Stemness, and Inhibits a 5hmC-independent Epithelial-Mesenchymal Transition, in Cervical Precancerous Lesions. *Cancer Lett.* 450, 53–62. doi:10.1016/j.canlet.2019.01.033

Sun, M., Song, C.-X., Huang, H., Frankenberger, C. A., Sankarasharma, D., Gomes, S., et al. (2013). HMGA2/TET1/HOXA9 Signaling Pathway Regulates Breast Cancer Growth and Metastasis. *Proc. Natl. Acad. Sci.* 110 (24), 9920–9925. doi:10.1073/pnas.1305172110

Szabó, B., Németh, K., Mészáros, K., Szücs, N., Czirják, S., Reiniger, L., et al. (2020). Demethylation Status of Somatic DNA Extracted from Pituitary Neuroendocrine Tumors Indicates Proliferative Behavior. *J. Clin. Endocrinol. Metab.* 105 (6), dgaa156. doi:10.1210/clinem/dgaa156

Taberlay, P. C., Statham, A. L., Kelly, T. K., Clark, S. J., and Jones, P. A. (2014). Reconfiguration of Nucleosome-Depleted Regions at Distal Regulatory Elements Accompanies DNA Methylation of Enhancers and Insulators in Cancer. *Genome Res.* 24 (9), 1421–1432. doi:10.1101/gr.163485.113

Tahiliani, M., Koh, K. P., Shen, Y., Pastor, W. A., Bandukwala, H., Brudno, Y., et al. (2009). Conversion of 5-methylcytosine to 5-hydroxymethylcytosine in Mammalian DNA by MLL Partner TET1. *Science* 324 (5929), 930–935. doi:10.1126/science.1170116

Taylor, M. A., Wappett, M., Delpuech, O., Brown, H., and Chresta, C. M. (2016). Enhanced MAPK Signaling Drives ETS1-Mediated Induction of miR-29b Leading to Downregulation of TET1 and Changes in Epigenetic Modifications in a Subset of Lung SCC. *Oncogene* 35 (33), 4345–4357. doi:10.1038/onc.2015.499

Thienpont, B., Steinbacher, J., Zhao, H., D'Anna, F., Kuchnio, A., Ploumakis, A., et al. (2016). Tumour Hypoxia Causes DNA Hypermethylation by Reducing TET Activity. *Nature* 537 (7618), 63–68. doi:10.1038/nature19081

Thomson, J. P., and Meehan, R. R. (2017). The Application of Genome-wide 5-hydroxymethylcytosine Studies in Cancer Research. *Epigenomics* 9 (1), 77–91. doi:10.2217/epi-2016-0122

Tian, X., Sun, B., Chen, C., Gao, C., Zhang, J., Lu, X., et al. (2018). Circulating Tumor DNA 5-hydroxymethylcytosine as a Novel Diagnostic Biomarker for Esophageal Cancer. *Cel Res* 28 (5), 597–600. doi:10.1038/s41422-018-0014-x

Tong, M., Gao, S., Qi, W., Shi, C., Qiu, M., Yang, F., et al. (2019). 5-Hydroxymethylcytosine as a Potential Epigenetic Biomarker in Papillary Thyroid Carcinoma. *Oncol. Lett.* 18 (3), 2304–2309. doi:10.3892/ol.2019.10531

Tsai, K.-W., Li, G.-C., Chen, C.-H., Yeh, M.-H., Huang, J.-S., Tseng, H.-H., et al. (2015). Reduction of Global 5-hydroxymethylcytosine Is a Poor Prognostic Factor in Breast Cancer Patients, Especially for an ER/PR-negative Subtype. *Breast Cancer Res. Treat.* 153 (1), 219–234. doi:10.1007/s10549-015-3525-x

Tsai, Y.-P., Chen, H.-F., Chen, S.-Y., Cheng, W.-C., Wang, H.-W., Shen, Z.-J., et al. (2014). TET1 Regulates Hypoxia-Induced Epithelial-Mesenchymal Transition by Acting as a Co-activator. *Genome Biol.* 15 (12), 513. doi:10.1186/s13059-014-0513-0

Tuaeva, N. O., Falzone, L., Porozov, Y. B., Nosyrev, A. E., Trukhan, V. M., Kovatsi, L., et al. (2019). Translational Application of Circulating DNA in Oncology: Review of the Last Decades Achievements. *Cells* 8 (10), 1251. doi:10.3390/cells8101251

Wan, J. C. M., Massie, C., Garcia-Corbacho, J., Mouliere, F., Brenton, J. D., Caldas, C., et al. (2017). Liquid Biopsies Come of Age: towards Implementation of Circulating Tumour DNA. *Nat. Rev. Cancer* 17 (4), 223–238. doi:10.1038/nrc.2017.7

Wang, P., Yan, Y., Yu, W., and Zhang, H. (2019). Role of Ten-Eleven Translocation Proteins and 5-hydroxymethylcytosine in Hepatocellular Carcinoma. *Cell Prolif* 52 (4), e12626. doi:10.1111/cpr.12626

Wang, Z., Du, M., Yuan, Q., Guo, Y., Hutchinson, J. N., Su, L., et al. (2020). Epigenomic Analysis of 5-hydroxymethylcytosine (5hmC) Reveals Novel DNA Methylation Markers for Lung Cancers. *Neoplasia* 22 (3), 154–161. doi:10.1016/j.neo.2020.01.001

Wu, B.-K., and Brenner, C. (2014). Suppression of TET1-dependent DNA Demethylation Is Essential for KRAS-Mediated Transformation. *Cel Rep.* 9 (5), 1827–1840. doi:10.1016/j.celrep.2014.10.063

Wu, J., Li, H., Shi, M., Zhu, Y., Ma, Y., Zhong, Y., et al. (2019). TET1-mediated DNA Hydroxymethylation Activates Inhibitors of the Wnt/β-Catenin Signaling Pathway to Suppress EMT in Pancreatic Tumor Cells. *J. Exp. Clin. Cancer Res.* 38 (1), 348. doi:10.1186/s13046-019-1334-5

Wu, M.-Z., Chen, S.-F., Nieh, S., Benner, C., Ger, L.-P., Jan, C.-I., et al. (2015). Hypoxia Drives Breast Tumor Malignancy through a TET-Tnfα-P38-MAPK Signaling Axis. *Cancer Res.* 75 (18), 3912–3924. doi:10.1158/0008-5472.can-14-3208

Xiao, Z., Wu, W., Wu, C., Li, M., Sun, F., Zheng, L., et al. (2021). 5-Hydroxymethylcytosine Signature in Circulating Cell-free DNA as a Potential Diagnostic Factor for Early-stage Colorectal Cancer and Precancerous Adenoma. *Mol. Oncol.* 15 (1), 138–150. doi:10.1002/1878-0261.12833

Xu, W., Yang, H., Liu, Y., Yang, Y., Wang, P., Kim, S.-H., et al. (2011). Oncometabolite 2-Hydroxyglutarate Is a Competitive Inhibitor of α-Ketoglutarate-Dependent Dioxygenases. *Cancer cell* 19 (1), 17–30. doi:10.1016/j.ccr.2010.12.014

Xu, Y.-p., Lv, L., Liu, Y., Smith, M. D., Li, W.-C., Tan, X.-m., et al. (2019). Tumor Suppressor TET2 Promotes Cancer Immunity and Immunotherapy Efficacy. *J. Clin. Invest.* 129 (10), 4316–4331. doi:10.1172/jci129317

Yan, Y.-L., Huang, Z.-N., Zhu, Z., Cui, Y.-Y., Li, M.-Q., Huang, R.-M., et al. (2020). Downregulation of TET1 Promotes Bladder Cancer Cell Proliferation and Invasion by Reducing DNA Hydroxymethylation of AJAP1. *Front. Oncol.* 10, 667. doi:10.3389/fonc.2020.00667

Yang, Q., Wu, K., Ji, M., Jin, W., He, N., Shi, B., et al. (2013). Decreased 5-hydroxymethylcytosine (5-hmC) Is an Independent Poor Prognostic Factor in Gastric Cancer Patients. *J. Biomed. Nanotechnology* 9 (9), 1607–1616. doi:10.1166/jbn.2013.1713

Zeng, C., Stroup, E. K., Zhang, Z., Chiu, B. C.-H., and Zhang, W. (2019). Towards Precision Medicine: Advances in 5-hydroxymethylcytosine Cancer Biomarker Discovery in Liquid Biopsy. *Cancer Commun.* 39 (1), 12. doi:10.1186/s40880-019-0356-x

Zhang, F., Liu, Y., Zhang, Z., Li, J., Wan, Y., Zhang, L., et al. (2016). 5-hydroxymethylcytosine Loss Is Associated with Poor Prognosis for Patients with WHO Grade II Diffuse Astrocytomas. *Sci. Rep.* 6, 20882. doi:10.1038/srep20882

Zhang, J., Han, X., Gao, C., Xing, Y., Qi, Z., Liu, R., et al. (2018). 5-Hydroxymethylome in Circulating Cell-free DNA as A Potential Biomarker for Non-small-cell Lung Cancer. *Genomics, Proteomics & Bioinformatics* 16 (3), 187–199. doi:10.1016/j.gpb.2018.06.002

Zhang, L.-Y., Han, C.-S., Li, P.-L., and Zhang, X.-C. (2016). 5-Hydroxymethylcytosine Expression Is Associated with Poor Survival in Cervical Squamous Cell Carcinoma. *Jpn. J. Clin. Oncol.* 46 (5), 427–434. doi:10.1093/jjco/hyw002

Zhang, Z., Jin, Y., Zhang, W., Chu, C., Zhang, K., Gao, X., et al. (2020). Values of 5mC, 5hmC, and TET2 for Identifying the Presence and Progression of Breast Precancerous Lesion. *J. Clin. Lab. Anal.* 34 (5), e23162. doi:10.1002/jcla.23162

Zhong, A., Tian, Y., Zhang, H., and Lai, M. (2018). DNA Hydroxymethylation of Colorectal Primary Carcinoma and its Association with Survival. *J. Surg. Oncol.* 117 (5), 1029–1037. doi:10.1002/jso.24978

Conflict of Interest: The authors declare that the research was conducted in the absence of any commercial or financial relationships that could be construed as a potential conflict of interest.

Publisher's Note: All claims expressed in this article are solely those of the authors and do not necessarily represent those of their affiliated organizations, or those of the publisher, the editors and the reviewers. Any product that may be evaluated in this article, or claim that may be made by its manufacturer, is not guaranteed or endorsed by the publisher.

Copyright © 2021 Xu, Zhou, Chen, Bissessur, Chen, Mao, Ju, Chen, Chen, Li, Zhang, Chen, Cao, Wang and Wang. This is an open-access article distributed under the terms of the Creative Commons Attribution License (CC BY). The use, distribution or reproduction in other forums is permitted, provided the original author(s) and the copyright owner(s) are credited and that the original publication in this journal is cited, in accordance with accepted academic practice. No use, distribution or reproduction is permitted which does not comply with these terms.

Advantages of publishing in Frontiers

OPEN ACCESS
Articles are free to read for greatest visibility and readership

FAST PUBLICATION
Around 90 days from submission to decision

HIGH QUALITY PEER-REVIEW
Rigorous, collaborative, and constructive peer-review

TRANSPARENT PEER-REVIEW
Editors and reviewers acknowledged by name on published articles

Frontiers
Avenue du Tribunal-Fédéral 34
1005 Lausanne | Switzerland

Visit us: www.frontiersin.org
Contact us: frontiersin.org/about/contact

REPRODUCIBILITY OF RESEARCH
Support open data and methods to enhance research reproducibility

DIGITAL PUBLISHING
Articles designed for optimal readership across devices

FOLLOW US
@frontiersin

IMPACT METRICS
Advanced article metrics track visibility across digital media

EXTENSIVE PROMOTION
Marketing and promotion of impactful research

LOOP RESEARCH NETWORK
Our network increases your article's readership